Hydrogen, Fuel Cells and Infrastructure Technologies Program

2002

Annual Progress Report

U.S. Department of Energy,
Energy Efficiency and Renewable Energy

ACKNOWLEDGEMENT

We would like to express our sincere appreciation to Argonne National Laboratory and QSS Group, Inc., for their artistic and technical contributions in preparing and publishing this report.

In addition, we would like to thank all our program participants for their contributions to the programs and all the authors who prepared the project abstracts that comprise this report.

U.S. Department of Energy
1000 Independence Avenue, S.W.
Washington, D.C. 20585-0121

FY 2002

Progress Report for Hydrogen, Fuel Cells, and Infrastructure Technologies Program

Energy Efficiency and Renewable Energy
Office of Hydrogen, Fuel Cells, and Infrastructure Technologies

Approved by Steven Chalk

November 2002

CONTENTS

CONTENTS (Continued)

CONTENTS (Continued)

CONTENTS (Continued)

CONTENTS (Continued)

CONTENTS (Continued)

I. INTRODUCTION

Developing Advanced Hydrogen and Fuel Cell Technologies for Transportation, and Stationary Power Systems

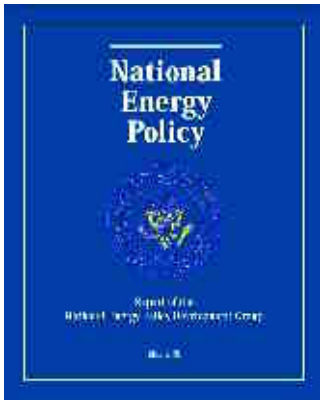

We are pleased to present the Fiscal Year (FY) 2002 Annual Progress Report for the Hydrogen, Fuel Cells, and Infrastructure Technologies Program. This new program office integrates activities in hydrogen production, storage, and delivery with transportation and stationary fuel cell activities. Under the Assistant Secretary for Energy Efficiency and Renewable Energy (EERE), the new Office of Hydrogen, Fuel Cells, and Infrastructure Technologies is responsible for research, development and demonstration of all aspects of hydrogen and fuel cells and was formed in response to a recommendation in the National Energy Policy to "focus research and development efforts … on integrating current programs … regarding hydrogen and fuel cells…"

In January 2002, as a further step toward implementation of the National Energy Policy, Secretary of Energy Spencer Abraham announced formation of the FreedomCAR Partnership, an ambitious, cost-shared cooperative research and development partnership between the Department of Energy (DOE) and the U.S. Council for Automotive Research, the precompetitive research organization of Ford, General Motors (GM), and DaimlerChrysler. The CAR in FreedomCAR stands for Cooperative Automotive Research. And the "Freedom" principle is framed by:

Secretary Abraham announces FreedomCAR

- Freedom from foreign petroleum dependence;
- Freedom from pollutant emissions;
- Freedom for Americans to drive where they want, when they want, in the vehicle of their choice; and
- Freedom to obtain fuel affordably and conveniently.

The long-term goal of the FreedomCAR Partnership is the achievement of vehicles and fuels that lead to a clean and sustainable energy future. Fuel cell vehicles running on renewable hydrogen offer a promising path toward achieving this vision. Thus, a major focus of FreedomCAR is the development of hydrogen and fuel cell technologies. The formation of FreedomCAR demonstrates the federal government's commitment to next generation transportation technologies including fuel cells and hydrogen. The FreedomCAR Partnership Plan can be downloaded from the internet at http://www.cartech.doe.gov.

President Bush and UTC Fuel Cells President William Miller discuss fuel cell technology

The U.S. Department of Energy has also initiated a National Hydrogen Vision and Roadmap process in response to recommendations made in the National Energy Policy. Energy Secretary Spencer Abraham stated, "The President's Plan directs us to explore the possibility of a hydrogen economy." The Vision Meeting, an important first step, took place November 15-16, 2001. The 53 business executives, Federal and State energy policy officials, and leaders of universities, environmental organizations, and National Laboratories who participated contributed to the development of the vision:

> ***Hydrogen is America's clean energy choice. It is flexible, affordable, safe, domestically produced, used in all sectors of the economy, and in all regions of the country.***

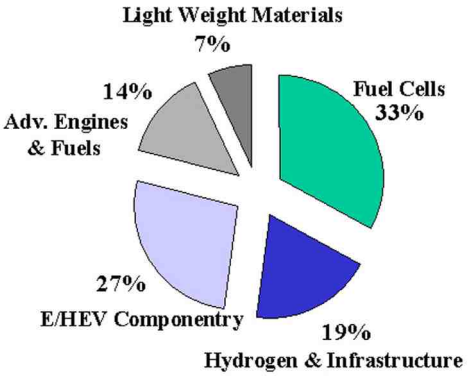

Shown above is the breakdown of DOE FreedomCAR funding ($150 million) by technology area. Industry share is an additional 20-50%.

Building on the work of the Vision Meeting, more than 200 participants representing hydrogen energy industries, academia, environmental organizations, federal and state government agencies, and National Laboratories met on April 2-3, 2002 for a National Hydrogen Energy Roadmap Workshop in Washington, DC. The purpose of the workshop was to identify the key activities that will have to take place to enable the vision to become reality. The intent was to identify the most important barriers and paths forward that should be addressed in order to achieve the Vision; the time frames for the top priority research and development and other efforts; and the respective roles of industry, government, universities, and National Laboratories in dealing with these issues. In his concluding remarks to the workshop participants, David Garman, Assistant Secretary for Energy Efficiency and Renewable Energy, stated: "There are two paths we need to follow: research and development, and public outreach to capture the imagination of the American people. This will be a long journey and process, and the Department of Energy will work with you as we move forward." The National Hydrogen Energy Roadmap Report is available on http://www.eren.doe.gov/hydrogen.

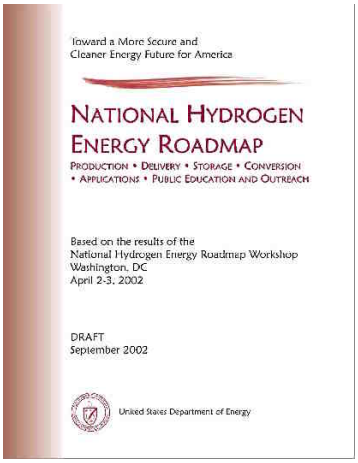

This report provides an overview of the nature, objectives, and progress of the Program; examines the remaining technical barriers to commercialization of the technology; and highlights the Program's future directions. While the primary purpose of this report is to document the progress made by the DOE Hydrogen, Fuel Cells, and Infrastructure Technologies Program during FY 2002 in overcoming the R&D barriers, it also highlights some of the major advances in fuel cell technology made through other private and public initiatives throughout the year. The reader is also referred to http://www.eren.doe.gov/hydrogen for additional information.

Transportation Highlights

In October 2001, Ford set a national record for fuel cell endurance by running a P2000 car continuously for 24 hours. The vehicle traveled 1,391 miles averaging 58 mph, including stops for refueling and driver changes. Average actual on-track speed was 65 mph. The P2000 uses an advanced lightweight Ford Research vehicle platform that offers interior space for 5 passengers while weighing only ~3,300 pounds. The P2000's

Ford P2000 Fuel Cell Vehicle

fuel cell system delivers 90 hp and accelerates the car from 0 to 60 in less than 14 seconds. The polymer electrolyte membrane fuel cells and electric drive powertrain were supplied by Ballard Power Systems.

DaimlerChrysler's NECAR 5 sedan completed the first transcontinental journey of a fuel cell powered vehicle in June 2002. The NECAR 5 is powered by a fuel cell engine designed by Ballard Power Systems and fueled by methanol. The 3,262-mile trip, which took 85 hours of driving over 12 days, ended at the DOE-sponsored Future Car Congress in Washington, D.C. in June, 2002. According to DaimlerChrysler, no components of the fuel cell engine had to be repaired during the journey. An electrical short caused by moisture delayed the trip for one day, and two belts, four fuel filters, and one water compartment had to be replaced.

DaimlerChrysler NECAR 5 and Jeep Commander Fuel Cell Vehicles

In January 2002, at the North American International Auto Show in Detroit, General Motors unveiled the Autonomy fuel cell concept car. The basic component of GM's plan for a fuel cell vehicle is a so-called "skateboard" platform that would include both the fuel cells and the vehicle's electronic powertrain. The platform would allow a variety of body types to be built and assembled to the chassis.

GM Autonomy Fuel Cell Car (left) and the "Skateboard" Platform (right)

To accelerate the development of fuel cell vehicles, the California Fuel Cell Partnership (CaFCP) was established in Sacramento, CA, in November 2000 (see http://www.fuelcellpartnership.org). The CaFCP 2002 technical achievements include:

- operation of 16 CaFCP fuel cell powered vehicles,
- installation of a methanol fuel station at the West Sacramento headquarters, and
- commencement of a second joint study examining hydrogen vehicle facility construction and use issues.

Technology Status and Challenges

Hydrogen Production

Hydrogen, like electricity, can be produced from many sources, including fossil fuels, renewable resources, and nuclear energy. The Department currently supports R&D on a number of different hydrogen production technologies, including biological-, biomass-, fossil-, nuclear-, and renewable-based processes. Future R&D will also address approaches for producing hydrogen utilizing waste heat from nuclear energy sources.

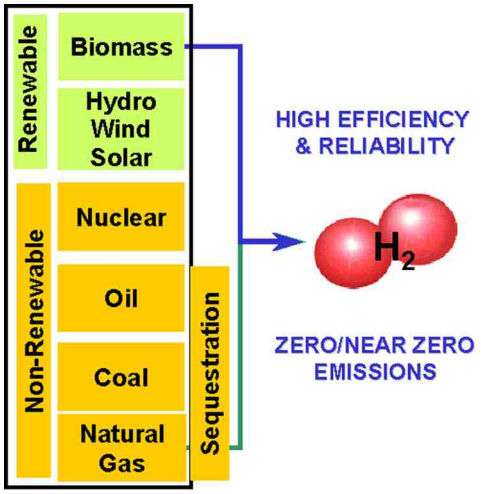

The FreedomCAR target for hydrogen production via natural gas reforming is presented in Table 1. Targets for hydrogen production, separation and purification, storage, and delivery are listed in Appendix A. Remaining technical challenges for hydrogen energy systems include:

- Reducing the cost of hydrogen production from renewable resources and fossil feedstocks
- Establishing "learning" hydrogen fuel infrastructure demonstrations to address technical and economic issues that will help refocus research
- Developing standards of safe practice, codes, and product certification to enable commercial production of hydrogen-based systems for mobile and stationary applications

Technology[1]	2002 Status	2010
Natural Gas Reforming	$6.00/gge[2]	$1.50/gge[3]
1. A thorough analysis will be performed in FY 2003 to establish technical targets for biomass and other hydrogen production pathways. 2. Status based on single, 215 kg/day unit. (gge=gasoline gallon equivalent) 3. Target based on projected cost for ~900 kg/day units, produced in volume of 100 units per year.		

Table 1. Hydrogen Production Status and Targets

Hydrogen Storage

The overarching technical challenge for hydrogen storage is how to store the necessary amount of hydrogen needed to fuel the vehicle for its required driving range (>300 miles), within the constraints of weight, volume, efficiency, and cost.

The Department is currently pursuing three approaches for on-board hydrogen storage: 1) physical storage, 2) reversible chemical storage, and 3) irreversible chemical storage. Physical storage involves the development of tanks for either compressed hydrogen gas or liquid hydrogen. Reversible chemical approaches store hydrogen in solid materials where the hydrogen can be released and refilled without physically removing the storage media from the vehicle. Potential reversible storage materials include metal hydrides and carbon materials such as carbon nanotubes. Irreversible chemical approaches release hydrogen via an on-board chemical reaction with the storage material. In this case, the storage media must be physically replaced with fresh material once it has become exhausted. The reaction of sodium borohydride with water is an example of this approach.

Table 2 gives the DOE hydrogen storage system goals for the year 2005 and compares these goals to the state-of-the-art hydrogen storage technology – 5,000 psi tanks, which have been certified. Development of compressed hydrogen tanks at 10,000 psi is near completion; certification activities are in progress. Materials to enable low pressure hydrogen storage are the focus of DOE hydrogen storage activities. Other hydrogen storage targets are listed in Appendix A.

Characteristic	2002 Status[2]	2005 Goal
Weight Percent	5.2	6
Specific Energy (W-h/kg)	1745	2000
Energy Density (W-h/liter)	813	1100
Cost ($/kWh)	50	5
1. 2010 targets are under review by the FreedomCAR Hydrogen Storage Technical Team 2. Status is based on certified 5,000 psi hydrogen tanks; 10,000 psi tanks have been developed – certification activities are underway		

Table 2. Comparison of Current Status[1] to 2005 Hydrogen Storage System Goals

Transportation Fuel Cells

Direct hydrogen PEM fuel cell systems are more technically mature and face fewer challenges than systems requiring an on-board fuel processor. Although the demonstrated performance and efficiency of direct hydrogen systems approach the anticipated goals, several issues remain. The primary barriers are lack of a refueling infrastructure and on-board hydrogen storage, cost, durability, size, and weight.

Remaining technical challenges for automotive fuel cell power systems include:

- Reducing component and system costs (including reducing precious metal requirements)
- Developing high-volume manufacturing capability
- Demonstrating component and system durability
- Reducing system start-up time, especially for gasoline-powered systems
- Developing high-efficiency air management subsystems

Technical and economic targets were developed for direct hydrogen transportation PEM fuel cell systems and they are indicated along with the status in Table 3, as well as in Appendix A. The targets and status of gasoline-fueled systems remain the same as in FY 2001. Note that the FreedomCAR fuel cell technical team is currently considering revisions to all technical targets.

Characteristic	2002 Status	2005	2010
Energy efficiency @ 25% of rated power (%)	59	60	60
Energy efficiency @ rated power (%)	50	50	50
Power density (W/L) excluding H_2 storage including H_2 storage	 400 140	 500 150	 650 220
Specific power (W/kg) excluding H_2 storage including H_2 storage	 400 250	 500 250	 650 325
Cost (including H_2 storage) ($/kW)	200	125	45
Transient response (time from 10% to 90% of rated power) (seconds)	3	2	1
Cold start-up time to maximum power (seconds) @ –20°C ambient temperature @+20°C ambient temperature	 120 60	 60 30	 30 15
Emissions	Zero	Zero	Zero
Durability (hours)	1000	2000	5000
Survivability (°C)	-20	- 30	-40

Table 3. Comparison of Targets for 50 kWe (net) Integrated Fuel Cell Power Systems Operating on Direct Hydrogen to Current Status

Major Go/No-Go Decision Planned

DOE is pursuing a dual pathway to evaluate fuels for fuel cell vehicles. As an alternative to the direct hydrogen approach, the Program is pursuing development of on-board fuel processors to reform gasoline and alternative fuels such as methanol, ethanol, and natural gas to produce the required hydrogen. An advanced petroleum-based fuel, which is "gasoline-like," would be an interim "transition" strategy. It would be compatible with the existing refueling infrastructure and eliminate the hydrogen storage barrier. However, on-board fuel processing has been presenting serious technical and economic challenges which may not be overcome in the required "transition" timeframe. Consequently, DOE is deciding whether to continue on-board fuel processing R&D beyond the end of FY 2004. Identification of decision criteria (such as energy required for start-up) and metrics is in the early stages.

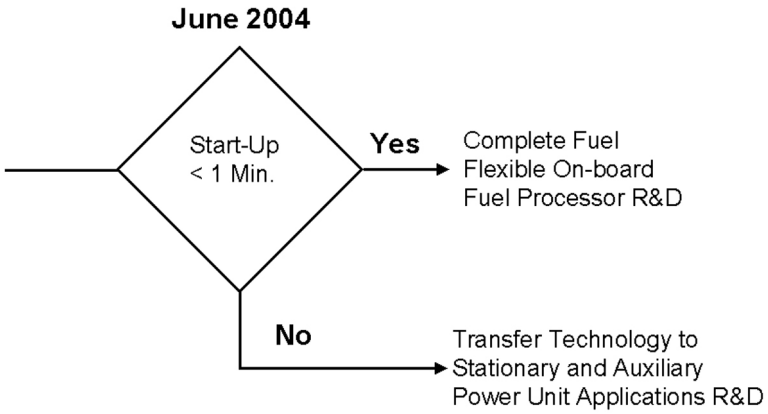

Stationary Fuel Cells

Because the buildings sector accounts for ~36% of the U.S. primary energy consumption and between 30% and 40% of all airborne emissions, DOE is developing high efficiency polymer electrolyte membrane (PEM) fuel cell power systems as an alternative power source to grid-based electricity for buildings. A successful stationary fuel cell program will not only save energy and reduce emissions, but its inherent flexibility will help address energy shortage issues through energy diversity. Industry cost-shared projects will cross-cut several technological areas addressing research needs in stationary fuel cell systems, fuel cells for back-up power, materials for high temperature membranes, fuel cell component durability, water and thermal management, fuel processing for stationary applications, platinum recycling, and non-precious metal catalysts.

Technical and economic challenges for natural gas-based stationary fuel cell R&D include:

- Improving energy efficiency
- Improving integrated system durability
- Reducing component and system cost
- Resolving interconnectivity issues with grid and developing codes/standards
- Developing fuel-cell systems with potential to meet cost-effective thermal energy needs for some or all of the building's heating/cooling requirements

In FY 2003, a study is planned to establish baseline performance and outyear targets for stationary PEM fuel cells for various market segments.

Research, Development and Demonstration (R,D&D) Highlights

Researchers supporting the Hydrogen, Fuel Cells, and Infrastructure Technologies Program continued to make significant progress in meeting R,D&D challenges during FY 2002. The summaries that follow are selected highlights of the progress made under the program.

Biological Organisms Replace Expensive Nickel Catalysts for Hydrogen Production The National Renewable Energy Laboratory has successfully shown that a unique photosynthetic organism can replace nickel catalysts in the water-gas-shift reaction for hydrogen production from synthesis gas. These organisms are able to produce hydrogen from water while converting carbon monoxide to carbon dioxide. Industrially, this reaction is normally performed using expensive nickel catalysts and at high temperatures. To date, these organisms have been able to perform with industrial synthesis gas and with gas from a biomass gasification process development unit. The organisms are robust under a variety of conditions. Work is now progressing on improving reactor design and reaction rates.

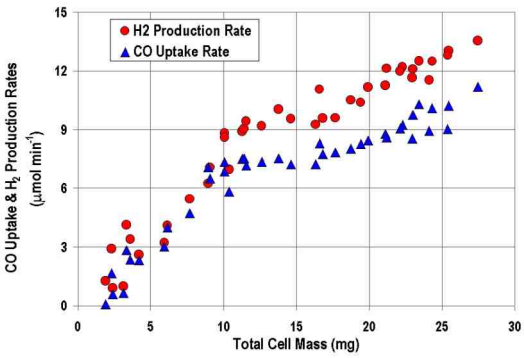

Hydrogen Production and Carbon Monoxide Uptake Rates vs. Total Call Mass

SNL Develops Defect-Free Thin Film Membranes for Hydrogen Separation and Isolation Even small amounts of carbon monoxide or other contaminants can poison a fuel cell. Sandia National Laboratories (SNL) is working on developing gas-selective thin film membranes to improve and lower the cost for hydrogen purification. Defect-free aluminosilicate and silicalite zeolite thin films supported on commercially available alpha and gamma alumina disk substrates were developed. In tests using SNL's permeation unit, which can test both pure and mixed gases from room temperature to 250°C, excellent separation values for hydrogen were achieved.

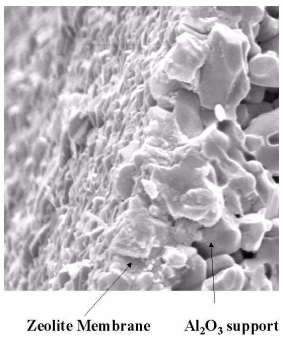

Cross section view by SEM of the micron thick Na/Al/Si ZSM-5 membrane on gamma-alumina substrate for hydrogen purification.

University, Industry and Laboratory Team Completes Reactor Testing and Produces Hydrogen from Peanut Shells Clark Atlanta University, Georgia Institute of Technology, Scientific Carbons Inc., Enviro-Tech Enterprises Inc. and the National Renewable Energy Laboratory (NREL) have partnered to move NREL's technology for the generation of hydrogen from biomass and agricultural residue into the commercial setting. This success marks the first application of a near-term economically viable option for renewable hydrogen production. During FY 2002, the team successfully tested a 1 kg per hour shift reactor on vapors from peanut shell pyrolysis, both at NREL and at the Scientific Carbons Inc. facility in Blakely, Georgia. The unit was also used to show that the fluidizable catalyst being developed by NREL in collaboration with CoorsTek in Golden, Colorado, is able to reform the pyrolysis vapors while maintaining its physical integrity. This technology is particularly interesting because it is applicable to all forms of biomass. This project is a showcase of the hydrogen economy vision that exemplifies stakeholder involvement throughout the energy chain (farmers, food processors, industrial commodity producers, energy/fuel consumers).

QUANTUM Technologies Tanks Validated for 5,000 and 10,000 psi On-Board Hydrogen Storage

The 5,000 and 10,000 psi tanks developed by QUANTUM Technologies have been validated to meet the requirements of DOT FMVSS304, NGV2-2000 (both modified for 10,000 psi hydrogen) and draft E.I.H.P standard. The tanks were submitted to typical safety testing, including: Burst Tests (2.35 safety margin), Fatigue, Extreme Temperature, Hydrogen Cycling, Bonfire, Severe Drop Impact Test, Flaw Tolerance, Acid Environment, Gunfire Penetration, Accelerated Stress, Permeation and Material testing. These QUANTUM "TriShield" tanks achieve 6% hydrogen by weight, 1,050 W-h/L, and 2,000 W-h/kg, meeting the percent weight and specific energy goals and nearly meeting the energy density goal of 1,100 W-h/L. Significant cost reductions are possible with further optimization. QUANTUM is now working with several automotive manufacturers to incorporate these tanks into hydrogen fuel cell vehicles.

QUANTUM TriShield™ Type IV Tank

World's First Hydrogen Station Co-Produces Fuel and Electricity A facility that will serve as a "learning" demonstration of hydrogen as a safe and clean energy alternative for vehicle refueling is under construction by Air Products and Chemicals, Inc., in partnership with Plug Power Inc. and the City of Las Vegas (CLV), Nevada. The facility includes small-scale, on-site hydrogen production technologies, a hydrogen/compressed natural gas blend refueling facility, and a 50-kW PEM fuel cell system which supplies electricity to the grid. The fueling station and power plant are co-located at the existing City of Las Vegas Fleet & Transportation Western Service Center. The CLV was given easement to public lands by the Bureau of Land Management, which also conducted the appropriate environmental analyses for the facility. All permits were approved and construction is nearly complete. Other partners include NRG Technologies in Reno, Nevada, who is retrofitting the 6 buses donated by the City of Las Vegas that will be refueled at this station, and the University of Las Vegas, who is modifying a bus to burn hydrogen in an internal combustion engine and to store the hydrogen in a compressed tank.

Hydrogen Technologies for Public Transportation in California's Coachella Valley The SunLine Services group continued to host what has been called the world's most complex hydrogen demonstration project to date. Buses running on hydrogen and hydrogen/natural gas mixtures were used for public transport and filled at SunLine's public access fueling island. Two different types of electrolyzers, one supplied by a photovoltaic grid and the other by a natural gas reformer, produced hydrogen on-site. A full training program, including a curriculum for the local community college, has been developed. More than 5,000 visitors a year from

Sunline Transit Clean Fuel Mall and Hydrogen Transit Bus Being Refueled

around the world have toured SunLine's facilities. SunLine's experience and leadership is instrumental in establishing a knowledge base and developing codes and standards for hydrogen production and use.

University of Miami Leads Hydrogen Safety Evaluation and Simulation Studies for Codes and Standards Development Using computer simulations and real-time safety studies, Dr. Michael Swain at the University of Miami evaluated the safety protocols at the California Fuel Cell Partnership (CaFCP) building in Sacramento, California. Two different hydrogen leak scenarios were used to evaluate building ventilation and potential ignition hazards, and to establish safety procedures in the event of a hydrogen leak. Dr. Swain also developed a simple method for visualizing the motion of gases from a hydrogen leak, which will be used to determine sensor placement for hydrogen leak detection. These and other tests being done at the University of Miami are being used by the International Code Council Ad Hoc Committee to develop codes and standards for the safe use of hydrogen.

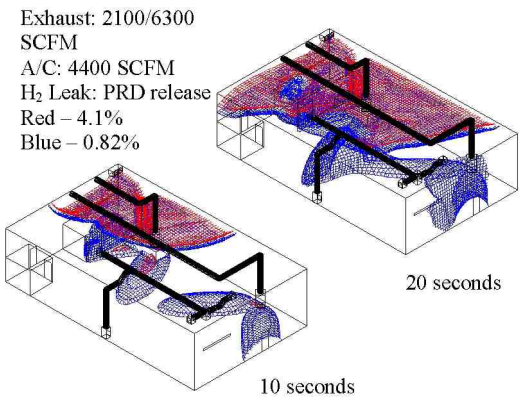

Transportation Fueling Infrastructure Analysis Completed Longitude 122 West completed its analysis of transportation fueling infrastructure costs and environmental impacts, looking at refueling alternatives (gaseous or liquid hydrogen); vehicle configuration and fuel alternatives (various hydrogen storage and power plant selections, and alternative fuels, including methanol and gasoline); cost variations for electricity, natural gas and hydrogen with economic conditions and over international boundaries; and future costs of upstream infrastructure. The analysis showed that various options for hydrogen infrastructure are possible and that the least costly option may vary with location, local pricing of gas or electricity, and technology maturity. Near-term options using hydrogen delivered from existing sources are quite feasible. The longer-term options include building new central production and distribution facilities. On-site generation requires development of commercial subsystems. The urgency of reduced local emissions can be met with hydrogen-fueled vehicles and clean hydrogen brought in by pipeline or produced by electrolysis.

Porvair Scales Up Oak Ridge Bipolar Plate Process During FY 2002, Porvair Fuel Cell Technology scaled up PEM bipolar plate fabrication technology licensed from Oak Ridge National Laboratory. The process involves fabricating porous carbon pre-forms which are subsequently impregnated with carbon by a chemical vapor impregnation or deposition process to the desired density. The plates can be embossed with the flow field pattern to eliminate machining. Porvair has scaled up production to 30 plates per day and is designing a semi-continuous process for 300 plates per day. As shown in the accompanying table, DOE material properties have been met. Plates designed by UTC Fuel Cells have been delivered to them for a 20-cell stack.

Property	Value	DOE Target
Electrical Conductivity (S/cm) (ASTM C611)	> 300	> 100
Density (g/cc)	1.00 – 1.30	-
Flexural Strength (psi)	5700	> 600 (crush)
Flexibility (%) (deflection at mid-span)	1.5 – 3.5	3-5
Nitrogen Permeability (cc/cm^2/sec) (ASTM D1434)	Not detected	<2x10^{-6} (Hydrogen)

Porvair Carbon/Carbon BiPolar Plates

Brookhaven National Laboratory Has Developed a Process for Low-Pt Electrodes Brookhaven National Laboratory has developed and demonstrated a new electrocatalyst structure and deposition process with higher mass-specific activity (amps/mole of Pt) for hydrogen oxidation and CO tolerance than commercial electrocatalysts with several times higher platinum loadings. The concept involves synthesis of electrocatalysts by spontaneous deposition of Pt on a Ru surface, resulting in a submonolayer of Pt on the Ru nanoparticles. Based on cell testing performed at Los Alamos National Laboratory, the Pt loading and Ru

loading of the new anode catalyst structure are 0.06 g/kW and 0.50 g/kW, respectively. The Pt loading is well below the DOE target of 0.2 g Pt/peak kW total for the MEA, and the Ru loading is at the level of the present state-of-the-art catalysts. Future work in this area includes replacement of the Ru with a non-precious metal such as tungsten to further reduce the precious metal loading and demonstration of the concept for oxygen reduction at the fuel cell cathode. Durability and scale-up issues will also be addressed.

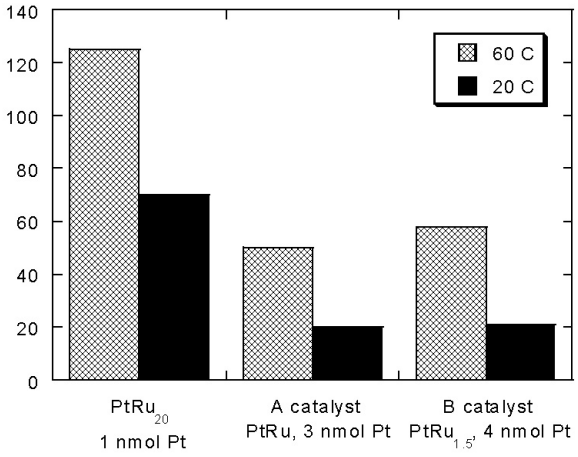

3M Develops High-Performance MEAs This 3M project is directed toward demonstrating high-performance, matching PEM fuel cell components that can be manufactured by integrated pilot processes, using a patented nano-structured thin-film catalyst support system, and reducing precious metal loadings. Progress during FY 2002 includes: development of a new Pt ternary cathode catalyst that gives the same performance with one-half the amount of Pt, producing 0.4 A/cm^2 at 0.8 V under 30/30 psig H_2/air with 0.2 mg/cm^2 total precious metal per MEA; identification of a non-precious metal replacement for Ru on the anode for reformate tolerance, which, with air bleed, gives equivalent performances within ± 10-20 mV; integration of multiple process steps for generating the nanostructured catalyst support films into a single pass, dry web-coating, pilot plant process; and verification of the uniformity of the processed roll-goods. The accompanying figure shows the excellent uniformity of 7 statistically sampled MEAs from a 450-lineal yard roll-good.

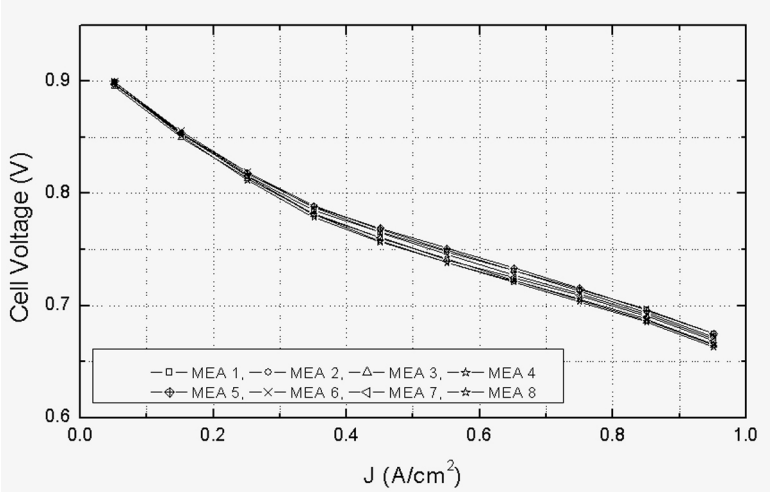

SwRI Demonstrates Pilot Manufacturing of Low-Pt Electrodes During FY 2002, Southwest Research Institute (SwRI), in cooperation with W.L. Gore and Associates, a leading supplier of MEAs for PEM fuel cells, completed scale-up and demonstration of a high-volume pilot manufacturing process for electrode material, a crucial (and currently costly) element in the high-volume production of fuel cell MEAs. The key component of this process is a vacuum coating unit capable of producing large quantities of high-performance, ultra-low platinum (0.1 mg/cm^2 total) per year and the potential for bringing MEA production costs below $10/kW. A pilot manufacturing facility was installed which has the capability of catalyzing more than 100,000 m^2 per year of electrode material on a 2-shift basis. Several thousand ft^2 of electrode materials at 40 linear feet per minute have been manufactured and fabricated into MEAs, which were tested on reformate and neat hydrogen in single cells. The continuously-

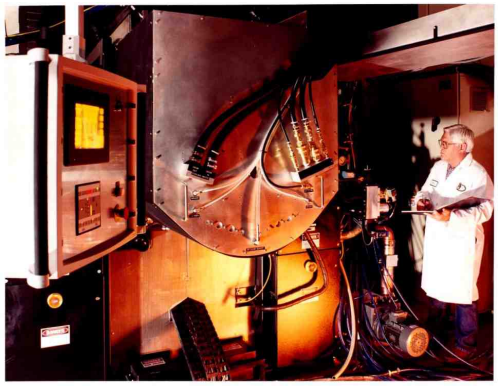

produced MEAs compare favorably with baseline MEAs with much higher Pt loadings. Future work will focus on the durability of the low-Pt MEAs.

McDermott Operates Integrated Gasoline Fuel Processor During a 100-hour test, McDermott Technology successfully demonstrated a large-scale, fully-integrated multi-fuel processor on gasoline to produce a fuel cell-quality gas containing 43% hydrogen. The fuel processor produces enough hydrogen for a 50-kW PEM fuel cell power plant, sufficient to provide propulsion power for a small vehicle or to supply hydrogen to a stationary fuel cell installation. The processor is based on a design which incorporates state-of-the-art autothermal reforming, liquid-phase desulfurization, and a medium-temperature shift reactor for CO clean-up to achieve compact size, simplified controls, and high efficiency. The system also includes a preferential oxidation (PrOx) unit supplied by Los Alamos National Laboratory and a steam generator based on microchannel heat exchanger technology developed by Pacific Northwest National Laboratory.

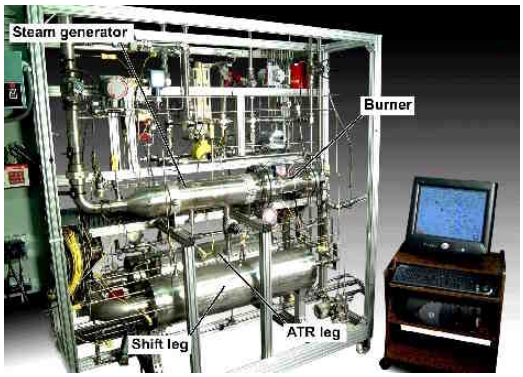

Caterpillar Operates PEM Fuel Cell stack on Ethanol Reformate Caterpillar, Nuvera Fuel Cells, and Williams Bio-Energy have teamed to develop and demonstrate a 15-kW ethanol-fueled PEM fuel cell system. The primary technical objectives of this project are to demonstrate performance, durability and reliability and to understand correlations and reduce gaps between stationary and transportation PEM fuel cell applications. Power module design specifications have been completed. The reformer has been tested for a short period of time (45 minutes) on ethanol at rated power, and 45- and 80-cell stacks have been successfully tested with output from the reformer.

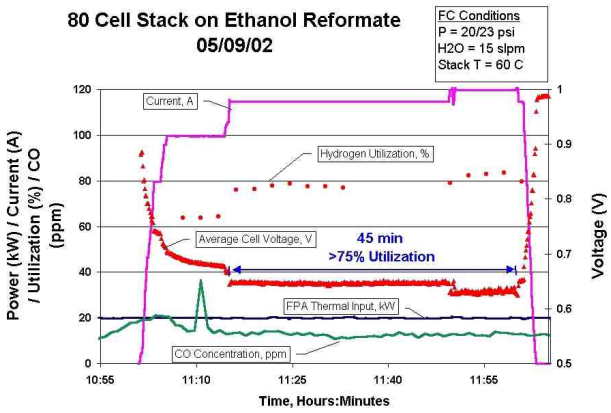

Programmatic Highlights

Hydrogen Storage Workshop On-board hydrogen storage is a "critical path" enabling technology because current technologies offer limited driving range and demand excessive cost, volume, and weight. A Hydrogen Storage Workshop (see http://www.eren.doe.gov/hydrogen/docs/2002storageworkshop.html) was held during FY2002 to discuss approaches to increasing the capacity and reducing the cost of hydrogen storage technologies. Sessions were held on carbon technologies, chemical storage, advanced/complex hydrides, and advanced concepts. Participants included representatives of industry, academia, and DOE/national Laboratories. As a result of the Workshop, a hydrogen storage solicitation is planned for FY2003.

High-Temperature Polymer Membrane Working Group It is desirable to operate PEM fuel cells at temperatures exceeding the currently typical 80°C. Operation at higher temperature would facilitate stack and system thermal management, increase CO tolerance, and improve electrode kinetics. A High-Temperature Polymer Membrane Working Group was established to address this challenging task and to coordinate industrial, government, and academic efforts on membrane design and synthesis, thermal stability, maintaining conditions beneficial to proton conduction in the polymeric medium, implementation of new "carrier" media to replace the function of water in Nafion, study of proton transfer dynamics, and understanding the fundamentals of the proton transfer and transport processes.

The formation and processing of MEAs from any new polymers, including any critical additives, is also being addressed. The oxygen reduction reaction (ORR) activity within MEAs containing different additives or other mechanisms of proton transfer must be understood as well.

The Working Group meets biannually in conjunction with the Electrochemical Society Meetings, allowing us to assess progress and to communicate issues and needs to the High-Temperature-Membrane community at large.

Fuel Cells for Buildings and Stationary Applications A workshop was held with DOE and industry stakeholders on April 10-11, 2002 to identify the issues related to fuel cells for buildings and stationary applications (see http://www.eren.doe.gov/hydrogen/pdfs/stationary_fc_proceedings.pdf). A solicitation, "Cooperative Research, Development, and Demonstration for Fuel Cells for Stationary and Automotive Applications", was issued (see http://www.energy.gov/HQPress/releases02/seppr/pr02193.htm) addressing the major issues raised during the workshop through DOE's "Industry Interactive Procurement System" (IIPS) web page (http://e-center.doe.gov under the "HELP" section of the website – DE-SC02-02EE11137). The solicitation also includes topics that address cross-cutting barriers to both stationary and automotive fuel cells.

Portable and Off-Road Fuel Cell Power Applications Portable power will likely be the first high-volume market for fuel cells because of their low power requirements and less-stringent cost target (~$5,000/kW). The manufacturing capability that develops for portable power fuel cells will help accelerate commercialization of fuel cells for stationary power generation and transportation. A joint DOE/industry Portable Power Workshop was held in January 2002 (see http://www.eren.doe.gov/hydrogen/docs/2002fcportablepowerworkshop.html). The focus of the Workshop was portable fuel cells for low-power (sub-watt to 20-50W) applications such as consumer electronics and high-power (20W to 5kW) applications such as auxiliary power units (APUs) (1-10kW) for hotel and refrigeration loads for long-haul trucks and recreational vehicles. A solicitation, "Research, Development, and Integration of Energy Efficient Technologies in Portable Power and Off-Road Fuel Cell Applications" (see http://www.golden.doe.gov/business%20opportunities/solicitations.html - DE-PS36-02GO92TBD) will be issued for R,D&D in proposed consumer electronics and auxiliary power unit fuel cell systems. The solicitation will also request proposals to assess technical issues and perform R&D to evaluate and demonstrate remedies specific to off-road fuel cell applications.

Reports to Congress The United States Congress, in November of 2001, directed the DOE to submit two reports addressing the status of fuel cell technologies (see http://www.eren.doe.gov/RE/hydrogen.html. The first of these reports, to be issued in November of 2002, addressed the need for public/private partnerships to demonstrate the use of fuel cells in commercial scale applications. This report identified two public-private partnership programs, one on Stationary and Distributed Generation and one on Transportation and Infrastructure, which would be required to enable commercial-scale demonstration and to realize the benefits of fuel cell technologies.

The second report requires DOE to report on "the technical and economic barriers to the use of fuel cells in transportation, portable power, stationary and distributed generation applications." The report is also expected to include "recommendations on program adjustments based on an assessment of the technical, economic and infrastructure requirements needed for the commercial use of fuel cells for stationary and transportation applications by 2012." This second report is in the early draft stage.

Future Directions

Worldwide interest in hydrogen and fuel cell technologies remains very strong for a broad range of transportation, stationary, and portable power applications. The U.S. DOE remains committed to contributing

to this progress in a significant way by supporting R&D activities that address the most critical barriers to the introduction of commercially viable PEM fuel cell systems and supporting fuel infrastructure.

Recent new DOE projects de-emphasize fuel cell system integration and full-scale stack development because industry has the capability to carry these efforts forward. The DOE program will focus on addressing the most critical issues of cost, durability, and performance of materials, components, and enabling technologies. Substantial progress was made during 2002 toward meeting the technical targets for fuel cell and fueling systems for light-duty vehicles; however, significant technical and economic challenges remain before fuel cell vehicles and the supporting infrastructure will achieve significant market penetration. As we move forward, we will continue to work with our government and industry partners to address these challenges. In addition to the contracts with industry and academia, the DOE national laboratories will continue to provide valuable support to the Hydrogen, Fuel Cells, and Infrastructure Technologies Program during FY 2003 (see Table 4). Through these efforts and other related projects, researchers in the Program will continue to improve cost, durability, efficiency, and overall system performance, allowing us to move closer to the commercial availability of fuel cell vehicles.

Table 4. DOE national laboratory R&D in support of Hydrogen, Fuel Cells, and Infrastructure Technologies program.

Laboratory	R&D Focus
Argonne National Laboratory	Systems Analysis Fuel Processor Catalysis Fast-Start Fuel Processing
Brookhaven National Laboratory	Low-Pt Electrodes
Lawrence Berkeley National Laboratory	Electrocatalysts
Lawrence Livermore National	Sensors Hydrogen Storage
Los Alamos National Laboratory	Sensors Improved Cathodes High-Temperature Membranes Durability Studies Fuels Effects
National Energy Technology Laboratory	Fuel Processing
National Renewable Energy Laboratory	Vehicle and Hydrogen Infrastructure Analyses Hydrogen Production Hydrogen Storage
Oak Ridge National Laboratory	Stack Materials/Components
Pacific Northwest National Laboratory	Microchannel Fuel Processing
Sandia National Laboratory	Hydrogen Purification Hydrogen Storage

As mentioned earlier, EERE's Hydrogen Program, Fuel Cells for Buildings Program, and Fuel Cells for Transportation Program were merged to form the Hydrogen, Fuel Cells and Infrastructure Program. The Program Office is organized as follows:

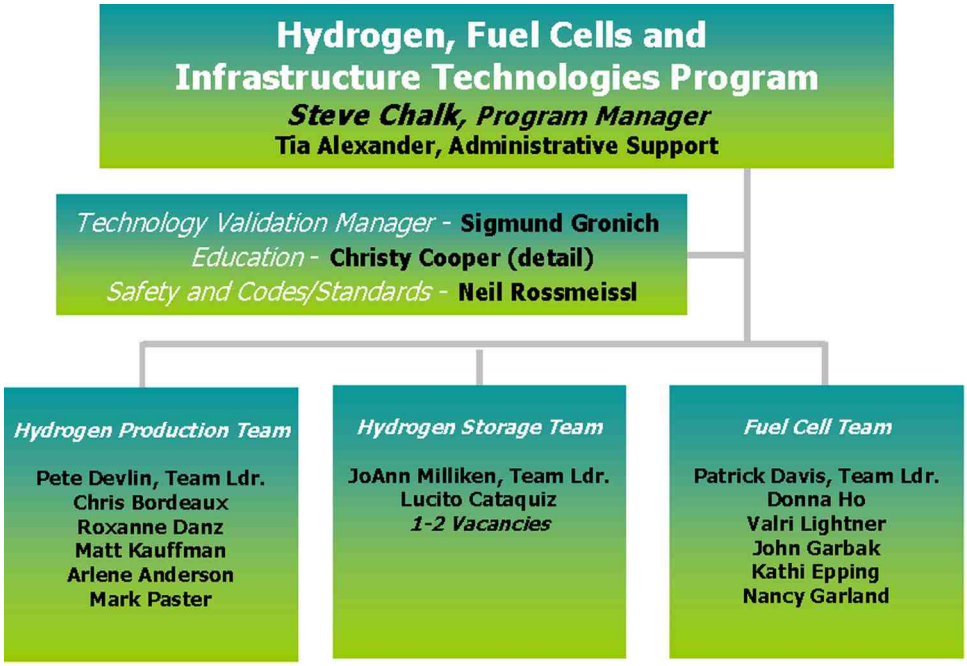

Programmatic responsibilities have been assigned as follows:

Hydrogen Production Team	
Pete Devlin (202) 586-4905 Peter.Devlin@ee.doe.gov	• Overall Hydrogen Production R&D • FreedomCAR Energy Industry Expansion
Roxanne Danz (202) 586-7260 Roxanne.Danz@ee.doe.gov	• Biological, Biomass, and other Renewable Hydrogen Production
Chris Bordeaux (202) 586-3070 Christopher.Bordeaux@ee.doe.gov	• Integrated Power Parks • Uninterruptible Power Systems • H_2 Infrastructure Validation • California Fuel Cell Partnership • International Outreach (non-IEA)
Matt Kauffman (202) 586-5824 Matthew.Kauffman@ee.doe.gov	• Cross-cutting Analyses • Electrolyzers
Arlene Anderson (202) 586-3818 Arlene.Anderson@ee.doe.gov	• H_2 Production: Natural Gas, Petroleum Feedstocks • Coordinate with Fossil Energy on Coal-Based H_2 Production • 5-Year R,D&D Plan Development • Platinum Mining & Recovery
Mark Paster (202) 586-2821 Mark.Paster@ee.doe.gov	• Overall Feedstock Strategy for H_2 production • High Temperature Thermochemical and Electroysis H_2 Production • Hydrogen Delivery

Hydrogen Storage Team	
Lucito Cataquiz (202) 586-0729 Lucito.Cataquiz@ee.doe.gov	• Support Service Contractor COTR • Cost/Financial Status • Pressurized Tanks & Hydrogen Compressors
JoAnn Milliken (202) 586-2480 JoAnn.Milliken@ee.doe.gov	• Overall Hydrogen Storage • Fuel Cell International Activities • FreedomCAR Storage & Vehicle Interface Tech Team
Fuel Cell Team	
Pat Davis (202) 586-8061 Patrick.Davis@ee.doe.gov	• Overall Fuel Cell Systems • FreedomCAR Fuel Cell Tech Team • Compressors/Expanders
Donna Ho (202) 586-8000 Donna.Ho@ee.doe.gov	• Transportation Fuel Cells • CARAT Program
Valri Lightner (202) 586-0937 Valri.Lightner@ee.doe.gov	• Fuel Processing • MEA R&D
John Garbak (202) 586-1723 John.Garbak@ee.doe.gov	• Fuel Cell Vehicle Demonstration • Liaison with 21st Century Truck • Fuel Cells for APUs
Kathi Epping (202) 586-7425 Kathi.Epping@ee.doe.gov	• Stationary Fuel Cells
Nancy Garland (202) 586-5673 Nancy.Garland@ee.doe.gov	• National Lab Fuel Cell R&D • Sensors • GATE Program
Cross-Cutting Functions	
Sig Gronich (202) 586-1623 Sigmund.Gronich@ee.doe.gov	• Overall Technology Validations for Transportation and Stationary Applications
Christy Cooper (202) 586-1885 christy.cooper@ee.doe.gov	• Education on Hydrogen and Fuel Cells
Neil Rossmeissl (202) 586-8668 Neil.Rossmeissl@ee.doe.gov	• H_2 Codes and Standards • H_2 Safety • Hydrogen Technical Advisory Panel • IEA H_2 Agreement

The Office of Hydrogen, Fuel Cells and Infrastructure Technologies has established the following FY 2003 priorities:

1. Develop an integrated 5-year R,D&D Plan to address challenges identified in the National Hydrogen Energy Roadmap.
2. Implement a "national" program in hydrogen storage that focuses on low pressure, solid-state materials.
3. Develop, with assistance of the National Academy of Sciences, a feedstock strategy for hydrogen production which can be used as a basis for cost effective implementation of hydrogen infrastructure.
4. Prepare an integrated DOE Hydrogen Plan to coordinate efforts among the Offices of Energy Efficiency and Renewable Energy, Fossil Energy, Nuclear Energy and Science.
5. Evaluate the feasibility and conduct planning for a fuel cell vehicle and hydrogen infrastructure test and evaluation program.
6. Engage the energy industry as formal partners in FreedomCAR.
7. Establish more comprehensive PEM stationary fuel cell activities. (Initiating new activities with a solicitation for fuel cell R,D&D, see graphic.)

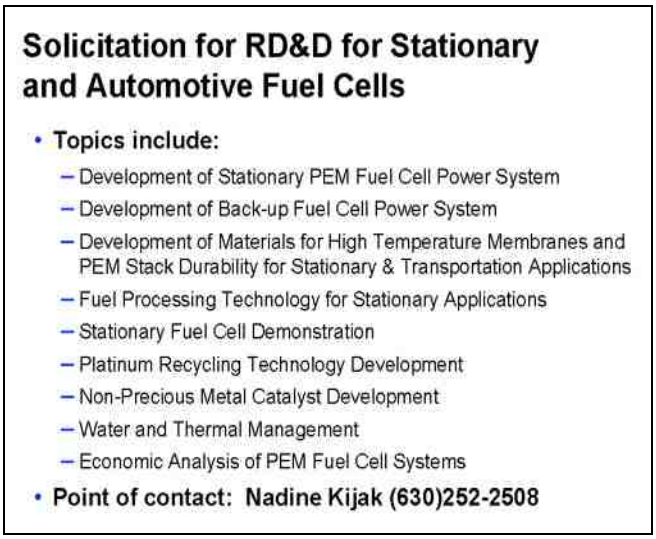

8. Publish a national plan for safety, codes and standards.
9. Develop a hydrogen education "campaign" as recommended in the President's National Energy Policy.
10. Establish closer relationships with states through EERE Regional Support Offices to execute hydrogen and fuel cell R,D&D.

The remainder of this report presents extended project abstracts that highlight progress achieved during FY 2002 under the Hydrogen, Fuel Cells, and Infrastructure Technologies Program. The extended abstracts summarize both industry and national laboratory projects, providing the major results of the work being conducted to overcome the technical barriers associated with the development of hydrogen production, storage, and delivery and fuel cell power systems.

Left to Right: Front Row: Donna Ho, Patrick Davis, Steve Chalk, Mark Paster, John Garbak
Middle Row: Christy Cooper, JoAnn Milliken, Roxanne Danz, Sigmund Gronich, Lucito Cataquiz, Arlene Anderson, Nancy Garland, Kathi Epping, Valri Lightner, Chris Bordeaux
Back Row: Neil Rossmeissl, Tia Alexander, John Petrovic (LANL), Reeshemiah Schuler (CSMI), Peter Devlin, Matt Kauffman, Bill Cleary (ANL)

We hope to see you at the next program review meeting to be held in Berkeley, California on May 19-22, 2003.

Steven G. Chalk, Program Manager
Office of Hydrogen, Fuel Cells, and Infrastructure Technologies
Energy Efficiency and Renewable Energy

Section II. Hydrogen Production and Delivery

II.A Biological Processes

II.A.1 Biological Water Gas Shift Development

Gary R. Vanzin, Sharon Smolinski, Karen Kronoveter, Pin-Ching Maness, Edward J. Wolfrum (Primary Contact), Andrew S. Watt, and Jie Huang
National Renewable Energy Laboratory
1617 Cole Blvd.
Golden, CO 80401
(303) 384-7705, fax: (303) 384-6363, e-mail: ed_wolfum@nrel.gov

DOE Technology Development Manager: Roxanne Danz
(202) 586-7260, fax: (202) 586-9811, e-mail: Roxanne.Danz@ee.doe.gov

Objectives

- Study the overall biological CO shift pathway at the physiological, biochemical, and genetic levels.
- Improve the rates and durability of H_2 production from CO by determining how CO regulates the overall water-gas shift (WGS) pathway by serving as an inducer, a substrate, and an inhibitor.
- Elucidate the genetic system of the CO shift reaction to (1) identify the various components involved and (2) allow manipulation of gene expression.
- Develop bioreactors that will promote an economic biological WGS reaction.
- Design, construct, and operate a bioreactor capable of operating at elevated system pressures.
- Measure the specific CO shift kinetics of the photosynthetic bacterium *Rubrivivax (Rx.) gelatinosus* CBS.

Approach

- Characterize the physiological and biochemical mechanisms in the CO shift reaction by which *Rx. gelatinosus* CBS produces H_2 from CO.
- Clone and characterize genes involved in the *Rx. gelatinosus* CBS CO shift pathway.
- Build on the understanding of the CO shift pathway, optimize the WGS process for maximum H_2 production.
- Develop reactor models and economic analyses to guide the research and development efforts of the biological WGS process.
- Scale up the WGS bioreactor design based on laboratory data, reactor modeling results, and economic analyses.

Accomplishments

- Completed physiological/biochemical study of the CO shift reaction and determined that CO acts as an inducer of the CO shift reaction at the gene transcription level and that at least 10% (v/v) CO is required to maximally induce the H_2 production activity.
- Identified several aspects of the CBS genome that will aid in the cloning of genes involved in H_2 production.
- Successfully operated trickle-bed bioreactors with volumes of 1L and 5L, and showed that the performance of the larger reactor could be predicted from the performance of the smaller one.

- Operated the 1-L bioreactor on a synthesis gas stream derived from biomass gasification, and investigated a number of materials for use as reactor supports.
- Determined the specific CO shift rate of *Rx. gelatinosus* CBS.
- Operated a 100-mL pressurized bioshift reactor at system pressure of 10 atm.
- Completed a "Work for Others" project with a refinery services company that demonstrated the ability of NREL-isolated microorganisms to effectively treat certain "real-world" refinery gas streams, and documented the attractive economics of the overall process. This work culminated in a National Renewable Energy Laboratory (NREL) Record of Invention (ROI).

Future Directions

- Determine if the CO shift reaction can serve as an energy-yielding step in darkness. If verified, this energy can be used to sustain cell growth and to induce new CO shift enzymes to support H_2 production for a longer duration without the need for light input.
- Investigate the enzymes and proteins involved in the initial CO oxidation step - namely the CO dehydrogenase (CODH) enzyme, its electron acceptor and electron mediators - to further understand the biochemistry of the CO shift pathway.
- Construct a large-insert genomic library in a broad host range plasmid. This will facilitate the cloning of CO-shift related genes as well as be useful in complementation experiments when a CO-shift mutant is obtained.
- Continue efforts to overcome the technical hurdles involved in operating the pressurized 1-L volume WGS bioreactor. Key issues to be resolved include system pressure control, in-place reactor sterilization, media addition and removal, and pH/ORP monitoring at elevated pressures.
- Once the bench scale system is optimized, design and construct a pilot-scale pressurized bioreactor at significantly increased scale.
- Continue to build on the specific rate measurement work completed, continuing experiments on the effect of trace levels of organic compounds on the specific CO shift rate of *Rx. gelatinosus* CBS.
- Determine how coproducts might affect the overall economics of biological hydrogen production, specifically on the co-production of single-cell protein (SCP).
- Continue work with industrial partners to investigate near-term applications for the biological water gas shift process.

Introduction

Microbial production of H_2 has gained substantial interest in recent years due to the wide variety of substrates microbes can use to generate H_2. These substrates can either be waste biomass or commercial waste streams containing organic compounds. Microbial H_2 production therefore has the dual benefits of generating a clean fuel and reducing waste. However, due to its heterogenous nature, biomass utilization by microbes is extremely slow. Instead, biomass can be gasified via a thermochemical process to generate a homogeneous synthesis gas, which contains hydrogen, carbon monoxide and carbon dioxide. The water-gas shift reaction, in which carbon monoxide is oxidized to carbon dioxide, and simultaneously water is reduced to hydrogen, is used to produce hydrogen from synthesis gas. The photosynthetic bacterium Rubrivivax gelatinosus CBS is one of a small number of organisms that can perform this reaction at ambient temperatures. This biologically-mediated shift reaction may be a cost-effective technology for the production of hydrogen from syngas.

Approach

Biological Hydrogen from Fuel Gases

To fully utilize the CO shift reaction as a renewable energy resource, it is necessary to understand the mechanism of how *Rx. gelatinosus*

CBS produces H_2 from CO. Carbon monoxide plays multiple roles in the microbial CO oxidation system, serving as a substrate, an inducer, and an inhibitor. In order to obtain optimal activity, we must understand how CO regulates the overall pathway, i.e., the effect and concentrations of CO on the maximal induction, synthesis, and maintenance of enzymatic activities in the CO pathway.

Another approach to gain insight into the CO shift is to clone and characterize genes involved in the pathway. For example, gene discovery will help in the understanding of the rate-limiting step during H_2 production, as well as how CO shift enzymes are produced and degraded.

Bioreactor Development for Biological Hydrogen Production

The overall goal of this part of the project is the scale-up of the low-temperature biological WGS reaction to provide a cost-effective technology for the conditioning of biomass-derived synthesis gas. Laboratory-scale data, reactor modeling results, and technoeconomic analyses are used to guide the development of the bioreactor and the biological WGS process. To date, these efforts indicate that favorable process economics are achievable if the WGS bioreactor can be operated at elevated pressures with improved volumetric mass transfer rates. The current approach is focused on examining the effect of reactor parameters on volumetric mass transfer rates, and designing and testing laboratory-scale bioreactors with higher system operating pressures. Once positive results are achieved in small-scale tests, a larger high-pressure reactor can be constructed to collect more detailed reactor data.

Results

Induction of CO Shift Activity by CO

A series of tests were conducted to determine if CO induces the CO-shift activity in *Rx. gelatinosus* CBS. Within two hours after adding CO to the gas phase of CBS cultures previously incubated in the absence of CO, CO consumption and H_2 production were detected (Figure 1). The addition of chloramphenicol (which inhibits new protein synthesis while exerting no effect on existing hydrogenase activity) along with the CO

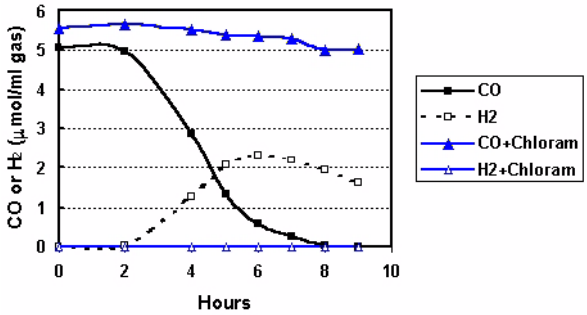

Figure 1. Effects of CO and a Protein Synthesis Inhibitor Chloramphenicol (Choloram) on Inducing CO Shift Activity

immediately stopped the appearance of the CO-shift activity for up to a seven-hour period (triangle), suggesting that CO acts as an inducer for the *de novo* synthesis of both carbon monoxide dehydrogenase (CODH) and hydrogenase of the CO-shift pathway. Consequently, in order to maintain CO shift activity, CO must be present to ensure that new enzymes are constantly being synthesized.

To determine if an optimal or minimal level of CO is required for maximal induction of the CO shift activity, *Rx. gelatinosus* CBS was cultured in various amounts of CO, ranging from 0%-50% (v/v). Data from Figure 2 suggests that at least 10% CO has to present at all times to ensure the maximal induction of the CO shift pathway.

Because CO facilitates the production of new CO shift enzymes, its constant presence is likely required to maintain steady-state levels of CO shift proteins. To verify this, two identical CBS cultures were

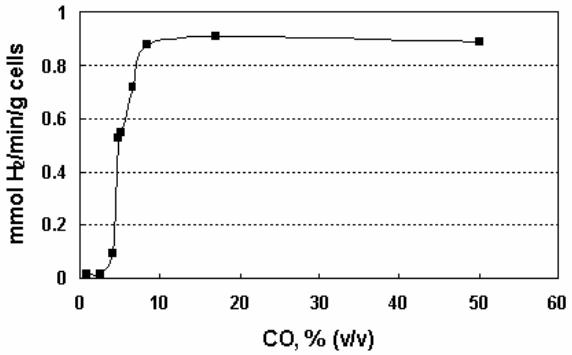

Figure 2. Effect of CO Concentrations on the Induction of Various Levels of CO Shift Activity

prepared and fed 20% CO during inoculation. To the control culture, no CO was fed once it was consumed within 10 hours, and to a parallel culture CO (20%) was fed daily. Results from Figure 3 indicate that, over a period of five days, the culture receiving CO daily was able to maintain a more constant CO shift rate, between day two and day five, 56% higher than that of the control without daily CO feeding.

Cloning the CO Shift Genes

To identify the genes involved in the CO shift pathway in *Rx. gelatinosus* CBS, a library of transposon mutants was created and then screened for CO shift activity. Mutants unable to either consume CO or produce H_2 would suggest that the gene(s) responsible for that function has been interrupted with the transposon insertion. After screening approximately 2000 mutants, two lines that were unable to consume CO or produce H_2 were identified. Biochemical analysis indicates that mutant GV1214 lacks the CODH activity, yet it still retains partial hydrogenase activity; mutant GV1762 retains 32% of the CODH activity, yet its hydrogenase activity is abolished completely. Sequence analysis suggests that the mutations occurred in a CODH gene and hydrogenase large subunit gene, respectively.

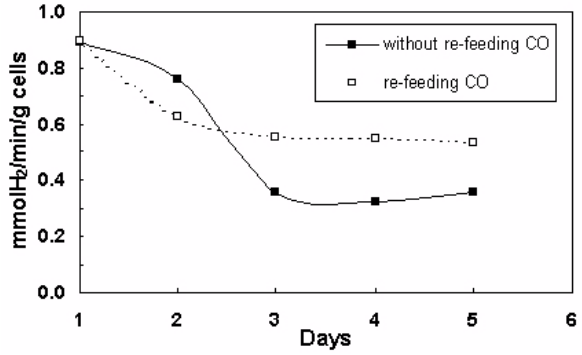

Figure 3. Effect of CO Feedings on Rates and Longevity of the CO Shift Reaction

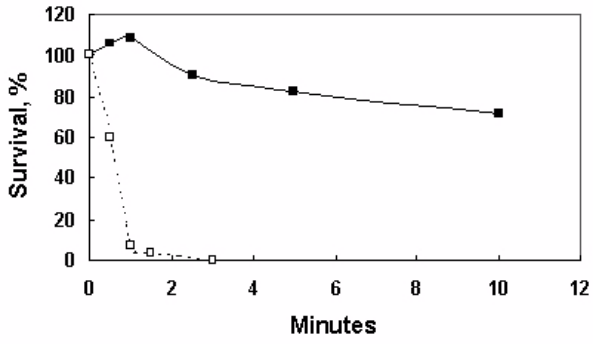

Figure 4. Photo-Oxidative Killing of Rx. gelatinosus

During the mutagenesis process, several mutants unable to produce carotenoid, the photoprotective pigment responsible for scavenging oxygen radicals, were identified. Without the carotenoid pigment, these colonies will die when exposed to both high light and O_2 simultaneously. Data from Figure 4 show that when a G1 culture was bubbled with air, the bulk of the cells were killed completely within one minute of illumination (open square). Little impact was observed with a parallel control containing CBS wild-type cells (closed square). Based on the susceptibility of the pigmented mutant to photo-oxidative killing, CO shift mutant can be selected from a population of cells cultured in CO as the sole carbon substrate.

Effect of Bioreactor Pressure and Inlet CO Concentration

Experiments were performed to investigate the effects of reactor pressure and carbon monoxide concentration on the volumetric productivity of trickle bed bioreactors. Figure 5 shows the apparent rate constant, k_{app} (a measure of reactor productivity), as a function of bioreactor operating pressure. As the system pressure is increased, the

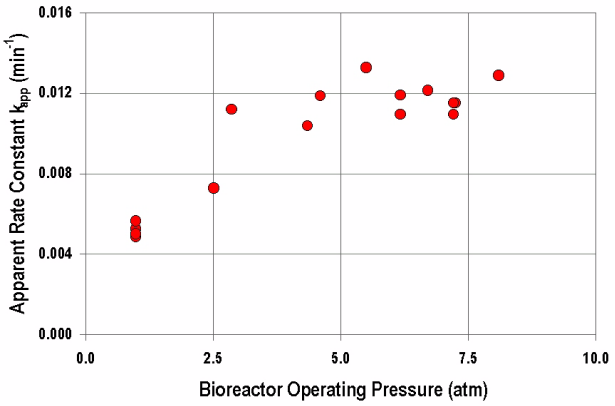

Figure 5. The effect of elevated operating pressure on the apparent bioshift rate constant k_{app}. At modest pressures, a significant increase in rate with pressure is seen. This effect appears to diminish at approximately 80 psia.

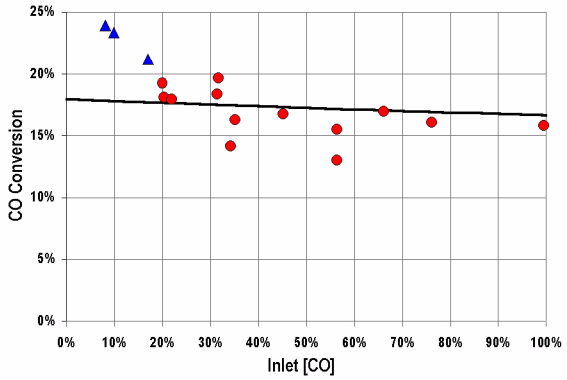

Figure 6. Effect of inlet CO concentration on CO conversion in a 1-L bioreactor. Curve is model prediction (Wolfrum 2002).

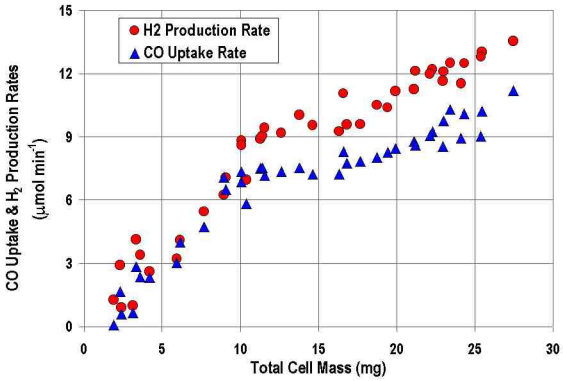

Figure 7. Hydrogen Production and Carbon Monoxide Uptake Rates vs. Total Cell Mass for Photosynthetic Bacterium *Rhodocyclus gelatinosus* CBS

apparent rate constant increases up to approximately 80 pounds per square inch absolute (psia), after which no further increase in reactor productivity occurs.

The effect of CO concentration on reactor performance was evaluated in a series of experiments in a 1-L bioreactor. The data in Figure 6 cover the range of CO inlet concentrations of 8% to 99%. The curve is a model fit using a previously developed reactor model (Wolfrum 2002). The data at low CO concentrations (triangle symbols) are believed to be unreliable because the measured concentration change is close to the repeatability of the analytical equipment (Agilent P200 gas chromatograph). The data in Figure 6 clearly indicate that the biologically-mediated CO-shift reaction is robust over a very wide range of inlet carbon monoxide concentrations; no poisoning of the microorganism occurred at high inlet CO concentrations.

Measurement of Specific H_2 Production Rate

The overall rate of CO uptake and H_2 production were measured at various cell densities.

Figure 7 shows a plot of hydrogen production and carbon monoxide uptake rates vs. the total cell mass for all experiments. When the total cell mass is less than approximately 0.012 g, there is a linear relationship between cell mass and H_2 production and CO uptake. At higher cell mass values, the CO uptake and H_2 production values do not appear to increase linearly with cell mass. This is an indication of bulk (gas-liquid) mass transfer limitations. The data in the linear region of the curves in Figure 7 were used to calculate the specific CO uptake rate and H_2 production rate.

The specific rate of H_2 production appears to be slightly higher than the specific CO uptake rate (0.80 vs. 0.73 mmol/min/g [millimole/minute/gram]), although theoretical stoichiometry predicts that they should be equal. However, at the 95% confidence level, the two parameters are equal. This is supported by the value of the H_2/CO ratio (1.07 ± 0.14), which cannot be distinguished from unity at the 95% confidence level.

Conclusions

- CO serves as an inducer for the CO shift reaction in *Rx. gelatinosus* CBS, and its constant presence is required to maintain this reaction both at a higher rate and for a longer duration.
- At least 10% CO has to be present at all times to ensure the maximal induction of the CO shift pathway in *Rx. gelatinosus* CBS.
- By identifying putative CO shift genes, researchers are beginning to understand, on the molecular level, how *Rx. gelatinosus* CBS responds to CO and produces H_2.
- A line of carotenoidless pigmented mutants has been isolated and could be incorporated

in a photo-oxidative killing scheme to enrich for CO-shift mutants.

- Inlet CO concentration has little impact on the bioreactor conversion efficiency over the range 8%-99% CO (v/v%).
- Increasing the system pressure increased the bioreactor productivity up to approximately 80 psia, after which no increase in productivity was seen.
- The specific CO uptake rate was activity 0.73 ± 0.10 mmol/min/g, while the specific H_2 production rate was 0.80 ± 0.13 mmol/min/g. These two rates cannot be distinguished from each other at the 95% confidence level.

FY 2002 Publications/Presentations

1. Maness, P.-C. and Weaver, P.F. "Evidence for Three Distinct Hydrogenase Activities in Rhodospirillum rubrum." Applied Microbiology and Biotechnology, 57, pp. 751-756 (2001).

2. Maness, P.-C., Smolinski, S., Dillon, A.C., Heben, M.J., and Weaver, P.F. "Characterization of the Oxygen Tolerance of a Hydrogenase Linked to a Carbon-Monoxide Oxidation Pathway in *Rubrivivax gelatinosus*." Applied and Environmental Microbiology, 68: 2633-2636 (2002).

3. Maness, P.-C. and Weaver, P.F. "Hydrogen Production from a Carbon-Monoxide Oxidation Pathway in Rubrivivax gelatinosus." International Journal of Hydrogen Energy. In press (October 2002).

4. Wolfrum, Edward J. and Watt Andrew S. "Bioreactor Design Studies for a Hydrogen-Producing Bacterium." Applied Biotechnology and Bioengineering, 98-100, pp. 611-625 (2002).

5. Maness, P.-C. "The Production of H_2 from a CO-Oxidation Reaction in the Photosynthetic Bacterium *Rubrivivax gelatinosus*." Lecture to the Graduate Program in Plant Physiology, Institute of Biological Chemistry, Washington State University (March 15, 2002) (Honorarium).

6. Wolfrum, E., Amos, W., and Hamel, B. "Method for the Recovery and Incremental Production of Hydrogen from Process Waste Streams in Refineries." (Record of Invention).

II.A.2 Maximizing Photosynthetic Efficiencies and H_2 Production in Microalgal Cultures

Tasios Melis (Primary Contact)
University of California at Berkeley
Plant & Microbial Biology
Berkeley, CA 94720-3102
(510) 642-8166, fax: (510) 642-4995, e-mail: melis@nature.berkeley.edu

DOE Technology Development Manager: Roxanne Danz
(202) 586-7260, fax: (202) 586-9811, e-mail: Roxanne.Danz@ee.doe.gov

Objectives

- Develop genetically engineered microalgae with enhanced photosynthetic solar conversion efficiencies and biomass/hydrogen production capabilities under mass culture conditions.
- Minimize absorption and wasteful dissipation of sunlight by the algae, a solution that requires reduction in the number of the chlorophyll (Chl) molecules in photosynthesis.
- Clone genes that determine the size of the Chl antenna in the model green alga *Chlamydomonas reinhardtii*. These genes could then be over-expressed or down-regulated to improve green alga solar conversion efficiency and biomass/hydrogen production.
- Create a library of genes conferring a 'truncated chlorophyll antenna size' in green algae.

Approach

- Apply DNA insertional mutagenesis and screening in the model green alga *Chlamydomonas reinhardtii* for the isolation of 'truncated Chl antenna' transformants.
- Apply biochemical, genetic and molecular analyses of the transformant cells, followed by DNA sequencing to identify genes that confer a 'truncated Chl antenna size'.

Accomplishments

- DNA analysis of the 'truncated Chl antenna size' *tla1* insertional transformant: Completed the DNA sequencing of the ARG7 insertion site in the *tla1* strain. Obtained full-length genomic DNA, cDNA and protein amino acid sequences for the *TLA1* gene.
- Initiate *tla1* mutant complementation studies: Successfully complemented the *tla1* strain with plasmid carrying the ble selectable marker and the isolated *TLA1* gene. Biochemical analyses are now under way to characterize the complemented strain. Initial results showed that the complemented strain has nearly wild type levels of Chl/cell and a low Chl *a* / Chl *b* ratio in its thylakoid membranes. The *Tla1* protein sequence analysis and the recovery of wild type phenotype provide a strong indication that the *TLA1* gene is a "Chl antenna size" regulatory gene. This is a first-time isolation and characterization of such a regulatory gene.
- Investigate mechanism of *CAO* (chlorophyll *a* oxygenase) gene expression: The *CAO* gene expression affects the biosynthesis and distribution of chlorophyll among the photosystems in green algae. The research proved that it is an important target for a truncated Chl antenna size in photosystem II (PSII). Beyond *CAO*, the work investigated the signal transduction pathway for the regulation of the Chl antenna size by irradiance. A novel molecular mechanism was discovered and analyzed.
- DNA insertional mutagenesis library: An additional 5,000 DNA insertional transformants were generated and screened by the Chl *a*/ Chl *b* ratio measurement. Among those, two putative "truncated

Chl antenna size" strains were identified. A biochemical and molecular analysis of these new transformants is now being undertaken.

- Solar conversion efficiency and H_2 production tests in wild type and *tla1* transformant: Scale-up tests were initiated under field conditions (in the University of California Berkeley [UCB] greenhouse) where photosynthetic productivity of wild type and *tla1* strains is conducted under mass culture conditions. Preliminary measurements of biomass accumulation and gas production (so far oxygen) support the notion of a better performance for the *tla1* versus the wild type strain.

Future Directions

- Functional analysis of the *TLA1* gene: Initiate a study of expression patterns for the *TLA1* gene under different irradiance conditions.
- Bring to a completion the *tla1* mutant complementation studies: Complete the biochemical analyses of the complemented strain by providing a full molecular and biochemical characterization of its properties.
- DNA insertional mutagenesis library: Proceed with the genetic, molecular and biochemical analysis of the two additional (recently isolated) putative "truncated Chl antenna size" strains that have been isolated.
- Solar conversion efficiency and H_2 production measurements in wild type and *tla1* mutant: Continue with the scale-up measurements under field conditions (in the UCB greenhouse) to fully assess photosynthetic productivity and H_2 production in wild type and *tla1* strains.

Introduction

Green algae growing under full sunlight, when photosynthetic productivity ought to be at a maximum, have disappointingly low solar conversion efficiencies. The reason for this inefficiency is that green algae have a genetic tendency to assemble large arrays of light absorbing chlorophyll antenna molecules in their photosystems [1]. At high solar intensities, the rate of photon absorption by the Chl antennae of the first few layers of cells in the mass culture far exceeds the rate at which photosynthesis can utilize them, resulting in dissipation and loss of the excess photons as fluorescence or heat. Up to 95% of absorbed photons could thus be wasted, reducing solar conversion efficiencies and cellular productivity to unacceptably low levels. In addition to the wasteful dissipation of excitation, and due to the high rate of photon absorption by the photosynthetic apparatus, cells at the surface of the mass culture are subject to severe photoinhibition of photosynthesis [2], a phenomenon that compounds losses in productivity. Moreover, cells deeper in the culture are deprived of much needed sunlight, as this is strongly attenuated due to filtering [1, 3, 4]. A genetic tendency of the algae to assemble large arrays of light absorbing chlorophyll antenna molecules in their photosystems is a survival strategy and a competitive advantage in the wild, where light is often limiting. Obviously, this property of the algae is detrimental to the yield and productivity in a mass culture.

The work aims to minimize the Chl antenna size of green algae and, thus, to maximize solar conversion efficiencies and the yield of biomass/ hydrogen production in mass culture.

Approach

A smaller, or truncated, chlorophyll antenna size in microalgae could alleviate the optical shortcomings associated with a fully pigmented Chl antenna, because it will minimize the over-absorption of bright incident sunlight by the photochemical apparatus of the algae. A truncated Chl antenna will diminish the over-absorption and wasteful dissipation of excitation energy by the cells, and it will also diminish photoinhibition of photosynthesis at the surface while permitting greater transmittance of light deeper into the culture. Such altered optical properties of the cells would result in much greater photosynthetic productivity and better solar conversion efficiency in the mass culture. Indeed, actual experiments [1, 5] showed that a smaller Chl antenna size results in a relatively higher

light intensity for the saturation of photosynthesis in individual cells but, concomitantly, in a 3-fold greater productivity of the mass culture. Thus, approaches by which to genetically truncate the Chl antenna size of photosynthesis in green algae merit serious consideration.

The Chl antenna size of the photosystems is not constant. In general, low light intensity during growth promotes a large Chl antenna size. Growth under high light intensities elicits the assembly of a smaller Chl antenna size [6-11]. Such adjustments of the Chl antenna size in response to irradiance are a compensation reaction of the chloroplast, as they are inversely related to the incident intensity. This regulatory mechanism functions in all organisms of oxygenic and anoxygenic photosynthesis [7, 12, 13]. It is possible to genetically interfere with this regulatory mechanism through DNA insertional mutagenesis and transformation of the algae and to direct the chloroplast biosynthetic/assembly activities toward a permanently truncated Chl antenna size.

Results

The foregoing suggests that, for purposes of biomass or H_2-production under ambient sunlight conditions, it is important to identify genes that confer a truncated Chl antenna size in the model green alga *Chlamydomonas reinhardtii*. Once a library of such genes is at hand, over-expression or down-regulation of expression of these genes, as needed, can be applied to other green algae that might be suitable for commercial exploitation and H_2-production.

The chlorophyll a oxygenase (*CAO*) gene encodes a chloroplast enzyme that catalyzes the last step in the Chl biosynthetic pathway, namely the conversion of Chl *a* into Chl *b*. A mutant with inactivated *CAO* was unable to synthesize Chl *b*, thereby lacking this auxiliary light-harvesting pigment. The assembly, organization and function of the photosynthetic apparatus was comparatively investigated in wild type and a Chl *b*-less mutant of *Chlamydomonas reinhardtii*, generated by DNA insertional mutagenesis [14]. It was shown that lack of Chl *b* diminished the photosystem II (PSII) functional Chl antenna size from 230 Chl (*a* and *b*) to about 95 Chl *a* molecules [15]. However, the functional Chl antenna size of photosystem I (PSI) remained fairly constant at about 290 Chl molecules, independent of the presence of Chl *b* (Table 1). This work provided evidence to show that transformation of green algae can be used as a tool by which to interfere with the biosynthesis of specific pigments and, thus, to generate mutants exhibiting a permanently truncated Chl antenna size. In support of the role of *CAO* in the Chl antenna size of photosynthesis, further work [11] showed that *CAO* gene expression is highly regulated in vivo according to the Chl antenna size needs of the organism. Thus, the *CAO* gene may be a target for a truncated Chl antenna size in PSII.

Chlamydomonas reinhardtii double mutant *npq2/lor1* lacks the β,ε-carotenoids lutein and loroxanthin as well as all β,β-epoxycarotenoids derived from zeaxanthin (e.g. violaxanthin and neoxanthin). Thus, the only carotenoids present in the thylakoid membranes of the *npq2/lor1* cells are β-carotene and zeaxanthin. The effect of these mutations and the lack of specific xanthophylls on the Chl antenna size of the photosystems was investigated [16]. In cells of the mutant strain, the Chl antenna size of PSII was substantially smaller than that of the wild type (Table 1). In contrast, the Chl antenna size of PSI was not truncated in the mutant. This analysis showed that absence of lutein, violaxanthin and neoxanthin specifically caused a smaller functional Chl antenna size for PSII but not for that of PSI. Thus, xanthophyll-biosynthesis genes, such as *lycopene* ε-*cyclase* and *zeaxanthin epoxidase* may be targets for a truncated Chl antenna size in PSII.

More recent DNA insertional mutagenesis and screening resulted in the isolation of a regulatory mutant, the phenotype of which was Chl deficiency and elevated Chl *a* /Chl *b* ratio [17]. This truncated light-harvesting Chl antenna (*tla1*) mutant apparently has a defect in the Chl antenna regulatory mechanism, the result of which is inability to produce a large Chl antenna size under any growth conditions. Table 1 shows that both the Chl antenna size of PSII and PSI were smaller in the *tla1* strain. This work provided further evidence to show that transformation of green algae can also be used as a tool by which to genetically interfere with the

molecular mechanism for the regulation of the Chl antenna size in green algae (Kanakagiri, Polle and Melis, unpublished).

The ultimate goal of our combined approaches is to develop customized strains of green algae which assemble only the minimum Chl antenna size of the PSII-core complex (37 Chl) and of the PSI-core complex (95 Chl molecules) (Table 1).

Table 1. Photosystem Chl antenna size in wild type and three *Chlamydomonas reinhardtii* mutant strains. The *cbs3* strain lacks Chl *b* and was isolated upon DNA insertional mutagenesis [15]. The *npq2/lor1* strain lacks all β,ε-carotenoids as well as the β,β-epoxycarotenoids. It contains zeaxanthin but lacks lutein, violaxanthin and neoxanthin from its thylakoid membranes [16]. The *tla1* strain was isolated upon DNA insertional mutagenesis [17]. Note that the *tla1* transformant has the smallest combined Chl antenna size of the three mutants described.

Table 1.

	Wild type	*cbs3* (Chl *b*-less)	*npq2/lor1* (Lut, Vio & Neo-less)	*tla1*	Goal (minimum Chl antenna size)
Chl-PSII	230	90	125	115[1]	37
Chl-PSI	290	289	294	160[1]	95

Notes:

Numbers show the Chl antenna size, i.e., the Chl (*a* and *b*) molecules specifically associated with each photosystem.
[1]Polle, Kanakagiri and Melis, unpublished.

Conclusions

Identification of three genes that confer a truncated Chl antenna size in the photosynthetic apparatus is a significant development in the direction toward cost-effective commercialization of green algae for biomass and H_2 production. Most promising in this respect is the cloning of the *TLA1* regulatory gene. A complete genomic and cDNA sequence of *TLA1* as well as the amino acid sequence of the *Tla1* protein are currently at hand (Kanakagiri and Melis, manuscript in preparation). It should be noted that this is a first-time isolation and characterization of a "Chl antenna size" regulatory gene. The *TLA1* gene may serve as a molecular tool in the elucidation of the function of the mechanism that regulates the Chl antenna size in photosynthesis. It may thus contribute to the identification of other genes that are important in this regulatory process. Further, *TLA1* may serve in the truncation of the Chl antenna size in a variety of green algae and, potentially, in non-oxygenic photosynthetic bacteria.

In conclusion, green algae with a truncated Chl antenna size are indispensable in efforts to substantially increase solar conversion efficiencies and the yield of biomass and H_2 production in photobioreactors under mass culture conditions.

References

1. Melis A, Neidhardt J and Benemann JR (1999) *Dunaliella salina* (Chlorophyta) with small chlorophyll antenna sizes exhibit higher photosynthetic productivities and photon use efficiencies than normally pigmented cells. J. appl. Phycol. 10: 515-525

2. Melis A (1999) Photosystem-II damage and repair cycle in chloroplasts. What modulates the rate of photodamage i*n vivo*? Trends in Plant Science 4: 130-135

3. Naus J and Melis A (1991) Changes of photosystem stoichiometry during cell growth in *Dunaliella salina* cultures. Plant Cell Physiol. 32: 569-575

4. Neidhardt J, Benemann JR, Zhang L and Melis A (1998) Photosystem-II repair and chloroplast recovery from irradiance stress: relationship between chronic photoinhibition, light-harvesting chlorophyll antenna size and photosynthetic productivity in *Dunaliella salina* (green algae). Photosynth. Res. 56:175-184

5. Nakajima Y and Ueda R (1999) Improvement of microalgal photosynthetic productivity by reducing the content of light harvesting pigment. J Appl Phycol 11: 195-201

6. Melis A (1991) Dynamics of photosynthetic membrane composition and function. Biochim. Biophys. Acta (Reviews on Bioenergetics) 1058: 87-106

7. Melis A (1996) Excitation energy transfer: functional and dynamic aspects of *Lhc* (cab) proteins. In, Oxygenic Photosynthesis: The Light Reactions" (DR Ort, CF Yocum, eds), Kluwer Academic Publishers, Dordrecht, The Netherlands, pp. 523-538

8. Maxwell DP, Falk S and Huner NPA (1995) Photosystem II excitation pressure and development of resistance to photoinhibition. 1. Light harvesting complex II abundance and zeaxanthin content in *Chlorella vulgaris*. Plant Physiol 107: 687-694

9. Huner NPA, Oquist G and Sarhan F (1998) Energy balance and acclimation to light and cold. Trends in Plant Science 3: 224-230

10. Escoubas JM, Lomas M, LaRoche J and Falkowski PG (1995) Light intensity regulation of cab gene transcription is signalled by the redox state of the plastoquinone pool. Proc. Nat. Acad. Sci. 92: 10237-10241

11. Masuda T, Polle JEW and Melis A (2002) Biosynthesis and distribution of chlorophyll among the photosystems during recovery of the green alga *Dunaliella salina* from irradiance stress. Plant Physiol. 128: 603-614

12. Webb MR and Melis A (1995) Chloroplast response in *Dunaliella salina* to irradiance stress. Effect on thylakoid membrane assembly and function. Plant Physiol. 107: 885-893

13. Tanaka A and Melis A (1997) Irradiance-dependent changes in the size and composition of the chlorophyll *a-b* light-harvesting complex in the green alga *Dunaliella salina*. Plant Cell Physiol. 38: 17-24

14. Tanaka A, Ito H, Tanaka R, Tanaka N, Yoshida K and Okada K (1998) Chlorophyll *a* oxygenase (*CAO*) is involved in chlorophyll *b* formation from chlorophyll *a*. Proc Natl Acad Sci USA 95: 12719-12723

15. Polle JEW, Benemann JR, Tanaka A and Melis A (2000) Photosynthetic apparatus organization and function in wild type and a Chl *b*-less mutant of *Chlamydomonas reinhardtii*. Dependence on carbon source. Planta 211: 335-344

16. Polle JEW, Niyogi KK and Melis A (2001) Absence of lutein, violaxanthin and neoxanthin affects the functional chlorophyll antenna size of photosystem-II but not that of photosystem-I in the green alga *Chlamydomonas reinhardtii*. Plant Cell Physiol. 42: 482-491

17. Polle JEW, Kanakagiri S, Benemann JR and Melis A (2001) Maximizing photosynthetic efficiencies and hydrogen production in microalga cultures. In, BioHydrogen II (J Miyake, T Matsunaga and A San Pietro, eds), Elsevier, Kidlington, Oxford, U.K., pp. 111-130

FY 2002 Publications/Presentations

1. Polle JEW, Niyogi KK and Melis A (2001) Absence of lutein, violaxanthin and neoxanthin affects the functional chlorophyll antenna size of photosystem-II but not that of photosystem-I in the green alga *Chlamydomonas reinhardtii*. Plant Cell Physiol. 42: 482-491

2. Polle JEW, Kanakagiri S, Benemann JR and Melis A (2001) Maximizing photosynthetic efficiencies and hydrogen production in microalga cultures. In, BioHydrogen II (J Miyake, T Matsunaga and A San Pietro, eds), Pergamon/ Elsevier Science, Kidlington, Oxford, U.K., pp. 111-130.

3. Masuda T, Polle JEW and Melis A (2002) Biosynthesis and distribution of chlorophyll among the photosystems during recovery of the green alga *Dunaliella salina* from irradiance stress. Plant Physiol. 128: 603-614

4. Masuda T, Tanaka A and Melis A (2002) Irradiance-dependent adjustments in the Chlorophyll antenna size of *Dunaliella salina* are regulated by coordinate expression of Chlorophyll *a* Oxygenase (*CAO*) and *Lhcb* genes in shared signaling pathways. Plant Mol. Biol., in press

5. Polle JEW, Niyogi KK and Melis A (2001) Annual Meeting of the American Society of Plant Biologists. Providence, Rhode Island, July 21-25, 2001.

6. Masuda T, Tanaka A and Melis A (2001). Annual Meeting of the American Society of Plant Biologists. Providence, Rhode Island, July 21-25, 2001.

7. Melis A, Polle JEW, Kanakagiri S and Masuda T (2001) International Photosynthesis Congress, Australia, Aug. 15-18, 2001.

8. Melis A (2002) British Royal Society Meeting, London. March 13-15, 2002.

9. Melis A (2002) BioHydrogen 2002 (An International Conference Held in The Netherlands). April 21-24 2002.

10. Polle JEW, Kanakagiri S, Jin E-S and Melis A (2002) BioHydrogen 2002 (An International Conference Held in The Netherlands). April 21-24 2002.

11. Kanakagiri S, Polle JEW and Melis A (2002) Tenth International Conference on the Cell & Molecular Biology of Chlamydomonas. University of British Columbia, Vancouver. June 11-16, 2002.

II.A.3 Efficient Hydrogen Production Using Enzymes of the Pentose Phosphate Pathway

Barbara R. Evans (Primary Contact), Jonathan Woodward (Retired), Hugh M. O'Neill (University of Tennessee, Knoxville), Eugene Pinkhassik (University of Memphis), and John P. Getty, Jr.
Oak Ridge National Laboratory
4500N Bethel Valley Road
Oak Ridge, TN 37831-6194
(865) 241-3185, fax: (865) 574-1275, e-mail: evansb@ornl.gov

DOE Technology Development Manager: Roxanne Danz
(202) 586-7260, fax: (202) 586-9811, e-mail: Roxanne.Danz@ee.doe.gov

Main Subcontractor: J.P. Getty Enterprise, Inc., Oak Ridge, Tennessee

Objectives

- Cloning and expression of thermophilic pentose phosphate pathway enzymes
- Immobilization and stabilization of enzymes and cofactors for bioreactor development
- High stoichiometric yields of hydrogen from sugars derived from renewable resources using the optimized pentose phosphate pathway enzymes

Approach

- Isolate genes for thermophilic enzymes by polymerase chain reaction (PCR) and subclone into expression vectors for production in mesophilic host
- Employ and analyze immobilization methods for optimal performance
- Determine enzyme kinetics separately and in combination to optimize hydrogen production

Accomplishments

- Demonstration of the production of hydrogen by combination of enzymes from different thermophiles
- Isolation and subcloning of two key enzymes, glucose 6-phosphate dehydrogenase and 6-phosphogluconate dehydrogenase, from the thermophile Thermotoga maritima
- Production of hydrogen by enzymes encapsulated in lipsomes

Future Directions

- Isolate, clone, and express the remaining pentose phosphate pathway enzymes
- Demonstrate hydrogen production with thermophilic pentose phosphate pathway enzymes and compare with mesophilic counterparts
- Improve liposome encapsulation and investigate additional immobilization methods

---

Introduction

The sugar glucose is the monomeric unit of which the major biomass components starch and cellulose are made. The abundant disaccharide sucrose, composed of glucose and fructose, is another common source of glucose. Methods to hydrolyze these bioproducts to glucose have been studied intensively by the food and bioethanol industries. But direct microbial production of hydrogen from glucose is generally not very efficient and often produces undesirable side products such as

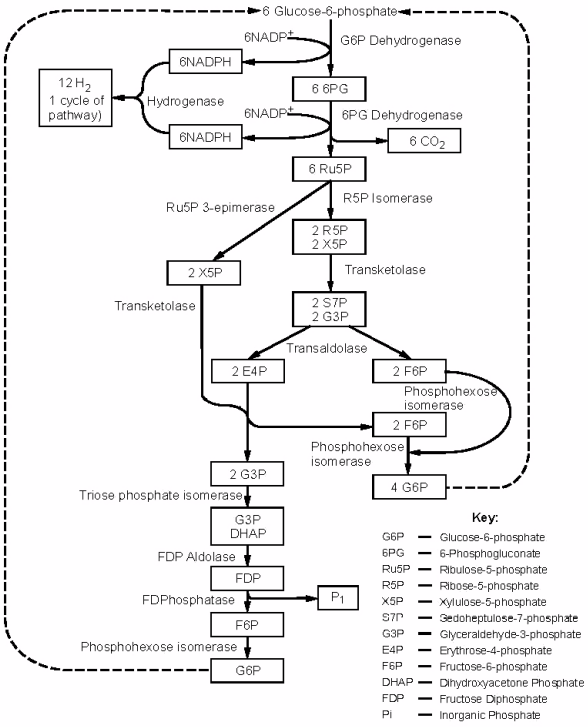

Figure 1. Production of Hydrogen from Glucose Using Pentose Phosphate Pathway Enzymes

hydrogen sulfide. Utilization of isolated enzymes has been shown to increase the efficiency of hydrogen production. Two enzymes, glucose dehydrogenase and hydrogenase, can be coupled through the cofactor nicotinamide adenine dinucleotide phosphate (NADP) to produce 1 mol H_2 per mol glucose (1, 2). By addition of the enzymes of the pentose phosphate pathway (Figure 1), a metabolic pathway found in all organisms, the yield can be increased to close to the theoretical value of 12 mol H_2/mol glucose. In this pathway, the cofactor NADP is reduced by the two enzymes glucose 6-phosphate dehydrogenase and 6-phosphogluconate dehydrogenase, then used by hydrogenase for production of hydrogen gas (3). Utilization of the pentose phosphate pathway enzymes is currently limited by their expense and lack of long-term stability, as well as the instability and expense of the cofactor NADP. Development of cost-effective enzyme catalysts, cofactor stabilization, and bioreactor design is essential for practical application of this method for hydrogen generation from biomass components.

A popular method for obtaining stable biocatalysts is the utilization of enzymes originating from thermophiles, microorganisms that grow at high temperatures. Many of these enzymes can be conveniently produced from recombinant DNA constructs in mesophilic hosts such as Escherchia coli laboratory strains. The recombinant versions offer the advantages of simpler culture conditions, high yields, and simplified purification compared to production from the original thermophiles. However, some enzymes, such as hydrogenases, require certain special metal groups or other features and cannot be produced in common laboratory host bacteria.

Utilizing specific DNA primers that flank the desired gene sequences, copying and amplification of target genes for cloning can be rapidly carried out using PCR. The cloning of thermophilic enzymes is simplified by the availability of the complete genomic sequences of thermophiles such as Methanococcus jannaschii (4) and Thermotoga maritima (5) as a result of the DOE Microbial Genome Program, as well as the availability of bacterial strains from the American Type Culture Collection.

Approach

Enzyme and whole cell activities of the thermophile Thermotoga maritima were examined for comparison with and complementation of the recombinant enzymes and the Pyrococcus hydrogenase.

The target genes were determined based on the successful production of hydrogen using commercially available pentose phosphate pathway enzymes originating from mesophilic organisms such as yeast and rabbits. Based on the published genomic sequences of thermophiles, DNA primers are designed and synthesized for amplification of the target genes by PCR. The amplified genes are then cloned into an expression vector so they can be produced in laboratory host strains of Escherichia coli. These recombinant thermophilic enzymes will be tested for activity, then combined with the hydrogenase produced by the thermophile Pyrococcus furiosus (M. M. Adams, University of

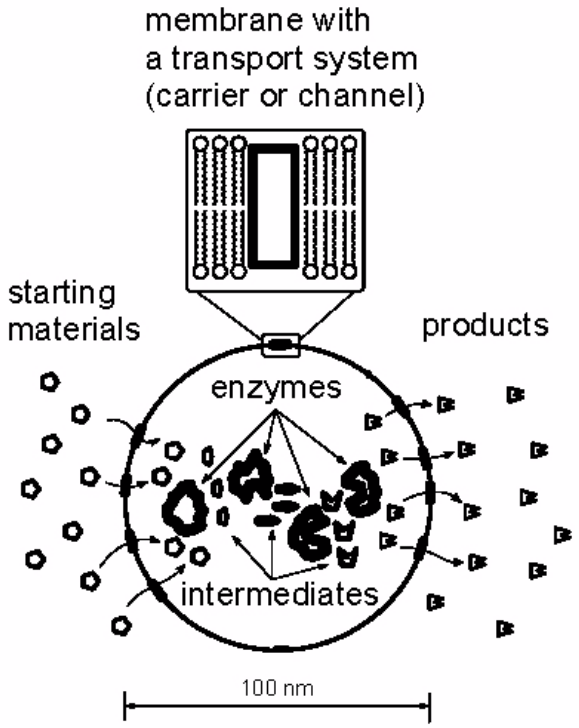

Figure 2. Liposomes as Nanobioreactors

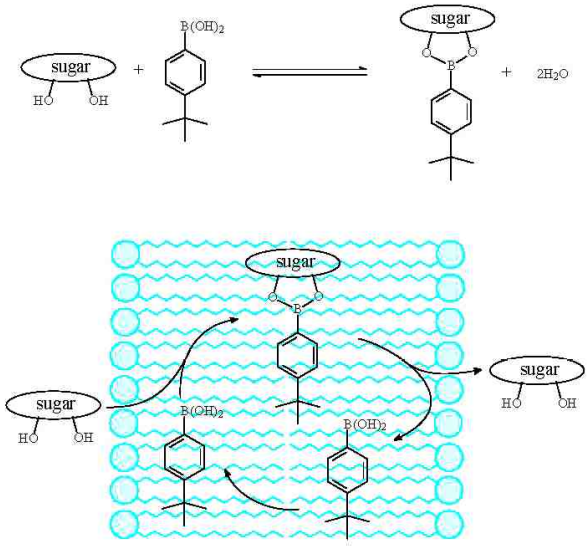

Figure 3. Glucose Transporter Mechanism

Georgia) and the cofactor NADP for optimization of the production of hydrogen from glucose.Parallel to the cloning endeavor, methods of immobilization and stabilization, as well as cofactor recycling, are being

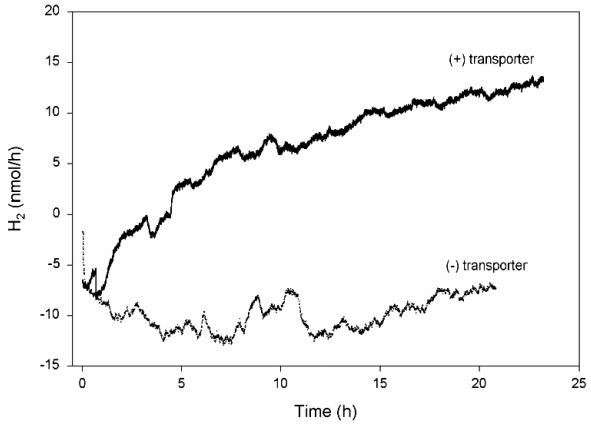

Figure 4. Production of Hydrogen from Glucose by Encapsulated Glucose Dehydrogenase, Hydrogenase, and NADP in Presence (+) or Absence of Glucose Transporter

investigated for suitability in a bioreactor for the production of hydrogen. Methods that are being examined include sol gel immobilization, NADP analogs, and liposome encapsulation. The formation of liposomes, small vesicles composed of lipid bilayers that enclose aqueous solutions, does not require covalent linking of enzymes and can easily entrap multiple enzymes and cofactors in one step.

Results

The intrinsic production of hydrogen by Thermotoga whole cells and cell extracts was found to be low. The cell extracts produced hydrogen at a rate of 0.1 µmol/h. The key enzyme glucose 6-phosphate dehydrogenase was detected in the cell extracts. Addition of Pyrococcus hydrogenase increased the rate of hydrogen production by the cell extract to 1.9 µmol/h.

Primers were designed and used to clone the genes for the pentose phosphate pathway enzymes glucose 6-phosphate dehydrogenase and 6-phosphogluconate dehydrogenase from genomic DNA prepared from T. maritima. Activity of the cloned enzymes was detected when the recombinant genes were expressed in E.coli.

Liposomes were prepared containing glucose dehydrogenase, hydrogenase, and the cofactor NADP+ encapsulated in lipid bilayers. The bilayers

are permeable to hydrogen gas but keep proteins and other water-soluble molecules inside the liposome, similar to natural cell membranes (Figure 2). The compound tertbutylphenyl boronic acid was incorporated into the liposomes to transport glucose across the lipid bilayer (Figure 3). Hydrogen production was demonstrated when this transporter was included in the liposomes with the two enzymes at an encapsulation efficiency of 1% (Figure 4). A modified procedure using dried, reconstituted lipid vesicles to encapsulate the enzymes increased the efficiency to 30-50%

Conclusions

The Thermotoga enzymes were demonstrated to be compatible with the Pyrococcus hydrogenase, indicating that the utilization of recombinant enzymes coupled with this hydrogenase will be successful. Without hydrogenase supplementation, Thermotoga whole cells and extracts produced hydrogen at a low rate. Cloning and expression of two of the pentose phosphate pathway enzymes from Thermotoga was accomplished. Liposome encapsulation was shown to be a promising method for immobilization of enzymes for the production of hydrogen. The enzymes and cofactor are kept inside the liposomes and are not diluted or lost, while hydrogen passes through the liposome membrane and is removed from the solution by the carrier gas.

References

1. Woodward, J., Mattingly, S. M., Danson, M., Hough, D., Ward, N., Adams, M. (1996) Nature Biotechnology 14, 872-874, "In vitro hydrogen production by glucose dehydrogenase and hydrogenase".

2. Woodward, J., Cordray, K. A., Edmonston, R. J., Blanco-Rivera, M., Mattingly, S. M., and Evans, B. R., "Enzymatic Hydrogen Production: Conversion of Renewable Resources for Energy Production", (2000) Energy & Fuels 14, 197-201.

3. Woodward, J., Orr, M., Cordray, K., Greenbaum, E. (2000) Nature 405, 1014-1015, "Enzymatic Production of Biohydrogen".

4. Bult, C. J., White, O., Olsen, G. L., Zhou, L., Fleischmann, R. D., Sutton, G. G., Blake, J. A., Fitzgerald, L. M., Clayton, R. A., Gocayne, J. D., Kerlavage, A. R., Dougherty, B. A., Tomb, J.-F., Adams, M. D., Reich, C. I., Overbeek, R., Kirkness, E. F., Weinstock, K. G., Merrick, J. M., Glodek, A., Scott, J. L., Geoghagen, N. S. M., Weidman, J. F., Fuhrman, J. L., Nguyen, D., Utterback, T. R., Kelley, J. M., Peterson, J. D., Sadow, P. W., Hanna, M. C., Cotton, M. D., Roberts, K. M., Hurst, M. A., Kaine, B. P., Borodovsky, M., Klenk, H.-P., Fraser, C. M., Smith, H. O., Woese, C. R., Ventner, J. C. (1996) Science 273, 1058-1073 (23 August), "Complete Genome Sequence of the Methanogenic Archeon, Methanococcus jannaschii".

5. Nelson, K. E., Clayton, R. A., Gill, S. R., Gwinn, M. L., Dodson, R. J., Haft, D. H., Hickey, E. K., Peterson, J. D., Nelson, W. C., Ketchum, K. A., McDonald, L., Utterback, T. R., Malek, J. A., Linher, K. D., Garrett, M. M., Stewart, A. M., Cotton, M. D., Pratt, M. S., Phillips, C. A., Richardson, D., Heidelberg, J., Sutton, G. G., Fleischmann, R. D., White, O., Salzberg, S. L., Smith, H. O., Venter, J. C. and Fraser, C. M. (1999) Nature 399(6734), 323-329, "Evidence for lateral gene transfer between Archaea and bacteria from genome sequence of Thermotoga maritima."

FY 2002 Publications/Presentations

1. Woodward, J., Heyer, N. I., Getty, J. P., O'Neill, H. M., Pinkhassik, E., Evans, B. R. "Efficient Hydrogen Production Using Enzymes of the Pentose Phosphate Pathway". Proceedings of the Annual Review Meeting, U. S. Department of Energy Hydrogen Program, Golden, CO, May 6-8, 2002.

2. O'Neill, H. M., Angley, C. V., Hemery, I., Evans, B. R., Dai, S., and Woodward, J., "Properties of carbohydrate-metabolizing enzymes immobilized in sol-gel beads: stabilization of invertase and -glucosidase by Blue Dextran", (2002) Biotechnol. Lett. 24: 783-790.

3. Heyer, N. I., O'Neill, H. M., Gerike, U., Woodward, J., Danson, M. J., Hough, D. W. Extremophiles (2002) in press.

Special Recognitions & Awards/Patents Issued

1. Getty, J. P., Orr, M. T., Woodward, J. USPO 6,395,252 (2002), "Method for the continuous production of hydrogen".

II.A.4 Biohydrogen Production from Renewable Organic Wastes

Shihwu Sung (Primary Contact), Dennis A. Bazylinski, and Lutgarde Raskin
Dept. of Civil and Construction Engineering
Iowa State University, Ames IA 50011
(515) 294-3896, fax (515) 294-8216, e-mail: sung@iastate.edu

DOE Technology Development Manager: Roxanne Danz
(202) 586-7260, fax: (202) 586-9811, e-mail: Roxanne.Danz@ee.doe.gov

Objectives

- Develop different strategies for selective growth of hydrogen producing bacteria (e.g., heat selection and pH control) in a mixed culture environment.
- Apply nucleic acid based technique to identify and quantify the hydrogen-producing bacterial population in a complex microbial community background.
- Optimize process to achieve sustainable hydrogen production in continuous flow bioreactors.

Approach

- Evaluate technical and practical feasibility of sustainable hydrogen production in continuous flow bioreactors.
- Investigate the effect of heat treatment of sludge on hydrogen production rate through batch and continuous experiments.
- Apply nucleic acid based techniques for microbial identification and quantification.
- Find the correlation between hydrogen yield and the *Clostridium* sp. in the continuous bioreactor.

Accomplishments

- Evaluated the effect of environmental factors on hydrogen production using mixed culture.
- Successfully enriched naturally available mixed seed to culture hydrogen producing bacteria.
- Enhanced the hydrogen production through preheat treatment of seed inoculum at 70-90^{o}C for 15 - 20 minutes followed by repeated heat treatment of settled returned sludge.
- Found positive correlation of hydrogen production with *Clostridium* sp. in the continuous bioreactor.

Future Directions

- Develop pilot-scale hydrogen production demonstration project using real wastes.
- Evaluate the full-scale plant design.
- Prepare design manual with detail guidelines for biohydrogen production from organic wastes.
- "Identify and quantify the hydrogen-producing bacterial population in a complex microbial community background using nucleic acid based techniques.

Introduction

As a sustainable energy supply with minimal or zero use of hydrocarbons, hydrogen is a promising alternative to fossil fuels. It is a clean and environmentally friendly fuel, which produces water instead of greenhouse gases when combusted. The waste streams from corn, soybean, and meat processing plants pose a major burden on the environment. Aerobic wastewater treatment of these wastes requires energy input to provide aeration, whereas anaerobic digestion processes can achieve the dual benefits of energy production in the form of hydrogen or methane, and waste stabilization. By using hardware similar to that used in industrial methane fermentation, the economics of hydrogen fermentation could be favorable due to its faster reaction rate.

For global environmental considerations, production of hydrogen by biological reactions from renewable organic waste sources represents an important area of bioenergy production. However, the viability of biohydrogen production using mixed culture in a continuous mode has not yet been evaluated. This study evaluated the potential application of mixed culture to produce hydrogen and also examined two important operating strategies, heat treatment, and pH, control to achieve sustainable hydrogen production.

Approach

The first phase of this study involved the design and development of a completely mixed bioreactor for continuous hydrogen production using mixed culture. The experimental setup is shown in Figure 1. The bioreactor was equipped with mixer, pH control unit, external settling tank and heating chamber. Upon successful start-up, operation of the bioreactor was optimized to maximize hydrogen production. The process optimization included determination of optimum operating pH, temperature, and duration of heating of settled biomass, and COD loading rate.

Detail microbial study is crucial to correlate hydrogen production to the microbial group involved. For this purpose, a nucleic acid based technique - terminal restriction fragment length polymorphism (T-RFLP) - was used to identify the abundant populations in the bioreactors in a complex microbial community background.

Figure 1. Experimental Setup of Continuous Bioreactor

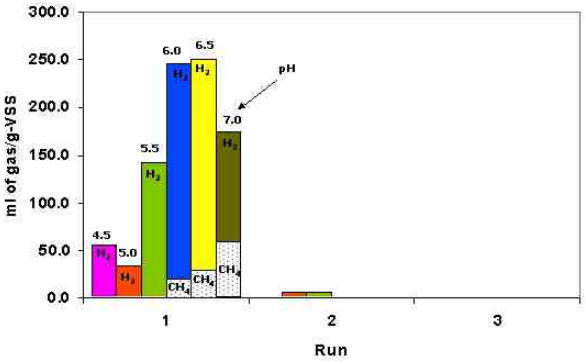

Figure 2. Effect of pH on Hydrogen Production in Batch Studies

Results

According to the batch test result in Figure 2, the pH of 5.5 was found optimum for hydrogen production without any detection of methane in the gas phase. This pH was therefore selected for all continuous phase research. Batch tests showed that heat treatment of seed inocula at 70-90^{o}C for 15-20

minutes enhanced the hydrogen production by more than five times with respect to the control (without heat treatment), as shown in Figure 3. Such an increase was likely due to more favorable conditions for spore-forming hydrogen producers by reducing nonspore-forming hydrogen consumers. An interesting observation was the occurrence of a lag phase during hydrogen production. Heat treatment could potentially damage the cells. Thus, the HRT should be longer than the lag time in the continuous operation so that hydrogen producers can adjust themselves to a new environment.

In the continuous operation, a substrate concentration of 20 g/L was chosen to improve hydrogen production because high substrate concentrations were favorable to hydrogen producers. The seed sludge was preheat-treated at 100°C for 15 minutes, whereas repeated heat treatment was applied only to returned sludge from reactor R1. After 10 days of operation (in steady-state), hydrogen production of reactor R1 was similar to that of reactor R2 but higher hydrogen content was maintained in reactor R1 (Figure 4). Methane was not detected in these two reactors. The average VFA concentrations were measured at 5,220 and 5,100 mg/L as acetic acid for reactors R1 and R2, respectively. Approximately 92% and 93% of sucrose were converted into H_2 and VFA in reactors R1 and R2, respectively. H_2 yield (0.113 m^3 H_2/kg COD) of reactor R1 was higher than that (0.075 m3 H_2/kg COD) of R2 based on maximum values. Repeated heat treatment was, therefore, effective in selecting or even activating spore-forming hydrogen-producers.

Microbial studies conducted at University of Illinois Urbana Champaign showed that *Clostridium butyricum, C. beijerinckii, C. botulinum, C. putrificum and C. sporogenes* were predominant in both reactors. Clostridia are obligate anaerobic acidogenic bacteria that can form spores (endospores) to protect themselves against unfavorable environmental conditions, such as high temperature, desiccation, radiation, or toxic chemicals; however, when favorable conditions return, they can germinate and become vegetative cells. Some of *Clostridia's* spores require heat treatment to increase the germination of spores.

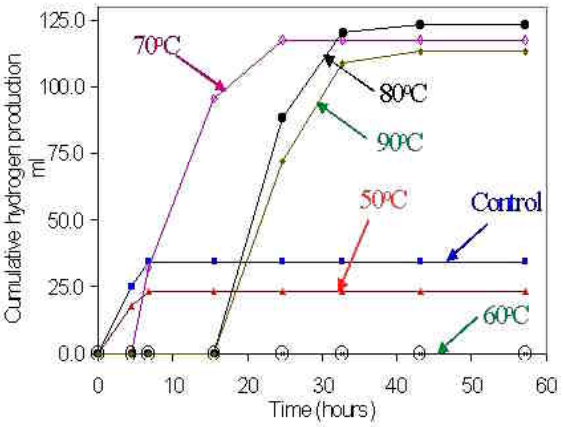

Figure 3. Effect of Heat Treatment on Hydrogen Production in Batch Studies

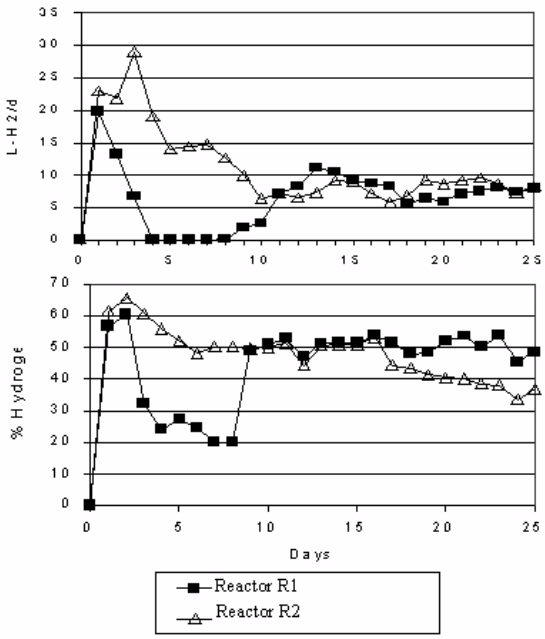

Figure 4. Hydrogen Production Rate and Percentage of Hydrogen in Biogas for Continuous Anaerobic Reactor with (Reactor R1) and Without (Reactor R2) Repeated Heat

Conclusions

- Both initial heat treatment of the inoculum and repeated heat treatments of the biomass during operation promoted hydrogen production by eliminating non-spore forming hydrogen consuming microorganisms and by selecting for hydrogen producing, spore forming bacteria.
- An operational pH of 5.5 was shown to be optimal for hydrogen production.
- Sustainable hydrogen production was possible with pH control and repeated heat treatment of settled sludge at 70-90^{o}C for 15-20 min.
- Terminal restriction fragment length polymorphism (T-RFLP) analysis showed that *Clostridium* and *Bacillus* species were the dominant populations in the bioreactors.
- A positive correlation was observed between the total abundance of *Clostridium* species and hydrogen production during part of an operational run.

Publications and Presentations

1. Duangmanee, T., Padmasiri, S., Simmons, J. J., Raskin, L. and Sung, S. (2002) Hydrogen production by anaerobic communities exposed to repeated heat treatment. Water Environment Federation 74th Conference, Chicago., Ilinois.

2. Duangmanee, T., Chyi, Y. and Sung, S. (2002) Biohydrogen production in mixed culture anaerobic fermentation. 14th World Hydrogen Energy Conference, Montreal, Canada.

3. Van Ginkel, S., Sung, S. and Lay, J. J. (2001) Biohydrogen production as a function of pH and substrate concentration. Environmental Science & Technology, 35:4726 - 4730.

4. Van Ginkel, S., Lay, J. J. and Sung, S. (2000) Biohydrogen production optimization using variable natural inocula. Proceedings of Water Environment Federation 73rd Annual Conference, Anaheim, California.

II.A.5 Photobiological Algal H_2 Production

Task 1: Molecular Engineering of Algal H_2 Production

Michael Seibert, Paul King, Liping Zhang, Lauren Mets, and Maria Ghirardi (Primary Contact)

Task 2: Cyclic Photobiological Algal H_2 Production

Maria L. Ghirardi, Sergey Kosourov, Anatoly Tsygankov, Andrew Rubin, and Michael Seibert
National Renewable Energy Laboratory
1617 Cole Blvd.
Golden, CO 80401
(303) 384-6312, (303) 384-6150 (fax), maria_ghirardi@nrel.gov

DOE Technology Development Manager: Roxanne Danz
(202) 586-7260, fax: (202) 586-9811, e-mail: Roxanne.Danz@ee.doe.gov

Objectives

Molecular Engineering of Algal H_2 Production

- Study two cloned *Chlamydomonas reinhardtii* hydrogenases at the molecular biology, biochemical and structural level.
- Use the information from these studies to design mutated genes with potentially higher tolerance to O_2.

Cyclic Photobiological Algal H_2 Production

- Build a new photobioreactor system with monitoring and feeedback control capability for key biophysical and biochemical parameters and determine the effect of chosen parameters (pH, light intensity, temperature) on inactivation of O_2 evolution and/or rates of H_2 photoproduction by sulfur-depleted *Chlamydomonas reinhardtii*.

Approach

Molecular Engineering of Algal H_2 Production

- Clone and sequence the [Fe]-hydrogenase genes (encoding for the enzymes that releaseH_2 gas), *hydA1* and *hydA2*, in *C. reinhardtii*.
- Raise antibodies specific against each of the enzymes to investigate differences in the physiological role of the two cloned algal hydrogenases and to decide which enzyme to target for mutagenesis.
- Use the antibodies in detailed protein expression studies.
- Characterize the differences between the purported amino acid sequences and structures of HydA1 and HydA2 to identify what specific regions of the protein to target for future mutagenesis in order to improve the O_2-tolerance of the system.

Cyclic Photobiological Algal H_2 Production

- Evaluate the effects of pH, light intensity, and temperature on the inactivation of photosynthetic O_2 evolution by sulfur-depleted algal cultures.

- Build a photobioreactor with feedback control to monitor biophysical and biochemical culture parameters.
- Determine the effects of adding controlled amounts of sulfate during H_2-production to maintain electron transport from H_2O to the hydrogenase at higher levels.

Accomplishments

Molecular Engineering of Algal H_2 Production

- Cloned and sequenced the *hydA1* and *hydA2* [Fe]-hydrogenase genes in *C. reinhardtii*.
- Developed a new high-throughput screening procedure based on a DNA plasmid, constructed to study the expression of *in vitro* mutated hydrogenases introduced into wild-type algae.
- Generated antibodies against oligopeptides specific to the HydA1 and HydA2 proteins to facilitate the expression studies. Heterologous expression of the two algal hydrogenases further confirmed the specificity of the antibodies.
- Completed biochemical studies of the physiological changes of *C. reinhardtii* upon anaerobic induction under photoheterotrophic and photoautotrophic conditions and correlated these results to the expression of the *hydA1* and *hydA2* transcripts.
- Completed preliminary structural modeling studies of the proteins encoded by *hydA1* and *hydA2*.

Cyclic Photobiological Algal H_2 Production

- Evaluated the effects of pH, high light and/or high temperature on the inactivation of photosynthetic O_2 evolution by sulfur-depleted algal cultures.
- Investigated the effects of adding controlled amounts of sulfate during H_2-production to maintain electron transport from H_2O to the hydrogenase at higher levels.
- Found that the residual PSII electron transport activity in sulfur-deprived cultures limits the rate of H_2 photoproduction by the system.
- Developed the use of a fluorescence method to externally monitor the health of the cultures in the bioreactors and to determine when they will start to produce H_2.

Future Directions

Molecular Engineering of Algal H_2 Production

- Continue to study mutant hydrogenase genes, differentiating between the roles of HydA1 and putative HydA2 in H_2 photoproduction under different physiological conditions. These studies will determine which of the enzymes should be the focus of future mutagenesis efforts to generate O_2-tolerant mutants.
- Study the regulation of HydA2 expression using the antibody developed this year. Correlate expression studies of HydA2 using activity assays, antibodies, and nucleic acid hybridization techniques.
- Improve the frequency of *C. reinhardtii* transformation by electroporation in NREL's laboratory.
- Generate mutant hydrogenase genes by either random or site-directed mutagenesis, based on information obtained from structural analyses.

Cyclic Photobiological Algal H_2 Production

- Complete a feasibility study on the operation of a new photobioreactor that produces H_2 for longer periods of time as an alternative to significantly increasing H_2-production rates.
- Design, construct, and test a photobioreactor with immobilized algal cells.

- Identify and test physical and chemical variables to optimize the H_2-production rates with the new photobioreactors.
- Eliminate the need for costly centrifugation as a means to change the growth medium from sulfur-replete to sulfur-depleted.

Introduction

Hydrogen metabolism, catalyzed by [Fe]-hydrogenases in green algae, was first observed 60 years ago in *Scenedesmus obliquus*. Since then, hydrogenase enzymes that either uptake or evolve H_2 have been found in many green algae. Hydrogen production by green algae has significant advantages over other photobiological systems: ATP is not required, high theoretical efficiencies are possible, and water is used directly as the source of reductant without the need to produce biomass or to store intermediary carbon metabolites. Research is underway in several areas to maximize the hydrogen production capabilities of green algae:

1. *Molecular Engineering of Algal H_2 Production.* Algal H_2 photoproduction is sensitive to O_2, a co-product of photosynthesis, and this sensitivity is one of the major factors currently limiting the use of algal systems for H_2 production. One research goal is to engineer the metabolic pathways in the green alga, *Chlamydomonas reinhardtii*, involved in H_2 photoproduction to decrease their O_2 sensitivity and eventually lead to development of a mutant hydrogenase gene that produces H_2 under aerobic conditions.

2. *Cyclic Photobiological Algal H_2 Production.* Previous research has shown that removing sulfate from the algal growth medium partially inactivates the photosynthetic H_2O-oxidizing activity of the cells and results in the establishment of anaerobic conditions in the culture. The resulting anaerobiosis leads to induction of the hydrogenase activity. This research effort is focused on further developing the sulfur-deprivation approach, elucidating the pathways involved in H_2-production under sulfur-deprivation, and developing approaches to improve the H_2-production yield of the process.

Approach

Molecular Engineering of Algal H_2 Production

Mutagenesis can be used to decrease the O_2 sensitivity of [Fe]-hydrogenases and thus lead eventually to a system that produces H_2 under aerobic conditions. The first step in the process is to clone and sequence the [Fe]-hydrogenase genes (encoding for the enzymes that releases H_2 gas), *hydA1* and *hydA2*, in *C. reinhardtii*. In order to investigate differences in the physiological role of the two cloned algal hydrogenases, antibodies specific against each of the two enzymes have been raised and will be used for detailed protein expression studies. This information will help us to determine which enzyme to target for mutagenesis in order to improve the O_2-tolerance of the system. Characterization of the differences between the purported amino acid sequences of HydA1 and HydA2, combined with structural modeling of the two enzymes, will be used to identify what specific regions of the protein to focus on in our mutagenesis studies, which will be done concomitantly with random error-prone PCR mutagenesis.

Cyclic Photobiological Algal H_2 Production

This work stems from past research that demonstrated the feasibility of using sulfur-deprived algal cultures to photoproduce H_2 continuously over a number of days. In this case, the approach is to control the environment in the photobioreactor to maximize the H_2-production activity of the system. This includes evaluating the effects of pH, light intensity, and temperature on the inactivation of photosynthetic O_2 evolution by sulfur-depleted algal cultures. A photobioreactor with feedback control was built to support this effort. *In situ* fluorometry is also being developed as a method to externally monitor the physiological state of the H_2-producing cultures. Finally, the effects of adding controlled amounts of sulfate during H_2-production to maintain electron transport from H_2O to the hydrogenase at higher levels are evaluated.

Results

Molecular Engineering of Algal H_2 Production

Two [Fe]-hydrogenase genes from *C. reinhardtii*, *hydA1* and *hydA2*, have been cloned and sequenced. The *hydA2* gene has a similar degree of homology to other [Fe]-hydrogenases as *hydA1*, and it contains all the motifs characteristic of other [Fe]-hydrogenases. Additional analysis shows that *hydA2* is a distinct nuclear gene that is located on a different chromosome from *hydA1* (see Figure 1A). Exposure of *C. reinhardtii* to anaerobic conditions is accompanied by the induction of hydrogenase activity. Figure 1B shows that the induced H_2 photoproduction reaches steady-state levels after about 90 minutes of anaerobic treatment. The *hydA1* and *hydA2* transcripts are induced almost equally under anaerobic conditions, when grown either photoheterotrophically (Fig. 1B) or photoautotrophically (not shown). Moreover, both transcripts are equally inactivated by exposure to O_2 (not shown).

Two oligopeptides containing sequences that are specifically found in either HydA1 or HydA2 were designed, coupled to a carrier protein and used as antigens to generate specific antibodies in rabbits. The specific antibody reaction to HydA1 and HydA2 was characterized using cell extracts from *E. coli*, and demonstrates that the anti-HydA1 antibody shows very little cross-reaction with the HydA2 protein and vice-versa. These antibodies are being tested against cell extracts from *C. reinhardtii* and will be used for detailed protein expression studies in the future.

The predicted structures of HydA1 and of the putative HydA2 hydrogenase were generated by homology modeling of the purported amino acid sequences against the known structure of the [Fe]-hydrogenase from the anaerobic bacterium, *Clostridium pasteurianum* (Cpl). The core regions of the HydA1 and HydA2 exhibit a very high degree of structural similarity with each other and with Cpl. Figure 2 shows a surface view of HydA1. Careful analyses of the model structures of the two algal hydrogenases will help to direct further efforts in the generation of O_2-tolerant mutants for sustained H_2 production under aerobic conditions.

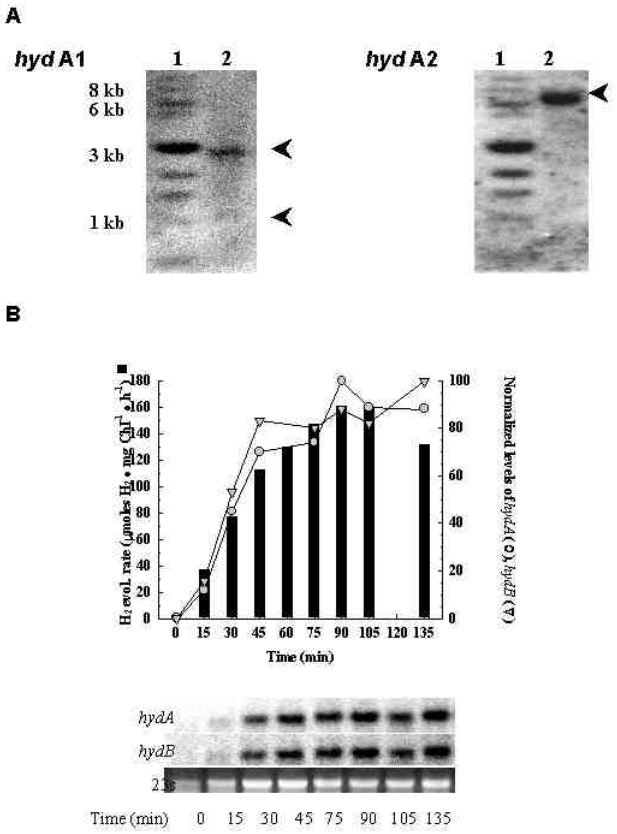

Figure 1. (A) Southern blot analyses of *PstI*-digested *C. reinhardtii* DNA probed with, respectively, *hydA1*- or *hydA2*-specific DNA probes. The arrows indicate the location of the restriction digest fragments. (B) Results from Northern blot analyses of RNA isolated from cultures grown photoheterotrophically and then anaerobically-induced for different periods of time and probed with *hydA1*- or *hydA2*-specific probes. The bars represent H_2-production activity measured concomitantly. Gels at the bottom show the original Northern blot data.

Cyclic Photobiological Algal H_2 Production

Sustained production of H_2 by green algae can be achieved by the reversible inactivation of photosynthetic H_2O-oxidizing activity, catalyzed by Photosystem II (PSII). Past research has shown that the removal of sulfate from the growth medium can accomplish this inactivation. Current research efforts are focused on the elucidation of the pathways involved in H_2-production under sulfur-deprivation

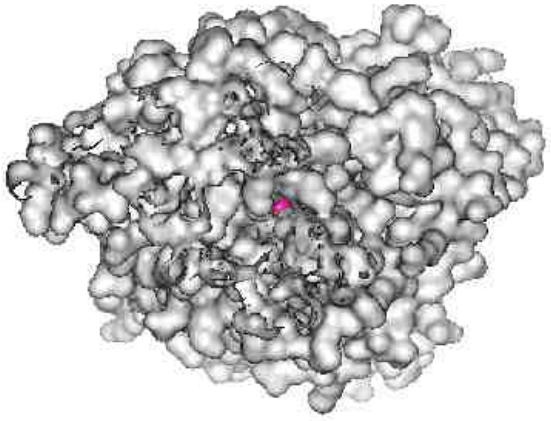

Figure 2. Surface model of HydA1. The red dot in the center of the structure represents the [2Fe2S] center of the catalytic H-cluster.

and on approaches to improve the H_2 production yield of the process.

First, a pH titration of various metabolic activities during sulfur-deprivation was used to identify those favoring H_2 production. The maximum yield and initial rates of H_2 photo-production by sulfur-deprived cultures were observed at pHs that favor the residual activity of PSII (Figure 3), strengthening previous observations that photosynthetic water oxidation is the main source of electrons for H_2 production. At the equivalent optimal initial pH of 7.7, hydrogenase activity is close to its maximum rate. In contrast, starch and protein degradation peak at acidic pHs, and generate fermentation products (acetate, formate, and ethanol). If fermentation products are desired, the algal system is robust enough to shift its metabolism to a fermentative mode upon lowering the pH inside the photobioreactor.

A second approach focused on the addition of limiting amounts of sulfate at different points during the process. When added at the start of anaerobiosis, a concentration of 5 µM sulfate will allow H_2 photoproduction to start at the expected time and to proceed at rates similar to those of samples to which no sulfate was re-added. However, addition of sulfate at concentrations of 1 µM or higher 14 h after the start of H_2 photoproduction will interrupt the process temporarily and result in lower final yields. These results show that it is possible to find a maximum concentration of sulfate that will not

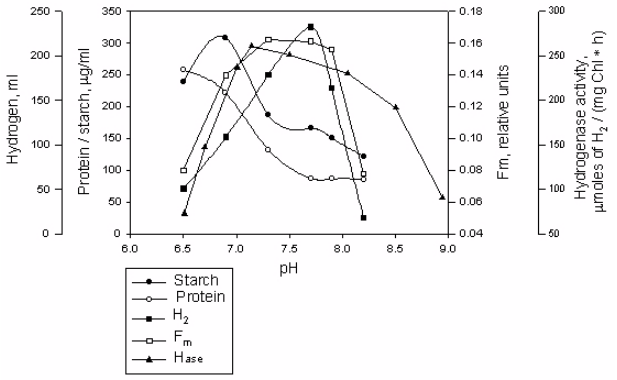

Figure 3. pH titrations of the amounts of starch and protein degraded, the amount of H_2 produced, the maximum Chl *a* fluorescence yield (a measure of PSII capacity) and the *in vitro* hydrogenase activity. As observed in the text, the pHs used in the titration of hydrogenase activity only were set to the actual values measured *in vitro*, and do not represent the initial pH at sulfur deprivation. In order to correlate them to the pH titrations of the other parameters, it is necessary to subtract 0.4 pH units from each value, which corresponds to the change in pH of the cultures from the start of sulfur deprivation to the early H_2 photoproduction phase.

inactivate H_2 photoproduction, and that this concentration is different depending on the time at which sulfate is added. These results open up the possibility of maintaining high PSII capacity during the H_2-production phase by continuously supplying the medium with specific amounts of sulfate.

To further understand factors that currently limit the rate of H_2 photoproduction, PAM fluorometry measurements were used to externally monitor the *in situ* PSII photochemical activity of the algal culture inside the photobioreactor vessels. These results show that during the early stages of sulfur deprivation (O_2-production and consumption phases), PSII photochemical activity gradually declines. However, at the time anaerobiosis is established, an additional, abrupt, and partially reversible down-regulation of PSII photochemical activity occurs, as shown in Figure 4. This drop begins at the exact time that the O_2 concentration in the culture suspension reached zero. These changes in PSII activity are characterized by complex

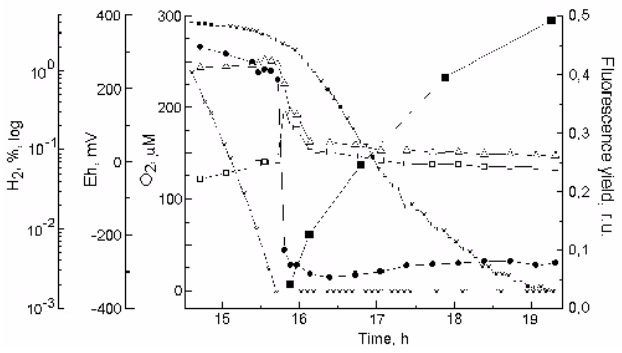

Figure 4. Time course of physiological parameters and H_2 production in *C. reinhardtii* cells during incubation under sulfur-deprived conditions. F_t (open squares), $D_\Delta F/F_m'$ (solid circles), F_m' (open triangles), dissolved oxygen (pO_2, crosses), redox potential (E_h, asterisks) and H_2 content (%) in the gas phase of the culture vessel (solid squares). Incubation in sulfur-deprived medium started at 0 h.

dynamics during the course of cell adaptation to the nutrient stress. The redox state of the PQ pool has been identified as the primary factor in regulating the activity of PSII water-splitting capacity during all stages of sulfur deprivation. Thus, the redox potential of the PQ pool depends on the relationship between the rates of photosynthesis, chlororespiration, respiration, and H_2 production.

Conclusions

Molecular Engineering of Algal H_2 Production

- Characterization of *hydA2* confirmed that it is expressed at the mRNA level and is located on a different gene than *hydA1*. In addition, its expression is regulated by anaerobiosis. The *hydA2* gene has a similar degree of homology to other [Fe]-hydrogenases as *hydA1*, and it contains all the motifs characteristic of these hydrogenases in algae.
- The *hydA1* and *hydA2* transcripts are induced almost equally under anaerobic conditions, and equally inactivated by exposure to O_2. The level of both transcripts is further modulated by the growth condition of the culture prior to the anaerobic treatment.
- Modeled structures of HydA1 and HydA2 are very similar to each other and to the core structures of the [Fe]-hydrogenase from the anaerobic bacterium, *Clostridium pasteurianum*, for which there is a solved X-ray crystal structure. A gas channel from the surface to the catalytic center of the enzyme was identified and will direct further mutagenesis work.

Cyclic Photobiological Algal H_2 Production

- H_2 production can be optimized by controlling the pH of the medium at the start of sulfur deprivation.
- Different maximum amounts of sulfate can be re-added to the system at different points of the sulfur-deprivation process without decreasing H_2 production.
- Overall, the rates of H_2-production in the system are limited by the rates of electron transport from the H_2O-oxidizing complex to hydrogenase under anaerobic conditions. H_2-production during sulfur-deprivation provides the means to reactivate residual photosynthetic electron transport capacity, which is rapidly down-regulated by the establishment of anaerobiosis.
- The technique of PAM fluorescence is a practical and inexpensive means to externally monitor the start of H_2 photoproduction by the cultures and could be further developed for use with future applied systems.

FY 2002 Publications/Presentations

Molecular Engineering of Algal H_2 Production

1. Seibert, M., Flynn, T. and Ghirardi, M.L. (2001) "Strategies for Improving Oxygen Tolerance of Algal Hydrogen Production". In *BioHydrogen II* (J. Miyake, T. Matsunaga, and A. San Pietro, Eds), Pergamon, Amsterdam, pp. 65-76 (2000, CD ROM 2000).

2. Forestier, M., Zhang, L., King, P., Plummer, S., Ahmann, D., Seibert, M., and Ghirardi, M. "The Cloning of Two Hydrogenase Genes from the Green Alga, *C. reinhardtii*". Proceedings of the *12th International Congress on Photosynthesis, 18-23 August 2001, Brisbane, Australia*, CSIRO Publishing, Melbourne, Australia. http://www.publish.csiro.au/ps2001 (2001).

3. Zhang, L., King, P., Seibert, M. and Ghirardi, M.L. "Direct Evidence for Different Electron Transport

Pathways Linked to H_2 production in the green alga *Chlamydomonas reinhardtii*". Abstracts of the *11th Western Photosynthesis Conference, January 3-6, 2002, Asilomar Conference Center, Pacific Grove, CA*, p. 44.

4. Forestier, P., King, P., Posewitz, M., Schwarzer, S., Happe, T., Zhang, L., Ghirardi, M.L., and Seibert, M. "A Second Putative [Fe]-Hydrogenase Gene (*hydA2*) in *C. reinhardtii* is Also Expressed Under Anaerobic Conditions". Submitted (2002).

5. Flynn, T., Ghirardi, M.L., and Seibert, M. "Accumulation of Multiple O_2-Tolerant Phenotypes in H_2-Producing Strains of *C. reinhardtii* by Sequential Application of Chemical Mutagenesis and Selection". *Int. J. Hydrogen Energy 27, 1421-1430*.

6. Ghirardi, M. "The Cloning of Two Hydrogenase Genes from the Green Alga *Chlamydomonas reinhardtii*". Invited plenary lecture at the *12th International Congress on Photosynthesis, 18-23 August 2001, Brisbane, Australia.*

Cyclic Photobiological Algal H_2 Production

1. Kosourov, S., Tsygankov, A., Ghirardi, M.L., and Seibert, M. "Sustained Hydrogen Photoproduction by *Chlamydomonas reinhardtii*—Effects of Sulfur Re-addition". Proceedings of the *12th International Congress on Photosynthesis, 18-23 August 2001, Brisbane, Australia*, CSIRO Publishing, Melbourne, Australia, (2001).

2. Kosourov, S., Ghirardi, M.L. and Seibert, S. "Influence of Extracellular pH on Hydrogen Photoproduction by Sulfur-Depleted *Chlamydomonas reinhardtii* Cultures". Abstracts of the *11th Western Photosynthesis Conference, January 3-6, 2002, Asilomar Conference Center, Pacific Grove, CA*, p. 33.

3. Antal , T. K., T. E. Krendeleva, T. V. Laurinavichene, V. V. Makarova, A. A. Tsygankov, M. Seibert, and A. B. Rubin (2001) "The Relationship between Photosystem 2 Activity and Hydrogen Production in Sulfur Deprived *Chlamydomonas reinhardtii* Cells'" *Doklady Akademii Nauk (Biochemistry and Biophysics)* 381, 371-375.

4. Kosourov, S., Tsygankov, A., Seibert, M, and Ghirardi, M.L. "Sustained Hydrogen Photoproduction by *Chlamydomonas reinhardtii*—Effects of Culture Parameters". *Biotechnol. Bioeng*. 78 p. 731-740 (2002).

5. Laurinavichene, T.V., Tolstygina, I.V., Galiulina, R.R., Ghirardi, M.L., Seibert, M., and Tsygankov, A. "Different Methods to Deprive *Chlamydomonas reinhardtii* Cultures of Sulfur for Subsequent Hydrogen Photoproduction". *Int. J. Hydrogen Energy 27, 1245-1249.*

6. Tsygankov, A., Kosourov, S., Seibert, M., and Ghirardi, M.L. "Hydrogen Photoproduction under Continuous Illumination by Sulfur-Deprived, Synchronous *Chlamydomonas reinhardtii* Cultures". *Int. J. Hydrogen Energy 27, 1239-1244*.

7. Seibert, M. "Hydrogen Gas Production in *Chlamydomonas*—Effects of Sulfate Re-addition to Sulfur-Deprived Cultures," Invited plenary lecture at the *Biohydrogen Joint Workshop of COST Action 841 and IEA Annex 15*, (September 2002).

Special Recognitions & Awards/Patents Issued

Molecular Engineering of Algal H_2 Production

1. Seibert, M., Flynn, T., and Benson, D. "Method for Rapid Biohydrogen Phenotypic Screening of Microorganisms Using a Chemochromic Sensor," U.S. Patent No. 6,277,589.

2. Seibert, M., Flynn, T. and Benson, D. "Apparatus for Rapid Biohydrogen Phenotypic Screening of Microorganisms Using a Chemochromic Sensor," U.S. Divisional Patent pending.

Cyclic Photobiological Algal H_2 Production

1. Seibert, M., Makarova, A., Tsygankov, A., and Rubin, A.B. "A Fluorescence Technique for On-line Monitoring of the Physiological State of Hydrogen-Producing Microorganisms," Patent application submitted.

II.B Biomass-Based

II.B.1 H_2 Production by Catalytic Reforming of Pyrolysis Vapors

R.J. Evans (Primary Contact)
National Renewable Energy Laboratory
1617 Cole Blvd.
Golden, CO 80401
(303) 384-6284, fax: (303) 384-6363, e-mail: bob_evans@nrel.gov

Task 1: Fluidizable Catalysts for Producing Hydrogen by Steam Reforming Biomass Pyrolysis Liquids, K. Magrini-Bair, S. Czernik, R. French, Y. Parent, M. Ritland, E. Chornet

Task 2: Production of Hydrogen from Post-Consumer Wastes, S. Czernik, R. French, C. Feik, E. Chornet

Task 3: Hydrogen from Biomass for Urban Transportation, Y.D. Yeboah, K.B. Bota, Z. Wang, M. Realff, D. Day, J. Howard, D. McGee

Task 4: Engineering Scale-Up of Renewable Hydrogen Production by Catalytic Steam Reforming of Peanut Shells Pyrolysis Products, R.J. Evans, S. Czernik, E. Chornet, C.J. Feik, R. French, S.D. Phillips

DOE Technology Development Manager: Roxanne Danz
(202) 586-7260, fax: (202) 586-9811, e-mail: Roxanne.Danz@ee.doe.gov

Objectives

Fluidizable Catalysts for Producing Hydrogen by Steam Reforming Biomass Pyrolysis Liquids

- Formulate a fluidizable particulate catalyst for the production of hydrogen (H_2) by reforming biomass-derived pyrolysis oils. The catalyst support must be able to withstand reforming conditions for extended operation.

Production of Hydrogen from Post-Consumer Wastes

- Develop a robust thermo-catalytic process for producing hydrogen from readily available non-recyclable post-consumer materials and residues, such as spent plastics, organic solid residues, and waste grease.
- Demonstrate the feasibility of the production of hydrogen from synthetic polymers and from waste grease with a yield of 80% of the stoichiometric potential.

Hydrogen from Biomass for Urban Transportation

- Demonstrate process to produce hydrogen from peanut shells and other agricultural residues for use in an urban bus/transportation demonstration.
- Integrate a pilot-scale version of the pyrolyzer that is currently used to produce activated carbon from peanut shells with the pilot-scale catalytic steam reformer designed and constructed in Phase I.

Engineering Scale-Up of Renewable Hydrogen Production by Catalytic Steam Reforming of Peanut Shells Pyrolysis Products

- Partner with interested parties to demonstrate that the thermochemical conversion of biomass to hydrogen is commercially viable over the next three years.
- Scale up the National Renewable Energy Laboratory's (NREL's) thermochemical biomass-to-hydrogen production process.
- Determine gas composition over the catalyst life cycle and compare the purity requirements needed for the shift reactors and pressure swing adsorption unit.
- Participate in Phase 2 testing work that will occur in Georgia at Scientific Carbon's activated carbon production facility.

Approach

Fluidizable Catalysts for Producing Hydrogen by Steam Reforming Biomass Pyrolysis Liquids

- Identify, refine, and optimize robust, available catalyst support materials.
- Formulate and evaluate multicomponent reforming catalysts made with the best supports.

Production of Hydrogen from Post-Consumer Wastes

- Identify and evaluate appropriate waste streams.
- Develop and refine the thermochemical processes (i.e., pyrolysis or partial oxidation followed by catalytic steam reforming) used to produce hydrogen from wastes.

Hydrogen from Biomass for Urban Transportation

- Develop decision models for selecting a feedstock, a process, and alternatives, and characterize the coproducts of the process.
- Design, construct, test, and integrate the pilot-scale pyrolyzer and the pilot-scale steam reformer, and begin long-term catalyst activity testing.
- Design a separation and storage system for hydrogen, and develop analytical systems for monitoring transportation system performance.
- Develop partnerships and collaborations for future bus/transportation demonstrations, the use of other feedstocks, and the development of new processes and markets for the co-products.

Engineering Scale-Up of Renewable Hydrogen Production by Catalytic Steam Reforming of Peanut Shells Pyrolysis Products

- In NREL's Thermochemical User's Facility (TCUF), scale up and shake down catalytic steam reforming process as derived from the bench-scale experimentation carried out at NREL to develop the process concept.
- Provide technical support for the shakedown of the pyrolyzer/reformer system in Georgia.
- Support the partnership development that will be necessary for the bus demonstration. Identify other biomass resources in the region that could be used to produce hydrogen.

Accomplishments

Fluidizable Catalysts for Producing Hydrogen by Steam Reforming Biomass Pyrolysis Liquids

- Tested 11 commercially-available spherical alumina catalyst supports to determine optimum particle size, surface area, and attrition resistance.

- Prepared and evaluated several viable catalysts from the two alumina supports that showed the best performance in simulated reforming operations.

Production of Hydrogen from Post-Consumer Wastes

- Demonstrated a fluidized bed catalytic steam reforming process for the production of hydrogen from "trap grease".
- Studied pyrolysis/reforming of several types of common plastics using a micro-reactor interfaced with a molecular-beam mass spectrometer (MBMS).
- Designed a bench-scale fluidized bed pyrolysis reactor.

Hydrogen from Biomass for Urban Transportation

- Collected bio-oil and determined solubility parameters and physical property estimation methods for the components of the bio-oil product of peanut shell pyrolysis.
- Completed the design and construction of a pilot-scale (1/8th-scale) pyrolyzer. Began integration of the pyrolyzer with the reformer.
- Prepared the catalyst and feed samples for the pyrolyzer-reformer integration shakedown and long-term catalyst testing at Scientific Carbons Inc.
- Acquired additional analytical instruments for determining and monitoring the composition of the pyrolyzer and reformer inlet and output streams.
- Developed partnerships with several institutions and organizations including the Federation of Southern Cooperatives (for feedstock/farmer training in future phases); Albany State University (summer student interns and community acceptability study); Dougherty County, City of Albany and Georgia's Water Gas & Light Commission (future bus/transportation demonstration).

Engineering Scale-Up of Renewable Hydrogen Production by Catalytic Steam Reforming of Peanut Shells Pyrolysis Products

- Developed a new heater control system to protect the reactor from overheating in case of heater malfunction.
- Successfully operated the 30-cemtimeter (cm) catalytic steam reformer on methane and peanut shell pyrolysis products at NREL.
- Experiments with peanut shell pyrolysis vapor reforming duplicated the 5-cm bench-scale unit results with the aqueous fraction of wood pyrolysis oil. This is the first time whole pyrolysis vapors have been processed in the fluid bed reforming process.
- Developed a computer system to to ensure that the unit in Georgia can be monitored during operation and utilize the new control strategy to protect the reactor.

Future Directions

Fluidizable Catalysts for Producing Hydrogen by Steam Reforming Biomass Pyrolysis Liquids

- Produce attrition-resistant alumina supports and develop an appropriate "recipe" for adding promoters during support preparation.
- Develop a "recipe" for producing a broad range of robust promoted nickel (Ni) fluidization catalysts, focusing on adding stabilization agents (magnesium [Mg], manganese [Mn]) to Ni to improve reforming performance.
- Provide the best catalysts to the Post-Consumer Waste Hydrogen Production project.
- Produce a pilot-scale quantity of catalyst for use in the scale-up evaluation for the Steam Reforming of Peanut Shell Pyrolysis Vapors project.

Production of Hydrogen from Post-Consumer Wastes

- Demonstrate the process concept for producing hydrogen by pyrolysis and subsequent reforming of plastics and achieve 80% of the theoretically possible conversion of plastics to hydrogen.
- Construct and demonstrate a bench-scale two-step pyrolysis reforming system.
- Continue using the MBMS reactor system to quantitatively evaluate the process performance.
- Demonstrate the "trap grease"-to-hydrogen process in long-duration tests using the attrition-resistant catalysts. An alternative reactor option that uses a circulating bed to prepare 80 μm catalyst particles will also be considered.
- Analyze the catalyst used in "trap grease" reforming tests to determine if it was affected by possible contaminants in the feed.

Hydrogen from Biomass for Urban Transportation

- Perform liquid-liquid equilibrium experiments on representative bio-oil compounds and develop property estimation methods.
- Develop models and heuristic solution methods for the network of process steps to account for feedstock, location, process and the uncertainties of these factors.
- Complete integration and testing of the pyrolyzer, reformer, analytical instruments, and accessories, and begin long-term catalyst testing at Blakely, GA.
- Design pressure swing adsorption (PSA) separation and hydrogen storage systems for the produced hydrogen.
- Establish additional partnerships to prepare for the urban bus demonstration, identify alternative feedstocks, and develop new markets for the coproducts.

Engineering Scale-Up of Renewable Hydrogen Production by Catalytic Steam Reforming of Peanut Shells Pyrolysis Products

- Complete detailed analysis of the product over the catalyst life cycle.
- Continue to provide technical support for the shakedown testing in Georgia. The goal is 100 hours of operation.
- Recommend a design and implementation plan for the shift and separation steps for the Phase 3 demonstration in Georgia in 2003.

Introduction

Fluidizable Catalysts for Producing Hydrogen by Steam Reforming Biomass Pyrolysis Liquid

Bio-oil reforming requires a multi-functional catalyst which can (1) steam reform the oil organic components into carbon dioxide (CO_2), carbon monoxide (CO) and H_2; (2) shift the produced CO with steam to make more CO_2 and H_2; (3) gasify carbonaceous residues formed on the catalyst surface mostly from non-volatile bio-oil components; and (4) resist attrition. CoorsTek Ceramics produces spherical aluminas, with a range of physical properties, which could meet these requirements. Nickel-based catalysts, the most widely used shift catalysts, with potassium and magnesium as additives to aid coke and shift gasification and stabilize nickel crystals, respectively, are being evaluated to optimize catalyst performance.

Production of Hydrogen from Post-Consumer Wastes

At present, hydrogen is mostly produced by catalytic steam reforming of hydrocarbons: natural gas and naphtha. The goal of this research is to develop a technology for producing hydrogen from alternative resources, specifically from two types of waste post-consumer materials: plastics and "trap grease". The concept proposed for plastics is a two-stage process: fast pyrolysis to convert polymers to a

gas/vapor stream of monomers and other low-molecular weight compounds, followed by catalytic steam reforming of this gas to yield hydrogen and carbon oxides. "Trap grease", a waste material recovered from traps on sewer lines, does not require a depolymerization step and can be directly steam reformed to produce hydrogen. The challenge is to efficiently convert plastic polymers and the constitutive molecules of "trap grease" (predominantly free fatty acids and glycerides) to hydrogen at a cost similar to that for the existing natural gas-based technologies.

Hydrogen from Biomass for Urban Transportation

Clark Atlanta University has teamed with the National Renewable Energy Laboratory (NREL) and other partners in Georgia to develop and demonstrate a biomass-to-hydrogen process that will use peanut shells as a biomass feedstock for hydrogen production, and then use this hydrogen as a transportation fuel. Specifically, a pilot-scale reactor on site at Scientific Carbons Inc., a company in Blakely, Georgia, that produces activated carbon by pyrolysis of densified peanut shells, is being used to test the concept. The vapor by-products from the pyrolysis, which are currently used as fuel for steam generation, will be converted to hydrogen using NREL's catalytic steam reforming process. In the transportation demonstration, the hydrogen produced from peanut shells will be combined with compressed natural gas to raise its energy density and create a more viable transportation fuel.

Engineering Scale-Up of Renewable Hydrogen Production by Catalytic Steam Reforming of Peanut Shells Pyrolysis Products

The steam reforming of biomass pyrolysis oil, when integrated with the production of high-value products, is a promising near-term approach to the production of renewable hydrogen. Based on bench-scale work at NREL, a team from Georgia is utilizing the NREL TCUF and its staff to develop a 7 kg/hr reactor that will be operated at NREL this year before being run at the production site in Georgia on densified peanut shells. The application in Georgia is at a plant that makes activated carbon from peanut shells and has pyrolysis by-products available for conversion. The key technical goals for the shakedown at NREL are to ensure the safety of the reactor and obtain preliminary performance data on the catalyst, especially physical attrition and deactivation.

Approach

Fluidizable Catalysts for Producing Hydrogen by Steam Reforming Biomass Pyrolysis Liquids

The mechanical strength of the fluidized catalyst is a significant process issue that must be solved. To address this operational problem, a two-step approach was taken to (1) identify and develop economical and attrition resistant support materials that could withstand high-temperature fluidization, and (2) prepare reforming catalysts from the best supports. The catalysts, containing nickel oxide (NiO), manganese oxide (MgO) and/or potassium oxide (K_2O), were then evaluated for attrition resistance and activity in a fluid bed system.

Production of Hydrogen from Post-Consumer Wastes

To prove this process concept, a two-stage micro-scale reactor interfaced with a molecular-beam mass spectrometer was used to qualitatively evaluate several types of plastic. Samples of plastics were pyrolyzed in the bottom part of the reactor; then the created gases and vapors were steam reformed in a fixed bed of a commercial Ni catalyst located in the upper part of the reactor. The product gas was analyzed by mass spectroscopy. "Trap grease" was catalytically steam reformed in a 2"-diameter fluidized bed reactor using the same commercial nickel catalyst. Observed catalyst losses, and the resulting hydrogen conversion efficiency losses, highlight the need for either further process evaluation using a fluidizable attrition-resistant catalyst, or reconfiguring the bed to allow the use of existing commercial catalysts.

Hydrogen from Biomass for Urban Transportation

In Phase 1 of this project, decision models for selecting a feedstock, a process, and alternatives were developed, and a 7 kg/hr fluidized-bed catalytic steam reformer system was designed and constructed. In Phase 2, the emphasis is on integrating and testing the pilot-scale pyrolyzer at

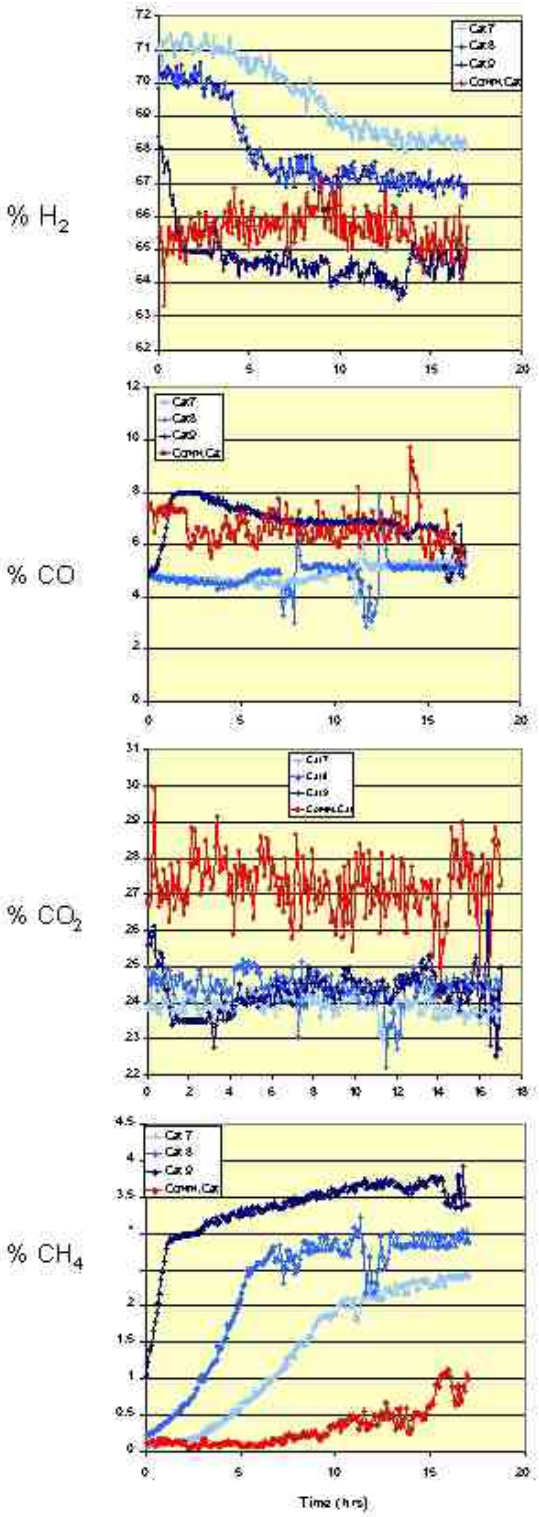

Figure 1. Reaction Gas Composition Data Versus Reaction Time for Catalysts 7-9 and CK-11 NK

Scientific Carbon's activated carbon production facility with the pilot-scale reformer constructed and tested in Phase 1. In addition, Phase 2 will involve engineering research and pilot-scale process development studies in the use of peanut shells as feedstock for the pyrolysis-steam reforming process to produce hydrogen. The hydrogen produced in Phase 3 will be blended with CNG and used to power a bus in nearby Albany, Georgia. Partnership-building and outreach play a key role in this collaborative project.

Engineering Scale-Up of Renewable Hydrogen Production by Catalytic Steam Reforming of Peanut Shells Pyrolysis Products

The peanut shell-to-hydrogen concept is a modification of the biomass-to-hydrogen process that has been under development at NREL since 1993. This process concept was first characterized at the bench scale to determine the concept viability and to define key process parameters. Based on past results with the bench-scale fluid bed reactor, a pilot-scale unit was constructed and tested in NREL's Thermochemical User's Facility (TCUF). The 20-kg/hr fluid bed pyrolysis unit at TCUF was used to feed the steam-reforming unit for the shakedown tests. The TCUF is designed to test new thermochemical process concepts by interfacing key unit operations in the existing TCUF facility. This approach minimizes risk and disruption by taking advantage of process control systems and analytical capabilities, which would not be available for shakedown or proof of concept in an industrial environment. By performing the initial system tests at NREL, the experience of the NREL researchers with the process and the analytical equipment of TCUF can be used to monitor and optimize the system performance.

Results

Fluidizable Catalysts for Producing Hydrogen by Steam Reforming Biomass Pyrolysis Liquids

Eleven commercial catalysts were tested for attrition resistance under simulated reforming conditions. Two alumina supports supplied by CoorsTek Ceramics (90% and 99% alumina) showed the best combination of attrition resistance and surface area. In addition, they consist of alpha

alumina, the desired support for reforming because of surface acid sites, which contribute to hydrocarbon cracking, and are readily available in the kg amounts required for testing. These materials were used to prepare several simple Ni-based catalysts to evaluate reforming and gasification activity with pyrolysis oil in the 2" fluidization reactor.

The sample catalysts, prepared from CoorsTek supports, were evaluated by comparing their performance with that of the industrial catalyst, C-11 NK. Preliminary evaluations (Catalysts 1-6) led to the development of Catalyst 7, which showed a slightly better short-term performance and a 20% improvement in the shift reaction when compared to C-11 NK. Catalyst 7 contained 1.8% Ni, 0.15% Mg, and 0.1% potassium (K), on 99% alumina with 0.2-1.4 m^2/g surface area. Two additional catalysts (Catalysts 8 and 9), with varying amounts of Ni, Mg, and K, were prepared in an effort to establish the boundary compositions for the three-component, multifunctional catalyst. Figure 1 plots H_2, CO, CO_2, and CH_4 concentration versus reaction time for Catalysts 7-9 and C-11 NK.

Production of Hydrogen from Post-Consumer Wastes

Pyrolysis and reforming of several types of common plastics (polyethylene, polypropylene, polyvinyl chloride, polyethylene terephthalate, polyurethane, and polycarbonate) were studied qualitatively, using a micro-reactor interfaced with a MBMS. Each type of plastic pyrolyzed at 550-750ºC. This was followed by steam reforming of vapors in a fixed bed of C-11 NK catalyst at 750-800ºC. The composition of the product gas (mass spectrum) was observed for different values of the steam-to-carbon ratio and space velocity that changed depending on the size of plastic samples. Preliminary tests showed that at process conditions similar to those used for reforming natural gas, polymers were almost completely converted to hydrogen and carbon oxides.

"Trap grease" was also evaluated as a low-cost feedstock for hydrogen production, via catalytic steam reforming. The suitable process conditions are similar to those for natural gas reforming. At 850°C,

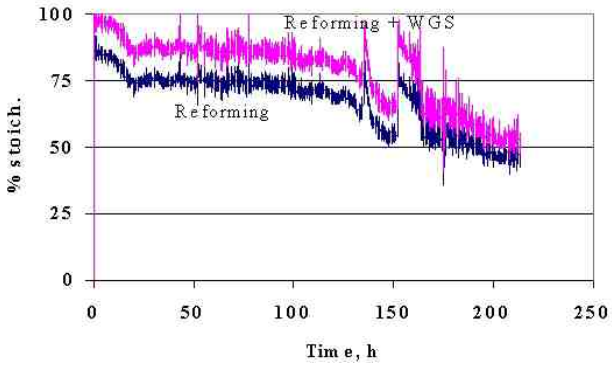

Figure 2. Yield of Hydrogen from Reforming "Trap Grease"; t=850°C, S/C=5, GC1 VHSV=970 h-1

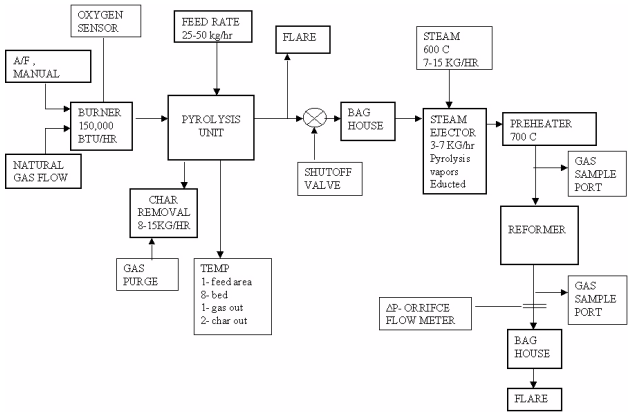

Figure 3. Schematic Flow Diagram of the Biomass Pyrolysis-Reformer Process

using steam-to-carbon ratio 5, and with a space velocity of 1000 h-1, hydrogen was produced with a yield of 25 grams (g) per 100 g of grease during 135 hours of continuous testing. This yield could be increased to over 28 g H_2/100 g grease (85% of the stoichiometric potential) if CO were further converted by water-gas shift. At the end of the testing, this yield decreased to 16.4 g/100 g grease (48% of the stoichiometric potential), as shown in Figure 2.

Hydrogen from Biomass for Urban Transportation

A schematic flow diagram of the biomass pyrolyzer-reformer designed and constructed for Phase 2 is shown in Figure 3. The pyrolyzer is designed to process up to 188 lbs (85 kg) per hour of pelletized biomass into char and pyrolytic off-gas.

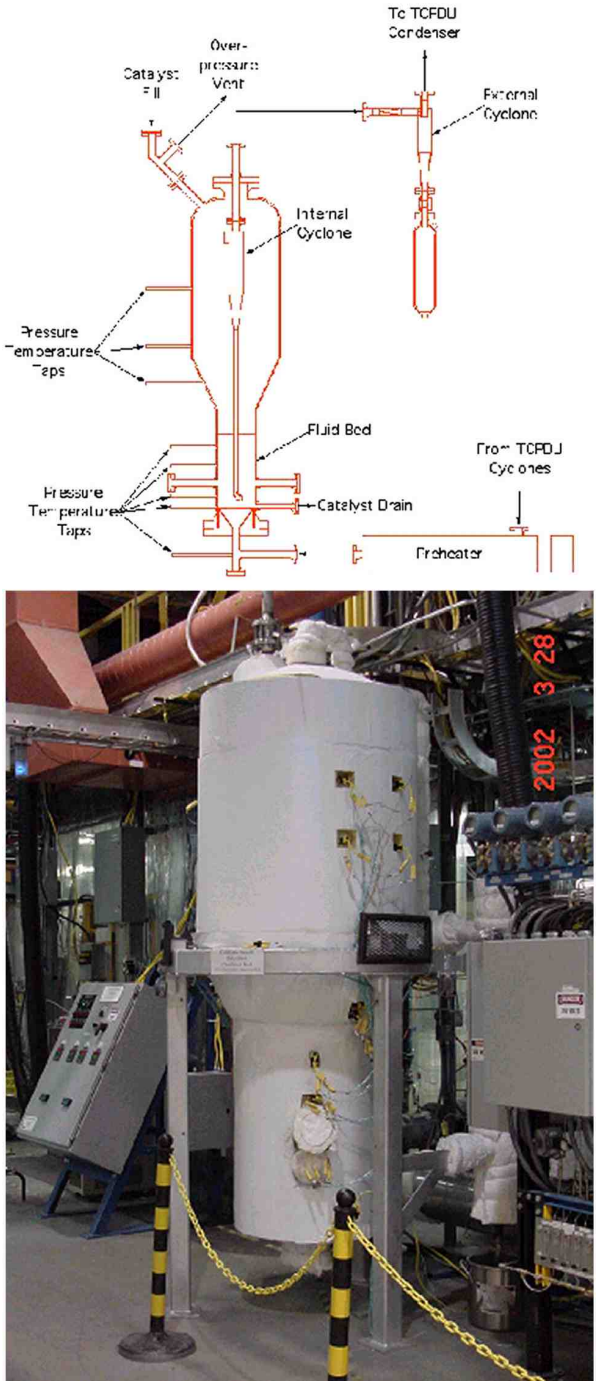

Figure 4. Catalytic Fluid Bed Steam Reforming Reactor

After carbon particulates are removed from the off-gas, it is heated to 700°C and then fed into the bottom of a steam reformer. Literature data and thermodynamic models were employed to evaluate a large number of organic solvents for the extraction of phenol from aqueous bio-oils. Propyl acetate and methyl isobutyl ketone (MIBK) were identified as good solvents as a result of this evaluation. These two solvents were used in extractions of bio-oil samples.

The hydrogen produced from peanut shells will be combined with compressed natural gas (CNG). This will require the development of a safe hydrogen-compressed natural gas storage system. Key design issues under evaluation include gas storage pressure, slow-fill versus fast-fill refueling stations, hydrogen/natural gas mixture, and materials of construction for storage cylinders. Given a target gas pressure of 3,600 psi and variable composition ranges from 75% to 85% CNG (i.e., 15% to 25% hydrogen), a tank volume of 1.78 cubic meters, diameter of 0.61 m, and length of 6.1 m is required. Due to the limitations placed on the system by the CNG distribution pipelines and the corrosive properties of hydrogen, the 80:20 mixture was selected.

Engineering Scale-Up of Renewable Hydrogen Production by Catalytic Steam Reforming of Peanut Shells Pyrolysis Products

A schematic and photograph of the pilot-scale catalytic fluid bed reformer are shown in Figure 4. The 30-cm catalytic steam reforming reactor was successfully operated on peanut pyrolysis vapor at a feed rate of 7 kg/hour of vapors. The results are in agreement with those obtained from the 5-cm bench-scale reactor used for the reforming of the aqueous fraction of pyrolysis oil. Typical gas compositions at the outlet of the reformer are shown in Figure 5. These data show that the yield of hydrogen is approximately 90% of maximum.

The fluid bed pyrolysis unit was fed at a maximum feed rate of 20 kg/hour of peanut shell pellets. Because peanut shells are high in lignin (32%) and protein (8%), the char yield was approximately 35%, which is higher than the yield from typical biomass. Vapor contact time was explored by varying the weight hourly space velocity (WHSV) (weight of feed/hr/weight of catalyst). A plot of H_2 yield on an oil basis versus the inverse of WHSV is shown in Figure 6. A smaller WHSV represents more catalyst contact; therefore, plotting

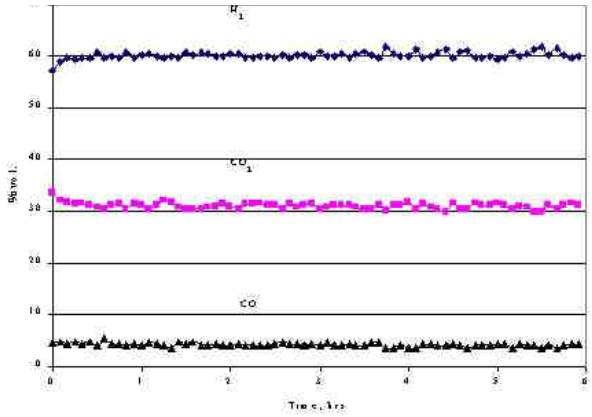

Figure 5. Gas Composition from Reforming Peanut-Shell Pyrolysis Vapors

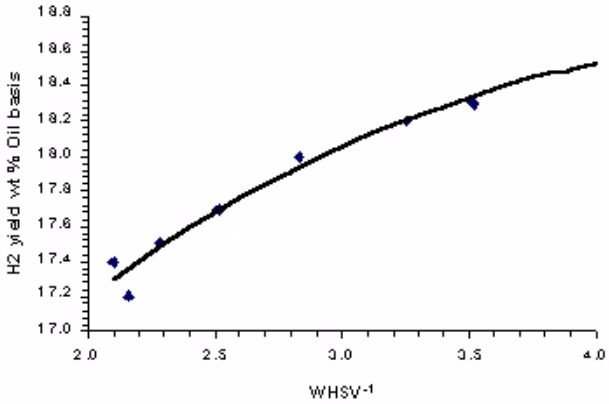

Figure 6. Variation in Estimated H_2 Yield based on Contact Time (inverse WHSV is proportional to contact time)

the inverse, which is proportional to contact time, presents a clearer picture of the effect of increasing catalyst contact. A 5% relative increase in H_2 yield was noted at higher contact time.

Conclusions

Fluidizable Catalysts for Producing Hydrogen by Steam Reforming Biomass Pyrolysis Liquids

- Most of the alumina materials tested exhibited improved attrition resistance under steam reforming conditions compared to that of commercial fluidized reforming catalysts though surface areas are about an order of magnitude less.
- The best support materials were CoorsTek 90% and 99% alumina particles with surface areas of 0.2-1.4 m^2/g. Attrition losses for the materials were less than 0.5 wt% per day.
- Catalysts made from the CoorsTek supports and containing Ni, Mg, and K oxides exhibit increased shift/gasification activity and significantly improved reforming ability compared to the industrial material for the first 3 hours of reaction. From 20-23 hours, we observed a reduction in shift/gasification activity for the NREL and commercial catalysts.
- While this new support/catalyst system works about as well as the commercial catalyst (C-11 NK), further optimization of support and catalyst composition may yield even more active and selective catalysts.

Production of Hydrogen from Post-Consumer Wastes

- Qualitative tests for producing hydrogen by pyrolysis/reforming of plastics showed promising results.
- NREL's fluidized bed catalytic steam reforming process for the production of hydrogen from "trap grease" also showed promising results in a bench-scale system.
- The fluidized bed process performance significantly decreased after 135 hours of uninterrupted operation. This low conversion to hydrogen was most likely due to the catalyst losses by attrition and elutriation from the reactor, though some deactivation effects cannot be excluded at this time.

Hydrogen from Biomass for Urban Transportation

- The project is ready to begin the shakedown and testing phase of the entire pyrolyzer/ reforming system at the Scientific Carbon facility in Blakely, Georgia.
- The hydrogen storage system design is underway, and some of the system constraints have been identified.
- The partnership efforts are building interest in the project and helping to lay the groundwork for the future bus demonstration.
- Engineering Scale-Up of Renewable Hydrogen Production by Catalytic Steam

Reforming of Peanut Shells Pyrolysis Products

- The 30-cm catalytic steam reforming reactor was successfully operated on peanut shell pyrolysis vapor at a feed rate of 7 kg/hour of vapors.
- Experiments with peanut pyrolysis vapor reforming duplicated the results in a 5-cm bench-scale unit with the aqueous fraction of wood pyrolysis oil.
- The whole vapors from peanut shells, which have a unique composition, i.e., high levels of lignin and protein, can be successfully reformed. Over the time on stream tested to date, no significant deactivation of the catalyst was noted.

II.B.2 Supercritical Water Partial Oxidation

Michael H. Spritzer (Primary Contact) and Glenn T. Hong
General Atomics
3550 General Atomics Court
San Diego, California 92121
(858) 455-2337, fax: (858) 455-4111, e-mail: michael.spritzer@gat.com

DOE Technology Development Manager: Roxanne Danz
(202) 586-7260, fax: (202) 586-9811, e- mail: Roxanne.Danz@ee.doe.gov

Main Subcontractor: General Atomics, San Diego, CA

Objectives

- Show feasibility of supercritical water partial oxidation (SWPO) in pilot-scale preliminary testing.
- Develop improvements to SWPO hardware.
- Optimize SWPO operating parameters and hydrogen yields.
- Demonstrate an integrated SWPO pilot-scale system including hydrogen separation.

Approach

- Test various feedstocks and reactor designs using existing General Atomics (GA) pilot plant.
- Identify suitable SWPO feedstocks.
- Identify improvements to reactor and system design.
- Implement and test improvements when possible.

Accomplishments

- Showed basic feasibility of SWPO at a pilot scale.
- Established suitable operating conditions, e.g. reactor and preheat temperatures.
- Confirmed prior laboratory-scale results showing high hydrogen yields.
- Identified suitable feedstocks.
- Attained reliable pumping of thick feed slurries.
- Identified improvements to reactor design.

Future Directions

- Update a Development Plan for commercializing SWPO (Phase I).
- Implement second-generation pilot-scale SWPO reactor (Phase II).
- Characterize SWPO operating parameters and hydrogen yields (Phase II).
- Demonstrate an integrated SWPO pilot-scale system including hydrogen separation (Phases III & IV).

Introduction

General Atomics is developing Supercritical Water Partial Oxidation (SWPO) for the efficient and environmentally advantageous gasification of and hydrogen production from low-grade fuels such as biomass, municipal/solid waste (MSW) and high-sulfur coal.

SWPO involves carrying out oxidative reactions in a supercritical water environment - akin to high-pressure steam - in the presence of limited quantities of oxidant, typically pure oxygen or air. The key potential advantage of the SWPO process is the use of partial oxidation in-situ to rapidly heat the gasification medium, resulting in less char formation and improved hydrogen yield. Another major advantage is that the high-pressure, high-density aqueous environment is ideal for reacting and gasifying organics. The high water content of the medium should encourage formation of hydrogen and hydrogen-rich products and is highly compatible with high water content feeds such as biomass materials. By the same token, the high water content of the medium is effective for gasification of hydrogen-poor materials such as coal. The pressurized nature of the SWPO process naturally lends itself to the liquefaction and sequestration of carbon dioxide (CO_2). The combination of high pressure and the cold sink available with a liquid oxygen oxidant enables ready liquefaction of CO_2. It may then be recycled, injected for oil recovery or otherwise handled to reduce greenhouse effects.

Approach

Figure 1 provides a representative process flow diagram for the gasification tests carried out. A number of different configurations were tested over the course of the project. The particular configuration shown is that used in conjunction with the "large" reactor vessel. This reactor has a volume of about 10 liters and at the flow rates tested provides a residence time of about 75 seconds at 650°C operating temperature and about 60 seconds at 800°C operating temperature. Figures 2 through 4 show photographs of three skids comprising the SWPO system.

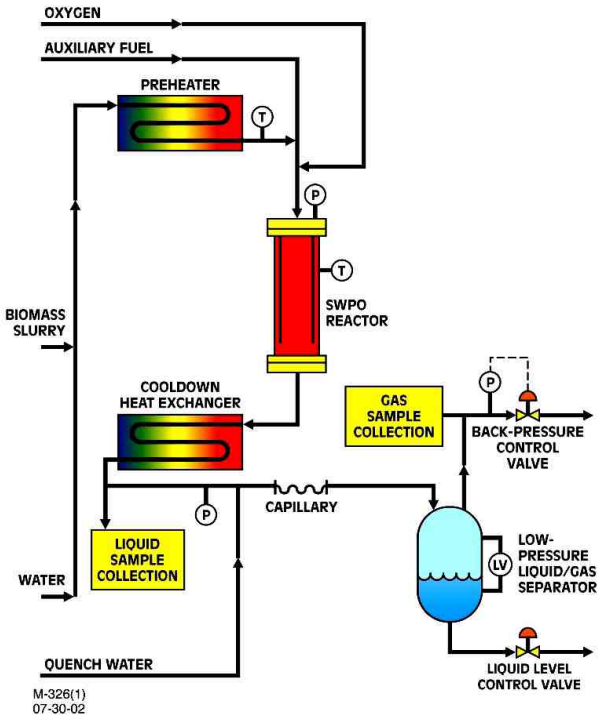

Figure 1. Process Flow Diagram for the SWPO System

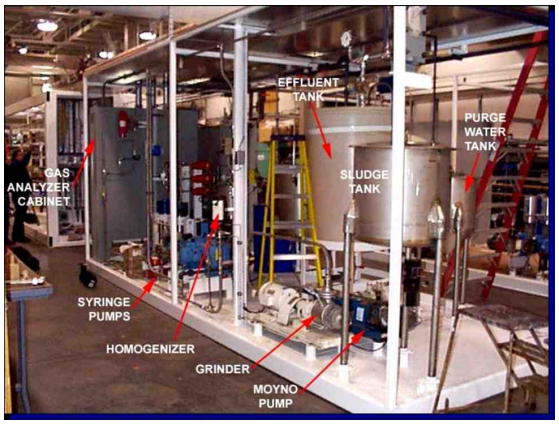

Figure 2. SWPO System Feed Skid

Pressurized slurry (or water during startup and shutdown) is fed to the preheater, where it is preheated to a temperature of 250°C, or other suitable temperature depending on the feed material. It was found during testing that slurry preheating had to be limited to avoid char formation and plugging of the preheater. In addition, the pumpable

concentration of biomass slurry was limited, for example to about 10-15 wt% for wood flour. Due to limited resources for advancing solutions to these limitations during the Phase I effort, it was decided to utilize a liquid fuel to help attain the desired reactor operating temperature. Thus, as shown in Figure 1, high-pressure auxiliary fuel (ethanol) and oxygen are combined with the preheated slurry at the reactor inlet. Oxidation of the organics results in a typical reactor temperature of 650°C. In the reactor, the feed is converted primarily to CO_2, H_2O, hydrogen gas (H_2), methane (CH_4) and CO. The liquid effluent is collected in a tank, while the gases are vented through the facility carbon filter and released to the atmosphere.

Table 1 provides a synopsis of the Phase I pilot-scale testing carried out. Several runs with composted municipal solid waste (MSW) were carried out with a pipe reactor in the absence of oxidant, i.e., they were indirectly heated and did not utilize partial oxidation. The pipe reactor had an ID of 0.815 inches and a length of about 90 feet.

Table 1. Summary of Gasification Runs

Feed	No. of Runs	Reactor Type	Run Conditions
40% corn starch	1	Small vessel	605°C
40% coal	2	Small vessel	530°C; 620°C
30-40% MSW compost	2	Small vessel	570°C
30-40% MSW compost	5	Pipe	620°C- 650°C
30% corn starch	1	Pipe	650°C, 300°C preheat
10% wood + 10% coal	2	Large vessel	800°C, 250°C preheat, EtOH fuel[2]
10% wood	3	Large vessel	650°C, 250°C preheat, EtOH fuel[2]
10% wood	3	Large vessel	800°C, 250°C preheat, EtOH fuel[2]
10% corn starch	4	Large vessel	650°C, EtOH fuel[2]
40% corn starch	2	Large vessel	650°C, EtOH fuel[2]
15% wood	2	Large vessel	650°C, 250°C preheat, EtOH fuel[2]
20% MSW compost	1	Large vessel	650°C, 250°C preheat, EtOH fuel[2]

Notes:
1. All tests are at 3400 psi.
2. Ethanol (EtOH) is oxidized with approxiately stoichiometric oxygen in the reactor to bring the preheated stream up to the target reactor temperature.

Results

The major results observed over the past year are as follows:

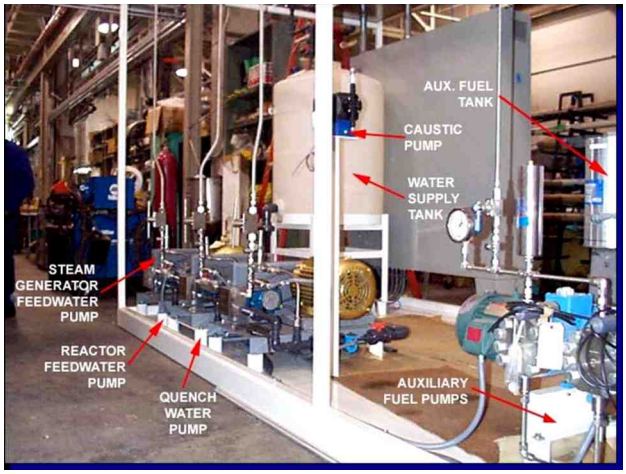

Figure 3. SWPO System Pump Skid

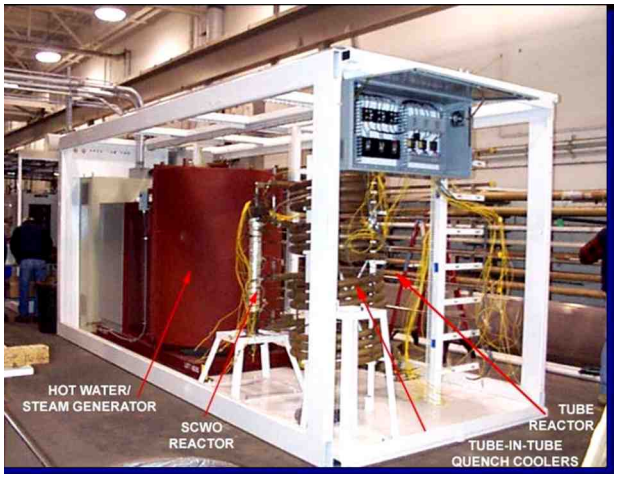

Figure 4. SWPO System Reactor Skid

1. Using direct mixing with supercritical water for heat-up of a biomass slurry entering the reactor is problematic because a relatively large amount of supercritical water is required. This dilutes the biomass slurry and requires oxidation of most of the biomass to attain the desired final temperature of about 650°C. Limited preheat and partial oxidation have been established as the preferred means of heat-up.
2. Significant effort was required to obtain reliable operation of a dual syringe pump for pumping thick slurries to high pressure. A number of improvements over the basic design were implemented, including magnetic sensing of the position of the driving pistons. The pump is now operating in highly reliable fashion.

3. The maximum pumpable concentration of wood flour slurries is in the range of 10-15 wt% dry basis. The maximum pumpable concentration of composted MSW is in the range of 30 wt% dry basis. A mixture of 10 wt% wood plus 10 wt% coal is readily pumpable.
4. Preheat temperatures in excess of about 250°C are conducive to charring with many biomass feeds. Preheating is being limited to 250°C.
5. A vessel reactor is preferable to a pipe reactor, allowing better temperature control and heat conservation and better ash and char handling.
6. Coal does not gasify well at 3400 psi and temperatures up to 800°C, but excellent oxidation has been achieved for coal at the same conditions.
7. Results for gasification of wood slurries have generally confirmed the high hydrogen yields reported in earlier laboratory testing at the University of Hawaii (UH). Table 2 compares the GA pilot scale results with UH's results. In addition to some temperature and pressure differences as shown in the table, the UH tests utilized an activated carbon catalyst with external heating, while the GA tests utilized no catalyst and partial oxidation with ethanol fuel. Hydrogen yields (Table 2, last column) are similar for both sets of tests, and both show a significant takeup of hydrogen from the water to make gaseous products.

Table 2. Comparison of GA Pilot-Scale Tests with UH Lab-Scale Tests

Organi-zation	Feed	T °C	P psi	% H_2	% CH_4	% C_2	% CO	% CO_2	g H/ 100g feed
GA	9% wood + CMC[1,2]	650	3400	44	33	0.3	7	16	9.9
GA	9% wood + CMC[1,2]	800	3400	38	30	0.2	4	28	10.8
UH Ref. 1	10.4% corn starch[3]	650	4061	45	14	0.0	2	35	9.1
UH Ref. 1	5% wood + 5.5% corn starch[3]	650	4061	34	23	0.2	3	45	8.2
UH Ref. 1	5% wood + 5.6% corn starch[3]	650	4061	50	10	0.0	4	39	11.4
UH Ref. 1	5% wood + 6/1% corn starch[3]	650	4061	43	14	0.2	3	37	9.3
UH Ref. 2	11% wood + 4.25% corn starch[3]	650	4061	57	6	NA	4	33	12.2

Notes:
1. CMC is carboxymethyl cellulose suspension agent.
2. Average of 3 runs, some ethanol fuel present.
3. Activated carbon catalyst used.

Conclusions

A versatile pilot plant for exploring gasification in supercritical water has been established at the General Atomics' facility in San Diego. Preliminary testing of the SWPO process has found hydrogen yields of about 10 grams per 100 grams of feed, comparable to those found in prior laboratory-scale work carried out at UH. As in that prior work, a significant amount of the hydrogen found in the gas phase products is derived from the water/steam matrix. Potential improvements to the SWPO process include higher energy feed injector nozzles for the reactor to achieve better dispersion of the incoming feed, second-generation reactor designs with higher solids residence times, and means for feeding more concentrated slurries or dry feed.

References

1. Antal, M.J., Jr. and X. Xu, "Hydrogen Production by the Total, Catalytic, Supercritical Steam Reforming of Wood Sawdust", 216th American Chemical Society National Meeting, Boston, August 23, 1998.

2. Xu, X and M.J. Antal, "Gasification of Sewage Sludge and Organics in Supercritical Water", American Institute of Chemical Engineers Annual Meeting, Los Angeles, 1997.

FY 2002 Publications/Presentations

1. Spritzer , M.H. and G.T. Hong, "Supercritical Water Partial Oxidation", Presented at the Annual Peer Review Meeting, USDOE Hydrogen Program, Golden, CO, May 2002.

2. Hong, G.T. and M.H. Spritzer, "Supercritical Water Partial Oxidation", 2002 Annual Report to USDOE Hydrogen Program, available at www.eren.doe.gov/hydrogen/docs/2002toc.html.

II.B.3 Biomass-Derived Hydrogen from a Thermally Ballasted Gasifier

Robert C. Brown (Primary Contact)
Center for Sustainable Environmental Technologies
Iowa State University
283 Metals Development Bldg.
Ames, IA 50011-3020
(515) 294-7934, fax: (515) 294-3091, e-mail: rcbrown@iastate.edu

DOE Technology Development Manager: Roxanne Danz
(202) 586-7260, fax: (202) 586-9811, e-mail: Roxanne.Danz@ee.doe.gov

Main Subcontractor: Iowa State University, Ames, Iowa

Objectives

- Determine whether switchgrass is a suitable fuel for the ballasted gasifier.
- Obtain time-resolved concentrations of important fuel components evolved.
- Identify process conditions that maximize the production of hydrogen (H_2).
- Evaluate methods for removing contaminants from the producer gas.
- Evaluate methods for mediating the water-gas shift reaction in the product gas.
- Estimate the economics of H_2 production from switchgrass.

Approach

- Prepare switchgrass fuel and feeder.
- Prepare 5-ton per day bubbling fluidized bed gasifier and a latent heat ballasting system.
- Prepare slipstream for upgrading producer gas.
- Prepare gas sampling and analysis system.
- Perform gasification trials.
- Perform cost estimate of the gasification system.

Accomplishments

- The 5-ton per day biomass gasifier has been modified to operate as a ballasted gasifier.
- The gas sampling system and a slipstream of the gasifier effluent have been prepared.
- The gas conditioning system has been designed and constructed.
- Analytical methods for measurement of trace contaminants (hydrogen sulfide [H_2S], Ammonia [NH_3], and hydrochloric acid [HCl]) have been established.
- Shakedown trials of the gasifier have been performed.
- Producer gas composition has been characterized for gasification of switchgrass.
- The steam reformer has been demonstrated to reduce total tar by 95% and condensable (heavy) tar by greater than 99%.
- The catalytic water-gas shift reactor has been demonstrated to reduce carbon monoxide (CO) to less than 0.5 %-vol.

Future Directions

- Design and construct multi-contaminant control system based on sorbent injection. This system will remove particulate, sulfur, and halogen contaminants.
- Improve trace contaminant instrumentation. These improvements will give on-line capability for sulfur, NH_3, and some tar species.
- Evaluate effectiveness of multi-contaminant control system.
- Evaluate additional catalysts for removal of tar and NH_3 and enriching H_2 content via water-gas shift reaction.
- Identify appropriate separation technology to purify H_2.
- Perform thermal system and cost estimate analyses.

Introduction

The goal of this project is to optimize performance of an indirectly heated gasification system that converts switchgrass into H_2-rich gas suitable for powering fuel cells. We have developed a thermally ballasted gasifier that uses a single reactor for both combustion and pyrolysis. Instead of spatially separating these processes, they are temporally isolated. The producer gas is diluted with neither nitrogen (N_2) nor the products of combustion. The heat released during combustion at 850°C is stored as latent heat in the form of molten salt sealed in tubes immersed in the fluidized bed. During the pyrolysis phase, which occurs at temperatures between 600 and 850°C, the reactor is fluidized with steam or recycled producer gas rather than air. Heat stored in the phase change material is released during this phase of the cycle to support the endothermic reactions of the pyrolysis stage.

Because air is not used during the gas-producing phase of the cycle, N_2 does not dilute the product gas, resulting in relatively high concentrations of H_2 and CO in the producer gas compared to conventional gasifiers. The CO, along with steam used to fluidize the reactor, can be shifted to additional H_2 by the water-gas shift reaction.

Approach

The approach to this project is to employ a pilot-scale (5-ton per day) gasifier to evaluate the thermally ballasted gasifier as a means for producing H_2 from switchgrass. Gasification at the pilot scale is important for obtaining realistic process data, especially for calculating energy flows through the system and assessing the practicality of feeding switchgrass into the gasifier. A series of gasification trials are being performed to evaluate the effect of biomass feed rate (fixed steam rate) and the effect of biomass/steam rate (fixed biomass feed rate) on H_2 production.

A slipstream from the gasifier will be used to evaluate gas cleaning and upgrading options during the first year of research. This slipstream will include a guard bed designed to remove H_2S and HCl and some tar, a steam reformer designed to crack the remaining tar and decompose NH_3, and high-temperature and low-temperature catalytic water-gas shift reactors to remove CO from the product gas and increase its H_2 content. A series of gasification trials will be performed to evaluate the effectiveness of these four reactors in removing tar and contaminants, and shifting producer gas towards increased H_2 and decreased CO.

Results

Most of the first year was consumed in constructing the experimental equipment required for the gasification system and the gas analysis system. The gasification system is illustrated schematically in Figure 1. The 5-ton per day bubbling fluidized bed gasifier was modified to operate as a ballasted gasifier. This entailed installation of the ballast system within the fluid bed reactor. The ballast system consists of 25.4 mm diameter stainless steel tubes 610 mm in length. Each of the ballast tubes was filled with 0.3 kg (0.66 lb) of Lithium Fluoride (LiF). An air pocket was left in each of the tubes to allow for expansion of the LiF. Forty-eight ballast tubes cover about 15% of the bed cross-sectional area. This represents a total latent heat storage capacity of 15,100 kJ.

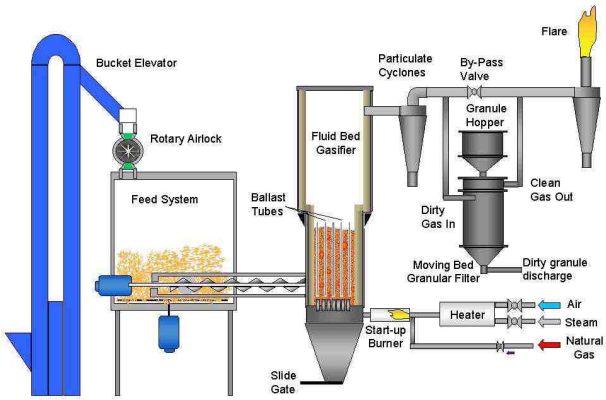

Figure 1. Schematic of the Gasifier System

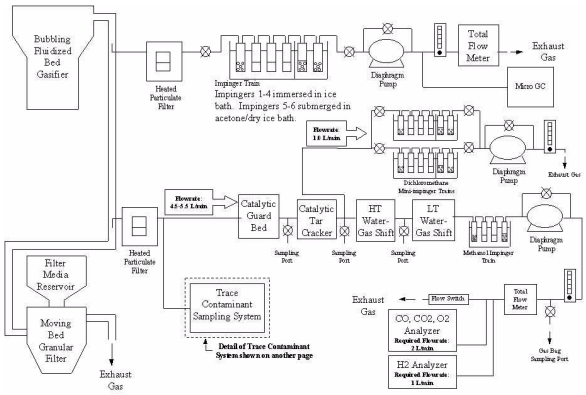

Figure 2. Overall Schematic of Gas Sampling System and Slipstream from Gasifier Effluent

Several other modifications have been made to the gasifier system. An additional fuel hopper was added to the system to enable the use of multiple fuels. Both fuel hoppers were outfitted with load cells to accurately measure fuel flow into the gasification reactor. The moving bed granular filter, which will be evaluated for hot gas cleanup of particulate material in the producer gas, has been improved by the addition of a new auger system to remove dirty filter media from the bottom of the filter. The exhaust system, which was in poor repair, was replaced and upgraded to minimize the impacts of temperature on the system. Additionally, an automated high-temperature valve was installed to enable division of the pyrolytic gases from the combustion gases.

Figure 2 is a flow diagram of the gas sampling system and the slipstream used on the producer gas effluent. Producer gas is extracted at two locations in the producer gas effluent. The first sampling point is positioned just downstream of the gasifier to provide raw gas characterization. This sampling is performed isokinetically to obtain a representative particulate loading. The isokinetically-sampled gas passes through a Mott Hyline porous metal filter operated at 600ºC to prevent condensation of tar. The gas then passes through a series of impingers containing varying combinations of dichloromethane (DCM) and glass beads. The impingers remove all condensable species, including tars and water. The Varian Micro-Gas Chromatograph draws a small portion of the sample stream in order to characterize the gas, specifically for H_2, CO, carbon dioxide (CO_2), N_2, methane (CH_4) and ethylene (C_2H_4). The remaining portion of the sample stream is passed through a total volumetric gas meter and exhausted to atmosphere.

The second extraction point is for the purpose of producing a slipstream of the gasifier effluent, which is used to evaluate an experimental gas conditioning system. A heated filter, similar to the one previously described, removes particulate matter, but gas is not sampled isokinetically, as is done in the first gas extraction location. After passing through the gas conditioning system, described in the next section, the producer gas passes through on-line gas analyzers that monitor CO, CO_2, Oxygen (O_2) and H_2. The slipstream also provides a particulate-free gas for the quantification of trace contaminants such as H_2S, HCl, hydrogen cyanide (HCN), and NH_3.

Based upon previous work on the catalytic conversion of tars, new reactors have been designed and constructed. Improvements include the addition of standard flanges for better leakage control, upgraded reactor materials for improved characteristics in high-temperature environments, and welded joints in all areas inside the heated enclosures to vastly reduce leakage potential. Two more reactors were added for high-temperature and low-temperature H_2 shift reaction purposes. Figure 3 shows the current design for the gas conditioning system. The reactor bodies are made of 1¼ inch pipes constructed with Haynes 230 and pre-manufactured flanges made of 304 stainless steel. The 3/8 inch inlet and outlet pipes are constructed

with Haynes 230 material and have 3/8 inch stainless steel tube adapters welded to them. Each reactor has a volume of approximately 16.5 cubic inches (270 cubic centimeters).

The trace contaminant sampling system draws a slipstream from the gas passing into the catalytic reactor system. This sample is drawn following the porous metal filter through which all of the gas passes. The slipstream progresses through a condensing coil to remove all tars. The flow is then split into two smaller streams. The first stream is passed through a nafion membrane to remove all moisture from the gas, and a sample is drawn with Draeger tubes to quantify H_2S content. The second stream passes through bubblers plumbed in parallel to each other to simultaneously quantify HCl, HCN and NH_3. Following sampling, these streams are exhausted to the atmosphere.

During the first year, most gasification trials were performed with the gasifier operated in conventional, air-blown mode. Experimental results included characterization of the gas obtained from gasification of switchgrass, preliminary evaluation of the performance of the steam reformer, and preliminary evaluation of the catalytic water-gas shift reactors.

Air-blown gasification of switchgrass produced tar loadings of 117 g/nM^3, which is within 10% of the tar loadings obtained from gasification of obsolete seed corn, the model fuel used in this test program. Particulate loadings from air-gasification of switchgrass were 19.3 g/nm^3. The steam reformer was able to reduce total tar by 95% and condensable (heavy) tar by greater than 99%. The catalytic water-gas shift reactor reduced CO to less than 0.5 %-vol.

Conclusions

Most of the first year was occupied in setting up the 5-ton per day pilot plant gasifier to operate in thermally ballasted mode and preparing the slip stream for gas conditioning studies.

Switchgrass was successfully gasified and shown to produce a gas with characteristics similar to producer gas from a model gasification fuel, namely obsolete seed corn.

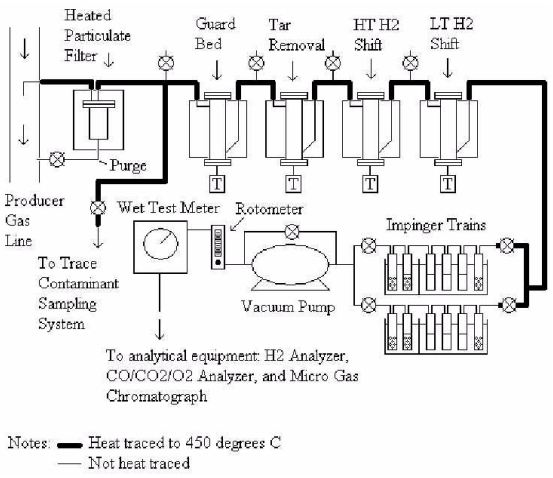

Figure 3. Gas Conditioning System

The steam reformer was able to eliminate up to 95% of heavy tars.

The water-gas shift reactors reduced CO in the producer gas to 0.5 %-vol.

FY 2002 Publications/Presentations

1. Cummer, K. and Brown, R. C., "Ancillary equipment for biomass gasification," accepted for publication in Biomass and Bioenergy, Fall 2001.

2. Pletka, R., Brown, R. C., and Smeenk, J., "Indirectly heated biomass gasification using a latent heat ballast. Part 1: Experimental evaluations," Biomass and Bioenergy 20, 297-305, 2001.

3. Pletka, R., Brown, R. C., and Smeenk, J., "Indirectly heated biomass gasification using a latent heat ballast. Part 2: Computational model," Biomass and Bioenergy 20, 307-315, 2001.

4. Zhang, R., Brown, R. C., Suby, A., Cummer, K., "Catalytic cleaning of hot producer gas," Fifth International Biomass of the Americas Conference, Orlando, FL, September 17-21, 2001 (conference cancelled because of national emergency).

5. Nunez, J. S., Cummer, K., Brown, R. C., Smeenk, J., "Use of a moving bed filter for cleanup of hot producer gas," Fifth International Biomass of the

Americas Conference, Orlando, FL, September 17-21, 2001 (conference cancelled because of national emergency).

6. Levin, D. B., Maness, P., Brown, R. C., "Integrated hydrogen energy system for power and transportation," Fifth International Biomass of the Americas Conference, Orlando, FL, September 17-21, 2001 (conference cancelled because of national emergency).

7. Cummer, K., Zhang, R., Suby, A., Norton, G., and Brown, R. C., "Improving prospects for gasification of wastes through gas conditioning: Tar removal," Renewable Energy and Organics Recycling Conference, Des Moines, IA, October 29-31, 2001.

8. Nunez, J., Cummer, K., Suby, A., Dvorak, B., Smeenk, J., Brown, R. C., "Improving prospects for gasification of wastes through gas conditioning: Dust removal," Renewable Energy and Organics Recycling Conference, Des Moines, IA, October 29-31, 2001.

9. Méridaa, W., Levina, D. B., Manessb, P. C., and Brown, R. C., "Enhanced hydrogen production and CO removal from indirectly heated biomass gasification," 11th Canadian Hydrogen Conference, Victoria, British Columbia, Canada, June 17-20, 2001.

10. Young, B. L. and R. C. Brown, "Application of biomass gasification to Chinese markets," Eco-Informa 2001, Argonne National Lab, Chicago, May 14-18, 2001.

II.B.4 Techno-Economic Analysis of Hydrogen Production by Gasification of Biomass

Francis Lau (Primary Contact), Dave Bowen, Robert Zabransky
Gas Technology Institute
1700 South Mount Prospect Road
Des Plaines, Illinois 60018
(847) 768-0592, fax: (847) 768-0600, e-mail: Francis.Lau@gastechnology.org

DOE Technology Development Manager: Peter Devlin
(202) 586-4905, fax: (202) 586-9811, e-mail: Peter.Devlin@ee.doe.gov

Main Subcontractors: Hawaii Natural Energy Institute, Honolulu, Hawaii, Electrical Power Research Institute, Palo Alto, California

Objectives

- To determine the economics of hydrogen production by gasification of three biomass candidates: bagasse, switch grass, and nutshells.
- To optimize hydrogen production for transportation use.
- To identify the economic and technical barriers associated with biomass gasification.

Approach

- Develop a simulation to quantify hydrogen production.
- Determine the optimization of hydrogen by testing various cases through simulation.
- Analyze research and simulation results to determine technical and economic feasibility.

Accomplishments

- Developed a model using a Hysis Simulation package.
- Explored the resource base for nutshells and bagasse to determine their availability.
- Gathered literature for an ultimate dry basis analysis of the feedstocks.

Future Directions

- Develop a more detailed process flow schematic with a complete gas cleanup system.
- Perform laboratory testing on biomass feedstocks and analyze hydrogen production.

Introduction

The future application of hydrogen as a non-polluting fuel is dependent on the convergence of cost effective technologies for its manufacture, delivery, and end-use. DOE is actively pursuing research in all these areas to enable the private sector to demonstrate the technical viability of hydrogen technologies. Once viable from a technical viewpoint, commercial acceptance requires that these technologies demonstrate cost effectiveness in the marketplace. Key markets for hydrogen technologies are the transportation, stationary industrial, residential, and commercial energy markets. The prime mover targeted for hydrogen is fuel cell systems that are capable of very efficient and clean conversion of hydrogen to electricity, either with or without byproduct heat recovery.

Approach

The object of this project is to assess the cost of hydrogen production from three candidate biomass feedstocks and identify the barriers for commercialization of this technology. This is to be accomplished by first assessing the resource base. A process flow scheme will be developed for each feedstock that includes the following sections: feed preparation, followed by gasification or pyrolysis, a reforming section to reduce heavy hydrocarbons in the gas, a shift conversion process to maximize hydrogen production, and a gas purification process to provide gas meeting end-use specifications. The process design will then be used to perform an economic analysis to determine the cost of producing hydrogen. Throughout this effort, possible barriers to implementation of the technology will be identified, and a cost sensitivity analysis examining the major cost elements of the process will be performed. The resultant package will identify areas where targeted research will have the greatest benefits. The project will also identify the current influence of government incentive programs for biomass production and recommend changes that will further stimulate integration of biomass as an energy feedstock.

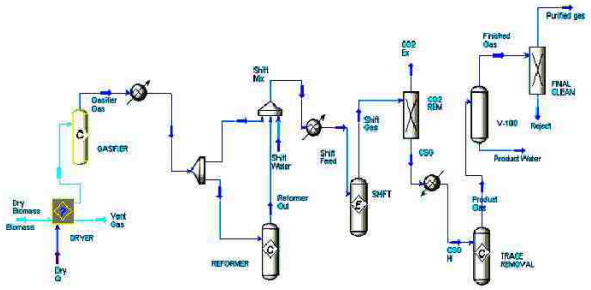

Figure 1. Hysis Simulation Flow Sheet

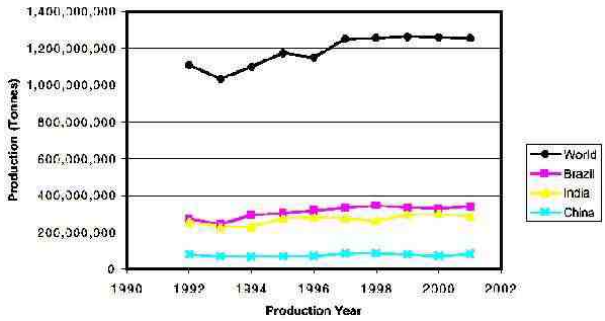

Figure 3. Sugar Cane Production for the World, Brazil, India, and China (1992 - 2001)

Results

This project is still in the analysis phase to determine the economics of hydrogen production from biomass. A process flow sheet has been developed (see Figure 1) and a resource base for nutshells and bagasse has been analyzed. Nut production varies, as with any agricultural crop, due to changing climates and weather conditions. Generally, the production of nuts has increased over the past 10 years. Heating values for nutshells range from 7500 - 9000 BTU/lb on a dry basis.

Bagasse is leftover material from the production of sugar cane. The majority of sugar cane production comes from Brazil, India, and China (the United States ranks tenth in world production of sugar cane). Data on world and major sugar cane producing countries can be seen in Figure 2. The majority (85%) of bagasse is used to meet the thermal demands of the processing factory. The remaining 15% can be used for power generation needs. During the crushing season in Brazil, there would be roughly 165 ton/day of bagasse fiber if a given factory operated at capacity. Based on this estimate, four plants have the ability to produce around 660 tons of bagasse per day for around 200 days per year, which would satisfy the needs of a small hydrogen production facility. The heating value of bagasse is around 7200 - 8000 BTU/lb on a dry basis.

Switchgrass is an energy crop being studied for its potential as a fuel source. Switchgrass is beneficial in that it has yet to be cultivated and therefore can potentially be grown in locations close to the gasifier and ultimately reduce hydrogen production costs by reducing transportation costs. Typical heating values for switchgrass range from 7700 - 8200 BTU/lb on a dry basis.

Conclusions

- Gasification technologies, in combination with advancements in hot gas cleanup technologies, allow for hydrogen production with little environmental impact.

- Biomass can be used as a valuable and environmentally clean product, instead of a waste product, if used to produce hydrogen.
- Hydrogen production costs for transportation use will be significantly higher than current fossil fuel prices, but hydrogen from biomass has potential to become a competitive fuel with various government incentives and advances in technology.
- Hydrogen from biomass yielded production values ranging from 5.7 - 9.1 scf H_2 / lb biomass during initial case studies (this is assuming that all the CO is shifted to H_2).
- A typical hydrogen from biomass plant will be able to operate economically at around 600 tons/day for bagasse. A plant producing hydrogen from nutshells will be significantly lower. Switchgrass has yet to be determined.

References

1. Woodruff, J.G. 1979. Tree Nuts: Production, Processing, Products. AVI Publishing, Westport, CN. http://www.fao.org/waicent/faoinfo/Economic/faodef/FDEF05E.HTM.

FY 2002 Publications/Presentations

1. F. Lau, R. Zabransky, D. Bowen, C. Kinoshita, S. Turn, and E. Hughes. Techno-Economic Analysis of Hydrogen Production by Gasification of Biomass. Proceedings of the 2002 US DOE Hydrogen and Fuel Cells Annual Program / Lab R&D Review, May 6-10, 2002, Golden Colorado. http://erendev.nrel.gov/hydrogen/pdfs/32405b5.pdf.

II.C Fossil-Based

II.C.1 Production of Hydrogen by Superadiabatic Decomposition of Hydrogen Sulfide

Francis S. Lau (Primary Contact), Rachid B. Slimane, Remon J. Dihu, and Mark Khinkis
Gas Technology Institute
1700 S. Mt. Prospect Rd., Des Plaines, Illinois 60018
(847) 768-0592, fax: (847) 768-0600, e-mail: francis.lau@gastechnology.org

Jacques Bingue, Alexei Saveliev, Alexander Fridman, and Lawrence Kennedy
University of Illinois at Chicago, Chicago, IL

DOE Technology Development Manager: Peter Devlin
(202) 586-4905, fax: (202) 586-9811, e-mail: Peter.Devlin@ee.doe.gov

Main Subcontractor: University of Illinois at Chicago, Chicago, IL

Objectives

- Demonstrate the feasibility of the superadiabatic partial oxidation concept as a basis for developing an innovative process for production of economically viable quantities of hydrogen through the thermal, noncatalytic decomposition of hydrogen sulfide (H_2S) in H_2S-rich waste streams into hydrogen and elemental sulfur, without the input of additional energy (and no additional carbon dioxide [CO_2] emissions).
- Outline a research and development strategy leading to the demonstration of an integrated process at an industrial site.

Approach

- Develop a numerical model for the superadiabatic H_2S decomposition reactor.
- Design, construct, and operate a bench-scale reactor system to demonstrate technical feasibility of the superadiabatic partial oxidation concept.
- Evaluate process economics and markets.
- Conduct thermodynamic and kinetic modeling studies to evaluate agreement between modeling predictions and experimental data, and to extend model applicability to conditions not tested experimentally.

Accomplishments

- Identified key process variables and optimum operating conditions, and developed reactor design guidelines.
- Prepared a design package for a bench-scale testing system.
- Performed preliminary confirmation of technical viability of the concept.
- Designed and constructed a state-of-the-art superadiabatic H_2S decomposition reactor system to carry out a rigorous demonstration of the technical feasibility of the superadiabatic decomposition approach.

Future Directions

- Determine the fate of feed gas impurities (i.e., CO_2, methane [CH_4], etc.) in the product gas, and their effect on reactor performance, especially with respect to hydrogen yield.
- Evaluate several product/byproduct separation schemes to separate the unreacted H_2S for recycle (to maximize the overall H_2S conversion), the hydrogen product for purification, and the tail gas for cleanup.
- Construct and operate a pilot-scale superadiabatic reactor system to provide for a more practical evaluation of the process and to develop large-scale plant data permitting more realistic engineering and economic analysis.
- Construct an integrated superadiabatic H_2S decomposition system for field-testing at an industrial site (e.g., refinery).

Introduction

In recent years, H_2S has come to be regarded as a mineral from which two valuable products (hydrogen and sulfur) can be extracted.[1] Technology is well established for the recovery of the sulfur component, with the Claus process being the most prominent. Although this technology also produces a low-quality steam, it does not fully utilize the potential of H_2S as a resource for hydrogen. Because of the significant amounts of H_2S available worldwide, efforts have been made in recent years for the production of hydrogen, in addition to sulfur, from H_2S through a number of approaches. It is widely recognized that the most direct process of converting H_2S into hydrogen (H_2) and sulfur is through thermal decomposition (catalytic or noncatalytic). However, because of energy considerations, this approach has been considered impractical at temperatures exceeding about 927°C (1200K). In addition to being endothermic, the equilibrium of the thermal decomposition of H_2S at these temperatures is relatively low, and the reaction does not proceed to an industrially important extent.[2] For example, based on thermodynamic equilibria, conversion of H_2S into H_2 is only about 20% at 1000°C and 38% at 1200°C. Temperatures exceeding 1375°C are needed to drive the H_2S decomposition reaction to conversions > 50%.

Because of these limitations and other considerations, such as strict environmental regulations on sulfur emissions, any process for the recovery of hydrogen, in addition to sulfur, from H_2S based on thermal decomposition or dissociation has to overcome a number of technical (and economical) hurdles. These include:

- Low yields even at high temperature (equilibrium limited)
- To maximize H_2 production, it is necessary to recycle unreacted H_2S
- Need to separate product gases
- Large recycle streams, unless conversion is reasonably high
- Rapid quenching of product gas may be necessary to block any recombination of H_2 and S_2 (decomposition reaction is reversible)
- Fate of impurities in feed gas has implications on emissions, tail-gas cleanup, and purity of the H_2 product.

Due to the high energy demands for thermal dissociation, other approaches were evaluated where attempts were made to carry out the decomposition reaction with equilibrium shift, such as by preferential removal of reaction products by membranes and thermal diffusion columns. Despite the advances made in these areas, no method of hydrogen sulfide decomposition can be considered commercially feasible today.

Approach

Working with the University of Illinois at Chicago (UIC) and other industrial partners, including Universal Oil Products and BP Amoco, the Gas Technology Institute (GTI) has been developing an innovative process that promises to overcome the limitations of the noncatalytic thermal decomposition approach. In this process, operation at significantly

high temperatures is made possible and economical by oxidation of part of the H_2S to provide the energy required for the decomposition reaction to proceed to a significant extent. Partial oxidation of H_2S in the H_2S-containing fuel gas is carried out in the presence of an inert, porous, high-capacity medium, and the intense heat exchange results in flame temperatures that significantly exceed the adiabatic flame temperature of the gas mixture. By coupling the partial oxidation of H_2S in the porous medium with the H_2S decomposition, temperatures as high as 1400^oC (1673K) can be achieved economically within a reaction zone without the input of external energy, and therefore, no additional CO_2 emissions. In this reaction zone, the self-sustaining conditions are very favorable for the decomposition reaction to proceed to an industrially significant extent, within a slowly propagating thermal wave (Figure 1). The superadiabatic partial oxidation concept is depicted in Figure 2 for a given set of operating conditions (i.e., 20% H_2S in the feed gas, 12 cm/s gas velocity, etc.).[3] It is clearly seen that in this case, for equivalence ratios > 1.5, the temperature achieved greatly exceeds the adiabatic temperature of the gas mixture. (Equivalence ratio is defined as the molar ratio of oxygen gas (O_2) supplied to the O_2 that is stoichiometrically required to burn all the H_2S.) It is conceivable that higher temperatures than shown in Figure 2 can be achieved by manipulating the operating conditions.

GTI has envisioned a process (Figure 3) comprising the superadiabatic H_2S decomposition reactor, product/byproduct separation schemes, hydrogen purification, and tail gas cleanup. Work has so far concentrated mainly on the superadiabatic reactor, and has comprised computational modeling and experimental studies to demonstrate the technical and economical feasibility of the superadiabatic H_2S decomposition concept, using H_2S-nitrogen (N_2)-O_2 gas mixtures.

Groundwork numerical modeling of the superadiabatic decomposition reactor has been performed, identifying key process parameters. These parameters include fuel gas composition (i.e., H_2S-rich and H_2S-lean), oxidant composition (air/enriched air/oxygen), equivalence ratio, superficial gas velocity, feed gas temperature (pre-heating effect), and product gas quenching (to avoid

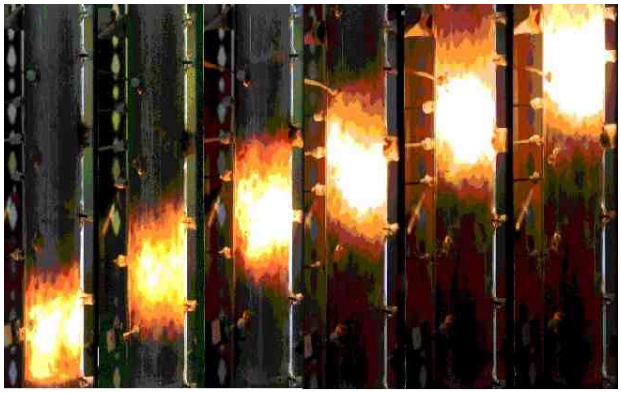

Figure 1. Propagating Superadiabatic Partial Oxidation Wave

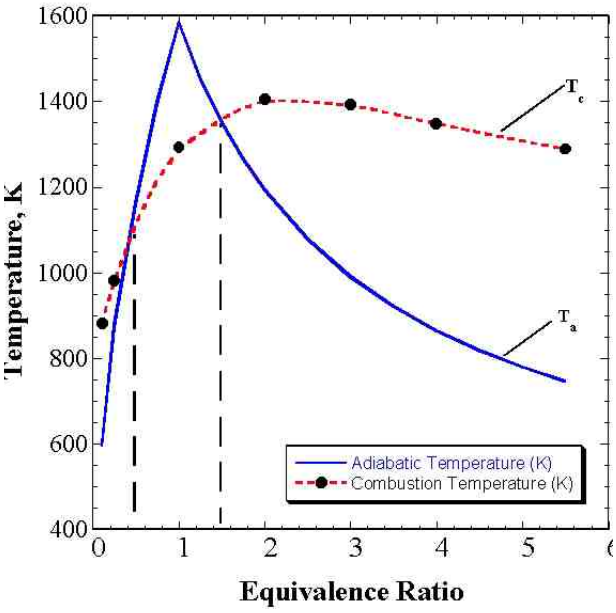

Figure 2. Partial Oxidation Temperature of H_2S (Gas Velocity= 12 cm/s)

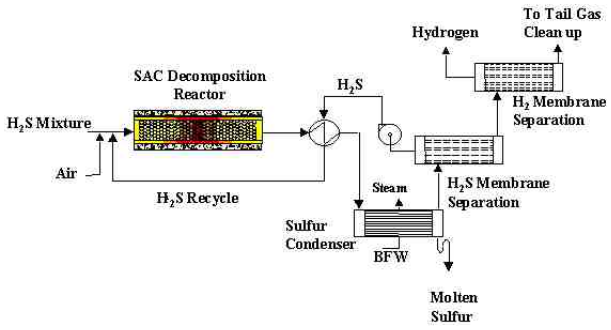

Figure 3. Conceptual Process Design for Hydrogen Production Based on the Superadiabatic Decomposition Concept

recombination of H_2 and S_2). Qualitative and quantitative determinations were made of the effects of these parameters, individually and in combination, on the performance of the superadiabatic decomposition reactor for production of hydrogen and elemental sulfur.[4,5]

Collaborative experimental investigations by GTI and UIC researchers on the generation of hydrogen-rich gases from hydrocarbons via superadiabatic partial oxidation have shown the high potential and practicality of this approach. To carry out a rigorous process evaluation, GTI designed and constructed a state-of-the-art superadiabatic H_2S decomposition reactor system (Figure 4). This reactor is currently being operated to demonstrate the technical feasibility of the superadiabatic decomposition process, to evaluate the agreement between modeling predictions and experimental results, and to reassess the economic potential of the process.

Results

The major findings from the numerical modeling work appear to indicate that by optimizing the porous body reactor configuration, equivalence ratio, and gas velocity, the overall H_2S decomposition in a single pass can be as high as 50%, with a conversion of H_2S to the desirable product hydrogen (H_2) reaching a level of 30%. It is estimated that the overall process performance can be substantially improved with respect to hydrogen production by membrane separation of product gases and recirculation of unreacted H_2S. It is estimated that in 4 to 5 passes nearly total H_2S decomposition into sulfur can be realized, with recovery of 30-40% of the hydrogen component.

The optimum numerical modeling scenario indicates that, with feed gases entering the reactor at ambient temperature, a maximum temperature of 1631 K (1394°C or 2541°F) can be achieved in the superadiabatic reactor, resulting in an overall H_2S conversion of 50%, with a hydrogen (H_2)/water (H_2O) selectivity of 57/43 and an elemental sulfur (S_2)/sulfur dioxide (SO_2) selectivity of 99/1.

Preliminary experimental testing has shown that stable self-sustained flames could be generated using

Figure 4. Overall Arrangement of GTI's Newly-Constructed Lab-scale H_2S Superadiabatic Decomposition Reactor

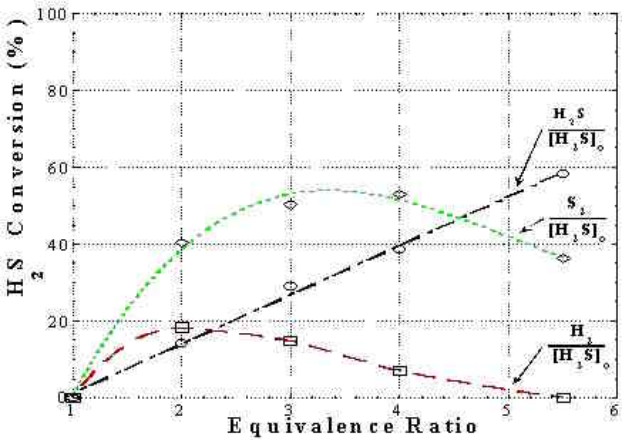

Figure 5. Hydrogen Sulfide Conversions (Vg= 12 cm/s)

H_2S-containing gases as a feedstock in the range of equivalence ratios from 2 to 5 with a hydrogen output at about 20%[6], as shown in Figure 5. The agreement between the groundwork experimental data developed to-date and modeling predictions is quite reasonable.

Figure 6. Sulfur Produced Through the Superadiabatic Decomposition of H_2S

The newly constructed superadiabatic H_2S decomposition reactor system is currently being operated to develop a data package to provide evidence of the technical feasibility of the superadiabatic partial oxidation concept for the production of hydrogen (and elemental sulfur) from H_2S. Successful tests have been made; a photo of the sulfur product, collected at the end of a typical test, is shown in Figure 6.

Conclusions

The superadiabatic partial oxidation concept appears to hold significant promise as a basis for developing a novel process for the production of low-cost hydrogen (and sulfur) by enhanced thermal decomposition of H_2S in H_2S-containing waste streams, without the input of external energy, and therefore, no additional CO_2 emissions. The process has potential to utilize significant quantities of hydrogen that are currently being wasted as water vapor by conventional sulfur recovery processes (e.g., Claus).

References

1. Zaman, J. and Chakma, A. "Production of Hydrogen and Sulfur from Hydrogen Sulfide," Fuel Processing Technology 41 (1995) 159-198.

2. Norman, J.H., "Hydrogen Production from In-Situ Partial Burning of H_2S," U.S. Patent Number: 4,481,181, 1984, Assigned to GA Technologies Inc., San Diego, CA.

3. Bingue, J.P., Saveliev, A.V., Fridman, A.A., and Kennedy, L.A., "Filtration Combustion of Hydrogen Sulfide," Proceedings of the 2000 Technical Meeting of the Central State Section of the Combustion Institute.

4. Slimane, R.B., Lau, F.S., and Abbasian, J. "Production of Hydrogen by Superadiabatic Decomposition of Hydrogen Sulfide," Final Technical Report, DOE Contract No.: DE-FC36-99GO10450, June 1, 1999 - September 30, 2000.

5. Slimane, R.B., Lau, F.S., and Abbasian, J., "Hydrogen Production by Superadiabatic Combustion of Hydrogen Sulfide," Proceedings of the 2000 U.S. DOE Hydrogen Program Review.

6. Bingue, J.P., Saveliev, A.V., Fridman, A.A., and Kennedy, L.A., Proceedings of the 2000 Technical Meeting, The Central State Section of the Combustion Institute, Indianapolis, IN, pp. 379-384, 2000.

FY 2002 Publications/Presentations

1. Slimane, R.B., Lau, F.S., et al. "Production of Hydrogen by Superadiabatic Decomposition of Hydrogen Sulfide," GTI Technical Progress Report for Contract No. DE-FC36-99GO10450, Submitted to DOE, June 2002.

2. Slimane, R.B., Lau, F.S., Dihu, R., Bingue, J.P., Saveliev, A.V., Fridman, A.A., and Kennedy, L.A., "Production of Hydrogen by Superadiabatic Decomposition of Hydrogen Sulfide," Paper presented and published in the 14th World Hydrogen Energy Conference, June 9-14, 2002, Montreal, Quebec, Canada.

3. Slimane, R.B., Lau, F.S., Dihu, R., "An Economical Process for the Utilization of H_2S from Natural Gas Upgrading Operations," Paper to be presented at the Natural Gas Technologies - What's New and What's Next Conference, Sept. 29 - Oct. 2, 2002, Lake Buena Vista, Florida.

4. Bingue, J.P., Saveliev, A.V., Fridman, A.A., and Kennedy, L.A., "Hydrogen Production in Ultra-Rich Filtration Combustion of Methane and Hydrogen Sulfide," International Journal of Hydrogen Energy, 27/6, 643-649, 2002.

II.C.2 Thermal Dissociation of Methane Using a Solar-Coupled Aerosol Flow Reactor

Alan W. Weimer (Primary Contact)
Department of Chemical Engineering
University of Colorado
Boulder, CO 80309-0424
(303) 492-3759, fax: (303)492-434, e-mail: alan.weimer@colorado.edu

DOE Technology Development Manager: Peter Devlin
(202) 586-4905, fax: (202) 586-9811, e-mail: Peter.Devlin@ee.doe.gov

Main Subcontractor: National Renewable Energy Laboratory (NREL), Golden, CO

Objectives

- Demonstrate a pilot scale solar-thermal transport tube reactor process to thermally dissociate methane to hydrogen (H_2) and carbon black.
- Develop a fundamental understanding of the reaction kinetics and transport heat and mass transfer processes to allow plant design of a scaled-up process for economic evaluation.
- Carry out an economic and environmental evaluation of the process in order to assess viability and to identify fruitful research areas where success would significantly impact the economics.
- Involve as many students and interested companies as possible in the project, nurture their interaction, and facilitate communication among all parties (students, NREL, and nine companies) to provide a framework for successful project completion and learning.

Approach

- A pilot reactor system was designed, constructed, and interfaced to the NREL High-Flux-Solar Furnace (HFSF).
- The process was successfully started up and has been operating for six months; a matrix of statistically designed experiments has been carried out to obtain data for fundamental understanding and process plant design scale-up.
- The produced carbon black has been evaluated internally and by Chevron-Phillips, the industry liaison interested in potentially marketing the carbon black.
- Four teams of senior chemical engineering students supervised by teams of the industry liaisons carried out plant designs and economic evaluations for four process scenarios - centralized hydrogen plant, distributed hydrogen plant, co-generation (H_2 and electricity) utility plant, and industrial semi-conductor hydrogen plant.

Accomplishments

- Demonstrated rapid methane dissociation exceeding 60% for residence times of 0.01 second at a temperature of 1900^{o}K (Kelvin) and without co-feeding carbon black.
- Demonstrated production of an amorphous (not graphitic), ash-free, fine sized (20 to 40 nanometer) carbon black powder suitable for tire production or conversion in a high-efficiency carbon conversion fuel cell [1] with no wall deposition in reactor.
- Demonstrated suitable materials of construction for a high-temperature solar-thermal process - reactor assembly constructed of exterior quartz and interior porous and solid graphite.

- Demonstrated a highly efficient process that requires ~ 40 times less heliostat (sun capture surface) area than photovoltaic cells powering electrolyzers to produce H_2.
- Carried out an economic assessment of the process indicating a 15% internal rate of return (IRR) for an out-the-gate hydrogen plant selling hydrogen at < $15/GJ (Giga-Joule).
- Over a three-year period, the project involved 26 undergraduate students, one Ph.D. student, one postdoctoral researcher, nine companies, and NREL.

Future Directions

- This is the final year of a three-year project and no future research is planned. However, DOE is currently considering a process extension proposal to support a solar-thermal process to rapidly dry reform waste landfill gas to hydrogen and carbon black. Independent of the outcome of that proposal, the following issues need to be addressed:
- The produced carbon black needs to be supplied in a large enough quantity for testing by tire manufacturers. The Goodyear Tire & Rubber Company has agreed to evaluate the carbon black. Extended reactor operations should be carried out to supply the carbon black powder to Goodyear for testing.
- Efforts should be directed to study the impact of transient effects (clouds passing over, etc.) on the process, and process control systems for operating the reactor under such transient conditions should be developed.
- An economic evaluation should be carried out for a one-step solar-thermal process to supply hydrogen-enriched natural gas (HCNG) for fleet vehicle fueling. In such a process, 35% H_2 in natural gas (NG) can be achieved at only 21% conversion by stripping some carbon out of the NG. The alternative steam-reforming process (oxygen added in the form of water) requires complete processing (many steps) to pure H_2 which is then blended with NG to obtain the desired composition.
- Methods should be evaluated for operating the solar-thermal process continuously to produce H_2. Two such methods are (1) design and construction of a reactor capable of operating with an electrically heated supplementary source of power and (2) development of and integration of the solar-thermal process with a high efficiency carbon conversion fuel cell to supply electricity to an electrolyzer for splitting water. In both instances, H_2 could be supplied off-sun. Development of a carbon conversion fuel cell would also provide a significant outlet (in addition to tire sales) for all of the carbon black that is produced while on-sun. The carbon black that is produced is a perfect feed for a carbon conversion fuel cell - fine sized, amorphous, and ash-free.
- Alternative H_2 production processes using concentrated sunlight to drive rapid reactions should be investigated. These reactions include the reforming of high CO_2 containing NG wells (i.e. "contaminated wells") that may be capped and not used, and waste landfill biogas that is currently being flared or simply burned to generate electricity.

Introduction

Sunlight can be concentrated with mirrors and used to achieve ultra-high temperatures that are otherwise only achievable using electricity or nuclear power. The use of such renewable solar-thermal processing has significant potential in the desert southwest United States (AZ, CA, CO, NM, NV, and UT) for heating specialized chemical reactors to produce H_2 from NG, biogas, or waste landfill gas. Since there is no energy conversion processing required (i.e. no efficiency losses to convert steam generated by combustion into electricity via a turbine or to convert sunlight to electricity via a photovoltaic cell and then use the electricity to split water by electrolysis), the sunlight is directly used to drive high temperature "brute force" chemical reactions - such as dissociation reactions - at high efficiency. Overall solar-thermal efficiencies approach 50%.

With the ultra-high temperatures (~ 2000^{o}K) achieved in the process, the chemical reaction rates are enormous and approximately 1000 times faster than rates achieved when operating at more conventional (~ 1000^{o}K) temperatures. The primary technical challenges for solar-thermal NG dissociation are related to (1) the ability to operate on an on/off mode with the sun, (2) the selection of suitable materials of construction and reactor design to achieve the ultra-high temperatures, (3) the ability to prevent carbon deposition on the inside wall of the reaction vessel, (4) the ability to heat and dissociate a gas that is transparent to radiation, and (5) the ability to operate continuously using supplementary energy or stored energy that is produced while on-sun.

In this project, a pilot scale solar-thermal reactor was constructed at the University of Colorado (Boulder, CO) and interfaced to the HFSF at NREL in nearby Golden, CO (see Figure 1). After experiments were done, the reactor was optimized. This was followed by significant experimentation to develop an understanding of the rate of reaction at ultra-high solar-thermal temperatures. Produced carbon black was evaluated for product quality (i.e. market price). A study was conducted to design a scaled-up plant for commercial processing (four scenarios), and profitability studies were carried out. Nine companies (BP, Chevron-Phillips, Chevron-Texaco, Electric Power Research Institute, General Motors, Harper International, Pinnacle West, PlugPower, and Siemens) are involved in the process and attended at least one of the two team meetings that were held during the year. Eight of the companies attended the final project review. The companies have been instrumental in guiding the research. One Ph.D. student is responsible for the fundamental understanding of the process. One chemical engineering postdoctoral researcher has been responsible for the applied aspects of the process. Ten undergraduate chemical engineering students (~ 50% female and/or under-represented minorities) were involved in the 2002 process design and profitability analysis as part of the senior chemical engineering plant design and economics course. The process appears feasible and potentially economical.

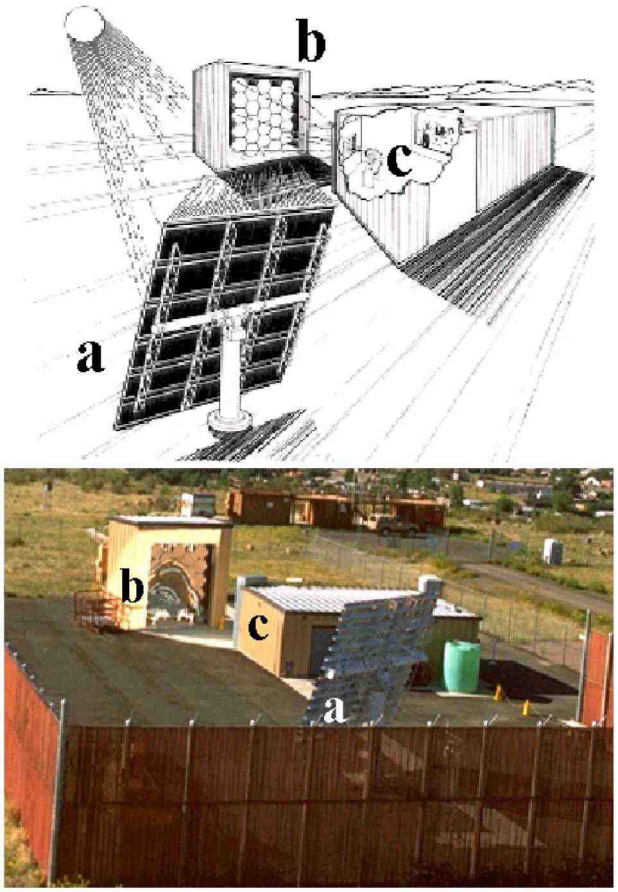

a) Heliostat b) Primary Concentrator c) Reactor

Figure 1. Schematic of Photo and HFSF at NREL, (Golden CO)

Approach

A vertical aerosol flow reactor was constructed and interfaced to the HFSF at NREL [2]. Argon flows in the annular region between the two tubes and provides an inert atmosphere that prevents oxidation of the graphite tube while preventing any decomposition products from depositing on the inner quartz wall. Feed methane gas flows downward through the graphite tube. The reactor was placed at the focal point of the primary concentrator that can deliver up to 10 kW (kilowatt) of power on-sun. A secondary concentrator enveloping the reactor allows temperatures greater than 2000^{o}K to be achieved.

The reactor is operated as a cold wall process because the beam is delivered directly on target.

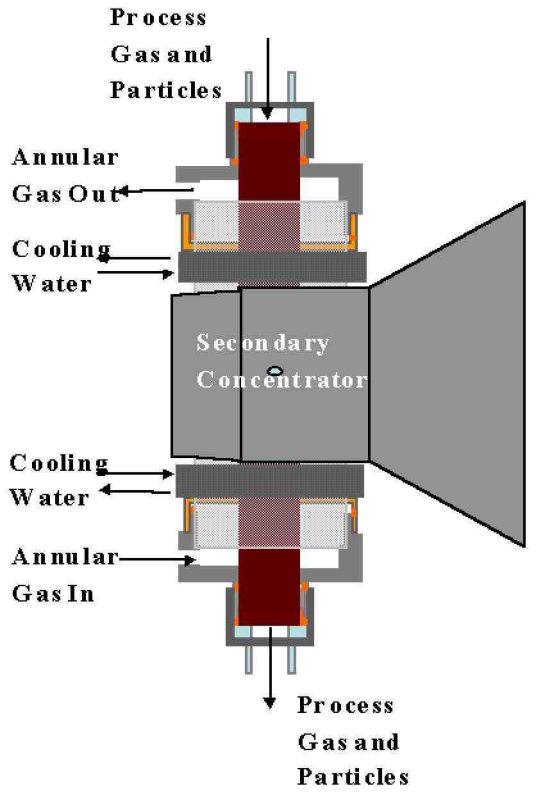

Figure 2. Solar-Thermal Aerosol Reactor (Top) Schematic, (Bottom) Installed

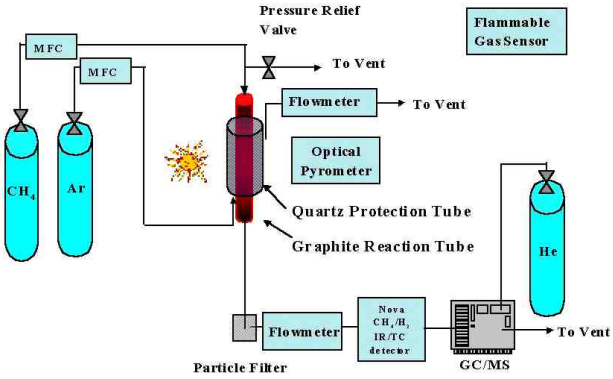

Figure 3. Schematic of Solar-Thermal Pilot Facility Interfaced to HFSF at NREL (Golden, CO)

The graphite and quartz design allows for on/off processing without thermal expansion or stress difficulties. The graphite reaction tube can be heated to reaction temperatures in a matter of seconds. A schematic of the reactor system and a photograph of the reactor that was taken after the system had been heated are shown in Figure 2. An overall pilot system schematic is shown in Figure 3.

Four process scenarios were considered for plant design/profitability studies and environmental impact: (1) a large scale plant where H_2 is being sent to a pipeline and carbon black is being sold, (2) a distributed industrial plant to supply H_2 to a semi-conductor processing facility in AZ, (3) a medium sized distributed plant where H_2 is used to fill fuel cell vehicles, and (4) a large scale utility co-generation facility where H_2 is being supplied to a pipeline and carbon black is being fed to a carbon conversion fuel cell to supply electricity to the grid.

Results

The process has been operated at temperatures as high as 2100^{o}K for high power levels (8.5 kW) and gas flows of 5 standard liters per minute (slpm). However, typical operating temperatures are in the range of 1700 to 1900^{o}K. The effect of varying the annular flow rate was examined during experiments. It was found that an increase in the argon flow rate between the quartz and solid graphite tube of from 7 to 10 slpm at high power levels had little effect on the gas phase temperature. A greater effect is seen at lower power levels, such as 2.5 kW. In general, the

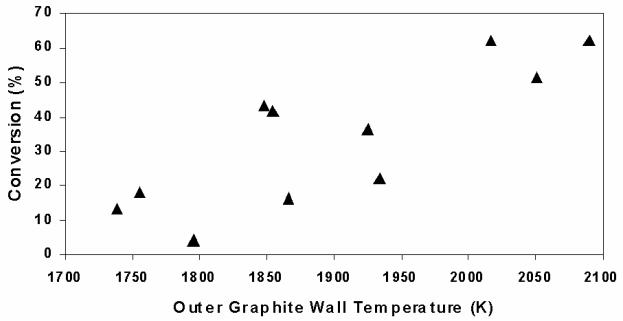

Figure 4. Experimental Dissociation Results (t = 0.01 to 0.02 sec)

amount of gas flowed between the quartz tube and the outer solid graphite tube will be very small and only enough to prevent deposition of any volatiles along the inside quartz wall.

Various experiments were run to determine the effect of temperature and residence time on conversion. In all cases, pure methane was fed to the reactor. As can be seen in Figure 4, conversions exceeding 60% have been obtained at 2000°K for residence times on the order of 0.01 second and with no co-fed carbon black to improve reactor heating. It should be noted that complete dissociation is expected at these temperatures and that the conversion was limited by heat transfer. Future experiments will include the co-feeding of fine carbon black particles to act as radiation absorbers for heating the gas. Math modeling has indicated that the co-feeding of carbon black particles has a substantial effect on the overall process throughput and reactor performance.

The quality of the carbon black powder (Figure 6) product was evaluated as it impacts the overall economics of the process. A transmission electron photomicrograh (TEM) of a carbon black powder produced at a power level of 8.5 kW (~ 2000°K) indicates a primary particle size of between 20 and 40 nanometers. In addition, the solar-thermally produced carbon black is compared to Shawinigan™ carbon black (tradename of Chevron-Phillips Corp.), the high quality world standard specialty carbon black. A comparative TEM image indicates that the carbon particles being formed have a similar chain-like structure as compared to the Shawinigan™ black. An X-ray diffraction pattern of the carbon

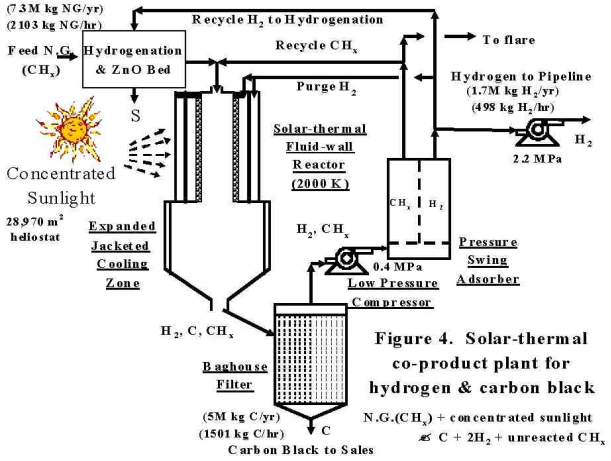

Figure 5. Solar-Thermal Co-product Plant for Hydrogen and Carbon Black

black and the TEM indicate that the solar-thermally produced carbon black is amorphous and has similar or reduced crystallinity compared to the Shawinigan™ black..

The solar-thermal process (Figure 5) for co-producing hydrogen (1670 t/yr [tonnes/year]) and carbon black (5000 t/yr) has been conceptualized and costed (± 30%; percentage of delivered equipment cost). The 16.6 Mega-Watt thermal plant has been designed for the Phoenix, AZ (USA) area (0.38 solar capacity factor). Produced carbon black will be sold into the carbon black market (world market is 7.9 M metric tonnes (t)/yr), and produced hydrogen will be supplied to a hydrogen pipeline at a pressure of 2.2 MPa. The plant will dissociate 7300 t/yr of natural gas (NG). The reactor is sized from the kinetics rate expression developed by Dahl et al [4].

The process has been simulated and priced using base cases from Spath and Amos [3] and appropriate scale factors. The selling price of H_2 is determined to be $13.80/GJ to achieve a 15% IRR when carbon black is sold at $0.66/kg. For a carbon black selling price of $0.80/kg, the price of H_2 to achieve the 15% IRR drops to $10/GJ. For a carbon black selling price of $1.10/kg, the price of the H_2 to achieve the 15% IRR drops to $5/GJ. It is important to note that most specialty carbon blacks sell for between $2 and $3.50/kg. The world market for these specialty blacks is 0.6 mega-t/yr. Hence, the 5000 t carbon black/yr co-product plant described here is 0.8% of

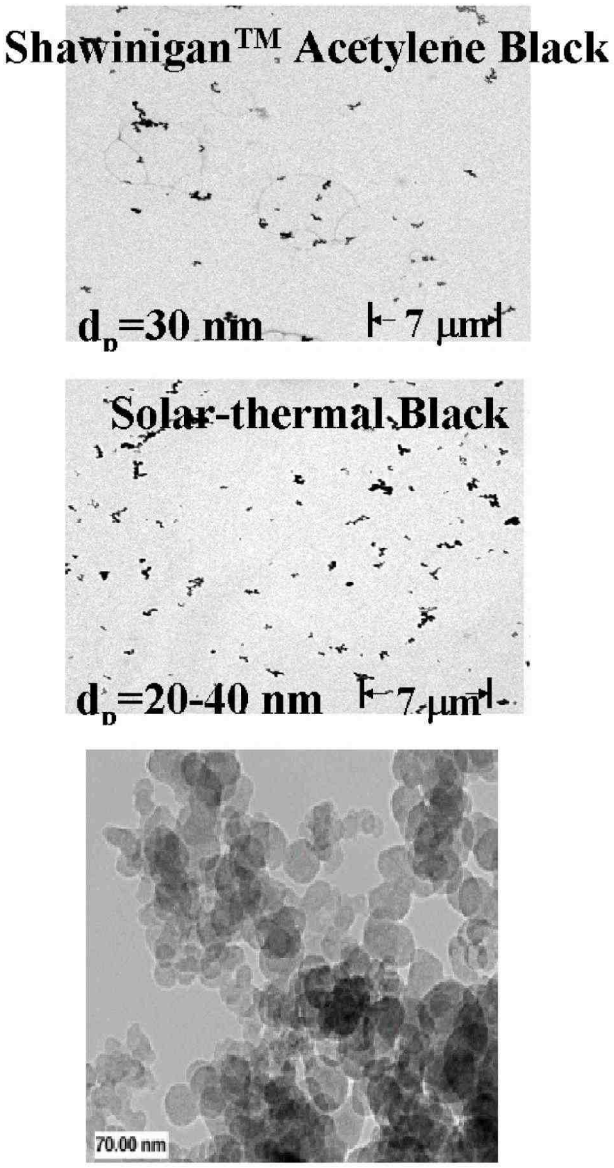

Figure 6. Comparison of Solar-Thermal Carbon Black with Commercial High Quality Standard (Chevron-Phillips Shawinigan Black™)

the world market for specialty blacks. The process has a 3rd year return on investment of 16% and a payback period of 6 years.

For the process scenario discussed, the solar-thermal process avoids 277 MJ fossil fuel and 13.9 kg-equivalent CO_2/kg H_2 produced as compared to conventional steam-methane reforming and furnace black processing.

Conclusions

The solar-thermal process is feasible: there are no technical show stoppers and there are no materials concerns. The fluid-wall reactor design allows continuous operation without inside wall deposition of carbon black. Reaction rates at the demonstrated ultra-high temperatures are enormous.

The solar-thermal process is environmentally friendly. The most environmentally friendly option is when selling carbon black into the tire carbon black market as the energy and pollution associated with normal carbon black production are avoided. If carbon is fed to a carbon conversion fuel cell, the total green house gas emissions are still ~ 60% of those of a steam reformer and the bulk of the released CO_2 is in a pure form so it can be easily sequestered.

The process is potentially economical in the desert southwest United States. However, an outlet for the carbon black is an integral part of the overall economics. Compared to photovoltaic conversion and electrolysis of water to produce H_2, the solar-thermal process requires ~ 40 times less heliostat surface, and the heliostats are lower cost mirrors rather than expensive photovoltaic cells. The solar-thermal process can produce HCNG at high rates in one step by efficiently and cleanly removing carbon from fed NG.

References

1. Cooper JF, Cherepy N, Berry G, Pasternak A, Surles T, Steinberg, M. Direct carbon conversion: Application to the efficient conversion of fossil fuels to electricity. Report no. UCRL-JC-140629. Lawrence Livermore National Laboratory: Livermore, CA, October 2000.

2. Lewandowski A. Performance characterization of the SERI high-flux solar furnace. Solar Energy Materials 1991; 24: 550-563.

3. Spath PL, Amos WA. Assessment of natural gas splitting with a concentrating solar reactor for hydrogen production, report no. NREL/TP-510-31949. National Renewable Energy Laboratory: Golden, CO, April 2002.

4. Dahl JK, Barocas VH, Clough DE, Weimer AW. Intrinsic kinetics for rapid decomposition of methane in an aerosol flow reactor. International Journal of Hydrogen Energy 2002; 27: 377-386.

FY 2002 Publications/Presentations

1. Dahl, JK, Barocas, VH, Clough, DE, Weimer, AW, "Intrinsic kinetics for rapid decomposition of methane in an aerosol flow reactor," International Journal of Hydrogen Energy 2002; 27: 377-386.

2. Dahl, JK, Tamburini, J, Weimer, AW, Lewandowski, A, Pitts, R, and Bingham, C, "Solar-thermal Processing of Methane to Produce Hydrogen and Syngas," Energy and Fuels, 15, 1227-1232 (2001).

3. Buechler, KJ, "Synthesis of Hydrogen through Solar-thermal Decomposition of Natural Gas," paper presented at the 2001 Annual Meeting of the American Institute of Chemical Engineers, November 6, 2001 (Reno).

4. Weimer, AW, "Ushering in the Hydrogen Economy," paper presented at the Center of the American West Program "Energy in the West: What Every Westerner Should Know", June 22, 2002 (Boulder).

5. Dahl, JK, "Solar-thermal Dissociation of Methane in an Aerosol Flow Reactor," paper presented at the Fourth World Congress on Particle Technology," Sydney, Australia, July 25, 2002 (Boulder).

6. Weimer, AW, "Solar-thermal Process for Rapid Natural Gas Dissociation," presented to the Department of Chemical Engineering - Graduate Seminar, University of Maryland (October, 2001).

7. Weimer, AW, "Rapid Process for the Benign Synthesis of Hydrogen," presented to the Department of Chemical Engineering - Graduate Seminar, Colorado School of Mines and Technology (November, 2001).

8. Weimer, AW, "Benign Hydrogen Synthesis Using Rapid Solar-thermal Processing of Natural Gas," paper presented at the 14th World Hydrogen Energy Conference, Montreal, Ontario, Canada (June 12, 2002).

9. Weimer, AW, "Distributed Hydrogen by Rapid Solar-thermal Dissociation of Methane," paper to be presented at the 224th American Chemical Society Meeting, Boston, MA (August 21, 2002).

10. Weimer, AW, "Rapid Solar-thermal Dissociation of Natural Gas," paper to be presented at the 11th International Symposium on Concentrated Solar Power and Chemical Energy Technologies, Zurich, Switzerland (September 5, 2002).

11. Dahl, JK, "Production of Hydrogen Using a Solar-thermal Fluid-wall Reactor," paper to be presented at the 2002 Annual Meeting of the American Institute of Chemical Engineers," Indianapolis, IN (November, 2002).

12. Weimer, AW and Lewandowski, S, "Thermal Dissociation of Methane Using a Solar-coupled Aerosol Flow Reactor," U.S. Department of Energy Hydrogen Program Review Presentation, Golden, CO (May 7, 2002).

FY 2002 Patent Applications

1. "Solar-thermal Aerosol Flow Reaction Process," International PCT Application Number PCT/US 01/15160 (filed February 12, 2002, priority date May 8, 2001).

2. "Solar-thermal Fluid-wall Reaction Processing," Provisional Patent Application filed March 7, 2002.

II.C.3 Thermocatalytic CO_2-Free Production of Hydrogen From Hydrocarbon Fuels

Nazim Muradov (Primary Contact)
Florida Solar Energy Center
1679 Clearlake Road, Cocoa, Florida 32922
(321) 638-1448, fax: (321) 638-1010, e-mail: muradov@fsec.ucf.edu

DOE Technology Development Manager: Peter Devlin
(202) 586-4905, fax: (202) 586-9811, e-mail: Peter.Devlin@ee.doe.gov

Objectives

- Develop an economically viable thermocatalytic process for production of hydrogen (H_2) and value-added carbon products from hydrocarbon fuels
- Obviate the concurrent production of carbon monoxide/carbon dioxide (CO/CO_2) byproducts and drastically reduce (preferably, eliminate) greenhouse gas emissions from the process
- Improve the process efficiency and reduce the cost of hydrogen production

Approach

- Investigate CO/CO_2-free production of hydrogen and carbon products via efficient thermocatalytic decomposition of hydrocarbon feedstocks over carbon-based catalysts in an air/water-free environment
- Improve the process efficiency and sustainability via in-situ generation of catalytically active carbon particulates
- Design, fabricate and test a bench-scale thermocatalytic reactor for CO/CO_2-free production of hydrogen-rich gas and carbon products
- Determine the effect of heavy hydrocarbons, moisture and sulfur compounds present in commercial hydrocarbon fuels on the process efficiency and the catalyst activity/stability
- Characterize carbon products of the process and evaluate their application areas and market value

Accomplishments

- Developed new approaches to improving the catalyst long-term stability and process sustainability
- Determined the effect of heavy hydrocarbons, moisture and H_2S present in commercial hydrocarbon feedstocks on the process efficiency and the catalyst activity and stability
- Designed, fabricated and operated a bench scale thermocatalytic reactor (TCR); demonstrated CO/CO_2-free production of hydrogen-rich gas with H_2 concentration up to 80 v.%
- Tested TCR in combination with a proton exchange membrane (PEM) fuel cell
- Analyzed carbon products of the process using a number of material characterization methods; assessed potential markets for carbon products (in collaboration with industry)
- Conducted techno-economic analysis of thermocatalytic decomposition of natural gas (in cooperation with the National Renewable Energy Laboratory [NREL])

Future Directions

- Fabricate and operate the scaled-up (up to 5 kW) multi-fuel thermocatalytic reactor coupled with a gas clean-up system using commercial hydrocarbon fuels.
- Reduce the amount of greenhouse gas emissions via optimization of the thermocatalytic process and utilization of carbon materials produced in the process
- Increase the yield of high-value carbon products and reduce the cost of hydrogen production
- Address safety and reliability issues related to the operation of the thermocatalytic reactor
- Evaluate new application areas for carbon products (with industrial partners)

Introduction

Thermocatalytic decomposition (TCD) of methane (CH_4) results in the formation of hydrogen (H_2) and elemental carbon:

$$CH_4 \rightarrow C + 2H_2 \qquad \Delta H^o = 75.6 \text{ kJ/mol } (CH_4)$$

The energy input requirements for TCD are significantly less than that of steam methane reforming (37.8 and 63.3 kJ/mol H_2, respectively). Due to the absence of oxidants (e.g., H_2O and/or O_2), no carbon oxides are formed in the reaction. The choice of an efficient and durable methane decomposition catalyst is vital for the development of a TCD process. Two major problems associated with existing catalysts relate to their rapid deactivation (due to carbon deposition) and co-production of large amounts of CO_2 during the catalyst regeneration step. The successful development of efficient and stable carbon-based catalysts for a methane decomposition process can solve both the catalyst deactivation and CO_2 emission problems.

Approach

The approach is based on thermocatalytic decomposition of hydrocarbon fuels over carbon-based catalysts in an air/water-free environment. The important feature of the process is that the reaction is catalyzed by carbon particulates produced in the process, so no external catalyst is required (except for the start-up operation). This results in the following advantages: (1) no CO/CO_2 byproducts are generated during the hydrocarbon decomposition stage, (2) no catalyst regeneration is required, (3) the catalyst is resistant to sulfur poisoning, (4) several valuable forms of carbon can be produced in the process, (5) overall CO_2 emissions could be drastically reduced (compared to conventional processes).

Results

Improvement in Catalyst Stability and Process Sustainability. The following new approaches to improving the catalyst long-term stability and the process sustainability have been developed: (i) the in-situ generation of catalytically active carbon species produced by co-decomposition of hydrocarbons, and (ii) activation of carbon catalysts via surface treatment with activating agents. The treatment of carbon particles with steam and CO_2 (outside the pyrolysis zone) resulted in a significant increase in methane decomposition rate (Figure 1).

Effect of Moisture and Sulfur on Methane Decomposition Rate. The presence of small amounts of moisture and H_2S (<3 v.%) in the hydrocarbon feedstock is not detrimental to the process efficiency. However, these impurities result in contamination of hydrogen with carbon oxides and H_2S, which could be removed from the product gas using methanation and H_2S scrubbing steps, respectively. Figure 2 demonstrates the removal of carbon oxides from hydrogen-rich gas via methanation reactions using Ru-catalyst.

Fabrication and Testing of Thermocatalytic Reactor. A bench-scale thermocatalytic reactor (TCR) for CO/CO_2-free production of hydrogen-rich gases was designed, fabricated and operated using methane or propane as feedstocks (Figure 3). The concentration of hydrogen in the hydrogen-containing gas reached up to 80 v.% (the balance methane). Since no carbon oxides were detected in the hydrogen gas, it was directly fed to a PEM fuel cell.

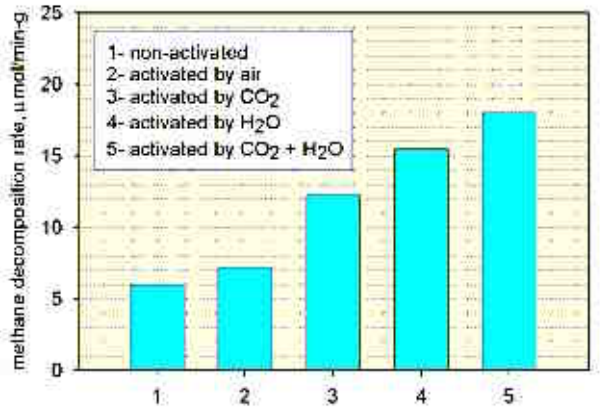

Figure 1. Effect of Carbon Catalyst Activation on Methane Decomposition Rate at 850°

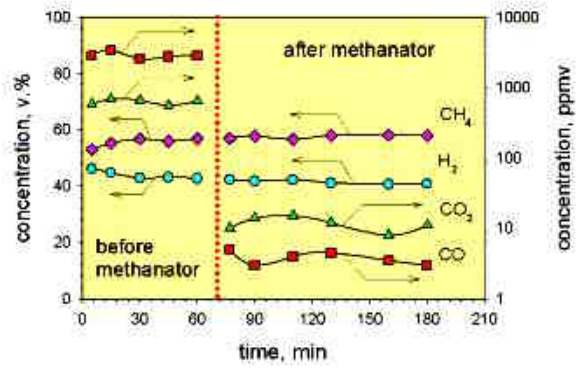

Figure 2. Removal of CO and CO_2 from H_2-CH_4 Stream via Methanation Reaction at 350°C

Structural and Surface Characterization of Carbon Products. Carbon products of the process were analyzed by a number of material characterization techniques, including x-ray diffraction, scanning electron microscopy, Auger electron spectroscopy, x-ray photoelectron spectroscopy, and others. X-ray diffraction studies revealed an ordered graphite-like (or turbostratic) structure of carbon products (Figure 4).

Techno-economic Evaluation of Hydrogen Production by Thermocatalytic Decomposition of Natural Gas. Techno-economic analysis of hydrogen production by thermocatalytic decomposition of natural gas was conducted in cooperation with

Figure 3. Experimental Set-Up with TCR, PEM Fuel Cell, Fuel Tank, and Testing Equipment

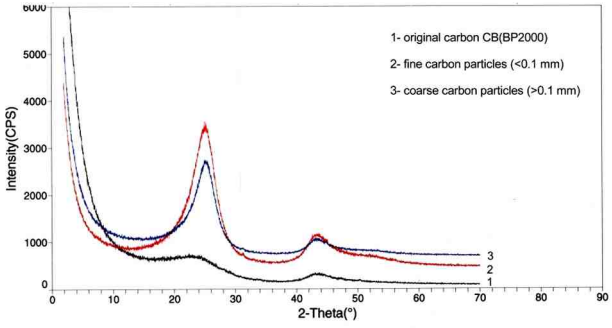

Figure 4. X-ray Diffraction Spectra of Carbon Particles Produced by C_3H_8 Decomposition Over CB(BP2000)

NREL. The hydrogen selling price varied in the range of $7-21/GJ (giga-Joule) depending on the cost of natural gas and carbon selling price.

Conclusions

New methods for improving the sustainability of the methane thermocatalytic decomposition process have been developed. Studies indicate that the presence of small amounts of moisture and H_2S (<3 v.%) in the hydrocarbon feedstock is not detrimental for the catalyst activity and process efficiency. This implies that commercial hydrocarbon fuels could potentially be employed as feedstocks for the process. A bench-scale thermocatalytic reactor was designed, fabricated and operated using methane and propane as feedstocks. The TCR produced hydrogen-rich gas free of CO/CO_2 impurities; the gas was directly fed to PEM fuel cell. Material characterization studies indicated that depending on operational conditions, carbon could be produced in several valuable forms including turbostratic carbon, pyrolytic graphite, spherical carbon particles, or filamentous carbon.

FY 2002 Publications/Presentations

1. Muradov, N. "Low-emission Fuel Reformers for Fuel Cell Applications", 14th World Hydrogen Energy Conference, Montreal, Canada, 2002.

2. Muradov, N. "Thermocatalytic CO_2-free Production of Hydrogen from Hydrocarbon Fuels", DOE Annual Hydrogen Program Review Meeting, Golden, CO, 2002.

3. Muradov, N. and Schwitter, A. "Formation of Conical Carbon Structures on Vapor-grown Carbon Filaments", Nano Letters, v.2, 673 (2002).

4. Muradov, N. "Emission-free Fuel Reformers for Fuel Cell Applications", Fuel Cells, Science and Technology 2002, Amsterdam, Netherlands, 2002.

5. Muradov, N. "Hydrogen via Methane Decomposition: an Application for Decarbonization of Fossil Fuels", Intern. Journal Hydrogen Energy, v.26, 1165 (2001).

6. Muradov, N. "Catalysis of Methane Decomposition over Elemental Carbon", Catalysis Communications, No.2, 89 (2001).

7. Muradov, N. "Thermocatalytic Production of Hydrogen via Pyrolysis of Hydrocarbon Fuels: from Methane to Residual Oil", Amer. Chem. Soc. Symposium: Energy for 21st Century: Hydrogen Energy, San Diego, 2001.

8. Muradov, N. "Thermocatalytic CO_2-free Production of Hydrogen from Hydrocarbon Fuels", DOE Annual Hydrogen Program Review Meeting, Baltimore, MD, 2001.

Special Recognitions & Awards/Patents Issued

1. Muradov, N. U.S. Patent Application No. 60/194,828 (2001) "Thermocatalytic Process for CO_2-free Production of Hydrogen and Carbon from Hydrocarbons".

2. Muradov, N. U.S. Patent Application No. 60/203,370 (2001) "Portable Hydrogen Generator".

3. Muradov, N. U.S. Patent Application No. 60/346,548 (2002) "A Method and Apparatus for Production of 3D Carbon Fibers".

II.C.4 Novel Catalytic Fuel Processing Using Micro-Channel Steam Reforming and Advanced Separations Technology

Patricia Irving (Primary Contact), Quentin Ming, Lloyd Allen, Todd Healey, and Andrew Lee
InnovaTek, Inc.
350 Hills Street
Richland, WA 99352
(509) 375-1093, fax: (509) 375-5183, e-mail: Irving@tekkie.com

DOE Technology Development Manager: Peter Devlin
(202) 586-4905, fax: (202) 586-9811, e-mail: Peter.Devlin@ee.doe.gov

Objectives

The goal of this project is to produce pure hydrogen from infrastructure fuels using cost-competitive, highly efficient catalytic steam reforming and membrane separation technology. The following objectives are identified to achieve this goal.

- Optimize InnovaTek's proprietary steam reforming catalyst composition and evaluate reforming conditions for diesel fuel and natural gas.
- Optimize the hydrogen-permeable membrane composition and operating procedures, and compare to water gas shift approach for CO clean-up.
- Develop efficient thermal management using microchannel heat exchangers and an internal burner.
- Integrate processes and components to achieve smallest size and most efficient thermal management.

Approach

- Conduct system analysis and design specification.
- Design and develop components.
- Test components.
- Design process configurations.
- Evaluate configurations with model simulation.
- Predict component and operational requirements with model simulation.
- Conduct iterative testing of integrated system.

Accomplishments

- Developed process model and used output to help size system components and select range for operating conditions.
- Developed sulfur-tolerant steam reforming catalyst that reforms current hydrocarbon fuels without the need for prior sulfur removal.
- Designed and tested advanced membrane technology that separates pure hydrogen from reformate, thereby enabling higher fuel cell power densities and eliminating potential for electrode poisoning.
- Utilized micro technology for reactor, heat exchanger, and fuel vaporizer to improve system efficiency through optimized thermal management and fluid dynamics.
- Completed a successful 500-hour demonstration of natural gas steam reforming and an 80-hour test of diesel fuel reforming.

Future Directions

- Scale up to at least 60 LPM hydrogen output – enough for a 5 kWe fuel cell.
- Complete micro-channel implementation.
- Automate start-up, operation, shut-down.
- Achieve more complete thermal integration.
- Focus on manufacturability, cost-reduction and high-volume production.
- Achieve full integration with at least one fuel cell model.
- Conduct thorough reliability testing.
- Incorporate enhanced controls – off-site monitoring, data mining, self-diagnostics.
- Complete documentation – drawings, bills of material, manufacturing routers.
- Prepare tooling – dies, molds, computer aided machining (CAM) programming etc.
- Obtain agency approval – Underwriters Laboratory, Canadian Standards Association, Consumer Electronics, etc.

Introduction

To be marketable now, fuel cells need to use primary fuel sources from existing production and distribution networks – i.e. natural gas, gasoline, diesel or jet fuels.

Fossil fuel-powered fuel cells or refueling stations can form the bridge to a future when renewable resources power fuel cells. When compared to compressed hydrogen, reformed hydrocarbon fuels offer a significant cost advantage in the delivery of power. The high energy density of these fuels will also contribute to increased run times per unit of fuel consumed, and size and weight reductions associated with fuel storage.

To meet this need, InnovaTek is integrating microreactor technology with advanced sulfur-tolerant catalysts and hydrogen membrane technology to create a fuel processor for hydrogen generation from hydrocarbons. The ultimate goal of this 4-year cooperative project is the development of a catalytic reactor heated by the combustion of membrane by-products (raffinate) for production of clean hydrogen by steam reforming hydrocarbon fuels, including fuels that contain sulfur. Advanced membrane technology is being used to remove CO and CO_2 from the reformate. The fuel processor being developed will provide a pure output stream of hydrogen that can be used without further purification for electrical generation by a PEM fuel cell.

Approach

Process simulation and analysis was performed for all possible system configurations to obtain an optimal system design and a complete mass and energy balance for every individual component of the system. These include flow rates, flow compositions, and temperatures for every stream in the system. The information provided a solid foundation for the design, fabrication, and testing of the reactor, heat exchangers, and combustor. The information will also guide us during the integration and demonstration of the complete system throughout the entire project period.

Proprietary components were designed and developed to achieve a technically superior fuel processor by solving specific problems related to several of the fundamental processes associated with fuel processing. These components will comprise a more efficient system that is sulfur tolerant and produces pure hydrogen while remaining compact and lightweight.

The individual components have been tested, and results of key tests are summarized below. The components are now being integrated into a bench-top system that will undergo additional testing, culminating in a prototype demonstration in late 2002 that produces 12 LPM of pure hydrogen, enough to power a 1 kWe fuel cell.

Results

The design and optimization of a fuel processing system is complex because of the number of required components and functions (Figure 1). The first step in developing an optimal system design is evaluating different process configurations using process simulation. Another objective is to develop the specifications for the design of the components used in the system. Special attention is paid to thermal management and water management, two of the most technically challenging issues of effective system operation and integration.

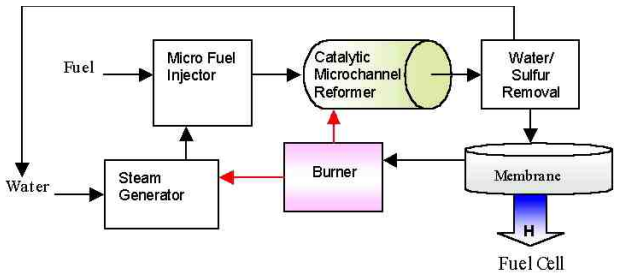

Figure 1. Flow Diagram of Major Fuel Processor System Components

A system process model was developed and used to track mass and enthalpy flows. Estimates of molar flows of reforming products were determined by solving for equilibrium concentrations at given temperatures and pressures. Thermodynamic properties were used to determine heat transfer, water removal, and air and heat required to achieve energy balance in the reforming reactor. A non-linear differential equation was used to determine membrane area for the desired hydrogen output at various temperatures and pressures. Model output helped determine the size of system components and select the range for operating conditions.

System components were designed, fabricated, tested, and optimized in an iterative process. Primary system components and their functions are listed in Table 1. Each component was tested, redesigned, and tested again until optimum geometries and formulations were determined. Then the components were integrated step by step and tested again. Complete system testing is now underway.

Component	Function	Product
catalytic reactor	catalytically reforms fossil fuels	Reformate (H, CO_2, CO)
catalyst	catalyzes the reforming reaction	reformate
combustor	burns raffinate to provide heat for the reforming reaction	Heat, CO_2, H_2O
fuel injector	injects and mixes fuel and steam into the reactor	Vaporized steam/fuel mixture
heat exchangers	provides the proper temperature for each component	Warmer or cooler gas streams
H-permeable membrane	converts reformate to pure hydrogen and produces raffinate (membrane reject stream) for combustor	Pure hydrogen, raffinate (H, CO_2, CO)

Table 1. Primary Components of InnovaTek's Fuel Processor

Initial tests were conducted to investigate the effect of reaction temperature on conversion and product gas composition using our proprietary catalyst ITC-3. Additional testing was conducted to optimize the catalyst for specific fuel types. After catalyst optimization, long-term tests for reforming natural gas were successfully conducted using InnovaTek's proprietary catalyst ITC #1148 (Figure 2). The hydrogen concentration in the reformate product was over 74% on a dry basis. CO and CO_2 concentrations were about 19% and 6%, respectively. No methane was detected, indicating 100% conversion during the entire testing period. The test was continuously conducted for 341 hours at the same conditions with the catalyst showing very high and stable activity. The reactor temperature was then set to 800°C and the tests were continued for another 100 hours with very stable performance. These results indicate that our catalyst composition has great potential for stable hydrogen generation from natural gas.

An 80-hour test with ultra-low sulfur (~5 ppm) diesel, a developmental product obtained from Chevron Phillips Chemical, was also successfully completed (Figure 3). The use of this product permits

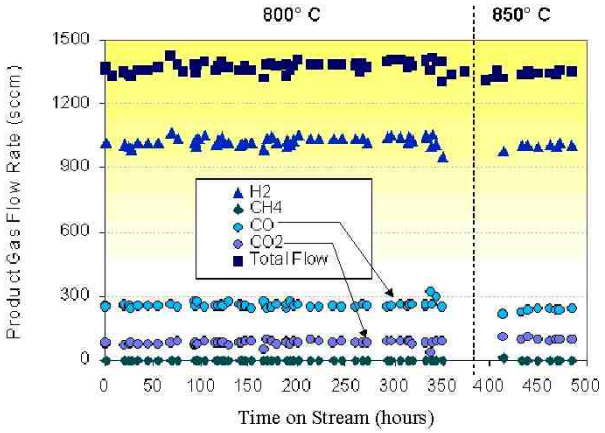

Figure 2. Steam Reforming of Natural Gas Using InnovaTek's Proprietary Catalyst, ITC-1145

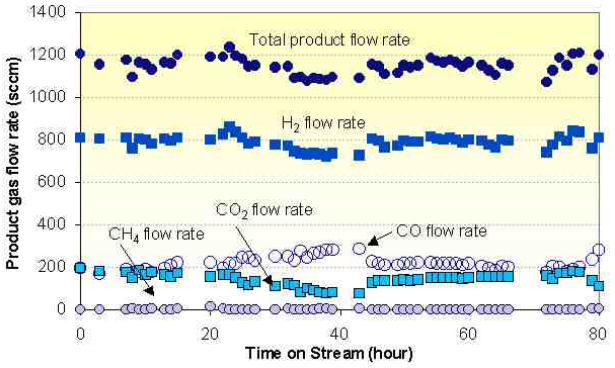

Figure 3. Steam Reforming of Low-Sulfur Diesel Fuel Using InnovaTek's Proprietary Catalyst

us to add controlled amounts of sulfur for testing sulfur tolerance. In an 8-hour test using this fuel with 100 ppm sulfur added, the catalyst had a 100% conversion rate. These test results indicate that our ITC catalyst #1145 has very high catalytic activity and selectivity to hydrogen production and tolerates the presence of sulfur in the fuel.

A radial concept is used for the integration of the combustor and catalytic reactor where concentric functional chambers build outward from a central core (Figure 4). The innermost sections comprise the combustor unit, where air is carried to the interior and raffinate gas from the membrane penetrates through the wall to form a combustion flame along the inner wall of the reaction chamber. Preheated and mixed steam and fuel enter the reaction chamber and are catalytically converted to reformate. Reformate exits the reactor and is then sent to the

Figure 4. Photo of InnovaTek's Steam Reformer with Integrated Raffinate Combustor

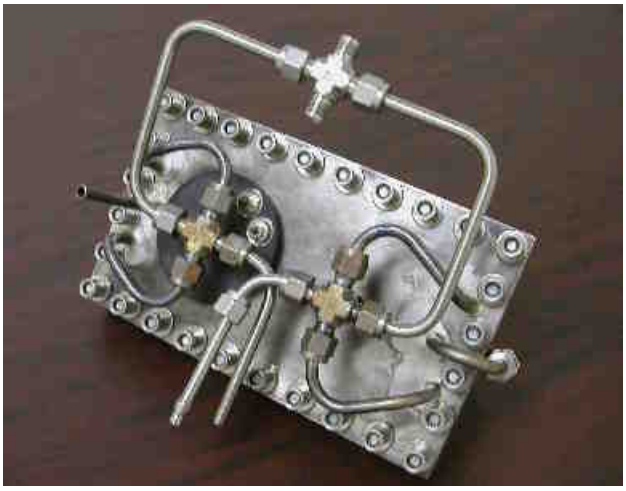

Figure 5. Photo of InnovaTek's Hydrogen-Permeable Membrane Component

membrane, where pure hydrogen is separated. Exhaust gas from the combustion chamber is carried back so that the hot gas passes over the outside of the reaction chamber, thereby providing uniform thermal conditions. This reactor, which is about 12 inches long, has a capacity for producing enough hydrogen for a 1 kWe fuel cell. It is currently being used for integrated system testing.

For purification of the reformate, hydrogen-permeable membranes were constructed using a flat-plate design that encased ultra-thin metal foils that are permeable only to hydrogen (Figure 5). InnovaTek is investigating several formulations of metal for these membranes, including sulfur-tolerant membranes. We were successful in producing several membrane prototypes for a range of hydrogen production rates. Work on membrane optimization is continuing as we examine variables such as pressure, temperature, and sulfur content of the reformate. One important finding is that hydrogen permeation

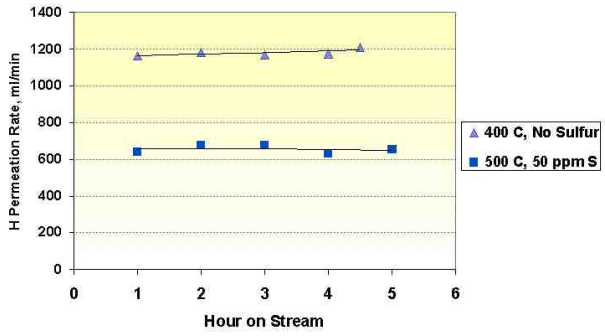

Figure 6. Hydrogen Permeation Rate through InnovaTek's S-Tolerant Membrane as a Function of Temperature and Sulfur Content

rate is reduced and higher membrane temperatures are required for processing sulfur-containing fuels (Figure 6). The membrane component has been integrated with the catalytic reactor component and testing is underway.

Conclusions

- A proprietary sulfur-tolerant catalyst developed by InnovaTek can reform natural gas, gasoline, and diesel fuels without need for prior sulfur removal, thereby greatly improving the prospects for commercialization of fuel cell technology.
- Advanced membrane technology for hydrogen separation produces nearly pure hydrogen output from reformate gas, enabling higher fuel cell power densities and eliminating potential for electrode poisoning.
- The use of micro technology for reactor, heat exchanger, and fuel vaporizer components improves system efficiency through optimized thermal management and fluid dynamics.
- The use of steam reforming and membrane purification combined with tight thermal integration can result in a highly efficient fuel processor that, when combined with a fuel cell, will produce at least twice the energy of a combustion engine for a given amount of fuel.

FY 2002 Publications/Presentations

1. Ming, Q., Healey, T., Allen, L., and Irving, P., "Steam Reforming of Hydrocarbon Fuels". Catalysis Today, in press, 2002.

2. Irving, P., Allen, L., Herron, T., and Stephens, R., "Diesel Fuel Reforming with Advanced Separations Technology for the Production of Pure Hydrogen". Proceedings of the 3rd Department of Defense Logistic Fuel Reforming Conference. Panama City Beach, FL, August 27-28, 2002.

3. Irving, P. "Fuel Processor for Generating Pure Hydrogen for Fuel Cells from Sulfur-Containing Fuels". Proceedings of the 4th Annual Knowledge Foundation's International Symposium, Small Fuel Cells 2002. Washington D.C., April 21-23, 2002.

Special Recognitions & Awards/Patents Issued

1. Hydrocarbon Fuel Reforming Catalyst and Use Thereof. U.S Non-Provisional Patent Application, Q. Ming, T. Healey, and P. Irving, pending.

II.C.5 ITM Syngas and ITM H_2: Engineering Development of Ceramic Membrane Reactor Systems for Converting Natural Gas to Hydrogen and Synthesis Gas for Liquid Transportation Fuels

Christopher M. Chen (Primary Contact), Michael F. Carolan, Steven W. Rynders
Air Products and Chemicals, Inc.
7201 Hamilton Boulevard
Allentown, PA 18195
(610) 481-3315, fax: (610) 706-6586, e-mail: chencm@apci.com

DOE Technology Deveopment Manager: Arlene Anderson
(202) 586- 3818, fax: (202) 586- 9234, e-mail: Arlene.Anderson@ee.doe.gov

Main Subcontractor: Air Products and Chemicals, Inc., Allentown, PA; Ceramatec, Inc. Salt Lake City, UT; ChevronTexaco, Richmond, CA; Eltron Research Inc., Boulder, CO; McDermott Technology Inc., Alliance, OH; Norsk Hydro, Oslo, Norway; Pacific Northwest National Laboratory, Richland, WA; Pennslyvania State University, University Park, PA; University of Alaska Fairbanks, Fairbanks, AK; University of Pennsylvania, Philadelphia, PA

Objectives

- Research, develop and demonstrate ion transport membrane (ITM) Syngas/ITM H_2 ceramic membrane reactor system for the low-cost conversion of natural gas to hydrogen and synthesis gas
- Scale-up the ITM Syngas/ITM H_2 reactor technology through three levels of pilot-scale testing and precommercial demonstration
- Obtain the technical, engineering, operating and economic data necessary for the final step to full commercialization of the ITM Syngas/ITM H_2 technologies

Approach

- This project is in Phase 2 of three phases. The approach in Phase 2 includes:
- Task 2.1 Commercial Plant Economic Evaluation
- Task 2.2 Materials and Seals Development and Evaluation
- Task 2.3 ITM Syngas/ITM H_2 Membrane and Module Design and Fabrication
- Task 2.4 Nominal 24 thousand standard cubic feet per day gas flowrate (MSCFD) ITM Syngas/ITM H_2 Process Development Unit (PDU)
- Task 2.5 Nominal 330 MSCFD ITM Syngas/ITM H_2 Subscale Engineering Prototype

Accomplishments

- Process design and economic evaluation of a 760 million standard cubic feet per day gas flowrate (MMSCFD) H_2 plant with CO_2 separation to provide a carbon-free "clean fuel" showed the potential for over 30% capital cost savings in the syngas production step
- Multiple tests of lab-scale tubular membranes and seals each operated continuously for over 6 months at 250 psig and 825°C with good performance stability
- A number of sub-scale thin film membranes were tested for over 1200 hours; oxygen fluxes of over 10 sccm/cm^2 were recorded

- PDU module seals demonstrated good performance at 425 psig and 900°C under static conditions and pressure/thermal cycling conditions
- Pilot-scale membrane modules were fabricated for PDU tests
- The PDU reactor system was commissioned at high temperature and pressure with synthesis gas
- Initial scope definition of SEP project was completed with vendor quotes
- Design of full-scale membranes for SEP was completed
- SEP membrane fabrication development commenced with the fabrication of SEP membrane components

Future Directions

- Evaluate the ITM Syngas/ITM H_2 processes using PDU data
- Conduct long-term stability tests of tubular membranes and seals at high pressure
- Demonstrate performance of pilot-scale membrane modules in PDU
- Complete membrane module design and select catalysts for the SEP
- Commission the ceramic Production Development Facility and fabricate SEP membranes
- Design and fabricate the SEP reactor

Introduction

Ion Transport Membranes (ITMs) are a revolutionary platform technology for producing hydrogen and synthesis gas for applications in power generation, transportation fuels, and chemicals. The ITM Syngas and ITM H_2 processes provide a lower-cost method for converting natural gas to hydrogen and synthesis gas by combining air separation and natural gas partial oxidation in a single-step ceramic membrane reactor, with the potential for capital cost savings of over 30%. If successful, this technology could be important to emerging hydrogen markets, such as hydrogen-based fuel cells for transportation and large-scale centralized hydrogen production facilities with CO_2 capture.

The new technology utilizes non-porous ceramic ITM membranes, fabricated from multi-component metallic oxides that have both high electronic and oxygen ion conductivity at high temperatures (greater than approximately 700°C). In operation, oxygen from a hot air stream is reduced at one surface of the ITM membrane to oxygen ions, which diffuse through the membrane under a chemical potential gradient. At the opposite surface of the membrane, the oxygen partially oxidizes a pre-reformed mixture of hot natural gas and steam to form syngas, a mixture of hydrogen and carbon monoxide. The ratio of hydrogen to carbon monoxide is in part dependent upon the amount of steam. The membrane material must show long-term stability in reducing and oxidizing atmospheres, and long-term compatibility with any oxygen reduction and reforming catalysts that are in contact with its surface.

Approach

The objective of this project is to research, develop and demonstrate a novel ceramic membrane reactor system for the low-cost conversion of natural gas to hydrogen and synthesis gas: the ITM Syngas/ ITM H_2 processes. Through a 9½ year, three-phase program, the ITM Syngas/ITM H_2 technology will be developed and scaled up to obtain the technical, engineering, operating and economic data necessary for the final step to full commercialization of the hydrogen and syngas generation technologies. Phase 2 of the program was initiated in FY2000 and will extend for 4½ years. Process concepts and performance will be validated in two stages of scale-up in Phase 2: the Process Development Unit (PDU), which began operation in 2002, and the Subscale Engineering Prototype (SEP), which will begin operation in 2004.

In Task 2.1, "Commercial Plant Economic Evaluation," advanced ITM Syngas/ITM H_2 processes will be developed, and the economics of operation at the commercial plant scale will be evaluated based on the results of the Phase 2 program. In Task 2.2, "Materials and Seals Development and Evaluation," membrane materials and seals will be tested at the laboratory scale under ITM Syngas/ITM H_2 process conditions to obtain statistical performance and lifetime data. In Task 2.3, "ITM Syngas Membrane and Module Design and Fabrication," membrane reactors will be designed for the ITM Syngas/ITM H_2 processes at the PDU, SEP and commercial scales. Pilot-scale membrane modules will be fabricated for testing in the PDU. Fabrication of the membrane reactor modules will be scaled up in a Production Development Facility to supply the requirements of the SEP.

In Task 2.4, "Nominal 24 MSCFD ITM Syngas/ ITM H_2 PDU," the components of the ITM Syngas/ ITM H_2 technology will be demonstrated in a laboratory Process Development Unit (PDU). The PDU will operate at an equivalent of 24 MSCFD of syngas capacity, and will performance test pilot-scale planar membranes under commercial process conditions. In Task 2.5, "Nominal 330 MSCFD ITM Syngas/ITM H_2 SEP, "a Sub-Scale Engineering Prototype (SEP) unit will be built to demonstrate the ITM Syngas/ITM H_2 technology using full-size membranes in sub-scale modules. The SEP will demonstrate the operation of the ITM Syngas/ITM H_2 processes at up to an equivalent of 330 MSCFD of syngas capacity.

Results

As reported previously, preliminary process design and economic evaluation for ITM H_2 in the "Distributed H_2" target range of 0.1 to 1.0 MMSCFD H_2 indicated the potential for up to 27% savings in production costs compared with trucked-in liquid hydrogen for 5000 psig fuel cell vehicle refueling applications. In addition, economic evaluation of the ITM Syngas process producing about 150 MMSCFD of a 2:1 mixture of hydrogen and carbon monoxide confirmed the potential for >33% capital cost savings compared with conventional technology based on an autothermal reformer and cryogenic oxygen supply.

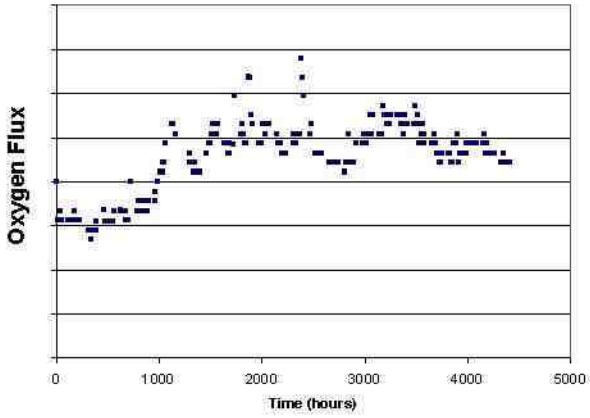

Figure 1. Six Month High Pressure Test of a Tubular Membrane

In an evaluation of advanced process concepts, the ITM H_2 process was developed for a large hydrogen production plant with CO_2 removal, producing 760 MMSCFD of fuel-grade hydrogen at 100 bar and 14,000 tonne/day of CO_2 at 80 bar for sequestration. For this application, the ITM H_2 process was compared to a conventional oxygen-blown Autothermal Reformer (ATR) with a cryogenic air separation unit to supply oxygen. Economic evaluation of the ITM H_2 process showed the potential for over 30% capital cost savings in the syngas generation process area and over 20% capital cost savings for the overall syngas/H_2/CO_2 production process. The ITM H_2 process also has a higher thermal efficiency of 74% compared to 71% for the oxygen-blown ATR process. The hydrogen product is a "clean" fuel suitable for centralized power generation (approximately 1300 MW) and for distribution to local stationary or mobile applications, including fuel cells.

Tubular membranes and seal assemblies were tested in high-pressure, high-temperature lab-scale units under ITM Syngas and ITM H_2 process conditions. In these tests, pre-reformed natural gas mixtures at process pressure were passed over the outer surface of the tubular membrane, while air at atmospheric pressure was fed to the inner surface of the tube. Multiple tests under ITM H_2 conditions each operated continuously for over 6 months at 250 psig and 825°C with good performance stability. The results of one of these six-month continuous tests are shown in Figure 1.

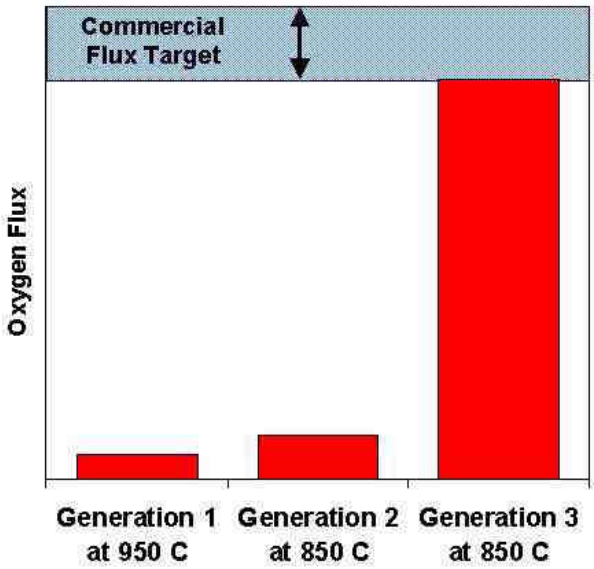

Figure 2. Advanced Catalyzed Membranes Approach Commercial Flux Target

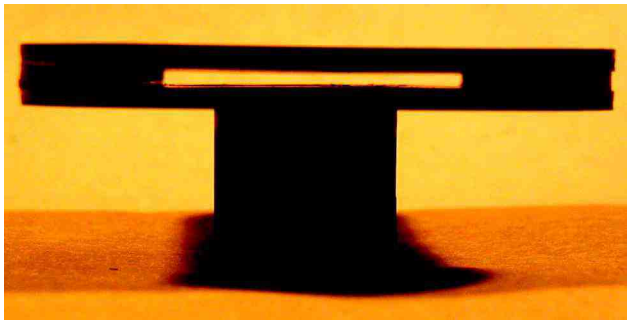

Figure 3. Process Development Unit Membrane Module

Sub-scale thin film membranes were also tested at atmospheric pressure for periods of over 1200 hours. Tests of advanced catalyzed membranes demonstrated oxygen fluxes that approach the commercial flux target range, as shown in Figure 2.

Pilot-scale PDU planar membrane modules were fabricated, an example is shown in Figure 3. Air at low pressure is passed through the inner support passages (not shown) constructed within the planar membrane, while the pre-reformed methane mixture is passed at high pressure over the surfaces of the membrane module, where partial oxidation takes place to produce syngas.

Figure 4. The ITM Syngas/ITM H_2 Process Development Unit

Installation of the PDU system was completed, and the PDU reactor system and PDU membrane modules were commissioned at high temperature and pressure with a syngas mixture. The PDU integrates the various components of the ITM Syngas/ITM H_2 reactor design and will be used to confirm the performance of the planar membrane modules and seals under commercial process conditions. The PDU reactor is shown in Figure 4.

The design of the full-scale membrane for the SEP was completed. SEP membrane fabrication development commenced with the fabrication of SEP membrane components. The rapid scale-up in in ceramic membranes is shown in Figure 5. Lab-scale membranes were developed in 1999-2000 in conjunction with initial materials development and were used to demonstrate oxygen separation performance. Pilot-scale membranes were developed in 2000-2001 and have a 40-fold increase in membrane area over the lab-scale membranes. The pilot-scale membranes are being used to demonstrate membrane performance at commercial process conditions in the PDU. Fabrication methods that were developed at the pilot scale are being scaled-up for full-size membranes. Full-size membranes are currently under development and have a 180-fold increase in membrane area over the lab-scale membranes.

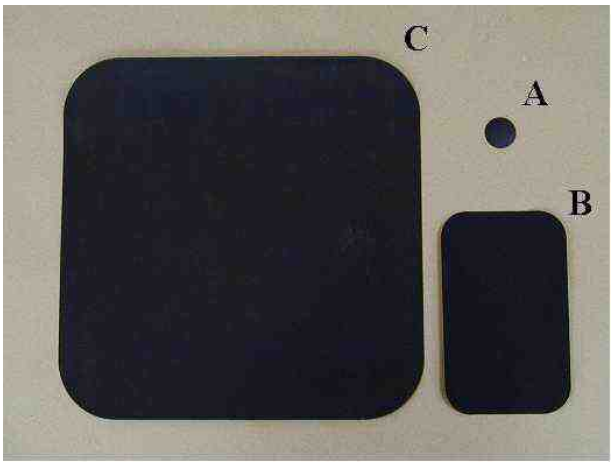

Figure 5. Scale-up of ITM Syngas/ITM H_2 Ceramic Membranes. (a) Lab-scale (b) Pilot-scale (c) Full-size

Initial scope definition of the SEP project was completed. Preliminary process flow diagrams were developed, and vendor quotes were received for major equipment items. In addition, preliminary design of the ITM Syngas/ITM H_2 SEP reactor was completed.

Conclusions

Significant progress has been made to develop the ITM Syngas/ITM H_2 technology. A database is being built up of performance data from several six-month long membrane tests. Membrane modules and seal assemblies have also been fabricated for testing in the PDU and ceramic fabrication scale-up is continuing the progression from lab-scale to full-size membranes. The PDU has been commissioned at high temperature and pressure. We continue to make excellent progress against the remaining technical challenges in the demonstration and scale-up of the ITM Syngas and ITM H_2 technology.

FY 2002 Publications/Presentations

1. C.M. Chen and P.N. Dyer, "Development of the ITM Syngas Process For GTL Conversion," American Chemical Society 222nd National Meeting, Ultra-Clean Transportation Fuels Symp., Chicago, IL, August 2001.
2. C.M. Chen, US DOE H2 Program Review, Golden CO, May 2002, "Engineering Development of Ceramic Membrane Reactor Systems for Converting Natural Gas to Hydrogen and Synthesis Gas for Liquid Transportation Fuels."

Patents Issued

1. US Patent 6214066, S. Nataraj, S.L. Russek, "Synthesis Gas Production by Ion Transport Membranes," April 2001.
2. US Patent 6302402, S.W. Rynders, E. Minford, R.E. Tressler, D.M. Taylor, "Compliant High Temperature Seals for Dissimilar Materials," October 2001.

II.C.6 Integrated Ceramic Membrane System for Hydrogen Production

Raymond F. Drnevich (Primary Contact), Minish M. Shah
Praxair, Inc.
P.O. Box 44
Tonawanda, NY 14151-0044
(716) 879-2595, fax: (716) 879-7091, e-mail: ray_drnevich@praxair.com

DOE Technology Development Manager: Arlene Anderson
(202) 586-3818, fax: (202) 586-923, e-mail: Arlene.Anderson@ee.doe.gov

Main Subcontractor: Argonne National Laboratory, Argonne, IL

Objectives

- Perform technoeconomic feasibility analysis of the integrated ceramic membrane system for hydrogen production.
- Define the development needed to prepare the concept for pilot testing and demonstration.

Approach

- Identify process options with potential for lower product costs.
- Evaluate performance of various process options by simulations.
- Carry out experiments to assess the performance of ceramic proton conducting membranes.
- Estimate capital and product costs.
- Select the process option that is most likely to be commercially viable.
- Identify development issues for the selected process option and prepare a development program for Phase II.

Accomplishments

- Two process options were identified: 1) Integrated oxygen transport membrane (OTM)-hydrogen transport membrane (HTM) reactor process that uses proton conducting ceramic membrane for hydrogen separation and 2) sequential OTM and HTM reactors process that uses a palladium (Pd) alloy based membranes for hydrogen separation. The efficiency hydrogen/methane (H_2/CH_4) of the sequential OTM and HTM reactor was higher at 79% (on higher heating value [HHV] basis) as compared to 76% for the integrated OTM-HTM reactor process.
- The hydrogen flux through the proton conducting membrane was much lower than for the flux required for commercial viability.
- The capital and product costs for the sequential reactor process were 10 - 12% lower than for the integrated reactor process.
- A process with sequential OTM and HTM reactors was selected for further development, and Pd alloy based membrane was identified as a major development item for Phase II efforts.

Future Directions

- Develop a composite membrane with a thin film of Pd alloy deposited on a porous support.
- Develop a suitable porous support with desired pore architecture for supporting a thin film of membrane and with necessary mechanical strength.

- Screen Pd alloy compositions for resistance to syngas and thermal cycling.
- Prepare tubes of composite membranes.
- Test a bench-scale membrane reactor for carrying out shift conversion and hydrogen separation.

Introduction

Hydrogen is expected to play a vital role in the transportation sector for the fuel cell vehicles (FCVs). One of the crucial factors for the successful introduction of FCVs on the U.S. roadways is a low-cost supply of hydrogen. The demand for hydrogen at fueling stations for FCVs is projected to be less than 10,000 standard cubic feet per hour (scfh). To be competitive with gasoline, the cost of hydrogen delivered to a vehicle must be below $20/MMBtu. A key challenge in achieving this hydrogen price is to reduce the capital costs of an on-site plant. The approach taken in this project is to reduce capital costs by reducing the complexity of the process and thus reducing the equipment needed to generate hydrogen.

Approach

Two process options were evaluated. In the first process option, both the OTM and the HTM were integrated into a single unit such that various processing steps (syngas generation, shift conversion and hydrogen purification) necessary for hydrogen production occur in a single reactor [1]. Since the OTM reactor operates at high temperatures (800 to 1100^{o}C), it is necessary to have the HTM operating at high temperatures. The ceramic proton conducting membranes can operate at temperatures up to 900^{o}C and they were considered as HTMs for this process option. (The Pd alloys are not suitable for high temperature operation.) In the second process option, OTM and HTM are placed in two separate reactors (Figure 1). By de-coupling these two membranes, the temperature constraint for the HTM is removed, and the HTM reactor can be operated at much lower temperatures (e.g. 300 to 600^{o}C) than the OTM reactor. The Pd alloy membranes were considered for this process option.

Air at low pressure (~25 pounds per square inch absolute [psia]) is passed to the retentate side of the OTM, and compressed natural gas (200 - 300 psia) and steam are passed to the permeate side of the OTM. Oxygen is transported across the OTM to the permeate side, where it reacts with natural gas to form syngas. A portion of natural gas also reacts with steam to form syngas. Additional hydrogen is formed by the water-gas shift reaction. The basic reactions involved in the process are:

$$CH_4 + 1/2O_2 \rightarrow CO + 2H_2 \text{ (Partial Oxidation)}$$

$$CH_4 + H_2O \rightarrow CO + 3H_2 \text{ (Reforming)}$$

$$H_2O + CO \rightarrow H_2 + CO_2 \text{ (Shift)}$$

A catalyst is incorporated in the reactors to promote the reactions. The syngas from the OTM reactor is cooled and then fed to the retentate side of the HTM reactor. In the HTM reactor, the shift reaction and the hydrogen separation through the HTM take place. Hydrogen is transported to the permeate side of the HTM by the partial pressure difference driving force. Due to removal of hydrogen from the reaction zone, more hydrogen is formed by the shift reaction. As much hydrogen as possible is recovered from the reaction zone by transport through the HTM to the permeate side. Eventually, a partial pressure pinch between the reaction zone and the permeate side is reached, limiting the amount of hydrogen that can be recovered. A process model was developed for the process with sequential OTM and HTM reactors. The Hysys simulation was used to evaluate the performance of the process.

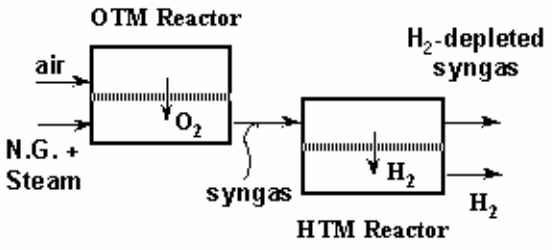

Figure 1. Sequential OTM and HTM Reactor System

Results

The overall efficiency of the plant is defined as follows:

H_2 efficiency = (energy recovered in H_2 (HHV) x 100)/(energy input in natural gas (HHV)).

Table 1 Summarizes utility consumption and the H_2 efficiency for the sequential reactor process.

Table 1. Performance Summary of the Sequential Reactor Process

Hydrogen Capacity, scfh	1,000
Natrual Gas, scfh	404
Power, kW	4.6
Water, gpm	1.1
H_2 Efficiency, %(HHV)	79%

The H_2 efficiency of the process with sequential reactors was estimated to be 79% (HHV). This compares with ~76% efficiency (HHV) for the process with the integrated OTM-HTM reactor. The higher efficiency for the process with sequential OTM and HTM reactors was due to lower temperature, which is favorable for shift reaction equilibrium.

The cost estimate developed for the process based on the integrated OTM-HTM reactor was used as a baseline cost, and the cost estimate for the process with the sequential reactors was developed by extrapolation. The hydrogen plant capacity was fixed at 1,000 scfh for the cost estimation. The capital costs for 2,000 and 5,000 scfh were estimated by using appropriate scale-up factors. For each capacity, costs were estimated for 10, 100, and 1,000 plants built/year. After reviewing the results, it was clear that the plants with capacities of 1,000 and 2,000 scfh will not be economically viable, because the cost of hydrogen from such plants is either comparable to or higher than the cost of liquid hydrogen. Therefore, the results for only 5,000 scfh plants are presented here.

The cost estimate presented last year for the integrated reactor process was reviewed and revised. The cost components with significant revisions were costs of reactor, instrumentation, natural gas and capital recovery. In addition, the costs related to contingency and safety were added. To estimate capital recovery costs, the method described in the Hydrogen Infrastructure Report [2] was used. The financial parameters listed in Table 2 were used.

Table 2. Financial Parameters

15% after-tax rate of return
38% corporate tax rate
15-year plant life
0% inflation rate

These parameters lead to capital-related charges of 23.5% of capital investment/year. In addition, the assumptions listed in Table 3 were made.

Table 3. Cost Estimation Assumptions

Natural Gas	$4/MMBtu (HHV)
Power	$0.05/kWh
Water	$0.01/1000 gal.
Maintenance and Replacement	3% of capital investment/yr
Capacity Utilization	80%

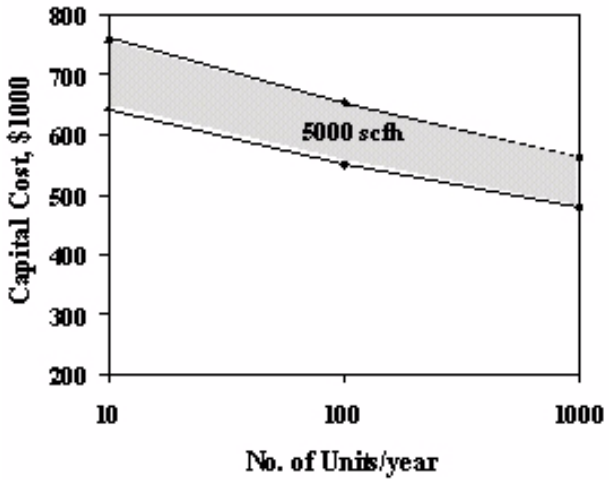

Figure 2. Capital Costs for the Integrated OTM-HTM Reactor Process

Figures 2 and 3 show the revised capital and product costs for the process with the integrated reactor. Figures 4 and 5 show capital and product costs for the process with the sequential reactors. The range in capital costs for any given point is due to the level of uncertainty in the cost estimate, especially in the costs of membrane reactors.

Comparing the costs for the two process options, the capital costs for the sequential reactor process are ~12% lower than the costs for the integrated reactor

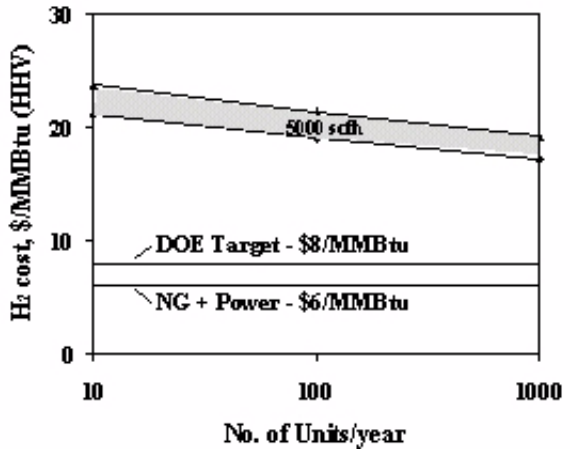

Figure 3. Product Costs for the Integrated OTM-HTM Reactor Process

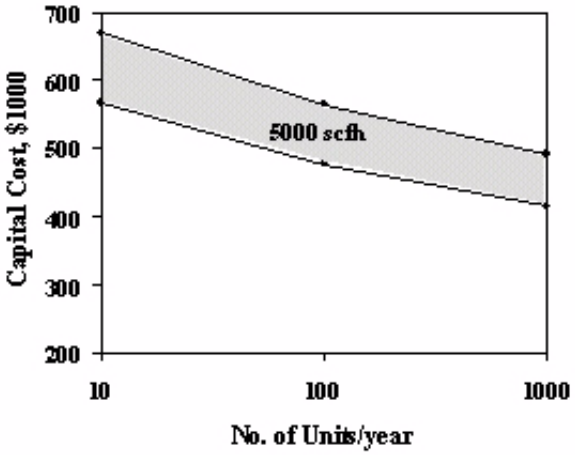

Figure 4. Capital Costs for the Sequential OTM and HTM Reactors Process

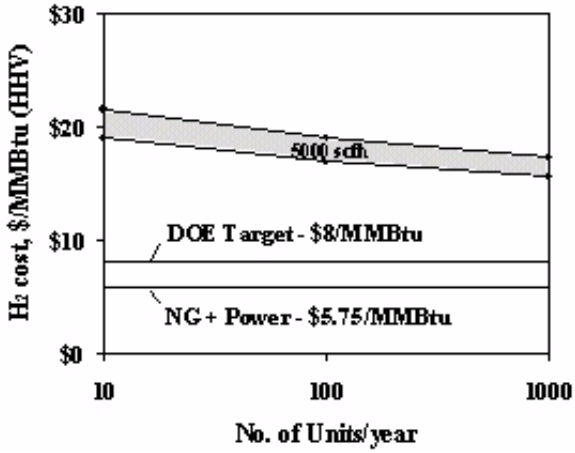

Figure 5. Product Costs for the Sequential OTM and HTM Reactors Process

process. Several factors contributed to lower costs for the sequential reactor process. The complexity of the reactor design is significantly reduced when there are two separate membrane reactors. Operation of the HTM reactor at lower temperature makes it possible to use less expensive materials of construction. The OTM reactor still operates at a high temperature; however, its size is significantly smaller than the size of the integrated OTM-HTM reactor. Finally, the hydrogen flux through a Pd alloy membrane (which is used in the sequential reactor process) is much higher than the flux through a proton conducting ceramic membrane (which is used in the integrated reactor process). As a result, less membrane area is required, which in turn reduces the size and cost of the HTM reactor.

The product hydrogen costs for the sequential reactor process were ~10% lower than the integrated reactor process. The cost of hydrogen production (at 15 psia) ranged from $15 to $21/MMBtu (HHV) depending on the number of plants built per year. These numbers do not include the costs of compression, storage and dispensing. At low production volume (10 units/year), the cost of hydrogen will be $19 to $21/MMBtu (HHV). With mass production (1000 units/year), the cost of hydrogen will drop down to $15 to $17/MMBtu (HHV). The capital cost reduction at higher production volume results from the volume discounts for the equipment purchases and reduction in assembly costs due to experience in building multiple identical plants.

Phase I indicated that the two-step reactor system with OTM reactor followed by integrated HTM shift reactor is the preferred approach for an economical hydrogen production system. Significant efforts are required in two areas for successful commercialization: development of cost-effective HTM and development of mass production approach to reduce capital costs. We are proposing a program with the emphasis on advancing the hydrogen separation technology. Any effort related to mass

production will be undertaken when the market for FCVs is more clearly visible.

The experimental work on the proton conducting materials based HTMs indicate that the hydrogen flux is not sufficient for commercial viability in the foreseeable future. Therefore, we have decided to focus on the Pd alloy based HTMs for further development efforts. The basis for the future work is the technology established by Research Triangle Institute to deposit thin, uniform, defect-free, Pd alloy membrane layer on the ceramic substrate and Praxair's ceramic membrane manufacturing technology.

Phase II of the program is expected to last three years, and it will be divided into two parts. The first part of Phase II will focus on developing a commercially viable HTM and will last two years. We expect to develop HTM and its sub-components during the first year and test a bench-scale membrane reactor (containing multiple membrane elements) with shift conversion in the subsequent year. The second part of Phase II will involve testing of critical balance of plant components such as OTM reactor, steam generator and high temperature heat exchangers.

Conclusions

The efficiency of the sequential reactor process is estimated to be 79% (HHV). The sequential OTM and HTM reactors process with the HTM reactor operating at lower temperature will result in lower hydrogen costs compared to the integrated OTM-HTM reactor process. The cost of hydrogen is estimated to range from $15 to $21/MMBtu (HHV) depending on the number of hydrogen plants built per year. The projected hydrogen costs from the proposed system are lower than the competing supply options, such as electrolysis and liquid hydrogen.

A Phase II plan has been defined. The sequential reactor process has been selected as a preferred process option. The first objective of Phase II is to develop a low-cost HTM (based on Pd alloy) with high hydrogen flux and tolerance for syngas components and thermal cycling. The next task will be to design and test a bench-scale membrane reactor to carry out shift conversion and hydrogen separation. Finally, other critical components such as OTM reactor, steam generator and high temperature heat exchangers will be tested.

References

1. Shah, M. M., Drnevich, R. F., Balachandran, U., Dorris, S. E. and Lee, T. H. 2001. "Technoeconomic Feasibility Analysis of Hydrogen Production by Integrated Ceramic Membrane System for Hydrogen Production", in the Proceedings of the DOE's 2001 Annual Hydrogen Review Meeting.

2. Thomas, C. E., James, B. D., Kuhn, I. F. Jr., Lomax, F. D., and Baum, G. N. 1997. Hydrogen Infrastructure Report, DOE Report No. DOE/CE/50389-504.

FY 2002 Publications/Presentations

1. Shah, M. M. and Drnevich, R. F., 2002. "Integrated Ceramic Membrane System for Hydrogen Production", Final Report Prepared for the DOE.

II.C.7 Low Cost Hydrogen Production Platform

Timothy M. Aaron (Primary Contact)
Praxair, Inc.
P.O. Box 44
Tonawanda, NY 14151-0044
(716) 879-2615, fax: (716) 879-7567, e-mail: tim_aaron@praxair.com

DOE Technology Development Manager: Arlene Anderson
(202) 586-3818, fax: (202) 586-9234, e-mail: Arlene.Anderson.ee.doe.gov

Main Subcontractors: Praxair, Inc., Tonawanda, NY; Boothroyd Dewhurst Inc., Wakefield, RI; Diversified Manufacturing Inc., Lockport, NY

Objectives

- Define process/equipment concepts and develop preliminary design suitable for mass production of a small on-site hydrogen systems.
- Perform a technoeconomic study for an on-site hydrogen production system for the transportation and industrial market (1,000 to 5,000 standard cubic feet per hour [scfh]).
- Develop business cases regarding the viability of the development project.
- Define the system in sufficient detail to develop a Phase II plan for the prototyping and system detail modeling of the major components.

Approach

- Use existing steam methane reformer (SMR) and purification process technologies as the base for the system.
- Develop design parameters for the system including natural gas, water and product specifications and pressures as well as setting goals for the mechanical details such as system footprint, shipping parameters and system setup time.
- Investigate current on-site hydrogen plant designs and develop component and overall cost breakdowns of the systems.
- Use design for manufacturing and assembly (DFMA) principles from the early stages of the design effort.
- Design the system with high volume manufacturing as an up-front design parameter.
- Select the system option that is most likely to be commercially viable when produced in high quantity production runs.
- Identify development issues for the selected design option and prepare a development plan for Phase II.

Accomplishments

- Design parameters for the system have been determined.
- A detailed review of current on-site options was completed, and a cost percentage breakdown of individual plant components has been developed. This information was then used to set goals for the overall system and component cost and design.

- Multiple process models of various reformer and purification options have been developed. These models served as a baseline to create the mechanical designs of the system.
- Three high potential conceptual designs were selected for further development. The selection process included design evaluations by the subcontractors.

Future Directions

- Complete the evaluation of the three current design concepts. Select highest potential concept(s) or combination of concepts for further development.
- Refine and optimize the selected concept(s) using DFMA techniques.
- Develop scale of economy analysis for the selected system design(s).
- Complete the techno-economic study for the system, including business model and competitive assessment.
- Develop plan for Phase II of project. Determine components requiring prototyping and/or advanced modeling/simulation in Phase II.

Introduction

Hydrogen is expected to play a vital role in the transportation sector with fuel cell vehicles (FCVs). A source of low cost hydrogen will be vital to the successful transition to a hydrogen based transportation economy and a key challenge to this goal is to reduce the overall cost for the small scale on-site generation of hydrogen. Praxair is an industry leader in the design, development and operation of hydrogen production facilities and is applying this extensive knowledge base, as well as advanced mass production, design and tooling experience provided by the subcontractors, to this development effort.

The overall goal of the Low Cost Hydrogen Production Platform (LCHPP) cooperative agreement is to develop an on-site hydrogen generation system, based on existing steam methane reformer technology, which will significantly lower the overall cost to produce hydrogen at low volumes. Praxair has, as partners in this project, Boothroyd-Dewhurst Inc. (BDI) and Diversified Manufacturing Inc. (DMI). BDI has expertise in the area of DFMA, and they have worked extensively with the automotive industry to lower the overall cost of production for mass produced systems. DMI is a design and fabrication facility with extensive experience in the areas of high temperature component design for both new designs and refurbishments, tooling design and manufacturing processes.

Approach

The requirement for industrial on-site hydrogen plants has typically been larger volumes than that of the LCHPP project. Achieving a competitive, lower volume plant offering has dictated the need to modularize plant components and streamline the installation and start-up process. The cost target of the LCHPP project is significantly lower than any previous goal set for the industrial market and to approach this goal, further integration, scale of economies and design optimization will need to be implemented. Rather than designing a system from a block flow process engineering approach, the system will be designed from the ground floor using DFMA techniques as well as a very high level of system integration. The system will also be designed for mass production and will therefore require the development of tooling and fixtures to aid in the assembly process. It will not be possible to build 0 - 10 of these units and approach the DOE cost goal. The economic viability of the system will only be achieved in large volume production runs.

The LCHPP project is structured in 3 distinct phases. Phase I is the engineering study and feasibility phase, which is scheduled to be completed in October 2002. A business plan and economic model will be developed as part of Phase I and will be updated as required during Phases II and III. Phase II is the system detail design, tooling development and prototype phase and is currently scheduled to begin in December 2002. Phase III is

the final phase where a demonstration unit will be developed and tested. The tooling required for the mass production of the system will also be developed in Phase III. Phase III is currently scheduled to begin in September 2004 and last for 1.5 years.

The process used for this project will be a SMR with a pressure swing adsorption (PSA) or membrane based purification system. The project does not include the hydrogen compression, storage or distribution system required for the high-pressure filling of FCVs. A process diagram of the system is shown in Figure 1.

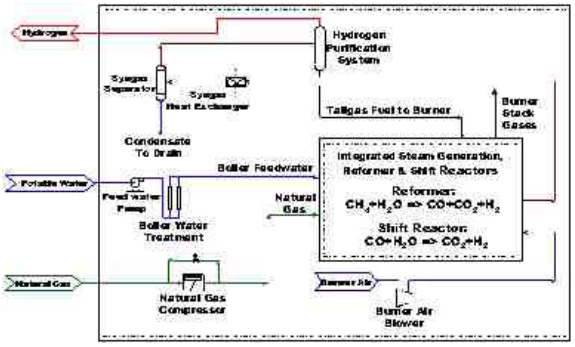

Figure 1. Low Cost Hydrogen Production Platform (LCHPP) Process Diagram

Results

Praxair previously developed what was then considered to be a small on-site hydrogen plant for the industrial market in the mid 1990s. The system capacity ranges from 12,000 to 30,000 scfh (340 to 850 Nm^3/hr) and generates hydrogen using a SMR with a PSA purification system. The system, although it has multiple skids requiring field assembly, demonstrates some of the potential positive effects of packaging all components on skids and limiting the field installed items to a few miscellaneous components. The installation cost percentage of the overall capital was less than one half of that of the larger systems, and the system was installed in less than 4 weeks. This is a significant improvement over the large plant approach, but the goals for the LCHPP will require additional installation and start-up cost reductions. The Praxair on-site hydrogen generating system (HGS) is shown in Figures 2 and 3.

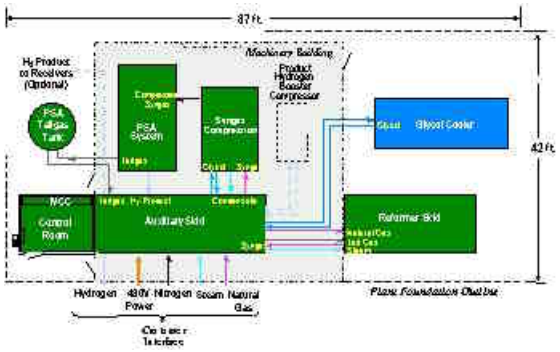

Figure 2. Praxair HGS On-Site Supply System

Figure 3. Praxair HGS On-Site Supply System (Seymour, Indiana)

Although the HGS system has been a success in the industrial market, with the system being over 97% reliable, the goals for the LCHPP project require a step change. The LCHPP will be approximately one-sixth the capacity, about one-fifth the footprint, and will lower the hydrogen product to about one-half that of the HGS system.

A detailed analysis of existing SMR based on-site hydrogen plants, including the HGS system detailed above, has been completed. The object of this analysis was to evaluate the current design methodology related to industrial on-site hydrogen plants. A cost matrix detailing the individual component costs as well as the project and operating costs associated with the plants was created. The data was collected from over 15 on-site hydrogen supply systems currently operated by Praxair. The

systems analyzed ranged from 10 to 100 times the capacity required in accordance with this project. Data from the analysis indicates that SMR hydrogen plants are typically custom designed with very low levels of integration. A significant percentage of the capital is required for the installation of the plant. The analysis also confirmed that typically over 50% of the installed capital cost is related to the reformer and shift components. With the cost matrix component breakdown, the areas of highest potential cost savings were clearly identified.

Results to date also include the development of detailed process models of SMR and purification systems. These models served as the baseline for the development of the mechanical design concepts. Options such as high/low pressure reforming, natural gas/syngas compression, PSA/membrane purification and various levels of thermal/process integration were modeled.

After the initial development of the process flow models, the mechanical design phase of the project began. As a result of the existing technology assessment discussed above, significant initial effort was placed in the cost reduction of the reformer and shift portion of the system. Initially, 6 mechanical design concepts were developed and evaluated. After discussions with the subcontractors, the six initial concepts were narrowed down to the three highest potential concepts. The three conceptual design options are currently being evaluated from the following three perspectives: 1) Praxair is developing 3D mechanical models as well as detailed process models of the various options, 2) DMI is reviewing the designs regarding manufacturability, single unit cost and higher quantity manufacturing costs, and 3) BDI is reviewing the options from a part count and system mechanical design optimization approach. Both a preliminary manufacturing cost summary of each concept for a single unit and the potential for cost savings in a mass production operation are being developed. At the conclusion of the preliminary analysis, the concepts will be narrowed down to the one (or possibly two) highest potential concept(s).

The purification system is also currently being evaluated. A PSA-based purification system appears to be the clear overall economic choice. Praxair has extensive experience in the area of PSA development and has developed advanced PSA cycles and system designs that will lower the overall cost of this component.

Conclusions

Development of a cost effective hydrogen supply infrastructure is a major issue facing the use of hydrogen in FCVs. Design-optimized, integrated small scale systems are likely to play an important role in the development of that infrastructure. The low cost hydrogen production platform project should lead to a cost effective SMR based system that can be an economical source of hydrogen for retail fueling stations. A report summarizing the findings of Phase I, as well as recommendations for Phase II will be developed at the end of Phase I of the agreement.

FY 2002 Publications/Presentations

1. Aaron, T. M., 2002. "Low Cost Hydrogen Production Platform", Presentation given to the DOE at the annual review meeting in Golden, CO, May 6-10, 2002.

II.C.8 Effects of Fuel Constituents on Fuel Processor Catalysts

John P. Kopasz (Primary Contact), Dan Applegate, Laura Miller, Shabbir Ahmed
Argonne National laboratory
9700 S. Cass Ave
Argonne, IL 60439
(630) 252-7531, fax: (630) 972-4405, e-mail: Kopasz@cmt.anl.gov

DOE Technology Development Managers:
Peter Devlin: (202) 586-4905, fax: (202) 586-9811, e-mail: Peter.Devlin@ee.doe.gov
Nancy Garland: (202) 586-5673, fax: (202) 586-9811, e-mail: Nancy.Garland@ee.doe.gov

Objectives

- Identify the effects of major constituents, additives, and impurities in petroleum-based fuels on reformer performance
- Evaluate the effects of fuel constituents and impurities on catalyst stability
- Collaborate with major oil companies for development of future fuels for fuel cells

Approach

- Investigate autothermal reforming of fuels and fuel constituents in microreactor
- Rate performance based on byproduct formation, catalyst deactivation, and dependence of hydrogen yield and conversion
- Test blends of fuel components to establish a composition/performance relationship matrix; compare results with those for pure components
- Use long-term (>1000 h) tests to determine effects on catalyst stability, poisoning and long-term degradation

Accomplishments

- Completed short-term testing of refinery blends from three oil companies and determined that fuels low in aromatic and naphthenic components can be reformed over a wider range of operating conditions.
- Completed short-term testing of paraffinic-aromatic and paraffinic-naphthenic blends and determined that aromatic and naphthenic components decrease the rate at which paraffinic species are reformed
- Determined effects of amine additives on reforming behavior
- Studied effect of composition on water requirements and water balance issues in fuel reformer-fuel cell systems
- Completed long-term tests on monolithic catalysts

Future Directions

- Investigate long-term effects of additives (e.g., detergents, antioxidants) and impurities
- Continue investigating reforming of blended fuels; determine composition/performance relationships from results
- Investigate differences in fuel reforming with different catalysts
- Make recommendations for fuel cell fuels

Introduction

On-board reforming of petroleum-based fuels, such as gasoline, may help ease the introduction of fuel cell vehicles to the marketplace. Although gasoline can be reformed, some constituents and impurities may have detrimental effects on the fuel processing catalysts, which may lead to compromised performance and decreased fuel conversion efficiency. In order to identify which constituents are beneficial and which are detrimental to the reformer, we have begun to test various components of gasoline and blends of gasoline streams under autothermal reforming conditions.

Prior work focused on the autothermal reforming of some of the major components of gasoline. We investigated the autothermal reforming of iso-octane, n-octane, octane, trimethylbenzene, toluene, methylcyclohexane, and methylcyclopentane. These chemicals represent the branched paraffins, straight chain paraffins, olefins, aromatics, and cyclic paraffins present in gasoline. We observed that trimethylbenzene required more severe reforming conditions than the other components.[1] The current work focuses on the effects of blends of components and on the effects of additives. Blends are being investigated to determine if the presence of some components can affect the reforming of others.

Approach

Fuel blends were obtained from three major oil companies. The blends were formulated to provide fuels with compositions of interest to the refineries. Reforming of the fuel blends was performed under constant O_2:C and H_2O:C ratios (0.42 and 1.4) on identical catalysts to allow for comparisons of the different fuels. Short-term (<20 h) tests were performed in a reactor containing ~2 g of catalyst. The fuel and water were vaporized, then mixed and sent to the reactor where oxygen was added. Four sampling ports allowed for testing at various positions (and space velocities) in the catalyst bed. A small portion (<1%) of the gas stream was diverted through one of these ports to the residual gas analyzer for analysis. The remainder of the gas stream continued through the reactor bed to the exit stream. Batch sampling was performed at the reactor exit.

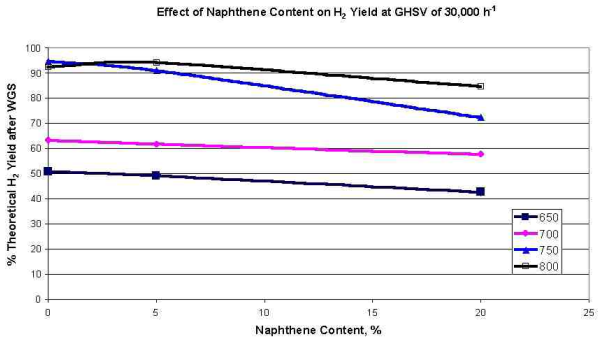

Figure 1. Effect of naphthene content on the hydrogen yield from reforming refinery blends.

Long-term (>1000 h) tests were performed in a separate reactor equipped with a solid-state on-line hydrogen sensor and infrared carbon monoxide and carbon dioxide detectors. Batch sampling was performed at the exit stream. This system allowed us to determine the durability of the autothermal reforming catalyst and to determine if there are any long-term problems (poisoning, coking) caused by the fuel components.

Results

Tests on the fuel blends indicate that fuels that are high in naphthenic components have a narrow window of operating conditions in which they provide good hydrogen yields. Figure 1 shows the dependence of hydrogen yield on naphthenic content for reforming at a GHSV of 30,000h^{-1} at 650, 700, 750 and 800°C. Increasing the naphthene content from 0 to 5% has very little effect; however, when the naphthene content is increased to 20%, hydrogen yield drops off substantially. To better understand the effects of naphthenes, we investigated the reforming of a binary mixture of isooctane and 20% methylcyclohexane. The partial pressures of cyclohexane, methylcyclohexane, and benzene, normalized to the partial pressure of a helium internal standard, are plotted as a function of the inverse of the space velocity in Figure 2. The inverse of the GHSV is proportional to the residence time in the reactor. At short residence times methylcyclohexane and cyclohexane (formed by removing a methyl group from methylcyclohexane) dehydrogenated to form aromatics. The aromatics then behaved as they did in the refinery blends with high aromatic content and the isooctane-xylene mixtures,[2] and decreased

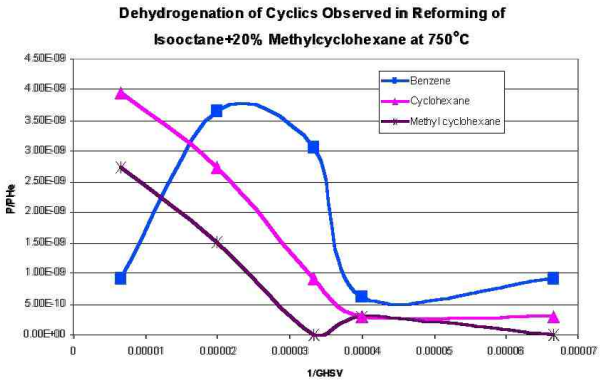

Figure 2. Methylcyclohexane, cyclohexane, and benzene content in the product gas from reforming isooctane+20%methylcyclohexane, showing conversion of cyclohexanes to benzene.

the rate of reforming of the paraffin. In addition, the dehydrogenation reaction is endothermic. This reduces the temperature at the front of the reactor and further decreases the reaction kinetics relative to those for pure isooctane.

Experiments were performed on solutions of isooctane with n-secbutylamine, a surrogate for isobutyleneamine detergents. The addition of n-secbutylamine decreased the hydrogen yield at temperatures below 750°C (see Figure 3). A closer investigation of the product gas revealed that, similar to the case for aromatics, the amine additive decreased the rate at which isooctane is reformed (Figure 4). However, with n-secbutylamine the effect is seen at much lower concentrations. A concern with amine additives is that they may form ammonia, which is a poison for PEM fuel cells at sub ppm levels. No ammonia was observed in the reforming of isooctane-n-secbutylamine solutions of 50 ppm n-secbutylamine. For solutions with 500 wppm n-secbutylamine, no ammonia was observed when the reforming was performed at 800°C; however, trace amounts (<250 ppb) were observed when the reformer was operated at 650°C. When the amine concentration was 1000 wppm, ammonia was observed in the product gas at levels of 1 ppm when the reactor was at 800°C and 1.5 ppm when the reactor was at 650°C.

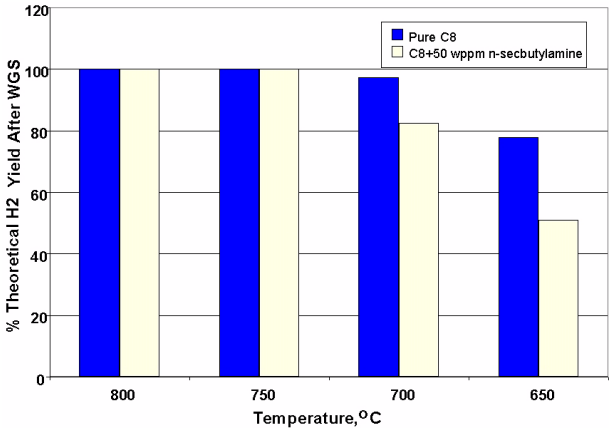

Figure 3. Effect of n-secbutyl amine on the hydrogen yield from reforming isooctane.

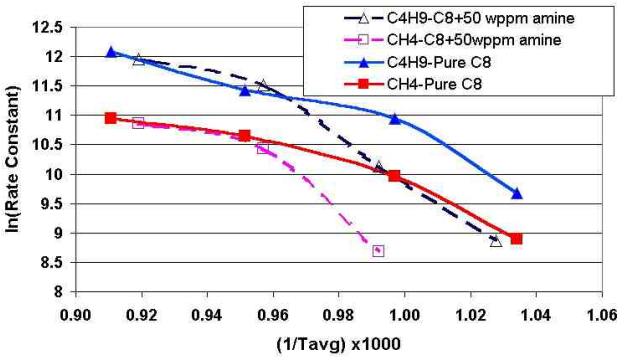

Figure 4. Effect of n-secbutylamine on the rate of disappearance of paraffinic species during isooctane reforming.

These results indicate that species that adsorb more strongly to the metal centers in the catalyst tend to decrease the rate at which the paraffinic species in the fuel are reformed. This is similar to results reported in combustion literature, where species such as aromatics have been observed to decrease the combustion of paraffins in a mixed stream.[3,4] It also suggests that other additives and impurities that have strong adsorption to platinum will decrease the rate of reforming.

Water Balance Issues

Where fuel cell systems use on-board fuel processing of available fuels, the fuel processor requires high-purity water. For transportation applications, the process water must be recovered from the fuel cell system exhaust gas. For such

applications, it is critically important that the fuel cell system be a net water-producing device. A variety of environmental conditions (e.g., temperature, pressure), fuel cell system design, and operating conditions determine whether the fuel cell system is water-producing or water-consuming. The fuel composition can also have a significant effect. We have performed calculations determining the water balance for an ambient pressure system with on-board reforming and water recovery, assuming fuel feed rates of 1 gmol/min. In the reformer the steam-to-carbon ratio is 1.5, and oxygen flow rates are adjusted to provide a temperature rise in the reactor of 200°C. For the condenser, we have assumed a design ambient temperature of 35°C (95°F) and an approach temperature of 11.1°C (20°F), leading to an exhaust gas temperature of 46.1°C (115°F). In the fuel cell we are assuming 80% fuel utilization and 40% oxygen utilization. Calculations for several different fuels are shown in Table 1. Methane is a net water producer under these conditions, while trimethylbenzene leads to a water deficit of 81 ml/min. In order to achieve water balance for trimethylbenzene under these conditions, the exhaust gas temperature would need to be lowered to 36.6°C (97°F), just 1.6°C above the ambient design temperature. Alternatively, the pressure can be increased. For trimethylbenzene, a pressure of 1.7 atm is needed to achieve water balance, while for isooctane a pressure of 1.2 atm is sufficient.

Fuel	Net water produced, ml/min	Exhaust temperature for water balance, °C (°F)
Gasoline	-38	42.0 (107)
Isooctane	-33	43.2 (109)
Trimethyl-benzene	-81	36.6 (97)
Methane	+5	49.2 (120)

Table 1. Fuel Calculations

Conclusions

These tests indicate that the fuel composition can have a large impact on reformer performance. Some fuel components can affect how other components are reformed. Species that adsorb more strongly to the metal centers in the catalyst, such as aromatics, tend to decrease the rate at which paraffinic species in the fuel reform. This is similar to results reported in combustion literature, where species such as aromatics have been observed to decrease the combustion of paraffins in a mixed stream.[3,4] This work also indicates that the fuel composition will have an impact on the water balance issues for the system. Fuels high in aromatics will need more aggressive conditions to be able to maintain a water balance. Future work will be directed towards understanding the interactions between the different types of components in multicomponent fuels.

References

1. J. P. Kopasz, S. Ahmed, M. Krumpelt, and P. Devlin, SAE Technical Paper Series 20001-01-1915, 2001.

2. J.P. Kopasz, D. Applegate, X. Wang, L. Miller, S. Ahmed, "Effects of Fuel Constituents on Fuel Processor Catalysts", 2001 Annual Progress Report, Fuels for Advanced CIDI Engines and Fuel Cells, U.S. Department of Energy, Office of Transportation Technologies, Washington D.C.

3. J. J. Spivey, Ind. Eng. Chem. Res. 1987, 26,2165-2180.

4. A. Barresi and G. Baldi, Ind. Eng. Chem. Res. 1994,33,2964-2974.

FY 2002 Publications/Presentations

1. Reforming Petroleum Based Fuels for Fuel Cell Vehicles: Composition-Performance Relationships, J. P. Kopasz, L. E. Miller, S. Ahmed, P. Devlin, and M. Pacheco, presented at 2002 Future Car Congress, Arlington, VA, June 3-5, 2002. SAE Technical Paper Series, 2002-01-1885, 2002.

2. Water Balance in Fuel Cells Systems, J. P. Kopasz, S. Ahmed, R. Kumar, M. Krumpelt, presented at 10th AIChE Spring National Meeting, New Orleans, LA, March 10-14, 2002.

3. Autothermal Reforming of New Gasoline for Fuel Cell Applications, J. P. Kopasz, M.A. Pacheco, S. Ahmed, X. Wang, M.A. Marquez, presented at the

7th Grove Fuel Cell Symposium, Westminster, London, UK, Sept. 11-13, 2001.

4. Reformability of Fuels and Fuel Constituents, J. P. Kopasz, presented at the IEA Annex XV Advanced Fuel Cell Meeting, Lucerne, Switzerland, July 1-2, 2001.

II.C.9 Separation Membrane Development

Kit Heung (Primary Contact)
Westinghouse Savannah River Technology Center
773-A, Savannah River Site
Aiken, South Carolina
(803) 725-3161, fax: (803) 725-2756, e-mail: leung.heung@srs.gov

DOE Technology Development Manager: Peter Devlin
(202) 586-4905, fax: (202) 586-9811, e-mail: Peter.Devlin@ee.doe.gov

Objectives

- Produce a sol-gel encapsulated metal hydride packing material that will absorb hyrogen selectively, not break down to fines, and tolerate reactive impurities.
- Evaluate selected packing material for hydogen separation in a small-scale column.

Approach

- Develop formulations and procedures to make silica encapsulated metal hydride composite material.
- Test selected samples in a laboratory scale separation column for hydrogen separation from feed streams of different compositions.

Accomplishments

- Produced hundred-gram size samples with three different procedures.
- Designed and installed an apparatus for gas separation tests.
- Conducted hydrogen separation from a nitrogen stream on two samples.

Future Directions

- Modify procedure to produce improved composite material to achieve required performance and reduce cost.
- Conduct hydrogen separation tests with feeds containing reactive impurities such as CO.
- Conduct cost analysis.

Introduction

For a hydrogen economy to become a reality, hydrogen production will have to be greatly increased from what it is today. According to U.S. DOE 1994 fuel use numbers, U.S. household transportation fuel use is a hydrogen equivalent of 0.55 billion lb/day. This is about 6 times the total U.S. hydrogen use of 0.1 billion lb/day today. Where will all the hydrogen come from? A definitive answer to this question is not yet known. One probable answer may be that hydrogen must come from multiple sources. These sources will include renewable (solar, wind, hydro, biomass, etc.) and non-renewable (fossil, nuclear, etc.) feedstocks. One sure thing is that hydrogen will have to be recovered from all kinds of gas streams. Many of the gas streams will contain low levels of hydrogen and undesirable impurities. Today's hydrogen recovery processes include the most commonly used pressure swing adsorption process, the cryogenic process, and the membrane process. Their use with low concentration feeds and high recovery are not efficient. A new hydrogen recovery process is still needed. This work is targeted at a new hydrogen recovery process that will be suited for hydrogen recovery from low hydrogen concentration gas streams.

Approach

When hydrogen content in a feed stream is high (more than about 50%), it is efficient to purify the hydrogen by adsorbing the impurities. This is the principle of the pressure swing adsorption process. When the hydrogen concentration is low (less than about 50%), it is more efficient to absorb the hydrogen from the feed stream. However, a practical absorbent for hydrogen is not yet available. Metal hydrides are a promising candidate because they absorb hydrogen reversibly at moderate conditions. One example is $LaNi_{4.25}Al_{0.75}$:

$$2\ LaNi_4.25Al_{0.75} + 5\ H_2 \leftrightarrows 2\ LaNi_{4.25}Al_{0.75}H_5$$

Each bulk liter of this material can absorb up to 18 moles of hydrogen reversibly. The hydrogen can be absorbed and desorbed by changing the hydrogen pressure, the temperature or both. This group of materials would have been well suited for hydrogen recovery from low concentration streams if not for two practical problems. Metal hydrides in general break down to fines after repeated hydrogen absorption and desorption. The fines are in the micron range that makes them very difficult to use in separation columns. Metal hydrides are sensitive to reactive impurities like oxygen and carbon monoxide. Levels at hundredths of a fraction can render them inactive toward hydrogen. Past efforts to deal with these problems can be represented by the works of Sandrock et al [1] and Suda et al [2].

In this work metal hydride particles are encapsulated in a porous silica matrix to form a composite material. The composite is then broken into granules of desired size for packing separation columns. Each granule is a matrix of porous silica with metal hydride particles uniformly distributed in it. The porous matrix is strong so that hydrogen absorption and desorption of the metal hydride particles does not cause breakage. The porosity of the matrix permits hydrogen to reach the metal hydride particles but prevents the larger size impurity molecules from penetrating. The composite granules can therefore withstand hydrogen absorption/ desorption without generating fines and can tolerate reactive impurities.

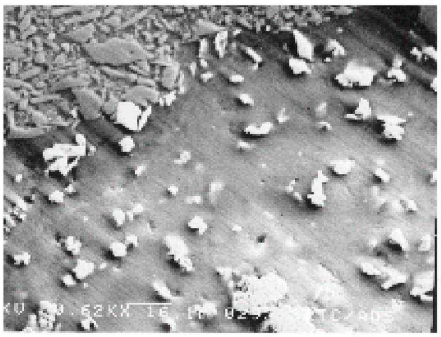

Polished surface, 620x

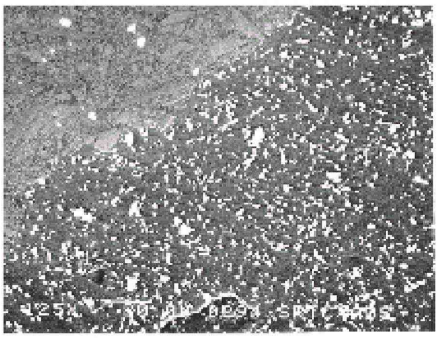

Polished surface, 125x
(bright spots are metal hydride)

Silica encapsulated

Figure 1. Silica Encapsulated Metal Hydride

Results

The fabrication of encapsulated metal hydride involves 3 main steps: 1) break the metal hydride to fine particles and stabilize the fines for handling in open air; 2) encapsulate the metal hydride particles in silica with the sol-gel method; 3) treat the composite with heat to obtain desired strength and porosity. Micrographs of a typical encapsulated sample are shown in Figure 1.

Samples of encapsulated $LaNi_{4.25}Al_{0.75}$ were tested for hydrogen absorption in a gas manifold with hydrogen from a known volume. The results showed that the encapsulated sample was easier to activate than the non-encapsulated metal hydride. The hydrogen absorption capacity of the encapsulated metal hydride did not change significantly. The encapsulated sample also retained its activity better than the non-encapsulated sample after exposure to air. After repeated absorption/desorption cycles, the granules did not generate fines as metal hydride did.

A laboratory scale separation apparatus was set up for testing the hydrogen separation properties of encapsulated metal hydride samples. The apparatus consists of a gas manifold, a packed column and a thermal conductivity detector (TCD). The gas manifold comprises supplies of hydrogen, nitrogen, methane, carbon dioxide and carbon monoxide. Mass flow controllers are used to generate gaseous mixtures to feed the separation column. The column is a U-shape ¾-inch diameter, 6-inch long stainless steel tube, packed with encapsulated metal hydride granules. On the outlet side of the column, a pressure-regulating valve keeps the pressure in the column constant. A side stream is directed to the TCD for measuring the hydrogen concentration. A top-open furnace and a water bath are use to heat or cool the column when needed.

A typical test involves a hydrogen absorption step and a regeneration step. In the absorption step, hydrogen and carrier gases at target rates are joined to form a feed stream to enter the column. The hydrogen is absorbed and the carrier gas is left passing through the column. As the absorption capacity of the packing material at the inlet end is saturated gradually, an absorption front is developed in the column. The absorption front is an inverse-S shaped concentration profile of hydrogen in the gas phase. This absorption front exits the column when the packing material is completely saturated. The hydrogen concentration measured by the TCD will show the absorption front to be an S-shaped curve of hydrogen concentration versus time. This curve is often called the breakthrough curve. The actual shape of the breakthrough curve is an indication of the kinetics of hydrogen absorption of the packing material. A steep rise of the curve indicates favorable kinetics for hydrogen separation. Hydrogen

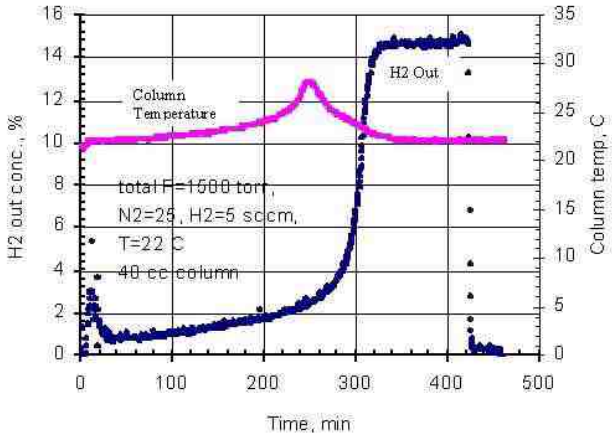

Figure 2. Breakthrough Curve of Hydrogen Absorption by Encapsulated Metal Hydride Packed

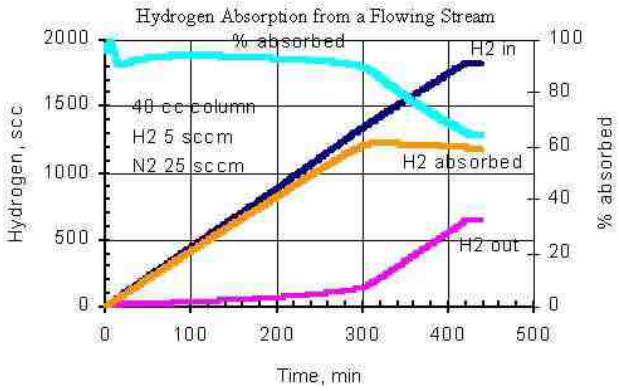

Figure 3. Hydrogen Removal from a Flowing Stream is about 95%.

absorption by metal hydride is an exothermic reaction. A thermocouple located in the column can measure the temperature peak indicating the location of the absorption front at a given time. A typical breakthrough curve and temperature peak is shown in Figure 2. This kind of data may be used to compare separation efficiencies and to design separation columns.

The efficiency of hydrogen removal can be shown by the difference in the amounts of hydrogen entering the column and the amounts of hydrogen leaving the column as a function of time. For a typical run, the results show that about 95% of the hydrogen entering the column is absorbed continuously until the column is saturated, see Figure 3.

For typical regeneration, the column is purged with nitrogen and is heated up to about 100°C at the same time. The hydrogen concentration at the exit stream is measured by the TCD. From this concentration data the partial pressure of the hydrogen can be calculated. The data in Figure 4 show that about half of the hydrogen can be recovered at 800 torr, and more than 95% can be recovered at 100 torr.

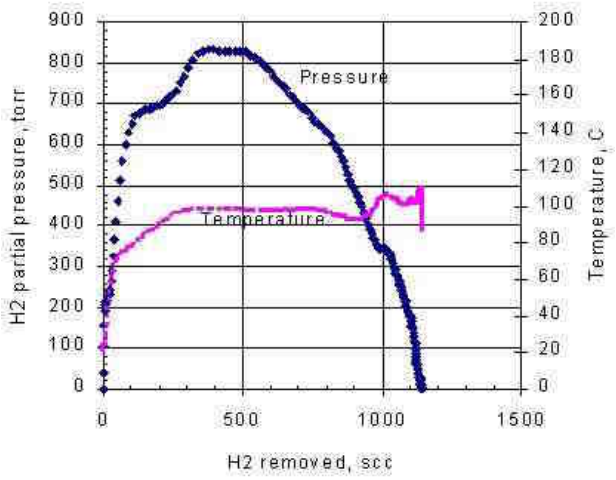

Figure 4. Hydrogen Recovery from the Column

Conclusions

Metal hydride powders can be encapsulated in a porous silica matrix using a sol-gel method. The encapsulated metal hydride retains its hydrogen absorption property with increased resistance to reactive impurities. Granules of encapsulated composite can withstand hydrogen absorption/ desorption cycles without producing fines. This makes them applicable in packed separation columns. Hydrogen recovery from a nitrogen stream has been demonstrated in a laboratory column with the encapsulated metal hydride. Hydrogen recovery from other gas streams such as methane, carbon dioxide and that containing carbon monoxide has been planned and will be tested. Encapsulated metal hydride is suited for hydrogen recovery from low concentration streams which will be needed in a hydrogen economy.

References

1. J. J. Sheridan III et al, Journal of the Less-Common Metals, 89 (1983) 447-455.

2. X.-L. Wang et al, Journal of Alloys and Compounds, 231 (1995) 860-864.

FY 2002 Publications/Presentations

1. Paper titled "Hydrogen Separation Using Encapsulated Metal Hydride" presented in 14th World Hydrogen Energy Conference, June 9th-13th, 2002.

Special Recognitions & Awards/Patents Issued

1. US patent number 6,262,328 issued.

II.C.10 Defect-Free Thin Film Membranes For H_2 Separation and Isolation

Tina M. Nenoff (Primary Contact)
Sandia National Laboratories
PO Box 5800, MS 0755
Albuquerque, NM 87185-0755
(505) 844-0340, fax: (505) 844-0968, e-mail: tmnenof@sandia.gov

DOE Technology Development Manager: Peter Devlin
(202) 586-4905, fax: (202) 586-9811, e-mail: Peter.Devlin@ee.doe.gov

Objectives

- Synthesize defect-free thin film zeolite membranes for H_2 isolation and purification, and use as water management membranes in proton exchange membranes (PEMs).
- Replace existing expensive and fragile Pt catalysts.
- Test the separations of light gases (pure and mixtures) through the membranes.
- Demonstrate effective light gas separations and commericalization potential of zeolite membranes.

Approach

- Synthesize defect-free thin film zeolite membranes and microporous bulk phases for future membrane applications.
- Model/simulate permeation of light gases through various frameworks/pores for optimized performance.
- Analyze flux and permeation of gases through membranes on unique in-house permeation unit.
- Validate modeling/simulation with actual permeation data to optimize membranes synthesized.

Accomplishments

- Synthesized defect-free zeolite membranes with different selectivities for various gas molecules; selectivity based upon a combination of molecular sieving through the pores and adsorption of the various composition frameworks.
- Designed and built a unique in-house permeation unit that can test both disk and tube membranes, with multiple pure or mixed gases, in a temperature range of 25-500°C.
- Analyzed selectivities of pure gases through various membranes; aluminosilicate (Al/Si) membranes are highly selective for hydrogen (H_2); all silica membranes are selective for carbon dioxide (CO_2).
- The Sandia aluminosilicate zeolite membranes have fluxes on the order of 10-6 mole/mole per meter squared Pascal secont (flux unit) (m^2Pa sec) and pure gas separations of $H_2/N_2 \geq 61$, $H_2/CO_2 \geq 80$, $H_2/CH_4 = 7$, $CH_4/CO_2 \geq 11$. H_2 (hydrogen), N_2 (diatomic nitrogen),CO_2 (carbon dioxide), CH_4 (methane).

Future Directions

- Synthesize and characterize of thin films and bulk novel microporous phases including of Al/Si zeolite thin films doped and/or ion exchanged with other elements, unsupported aluminosilicate zeolite membranes, and silicotitanate phases.
- Synthesize membranes on (commericaly viable) oxide-coated porous stainless steel supports.
- Model separation values by molecular dynamics calculations for pure and mixed light gases interacting with differing zeolite type membranes (ie., comparing ZSM-5 to ZSM-22).

- Perform permeation and flux studies of pure and mixed gases through membranes (H_2, CO, CO_2, CH_4, N_2, and sulfur hexafluoride [SF_6]).
- Build a partnership with a membrane company. Initiate an agreement for product development with an industrial partner.

Introduction

There is a great need for robust, defect-free, highly selective molecular sieve (zeolite) thin film membranes for light gas molecule separation ratios in hydrogen fuel production from CH_4 or H_2O sources. In particular, we are interested in (1) separating and isolating H_2 from H_2O and CH_4, CO, CO_2, diatomic oxygen (O_2,) and N_2 gases; (2) water management in PEMs, and (3) as replacing for expensive Pt catalysts needed for PEMs. Current hydrogen separation membranes are based on Pd alloys or on chemically and mechanically unstable organic polymer membranes. The use of molecular sieves brings a chemically and mechanically stable inorganic matrix to the membrane. The crystalline frameworks have "tunable" pores that are capable of size exclusion separations. The frameworks are made of inorganic oxides (e.g., silicates, aluminosilicates, phosphates) that bring different charge and electrostatic attraction forces to the separation media. The result is materials with high separation abilities plus inherent thermal stability over 600°C and chemical stability. Furthermore, the pore sizes and shapes are defined crystallographically (<1Å deviation) which allows for size exclusion of very similarly sized molecules. In comparison, organic polymer membranes are successful based on diffusion separations, not size exclusion. We envision positive results from this project in the near term with hydrocarbon fuels, and long term with biomass fuels.

Approach

The approach for this program is the development of defect-free thin film zeolite membranes and new bulk microporous phases for the selective separation of light gases. The development of these membranes includes synthesis, modeling/simulation, permeation studies and validation for separation and isolation of H_2. The permeation of pure and mixed gases through membranes is studied at room temperature and 80°C. The modeling and simulation work helps determine improved pore size and composition for sieving. The validation involves comparing modeling/simulation data with actual permeation values to determine needed improve upon the membranes synthesized.

Previous work at Sandia has successfully shown the ability to grow defect-free aluminosilicate and phosphate-based molecular sieve membranes. The focus now is on the enhancement and optimization of the type of molecular sieve for separation, the methodology of film growth, and the type of supports upon which to grow membranes (and remain commercially viable). We are studying aluminosilicate frameworks and metal doped frameworks to better determine the relationship between adsorption, sieving and then permeation. To study the effect and prerferability of support types, we are studying and comparing unsupported film growth versus film growth on ceramic supports. We are also beginning studies on newly available ceramic coated stainless steel supports (allowing for phase match on the ceramic, with the durability of stainless steel). With all materials synthesized, we perform characterization in-house to better understand structure-permeability relationships. These include X-ray diffraction, thermal analyses, elemental analysis and permeation studies. Our in-house permeation unit is capable of fitting both disk and tubular membrane supports, either of ceramic oxide or stainless steel materials. This unique unit can be run from room temperature to elevated temperatures ($\leq$ 500°C), though we only plan to run as high as 80°C. The unit also contains a residual gas analyzer, enabling us to monitor and identify ratios of the permeate mixtures. We also are able to leverage end sealant technology patented through Sandia. The gases we plan to test for this project include H_2, helium (He), CH_4, CO, CO_2, CH_4, O_2, N_2, and SF_6, plus mixtures of these gases.

Results

In the area of thin film membranes we have successfully synthesized micron thick aluminosilicate zeolite membranes on alumina disks (see Figure 1). Our permeation testing (see Figure 2) of the material shows that these membranes are defect-free. Defect free is denoted by permeation selectivity due to size exclusion by molecular sieving through the zeolite pores, and not through crystalline defect sites, pin holes, or crystallite mismatches (pores of this zeolite are 5.5 Å). Molecules used for this test are He (kinetic diameter = 2.6 Å) and SF_6 (kinetic diameter = 5.5 Å). Pure gas studies are run at room temperature. The only consistent problem has been that membranes have grown on both sides of the disk support, even when seeding occurs on one side. As a result, flux through the membrane/support is slightly diminished from what it would be with only one side membranes.

Once the membrane is determined to be defect-free, testing on pure gases vital to the steam reforming cycle for natural gas to hydrogen fuels can begin. Pure gas data presented in Table 1 show the results achieved by our membranes, and compares them to literature values [1,2]. Most importantly, the Sandia aluminosilicate zeolite membranes have flux values superior to those observed elsewhere. In particular, the Sandia membranes have fluxes on the order of 10-6 mole/(m^2Pa sec) and separations of $H_2/N_2 \geq 61$, $H_2/CO_2 \geq 80$, $H_2/CH_4 = 7$, $CH_4/CO_2 \geq 11$ (see Table 1) [3]. Also, the all-silica zeolite membranes have superior CO_2 separation from smaller light gases (such as H_2) [3,4]. Though not completely understood, these results indicate that we can tune the membrane materials to have selectivity for various light gases. This is even more valuable as it is with crystalline inorganic zeolite membranes that are chemically, thermally and mechanically robust and stable. In comparison to Pd alloy films, the zeolite membranes perform well. According to the literature [5], Pd on alumina had relative ratios of light gas separations of $H_2/N_2 = 110$ at elevated temperature of 350°C. The flux was also low (2 x 10^{-7} mole/m^2Pa sec). Furthermore, we have synthesized defect-free aluminosilicate zeolite thin films supported on commercially available oxide coated stainless-steel supports (SS316); industry needs stainless steel to make membranes an economically viable technology.

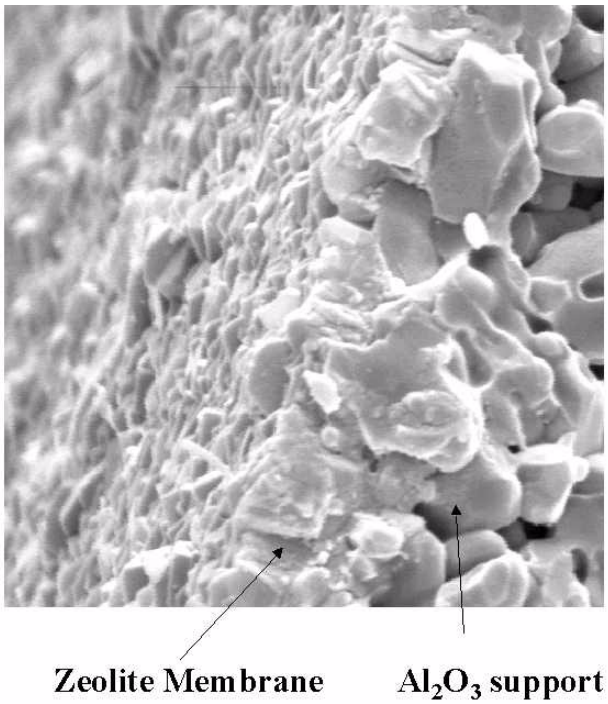

Figure 1. Cross Section View by Scanning Electron Microscope of the Micron Thick Zeolite Membrane on Gamma-Alumina Substrate

SNL All Silica (2-sided), $10^{-6} - 10^{-7}$ mole/(m^2 Pa sec)		
$H_2/N_2 = 1.4$		
$H_2/CH_4 = 0.625$	$CO_2/N_2 = 4.2$	
$He/N_2 = 1.1$	$CO_2/O_2 = 4.9$	
$CH_4/N_2 = 2.28$	$CO_2/H_2 = 3.0$	
$H_2/CO_2 \geq 0.34$	$CO_2/CO = 4.2$	
$H_2/O_2 = 1.7$	$CO_2/CH_4 = 1.8$	
$CH_4/CO_2 = 0.54$		
$H_2/CO = 1.43$		
SNL Na/Al/Si (2-sided) 10^{-6}mole/(m^2 Pa sec)	**Knudsen Selectivity**	**Lit. (values for Al/Si)** [1,2] **10^{-7}-10^{-10} mole/(m^2Pa·s)**
$H_2/N_2 \geq 61$	$H_2/N_2 = 3.73$	$H_2/N_2 = 3.91$
$H_2/CH_4 = 7$	$N_2/CO_2 = 1.00$	$N_2/CO_2 = 0.625$
$He/N_2 \geq 7$	$He/N_2 = 2.64$	$H_2/N_2 = 100$; 150°C
$CH_4/N_2 \geq 1.4$	$CH_4/N_2 = 1.32$	10^{-10} perm
$H_2/CO_2 \geq 80$		
$H_2/O_2 \geq 11$		
$CH_4/CO_2 \geq 11$		

Table 1. Permeation Values for Pure Gases at Room Temperature

Another avenue of research is bulk novel molecular sieve materials, with the goal of "tuning" pore sizes to molecular sieving needs. In this arena, we have successfully synthesized many new phases,

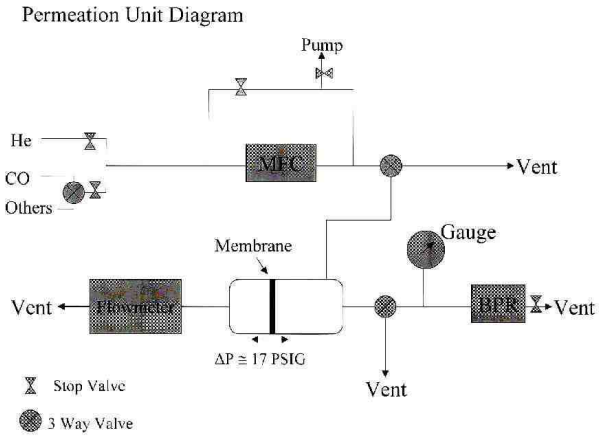

Figure 2. Sandia Permeation Unit for Light Gases (including CO), Pure and Mixed (the equipment diagram)

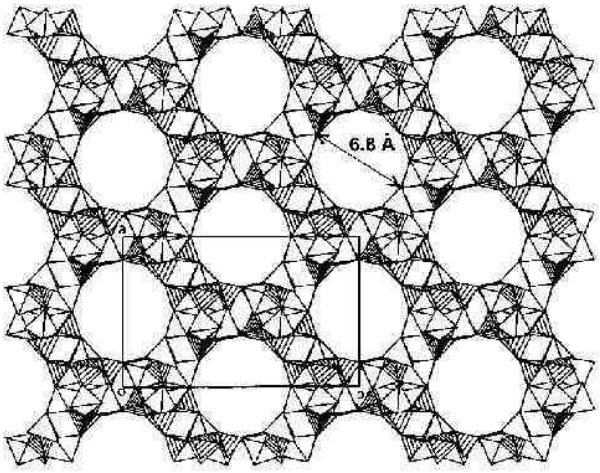

Figure 3. 3D Framework of 12-ring Gallo Fluorophosphate Microporous Phase

a number of which are promising for light gas separations. In particular, we have a novel crystalline 12-ring microporous fluorogallophosphate material. [6] Its pore sizes are the in range for light gas separations, as shown in Figure 3. We are now attempting to synthesize this as a thin film membrane.

Conclusions

There is a great need for robust, defect-free, highly selective molecular sieve (zeolite) thin film membranes for light gas molecule separations in hydrogen fuel production from CH_4 or H_2O sources. They contain an inherent chemical, thermal and mechanical stability not found in conventional membrane materials. Our goal is to utilize those zeolitic qualities in membranes for the separation of light gases, and to eventually partner with industry to commercialize the membranes. To date, we have successfully:

- Demonstrated (through synthesis, characterization and permeation testing) both the ability to synthesize defect-free zeolitic membranes and use them as size selective gas separation membranes;
- Built and operated our in-house light gas permeation unit;
- Synthesized membranes on commercially available disks (this is in addition to successes we have had in synthesizing zeolitic membranes to tubular supports [7]);
- Synthesized a number of new microporous bulk phases, including the novel 12-ring fluorogallophosphate; and
- Work continues in the synthesis of these novel materials as thin film membranes.

References

1. Tavolaro, A.; Julbe, A.; Guizard, C.; Basile, A.; Cot, L.; Drioli, E. "Synthesis and characterization of a mordenite membrane on an Al_2O_3 tubular support". J. Mater. Chem. 2000, 10, 1131.

2. Lai, R.; Gavalas, G. R. "ZSM-5 membrane synthesis with organic-free mixtures". Microporous and Mesoporous Materials, 2000, 38, 239.

3. Nenoff, T. M.; Bonhomme, F. "Defect-free thin film membranes for Hydrogen separation and isolation". 14th World Hydrogen Energy Conference Proceedings, Montreal, Canada, 2002, in press.

4. Bonhomme, F.; Nenoff, T. M. "Defect-free zeolite membranes for CO_2 separations".

Microporous and Mesoporous Materials, 2002, in preparation.

5. Chou, K. S.; Wang, S. M. "Studies on the preparation of Pd/alumina/porous stainless steel membranes for hydrogen separation". J. Chinese Inst. Chem. Eng., 2000, 31, 499.

6. Bonhomme, F., Thoma, S. G., Rodriguez, M. A., Nenoff, T. M. "$Ga_4(PO_4)_4F{\cdot}N_2C_7H_{11}{\cdot}\ 0.5H_2O$, A 3D Open Framework with 12-member Pores and "bowl-shaped" Building Units". Chem. Mater., 2001, 13(6), 2112.

7. Thoma, S. G.; Nenoff, T. M. "A New Method for Synthesizing Defect-Free Thin Film Membranes: Composite Zeolite/Sol-gel Membranes". SD-6222, US Patent Submission, 2000.

FY 2002 Publications/Presentations

1. Nenoff, T. M.; Bonhomme, F. "Defect-free thin film membranes for Hydrogen separation and isolation". 14th World Hydrogen Energy Conference Proceedings, Montreal, Canada, 2002, in press.

2. Bonhomme, F.; Thoma, S. T.; Nenoff, T. M. "Two ammonium templated gallophosphates: Synthesis and structure determination from powder diffraction data of 2D and 3D-GAPON". Micro. & Meso. Materials, 2002, 53, 87.

3. Bonhomme, F.; Thoma, S. G., Rodriguez; M. A.; Nenoff, T. M. "$Ga_4(PO_4)_4F{\cdot}N_2C_7H11{\cdot}\ 0.5H_2O$, A 3D Open Framework with 12-member Pores and "bowl-shaped" Building Units". Chem. Mater., 2001, 13(6), 2112.

4. Bonhomme, F.; Thoma, S. G.; Rodriguez; M. A., Nenoff, T. M. "Piperazine templated 3D flurogallophosphate: Synthesis and characterization of $Ga_5(PO_4)_5F_4$-$2[N_2C_4H_{12}]$". Micro. & Mesoporous Materials, 2001, 47(2-3), 185.

5. Bonhomme, F.; Thoma; S. G., Nyman; M., Rodriguez; M. A., Nenoff, T. M. "Synthesis and Crystal Structure of Guanidinium Tetrafluoro(trans-) dipyridinechromate(III), $[CrF_4(C_5H_5N)_2]^-CN_3H_6^+$". J. Fluorine Chem., 2001, 108, 73.

6. Mitchell, M. C.; Autry, J. D.; Nenoff, T. M. "Molecular Dynamics Simulations of Binary Mixtures of Methane and Hydrogen in Zeolite A and a Novel Zinc Phosphate". Mole. Physics, 2001, 99(22), 1831.

7. Bonhomme, F.; Thoma, S. G.; Nenoff, T. M. "A linear DABCO templated fluorogallophosphate: Synthesis and Characterization of $Ga(PO_4H)_2F{\cdot}[N_2C_6H_{14}]$". J. Mater. Chem. 2001, 11(10), 2559.

8. T. M. Nenoff, F. Bonhomme, "Defect-Free Thin Film Membranes for H_2 Separation and Isolation", 14th World Hydrogen Energy Conference, Montreal, Canada, June 10, 2002.

Special Recognitions & Awards/Patents Issued

1. T.M. Nenoff; F. Bonhomme; "Zeolite Membranes with High CO_2 Selectivity". US Patent submitted to Sandia National Laboratories, August 2002.

II.C.11 DFMA Cost Estimates of Fuel-Cell/Reformer Systems at Low/Medium/ High Production Rates

Brian D. James (Primary Contact), Gregory D. Ariff, Reed C. Kuhn
Directed Technologies, Inc.
3601 Wilson Blvd., Suite 650
Arlington, VA 22201
(703) 243-3383, fax: (703) 243-2724, e-mail: Brian_James@DirectedTechnologies.com

DOE Technology Development Manager: Sigmund Gronich
(202) 586-1623, fax: (202) 586-5860, e-mail: Sigmund.Gronich@ee.doe.gov

ANL Technical Advisor: Walter Podolski
(630) 252-7558, fax: (630) 972-4430, email: podolski@cmt.anl.gov

Objectives

- Develop realistic and internally consistent detailed designs for automotive gasoline fuel processors and direct hydrogen PEM fuel cell systems based on current-year technology.
- Apply Design for Manufacture and Assembly (DFMA) design and costing techniques to compare system designs at low, medium, and high annual production rates.

Approach

- Update design and cost estimate for baseline 0.7 V/cell peak-power reformer/fuel cell system.
- Develop detailed designs for three additional 50 kW_{net} PEM fuel cell systems: 0.6 V/cell reformer system, 0.7 V/cell direct hydrogen system, 0.6 V/cell direct hydrogen system.
- Apply DFMA techniques to assess manufacturing methods and costs for each system for comparison to baseline.

Accomplishments

- Completed detailed baseline design and thermodynamic modeling.
- Performed annual update to cost estimates of baseline system with more detailed estimates of peripheral components.
- Completed cost estimates of additional reformer and direct hydrogen systems for comparison to baseline.

Future Directions

- Update baseline reformer and fuel cell cost estimates to reflect advances in technology and additional manufacturing and design improvements. Conduct a series of in-depth trade studies on selected issues to assess pathways to lower cost systems.

Introduction

Directed Technologies Inc. (DTI) has performed a DFMA-style cost estimation for an onboard gasoline reformer and fuel cell system at several annual production volumes. The DFMA technique is a rigorous design/redesign and cost estimation methodology developed by Boothroyd and Dewhurst[1] and adapted by DTI. In a previous report[2], DTI analyzed the cost of a 50 kW_{net} baseline

system. The current report presents refined costs for the baseline system as well as comparisons to an alternate reformer/fuel cell system and two direct hydrogen fuel cell systems.

Approach

The contract statement of work defines four tasks to be completed by DTI. Having completed and reported the results for Task 1 and Task 2, our efforts are currently focused on Tasks 3 and 4. In Task 1, DTI specified the basic layout of the system and operating conditions. In Task 2, DFMA was used to identify the low-cost design and production methods and provide estimated material, manufacturing, and assembly costs. These results were reported in the "Fuel Cells for Transportation 2001 Annual Progress Report". Task 3 consists of annual updates and refinements of the system cost to reflect changing technology and new information. In Task 4, a variety of trade-off studies will be used to elaborate on basic system architecture and operating modes.

For this report, the DFMA methodology was applied to refine costs for the baseline 0.7 V/cell reformer/fuel cell system at production rates of 500, 10,000, 30,000, and 500,000 units per year. Additionally, three other systems were analyzed for comparison to the baseline: a gasoline reformer/fuel cell system operating at 0.6 V/cell (at peak power), a direct hydrogen system operating at 0.7 V/cell, and a direct hydrogen system operating at 0.6 V/cell. Each system is designed to provide 50 kW of net electrical power. The bills of materials for reformer/fuel cell systems and direct hydrogen systems are shown in Table 1. Items specifically not included in this analysis are the Traction Inverter Module, the main automotive electric motor, and any peak-power or load-leveling battery system.

Results

Reformer/fuel cell system definition

Figure 1 shows the system schematic for a gasoline reformer/fuel cell system. The drawing applies to both the 0.7 V/cell and 0.6 V/cell systems, which only differ dimensionally. In these systems, California reformulated gasoline is pumped from the fuel tank and injected into the integrated autothermal

Subsystem	Reformer/FC	Direct hydrogen
Fuel Loop	Fuel tank assembly High-pressure fuel pump High-pressure fuel injector	Compressed H_2 tank H_2 recirculation ejector H_2 intank solenoid & PRD
Fuel Cell Stacks	MEA and bipolar plate Endplates and brackets	MEA and bipolar plate Endplates and brackets
Air Loop	Air compressor/ expander Air mass flow sensors Air throttle body Air humidifier	Air compressor/ expander Air mass flow sensor Air humidifier
Water Loop	Water pump & reservoir Knock-out drum, condensers High-pressure rail system Water deionization filter	Water pump & reservoir Knock-out drum, condensers High-pressure rail system Water deionization filter
Coolant Loop	Pump, motor, controller Radiator assembly Thermostat, bypass valve	Pump, motor, controller Radiator assembly Thermostat, bypass valve
Controls	Electronic engine controller CO sensors	Electronic engine controllers
Misc./ Balance of Plant	Start-up battery Electrical System mounting Misc.	Start-up battery Electrical System mounting Misc.
Integrated ATR Assembly	Autothermal reactor Water gas shift reactors Sulfur removal Water boiler	N/A
Reformate Loop	PrOx unit Air control solenoid Catalytic burner Condenser	N/A

Table 1. Bill of Materials for Gasoline Reformer and Direct Hydrogen Fuel Cell Systems

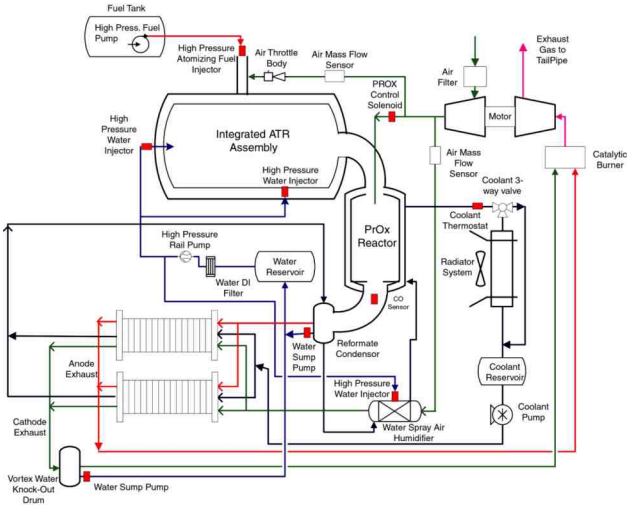

Figure 1. Gasoline Reformer/Fuel Cell System Schematic

reformer (ATR) assembly (which includes an ATR section, high and low temperature water-gas shift sections, and sulfur removal bed) where it is mixed with air and steam to generate a hydrogen-rich reformate stream. This gas stream is then sent to the preferential oxidation reactor (PrOx) to convert water and carbon monoxide to additional hydrogen and carbon dioxide. After the remaining water is condensed for removal, the reformate enters the PEM fuel cell where the hydrogen reacts with oxygen from air to generate electricity and heat. The unreacted fuel and air streams are mixed and burned in a catalytic burner and expanded in an exhaust gas expander to derive power for the air compressor.

The fuel cell system has four stacks containing 110 cells each. Table 2 provides details of each stack and its parameters. Because the reformate contains small amounts of carbon monoxide (<50 ppm) which can poison the platinum membrane catalyst, the catalyst loadings are significantly higher than for direct hydrogen systems (0.7 g/cm^2 versus 0.15 g/cm^2). The fuel cell performance is further hindered by the dilution of hydrogen due to the CO_2 and N_2 in the reformate stream, resulting in lower power densities (higher membrane areas).

Direct Hydrogen system definition

Figure 2 shows the system schematic for a direct hydrogen reformer/fuel cell system. Compressed hydrogen is stored in a carbon-fiber wrapped composite vessel at pressures up to 340 atm. It is fed through a control valve to the fuel cell at 2 atm, where it reacts with oxygen from air to generate electricity and heat. Unreacted hydrogen is

Peak Power Conditions	**0.7 V/cell ATR (baseline)**	**0.6 V/cell ATR**	**0.7 V/cell Direct H_2**	**0.6 V/cell Direct H_2**
Gross Power (kW)	55	56	56	57
Net Power (kW)	50	50	50	50
Cell Voltage (V)	0.7	0.6	0.7	0.6
Current Density (mA/cm^2)	400	650	600	1076
Nom. Operating Pressure (atm)	2.2	2.2	2.2	2.2
Power Density (mW/cm^2)	280	390	420	646
No. of strands	1	1	1	1
No. of stacks/strand	4	4	4	4
No. of cells/stack	110	110	110	110
Total active membrane area (m^2)	19.64	14.36	13.33	8.83
Active area/cell (cm^2)	446	326	303	201
Peak voltage (@ 0.92 V/cell) (V)	405	405	405	405
Min. voltage (@ peak power) (V)	308	264	308	264
Max current (@ peak power) (A)	178.6	212.1	181.8	215.9
Catalyst loading				
Cathode (mg/cm^2)	0.3 Pt	0.3 Pt	0.10 Pt	0.10 Pt
Anode (mg/cm^2)	0.4 Pt 0.2 Ru	0.4 Pt 0.2 Ru	0.05 Pt	0.05 Pt
Stack efficiency*	41.5%	35.1%	51.1%	43.1%
Onboard System efficiency*	33.4%	28.2%	51.1%	43.1%

* Stack efficieny is the electrical power output of the fuel cell stack divided by the lower heating value (LHV) per unit time of hydrogen entering the stack. System efficiency is the net electrical power of the system divided by the LHV per unit time of the fuel feed (gasoline for reformer system, hydrogen for direct hydrogen system).

Table 2. Operating Parameters for ATR and Direct H_2 Fuel Cell Systems

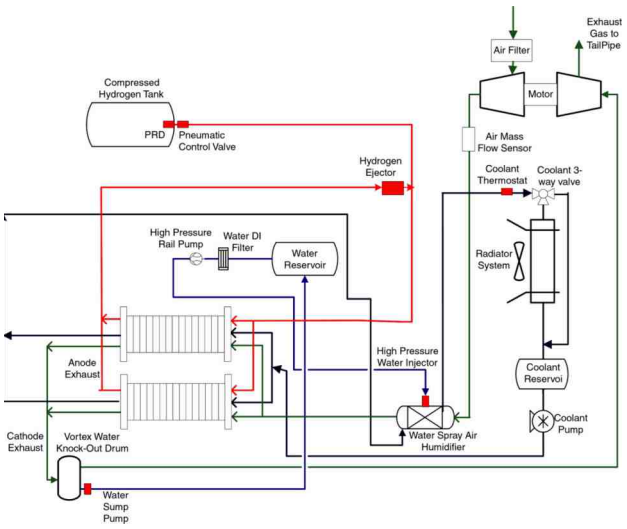

Figure 2. Direct Hydrogen Fuel Cell System Schematic

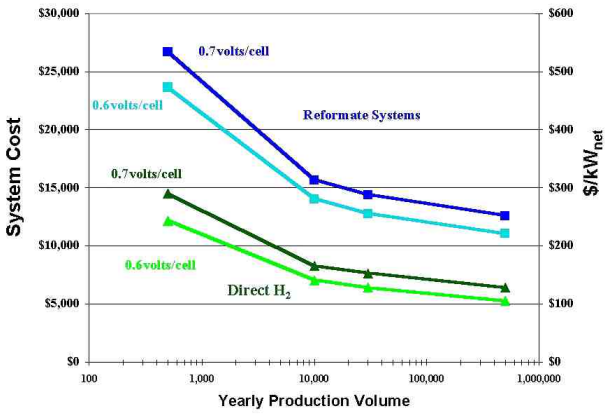

Figure 3. Power System Cost vs. Production Rate for ATR and Direct Hydrogen Systems (50 kW)

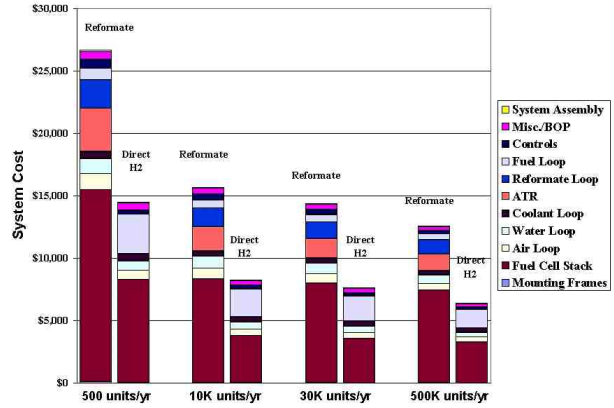

Figure 4. Comparison of 0.7 V/cell ATR and Direct H_2 System Costs (50 kW)

recirculated to prevent loss of hydrogen from the system, while the oxygen-depleted air stream is exhausted.

Like the reformer systems, four PEM fuel cell stacks of 110 cells each are used. These stacks are smaller and have lower catalyst loading than those for the reformer systems because the hydrogen is 99.99% pure, containing less than 10 ppm carbon monoxide. Stack parameters for the direct hydrogen systems are compared to those for the reformer systems in Table 2.

Cost estimates

Cost estimates for each system at each of the four production levels are the sum of materials, manufacturing, and assembly costs, as well as a manufacturer's markup and a 10% cost contingency (as is standard automotive cost estimation practice). As might be expected, cost of the finished system decreases with increasing production volume.

Figure 3 shows the cost of each of the four systems at four different production volumes. The reformer/fuel cell system designed for peak power at 0.6 V/cell offers some cost reductions compared to the baseline, but both direct hydrogen fuel cell systems are significantly less expensive than either of the reformer/fuel cell systems. This cost reduction is primarily due to the decreased size and cost of the fuel cell stack, as can be seen in Figure 4. The reformate loop and ATR are also eliminated in the direct hydrogen systems, but the fuel loop bears the cost of the fiber-wrapped composite tank for compressed hydrogen.

In all four systems studied and at all production rates, the fuel cell stack accounts for more than half of the total system cost. The cost of the stack is dominated by the membrane electrode assembly (MEA), as shown in Figure 5 for the 0.7 V/cell reformate fuel cell. The membrane material and catalyst account for roughly 85% of the MEA cost in the reformate systems and 62-76% in the direct hydrogen systems (low-high production volumes).

Differences in cost between the updated baseline system reflected in this report and preliminary costs

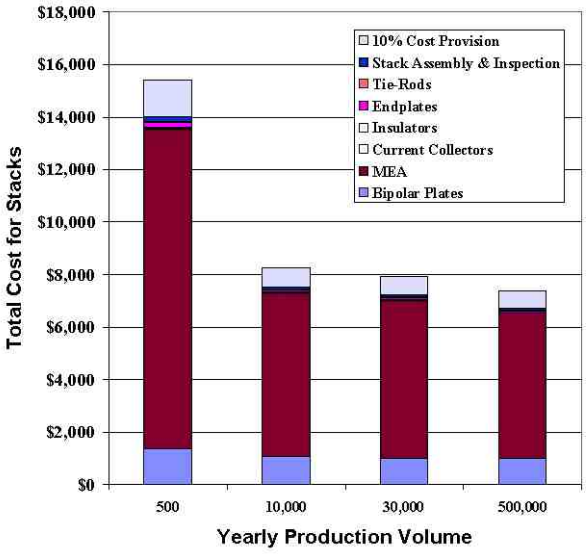

Figure 5. Cost Breakdown for Fuel Cell Stacks in 0.7 V/cell ATR System (50 kW)

from the previous report are the result of the more rigorous and thorough cost methodology performed in the past year. The updated costs, however, result in only a 3-4% change in total system cost for all production rates.

Conclusions

Capital costs for fuel cell power systems vary with production rates, peak power voltage conditions, and hydrogen source (reformate vs. direct). As with most manufactured products, the cost of materials, manufacturing, and assembly decrease with increasing annual production volumes. Designing the fuel cell stack to operate at lower voltages at peak power (0.6 V/cell vs. 0.7 V/cell) offers capital cost savings at the expense of system efficiency.

Power systems for hydrogen fuel cell vehicles are costly, with approximately half the cost coming from the fuel cell stacks. Because the MEA accounts for sixty to ninety percent of the stack cost, the cost of the entire power system is highly dependent on the total membrane area of the system. Due to the low hydrogen quality of the fuel stream in reformate/fuel cell systems, the membrane area and catalyst loadings in such systems significantly exceed those in direct hydrogen systems, driving up the cost of the power system. This cost difference is true at all production levels, from initial introduction of fuel cell vehicles through full public acceptance. Overall system costs range from $105/kW to $243/kW for the 0.6 V/cell direct hydrogen system and $221/kW to $472/kW for the 0.6 V/cell reformate system. Comparable systems operating at 0.7 V/cell cost approximately 12% to 22% more than the 0.6 V/cell versions.

References

1. Boothroyd, G., Dewhurst, P., and Knight, W. *Product Design for Manufacture and Assembly, Second Edition*. Marcel Dekker, Inc. New York, 2002.

2. James, B., Thomas, C.E., Ho, J., and Lomax, F. "DFMA Cost Estimates of Fuel-Cell/Reformer Systems at Low/Medium/High Production Rates" in *Fuel Cells for Transportation: 2001 Annual Progress Report*. U.S. Department of Energy, Office of Advanced Automotive Technology. Washington, D.C., 2001.

Presentations

1. This work was presented by Brian D. James at the SAE Future Car Congress in Washington, D.C. on June 7, 2002.

II.D Electrolytic Processes

II.D.1 Photoelectrochemical Systems for Hydrogen Production

Ken Varner, Scott Warren, J.A. Turner (Primary Contact)
National Renewable Energy Laboratory
1617 Cole Blvd.
Golden, CO 80401
(303) 275-4270, fax: (303) 275-3033, e-mail: john_turner@nrel.gov

DOE Technology Development Manager: Roxanne Danz
(202) 586-7260, fax: (202) 586-9811, e-mail: Roxanne.Danz@ee.doe.gov

Objectives

- Identify and characterize possible semiconductor materials that have appropriate bandgaps and are stable in aqueous solutions.
- Study multi-junction semiconductor systems for higher efficiency water splitting.
- Develop techniques for the preparation of transparent catalytic coatings and their application to semiconductor surfaces.
- Identify environmental factors (i.e., pH, ionic strength, solution composition, etc.) that affect the energetics of the semiconductor, the properties of the catalysts, and the stability of the semiconductor.
- Develop techniques for the energetic control of the semiconductor electrolyte interphase.

Approach

- Identify new semiconductor materials with bandgaps in the ideal range.
- Catalyze the surfaces and engineer the bandedges of the identified semiconductor materials as required.
- Determine if existing photovoltaic (PV) device structures could be easily modified to effect the direct splitting of water.

Accomplishments

- Work on the stability and efficiency characteristics of amorphous silicon structures for direct water splitting systems clearly showed that it is feasible to utilize amorphous silicon devices in direct contact with aqueous electrolytes without additional protective coatings.
- Work on the study of gallium indium nitride materials for water splitting showed that if the bandgap can be reduced, these materials have very promising bandedge energetics and stabilities.
- Studies of bandedge engineering of gallium indium phosphide (p-$GaInP_2$) have shown that the bandedges can be controlled within a small range of pHs.

Future Directions

- Continue to evaluate samples of new semiconducting materials with appropriate bandgaps.
- Continue to design and test additional multi-junction systems (CuGaInSSe, GaPN, and GaInN materials, and a-Si triple junction systems) for possible photoelectrochemical water splitting.

- Study the stability of semiconductor materials and coatings for protection against corrosion.
- Develop techniques for controlling the semiconductor energetics so that the bandedges are matched for water splitting, and identify factors that influence the catalysts of hydrogen and oxygen.

Introduction

The goal of this research is to develop a stable, cost-effective, photoelectrochemical (PEC)-based system that will split water upon illumination, producing hydrogen and oxygen directly, using sunlight as the only energy input. Past work has shown that PEC hydrogen producing devices can have an efficiency 30% higher than separated PV electrolysis devices, and analysis work has shown that the cost of PEC hydrogen can be lower than PVelectrolysis. For direct photoelectrochemical decomposition of water to occur, the following conditions must be met:

- The semiconductor system must generate sufficient voltage to split water.
- The energetic of the semiconductor must overlap those of the hydrogen and oxygen redox reactions.
- The semiconductor system must be stable in aqueous electrolytes.
- The charge transfer from the surface of the semiconductor must be fast enough to prevent corrosion and reduce energy losses due to overvoltage.

In developing PEC hydrogen systems that will meet these requirements, research efforts are focused in two areas: (1) chemical modification of the semiconductor electrode surface material to improve system energetics, and (2) evaluation of triple-junction amorphous silicon structures as low-cost thin-film water splitting systems.

Approach

Surface Modification of Semiconductor Material

Gallium indium phosphide (p-$GaInP_2$) is a semiconducting material that meets the bandgap energy criteria, but does not meet the bandedge overlap criteria required for PEC hydrogen production. This electrode also accumulates photogenerated charges at its surface, contributing to surface corrosion and bandedge migration away from the desired electrode energetics. In this research, p-$GaInP_2$ surfaces were modified by adsorption of metallated porphyrins and transition metals with the aim of moving bandedge energies and catalyzing interfacial charge transfer for PEC hydrogen generation.

Characterization of Triple-Junction Amorphous Silicon Systems

Low-cost solid state multi-junction systems, based on triple-junction amorphous silicon (a-Si) solar cells, have voltages sufficient for water splitting, and the cells can be tailored to produce voltages matched to the energetic requirements of the water splitting reaction. In this research, efforts focused on characterization of various a-Si triple junction samples. These samples underwent current-voltage tests, corrosion measurements, and metal-ion catalyst treatments. Because of the instability of a-Si in an aqueous environment, research efforts included evaluation of a surface coating of amorphous silicon carbide (a-SiC) to stabilize and protect the system. The a-SiC samples were tested for their effect on the overall efficiency of water splitting and their effectiveness in protecting the underlying semiconducting material from corrosion.

Results

Surface Modification of Semiconductor Material

After initial characterization of the p-$GaInP_2$ electrode material, seven different porphyrin treatments were evaluated for their ability to modify the surface of the p-$GaInP_2$ electrode. All of the porphyrins show a statistically significant shift in flat band potential, with the ruthenated porphyrins showing the greatest shift. The bandedges shifted into overlap conditions about 20% of the time with ruthenium octaethyl porphyrin carbonyl RuOEP CO. The variability observed in the flat band potential was attributed to the porphyrin application method and/or the age of the electrode, both of which affect the amount of porphyrin on the p-$GaInP_2$ surface.

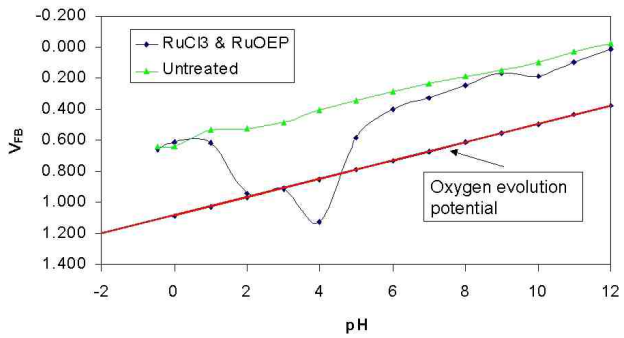

Figure 1. The effect of pH on the flat band potential of an untreated electrode and an electrode treated with both ruthenium chloride ($RuCl_3$) and RuOEP CO. Dip-coating an untreated electrode with $RuCl_3$ and then drop-evaporating RuOEP CO vastly improves charge catalysis properties up to a photocurrent of 1 mA/cm^2. Testing is in a 4 pH buffer. The most substantial shift in flat band potential occurs at pH 4, hence the testing at that pH.

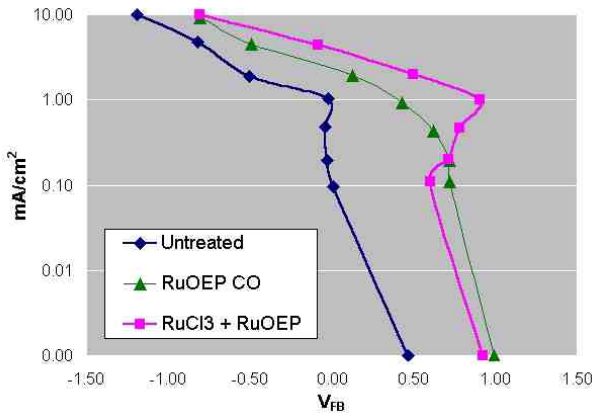

Figure 2. Charge transfer catalysis of various treatments. Testing performed in pH 4 buffer.

When combining the RuOEP CO with a transition metal, such as ruthenium or platinum, the bandedge shift increases up to 0.48 electron volts (eV) in the positive direction. These combination treatments allowed overlap of the water redox potentials to occur in the dark. The effect of pH on the flat band potential of an untreated electrode and

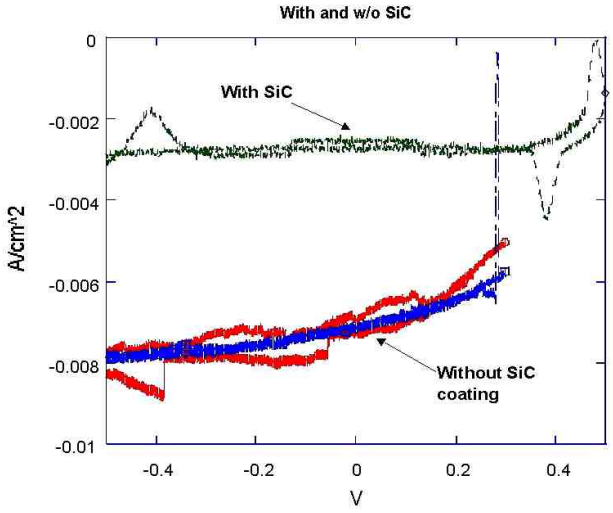

Figure 3. Comparison of the photocurrent for coated and uncoated samples in acid.

an electrode treated with RuOEP CO in combination with transition metals is shown in Figure 1. The largest shifts in flat band potential occurred at a pH of 4. Adding platinum or ruthenium to the porphyrin also significantly improves the charge transfer catalysis properties under light irradiation up to a photocurrent of 1 mA/cm^2, as shown in Figure 2. Despite the improved placement of bandedges, no significant change in the two-electrode current-voltage curve was perceptible. In addition, differences in open circuit cell potential between modified and unmodified systems were not statistically significant.

Characterization of Triple-Junction Amorphous Silicon Systems

In order to evaluate the effectiveness of a-SiC as a protective layer on a triple-junction a-Si device, triple-junction a-Si devices, both with and without a-SiC deposited on the surface, were exposed to chemically aggressive basic (1 molar [M] potassium hydroxide [KOH]) and acidic (1 M sulfuric acid) solutions. Current density measurements showed that the a-SiC coating provided some protection in the basic solution, but in acid, no noticeable difference occurred between the protected and non-protected samples. This suggests that a-SiC may not be necessary to protect the device, especially when the electrolyte solution is acidic.

However, as shown in Figure 3, in some cases, the a-SiC actually decreases the current density as compared to an unprotected sample. Because the a-SiC is deposited on the surface of the electrode, its physical and optical properties must be optimized to work with the a-Si triple junction it is designed to protect. Researchers determined that for a-SiC to be effective in this device without hindering the photocurrent, bandgaps in the 2.5 eV range and higher would be ideal. In addition to the light, electrons must also be able to move through the a-SiC to effect water splitting. Because it has a finite thickness, there will be some resistance associated with it. The resistance of a-SiC samples ranged from 0.8-1.0 ohm (Ù). At 15 milliamps per centimeters squared mA/cm^2 (typical photocurrent values), a 1 Ù resistance causes a 15 millivolts (mV) decrease in voltage, which would drop the current and corresponding hydrogen production by a factor of 2.5. Much additional work needs to be done to optimize this material before it can be used as a protective coating, including increasing the a-SiC's bandgap and decreasing the resistance, or possibly integrating the top cell in the device with a-Si and a-SiC.

Conclusions

- The surface of p-GaInP$_2$ can be modified by adsorption of metallated porphyrins and transition metals, resulting in improved energetics and catalysis for PEC water splitting.
- It is feasible to utilize amorphous silicon devices in direct contact with aqueous electrolytes without an additional protective coating.
- The combination of an optimized protective coating and an inherent underlying stability in the semiconductor material itself can lead to an extended lifetime in operation, because a breach in the protective layer would not be fatal to the device.
- Continued work with Energy Conversion Devices, Inc. to optimize the triple junction for increased efficiency and to tune the top layer for optimum stability is clearly indicated.

FY 2002 Publications/Presentations

1. Breach, J.D., Al-Thani, H., McCray, S., Collins, R.T., and Turner, J.A. "Bandgaps and Lattice Parameters of 0.9 ìm thick $In_xGa_{1-x}N$ Films for $0 \leq x < 0.140$," Journal of Applied Physics, 91 (May 1, 2002).

2. Aroutiounian, V.M., Arakelyan, V.M., Shahnazaryan, G.E., Stepanyan, G.M., Turner, J.A., and Khaselev, O. "Investigation of Ceramic Photoelectrodes Fe_2O_3<Ta> For Solar Energy Photoelectrochemical Converter," International Journal of Hydrogen Energy, 27, pp. 33-38 (January 2002).

3. Sebastian, P.J., Mathews, N.R., Pattabi, X., and Turner, J.A. "Photoelectrochemical Characterization of SiC," International Journal of Hydrogen Energy, 26, p. 123 (2001).

4. Turner, John A. "Renewable Energy: Generation, Storage, and Utilization," in Carbon Management: Implications for R&D in the Chemical Sciences Technology: A Workshop Report to the Chemical Sciences Roundtable, National Academy Press (2001).

5. Mathew, X., Bansal, A., Turner, J.A., Mathews, N.R., and Sebastion, P.J. "Photoelectrochemical Characterization of Surface Modified CdTe for Hydrogen Production," submitted to International Journal on New Materials for Electrochemical Systems.

6. Fernández, A.M. and Turner, J.A. "Preparation and Photocharacterization of Cu-Sb-Se Films Prepared by Electrodeposition," submitted to Solar Energy Materials and Solar Cells.

7. The Energy Council's 2001 State Trends in Energy and the Environment, entitled "Long Term Research on Solar Production of Hydrogen", June 30, 2001.

8. American Chemical Society meeting in Chicago, IL entitled "Renewable Energy: Sustainable Energy for all Future Generations", August 26, 2001.

9. General Motors Corporation, entitled "Renewable Energy, Hydrogen, and Direct Water-Splitting Systems", September 17, 2001.

10. Chemistry Department of the Colorado School of Mines entitled "Photoelectrochemical Direct Water Splitting Systems", October 4, 2001.

11. North Carolina State University entitled "Photoelectrochemical Systems for Hydrogen Production via Direct Water Splitting", October 30, 2001.

12. Lecture on basic fuel cell technology and operation at the ICBO/SBCCI Conference in Greensboro, NC, November 1, 2001.

13. National Academy of Sciences/National Research Council Workshop on Carbon Management, entitled "Renewable Energy: Generation, Storage and Utilization", January 8, 2002.

14. The USDOE Hydrogen Program's first Quarterly Program Performance and Results Briefing, for upper DOE management entitled "Advances in Photoelectrochemical Hydrogen Production Technologies", February 20, 2002.

15. American Institute of Chemical Engineers' Spring meeting, in a session on climate change, entitled "The Renewable Energy and Hydrogen Infrastructure", March 12, 2002.

16. American Physical Society's Spring meeting, in a session on climate change, entitled "Renewable Energy: Energy Security and Sustainability", March 19, 2002.

II.D.2 Photoelectrochemical Hydrogen Production

Eric L. Miller (Primary Contact), Richard E. Rocheleau
Hawaii Natural Energy Institute, University of Hawaii, Manoa
1680 East-West Road, POST 116
Honolulu, HI 96822
(808) 988-5337, fax: (808) 956-2336, e-mail: ericm@hawaii.edu

DOE Technology Development Manager: Roxanne Danz
(202) 586-7260, fax: (202) 586-9811, e-mail: Roxanne.Danz@ee.doe.gov

Main Subcontractor: University of Toledo, Toledo, OH

Objectives

- To develop high efficiency, cost-effective photoelectrochemical processes for the production of hydrogen.
- To engineer stable multi-junction photoelectrodes based on low-cost materials [such as stainless steel (SS) foil, amorphous silicon/germanium (a-Si:Ge), copper-indium-gallium-diselenide (CIGS), iron oxide (Fe_2O_3), etc.] that match energy requirements for efficient hydrogen production.
- To design, fabricate and test optimized photoelectrodes suitable for eventual commercial-scale use.

Approach

- Develop multi-junction a-Si:Ge and CIGS photovoltaic structures incorporating additional catalyst and protective thin film layers for use as hydrogen photoelectrodes.
- Establish industry and university partners to accelerate development of advanced thin-film materials and devices for photoelectrode use.
- Upgrade in-house fabrication facilities for advanced materials and devices.
- Adapt integrated electronic/optical/electrochemical models for analysis of advanced a-Si:Ge and CIGS photoelectrode configurations, including "hybrid" devices combining solid-state and photoelectrochemical junctions.
- To design, fabricate and test prototype photoelectrode systems for efficiency and stability.

Accomplishments

- Maintained present and established new university and industrial partnerships for developing advanced a-Si:Ge and CIGS materials and devices.
- Upgraded University of Hawaii (UH) in-house a-Si:Ge and CIGS deposition systems.
- Demonstrated 12% efficiency in in-house fabricated CIGS solar cells (2" x 4").
- Established partnerships for development of Fe_2O_3, WO_3 and TiO_2 for use in hybrid photoelectrode designs.
- Adapted models for hybrid photoelectrode analysis.
- Performed initial modeling of hybrid photoelectrodes using published data for nano-structured Fe_2O_3, WO_3 and TiO_2 films.
- Selected Fe_2O_3 for initial hybrid photoelectrodes based on model results.
- Initiated program to develop Fe_2O_3 in-house, and with Duquesne University.

- Completed an evaluation of a-Si:Ge devices deposited on various metal-foil substrates for determining optimal yield (with the University of Toledo).
- Fabricated initial set of multi-junction a-Si:Ge devices for use in preliminary hybrid photoelectrode tests (with the University of Toledo).

Future Directions

- Complete fabrication and testing of initial hybrid photoelectrode prototypes.
- Identify materials and design issues needed for improving hybrid photoelectrode performance.
- Continue cooperative partnerships with research organizations to further develop optimized a-Si:Ge, CIGS, Fe_2O_3, WO_3 and TiO_2 materials.
- Design, fabricate and evaluate optimized multi-junction a-Si:Ge hybrid photoelectrodes.
- Design higher-efficiency hybrid photoelectrodes using advanced CIGS tandem configurations.

Introduction

In recent years under the sponsorship of the U.S. Department of Energy (DOE), the Thin Films Laboratory at the Hawaii Natural Energy Institute of the University of Hawaii (UH) has been developing high-efficiency, potentially low-cost, photoelectrochemical (PEC) systems to produce hydrogen directly from water using sunlight as the energy source. The main thrust of the PEC systems research at UH has been the development of integrated multi-junction photoelectrodes, comprising semiconductor, catalytic, and protective thinfilms deposited on inexpensive substrates (such as stainless steel), for solar hydrogen production [1].

Figure 1a shows sunlight shining on photoactive regions of a generic photoelectrode, producing electric current to drive the hydrogen and oxygen evolution reactions at opposite surfaces. In the conceptual design for a large-scale reactor shown in Figure 1b, arrays of photoelectrodes are arranged in tubular reactors, and electrolyte is circulated to extract the high-purity hydrogen and oxygen gases produced, which are separated using membranes (as shown in Figure 1c). In order to meet the DOE's goals, the photoelectrode system must be low-cost and must be capable of operating stably in corrosive aqueous electrolyte environments with solar-to-hydrogen (STH) conversion efficiencies greater than 10%.

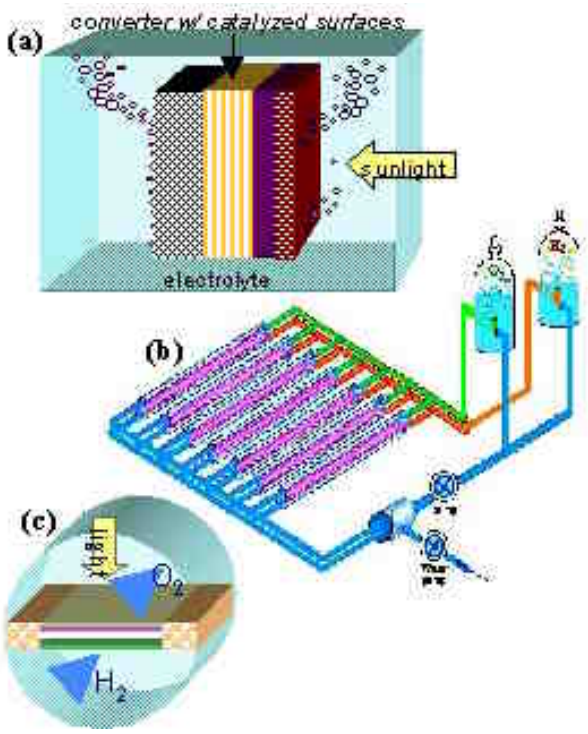

Figure 1. (a) Integrated planar photoelectrode for H_2 production; (b) Conceptual design of large-scale reactor; (c) Photoelectrode installed in collection tubes with separating membrane

Approach

Numerous approaches involving a variety of semiconductors have been explored for hydrogen photoelectrolysis since the early 1980s, but none

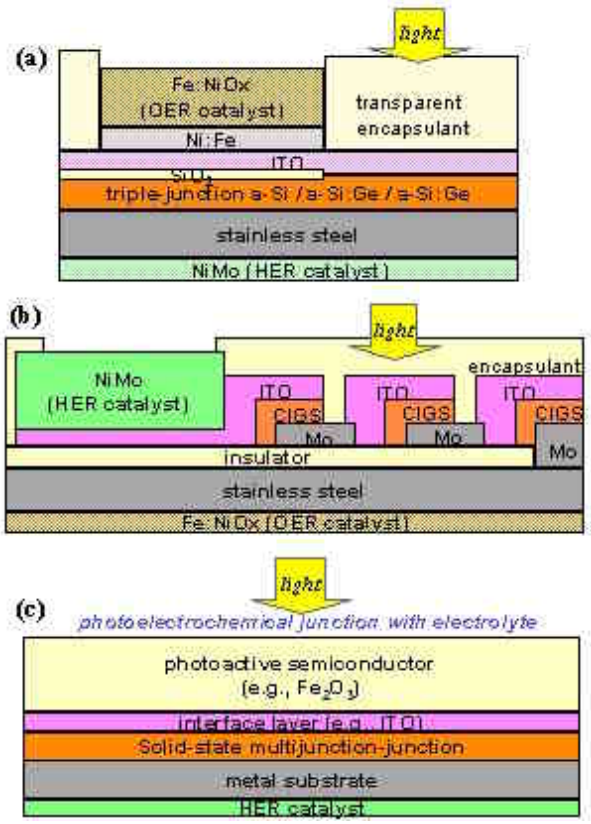

Figure 2. Encapsulated triple-junction photoelectrodes using (a) a-Si:Ge; (b) CIGS; and (c) basic structure of a hybrid solid-state/ photoelectrochemical photoelectrode

Note: HER = hydrogen evolution reaction
OER = oxygen evolution reaction

have successfully met both efficiency and stability goals. A photoelectrode design approach developed at UH incorporates multi-junction thin-film photoconvertors for high voltage along with thin-film catalyst and protective layers for stability. This research approach has relied on continued use of integrated models for photoelectrode design; establishment of industry and university partners with materials expertise and fabrication capabilities; and fabrication and evaluation of photoelectrode test structures for photoactivity and stability.

Examples of photoelectrode designs developed using this approach are shown in Figure 2, including (a) monolithically-stacked amorphous silicon/ germanium (a-Si:Ge), and (b) side-by-side stacked copper-indium-gallium-diselenide (CIGS) encapsulated triple-junction devices [2]. An important recent advance has been the design of a "hybrid" photoelectrode structure, shown in Figure 2c, combining solid-state multi-junctions with stable, photoactive semiconductor outer layers. Significant advantages of this hybrid design include elimination of lateral current collection, simplification of device geometry for ease of fabrication, and improved stability based on the thick, seamless outer oxide layer. Development of high performance hybrid photoelectrode structures using low-cost materials such as a-Si:Ge, CIGS and photoactive nano-structured iron oxide (Fe_2O_3) is currently the primary focus of our work.

Results

To date, significant progress has been made in the advancement of a-Si:Ge and CIGS materials and devices for use in photoelectrode applications, and in the initial development of hybrid photoelectrode designs. Important industry and academic partnerships have been established, in-house materials fabrication facilities have been significantly upgraded, and integrated models have been adapted for the design of prototype hybrid photoelectrode structures.

This past year, while maintaining close ties with the Institute for Energy Conversion (IEC) at the University of Delaware, who have recently reported progress in several key areas of CIGS research (including deposition of high-performance cells onto lightweight polyamide substrates [3]), and with the University of Toledo, who has reported photovoltaic efficiencies approaching 13% in multi-junction a-Si:Ge devices [4], we've also established a critical industry partnership with Daystar Technologies, whose principal scientist has reported record efficiencies approaching 19% in thin-film CIGS devices [5]. Another important new partnership established this year has been with Dr. Shahed Khan at Duquesne University, who has demonstrated nanostructured Fe_2O_3 films with good photoactivity deposited by spray pyrolysis [6], and who has been enthusiastic to participate in our hybrid photoelectrode research.

Partly with the help of our industry and university partners, we have successfully completed

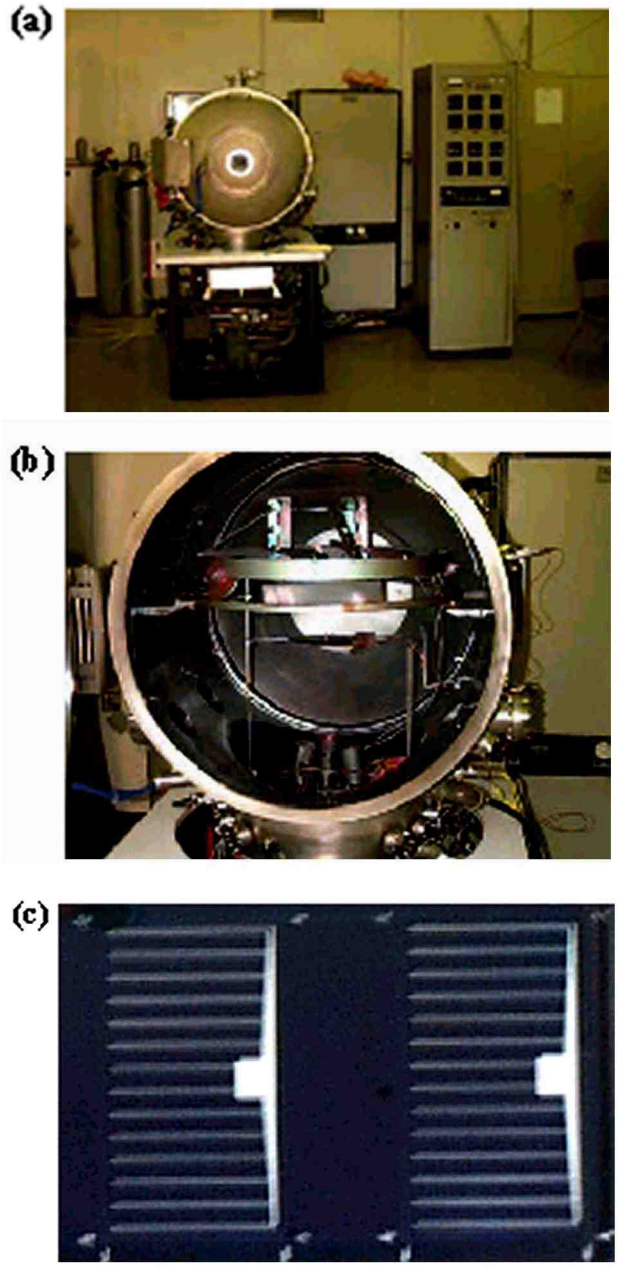

Figure 3. (a) CIGS deposition system at UH; (b) Interior view; (c) Completed CIGS PV device

important upgrades of our in-house materials fabrication equipment. The upgraded plasma-enhanced chemical vapor deposition (PECVD) system for a-Si:Ge films now includes a pulsed plasma generator for improved material properties. The upgraded CIGS system, pictured in Figures 3a and 3b, produces device-quality films over

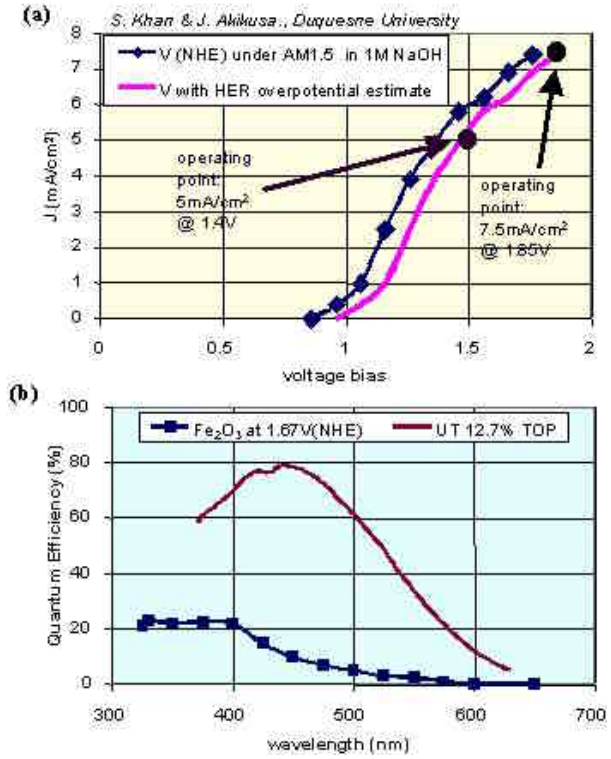

Figure 4. Hybrid design based on (a) Photocurrent response and (b) QE of nanostructured Fe_2O_3 films

approximately a 4" x 4" area. A significant achievement has been the in-house fabrication of CIGS photovoltaic devices onto 2" x 4" metal foil substrates (completed device shown in Figure 3c) with efficiencies exceeding 12%.

Also this year, we adapted our integrated electronic/optical/electrochemical models for the analysis of hybrid photoelectrode systems. Hybrid modeling using published data for nano-structured Fe_2O_3, WO_3 and TiO_2 films was performed, and based on this analysis (which utilizes current-voltage and quantum-efficiency film characteristics, as shown in Figure 4 for iron oxide films), Fe_2O_3 was selected for the initial hybrid prototypes. As a result, we initiated an Fe_2O_3 film development program focusing on the spray-pyrolysis material fabricated at Duquesne University and on sputter-deposited material fabricated in-house at UH. Preliminary hydrogen-reaction activity and surface morphology

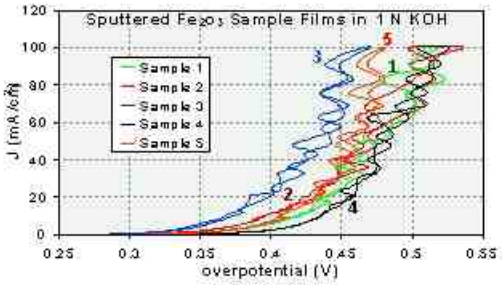

(a) hydrogen evolution activity in sputtered films

(b) sputtered film morphology

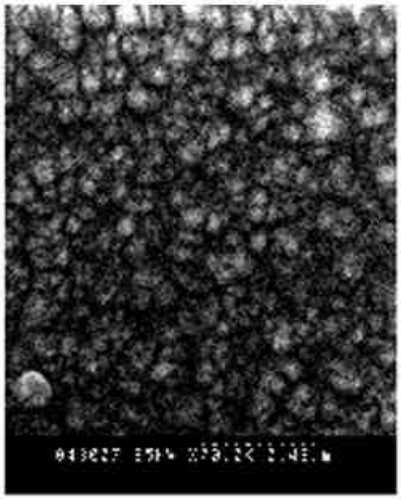

(c) pyrolysis film morphology

Figure 5. (a) OER overpotentials in sputtered Fe_2O_3; (b) scanning electron microscopy (SEM) of sputtered Fe_2O_3; (c) SEM of photoactive spray-deposited Fe_2O_3

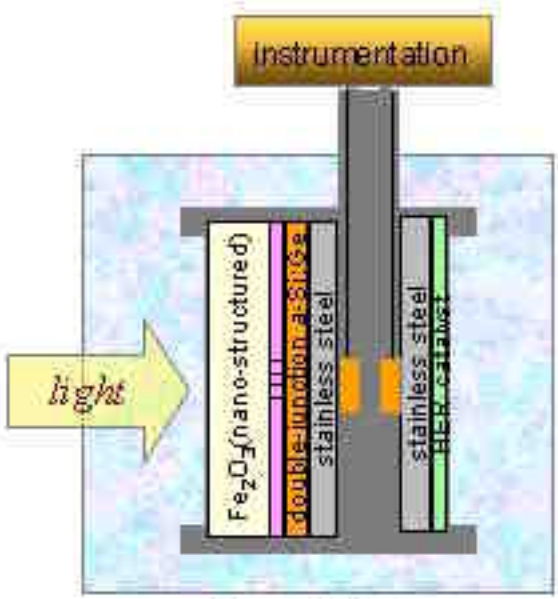

(a) test jig design

(b) implementation

Figure 6. Photoelectrode testing jig for monitoring current under different biases: (a) Cross section of design; (b) Implementation with prototype hybrid photoelectrodes

data for various iron-oxide films is shown in Figure 5.

Efforts are currently underway to fabricate and test prototype a-Si:Ge/Fe_2O_3 hybrid devices. With the University of Toledo, we completed an evaluation of a-Si:Ge device yield on different metal-foil substrates, and a series of multi-junction devices

for use in hybrid photoelectrode experiments was deposited on the highest-yield foil. The test jig shown in Figure 6 was designed and fabricated to facilitate evaluation of hybrid photoelectrode performance.

Conclusions

With this year's work, we have continued our emphasis on developing high-performance multi-junction hydrogen photoelectrodes based on low cost semiconductor and catalyst films. Significant progress was made in the advancement of amorphous silicon/germanium and copper-indium-gallium-diselenide materials for solid-state photojunctions, and great strides were made in the research and development of the 'hybrid' photoelectrode concept, including important initial work on nanostructured wide-bandgap semiconductor films for the photoelectrochemical interface. As a result of preliminary research and modeling efforts, iron oxide was selected as the most promising material for incorporation into first prototype hybrid devices. Development efforts to optimize Fe_2O_3 films, to design a-Si:Ge tandems with the correct optical and electronic properties, and to fabricate and evaluate test-structures combing the materials are currently underway. The conceptual design for higher efficiency hybrid devices using novel tandem CIGS configurations (in place of the a-Si:Ge tandems) with Fe_2O_3 outer layers is also under development.

References

1. Rocheleau, R., Miller, E., and Misra, A. 1998. "High-Efficiency Photoelectrochemical Hydrogen Production Using Multijunction Amorphous Silicon Photoelectrodes". Energy and Fuels 12:3-10.

2. Miller, E., Rocheleau, R. and Deng, X. 2002. "Design Considerations for a Hybrid Amorphous Silicon/Photoelectrochemical Multijunction Cell for Hydrogen Production" International Journal of Hydrogen Energy in press.

3. Hanket, G. et al. 2002. "Pilot-scale Manufacture of Cu(InGa)Se_2 Films on a Flexible Polymer Substrate", In Proceedings of the 29th IEEE Photovoltaics Specialists Conference, New Orleans, LA: IEEE.

4. Wang, W., et al. 2001. "Triple-Junction a-Si-Based Solar Cells with All Absorber Layers Deposited at the Edge of a-Si to μc-Si Transition." <http://www.physics.utoledo.edu/~dengx/ref3.pdf>.

5. Tuttle, J., et al. 1995. "Thin-Film Cu(In,Ga)Se_2 Materials and Devices: A Versatile Material for Flat Plate and Concentrator Photovoltaic Applications." Society of Photo-Optical Instrumentation Engineers, 2531:194-200.

6. Khan, S. U. M. and Akikusa, J. 1999. "Photoelectrochemical Splitting of Water at Nanocrystalline n-Fe_2O_3 Thin-film Electrodes, Journal of Physical Chemistry B, 1999, 103: 7184-7189.

FY 2002 Publications/Presentations

1. International Conference on Advanced Materials (ICAM 2001): Invited Lecture on Hybrid Photoelectrode Design.

2. "Design Considerations for a Hybrid Amorphous Silicon/Photoelectrochemical Multijunction Cell for Hydrogen Production" (in press: International Journal of Hydrogen Energy).

3. "Evaluation of RF-Sputtered Indium-Tin Oxide Films for Photoelectrochemical Applications" (submitted to the Journal of the Electrochemical Society).

Special Recognitions & Awards/Patents Issued

1. Patent Disclosure: "Hybrid Solid-State/ Electrochemical Photoelectrode for Hydrogen Production".

II.D.3 Photoelectrochemical Hydrogen Production Using New Combinatorial Chemistry Derived Materials

Eric W. McFarland (Primary Contact), Sung Hyeon Baeck, Kyoung-Shin Choi, Anna Ivanovskaya, Thomas F. Jaramillo
Department of Chemical Engineering
University of California, Santa Barbara, CA 93106-5080
(805) 893-4343, fax: (805) 893-4732, e-mail: mcfar@engineering.ucsb.edu

DOE Technology Development Manager: Roxanne Danz
(202) 586-7260, fax: (202) 586-9811, e-mail: Roxanne.Danz@ee.doe.gov

Main Subcontractor: University of California, Santa Barbara, CA

Objectives

- Design and construct a versatile automated system and methodologies for automated electrochemical synthesis of combinatorial libraries of mixed metal oxides
- Define electrosynthetic routes amenable to the automated electrochemical deposition system for synthesizing for doped and mixed metal
- Develop an automated high-throughput photoelectrochemical screening system
- Create and screen libraries of materials
- Complete the development of a chemo-optical detection system based on optical sensing of the reduction of tungsten oxide as a high-throughput screening system for monitoring hydrogen production
- Begin exploratory synthesis and screening of new metal-oxide systems and begin to examine composition-structure-function relationships
- Design and synthesize libraries of potential patterned metal oxides using diverse types of structure directing agents under a variety of deposition conditions

Approach

- Create synthesis and screening systems for rapid automated combinatorial synthesis of materials suitable for photoelectrochemical hydrogen production
- Develop chemical synthesis routes amenable to automated high-throughput experimentation
- Utilize the automated synthesis systems to create libraries of potential hydrogen photocatalysts
- Rapidly screen libraries for potential materials with high photoelectrocatalytic activity
- Synthesize in conventional manner selected materials for detailed analysis

Accomplishments

- Designed and built several prototype systems for electrosynthetic deposition of metal oxides, including both parallel and automated serial systems
- Developed direct cathodic routes to oxides of several metals including tungsten (W), nickel (Ni), niobium (Nb), titanium (Ti), Fe, copper (Cu), colbalt (Co), molybdenum (Mo), and zinc (Zn) by stabilization with several ligand types, and preliminary studies with libraries which have shown general trends

- Completed our chemo-optical high throughput screening system and demonstrated the first thin film results with zinc oxide (ZnO)
- Preliminary work on electrosynthesis of mesoporous tungsten trioxide (WO_3) and titanium dioxide (TiO_2) films from a peroxo-stabilized electrolyte using ionic surfactants has at last shown definitive evidence of highly structured materials (July 2002)
- From libraries of pulsed electrodeposited platinum (Pt) doped WO_3, whereby a new means of creating nanoparticles has been developed. The nanoparticles show high activity for methanol oxidation without the poisoning problems of Pt

Future Directions

- Explore the composition-function relationships of dopants in ZnO hosts
- Investigate metal oxide libraries for electrocatalytic hydrogen production and expand our high-throughput screening to include relative electrocatalytic overpotential as a routine screen
- Develop a high-throughput optical screening system to measure the effective bandgap of metal oxides in libraries
- Synthesize and screen model libraries optically for bandgap as a primary screen and create secondary libraries of compositions
- Investigate library designs for synthesis of semiconductor heterostructures utilizing two-photon absorption processes
- Continue and expand investigations of nanoporous materials with emphasis on the ZnO, WO_3 and TiO_2 hosts.

Introduction

The overall project objective is the development and application of combinatorial methods to discover an efficient, practical, and economically sensible material for photoelectrochemical production of hydrogen from water and sunlight. We will introduce a shift in the research paradigm from the present method of conventional serial chemical research to a combinatorial approach featuring a systematic and deliberate high-speed exploration of the composition-structure-property relationship of new metal-oxide based solid-state materials to discover new and useful energy producing materials as well as better understand the fundamental mechanisms and composition-structure functional relationships of these materials.

Approach

Our studies have focused on the development of automated chemical synthesis and screening systems, then on the preparation and analysis of diverse photoelectrochemical libraries of metal-oxides with semiconducting and other properties suitable for photoelectrocatalysis. Diversity has included: 1) variations in composition (by variable doping, electrochemical synthesis conditions, and surface redox catalysts) and 2) variations in structure (by deliberate and diverse ionic and non-ionic templating agents, synthesis conditions, and doping). The libraries are screened directly for hydrogen production using a two-dimensional chemo-optical sensor array.

Results

Specific Aim 1

Automated electrochemical synthesis routes are used to create libraries of mixed metal oxides, and we have designed and constructed the necessary apparatus and developed the detailed methodology to do so. Figure 1 schematically illustrates how our synthesis systems operate.

Combinatorial methods only make sense when very large numbers of different materials are made and screened quickly. Compositional diversity across a library is obtained by varying the

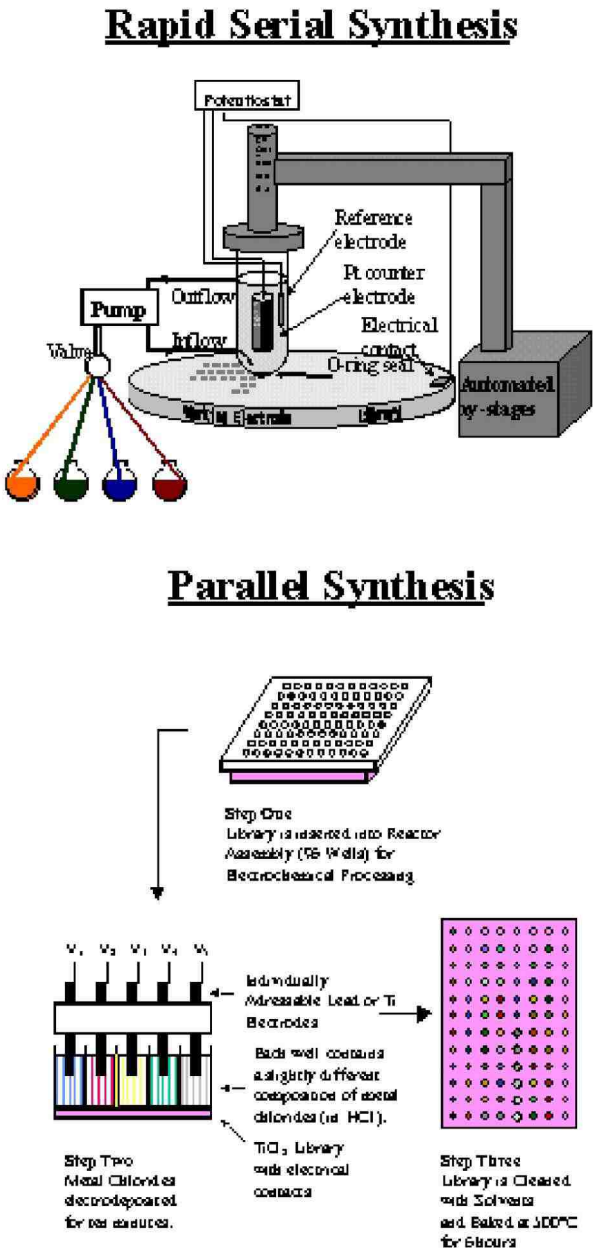

Figure 1. Schematic illustration of combinatorial synthesis by electrochemicaldeposition. The parallel approach is faster, but the rapid serial methodoffers greater control for each deposition.

electrochemical deposition conditions of time, voltage, current, surfactant additives and electrolyte. In the parallel system, the substrate (which is a common working electrode) has individual electrochemical cells isolated from each other by virtue of a perforated polypropylene block that is sealed to the substrate with an array of o-rings. This provides for different synthesis conditions at each library position; each cell constitutes an individual two-electrode system and is filled with a compositionally unique electrolyte. Clearly, synthesis speed is the advantage in a parallel scheme since all depositions occur simultaneously. In the rapid serial system, a complete three-electrode probe is scanned over the surface of the library substrate by an automated, computer-controlled set of x-y-z stages. The probe contains an o-ring at the bottom which forms a seal at the substrate. Electrolyte of choice flows into the cell by a computer-controlled pump, and a highly controlled deposition is conducted at each location by a potentiostat/ galvanostat. Several material systems have exhibited extraordinary sensitivity to deposition voltage.

Specific Aim 2

We have developed new electrochemical synthesis routes and extended existing ones to create routes amenable to our automated synthesis system for the generation of mixed metal oxides.

A number of metal hydroxides have been deposited by cathodic reduction. Metal oxides (WO_3, MoO3, TiO_2, ZnO, Fe_2O_3, Co_3O_4…) can be produced from the metal hydroxide by thermal annealing. In some cases, metal (Ni, Zn, Mn . . .) can be deposited by cathodic reduction and, after thermal annealing or electroanodization, a metal oxide can be obtained. We have also used electrochemical anodization for the synthesis of Al_2O_3 to roughen the surface and create a porous base material [13]. Our approach has been to stabilize the metal cations with ligands to allow for direct metal oxide deposition and the co-deposition of dopant cations. Several ligands we have used include hydrogen peroxide, citric acid, lactic acid, and acetic acid. WO_3, TiO_2, Nb_2O_5, and MoO_3 have been cathodically deposited from metal-peroxo solution. We have found that mixed metal oxides, such as WO_3-MoO_3, and WO_3-TiO_2 can be synthesized by mixing metal peroxo electrolytes. Pt or Ru doped tungsten oxide has been directly deposited under cathodic conditions in the presence of hydrogen peroxide, and diversity has been achieved by changing the concentration of the dopants in the electrolyte solution or by varying deposition potential. We have also stabilized the

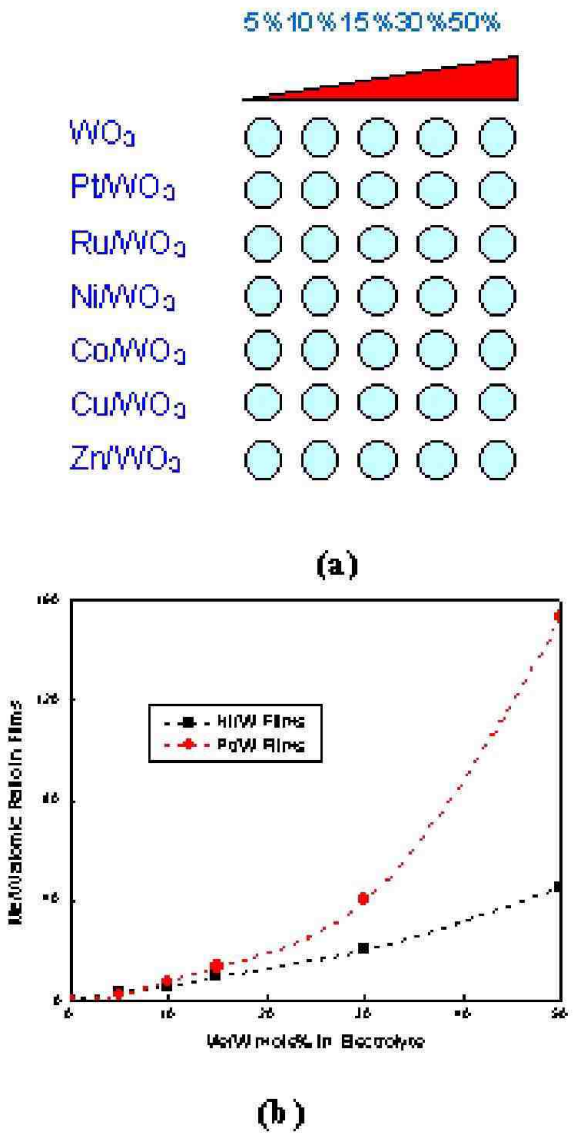

Figure. 2. Metal-doped WO_3 binary library. (a) Library design: variation indoping density is achieved by varying dopant concentration in theelectrolyte. (b) Relationship between dopant concentration in thedeposited film versus dopant concentration in the electrolyte.

metal cations in basic media using a complexing agent such as citric and lactic acid.

Specific Aim 3

We have developed two major systems for automated high-throughput photoelectrochemical screening designed to measure electrochemical and photoelectrochemical responses of combinatorially prepared photocatalyst libraries. The system in its electrochemical screening configuration allows for measuring cyclic voltammograms (I-V curves) and Mott-Schottky plots, which reveal flatband potential and sample dopant concentrations. The system is modular in nature - easy to set up for the experiment of interest by connecting the appropriate programmable source/measure devices: potentiostat, digital multimeter, data acquisition board, impedance analyzer and lock-in amplifier. This configuration allows for varying electrolytes for different samples by filling the wells of a perforated polypropylene block with a programmable pipette.

Specific Aim 4

We created a pair of libraries of WO_3 doped with different transition metals (at a variety of doping densities) with the aim of improving upon the photocatalytic activity of pure WO_3. The first library design is shown in Figure 2(a). The library incorporates Pt, Ru, Ni, Co, Cu, and Zn as dopants within polycrystalline WO_3. The materials were each co-deposited with WO_3 electrochemically from a mixture of 50 mM metal chloride solution and a W-peroxo solution. Altering the metal-chloride concentrations in the electrolyte, from 0% to 50% allowed for variation of doping concentrations within the deposited films. Figure 2(b) shows the relationship between doping density in the deposited film versus the concentration in the electrolyte for Pt and Ni as determined by Electron Dispersive X-Ray (EDX). Figure 3(a) illustrates the zero-bias photocurrent for the library members, and Figure 3(b) shows a cyclic voltammogram taken of the pure WO_3 film. We expect several photocurrent trends from this library. First of all, Ni has been shown to be an excellent absorber of visible light when doped into large band-gap oxide hosts, such as WO_3, so we expect an increase in photocurrent from that row. Similarly, we would expect better photocurrent from Pt and Ru dopants, since Pt is an excellent reduction catalyst and RuO_2 is a well-known oxidation catalyst. Figure 3(a) shows that, indeed, Ni doping increased photocurrent significantly compared to pure WO_3, with a maximum photocurrent achieved for 10% Ni. Pt and Ru dopants show a different trend. Seemingly, a greater doping concentration of either element decreases the photoactivity of WO_3.

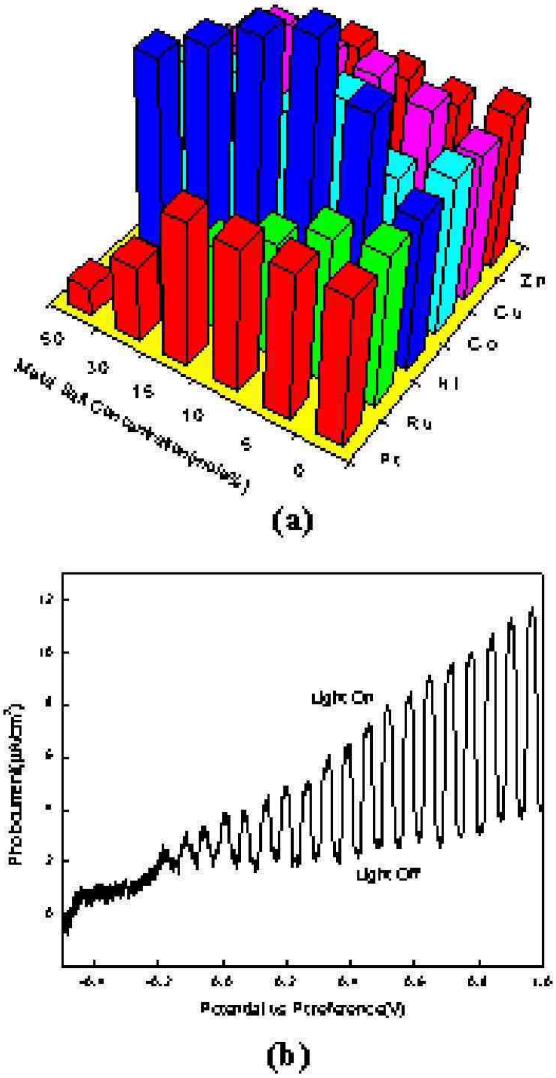

Figure 3. High-throughput photocurrent screening of the WO_3 library at zero bias.(a) Photocurrent trends in the library. (b) Cyclic voltammogram of pure WO_3 (0.2 cm^2) under chopped illumination from a 150 W Xe lamp (2.3 mW/cm^2).

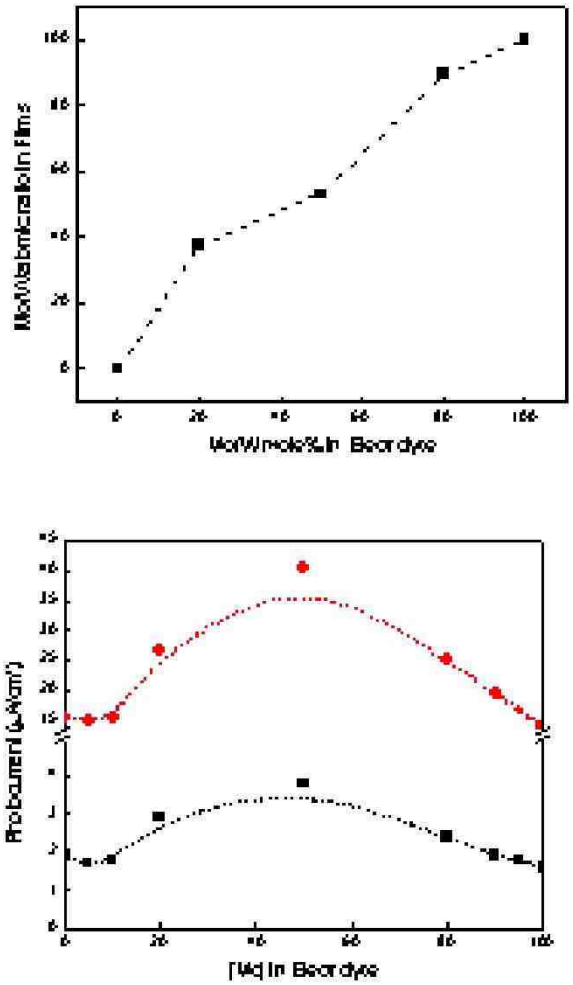

Figure 4. (a) EDS measured atomic ratio of Mo to W in films as a function of Mo concentration in electrolyte. (b) Photocurrents in 0.1 M sodium acetatesolution at zero bias(=)and 1 V bias(<) for WO_3-MoO_3 mixed oxides as a function of Mo concentration in electrolyte.

Specific Aim 5

We have engineered a high-throughput screening system for monitoring H_2 production based on a chemo-optical H_2 sensor [14-16]. This colorimetric sensor utilizes a Pd/WO_3 bilayer, whereby molecular H_2 dissociates on the Pd surface and diffuses as atomic hydrogen to reduce WO_3 to a tungsten bronze, H_yWO_{3-x}. The reduced tungsten oxide is photometrically distinct from WO_3 due to a decreased index of refraction. The reduction is reversible and the sensor can be regenerated in O_2. Details are presented in our published papers.

Specific Aim 6

A library consisting of a 45-member (5 x 9 array) WO_3-MoO_3 mixed binary oxide library, with diversity achieved by variations in deposition voltage and Mo concentration in the electrolyte was synthesized. The concentration of Mo was varied

from 0 to 100 mol% and all films were deposited for 10 minutes. After deposition, the library was calcined at 450°C for 4 hours in air.

The film compositions were determined by EDX for fifth row (prepared from 50% W- 50% Mo mixture) and fourth column (electrodeposited at -1.0 V). As expected, with increasing concentration of molybdenum in solution, the atomic fraction of molybdenum in the film increased (Figure 4(a)). However, the atomic ratio was independent of deposition voltage (-0.2 ~ -1.5 V, not shown). A trend in photoresponse as a function of molybdenum concentration in electrolyte was clearly observed. Figure 4(b) shows photocurrent at 0 and +1 V bias for the WO_3-MoO_3 mixed oxide. The photoresponse increased and reached a maximum when 50% Mo and 50% W concentration in electrolyte was used, and then decreased as concentration of Mo in electrolyte increased. In the cases where MoO_3 concentration was below 10% or above 90%, there is no enhancement of photoactivity compared to either pure WO_3 or pure MoO_3. Interestingly, in the range of 20 ~ 80% MoO_3, an increase of photoactivity was observed.

Nano-particulate tungsten oxide films were also synthesized by pulsed electrodeposition in libraries. Particle sizes between 45 ~ 330 nm were achieved by varying pulse duration from 5 ms to 500 ms. Films prepared by continuous electrodeposition had an average particle size of approximately 375 nm. As the pulse time decreased, particle size decreased as well. For a 5 msec pulsed deposition, the average particle size was approximately 45 nm. We checked the particle size with respect to deposition time (30 sec to 30 min, that is 3,000 to 180,000 pulses) and found that particle size was independent of total number of pulses; the total number of pulses seemed to affect only film thickness and not the final particle size.

We discovered that metal oxides (WO_3, MoO_3, TiO_2, Nb_2O_5) can be synthesized from peroxo-stabilized solution onto Cu foil by electroless deposition. The deposition rate was found to be strongly dependent on temperature, electrolyte concentration, and deposition time. As-synthesized films were amorphous and showed weak p-type photocurrent due to the formation of Cu_2O on the surface of Cu foil. After calcination at 450°C, metal oxide films were found to be crystalline. A 27-member (3 x 9 array) WO_3-MoO_3 mixed oxide library was prepared by electroless deposition on Cu foil, with diversity achieved by variations in deposition time and Mo concentration in electrolyte.

Specific Aim 7

In addition to our effort of finding better performance photocatalysts by tuning the composition of the films, we have been developing a general method for the production of high surface area nanostructured films by utilizing electrochemically driven self-assembly of surfactants at solid-liquid interfaces. We combined potential-controlled surface assembly with an electrodeposition process to fabricate nanostructured films. We have successfully electrodeposited mesoporous platinum and zinc oxide films by controlling deposition potentials and electrolyte compositions. The nanostructures of these films have been confirmed by transmission electron microscopy (TEM). The hexagonal structure of the Pt films, with the pores perpendicular to the substrate and the lamellar structure of ZnO, with the normal direction of the layers parallel to the substrate, are expected to allow facile access of the guest molecules and analytes to the pores and interlayers. The electrocatalytic properties of mesoporous Pt films, towards methanol oxidation were measured in order to confirm the increased effective surface areas and to evaluate a potentially important application of these films (i.e. direct methanol fuel cell applications).

Conclusions

Our work during the first 9 months of this project has focused on the development of combinatorial methods to rapidly synthesize and high-throughput screen mixed metal oxides, and on using these systems to begin to investigate new materials for photocatalytic hydrogen production. We have designed and constructed much of the combinatorial infrastructure (automated parallel and rapid serial synthesis and screening systems), and we have developed synthesis routes (based on electrochemistry) amenable to our combinatorial instruments. Rapid synthesis and functional

screening of mixed metal oxides of W, Cu, Ti, and Fe hosts has been demonstrated, and new electrosynthetic routes to W-Mo-oxide and nanoporous WO_3 have been developed. Recent data from $W_x(Mo,Ni,Pt)_yO_z$, $Cu_x(Zn_yNi_y)O_z$ and $Fe_x(Ti)_yO_z$ show (reserved) promise as improved materials.

References

1. Gaffron, H and Rubin, J., J. Gen. Physiol., 26, 219 (1942).

2. Fujishima, A. and Honda, K, Nature, 238, 37 (1972).

3. Herriman, A. and West, M. A., editors, "Photogeneration of Hydrogen", Royal Institution Symposium, Academic Press (1982).

4. Domen, K., Kondo, J. N., Hara, M., and Takata, T., Bull. Chem. Soc. Jpn., 73, 1307 (2000).

5. Gratzel, M. A., "Energy Resources through Photochemistry and Catalysis", Academic Press, New York (1983).

6. Hanak, J. J., J. Mater. Sci., 5, 964 (1970).

7. Hanak, J. J., Gittleman, J. I., Pellicane, J. P., and Bozowski, S., Phys. Lett., 30(3), 210 (1969).

8. Danielson, E., Golden, J. H., McFarland, E. W., Reaves, C. M., Weinberg, W. H., and Wu, X. D., Nature, 389, 944 (1997).

9. Danielson, E., Devenney, M., Giaquinta, D. M., Golden, J. H., Haushalter, R. C., McFarland, 10. E. W., Poojary, D. M., Reaves, C. M., Weinberg, W. H., and Wu, X. D., Science, 279, 837 (1998).

10. Therese G. H. A. and Kamath, P. V., Chem. Mater., 12, 1195 (2000).

11. Meulenkamp, E. A., J. Electrochem. Soc., 144, 1664 (1997).

12. Hutchins, M. G., Kamel, N. A., El-Kardy, W., Ramadan, A. A., and Abdel-Hady, K., Phys. Stat. Sol. A ,175, 991(1999).

13. Brandli, C., Jaramillo, T. F., Ivanovskaya, A., and McFarland, E. W., Electrochimica Acta, 47, 553 (2001).

14. Ito, K. and Ohgami, T., Appl. Phys. Lett., 60, 938 (1992).

15. Ito, K. and Kubo, T., Proceedings of the 4th Sensor Symposium, Tokyo, 153 (1984).

16. Tamura, H., Hashimoto, Y., and Ito, K., Solid State Phenom., 51-52, 429 (1996).

17. Shen, P., Chi, N., and Chan. K. Y., J. Mater. Chem., 1, 697 (2000).

18. Burgess, I., Jeffrey, C. A., Cai, X., Szymanski, G., Galus, Z., and Lipkowski, J., Langmuir, 15, 2607 (1999).

FY 2002 Publications/Presentations

1. S.H. Baeck, T.F. Jaramillo, C. Brandli, and E. McFarland, "Combinatorial Electrochemical Synthesis and Characterization of Tungsten-based Mixed Metal Oxides", J. Combi. Chemistry, (accepted and in press 2002).

2. S.H. Baeck, T.F. Jaramillo, G.D. Stucky, and E. McFarland, "Controlled Electrodeposition of Nanoparticulate Tungsten Oxide", Nano Letters, (accepted and in press 2002).

3. S.H. Baeck and E.W. McFarland, "Combinatorial Electrochemical Synthesis and Characterization of Tungsten-Molybdenum Mixed Oxides", Korean.J.Chem.Eng., (accepted and in Press 2002).

4. S.H. Baeck, T.F. Jaramillo, and E. McFarland, "Influence of Composition and Morphology on Photo and Electrocatalytic Activity of Electrodeposited Pt/WO_3", 224th National ACS Conference Proceedings, Boston, MA (2002).

5. Invited Seminar October 2001 "Combinatorial Methods of New Materials Discovery For Photocatalytic Hydrogen Production: A Long Way to a Million Million Watts", Department of Nuclear Engineering, MIT.

6. Invited Talk November 2001 "Combinatorial Electrosynthesis and Photoelectrocatalytic Screening of New Materials for Hydrogen Photosynthesis", AICHE Annual Meeting, Reno, Nevada.

II.D.4 Combinatorial Discovery of Photocatalysts for Hydrogen Production

Brent MacQueen (Primary Contact), Al Hirschon, Ted Mill, Mike Coggiola
SRI International
333 Ravenswood Ave
Menlo Park, CA 94025
(650) 859-5286, fax: (650) 859-4321, e-mail: brent.macqueen@sri.com

DOE Technology Development Manager: Roxanne Danz
(202) 586-7260, fax: (202) 586-9811, e-mail: Roxanne.Danz@ee.doe.gov

Objectives

- Develop a high throughput system for evaluating photocatalytic materials for hydrogen production
- Develop a methodology to produce a database of photocatalytic materials
- Discover new photoactive materials capable of producing hydrogen using solar radiation

Approach

- Construct automated high throughput testing equipment to evaluate physical properties and measure solar hydrogen production of photoelectrochemical systems
- Evaluate the effectiveness of nanosized materials for hydrogen generation from water using visible light
- Develop database useful for all researchers

Accomplishments

- Built and calibrated a light source for use as a solar simulator
- Built and tested a 4-cell reactor with pressure transducers for measuring hydrogen production from photocatalysts
- Modified and programmed a Gilson sampler for pressure transducer activated automated analysis of hydrogen production
- Synthesized and screened semiconductor materials, including nanosized titanium dioxide (TiO_2) materials, for water splitting using visible light
- Designed and constructing a 25-cell combinatorial reactor for screening photocatalysts for hydrogen production

Future Directions

- Develop a prototype multi-cell reactor for high throughput evaluation of the electrochemistry of photocatalytic materials
- Optimize the high throughput tools for discovery of water splitting catalysts
- Evaluate new nanoparticle materials synthesized as candidate photocatalysts
- Design and synthesize new materials which can produce hydrogen using visible light based on experimental results

Introduction

The conversion of the dominant energy source from one that is petroleum-based to one based on hydrogen will have a profound effect on the reduction of greenhouse gases being emitted by current technologies. Furthermore, if the hydrogen is generated from a non-carbon containing feedstock, such as water, using an energy source that is not carbon-based, such as solar radiation, the reduction in emitted gases will be enhanced even further. The key hurdle to overcome the obstacles to such a technology, photolytic generation of hydrogen from water, is a materials related issue and can be solved by the discovery of materials with the appropriate energetics and stability upon solar irradiation. A key aspect of this project is that it incorporates a nanoparticulate semiconductor producer, NanoGram, with a research institute, SRI International, with the required capabilities to be successful in this very important endeavor. The combination of NanoGram's synthetic process, which is scalable to Kg/hour quantities, with SRI's high throughput screening capabilities has the potential to make breakthrough discoveries with respect to the photolytic generation of hydrogen from water.

The goal of this effort is to develop more efficient ways to discover photocatalysts for the economical and environmentally sound production of hydrogen by splitting water with sunlight. SRI is developing combinatorial tools to identify new semiconductor compositions, surface modification(s), and experimental conditions that lead to efficient hydrogen production with visible light. Our specific objective in Year 1 of this effort has been to develop and validate a combinatorial workstation that can be used to rapidly screen an array of materials in terms of electrochemical properties and photocatalysis. To that end we have constructed a combinatorial system consisting of a simulated sunlight source, a multi-cell reactor with pressure and sampling capabilities and a programmed sample handler.

Approach

We are using a combinatorial approach to discover new photocatalytic materials, which can generate hydrogen using visible light. By first constructing combinatorial tools to quickly screen for effective photocatalysts, we can then investigate new materials as photocatalysts, including nanoparticulate semiconductors prepared by NanoGram, Corp., with whom we are collaborating on this project. Our approach is divided into three tasks as follows:

In Task 1 we are developing tools for combinatorial evaluation of the photoelectrochemical properties of semiconductors relevant to photogeneration of hydrogen. The objective of Task 1 is to develop plug and play components that will allow the rapid screening to find photocatalysts that generate hydrogen efficiently with visible light.

The goal of Task 2 is to synthesize photocatalysts for combinatorial screening for rapid hydrogen generation. We plan to use a rational design for materials synthesis that leverages the particle fabrication capabilities of our partner in this project, NanoGram, Corp, with SRI's chemistry and engineering capabilities. Systems level investigation will include modified commercial materials as well as new materials such as nanophase powders produced by NanoGram with various particle sizes, phases, and dopant levels using their proprietary synthetic process.

The goals of Task 3 are to identify photocatalysts that merit further investigation as evidenced by the combinatorial screen results and to begin a systematic evaluation of the materials identified in Task 2 using the tools developed in Task 1.

Results

We have modified a 1 kW Oriel xenon light source to provide an 8 inch illuminated circle with light between 300 and 1,000 nm to simulate sunlight for our prototype device. We have measured the light intensity distribution in the circle so that we can correct for effects of non-uniformity in the light field on the performance of photocatalysts.

We have developed two modular designs for the combinatorial screening of photocatalysts. One design focuses on hydrogen production from particles suspended in water and the other measures the electrochemical properties of monolithic (solid) substrates. The latter design provides a more detailed

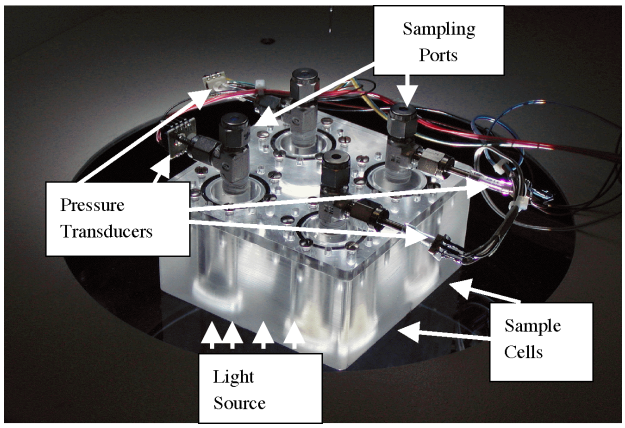

Figure 1. 4-cell Prototype of Photolysis Product Analysis Module

Figure 2. Gilson Autosampler and 4-cell Analysis Module

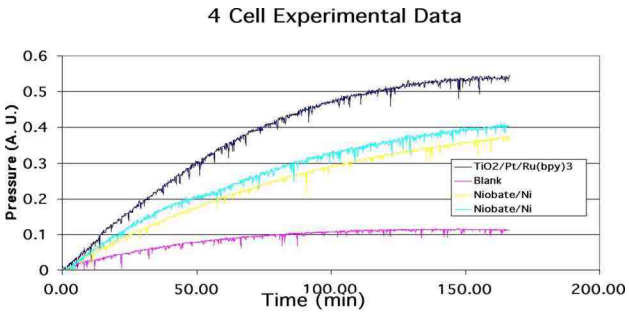

Figure 3. Pressure Transducer Output from 4-cell Module

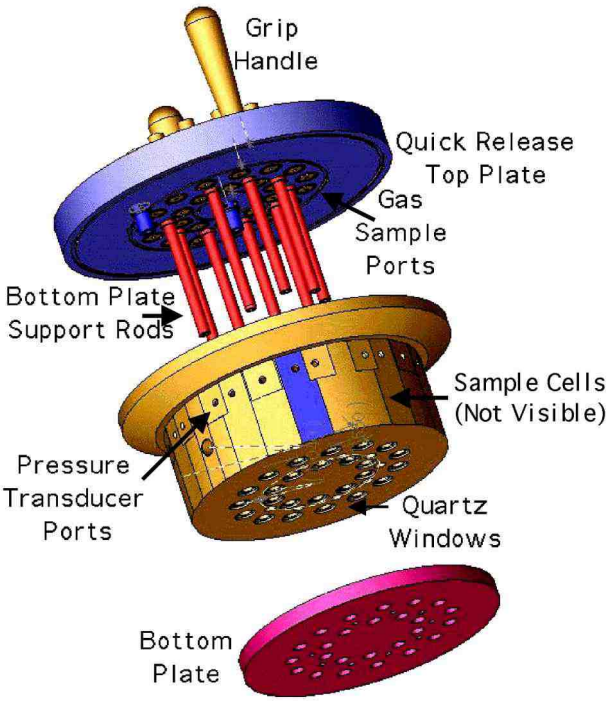

Figure 4. Design of 25-cell Analysis Module Currently Under Construction

analysis of the physical properties of the photocatalysts as a result of electrical (ohmic) contact to the measuring system, while the former design allows for rapid screening of particle dispersions to find active catalysts to be investigated in detail.

A 4-cell prototype of the particle suspension analysis design has been constructed (Figure 1). Individual cells are illuminated from the bottom, and each cell has a septum port and a micropressure transducer to detect evolution of gaseous products (i.e. H_2/O_2). A Gilson X-Y sampler (Figure 2) was programmed for autosampling based on the response of the micropressure transducers. The sampler injects the gas into a gas analyzer to determine how much hydrogen and oxygen were formed from any catalyst. Figure 3 shows typical data obtained during the course of a photolysis experiment. We are building a larger prototype with 25 cells, which has advantages in ease of assembly suitable for combinatorial use. The design of this multi-cell reactor is illustrated in Figure 4. A three-electrode system will be used for

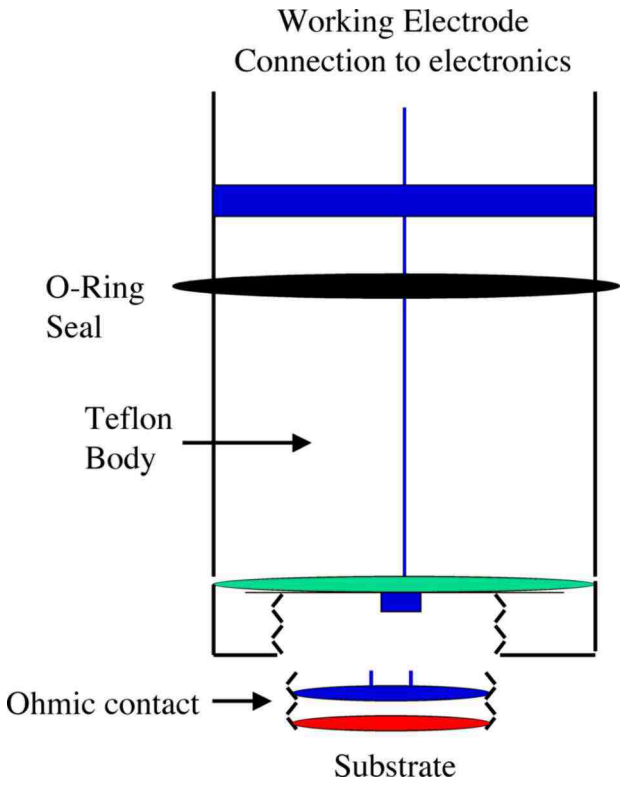

Figure 5. Design of Electrode Assembly Used for Electrochemical Analysis Module

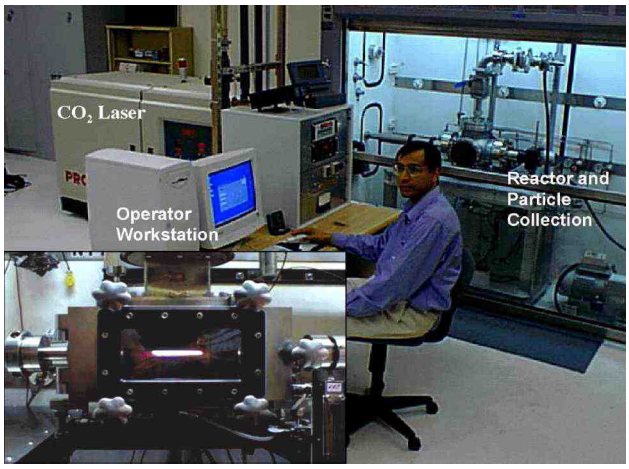

Figure 6. NanoGram Synthesis Workstation with Insert ShowingLaser Pyrolysis Reaction Zone

electrochemical measurements on monolithic materials. This module is attached to a common top that can be inserted onto the cell system designed for the particulate analysis (Figure 5). Thus, electrochemical properties of active semiconductor catalysts can be measured by switching the top plate of the analysis module.

The particle synthesis is progressing with the use of NanoGram's proprietary laser pyrolysis nanoparticulate synthesis technology (Figure 6).

Conclusions

We have made a great deal of progress in assembling the components necessary to conduct high throughput screening of materials for photocatalytic generation of hydrogen from water. This includes building a solar simulator, assembling and modifying the sample collection and sample analysis equipment, and designing, constructing analysis cells. When completed our equipment will allow us to facilitate the discovery of new photocatalysts able to produce hydrogen using solar radiation.

Special Recognitions & Awards/Patents Issued

Invention disclosure on quick release top plate design in progress.

II.D.5 Low Cost, High Efficiency Reversible Fuel Cell Systems

Christopher Milliken (Primary Contact), Dr. Robert Ruhl
Technology Management, Inc.
9718 Lake Shore Blvd.
Cleveland, OH 44108
(440) 995-9500, fax: (440) 720-4527, e-mail: milliken@stratos.net

DOE Technology Development Manager: Sigmund Gronich
(202) 586-1623, fax: (202) 586-5860, e-mail: Sigmund.Gronich@ee.doe.gov

Main Subcontractor: Technology Management, Inc., Cleveland, OH

Objectives

- Improve performance of reversible stacks (capable of operating in both fuel cell and electrolysis modes) by reducing area specific resistance, rate of degradation, and seal leakage.
- Demonstrate an integrated fuel cell hot subassembly opeating with a stack of about 50 reversible type cells operating on natural gas.
- Evaluate the economic impact of the reversible solid oxide fuel cell /solid oxide electrolyzer system and consider applications where a competitive advantage may be achieved.

Approach

- Evaluate alternate materials and geometric factors to reduce cell resistance.
- Reduce operating temperature to improve life and performance.
- Design and fabricate an integrated test station capable of testing reversible stacks (nominally 50 cells).

Accomplishments

- Optimized cell geometry by modeling the stack and system.
- Designed, fabricated, and evaluated performance of reversible stack over a range of temperatures and operating conditions.
- Demonstrated stable operation for >1200 hours in small reversible stacks at acceptable efficiency.
- Completed preliminary economic analysis and identified applications where reversible electolyzer/fuel cell systems may have a competitive advantage.

Future Directions

- Design, fabricate, and commission an integrated test system.
- Scale up fabrication to produce 50 cell stacks using standardized processes.
- Complete evaluation of alternate materials for improved life and performance.

Introduction

The Technology Management, Inc. (TMI) reversible (fuel cell - electrolyzer) system employs a high temperature solid-oxide based electrochemical process to produce either electricity from common hydrocarbon fuels (e.g., natural gas, propane, and bio-derived fuel) or hydrogen from supplied electricity. In electrolyzer mode, the reversible system uses electricity and thermal energy to convert pure water into fuel (hydrogen and oxygen). TMI's reversible system uses the waste thermal energy produced during electricity generation mode to achieve high system efficiency during electrolysis

mode, ultimately lowering product life cycle costs for the combined system. To further increase system efficiency, TMI has implemented a 'passive' (cell) system design which reduces the number and complexity of the balance of plant components.

During the current phase of the program, TMI has demonstrated reversible cells and stacks which met many of the performance targets including reversible efficiency and life. Several conditions were evaluated to understand the sensitivity of performance on operating variables such as temperature and current density. The highest reversible efficiency ($DC_{Volts\text{-}Out}$ / $DC_{Voltage\text{-}In}$) measured was 90.8% at 925°C and 50 mA/cm^2. A five cell stack was operated at < 2% / 1000 hours voltage degradation in fuel cell mode for over 1200 hours. Data from this work was used to expand economic and engineering studies completed earlier. An outcome of this was the concept for a system capable of delivering 5000 pounds per square inch (psi) pure hydrogen (e.g., needed for vehicle uses) in addition to electric power and recovered usable heat. The proposed systems would be configured in redundant modules to ensure high reliability and could be sized for either residential or commercial applications (including "power parks") being fed by electric power (renewable or low-cost grid) and/or fuel (fossil or biomass-derived).

Approach

Reversible stacks goals require negligible gas leakage rates, low polarization voltages, stable microstructures, and reproducible fabrication techniques to meet the goals. Low gas leakage rates have been demonstrated in limited tests that will continue. The DOE has suggested an alternate sealing technology that may be applicable if it can be adapted.[i] Low polarization voltages will be sought by optimizing the electrode microstructure and by continuing to improve the separator interface. Microstructure stability will be addressed through materials and processing improvements. Reproducible fabrication will be achieved through the following: enhanced inspection techniques, data analysis, and mechanized production methods. Finally, the design of the hot subassembly will be based on proven engineering designs developed by TMI over the past 10 years.

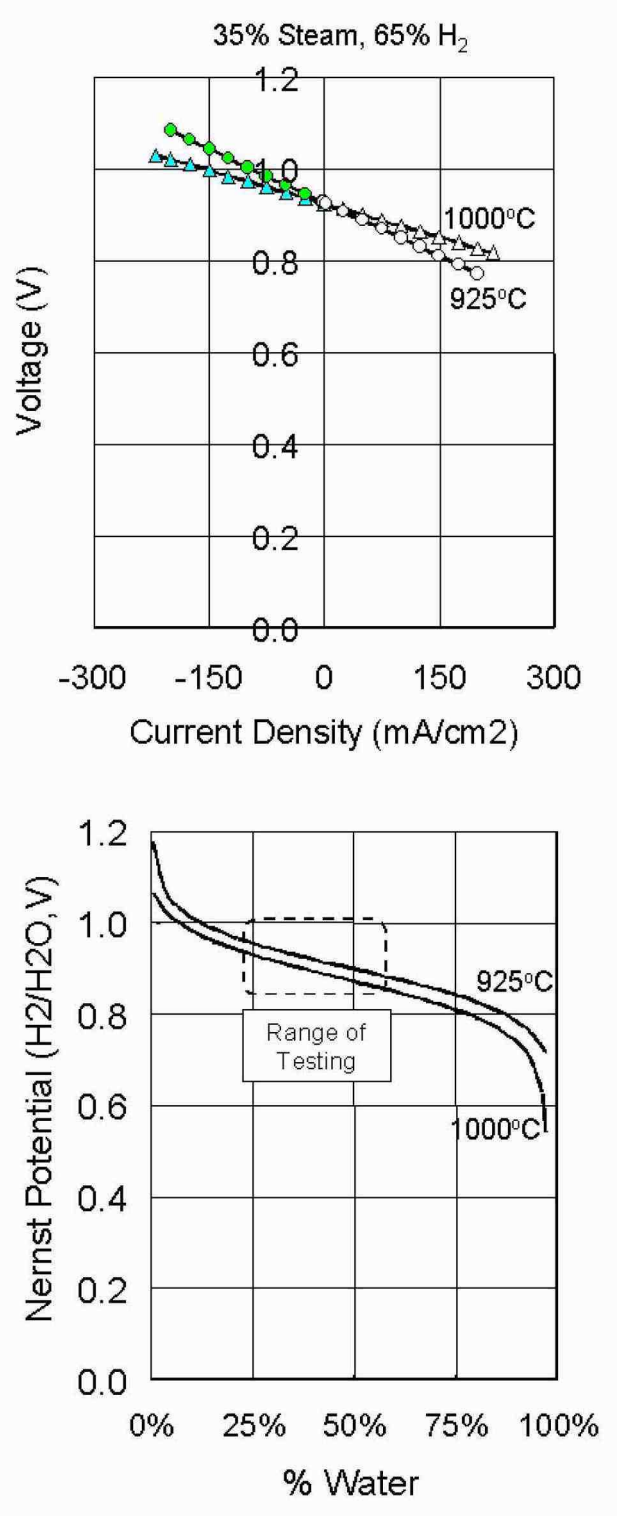

Figure 1. Reversible Testing of Cells

Results

Cell Component Development

The goal of the cell testing task was to validate the passive mode of operation and characterize performance. Temperature and gas phase concentration gradients are of particular interest because the processes are driven by gaseous diffusion.

Evolutionary improvements and modifications were made to existing TMI materials specifications, fabrication methods, and cell dimensions to accommodate this design. Minor modifications of standard TMI fabrication procedures were sufficient to produce thicker fuel + oxygen electrodes. Larger diameter, thicker seals were made using methods from internally funded programs. Fifty-percent thinner electrolytes were procured and used in some of the trials.

Figure 1 shows data from cells operated with a 65% hydrogen/35% steam mixture at two different temperatures. Operation was primarily in electrolysis mode with daily intervals in fuel cell mode. The mixture choice of fuel composition corresponds to the approximate midpoint in oxygen potential in a complete system as shown in the second part (b) of the figure. Characterization at extreme conditions was not considered during this phase.

The lack of offsets or slope changes near zero current indicates that no significant activation polarization exists in these cells (in marked contrast to proton exchange membrane [PEM] cells). The plot also shows that practical electrolysis current densities (100-200 mA/cm^2) required electrolysis voltages under 1.1 Volts --- far lower than PEM electrolyzers (which typically operate near 1.9 Volts) -- thus enabling higher electrolysis efficiencies when using TMI's solid oxide cells. Trends were consistent for similar materials and construction. The most likely sources of variability were fabrication quality and processing parameters. Because of the short program duration, fabrication condition optimization could not be explored. Finding an optimal set of fabrication conditions is essential for reproducible results.

Reversible cell efficiency is the ratio of fuel cell to electrolysis voltage at the same cell current and hydrogen/steam feed. It is a measure of the maximum possible energy storage efficiency for a reversible system using the cell (system efficiencies will be lower than cell efficiencies). The highest reversible cell efficiency observed was 90.8% (at 925°C and 50 mA/cm^2).

Engineering Studies

A modular system design producing both electricity and hydrogen was studied in the context of several assumptions. In this concept, AC power could be produced for local needs with possible sale of surplus power to the grid. High pressure (e.g., 5000 psi) pure hydrogen could also be produced for later use in vehicles after temporary storage in adjacent tanks. Hot water would be produced as a useful byproduct when operating from natural gas fuel augmented by renewable electricity where applicable. The exhaust would be extremely clean, and CO_2 emissions would be minimized during operation due to the high efficiency of the system.

Individual module sizes considered ranged from 1 to 30 kW. For each kilowatt of capacity, a module could either produce up to 1.0 AC kilowatt or up to 12.1 standard cubic feet per hour (scfh) of hydrogen (enough to power fuel cell cars for 21,200 miles per year) or a combination of electricity and hydrogen. The fuel cell subsystem would operate at atmospheric pressure, and the electrolysis subsystem would operate up to 5000 psi. Batteries could provide high power when needed for load-following, and surges would only require a small energy storage capacity. Mechanical auxiliary devices include a high-pressure water pump and compact heat exchangers. Complete systems assembled from two or more identical modules would have the added benefits of redundancy and ease of service. In multiples, overall system capacities could range from an individual residence to large vehicle filling stations or "power parks". Energy storage capacity can be supplanted by producing hydrogen at steady-state for later use in vehicles, thereby eliminating "round trips" and increasing overall efficiency.

For some special applications, an electrolyzer-only module could be sufficient, operating on DC

input power plus water and delivering high pressure pure hydrogen. Such a module would have much lower installed cost than the above but the same DC to hydrogen efficiency given in Table 1.

Table 1. Projected Efficiencies for Several Systems

Operating Mode	Electrical Efficiency at 60% Output	Electrical Efficiency at 100% Output	Energy Efficiengy
Renewable DC to AC	96%	96%	
Natural Gas to AC	72%	65%	97%
Renewable DC to Hydrogen	95%	95%	
Natural Gas to Hydrogen	83%	75%	97%

Conclusions

The project has met or exceeded all technical objectives (as revised by DOE Hydrogen Program management) on budget and on time. Experimental results have been promising. The economic / engineering studies indicate the potential for reversible systems to set new standards of performance, achieving lower cost of H_2 production, lower pollution levels, and potentially serving as an enabling technology for hydrogen fuel cells. At the system level, a demonstration reactor of sufficient size to demonstrate technology proof-of-concept will be designed, built, and operated. The design of the hot subassembly will be advanced based upon engineering designs developed by TMI over the past 10 years and will include the understandings from the work presented above and learning from advanced stack development.

References

1. Private communication with Neil Rossmeissl, Hydrogen Technology Development Manager, Office of Power Delivery Systems, December 2000

FY 2002 Publications/Presentations

1. Hydrogen/Fuel Cells for Transportation/Fuels for Fuel Cells, DOE 2002 Annual Meeting, Denver Colorado, May 6-10, 2002.

II.D.6 High-Efficiency Steam Electrolyzer

Ai-Quoc Pham (Primary Contact), Ervin See, David Lenz and Robert Glass
Lawrence Livermore National Laboratory
P.O. Box 808, L-350
Livermore, CA 94551
(925) 423-339, fax: (925) 422-6892, e-mail: pham2@llnl.gov

DOE Technology Development Manager: Sigmund Gronich
(202) 586-1623, fax: (202) 586-5860, e-mail: Sigmund.Gronich@ee.doe.gov

Objectives

- Develop a novel steam electrolysis approach for highly efficient hydrogen production.
- Demonstrate the concept of using natural gas as anode depolarizer to reduce the electrical energy consumption.
- Develop the materials, processes and engineering designs for the natural-gas-assisted steam electrolyzer (NGASE).
- Build and demonstrate prototype electrolyzers.

Approach

- Investigate the depolarizing effect of natural gas using disk type samples.
- Evaluate new materials for the electrolyzer anode and cathode.
- Study the effect of microstructure on electrode performance.
- Develop low cost electrolyzer tube fabrication processes.
- Develop ceramic-to-metal seal for easy gas manifolding.
- Design tubular electrolyzer stack for high-pressure operation.
- Build and test several electrolyzer prototypes.

Accomplishments

- Demonstrated feasibility of using methane to reduce the electrical energy consumption in high-temperature steam electrolyzer.
- Developed high performance anode and cathode.
- Developed a low-cost but highly reliable thin-film coating technique.
- Explored various tube fabrication techniques, including cold isostatic pressing and low-pressure injection molding.
- Demonstrated a metal-to-ceramic seal that withstands 150 psi pressure differential.
- Built the first electrolyzer stack capable of producing 700 sccm hydrogen.

Future Directions

- Develop better tube-to-tube series connections for high voltage, low current operation.
- Study the long-term stability of the electrodes.
- Design and build 1 and 3 kW electrolyzer stacks.
- Work with our industrial partner to do system integration.

Introduction

Currently, most hydrogen demand is met by hydrogen production from fossil fuels, i.e., by steam reforming of natural gas and by coal-gasification. It is unlikely that the same approach can be used for producing and delivering hydrogen for a hydrogen-based transportation system because of the absence of an adequate hydrogen distribution infrastructure. Hydrogen produced on-site would be much more attractive and would require less costly initial investments. Unfortunately, distributed hydrogen production using small-scale conventional steam reforming is not a viable option because of the high cost and low efficiency of the reactors at small scales. More interesting approaches, such as auto-thermal reforming, micro-channel steam reforming, as well as partial oxidation processes, are currently being pursued. However, these approaches are fairly complex, involving several additional steps, such as high-temperature shift, low-temperature shift, and preferential oxidation or hydrogen gas separation.

Hydrogen can be produced from water using the simple electrolysis reaction. Because of the modularity of the electrolyzer, electrolysis can be done at large central plants, at a refueling station, or even at home. However, water electrolysis has not had a significant commercial impact because of the high electrical energy consumption and the resulting high cost. Furthermore, using the grid electricity that is produced by burning coal and natural gas will result in high greenhouse gas emissions, which would defeat the purpose of the hydrogen program.

In the near-term, fossil fuels will still be a major source for hydrogen production. The challenge is to make the production efficient and suitable for a distributed generation scenario. The purpose of this project is to develop a system that has the simplicity of conventional electrolysis while being compatible with the existing fuel infrastructure and having high efficiency with respect to primary energy, and thus having low greenhouse gas emissions.

Approach

Our approach to decrease the electrical energy input requirements for electrolysis is to use natural gas as an anode depolarizer. This approach essentially replaces one unit of electricity by one equivalent energy unit of natural gas at one-fourth the cost. There are two possible modes of operation. In the total oxidation mode, i.e. when methane is just used to reduce the electrochemical potential difference across the two sides of the electrolyzer membrane, the system does not require any gas separation and has the potential to produce pure hydrogen at high pressures. In the partial oxidation mode, methane is converted to hydrogen and carbon monoxide, which is subsequently converted to hydrogen via the water-gas shift reaction. We choose to focus our current efforts on the development of a system operating in the total oxidation mode because of its simplicity. Using an appropriate system design, it is possible to electrochemically compress hydrogen in-situ, thus eliminating the need for an expensive hydrogen compressor.

Results

We have demonstrated the proof-of-concept of the NGASE approach using single cells. A voltage reduction of 1 V was observed when methane was used in the anode side. The electricity consumption was estimated to be about one order of magnitude lower than in conventional electrolyzers. Using thin film and novel catalyst materials, we subsequently demonstrated very high performance, up to 1 A/cm^2 at only 0.5 V at 700°C. At 900°C, cell current density was as high as 2.4 A/cm^2. For electrolyzer stack development, we selected the tubular approach since tubular structures have good mechanical integrity (relative to planar designs) while enabling operation at high pressure differentials.

During FY02, we continued to improve the tube performance by improving the tube microstructure. Figure 1 shows the current-voltage characteristics for various electrolyzer tubes as compared to disk data.

We have evaluated several ceramic tube fabrication techniques. The cold isostatic approach turned out to be inadequate for the present purpose because of the difficulties to incorporate sufficient porosity in the structure. A low pressure injection molding technique was successfully developed to fabricate green tubes with lengths up to sixteen inches (Figure 2).

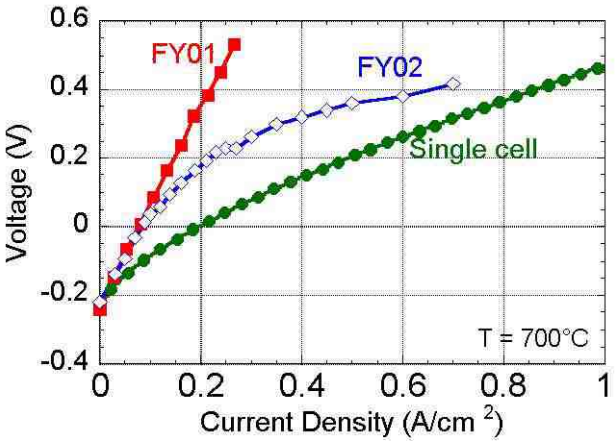

Figure 1. Current-Voltage Curves of Various Electrolyzer Tubes and of Single Disk

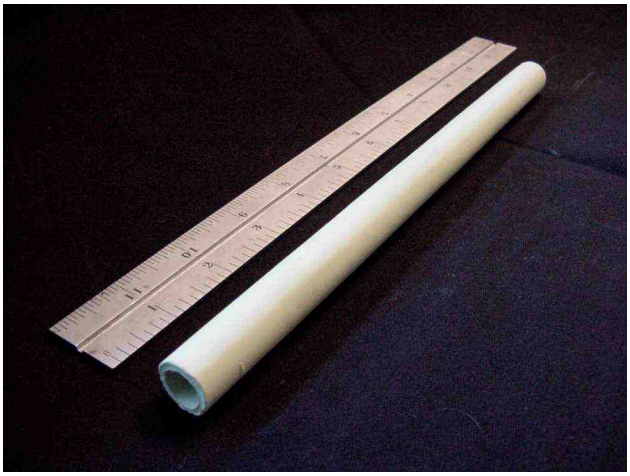

Figure 2. An Injection-Molded Electrolyzer Tube

Figure 3. Metal-to-Ceramic Seal

Figure 4. A 4-tube Electrolyzer Stack Prototype

Although the tubular design reduces significantly the issues typically encountered with sealing, there is still a need to seal the two ends of the tubes in order to avoid potential CO contamination and to enable operation with a pressure differential across the tube. We successfully developed a metal-to-ceramic seal that is leak-free up to 150 psi pressure differential (Figure 3).

Four electrolyzer tubes were assembled in parallel to form a prototype stack (Figure 4). When operated at 750°C, the stack produces 700 sccm hydrogen standard temperature and pressure. The stack performance was somewhat lower than what was expected from single tube results. The difference could come from the resistive loss in the cables because of very high current in the stack. This observation suggests that a series design with lower current and higher voltage is more desirable. A new stack design is being developed.

Conclusions

The electricity required for steam electrolysis can be reduced significantly if natural gas is used as anode depolarizer. The efficiency of the NGASE was estimated to be between 60 to 75%, depending on the current density. That number is significantly higher than the typical 40% efficiency for conventional electrolysis using average grid electricity.

We have demonstrated the concept and have developed the materials and initial system design. The development of the first electrolyzer stack prototype indicated that a number of issues remain to be improved. Most important of all are the long-term stability and the electrical connection between tubes.

FY 2002 Publications/Presentations

1. DOE Annual Program Review for 2002, May 8, 2002, Denver, CO

II.D.7 Enabling Science for Advanced Ceramic Membrane Electrolyzers

Fernando Garzon (Primary Contact), Rangachary Mukundan, and Eric Brosha
Los Alamos National Laboratory
MS D429, MST-11 Group
Los Alamos, New Mexico, 87545
(505) 667-6643, fax: (505) 665-4292, e-mail: garzon@lanl.gov

DOE Technology Development Manager: Sigmund Gronich
(202) 586-1623, fax: (202) 586-5860, e-mail: Sigmund.Gronich@ee.doe.gov

Main Subcontractor: Los Alamos National Laboratory, Los Alamos, New Mexico

Objectives

- Evaluate proton-conducting ceramic membranes for use in electrolyzers.
- Fabricate dense ceramics of cerates and zirconates and measure the bulk hydrogen conductivity using AC impedance spectroscopy and DC conductivity measurements; demonstrate water electrolysis using these materials.
- Synthesize electrode materials for electrolysis and characterize their polarization behavior using electrochemical methods.

Approach

- Synthesize cerate and zirconate proton-conducting oxides from the component oxides.
- Evaluate the structure and composition of the cerate and zirconate ceramics using X-ray diffraction and X-ray fluorescence techniques.
- Characterize the bulk hydrogen conductivity of the sintered proton-conducting ceramics using AC impedance spectroscopy and DC conductivity measurements.
- Obtain tubes of the proton-conducting ceramics and apply electrodes to these proton-conducting tubes.
- Design an experimental setup to demonstrate water electrolysis and hydrogen generation.
- Optimize electrode materials for electrolysis and characterize their polarization behavior using electrochemical methods.

Accomplishments

- Synthesized $SrCe_{0.95}Yb_{0.05}O_{3-x}$ and $SrZr_{0.9}Y_{0.1}O_{3-x}$ proton-conducting oxides.
- Confirmed the orthorhombic crystal structure of the proton-conducting oxides using X-ray diffraction. The lattice parameters of the proton-conducting oxides were also measured.
- The composition of the oxides was verified using X-ray fluorescence.
- Dense sintered proton-conducting ceramics were prepared, and their electrical conductivity was characterized using AC impedance spectroscopy and DC conductivity measurements.
- Tubes of the proton-conducting ceramic $SrCe_{0.95}Yb_{0.05}O_{3-x}$ were obtained from TYK Ceramics, and platinum electrodes were applied to the inner and outer sides of these tubes.
- An experimental setup to demonstrate water electrolysis and hydrogen generation has been designed by modifying a furnace to fit the electrolyzer tubes and by using an HP 5890 Series II chromatograph to analyze the evolved gases.

Future Directions

- The hydrogen evolution from the $SrCe_{0.95}Yb_{0.05}O_{3-x}$ tubes will be characterized under various conditions of temperature, water vapor and oxygen partial pressure.
- The polarization due to the platinum electrodes will be evaluated using AC impedance techniques.
- Alternative oxide electrodes to replace the platinum electrode will be prepared and evaluated.

Introduction

Efficient and economical electrolysis of water to hydrogen and oxygen gases is of great importance to renewable hydrogen energy programs. Combined fuel cell/electrolyzer systems offer the potential for efficient energy storage and conversion. Unfortunately, low-cost and low-maintenance electrolyzer technologies are not commercially available. Current alkaline and polymer membrane based electrolysis systems suffer from the following disadvantages:

- The hydrogen product gas is saturated with water vapor; the gas must be dried before the hydrogen can be stored in a hydride bed.
- Both technologies require high loadings of precious metal catalysts to reduce the overpotential losses.
- Neither technology is amenable to high-pressure operation. It is very difficult to pressurize wet alkaline electrolyte cells. Polymer membrane cells allow high crossover rates of gases across the membranes at elevated pressures.
- Long-term stability and contamination is a problem with both alkaline and polymer membrane electrolysis electrolytes. Alkaline electrolytes adsorb carbon dioxide readily and form carbonates. Polymer membrane systems must use very pure de-ionized water or they will accumulate cations that displace protons and increase the cell resistance over time.

A promising alternative to liquid and polymer membrane electrolytes is a proton conducting ceramic solid electrolyte technology. These materials offer a number of potential advantages over current systems:

- The ceramic electrolyzers are solid-state devices with no polymer or liquid electrolyte to contaminate, and they are well suited to operate at elevated pressures.
- The devices should operate with steam without expensive cation removal/carbon dioxide pretreatment.
- The ceramic cells operate at temperatures from 450-800°C and thus at a lower thermodynamic potential than the low-temperature systems.
- The elevated operating temperatures enable the use of non-precious metal electrodes, and electrode reaction kinetics may also be faster at these elevated temperatures.
- Temperatures in this range are directly compatible with solar furnace operating temperatures, offering potentially attractive integrated hybrid electrical/hydrogen generation systems.

Finally, this technology is intrinsically different from the other solid-state technology using zirconia-based oxygen ion electrolyzers in that the transported (separated) species is hydrogen rather than oxygen. The zirconia oxide ion systems produce a wet hydrogen product stream. The proton conducting ceramic electrolyte does not suffer from this disadvantage and produces a dry hydrogen stream with no further purification needed. The electrolysis of water vapor on oxygen ion and proton conducting ceramics is illustrated in Figure 1. We propose to demonstrate the feasibility of water electrolysis using solid-state electrochemical cells based on proton ion conducting solid electrolytes.

Approach

The principal goal of this project is to demonstrate electrolysis technology using ceramic electrochemical cells based on solid oxide proton conductors. Los Alamos National Laboratory (LANL) has experience in solid-state bulk and thin

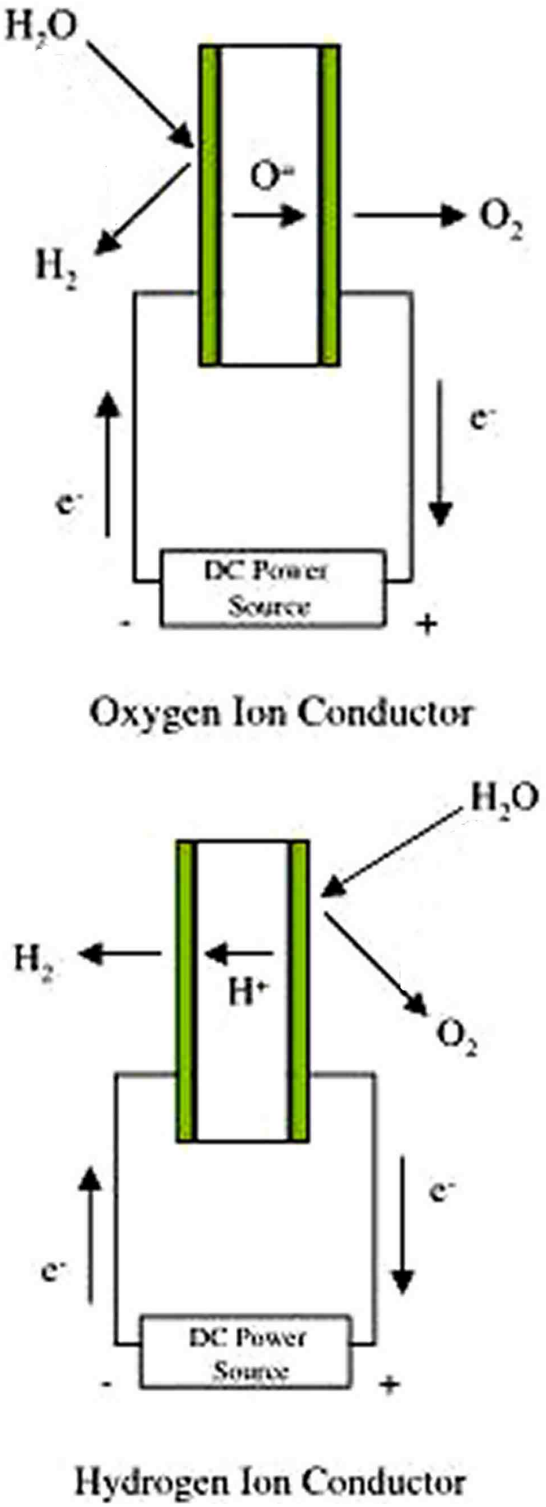

Figure 1. Schematic Illustration of Water Electrolysis on an Oxygen Ion Conducting Electrolyte (top) and a Hydrogen Ion Conducting Electrolyte (bottom).

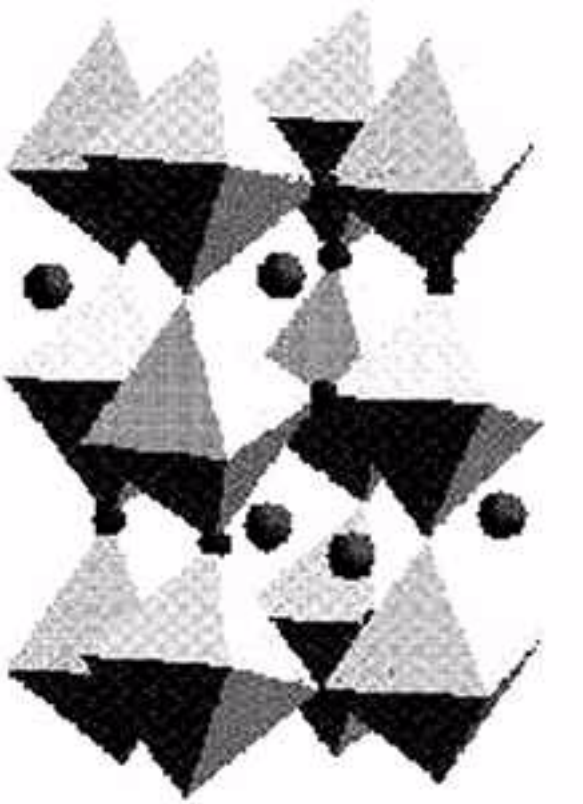

Figure 2. Polyhedral representation of the $(Sr,Ba)(Zr,Ce)(B)^{3+}O_{3-y}$ perovskites where $(B)^{3+}$ designates a trivalent substituted cation. The (Sr,Ba) occupy the A site; $(Zr,Ce)(B)^{3+}$ occupy the B center positions of the octahedrally coordinated oxygen.

film materials synthesis and characterization capability. We will synthesize and characterize electrolyte and electrode materials and fabricate test cell apparatus. Characterization methods available in the Electronic and Electrochemical Materials and Devices Group include X-ray diffraction, thermo gravimetric analysis, energy dispersive X-ray analysis, scanning electron microscopy and AC impedance and DC cyclic voltammetry electrochemical methods.

Recently, a number of perovskite structure ceramic proton separation membranes have been developed and reported by Iwahara et. al. [1]. These materials exhibit good stability, high ionic transport rates for protons and also operate in the 600-900°C temperature range which is optimal for insitu

catalysis reactions. The materials are also of great value for high temperature fuel cell technologies, isotope separation systems, sensor applications and heterogeneous catalysis [2,3].

The proton conducting materials are rare earth cerate and zirconate ABO_3 formula oxides, e.g. (Sr,Ba) (Zr,Ce)$(B)^{3+}O_{3-y}$, where $(B)^{3+}$ is a three valent yttium or lanthanide cation. The crystal structures of all of these materials are typically orthorhombic distortions of the cubic perovskite structure due to a tilt of the oxygen coordinated octahedra as illustrated in Figure 2. The perovskite materials contain oxygen ion vacancies introduced by the $(B)^{3+}$ substituting for four valent zirconium or cerium. Exposing these materials to steam at elevated temperatures causes water to hydrolyze and fill the vacancies with oxygen and two mobile protons.

Since these first reports, Iwahara and other investigators have studied the conductivities (both ionic and electronic), conduction mechanism, deuterium isotope effect, and thermodynamic stability of these materials. The motivation for most of this work derives from the desire to utilize these materials for high temperature, hydrogen-fueled solid oxide fuel cells. In a reverse operation mode, if metal or metal oxide electrodes are deposited onto a dense pellet of this material and heated to temperature T, the application of an electric potential to the electrodes will cause a hydrogen partial pressure difference across the pellet according to the Nernst equation:

$$\Delta V = \frac{RT}{zF} \ln \frac{P'_{H2}}{P_{H2}}$$

where F is Faraday's constant and z is the number of electrons transferred upon oxidation and reduction. For example, at 500°C the application of 1.5 V would produce a hydrogen partial pressure difference across a pellet on the order of 1020. These differences in hydrogen activity are high enough to decompose water at elevated temperatures.

The Sr and Ba-doped cerate electrolytes exhibit the highest proton conductivities; however, recent reports question the thermodynamic stabilities of the Ba compounds at intermediate temperatures and in the presence of high partial pressures of CO_2 and H_2O. It is unclear whether this will present a problem for electrolysis applications; therefore, we will evaluate the thermodynamic stability of these materials and study the stability of potential substitute candidates.

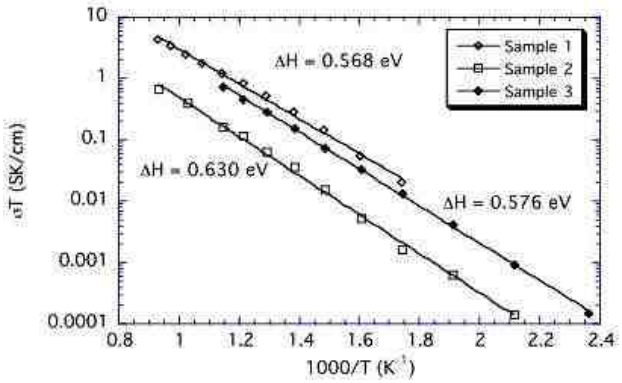

Figure 3. The Conductivities of Three $Sr_{0.95}Yb_{0.05}CeO_{3-x}$ Ceramic Samples Produced Using Differing Ceramic Processing Methods

Results

Consequently, we are in the startup phase of our program. Our first task was to identify candidate perovskite oxide materials with high protonic conductivities. We have identified ytterbium doped strontium cerate and yttrium doped strontium zirconate materials as possible electrolyte materials. Barium cerate perovskites exhibit higher protonic conductivity, but the reactivity with carbon dioxide would require pretreatment of the steam.

We have designed and assembled a high temperature AC impedance system for measurement of protonic conductivities. Our measurements of candidate ceramic protonic conductivities indicate that the electrolyte resistance in thin membrane form should not impose a large internal resistance (IR) loss on the electrolysis cell. However, ceramics processing also plays an important role in determining the conductivities of these materials. Figure 3 displays the conductivities of three $Sr_{0.95}Yb_{0.05}CeO_{3-x}$ samples made using differing starting powders and sintering schedules.

Figure 4. Ceramic Electrolyte Tube of $SrCe_{0.95}Yb_{0.05}O_{2.975}$ Custom Fabricated for LANL by TYK Corporation

We have identified and contracted a ceramics supplier, TYK Corporation, to fabricate electrolyte tubes for prototype electrolyzer research studies. The supplier has successfully manufactured and delivered closed end electrolyzer membrane tubes to LANL. The composition of the tubes is $SrCe_{0.95}Yb_{0.05}O_{2.975}$, and the tubes are 200 mm in length with an inner diameter of 12 mm and an outer diameter of 15 mm. Although the membrane thickness of 1.5mm could lead to significant IR losses (20-30 Ω cm^2 specific resistance), these tubes are ideally suited for the evaluation of these proton-conducting membranes as electrolyzers. Figure 4 is a photograph of a recently manufactured electrolyzer tube.

Platinum electrodes have been painted on an electrolyzer tube, and an experimental setup has been designed and built to evaluate the hydrogen permeation. The electrolyzer tube is placed in a modified Lindberg/BlueM furnace, and the gases are fed into an HP 5890 Series II gas chromatograph for analysis.

Conclusions

- $Sr_{0.95}Yb_{0.05}CeO_{3-x}$ has been selected as the first protonic conductor to be evaluated as an electrolyzer membrane.
- The conductivity of the ceramics reveals that thin films (<100 μm) of this material should be suitable for the manufacture of a practical electrolyzer.
- Tubes of the $Sr_{0.95}Yb_{0.05}CeO_{3-x}$ ceramic have been obtained and will be evaluated with the experimental setup that has been designed and built.

References

1. H. Iwahara, T. Esaka, H. Uchida and N. Maeda, Solid State Ionics, 3/4, 359 (1981)

2. A. S. Nowick and A. V. Vaysleyb, Solid State Ionics, 97, 17 (1997)

3. R. Mukundan, E.L. Brosha, S. A. Birdsell, A. L. Costello, F. H. Garzon, and R.S. Willms, Journal of the Electrochemical Society, 146, no.6, 2184-7(1999)

FY 2002 Publications/Presentations

1.Applications of Proton Conducting Perovskites, Rangachary Mukundan, Eric L. Brosha, and Fernando H. Garzon, A symposium in Honor of the 65th Birthday of Professor Wayne L. Worrell, PV 2002-5, pp. 142-147 (2002) The Electrochemical Society Inc.

II.D.8 Hydrogen Production Through Electrolysis

Robert J. Friedland (Primary Contact), A. John Speranza
Proton Energy Systems, Inc.
10 Technology Drive
Wallingford, CT 06492
(203) 678-2000, fax: (203) 949-8078, e-mail: rob.friedland@protonenergy.com

DOE Technology Development Manager: Sigmund Gronich
(202) 586-1623, fax: (202) 586-5860, e-mail: Sigmund.Gronich@ee.doe.gov

Objectives

- Reduce the cost of proton exchange membrane (PEM) electrolysis to levels of $1250/kW for 10,000 standard cubic feet per day (scfd) at production levels of 10,000 units per year.
- Reduce the cost of smaller units (1,000 scfd) of $2500/kW in production volumes of 10,000 units per year.
- Evolve the use of PEM electrolysis as an energy storage device to enable renewable energy technology as a sustainable source of electricity.

Approach

- Validate the design and cost reductions for the hydrogen oxygen generator (HOGEN®) 40 generator control board and advance that design into the more complicated controls of the HOGEN® 380 hydrogen generator.
- Design a cell stack compression scheme that reduces the material and labor cost associated with the manufacture of the cell stack.
- Investigate low cost power conversion options for use across the line of hydrogen generators.
- Test a renewables interface to a HOGEN® 40 generator and collect data to understand how the system interacts with the renewable (photovoltaic- or wind-powered) device.

Accomplishments

- Completed the validation of the HOGEN® 40 generator control board and the design specification for the HOGEN® 380 hydrogen generator control board. Savings of at least $3,500 of material and 40 hours of labor were removed from the HOGEN® 40 generator.
- Reduced the number of parts in the cell stack compression from 1344 to 15, assembly time from 75 minutes to 5 minutes, and overall volume by over 30%.
- Determined that a non-isolated power converter with minimal energy storage can get to between $.033-$.05/watt for the generators.
- Developed a 5 kW converter for photovoltaic (PV) and wind systems and tested the converter at Northern Power Systems.

Future Directions

- Validate the design of the control board for the HOGEN® 380 generator.
- Analyze additional power electronics options for the HOGEN® 380 generator.
- Conduct additional testing using a PV array coupled to a HOGEN® 40 generator.

Introduction

Proton's goal is to drive the cost of PEM electrolysis to levels of $1250 per kilowatt for 10,000 scfd and $2500 per kilowatt for 1,000 scfd of hydrogen gas output. Both of these costs assume a manufacturing volume of 10,000 units per year, and the cost per kilowatt is based on electrical power into the electrolyzer. In addition, this project will evolve the use of PEM electrolysis as an energy storage device to enable renewable energy technology as a sustainable energy source.

For this past fiscal year, Proton has focused on several aspects associated with these cost reduction efforts. First, all of the previous cost reductions on the HOGEN® 40 generator (see Figure 1) needed to be fully validated by testing to show they would meet the technical requirements of the product and support the customer and market requirements. Second, the control board on the HOGEN® 40 was to be advanced into the HOGEN® 380 generator product (see Figure 2). Third, investigation work was to be conducted on power supply options for the HOGEN® 380 generator based on some of the work on the HOGEN® 40 generator, but advanced to incorporate the higher power levels required on the larger units. Fourth, cell stack cost reduction activities on compression hardware was to be advanced and cost traded with traditional spring washer approaches. Finally, data was to be collected on renewable power inputs using power conditioning equipment developed by the project.

Approach

The HOGEN® 40 generator was chosen as the model for cost reduction for two reasons. First, the smaller size of the HOGEN® 40 generator made cost reduction activities and hardware purchases less costly, and thus enabled a larger scope of effort and impact on return. Second, advances are scalable. In other words, improvements and cost reductions made on the HOGEN® 40 generator can be scaled to the larger HOGEN® 380 generators with less financial and project related risk. The specifics of this approach were outlined in the Technical Paper submitted for that year's annual review[2].

Figure 1. HOGEN® 40 Hydrogen Generator

Figure 2. HOGEN® 380 Hydrogen Generator

The cost reduction effort targeted the electrical controls and mechanical systems that were common across the range of hydrogen generators and would need to be used for future products involving renewable energy technologies. The control board design and development done in this project yielded significant reductions in both material and labor costs. In addition, mechanical system

Figure 3. Current Cell Stack Compression Configuration

Figure 4. Improved Cell Stack Compression Configuration

simplifications, plumbing and fitting reductions and part substitutions also played a large role in the cost reduction effort for both labor and material. These modifications coupled with new technology developments like a power interface for renewable energy input successfully moved the HOGEN® 40 generator product towards renewable energy utility. By the end of FY2001 many of these design improvements and cost reductions had been developed but not fully validated[3].

Results

Cell Stack Compression

This task was to study the cost and performance differences of changing the methodology of compressing the electrolysis cell stack from a large number of spring washers (see Figure 3) to a fewer number of larger spring washers (see Figure 4). This change has yielded some impressive results. Changing to the large diameter spring reduces the assembly time of the washers from 75 minutes to 5 minutes, and reduces the parts count from 1344 pieces to 15. From a manufacturing standpoint, these are very impressive reductions that also have a tremendous impact on quality and consistency of assembly. Each of the smaller springs needs to be oriented in a certain way and with a certain ordering configuration on each rod. This complicated assembly is prone to mistakes that cause rework and could possibly jeopardize the sealing integrity of the cell stack.

Control System Cost Reduction

The HOGEN® 40 generator control board design represents a significant cost reduction to the overall electrolyzer control system. The material cost for the control system has been reduced from over $3,500 to less than $300 with a 40 hours to one hour reduction in labor (see Figures 5 and 6). This year's effort was focused on validating the design changes that were made to cost reduce the electrolyzer control system

in order to insure that the integrity and reliability of the product was not compromised. The control board was developed beyond the prototype stage and underwent extensive design validation testing prior to production release. Validation of the control board included Highly Accelerated Life Testing (HALT), which exposed the board to environmental extremes in order to identify hardware limitations. The results of the HALT testing were fed back into the design process to further enhance the robustness of the control board design. Validation testing also included agency safety/EMC testing and equivalent certifications for Underwriters Laboratory, CSA, and CE. The control board also underwent operational testing to insure that the electrolyzer operated within design specifications through all modes of operation.

The cost reduction efforts on the HOGEN® 380 generator control system have resulted in a greater than 90% control system cost reduction. The fact that the HOGEN® 380 generator control board was developed off of the HOGEN® 40 generator control board design and was able to maintain the same basic architecture and function has resulted in a much more dramatic hardware cost reduction. The current HOGEN® 380 generator control system costs in excess of $10,000. The projected cost of the production control board in modest volumes is less than $500. The validated HOGEN® 40 generator control board was used as the base platform for the HOGEN® 380 generator control board.

The HOGEN® 380 generator control board specification was drafted and a prototype board was delivered for functional testing early this year. The prototype board was then incorporated into an electrolyzer system to verify the design and test the basic functionality of the cost-reduced system. Basic design verification testing was completed, and the board design was modified to incorporate the changes that resulted from the verification testing. The beta board will be delivered this year and undergo extensive validation testing

HOGEN® 380 Generator Fluid Management Cost Reduction

Following the same strategy as was used on the control board development, a tremendous amount of cost reduction has been realized on the HOGEN® 380 generator fluids system with a minimal amount of reengineering. The components that were developed for the HOGEN® 40 generator were used as the platform for further cost reductions on the HOGEN® 380 generator. The development efforts on gas drying for the HOGEN® 380 generator have resulted in a low-cost pressure swing absorption dryer that can be manufactured in low quantities for under $4,000 compared to the previous design that was

Figure 5. Current Discreet Electrical Component Layout

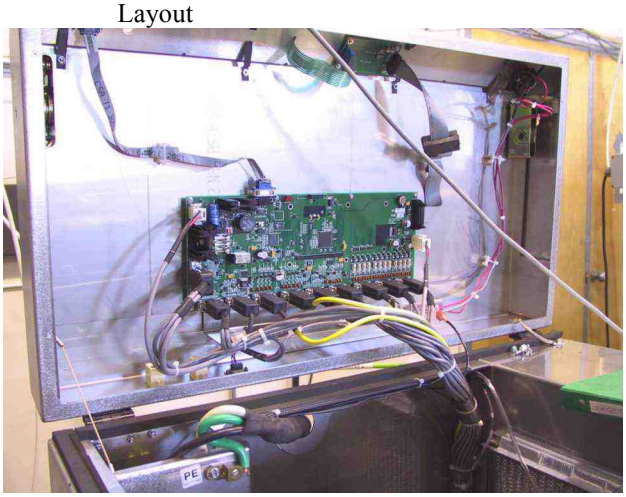

Figure 6. New Control Board Design

over $8,000. In higher volumes the cost of this dryer will be well under $2,000.

Power Conversion Cost Reduction

One of the first efforts that needed to occur, for the power conversion cost reduction to be successful, was a cell stack electrical characterization study. This task helped to understand the electrolysis cell stack as a power load.

Utility Grid Converter

With the cell stack characterization complete, a feasibility study and paper design based on a power electronics cost reduction effort for the HOGEN® 40 hydrogen generator was conducted. It was concluded that the high cost of power conversion of these units is due mainly to two factors: buying an "off-the-shelf" design that is not optimized for the electrolysis application and providing galvanic isolation to the electrolysis cell. The study concluded that a non-isolated power converter with minimal energy storage has the potential to achieve $.033/watt for the HOGEN® 40 generator and $.05/watt for the HOGEN® 380 generator.

Based on the initial results of the feasibility study, the design and development of a cost reduced power electronics package appears feasible. The path to the lowest cost for power electronics is in a design that is optimized for the electrolysis process, and the best approach to accomplish this is to develop the design "In House" or in cooperation/collaboration with a third party.

Presently, the HOGEN® 40 generator power electronics costs $0.30/watt and delivers DC power at an average efficiency of 85%. The feasibility study identifies a design path with the ability to reduce the cost of power electronics to less than $0.10/watt and an average efficiency of 94%.

Renewable Energy Interface Converter

Sustainable Energy Technologies (SET) was contracted to develop an interface converter with the capability to accept a power input from a photovoltaic or wind source. SET delivered two 5 kW photovoltaic interface converters that were tested by Northern Power Systems in Waitsfield, Vermont and found to meet the basic specifications of the design. SET also delivered an interface converter that was capable of accepting a wind turbine input, but due to the inability to interface directly to a wind turbine the converter was never tested beyond the basic power test. One of the PV converters has been delivered to the Illinois Institute of Technology for integration into a renewable energy system utilizing one of Proton's HOGEN® 40 hydrogen generators.

Conclusions

A sustainable energy system utilizing renewable energy technology must have the fundamental capability of storing excess renewable energy when it is available so it can be utilized on demand. Renewable energy technology is inherently intermittent based on the fundamental fact that the wind does not always blow and the sun does not always shine. Electrolyzer technology has great promise for helping to bridge the gap and make electricity available twenty-four hours a day, seven days a week. Proton's hydrogen generators also follow the load extremely well and can respond virtually instantaneously to fluctuations in power levels from the renewable energy device. However, the cost challenges associated with electrolysis must be overcome. This project has made tangible progress on reducing cost through various design initiatives and bringing those designs forward into products

References

1. Friedland, R., Smith, W., Speranza, A., January 2000. Integrated Renewable Hydrogen Utility System, Phase I Final Technical Report and Market Assessment PES-T-99014.

2. Friedland, R., May 2000. Integrated Renewable Hydrogen Utility System, Phase II Technical Paper for Annual Technical Peer Review.

3. Friedland, R., Speranza, A., May 2001. Hydrogen Production Through Electrolysis, Phase II Technical Paper for Annual Technical Peer Review.

II.E Hydrogen Fueling Systems and Infrastructure

II.E.1 Development of a Turnkey Commercial Hydrogen Fueling Station

David E. Guro (Primary Contact)
Air Products and Chemicals, Inc.
7201 Hamilton Blvd.
Allentown, PA 18195-1501
(610) 481-4625, fax: (610) 481-4260, e-mail: gurode@apci.com

DOE Technology Development Manager: Arlene Anderson
(202) 586-3818; fax (202) 586-9234, e-mail: Arlene.Anderson@ee.doe.gov

ANL Technical Advisor: William Swift
(630) 252-5964, fax: (630) 972-4473, e-mail: swift@cmt.anl.gov

Subcontractors: H2Gen Innovations, Inc., Alexandria, Virginia; Pennsylvania State University, University Park, Pennsylvania; QuestAir Technologies Inc. (under negotiation), Burnaby, British Columbia, Canada

Objective

Demonstrate the potential for an economically viable stand-alone, fully integrated hydrogen (H_2) fueling station based upon the reforming of natural gas by striving to:

- Develop a cost-effective solution to the reforming of natural gas to produce a reformate stream;
- Develop an efficient, cost-effective means to purify the hydrogen-rich reformate to pure hydrogen employing pressure swing adsorption (PSA) technology;
- Develop an optimum system to compress, store, meter, and dispense hydrogen into vehicles;
- Efficiently integrate the process steps mentioned above into a safe, user-friendly, cost-effective fueling station;
- Demonstrate the operation of the fueling station at Penn State University;
- Maintain safety as the top priority in the fueling station design and operation; and
- Obtain adequate operational data to provide the basis for future commercial H_2 fueling stations.

Approach

This nine-quarter project is being managed in three phases, with Stage Gate reviews between each phase. These phases overlap in time in order to make efficient use of resources and minimize costs.

- In Phase 1, conceptual design and preliminary cost evaluations for each major sub-system in the fueling station will be completed.
- In Phase 2, sub-system R&D will be performed to test the concepts put forth in Phase 1. Technical viability and fueling station costs will be validated.
- Phase 3 will include fabrication, installation, and testing of the full-scale H_2 generator and dispenser at Penn State University. This H_2 fueling station will be designed to deliver 50 nm^3/hr H_2.

Accomplishments

- Kicked off development work on the novel reforming system.
- Began the process and cost study of the various reforming options available.
- Initiated the H_2 PSA development program at Air Products and Chemicals, Inc. (APCI) and the engineering services study at QuestAir.
- Built a prototype H_2 PSA system to be installed for testing at an Air Products H_2 production facility.
- Started engineering work on the compression and dispensing systems.
- Equipped a laboratory to test H_2 flow meters for use within the dispenser.

Future Directions

In the near term, the development team will conclude the Phase 1 work and hold a Stage Gate review meeting with DOE management. Then, work on all aspects of Phase 2 will commence, followed by Phase 3. The expected schedule for these Phases is outlined in the table below:

Task	Date
Phase 1 Pre-Contract Technical Development	Oct 2001 – March 2002
Cooperative Agreement Award	29 March 2002
Phase 1 Conceptual Design and Economic Evaluation	April 2002 – June 2002
Phase 2 Subsystem Development	July 2002 – March 2003
Phase 3 System Deployment	April 2003 – December 2003
Phase 3 System Deployment – Operation & Testing	January 2004 – June 2004

Introduction

The transition to hydrogen as a fuel source presents several challenges. One of the major hurdles is the cost-effective production of hydrogen in small quantities. In the early demonstration phase, hydrogen can be provided by bulk distribution of liquid or compressed gas from central production plants; however, the next phase to fostering the hydrogen economy will likely require onsite generation to institute a pervasive infrastructure. Providing inexpensive hydrogen at a fleet operator's garage or local fueling station is a key step toward enabling commercialization of direct hydrogen fuel cell vehicles (FCVs). The objective of this project is to develop a comprehensive, turnkey, stand-alone hydrogen fueling station for FCVs with state-of-the-art technology that is cost-competitive with current hydrocarbon fuels. Such a station will promote the advent of the hydrogen fuel economy for buses, fleet vehicles, and ultimately personal vehicles.

Approach

The development efforts are expected to build on preliminary work accomplished by the major partners. Air Products, as the overall project manager, is responsible for the total system integration and final development of the installed equipment. As the system integrator, Air Products will ensure that the system is fully optimized and that all of the individual components are compatible to deliver the lowest cost H_2 fuel. This nine-quarter project is being managed in three phases, with Stage Gate reviews between each phase.

During Phase 1 of the program, subsystem conceptual designs will be formulated and costed. Options will be developed and compared for the

reformer system, PSA system, compression, storage, and dispenser. Air Products will work with H2Gen to develop and to evaluate the applicability of a novel convective steam methane reforming (SMR) based reforming system. At the end of Phase 1, we will confirm the preliminary feasibility of cost targets via an initial, pre-developmental definition of scope and execution costs and will identify the partners for further development of components.

In Phase 2, the most promising subsystem designs assessed and selected in Phase 1 will be further developed. Lab testing of certain components will be carried out. Recommendations for the optimal fueling station components will be made. Air Products engineers, working with the selected reforming partner, will optimize the design of the reformer and PSA systems, and build and test components of the systems in laboratories. Air Products will be directly responsible for the design of the dispenser, which will be tested in a shop prior to installation on site. Finally, Air Products will act as the system integrator to pull together the various pieces into a comprehensive turnkey unit and to minimize the total cost of delivered H_2.

During Phase 3, scale-up and detailed engineering design of all equipment will be completed. The engineered system will be analyzed for Design for Manufacture and Assembly (DFMA), and the assembled system will include instrumentation for data collection and provisions for remote monitoring of operation. Fabrication of all equipment and installation at Penn State University will follow. The fueling station will be started up and put into operation, beginning with 6 months of operation and testing. Finally, the cost of H_2 delivered from the installed fueling station will be validated, taking into account the impact of mass-producing components.

Results

As shown in Figure 1, hydrogen can be delivered for use at a refueling station in several ways. It can be piped to the station via a pipeline, delivered in cryogenic liquid form and then vaporized, delivered in compressed gaseous form and stored in on-site tanks, generated on-site via reforming of hydrocarbon feedstocks such as natural gas, or

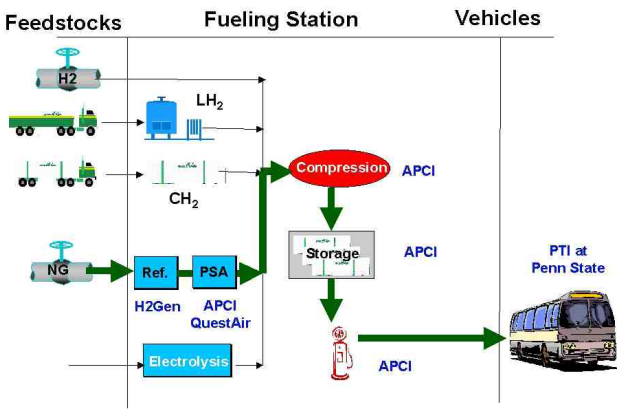

Figure 1. Hydrogen Fueling Station

produced via electrolysis of water with power input. The scope of this program is to develop the route highlighted with the bold arrows in Figure 1 – the reforming of natural gas followed by H2 purification with PSA technology. Subsequently, the high purity H2 will be compressed and stored prior to final dispensing into the H_2 vehicles.

Also highlighted in Figure 1 next to each process unit operation is the development partner responsible to contribute to the development or engineering of that piece of equipment. The development team began work addressing the technical challenges in October 2001. Below is a summary of progress to date:

Regarding aggreements and contracts, the cooperative agreement between DOE and APCI was signed on 29 March 2002. Subsequently, the subcontract with H2Gen was signed for development of the reformer. The subcontract with QuestAir is in review for supply of an improved H_2 PSA purifier design, and the subcontract with Penn State University has been completed for siting of the fueling station.

In the reforming area, H2Gen development work kicked off in October 2001. Catalyst characterization work has begun, and the first prototype reformer is being built. Components have been tested, and the burners have been sized and tested in the lab. In addition, APCI began its engineering study in April 2002 to update the comparison of autothermal reforming (ATR), partial oxidation (POX), and SMR technologies to

determine the optimum route to small-scale H_2 production. This kicked off the "Phase 1" portion of the development program.

As part of this Phase 1 study, APCI prepared and sent out a Request For Quotation (RFQ) for the reforming system to several reformer vendors. Included in the RFQ were companies offering SMR, ATR, and catalyst systems.

The development of a H_2 PSA at APCI began in October 2001. Adsorbent development has commenced and step-out approaches to achieving compact PSA designs have been identified. PSA cycle development work is underway to fully utilize the adsorbents' capabilities. Laboratory experiments are underway. Additionally, development of new PSA valves, vessels, and other mechanical components has been initiated; testing plans have been formulated; and laboratories are being equipped for component testing. To hasten the introduction of some of these new concepts, APCI completed detailed design of a prototype H_2 PSA unit to be evaluated at one of APCI's H_2 production facilities. The data collected on this PSA unit will serve to verify several of the significant technical "step-outs" being taken in the new PSA design being developed by the APCI team. Fabrication of this PSA skid was completed in early June, and the system is being installed on site. Finally, in anticipation of an engineering services sub-contract, QuestAir began work to improve their HyQuestor H_2 purifier in October 2001. Their preliminary design and cost summaries are nearing completion.

APCI's compression, storage, and dispensing development work began in October 2001. To date, APCI has completed the preliminary engineering work to determine the optimum configuration and selection of components for the H_2 dispenser. Also, laboratory equipment to test H_2 flow meters for use in the dispenser has been purchased and is being installed.

APCI has completed the initial conceptual process flow diagram (PFD) for the integrated fueling station. This will serve as the basis for engineering discussions related to the Penn State fueling station. To date, process specifications for all major components in the fueling station have been issued. Regarding utilities, APCI has defined a natural gas specification based on North American averages, has defined a potable water specification, and has identified Penn State's specific natural gas and potable water specifications for use as the design basis for the system to be placed there.

Conclusions / Future Directions

Work has begun on this aggressive project to determine the viability of a commercial turnkey H_2 fueling station. Initial conclusions will be communicated at the completion of the Phase 1 tasks and will be included in the Phase 1 report.

II.E.2 Autothermal Cyclic Reforming Based Fueling System

Ravi V. Kumar (Primary Contact), George N. Kastanas, Shawn Barge, Vladimir Zamansky, and Randy Seeker
GE Energy and Environmental Research Corporation
General Electric Co.
18 Mason
Irvine, CA 92618
(949) 859-8851 ext. 159, fax: (949) 859-3194, e-mail: Ravi.Kumar@ps.ge.com

DOE Technology Development Manager: Sigmund Gronich
(202) 586-1623, fax: (202) 586-5860, e-mail: Sigmund.Gronich@ee.doe.gov

ANL Technical Advisor: Thomas G. Benjamin
(630) 252-1632, fax: (630) 252-1632, e-mail: Benjamin@cmt.anl.gov

Subcontractors: Praxair and BP

Objectives

- Design, fabricate, and install a reliable and safe H_2 refueling system, based on autothermal cyclic reforming (ACR), that is capable of producing at least 40 kg/day of H_2 (450 std m^3 per day of H_2), which is sufficient for refueling at least 1 bus or 8 cars per day.
- The current target cost for generation and refueling of hydrogen is $19.2/GJ of hydrogen for a 900 kg/day of H_2 (10,000 std m^3 per day of H_2) system, based on the lower heating value (LHV) of hydrogen. The future target cost is expected to decrease to $17.2/GJ by 2005 and $16.2/GJ by 2010.

Approach

- Phase I (2002): Complete the design of the integrated system and assess the technical and economic feasibility of the design.
- Phase II (2003-4): Perform subsystem development.
- Phase III (2004-5): Demonstrate the fully integrated system.

Accomplishments

- An optimal process configuration was selected, process flow diagrams were developed and efficiencies were calculated.
- In collaboration with another ongoing DOE project, "Fuel Processing Based on ACR for Stationary PEM Fuel Cells" (contract No. DE-FC02-97EE50488), the component design of a fuel processor has been completed and the system is being fabricated. The fabrication is expected to be complete by July 2002.
- A detailed safety assessment including personnel hazard analysis (PHA), hazardous operations (HAZOP) and failure mode and effects analysis (FMEA) has been performed.
- An economic analysis for the hydrogen refueling station is being performed. Based on information from the literature, the cost of each subsystem of the refueling station was expressed as a function of the quantity manufactured and the hydrogen capacity. Preliminary estimates were made for cost of H_2.

Future Directions:

- Complete the system design.
- Complete the economic analysis.
- Develop a plan for Phase II.

Introduction

Autothermal Cyclic Reforming (ACR) is a GE patented technology for converting hydrocarbons to a hydrogen-rich stream. The ACR process operates in a three-step cycle that involves steam reforming the fuel on a nickel catalyst (reforming step), heating the catalyst bed through oxidizing the nickel catalyst to nickel oxide (air regeneration step), and finally reducing the catalyst to its original metal state (fuel regeneration step). The heat required for the endothermic reforming reaction is provided during the exothermic oxidation of nickel to nickel oxide.

Approach

A system design is being developed for the integrated hydrogen refueling system, and the technical and economic feasibility of the design is being assessed. The developmental activities and test work that are needed to both validate the design and identify a viable business model for commercialization, within the capital cost target, will be completed during the remaining part of Phase I (2002).

During Phase II (2003-4), the critical components and subsystems will be developed and tested to achieve the performance goals.

During Phase III (2004-5), the integrated H_2 refueling station will be fabricated, installed and operated. GE will develop the reformer and integrate the full system. Praxair will develop the pressure swing adsorption (PSA) unit, the H_2 compressor, and the H_2 storage tanks. BP will analyze the refueling logistics and safety.

Results

Process Analysis

A preliminary process analysis of the fuel processor, which includes the reformer, shift reactor and PSA unit, has been completed. The major subsystems of the hydrogen refueling station are shown in Figure 1, and they are: 1) autothermal cyclic reformer and PSA unit, 2) hydrogen compressor, 3) hydrogen storage system, and 4) hydrogen dispenser.

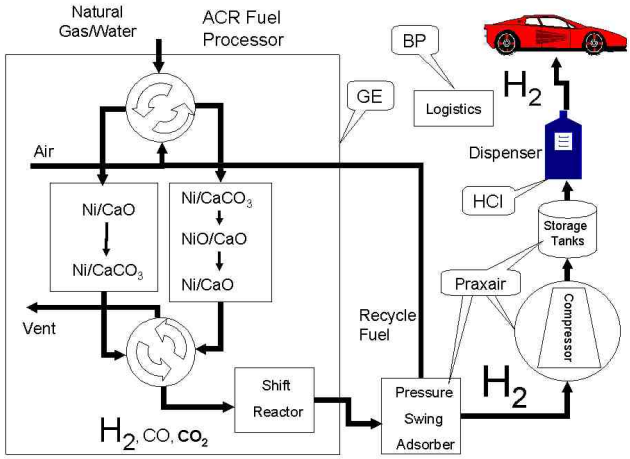

Figure 1. Major Subsystems of a Hydrogen Refueling Station

The efficiency of the fuel processor is defined as the ratio of the lower heating value (LHV) of the hydrogen produced to the LHV of the fuel consumed by the fuel processor. The major factors affecting the efficiency are: 1) the conversion in the reformer and shift reactors, 2) the recovery of hydrogen in the PSA, 3) the recovery of the process heat, and 4) the minimization of heat losses and parasitic requirements in compressors.

Several heat exchanger and compressor configurations were considered, since the thermal integration of the system has a significant impact on the efficiency. An optimal process configuration was selected, and the process flow diagrams were developed. As shown in Table 1, the efficiency of the optimal configuration is 75.2%. Compressor calculations showed that electricity required was

H_2 Recovery in PSA	80%
Electricity Consumed / LHV of fuel	1%
Mol H_2 Produced / Mol Fuel Fed	2.50
Efficiency= LHV of H_2 Produced / LHV Fuel Fed	75.2%

Table 1. Efficiency for the Optimal ACR Fuel Processor Configuration

around 1% of the LHV of the fuel. The operating conditions for the PSA are 7.9 bar (100 psig) and 50°C with 80% hydrogen recovery.

Fabrication of Integrated Fuel Processor

In coordination with another ongoing DOE project, "Fuel Processing Based on ACR for Stationary PEM Fuel Cells" (contract No. DE-FC02-97EE50488), the component design, fabrication and installation of the fuel processor have been completed (see Figure 2). The system can produce 90 kg of H_2 per day (127 kW on a LHV basis). The component design will be modified for hydrogen refueling applications, based on input from Praxair on integration of the PSA.

Figure 2. Prototype ACR Fuel Processor

Safety Analysis and Permitting

A detailed safety assessment including personnel hazard analysis (PHA), hazardous operations (HAZOP) and failure mode and effects analysis (FMEA) has been performed. The assessment will be expanded to ensure that the system is compliant with all applicable building, fire and electrical codes.

Economic Analysis

Based on a literature search, the capital cost for each major subsystem was estimated and then expressed as a function of the quantity manufactured and the hydrogen capacity of the refueling station. Cost models available in the literature for the hydrogen compressor, dispenser and storage subsystems have fairly good agreement. However, there is disagreement among various cost models for reformers. In general, small capacity reformers with optimized thermal integration are expected to cost less than conventional steam methane reformers.

Table 2 shows the information available in the literature[1-4] for capital costs of the reformer (excluding the PSA), hydrogen compressor, storage tanks and dispenser island scaled to a hydrogen capacity of 10,000 std m^3 per day (900 kg of H_2 per day or 1249 kW of H_2 on a LHV basis). Scaling factors were applied to determine the costs of the units as the manufactured quantities increase. The relationships between hydrogen capacity and subsystem capital cost are also shown in Table 2.

The projected preliminary estimate for the cost of a commercial hydrogen generation system based on ACR excluding cost of compression, storage and dispensing is presented in Table 3. The system capacity is 900 kg/day of H_2 (10,000 std m^3 per day of H_2), which can refuel 300 vehicles per day.

The cost of hydrogen was estimated by considering the capital costs, capital recovery factor, the operating expenses of the refueling station, the cost of utilities (fuel and electricity), and the cost of catalysts. The natural gas cost was assumed to be $5/GJ on a higher heating value (HHV) basis, and the electricity cost was assumed to be 7¢/kWhr. The efficiency of the system (75% on a LHV basis) was used to determine the required amount of natural gas. A capacity factor of 90% for plant utilization was used. The capital recovery factor was determined as 13.1%, assuming 10% interest rate over 15 years. The cost of H_2 generation was estimated to be $16.0/GJ. This preliminary cost analysis did not consider the cost reduction due to mass production, and did not consider the cost of hydrogen compression, storage and dispensing. These costs are currently being analyzed.

	Capital Cost	10 Stations	100 Stations	1,000 Stations	10,000 Stations
Fuel Processor (not including PSA)	$.88*10^{6}*(Kg/hr*9.5*10^{-3})^{0.7}$ @10 units	$424,716			$115,799
H2 Compressor	1341*(Kg/hr)+20896 @1,000 units	$141,506		$70,753	
H2 Storage Tanks	7708.8*(Kg/hr)+228 @10 units	$286,835		$200,784	
H2 Dispenser Island	850+1327.56*(Kg/hr) @10,000 units	$439,043	$149,484		$50,208

Table 2. Capital cost for refueling station subsystems as a function of the manufactured quantities. The delivered hydrogen capacity is 67 kg/day.

REFORMER H2 GENERATION CAPACITY		1249	LHV kW
CAPITAL INVESTMENT			
Total Plant Cost (TPC)		$992,162	
Allowance for Funds During Construction (AFDC)	6.3% of TPC	$62,506	
Total Plant Investment (TPI)		$1,054,668	
Royalty Allowance	2.6% of TPI	$27,421	
Inventory Capital	0.8% of TPI	$8,437	
Total Capital Requirement (TCR)		$1,090,527	
LEVELIZED CAPITAL CARRYING CHARGES (ANNUAL BASIS)			
Capital Recovery Factor	13.1% of TCR		$143,376
OPERATING AND MAINTENANCE COSTS (ANNUAL BASIS)			
Operating Labor	1.0% of TCR	$10,905	
Maintenance Labor	0.9% of TCR	$9,815	
Maintenance Material	1.2% of TCR	$13,086	
Administrative and Support Labor	0.5% of TCR	$5,453	
Total Operation and Maintenance			$39,259
SYSTEM EFFICINECY	80% (HHV)		
SYSTEM EFFICIENCY	75% (LHV)		
FUEL & ELECTRICITY COSTS (ANNUAL BASIS)			
Natural Gas Feed	55,150.0 MMBtu/year		
Natural Gas cost per year	$5.3 per MMBtu HHV		
Natural Gas cost per year	$5.0 per GJ HHV	$292,295	
Electricity Required/HHV of Fuel	4.4%		
Electricity Required	711,155.5 kW-hr		
Electricity Unit Cost	7 cents/kW-hr	$49,781	
Catalysts		$83,787	
Total Cost of Fuel & Electricity & Catalysts, accounting for capacity factor			$383,276
NET REVENUE REQUIRED (ANNUAL BASIS)			$565,911
HYDROGEN GENERATED	GJ/day (LHV)		107.89
CAPACITY FACTOR			90%
COST OF HYDROGEN	$/GJ (LHV)		$16.0
COST OF HYDROGEN	$/kg		$1.93

Table 3. Estimation of cost of hydrogen generation for a one-of-a-kind 900 kg/day of H_2 system (10,000 std m^3 per day of H_2; excludes cost of compression, storage and dispensing; does not consider mass production)

Conclusions

The thermal integration of the system has a significant impact on the fuel conversion efficiency of the hydrogen production system. An optimal process configuration that generates the process steam with minimum parasitic losses was selected, and the fuel conversion efficiency on an LHV basis was estimated to be 75.2%. Compressor calculations showed that electricity required was around 1% of the LHV of the fuel.

The preliminary analysis indicates that for a 900 kg/day of H_2 (10,000 std m^3 per day of H_2) one-of-a-kind commercial system, the cost of H_2 generation is $1.93/kg ($16.0/GJ) excluding the costs of hydrogen purification, compression, storage and dispensing. Mass production is expected to reduce the cost of hydrogen significantly.

References

1. J.M. Ogden, T. Kreutz, S. Kartha, L. Iwan, *"Hydrogen Energy Systems Studies",* Final Technical Report submitted to NREL, Contract # DE-FG04-94AL85803, August 13 1996.

2. C.E. Thomas, J.P. Barbour, B.D. James, *"Analysis of Utility Hydrogen Systems @ Hydrogen Airport Ground Support Equipment"*, from the Proceedings of the 1999 DOE Hydrogen Program Review.

3. C.E. Thomas, J.P. Reardon, F.D. Lomax Jr., J. Pinyan, I.F. Kuhn Jr., *"Distributed Hydrogen Fueling Systems Analysis"*, from the Proceedings of the 2001 DOE Hydrogen Program Review.

4. J.M. Ogden, *"Developing an Infrastructure for Hydrogen Vehicles: A Southern California Case Study"*, International Journal of Hydrogen Energy, **24** (1999) 709-730.

5. K. M. Guthrie, *"Process Plant Estimating Evaluation and Control"*, 1974.

6. J.M. Ogden, *"Data for Conventional Steam Reformers (Source Prospects for Building a H_2 Energy Infrastructure)"*, Annu. Rev. Energy Environ., **24** (1999) 227-279

2002 Publications and Presentations:

1. R.V. Kumar, "Autothermal Cyclic Reforming Based Hydrogen Refueling System", IEA Annexe XV Fuel Cells for Transportation Meeting, 2002, Sacramento, California.

2. R.V. Kumar, G. Kastanas, S. Barge, V. Zamansky, R. Seeker, "Autothermal Cyclic Reforming Based Hydrogen Refueling System", DOE Annual Hydrogen Program Review, 2002, Golden, Colorado.

3. R.V. Kumar, G. Kastanas, P. Kulkarni, C. Moorefield, S. Barge, V. Zamansky, R. Seeker, "Hydrogen Energy Park Based on Autothermal Cyclic Reforming", Fuel Cell Seminar, 2002, Palm Springs, California.

II.E.3 Development of a Natural Gas to Hydrogen Fuel Station

William E. Liss, Mark Richards
Gas Technology Institute
1700 S. Mount Prospect Road
Des Plaines, IL 60018
William E. Liss: (847) 768-0753, fax: (847) 768-0501, e-mail: william.liss@gastechnology.org
Mark Richards: (847) 768-0530, fax: (847) 768-0501, e-mail: mark.richards@gastechnology.org

DOE Technology Development Manager: Peter Devlin
(202) 586-8012, fax: (202) 586-9811, e-mail: Peter.Devlin@ee.doe.gov

ANL Technical Advisor: Thomas Benjamin
(630) 252-1632, fax: (630) 252-4176, e-mail: Benjamin@cmt.anl.gov

Subcontractor: FuelMaker Corporation

Objectives

- Develop cost-competitive technology for high-pressure, hydrogen-based fueling systems.
- Design a fast-fill natural gas-to-hydrogen fueling system with 40-60 kg/day delivery capacity that meets the DOE goal of providing hydrogen at a cost of $2.50/kg or less.

Approach

- Use innovative, compact natural gas steam reforming system and appliance-quality hydrogen compressor technologies.
- Undertake system design and analysis to find pathways for meeting cost and performance targets.
- Conduct development and lab testing to confirm subsystem operation.
- Integrate system and incorporate controls.
- Conduct lab and field testing to validate system performance and reliability.

Accomplishments

- Developed comprehensive model for analyzing hydrogen fueling station costs, including capital, operating, and maintenance cost elements. Included Monte Carlo techniques to account for uncertainty and variability in cost drivers.
- Prepared and presented paper on hydrogen fueling system economics to World Hydrogen Energy Conference.
- Constructed a state-of-the-art high-pressure hydrogen testing environmental chamber. System contains a full-size hydrogen three-bank storage cascade that can be run from –45^{o}C to 85^{o}C.
- Developed a first-principle model for understanding the fast-fill behavior of hydrogen and the effects of temperature rise on cylinder fill performance.

Future Directions

- Complete design phase, including revised estimates of system capital, operating, and maintenance costs.

- Begin work to document the fast-fill behavior of hydrogen over a range of temperatures and starting and ending conditions using cylinders of different construction.
- Begin long-term testing to evaluate and confirm the ability of various advanced materials to provide greater durability under dry gas conditions.

Introduction

A key barrier to expanded fuel cell vehicle use is fueling infrastructure. Along with onboard liquid hydrocarbon fuel reformers, a parallel DOE strategy is development of cost-competitive technology based on high-pressure, hydrogen-based fueling systems and on-board hydrogen storage. This project builds on experience gained with compressed natural gas coupled with targeted research on natural gas-to-hydrogen reformation processes and innovative strategies to meet hydrogen fuel quality requirements (water, carbon dioxide, and carbon monoxide levels). An additional core effort is development of a hydrogen dispenser with an advanced filling algorithm that will permit accurate and complete filling of compressed hydrogen vehicles under a range of conditions.

These advanced subsystems – reforming, fuel cleanup, compression, storage, and dispensing – will be incorporated into an integrated and cost-competitive small natural gas-to-hydrogen fueling station that will support hydrogen fueling infrastructure development and expansion.

The specific goal is a fast-fill natural gas-to-hydrogen fueling system with 40-60 kg/day delivery capacity. DOE goals include providing hydrogen at costs of $2.50/kg or less.

Approach

This project is based on leveraging developments at GTI in the stationary PEM fuel cell and compressed natural gas vehicle market sectors. GTI has been developing high-efficiency steam methane reformers for stationary fuel cells, including design approaches to achieve compact size, reduced cost, and simplified control and operation. Modification of this reformer—as a hydrogen generator with advanced controls—will comprise a core element of this system.

In addition, GTI is building upon its experience with high-pressure natural gas fueling systems and working with key partners to develop hydrogen-capable and compatible versions of our fueling products—including compressors, dispensers, and cascade storage vessels. GTI sees this strategy of product line extension as a near-term pathway for achieving cost reduction and product availability to support early establishment of a hydrogen fueling infrastructure.

In this regard, GTI is working with FuelMaker Corporation to develop a high-pressure hydrogen version of their vehicle refueling appliance (VRA). The FuelMaker VRA is a high-quality appliance-like compression unit that is completely oil free—an important consideration for contaminant sensitive PEM fuel cell stacks.

The project approach includes three phases: 1) Design, 2) Development and Lab Testing, and 3) Field Testing. Through these progressive phases, GTI anticipates having a proven small natural gas-to-hydrogen fueling system that can support the development and expansion of a distributed hydrogen fueling infrastructure.

Results

The project began in February 2002, with a focus on subsystem and system design.

GTI has developed a comprehensive model for hydrogen fueling systems that takes into account all capital, operating, and maintenance cost elements. The model can also be used to assess the effects of factors such as grants and tax incentives. The output, among other dimensions, is the levelized cost for hydrogen.

GTI currently sees capital and energy costs (including the cost of natural gas consumed in the steam reformer and electricity for compression) as the dominant cost factors (see Figure 1). The cost of

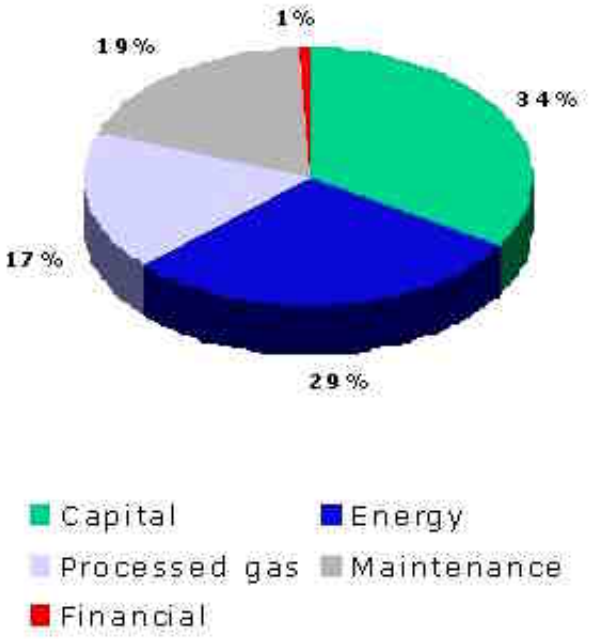

Figure 1. Hydrogen Station Costs

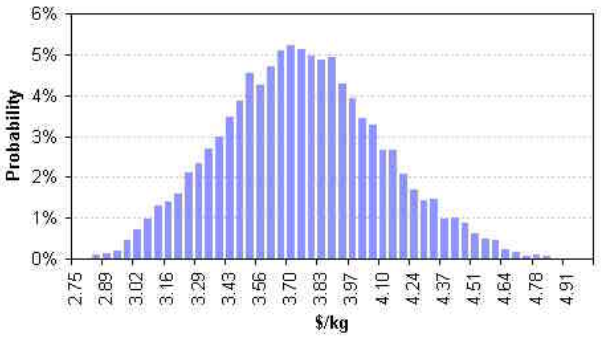

Figure 2. Hydrogen Fuel Station Cost Distribution

"processed gas"—that is, the gas reformed into hydrogen—is less than 20% of the cost of production.

Monte Carlo techniques were used to account for uncertainty and variability in individual cost elements—a facet of the nascent nature of this technology. Figure 2 shows the model results for expected cost. Levelized hydrogen costs are estimated at around $3.70/kg. Further work will be undertaken during the design phase to review these cost factors and revise the model.

GTI is also developing analytical and empirical information on the filling behavior of hydrogen

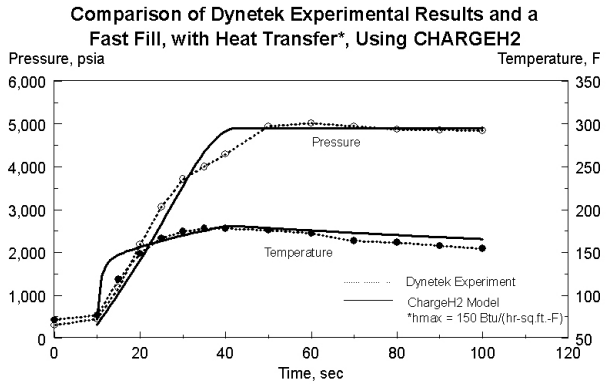

Figure 3. Hydrogen Fast Fill Data and Model

under fast-fill conditions. Work has shown that hydrogen experiences a significant temperature rise under these conditions. GTI has developed a first-principle model called CHARGE H2 that can be used as a predictive tool for this phenomenon. Figure 3 shows early results in comparing this model with empirical data. In this testing, a Dynetek carbon-wrapped, aluminum lined hydrogen cylinder rated at 345 bar (5000 psig) was "fast filled" in a period of less than 60 seconds. This cylinder had an internal water volume of 34 liters. At 345 bar, this implies a total hydrogen storage capacity of about 0.75 kg for this cylinder.

Of note is the nearly 55°C *in situ* gas temperature rise during cylinder filling. While some heat transfer from the gas phase to the cylinder liner occurs, the short duration of the fill process limits the amount of heat that can be dissipated. Longer fill times—for example, 3 to 5 minutes—may somewhat increase the amount of heat transferred. Preliminary indications show the initial cylinder internal heat transfer coefficient may be as high as 6 to 8 times greater than for natural gas.

The temperature rise phenomenon seen in hydrogen as well as natural gas reduces gas density and energy content and ultimately can result in reduced vehicle driving range. GTI will conduct comprehensive testing under a variety of conditions and using cylinders of differing construction to document this behavior and compare the resulting data with its CHARGE H2 model. To counteract this effect, GTI will develop a hydrogen dispenser control algorithm to more accurately fill cylinders and

provide underfill compensation that largely offsets this phenomenon.

To conduct this unique hydrogen testing, GTI has constructed a state-of-the-art high-pressure hydrogen environmental chamber. This system contains a full-size hydrogen three-bank storage cascade that can be run from –45°C to 85°C (see Figure 4). The chamber is fully instrumented and connected to a high-speed data acquisition system. Fast-fill hydrogen tests will be run over a wide range of temperature and pressure conditions using cylinders constructed with steel, aluminum, and plastic liners.

Figure 4. GTI Hydrogen Testing Environmental Chamber

Conclusions

Work was begun on this program in February 2002. Preliminary indications are that a natural gas to hydrogen fueling system with reduced cost capabilities is possible. Achieving the stated cost targets of $2.50/kg will be a challenge.

The strategy of leveraging developments in PEM reformers for stationary applications and compressed natural gas vehicle technology appears to be a promising pathway for leveraging technology, experience, and market channels.

References

1. Richards, M. and Liss, W., "Reformer-based Hydrogen Fueling Station Economics." World Hydrogen Energy Conference, June 11, 2002.

II.E.4 Distributed Hydrogen Fueling Systems Analysis: Cost and Performance Comparison of Stationary Hydrogen Fueling Appliances

Brian D. James (Primary Contact), Duane B. Myers, Gregory D. Ariff, John S. Lettow, C.E. (Sandy) Thomas, & Reed C. Kuhn
Directed Technologies
3601 Wilson Blvd., Suite 650
Arlington, Virginia 22201
(703) 243-3383, fax: (703) 243-2724, e-mail: Brian_James@DirectedTechnologies.com

DOE Technology Development Manager: Sigmund Gronich
(202) 586-1623, fax: (202) 586-5860, e-mail: Sigmund.Gronich@ee.doe.gov

Objectives

- Quantify the costs of hydrogen fueling appliances (HFAs) using two natural gas reforming technologies (autothermal reforming versus steam methane reforming) and two gas cleanup technologies (pressure swing adsorption versus metal membrane gas separation) to provide on-site hydrogen for a community of 183 hydrogen fuel cell vehicles (FCVs) (equivalent to 20 refuelings per day or a capacity of 115 kilograms (kg) of hydrogen (H_2) per day (with a 69% capacity factor).
- Estimate the cost of hydrogen using each combination of technologies.
- Estimate the cost reductions from scaling the least expensive technology to a larger unit providing 160 fuel cell vehicle refuelings per day.

Approach

- Design the chemical process, physical implementation, and manufacture and assembly methods for each of the four HFA technology combinations, produced in quantities of 250 units/year.
- Use Design for Manufacture and Assembly (DFMA) cost analysis techniques to estimate the capital costs of each HFA design.
- Apply discounted cash flow analysis to determine a cost per kilogram of hydrogen.
- Use common chemical engineering scale-up factors to scale-up the design producing lowest-cost hydrogen by 8x.

Accomplishments

- Designed complete 115 kg/day capacity HFA systems for low-cost hydrogen from four combinations of reforming-cleanup technologies: steam methane reforming (SMR) with pressure swing adsorption (PSA), autothermal reforming (ATR) with PSA, SMR with metal membrane gas separation, and ATR with metal membrane gas separation.
- Estimated costs of materials, manufacture, and assembly using an adapted DFMA methodology to arrive at capital costs for each HFA design.
- Using discounted cash flow analysis, identified the SMR-PSA system as the technology to provide lowest cost hydrogen ($3.38/kg) for small-scale, small production volume HFAs.
- Estimated up to 45% reduction in cost of hydrogen ($1.87/kg) from scaling HFA size up by 8x.

Future Directions

- Evaluate the cost of renewable hydrogen for transportation applications in the 2030-2050 time frame based on a variety of renewable resources (wind, biomass, geothermal, solar, etc.), transportation, and storage options.
- Determine the most practical and economically feasible plan for the supply of 10 Quads/year of renewable hydrogen for transportation applications in 2030-2050.

Introduction

Over several studies, Directed Technologies, Inc. has analyzed the costs of representative HFAs to supply the early-introduction hydrogen powered FCVs and the cost of hydrogen produced by these HFAs. In previous studies we evaluated the impact of fuel choice on FCV, the cost of other sizes and quantities of HFA's, and the infrastructure maintenance costs of various fuels. In this study we analyzed the costs for an intermediate production rate (250/year) of HFAs sized to support communities of 183 vehicles each (about one-eighth the size of the typical new gasoline station). This small HFA is chosen to allow economical hydrogen production in the early years when there are low numbers of FC's present in any geographical area. While the focus of this report is on the economics of hydrogen production at this small unit size, it is noted that significant hydrogen cost reductions can be achieved by scaling the HFA unit to a larger size.

For the baseline HFA, we compared the costs and efficiencies of two hydrogen-generation technologies (steam methane reforming and autothermal reforming) and two hydrogen purification technologies (pressure swing adsorption and metal membrane gas separation). Each HFA includes components for natural gas desulfurization, reformation, hydrogen purification, compression, storage, and dispensing. The processing options chosen for this comparison emphasize the relative strengths of each process, with the result that there are many other potential variations that involve tradeoffs between capital cost and efficiency.

Approach

Each HFA system required a careful chemical and mechanical engineering analysis to capture the appropriate performance parameters and cost factors. Once moderately detailed mechanical designs and material and energy balances were created for all system components, a complete system Bill of Materials was generated. This Bill of Materials allowed a line-by-line, element-by-element cost assessment to be conducted using a Design of Manufacturing and Assembly (DFMA) costing approach. This methodology is used extensively by industry for product cost estimation and to compare the relative cost of competing manufacturing and assembly approaches. The DFMA methodology is both a rigorous cost estimation technique and a method of product redesign to achieve lowest cost.

Once the capital costs for each design were determined, a discounted cash flow analysis was used to compare reforming options with differing initial investments and operating expenses. The cost of hydrogen was determined by calculating the cost of hydrogen that results in a net-present value of $0 for the HFA over ten years of operation. Solving for the cost of hydrogen at $0 net-present value yields the "wholesale price" at which the reformer operator realizes an after-tax return on investment equal to the cost of capital. The cost of hydrogen calculated in this analysis is somewhere between the wholesale and retail level. We have included the capital cost for storage and dispensing, which would not typically be reflected in the wholesale costs of other fuels, but have excluded retail markup and profit for the HFA operator.

Results

Each HFA system was designed such that the reforming system ([RS], not including hydrogen compressor, storage, and dispenser) could be contained on a skid-mounted pallet (see Figure 1). This pallet has an approximately 8 ft by 13 ft footprint, stands roughly 10 ft tall, and may be enclosed by a canopy and chain-linked fence. The compressor, hydrogen storage tanks, and dispenser would be housed separately.

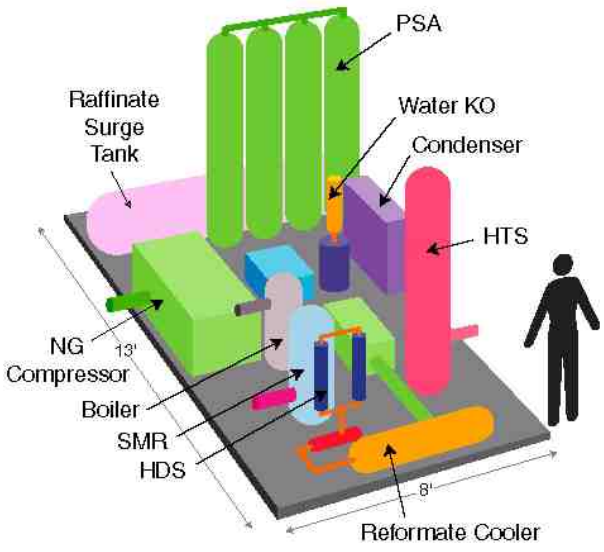

Figure 1. Proposed Layout of 10 atmospheres Steam Methane Reformer System

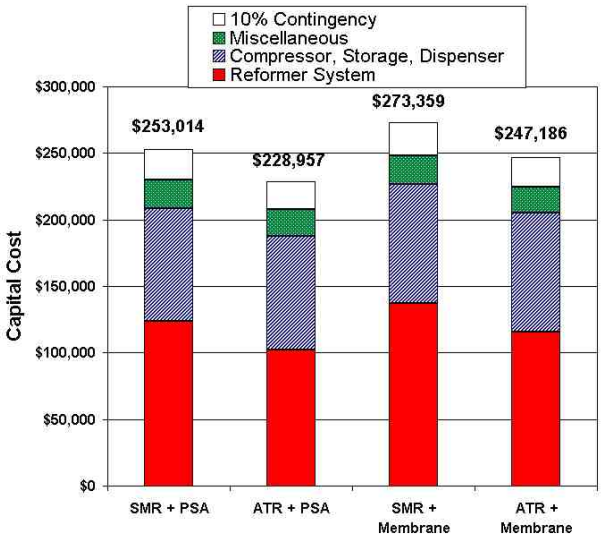

Figure 2. Contribution of Subsystems to Capital Cost for 115 kg/day HFAs. (The "Miscellaneous" category includes on-site installation, freight, taxes & insurance, and initial spares. The "Reformer System" category includes the hydrogen production and gas cleanup subsystems.)

Table 1. Cost of Hydrogen Produced from the 115 kg/day HFA Options

Costs in $/kg H_2	SMR/ PSA	ATR/ PSA	SMR/ Membrane	ATR/ Membrane
Hydrogen Cost	**$3.38**	**$3.59**	**$3.74**	**$4.28**
Capital Recovery	1.66	1.50	1.78	1.62
Natual Gas	0.95	1.17	1.01	1.44
Electricity	0.23	0.41	0.37	0.68
O&M	0.33	0.31	0.33	0.33
Taxes & Insurance	0.23	0.20	0.24	0.22
Gasoline Equivalent ($/gal)	**$1.55**	**$1.65**	**$1.72**	**$1.96**

HFA is assumed to run an average of 69% of capacity with 98% availability.
Capital Recovery assumes a 10% after-tax return on investment over its 10-year life.
A 38% marginal tax rate (34% federal, 4% state and local) is included in the return on investment calculation.
Natural gas price is based on the 19-year national average commercial rate of $5.34 per thousand scf.
Electricity price is based on the 19-yar national average commercial rate of 7.5 cent per kW hr.
The cost for water usage is negligible.
O&M inclludes yearly hydrogen desulfurization bed replacement and reformer and shift catalyst replacement after five years. It also includes general maintenance for compressors, valves, etc.
Tax and Insurance costs refer to annual property taxes at 1.5% of capital investment and annual insurance premiums at 1% of capital investment. Highway/road sales taxes are not included.
Gasoline equivalent price is based on an efficiency gain of 2.2 hydrogenc FCVs over current gasoline internal combustion engine vehicles.

While the cost of the RS varies considerably depending on the reformation and cleanup technologies employed, the cost of the hydrogen compressor, storage, and dispenser, as well as unit installation, are independent of RS design. A cost breakdown for each 115 kg/day HFA design and the resulting cost of hydrogen are provided in Figure 2 and Table 1, respectively. Based on this study, we find that the most cost-effective option as determined by the wholesale cost of hydrogen is SMR coupled with PSA hydrogen purification. The initial capital cost to install the preferred SMR-PSA to support 183

Table 2. Cost of Hydrogen from 920 kg/day (8x) SMR/ PSA HFA with Optimistic Assumptions

Costs in \$/kg H_2	16,000 scfh SMR/PSA HFA
Hydrogen Cost	**\$1.87**
Capital Recovery	\$0.77
Natual Gas	\$0.59
Electricity	\$0.15
O&M	\$0.24
Taxes & Insurance	\$0.13
Gasoline Equivalent (\$/gal)	\$0.85

Estimates are based on a scaled-up version of a 2,000 scfh HFA. Scale-up may not retain accuracy of original analysis.
HFA is assumed to run an average of 69% of capacity with 98% availability.
Capital Recovery assumes a 10% after-tax return on investment over a 15-year life.
A 38% marginal tax rate (34% federal, 4% state and local) is included in the return on investment calculation.
Natural gas price is based on the 19-year national average industrial rate of \$3.30 per thousand scf.
Electricity price is based on the 10-yar national average industrial rate of 4.65 cent per kW hr.
The cost for water usage is negligible.
O&M includes yearly hydrogen desulfurization bed replacement and reformer and shift catalyst replacement after five years. It also includes general maintenance for compressors, valves, etc.
Tax and Insurance costs refer to annual property taxes at 1.5% of capital investment and annual insurance premiums at 1% of capital investment. Highway/road sales taxes are not included.
Gasoline equivalent price is based on an efficiency gain of 2.2 hydrogen FCVs over current gasoline internal combustion engine vehicles.

vehicles is \$253,014 per unit. The wholesale cost of hydrogen for this option, including storage and dispensing but excluding sales taxes and retail markup, is \$3.38/kg, or \$1.55 per gallon of gasoline equivalent. Autothermal reforming (ATR) of natural gas is a lower initial-cost option (\$228,957), but the resulting cost of hydrogen is higher (\$3.59/ kg) because the ATR uses more natural gas and electricity than the SMR to produce the same quantity of hydrogen.

Based on the results of the baseline HFA analysis, we estimated the potential hydrogen cost reduction that would result from increasing the size of the HFA from 115 kg/day to 920 kg/day. An HFA of this size would support roughly 1464 vehicles, which is comparable to large modern gasoline stations. A breakdown of the estimated cost of hydrogen for this HFA is given in Table 2. Using scale-up factors common to chemical processes, the capital cost of this 8x HFA was estimated to be \$1.16 million, resulting in a hydrogen cost of \$1.87-\$2.48/ kg (dependent on assumptions about utility discounts, natural gas feedstock cost, and equipment life). Thus, the "small" HFA derived hydrogen cost of \$3.38/kg is appropriate when discussing the early introduction of fuel cell vehicles, and the significantly lower hydrogen cost of \$1.87-\$2.48/kg, produced by a "large" HFA, is appropriate for the future years when the FCV population and population density are much higher.

Conclusions

For HFA's of the baseline capacity (115 kg/day) and production volume (250 units/year), there are two general conclusions that can be taken from this analysis:

- Steam methane reforming is more efficient than autothermal reforming, and the efficiency benefit results in a lower cost of hydrogen over a ten-year system lifetime even with a slightly higher initial capital cost (\$253,014 for SMR vs. \$228,957 forATR). The difference between the SMR and ATR costs of hydrogen shrinks as the cost of the natural gas feedstock decreases, but only with zero-cost natural gas (i.e. free) does the ATR match the SMR. For a given cost of hydrogen the SMR and ATR economic returns are equal by the fourth year of operation, with the SMR advantage increasing every year thereafter.
- PSA is a more economical and reliable option than any other hydrogen cleanup system at this time. Significant reductions in the cost and reliability of membrane purification systems are required to make them competitive with PSA.

The wholesale cost of hydrogen from the SMR-PSA HFA is \$3.38/kg, which is the equivalent of \$1.55/gallon of gasoline for an internal combustion

engine vehicle after adjustment for the higher efficiency of the fuel cell engine. (Note that the hydrogen price provided does not include the taxation currently applied to gasoline.) This equivalent gasoline cost is at the upper end of current retail gasoline costs. When there are sufficient FCVs to justify a larger number of higher-volume stations, the cost of hydrogen will decrease by taking advantage of economies of scale in both HFA manufacture and the reforming process.

FY 2002 Publications/Presentations

1. "Cost and Performance Comparison of Stationary Hydrogen Fueling Appliances", submitted to Hydrogen Program Office, Office of Power Technologies, U.S. Dept. of Energy, under Grant No. DE-FG01-99EE35099, April 2002.

2. "Distributed Hydrogen Fueling Systems Analysis-Cost and Performance Comparison of Stationary Hydrogen Fueling Appliances", presentation made by Brian D. James at 2002 DOE Annual Hydrogen Program Review on May 6, 2002.

II.E.5 Technical Analysis: Integrating a Hydrogen Energy Station into a Federal Building

Stefan Unnasch (Primary Contact), Scott Fable
TIAX, LLC
1600 De Anza Blvd., Suite 100
Cupertino, CA 95014
(408) 517-1563, fax: (408) 517-1553, e-mail: unnasch.stefan@tiax.biz

DOE Technology Development Manager: Matthew Kauffman
(202) 586-5824, fax: (202) 586-5860, e-mail: Matthew.Kauffman@ee.doe.gov

Main Subcontractor: Bevilacqua-Knight, Inc., Sacramento, CA

Objectives

- Evaluate combined fuel cell power/hydrogen production systems (Energy Stations):
  - Analyze energy station systems with 50 kilowatt (kW) proton exchange membrane fuel cells (PEMFCs) that are suitable for installation in Federal buildings
  - Analyze options for system components, including direct hydrogen and reformate fuel cells and various storage, power production, and hydrogen usage configurations
  - Determine cost and energy efficiency for different system configurations
- Assess integration with buildings and potential for cogeneration:
  - Analyze potential for heat recovery from fuel cell/hydrogen production systems
  - Identify potential for cogeneration in Federal building applications
- Identify potential fleets to use hydrogen for vehicle operation
- Establish partnerships for hydrogen fueling and power sales
- Identify barriers to hydrogen use
- Make recommendations for future development
- Identify potential opportunities to develop fuel cell energy stations

Approach

- Analyze system cost and performance
- Assess public/private fleet size and locations
- Evaluate building integration

Accomplishments

- Developed list of possible components that will comprise hydrogen generation and dispensing station
- Developed list of relevant system configurations from possible components, with detailed description and schematics of proposed system configurations
- Selected a baseline system configuration, and initiated a detailed system cost and performance analysis
- Prepared a comprehensive list of potential operating configurations
- Surveyed potential public/private fleets and federal buildings for siting a hydrogen energy station

- Initiated evaluation of building integration and prepared comprehensive list of potential building interfaces

Future Directions

- Continue the analysis and identification of energy station applications in Federal buildings:
  - Explore specific public and private partnerships to support the establishment of a hydrogen energy station in a Federal facility
  - Analyze the cost, emissions, and energy utilization benefits of integrated power and vehicle refueling
  - Identify the key technology, cost, and public perception barriers to hydrogen use
  - Make recommendations for future development

Introduction

The purpose of this project is to analyze the development of a hydrogen infrastructure for transportation applications through the installation of a 50-75 kW stationary fuel cell-based energy station at federal building sites. The various scenarios, costs, designs and impacts of such a station are quantified. It uses a natural gas reformer to provide hydrogen fuel for both the fuel cell stack and a limited number of fuel cell powered vehicles, with the possibility of using cogeneration to support the building heating load.

Approach

The project has three major tasks:

Task 1. Analyze System Cost and Performance

The first task conducted in this project is to evaluate all of the competing technologies that could be utilized for each of the components in the entire fuel cell and vehicle fueling system based on the criteria of cost, performance, and technical feasibility. The goal of this initial, broad-based assessment is to select the most promising (four to five) system designs and technologies on the basis of the above criteria.

Task 2. Assess Public/Private Fleet Size/Locations

Data on the potential for energy stations with fleets is being collected from a representative and diverse composition of stakeholders. We are coordinating with automakers to obtain information about fuel cell vehicle fleet size, location and type projections. Another key source of information for projecting hydrogen vehicle fleet size and location are the Energy Policy Act (EPAct) fleet administrators, who will help us determine their current and projected alternative fuel vehicle (AFV) fleet practices. Finally, other policies, such as the California Zero-Emission Vehicle Mandate and the California Air Resources Board transit fleet regulation, that will either directly or indirectly encourage hydrogen fleets, are being analyzed for their potential impacts.

Task 3. Evaluate Building Integration

Using the results of Task 1 and a limited number of system designs and technologies selected for further analysis, the likely amounts and grades of waste heat that will be produced from the reformer and fuel cell stack(s) will be determined. With this information, cogenerative heat uses and technologies are being researched and evaluated with respect to beneficial utilization in a commercial/government building setting, as well as the cost and technical feasibility of those applications.

Results

Analysis of System Performance (Task 1)

A hydrogen-producing energy station would reform an input fuel to produce hydrogen for fuel cell operation and for dispensing to hydrogen-powered vehicles. The electrical power generated by the fuel cell and/or the residual heat from the system processes may be used to support energy station and nearby building power and heating loads. The fraction of reformer output used for hydrogen

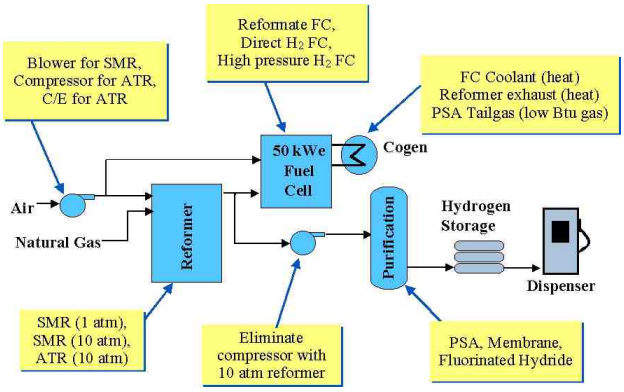

Figure 1. Several Technology Options Exist for System Configuration

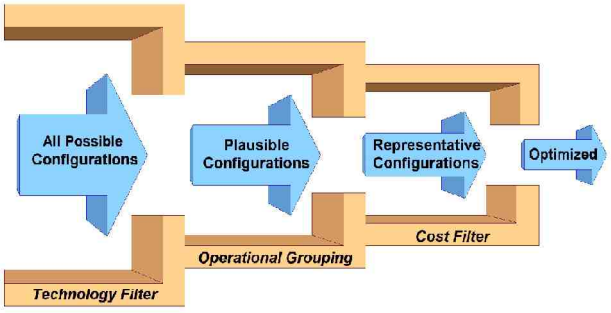

Figure 2. Application of Filters to Determine Optimal Configurations for Analysis

vehicles would be purified and stored for dispensing upon demand. Figure 1 shows the various major components that make up a hydrogen energy station.

In order to determine which system configurations and operational patterns are most viable for an energy station, TIAX developed several criteria for selecting a representative set of technology configurations. TIAX applied these criteria to all possible technology configurations to determine an optimized set, as shown in Figure 2. The remaining cases best illustrate the range of viable energy station configurations and operational profiles. These representative configurations, along with the baseline case, will be used to develop a representative cost and energy output estimate for the energy station (see Figure 3).

The possible operational scenarios for each of the station configurations include peak power

System Attributes	Major Components
Conventional Systems	Air Blower, SMR, PrOx, Reformate Fuel Cell, PSA
Lower-cost Fuel Cell	Air Blower, SMR, PSA, Direct Hydrogen Fuel Cell
Small Scale Purificaiton	Compressor / Expander, ATR, PrOx, Reformate Fuel Cell, Fluorinated Metal Hydride Purification
Simple Cogeneration	Air Compressor, ATR, PSA, Direct Hydrogen Fuel Cell

Figure 3. Representative Energy Station System Component Configurations

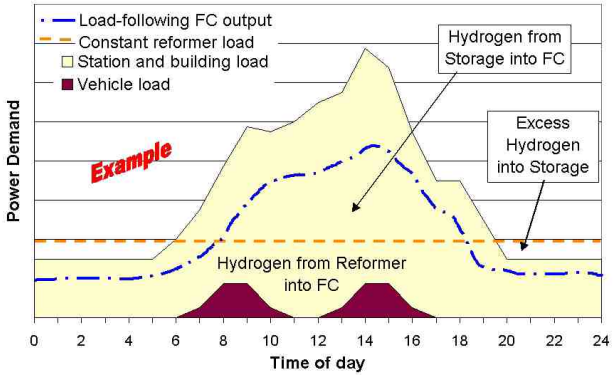

Figure 4. Example Fuel Cell and Reformer System Operation Scenarios

shaving, constant baseload operation, scheduled operation, on demand operation, and/or load following. These options are not necessarily exclusive - in some cases they may be used in combination. Figure 4 shows an example operational mode where the reformer load remains constant,

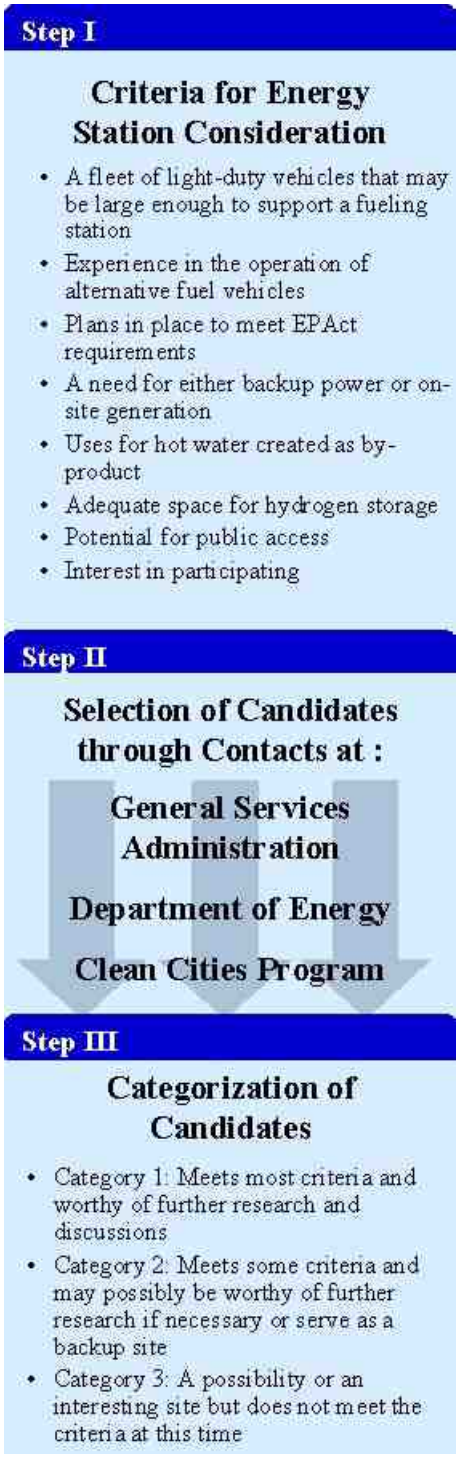

Figure 5. The Process for Choosing Facilities that Would Most Likely Benefit from an Energy Station

while the fuel cell load follows the combined station and building loads.

Assessment of Public and Private Fleet Size and Locations (Task 2)

In its effort to identify candidate federal facilities for the placement of a hydrogen fueling station, TIAX worked with its subcontractor, Bevilacqua-Knight, Inc. (BKI), to create a list of characteristics that the ideal location should possess. These characteristics, shown in Figure 5, formed the criteria by which the facilities would be judged.

For each federal agency contacted, BKI attempted to speak with both the fleet manager and the facility's energy manager. Fleet managers were asked about their existing vehicle fleet, experience with AFVs and plans for future acquisitions. TIAX was particularly interested in facilities that currently operate compressed natural gas (CNG) vehicles since CNG is a gaseous fuel with many properties similar to those of hydrogen. In addition, each agency was asked about how their vehicles were acquired. Lastly, TIAX asked how the facility planned to meet future EPAct requirements.

Evaluation of Building Integration (Task 3)

In order to take advantage of potential cogenerative heat uses and technologies, the likely amounts and grades of waste heat that will be produced from the reformer and fuel cell stack(s) will need to be determined. Using the representative technology configurations above, the opportunities for cogeneration are currently being examined. We are evaluating the potential cogeneration heat requirements in terms of heat load and seasonal variations as well as the hardware requirements required to integrate an energy station into a building.

Conclusions

- TIAX has identified a set of representative technologies and representative operational scenarios that are being analyzed to estimate the size, power output, and cost of a hydrogen energy station.
- Several options have been identified for system configuration and operation, with

each focusing on a different benefit: conventional system components, lower cost, small-scale operation, and design simplicity.

- Several Federal facilities have been identified as potential host sites, meeting most of the energy station host criteria developed as a part of this project. Energy and cost estimates will be presented in the final report of this project.

II.F Crosscutting Hydrogen Production and Delivery Analysis

II.F.1 Hydrogen Technical Analysis

Stephen Lasher (Primary Contact), Masha Stratonova, and Johannes Thijssen
TIAX LLC
Acorn Park
Cambridge MA, 02140
(617) 498-6108, fax: (617) 498-7054, e-mail: lasher.stephen@tiax.biz

DOE Technology Development Manager: Matthew Kauffman
(202) 586-5824, fax: (202) 586-5860, e-mail: Matthew.Kauffman@ee.doe.gov

Objectives

- Identify promising hydrogen (H_2) purification technologies that DOE does not currently fund
- Characterize technical maturity and risks of selected technologies
- Perform detailed performance and cost analysis for the selected purification technologies integrated into a hydrogen fueling station concept and compare to baseline technologies
- Identify key barriers and possible development paths for promising alternative purification technologies

Approach

- Screen purification technologies and select three for detailed analysis
- Evaluate current and projected performance and cost of the selected purification technologies
- Develop system models for each purification technology with various hydrogen fueling station design concepts
- Calculate overall costs and primary energy use based on system model results and capital cost estimates from developers and internal analyses

Accomplishments

- Selected amorphous membranes without noble metals (Zirconium-Nickel [Zr-Ni] alloy), dry fluorinated metal hydrides and the application of this fluorinated metal hydride in a slurry as the three most promising non-DOE funded purification technologies
- Projected future performance and cost parameters for the selected purification technologies based on developers' input and internal analyses
- Calculated overall system efficiencies and hydrogen costs for each purification technology integrated with various reformer types and storage options
- Identified fluorinated metal hydrides as the most attractive option to pursue further, especially in a slurry-based system. Identified need to examine system-level interactions on production / purification technology in hydrogen energy mini-grid

Future Directions

- Evaluate combined fueling and power concepts utilizing central production and storage for both direct-hydrogen vehicle fueling and direct-hydrogen PEMFC power systems

- Evaluate the use of fluorinated metal hydride slurries in a mini-hydrogen grid concept for enhancing co-gen opportunities from combined fueling and power systems
- Determine if combined fueling and power or mini-hydrogen grid concepts provide cost or efficiency savings or other benefits that could encourage hydrogen and PEMFC use

---

Introduction

There is increasing interest in the development of small-scale (< 1 million standard cubic feet per day) hydrogen fueling stations to support direct hydrogen fuel cell vehicles when and if these vehicles capture a significant fraction of the U.S. passenger vehicle fleet. Hydrogen for fuel cell vehicle refueling could be generated from conventional or emerging fuels at the fueling station with an on-site system including a reformer, hydrogen purification, storage, and dispensing, along with the necessary safety systems and controls. For this purpose, both higher pressure (around 10 atmospheres [atm]) and lower pressure reformers are being designed. Higher pressure systems would integrate well with the pressure requirements of conventional purification technologies (pressure swing adsorption [PSAs] and membranes). Lower pressure reformers (1-3 atm) would take advantage of designs originally intended for integrated reformer/fuel cell systems for automotive and stationary power applications and could result in lower cost due to synergies with those systems, though they would require the use of expensive and inefficient reformate compressors for integration with conventional purification technologies. It is thus clear that purification technology drives component and system design decisions.

Approach

Three small-scale purification technologies not currently being funded by DOE for on-site hydrogen production at vehicle refueling stations were evaluated. They were analyzed in the context of a larger (690 kilograms [kg] H_2/day) and a smaller (69 kg H_2/day) refueling station and in the context of high and low pressure on-board storage technologies. The analysis included assessments of technical maturity and risks, performance, cost, and a comparison to baseline technologies, as well as the identification of key barriers and an evaluation of possible development paths. We developed detailed flowsheet models for each of the options considered. These were used to estimate the conditions, flowrates, power requirements, and heat duties needed for sizing the necessary equipment. Based on the equipment sizes so calculated, we developed cost estimates from a combination of quotes and existing bottom-up cost models. The three purification technologies selected for analysis are:

Fluorinated Metal Hydrides (Dry)

If properly protected from certain impurities, metal hydrides could purify reformate streams at much lower pressure than conventional technology. Forming a porous fluoride film on the surface of metal hydride particles is a promising way to protect the metal hydride from poisoning by non-hydrogen species that are less likely to penetrate through the fluoride film than hydrogen molecules (particularly carbon monoxide and water). Combining this low pressure purification with hydrogen storage in the same metal hydride has the potential to simplify system integration and improve efficiency and cost for fueling metal hydride vehicles.

Metal Hydride Slurries

Utilizing fluorinated metal hydrides in slurries could improve system integration even further. The metal hydride slurry is pumpable, allowing for its use as a medium for hydrogen purification, storage and transportation simultaneously. Slurry systems also have faster absorption/desorption times than dry metal hydrides, allowing them to be used for purification only with compressed H_2 storage and dispensing. The fast absorption/desorption time also reduces the amount of metal hydride material required for purification, thus minimizing capital cost of the purification process.

Non-Palladium Metal Membranes

Non-palladium metal membranes are a potential low-cost alternative to palladium-based membranes currently in use. Japanese researchers have

Purification Attributes	Units	Small-scale PSA	Zr-based Membranes	Fluorinated MH[1,4]	Fluorinated MH Slurry[1]
Demonstrated Performance					
Inlet pressure	atm	10-20	3[2]	15 (initial)	NA
H_2 Outlet pressure	atm	9-19	~1[2]	1	NA
Operating temperature	°C	0-50	250-350	60, 80	NA
Hydrogen recovery[3]	%	70-90	40-60[2]	85	NA
Assumed Performance					
Inlet pressure	atm	10	10	1.5-10	1.5-10
H_2 Outlet pressure	atm	9	~1	5	5
Operating temperature	°C	40	350	40-110	40-110
Hydrogen recovery[3]	%	70-76	78-86	65-94	64-92

[1] Based on the material and processes investigated in this study. Attributes vary significantly with material.
[2] Current performance with 2 atm (30 psia) pressure difference across the membrane. Hydrogen recovery increases with increasing pressure difference.
[3] Varies depending on inlet pressure and reformate composition (SR versus ATR).
[4] Demonstrated performance based on: Wang, et al 1995.

Figure 1. Demonstrated and Assumed Purification Performance

promising results from amorphous alloy membranes without noble metals (Zr-Ni). Alloys without noble metals may be two orders of magnitude cheaper than palladium-based materials on a weight basis (Hara 2000).

Results

Hydrogen Recovery (Figure 1)

Hydrogen recovery was estimated for each purification technology and inlet condition. Demonstrated performance and our assumptions for inlet and outlet pressures, operating temperature, and hydrogen recovery are shown in Figure 1. Hydrogen recovery for the PSA case was based on vendor quotes for typical autothermal reformer (ATR) and steam reformer (SR) impurity concentrations. Zr-based membrane recovery was estimated based on current and estimated membrane performance characteristics, hydrogen pressure gradient across the membrane, and assumed permeability decrease due to carbon monoxide presence in the feed stream. Fluorinated metal hydride recovery was estimated based on the operating conditions and metal hydride cycling hydrogen capacity.

Efficiency (Figures 2 and 3)

- Steam reformer based systems result in lower primary energy use than autothermal reformer systems largely because steam reformers can utilize the non-recovered hydrogen from the purification step.
- For high-pressure dispensing options (compressed H_2 vehicles), PSA purification with a high-pressure steam reformer results in the lowest primary energy use, provided highly efficient waste heat integration is possible.
- PSA and membrane purification for use with low pressure reformers tend to have higher power-based primary energy use due to the need for compression prior to purification.
- Fluorinated metal hydride (Fl MH) purification options achieve very high hydrogen recovery rates compared with a PSA; but dehydriding energy requires an auxiliary burner for use with steam reformers, raising energy consumption.
- Autothermal reformers have enough waste heat to significantly reduce or eliminate an auxiliary burner for use with Fl MH systems, provided a significant fraction of the waste

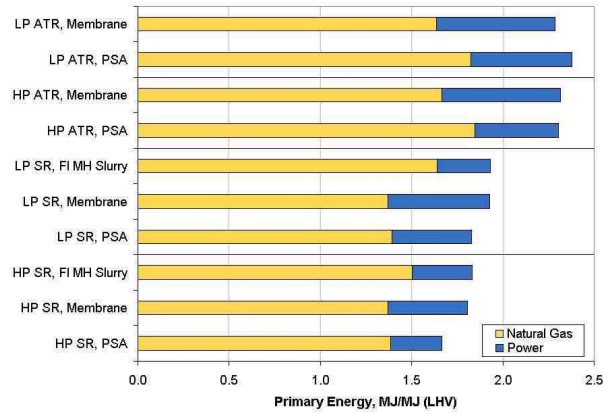

Figure 2. Primary Energy Use for Compressed H_2 Vehicle Fueling Stations

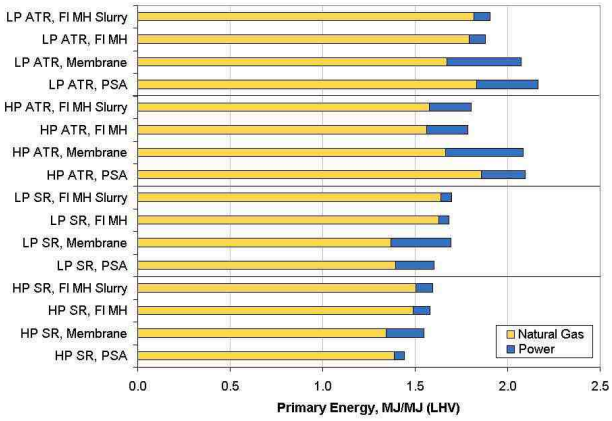

Figure 3. Primary Energy Use for MH Vehicle Fueling Stations

heat can be stored and used as needed during fueling.

With Fl MH purification, hydrogen recovery does not strongly depend on reformate quality, and hence is the preferred option with ATRs and purification of syngas streams from renewable sources (e.g. biomass gasification or pyrolysis).

Hydrogen Cost (Figures 4 and 5)

Notes on figures: purification category includes reformate compressor costs for low-pressure reformers with PSA and membrane purification. Cost categories include energy, maintenance, and capital recovery costs. "Other" costs include labor, rent, utilities, profit, and capital recovery for site preparation and central controls and safety.

- Under our cost assumptions, low-pressure (high production volume) reformers are cheaper than high-pressure (low production volume) reformers, but result in about the same overall cost for hydrogen due to higher purification costs.
- Although membrane cost may ultimately be low for non-palladium membrane purification, compression costs off-set the benefits this provides compared with PSA purification, except for use with low-pressure ATRs.
- Unlike PSAs and membranes, Fl MH systems are projected to have very similar purification cost regardless of reformate composition, making them particularly suitable for ATR and renewable-based hydrogen production.
- Fl MH purification scales down in size better than the other purification options, making it a more attractive technology for small fueling stations, though low-capacity stations still cost at least 50% more than large-capacity stations (not shown in figures).
- Liquid hydrogen delivery is projected to have the lowest cost of the central hydrogen production options, and the lowest cost of all compressed H_2 options provided transportation distances are short (delivery distance is assumed to be 50 miles).

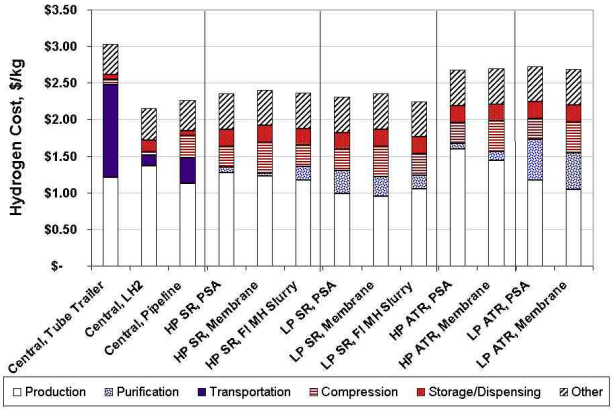

Figure 4. Hydrogen Cost for Compressed H_2 Vehicle Fueling - 690 kg H_2/day Capacity

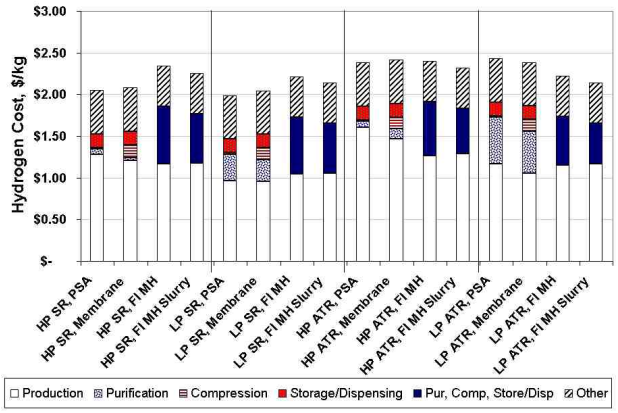

Figure 5. Hydrogen Cost for MH Vehicle Fueling - 690 kg H_2/day Capacity

However, central options could not be used ubiquitously, because costs will increase significantly with transportation distance.

Conclusions

Our analysis indicates that the use of fluorinated metal hydrides in slurry form could reduce overall hydrogen cost, especially if the slurry is used for purification only. In addition, if high-pressure storage is of concern due to safety or regulatory issues, Fl MH purification and storage could provide significant benefits. Slurries could also provide benefits in terms of hydrogen transmission to decentralized fuel cell power systems in a mini-hydrogen grid. It is not likely that significant energy savings can be expected over a well-integrated PSA combination, though improvements over the state-of-

the-art systems are possible. Some technology development will be required to optimize the slurry system, and significant development will be required to develop a stable and effective fluorinated metal hydride that can be produced cost-effectively.

References

1. Hara, S., K. Sakaki, N. Itoh, H.-M. Kimura, K. Asami, and A. Inoue. 2000. "An Amourphos Alloy Membrane without Noble Metals for Gaseous Hydrogen Separation." Journal of Membrane Science, 164:289-294

2. Wang, X.-L., K. Iwata, and S. Suda. 1995. "Hydrogen Purification using Fluorinated LaNi4.7Al0.3 Alloy." Journal of Alloys and Compounds, 231:860-864

FY 2002 Publications/Presentations

1. Weber, B., "Future of Hydrogen Fuels, Fuel Cells and Alternative Energy Technology", presented at 7th ASCOPE (ASEAN Council on Petroleum), Kuala Lumpur, Malaysia, November 5-8, 2001

II.F.2 Hydrogen Infrastructure Studies

Susan M. Schoenung (Primary Contact)
Longitude 122 West, Inc.
1010 Doyle Street, Suite 10
Menlo Park, CA 94025
(650) 329-0845, fax: (650) 329-9951, e-mail: schoenung@aol.com

DOE Technology Development Manager: Neil Rossmeissl
(202)586-8668, fax: (202) 586-5860, e-mail: Neil.Rossmeissl@ee.doe.gov

Objectives

- Address energy efficiency, cost competitiveness and environmental impact of integrated hydrogen systems through participation in three integrated system teams as called for by the International Energy Agency's (IEA) Hydrogen Agreement Annex 13: "Design and Optimization of Integrated Systems."

Approach

- Provide independent modeling and assessment of integrated hydrogen systems, with an emphasis on spreadsheet models
- Maintain consistency among the three teams with respect to assumptions of cost and performance
  - Lead the Transportation Applications analysis, focusing on hydrogen refueling infrastructure - particularly the production sources, distribution, and storage of hydrogen. The effort addresses several general areas:
  - Cost of hydrogen fuel dispensed to the vehicle
  - Sensitivity of that cost to numerous assumptions, including future hydrogen production and delivery options
  - Emissions (tailpipe and station), compared with alternative vehicle types
  - The impact of codes and standards on hydrogen storage footprints
- Attend Expert Team meetings and Task Definition Workshops
- Interact with the U.S. Operating Agent (Cathy Gregóire Padró), as needed

Accomplishments

- The transportation infrastructure analysis has been completed, including the following sensitivity studies:
  - Station utilization
  - Station size
  - Projected component costs for on-site hydrogen generation
  - Costs of natural gas and electricity (including renewables)
  - Upstream infrastructure costs (new central reformers and pipelines)
  - Transport distances
- The fuel economy and emissions analysis evaluated the following for alternative vehicle and fuel types:
  - Fuel economy

  - Cost of a 300-mile fill-up
  - Tailpipe emissions, gallon/mile
  - Major local / station emissions (kilogram [kg]/year)
  - Minor local / station air pollutants (kg/year)
- The final report on this analysis has been submitted and is part of an overall IEA package including all three project reports and a cost model
- A topical analysis and report of relevant (and changing) fire codes and the impact on station footprints were also completed

Future Directions

- Annex 13 was concluded at the end of June 2002. New tasks for a new Annex were proposed through two Task Development Workshops and are currently being developed for approval by the IEA Executive Committee. A new Annex or study task could address the following issues:
  - Validation of models using data from case studies
  - Use of models to assist in the design and optimization of demonstrations / projects
  - An analysis of legacy projects that lead from demonstration to commercial practice
  - An assessment of the impact of portable hydrogen system development (i.e., small devices) on larger system needs
  - Additional analysis of the impact of codes and standards on system design and cost
  - Comparison of different countries' demands, supplies, experiences and policies

---

Introduction

The U.S. Department of Energy participates in various activities of the International Energy Agency (IEA) through an Implementing Agreement and its Annexes. Hydrogen Agreement Annex 13, "Design and Optimization of Integrated Systems," calls for the U.S. to participate in three integrated system teams. The three teams and their projects are:

- Remote Power Systems
- Home/Residential Systems
- Transportation Applications
- Longitude 122 West serves as U.S. Team leader for Annex 13 activities

The goal of the analysis has been to provide independent modeling and assessment, especially of capital and operating costs, for the integrated systems. The current emphasis is on spreadsheet modeling, to make comparisons between system configurations and technologies easier. Other factors being considered are efficiency, environmental impact, and the role of codes and standards. The present task addresses infrastructure to support transportation applications.

Approach

The analysis of capital costs, operating costs, and footprints, fuel economy and emissions has been conducted using Excel spreadsheet modeling. Data sources included vendor data sheets and website information, vendor quotes and communications, case study experience, published literature (including Environmental Protection Agency data), theses, and engineering estimates. Major assumptions for the analysis include:

- Station serves 100 vehicles per day
- Each hydrogen fueling event delivers 4 kg of hydrogen
- Station operates 24 hours/day, 365 days per year
- Liquid hydrogen is delivered weekly; round trip delivery distance is 1,000 miles; storage is oversized by 30%

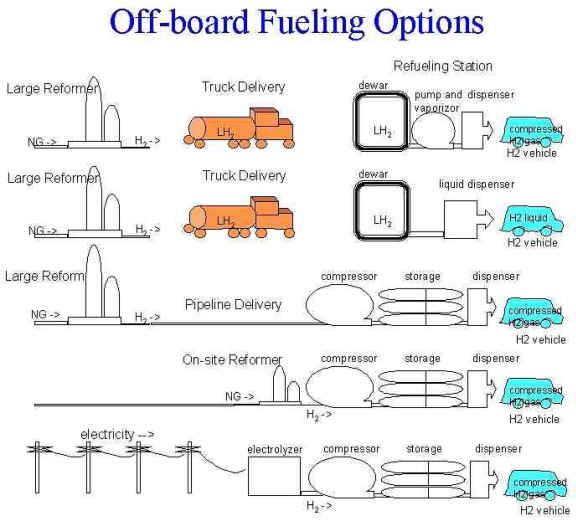

Figure 1. Refueling Station Alternatives Studied in this Work

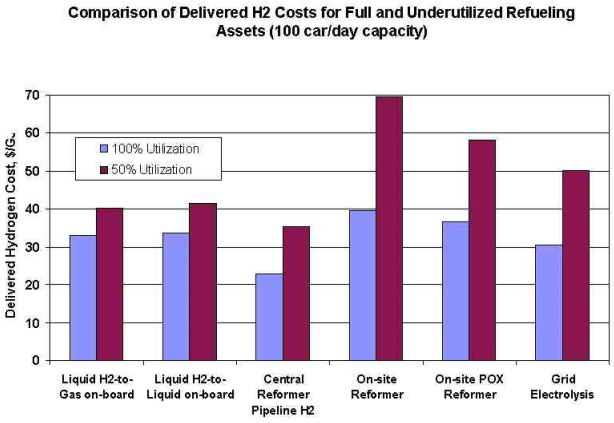

Figure 2. Cost of Dispensed Hydrogen ($/GJ) for Base Case and Station Utilized at 100% and 50% (100 Cars/Day Capacity)

- Gaseous hydrogen is delivered by pipeline or generated on-site; storage is sized for one day's service plus 40%
- On-site generators are sized / rated to fill storage in 18 to 24 hours, depending on electricity rates

The 6 scenarios differ by whether the hydrogen is produced off-site and transported by truck or pipeline, or whether the hydrogen is produced on-site by steam methane reformer (SMR), partial oxidation POx) reforming, or grid electrolysis. The scenarios are depicted in Figure 1.

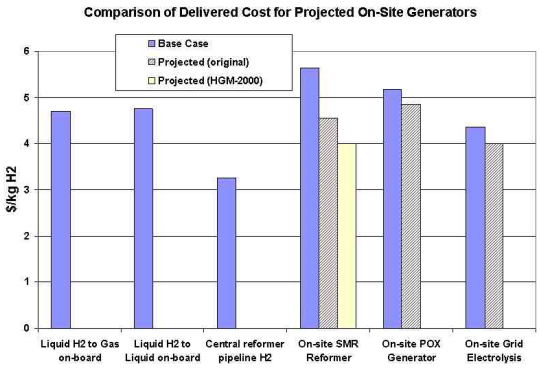

Figure 3. Sensitivity of Cost Results to Projected Costs of On-Site Generation Technologies

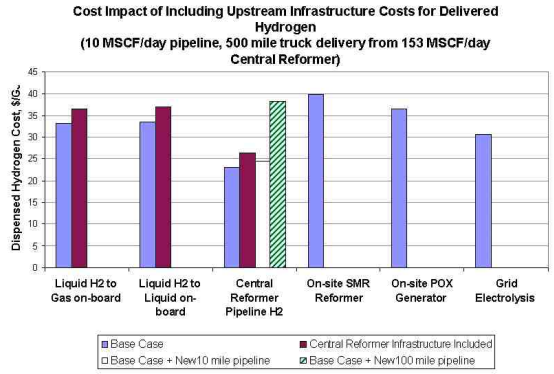

Figure 4. Sensitivity of Cost Results to the Inclusion of Upstream Infrastructure Costs

Results

Key results are the cost of dispensed hydrogen for the 6 cases. These are compared for a number of important parametric variations. The sensitivity to station utilization factor is shown in Figure 2, for both the base case of 100% utilization and under-utilization at 50%. The results are also sensitive to the projected cost of on-site production equipment, as shown in Figure 3. [1,2]

Another key result is that the construction of upstream production and delivery infrastructure (central SMR and pipelines) is not ruled out by including the amortization of these costs in the dispensed hydrogen cost, as shown in Figure 4.

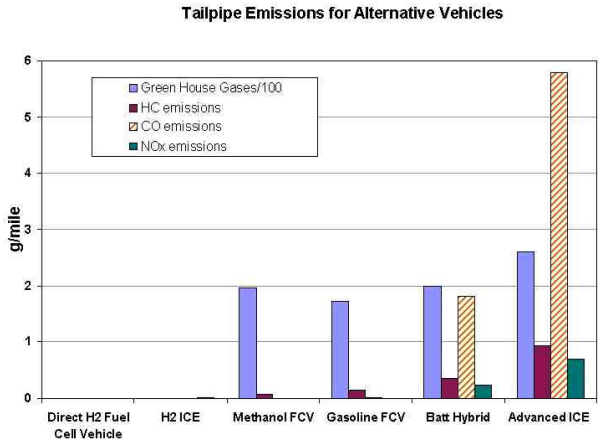

Figure 5. Tailpipe Emissions for Alternative Vehicles and Fuels

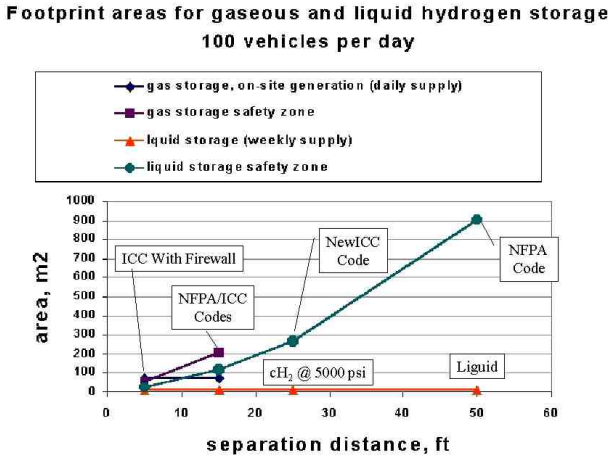

Figure 6. Footprints of Station Alternatives Showing Impact of Varying Fire Codes for Hydrogen Storage

Major and minor emissions from the tailpipe of alternative vehicles and the different refueling station options were calculated. The results show the pipeline and on-site electrolyzer to be the cleanest local approaches. Tailpipe emissions for alternative vehicles and fuels are shown in Figure 5.

Footprints are strongly dependent on the interpretation and implementation of fire codes and standards for local hydrogen storage [3]. As shown in Figure 6, a conservative safety stand-off zone requires a significantly larger footprint than a more practical standard.

Conclusions

Hydrogen refueling infrastructure can be provided for passenger vehicles by several alternative means, including bulk delivery of hydrogen to a station via truck or pipeline, or on-site generation using electrolysis or reforming techniques. The price of the various alternatives can be comparable, depending on the transport distance and production capacity.

References

1. Schoenung, S. M., "Hydrogen Technical Analysis on Matters Being Considered by the International Energy Agency - Transportation Infrastructure," Proc. DOE Annual Hydrogen Review, May, 2002

2. Thomas, C.E., Directed Technologies, Inc., personal communication based on report to Ford Motor Company, May 2001

3. Schoenung, S. M., "The Impact of Fire Code Specifications on Hydrogen System Footprints for IEA Integrated System Cases," draft report submitted to DOE Golden Field Office, June, 2002

FY 2002 Publications/Presentations

1. Susan M. Schoenung, "Hydrogen Vehicle Fueling Alternatives: An Analysis Developed for the International Energy Agency," in SAE Publication SP-1635: Fuel Cells and Alternative Fuels / Energy Systems, 2001.

2. Susan M. Schoenung, "A Comparison of Hydrogen Vehicle and Refueling Infrastructure Alternatives: An Analysis Developed for the International Energy Agency," proceedings 14th World Hydrogen Energy Conference, Montreal, Canada, June 2002

3. Technical staff seminar at South Coast Air Quality Management District, October 2002

Section III. Hydrogen Storage

III.A High Pressure Tanks

III.A.1 Hydrogen Composite Tank Program

Neel Sirosh (Primary Contact), Andy Abele, Alan Niedzwiecki
QUANTUM Technologies
17872 Cartwright Road
Irvine, CA 92614
(949) 399-4698, fax: (949) 399-4600, e-mail: nsirosh@qtww.com

DOE Technology Development Manager: Lucito Cataquiz
(202) 586-0729, fax: (202) 586-9811, e-mail: Lucito.Cataquiz@ee.doe.gov

Objectives

- Develop, demonstrate and validate 5,000 pounds per square inch (psi) 7.5 wt % and 8.5 wt% Type IV composite hydrogen storage tanks of specified sizes
- Develop and validate 5,000 psi in-tank-regulators
- Build, assemble, test and supply tank assemblies for DOE Future Truck and Nevada hydrogen bus programs
- Demonstrate 10,000 psi storage tanks

Approach

- Optimize materials, design and processes related to QUANTUM "TriShield" composite fuel storage tank technology to achieve high gravimetric efficiencies
- Develop tanks for specific sizes and perform safety verification and validation tests based on NGV2-2000, modified for high pressure hydrogen
- Supply fully validated tank assemblies to DOE

Accomplishments

- Achieved "World Record" hydrogen storage mass efficiency of 11.3 wt% on a prototype 5,000 psi tank, with Lawrence Livermore National Laboratory and Thiokol Propulsion
- Developed and demonstrated 7.5 wt % and 8.5 wt% Type IV composite hydrogen storage tanks of specified sizes
- Commenced shipping high efficiency TriShield^{TM} hydrogen storage tanks for a number of automotive and stationary applications
- Supplied tanks for Hyundai Santa Fe fuel cell electric vehicle, the first to fill to 5,000 psi hydrogen
- Achieved European Integrated Hydrogen Project (EIHP) specifications for 5,000 psi hydrogen storage tank, the first all-composite tank to achieve this
- Achieved Canadian Standards Association certification for industry's first 5,000 psi (350 bar) in-tank regulation system under NGV 3.1 standards
- Designed and developed industry's first hydrogen 10,000 psi (700 bar) in-tank regulation system
- Shipped tanks for DOE Future Truck and Nevada bus programs

Introduction

The objective of the DOE Hydrogen Composite Tank Project was to design, develop, validate, fabricate, and manufacture hydrogen fuel tanks (Figure 1) and in-tank regulators (Figure 2) along with vehicle integration brackets and isolators and have them delivered to Virginia Tech University and Texas Tech University in support of the Future Truck competition.

This project is part of the DOE program to demonstrate the feasibility of the use of compressed hydrogen as an automotive fuel. However, the lack of convenient and cost-effective hydrogen storage, particularly for an on-board vehicular system, is a major impediment to its widespread use. Improvements in the energy densities of hydrogen storage systems, reductions in cost, and increased compatibility with available and forecasted systems are required before viable hydrogen energy use will be realized. Possible approaches to hydrogen storage include: compression, liquefaction, chemical storage, metal hydrides, and adsorption. Although each storage method has desirable attributes, no approach currently satisfies all the efficiency, size, weight, cost, and safety requirements for transportation or utility use. Research continues in these areas, with progress being made in all approaches.

Currently there is a strong demand in the automotive market for cost-effective and efficient high-pressure hydrogen storage systems. The world's premier automotive original equipment manufacturer (OEMs) developing fuel cell vehicles have demonstrated significant interest in compressed hydrogen storage systems developed and validated by QUANTUM Technologies. The currently validated QUANTUM "TriShield" tank technology achieves 6% hydrogen by weight, 1,050 W-h/L, and 2,000 W-h/kg, meeting the DOE targets for percent weight and specific energy, and almost meeting the energy density target of 1,100 W-h/L. Significant cost reductions are possible with further optimization.

Figure 1. TriShield™ Hydrogen Storage Tank

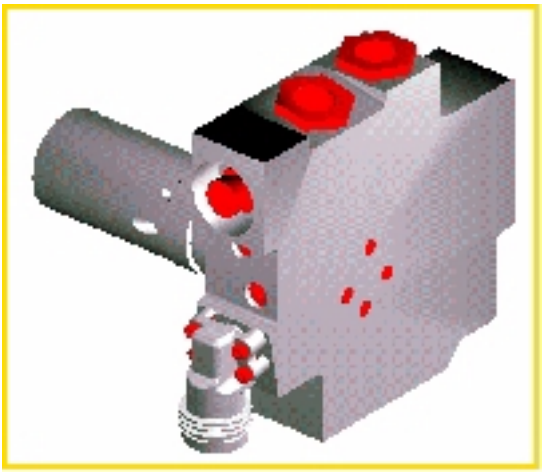

Figure 2. In-Tank High Pressure Regulator

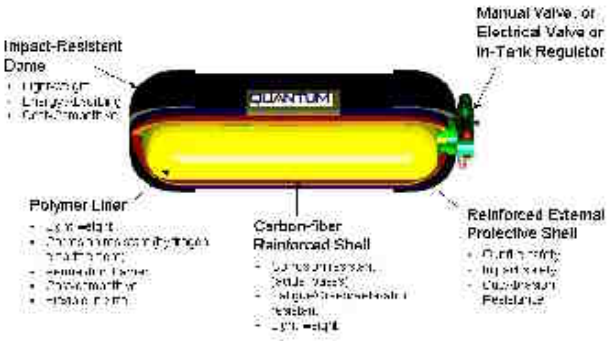

Figure 3. TriShield™ Tank Construction

Approach

The QUANTUM advanced composite tank technology incorporates a "TriShield™" design philosophy. The QUANTUM Type IV TriShield™ cylinder, as illustrated Figure 3, is comprised of a seamless, one piece, permeation resistant, cross-linked ultra-high molecular weight polymer liner that

is over wrapped with multiple layers of carbon fiber/ epoxy laminate and a proprietary external protective layer for impact resistance. TriShield™ hydrogen tanks feature a single-boss opening to minimize leak paths. The path to achieving high gravimetric efficiency is optimization in materials, design and processes. Numerical methods including the finite element method (see Figure 4) were employed to optimize the structural shell.

The TriShield™ hydrogen tank is designed to accommodate QUANTUM's patented in-tank regulator, which confines high gas pressures within the tank and thus, eliminates high-pressure fuel lines downstream of the fuel storage subsystem. By combining a check valve to assist tank filling, fuel filtering, fuel tank pressure and temperature monitoring, pressure relief device and tank lock-off in the regulation module, the system cost can be significantly reduced.

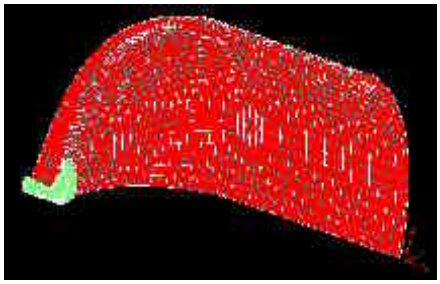

Figure 4. Composite Shell Finite Element Model

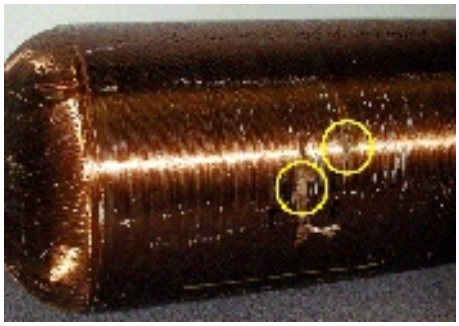

Figure 5. Gunfire Test Example

Figure 6. Bonfire Test Example

Results

The 5,000 and 10,000-psi tanks developed by QUANTUM Technologies have been validated to meet the requirements of DOT FMVSS304, NGV2-2000 (both modified for hydrogen) and the draft EIHP standard. Typical safety tests completed, in order to ensure safety and reliability in an automotive service environment included burst tests (2.35 safety margin), fatigue, extreme temperature, hydrogen cycling, bonfire, severe drop impact test, flaw tolerance, acid environment, gunfire penetration, accelerated stress, permeation and material tests (Figrues 5 and 6). The developed "In-Tank-Regulators" meet the requirements of NGV3.1 and EIHP.

Hydrogen poses challenges, both real and perceived, as a transportation fuel. The most challenging application is the light-duty vehicle or, more specifically, the automobile. Automobiles impose the greatest constraints with respect to available space on-board the vehicle and consumer expectations for vehicle range. In the near-term, fuel cell vehicles will likely first be introduced for fleet applications in 2003-05. Fleet applications will likely have centralized refueling available, so a vehicle range of 100 - 150 miles (160 - 241 km) would be acceptable. In terms of mass of hydrogen, this range could be achieved with about 3 kg of hydrogen supplying a fuel cell vehicle. Mature compressed and liquid hydrogen storage technologies of reasonable size and weight could achieve this short-term goal, as shown Table 1. Metal hydrides, although providing more compact storage, would impose a significant weight penalty.

Table 1. Current Status of Potential Short-term Hydrogen Storage Technologies for Volume and Weight Storing 3 kg H_2

Technology	Storage System Volume	Storage System Weight
5,000 psi Compressed H_2 Tanks	145 L	45 kg
10,000 psi Compressed H_2 Tanks	100 L	50 kg
Metal Hydrides	55 L	215 kg
Liquid H_2	90 L	40 kg

Short-term Goal: 3 kg H_2 (215 km)

In the long-term, average consumers will expect fuel cell vehicles to be transparent compared to the gasoline-powered vehicles they drive today with respect to cost, convenience and operation. In fact, it is likely that fuel cell vehicles will have to offer a significant value proposition to encourage consumers to adopt a new technology rather than continue with something that is tried and true. Vehicle range will be an important factor to consumers, especially as a hydrogen-refueling infrastructure begins to develop. Fuel cell vehicle range of over 400 miles (644 km) will be needed, or roughly 7 kg of hydrogen stored on-board. Advanced storage materials, including alanate hydrides and carbon nano-structures, will have to emerge from the current conceptual stage to reduce hydrogen storage system size and weight, as shown in Table 2. However, both of these solid-state storage media are years from commercialization. QUANTUM's 10,000 psi TriShield^{TM} could potentially meet this long-term goal without significantly impacting either the passenger or storage compartments.

Table 2. Current Status of Potential Long-term Hydrogen Storage Technologies for Storing 7 kg H_2

Technology	Storage System Volume	Storage System Weight
5,000 psi Compressed H_2Tanks	320 L	90 kg
10,000 psi Compressed H_2 Tanks	220 L	100 kg
Metal Hydrides	200 L	222 kg
Nanotubes	~130 L	~120 kg

Long-term Goal: 7 kg H_2 (700 km)

Conclusions

The technologies developed and validated under the DOE Hydrogen Composite project have played a key role in the commercialization of QUANTUM TriShield^{TM} tanks. In the near term, the markets for high-pressure hydrogen storage technology appear to be growing. Major automotive OEMs and bus OEMs are expected to be the major markets for this technology. In addition, QUANTUM sees growing interest in stationary and, especially, hydrogen refueling infrastructure applications for its advanced TriShield^{TM} storage tanks.

Presentations

1. Neel Sirosh, "Breakthroughs in Compressed Hydrogen Storage", Carbon Fiber 2000, San Antonio (2000)

2. Andris R. Abele, "Quantum's Experience - Leveraging DOE Funding to Accelerate Technology Development and Commercialization of Advanced Hydrogen Storage", NHA 12th Annual U.S. Hydrogen Meeting, Washington D.C. (2001)

3. Alan P. Niedzwiecki, "Advanced Hydrogen Storage to Enable Fuel Cell Vehicles", 14th World Hydrogen Energy Conference, Montreal, Quebec (2002)

4. Neel Sirosh, "Compressed Hydrogen Storage Technology", Hydrogen Storage: Gateway to Energy Security Workshop, Hilton Head Island (2002)

III.A.2 Hydrogen Storage Using Lightweight Tanks

Andrew Weisberg (Primary Contact), Blake Myers, Gene Berry
Lawrence Livermore National Laboratory
P.O. Box 808
Livermore, CA 94551
(925) 422-7293, fax (925) 424-3731, e-mail: weisberg1@llnl.gov

DOE Technology Development Manager: Lucito Cataquiz
(202) 586-0729, fax : (202) 586-9811, e-mail : Lucito.Cataquiz@ee.doe.gov

Objectives

- Learn how to build and operate the best hydrogen container technologies
- Explore the performance of recently discovered non-pressure-vessel structural containment options for compressed hydrogen
- Demonstrate fundamental improvements in hydrogen containment safety

Approach

- Quantify optimality with valid (correct Dimensional Analysis) consumer-preferred mixtures of volume, mass, and cost
- Fix computer aided engineering models to include 3D effects, conserve fibers, and predict matrix strength effects
- Continue to push the limits of mass performance through experiments with the smallest representative test articles
- Adopt process research based on statistical performance to save a predicted 30% in mass and cost

Accomplishments

- Engineered minimal diameter (4.5 inch) pressure vessel representative of all larger scales based on Balanced Ovaloid end dome contour
- Pioneered first use of recent computer aided manufacture (CAM) prototyping techniques for tank manufacture employing XLS, VBA, TCW, DWG, and STL computer languages
- Developer wider, more fundamental flavor of analyses applicable to new systems (including hydrogen infrastructures), as well as motor vehicles

Future Directions

- Account for the "missing 7%" in the record-breaking tanks burst in July 2000, then extend models to forecast performance across wide classes of hydrogen containment structures
- Observe spectacular "turn to dust" failure modes with real time instrumentation
- Conduct a statistical hydroburst test program to demonstrate substantial cost and mass savings

---

Introduction

The easiest near-term solution to storing hydrogen onboard motor vehicles may also be the best long-term solution for most hydrogen vehicles and infrastructure options. Compressed hydrogen must be contained in structures that can safely hold high pressures with low permeation. Pressure vessels that satisfy numerous hydrogen vehicular safety standards at pressures up to 5,000 pounds per square

inch (psi) are already commercially available. More advanced compressed hydrogen containment technologies have been the objective of research at Lawrence Livermore National Laboratory (LLNL) for almost a decade. Our research has been responsible for the most advanced pressure vessels (capable of safely containing 5,000 psi hydrogen) now nearing commercialization.

Recent theoretical results suggest that the best hydrogen containment solutions must store gas at pressures as high as 15,000 psi. LLNL has been seeking the lowest mass hydrogen storage technologies. Until 2002, the best hydrogen gas storage solutions employed pressure vessels (colloquially called tanks) that carry the high stresses due to high internal pressure in composite materials wound around almost impermeable liners. New structural containment solutions need not resemble tanks carrying stresses through their interiors in mass produced structural components rather than around them in strong shells. Both new and proven conventional solutions rely on advanced materials and analyses to deliver improved mass and cost performance.

Approach

Recently, record-breaking and mass-performance leading commercializable hydrogen tanks were developed from LLNL specifications with DOE funding. Because LLNL tank development to date has employed expensive aerospace manufacturing processes, continued experimentation progress on the frontiers of hydrogen tankage mass-performance has been jeopardized by the high cost of test articles. For the past year, LLNL advanced compressed hydrogen storage has therefore been directed at prototyping affordable test articles.

The prototype tanks LLNL is developing solve vehicle component cost problems as well as experimental tank affordability. Their small size does more than conserve costly advanced structural materials, direct costs, and fabrication costs - it prevents them from competing with existing or planned commercial products. They have been sized at the minimum scale that will yield experimental data relevant to calibrated predictions at all larger scales (4.5" diameter ~12" long), yet they remain applicable in future vehicle integration demonstration projects for strategic (no barriers to adoption) small vehicles: wheelchairs, motorcycle scooters, skidoos, etc.

Tank prototyping provided an opportunity to employ modern CAM techniques (developed in the 1990s), which have yet to be adopted in aerospace or industrial tank manufacture. These techniques conserved costly LLNL manpower and would have shortened the protected design process, if not for a sequence of increasing fundamental discoveries their fresh application unleashed. Details of the shape calculated for prototype tank end dome contours received detailed examination before substantial investments could be made responsibly in liner mold tooling. That scrutiny uncovered an implicit violation in assumptions used to derive the Balanced Ovaloid contour, especially in regions of negative curvature (where the end dome is convex in one direction and concave in the other). More consideration of those violated assumptions raised the possibility of deliberately manufacturing composite structures with regions of negative curvatures that would allow them to 'nest' in replicated geometries that fill space. Questions asked by LLNL colleagues about the advantages of such space filling structures lead to new forms of analysis that are widely applicable to hydrogen storage onboard vehicles and in future infrastructures. These forms of analysis will be explored and calibrated with experiments.

Results

Mass efficient compressed hydrogen containers will be the most cost efficient for any chosen structural material, although the highest strength materials cannot repay their high cost with mass savings. Container volume remains the greatest challenge to storing hydrogen onboard motor vehicles due to the low density of hydrogen in any of its storable forms (chemically bound, gas, or liquid). Structural improvements can deliver slight volume reduction, but storage volumes can be dramatically improved by increasing stored hydrogen pressure (and by decreasing temperature). These improvements reach diminishing returns above roughly 15,000 psi, and continued structural innovations will be required to withstand these higher pressures with affordable mass and cost. The

fundamental improvements LLNL is making in vehicle and infrastructure analyses allow mass, volume, and cost performance that reflect consumer preferences (e.g. gasoline vehicle range) to be assessed.

Preliminary results suggest volume improvements will be roughly twice as valuable as mass improvements (as ratios to existing technology). Increases in container mass required to hold higher pressures can be offset by the structural, operating, design, and materials improvements LLNL is investigating with small prototypes. Figure 1 points to locations in those prototypes (on their end dome cross section solid models) where discoveries have already emerged (in early 2002) from LLNL prototyping. That prototyping was intended to demonstrate predicted 30% savings in cost and mass that LLNL expects from Statistical Process Research, which must hydroburst (test to destruction) large (>25) numbers of test articles. Experimental statistics are expected to replace much of the controversial uncertainty in current structural "safety factors" with quantitative reliability methods. These methods, shown in Figure 2, were developed in the 1980's for maximizing mass in solid rockets, and for minimizing the cost of semiconductors.

Discoveries made during tank prototyping have begun to explain the rule of thumb used in modern finite element analysis tank design methods to avoid high-variance (and quite unsafe) failures in end domes. Actual wound tanks depart from the assumptions of axial symmetry embedded in their 2D design, in ways that can stress their composite's matrix with excessive local variations (in 3D) unless 40-80% excess fiber is used in helical windings. These discoveries, and LLNL colleagues' questions about their implications, led to a new formalism capable of mixing mass, volume, and cost performance. That formalism dissects an application into a hierarchy of components that can be quantitatively described by dimensionless ratios, which can be arbitrarily manipulated with nonlinear functions. The Calculus of Variations can be applied on top of such models to constrain consumer preference computables, such as vehicle range, while optimizing other consumer preferred performance measures (i.e. cost-per-mile or vehicle capital cost).

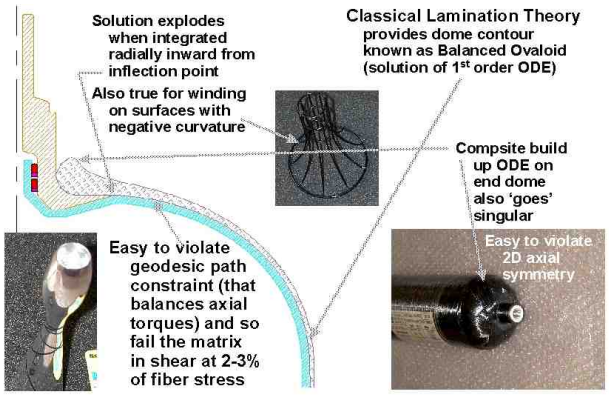

Figure 1. Locations of Discoveries Made by Tank Prototyping Based on Methods Predating Finite Element Analysis

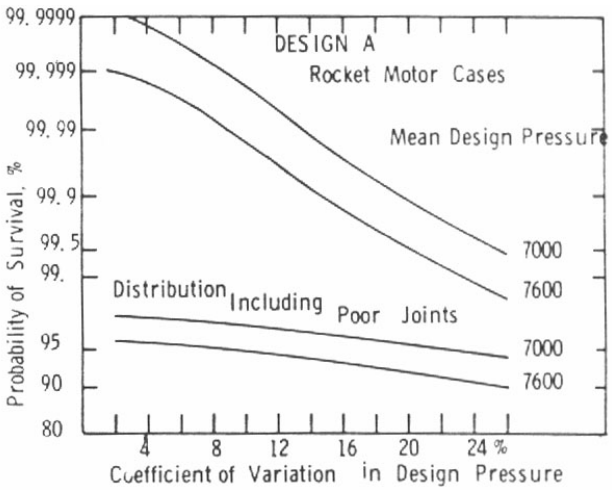

Figure 2. Statistical Methods Developed for Solid Rockets Provide the Basis for Predicted Savings

Figure 3 illustrates several of the structural innovations that emerged from the discoveries made at LLNL in the first half of 2002. It remains to be seen which of these innovations are best and/or affordably testable in the near term, but all are likely to improve on conventional tanks. Several important 'holes' in current theory and analyses emerged during the recent discovery process. These 'holes' are big enough that several PhD theses may not suffice to fill each one. Fiber number flex conservation, departures from constant (assumed) fiber/matrix ratio, and actual curvilinear (non-axisymmetric, nongeodesic) fiber trajectories will contribute arduous but necessary improvements to current composite design methods.

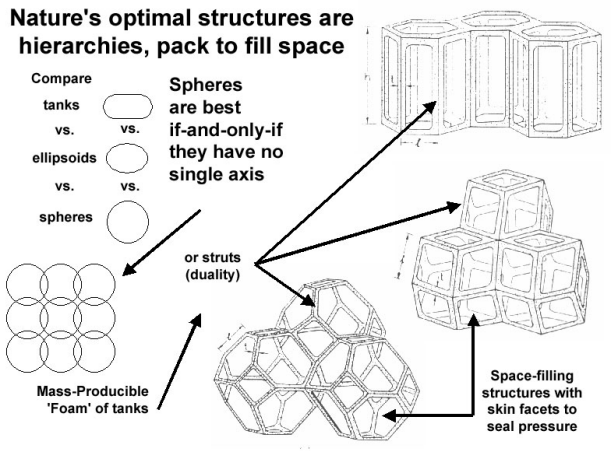

Figure 3. Forms of Hydrogen Storage Can Use Containment Structures That Do Not Resemble Tanks

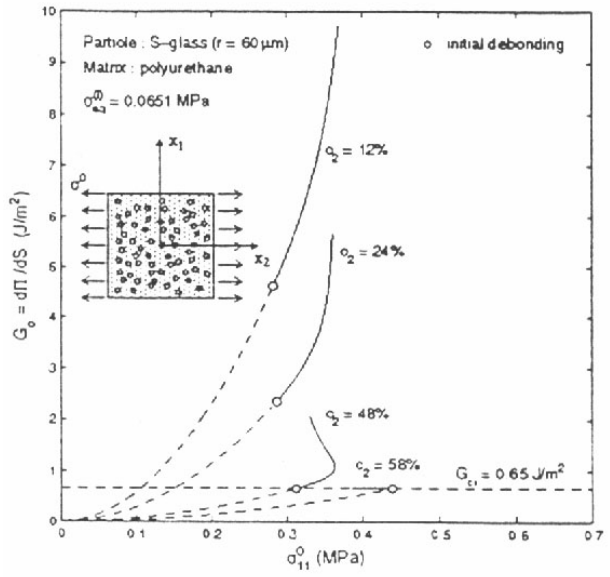

Figure 4. Recent Discoveries Include Debonding Waves First Observed in Particulate Composites

Experiments will be necessary to prove the existence, behavior, and engineering of a new class of physical instability. Tensor solitary waves have been hypothesized that are related to debonding instabilities first detected in particulate composites in the early 1980's. Figure 4 shows the characteristics of that simpler instability. Figure 5 captures a mysterious, ultrafast failure mode first observed in 2000, whose explanation may be similar to Figure 4's particulate (not fiber) composite results, but whose

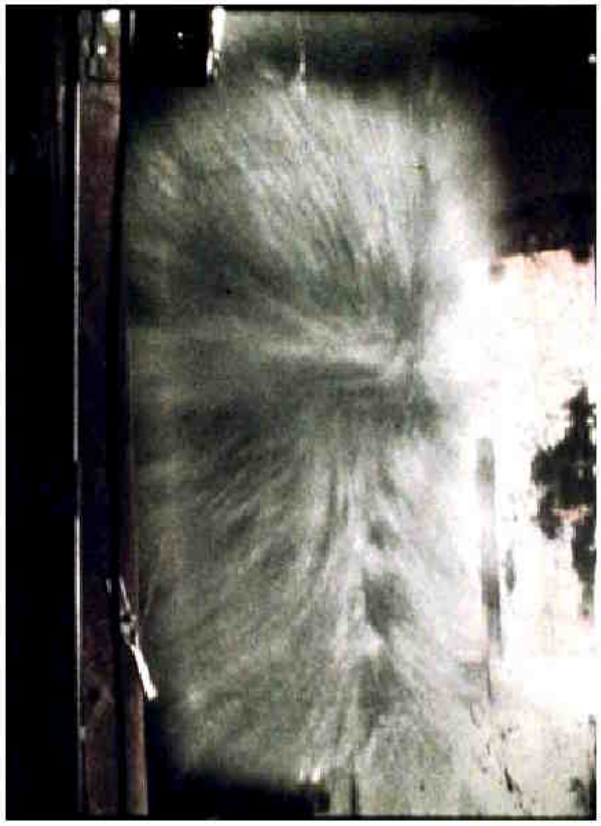

Figure 5. Observed Failure Modes Can Turn Tanks to Dust, Dissipating Stored Structural Energy Very Rapidly (< 200 Microseconds in this Frame), and Potentially Providing a Safety Breakthrough

morphology differs due to the extreme anisotropy of carbon fiber composites. LLNL structural hydrogen storage research has made progress in 2002 towards explaining the consistent fiber strain at failure loss of 7% observed during the same 2000 experiments. (This loss departed from Thiokol's data base of over 10,000 bursts performed with the same composite and winding techniques.) LLNL efforts have a longer-term goal of understanding and harnessing this failure mode into a safety breakthrough, dissipating the significant mechanical stored energy (implicit in high-pressure containment) during an accident.

Conclusions

Higher pressures are likely optimal for compressed hydrogen storage onboard motor vehicles, and hydrogen permeability must be

measured at those pressures for appropriate barrier materials to confirm their feasibility.

New analytic formalisms can provide a valid basis for optimizing consumer benefits from many forms of advanced hydrogen containment, including recent structural innovations unlike conventional pressure vessels.

Unmodeled departures from assumed axial symmetry, combined with low matrix shear strength in epoxy matrix composites, potentially accounts for consistent 7% strength loss in the record-settings tanks LLNL built and tested in mid 2000; and is expected could handicap conventional tank designs mass performance as pressure ratings increase.

References

1. Composite Reliability, E.M. Wu, ASTM STP 580 (Conf. Las Vegas 1974).

2. A Statistical Theory of the Strength of Materials, Weibull and Waloddi, Ingeniors Vetenskops Akadamien-Hawdlingar, Stockholm 1939, No. 151, p. 1-45.

3. Cellular Solids, Lorna J. Gibson and Michael F. Ashey, Pergammon Press, Oxford 1988.

FY 2002 Publications/Presentations

1. DOE Annual Program Review for 2002, May 8, 2002, Denver, CO

III.A.3 Hydrogen Storage in Insulated Pressure Vessels

Salvador M. Aceves (Primary Contact)
Lawrence Livermore National Laboratory
PO Box 808, L-644
Livermore, CA 94551
(925) 422-0864, fax: (925) 423-7914, e-mail: saceves@llnl.gov

DOE Technology Development Managers: Lucito Cataquiz
(202) 586-0729, fax: (202) 586-9811, e-mail: Lucito.Cataquiz@ee.doe.gov

Objectives

- Demonstrate the advantages of insulated pressure vessels for hydrogen storage in terms of improved packaging, reduced evaporative losses and reduced costs.
- Write standards for assuring the safety of insulated pressure vessels.
- Demonstrate the insulated pressure vessel technology in two pickup trucks.

Approach

- Conduct experiments and analysis to verify safety of insulated pressure vessels.
- Study existing standards for hydrogen storage in vehicles.
- Test performance of two insulated pressure vessels on pickup trucks.

Accomplishments

- Acquired funding from the South Coast Air Quality Management District to perform a demonstration project where we will install insulated pressure vessels in two trucks.
- Built 6 full size (130 liter internal volume) insulated pressure vessels according to our current design.
- Generated a preliminary list of tests for certification of insulated pressure vessels.
- Conducted the ISO/Department of Transportation (DOT) drop test and bonfire test on our pressure vessels. Our tanks passed both tests.

Future Directions

- Conduct a demonstration project at SunLine transit, where the insulated pressure vessels will be installed in two trucks.
- Generate a draft document proposing a set of rules for certification of insulated pressure vessels.
- Start work on building 12 additional insulated pressure vessels according to our current design.
- Subject tanks to the Society of Automotive Engineers (SAE) cryogenic drop and bonfire tests.

Introduction

The goal of this project is to develop a hydrogen storage technology that can satisfy light-duty vehicle storage needs in a cost-effective way. This high pressure, low temperature vessel has the packaging advantages of liquid hydrogen tanks (low weight and volume) with much reduced evaporative losses, infrastructure flexibility, lower energy consumption, lower cost, enhanced user convenience, and safety.

Insulated pressure vessels are being developed as an alternative technology for storage of hydrogen in light-duty vehicles. Insulated pressure vessels can be fueled with either liquid hydrogen or compressed hydrogen. This flexibility results in advantages compared to conventional hydrogen storage technologies. Insulated pressure vessels are lighter than hydrides, more compact than ambient-temperature pressure vessels, and require less energy for liquefaction and have less evaporative losses than liquid hydrogen tanks.

We plan to demonstrate that insulated pressure vessels that have packaging characteristics similar to liquid hydrogen and that are superior to ambient temperature pressure vessels. Compared with liquid hydrogen, insulated pressure vessels give increased flexibility to the fueling infrastructure, since the vehicle can be fueled with liquid hydrogen for long trips, or with less-energy-intensive ambient temperature hydrogen for daily driving. The high-pressure capability of the pressure vessel and the thermodynamic properties of hydrogen result in virtually zero boil-off losses for insulated pressure vessels. Finally, due to their high-pressure capability, insulated pressure vessels never run out of hydrogen after a long period of parking. This may be a major issue for liquid hydrogen tanks that can lose all the hydrogen due to evaporation.

Approach

We are conducting experiments and analysis to verify that insulated pressure vessels are a safe technology for vehicular storage of hydrogen. We have conducted a long list of DOT/ISO tests and we are planning to conduct two SAE tests that apply to cryogenic pressure vessels.

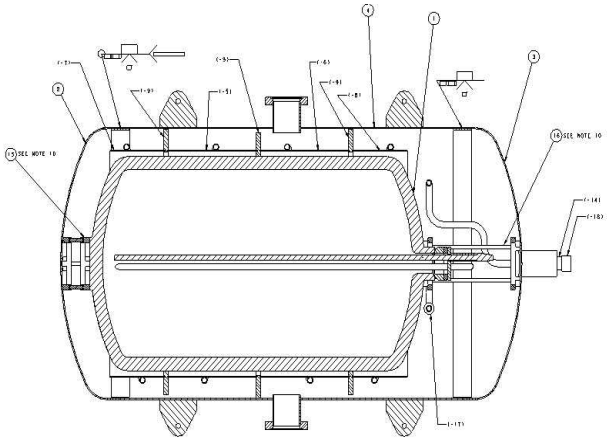

Figure 1. Insulation design for pressure vessel. The figure shows a vacuum space for obtaining good performance from the multilayer insulation, instrumentation for pressure, temperature and level, and a vapor shield for reducing hydrogen evaporative losses.

We are planning demonstration experiments to prove the feasibility of insulated pressure vessels in vehicles. To accomplish this task, we have secured funding from the South Coast Air Quality Management District, SCI and SunLine.

Results

During this year, we prepared a proposal to the South Coast Air Quality Management District to obtain funding to perform a demonstration project at SunLine Transit, where we will install insulated pressure vessels in two of the SunLine fleet trucks. The proposal has been approved and we will use these funds to complement the budget received from the hydrogen program.

We also have built 6 full-size (130-liter internal volume) insulated pressure vessels according to our current design (see Figures 1 and 2). Two of these vessels will be used for the SAE cryogenic drop and bonfire tests, while the other vessels will be used for vehicle demonstration at SunLine Transit.

We have generated a preliminary list of tests for certification of insulated pressure vessels. The list of tests will be sent to pressure vessel manufacturers for their comments. We have conducted all of the DOT/ISO tests for pressure vessel certification.

Finally, we are working on testing 5000-psi tanks for application in insulated pressure vessels. As a part of this work, we cycle tested two 5000-psi tanks 100 times down to liquid nitrogen temperatures. The tanks were then burst tested. The tanks failed at a pressure high enough to satisfy the DOT/ISO standards.

Conclusions

For reduced cost and complexity, it is desirable to use commercially available aluminum-fiber pressure vessels for insulated pressure vessels. However, commercially available pressure vessels are not designed for operation at cryogenic temperature. A series of tests has been carried out to verify that commercially available pressure vessels can be operated at cryogenic temperature with no performance losses. All analysis and experiments to date indicate that no significant damage has resulted. Future activities include a demonstration project in which the insulated pressure vessels will be installed and tested on two vehicles. A draft standard will also be generated for obtaining certification for insulated pressure vessels.

FY 2002 Publications/Presentations

1. Performance Evaluation Tests of Insulated Pressure Vessels for Vehicular Hydrogen Storage, S. M. Aceves, J. Martinez-Frias, F. Espinosa-Loza, Proceedings of the World Hydrogen Conference, Montreal, Canada, June 2002.

2. Insulated Pressure Vessels for Vehicular Hydrogen Storage: Analysis and Performance Evaluation, S. M. Aceves, J. Martinez-Frias, O. Garcia-Villazana and F. Espinosa-Loza, Paper IMECE2001/AES-23668, Proceedings of the 2001 ASME International Mechanical Engineering Congress and Exposition, November 11-16, New York, NY.

3. Certification Testing and Demonstration of Insulated Pressure Vessels for Vehicular Hydrogen Storage, S. M. Aceves, J. Martinez-Frias and F. Espinosa-Loza, Proceedings of the U.S. DOE Hydrogen Program Review Meeting, Denver, Colorado, May 2002.

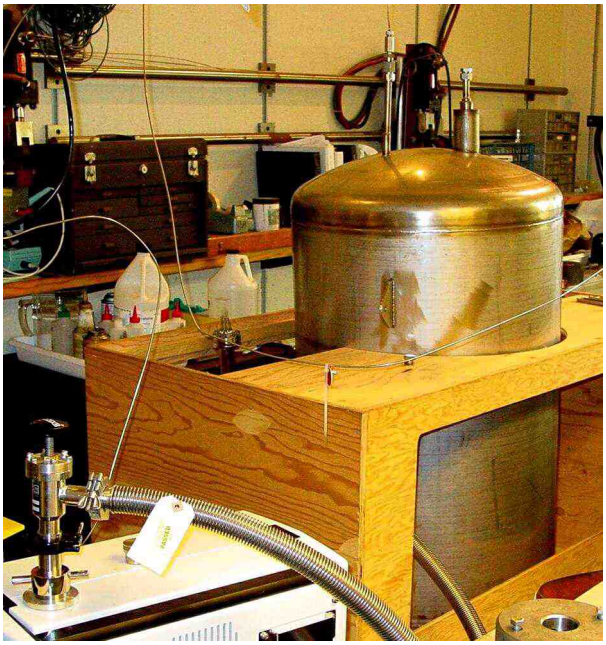

Figure 2. Finished Insulated Pressure Vessel being tested at the Lawrence Livermore National Laboratory High-Pressure Laboratory

4. Certification Testing and Demonstration of Insulated Pressure Vessels for Vehicular Hydrogen and Natural Gas Storage, Salvador M. Aceves, Joel Martinez-Frias and Francisco Espinosa-Loza, Randy Schaffer, William Clapper, Proceedings of the 8th International Conference and Exhibition on Natural Gas Vehicles, Washington, DC, October 8-10, 2002.

Special Recognitions & Awards/Patents Issued

1. Project was featured in the cover and in a 2-page article in "Mechanical Engineering" Magazine in February 2002.

III.A.4 Advanced Thermal Hydrogen Compression

David H. DaCosta (Primary Contact), Mark Golben
Ergenics, Inc.
373 Margaret King Ave.
Ringwood, NJ 07456
(973) 728-8815, fax: (973) 728-8864, e-mail: dacosta@warwick.net

DOE Technology Development Manager: Lucito Cataquiz
(202) 586-0729, fax: (202) 586-9811, e-mail: Lucito.Cataquiz@ee.doe.gov

Objectives

- Develop a hydride thermal hydrogen compressor that operates in conjunction with advanced hydrogen production technologies and improves the efficiency and economics of the compression process.
- Determine to what extent the hydride compression process can perform the dual function of compression with purification, to remove impurities that adversely affect fuel cells.

Approach

- Construct a single stage hydride compressor that employs miniature hydride heat exchangers and three purification technologies (passive purification for water vapor and diatomic oxygen [O_2], inert gas purification, and elevated temperature desorption for carbon monoxide [CO] and carbon dioxide [CO_2]).
- Test the compressor on impure hydrogen streams to determine threshold contamination levels (levels at which compressor performance is affected) for water (H_2O), O_2, CO, and methane (CH_4).
- Investigate compressor capabilities to perform the dual function of compression with purification for impurities that adversely affect fuel cell operation (CO and diatomic nitrogen [N_2]).
- Engineer and test hydride alloys suitable for long term operation at high pressures over 5,000 pounds per square inch gauge (psig).
- Validate the entire compressor process in a multi-stage, pilot scale system.

Accomplishments

- Demonstrated operation over 5,000 psig with hydride alloys from two separate "families," providing versatility to meet application-specific needs.
- Modified design operating conditions to increase efficiency, reduce energy consumption and reduce complexity, with a corresponding economic improvement via lower capital and operating costs.
- Engineered hydride alloys that can endure cycling at elevated temperatures without damage.

Future Directions

- Complete construction of a single stage hydride compressor and compressor test stand. The compressor includes hydrogen purification capabilities and the test stand includes fast response, continuous impurity monitors for the gathering of real-time operating information.
- Quantify the hydride compressor's tolerance to impurities in tests occuring in the Fall of 2002.
- Validate the entire thermal compression process in a pilot scale system that includes purification provisions and boosts hydrogen pressure to over 5,000 psig. The flow rate capability of the pilot-scale system will be similar to that required for overnight refueling of a hydrogen fuel cell automobile.

- Evaluate the commercial viability of the hydride compression process compared to existing mechanical compression and hydrogen purification technologies.
- Following a successful conclusion to this portion of the project, build and field demonstrate a full-scale compressor prototype sized for a hydrogen vehicle refueling station, and compare side-by-side with a mechanical compressor.

Introduction

Ergenics is investigating the application of its novel hydride hydrogen compression process to hydrogen produced from renewable resources. Hydride hydrogen compressors have offered significant operational and economic advantages over traditional mechanical compressors when the hydrogen is pure and flow rates are relatively low. However, hydrogen produced from renewable resources can contain impurities that might damage a hydride compressor and, if hydride compressors are to play a major role as hydrogen becomes an increasingly important part of America's energy supply, increased flow rate capabilities must be economical.

The primary focus of this project is to develop methods that allow hydride alloys to absorb non-pure hydrogen streams likely to result from renewable hydrogen production processes (DaCosta 2000). Three hydrogen purification techniques have been identified and will be tested during the fall of 2002. Increased flow capability will be accomplished by using miniature hydride heat exchangers (Golben 2001).

During the course of hydride compressor development, a number of additional insights have been gained regarding requirements for commercial hydride compressor viability. These insights are important for the overall success of the project and have been included in the project scope:

- Compression with purification may mitigate fuel cell degradation from CO. If the purification techniques used to protect the compressor's hydride alloys can be used to eliminate CO from hydrogen streams, alternative methods of extending fuel cell life may be unnecessary. A secondary benefit would be to remove impurities that damage the new hydrogen storage media now under development, such as sodium aluminum hydride and carbon nanotubes.

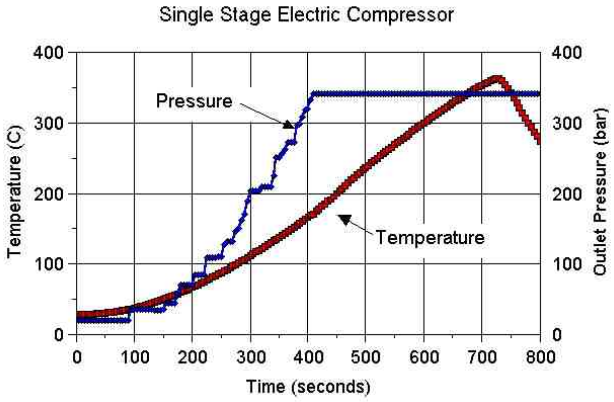

Figure 1. A Single stage Hydride Compressor Boosts Outlet Pressure to over 5,000 psi (350 bar) for Vehicular Storage

- Hydride compressors can compress hydrogen to the very high pressures under consideration for vehicular storage (5,000 to 10,000 pounds per square inch [psi]) much easier than mechanical compressors. For example, an electrically heated hydride compressor can achieve very high compression ratios in a single stage, as shown in the performance curve in Figure 1.
- Using natural gas as the energy source for a hydride compressor reduces energy costs to less than half that of a mechanical compressor. Lower compression energy cost reduces gasoline-equivalent hydrogen cost by 14 to 20 cents per gallon.
- The third insight has proven to be important for commercial viability. The ability to compress hydrogen using the low-grade heat energy in hot water is a compelling advantage of the hydride compression process. However, many applications either do not have adequate waste heat or solar hot water, or the waste heat or solar hot water is difficult to access economically. In these cases, traditional fuels can be used to provide compression energy, but the relatively low

operating efficiency of the hydride compression process must be increased by using higher temperatures. A new class of hydride alloys that will perform the compression function at elevated temperatures have been identified.

Approach

The hydride compressor is a form of "heat engine" based on the Carnot cycle. Its energy efficiency is about 50% of Carnot efficiency. Carnot efficiency is based on the temperature difference between the hot energy source and the cold heat sink. Efficiency plotted as a function of hot water (energy source) temperature appears in Figure 2.

Waste heat is usually available in the 80 to 90°C range. With a 30°C cooling water temperature, Carnot efficiency is from 13 to 16 percent and hydride compressor efficiency is from 4½ to 6½ percent. If waste heat is free, cycle economics can endure this level of efficiency.

By using a traditional form of heat energy, such as natural gas, cycle economics will benefit from an increase in hot water temperature. Using a heat transfer fluid from a gas fired heater at 130°C, Carnot efficiency is almost 25 percent, and hydride compressor efficiency increases to 15 percent. While 15 percent is about 1/2 that for a mechanical compressor, electricity is about 6 times costlier than natural gas, so the hydride compressor will enjoy a 67% lower energy cost. A simplified schematic of a natural gas powered hydride compressor appears in Figure 3.

An added benefit of higher temperature operation is a substantial reduction in the number of stages needed for a given compression ratio. Operation at 130°C in lieu of 90°C cuts by half the number of stages, with an associated reduction in system complexity, size and capital cost.

Unfortunately, when hydride alloys traditionally used for compressors are cycled at temperatures over 100°C, their performance can deteriorate through a process termed "disproportionation." In relatively few cycles, reversible hydrogen absorption capacity is lost, which would cause a hydride compressor to stop working.

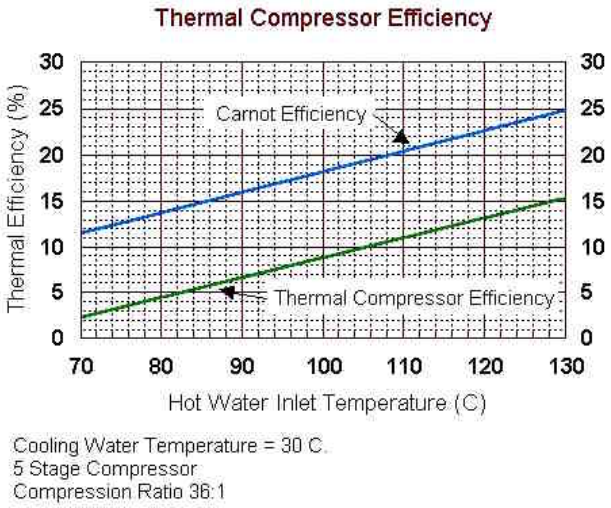

Figure 2. Increasing Hot Water Temperature Increases Compressor Efficiency

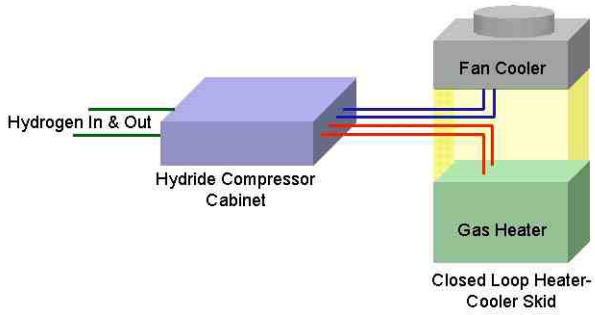

Figure 3. Simplified Schematic of a Natural Gas Powered Hydride Thermal Hydrogen Compressor

Ergenics pioneered the development of high temperature, disproportionation resistant alloys in 1995, while applying a hydride heat storage system to heat an automotive catalytic converter when the car was started. A hydride heater bed was placed in the exhaust pipe between the exhaust manifold and the catalytic converter. When activated, the heater bed temperature would increase from ambient to 400°C in a few seconds. The bed would be heated to over 500°C during normal driving. The alloy used in the heater bed had to endure these high temperatures for 25,000 start cycles and over the time it takes to travel 100,000 miles. Ergenics has extended its

original disproportionation-proof alloy development to the search for compressor alloys that can survive elevated temperatures.

Starting with the alloy family used in the catalytic converter heater, Ergenics modified alloy formulations to adjust the pressure-temperature performance. A correlation was developed between the formulations and pressure-temperature performance to permit the engineering of alloys appropriate for the different pressure stages in a hydride compressor. The alloys were then tested for resistance to disproportionation.

Results

During its original high temperature alloy development work in the mid 1990's, Ergenics developed a "Soak Test" procedure to screen alloy candidates. An alloy sample is placed within a test reactor vessel and is fully hydrided at high pressure. The test vessel is then held at high temperature for an extended duration to try to induce disproportionation. Pressure is monitored during the test. The temperature is high enough that a small amount of hydrogen is lost via diffusion through the reactor vessel wall. This diffusion loss is manifested by a small pressure decrease during the test. A pressure decrease in excess of the amount anticipated for diffusion may indicate alloy disproportionation.

The test reactor is subsequently weighed to rule out whether pressure loss not due to diffusion might be attributed to leakage. Finally, the sample is refilled with hydrogen to ascertain cycle-ability.

Figures 4 and 5 show the soak test results for two alloy candidates, one that experienced performance loss (Figure 4) and one with a new formulation that did not (Figure 5).

Conclusions

Increasing the heating fluid temperature of a hydride "thermal" hydrogen compressor from 80°C to 130°C more than doubles efficiency while reducing system complexity, size and cost. If natural gas is available as the heating source, energy costs can be three times lower than for an electric-motor-driven mechanical compressor.

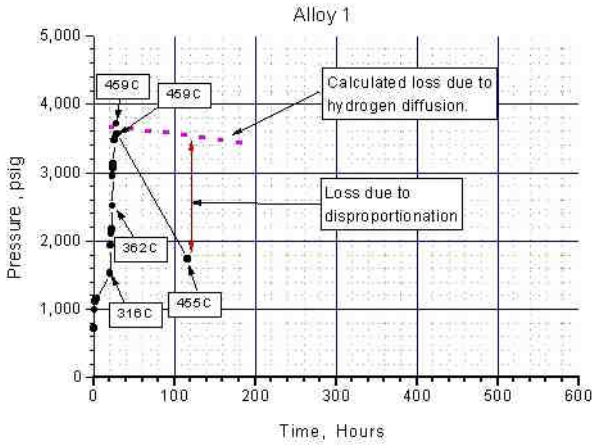

Figure 4. Soak Test Results Showing Alloy Disproportionation at Elevated Temperatures

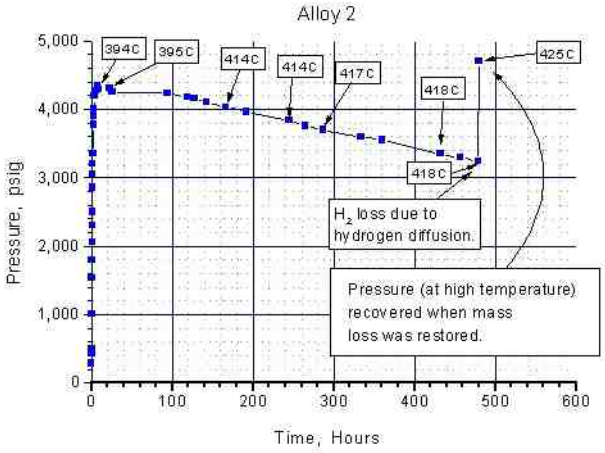

Figure 5. Soak Test Results for an Alloy that is Stable at Elevated Temperatures

Disproportionation-proof alloys that will survive elevated temperature operation have been engineered.

References

1. DaCosta, David H. 2000. "Advanced Thermal Hydrogen Compression." In Proceedings of the 2000 U.S. DOE Hydrogen Program Review, 720-727. San Ramon, CA: NREL/CP-570-28890.

2. Golben, M., DaCosta, D.H. 2001. "Advanced Thermal Hydrogen Compression." In Proceedings of the 2001 U.S. DOE Hydrogen Program Review, Baltimore, MD: NREL/CP-570-30535.

FY 2002 Publications/Presentations

1. D. DaCosta, M. Golben. "Disproportionation Resistant Alloy Development for Hydride Hydrogen Compression", Proceedings 2002 U.S. Department of Energy Hydrogen Program Annual Review Meeting, Golden, May 6-8, 2002, NREL.

2. D. DaCosta, M. Golben, D.C. Tragna. "Metal Hydride Thermal Hydrogen Compression", Proceedings 14th World Hydrogen Energy Conference, Montreal, June 9-13, 2002.

3. D. DaCosta, M. Golben. "Thermal Hydrogen Compression with Purification", International Energy Agency Hydrogen Implementing Agreement, Task 17 - Solid and Liquid State Hydrogen Storage Materials Workshop, Seattle, WA, February 21-22, 2002.

III.A.5 Development of a Compressed Hydrogen Gas Integrated Storage System for Fuel Cell Vehicles

Mr. John Wozniak (Primary Contact)
Johns Hopkins University Applied Physics Laboratory
11100 Johns Hopkins Road
Laurel, Maryland 20723-6099
(240) 228-5744, fax: (240) 228-5512, e-mail: john.wozniak@jhuapl.edu

DOE Technology Development Manager: Lucito Cataquiz
(202) 586-0729, fax: (202) 586-9811, e-mail: Lucito.Cataquiz@ee.doe.gov

Main Subcontractor: General Dynamics Armament & Technical Products (GDATP), Lincoln, Nebraska

Objectives

- Advance the technology elements required to develop a semi-conformal, Compressed Hydrogen Gas Integrated Storage System (CH2-ISS) for light-duty fuel cell vehicles (FCVs)
- Conduct engineering research to:
  - Develop materials and treatments to reduce hydrogen gas permeation through tank liners
  - Develop an optimized carbon fiber/epoxy resin tank overwrap
  - Determine alternative designs and materials for constructing the unifying elements of the integrated storage system

Approach

- Develop baseline CH2-ISS design consistent with notional FCV packaging and driving range requirements
- Develop tank liner surface treatments and measure hydrogen gas permeation
- Build and performance test all-carbon overwrap tanks with alternative toughened epoxy resin systems
- Explore with manufacturers alternative materials and means for low-cost production of the ISS outer shell and unitary gas control system
- Develop a roadmap identifying the steps needed to prototype the CH2-ISS and safety certify the container for FCV applications

Accomplishments

- Developed computer-aided drafting (CAD) models of alternative ways to construct the CH2-ISS
- Developed a process for surface treating the high density polyethylene (HDPE) tank liner to reduce hydrogen gas permeation
- Measured gas permeation and met allowable with acceptable margin
- Built a series of all-carbon overwrap hydrogen gas tanks with alternative toughened epoxy resin systems and conducted burst and gunfire tests
- Established an all-carbon overwrap design that passes gunfire test at the minimum factor of safety (2.25)

- Conducted a manufacturing trade study of alternative means and materials for fabricating the CH2-ISS outer protective shell
- Designed two alternative means for building the CH2-ISS unitary gas control unit

Future Directions

- Continue to develop liner materials and processing (metalization and surface coatings) to further reduce hydrogen gas permeation
- Optimize tank overwrap toughened resin system with respect to cost, minimizing impact on service temperature and tank manufacturability
- Conduct series of tests to quantity the performance of the CH2-ISS tank design
- Conduct flammability and impact tests on alternative CH2-ISS outer shell materials; select optimum for prototype build
- Detail design and prototype build the unitary gas control system

---

Introduction

FCVs are identified by the DOE, and virtually every major automaker, as a potential solution to problems of air quality and dependency on foreign fuel. Fuel cells produce electricity by combining hydrogen with oxygen from air to produce electrical power and give off only water vapor. The onboard storage of hydrogen fuel can consist of compressed hydrogen gas (cH_2) systems, cryogenic liquid hydrogen tanks or chemical or metal hydride storage systems. Another source of hydrogen is derived from gasoline, diesel, methane, or natural gas by using an onboard reformer. Of the many means of carrying hydrogen, cH_2 is one of the most attractive technologies because of fast refueling times, unlimited refueling cycles, ease of low temperature startup, superior long-term stability, and true zero vehicle emissions.

The storage of cH_2, however poses challenges in the areas of relatively low energy density, system cost, crashworthiness, and vehicle packaging. A solution to these challenges is offered by the Integrated Storage System (ISS) technology (U.S. Patent No. 6,257,360 issued July 2001) jointly developed by Johns Hopkins University Applied Physics Laboratory (JHU/APL) and General Dynamic Armaments and Technical Products (GDATP) (formerly Lincoln Composites). Under DOE Cooperative Agreement DE-FC36-01G011003 the ISS technology is being advanced to support development of a 5,000 pounds per square inch (psi) hydrogen gas service pressure, 5% or better gas mass fraction system that meets safety, vehicle packaging, and production cost objectives.

Technical Approach

ISS uses Type IV all-composite tanks constructed with a high-density polyethylene (HDPE) thermoplastic liner structurally overwrapped with carbon fiber and epoxy resin. The tanks are encapsulated within a high-strength outer shell unitizing the individual cylinders into a single container and providing protection from environmental exposure. Additional physical protection of the tanks is provided by urethane foam surrounding the tank dome region (location of highest stress concentration during impact). A unitized gas control module is incorporated into the ISS package and provides all necessary gas flow control and safety features. Figure 1 is a CAD image of the CH2-ISS design. The objective of this project is to advance the technologies needed to support development and safety certification of a CH2-ISS.

There are four specific tasks: (1) HDPE treatment and development of alternative tank liner materials for hydrogen gas permeation reduction; (2) enhancing epoxy resin toughness to improve the tank carbon fiber overwrap performance; (3) materials and process evaluation for manufacturing the ISS protective shell; and (4) engineering an optimized unitary gas control module. An additional task (5) is the formulation of a roadmap for prototyping and

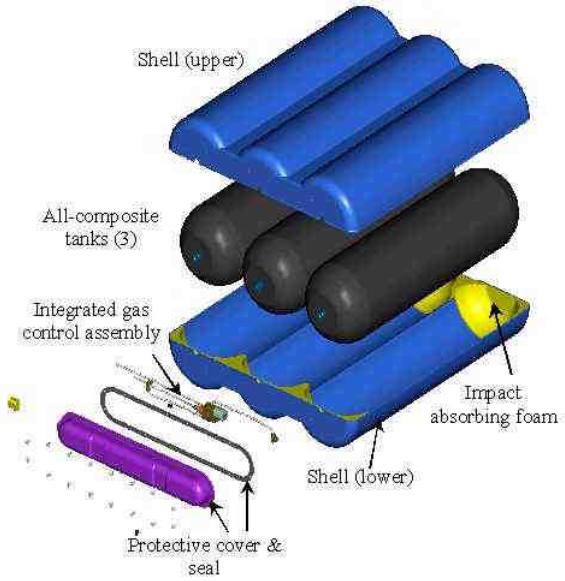

Figure 1. Assembly View of the CH2-ISS

Figure 2. High Density Polyethylene Liner

safety certifying the CH2-ISS for potential mass production.

Result

Task (1) ISS uses Type IV high-pressure gas storage tanks using a HDPE thermoplastic liner, (see Figure 2) overwrapped with carbon fiber and epoxy resin. The liner serves as a permeation barrier, mechanical interface to aluminum bosses, and a stable mandrel for the filament winding process. The main focus of the permeation task has been to quantify and control the hydrogen gas permeation rate through the HDPE. In FY02 a low-cost, proprietary surface treatment process was developed to reduce the hydrogen permeation. The tests were conducted on both the untreated and surface treated

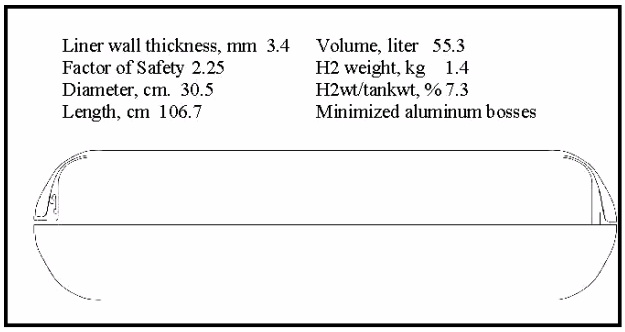

Figure 3. CH2-ISS Tank Preliminary Design

HDPE liners. Testing at 5,000 psi indicated a permeation rate of about 0.8 standard cubic centimeters per hour per liter (scc/hr/l) for the untreated HDPE and about 0.2 scc/hr/l for the treated. The current draft standard (e.g. ISO/DIS 15869) allows a permeation rate of 1.0 scc/hr/l. Additional work was done to develop a process for applying a coating to the surface of the HDPE liner. The permeation rate through the propriety surface coating has yet to be quantified.

Task (2) In FY02, a series of Type IV, all-carbon (T-700) tanks were designed, fabricated and performance tested. The objective was to develop the technology to construct small-diameter tanks for an operating pressure of 5,000 psi that would pass the critical gunfire test at the minimum allowable burst factor of safety (FOS) of 2.25. The overwrap technology investigation involved using winding patterns that maximize interspersion between helical and hoop layers. In addition, series of resin formulations were evaluated to assess their impact on tank gunfire performance. The brittle nature of structural epoxy resins is suspected of contributing to localized delaminating of the overwrap, resulting in catastrophic tank rupture under gunfire testing. Two toughening agents, polyether sulphone and amine-terminated butadiene acrylonitrile, formulated into GDATP's standard resin, in combination with the enhanced winding pattern, led to successful gunfire tests for an all-carbon fiber, 2.25 FOS tank construction. Based on this work, a preliminary tank design was developed (see Figure 3) for the CH2-ISS application.

Task (3) The ISS uses a high-strength, lightweight shell/cover in conjunction with flexible

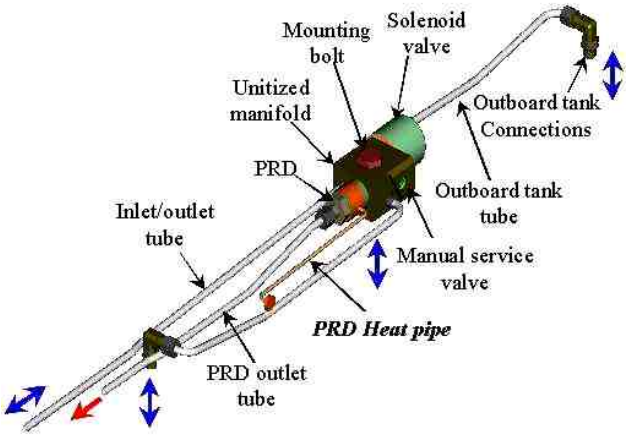

Figure 4. Unitary Gas Control Module Design

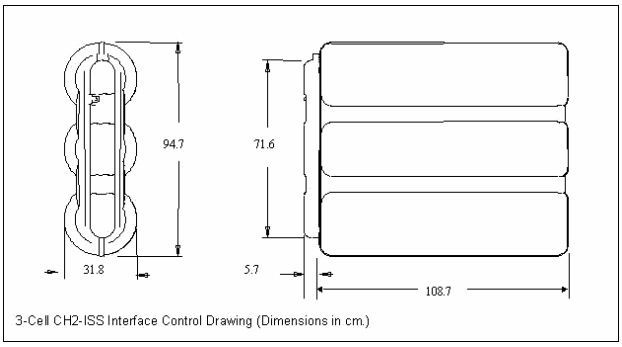

Figure 5. Estimated CH2-ISS Characteristics

CH2-ISS Performance Estimate

Total Empty Weight	73 Kg
Service Perssure	340 bar
Total Hydrogen Capacity	4.2 Kg
Gas/Container Mass Fraction	5.7%
External Volume	266 liter
Internal Gas Volume	166 liter

urethane impact-absorbing foam to encapsulate and protect the individual tanks into a single unitized container. In FY02, the shell technology work focused on identifying a manufacturing process and materials that result in the optimum combination of component strength, toughness, weight, tooling and part cost, trimming and assembly cost, and chemical resistance. Two Pro/ENGINEER CAD designs were developed to support an evaluation of alternative means for high-volume production of the CH2-ISS outer shell and gas control cover. Working with industry, a trade study was performed that examined a number of materials/processes and resulted in a downselect of two alternatives for further investigation - fabrication via (1) compression molding with Sheet Molding Compound (SMC) and (2) preform fabrication using Directed Fiber Preform combined with Structural Reaction Injection Molding.

Task (4) The ISS is assembled as a single, inseparable container, requiring only one manual service valve, one solenoid, and one thermally activated pressure relief device, all incorporated into a gas control module (see Figure 4). The added cost and complexity of redundant components when using multiple, separable cH_2 tanks is avoided by this approach. The gas control system is safeguarded from physical damage with impact absorbing foam within a high-strength protective cover. In FY02, two alternative Pro/ENGINEER CAD notional models were developed focused on a fully unitize affordable gas control module. The two designs are variants of JHU/APL's patented design "Compressed Gas Manifold" (U.S. patent # 6,321,775, dated November 27, 2001).

Task (5) The technology tasks completed in FY02 and the work needed to continue development was assembled into an overall project roadmap. The roadmap identifies out-year tasks needed to fully develop and safety-certify a CH2-ISS for potential mass production. The roadmap identifies important studies and/or subsystem developments and tests that minimize the risk of undertaking the full CH2-ISS development.

Conclusions

Substantial progress has been made in developing a high energy density, near-rectangular, safety-certified and affordable container for the onboard storage of compressed hydrogen gas for use in FCVs. The work has focused on the Integrated Storage System design, hydrogen tank permeation

reduction and overwrap development, and a trade-off study of protective shell and gas control manufacturing options. The information developed has been formulated into a preliminary CH2-ISS design with performance estimated (see Figure 5). Continued component development and critical tests are proposed for FY03 which will enable future full development of a CH2-ISS and its safety certification.

FY 2002 Publications/Presentations

1. Development of a Compressed Hydrogen Gas Integrated Storage System (CH2-ISS) for Fuel Cell Vehicles- Midterm Report, ADS-02-014, April 2002

2. Development of a Compressed Hydrogen Gas Integrated Storage System (CH2-ISS) for Fuel Cell Vehicles- Peer Review Presentation CD/ ROM Report, June 19, 2002

Special Recognition & Awards/Patent Issued

1. U.S. patent No. 6,418,962 entitled "Low Cost Compressed Gas Fuel Storage System", awarded July 16, 2002

III.A.6 Low Permeation Liner for Hydrogen Gas Storage Tanks

Paul A. Lessing (Primary Contact)
Idaho National Engineering & Environmental Laboratory (INEEL)
P.O. Box 1625
Idaho Falls, ID, 83415-2218
(208) 526-8776, fax: (208) 526-0690, e-mail: pal2@inel.gov

INEEL Technical Advisor: Raymond P. Anderson
(208) 526-1623, fax: (208) 526-9822, e-mail: anderp@inel.gov

DOE Technology Development Manager: Lucito Cataquiz
(202) 586-0729, fax: (202) 586-9811, e-mail: Lucito.Cataquiz@ee.doe.gov

Main Subcontractor: University of California at Los Angelos, Los Angeles, CA

Objective

- Develop a polymer liner that greatly limits hydrogen losses from commercial, light-weight, composite, high-pressure hydrogen tanks.

Approach

- Select and fabricate polymeric materials with the necessary electron and proton conducting properties
- Fabricate a "bench-top" model of a tri-layer, electrochemically-active protection device that greatly reduces hydrogen permeation through polymer "substrates"
- Demonstrate the successful functioning of the bench-top device
- Demonstrate a successful prototype of an active, electrochemical hydrogen barrier system within a high-pressure, polymer-lined, composite hydrogen storage tank

Accomplishments

- Invented a unique concept for an electrochemically active, tri-layer device to prevent hydrogen permeation through a polymeric tank liner
- Negotiated a cooperative agreement with a high-pressure hydrogen tank manufacturer
- Negotiated a statement of work for a major subcontract with a university that is actively engaged in research on conductive polymer compositions

Future Directions

- Select the proper materials of construction
- Fabricate tri-layer coatings having the necessary structural and electrochemical properties
- Experimentally verify that operation of the barrier provides hydrogenation/permeation protection

Introduction

State-of-the-art high-pressure gas storage tanks consist of an inner liner, made from a polymer such as cross-linked polyethylene or nylon, overlaid with a continuous graphite fiber/epoxy reinforcement layer. These tanks have successfully stored high-pressure methane gas. It is desired to extend the application of this type of tank to high-pressure hydrogen. However, hydrogen has a significantly higher permeability rate through these polymer liners than does methane. Permeation leads to a gradual loss of hydrogen pressure, and the hydrogen is thought to damage and weaken the reinforcement layer.

This project was recently begun to develop a hydrogen diffusion barrier that can be applied to the interior of the polymer liner. To be effective, the barrier must have the following attributes: (1) low permeability of hydrogen, (2) good adherence to the polymer liner, (3) stiffness (modulus) of the coating that matches the underlying polymer to avoid cracking when the tank is pressurized, (4) an application method that allows for coating inside a tank with a narrow neck and results in hermetic (gas-tight) coatings that are devoid of pin-holes, and (5) a material and coating method that does not appreciably add to the overall cost or weight of the tank.

Approach

An electrochemically "active" hydrogen barrier, fabricated from polymers, will be developed. A schematic of this barrier is shown in Figure 1.

The development plan includes the following:

- The barrier is to be constructed of three layers of polymers consisting of a proton-conducting electrolyte (electronic insulator) sandwiched between electronically conductive polymer electrodes. Candidate polymer compositions will be selected based upon existing knowledge. If this knowledge is not sufficient, new or modified compositions will be developed. Appropriate catalyst materials will be added at the electrolyte/electrode interfaces.

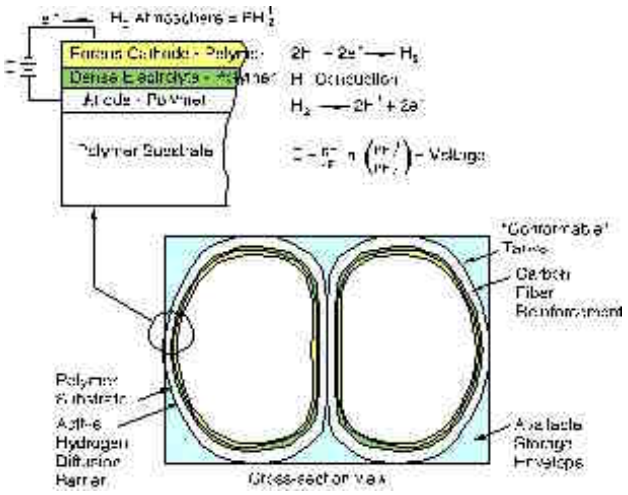

Figure 1. Schematic Showing Tri-layer Hydrogen Barrier Concept

- The methods to manufacture the layers will be adapted from existing techniques or developed during the project. This could include dip coating or spraying of monomers followed by polymerization. Other possibilities will be explored and successful manufacturing technologies will be developed.
- The device is designed as a galvanic-type device that functions to prevent hydrogen permeation through application of a small direct current (dc) voltage using small currents. Methods to provide attachment of the dc voltage will be developed.

The hydrogen partial pressure established by the voltage is extremely low at the underlying polymer interface. The hydrogen partial pressure can be calculated using the Nernst equation (relates the voltage of a cell to its thermodynamic properties), as shown in Figure 1. An appropriate level of voltage will be calculated and experimentally verified.

Results

This project has only recently begun, having been funded late in FY 2002. A patent application was drafted and submitted to the U.S. Patent Office. The application covers the basic concept, designs, and possible manufacturing methods. An initial literature search was conducted for the polymeric

materials that are intended to comprise the 3 layers of the electrochemically active coating.

A Cooperative Research and Development Agreement was negotiated between an industrial partner that manufacturers composite, high-pressure, INEEL (Bechtel BWXT Idaho). Additionally, a statement of work was negotiated with a university subcontractor (University of California at Los Angeles).

Conclusions

The project is just beginning, so conclusions are not yet available.

Patent

1. U.S. Patent Application: Paul A. Lessing, "Polymeric Hydrogen Diffusion Barrier, High-Pressure Storage Tank so Equipped, Method of Fabricating a Storage Tank, and Method of Preventing Hydrogen Diffusion", September, 2002.

III.B Carbon Materials

III.B.1 Hydrogen Storage in Carbon Single-Wall Nanotubes

A.C. Dillon, K.E.H. Gilbert, P.A. Parilla, J.L. Alleman, G.L. Hornyak, K.M. Jones, and M.J. Heben (Primary Contact)
National Renewable Energy Laboratory
1617 Cole Blvd.
Golden, CO 80401
(303) 384-6641, fax: (303) 384-6655, e-mail: michael_heben@nrel.gov

DOE Technology Development Manager: JoAnn Milliken
(202) 586-2480, fax: (202) 586-9811, e-mail: JoAnn.Milliken@ee.doe.gov

Objectives

- Determine the extent to which carbon single-wall nanotubes (SWNTs) can reversibly store hydrogen.
- Discover the mechanism of hydrogen storage in SWNTs.
- Develop simple, reproducible, and potentially scalable processes for producing SWNTs.

Approach

- Decouple the two steps in the ultrasonication process used to activate SWNTs for hydrogen storage, i.e., cutting and metal hydride introduction, to improve process control and to determine the relative contribution of each to the hydrogen storage capacity.
- Develop new methods for cutting SWNTs that avoid the introduction of the metal alloy and develop separate processes to introduce metal hydrides to the SWNTs in a controlled manner.
- Develop techniques to determine and measure the key characteristics of SWNTs that yield high hydrogen storage capacities.

Accomplishments

- Developed two different dry cutting methods for cutting SWNTs, which are in the process of being patented. Neither process involves sonication and therefore, cut samples that are free from metals can be produced.
- Improved control over pulsed laser synthesis of SWNTs, producing samples with hydrogen storage capacities of 4 weight percent (wt%).
- Developed a Raman analysis technique that can be used to characterize the purity and defects in SWNT materials. Raman analysis can also be used to determine the degree of cutting in bulk SWNT samples.

Future Directions

- Correlate the degree of SWNT cutting with hydrogen storage capacities in order to understand the hydrogen adsorption mechanism more completely.
- Probe possible adsorption pathways in order to explain why only specific nanotubes appear to be optimal for hydrogen storage applications.

- Develop a method for the controlled incorporation of metal catalyst particles of discrete sizes and in specific locations so that SWNT hydrogen storage capacities may be reproducibly optimized.
- Optimize the purity, production rate, diameter, and chirality of the laser-generated SWNT samples to reliably achieve 6-7 wt% hydrogen storage.

Introduction

Hydrogen storage technology must be significantly advanced in performance and cost effectiveness if the U.S. is to establish a hydrogen-based transportation system. Gas-on-solid adsorption is an inherently safe and potentially high energy density hydrogen storage method that could prove to be more energy efficient than other hydrogen storage methods under evaluation, such as chemical or metal hydrides and compressed gas storage. Carbon single-wall nanotubes (SWNTs) and other nanostrucured carbon materials are being evaluated for this application. The long-term goal is to scale up production of optimized SWNT materials to enable efficient adsorption of hydrogen at ambient temperature and pressure and at system energy densities specified by the DOE Hydrogen, Fuel Cells, and Infrastructure Technologies Program (6.5 wt% and 62 kg/m^3).

Approach

Currently, the high-power ultrasonication method used to activate SWNTs for hydrogen storage simultaneously cuts purified SWNTs into shorter segments and introduces a metal hydride alloy ($TiAl_{0.1}V_{0.04}$) into the SWNTs. However, the sonication process does not provide for detailed or independent control of either cutting or metal incorporation. Differing degrees of cutting, amounts of metal, and metal particle sizes are found in processed samples even when identical sonication parameters (sonication time, sonication power, acid concentration, hydrodynamics, etc.) are employed. This lack of process control leads to variability in the performance of the final SWNT materials, which show hydrogen storage capacities on the tube fraction ranging from 0 to 8 wt%.

This research project is focusing on increasing control of the process used to activate the SWNTs for hydrogen, as well as developing reliable methods to determine and control the characteristics necessary for optimizing the hydrogen storage capacity of SWNTs.

Results

Control of Laser-Production of Tailored SWNT Size and Type Distributions

Currently, SWNT materials are synthesized using a laser vaporization process. Samples with hydrogen storage capacities of ~7 wt% have been produced in a free running Nd:YAG laser (1064 nanometer [nm]) synthesis. Initial samples made with the Alexandrite laser (755 nm) showed less than 1 wt% storage. Multi-colored Raman measurements show that the Alexandrite laser was producing SWNTs that differ in diameter and chirality from those produced by the Nd:YAG laser. Past research on laser-generated SWNTs established that as the laser peak pulse power increases, SWNT diameter distributions shift to smaller diameters and SWNT chirality distributions result in semiconducting (rather than metallic) material properties. Using these two findings together, researchers have produced nanotube diameter and type distributions with the Alexandrite laser that are nearly identical to the Nd:YAG laser, as illustrated in Figure 1. Subsequent syntheses with the same peak power showed that the production of this SWNT size and type distribution is highly reproducible. With better control over SWNT production, samples with hydrogen storage capacities of 4 wt% have been fabricated with the Alexandrite laser.

Poor Repeatability of High Hydrogen Adsorption Capacities

The hydride alloy ($TiAl_{0.1}V_{0.04}$) accounts for a portion of the hydrogen storage capacity of the alloy/nanotube composite material that is formed in the ultrasonication process. Figure 2 displays a plot of hydrogen storage capacity versus alloy metal content for numerous purified SWNT samples that were treated with the ultrasonic probe process. About one-

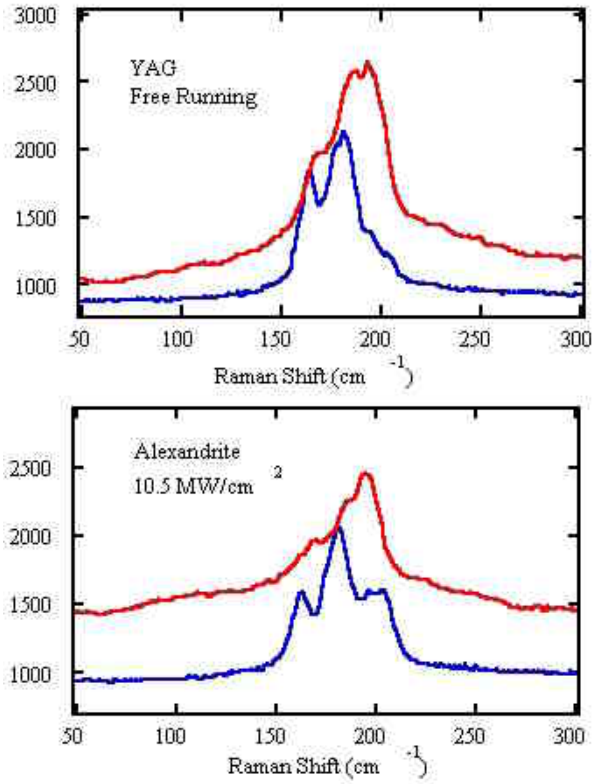

Figure 1. Raman spectra in the radial breathing mode region for a) a Nd:YAG-produced sample with a H_2 adsorption capacity of ~7 wt%, and b) a sample produced with the Alexandrite laser operating with a 200 ns pulse width at a peak power of 10.5 MW/cm^2. The red curves (highest curve on each figure) are for Raman excitation at 632.8 nm and show the SWNT size distribution for excited metallic and semiconducting tubes. The blue curves (lowest curve on each figure) were obtained at 488 nm and show predominantly semiconducting tubes.

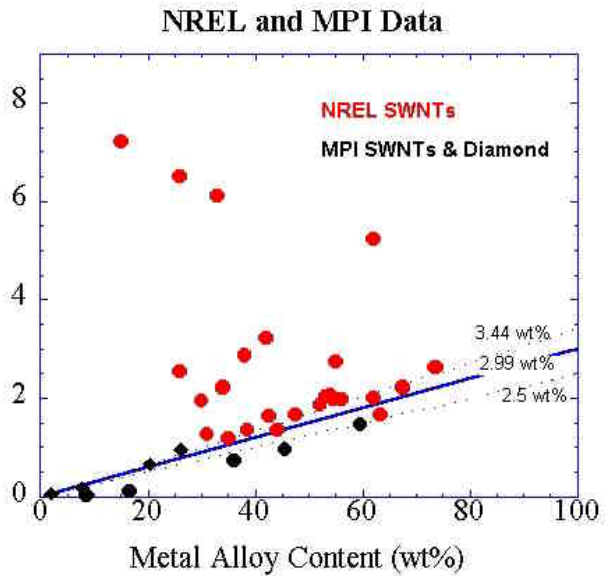

Figure 2. Plot of total sample hydrogen wt% content versus metal alloy content for SWNT samples following high energy sonication in HNO_3 with an ultrasonic probe. Lines are drawn as a guide to the eye to show the anticipated hydrogen storage based on metal alloy content alone.

half of the samples show hydrogen adsorption capacities that are too high to be explained by the presence of the alloy alone, indicating that these SWNTs have been activated for hydrogen storage. Assuming the hydrogen storage capacity of the $TiAl_{0.1}V_{0.04}$ alloy is 2.99 wt%, the SWNTs have hydrogen storage capacities between 0-8 wt%, with ~8 wt% being a maximum value, independent of the amount of alloy present. Possible explanations for the observed variability include (1) the extent of destruction to the SWNTs caused by the ultrasonic cutting process and (2) the size of the metal alloy particles incorporated.

Development of Controlled Cutting Method Without Metal Hydride Incorporation

To reduce the variability in the performance of the activated SWNTs, research has focused on decoupling the cutting and metal introduction processes. Controlled cutting of carbon single-wall nanotubes has been achieved via a new cutting method that does not employ ultrasonication. Transmission electron microscopy analyses and Raman spectroscopy show that significant cutting occurs without significant damage to the SWNTs. Figure 3 compares hydrogen temperature programmed desorption spectra of a purified SWNT sample and a SWNT sample cut with the new method. The spectrum of the cut sample shows an additional hydrogen desorption peak at ~65ºC, indicating the presence of hydrogen that is stabilized at ambient temperatures. This is the first time high-temperature adsorbed hydrogen has been observed

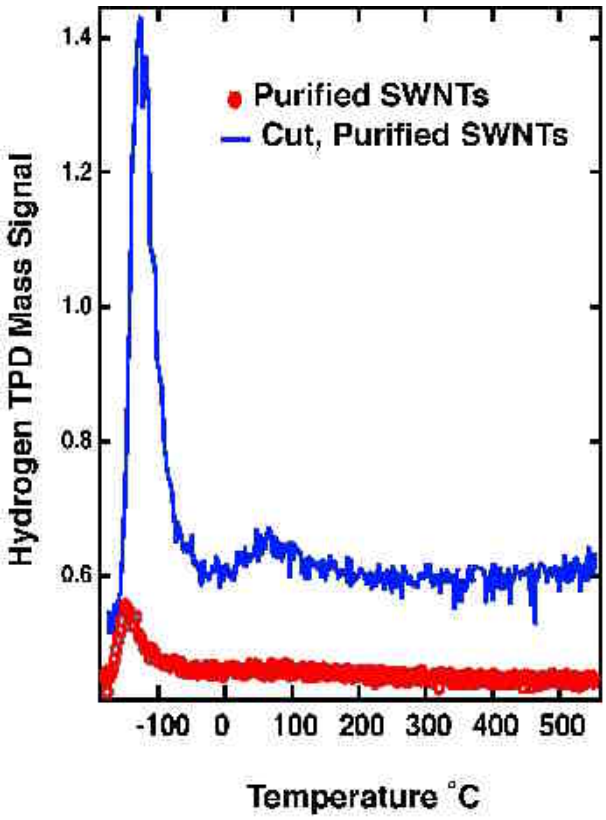

Figure 3. Temperature programmed desorption spectroscopy of purified SWNT materials before and after dry cutting process. The signal at 65 ºC for the cut sample is similar to the one we reported previously for arc-discharge SWNTs, but it occurs at a temperature which is ~65 degrees higher.

on laser-generated materials without using the sonication activation process.

A Simple Method to Determine Degree of SWNT Cutting

In order to establish if a relationship exists between cutting and hydrogen storage capacities, a Raman spectroscopy technique was developed to quantify the degree of cutting obtained in macroscopic SWNT samples. Using an analysis of the SWNT Raman mode at 1350 cm^{-1}, labeled the nanotube D-band, and the mode at 1593 cm^{-1}, or nanotube G-band, the degree of cutting can be tracked. The D-band increases when the nanotubes are cut and new defects are introduced. An increase of ~25% is observed for the D-band intensity in the

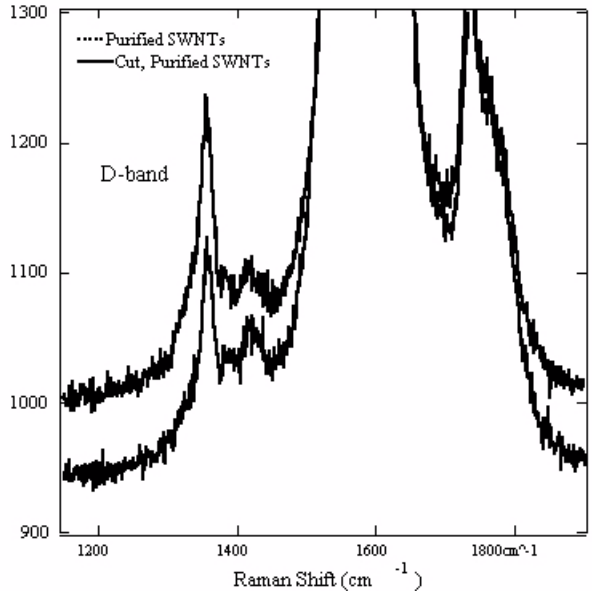

Figure 4. Raman spectra at 488 nm for a purified and purified/cut sample. The spectra are normalized to the G-band intensity at ~1593 cm^{-1}, which is off-scale. The D-band intensity is enhanced relative to the G-band intensity in the cut sample.

spectrum of the cut SWNTs in Figure 4. The SWNT G-band feature serves as a useful spectral feature for normalization because it does not change in intensity with cutting or the introduction of new defects. Figure 5 shows that the D/G ratio is nearly the same for three samples before and after identical cutting procedures, suggesting that the D/G ratio is correlated with the degree of cutting.

Conclusions

- Obtaining activated SWNT hydrogen storage materials with highly reproducible adsorption capacities has not yet been achieved. One reason may be that hydrogen storage is only optimized for a very specific and narrow distribution of SWNTs of distinct types and diameters.
- Laser synthesis conditions that reproducibly produce SWNTs with size and type distributions previously found to have optimal hydrogen storage capacities of ~7 wt% have been established.

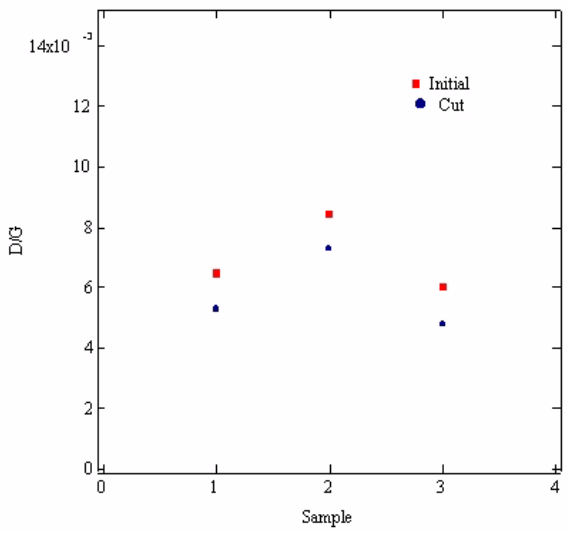

Figure 5. The ratio of the D-band intensity to the G-band intensity for a few samples before and after cutting. The D/G intensity ratio increases by a fixed amount after the same cutting procedures were applied.

- A new controlled dry cutting method that non-destructively cuts nanotubes without incorporating a metal hydride alloy has been developed.
- A new Raman spectroscopy-based technique that promises to allow the extent of SWNT cutting to be quantified has been developed.

FY 2002 Publications/Presentations

1. Dillon, A.C.; Gilbert, K.E.H.; Parilla, P.A.; Alleman, J.L.; Gennett, T.; Grigorian, L.; Jones, K.M.; Heben, M.J. "Hydrogen Storage in Single-Wall Carbon Nanotubes." In Proceedings of the 14th World Hydrogen Energy Conference Montreal, Quebec, Canada, June 2002.

2. Hornyak, G.L.; Grigorian, L.; Dillon, A.C.; Parilla, P.A.; Jones, K.M.; Heben, M.J. "A Temperature Window for Chemical Vapor Decomposition Growth of Single-Wall Carbon Nanotubes." J.Phys. Chem B 2002, 106, 2821-2825.

3. Dillon, A.C.; Parilla, P.A.; Gennett, T.; Alleman, J.L.; Jones, K.M.; Heben, M.J. "A Narrow and Defect-activated Raman D-Band in Pure Bulk Carbon Single-wall Nanotubes." Submitted to Phys. Rev. Lett.

4. Grigorian, L.; Hornyak, G.L.; Dillon, A.C.; Parilla, P.A.; Heben, M.J. "Synthesis of All Zig-Zag Single-Wall Carbon Nanotubes by CVD." Manuscript in preparation.

5. Maness, P.-C.; Smolinski, S.; Dillon, A.C.; Heben, M.J.; Weaver, P.F. "Characterization of the Oxygen Tolerance of a Hydrogenase Linked to a Carbon Monoxide Oxidation Pathway in Rubrivivax gelatinosus." To appear in Appl. Env. Microbiology.

Special Recognitions & Awards/Patents Issued

1. Grigorian, L.; Hornyak, G.L.; Dillon, A.C.; Heben, M.J. "Continuous Growth of SWNTs by CVD."

2. Dillon, A.C.; Parilla, P.A.; Heben, M.J. "Bulk Cutting of SWNTs." In preparation.

III.B.2 Doped Carbon Nanotubes for Hydrogen Storage

Ragaiy Zidan (Primary Contact)
Savannah River Technology Center
773-41A, Savannah River Site
Aiken, South Carolina
(803) 725-1726, fax: (803) 725-4129, e-mail: ragaiy.zidan@srs.gov

DOE Technology Development Manager: JoAnn Milliken
(202) 586-2480, fax: (202) 586-9811, e-mail: JoAnn.Milliken@ee.doe.gov

Objectives

- Develop reversible high-capacity hydrogen storage material with the following properties:
  - Hydrogen capacity greater than 6 weight %
  - Favorable thermodynamic and kinetics suitable for transportation applications
  - Stable with hydriding/dehydriding cycling
  - Resistant to trace contaminates

Approach

- Create a weak covalent bond between hydrogen and carbon by doping carbon nanotubes with metals to manipulate the electronic structure
- Produce consistent size metal dopants and structures of carbon nanotubes
- Control the type and size of the tubes and clusters inside the tubes
- Tune the material for hydrogen sorption to occur at desired temperatures and pressures
- Conduct thermodynamic and energetic characterization on hydrogen sorption
- Conduct spectroscopic characterization and elemental analysis to guide the effort

Accomplishments

- Developed Dopant Encapsulation, a novel method for producing metal doped carbon nanotubes with controlled size and structures (patent is applied for), which allows gram quantities of doped nanotubes with high purity to be produced
- Produced samples with different dopants, alloyed dopants
- Preliminary hydriding and dehydriding of samples showed hydrogen uptake and release of about 1.0 by weight % (more than expected from physisorption)
- Preliminary testing of cycling of hydrogen uptake and release showed consistent uptake and release over 10 cycles

Future Directions

- Continue producing nanotubes with different dopants and configurations using Dopant Encapsulation method
- Tune structure and control amount of dopants to optimize hydrogen binding energy (via achieving dihydrogen bonding)
- Conduct thermodynamic characterization of hydrogen uptake and release

- Utilize different spectroscopic methods (e.g. scanning electron microscopy [SEM], transmission electron microscopy [TEM], energy dispersive spectroscopy [EDS], etc.) to identify the type and size of nanotubes and clusters of dopants that result in a reversible high hydrogen capacity
- Tune conditions that result in a high yield of material possessing favorable characteristics such as storage capacity greater than 6 weight % hydrogen
- Perform cycling tests on material and investigate the effect of contaminants on hydrogen sorption
- Coordinate research and development effort with other DOE Laboratories and organizations working on carbon for hydrogen storage

---

Introduction

A major obstacle to a transition to a hydrogen economy has been the absence of a practical means for hydrogen storage. The goal of researchers has been to develop a high-density hydrogen storage system that can release hydrogen at temperatures lower than 100°C. It has been recognized that developing a suitable solid-state hydrogen storage material will be ideal for engineering a practical storage system. Carbon nanotubes represent a new direction for solid hydrogen storage, especially if these materials can be altered to store large amounts of hydrogen at room temperature. Widespread research activity into the properties and applications of the nanometer scale cylindrical carbon tubes has been reported [1-3], with much focus on the use of carbon nanotubes for hydrogen storage [4-8].

Simple mechanisms for hydrogen uptake and release involving physisorption and/or chemisorption cannot account for the unusual sorption of hydrogen by carbon nanotubes. In some cases, however, the unique nanotube structure and configurations could give rise to polarization and condensation of hydrogen inside the tubes. The research presented here is focused on modifying carbon nanotubes in an attempt to enhance and tune their hydrogen storage capabilities using metal dopants. The objective of this research has been to introduce transition metals and/or metal clusters inside the tubes that allow for hydrogen uptake and release. Establishing a relatively weak nanotube-hydrogen bond (not as weak as physisorption bond) should allow hydriding/ dehydriding to occur at mild conditions of temperature and pressure. Producing consistent structures is also necessary for reliable results and reproducible data.

Approach

Introducing nano-particles (dopants) to carbon nanotubes to create a weak covalent bond has been the general approach of this work. The goal has been to establish an interaction between hydrogen and carbon nanotubes based on a weak covalent bond where the electron donation from the (σ) orbital of hydrogen to the doped tubes weakens but does not break the hydrogen-hydrogen bond [9,10]. The unique strategy of this research is not just to dope carbon nanotubes with metals, but also to control the type and size of the tubes and the encapsulated metal clusters. This allows the electron density to be manipulated and the material to be tuned for hydrogen sorption at desired temperatures and pressures. The process is intended to take advantage of the nano scale properties of the system. This research is also aimed at producing gram quantities of consistent structures and sizes. Scanning and transmission electron microscopy are used to investigate configuration of tubes and dopants and to guide the development of the materials. Thermogravimetric and thermovolumetric analyzers are used to measure and quantify hydrogen uptake and release.

Results

The synthesis of different doped carbon nanotubes has been achieved using the Dopant Encapsulation method we developed. This method was used to dope the tubes not only with metals, but also with alloyed clusters of different metals. The Dopant Encapsulation method was utilized to produce large quantities of metal doped carbon nanotubes of consistent structure (see Figures 1 and 2). A thermogravimetric system capable of operating at a wide range of temperatures was used to measure

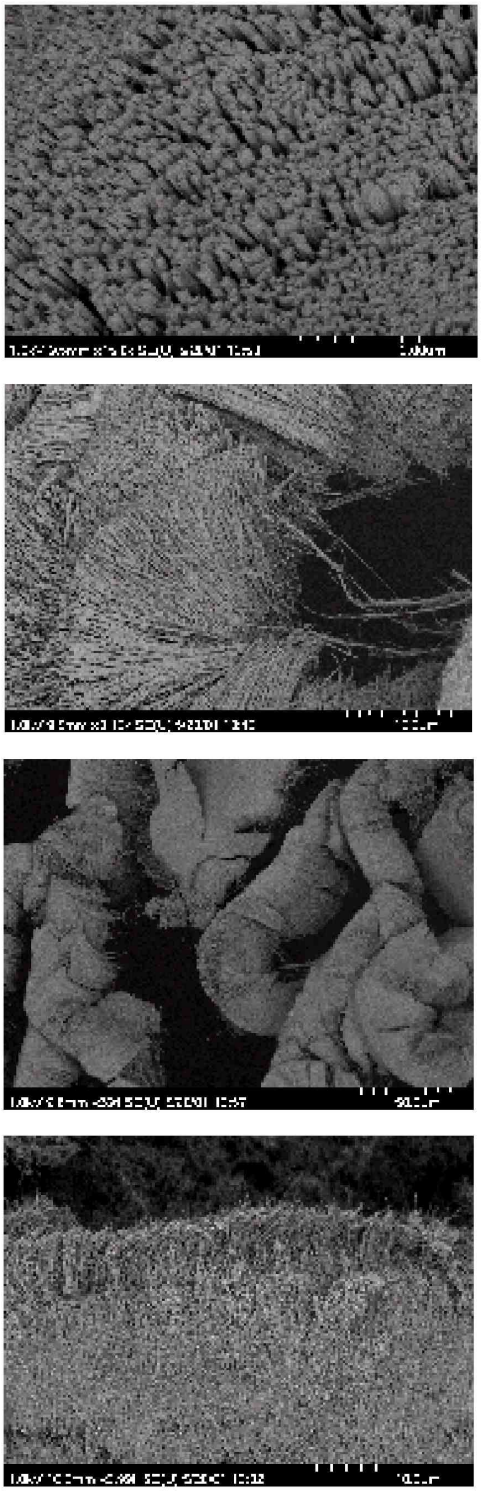

Figure 1. Shows SEM Images of Large Quantities of Nanotubes Doped with Different Metals (Gram Quantity Samples were Produced).

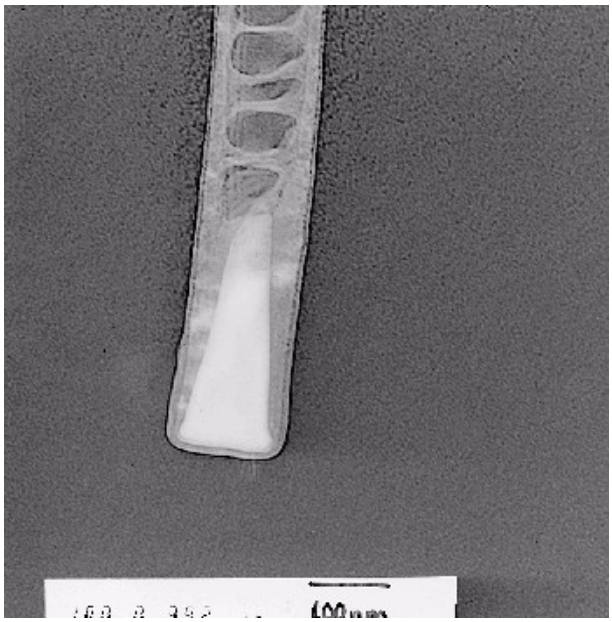

Figure 2. Shows the Tip of a Nanotube with Encapsulated Metal Particle

hydrogen uptake and release. The system was enclosed in an inert atmosphere glove box to avoid contamination from water and reactive gases. Preliminary results showed consistent hydrogen uptake and release of 1% by weight. The sample was cycled 10 times without deterioration of hydrogen capacity.

Conclusions

The immediate objective of this work was to produce large quantities of carbon nanotubes with consistent structures that can be modified as needed. Therefore, a novel method for producing and controlling configuration and structure of carbon nanotubes was developed and demonstrated. The Dopant Encapsulation method enables the production of doped carbon nanotubes with transition metals and alloys that can give rise to weak covalent bonds similar to dihydrogen. The encapsulation of a metal at the tip of the tube eliminates the need for opening or cutting the tube. Preliminary results, using a thermogravimetric analyzer, showed hydrogen uptake and release of 1% by weight.

Acknowledgement

This research work was done in collaboration with Dr. Apparao M. Rao, Department of Physics, Clemson University, South Carolina.

References

1. S. Iijima, Nature, 354 (1991) 56

2. S. Iijima and T. Ichihashi Nature, 363 (1993) 603

3. D. S. Bethune, C.H. Kiang, M. S. de Vries, G. Gorman, R. Savoy, J. Vazquez and R. Beyers, Nature, 363 (1993) 605

4. A.C. Dillon, K. M. Jones, T. A. Bekkedahl, C.H. Kiang, D. S. Bethune and M.J. Heben Nature, 386 (1997) 377

5. Y. Ye, C.C. Ahn, C. Witham, B. Fultz, J. Liu, A.G. Rinzler, D. Colbert, K.A. Smith, and R.E. Smalley, Applied Physics Letters 74, 2307 (1999)

6. C. Liu, Y.Y.Fan., M. Liu, H.T. Cong, H.M. Cheng, and M. Dresselhaus, Science 286, 1127 (1999)

7. P.,Chen, X. Wu, J. Lin, and K.L. Tan, Science 285, 91 (1999)

8. R. Chahine and P. Bénard, IEA Task 12: Metal Hydrides and Carbon for Hydrogen Storage (2001)

9. G.J Kubas, R.R. Ryan B. I. Swanson, P.J. Vergamini, and .J. Wasserman, J. Am. Chem. Soc. 106, 451 (1984)

10. G.J. Kubas, Acc. Chem. Res. 21, 120 (1988)

III.B.3 Hydrogen Storage in Metal-modified Single-Walled Carbon Nanotubes

Channing Ahn (Primary Contact)
California Institute of Technology
1200 E. California Blvd, MS 138-78
Pasadena, CA 91125
(626) 395-2174, fax: (626) 795-6132, e-mail: cca@caltech.edu

DOE Technology Development Manager: JoAnn Milliken
(202) 586-2480, fax: (202) 586-9811, e-mail: JoAnn.Milliken@ee.doe.gov

Objectives

- Alter adsorption enthalpy of hydrogen on single walled nanotubes (SWNTs) by use of a potassium intercalant.
- Increase number of adsorption sites in SWNTs by increasing the surface area through the use of intercalant.
- Improve the hydrogen storage capacity of SWNTs.

Approach

- Investigate potassium intercalation synthesis procedures and measure sorption behavior of flaked graphites.
- Apply synthesis "recipes" to SWNT intercalation.
- Use Sieverts apparatus to measure hydrogen sorption isotherms.

Accomplishments

- Optimized synthesis procedures for KC_{24} and KC_{48} intercalated graphites.
- Performed neutron powder diffraction of as-prepared and deuterided intercalated graphites.
- Showed for the first time that K-intercalated graphites undergo 5% lattice expansion beyond the 5.35 Å intercalated layer spacing when deuterided, indicating slit-pore sorption behavior for this system.
- Determined preliminary structure verifying 8.49Å a-b spacing for potassium dodecal structure within graphene planes.Å

Future Directions

- Purification and intercalation of SWNTs.
- Structural characterization of purified and intercalated SWNTs.
- Volumetric hydrogen adsorption measurements of SWNTs.

Introduction

Hydrogen physisorption on pure carbon materials will not meet DOE targets, owing to the thermodynamic enthalpy of hydrogen adsorption on carbon. For instance, our previous work on SWNTs yielded a value of 38 milli-electron volt [1] or 3.6 kilojoule per mole (kJ/mole), values consistent with adsorption on a graphene surface [2]. Our work for this project has concentrated on the use of potassium to increase the adsorption enthalpy in a way that will allow us to reduce the high pressures, and increase the low temperatures presently required for high hydrogen gravimetric densities. An issue of nearly equal importance is the number of sites for hydrogen sorption, since this sets the ultimate hydrogen storage capacity.

Potassium-intercalated graphite can readily adsorb and desorb hydrogen at ~1 weight % [3]. The level is much higher than can be attained in pure graphite, due to a larger thermodynamic enthalpy of absorption. Increased enthalpy allows hydrogen sorption at higher temperatures. Potassium also has beneficial effects that enable the design of a new material that include: a) Increased absorption enthalpy in potassium-intercalated graphite compared to pure graphite reduces the pressure and increases the temperature required for a given fractional coverage of hydrogen absorption. We expect the same effects in potassium-intercalated SWNTs and; b) As an intercalant, potassium separates c-axis planes in graphite. Potassium also separates the individual tubes of SWNTs ropes producing swelling and increased surface area. Increased surface area provides more adsorption sites, giving a proportionately higher capacity.

Intercalation of graphene planes separates the normal a-b spacing from 3.35 Å to a potassium containing graphene spacing of 5.35 Å. These potassium-containing planes form a dodecal structure, which, on the basis of space filling arguments, is capable of accommodating four hydrogen molecules, yielding 1.2 weight % gravimetric density. The hydrogen sorption energies for KC_{24} are ~40 kJ/mole [4], roughly an order of magnitude greater than for hydrogen on a graphene surface.

Adopting the approach of increasing the adsorption enthalpy for graphites should have a similar effect for SWNTs, and also have the effect of increasing the surface area of SWNTs. Nanotubes typically form rope structures due to van der Waals interactions which promote rope formation, limiting the surface area to ~300 m^2/gm (interior and exterior surface areas for a SWNT material should be above 2,600 m^2/gm). Potassium intercalation of SWNTs will separate the individual tubes. Computational work on SWNTs shows that under certain conditions, increasing the van der Waals gap will increase the amount of hydrogen that can be adsorbed [5].

Approach

We have been exploring 2-zone furnace procedures for the synthesis of KC_{24} and KC_{48}. Following 30-year-old synthesis techniques, we have used 2 different battery grade graphites deemed suitable for intercalation work. One is a high-purity plated graphite from Diemasters product G-1 and the other is a milled graphite from Superior Graphite designated SL-20. Having anticipated the importance of the analysis of these materials, we applied for beamtime at the Neutron Powder Diffractometer (NPD) at the Lujan Center at Los Alamos National Laboratory (LANL).

The initial goal of our work was to find the occupancy sites of deuterium atoms. Unlike hydrogen, deuterium is an effective coherent scatterer for neutrons, while its thermodynamic behavior with respect to carbon is similar to that of hydrogen. Thus, we would expect the presence of deuterium to alter the neutron diffraction pattern in a way that would reveal its location in the lattice. Deuterium is similar enough in size and physical behavior that such information would guide strategies for determining optimal positions for potassium on a graphite lattice, and provide a suitable foundation from which to calculate and understand hydrogen uptake in these intercalated graphites.

Three vanadium can assemblies, for the sample environment on the NPD at the LANL, were designed and constructed at Caltech. These assemblies incorporated conflat and VCR fittings (special fittings designed for high temperatures and pressures) in such a way as to accommodate the large temperature range available to us using the displex cooler on NPD. The vanadium cans were purchased from B&J Enterprises, a company that specializes in the manufacture of vanadium cans for neutron diffraction work. The stainless components were purchased from Norcal. All components were silver-soldered except for the vanadium-to-stainless joint, which was assembled using a high performance strain-gauge epoxy, M-bond 610 from Micro-measurements. These assemblies were tested to 77 degrees Kelvin and 10 bar pressure of hydrogen. In addition, a gas manifold was assembled at Caltech in order to provide a range of D_2 overpressures, necessary to accommodate absorption during sample cooling.

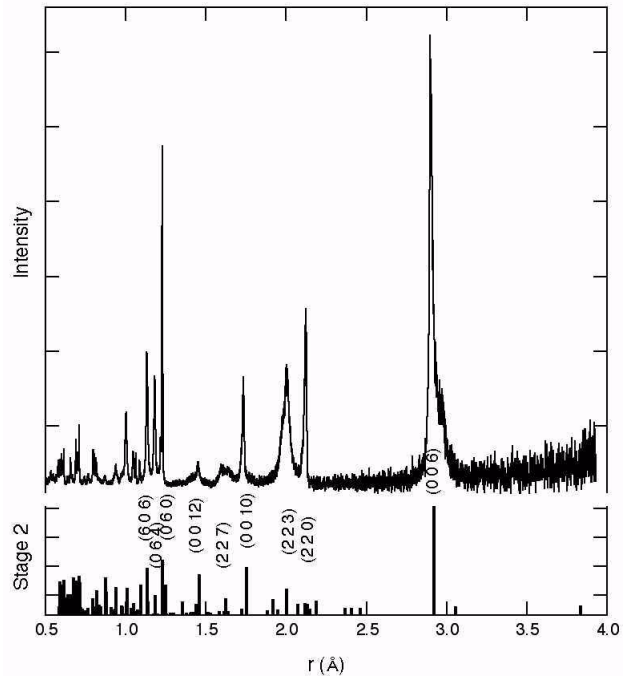

Figure 1. NPD initial run of KC_{24} intercalated graphite compound. Simulated data is shown in the lower trace with major planar indices as noted.

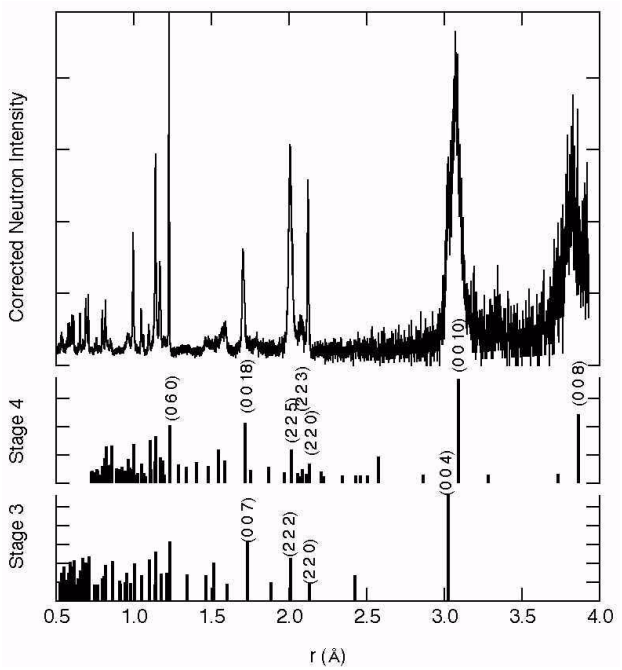

Figure 2. Neutron diffraction pattern from Stage 4 intercalated graphite. Indexed simulated peaks appear in the lower traces. Reflections from a Stage 3 phase (0 0 4) at 3.02 Å overlap with the Stage 4 (0 0 10) reflection at 3.09 Å. Lattice spacing measurements were determined by gaussian deconvolution.

Approximately 1 gram of each of these samples was loaded into the vanadium assemblies under Ar atmosphere in our glove box at Caltech and sealed and shipped to LANL.

Results

Figure 1 shows one of the first runs of the Stage 2 compound taken over a period of ~4 hours. The lower trace shows a simulation of diffraction data for a perfect crystal of the KC_{24} compound. Lack of the basal plane graphite reflection at 3.35 Å indicates that no decomposition or air exposure of this sample occurred.

The NPD data for the 300 degrees Kelvin run of the Stage 4 compound is seen in Figure 2. While the synthesis conditions used to make this sample were similar to the conditions used to make the Stage 2 compound, we believe that subtle differences in the nature of the starting graphite resulted in slower intercalation kinetics. In fact, this sample also contained a small amount of Stage 3 material. Both the (0 0 10) reflection from the Stage 4 phase as well as the (0 0 4) reflection corresponding to the Stage 3 phase can be observed in simulated and indexed diffractions for both phases in the lower traces.

Our analysis of the diffraction data upon cooling is shown in the lower traces of Figure 3 and reveals the normal lattice contraction expected for the c-axis. The upper traces show the lattice expansion in the deuterided material, and we can infer from a comparison of Stage 2 with Stage 4 data that the lattice expansion is consistent with deuterium only residing on the potassium-containing planes.

We have begun an initial set of computations for pair distribution analysis of our data with the hope that specific correlations can be drawn regarding the precise location (if any) of the deuterium molecules. In any event, these data do show deviations between 35 degrees Kelvin data sets for vacuum and deuterided KC_{24} as shown in Figure 4. These deviations begin beyond the 5.35 Å spacing of the

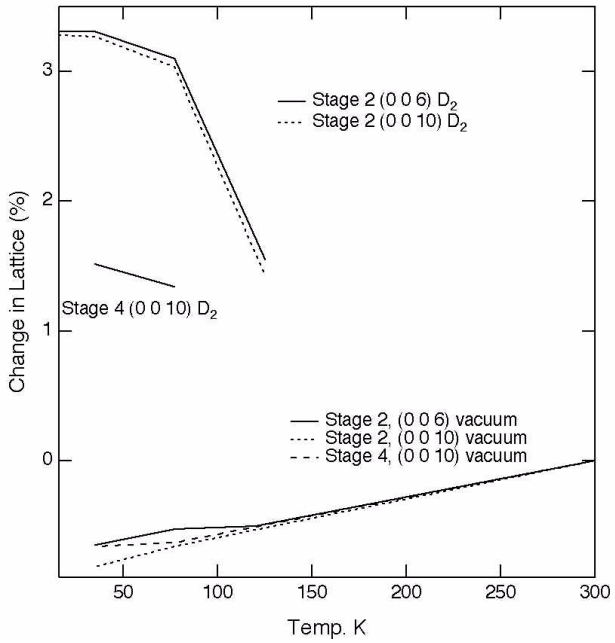

Figure 3. Basal plane lattice parameter changes as a function of temperature for Stage 2 and Stage 4 compounds under vacuum (lower traces) and deuterided (upper left traces).

potassium containing graphine distance, as shown in the residual in the lower trace.

Conclusions

The lattice expansion associated with deuteriding shows the dependence of absorption on potassium-containing planes in intercalated graphite and the importance of this system in serving as a suitable baseline for our subsequent measurements on SWNTs.

References

1. Y. Ye, C. C. Ahn, C. Witham, B. Fultz, J. Liu, A. G. Rinzler, D. Colbert, K. A. Smith and R.E. Smalley, Appl. Phys. Lett. 74, 2307 (1999).

2. E. L. Pace and A. R. Siebert, J. Phys. Chem. 63, 1398 (1959).

3. M. Colin and A. Herold, Bull. Soc. Chim. Fr., 6, 1982 (1971).

4. K. Ichimura, E. Takamura and M. Sano, Synth. Met., 40, 355, (1991).

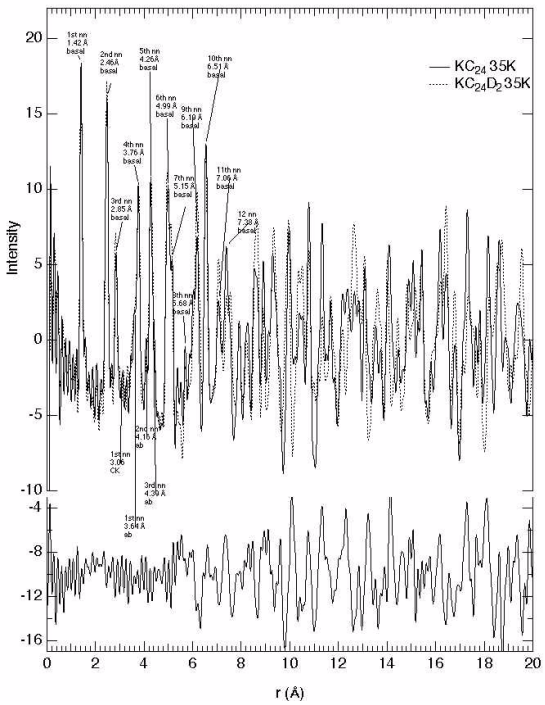

Figure 4. Pair distribution functions for Stage 2 intercalated graphite, extracted from NPD data for sample held under vacuum and deuterided. A plot of the difference between these two PDFs is shown in the lower trace.

5. V. V. Simonyan, J. K. Johnson, J. Alloys Comp. 330-332, 659 (2002).

FY 2002 Publications/Presentations

1. Hydrogen Storage and Neutron Powder Diffraction of Deuterided KC_{24}. C. C. Ahn, J. J. Vajo, R. Yazami, B. Fultz and D. W. Brown, Oral Presentation in symposium V (Materials for Energy Storage, Generation, and Transport), 2002 Spring Meeting, Materials Research Society.

2. Hydrogen Storage and Neutron Powder Diffraction of Deuterided KC_{24} and KC_{48}, C. C. Ahn, Invited Presentation, in Symposium S2 (Hydrogen Storage Materials and Hydrogen Generators), 201st Meeting of the Electrochemical Society in Philadelphia, May, 2002.

3. Hydrogen Storage in Carbons, C. C. Ahn, Invited Presentation, American Nuclear Society Annual Mtg., November 2002, Washington, D. C.

III.C Hydrides

III.C.1 Catalytically Enhanced Hydrogen Storage Systems

Craig M. Jensen (Primary Contact), Dalin Sun, Sesha Raman, Michael Eberhard, Keeley Murphy, Zhaohui Wang, Kristin Kumashiro, Walter Neimczura
University of Hawaii
Department of Chemistry
Honolulu, Hawaii 96822
(808) 956-2769, fax: (808) 956-5908, e-mail: jensen@gold.chem.hawaii.edu

DOE Technology Development Manager: JoAnn Milliken
(202) 586-2480, fax: (202) 586-9811, e-mail: JoAnn.Milliken@ee.doe.gov

Objectives

- Develop hydrogen storage materials based on complex aluminum hydrides that: a) have a hydrogen cycling capacity > 6 weight %; b) undergo dehydriding and rehydriding at temperatures below 100°C at rates that are sufficient for vehicular applications; and c) maintain >95% of their hydrogen capacity through >200 dehydriding/rehydriding cycles.
- Determine the kinetics and mechanism of the fundamental dehydriding and rehydriding reactions occurring in the doped hydride.
- Develop a catalyst that can affect the reversible dehydrogenation of cycloalkanes to arenes at rates that are sufficient for vehicular applications at temperatures of $\geq$100°C.

Approach

- Determine the minimum dopant levels to affect dehydriding of $NaAlH_4$ at adequate rates.
- Determine energetic barriers to the dehydrogenation of $NaAlH_4$ to Na_3AlH_6/Al and Na_3AlH_6 to NaH/Al and the reverse hydrogenation reactions by volumetric techniques.
- Differentiate hydride species present in doped hydride by solid state nuclear magnetic resonance (NMR) spectroscopy.
- Identify active catalyst through solid state NMR spectroscopy.
- Determine the activity of the iridium arsino pincer complex as a catalyst for alkane dehydrogenation.

Accomplishments

- Measured the rates of dehydrogenation of 2 mol % Ti and Zr doped $NaAlH_4$ to Na_3AlH_6/Al at 80-110°C and Na_3AlH_6 to NaH/Al at 120-150°C under 1 atm of H_2.
- Determined activation enthalpies, $\Delta H‡$, for the dehydrogenation for Ti and Zr doped hydride as 78 and 116 kJ/mol, respectively.
- Discovered through solid state 1H NMR spectroscopy that there are two distinguishable populations of hydrogen in both doped and undoped $NaAlH_4$, the minor population having unusually high solid state mobility.
- Discovered that the doping of the hydride results in the changes in the **bulk** structure of the hydride rather than the introduction of surface localized catalytic sites.

- Developed a model of the doped hydride in which doping entails substitution of Na^+ ions by M^{4+} at low ($\leq$2 mol %) doping levels and M^{3+} at higher doping levels together with the requisite number of lattice vacancies.
- Directly observed Ti^{3+} in 6 mol % Ti doped $NaAlH_4$ by electron spin resonance (ESR) spectroscopy studies conducted in collaboration with Sandia National Laboratory.
- Determined that ~20% conversion of cycloalkanes to arenes can be achieved with the iridium arsino pincer catalyst than is obtained with the analogous phosphino catalyst.

Future Work

- Determine the hydrogen cycling kinetics of $NaAlH_4$ to NaH/Al of hydride that is doped solely with Ti^{3+}, Ti^{4+}, Zr^{3+}, and Zr^{4+}.
- Detect and quantify the amount of M^{3+}, M^{2+}, and/or M^0 that are present in 1 and 6 mol % Ti and Zr doped hydride.
- Characterize the "mobile hydrogen" in $NaAlH_4$ by solid state NMR spectroscopy, inelastic neutron scattering, optical spectroscopy and neutron diffraction studies.

Introduction

During the initial dehydriding reaction of $NaAlH_4$, seen in equation 1, $NaAlH_4$ rapidly evolves

$$3\ NaAlH_4 \text{ ----------> } Na_3AlH_6 + 2\ Al + 3\ H_2 \qquad (1)$$

hydrogen at moderate temperatures upon doping with 2 mole percent $Ti(O^nBu)_4$ [1-13]. At 100°C, hydrogen flow rates of 0.01 g H_2/s per kg under a constant pressure of 1 atm have been measured to evolve from hydride doped through methods developed in our laboratory [2,3]. This dehydriding performance is adequate to meet the demands of a fuel cell operating under practical conditions. We have also found that NaH and Al doped with 2 mole percent $Zr(O^nPr)_4$ absorbs 4.4 weight percent hydrogen within 15 minutes at 120°C under 125 atm of hydrogen. However, despite this progress in maximizing the catalytic enhancement of both the dehydriding and rehydriding process, it has not yet been demonstrated that ~5 weight percent hydrogen can be reversibly released from these materials under conditions that are required for the practical operation of an onboard fuel cell. Most notably, the rates of the second dehydriding reaction, seen in equation 2,

$$Na_3AlH_6 \text{ ----------> } 3\ NaH + Al + 3/2\ H_2 \qquad (2)$$

and the reverse, hydriding of NaH and Al to $NaAlH_4$, are impractical for hydride that is doped with titanium, and materials which exhibit improved kinetics in this second dehydriding reaction must be produced to achieve commercial viability.

The PCP pincer complex, $IrH_2\{C_6H_3\text{-}2,6\text{-}(CH_2PBu^t_2)_2\}$, is the first reported homogeneous catalyst for the dehydrogenation of cycloalkanes to arenes [14-19]. Unlike the heterogeneous catalysts for this reaction, it shows appreciable activity at low concentrations at temperatures as low as 100°C. The pincer complex also catalyzes the hydrogenation of arenes to cycloalkanes under moderate (10 atm) pressures of hydrogen. The two-way, hydrogenation/dehydrogenation activity of the catalyst suggests its application in a hydrogen storage system. Such a system meets the criteria of low cost and high hydrogen density (>6 wt %) required for a practical hydrogen storage system. The major drawback of a system based on cycloalkanes and the PCP pincer catalyst is that pronounced product inhibition occurs after about 10% dehydrogenation of cycloalkanes. Thus, an improved catalyst must be developed.

Results

Determination of the Energy Barriers Heights of the Fundamental Reactions

We have measured the rates of dehydrogenation of 2 mol % Ti and Zr doped $NaAlH_4$ to Na_3AlH_6/Al at 80-110°C and Na_3AlH_6 to NaH/Al at 120-150°C under 1 atm of H_2. Eyring plots of the data show that the $\Delta H‡$ of dehydrogenation reactions are 78 and 116

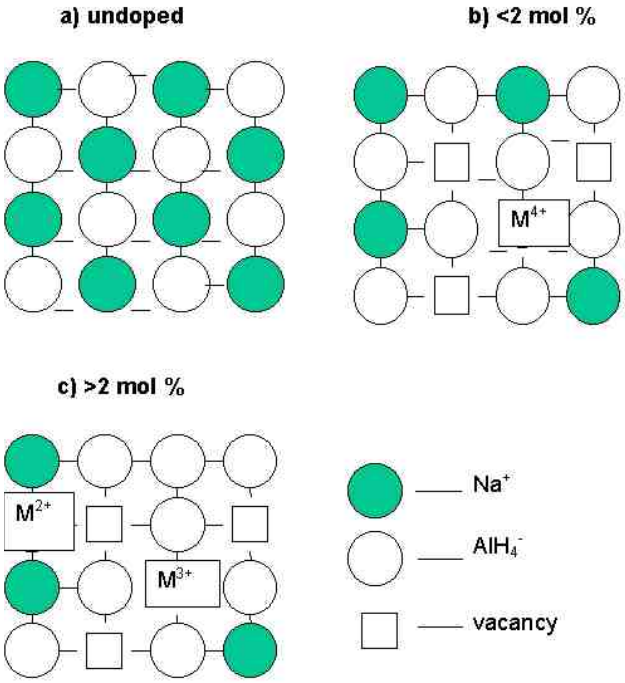

Figure 1. Energy-Reaction Profile for the Reversible Dehydrogenation of $NaAlH_4$ to NaH + Al

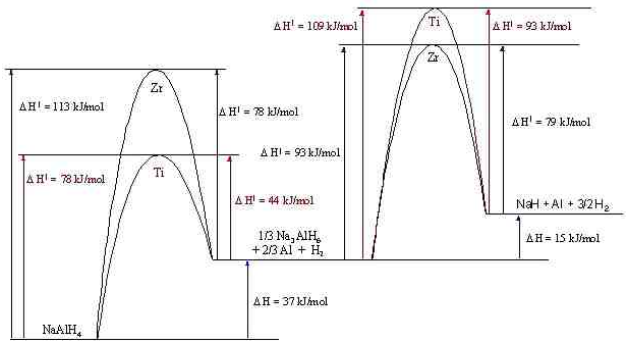

Figure 2. Schematic Illustration of the Changes in the $NaAlH_4$ Lattice upon Increased Level of Doping (a) Undoped hydride; (b) Substitution of Na^+ by M^{4+} and requisite formation of 3 Na^+ vacancies upon doping with 2 mol % M^{4+}; (c) increasing substitution without increasing Na^+ vacancies requires M to be present as M^{3+} or M^{2+} at higher doping levels.

kJ/mol respectively for the Ti doped hydride and 113 and 93 kJ/mol for the Zr doped hydride. We obtained predictions for the ΔH‡ of the reverse, hydrogenation reactions from reaction profile diagrams that were constructed using the values of ΔH‡ obtained from our studies and ΔH that were previously established for these reactions. We have also measured the rates of hydrogenation reactions and determined the activation enthalpy for ΔH‡ from Eyring plots of the data. As illustrated in Figure 1, we find that the experimentally determined values of ΔH‡ closely match the predicted by the reaction profile diagrams. This demonstrates that the kinetics of both hydriding reactions are limited by the micro-reverse of the fundamental Al-H bond breaking process. This data also confirms our earlier conclusion [3] that the best kinetic performance for the reversible dehydriding of $NaAlH_4$ to Na_3AlH_6/Al is achieved by Ti doping, while the best kinetic performance for the reversible dehydrogenation of Na_3AlH_6 to NaH/Al is achieved by Zr doping.

Solid State NMR and ESR Studies

The extremely narrow signal that is observed for one of the hydrogen species establishes that it has unusually high solid state mobility. This finding is in agreement with recent X-ray diffraction studies we conducted with the National Institute of Advanced Industrial Sciences and Technology that have shown that the doping results in the changes in the **bulk** structure of the hydride rather than the introduction of surface localized catalytic sites [13]. As illustrated in Figure 2, we have hypothesized that structural changes result from substitution of Na^+ ions by M^{4+} and M^{3+} ions together with the requisite number of lattice vacancies. The presence of Ti^{3+} in 6 mol % Ti doped $NaAlH_4$ has recently been confirmed by electron spin resonance spectroscopy studies that were conducted in collaboration with Sandia National Laboratory.

Testing of Arsino Pincer Catalyst

We have found that the higher levels of conversion of cycloalkanes to arenes can be achieved with the iridium arsino pincer complex, $IrH_2\{C_6H_3$-2,6-$(CH_2AsBu^t_2)_2\}$ than are obtained with the analogous phosphino catalyst. However, inhibition of the arsino pincer catalyst is observed at the ~20% dehydrogenation level for methylcyclohexane, decalin, and dicyclohexyl.

Conclusions

Our studies of doped $NaAlH_4$ have given important insights into the highly promising but enigmatic hydrogen storage properties of this material. Our kinetic studies strongly suggest that the rate of the dehydrogenation and hydrogenation reactions are limited by the micro-reverse of the fundamental Al-H bond breaking process. Our X-ray diffraction and solid state NMR studies have shown that doping results in bulk changes to the crystal lattice of the hydride rather than the generation of surface isolated catalytic sites [1,4,5,9,11]. This structural augmentation of the hydride affects bulk perturbation and mobilization of hydrogen. These observations that bulk structural changes occur upon doping the hydride have led us to develop a new model of the doped hydride which accounts for the structural changes as the result of substitution of Na^+ ions by M^{4+} and M^{3+} ions. In support of this "Na^+ substitution" model, the presence of Ti^{3+} in samples $NaAlH_4$ that were doped with a variety of titanium precursors has been confirmed through electron spin resonance studies.

We have attempted to develop a hydrogen storage system based on the reversible dehydrogenation of cycloalkanes to arenes utilizing iridium "pincer" complexes, $IrH_2\{C_6H_3\text{-}2,6\text{-}(CH_2AsBu^t_2)_2\}$ and $IrH_2\{C_6H_3\text{-}2,6\text{-}(CH_2PBu^t_2)_2\}$. These complexes show appreciable catalytic activity at low concentrations at temperatures as low as 100°C. The complexes also show appreciable catalytic activity for hydrogenation of arenes to cycloalkanes under moderate (10 atm) pressures of hydrogen. Despite this two-way hydrogenation/ dehydrogenation activity, their practical application in a hydrogen storage system seems unlikely as the dehydrogenation activity of the pincer catalysts was found to be inhibited by the arene products of all of the substrates tested after about 10-20% conversion.

References

1. B. Bogdanovic, M. Schwickardi, *J. Alloys Comp.* **1997** *253*, 1.

2. C.M. Jensen, R.A. Zidan, N. Mariels, A.G. Hee, C. Hagen, Int. J. Hydrogen Energy **1999,** *24*, 461.

3. R.A. Zidan, S. Takara, A.G. Hee, C.M. Jensen, *J. Alloys Comp.***1999** *285*, 119.

4. B. Bogdanovic, R.A. Brand, A. Marjanovic, M. Schwickardi, J. Tolle, *J. Alloys Comp.* **2000**, *302*, 36.

5. K.J. Gross, S. Guthrie, S. Takara, G. Thomas, *J. Alloys Comp.* **2000** *297*, 270.

6. A. Zaluska, L. Zaluski, J.O. Ström-Olsen, *J. Alloys Comp.* **2000** *298*, 125.

7. C.M. Jensen and K.J. Gross, *Appl. Phys. A.* **2001** *72,* 213.

8. B. Bogdanovic and M. Schwickardi, *Appl. Phys. A.* **2001** *72*, 221.

9. K.J. Gross, C.M. Jensen, G.J. Thomas, *J. Alloys Comp.* **2002** *330-332*, 683.

10. G. Sandrock, K. Gross, G. Thomas, C. Jensen, D. Meeker, S. Takara, *J. Alloys Comp*. **2002** *330-332*, 696.

11. G.J. Thomas, K.J. Gross, N.Y.C. Yang, C. M. Jensen, *J. Alloys Comp.* **2002** *330-332*,702.

12. G.P. Meisner, G.G. Tibbetts, F.E. Pinkerton, C.H. Olk, M.P. Balogh, *J. Alloys Comp.* **2002** *337*, 254.

13. D. Sun, T. Kiyobayashi, H. T. Takeshita, N. Kuriyama, C. M. Jensen, *J. Alloys Comp.* **2002** *337*, L8.

14. M. Gupta, C. Hagen, W.C. Kaska, R. Flesher, and C.M. Jensen, *J. Chem. Soc. Chem.Commun*., **1996** 2083.

15. M. Gupta, C. Hagen, W.C. Kaska, R.E. Cramer, C.M. Jensen, *J. Am. Chem. Soc.*, **1997,** 119, 840.

16. M. Gupta, W.C. Kaska, and C.M. Jensen, *J. Chem. Soc., Chem. Commun*., **1997**, 461.

17. X. Xu, G.P. Rosini, M. Gupta, C.M. Jensen, W.C. Kaska, K. Krough-Jespersen, and A.S. Goldman, *J. Chem. Soc. Chem. Commun*., **1997**, 2273.

18. C.M. Jensen, *J. Chem. Soc., Chem. Commun.*, **1999**, 2443

19. Liu, E.B. Pak, B. Singh, C.M. Jensen, and A.S. Goldman, *J. Am. Chem. Soc*. **1999**, *121*, 4086.

FY 2002 Publications

1. "Development of Catalytically Enhanced Sodium Aluminum Hydride as a Hydrogen Storage Material." Craig M. Jensen and Karl J. Gross, *Appl. Phys. A.* **2001,** *72*, 221.

2. "Catalyzed Alanates for Hydrogen Storage." K.J. Gross, C.M. Jensen, S. Takara, D. Meeker, and G.J. Thomas, *J. Alloys Comp.* **2002,** *330-332*, 683.

3. "Engineering Considerations in the Use of Catalyzed Sodium Alanates for Hydrogen Storage." G. Sandrock, K. Gross, G. Thomas, C. Jensen, D. Meeker, and S. Takara, *J. Alloys Comp.* **2002**, *330-332*, 696.

4. "Microstructural Characterization of Catalyzed $NaAlH_4$." G.J. Thomas, K.J. Gross, N.Y.C. Yang, C.M. Jensen, *J. Alloys Comp.* **2002**, *330-332*, 702.

5. "X-ray Diffraction Studies of Titanium and Zirconium Doped $NaAlH_4$: Structural Basis of the Enhanced Hydrogen Storage Properties Resulting Upon Doping." Dalin Sun, Hiroyuki T. Takeshita, Tetsu Kiyobayashi, Nobuhiro Kuriyama, and Craig M. Jensen, *J. Alloys Comp.* **2002**, *337*, 8.

FY 2002 Presentations

1. "Recent Progress in the Development of PCP Pincer Complexes as Catalysts for Organic Transformations." 2000 International Chemical Congress of the Pacific Basin Societies, Honolulu, Hawaii, 12/17/01.

2. "PCP Pincer Complexes as Catalysts for Novel Organic Transformations." University of Utah, 10/25/01.

3. "Recent Advances in the Development of Doped $NaAlH_4$ as a Hydrogen Storage Material: X-ray Diffraction and Solid State ^{1}H, ^{27}Al, and ^{23}Na NMR Studies." The 2nd International Symposium on New Protium Function, Miyazaki, Japan, 12/14/01.

4. "Solid state ^{1}H, ^{27}Al, and ^{23}Na NMR Studies of Doped and Undoped $NaAlH_4$." Symposium on the Fundamentals of Advanced Materials for Energy Conversion, 2002 meeting of the Minerals, Metals, and Materials Society, Seattle, Washington, 2/20/02.

5. "PCP Pincer Complexes as Catalysts for Novel Organic Transformations." University of Washington, 2/24/02.

6. "PCP Pincer Complexes as Catalysts for Novel Organic Transformations." 81st meeting of the Chemical Society of Japan, Tokyo, Japan, 3/27/02.

7. "Recent Advances in the Development of Doped $NaAlH_4$ as a Hydrogen Storage Material: X-ray Diffraction and Solid State ^{1}H, ^{27}Al, and ^{23}Na NMR Studies." Symposium on Hydrogen Storage Materials and Hydrogen Generators, 201st meeting of the Electrochemical Society, Philadelphia, PA, 5/13/02.

8. "Sodium Aluminum Hydride: Fundamental Studies and Development of a Promising New Hydrogen Storage Material." Universal Oil Products, 8/13/03.

III.C.2 Complex Hydrides for Hydrogen Storage

Darlene K. Slattery (Primary Contact), Michael D. Hampton
Florida Solar Energy Center
1679 Clearlake Road
Cocoa, FL 32922
(321) 638-1449, fax:(321) 638-1010, e-mail: dkslatt@fsec.ucf.edu

DOE Program Managers: JoAnn Milliken
(202) 586-2480, fax: (202) 586-9811, e-mail: JoAnn.Milliken@ee.doe.gov

Objectives

- Identify and prepare a complex hydride that reversibly stores at least 6.0 wt% hydrogen
- Optimize kinetics by the addition of a catalyst

Approach

- Determine hydrogen uptake and release characteristics of each compound in pure and catalyzed form
- Study mechanisms of catalyst action using physical methods such as x-ray photoelectron spectroscopy (XPS), Auger electron spectroscopy (AES) and x-ray diffraction (XRD)

Accomplishments

- Characterized uncatalyzed materials using differential scanning calorimetry (DSC) and thermovolumetric analysis (TVA)

Future Directions

- Develop method to synthesize solvent- and by-product-free complex hydrides
- Characterize these pure complexes for suitability
- Identify "best" candidate for further testing
- Initiate extended cycling tests

Introduction

A major obstacle to the implementation of a hydrogen economy is an efficient, safe and economical method for storing hydrogen for automotive applications. An acceptable storage system should allow for a range of 300 miles per charge and should be reversible. Complex hydrides, such as sodium aluminum hydride, show great promise, but there are still problems with kinetics and weight percent of available hydrogen.

Complex hydrides were previously thought to be irreversible. However, Bogdanovic and Schwickardi (1) showed that the addition of a catalyst, such as titanium, facilitated rehydrogenation. The primary problem is that, upon heating, the decomposition products are sodium hydride, aluminum and hydrogen. The hydrogen that remains tied up as sodium hydride is unavailable for use as a fuel and, as a result, the reversible hydrogen is only 5.5 wt%.

Approach

While sodium aluminum hydride was the first complex hydride shown to be reversible, there is a family of these compounds with high hydrogen content (Figure 1). In order to develop a system that meets the DOE target of greater than 6.0 wt% hydrogen, it is necessary either to start with a complex hydride containing a greater hydrogen density, or to develop a catalyst that will facilitate the release of the hydrogen from the decomposition product, sodium hydride. Sodium hydride has been

Complex Hydride	Wt %
$LiAlH_4$	10.5
$LiBH_4$	18.2
$Al(BH_4)_3$	20.0
$LiAlH_2(BH_4)_2$	15.2
$Mg(AlH_4)_2$	9.3
$Mg(BH_4)_2$	14.8
$Ca(AlH_4)_2$	7.7
$Ca(BH_4)_2$	11.4
$NaAlH_4$	7.5
$NaBH_4$	10.5
$Ti(BH_4)_3$	12.9
$Ti(AlH_4)_4$	9.3
$Zr(BH_4)_3$	8.8
$Fe(BH_4)_3$	11.9

Figure 1. Available Hydrogen in Select Complex Hydrides

long known and extensively studied, with no progress toward reducing its stability. The option of investigating other complex hydrides appears to be the more judicious approach.

Four of the complex hydrides of interest are commercially available. The others require synthesis, either by literature methods or by methods to be developed in-house. In order to determine the effect of the newly recognized hydrogenation/ dehydrogenation catalysts, it was necessary to investigate the compounds in their pure state. Only by having these baseline measurements would it be possible to ascertain the effect of an added catalyst.

Also of importance in the study of hydrogen storage materials is an understanding of the mechanism of any catalyst. Only by understanding how a catalyst functions is it possible to improve upon its performance. The catalyst mechanism may be surmised by determining the fate of the catalyst in the storage compound, which maybe accomplished using techniques such as XPS, AES and XRD.

Results

As a new project, it was necessary to first refurbish and update the instrumentation necessary for characterizing the hydrides. While the equipment

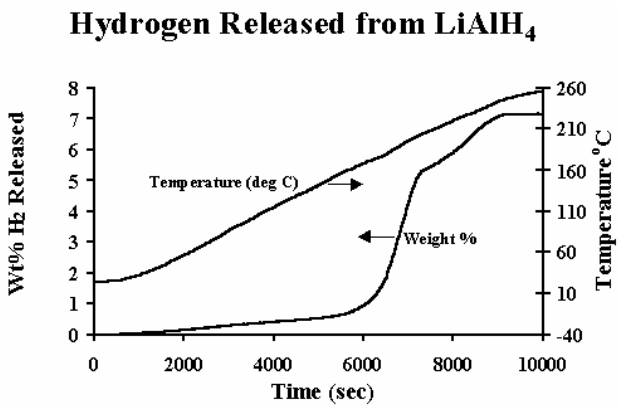

Figure 2. Thermovolumetric Analysis of LiAlH4

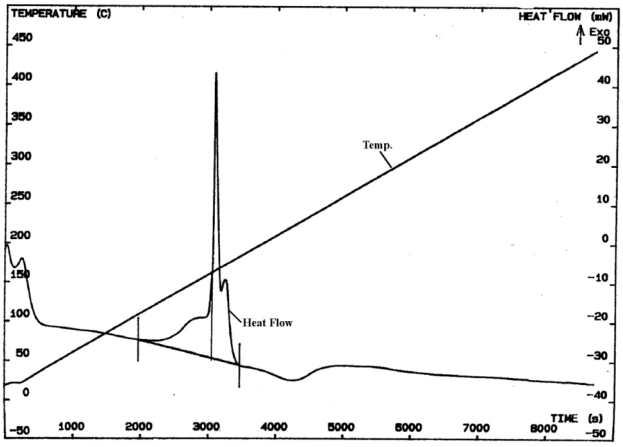

Figure 3. DSC Thermogram of LiAlH4

was being updated, the synthesis of materials with literature preparations was begun. It has been determined that some of the literature reports contain erroneous information, resulting in synthetic difficulties. The literature preps for many of these compounds also result in a product that is contaminated with solvent and, therefore, the hydrogen released is contaminated. Additionally, these products are frequently contaminated with byproducts that neither react with hydrogen nor facilitate the reaction with hydrogen and, thus, decrease the apparent hydrogen capacity of the product. This effort has demonstrated the necessity to develop new methods for preparing contaminant-free hydrides.

The purchased hydrides were all subjected to characterization in their as-received state, using both differential scanning calorimetry (DSC) and thermovolumetric analysis (TVA). The baseline data from the two methods of characterization, shown in

Figures 2 and 3, were found to corroborate the data in the literature. The dehydriding proceeds via a two-step mechanism and, without a catalyst, is not reversible. The TVA data, in addition to illustrating the kinetics of the hydride, allowed the calculation of the weight percent of hydrogen released from the material. The TVA data for the sodium aluminum hydride and the lithium aluminum hydride showed obvious release temperatures, while the corresponding borohydrides did not. It was also determined that the TVA and the DSC are complimentary techniques, providing data that match literature values while operating on significantly different sample sizes and theoretical principles.

Conclusions

- Analysis using DSC and TVA gives complementary information.
- Baseline studies were consistent with literature reports.
- Literature methods for synthesizing complex hydrides result in materials of low purity. New methods need to be developed.

References

1. Bogdanovic, B., and Schwickardi, M. J. Alloys andCompounds,(1997)253,1-9.

FY 2002 Publications/Presentations

1. Slattery, D.K. and Hampton, M.D., "Complex Hydrides for Hydrogen Storage," Semi-annual contract report submitted to DOE under cooperative agreement DE-FC36-01GO11094. May 2002.

2. Slattery, D.K. and Hampton, M.D., "Complex Hydrides for Hydrogen Storage," Proceedings of the U.S. DOE Hydrogen Program Annual Review, Golden, CO, May 6-8, 2002.

3. Hampton, M.D and Slattery, D.K., "Complex Hydrides for Hydrogen Storage," Presented at the Alanate Working Group Meeting, January 31, 2001.

III.C.3 High-Density Hydrogen Storage Demonstration Using $NaAlH_4$ Based Complex Compound Hydrides

Donald Anton (Primary Contact), Daniel Mosher
United Technologies Research Center
MS 129-22
411 Silver Lane
East Hartford, CT 06108
(860) 610-7174, fax: (860) 610-7253, e-mail: antondl@utrc.utc.com

DOE Technology Development Manager: JoAnn Milliken
(202) 586-2480, fax: (202) 586-9811, e-mail: JoAnn.Milliken@ee.doe.gov

ANL Technical Advisor: Thomas Benjamin
(630) 252-1632, fax: (630) 252-4176, e-mail: Benjamin@cmt.anl.gov

Subcontractors: Hydrogen Components, Inc. (HCI), Littleton, CO; QuesTek Innovations, LLC, Evanston, IL

Objectives

- Improve the charging and discharging rates of the $NaAlH_4$ based hydrogen storage medium. Specifically, in collaboration with other efforts,
  - Increase the reversible weight fraction of hydrogen stored to 7.5% from the current 5.5%.
  - Enhance the hydrogen evolution rate from 0.1 wt%/hr. at 80°C to 0.55 wt%/hr. to meet steady-state fuel cell demand.
  - Increase the regeneration rates from the documented 0.5 wt%/hr to the 90 wt%/hr to achieve five minute refill requirement.
- Determine the safety and risk factors associated with the enhanced compositions.
- Design, develop and evaluate a hydrogen storage system having a 5 kg hydrogen capacity and installation capability in a fuel cell-powered mid-size sedan.

Approach

- Create thermodynamic models of the $NaAlH_4$ system to determine optimum catalyzed compositional ranges designated as Complex Compound Hydrides (CCH).
- Cyclically evaluate selected CCH compositions to determine degradation mechanisms and ameliorations as well as compatibility with construction materials.
- Conduct standardized safety testing related to the classification of hazardous materials.
- Develop preliminary designs through the evaluation of existing systems, generation of weight/volume/cost improvements, and high-level optimization to balance automotive demands.
- Perform heat and mass flow modeling for detailed optimization of the required system volume and mass. Evaluate methods to enhance heat conduction into the CCH powder.
- Fabricate and evaluate 1-kg H_2 and 5-kg H_2 capacity hydrogen supply systems in conjunction with proton exchange membrane fuel cell (PEMFC) systems.
- Conduct preliminary performance modeling of the combined PEMFC and hydrogen supply system under steady-state and transient conditions to establish dynamic control requirements.

Accomplishments

This project is in the early stages, having received contract finalization two weeks prior to the writing of this report with some anticipatory work having been conducted at a reduced level over the past two months.

- Safety testing procedures have been selected and the majority of the unique test fixturing has been fabricated.
- An assessment of system preliminary design options has been initiated along with first order cost modeling for high volumes of 1 million units per year.

Future Directions

- Sufficient material to perform the safety analysis and cyclic testing will be prepared by ball milling utilizing a composition of 2m% $TiCl_3$ catalyzed $NaAlH_4$, designated CCH#0.
- Continue development of safety testing procedures and conduct initial tests on the CCH#0 composition.
- Generate additional concepts for the storage system tank to reduce system volume, weight, and cost.
- Conduct analytical, numerical, and experimental studies on a variety of heat conduction enhancement methods (metal foams, screens, wires, wools).

Introduction

One of the most significant barriers to the widespread application of hydrogen-based propulsion is the development of on-board storage systems which can provide the needed quantity of hydrogen with acceptable volume, weight, cost, and safety risk. The major classes of established hydrogen storage methods–compressed gas, liquid, metal hydrides and chemical hydrides–all have advantages and disadvantages, but none are clearly superior for automotive applications. In particular, a disadvantage of metal hydrides is their low hydrogen capacities of less than 2 wt% for alloys with discharge temperatures where the waste heat of a PEMFC (~ 90 deg. C) can be used to release the hydrogen. Many chemical hydride materials, while having high capacities, are classified as irreversible, which requires that the entire material be replaced during refueling rather than simply charging with hydrogen gas. The current project is focusing on the reversible chemical hydride, $NaAlH_4$, with a theoretical hydrogen capacity of 5.5 wt%, and seeks to enhance the material for improved charging and discharging rates as well as increased capacity. The project seeks to apply this material in the development of a system which will reversibly store a high wt% of hydrogen at low pressure for an indefinite amount of time. Safety studies of the enhanced material will also be conducted to support the technology as it is driven toward commercialization.

The storage system which contains the CCH powder must serve two primary functions: (1) exchange heat between the powder and a working liquid to drive the absorption/desorption of hydrogen and (2) support elevated hydrogen pressure during refueling. These functions must be performed with a minimum of weight, volume and cost. In addition, there are other secondary characteristics such as (i) allowing for significant volumetric change of the powder, (ii) exchanging hydrogen without the loss of the fine CCH powder particles, (iii) maintaining chemical compatibility with the CCH powder and hydrogen, (iv) producing minimal impurities going to the PEMFC, and (v) fitting into a conformable volume.

Approach and Results

Over 200 kg of catalyzed $NaAlH_4$ will be required for this project. An acceptable vendor has been identified to furnish the pure material within the budget of the project, and an order has been placed with a two month lead time which will slightly impact project schedule.

Determination of the charging and discharging reaction rates for catalyzed $NaAlH_4$ are well under way, both under internal UTC funding and through other DOE contracts by other investigators. Hydrogen discharge rates sufficient to deliver hydrogen to PEMFC powered vehicles at ~20 mph using 80°C water have been readily achieved. Hydrogen charging rates required to achieve 2 hr charging times are also within reach with significant improvements in this area foreseen.

Safety issues related to accidental damage of CCH systems and subsequent environmental exposure are a concern, and little information is available in the open literature. Safety studies examining how this material will react upon sudden exposure to heat, moist air, water or sudden impact are being examined by the subcontractor HCI. These tests will be based on the United Nations document "Recommendations on the Transport of Dangerous Goods - Manual of Tests and Criteria" (Reference 1) that serves as the basis for U.S. Department of Transportation (DOT) Hazardous Materials (HAZMAT) shipping classifications. While these tests are not specific to automotive fuel tanks, following these established procedures will put catalyzed $NaAlH_4$ into perspective with a large database of other flammable, self-heating and water reactive materials. The equipment has been constructed for the burn rate, self-heating, pyrophoricity and water reaction tests. Figure 1 shows a powder train of surrogate material produced by standardized sizing and settling procedures. The burn rate is determined by the time the flame takes to travel between the 80 mm and 180 mm marks.

To address the system needs, existing designs, such as the one from SRTC sketched in Figure 2, will be evaluated and novel ideas generated to improve upon the performance/cost as well as to better integrate with the particular characteristics of the CCH powder and PEMFC. Since the material characteristics are being modified, the required charging pressure to achieve the desired refueling rate has yet to be determined. Therefore, a number of pressure conditions will be examined using the design guidelines of the ASME Pressure Vessel Code.

Figure 1. Photograph of the safety test set up measuring powder burn rate.

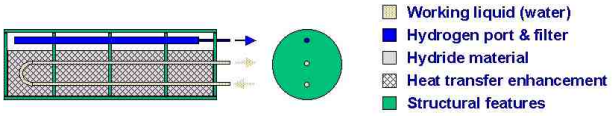

Figure 2. Sketch of an existing baseline design from SRTC indicating the major storage system elements.

During the discharging of hydrogen, heat must be provided to the CCH powder in order to release hydrogen, and during charging, heat must be removed rapidly to prevent the powder from melting. However, the powder has a very low thermal conductivity which is on the order of 1/1000th that of aluminum. Different types of heat transfer enhancement will be examined to improve conduction into the hydride powder. Analytical and numerical models using the ABAQUS finite element code will be constructed, and experiments will be performed which evaluate the heat transfer performance of different enhancement methods including metal foams, screens, wires and wools. Cost, weight and chemical compatibility will also be factored into the selection of the method.

Conclusions

Significant progress has been made in hydrogen charging and discharging kinetics in a relatively short time. It is not anticipated that kinetics will be limiting for this material.

A reasonable set of safety guidelines and experiments have been identified which will be used to classify the chemical hazards associated with utilizing $NaAlH_4$ type compounds.

References

1. "Recommendations on the Transport of Dangerous Goods - Manual of Tests and Criteria," 3rd edition, 1999, United Nations Publication ST/SG/AC.10/11/Rev.3.

Presentations

1. Winter 2002 IEA Working Group on Hydrogen Storage, Annex 17, Seattle, WA, February, 2002.

2. DOE Alanate Working Group Meeting, Livermore, CA, January 2002.

III.C.4 Standardized Testing Program for Emergent Chemical Hydride and Carbon Storage Technologies

Richard A. Page (Primary Contact) and Michael A. Miller
Southwest Research Institute™
P. O. Drawer 28510
6220 Culebra Road
San Antonio, TX 78228-0510
(210) 522-3252, fax: (210) 522-6220, e-mail: rpage@swri.org

DOE Technology Development Manager: JoAnn Milliken
(202) 586-2480, fax: (202) 586-9811, e-mail: JoAnn.Milliken@ee.doe.gov

ANL Technical Advisor: William Swift
(630) 252-5964, fax: (630) 972-4473, e-mail: swift@cmt.anl.gov

Subcontractors: Teledyne Energy Systems, Hunt Valley, MD; The National Hydrogen Association, Washington, D.C.; Energy Conversion Devices, Inc., Troy, MI

Objectives

- Develop and operate a standard testing and certification program specifically aimed at assessing the performance, safety and life cycle of emergent chemical hydride and carbon adsorption/desorption hydrogen storage materials and systems.
- Work with industry and the U.S. government to develop an accepted set of performance and safety evaluation standards.

Approach

- Task 1: Perform a comprehensive review of the current accepted practices for testing the performance of chemical hydride and carbon storage media.
- Task 2: Define the equipment and test protocols that will be used in the standardized testing program.
- Task 3: Design and construct the test facilities for characterizing the performance of chemical hydride and carbon storage media.
- Task 4: Develop a chemical process-engineering model that can be used to compute the thermal and chemical performance of storage systems at any scale.
- Task 5: Evaluate the operation of the test facility with actual sample materials to verify that all components operate correctly pursuant to the test protocols developed in Task 2.
- Task 6: Validate and optimize the performance model so that the performance characteristics of most any chemical hydride or carbon storage media can be viewed independently of scale.
- Task 7: Analyze a select number of emergent chemical hydride and carbon storage materials in accordance with the protocols established in Task 2.
- Task 8: Work for the adoption of the test protocols developed in this program by a recognized national or international standards organization.

Accomplishments

- A comprehensive review of current accepted practices was initiated.

- Discussions with potential suppliers of test equipment have been initiated.
- Participated in the May 21, 2002 ISO TC 197 US TAG Meeting on standards for hydride storage systems.

Future Directions

- Based on the review of current accepted practices, a report detailing the proposed test protocols will be submitted to DOE.
- Following DOE approval of the test protocols, design and construction of the test facility will commence.

Introduction

The choices of viable hydrogen storage systems at this time are limited to compressed hydrogen gas (CH_2), cryogenic liquid hydrogen (LH_2), chemical hydride adsorption, and carbon hydrogen adsorption. While each of these enabling storage technologies have specific advantages and disadvantages, chemical hydride and carbon adsorption storage systems may offer advantages in terms of storage capacity and, most importantly, safety.

The realization that chemical hydride and carbon storage systems will most efficiently meet the storage capacity and safety requirements of a hydrogen-based infrastructure has led to significant interest and monetary investment to accelerate the development of complete hydrogen adsorption storage systems. However, there are no standard guidelines, dedicated facilities, nor certification programs specifically aimed at testing and assessing the performance, safety and life cycle of these emergent systems. The development of a standardized protocol and testing system for assessing the performance of these materials and systems would allow both DOE and the R&D organizations to assess the potential performance of the wide array of materials and systems and focus their efforts on those that show the most promise.

Approach

In anticipation of the availability of many new materials and technologies for hydrogen storage, the purpose of the present effort is to develop an evaluation facility with established evaluation protocols and standards for the testing and assessment of these emergent chemical hydride and carbon storage materials and systems. Upon thorough validation of the experimental apparatuses and associated protocols, the testing facility and the technical staff that supports it will be available as the focal testing center to any prospective innovator of chemical hydride or carbon hydrogen storage materials or systems. Although the final form of the test protocol and equipment will be defined from the survey results, it is anticipated that the test system will be centered around hydrogen sorption/desorption measurements of smaller quantities of storage media. These measurements may be performed using a magnetically coupled thermogravimetric analyzer, as shown in Figure 1. An ability to test complete storage systems will also be included. Testing of complete systems is required in order to validate the system performance models that are developed as part of the project.

The performance characteristics of candidate materials will be determined through a comprehensive materials characterization and systems testing approach. This approach will encompass the elements described below.

Certification of Chemical Composition and Crystallographic Properties

Materials selected for evaluation will be analyzed to determine or verify their elemental composition and crystallographic properties using appropriate analytical capabilities: atomic adsorption spectroscopy (AAS), X-ray fluorescence (XRF), Raman spectroscopy, Fourier transform infrared spectroscopy (FTIR), and powder X-ray diffraction.

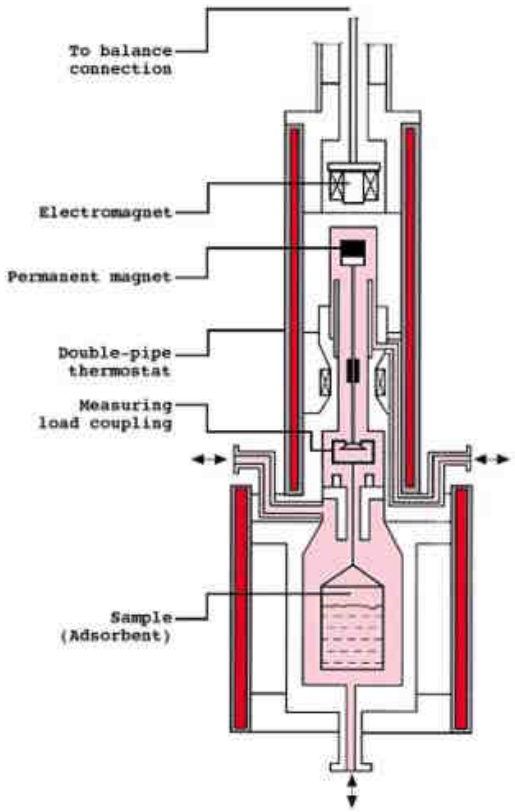

Figure 1. Magnetically Coupled Thermogravimetric Analyzer

Evaluation And Certification Of Performance Parameters

The intrinsic thermodynamic characteristics of candidate storage materials, where existing data is not available, will be evaluated by modulated differential scanning calorimetry (MDSC). Data of this sort that has already been generated by others will be used to the extent that it is relevant to the specific goals of the present study. The intrinsic thermodynamic characteristics that will be derived from the MDSC analysis include the following:

- Determination of first- and second-order phase transitions
- Heat of transition
- Transition temperature
- Non-reversible transitions (such as in decomposition)
- Decomposition temperature
- Decomposition exotherm
- Crystalline versus amorphous compositions

Once the intrinsic thermodynamic characteristics are firmly established, the storage materials will be subjected to the performance assessment test protocols. The performance parameters and conditions that will be derived from the testing regime are as follows.

- Specific energy contained in storage system (LHV H_2 per mass of total system)
- Sorption/desorption cycle life
- Resistance to exogenous contaminates
- Average refueling time
- Most favorable thermal-cycle conditions
- Impact resistance (only applicable to complete hydrogen storage container technologies)
- Vibration resistance (only applicable to complete hydrogen storage container technologies)
- Fire resistance (only applicable to complete hydrogen storage container technologies)

Results

The project is a new start and has been underway for only two months. During that period the comprehensive review of current accepted practices was initiated. Discussions with potential suppliers of test equipment were also initiated.

Future Work

Effort in the immediate future (6-9 months) will focus on completion of the review of current accepted practices and initiation of the definition and design of the test facilities. Visits to a number of leading laboratories in hydrogen storage measurement will be included as part of the review of current practices.

FY 2002 Presentations

1. Project overview presented at International Hydrogen Infrastructure Program Meeting, August 23, 2001, Washington, D.C.

2. Project overview presented at DOE New Project Kick-Off Meeting, October 30, 2001, Washington, D.C.

3. Project overview presented at Hydrogen Program Annual Review, May 6-8, 2002, Golden, CO.

III.C.5 Hydrogen Fueled ICE Scooter with On-Board Metal Hydride Storage

Krishna Sapru (Primary Contact), S. Ramachandran, Z. Tan and P. Sievers
Energy Conversion Devices, Inc.
1621 Northwood Dr, Troy, MI 48084
(248) 362-4780, fax: (248) 362-0012, e-mail: ksapru@ovonic.com

DOE Technology Development Manager: JoAnn Milliken
(202) 586-2480, fax: (202) 586-9811, e-mail: JoAnn.Milliken@ee.doe.gov

Objectives

- Convert a gasoline internal combustion engine (ICE) scooter into a commercially viable hydrogen fueled scooter.
- Design and fabricate a metal hydride storage system (MHSS) for on-board hydrogen storage.
- Integrate the MHSS into the scooter for optimum utilization of the exhaust waste heat to release the stored hydrogen.
- Minimize backfiring and nitrogen oxide (NO_x) emissions. Optimize power, range, and overall efficiency/vehicle performance.
- Develop preliminary business plan to involve scooter manufacturers, hydrogen producers and other entities needed for commercialization.

Approach

- Convert 80-250 cc four-stroke, gasoline-ICE scooters to operate on hydrogen, which involves making changes to the fuel delivery and ignition systems.
- Maximize engine power output with minimum emissions by optimizing suitable air/fuel ratio and ignition timing.
- Design improved metal hydride storage system and integrate into the exhaust system of the hydrogen-ICE (H-ICE) scooter.
- Perform chassis dynamometer tests under steady-state conditions, and road tests to evaluate fuel consumption and drivability.
- Install and operate an electrolyzer to deliver hydrogen as one means to charge the metal hydride storage system on-board the scooter.
- Perform a market study to determine the feasibility of introducing H-ICE scooters in developing countries.

Accomplishments

- Successfully converted and demonstrated a working hydrogen ICE Scooter.
- Designed, fabricated, and integrated an air-cooled metal hydride storage system into the H-ICE scooter.
- Performed extensive dynamometer and road testing.
- Acquired, installed and operated an electrolyzer which produces 10 normal cubic meters per hour (approximately 1 kilogram per hour) hydrogen. Tested the purity, dryness, flow rate, and hydrogen delivery pressure, for compatibility with Energy Conversion Devices, Inc.'s (ECD's) (Ovonic) metal hydrides.

- Completed an extensive market study, which indicates a very large market for H-ICE small vehicles in developing countries. Used India as a case study.
- Study performed to determine the availability and cost of hydrogen from various renewable sources.
- Generated substantial awareness and interest in hydrogen for both transportation and distributed power generation as a result of meetings and presentation in India to automotive manufacturers, hydrogen producers and several key government agencies.

Future Directions

- Use knowledge/experience gained to improve overall H-ICE efficiency. This will be accomplished by further research on the engine/vehicle performance (increase power, fuel economy and reduce NO_x emissions).
- Identify optimal engine operational parameters such as air-flow, compression ratio, spark/fuel control, and valve timing, and develop an on-board fuel gauge.
- Incorporate improved metal hydride alloys and improve heat exchanger design along with additional engine work to increase the range from present 35 kilometers (km) to greater than150 km .
- Perform accelerated testing to check the compatibility between hydrogen and materials (i.e. corrosion and embrittlement) of various engine parts.
- Convert a liquid cooled 250 cc scooter to simulate the size of a 3-wheeler taxi in developing countries. Liquid heat exchange between engine coolant and metal hydride should provide better heat transfer.
- Leverage knowledge gained with hydrogen engine development for small vehicles (2 and 3 wheelers) and demonstrate H-ICE for distributed power generation.
- Explore federal/private partnerships for demonstrations and optimization.

Introduction

The global 2- and 3-wheeler fleet is in excess of 300 million units, most of them in highly polluted and rapidly developing nations such as China and India. While the Organization for Economic Cooperation and Development (OECD) countries are currently the largest contributors to greenhouse gas emissions, the Asia and Pacific regions are expected to replace OECD countries as the largest source of greenhouse gas emissions worldwide by about 2015. Development of small vehicles and power generation devices to run on hydrogen would result in dramatic improvement in air quality, in addition to economic and energy security benefits for all.

Developing clean hydrogen combustion technologies will not defer, but speed up a global transition to fuel cell technologies by promoting early hydrogen infrastructure development. Fuel cell power will be more energy efficient in the long run, but it is at least 15-20 years away from commercialization, especially in the industrialized nation where the per capita energy demand and performance expectations are very high. ICE manufacturing and maintenance capabilities are already established and only minimal re-tooling is needed. In addition to hydrogen conversion technologies, widespread availability of cost effective hydrogen fuel is required. A study was undertaken to compare the cost and availability of hydrogen from renewable sources in India. This study showed three possible sources:

- Use of low cost electricity from the bagasse co-generation in sugar mills to produce hydrogen via electrolysis of water
- Hydrogen by-product from the chlorine-caustic industry
- Direct gasification of biomass to hydrogen

Metal hydrides that reversibly store and deliver hydrogen at low temperatures and pressures offer a compact and safe means to carry hydrogen on-board small vehicles. Storage of hydrogen as a solid offers superior safety and volumetric advantages versus gaseous or liquid storage. In addition, large-scale metal hydride production facilities are already in

place (due to commercialization of the nickel/metal hydride battery technology), and this investment can be leveraged to produce alloys for hydrogen storage.

Approach

Our approach is to work with small ICE vehicles with engines in the 80-250 cc range, since this covers the broadest segment of the market. Vehicle conversion involves making changes to the fuel delivery and ignition systems. We will work on the vehicle to obtain maximum engine power with minimum emissions by determining suitable air/fuel ratio and ignition timing over the operating range of the engine.

In addition to vehicle optimization, we will use higher capacity metal hydride alloys developed at ECD, coupled with improved heat exchangers. This improved metal hydride storage system will be integrated into the vehicle for optimum utilization of waste heat. Detailed performance characteristics under different sets of driving conditions will determine areas of further improvement if necessary.

Results

We successfully converted an 80 cc gasoline ICE scooter to run on hydrogen fuel (Figures 1 and 2). This scooter was demonstrated at the U.S. DOE Annual review meeting in Denver, Colorado in May, 2002, and also at the World Hydrogen Energy Conference in Montreal in June, 2002. The conversion was achieved by making changes to the fuel delivery system and the ignition system. The scooter uses a fuel injector controlled by an engine control unit. The carburetor was removed and a throttle body was designed to replace the carburetor.

A driving test was done on a warm day in Michigan when the temperature was 92^{o} F, the barometric pressure 30 inches of mercury and humidity range of 46-55%. The on-board metal hydride storage system was charged with 140 grams of hydrogen and a range of 35 kilometers was obtained, with an approximate fuel consumption of 3.8 grams of H_2 per kilometer. The average speed during this test run was 32 km/hour and the top speed was 40 km/hour.

Figure 1. 80 cc, Four-Stroke, Single Cylinder Scooter Converted to Run on Hydrogen

Figure 2. ECD's Proprietary Metal Hydride Storage System On-Board, Under the Seat

The metal hydride used in the 80 cc scooter had 1.5 weight % reversible hydrogen-storage capacity. Within the geometrical constraints, using the same alloy, up to 240 grams of hydrogen can be carried on-board resulting in a range increase from the present 35 km to 60 km. Additionally, we recently developed new alloys having reversible hydrogen-storage capacities of 2.6 weight % (Figure 3). Using these

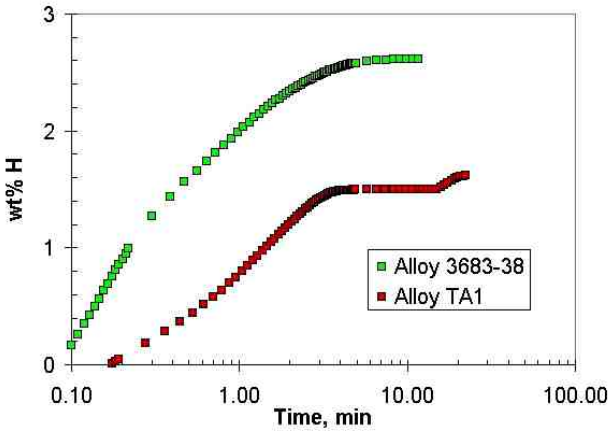

Figure 3. Hydrogen Desorption Kinetics of Proprietary Ovonic Hydrogen Storage Alloys at 100°C FY 2002

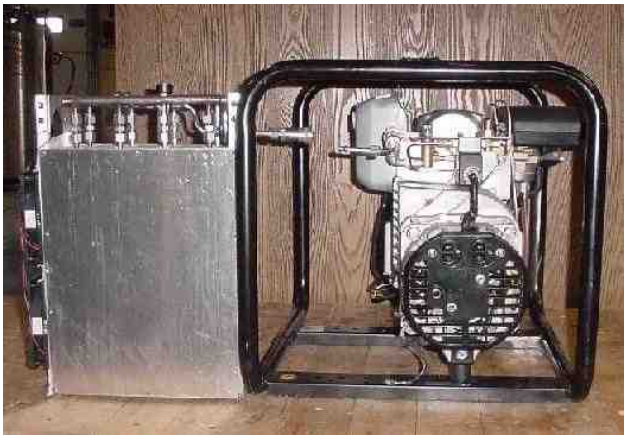

Figure 4. Laboratory Model of Ovonic Hydrogen ICE Generator Powered by Metal Hydride Storage Providing 3 hours of Back-Up Power at 2 kilo watts electrical

new alloys along with planned improvements in engine/vehicle performance will allow us to increase the vehicle range to 150 km. A 50 km to100 km vehicle range could be commercially acceptable in many developing countries, where the average daily driving range is less than 20 km, and gasoline prices are between U.S. $4 to $5 per gallon. These are also regions where air quality is among the worst in the world.

Distributed Power Generation for Portable and Stationary Use

It is estimated that 40% of the world's population is without electric power. These non-electrified regions of the world are potential markets for distributed small-scale (0.5-3 kilowatt) power systems. Also, because of severe power shortages and frequent outages in regions that do have electricity, there is a need to replace highly polluting diesel engines, gasoline and kerosene generators currently being used extensively; thus, the demand for hydrogen for power generation can be enormous. Figure 4 shows ECD's laboratory prototype of a H-ICE generator.

Conclusion

With support from the U.S. DOE hydrogen program, ECD has demonstrated the viability of H-ICE scooters with metal hydride for on-board hydrogen storage. Hydrogen fueled small ICE vehicles and distributed power generation devices can improve global air quality and reduce our dependence on fossil fuels. These products can be commercialized in a relatively short time frame (3-5 years) and pave the way to a hydrogen economy. However, additional research and demonstration projects are needed. Research should focus on improving fuel economy, reducing nitrogen oxides, improving power and vehicle range, materials compatibility and reducing overall cost.

Presentations

1. K. Sapru, S. Ramachandran, Z. Tan, 12th Annual US National Hydrogen Association, March 6-8, 2001, meeting in Washington, DC.

2. K. Sapru, S. Ramachandran, Z. Tan "Hydrogen- The New Oil- for Sustainable Transportation & Distributed Power Generation", invited talk at "International Symposium & Exposition on Alternative Energy Vehicles", Indian Institute of Technology, November 23-25, 2001, Kanpur, India.

3. K. Sapru, "*Hydrogen –The New Oil***.** Near Term Business Opportunities for Hydrogen in Developing Countries", The 2002 Hydrogen Investment Forum, April 3-4, 2002, Washington, DC,

4. K. Sapru, Hydrogen – "The New Oil", Hydrogen for Transportation and Distributed Power for

India, invited talk presented at the Science & Technology India Conference, April 10-12, 2002, New Delhi, India.

5. Z. Tan and K. Sapru, "Calcium Lithium Based Hydrogen Storage Materials", Canadian Hydrogen Storage Workshop sponsored by Canadian NRC, February, 2002, Ottawa, Canada.

6. K. Sapru, First Indo-US Fuel Cell Meeting, June 2-4, 2002, Washington, DC.

Patent Applications

During 2001-2002, the following patent applications have been filed:

1. S. Ramachandran, P. Sievers, K. Sapru and Z. Tan, A Hydrogen Powered Scooter, US patent pending.

2. Z. Tan and K. Sapru, High Capacity Calcium Lithium Based Hydrogen Storage Material and Method of Making the Same, US patent pending.

3. K. Sapru, Z. Tan, M. Bazzi, and S. Ramachandran, High Capacity Transition Metal Ti-V-Cr-Mn based Hydrogen Storage Materials, US patent pending.

III.C.6 Hydride Development For Hydrogen Storage

Karl Gross (Primary Contact), E. Majzoub, G.J. Thomas, G. Sandrock
Sandia National Laboratories
P.O. Box 969
Livermore, CA 94551
(925) 294-4639, fax: (925) 294-3410, e-mail: kjgross@sandia.gov

DOE Technology Development Manager: JoAnn Milliken
(202) 586-2480, fax: (202) 586-9811, e-mail: JoAnn.Milliken@ee.doe.gov

Objectives

- Develop new complex hydride materials with 6 weight percent system hydrogen capacity.
- Improve the kinetics of absorption and desorption and thermodynamic plateau pressures of Ti-doped sodium alanate metal hydrides.
- Improve processing and doping techniques of Ti-doped sodium alanate which will lower cost.

Approach

- Developing new complex hydrides to achieve higher capacities.
- Innovate methods to synthesize the complex hydrides and improve the doping process to improve both rates and capacity. Test different Ti-halide catalyst-precursor materials and other Ti-containing alloys and hydrides to determine the efficacy of Ti-doping with other starting materials.
- Characterize the material properties of each new generation of complex hydrides to aid in further improvements. Compare different material responses using kinetics experiments coupled with analytic techniques such as X-ray, electron spin resonance (ESR), nuclear magnetic resonance (NMR), Auger spectroscopy, etc.
- Determine the hydriding mechanisms through experimental analysis and modeling. Using Sievert's apparatus, measure rates of absorption and desorption of hydrogen from Ti-doped sodium alanate. Determine Arrhenius behavior and find activation energies and rate constants. Compare these results with mechanistic studies including neutron diffraction and ab initio calculations (electronic structure calculations.
- Evaluate the behavior of the materials on an engineering scale to ensure that they are on track for eventual commercialization.

Accomplishments

- Improved reversible capacities with the use of direct material synthesis and lower weight titanium (Ti)-halides such as titanium dichloride ($TiCl_2$) as catalyst precursors now give 4.3 weight % hydrogen (H_2).
- Discovery that Ti-halides with Ti valency of 2+, 3+, and 4+ work as catalysts in the sodium alanate system.
- Simplification of processing procedure for manufacture of Ti-doped sodium alanate from raw materials of Na, Al, and Ti-halide, resulting in a patent application.

Future Directions

- Find new complex metal hydrides and catalysts using procedures and techniques developed during the sodium alanate investigations.

- Determine the mechanism of action of the Ti in the material for the enhanced kinetics.
- Find new methods to introduce Ti into sodium alanate that may be more beneficial and economical than Ti-halide introduction.

Introduction

Ti-doped alanates offer an entirely new prospect for lightweight hydrogen storage. These materials have nearly ideal equilibrium thermodynamics, good packing densities, moderate volume expansion and useful sintering properties. However, there is much room for improving both absorption and desorption kinetics, and the less-than-theoretical reversible capacities. Our work has focused on finding solutions to these problems to achieve the performance requirements needed to supply onboard hydrogen for PEM fuel cell powered vehicles.

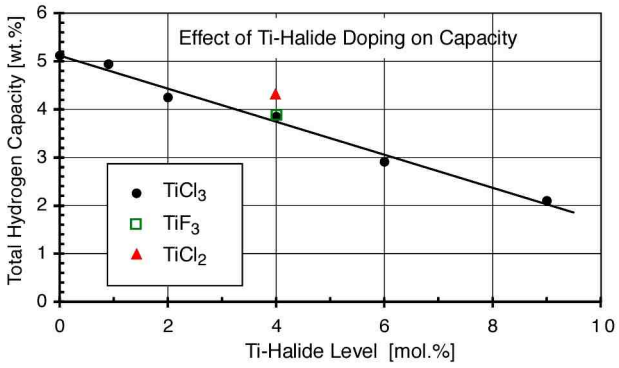

Figure 1. Reversible Hydrogen Capacity as a Function of $TiCl_3$ Content

Approach

Dehydriding and hydriding rates and capacities were obtained volumetrically using a Sieverts' apparatus and a cylindrical 316L stainless steel reactor (1.3 centemeter [cm] outer diameter by 0.12 cm wall thickness and length of 12 cm) containing about 1.5 gram of catalyzed samples. A thermocouple well in the center of the vessel allows for accurate temperature measurements during cycling. Absorption pressure changes were quantified with a calibrated 200 atmosphere absolute (atma) pressure transducer and desorption pressures with a 1000 Torr (1.3 atma) Baratron® capacitance manometer. Data were recorded via computer, and measurements lasted from minutes to several days, depending on the Ti-doping level, test pressure, and temperature conditions.

During absorption, the applied H_2 pressure was generally in the 80-90 atm range, well above the 30-40 atma plateau pressure for sodium tetrahydroaluminate ($NaAlH_4$) at 125°C. For the desorption experiments, the back-pressure during $NaAlH_4$ decomposition was kept below 1 atma and during trisodium hexahydroaluminate (Na_3AlH_6) decomposition below 0.25 atma, well below the Na_3AlH_6 plateau pressure of about 2 atma. Hydrogen capacity data are presented in Figure 1 as weight % with respect to the total sample weight, including the catalyst.

Isothermal arrhenius analysis were performed as follows. Measurements were started after several hydriding/dehydriding cycles with samples in the fully hydrided condition and cooled to room temperature. The pressure rise from desorption into a known volume at a given temperature was measured; and the temperature was then increased. Desorption rates were determined at each temperature from the slope of the essentially linear increase in pressure with time. This procedure was continued up to 150°C. The sample was held at this temperature until the $NaAlH_4$ decomposition step was finished. The rate data are presented as moles of desorbed hydrogen per mole active sodium per hour as shown in Figure 2.

Results

To improve capacity we have investigated the use of Ti-halides other than $TiCl_3$ to catalyze hydrogen absorption and desorption in $NaAlH_4$. Titanium triflouride (TiF_3) and $TiCl_2$ appear to work equally as well as $TiCl_3$ and reduce the overall capacity loss due to the formation of sodium chloride (NaCl) or sodium flouride (NaF).

Two new generations of materials have been developed. These are Generation III and Generation IV Ti-doped sodium alanates that are synthesized

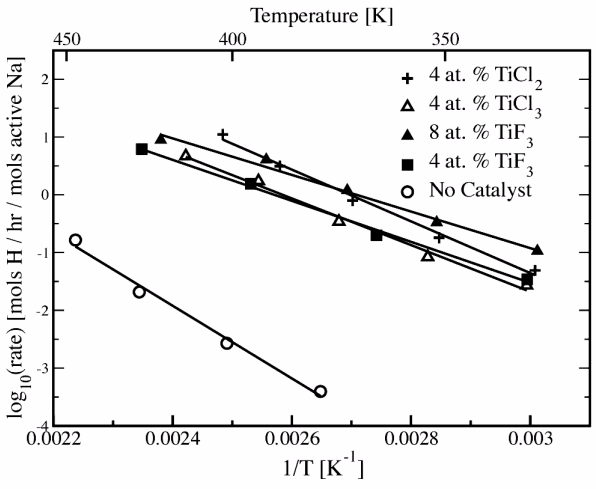

Figure 2. Arrhenius Plot of the Hydrogen Desorption Rates vs. 1/T for the Decomposition of $NaAlH_4$

directly from sodium hydride (NaH), Al, Ti-dopant and Na-metal, Al, Ti-dopant, respectively. These materials have demonstrated better kinetics than materials produced using earlier methods. In addition, the direct synthesis is performed without the use of solvents.

The result is a hydrogen storage material that is less-expensive to produce and delivers hydrogen free of hydrocarbon impurities.

Conclusions

We developed a synthesis route to produce Na_3AlH_6 and $NaAlH_4$ directly from Na and Al metals (patent application submitted).

We discovered that it is the titanium that contributes to the enhanced kinetics; the Ti-halide precursor gives the same results independent of the halide that is used. For that reason, the use of Ti-fluorides or lower Cl content chlorides will provide an incremental improvement in the reversible weight capacity.

A preliminary investigation shows that the direct synthesized alanates undergo an activation consisting of 2-3 cycles. Following this, it appears that the capacity and rates are quite stable after many cycles.

Aluminum is consumed in forming the alanates. It was found that it doesn't matter where the aluminum comes from (i.e. sorption materials or container vessel walls). However, the use of alanates that are not aluminum deficient did not appear to degrade the strength of aluminum-based alloys when tested under long-term cycling conditions.

In summary, these results demonstrate that solid progress is being made on the development of alanates for mobile hydrogen storage applications.

References

1. Bogdanovic, B. and Schwickardi, M. 1997. "Ti-doped alkali metal aluminum hydrides as potential novel reversible hydrogen storage materials", J. Alloys and Compounds, 253:1.

2. Bogdanovic, B., Brand, R.A., Marjanovic, A., Schwikardi, M., and Tölle, J. 2000. "Metal-doped sodium aluminum hydrides as potential new hydrogen storage materials", J. Alloys and Compounds, 302:36.

3. Bogdanovic, B., Schwickardi M. 2001. "Ti-doped $NaAlH_4$ as a hydrogen-storage material – preparation by Ti-catalyzed hydrogenation of aluminum powder in conjunction with sodium hydride", Applied Physics A, 72 (#2):221.

FY 2002 Publications/Presentations

1. Gross, K. J., Thomas, G. J. and Jensen, C. M., "Catalyzed Alanates for Hydrogen Storage", Journal of Alloys and Compounds, review article, 330-332 (2002) 683.

2. Gross, K. J., Sandrock, G., and Thomas, G. J., "Dynamic In Situ X-ray Diffraction of Catalyzed Alanates", Journal of Alloys and Compounds, 330-332 (2002) 691.

3. Gross, K. J., Majzoub, E.H., Thomas, G. J., and Sandrock, G. 2002 " Hydride Development for Hydrogen Storage", Proceedings of the 2002 U.S. DOE Hydrogen Program Review NREL/CP-610-32405.

4. Majzoub, E.H., Somerday, B.P., Goods, S.H., and Gross, K.J. 2002. "Interaction between Sodium

Aluminum Hydride and Candidate Containment Materials", Proceedings of the Conference on Hydrogen Effects on Material Behavior, Jackson Hole Wyoming, N. Moody editor.

5. G. Sandrock, K. J. Gross, and G. J. Thomas, "Effect of Ti-Catalyst Content on the Reversible Hydrogen Storage Properties of the Sodium Alanates", Journal of Alloys and Compounds, 339 (2002) 299-308.

6. G. J. Thomas, G. Sandrock, N. Yang, and K. J. Gross, 'Microstructural Characterization of Catalyzed $NaAlH_4$', Journal of Alloys and Compounds, 330-332 (2002) 702.

7. G. Sandrock, K. J. Gross, G. J. Thomas, C. M. Jensen, D. Meeker, and S. Takara, "Engineering Considerations in the Use of Catalyzed Sodium Alanates for Hydrogen Storage", Journal of Alloys and Compounds, 330-332 (2002) 696.

8. Gross, K. J., Majzoub, E.H., "New Reversible Complex Hydrides for Practical Hydrogen Storage", presentation World Hydrogen Energy Conference, Montreal, Canada, June 9th-13th, 2002.

9. Gross, K. J., Majzoub, E.H., and Sandrock, G. "Complex Hydrides for Light-Weight Hydrogen Storage", presentation TMS Annual Meeting, Seattle WA, February 20, 2002.

Special Recognitions & Awards/Patents Issued

1. DOE OPT Young Investigator Award – K. J. Gross.

2. Patent application. "Direct synthesis of lightweight catalyzed hydride for hydrogen storage." May 3, 2001.

Section IV. Fuel Cells

IV.A Transportation Power Systems

IV.A.1 Atmospheric Fuel Cell Power System for Transportation

Murdo J. Smith
UTC Fuel Cells
195 Governor's Highway
South Windsor, CT 06074
(860) 727-2269, fax:(860) 727-2399, e-mail: murdo.smith@utcfuelcells.com

DOE Technology Development Manager: Patrick Davis
(202) 586-8061, fax: (202) 586-9811, e-mail: Patrick.Davis@ee.doe.gov

ANL Technical Advisor: Walter Podolski
(630) 252-7558, fax: (630) 252-4176, e-mail: podolski@cmt.anl.gov

Objectives

- Deliver the following to DOE/Argonne National Laboratory (ANL) for functional demonstration testing:
  - A 50 kW-equivalent gasoline fuel processing system
  - A fully integrated, gasoline-fueled 50 kW proton exchange membrane (PEM) power plant
  - A fully integrated, gasoline-fueled 75 kW advanced PEM power plant
- Although focused on gasoline operation, the fuel processing system will utilize fuel-flexible reforming technology that can be modified to accommodate fuels such as methanol, ethanol and natural gas

Approach

- Deliver and test an autothermal fuel processor
- Deliver and test a 50 kW, ambient-pressure integrated power subsystem
- Deliver and test a 75 kW advanced ambient-pressure integrated power subsystem

Accomplishments

- Delivered and tested a 50 kW-equivalent gasoline fuel processing system
- Delivered and tested a 50 kW integrated power plant configured for system verification testing at UTC Fuel Cells (UTCFC) and delivered the power plant to DOE for follow-on testing at ANL

Future Directions

- Completely tear down and analyze the 50 kW power plant
- Deliver and test the 75 kW power plant at UTCFC and deliver to DOE for follow-on testing at ANL

Introduction

The focus of UTCFC's program is an ambient pressure PEM power plant system operating on gasoline fuel and delivering 75 kW net dc power to the automotive electrical system.

UTCFC will deliver to DOE a 50 kW-equivalent gasoline fuel processing system, a 50 kW PEM power plant, and a 75 kW advanced PEM power plant.

Approach

Figure 1 provides a schematic of the gasoline fuel cell power plant. The major subsystems include the Fuel Processing Subsystem, the Power Subsystem and the Balance of Plant. The Balance of Plant includes the Thermal Management Subsystem, the Air and Water Subsystems and the Controller and associated electrical equipment.

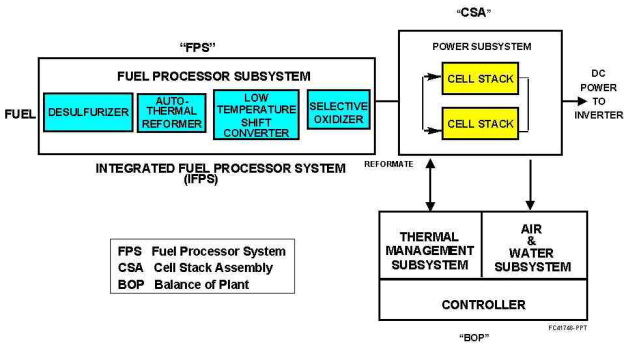

Figure 1. Power Plant Schematic

Results

50 kW Power Plant

Figures 2 and 3 are photographs of the fully integrated 50 kW, ambient pressure, gasoline-fueled power plant showing the locations of major components.

The power plant was installed for demonstration testing at UTCFC's facilities in South Windsor, Connecticut. A California Phase II reformulated gasoline (RFG) fuel was used throughout the test program.

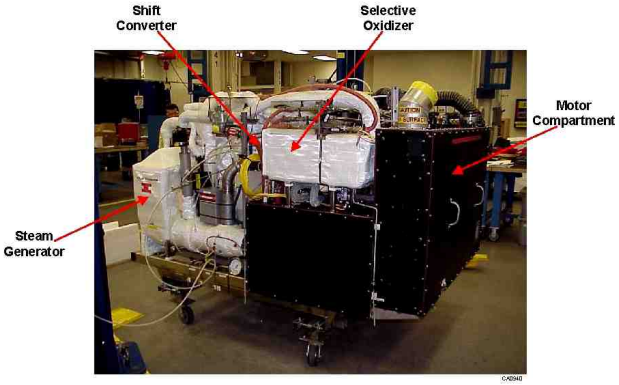

Figure 2. 50 kW Gasoline Fueled Power Plant – side view

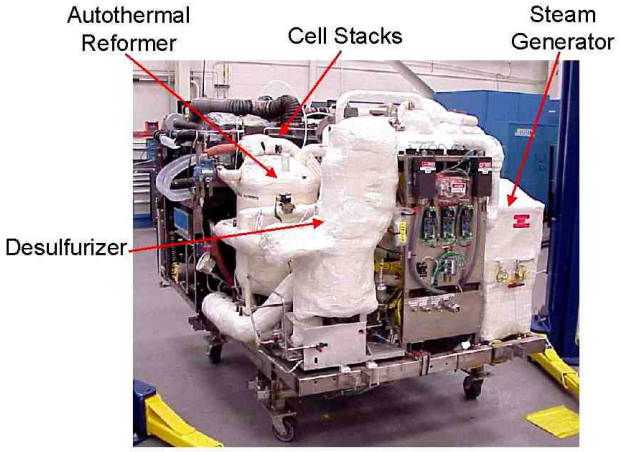

Figure 3. 50 kW Gasoline Fueled Power Plant – end view

A summary of the demonstrated system characteristics is shown in Table 1.

Table 2 provides selected comparative DOE Technical Targets for a 50 kWe (net) integrated fuel cell power system operating on Tier 2 gasoline containing 30 ppm sulfur.

Comparing the two tables, the UTCFC power plant demonstrated an efficiency level close to the DOE "2001 status" for 25% of rated power but was lower at rated power. The volume and weight numbers are significantly different, with the UTCFC power plant being larger and heavier.

Characteristic	Anticipated	Demonstrated
Rated net power	≥50 kWe	53 kWe
Efficiency at 50 kWe	---	25%
Efficiency at 25% rated power	≥32%	32%
Specific power based on wet weight	1550 lbs.	1825 lbs.
Power density ft^3 kW	28.5 ft^3	30.7 ft^3
Fuel compatibility	CA Phase II RFG	CA Phase II RFG
Start time to full power	45 min.	>45 min.
Voltage range	≤220 voltage ≤400 Vdc	≤250 voltage ≤420 Vdc

Table 1. Power Plant System Characteristics

Characteristic	Units	2001 Status	2005	2010
Energy Efficiency @ rated power	%	31	33	35
Energy Efficiency @25% of rated power	%	34	40	45
Power Density	W/L	140	250	325
Specific Power	W/kg	140	250	325

Table 2. DOE Fuel Cell Power System Technical Targets

Following testing at UTCFC, the power plant was delivered to DOE's Argonne National Laboratory. Figure 4 shows the power plant installed in the ANL test facility. Testing at ANL included steady-state and transient operation and provided experience in the new test facility.

The power plant has been returned to UTCFC after completion of the ANL test program. It will be torn down and specific components analyzed to better understand the impact of operation on their physical characteristics. These analyses will focus on the cell stack and fuel processing system.

Figure 4. 50 kW power plant installed in ANL test facility

75 kW Power Plant

In the second phase of the project, UTCFC will deliver to DOE an advanced 75 kW, gasoline-fueled PEM fuel cell power plant. This power plant will address opportunities for distributing components throughout the automobile structure.

Conclusions

A fully-integrated, ambient-pressure, 50 kW PEM power plant was assembled and tested at UTCFC and then delivered to ANL for follow-on testing. The power plant has been returned to UTCFC for teardown and analysis. Under Phase 2 of the project, UTCFC will deliver to DOE an advanced 75 kW gasoline-fueled ambient pressure PEM power plant.

IV.A.2 Fuel Cell Systems Analysis

Romesh Kumar (Primary Contact), Rajesh Ahluwalia, E. Danial Doss, and Michael Krumpelt
Argonne National Laboratory
9700 South Cass Avenue
Argonne, IL 60439-4837
(630) 252-4342, fax: (630) 252-4176, e-mail: kumar@cmt.anl.gov

DOE Technology Development Managers:
JoAnn Milliken: (202) 586-2480, fax: (202) 586-9811, e-mail: JoAnn.Milliken@ee.doe.gov
Nancy Garland: (202) 586-5673, fax: (202) 586-9811, e-mail: Nancy.Garland@ee.doe.gov

Objectives

- Identify key design parameters and operating efficiencies of direct hydrogen and reformed gasoline-fueled automotive fuel cell systems.
- Assess design-point, part-load, and dynamic performance of automotive fuel cell systems and system components.

Approach

- Develop, document, and make available an efficient, versatile system design and analysis code.
- Develop models of different fidelity (mechanistic detail) for fuel cells, stacks, and balance-of-plant components, such as reactors, condensers, and radiators.
- Apply models and modeling to issues of current interest as they evolve.

Accomplishments

- Developed new models:
  - An application package for the analysis of kinetic data from microreactors;
  - A generic model for metal hydrides, including kinetics with heat transfer;
  - A model for a desulfurizer based on zinc oxide sorbent; and
  - A kinetic model for the autothermal reforming of iso-octane using the Argonne catalyst.
- Developed a variety of GCtool-ENG models of fuel cell system components based on GCtool architecture for the speed and accuracy appropriate for fast transients in vehicle simulations by PSAT and similar MATLAB-based models.
- Working with DOE and others, developed R&D targets for the direct hydrogen fuel cell systems and components.
- Analyzed an 80-kW pressurized direct hydrogen system for efficiency and for heat and water management in an SUV application.

Future Directions

- Validate models with data from the Nuvera fuel processor system.
- Analyze the performance of ambient-pressure direct-hydrogen systems.
- Analyze reformed liquid-fueled systems on drive cycles.
- Model fast-start and load-following fuel processors.
- Analyze high-temperature-membrane fuel cell systems.

Introduction

While different developers are addressing improvements in individual components and subsystems in automotive fuel cell propulsion systems (e.g., cells, stacks, fuel processors, balance-of-plant components), we are using modeling and analysis to address issues of thermal and water management, design-point and part-load operation, and component-, system-, and vehicle-level efficiencies and fuel economies. Such analyses are essential for effective system integration.

Approach

We use Argonne's GCtool software package to devise and analyze system configurations and operation. We develop additional component models as needed to address evolving issues.

Results

During FY 2002, one of our major activities was to model and analyze an 80-kW pressurized direct hydrogen fuel cell system, potentially for an SUV application. The modeled system used compressed hydrogen fuel and operated at 3 atm, 80ºC, and a cell potential of 0.7 V at the rated power point. Performance data for the compressor-expander module (CEM) were obtained from a DOE development program. The fuel cell stack polarization curve was based on data from Los Alamos National Laboratory, extrapolated to various pressures and temperatures by the detailed fuel cell model in GCtool. The anode and cathode feed gases were heated/cooled to 70ºC and humidified to 90% relative humidity at the stack temperature. The modeled fuel cell system was analyzed for water and heat management issues, parasitic losses and system efficiency at normal and high ambient temperatures and elevations, and startup and dynamic response and efficiency in drive cycles.

Water Management

At the rated power, the dew point of the cathode exit gas that is needed to maintain water self-sufficiency is higher than the stack operating temperature, so no condensation of the water from the exhaust gas is needed. As the system operates at part load, however, the pressure ratio decreases from 3 toward 1. At pressure ratios below about 1.8, the required dew point decreases below 80ºC (the stack temperature), indicating that condensation of water from the exhaust is needed. The needed dew point as a function of the pressure ratio is shown in Figure 1. The figure shows the base case for 25% ambient relative humidity and 1 atm ambient pressure (at mean sea level), as well as cases for 100% relative humidity and 0.75 atm ambient pressure (at elevated locations, such as Los Alamos, New Mexico).

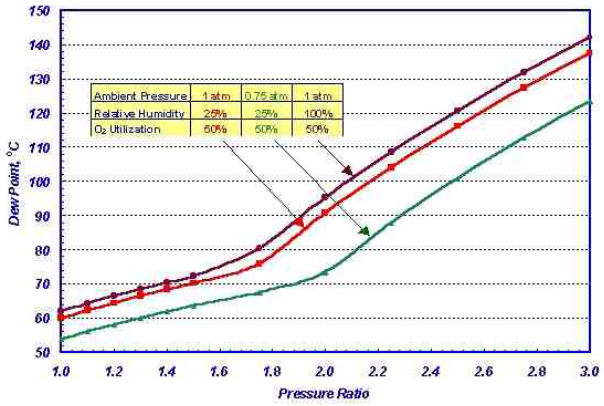

Figure 1. Dew point of the cathode exhaust required for water self-sufficiency in the fuel cell system. Dew points lower than the stack temperature must be achieved by condensing out some of the water from the exhaust. Operation at higher elevations requires more water to be recovered.

The corresponding heat duty of the condenser is shown in Figure 2. As discussed above, the condenser is needed only at pressure ratios less than about 1.8. The condenser duty increases with decreasing pressure ratios from ~1.8, reaching a maximum at a pressure ratio of ~1.2. At still lower pressure ratios, the condenser duty decreases due to the reduced air flow rates. Figure 2 also shows the effect of varying the oxygen utilization from 60% to 30% (50% is the base case). With decreasing oxygen utilization, the condenser duty increases; the maximum condenser duty more than doubles for operation with 40% oxygen utilization versus operation with 60% oxygen utilization.

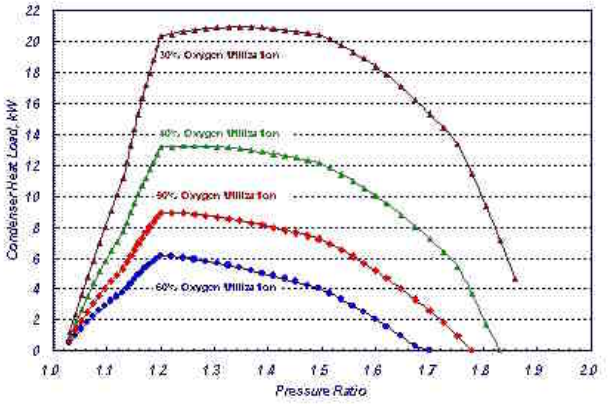

Figure 2. Condenser heat duty in the 80-kW system as a function of pressure ratio and oxygen utilization. The heat duty reaches a maximum at part load.

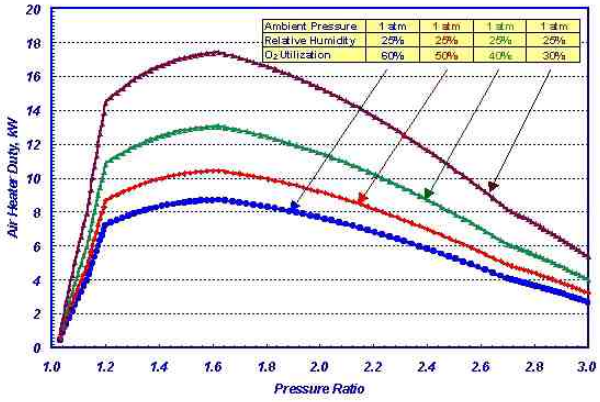

Figure 3. Heat duty of the air heater/humidifier in the 80-kW system as a function of pressure ratio and oxygen utilization. The maximum heat duty is required at part load.

Air Heater/Humidifier Duties

As is the case for the condenser, the maximum heat duty required at the cathode feed air heater/ humidifier is not at the rated power point; rather, the maximum heat transfer requirement occurs at the part-load pressure ratio of approximately 1.6, as shown in Figure 3. At higher pressure ratios, the compression itself provides the major portion of the heating and humidification heat duty. The compressor contributes a successively lesser fraction of the needed heating as the pressure ratio decreases from 3 at the rated power point toward 1.6 at approximately 20% of full load. Figure 3 also shows that the maximum heat duty increases with decreasing oxygen utilization, with the maximum air heater duty with 30% oxygen utilization being about twice the heat duty with 60% oxygen utilization.

Parasitic Losses and Efficiencies

In the pressurized direct hydrogen fuel cell system, the two major parasitic power consumers are the CEM and the radiator fan. Parasitic power consumption becomes significantly greater as the ambient temperature increases from the nominal 300 K (27°C, 80°F) to 320 K (47°C, 116°F), as shown in Figure 4. At the lower ambient temperature, the total parasitic power consumption at the rated power is approximately 6 kW (for an 80-kW net power system), most of which is due to the power consumed

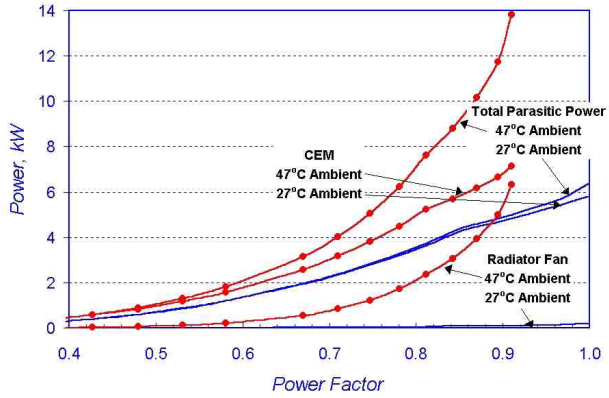

Figure 4. The compressor module and the radiator fan are the biggest parasitic power consumers in the system.

by the CEM. At the higher ambient temperature, the system is unable to deliver the full rated power of 80 kW net. At 90% of the rated power, the CEM and the radiator fan each consume over 6 kW, with a total parasitic power consumption of nearly 14 kW (for a net 72 kW delivered by the system).

The cell and overall system efficiencies (based on the lower heating value of hydrogen) at various power factors are shown in Figure 5. At the rated power and the nominal 300 K ambient temperature, the cell and system efficiencies are approximately 58% and 52%, respectively. The corresponding cell and system efficiencies at 320 K and 90% of rated power are approximately 57% and 46%, respectively.

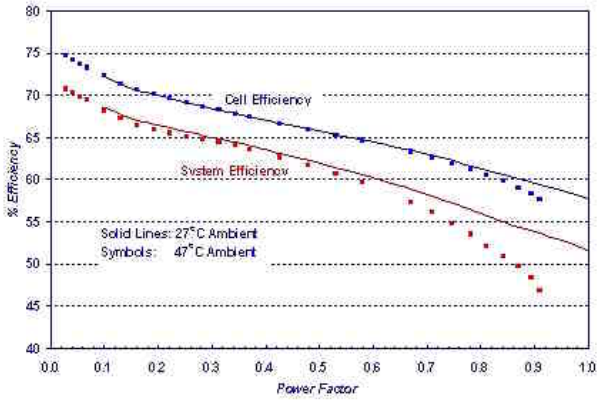

Figure 5. Fuel cell and system efficiencies as a function of power factor and ambient temperature.

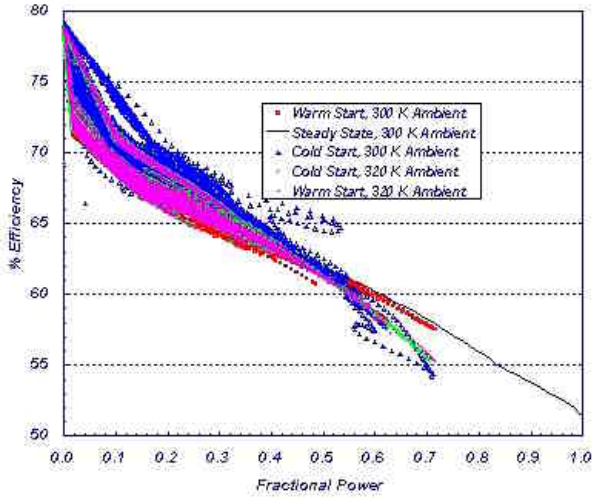

Figure 6. System efficiency at various power factors for different ambient temperatures and different cold and warm start conditions.

Startup and Dynamic Response on Drive Cycles

We have analyzed the performance of the pressurized direct hydrogen system during cold and warm startup at 300 K and at 320 K. Figure 6 shows the calculated efficiencies at various power factors for different operating conditions. In particular, at power factors less than about 0.5, i.e., at net power deliveries of 40 kW or less [the power most commonly called for from the 80-kW fuel cell system on the Federal Urban Driving Schedule (FUDS) and the Federal Highway Driving Schedule (FHDS)], the system efficiency can vary by more than 5 percentage points, depending on the state of the fuel cell system and the ambient conditions.

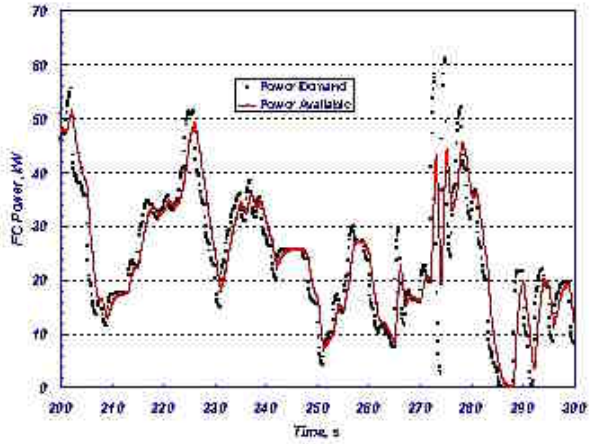

Figure 7. Dynamic response of the system on a portion of the FUDS. The fuel cell system's power generation lags behind the driving schedule's power demand during rapid power up-ramps.

The key factors for the dynamic performance of the fuel cell system are the response characteristics of the CEM and of its controller. An example of the system's dynamic response is given in Figure 7, which shows the power demand for the SUV and the power available from a warmed-up fuel cell system during a 100-second portion of the FUDS. During rapid power up-ramps, the power generation by the fuel cell lags behind the demand. The magnitude of this difference depends primarily on the response time of the CEM and the operating logic of its controller.

Conclusions

Our analysis of the pressurized direct hydrogen system shows that:

- A condenser is required at part load for water self-sufficiency.
- The condenser and the air heater/humidifier must be designed for the maximum heat duties, which occur at part load rather than at the system's design operating point.
- The compressor-expander module and the radiator fan are the biggest parasitic power consumers in the system, taking up nearly 15% of the gross power generated.
- Efficiencies of the system range from ~45% at the rated power to ~65% at part load.

- In load-following mode, the response characteristics of the CEM and its controller cause the power delivered to lag behind the power demand during the sharp transients of the FUDS.

FY 2002 Publications/Presentations

1. Ahluwalia, R. K., Doss, E. D., and Kumar, R., "Performance and Specific Power Attributes of PEFC Systems for Transportation," IEA Annex XV Meeting, Sacramento, CA, December 10–11, 2001.

2. Kumar, R., Ahluwalia, R., Doss, E., Krumpelt, M., “Fuel Cell Systems Analysis,” 2002 Annual National Laboratory R&D Meeting, DOE Fuel Cells for Transportation Program, Golden, CO, May 9–10, 2002.

3. Ahluwalia, R. K., Doss, E. D., and Kumar, R., “Performance of High-Temperature Polymer Electrolyte Fuel Cell Systems,” IEA Annex XI Phase II Meeting, Philadelphia, PA, May 17–18, 2002.

4. Ahluwalia, R. K., DeVille, B., Zhang, Q., Doss, E. D., Rousseau, A., and Kumar, R., "Performance of Hydrogen Fuel Cell Systems and Vehicles," IEA Annex XV Meeting, Dusseldorf, Germany, June 28, 2002.

5. Rousseau, A. and Ahluwalia, R. K., "Modeling and Control of Fuel Cell Vehicle Transient Behavior," Future Car Congress, June 3–5, 2002.

IV.A.3 Fuel Cell Vehicle Systems Analysis

Keith Wipke (Primary Contact), Tony Markel
National Renewable Energy Laboratory
1617 Cole Blvd.
Golden, CO 80401
(303) 275-4451, fax: (303) 275-4415, e-mail: keith_wipke@nrel.gov

DOE Technology Development Managers:
JoAnn Milliken: (202) 586-2480, fax: (202) 586-9811, e-mail: JoAnn.Milliken@ee.doe.gov
Nancy Garland: (202) 586-5673, fax: (202) 586-9811, e-mail: Nancy.Garland@ee.doe.gov

Objectives

- Develop and validate models and simulation programs to predict fuel economy and emissions and aid in setting performance targets for fuel cell electric and fuel cell hybrid electric vehicles
- Provide DOE and industry with modeling tools and early design insights that lead to introduction and application of advanced technology
- Quantify benefits and impacts of DOE fuel cell technology development efforts at the vehicle level

Approach

- Apply vehicle systems analysis expertise and software tools to study the impacts of DOE component technology development programs and a variety of design scenarios
- Develop and link existing component and vehicle models to enhance systems analysis capabilities
- Collect experimental data and models from DOE contractors to validate system model predictions and to provide systems level insights to component developers

Accomplishments

- Completed a series of three technical papers that evaluated how several vehicle and component characteristic parameters could influence the optimal vehicle design for neat and hybrid fuel cell vehicles
- Released a vehicle simulation model, ADVISOR 2002, with a reorganized, configurable subsystem fuel cell model library
- Enhanced fuel cell system thermal network model developed by Virginia Tech based on FutureTruck competition vehicle
- Initiated fuel cell component data collection effort with DOE contractors and received data from several parties
- Contributed to the development of Society of Automotive Engineers (SAE) recommended practice for measuring fuel economy and performance of a fuel cell hybrid electric vehicle

Future Directions

- Optimize fuel cell hybrid vehicle system, considering a variety of energy storage options and system operating characteristics, including fuel cell idling and start-up/shut-down
- Continue to collect available data and models from fuel cell program contractors to enhance modeling capabilities
- Evaluate options for enhancing fuel cell system performance and reducing cost in a vehicle application

- Complete the enhanced fuel cell system thermal model under development at Virginia Tech
- Work with industry partners to validate model predictions and perform studies that support fuel cell technology introductions

Introduction

The U.S. Department of Energy has supported the development of vehicle and subsystem computer models to provide research and development program guidance for promising future research directions and to evaluate applications of existing advanced technologies. The vehicle simulation model ADVISOR (Advanced Vehicle Simulator) has been developed and is supported by the staff of the National Renewable Energy Laboratory. The model uses the MATLAB/Simulink programming environment and has an easy-to-use graphical user interface. ADVISOR is used mainly for target setting, systems analysis, and optimization.

In this project, ADVISOR was used to simulate different fuel cell vehicle design scenarios and to quantify the impacts of several influential parameters. The effects of designing for a specific drive cycle were analyzed. Likewise, vehicle scenarios for optimal fuel economy were derived for vehicles with a range of fuel cell system performance attributes. These studies have established the groundwork for future studies to be performed based on existing and planned technology deliverables in the DOE Fuel Cells for Transportation Program.

Approach

This analysis effort has focused on two areas: 1) model enhancement and validation with data collected from DOE contractors and 2) application of the model to understand some of the design trade-offs associated with fuel cell vehicles. The approach has been to work closely with industry partners to ensure that the models are accurate, to focus on appropriate systems issues, and to disseminate the study results in peer reviewed forums when possible.

Results

Data Collection and Analysis

The vehicle systems modeling tools can be used to understand the impacts, specifically on fuel economy and performance, of single or multiple component characteristics. Characteristic performance data will be collected from the several DOE contractors working on developing technologies for fuel cell systems. The data being requested includes attributes like the fuel cell polarization curve, the load vs. flow rate for an air compressor or compressor/expander unit, or the fuel usage vs. the net power out of the complete system.

After the component data has been imported into ADVISOR, a variety of studies can be performed. For example, if the use of a different catalyst improves a portion of the polarization curve but has no impact on other operating regions, does this have any impact on the overall vehicle performance? Such questions as “under what design scenarios will a change have an impact and what is the value of the impact?” can be investigated.

Data has been collected from several air compressor suppliers and from a fuel cell system supplier. The air compressor data provides realistic inputs to estimate the parasitic load placed on the fuel cell stack for pressurized operation. The fuel cell system data is being used to investigate several options to overcome the start-up issues of current fuel cell systems.

Fuel Cell Vehicle Optimization Studies

At the vehicle systems level, there are thousands of interacting parameters that can influence the performance of a fuel cell vehicle. ADVISOR makes the task of quantifying the impacts of these parameters easier. However, studies that go beyond one or two parameters are difficult to do through manual iteration. Optimization tools have been incorporated into ADVISOR by NREL to automate the process of multi-dimensional analysis of fuel cell hybrid vehicles.

Two fuel cell vehicle analysis studies have been completed using ADVISOR and optimization techniques. In both studies, the optimizer was allowed to vary component parameters including fuel

cell peak power, the motor peak power, the battery power, and the battery capacity. In addition, the optimizer was allowed to adjust energy management parameters including minimum and maximum fuel cell power settings, minimum off time for the fuel cell, and the maximum charge power to be requested from the fuel cell. In each case, the vehicle was required to meet or exceed a set of performance constraints that were derived from the comparable baseline conventional vehicle. The performance constraints are summarized in Table 1.

Type	Description	Condition
Acceleration	0-96.5 km/h (0-60 mph)	<= 11.2 s
	64-96.5 km/h (40-60 mph)	<= 4.4 s
	0-137 km/h (0-85 mph)	<= 20.0 s
Gradeability	@ 88.5 km/h (50 mph) for 20 min. at Curb Weight + 5 passengers and cargo (408 kg)	>= 6.5%
Drive Cycle	Difference between drive cycle requested speed and vehicle achieved speed at every second during the drive cycle	<= 3.2 km/h (2 mph)
SOC Balancing	Difference between final and initial battery state of charge	<= 0.5%

Table 1. Performance Constraints for Fuel Cell Vehicle Studies

In the first study, optimal component and control strategy parameters were derived to provide the best fuel economy on 4 individual drive cycles. The drive cycles included

- Comp. - City/Highway composite, a weighted value composed of the results of one highway cycle and one Federal Test Procedure (FTP) cycle
- US06 – high speed, high acceleration rate profile to be used in the U.S. Environmental Protection Agency Supplemental Federal Test Procedure (SFTP)
- NEDC – New European Drive Cycle including both low speed urban and high speed highway driving
- 1015 - Japan 1015 Mode Cycle, representing congested urban driving typical in Japan.

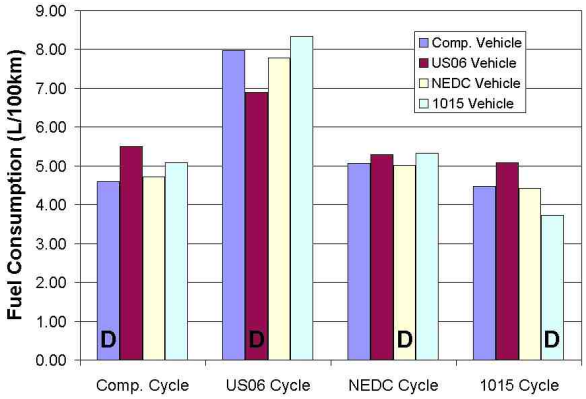

Figure 1. Fuel Consumption of Fuel Cell Vehicles Over Both On- and Off-Design Drive Cycles

The four optimized vehicles were then simulated over the other three cycles. The fuel consumption results are summarized in Figure 1. In all cases, the vehicle designed for the cycle (indicated with a "D") was better (lower fuel consumption) than all other vehicles over the drive cycle for which it was designed. Additionally, it was observed that the vehicle designed for the NEDC cycle was always the next best vehicle over the off-design cycles. This indicates that designing for the NEDC provides a reasonable vehicle design that is robust to variance in fuel economy.

It was assumed in the drive cycle study that the fuel cell system could respond to a transient power request from 10-90% peak power in 2 seconds, based on current DOE R&D Plan technical targets. In the follow-on study, all other assumptions were held the same while the transient power response capability was varied between 0 seconds (fast response, i.e. direct hydrogen) to 40 seconds (slow response, i.e. gasoline reformed system). Again the optimizer was allowed to vary the component sizes and the energy management parameters to find the design scenario that provided the best fuel economy while satisfying the performance constraints.

Figure 2 summarizes the key results of the response time study. It provides the vehicle fuel economy (squares) and the fuel cell specific power (triangles) data for three vehicle designs, an ICE conventional vehicle, a neat (no energy storage) fuel cell vehicle, and a fuel cell hybrid vehicle. The key conclusion to be drawn from these results is that the

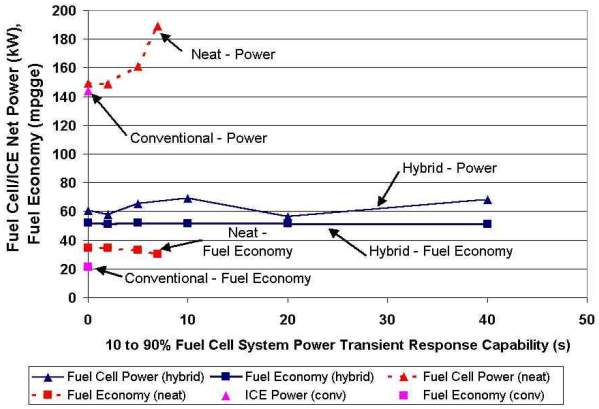

Figure 2. Impacts of Transient Response Capability for Hybrid and Neat Fuel Cell Vehicles on Combined City/Highway Driving Fuel Economy

flexibility of a hybrid design can be used to provide the same fuel economy performance independent of the fuel cell system response capability. However, as response time increases (the fuel cell system responds more slowly) the size of the fuel cell system grows rapidly, and the fuel economy begins to decline significantly in the case of a neat fuel cell vehicle. The neat option does provide about a 65% fuel economy improvement over a conventional internal combustion engine vehicle. An additional 50% improvement over the neat fuel cell vehicle case is available through regenerative energy and other techniques when the fuel cell vehicle is hybridized.

Conclusions

The results of the fuel cell vehicle optimization studies completed this year have contributed substantially to the bulk of knowledge on fuel cell vehicle design for both neat and hybrid design scenarios. It was concluded that the drive cycle can have a significant influence on the optimal design and that designing for the NEDC cycle actually provides a fairly robust vehicle design. Additionally, it was observed that hybridization provides substantial benefits and flexibility in overcoming possible shortfalls in fuel cell system performance caused by slow transient response capability.

A data collection effort was initiated with fuel cell program partners. Component data, including polarization curves, fuel cell system efficiency, air compressor loads, and system response characteristics have been collected. The experimental data and predictions are being used to 1) validate the existing models and 2) quantify the system level benefits of the technology developments and the progress being made toward satisfying the DOE technical targets.

Publications/Presentations

1. Markel, T.; Wipke, K. "Optimization Techniques for Hybrid Electric Vehicle Analysis Using ADVISOR." Proceedings of ASME International Mechanical Engineering Congress and Exposition. New York, New York. November 11-16, 2001.

2. Markel, T.; Wipke, K.; Nelson, D. "Vehicle System Impacts of Fuel Cell System Power Response Capability." *SAE Future Car Congress*. Arlington, Virginia. June 3-6, 2002.

3. Wipke, K.; Markel, T.; Nelson, D. "Optimizing Energy Management Strategy and Degree of Hybridization for a Hydrogen Fuel Cell SUV." *18th International Electric Vehicle Symposium*. Berlin, Germany. October 20-24, 2001.

IV.A.4 Cost Analyses of Fuel Cell Stack/Systems

Eric J. Carlson (Primary Contact) and Dr. Johannes H.J. Thijssen
TIAX LLC
Acorn Park
Cambridge, MA 02140-2390
(617) 498-5903, fax: (617) 498-7012, e-mail: carlson.e@tiax.biz

DOE Technology Development Manager: Nancy Garland
(202) 586-5673, fax: (202) 586-9811, e-mail: Nancy.Garland@ee.doe.gov

ANL Technical Advisor: Robert D. Sutton
(630) 252-4321, fax: (630) 252-4176, e-mail: sutton@cmt.anl.gov

Objective

- To develop an independent cost model for proton exchange membrane fuel cell (PEMFC) systems for transportation applications and to assess cost reduction strategies for year 2000 to 2004 development programs.

Approach

- In the first two years, develop a baseline system configuration and cost estimate based on best available and projected technology and manufacturing practices, and assess the impact of potential technology developments on system cost reduction
- In the subsequent four years, annually update the baseline cost model and system scenarios based on assessments of developments in PEMFC system technologies and manufacturing processes.

Accomplishments

- Assessed the potential for reductions in platinum loading by conducting an electrochemical kinetic analysis of the impact of catalyst loading, temperature, and pressure on polarization of the cathode.
- Developed future cost projections for reformer and direct hydrogen systems.

Future Direction

- Develop projections of future system performance and cost based on continued industry feedback, alternative system scenarios, and projected technology developments.

Introduction

In 1999, a baseline cost estimate for a 50 kilowatt (kW) PEMFC system for passenger vehicles was developed based on technology available in the Year 2000, using a high production volume scenario (i.e., 500,000 units per year). In Year 2000, we solicited feedback from system and component developers on the system configuration, design and performance parameters, and manufacturing process and costing assumptions. The impact of alternative system design approaches were also assessed, including the impact of sizing the stack at the high power point rather than 0.8 volts, and the impact of hybridization, i.e., reducing or increasing rated power, on the fuel cell system power cost ($/kW). In Year 2001, we focused on the development of future costs based on projected technology. In 2002, an electrochemical model for the relationship between catalyst loading, temperature, pressure, and power density was combined with the cost model to understand the tradeoffs between catalyst loading

and cost of the stack. The cost model was used to develop projections for direct hydrogen fueled systems.

Approach

The factors influencing platinum loading were assessed to develop an estimate of future fuel cell stack cost for reformate and hydrogen systems. Projections of minimum platinum requirements were estimated based on an analysis that considered:

- Impact of catalyst particle size and catalyst activity on kinetics
- Impact of electrolyte adsorption on catalyst kinetics
- Development of polarization curves based on electrochemical kinetics
- Impact of ohmic resistance losses on polarization curve

The assumption of relatively high unit cell voltages (e.g., 0.8 volts) to achieve overall system efficiency targets simplified the analysis because cathode kinetics then dominate the voltage losses within the stack. Tafel kinetics were used to assess the effect of operating conditions and cathode voltage losses. Voltage drops were then assigned to the anode and ohmic components based on experimental data.

The polarization curves and functional relationships between platinum loading and performance were then combined with the stack cost model to assess the relationship between platinum loading and materials cost. Several overall assumptions are important to understanding the basis of the analysis. First, we assumed the performance of the catalyst is not limited by diffusion, the structure of the electrode, or the dispersion of the catalyst. In the early days of PEMFC development, significant performance gains were made while significantly decreasing the catalyst loadings. In our analysis, reduction in platinum loading leads to lower power density. Second, introduction of ohmic resistance losses into the analysis reduces the power density that can be achieved by increasing catalyst loading or by decreasing the cell voltage. Voltage losses across the ohmic resistances (I^2R) in the system reduce the voltage available to perform useful work at the electrodes. Third, in the baseline cost estimate, the fuel stack materials represent over 90% of the stack cost. Consequently, in the following analysis, we only consider the cost of materials in the stack (i.e., MEA, gas diffusion layer, and bipolar plate). The assumptions used to make the future projections are summarized in Table 1.

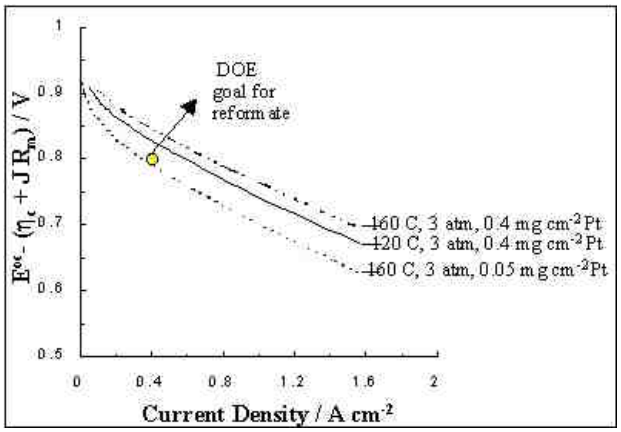

Figure 1. Polarization Curve at Different Temperatures and Platinum Loadings at 3 Atmospheres and with 3.5 nanometer Catalyst Particle Size

Table 1. Assumptions Used to Project Future Fuel System Costs

Parameter	Baseline	Future Reformate	Future Hydrogen
Stack Improvements			
◆ Current Density (mA/cm^2)	310	500	750
◆ Cathode Pt (mg/cm^2)	0.4	0.2	0.2
◆ Anode Pt (mg/cm^2)	0.4	0.2	0.1
◆ Anode Ru (mg/cm^2)	0.2	0.0	0.0
◆ Stack Temperature (° C)	80	160	160
Fuel Processor Improvements	◆ ATR ◆ Sulfur bed ◆ PrOX ◆ Year 2000 Cost Study Parameters	◆ Short contact time reactor ◆ Improved shift catalysts ◆ No sulfur bed ◆ No PrOX	◆ No fuel processor ◆ Compressed H_2 storage ◆ Simplfied tailgas burner
System and Material Cost Reduction		Reduced Sensor, CEM, and Membrane costs	

Results

Figure 1 shows polarization curves generated for different platinum loadings and temperatures assuming 3.5 nanometer catalyst particle size and 3 atmospheres pressure. The DOE fuel cell target for current density and voltage is highlighted by the circle. The polarization curve for the stack must lie above this circle to allow for additional voltage losses from the electrolyte, bipolar plates, and anode.

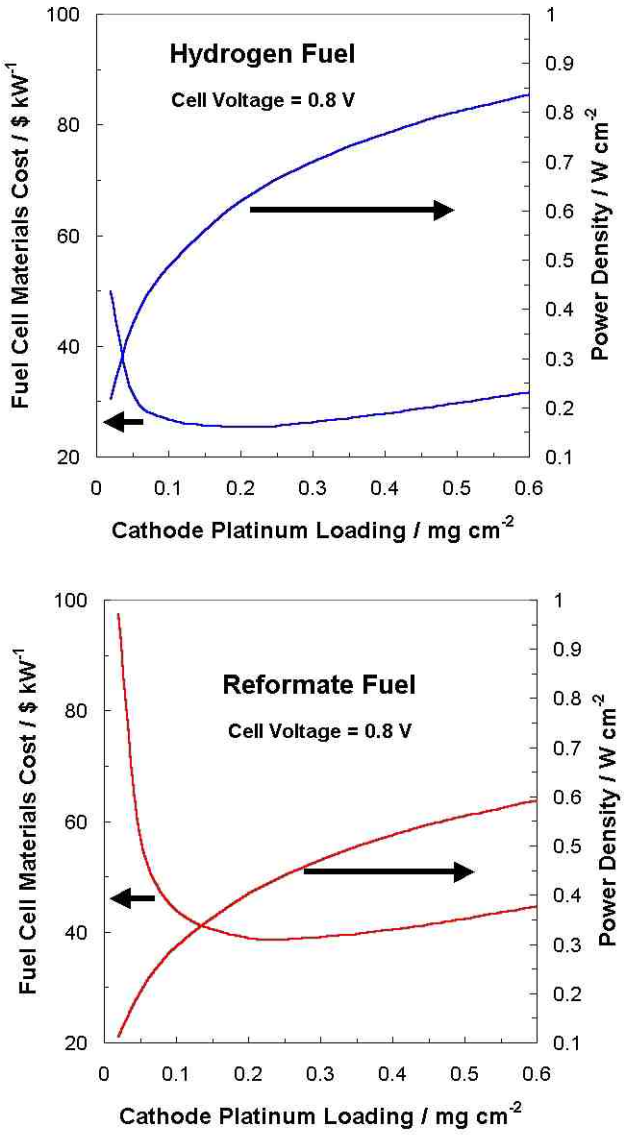

Figure 2. Fuel Cell Stack Material Cost versus Cathode Platinum Loading

Figure 2 shows the material cost ($/kilowatt electrical [kWe]) versus cathode platinum loading for stacks operating at 3 atmospheres, 160°C, and 0.8 volts with direct hydrogen and reformate. Assumptions in this analysis include use of an alloy catalyst having a kinetic activity two times that of platinum, a unit cell resistance of 0.1 ohm centimeter squared (cm^2), and an anode catalyst loading equal to one half the cathode loading.

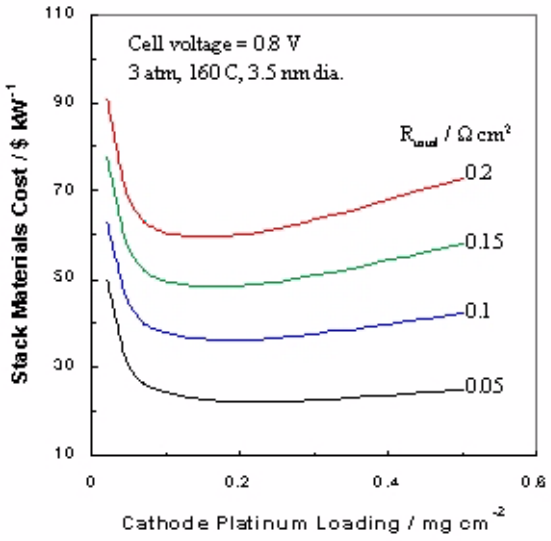

Figure 3. Impact of Ohmic Resistance on the Cost versus Platinum Loading Relationship

The analysis produced an "L" shaped curve where material costs rise sharply at low platinum loadings (low power density) and then show weak dependence with increasing platinum loading. Figure 3 shows the flat portion of the curve for various values of ohmic resistance. Independent of the resistance value, all of the curves have a minimum cost in the region of 0.1 to 0.3 mg/cm^2.

Figure 4 shows the cost projections for the future system scenarios. The contribution of precious metal cost to each system is broken out separately to highlight its impact on system cost. This analysis compares the cost of reformate and direct hydrogen systems on a 50 kWe basis. In practice, the lighter weight of direct hydrogen systems will produce equivalent vehicle performance (e.g., acceleration, hill climb) at lower net system power. The higher efficiency of the hydrogen system may also lead to operation of the stack at lower voltages (higher power density) leading to lighter, less costly stacks. Hence, the cost of the hydrogen system could be reduced further relative to the reformate system.

Conclusions

The analysis of minimum platinum loading and projection of cost for future scenarios provided several important insights, including:

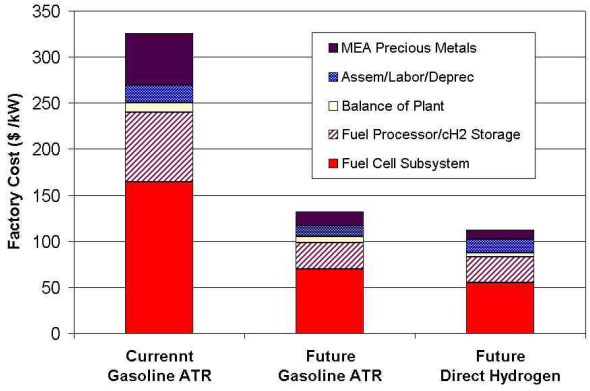

Figure 4. Projections of Future Reformate and Direct Hydrogen System Costs for a 50 kW System Produced in Large Volume (500,000 units per year)

- Analysis of a series of scenarios involving catalyst loadings, pressures, and temperatures led to the conclusion that the stack would have to operate at high temperature (e.g., 160^{o}C) and elevated pressure (e.g., 3 atmospheres) to satisfy DOE fuel cell power density (kW/cm^{2}) goals.

- The cost of non-active materials (gas diffusion layer, membrane, and bipolar plates) dominate stack cost at very low platinum loadings, while ohmic losses limit the benefit of increasing platinum loading beyond some point.

- The future fuel system costs presented here are significantly lower than earlier cost estimates based on near-term technology. However, the projected costs for reformate and hydrogen systems are still higher than FreedomCAR goals of $45/kWe. The direct hydrogen system is closest to the FreedomCAR target, but it will need technology advances in high temperature membranes and further reduction in material and component costs to achieve the cost goals.

IV.B Stationary Power Systems

IV.B.1 Alkaline Fuel Cell Development

Timothy Armstrong (Primary Contact), Dane Wilson, Lynn Klett
Oak Ridge National Laboratory
PO Box 2008
Oak Ridge, TN 37831-6084
(865) 574-7996, fax: (865) 574-4357, e-mail: armstrongt@ornl.gov

Wayne Smith (Primary Contact)
Los Alamos National Laboratory
PO Box 1663
Los Alamos, NM 87545
(505) 667-2635, fax: (505) 665-4292, e-mail: wsmith@lanl.gov

DOE Technology Development Manager: Nancy Garland
202-586-5673, fax: (202) 586-9811, e-mail: Nancy.Garland@ee.doe.gov

Objectives

- Jointly develop alkaline fuel cell research and development (R&D) roadmap
- Improve existing alkaline fuel cell anode by eliminating platinum
- Improve power density of alkaline fuel cell

Approach

- Address needed improvements in current technology and propose research breakthrough technologies based on evaluation of all existing alkaline fuel cell documentation and company site visits
- Evaluate new polymer-based hydroxyl conducting membranes
- Determine CO_2 tolerance of other aqueous and molten salt based alkaline electrolytes
- Evaluate new anode catalysts to promote high efficiencies and operating temperatures
- Develop high conductivity composite bipolar plates to allow high power density designs to be developed

Accomplishments

- Draft R&D roadmap completed in August 2002

Future Directions

- Evaluate new polymer-based hydroxyl conducting membranes
- Determine CO_2 tolerance of other aqueous and molten salt based alkaline electrolytes
- Evaluate new anode catalysts for high efficiencies and operating temperatures
- Develop high conductivity composite bipolar plates to allow high power density designs to be developed

Introduction

Alkaline fuel cells are potentially the lowest cost fuel cell due to the materials and manufacturing processes used to make them. They are efficient (51% system), restorable (replacing the electrolyte restores output to near new), and recyclable. The reliability of alkaline fuel cells has been demonstrated convincingly over 30 years of service in space missions. The new low-cost alkaline fuel cells being developed by other manufacturers are equally reliable but at a fraction of the cost. They are fabricated from relatively inexpensive components and catalysts, and can be manufactured using simple production techniques in an inexpensive factory. Their low cost, even in small volume production, will enable the alkaline fuel cell to be used in niche markets (i.e., peaking and/or stationary power) before the mass production envisioned for other fuel cell types (proton exchange membrane [PEM], solid oxide fuel cell [SOFC]) brings the price of these technologies to a competitive level. However, additional development is needed to improve the sensitivity of alkaline fuel cells to atmospheric CO_2, increase their efficiency, and to improve their power density.

Approach

This is a new project initiated in early spring 2002. The initial goal is to develop an understanding of the development needs of alkaline fuel cells through visits to developers and by analysis of published records and literature. Upon completion of this analysis, development of critical materials or components will commence with the emphasis on advancing current alkaline technology. To obtain higher temperature, higher power density cells and stacks in the future.

Results

A collaborative laboratory effort between Oakridge National Laboratory and Los Alamos National Laboratory has recently been undertaken to evaluate the alkaline fuel cell literature and develop a research and development program plan. To date, the team evaluated the literature and drafted a review of the state-of-the-art. Based on this and input from industrial participants, a research plan is being drafted and will be presented to the Office of Hydrogen, Fuel Cells and Infrastructure Technologies in August 2002.

IV.B.2 Development of Advanced, Low-Cost PEM Fuel Cell Stack and System Design for Operation on Reformate

Michel Fuchs
Teledyne Energy Systems, Inc.
1501 Northpoint Parkway, #101
West Palm Beach, FL 33407
(561) 688-0506 x239, fax: (561) 688-0766, e-mail: michel.fuchs@teledynees.com

DOE Technology Development Manager: Donna Ho
(202) 586-8000, fax: (202) 586-9811, e-mail: Donna.Ho@ee.doe.gov

ANL Technical Adivsor: William Swift
(630) 252-5964, fax: (630) 252-4176, e-mail: Swift@cmt.anl.gov

Objectives

- Design and demonstrate a reformate-capable fuel cell stack, utilizing CO-tolerant membrane electrode assemblies (MEAs) and low cost bipolar collector plates.
- Design, integrate and demonstrate a natural gas fueled 7-kW_{net} fuel cell power plant.

Approach

- Phase I: Demonstration and delivery of a PEM ten cell stack with reformate capability and ten additional bi-polar plates manufactured by the compression molding process.
- Phase II: Demonstration and delivery of a high efficiency reformate tolerant 7-kW_{net} fuel cell stack and power plant utilizing molded bipolar plates and natural gas fuel processor to Argonne National Laboratory for independent testing and verification.

Accomplishments

- Built and operated a 3-kW_{net} fuel cell power plant with integrated natural gas reformer.
- Began construction of second 3-kW_{net} fuel cell power plant with advanced features and controls.
- Built and tested reformate tolerant 60-cell 5.0-kW_{gross} Teledyne Perry NG2000 stack.
- Have accumulated over 2500 hours of 10-cell stack operation on synthetic reformate.
- Developed control architecture capable of compensating for reformer response and effectively meeting transient power demands.
- Developed system design that utilizes improvements generated from 3-kW_{net} plant testing.
- Established design criteria to achieve neutral water balance.

Future Directions

- Develop a 7-kW_{net} fuel cell system with integrated natural gas fuel processor.
- Continue evaluations of new MEA materials for optimal reformate performance and longevity.
- Fabricate, assemble and test 7-kW_{net} power plant and prepare it for delivery.

Introduction

Current work is associated with the development of a 7-kW_{net} fuel cell power plant with integrated natural gas reformer based on Teledyne Energy Systems's 3-kW_{net} prototype stationary power plant. The development effort will focus on a systems approach broken down into three areas: PEM fuel cell stack, natural gas reformer and integrated system.

Approach and Results

PEM Fuel Cell Stack

Taking into account commercial objectives and goals, a Teledyne Perry NG2000 stack configuration was chosen to meet requirements for the 7-kW_{net} power plant. Two 60-cell stacks rated at 5.0-kW_{gross} (Figures 1 and 2), electrically connected in parallel, will be utilized to meet total power demands.

The NG2000 has an active area size of 300 cm^2 and is designed to operate on pure hydrogen or reformate, e.g. 45% H_2, 35% N_2, 20% CO_2, 10 ppm CO. The MEAs are designed for continuous operation with CO concentrations of 10 ppm and can tolerate transients approaching 100 ppm. Excellent cell-to-cell consistency has been demonstrated throughout the stack's operating range (Figure 3). Running on reformate, the NG2000 can be scaled to meet a variety of power requirements from 360-W to 10-kW_{gross}.

The NG2000 is capable of operating between 0.2 and 3 atm and up to 70°C. Tables 1 and 2 show specifications and capabilities of the 60-cell stack respectively. Ongoing work is focused on attaining 10,000 hours of operation in the near-term with a final objective of 40,000 hours. So far over 2500 hours of continuous operation has been demonstrated on a 10-cell NG2000 stack running on synthetic reformate.

A duplicate of the 60-cell stack that will be used in the power plant was recently constructed and then tested on synthetic reformate. Figures 4 and 5 show the performance of the stack on hydrogen and synthetic reformate respectively. Operating on reformate, the 60-cell exhibits near pure hydrogen performance.

In situ evaluation of a 60-cell stack was demonstrated in Teledyne Energy Systems's 3kW_{net}

Figure 1. Teledyne Perry NG2000 60-Cell Stack

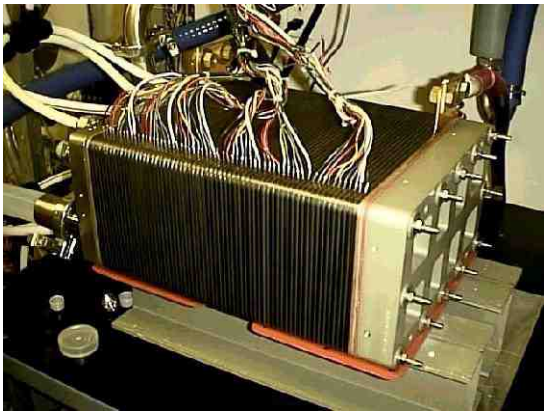

Figure 2. Teledyne Perry NG2000 60-Cell Undergoing Testing

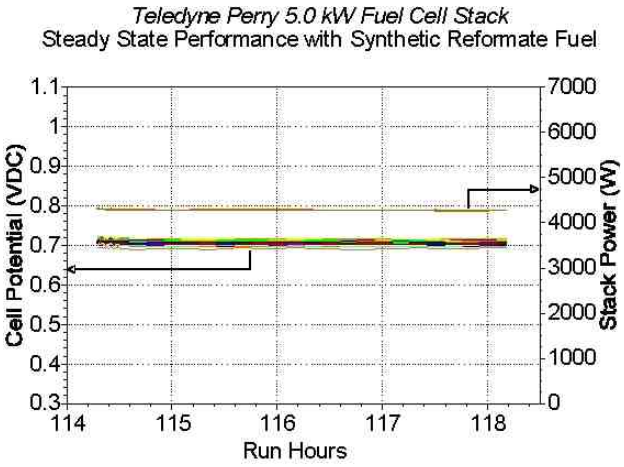

Figure 3. Teledyne Perry NG2000 60-Cell Steady-State Performance with Synthetic Reformate

prototype stationary power plant which incorporated a 7-kW natural gas reformer (Figure 6).

Table 1. Teledyne Perry, NG2000 60-Cell Stack Specifications

Reactants:	Air/Reformate
Active area	292 cm^2
Operating volt. range	38-57 V
Operating pressure	0.2 to 3.0 atm.
Operating temperature	60 to 70°C
Stack volume	21.2 Liters
Stack weight	50 kg

Table 2. Teledyne Perry, NG2000 60-Cell Stack Performance

Max cont. power	5.4-kW @ 38 VDC
Power density	255 W/L
Reformate composition as tested	45% H_2, 35 % N_2, 20% CO_2, 10 ppm CO

Reformer

A 10-kW natural gas fuel processor will be integrated into the power plant. The processor is capable of starting up and producing fuel cell quality reformate in less than 60 minutes. Furthermore, it is able to transition from minimum power to full power (2 kW to 10 kW) in less than 60 seconds. The reformer is a larger version of the unit used in the 3-kW_{net} stationary plant, which has demonstrated good transient response and low CO output (less than 50 ppm throughout its operating envelope).

Integrated System

The 7-kW_{net} system will consist of the fuel cell, reformer and ancillary systems. The final packaged system will be optimized for laboratory use and outfitted with an extensive, PC based, data acquisition system.

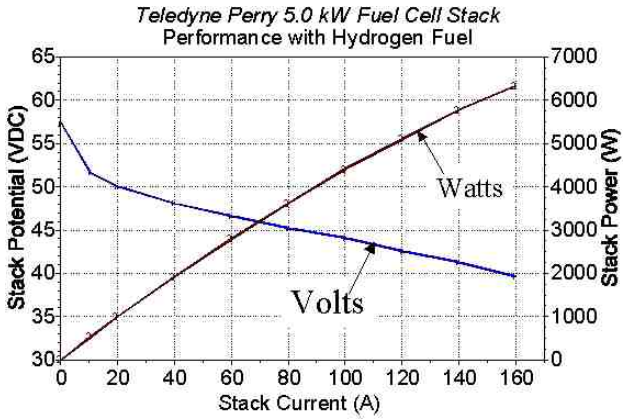

Figure 4. Teledyne Perry NG2000 60-Cell Performance with Hydrogen Fuel

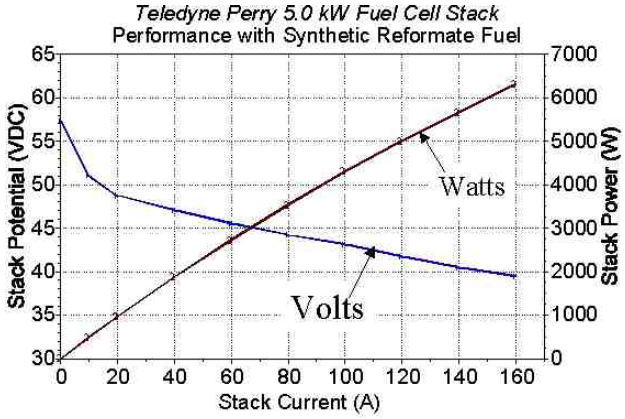

Figure 5. Teledyne Perry NG2000 60-Cell Performance with Synthetic Reformate Fuel

To compensate for the response of the fuel processor, a control architecture was developed to allow a battery system to provide for peak power demands. The power plant has been designed to maintain the batteries' state of charge at an optimal level while the batteries provide the capacitance necessary to meet any load topography. In this configuration, the transient-following capabilities of the power plant are greatly enhanced.

The ancillary systems are designed to track the load demands placed on the power plant. For instance, compressors, pumps and fans will be operated to provide only the conditions necessary to allow the stack to meet a given power demand. This will enable optimal efficiency to be maintained at all operating conditions.

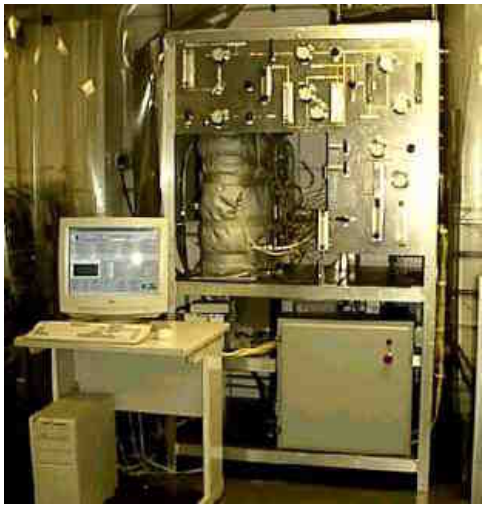

Figure 6. 7-kW Reformer Test Stand

A model based on the performance on the 3-kW_{net} stationary power plant was developed to assist in designing the 7-kW_{net} system. Table 3 shows results obtained from the model at various operating conditions.

Table 3. 7-kW_{net} Fuel Cell Power Plant Model Results

Parameter	@ 7kW_{net}	@ 5kW_{net}	@ 2kW_{net}
Stack array pwr	9.2 kW	6.5	2.7
Stack array volt	41.1 V	43.9 V	47.8 V
Ancillary load	2.2 kW	1.5 kW	0.7 kW
Stack thermal Eff. (LHV)	55%	58%	63%

Sensitive to the necessity to reduce costs critical to the successful commercialization of fuel cell technology, a concerted effort has been placed on designing a system that is as simple as possible and that strives to implement components from well established industries, e.g. automotive and appliance.

Conclusion

Teledyne Energy Systems, Inc. will construct a 7-kW_{net} stationary fuel cell power plant that will utilize natural gas and enable an in-depth evaluation of a fuel cell and reformer package. The design of the system will be based on Teledyne Energy Systems's commercially oriented 3-kW_{net} stationary product, which is currently under development.

Presentations/Publications:

1. M. Fuchs, F. Barbir and M. Nadal, "Performance of Third Generation Fuel Cell Powered Utility Vehicle #2 with Metal Hydride Fuel Storage", presented at the 2001 European Polymer Electrolyte Fuel Cell Forum, Lucerne, Switzerland, July 2001

2. F. Barbir and J. Braun, "Development of Low Cost Bi-Polar Plates for PEM Fuel Cell", Proc. Fuel Cell 2000 Research & Development, Strategic Research Institute Conference, Philadelphia, PA, September 2000

3. M. Fuchs, F. Barbir and M. Nadal, "Fuel Cell Powered Utility Vehicle with Metal Hydride Fuel Storage", presented at the GlobeEx 2000 Conference, Las Vegas, NV, July 2000

4. F. Barbir, "Recent Progress and Remaining Technical Issues in PEM Fuel Cell Development", submitted to the World Hydrogen Energy Conference, WHEC XIII, Beijing, China, June 2000

5. F. Barbir, "Air, Water and Heat Management in Automotive Fuel Cell Systems", presented at the Intertech Conference Commercializing Fuel Cell Vehicles 2000, Berlin, Germany, April 2000

6. M. Fuchs, F. Barbir, A. Husar, J. Neutzler, D. Nelson and M. Ogburn, "Performance of Automotive Fuel Cell Stack", presented at the 2000 Future Car Congress, Arlington, VA, April 2000

7. F. Barbir, "Bi-polar Plates, Flow Fields and Stack Design Criteria", presented at the American Physical Society Meeting, Minneapolis, MN, March 2000

8. F. Barbir, M. Fuchs, A. Husar and J.Neutzler, "Design and Operational Characteristics of Automotive PEM Fuel Cell Stacks", Fuel Cell Power for Transportation, SAE SP-1505, Proc. SAE International Congress & Exhibition, Detroit, March 2000, pp. 63-69, SAE, Warrendale, PA, 2000

9. V. Gurau, F. Barbir and H. Liu, "An Analytical Solution of a Half-cell Model for PEM Fuel Cells", Journal *of Electrochemical Society*, Vol. 147(7), 2000

IV.B.3 Proton Exchange Membrane Fuel Cell Power System on Ethanol

Ahmed Amrani (Primary Contact), Thomas Richards
Caterpillar Inc.
Technical Center, P.O. Box 1875
Peoria, Illinois 61656 - 1875
(309) 578-3913, fax: (309) 578-9900, e-mail: Amrani_Ahmed@cat.com

DOE Technology Development Manager: Kathi Epping
(202) 586-4725, fax: (202) 586-9811, e-mail: Kathi.Epping@ee.doe.gov

ANL Technical Advisor: William M. Swift
(630) 252-5964, fax: (630) 972-4473, e-mail: swift@cmt.anl.gov

Main Subcontractors: Nuvera Fuel Cells, Cambridge, Massachusetts; Williams Bio-Energy, Pekin, Illinois

Objectives

- Caterpillar, Nuvera Fuel Cells, and Williams Bio-Energy have teamed up to develop and demonstrate a 15 kilowatt (kW) ethanol-fueled proton exchange membrane (PEM) fuel cell system. The primary objectives of this project are to:
  - Demonstrate performance, durability and reliability
  - Remove technical uncertainties
  - Understand correlation and reduce gaps between stationary and transportation application
  - Collect data to evaluate economic feasibility
  - Assess commercial viability of total system

Approach

- Nuvera will assess and modify advanced fuel cell power module designs that are now under development in separate projects to develop the power module for this project.
  - Caterpillar will design the power converter module and will integrate the system.
  - Williams will supply the ethanol and host the site to test the unit and conduct endurance testing.

Accomplishments

- A preliminary design review between Nuvera, Williams and Caterpillar took place May 20 - 21, 2002.
- Power module design specifications have been completed.
- The ethanol reformer has been tested for a short period of time at rated power.
- The fuel cell stack has been tested for a short period of time at ¼ rated power with output from the reformer.
- Power converter specifications have been completed.
- The design and release of the power converter is near completion.
- Preliminary site specifications exist and a safety codes and standards review has been scheduled.

Future Directions

- Prepare and conduct a final design review with cooperative team and sponsors
- Conduct independently the functional test of both the power module and the power converter. This is targeted for January-February 2003.
- Prepare the test site building, which will be the endurance-testing place for the fuel cell system. This is targeted to be completed in the January 2003 time frame.
- Ship the functional unit to the test site and start the endurance-testing phase. This is targeted to start in February 2003.

Introduction

Nuvera will design, build, test, and deliver a 15 kilowatt electrical (kWe) direct current (DC) fuel cell power module that will be specifically designed for stationary power operation using ethanol as a primary fuel. Two PEM fuel cell stacks in parallel will produce 250 amps and 60 volts at rated power. The power module will consist of a fuel processor, carbon monoxide (CO) clean-up, fuel cell, air, fuel, water, and anode exhaust gas management subsystems. A state-of-the-art control system will interface with the power system controller and will control the fuel cell power module under start-up, steady-state, transient, and shutdown operation. Temperature, pressure, and flow sensors will be incorporated in the power module to monitor and control the key system variables under these various operating modes. The power module subsystem will be tested at Nuvera and subsequently be delivered to the Williams Bio-Energy Pekin, Illinois site.

Approach

Nuvera plans to modify advanced fuel cell power module designs that are now under development in separate projects for use in this project. They will start with a power module design that is a multi-fuel, 1 atmosphere, 20 kWe power module designed for transportation (light duty vehicle) applications. The purpose of using this design baseline is twofold.

- By using an existing design, much of the design effort and technical risk associated with a completely new power module design will be avoided.
- By using a transportation-based design, this demonstration will simultaneously illustrate that renewable ethanol can be used in fuel cell power systems applied to stationary power generation as well as transportation.

Caterpillar will design, build, test and deliver a power converter module that converts the DC output of the power module into AC power. Caterpillar will also provide system level control to insure all major subsystems work in harmony and provide constant power (14 kWe) to the industrial load on site. The fuel cell system will add power to the overall power at the Williams Bio-Energy ethanol production site in Pekin, Illinois.

The power converter design will rely on Caterpillar's experience with state-of-the-art solid-state power converters that employ switches, inverters and pulse width modulation to shape a sinusoidal voltage and current in time with the existing power source on site.

Caterpillar also aims to demonstrate technology to the greatest extent possible that can meet the dual requirements of the transportation industry and the stationary electric power generation industry. In addition to low levels of emissions, we intend to demonstrate high efficiency, durability and reliability. These technical objectives will enable us to calculate the cost of electricity ($/kW-hr) for transportation and stationary power applications.

Williams Bio-Energy will host the industrial site for this demonstration. Williams works with Nuvera and Caterpillar to provide them with site electrical load requirements. They will prepare the site to ensure that the fuel cell system links to their power network and will supply ethanol fuel and other utilities. During the demonstration, Williams' personnel will monitor and service equipment and permit visitors to witness the demonstration in comfort and safety.

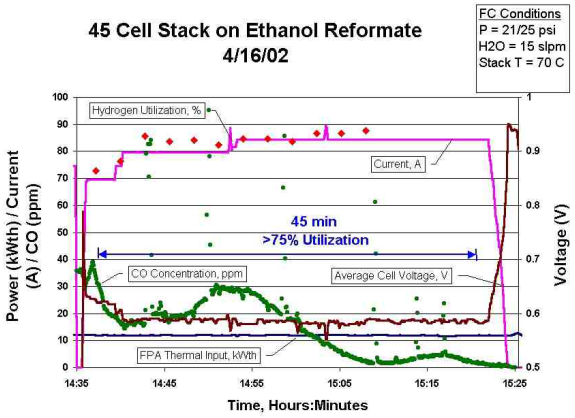

Figure 1. System Level Block Diagram

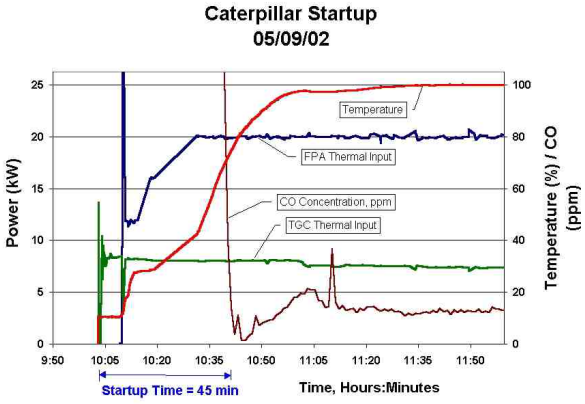

Figure 2. Startup Profile of Reformer System

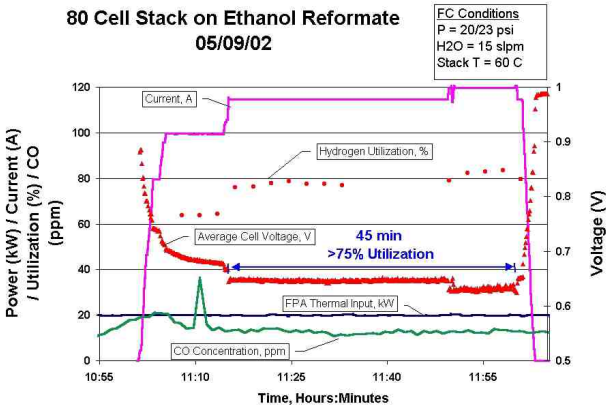

Figure 3. Stack Performance at Full Power Cell Conditions

Results

The cooperative team has demonstrated several milestones.

Power Converter

The overall system block diagram, system level wiring diagram, and power converter diagram have all been finalized. This is depicted in Figure 1. The overall schematic and bill of material have identified the long lead items, which are now being procured. A system level functional specification is being revised with a baseline allowing configuration control and management.

Power Module

Several rig tests to study contaminant formation from ethanol reforming were conducted to finalize the selection of the proper catalyst, and a burner was re-engineered and sized to meet the different power requirement.

Cold start testing of the reformer using ethanol was completed at half power and operability of the reformer using new sensors and controllers was demonstrated at full power, resulting in reformate with less than 20 parts per million CO and with 37% of hydrogen (H_2) under stable condition. (See Figures 2 and 3.)

A 45-stack baseline system test (fuel cell stack and reformer) was conducted to demonstrate stability and high H_2 utilization (75%-80%). This was followed by an 80-stack design test at full power for over 45 minutes, resulting in high H_2 utilization. Cold start of the reformer without afterburner was completed.

The overall process and instrumentation diagram as well as the interface diagram are now completed.

Conclusions

A preliminary design review was held at Nuvera in Cambridge on May 20, 2002, focusing on refining the project plan with milestones, target critical design review dates and visiting the existing building where the fuel cell system will be hooked up and tested.

Also reviewed were the power converter and module specifications, power topology, power flow requirement, a common data acquisition system, the different control flow charts, the system wiring diagrams, and the different protocols for data acquisition and monitoring.

The cooperative team has also established a common FMEA (Failure Mode Evaluation and Analysis) system using the power converter FMEA from Caterpillar as a template, and expanding this approach to define a preliminary HazOps analysis to be conducted in the future.

At this phase no technical hurdles are anticipated. Future actions include conducting a safety design review (HazOps analysis), establishing an activity-based target date for a critical design review, and generating a system level functional specification document which will help define the research boundaries for this project.

Procurement of critical long lead hardware will continue. This will allow a sound forecasting in planning the shakedown testing of the power module and the power converter separately. The unit will be then assembled and ready for the endurance testing.

IV.B.4 Fuel Cell Distributed Power Package Unit: Fuel Processing Based on Autothermal Cyclic Reforming

George Kastanas, Court Moorefield, Parag P. Kulkarni, Shawn Barge, Vladimir Zamansky, Ravi Kumar (Primary Contact)
GE Energy and Environmental Research Corporation
General Electric Company
18 Mason
Irvine, CA 92618
(949) 859-8851 ext.159, fax: (949) 859-3194, e-mail: ravi.kumar@ps.ge.com

DOE Technology Development Manager: Kathi Epping
(202) 586-7425, fax: (202) 586-9811, e-mail: Kathi.Epping@ee.doe.gov

Goals and Objectives

- The overall goals of the project are to:
  - Design, fabricate and operate a precommercial integrated fuel processor;
  - Create a design for mass manufacturing of the system;
  - Assess the performance of the system in terms of total efficiency, electrical production efficiency, and cogeneration value; and
  - Assess the economics of the design.

- The specific performance objectives of the fuel processor are to:
  - Convert natural gas to a proton exchange membrane (PEM) fuel cell grade hydrogen-rich stream (< 10 ppm CO);
  - Achieve fully automatic operation during normal, start-up, shut-down and stand-by modes;
  - Operate in a fully automatic mode for over 100 hours;
  - Achieve 75% fuel processor efficiency on a higher heating value (HHV) basis; and
  - Achieve a capital cost target that is less than $1000/kW and electricity cost that is less than $0.06/kWh, when the system is mass produced.

Approach

- Design a 50 kW fuel processor capable of producing PEM fuel cell grade hydrogen-rich stream.
- Fabricate and operate a fully automated 50 kW fuel processor capable of operating on natural gas.
- Conduct an economic and manufacturability analysis to reduce costs for the system and to provide information on the high volume manufacturing cost of the fuel processor.

Accomplishments

- Design of 50 kW integrated fuel processor, which includes reformer, shift reactor, steam generator and preferential oxidation reactor.
- Fabrication of reformer, shift reactor, and steam generator.
- Design and programming of automated control system.
- Shakedown of steam generator, valves and feed metering systems
- Preliminary economic analysis.

Future Directions

- Fabricate preferential oxidation reactor.
- Operate and optimize the fully integrated fuel processor.
- Analyze the reliability of the fuel processor.
- Perform a detailed economic analysis.

Introduction

GE Energy and Environmental Research Corporation (GE EER) is developing a PEM fuel cell based distributed power generation (DPG) system. The DPG system uses a proprietary fuel processor to convert fossil fuels to a hydrogen-rich gas for use in the fuel cell. The project is currently in Phase II, which is a demonstration of the integrated fuel processor operating in a fully automatic mode for over 100 hours to continuously generate a PEM fuel cell grade hydrogen-rich stream (<10 ppm CO) with thermal efficiency of 75% on a HHV basis.

GE EER will design, fabricate and operate a pre-commercial integrated fuel processor, develop a design for mass manufacturing of the system, and assess the potential cost and performance.

Approach

A precommercial, integrated 50 kWe fuel processor that can produce a PEM fuel cell grade hydrogen-rich stream will be designed and fabricated. The Autothermal Cyclic Reforming (ACR) and Low Temperature Shift (LTS) technologies that have been successfully demonstrated during the earlier part of the project will be used. In order to reduce the concentration of CO to less than 10 ppm, GE EER will only consider technologies that are commercially available or are close to commercialization. The technologies that are commercially available are Pressure Swing Adsorption (PSA) and Selective Hydrogen Membrane Permeation. The technologies that are in the developmental stage but potentially are near commercialization are Preferential Oxidation (PROX) of Los Alamos National Laboratory and Methanation. The major deliverable will be a report on continuous operation of the fuel processor in fully automatic mode for over 100 hours. An economic analysis will be conducted to identify the opportunities for reducing costs of the system and to provide improved information on the high volume manufacturing cost of the fuel processor.

Figure 1. 50 kW Integrated Fuel Processor

Results, Conclusions, and Future Directions

The autothermal cyclic reformer, LTS reactor, steam generator and desulfurizer have been designed, fabricated and installed on the skid. The desulfurizer absorbs sulfur components from the natural gas upstream of the reformer. A conventional Copper/ Zinc catalyst was selected for the LTS reactor. The PROX reactor, which reduces CO level to less than 10 ppm in the hydrogen-rich gas, has been designed. The PROX catalyst was selected and has been ordered. The skid platform, the flow panels and the feed metering systems have been fabricated. The piping to all vessels has been installed and leak checked. The flow control system, control hardware and independent safety systems have been installed. The automatic control system has been designed and programmed. The shakedown of the steam generator, valves and feed metering systems has been completed. The PROX reactor will be fabricated and the integrated fuel processor will be operated and optimized. The 50 kW fuel processor is shown in Figure 1.

The results to date are highly promising and indicate that the GE reforming technology is on the road to success to meet DOE goals. The fuel processor promises to advance the current state of fuel cell technology and will provide clean hydrogen generation, allowing for distributed reforming at high efficiency, with reduced pollutant emissions, and fuel flexibility, at lower cost. The development and commercialization of ACR-based fuel processors will remove the barriers for fuel cell development, which is presently being stifled by the lack of small scale reformers and the lack of hydrogen distribution systems.

A template for calculating cost of electricity has been developed. The analysis considers efficiency, capital costs, operating and maintenance costs, capital recovery factor, availability, fuel price and other factors. A detailed economic analysis will be performed.

GE EER and GE's Global Research Center (GRC) will analyze the design for reliability (DFR) of the fuel processor. The components that require a design review to reduce capital costs have been identified. DFR templates that have been developed by GRC to record all failures will be used. This data will be analyzed and all identified reliability issues will be addressed during the design of the next system. The DFR plan also includes component testing that will help identify failures of subsystems and components. Information from DFR analysis will be combined with the economic analysis to determine the economic benefits of the advanced fuel processor system.

FY 2002 Publications and Presentations

1. R.V. Kumar, "Autothermal Cyclic Reforming Based Hydrogen Refueling System", IEA Annex XV Fuel Cells for Transportation Meeting, 2002, Sacramento, California.

2. R.V. Kumar, G. Kastanas, S. Barge, V. Zamansky, R. Seeker, "Autothermal Cyclic Reforming Based Hydrogen Refueling System", DOE Annual Hydrogen Program Review, 2002, Golden, Colorado.

3. R.V. Kumar, G. Kastanas, P. Kulkarni, C. Moorefield, S. Barge, V. Zamansky, R. Seeker, "Hydrogen Energy Park Based on Autothermal Cyclic Reforming", Fuel Cell Seminar, 2002, Palm Springs, California.

IV.B.5 Research and Development on an Ultra-Thin Composite Membrane For High-Temperature Operation in Proton Exchange Membrane Fuel Cells

Chao-Yi Yuh (Primary Contact)
FuelCell Energy, Inc.
3 Great Pasture Road
Danbury, CT 06813
(203) 825-6112, fax: (203) 825-6273, e-mail: cyuh@fce.com

DOE Technology Development Manager: Kathi Epping
(202) 586-7425, fax: (202) 586-9811, e-mail: Kathi.Epping@ee.doe.gov

Main Subcontractors: University of Connecticut, Storrs, Connecticut and Ion Power, Inc., Bear, Delaware

Objectives

- Develop an ultra thin, durable membrane (< 75 μm) capable of operation at 100-140°C with the following properties:
  - <0.2 Ωcm^2 (Ohm-centimeter-squared) membrane ohmic resistance and <1% crossover
  - High ionic conductance with negligible electronic conductivity
  - High mechanical strength
  - >0.6 volts (V) performance at 400 mA/cm^2 (milliamps/centimeters squared) under ambient reformate/air operation at 120°C

Approach

- Develop a solid superacid-Nafion®composite membrane electrode assembly (MEA) with the following components:
  - Solid superacids as high-temperature proton conductors and moisture retainers
  - Nafion® phase as proton conducting binder phase
  - Inert support phase may be added to enhance strength

Accomplishments

- Demonstrated atmospheric MEA performance of ~600 mV at 400 mA/cm^2 under actual system operating conditions (atmospheric, low relative humidity, high utilizations) at 120°C for 500 hours (h)
- Achieved membrane ohmic resistance and cross-over objectives

Future Directions

- Optimization of the promising membrane-electrode assembly
- Scale-up to nominal 300 cm^2 and validation in single cell
- 300 cm^2 short stack evaluation

Introduction

Fuel cells offer the best alternative to conventional power generation technologies. They are inherently very efficient and clean. For fuel cells to be commercially competitive, issues such as cost, size, and functionality need to be addressed. The specific goal of this fuel cell for buildings applications project is to develop an atmospheric-pressure natural gas-fueled proton exchange membrane fuel cell (PEMFC) system with >35% efficiency (higher heating value), >100°C operation for cogeneration, simple construction, >40,000 h reliable life, and <$1500/kW system cost. For the PEMFC to be commercially viable, the performance of critical components, such as the polymer electrolyte membrane in particular, needs to be improved.

At present, the state-of-the-art PEMFC is operated at ~80°C. Carbon monoxide (CO) poisoning of the PEMFC anode's precious metal catalyst is a major technical barrier for utilizing hydrocarbon feedstocks such as natural gas. CO clean-up from the fuel stream requires a complicated and expensive fuel processor. Since the chemisorption of CO on the anode catalysts is exothermic and therefore weakens considerably with temperature, one approach to mitigate the CO poisoning is to operate the PEMFC at higher temperatures. Many other advantages can also be realized, such as faster electrode kinetics, lower voltage loss, higher quality waste heat for cogeneration, cathode flooding mitigation, and greater ability to remove waste heat.

The baseline Nafion® membrane is deficient in terms of ionic conductivity above 100°C and at low relative humidity required for atmospheric-pressure building applications. Such conditions tend to dry out the membrane, drastically reducing membrane proton conductivity. Furthermore, the loss of water causes membrane embrittlement, resulting in membrane cracking, reactant cross-leakage and poor electrode-membrane contact. Therefore, a cost-effective membrane, with proton conductivity that is less sensitive to change in water content, is needed.

Another important issue for >100°C operation is cell voltage loss. Only a minor portion of the cell voltage loss is in fact caused by the membrane ohmic resistance increase. The majority of the voltage loss increase is due to the increase in cathode polarization. In order to achieve the high-temperature cell performance goal, cathode performance improvement is essential.

Based on the literature survey, no membranes or MEAs reported so far can achieve all the above required goals. This research is directed at developing novel high-temperature, composite proton exchange membrane-electrolyte assemblies for PEMFC for building applications.

Approach

The overall objective is to operate PEMFCs at 100-140°C to improve CO tolerance, mitigate water and thermal management challenges and reduce membrane cost. The basic approach is to develop a composite membrane consisting of mechanical support and high-temperature proton conduction phases. In order to improve cathode performance, modification of cathode formulation and structure is on-going. Promising solid superacids are incorporated into the cathode.

Results

A number of composite membranes and MEAs have been developed to improve water retention and proton conduction at 120°C. Additives/modifiers with specific properties have been synthesized. The performance of the fabricated MEAs in laboratory-scale cells has been characterized to screen promising formulations. The negligibly low anode polarization loss at >100°C has been verified. Significant improvements in 120°C performance and endurance have been achieved. The ohmic resistance and cross-over goals of the membrane have been met. MEA performance of ~0.6 V at 400 mA/cm^2 under realistic system operating conditions (atmospheric, low relative humidity, high utilizations) has been achieved in a 500 h 25-cm^2 cell endurance test (Figure 1). The MEA Pt loading was 0.4 mg/cm^2 for each electrode. This represents one of the best cell performances ever reported in the literature. Performance of >750 mV at 120°C was also achieved under pressurized operating condition (30 psig). These results are highly promising.

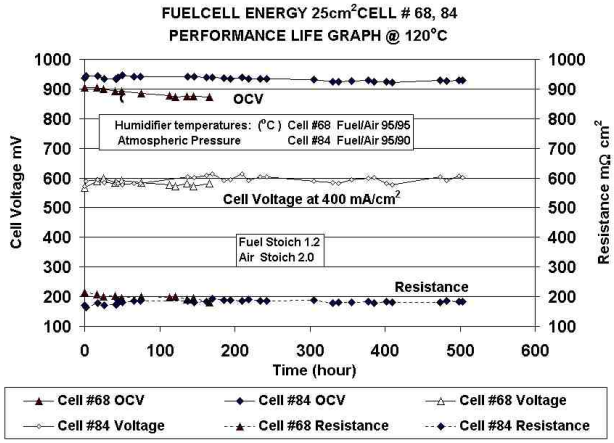

Figure 1. MEA performance of ~0.6 V at 400 mA/cm^2 under realistic system operating conditions (atmospheric, low relative humidity, high utilizations) has been achieved in a 500 h 25-cm^2 cell endurance testing.

The main activities for the remaining part of this program will focus on optimization of the promising membrane-electrode assembly, scale-up to nominal 300 cm^2 and validation in single cells followed by short stack evaluation. The program is scheduled to be completed in February 2003.

Conclusions

An MEA performance of ~600 mV at 400 mA/cm^2 under realistic system operating conditions has been demonstrated, representing a major milestone towards developing a viable atmospheric PEMFC system. To further enhance cell performance (to desired operating conditions of 0.8 V at 400 mA/cm^2), optimization of cathode structure and formulation to enhance proton conduction and cathode catalyst utilization is required.

Publications/Presentations

1. C. Yuh, P. Patel, R. Kopp, S. Katikaneni and S. Grot, "Novel Composite Membrane-Electrode Assembly for High-Temperature PEMFC," 3rd International Symposium on Proton Conducting Membrane Fuel Cells, The Electrochemical Society Fall Meeting, Salt Lake City, Utah, October 20-24, 2002.

2. C. Yuh, "R&D on an Ultra Thin Composite Membrane for High-Temperature Operation in PEMFC," Annual Report to US DOE, for the Period of September 1999 to August 2000.

IV.C Fuel Processing Subsystem and Components

IV.C.1 Next Millennium Fuel Processor™ for Transportation Fuel Cell Power System

Prashant S. Chintawar (Primary Contact), James Cross, Brian Bowers, Robert Rounds, and Zhi-Yang Xue
Nuvera Fuel Cells, Inc.
35 Acorn Park
Cambridge, MA 02140
(617) 498-6577, fax: (617) 498-6664, e-mail: chintawar.p@nuvera.com

DOE Technology Development Manager: Patrick Davis
(202) 586-8061, fax: (202)586-9811, e-mail: Patrick.Davis@ee.doe.gov

ANL Technical Advisor: Walter Podolski
(630) 252-7558, fax: (630) 972-4430, e-mail: podolski@cmt.anl.gov

Subcontractors/Partners: SudChemie, Inc.; STC Catalysts, Inc.

Objectives

- Validate Argonne National Laboratory (ANL) computer models by integrating existing fuel processing technology into a 10 kWe multi-fuel power system.
- Utilize integrated STAR (Substrate based Transportation application Autothermal Reformer) fuel processor, MPR (Modular Pressurized Reformer – a disintegrated fuel processor), high temperature material test facility, and microreactors to perform endurance testing that will identify and address component and fuel processor degradation mechanisms.
- Design and test the 50kWe STAR fuel processor.

Approach

- Integrate fuel processing (existing Model B based technology) and fuel cell sub-systems.
- Develop control strategies on 10 kWe fully automated fuel cell power system (FCPS) and deliver to ANL.
- Perform automotive system analysis and identify strategies for STAR to meet FreedomCAR targets.
- Set targets and develop key technologies and components to be used in STAR.
- Design and test STAR on four fuels and investigate efficiency, emissions, steady state and transient performance, and reformate purity.
- Integrate STAR fuel processor and fuel cell, investigate the performance of the power system, and identify system level integration issues. Deliver the integrated fuel processor system to ANL.
- Investigate and address degradation and durability issues of STAR fuel processor both on the component and integrated fuel processor level.

Accomplishments

- Tested the fuel cell sub-system and fuel processor sub-system.
- Developed sub-system and integrated power plant control strategies.
- Performed steady state and transient testing on gasoline and delivered integrated FCPS to ANL.
- Developed design criteria for scrubber media and validated them during full-scale operation of fuel processor and STAR systems.
- Selected materials for high temperature zones of the fuel processor and designed test facility to investigate long term stability of such materials.
- Performed deactivation studies of the STAR catalyst suite in microreactor.
- Tested >100 catalysts for STAR and selected final candidates.
- Designed substrate-only fuel processor and devised control strategies for fuel processor and FCPS.
- Tested partially integrated fuel processor (version 1) and demonstrated 74% H_2 efficiency (at high temperature shift exit).
- Tested partially integrated fuel processor (version 2) and demonstrated improvements in thermal stress and serviceability over version 1, and 80% syn gas efficiency (at high temperature shift exit).
- Designed and characterized reformate tolerant fuel cell on hydrogen.

Future Directions

- Support ANL's testing efforts and modeling studies, and provide necessary assistance.
- Bring the high temperature material test facility on-line.
- Complete the long term stability studies of the STAR catalyst suite and deduce equations to describe degradation.
- Perform long term stability studies of the integrated STAR fuel processor with gasoline.
- Demonstrate ≥50 kWe power from an integrated FCPS and characterize fuel processor on four fuels.
- Perform emission characterization of integrated FCPS.
- Deliver fuel processor system to ANL.

Introduction

Nuvera is working with the Department of Energy to develop efficient, low emission, on-board multi-fuel processors for the transportation application. The fuels include gasoline, methanol, ethanol, and natural gas.

In the first part of the project, Nuvera integrated an existing fuel processing technology into a 10 kWe multi-fuel power system in order to allow validation of computer models developed by ANL. This integrated fuel cell power system was delivered to ANL in June 2002.

The Substrate based Transportation application Autothermal Reformer (STAR) will contain high-activity, low-cost, transportation specific catalysts and substrates to address power density, specific power, and start-up tie issues. To address the issue of system durability, we are developing fuel purification (sulfur removal) and reformate clean-up technologies.

Results

Based on component technologies produced in previous years, we completed design of the STAR fuel processor in the reporting period (Figures 1 and 2). The design shown contains all the reaction zones and has a volume of ~70 L. This fuel processor also has the shape factor necessary for installation in the fuel cell vehicle.

We have collected operation data from the partially integrated STAR fuel processor (Figure 3). Gasoline was used as a fuel in this testing at 175 kWth feed rate and we expect the maximum feed rate to be ~200 kWth. The H_2 efficiency and CO concentration approach equilibrium values

Figure 1. Conceptual Design of STAR Fuel Processor

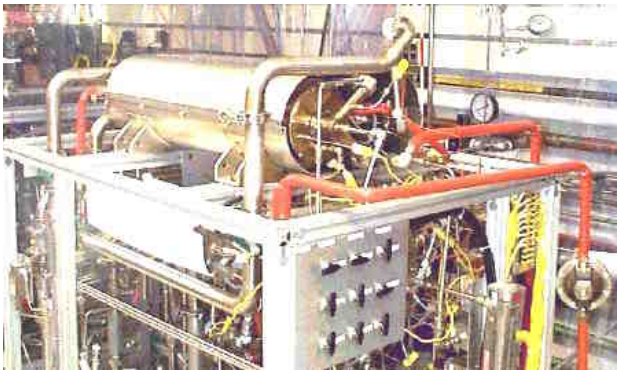

Figure 2. STAR Fuel Processor on Test Cart

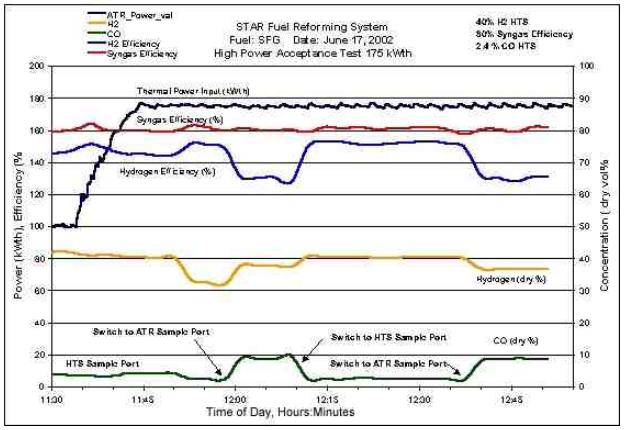

Figure 3. Performance Data of Partially Integrated STAR Fuel Processor

Technical targets: fuel processors[a] to generate hydrogen-containing fuel gas from reformulated gasoline containing 30 ppm sulfur, average, for 50 kWe (net) fuel cell systems

(Excludes fuel storage; includes controls, shift reactors, CO cleanup, heat exchangers)

Characteristics	Units	Calendar year		
		2001 status[b]	2005	STAR 2002[c]
Energy efficiency[d]	%	78	78	78
Power density	W/L	500	700	836
Specific power	W/kg	450	700	585
Cost[e]	$/kW	85	25	65
Cold start-up time to maximum power @+20 °C ambient	min	<10	<1	<10
Transient response (time for 10% to 90% power)	sec	15	5	15
Durability[f]	hours	1000[g]	4000[h]	1000
Survivability[i]	°C	TBD	–30	TBD
CO content in product stream[j]				
steady state	ppm	10	10	<50
transient	ppm	100	100	<100
H_2S content in product stream	ppb	<200	<50	<100
NH_3 content in product stream	ppm	<10	<0.5	<1

[a]With catalyst system suitable for use in vehicles.
[b]Projected status for system to be delivered in late 2002: 80% efficiency, 900 W/L, 550 W/kg.
[c]Projected status for STAR fuel processor in 2002.
[d]Fuel processor efficiency = total fuel cell system efficiency/fuel cell stack system efficiency, where total fuel cell system efficiency accounts for thermal integration. For purposes of testing fuel-processor-only systems, the efficiency can be estimated by measuring the derated heating value efficiency (lower heating value of $H_2 \times 0.95$/ lower heating value of the fuel in) where the derating factor represents parasitic system power losses attributable to the fuel processor.
[e]High-volume production: 500,000 units per year.
[f]Time between catalyst and major component replacement; performance targets must be achieved at the end of the durability period.
[g]Continuous operation.
[h]Includes thermal cycling.
[i]Performance targets must be achieved at the end of an 8-hour cold-soak at specified temperature.
[j]Dependent on stack development (CO tolerance) progress.

Table 1. Comparison of FreedomCAR Targets and STAR Performance Projections

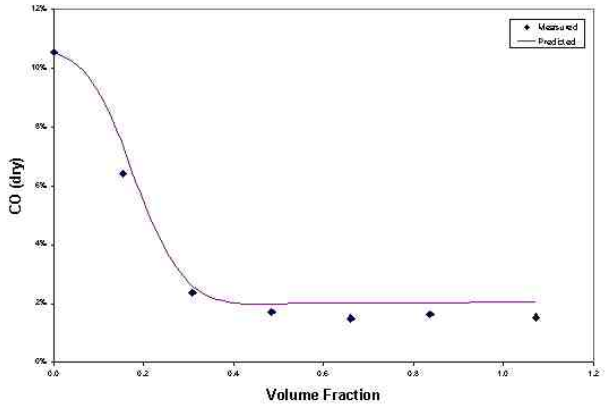

Figure 4. Comparison of Expected vs. Obtained Performance of WGS Catalyst in MPR

suggesting the validity of our design basis. We have accumulated >50 hrs of gasoline operation on STAR fuel processor (version 2) and have subjected it to >30 thermal cycles. Table 1 compares Nuvera's projections of the STAR fuel processor performance and FreedomCAR targets.

The STAR fuel processor represents a culmination of three years of intensive R&D and design efforts. Prior to their use in the integrated fuel processor, all components were tested in the MPR. Figure 4 compares the expected and obtained performance of the water-gas-shift catalyst in the MPR. Similarly, the MPR testing validates the desulfurizer performance data collected on the bench scale reactor (Table 2). The sulfur capacity was the same in both the MPR and the bench scale reactor.

Parameter	Bench-Scale	MPR
Adsorbent Weight (g)	9	3330
Physical Form	Powder	Structured

Table 2. Comparison of Bench-Scale and MPR Performance of Desulfurizer

The STAR fuel cell stack, shown in Figure 5, was characterized via H_2/air operation (Figure 6). Figure 6 data are limited to 66 kWe although the stack is capable of higher power – load bank limitations have prevented us from higher power operation.

The performance of adsorbent clean-up media was evaluated and validated. We anticipate the use

Figure 5. STAR Fuel Cell Stack

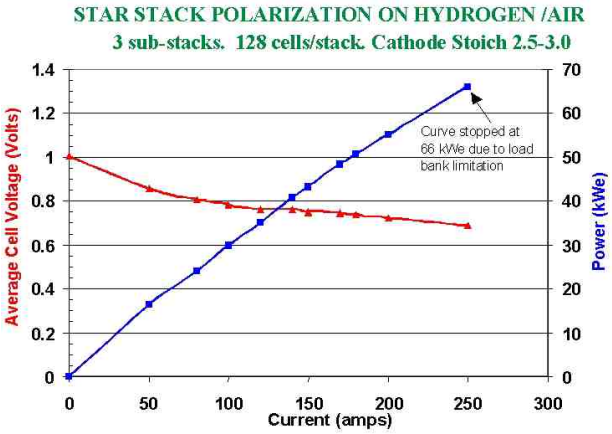

Figure 6. Polarization Data on STAR Fuel Cell for H_2/ Air Operation

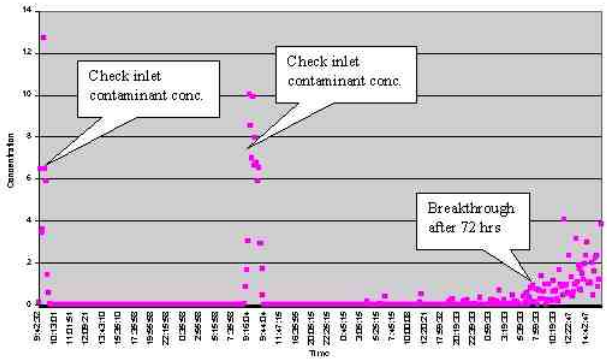

Figure 7. Performance of Adsorbent "A" after Being Used on Fuel Cell Power System for 30 hours

of such media between the fuel processor and fuel cell sub-systems to safeguard the fuel cell from various trace species generated and/or present in gasoline. Figure 7 shows the performance of medium "A" after being used on the fuel cell power system for 30 hrs. We have also carried out extensive short-term and long-term durability testing of the STAR catalyst suite (Figure 8).

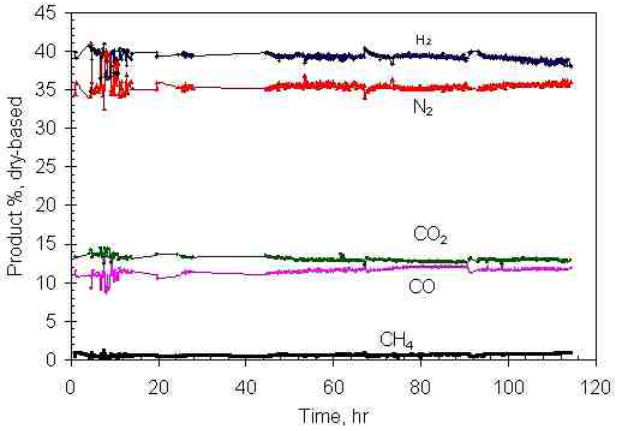

Figure 8. Longevity of STAR ATR Catalyst

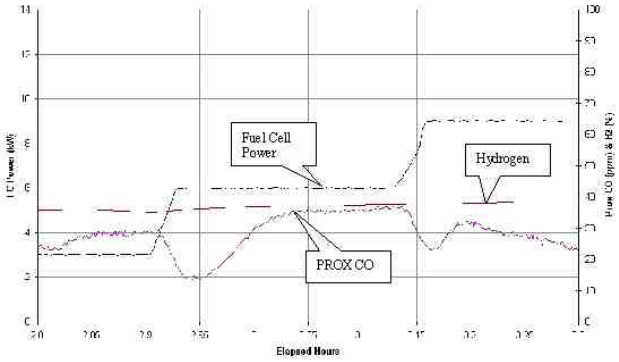

Figure 9. Fuel Cell Power System Performance on Gasoline

Over the last year, we retrofitted the existing fuel processor sub-system, designed the fuel cell sub-system, and integrated the two units. The integrated power plant was delivered to ANL in June 2002. Figure 9 shows typical performance of the integrated system on gasoline.

Conclusions

- A substrate only multi-fuel processor has been designed and tested. Preliminary data on gasoline indicate 80% efficiency (at HTS exit). Detailed testing is expected to validate the performance projections of specific power, power density, and emissions.
- Thermal stress and fluid flow distribution constitute major design challenges with such fuel processors.

IV.C.2 Multi-fuel Processor for Fuel Cell Electric Vehicle Applications

Tom Flynn (Primary Contact)
McDermott Technology, Inc.
1562 Beeson Street
Alliance, OH 44601-2196
(330) 829-7622, fax: (330) 829-7283, e-mail: tom.j.flynn@mcdermott.com

Brian Engleman
Catalytica Energy Systems, Inc.
430 Ferguson Drive
Mountain View, CA 94043-5272
(650) 940-6391, fax: (650) 960-0127, e-mail: bde@catalyticaenergy.com

DOE Technology Development Manager: Nancy Garland
(202) 586-567, fax: (202) 586-9811, e-mail: Nancy.Garland@ee.doe.gov

ANL Technical Advisor: Walter Podolski
(630) 252-7558, fax: (630) 972-4430, e-mail: podolski@cmt.anl.gov

Main Subcontractors: Catalytica Energy Systems and NexTech Materials, Ltd. (NexTech)

Objectives

- Design, build and demonstrate a fully integrated, 50-kilowatt electric (kWe) catalytic autothermal fuel processor system. The fuel processor will produce a hydrogen-rich gas for direct use in proton exchange membrane (PEM) fuel cell systems for vehicle applications.

Approach

- Develop preliminary design of 50-kWe fuel processor system and performance goals for individual components.
- Evaluate alternate approaches for the major catalytic components (e.g., desulfurizer, reformer, shift reactor and selective oxidation reactor).
- Conduct subsystem testing of major components utilizing best catalyst approach.
- Develop final design of overall system and design specifications for individual components.
- Assemble 50-kWe fuel processor system.
- Perform demonstration testing on gasoline and methanol.
- Ship fuel processor system to Argonne National Laboratory.

Accomplishments

- Completed peer review of final design.
- Produced required amount of Catalytica Energy System's autothermal reformer (ATR) catalyst.
- Produced required amount of NexTech platinum (Pt)/ceria medium-temperature-shift (MTS) catalyst.
- Obtained Los Alamos National Laboratory preferential oxidation (PROX) reactor.
- Obtained Battelle/Pacific Northwest National Laboratory micro-channel steam generator.
- Obtained Precision Combustion, Inc. dual-fuel catalytic burner.

- Completed fabrication and assembly of fuel processor system.
- Completed checkout of components, controls and instrumentation.

Future Directions

- Conduct performance tests of fuel processor system.
- Ship fuel processor system to Argonne National Laboratory for further evaluation and testing.

Introduction

Development of a compact, efficient and low-cost processor for converting carbon-based fuels to hydrogen is an important aspect of the successful implementation of fuel cells for transportation applications. A catalyst-based reforming approach for fuel processing can provide fast start-up and transient response, high efficiency and compactness. When coupled with a liquid-fuel desulfurizer, the multi-fuel processor under development by McDermott Technology, Inc./Catalytica Energy Systems promises to approach the FreedomCAR fuel processor targets.

Approach

The fuel processor consists of a liquid-phase desulfurizer, a catalytic reformer, two stages of water-gas-shift reaction, a selective oxidizing unit, and ancillary components including pumps, heat exchangers and controls [1]. A general arrangement concept drawing of the fuel processor system is shown in Figure 1. The project consists of 5 major tasks: preliminary design, catalyst development, subsystem testing, final design, and prototype assembly and demonstration.

The liquid fuel desulfurizer reduces sulfur in gasoline to less than 3 parts per million (ppm). The reformer unit operating at an average temperature of 800°C produces a hydrogen-rich gas from the fuel feed. Two reformer approaches were evaluated - a packed bed comprising a single catalyst and a plate-based catalyst system. A bi-functional ATR catalyst developed by Catalytica Energy Systems was selected for use over the plate-based design. The plate design showed possible advantages in size but could not be developed in the contract time frame. The ATR is followed by a shift reactor consisting of two stages. The first stage contains a medium-temperature-shift catalyst developed by NexTech. The second stage contains a commercial low temperature shift (LTS). The shift reactors reduces the CO concentration in the reformate gas to approximately 2,000 ppm. Final reduction of CO is achieved in a preferential selective oxidation reactor.

McDermott Technology, Inc. developed the overall system design including heat integration, mechanical design, ancillary equipment, and instrumentation/controls. Catalytica Energy Systems developed the catalytic components, including a state-of-the-art autothermal reforming catalyst. NexTech contributed its expertise and technology in the area of shift catalysts.

Results

During this reporting period, a peer review of the final design was completed. The review was performed by independent experts and was attended by DOE and team members. The reviewers approved the final design. Following the review, general arrangement drawings for the system and detailed fabrication drawings of the U-tube pressure vessel and internal components were completed.

The predicted performance of the system is summarized in Table 1. Three loads were used to develop the design. The maximum efficiency design point is 25% load (12.5 kWe). Thermal integration was optimized around the 60% load (30 kWe) case. The maximum continuous rated design point is 50 kWe. The predicted fuel processor efficiency is 80.6% at 25% load assuming 80% hydrogen utilization and 50% efficiency in the fuel cell.

Size and weight predictions are summarized in Table 2. The system power density and specific power are 283 W/L and 165 W/kg, respectively. The size and weight are actual size and weight using commercially available components or

Table 1. Predicted Performance for Authothermal Processor System

Characteristic	Units	Predicted Performance		
		Nominal	Design	Maximum
Load	kWe (net)	12.5	30	50
Reformer S/C Ratio		2.00	2.00	2.00
Total S/C Ratio		2.58	2.89	3.31
Total A/F Ratio (includes PrOx)		13.4	14.5	16.1
Reformer Stoichiometry		0.23	0.25	0.28
Fuel Equivalence Ratio		4.31	3.98	3.58
Fuel Value of Gasoline, LHV	kW	35.1	92.7	167.2
Fuel Value of H_2 to Fuel Cell, LHV	kW	31.2	80.4	141.0
Electrical Output	kWe (gross)	13.97	35.81	62.86
Electrical Output	kWe (net)	12.74	30.68	50.38
Carbon Conversion	%	99.82	99.45	99.76
Cold Gas Efficiency (LHV)	%	88.92	86.74	84.37
Fuel Processor Efficiency	%	80.58	82.42	81.99
Overall System Efficiency (LHV)	%	32.84	31.43	29.26
Compressor Efficiency	%	67.0	74.4	73.0
Expander Efficiency	%	75.7	81.8	85.0
Expander Output	kWe	0.4	2.3	4.0
Parasitic Loads	kWe	1.6	7.5	16.5
Radiator Heat Rejection	kW	13.8	34.6	63.5
Fuel Cell Operating Temperature	°C	60	60	60
Fuel Cell Voltage (Assumed)	V	0.7	0.7	0.7
Fuel Cell H_2 Utilization	%	80.11	79.83	79.86
Fuel Cell O_2 Utilization	%	50.07	49.90	49.91
Fuel Cell Efficiency, LHV	%	44.78	44.54	44.58
PrOx O_2/CO Ratio		0.98	0.98	0.98
PrOx Selectivity		0.51	0.51	0.51
PrOx CO Conversion	%	99.78	99.66	99.47
Sy Pressure Drop	KPa	6.74	15.75	38.69

developmental components for control and thermal management. The compressor/expander and start-up

Table 2. Summary of Sized and Weights of Components and System

Subsystem Totals	Size (L)	Weight (kg)
Reformate Generator	128.00	28-.0.25
Steam Regenerator	6.50	7.70
Reformate Conditioner	45.00	30.00
Fuel Supply	11.28	22.63
Water Supply	18.80	40.70
Controls & Piping (1/10 demonstration unit)	19.48	15.15
Overall Total	222.38	380.63
Power kWe (Gross	62.86	62.86
Power Density/Specific Power	283	165
DOE FreedomCAR 2000 Target (W/L, W/kg)	600	600
DOE FreedomCAR 2004 Target (W/L, W/kg)	750	750

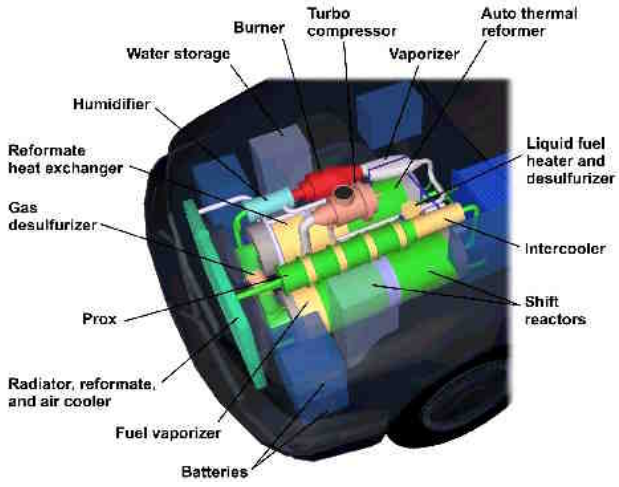

Figure 1. Schematic of McDermott's Fuel Processor

burner are excluded from the totals. A humidifier is included in the fuel processor scope as part of the water management system.

The catalyst scheme is summarized in Table 3. The required amount of Catalytica Energy Systems ATR catalyst was produced and installed in the reactor. The required amount of NexTech shift catalyst was produced and installed in the first stage shift reactor. The NexTech shift catalyst is a medium-temperature shift catalyst that remains active in the oxidized or reduced state and is less sensitive to condensed moisture [2]. All catalysts are currently in pellet form; however, noble metal wash coating on monolith substrates is existing technology. Therefore, once the catalyst and system performance are verified, it will be straightforward to convert these catalysts to monoliths. The reactors

have been designed to accommodate standard monolith sizes.

Table 3. Catalyst Scheme

	Catalyst Beds				Clean-up Beds	
Parameter	**ATR**	**MTS**	**LTS**	**PROX**	**Sulfur Removal**	**NH_3 Removal**
Temperature (^oC)	807	399	263	94	322	None
Catalyst	Rh	Pt	Cu/ ZnO	Pt	ZnO	None
Support	Alumina	Ceria/ Zirconia	ZnO/ Al_2O_3	Alumina	None	None
GSHV (1 hour)	9.165	13,833	13,623	25,000	134,405	None
Bed Volume (L)	10.0	10.0	11.2	7.4	1.0	None
Bed Weight (kg)	14.4	15.0	15.0	2.23	1.4	None

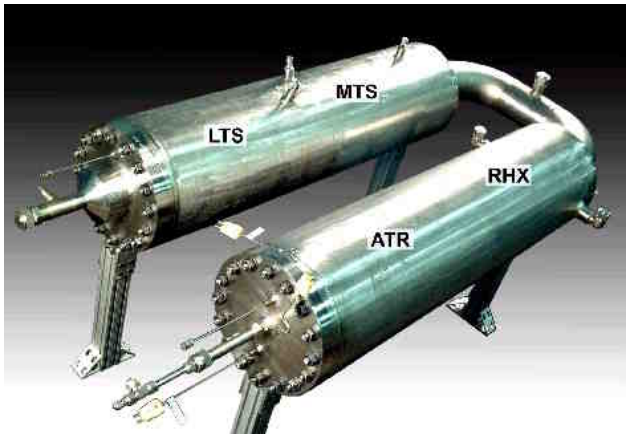

Figure 2. Fuel Processor Tube Pressure Vessel

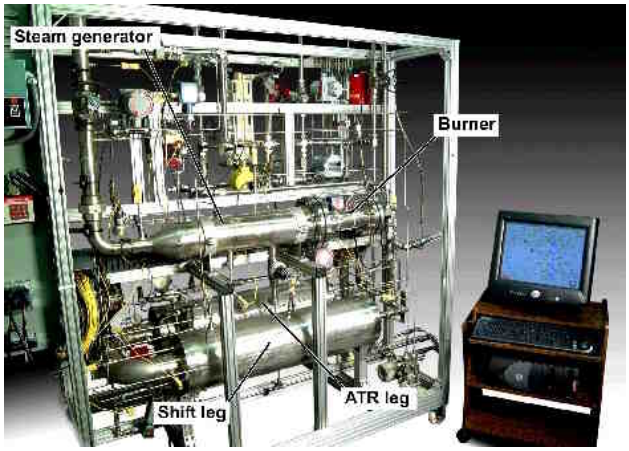

Figure 3. Integrated Fuel Processor Test Stand

Los Alamos National Laboratory provided a preferential oxidation reactor suitable for demonstration with monolith catalysts. Pacific Northwest National Laboratory provided a steam generator based on micro-channel heat exchanger technology. Precision Combustion, Inc. provided a dual-fuel catalytic burner.

The tube pressure vessel and its internals were fabricated and assembled as shown in Figure 2. The tube pressure vessel thermally integrates many major components including the ATR reactor, reformate heat exchanger, gas desulfurizer, fuel vaporizer, and MTS and LTS reactors. In addition, internal water spray cooling is used for temperature control. Upon completion of the pressure vessel and receipt of vendor-supplied components, the fuel processor system was assembled on a test stand as shown in Figure 3 with controls and instrumentation. To date, all components, controls and instrumentation have been checked out.

Conclusions

A fully integrated autothermal fuel processor based on a bi-functional ATR catalyst has been designed, fabricated and checked out. The unit continues to show progress towards the FreedomCAR targets and will be tested in the summer of 2002.

References

1. Flynn, T. J., Privette, R. M., Perna, M. A., Kneidel, K. E., King, D. L. and Cooper, M., "Compact Fuel Processor for Fuel Cell-Powered Vehicles," International Congress and Exposition, Detroit, MI, March 1-4, 1999, SP-1425, pp 47-53.

2. Swartz, Scott, L. "Nanoscale Water-Gas-Shift Catalysts," Snapshots of Cooperative Automotive Research for Advanced Technologies Projects, Phase 2, published by Argonne National Laboratory, Transportation Technology R&D Center, March 2000, pp 11-12.

FY 2002 Publications

1. Flynn, T. J., Privette, R. M., Perna, M. A., Kneidel, K. E., King, D. L. and Cooper, M., "Compact Fuel Processor for Fuel Cell-Powered Vehicles," International Congress and Exposition, Detroit, MI, March 1-4, 1999, SP-1425, pp 47-53.

IV.C.3 Quick-Starting of Fuel Processors

S. Ahmed (Primary Contact), C. Pereira, H.K. Liao, S. Lottes, M. Krumpelt
Argonne National Laboratory,
9700 S. Cass Ave., Argonne, IL 60439
(630) 252-4553, fax: (630) 972-4553, email: ahmed@cmt.anl.gov

DOE Technology Development Managers:
JoAnn Milliken: (202) 586-2480, fax: (202) 586-9811, e-mail: JoAnn.Milliken@ee.doe.gov
Nancy Garland: (202) 586-5673, fax: (202) 586-9811, e-mail: Nancy.Garland@ee.doe.gov

Objectives

- Develop strategies to meet the rapid-start targets for on-board fuel processors in gasoline-fueled fuel cell vehicles.

Approach

- Identify constraints that limit fuel processors from reaching rated hydrogen production capacity within 30 seconds.
  - Identify the fundamental technical barriers – thermal mass, fuel consumption, feed limitations, etc.
  - Set up component and hardware models, and validate with experimental study of rapid heat-up behavior.
- Develop a heat-up strategy to enable 30-second start-up of the fuel processor.
- Demonstrate fast-start strategy in a laboratory-scale fuel processor.

Accomplishments

- Evaluated burner feeds and heat load required to warm up the fuel processor to full capacity.
  - The mid-temperature (200-400°C) zones represent ~70% of the total heat load.
  - Air flows required at the burner for meeting the appropriate hot gas temperatures in the various zones are nearly five times that required for operation in reforming mode at rated power.
  - Parallel heating of the various components is preferable to sequential heating, since parallel heating allows better temperature control of the hot gas and permits starting the fuel processor at partial capacity.
- Developed a computational fluid dynamics (CFD) model to simulate heat-up of individual reactor zones.
- Designed, fabricated, and installed a generic fuel processor and test stand to study the heat transfer characteristics of monolith loaded reaction zones.
  - Initiated experiments to validate the CFD model.

Future Directions

- Study the effect of hot gas temperature, gas hourly space velocity, adjacent environments, and flow patterns (adjacent zones with co- or counter-current flow, parallel vs. series heating, etc.) on the heat-up rates.
- Validate model with experimental data and use model to design a fuel processor capable of rapid start.
- Establish a start-up strategy (identify necessary components, hot gas and flow specifications, heating sequence, etc.) to achieve fast start
- Demonstrate rapid start-up of an engineering-scale (~5 kilowatts electrical [kWe]) fuel processor.

Introduction

To achieve significant market penetration, fuel cell vehicles will have to meet or exceed the performance baseline established by today's spark-ignition engine vehicles. These performance criteria include improved gas mileage, rapid acceleration, and turn-key start-up. The goal of this work is to develop strategies that will result in demonstration of a fuel processor for fuel cell vehicles that starts rapidly. The Department of Energy has set a start-up time of 30 seconds (from 20°C to maximum power) for the year 2010.

Approach

This project will identify the constraints that prevent existing fuel processors from reaching rated capacity in 30 seconds or less. A fundamental technical barrier is the thermal mass of the catalysts and structural materials. Reductions in thermal mass require improvements in catalyst materials and effective heat transfer. Other limiting factors are related to auxiliary equipment and process design, such as available gas blowers and burners, the fuel injection system, sensor response, and hot gas distribution within the processor.

The development approach will be to set up component and hardware models for rapid heat-up and to validate the models experimentally. The models will then be used to determine optimal feed distributions, anisotropies in gas flow, and patterns of heat transfer. Further experiments will be conducted to validate the models. The initial goal is a thorough understanding of the heat transfer characteristics of monolithic catalysts. Studies will include the effect of geometry, flow and distribution of the heating medium, and material compositions.

Fundamental studies of heat transfer, combined with a basic understanding of the underlying kinetics of the combustion process, will be used to develop a model of the fast-start reactor. The model will then be used to design a fast-start reactor that can meet the prescribed operational targets.

Accomplishments

As a first step in development, the heating requirements for a fast-start reactor were defined.

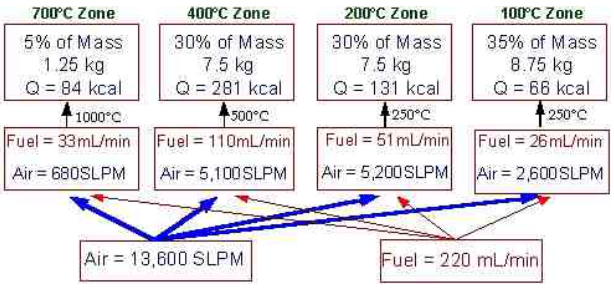

Figure 1. Fuel Requirements for a 50-kW Processor

The processor was sized according to existing catalyst technology, and the design was based on our previous fuel processor's test systems.

The processor can be divided into four zones based on the operating temperature: reformer, scrubber-high temperature shift (S-HTS), low temperature shift (LTS), and preferential oxidation (PROX). Operating temperatures are nominally 700°C in the reformer, 400°C in the S-HTS, 200°C in the LTS, and 100°C in the PROX. In actual operation, temperatures are not discrete; rather, there is a gradual decrease between each zone. The middle zones, S-HTS and LTS, comprise ~70% of the total heat required during start-up. The fuel requirements and heat flow for a 50-kilowatt (kW) processor are shown in Figure 1.

Two primary options for heating the fuel processor were considered: heating the different components in sequence or in parallel. Heating the components in parallel is preferable to heating them sequentially since it allows direct temperature control of the hot gas within each zone. A parallel system also avoids sending all of the hot gas through the reformer catalyst. A negative feature is the requirement of multiple injection points.

For a parallel system with a central burner, the air flow required to achieve the appropriate temperatures during start-up is nearly five times that required for steady operation at the rated reforming capacity. The additional air is required to maintain temperatures within allowable ranges for each of the various zones. A possible design for a parallel heating system utilizing a fuel burner is shown in Figure 2.

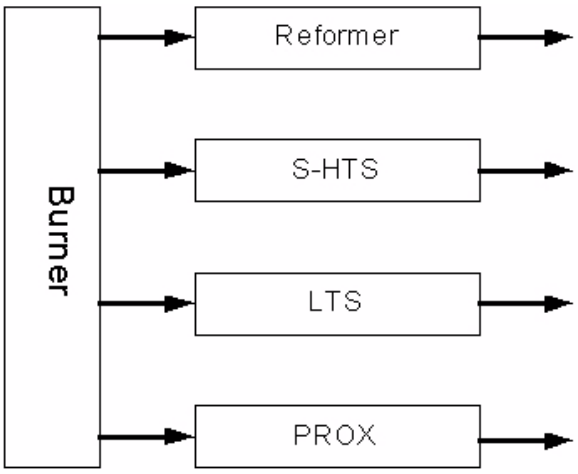

Figure 2. Parallel Heating of the Fuel Processor Components

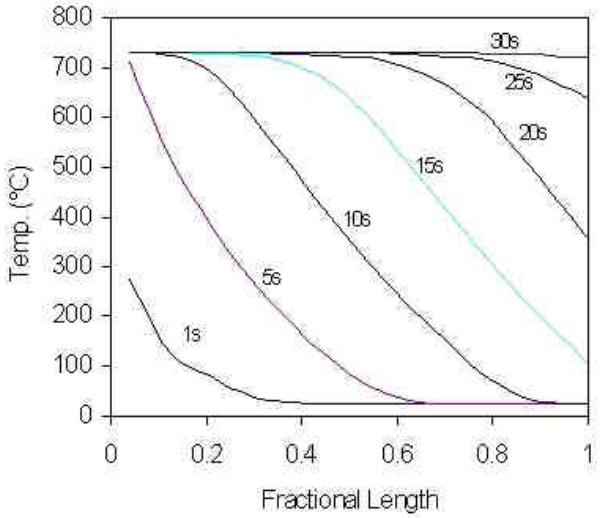

Figure 3. Initial Temperature Progression in Reformer

A CFD model was developed to simulate heat-up of a generic fuel processor based on a cylindrical geometry. The model was based on a simplified fuel processor design that consisted of three concentric zones bounded and separated by three concentric cylinders. The adjacent zones can represent either a layer of insulation or another catalyst bed. The heat transfer characteristics are studied by varying the weight of catalyst in each zone, the temperatures of the hot gases used to heat up the zones, and the direction (co- or counter-current) of flow of the hot gases in adjacent zones.

Figure 4. A test reactor is used to validate the CFD model.

Figure 3 shows the temperature progression from the CFD model for a cylindrical reactor containing a cordierite monolith that is heated to 700°C. This result suggests that the reformer monolith can attain its desired temperature in 30 seconds if a hot gas at 730°C is fed at a space velocity of 45,000 per hour (h^{-1}), assuming no heat losses. Similar start-up scenarios can be obtained for the other zones.

To validate the CFD model, a generic reactor, shown in Figure 4, was fabricated and is being used for the heating studies. Electrically heated air rather than hot combustion gas, is used to heat the catalyst beds.

As in the CFD model, the three concentric zones were loaded with monoliths and insulation. Other structural forms such as heat exchangers can be installed as needed to study their heat-up characteristics (rate, heat transfer effectiveness, temperature distribution, etc. The model is being updated to account for deviations between simulated and experimental data.

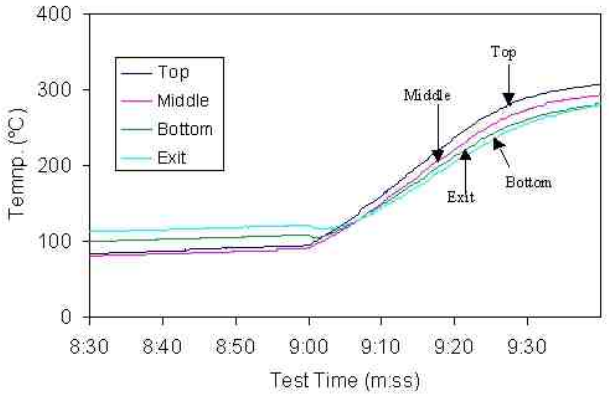

Figure 5. Heat-up of a Cylindrical Zone using Hot Gas, Flowing at a Space Velocity of 60,000 h^{-1}

Conclusion

Analysis of thermal requirements to attain operating temperatures in the fuel processor indicates that, at the space velocities required in fuel processors typical today, the shift reactor zone represents the largest thermal mass. The hot zones in the fuel processor can be heated up with hot combustion gas. Parallel heating of the various zones is preferable to sequential heating because it allows individual control of the hot gas streams into each zone. The total air required to limit the combustion gas temperatures within the bounds of tolerance of the catalyst zones is significantly higher than during reforming operations, and the air blower needs to be sized accordingly. Similarly, the cross-sectional area of each zone must be large enough to accommodate the larger flow during heat-up.

Future Directions

The fast-start test reactor will be used to determine the effect of hot gas temperature, gas hourly space velocity, adjacent environments, and flow patterns on the heat-up rates of catalysts and materials. The temperature progression within the reactor will be a function of the effectiveness of heat transfer between the hot gas and the catalyst. Variations in flow patterns that will drive the design of a fast-start processor include the effect of counter-current versus co-current flow of the gas streams in adjacent zones and of heating the zones in series versus parallel. The temperature distributions in adjacent zones will determine the insulation requirements and drive the design of the heat exchangers.

The results of these tests will be used to validate the heat transfer model. Once the heat transfer characteristics are understood, the model will be expanded to include the effects of using a fuel:air combustion mixture to generate the hot gas to heat up the system. An overall start-up strategy will be defined that will achieve rapid start and transition to steady-state operation. The strategy will identify the necessary components, the hot gas flow specifications, and the heating sequence. These data will be incorporated into the design of a 5-kWe engineering-scale fuel processor that will demonstrate a start-up time of 2 minutes or less.

Fy 2002 Publications

1. C. Pereira, S.H.D. Lee, T.D. Kaun, S. Ahmed and M. Krumpelt, “Fuel Processor for Fuel Cell Systems,” presented at the Annual Meeting of AIChE, Reno, NV, November 2001.

2. C. Pereira, S. Ahmed, S.H.D. Lee, and M. Krumpelt, “Integrated Fuel Processor Development,” 2002 Future Car Congress Proceedings, Arlington, VA, June, 2002.

IV.C.4 Microchannel Fuel Processor Development

Kriston P. Brooks, James M. Davis, Chris M. Fischer, Adam R. Heintzelman, David L. King, V. Susie Stenkamp, Ward E. TeGrotenhuis, Robert S. Wegeng, Greg A. Whyatt, and Larry R. Pederson (Primary Contact)
Pacific Northwest National Laboratory
PO Box 999
Richland, WA 99352
(509) 375-2731, fax: (509) 375-2167, e-mail: larry.pederson@pnl.gov

DOE Technology Development Managers:
JoAnn Milliken: (202) 586-3480, fax: (202) 586-9811, e-mail: JoAnn.Milliken@ee.doe.gov
Nancy Garland: (202)586-5673, fax: (202) 586-9811, e-mail: Nancy.Garland@ee.doe.gov

Objectives

- Develop a compact, steam reformation-based fuel processing system for the onboard reformation of hydrocarbon fuels that meets FreedomCAR performance targets for energy density, efficiency, residual CO content, durability, rapid start-up, and transient response.
- Develop highly effective reactors, fuel and water vaporizers, recuperative heat exchangers, and condensers broadly applicable to fuel processing and fuel cell systems.

Approach

- Emphasize endothermic steam reformation to best take advantage of unique heat and mass transfer advantages available in engineered microstructures.
- Utilize a differential temperature approach for the water gas shift reactor to provide an optimum balance of rapid kinetics at high temperature and favorable thermodynamics at lower temperature.
- Use a two-stage preferential oxidation reactor to reduce CO concentrations to acceptable levels, with active heat exchange for superior temperature uniformity.
- Achieve high efficiency through integration of steam reforming, water gas shift, and preferential oxidation reactors with microchannel recuperative heat exchangers, fuel and water vaporizers, condensers, and separators.

Accomplishments

- Fuel flexibility of the fuel reforming subsystem was demonstrated using methane, propane, butane, methanol, ethanol, isooctane, and benchmark gasoline. A 1000-hour catalyst and reactor durability test was completed using benchmark gasoline. Warm transient response of less than 5 seconds was achieved for 10 to 90% of full reformer capacity. A three-fold increase in reformer productivity was achieved compared to the previous year, due to improved catalyst performance and more uniform flow within the reactor. Reactor concepts that would meet FreedomCAR's rapid start-up targets were developed.
- A differential temperature water gas shift reactor was designed based on tests performed with engineered catalysts in a microchannel configuration. Conversion rates in the differential temperature reactor were higher than achievable in two isothermal stages.
- Residual CO concentrations less than 15 ppm were achieved in two microchannel preferential oxidation stages at gas hourly space velocities greater than 200,000 using catalysts obtained from commercial developers.

- Heat exchangers and vaporizers with very low pressure losses have been developed and are being supplied to interested collaborators for evaluation. A low pressure-drop water vaporizer sufficient to supply a 50 kWe autothermal reformer was designed, constructed, and delivered to McDermott Technology, Inc. Vaporizers and heat exchangers were provided to other industrial partners as well.

Future Directions

- Demonstrate rapid reformer start-up based on low pressure-drop concepts. This reactor design should also provide improved transient response characteristics.
- Incorporate a sulfur management subsystem into the steam reformer.
- Complete optimization of the reformer, water gas shift, and preferential oxidation catalyst compositions and forms.
- Complete integration of the steam reforming, water gas shift, and preferential oxidation subsystems.
- Conduct lifetime testing of reactors, heat exchangers, and catalysts using transportation fuels.
- Continue to engage industrial partner(s) to facilitate reformer system development.

Introduction

Steam reforming is an attractive fuel processing option for several reasons. Steam reforming is endothermic and thus can make use of heat from the catalyzed combustion of unutilized fuels in the fuel cell exhaust. The hydrogen content in the reformate stream is higher than obtained using other fuel processing options because it is not diluted by nitrogen from air. High reformate pressures can be efficiently generated by pumping fuel and water in liquid form; compression of air is not necessary. While conventional hydrocarbon steam reformation requires long residence times and relatively large reactor sizes because of heat transfer limitations, the heat and mass transfer advantages offered by engineered microchannels allow steam reformation to be conducted in a compact, energy-efficient system. Rapid kinetics for steam reforming in heated microchannels was first demonstrated by PNNL in 1999. Steam reforming reactors in the 10-20 kWe range were later demonstrated, coupled with a network of microchannel heat exchangers that significantly improved energy efficiency (Whyatt et al. 2001).

Approach

A modular, steam-reforming test stand with an internal volume of 51 cc that would support fuel processing rates in the 50 to 1000 We range was designed to conduct fuel flexibility and long-term durability testing (Figure 1). A network of microchannel heat exchangers was included in the test stand for water and fuel vaporization, recuperation of reformate to preheat reactants and for preheating of combustion air using the combustion exhaust. The heat exchangers were fabricated as

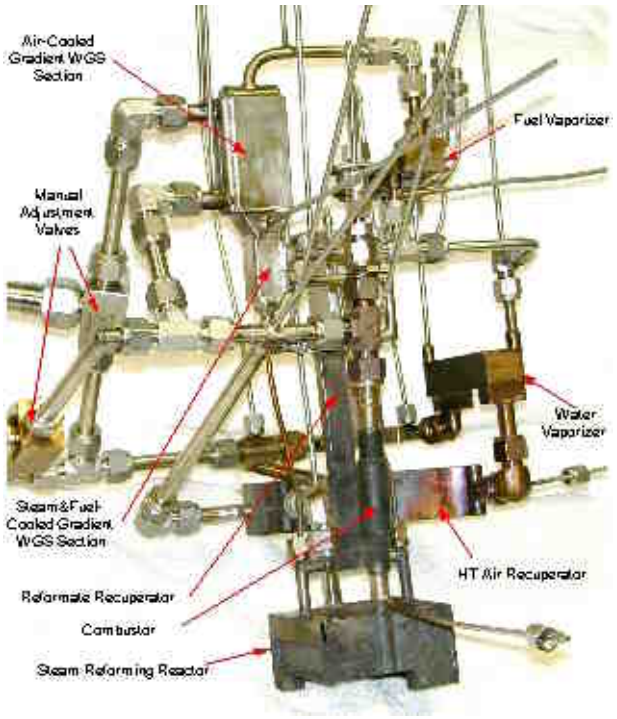

Figure 1. Modular Steam Reforming Test Stand Capable of Testing in the 100 to 1000 We Capacity Range

individual components and then connected via tubing.

The superior heat transfer achievable in engineered microchannels can be used to optimize temperature profiles in a reactor, which can lead to smaller reactor sizes and improved conversion. For reversible exothermic reactions such as water gas shift, the microchannels make it possible not only to remove the heat of reaction, but also to reduce the reaction temperature. By maintaining heat transfer length scales on the order of 100 microns, minimal temperature gradients across the catalyst were maintained while achieving precise control of temperature down the reactor. This approach provides an optimum balance between rapid kinetics at high temperature and favorable thermodynamics for conversion as the temperature is reduced.

Results

Steam Reforming Subsystem

Through improvements in gas flow characteristics and engineered catalyst performance, the volumetric productivity of the steam reforming reactor was improved by approximately a factor of three compared to our previous efforts. The catalyst that was used in these tests is a proprietary formulation obtained from Battelle Memorial Institute. For a full-sized, complete fuel processing system, projected power densities are more than double FreedomCAR targets, as shown in Table 1. To meet FreedomCAR targets for specific power, the mass of the system will need to be reduced, expected to be met through further improvements in reactor productivity and the use of lightweight alloys where appropriate.

The steam reforming subsystem was shown to exhibit good fuel flexibility. Tests were conducted using multiple fuels, including methane, propane, butane, methanol, ethanol, isooctane, and benchmark gasoline, a mixture of isooctane, xylene, methyl cyclohexane, and 1-pentene. The results of these tests are given in Figure 2, which shows conversion versus gas hourly space velocity (GHSV). The steam to carbon ratio was maintained at 3 to 1 for all non-alcohol fuels. For alcohols, the oxygen to carbon ratio was maintained at 3 to 1. Methanol was the most easily reformed, and was completely reacted to the highest space velocities tested. A conversion greater than 99.9% is necessary for fuels such as gasoline to prevent downstream condensation, whereas lower conversion may be acceptable for volatile fuels such as methane.

Performance Criteria	Current Performance	2005 FreedomCAR Target	Explanation
50 kWe System Volume	<1 cubic foot (<28 L)	2.5 cubic feet (71 L)	Projected from tests conducted on a smaller scale.
Energy Efficiency	81%	78%	High efficiency is the result of extensive thermal integration using effective heat exchangers.
Durability	>1000 h	4000 h	Testing beyond 1000 hours not conducted; expanded durability testing planned for FY 2003.
Power Density, Specific Power	1800 W/L, 320 W/kg	700 W/L, 700 W/kg	Improvements in specific power expected from improved productivity and use of lightweight alloys for components intended for low temperature operation.
Transient Response	5 s	5 s	Further improvements expected with incorporation of low pressure-drop components.
Start-Up to Full Power, 20^{0}C	30 s (low dP) projection 15 min current	<1 min	Low combustion-side pressure drop is key to start-up; redesign of reactors using low pressure-drop concepts is expected to meet start-up goals.

Table 1. Comparison to FreedomCAR Performance Targets

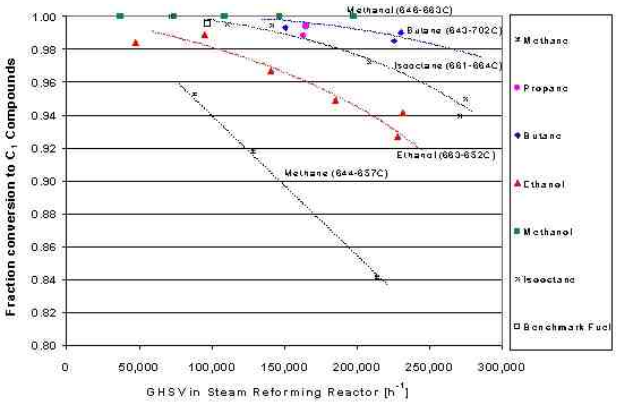

Figure 2. Conversion versus Space Velocity for Multiple Fuels

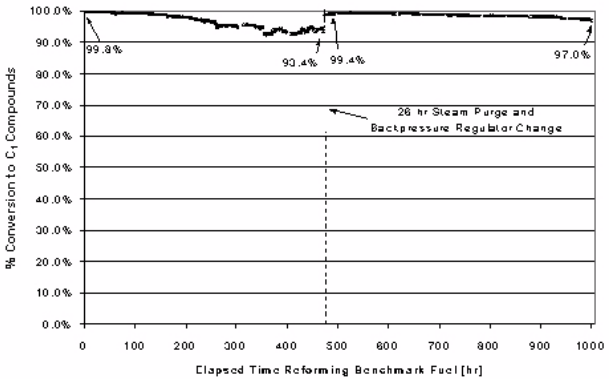

Figure 3. Conversion of Benchmark Gasoline versus Time in a Steam Reforming Reactor

To evaluate the durability of both the reactor and reforming catalyst, a 1000-hour test was performed using benchmark gasoline containing 10 ppm sulfur. The space velocity was chosen to obtain a small fraction of unconverted fuel (0.2%) at the start of the test, which aided in tracking changes in conversion versus time. Conversion fell by several percent over the first 500 hours, as shown in Figure 3, believed due to the effects of sulfur. The catalyst was then re-activated in clean hydrogen and steam, which returned the performance to near initial levels.

Warm transient response characteristics of the steam reforming subsystem were evaluated, shown in Figure 4. Fuel inflow was varied from 10 to 100% of full-scale, and reformate outflow was measured versus time. Because the residence time for fuel in this reactor and heat exchangers is very short, these

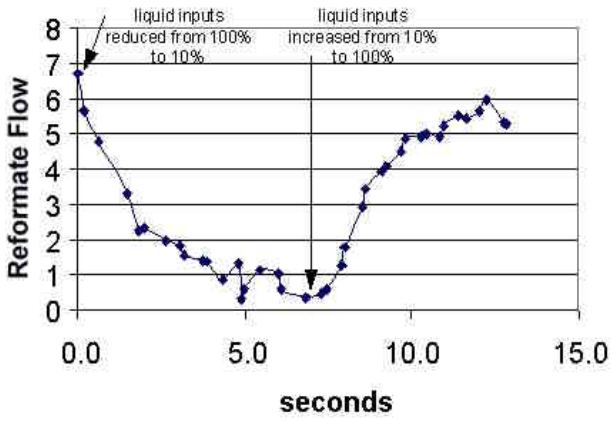

Figure 4. Warm Transient Response of the Steam Reforming Reactor from 10 to 100% of Full Capacity

portions of the system are capable of very rapid transient response. Major limiting factors are associated with fuel and water vaporizers. Scale-up is not expected to diminish transient response characteristics since a greater number of microchannels with similar aspect ratios would be used.

Water Gas Shift Subsystem

Research supporting the development of a compact water gas shift (WGS) reactor subsystem included catalyst screening studies, kinetic model development, and test reactor design and performance evaluation. Water gas shift catalysts obtained from commercial and other developers were converted into an engineered form and tested versus temperature, space velocity, and steam-to-gas ratio in single-channel reactors. Both base metal and precious metal catalyst formulations were included in the studies.

While both base metal and precious metal catalyst formulations performed well in a simulated high temperature WGS feed stream (~15% CO), precious metal catalysts were clearly superior when tested with a low temperature WGS feed stream (~5% CO). Results for a Süd-Chemie copper zinc catalyst (T2650) and a Süd-Chemie precious metal-ceria catalyst (PMS5) are shown in Figure 5, tested in a simulated low temperature WGS feed stream. Equilibrium was achieved for the PMS5 catalyst for

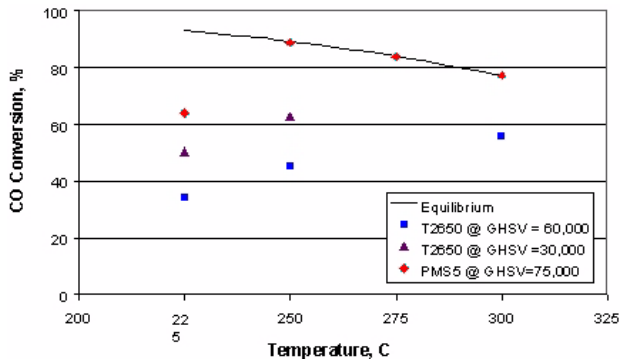

Figure 5. Conversion of CO versus temperature for engineered forms of Sud-Chemie T2650 (copper-zinc) and PMS5 (precious metal ceria) catalysts. Results correspond to a simulated low temperature WGS feed stream at a steam to gas ratio of 0.5.

temperatures greater than 250°C at a gas hourly space velocity of 75,000, whereas the T2650 copper-zinc catalyst gave more modest performance. Thus, the PMS5 catalyst was used primarily in additional testing.

A kinetic model was developed from the results of catalyst screening studies that relates reaction rates to temperature, space velocity, and steam to gas ratio. A finding of kinetic modeling studies is that conversion of carbon monoxide could be enhanced in a thermal gradient compared to reactions conducted isothermally. By managing the temperature profile of a reactor, reactants can be fed at a high temperature where rapid kinetics promotes an initial approach to equilibrium. As the reaction mixture is cooled, conversion is increased due to more favorable thermodynamic driving forces.

To optimize the performance of a microchannel-based water gas shift reactor, the temperature profile of the reactor was adjusted as a means to provide the best trade-off of rapid kinetics at high temperature and favorable thermodynamics at low temperature. A schematic for one microchannel configuration is shown in Figure 6, where catalytic monoliths are located at the center of an array of reaction channels, interleaved with heat exchange channels. A heat exchange fluid flowing co- or counter-current (shown in Figure 6) to the reaction flow removes the heat of reaction and cools the gas, thereby

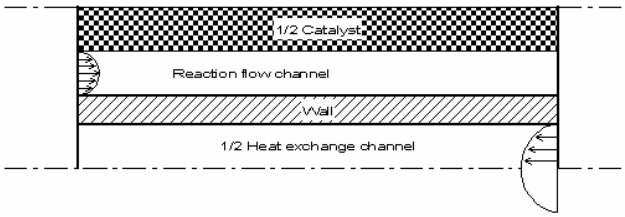

Figure 6. Two-dimensional schematic of a repeat unit for a microchannel reactor with counter-current heat exchange. Dashed lines indicate symmetry planes.

establishing a temperature trajectory for the reaction. The choice of coolant, the temperature and flow of the coolant, and the geometry are all design variables for achieving an optimal temperature profile to maximize the productivity of the catalyst.

An experimental validation of modeling predictions is given in Figure 7, comparing the performance of a reactor run in a differential temperature mode versus isothermally. This experiment was performed using a low temperature feed stream, corresponding to an initial CO concentration of 4.9% (wet basis). For a space velocity of 76,000 hr^{-1}, as steam to dry gas ratio of 0.52, and an initial temperature of 350°C dropping to 280°C, a CO concentration at the outlet of 0.84% was achieved. Conversion was always less when performed isothermally in the same reactor at an identical space velocity.

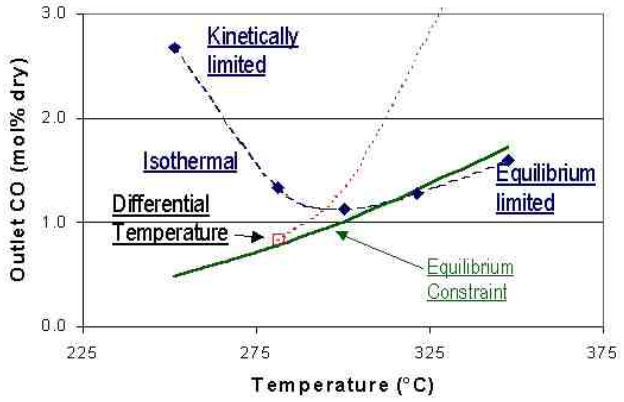

Figure 7. Comparison of a Microchannel WGS Reactor Run in Isothermal and Differential Temperature Modes on a Simulated Low Temperature Feed Stream

Preferential Oxidation Subsystem

Microchannel reactor designs may hold advantages for use in the preferential oxidation subsystem because of the ability to operate under strictly isothermal conditions and because of the ability to suppress undesired reactions (methane formation and reverse water gas shift) through the use of short residence times. Engineered forms of precious metal and base metal preferential oxidation catalysts obtained from commercial suppliers were evaluated in a microchannel reactor to show whether this approach is a viable means to meet FreedomCAR targets for conversion and selectivity. We have shown that less than 15 ppm CO in a 2 stage microchannel reactor can be obtained. For the first stage, operation at approximately 200°C, oxygen to carbon ratio = 1.0, and GHSV greater than 200,000 resulted in a reduction of CO from approximately 1% to approximately 500 ppm (0.05%). For the second stage, operation at 100°C, oxygen to carbon ratio = 4.0, and GHSV = 200,000 resulted in conversion of CO to below 15 ppm. To date, these two stages have not been tested together, nor has the catalyst durability been established. Discussions with catalyst vendors indicate that improved catalysts over what we have already tested are available, and such catalysts will be evaluated.

Water Vaporizer

A full-scale water vaporizer exhibiting extremely low gas-side pressure drop has been developed during the past year and provided to industrial collaborators for evaluation. Sufficient to support a 50 kWe autothermal reforming system, the dimensions of the vaporizer panels are 22.2 cm x 10 cm x 1.8 cm, with a weight of 2.4 kg when constructed using 316L austenitic stainless steel, as shown in Figure 8. At the maximum operating point, the heat exchanger duty is 24.6 kW, with a heat exchange intensity of 60 W/cm^3. The pressure drop on the gas side was minimized by making the flow distance very short and by providing a large cross-sectional area for gas flow. Multiple vaporizer panels were fabricated in a single diffusion bonded stack, separated using wire electric discharge machining methods. One of the steam generator panels is currently undergoing testing by McDermott Technology Inc. in a 50 kWe autothermal steam

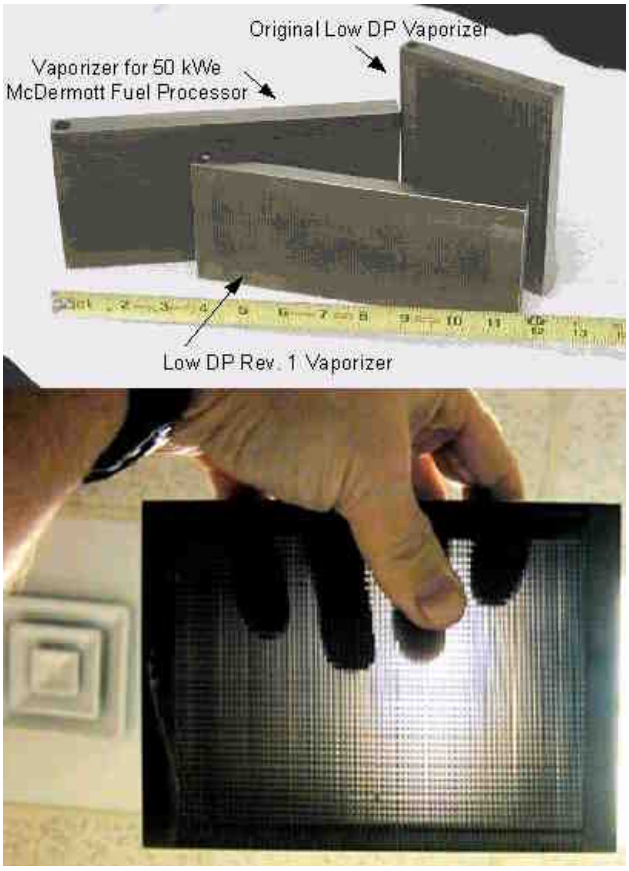

Figure 8. Microchannel Steam Generator Panel Sufficient to Support a 50 kWe Autothermal

reforming system. This particular panel was designed to vaporize more than 4 g/s water to produce steam at 225°C and 425 kPa. The expected combustion-side pressure drop is approximately 250 Pa.

Conclusions

- Power densities in excess of FreedomCAR targets, fuel flexibility, greater than 1000-hour reactor and catalyst life, and less than 5 second transient response have been demonstrated in a microchannel-based steam reformer. Future development activities will focus on rapid start-up and improving specific power.
- A differential temperature water gas shift reactor was developed that provides an optimum balance between fast kinetics at high temperatures and favorable thermodynamics at low temperatures.
- Residual CO concentrations less than 15 ppm were achieved in two microchannel preferential

oxidation stages at gas hourly space velocities greater than 200,000.
- Heat exchangers and vaporizers exhibiting very low pressure losses have been developed and are being supplied to interested collaborators for evaluation, including a unit sufficient to supply a 50 kWe autothermal reformer provided to McDermott Technology, Inc.

References

1. Whyatt, G. A., W. E. TeGrotenhuis, J. G. H. Geeting, J. M. Davis, R. S. Wegeng, and L. R. Pederson. "Demonstration of Energy Efficient Steam Reforming in Microchannels for Automotive Fuel Processing," Proceedings of the 5th International Conference on Microreaction Technology, May 27-30, 2001.

2. Van Herwinen, T. and W. A. DeJong. J. Catalysis 63, 3 (1980).

FY 2002 Publications/Presentations

1. TeGrotenhuis, W. E., D. L. King, K. P. Brooks, B. J. Golladay, and R. S. Wegeng. "Optimizing Microchannel Reactors by Trading-Off Equilibrium and Reaction Kinetics Through Temperature Management," IMRET 6 – 6th International Conference on Microreaction Technology, AIChE, New Orleans, March 10-14, 2002.

2. Whyatt, G. A., C. M. Fischer, and J. M. Davis. "Progress on the Development of a Microchannel Steam Reformer for Automotive Applications," IMRET 6 – 6th International Conference on Microreaction Technology, AIChE, New Orleans, March 10-14, 2002.

Special Recognitions and Awards/Patents Issued

1. "Active Microchannel Fluid Processing Unit and Method of Making", USP 6,192,596

IV.C.5 Plate-Based Fuel Processing System

Ralph Dalla Betta (Primary Contact and Principal Investigator)
Catalytica Energy Systems
430 Ferguson Drive
Mountain View, CA 94043
(650) 940-6310, fax: (650) 965-4345, e-mail: rdallabetta@catalyticaenergy.com

DOE Technology Development Manager: Donna Ho
(202) 586-8000, fax: (202) 586-9811, e-mail: donna.ho@ee.doe.gov

ANL Technical Advisor: Walter Podolski
(630) 252-7558, fax: (630) 972-4430, e-mail: podolski@cmt.anl.gov

Subcontractors: National Fuel Cell Research Center, Irvine, CA

Objectives

- Design, build and demonstrate a fully integrated, plate-based fuel processor system that will convert EPA Tier 2 gasoline into a hydrogen-rich gas for direct use in proton exchange membrane (PEM) fuel cell systems for vehicular applications.

Approach

Phase 1

- Complete conceptual design of plate-based reformer, water gas shift and preferential oxidation reactors and simulation models of each reactor using available catalyst kinetics. Begin optimization studies and parametric sensitivity analysis.
- Obtain catalyst performance data and kinetic data as required, including initial data on catalyst deactivation rate.
- Assess feasibility of reactor configurations, understand performance advantages, and develop initial cost analysis of reactor components.

Phase 2

- Perform prototype proof of concept testing at about 2-kW scale for laboratory component reactors.

Phase 3

- Develop 50-kW component reactors and assemble complete integrated fuel processor. Evaluate performance.

Accomplishments

- Identified sources of high local stresses in the plate reformer design that would result in short cyclic life. Developed improved designs with cyclic life approaching 250,000 cycles.
- Identified the need for a unique reactor design that would allow close control of reaction temperature under conditions typical of the reactor concepts being developed.
- Developed detailed reactor models for steam reforming, water gas shift and preferential oxidation reactor designs.

- Developed new proprietary catalyst for the water gas shift reaction that is non-noble metal, non-pyrophoric, and does not require pre-reduction.
- Began development of a fuel processor simulation tool to assess the overall integration and performance of the complete fuel processor utilizing the novel component reactors being developed.

Future Directions

- Establish kinetic models for the primary catalyst candidates for each of the component reactors (steam reforming, water gas shift, and preferential oxidation). Update the reactor models for the component reactors and establish performance for the various reactor configurations.
- Use the fuel processor simulation tool to evaluate the performance of a fuel processor based on the reactor design and establish catalyst performance criteria required for optimum performance of the component reactors and desired performance of the fuel processor.
- Complete initial catalyst stability studies for each of the component reactors. Establish catalyst stability improvement targets if required.
- Develop mechanical design for a steam reformer meeting the durability requirements including cyclic life.

Introduction

The Catalytica Energy Systems, Inc. (CESI) project is directed at developing unique reactor designs and the associated catalyst materials that will provide advantages toward meeting the DOE performance goals. The general approach is to utilize where feasible a plate-based reactor design that closely integrates heat exchange with the catalytic process to optimize component and system performance. The program consists of 3 phases as described above, with the first phase concentrating on component conceptual design and catalyst development.

Approach

The approach taken in this project is to utilize 1) steam reforming of gasoline as the first step to produce a reformate that has a high concentration of hydrogen, followed by 2) sulfur removal, 3) water gas shift, and 4) preferential oxidation to yield PEM fuel cell quality hydrogen. Work is ongoing on each of these four catalytic processes, including the development of a process simulation model that includes catalyst reaction kinetics, heat and mass transfer effects, etc. to adequately model the important aspects of the reactor design. Kinetics are either taken from the literature or are measured experimentally.

Results

Plate Reactor Design Development

In previous work, a prototype plate reactor was developed for methane steam reforming. This unit was operated for 400 hours at 100% load but with minimal (approximately 20) slow start-up cycles. An automotive fuel processor would have to demonstrate significantly higher levels of durability, including a large number of fast start-up cycles. It was assumed that the system would undergo 250,000 start-up and load transients as a worst case scenario (5,000 hours fuel processor life, one cycle every 1.2 minutes and similar stress levels from start-up and load transients). For a typical ferritic steel, this would require that the strain levels remain below 0.25%. Finite element analysis of a very fast start-up transient (30 seconds) resulted in high local stresses, in the range of 0.5 to 0.8% in the baseline reactor design. Alternative mechanical designs were evaluated, including designs that would provide a more realistic gas flow path and flow distribution. A derivative design was developed that gave a calculated strain of 0.28%, close to the target value and in an acceptable range.

Gasoline Steam Reforming Catalyst Evaluation

Initial catalyst development for direct steam reforming of gasoline was done in an integral reactor

system operating at design conditions including pressure and space velocity as shown below. In these tests, the H_2 and CO levels at the reactor exit are near the expected equilibrium values.

Conditions

Gasoline flow rate (as C_8H_{18})	0.522 mmol/min
Steam to carbon ratio (S/C)	3.1
Pressure	3 atm
Catalyst amount	2.0 g
Weight hourly space velocity	1.75 g/g/hr
Reactor outlet temperature	795°C

Results

Conversion (based on C species)	95.6%
Carbon mass balance	100.6%
Product composition (dry basis)	mole fraction
H_2	0.666
CO	0.158
CO_2	0.160
$CH_4 + C_{2+}$	0.016

It should be noted that these space velocities are similar to those typically found in autothermal reforming (ATR) so that catalyst volumes will not be excessive compared to autothermal reforming processes. Catalyst activity was found to be reasonably stable for the short duration tests in this work. However, the extremely endothermic nature of the reaction and the integral operation of the test reactor made it difficult to extract reaction kinetics. A new test reactor design was developed and fabricated, and work is in progress to obtain simplified kinetics for the gasoline steam reforming reaction adequate to model the catalytic process in the plate reactor simulation.

Water Gas Shift Catalyst Development

CESI is developing an improved water gas shift catalyst formulation that targets transportation applications with catalyst characteristics such as 1) no pre-conditioning requirement, 2) no air sensitivity, 3) preferably non-precious metal based, and 4) low sensitivity to condensed water. For the data analysis, the integral fixed bed reactor design equation was used with an empirical rate expression and a first-order deactivation model. Catalysts were quantitatively compared on the basis of the initial activity, *k'* [=] moles/(gram cat.-hr-atm^2), and the deactivation constant, k_d [=] hr^{-1}. The best Pt-based material tested did exhibit reasonable initial activity (*k'* = 0.287 at 250ºC), but rapid deactivation was observed throughout the temperature window of 250ºC to 350ºC. The value of k_d = 0.008 for that catalyst indicates a 50% loss of activity in just 87 hours time-on-stream, implying a very rapid loss in activity with time, making these catalysts inappropriate for commercial application [1-2].

Significant work during this period was directed at developing a non-precious metal-based or base metal water gas shift catalyst (Figure 1). The initial activity, *k'*, and the deactivation rate, k_d, are determined from a fit of the measured conversion curve shown in Figure 1 after the first 5 to 10 hours. These k_d and *k'* values for these catalysts are summarized in Table 1 with the Pt catalyst reported in Reference 2 included for comparison.

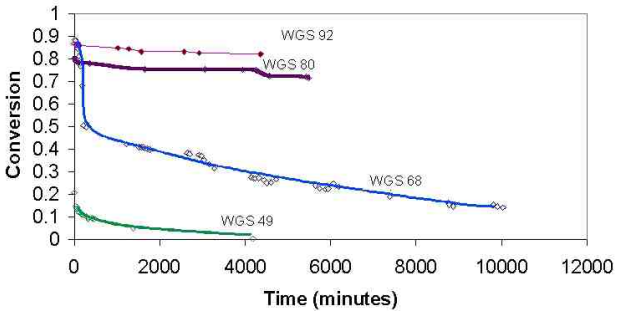

Figure 1. Catalyst Performance Test Results for Water Gas Shift Catalyst Materials

Catalyst	k_d	*k'*	Half life
	hr^{-1}	mol/(g-hr-atm^2)	hr
WGS 49	0.0812	0.014	8.5
WGS 68	0.0047	0.44	147
WGS 80	0.0022	1.39	315
WGS 92	0.0016	1.21	433
Pt-catalyst	0.008	0.287	86.6

Table 1. Performance of Base-Metal and Pt-Based Water Gas Shift Catalysts after 5 to 10 Hours on Stream

Currently, the best base-metal catalyst developed by CESI possesses much better activity and stability than the reported Pt-based catalyst and is comparable to commercial catalysts in long term activity. However, while the WGS 92 catalyst shows very good stability, the k_d value of 0.0016 still implies a half life of about 433 hours, and if this deactivation rate is maintained throughout 2,000 hours of operation, the catalyst activity would decrease by 25 fold. Work is in progress to develop static aging procedures to measure activity out to 5,000 hours and to accelerate the development of more stable catalyst systems.

Preferential CO Oxidation

A detailed computational model was developed for several different innovative designs for the preferential carbon monoxide (CO) oxidation reactor using a kinetic mechanism and reaction sequence derived from a micro-kinetic model and literature data for the specific adsorption coefficients and kinetic parameters for a platinum-based catalyst. The course of the reaction calculated by such a kinetic model is shown in Figure 2, where the space time is varied over a wide range in an isothermal reactor operating at 150°C. At nearly 100% CO conversion, the selectivity is high due to the selective adsorption of CO over H_2; it drops as H_2 begins to oxidize.

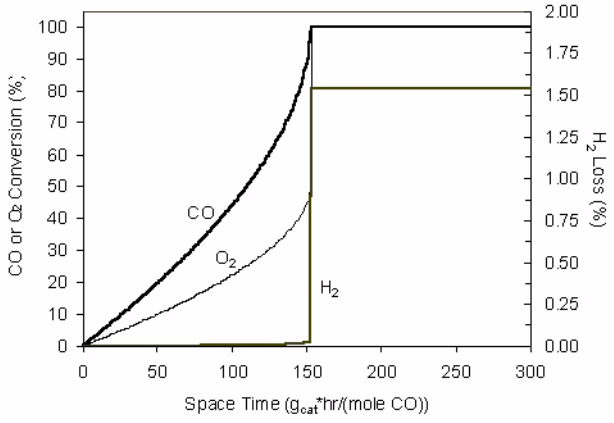

Figure 2. Reaction profile during the preferential oxidation of CO using the simulation model described in the text. This models an isothermal reactor operating at 150°C with a 1% CO reformate stream typical of the exit composition from the water gas shift reactor.

The results of a parametric study exploring the effect of mass transport limitations on this reaction gave the results shown in Figure 3. For this study, the reactor was assumed to be isothermal, and the conversion data of Figure 3 show the final composition exiting the reactor. The ideal (kinetics only) result gives the expected high conversion and selectivity due to the selective CO reaction. As mass transport limitation is added, the maximum CO conversion drops (Table 2) due to CO depletion near the surface since O_2 is in excess.

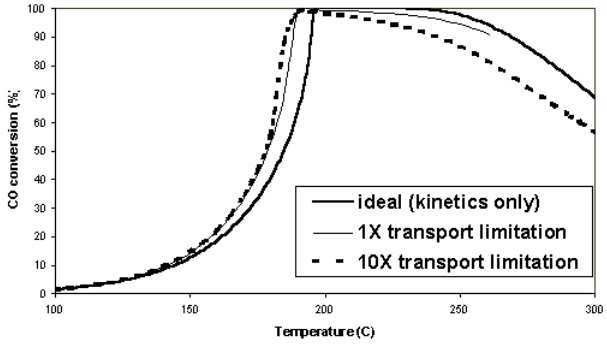

Figure 3. Simulation model results showing the effect of transport limitations on the preferential oxidation of CO. This models an isothermal reactor operating at 150°C with a 1% CO reformate stream typical of the exit composition from the water gas shift reactor.

Simulation conditions	Minimum CO level
Kinetics only	~0 ppm
1X mass transport limitations	30 ppm
10X mass transport limitations	140 ppm

Table 2. Effect of Mass Transport Limitations on the Minimum Level of CO that Can Be Obtained in the Preferential Oxidation of CO

These results and other parametric studies show the importance of the reactor and catalyst design. However, some of these results deviate from measured kinetics and CO selectivity and suggest that the assumed kinetics may not be fully representative of reality. The strong dependence of the results on the kinetic and equilibrium parameters suggest that it is absolutely essential that the kinetic parameters be validated by experimental tests, and this work is in progress.

Conclusions

Initial work on the steam reforming of Tier 2 gasoline demonstrated that equilibrium composition reformate can be obtained with space velocities typical of autothermal reforming catalysts, supporting the feasibility of a compact and effective gasoline steam reforming reactor. A new reactor design has been developed to obtain kinetics under well controlled conditions for highly exothermic or endothermic reactions.

A water gas shift catalyst has been developed that is very active and reasonably stable, does not require pre-reduction, is non-pyrophoric, and does not contain precious metals. The kinetics of this catalyst are being more fully explored to allow process and reactor modeling, including modeling in a plate reactor configuration, and work has been initiated to develop a long-term, cost effective aging process to estimate performance at the target 2,000 to 5,000 hour life.

A process simulation tool for the full fuel processor has been developed, and parametric studies have shown the importance of catalyst and reactor design in obtaining the target CO levels of 10 ppm.

References and Publications

1. Zalc, J.M., Park, T., Sokolovskii, V.D., and Löffler, D.G., "Optimal Design of a Water-Gas Shift Reactor for Use in Automotive Applications," American Institute of Chemical Engineers Annual Meeting, Reno, Nevada, November 6, 2001, Paper 167a.

2. Zalc, J.M., Sokolovskii, V.D. and Löffler, D.G., "Are Noble Metal-Based Water-Gas Shift Catalysts Practical for Automotive Fuel Processing?" Journal of Catalysis, 206[1], 169-171, 2002.

IV.C.6 Fuel Processors for PEM Fuel Cells

Levi Thompson (Primary Contact)
University of Michigan
Department of Chemical Engineering
3026 H.H. Dow Building
Ann Arbor, MI 48109-2136
(734) 647-7150, fax: (734) 763-0459, e-mail: ltt@umich.edu

DOE Technology Development Manager: Patrick Davis
(202) 586-8061, fax: (202) 586-9811, e-mail: Patrick.Davis@ee.doe.gov

Subcontractor: Ricardo, Inc. Plymouth, MI

Objectives

The key objectives of this project are to:

- Demonstrate high performance desulfurizer, catalyst, microreactor and microcombustor/ microvaporizer concepts that will enable production of compact fuel processors for proton exchange membrane (PEM) fuel cells;
- Design, fabricate and evaluate a 1 kW fuel-flexible (including EPA Phase II reformulated gasoline) fuel processor; and
- Design, fabricate and evaluate a fuel-flexible (including EPA Phase II reformulated gasoline) fuel processor capable of producing a hydrogen-rich stream for up to a 10 kW PEM fuel cell.

The 1 kW fuel processor will be completed during the first 36 months of the project. Following a go/no-go decision, the larger fuel processor will be completed within 48 months.

Approach

Tasks devised to accomplish the program objectives include:

- Component design and modeling;
- Sorbent development;
- Catalyst development and catalyst/microreactor integration;
- Microcombustor/microvaporizer development;
- Microchannel reactor system development;
- Component evaluations;
- Fuel processor design, modeling, fabrication and evaluation; and
- Cost analysis.

Accomplishments

- Models have been developed for the entire fuel processor system (ASPEN) and several of the microchannel reactors (FEMLAB and FLUENT).
- Demonstrated that π-complexation sorbents out-perform commercial sorbents by a wide margin for the adsorption of model sulfur compounds like thiophene.
- High activity carbide and supported gold water gas shift (WGS) catalysts have been demonstrated. Some of the materials possess rates that exceed those for Cu-Zn-Al commercial catalysts.
- Fabricated and tested several micro-reactors.

Future Directions

- We are in the first year of the project. We have not identified better strategies; therefore, we plan to execute the tasks outlined above.

Introduction

Fuel cells are being developed to power cleaner, more fuel efficient automobiles. The fuel cell technology favored by many automobile manufacturers is proton exchange membrane (PEM) cells operating with H_2 from liquid fuels like gasoline and diesel. A key challenge to the commercialization of PEM fuel cell based powertrains is the lack of sufficiently small and inexpensive fuel processors. Improving the performance and cost of the fuel processor will require the development of better performing catalysts and new reactor designs, as well as better integration of the various fuel processing components.

Approach

Prototype gasoline fuel processors will be produced and evaluated against the Department of Energy technical targets. Significant improvements over the present state-of-the-art will be achieved by integrating low-cost microchannel systems, high activity catalysts, π-complexation sorbents, and high efficiency microcombustors/microvaporizers being developed at the University of Michigan. The microchannel system will allow (1) more efficient thermal coupling of the fuel processor components and minimization of the heat exchanger requirements, (2) improved catalyst performance due to optimal reactor temperature profiles and increased heat and mass transport rates, and (3) better cold start and transient responses. The project will be accomplished in 3 phases. The Phase I effort will focus on demonstrating compact desulfurizer, microreactor and microcombustor/microvaporizer components for a 1 kW fuel processor, and developing low-cost microdrilling and micromilling methods for the production of microchannel systems. The components will be third-party tested and will provide the basis for design and fabrication of an integrated 1 kW ethanol or gasoline fuel processor during Phase II. We will scale-up the smaller processor to 10 kW during Phase III.

Results

Component design and modeling. ASPEN, a chemical process simulator, is being used to model the fuel processor system. These simulations will allow determination of the equilibrium constraints and heat duties for the different components in the fuel processing system. Performance of the micro-reactors is being simulated using FEMLAB, a finite-element software package, and FLUENT, a package that is capable of handling multi-component transport in a flow fluid simultaneously with surface reactions. The FEMLAB simulations demonstrated that one can control heat transfer in microchannel reactors by properly designing thermal bridges within the microfabricated system. The FLUENT results are being cross-validated against the FEMLAB results.

Sorbent development. During liquid-phase experiments, π-complexation sorbents adsorbed more sulfur (e.g. thiophene) at low concentrations than commercial sorbents. Table 1 compares the performance of selected sorbents.

.

	NaY (commercial)	π-Complexation Adsorbent
Solvent	Saturation Amount (mmol/g)	
Benzene	0.102	0.171
n-Octane	----	0.898

Table 1. Thiophene Adsorption Amounts upon Saturation

Catalyst development and catalyst/ microreactor integration. Several ATR, WGS, and PrOx catalysts have been prepared. The ATR catalysts include beta-alumina supported nickel. These catalysts are being evaluated. Transition metal carbide and oxide supported gold catalysts were demonstrated to be highly active for the WGS

reaction. The carbide catalysts were more active and durable than the oxide supported catalysts. The oxide supported gold catalysts deactivated dramatically during the first 10 hours on stream (see Figure 1). The deactivation appears to be a consequence of over-reduction of the support by CO. We are modifying the supports to improve their durability. Preferential oxidation catalysts consisting of 5% Pt/15% ceria-85% alumina wash-coated onto honeycomb monoliths have been prepared. These materials are currently being tested.

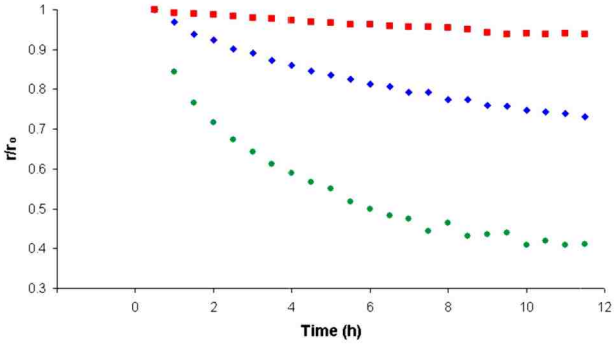

Figure 1. Deactivation Patterns for the Oxide Supported Gold Catalysts

Microchannel reactor system development. A prototype micro-reactor with concentric tubes has been fabricated. The main body is made of aluminum with 4 channels produced by deep hole micro-drilling. These channels have diameters of 3 mm and depths of 50 mm. Tubes with outer diameters of 650 µm and inner diameters of 300 µm were fitted into the channels. The structure included 4 stainless steel end caps made by milling and micro-drilling processes. The prototype reactor is illustrated in Figures 2 and 3.

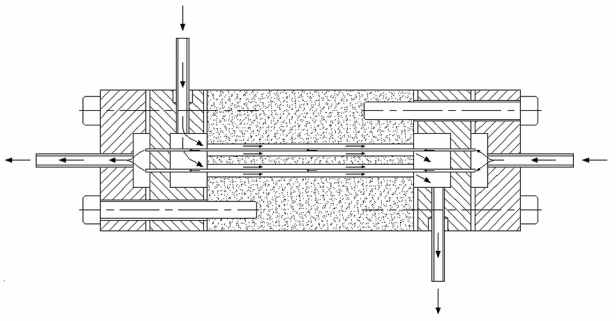

Figure 2. Schematic of the Prototype Micro-Reactor

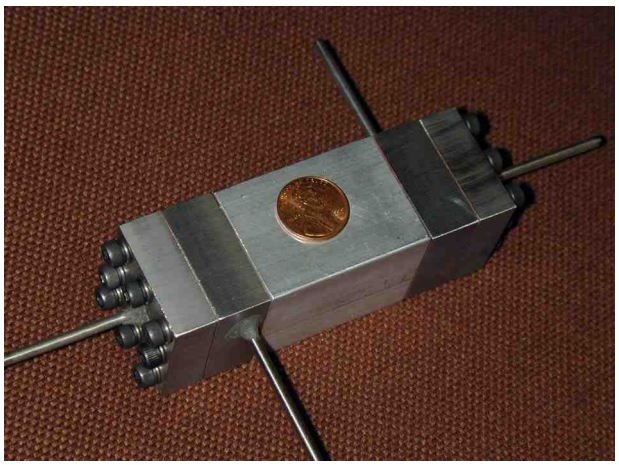

Figure 3. Photograph of the Prototype Micro-Reactor

Conclusions/Future Work

While this project is relatively new, significant progress has been made regarding the component design and modeling, sorbent and catalyst development and microchannel system development tasks. We will continue to focus on these tasks and microcombustor/vaporizer development. In addition, methods will be demonstrated to integrate catalysts into the micro-reactors.

IV.C.7 Evaluation of Partial Oxidation Fuel Cell Reformer Emissions

Stefan Unnasch (Primary Contact), Scott Fable
TIAX, LLC.
1600 De Anza Blvd., Suite 100
Cupertino, CA 95014
(408) 517-1563, fax: (408) 517-1553, e-mail: unnasch.stefan@tiax.biz

DOE Technology Development Manager: Nancy Garland
(202) 586-5673, fax: (202) 586-9811, e-mail: Nancy.Garland@ee.doe.gov

ANL Technical Advisor: Walter Podolski
(630) 252-7558, fax: (630) 972-4430, e-mail: podolski@cmt.anl.gov

Subcontractors: Nuvera Corporation, Cambridge, MA; Air Toxics, Ltd., Sacramento, CA; Clean Air Vehicle Technology Center, Hayward, CA

Objectives

- Measure the emissions from a partial oxidation/autothermal fuel processor for a proton exchange membrane (PEM) fuel cell system under both cold-start and normal operating conditions.
- Assess the feasibility of meeting emissions standards for automobiles and light-duty trucks through the use of a fuel cell vehicle with a gasoline reformer.

Approach

- Define a representative test cycle consisting of both cold-start and normal operating conditions.
- Use the established test cycle to quantify emissions from a partial oxidation reformer before and after anode-gas-burner treatment.
- Measure emissions with continuous monitor measurements supplemented with laboratory analyses of speciated hydrocarbons.
- Use reasonable approximations and estimates to convert emissions data from a grams/unit fuel basis to a predicted grams/mile basis.

Accomplishments

- Measured emissions from a fuel processor (without fuel cell) over several operating conditions including cold-start.
- Speciated total hydrocarbon data before and after the anode gas burner.
- Assessed the sensitivity of monitoring equipment over a range of operating conditions.
- Analyzed data to report emissions on a g/kg fuel basis.
- Established testing plans for two additional reformer systems.

Future Directions

- Perform extensive emissions testing of a fuel cell/reformer system to include particulate, formaldehyde, and ammonia as well as NO_x, hydrocarbons, and CO.
- Develop control strategies to minimize emissions.
- Test emissions from McDermott Technologies fuel processor in August 2002.
- Evaluate on-road emissions from fuel cell vehicles with on-board reformers.

Introduction

Fuel reformer operation is generally divided into two operating modes: start-up and normal partial oxidation. During start-up, the fuel processor burns fuel at near stoichiometric conditions until critical system temperatures and pressures stabilize to target values. Once the target conditions are reached, the reformer operates in normal mode in which the fuel processor burns fuel at very rich conditions. Since these modes are comprised of considerably different operating conditions, it follows that the emissions associated with each of these modes are also considerably different.

Since the combustor is typically cold under start-up conditions, the emissions produced during this brief period (target times are under 30 seconds) can be substantially higher than those produced during the remaining, much longer portion of the driving cycle. The pollutant emissions produced during this operating mode include NO_x, CO, formaldehyde, and organic compounds. These organic compounds, which include hydrocarbons, alcohols, and aldehydes, are regulated in California and referred to as non-methane organic gases (NMOG).

Under normal operating conditions, in which the combustor is sufficiently warm and operated under fuel rich conditions, virtually no NO_x is formed, although the formation of ammonia is possible. Most hydrocarbons are converted to carbon dioxide (or methane if the reaction is incomplete); however, trace levels of hydrocarbons can pass through the fuel processor and fuel cell. The shift reactors and the preferential oxidation (PrOx) reactor reduce CO in the product gas, with further reduction in the fuel cell. Thus, of the criteria pollutants (NO_x, CO, and non-methane hydrocarbons [NMHC]), NO_x and CO levels are generally well below the most aggressive standards. NMOG concentrations, however, can exceed emission goals if these are not efficiently eliminated in the catalytic burner.

Approach

In this study, a gasoline fuel processor is operated under conditions simulating both cold start and normal operation. Emissions are measured before and after the anode gas burner in order to quantify the effectiveness of the burner catalyst in controlling startup emissions. The emissions sampling system includes continuous emissions monitors (CEMs) for O_2, CO_2, CO, NO_x, and total hydrocarbons (THC). Also, integrated gas samples are collected in Tedlar bags for hydrocarbon speciation analysis via gas chromatography (GC). This analysis yields the concentrations of the hydrocarbon species required for the California NMOG calculation. The particulate matter (PM) concentration in the anode burner exhaust is measured through either isokinetic sampling or the placement of a filter in the exhaust stream.

Concentrations of the aforementioned species are obtained using the emission sampling system shown in Figure 1. Since emissions vary significantly between startup and normal operation, a wide range of analyzer capability is required.

Emission data will be used to assess on-road emissions from fuel cell vehicles and will be characterized in terms of cold-start on reforming modes. Current fuel processor technologies are not configured to follow a vehicle load and may be

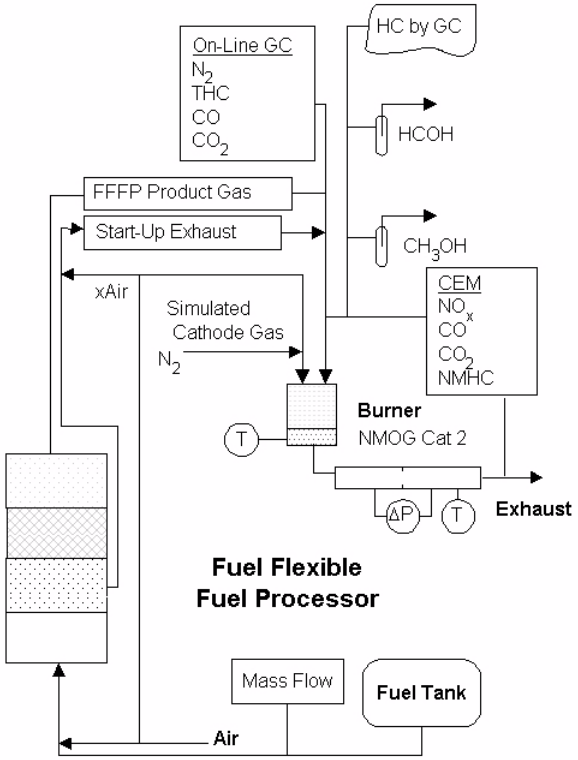

Figure 1. Fuel Processor Schematic

integrated with a hybrid vehicle. For this project, the fuel processor is operated at several steady-state points while emissions are monitored for the steady-state conditions and transients between load changes. The combination of data during start-up, different loads, and transients will be inputs to a vehicle emissions model. The model for determining vehicle emissions estimates the emissions for each second in a driving cycle based on load. Start-up emissions are also added to the total driving emissions. The data will also be provided to the National Renewable Energy Laboratory to support their efforts in vehicle emissions modeling.

Results

Our previous report summarized the results of a preliminary emissions test of an autothermal fuel processor operating without a fuel cell. The test focused on NO_x and hydrocarbon emissions, including speciation of hydrocarbon components. Figure 2 shows NO_x and THC emission levels as the reformer was started up and operated over a duty cycle. The testing did not attempt to follow a vehicle driving cycle but rather followed a series of steady-state conditions with load changes. THC emissions were high during start-up and then varied during the test, with spikes occurring when the load was increased.

During reforming, over 90 percent of the THC emissions were methane. The composition of the hydrocarbons was analyzed and the presence of toxic contaminants determined. Figure 3 shows the hydrocarbon fractions from fuel processor tests in terms of methane and NMHCs. Samples from these tests were also analyzed to determine the speciated hydrocarbon emissions profile over various operating loads. Figure 4 shows the results of the speciation analysis, in terms of the fraction of olefins and saturated and aromatic hydrocarbons that comprise the NMHCs. Aromatics and saturated hydrocarbons comprise almost all of the NMHC emissions. The fraction of NMHC as aromatics was close to the fraction of aromatics in the test gasoline for several samples taken from the PrOx and the tail gas combustor (TGC). The TGC burned reformer product gas.

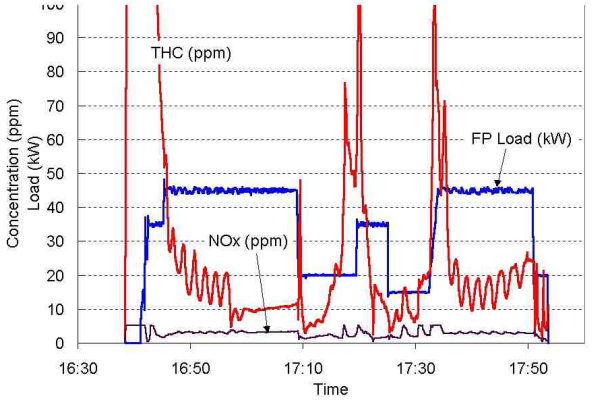

Figure 2. THC and NOx Concentrations Compared with Fuel Processor Load over Time

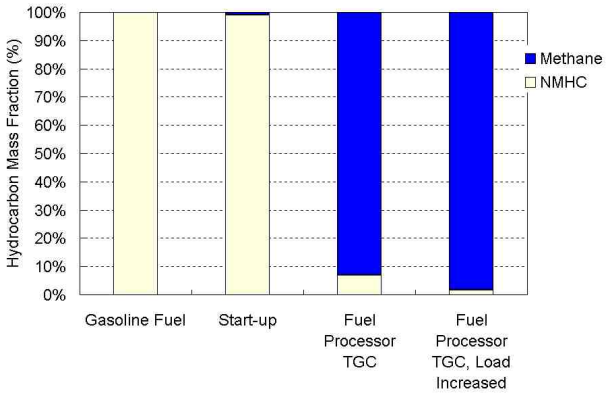

Figure 3. Hydrocarbon Mass Fraction of Fuel Processor Emissions at Various Stages

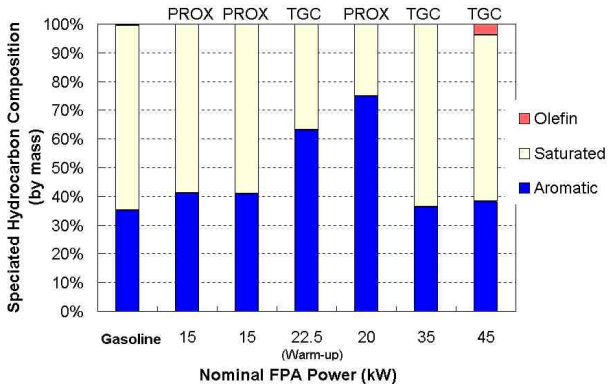

Figure 4. Speciated Hydrocarbon Composition of Air Toxics Samples from the Fuel Processor or Tail Gas Combustor at Various Fuel Processor Loads

During warm-up and one mid-power PrOx sample (20-22.5 kW), the fraction of NMHC as aromatics was higher. Olefins were typically less than 1 percent of NMHC in the PrOx and TGC samples and also represented less than 1 percent of the gasoline. However, for one test point, olefins comprised 4% of the NMHC. The presence of the toxic components benzene and 1,3-butadiene were less than 1 ppm.

Conclusions

Preliminary emissions data were measured from the PrOx and a TGC that combusted all of the reformer products. The fuel processor and the combustion of reformer products did not represent an optimized fuel cell vehicle configuration. Even with these limitations, the following conclusions can be drawn from the data.

NO_X emissions measured from a TGC ranged from less than 1 ppm to 5 ppm. These emission levels would correspond to approximately 0.01 g/mi of NO_X over a vehicle driving cycle. These emissions would be as low if the TGC were burning hydrogen-depleted anode gas.

NMHC emissions during start-up were over 100 ppm. In order to meet stringent emission standards, the start-up duration will need to be minimized. More data on start-up with an optimized fuel processor is required before on-road NMHC emissions can be estimated.

During reforming, hydrocarbon emissions are typically 90 percent methane, which will help reduce the NMHC contribution of the fuel processor.

IV.C.8 Catalysts for Autothermal Reforming

Theodore Krause (Primary Contact), Jennifer Mawdsley, Cecile Rossignol, John Kopasz, Daniel Applegate, Magali Ferrandon, J. David Carter, and Michael Krumpelt
Argonne National Laboratory,
9700 South Cass Ave.
Argonne, IL 60439
(630) 252-4356, fax: (630) 972-4463, e-mail: krause@cmt.anl.gov

DOE Technology Development Managers:
JoAnn Milliken: (202) 586-2480, fax: (202) 586-9811, e-mail: JoAnn.Milliken@ee.doe.gov
Nancy Garland: (202) 586-5673, fax: (202) 586-9811, e-mail: Nancy.Garland@ee.doe.gov

Objectives

- Improve catalytic activity and reduce the cost of autothermal reforming (ATR) catalyst to decrease the size of the fuel processor and reduce start-up time.
- Develop a better understanding of reaction mechanisms in order to optimize catalytic activity, minimize deactivation, and improve sulfur tolerance.

Approach

- Synthesize materials that meet Argonne National Laboratory (ANL) selection criteria and DOE cost goals.
- Determine H_2, CO, CO_2, CH_4, and C_nH_m yields versus temperature and space velocity.
- Work with catalyst manufactures to optimize catalyst performance and to support the catalyst on structured forms such as a monolith.
- Conduct fundamental studies to gain insight into reaction mechanisms.

Accomplishments

- Demonstrated the performance of Rh-, Ni-, and Pt-CGO (gadolinium-doped ceria) supported on a cordierite monolith.
- Demonstrated that the oxidation and reforming reactions are “decoupled.”
- Transferred technology to Süd-Chemie, Inc. under a CRADA to optimize the performance of the CGO-based catalyst.
- Demonstrated that modified $LaNiO_3$ and $LaCoO_3$ perovskites are active for autothermal reforming and appear to be structurally stable under autothermal reforming conditions.

Future Directions

- Optimize the choice of metals and metal loadings for the CGO-based catalysts supported on structured forms, such as monoliths or foams.
- Work with Süd-Chemie, Inc. to optimize the performance of the CGO-based catalysts.
- Increase the activity of the perovskite catalysts.
- Improve the sulfur tolerance of non-Pt catalysts.
- Continue to work with academic collaborators to gain better insight into reaction mechanisms.

Introduction

Catalytic autothermal reforming (ATR) of hydrocarbon fuels was first proposed by Argonne National Laboratory (ANL) several years ago and has been widely accepted as the most promising route to meet the efficiency, volume, and cost goals of the DOE Hydrogen, Fuel Cells and Infrustructure Technologies Program. ANL has developed a new family of reforming catalysts that are modeled after solid oxide cathode materials. Unlike typical industrial steam-reforming catalysts that consist of nickel supported on a modified alumina substrate, the ANL catalyst consists of selected Group VIII transition metals, such as platinum, rhodium, or nickel, supported on an oxide ion-conducting substrate, such as gadolinium- or samarium-doped ceria. The ANL catalyst has demonstrated near-equilibrium yields of H_2 from a number of hydrocarbon fuels, including natural gas, gasoline, and diesel, exhibiting high catalytic activity and resistance to coking. The platinum catalyst has been shown to exhibit long-term tolerance to sulfur at a concentration of 50 ppmw, which is typical of the sulfur content in Tier II gasoline. Süd-Chemie, Inc., of Louisville, Kentucky, produces the ANL catalyst under a licensing agreement. Because of concern over the cost of platinum and rhodium, we have initiated an effort to develop mixed non-noble metal oxides with the ABO_3 stoichiometry and the perovskite structure as reforming catalysts. Perovskites were selected because many are good oxygen ion conductors and/or good mixed electronic conductors.

High reforming activity has been exhibited by lanthana-based perovskites that have been doped on the A-site to improve catalytic activity and on the B-site to provide structural stability in reducing environments.

Approach

Gadolinium-doped ceria (CGO) substrates are prepared from nitrate salt precursors by either coprecipitation or glycine-nitrate combustion techniques. Pt, Rh, or Ni is loaded onto the CGO using the incipient wetness technique. Typical weight loadings are 1 wt% or less for Pt and Rh and up to 10 wt% for Ni. Pt-, Rh-, and Ni-CGO supported on cordierite monoliths were prepared by Süd-Chemie. Core samples from the monoliths were tested in a microreactor system for the reforming of isooctane and benchmark fuel (74 wt% isooctane, 20 wt% xylenes, 5 wt% methylcyclohexane, and 1 wt% 1-pentene). Temperature-programmed reaction studies were performed by exposing powder samples (~50 mg) of the catalysts to isobutane (C_4H_{10}), O_2, H_2O, and N_2 at the desired feed ratios over a temperature range of 100-800ºC using a Zeton Altamira Chemisorption Instrument Model AMI-100 equipped with a mass spectrometer. Lanthana-based perovskites were prepared by mixing selected nitrate salt precursors at the appropriate ratios using the glycine-nitrate combustion technique. Powder samples were tested for isooctane and benchmark fuel reforming in a microreactor system. The structural stability of the materials was evaluated by comparing the X-ray diffraction pattern of samples before and after reforming.

Results

Rh-, Ni-, and Pt-CGO Catalysts Supported on a Cordierite Monolith

As shown in Figure 1, Rh- or Ni-CGO supported on a cordierite monolith were observed to be more active than Pt-CGO supported on a cordierite monolith based on the higher H_2 yield observed with

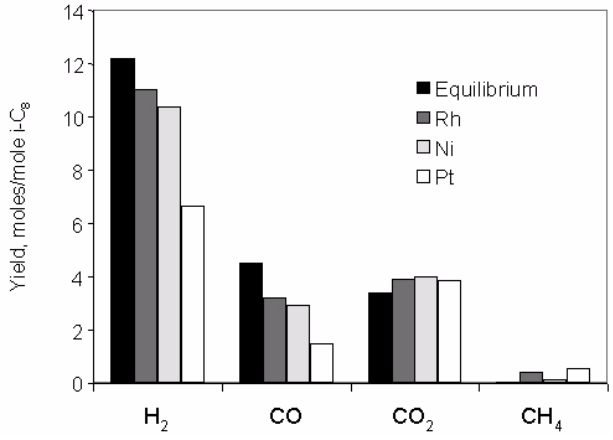

Figure 1. Yields of H_2, CO, CO_2, and CH_4 (mole/mole of isooctane) from Reforming Isooctane Catalyzed by Rh-, Ni-, or Pt-CGO Supported on a Cordierite Monolith. Conditions: 700°C, O_2/C=0.5, H_2O/C=1.2, GHSV=11,000 h^{-1}.

Rh-CGO (11.0 moles/mole of isooctane) or Ni-CGO (10.4 moles/mole of isooctane) compared with Pt-CGO (6.7 moles/mole of isooctane) for isooctane reforming at 700°C. The 11.0 moles of H_2 per mole of isooctane produced by Rh-CGO were slightly less than the 12.2 moles of H_2 predicted by thermodynamic equilibrium at 700°C. The higher H_2 yield observed with Rh- or Ni-CGO compared to Pt-CGO is attributed to Rh and Ni being more active than Pt for steam reforming. A comparison of the temperature-programmed isobutane reforming reaction profiles for Rh-, Ni-, and Pt-CGO (Figure 2) shows that the temperature at which 50% of the maximum H_2 yield is observed for Rh-CGO (381°) or Ni-CGO (512°) is considerably lower than for Pt-CGO (615°C). For Rh-, Ni-, and Pt-CGO, the oxidation reactions involving O_2 occur at a lower temperature than the reforming reactions, which produce H_2 and CO (not shown in Figure 2). While it is possible that H_2 and CO may be produced by partial oxidation reactions, they are rapidly oxidized to H_2O and CO_2, respectively, as long as O_2 is still present. For isooctane reforming, the fact that the CO_2 yield for all three metal catalysts is essentially the same (3.9-4.0 moles per mole of isooctane), as shown in Figure 1, and the lack of O_2 in the reformate suggest that all three metals are very active oxidation catalysts.

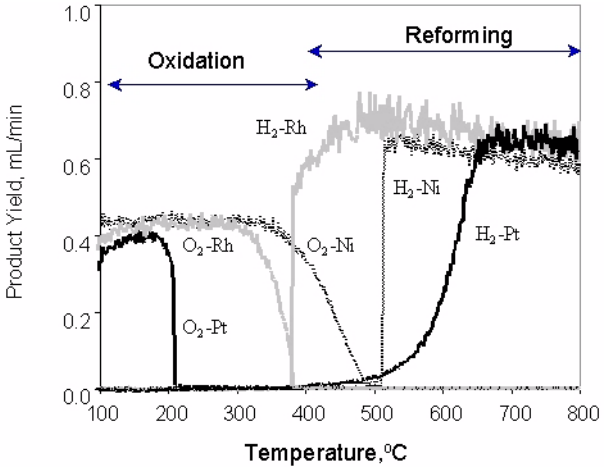

Figure 2. Temperature-Programmed Reaction Profile for the Flowrate of O_2 and H_2 in the Reformate Produced from Reforming Isobutene Catalyzed by Rh-, Ni-, or Pt-CGO in Powder Form. Conditions: O_2/C=0.5, H_2O/C=1.0, GHSV=~50,000 h^{-1}, total flowrate is 50 mL/min (balance He).

In long-term testing, Rh-CGO supported on a cordierite monolith exhibited relatively stable performance over a 1000-hr period, producing a reformate containing ~30-38 vol% H_2 from the benchmark fuel at 700°C, as shown in Figure 3. Initially, Pt-CGO supported on a cordierite monolith exhibited activity similar to Rh-CGO, producing a reformate containing ~38 vol% H_2 at 675°C (Figure 3); however, the concentration of H_2 in the reformate decreased by ~50% after only a few hours on stream. This initial rapid decrease in activity was followed by a much slower, continuing decrease in activity. After 250 hr, the concentration of H_2 in the reformate was <10 vol%. Increasing the reaction temperature to 725°C resulted in an increase in the H_2 concentration to ~20 vol%.

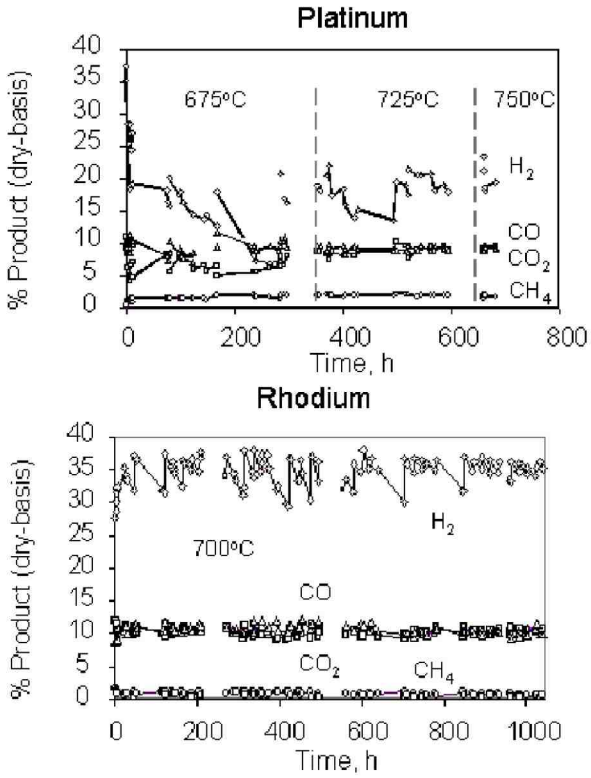

Figure 3. Yields of H_2, CO, CO_2, and CH_4 (mole/mole of fuel) from Reforming Benchmark Fuel Catalyzed by Rh- or Pt-CGO Supported on a Cordierite Monolith. Conditions: O_2/C=0.44, H_2O/C=1.6, GHSV=9,000 h^{-1}.

Mixed Metal Oxides with the Perovskite Structure

Simple lanthana-based perovskites ($LaNiO_3$, $LaCoO_3$, $LaCrO_3$, $LaFeO_3$, and $LaMnO_3$) were tested for reforming activity using isooctane at 700°C. Yields of 14.3 and 11.3 moles of H_2 per mole of isooctane were observed with $LaNiO_3$ and $LaCoO_3$, respectively. The X-ray diffraction patterns of $LaNiO_3$ and $LaCoO_3$ after testing suggested that the oxides had decomposed into La_2O_3 and metallic Ni and Co, respectively, under the reaction conditions. Yields of 2.6 and 2.5 moles of H_2 per mole of isooctane were observed with $LaCrO_3$ and $LaMnO_3$, respectively, while the H_2 yield of $LaFeO_3$ was 6.4 moles per mole isooctane. The X-ray diffraction patterns of $LaCrO_3$, $LaFeO_3$, and $LaMnO_3$ after testing suggested that these compounds maintained the perovskite structure under the reaction conditions.

In order to stabilize $LaNiO_3$ or $LaCoO_3$, we substituted a portion of Ni or Co with selected transition metals, termed "B-site modifying". Although the B-site-modified $LaNiO_3$ appeared to be structurally stable under reducing conditions (based on a comparison of the X-ray diffraction pattern of the oxide before and after testing), a decrease in the H_2 yield was observed compared with the unmodified $LaNiO_3$, as shown in Table 1. The H_2 yield of the B-site-modified $LaNiO_3$ could be improved by substituting a portion of the La with a lower valent cation, termed "A-site modifying," which introduces oxide ion vacancies (Table 1). An "A,B-site-modified" $LaNiO_3$ exhibited relatively stable performance over a 300-hr period, producing a reformate containing ~35 vol% H_2 from the benchmark fuel at 700°C, as shown in Figure 4. The "A,B-site-modified" $LaNiO_3$ deactivated rapidly when exposed to the benchmark fuel containing 50 ppmw sulfur added as benzothiophene.

Perovskite	Moles of H_2/Mole of Isooctane	
	700°C	600°C
$LaNiO_3$	14.3	10.8
B-site modified $LaNiO_3$	12.6	10.0
A,B-site modified $LaNiO_3$ (I)	13.1	13.5
A,B-site modified $LaNiO_3$ (II)	13.2	11.3

Table 1. Effect of A- and B-Site Modification of $LaNiO_3$ on the Moles of H_2 Produced per Mole of Isooctane for Reforming Isooctane. Conditions: O_2/C=0.5, H_2O/C=1.2, GHSV=~5,000 h^{-1}.

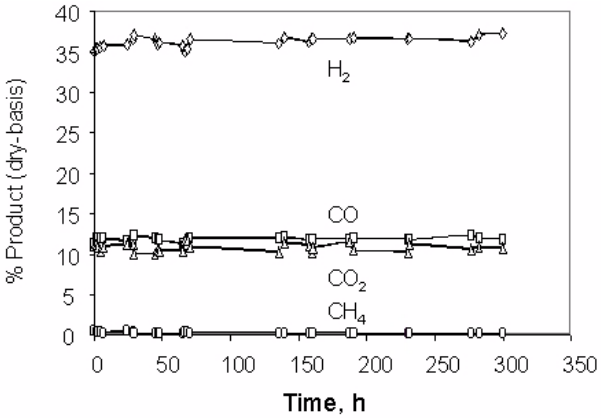

Figure 4. Yields of H_2, CO, CO_2, and CH_4 (mole/mole of fuel) from Reforming Benchmark Fuel Catalyzed by an A,B-Site-Modified $LaNiO_3$ in Powder Form. Conditions: O_2/C=0.44, H_2O/C=1.6.

Conclusions

Rh- or Ni-CGO supported on a cordierite monolith produced reformates with a higher H_2 concentration than Pt-CGO supported on a cordierite monolith. The better performance of the Rh- and Ni-CGO compared with Pt-CGO is attributed to the higher steam reforming activity of Rh and Ni. Sulfur tolerance is still an issue, since only Pt-CGO has shown sulfur tolerance when reforming fuels with sulfur concentrations in the 30-80 ppmw range. We are working with Süd-Chemie under a CRADA to optimize the activity of the CGO-based catalysts.

A,B-site modified $LaNiO_3$ and $LaCoO_3$ were demonstrated to be active autothermal reforming catalysts and appear to be structurally stable under the reducing reaction conditions. Sulfur tolerance is still an issue based on the rapid decrease in the H_2 concentration in the reformate when reforming sulfur-containing fuels. Future work will focus on improving the activity and the sulfur tolerance of these perovskite catalysts.

Publications/Presentations

1. M. Krumpelt, T. R. Krause, J. D. Carter, J. P. Kopasz, and S. Ahmed, "Fuel Processing for Fuel Cell Systems in Transportation and Portable Power Applications," *Catalysis Today* (submitted for publication).

2. T. Krause, J. Kopasz, C. Rossignol, J. D. Carter, and Michael Krumpelt, "Catalytic Autothermal Reforming of Hydrocarbon Fuels for Fuel Cell Systems," 224th American Chemical Society National Meeting, Boston, MA, August 18-22, 2002.

3. A. L. Wagner, J. P. Wagner, T. R. Krause, and J. D. Carter, "Autothermal Reforming Catalyst Development for Fuel Cell Applications," 2002 Future Car Congress, Arlington, VA, June 3-5, 2002.

4. C. Rossignol, T. Krause and M. Krumpelt, "Role of Metal-Support Interactions on the Activity of Pt and Rh Catalysts for Reforming Methane and Butane," American Institute of Chemical Engineers Spring National Meeting 2002, New Orleans, LA, March 10-14, 2002.

5. M. Krumpelt, T. Krause, J. Kopasz, J. D. Carter, and S. Ahmed, "Catalytic Autothermal Reforming of Hydrocarbon Fuels For Fuel Cells," American Institute of Chemical Engineers Spring National Meeting 2002, New Orleans, LA, March 10-14, 2002.

Patents

1. K. W. Kramarz, I. D. Bloom, R. Kumar, S. Ahmed, R. Wilkenhoener, and M. Krumpelt, "Steam Reforming Catalyst," US Patent 6,303,098 issued October 16, 2001.

2. S. Ahmed, R. Kumar, and M. Krumpelt, "Methanol Partial Oxidation Reformer," US Patent 6,244,367 issued June 12, 2001.

Special Recognitions & Awards

1. R&D Magazine – R&D 100 Award (2001) for Autothermal Reforming Catalyst Technology; Federal Laboratory Consortium Award (2002) for excellence in technology transfer.

IV.C.9 Fuel Processing of Diesel Fuel for Auxiliary Power Units

David A. Berry (Primary Contact), Dushyant Shekhawat, Todd H. Gardner, and William Rogers
U. S. Department of Energy
National Energy Technology Laboratory
P. O. Box 880
3610 Collins Ferry Road
Morgantown, WV 26507-0880
(304) 285-4430, fax: (304) 285-4403, e-mail: david.berry@netl.doe.gov

DOE Technology Development Managers:
JoAnn Milliken: (202) 586-2480, fax: (202) 586-9811, e-mail: JoAnn.Milliken@ee.doe.gov
Nancy Garland: (202) 586-5673, fax: (202) 586-9811, e-mail: Nancy.Garland@ee.doe.gov

Objectives

- Develop understanding of system integration issuesfor diesel fuel powered auxiliary power units (APUs) and provide necessary tools (models) and information to fuel cell/fuel process developers and system integrators for performance optimization and system control.

Approach

- Conduct a systems analysis to understand reformer integration and operational requirements.
- Utilize computational fluid dynamics (CFD) models to understand and address heat and mass transfer issues and reactor performance for steady-state and transient analysis.
- Conduct kinetic rate determination studies in the laboratory to allow for predictive modeling and design of diesel fuel reformers.

Accomplishments

- Identified diesel-based 5-kWe fuel cell auxiliary power unit (APU) system with >50% electrical conversion efficiency
- Developed a prototype CFD model including all the key elements of auto-thermal reforming (ATR)
- Developed a model that accounts for fuel atomization and vaporization, partial oxidation, steam gasification, and anode exhaust gas combustion
- Tested the convergence behavior of the model
- Conducted laboratory kinetic experiments
- Tested platinum (Pt), palladium (Pd), and ruthenium (Ru) catalysts
- Initial rate measurements made for hexadecane and diesel fuel

Future Directions

- Develop a predictive CFD model (Fluent) for diesel reforming
- Conduct steady-state simulations and validate model with ATR experimental data
- Conduct transient analysis
- Use benchmark fuel for kinetic modeling experiments
- Develop a complex reaction model and validate with CFD
- Ultimately, develop a kinetic rate methodology for diesel autothermal reforming catalyst systems

Introduction

The U.S. Department of Energy is sponsoring development of high temperature fuel cell power systems based on solid oxide technology through its Solid State Energy Conversion Alliance (SECA) program. The program is geared at mass manufacturing of fuel cells for high volume markets and multiple applications. One of those markets/ applications is a diesel-fueled auxiliary power unit (APU) for long-haul truck transportation. The fuel processor is a critical component of this system and must be able to provide a clean, tailored synthesis gas to the fuel cell stack for long-term operation. Key characteristics desired for the processor (and the system) include low cost, high efficiency, maximum thermal integration, low maintenance intervals, and acceptable startup and transient response. There are several barrier issues that must be overcome to achieve these characteristics. Carbon formation, particularly upon startup, must be minimized to avoid coking of the catalysts in the reformer and downstream fuel cell. Fuels containing sulfur can poison both the reforming catalysts and the fuel cell anode. High thermal mass components (some of which may have heat-ramp restrictions) can limit startup times and transient response. Finally, cost targets must be achieved to ensure commercial success. Depending on the system approach taken, technology is needed to resolve these barriers.

Approach

The objective of this work is to develop understanding of system integration issues for diesel fuel powered APUs and provide the necessary tools (models) and information to fuel cell/fuel process developers and system integrators for performance optimization and system control. A systems analysis was the first activity conducted to help understand reformer integration and operational requirements for the system. One of the more important underlying assumptions of the study is that the reforming catalyst can handle any sulfur content of the fuel, but the sulfur must be removed prior to the fuel gas entering the fuel cell. This may or may not be eventually achieved, but there is some evidence that a viable degree of sulfur tolerance can be attained in the reformer, especially as sulfur content of the diesel itself is being dramatically reduced through Environmental

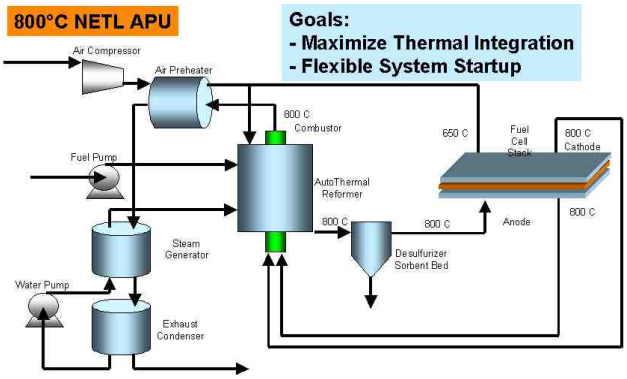

Figure 1. High Efficiency Integral Combustor/Reformer

Protection Agency regulations. This assumption could greatly impact the cost/efficiency trade-off of dealing with sulfur in the system. One goal of the systems analysis is to reduce the number of components to keep the system compact and economical, while still having the enough thermal integration to maximize system efficiency.

The next task was to model the reformer itself to understand design issues and be able to predict performance of various reactor/catalyst types and transient behavior. However, upon trying to obtain kinetic rate expressions for the reforming reactions, it was found that very little information existed in the public domain. This led to the decision/need to develop reaction kinetics for catalytic partial oxidation and steam reforming at National Energy Technology Laboratory's (NETL's) onsite research facility.

Results

Systems Analysis: Figure 1 shows a concept identified by NETL for a integrated fuel processor/ fuel cell system targeted for diesel APUs. There are several favorable attributes of this system. For example, startup occurs by firing an internal combustor in the dual reactor reformer. This provides heat to the ATR reformer (via conduction) as well as supplying heat to the fuel cell cathode via direct exhaust from the combustor or preheated air from the heat exchanger (optional). If necessary, the ATR is fired in a partial oxidation mode to aid in heatup and to provide heat to the anode side of the

fuel cell. At steady-state, all fuel is diverted to the reformer, and the internal combustor acts as a polishing bed to fully oxidize any remaining unburned hydrocarbons from the fuel cell. The figure also depicts a bed of zinc oxide that serves as a polishing bed to remove sulfur from the fuel gas entering the fuel cell. This is just one of several configurations that is being evaluated for this particular system. Depending on the rate of technology development (e.g., sulfur-tolerant reforming catalysts), the system could evolve along one of several pathways. Table 1 shows the effect of system integration of the fuel processor on the efficiency of the overall fuel cell system when compared to stand-alone reformer with external (non shared heat) combustion of anode exhaust. The comparison shows an approximate 7% efficiency improvement due primarily to better thermal integration in the shared heat reformer concept. Fuel flow was kept constant, but it was necessary to vary the fuel/air (F/A) ratio of the non-shared heat system in order to keep the reformer and fuel cell at reasonable temperatures. Increased efficiency of the non-shared case could also be obtained with the addition of another heat exchanger for independent preheat of the reformer and fuel cell inlet air. Unfortunately, this leads to higher cost, footprint, and complexity.

Table 1. Effect of System Analysis on System Efficiency

	Shared Heat	Non-Shared Heat
Fuel (kg/hr)	0.834	0.834
Air – stoichiometric units in	5	5.2
ATR F/A Ratio	9	3.5
Steam/Carbon Ratio	0.8	0.8
Efficiency	50.21	42.39
Net Power	5.0	4.221
ATR Temperature	800	800
Fuel Cell Tempera-ture	805	813

Reformer Modeling: NETL is also developing a CFD model in Fluent to understand and address the heat and mass transfer issues and reactor performance for steady-state and transient analysis.

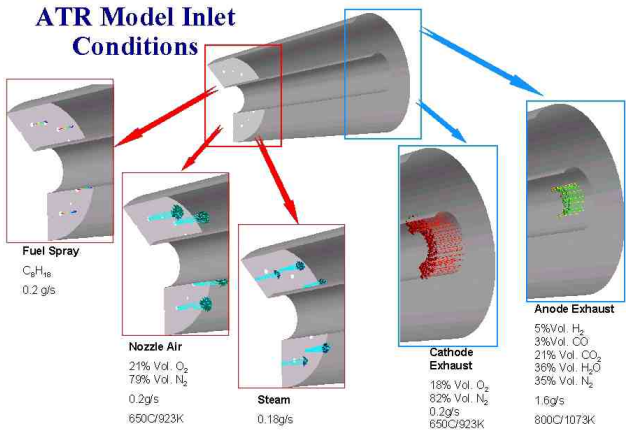

Figure 2. ATR Model Inlet Conditions

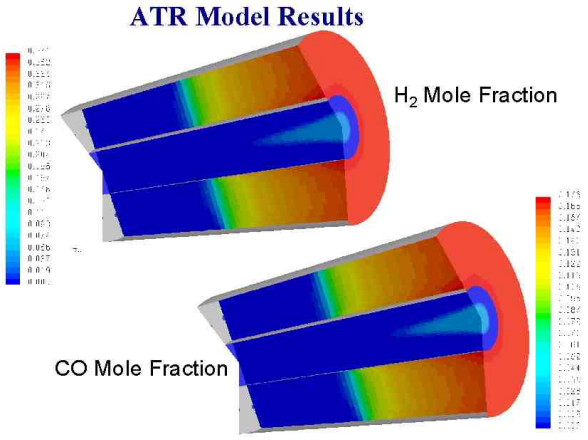

Figure 3. ATR Model Results

This model accounts for fuel atomization and vaporization, partial oxidation, steam reforming, and anode exhaust combustion. It is asumed that the partial oxidation reaction is very fast and occurs at the top of the catalyst bed along with fuel atomization and vaporization. It is also assumed that the steam reforming initiates after all O_2 is consumed in the partial oxidation reaction. Therefore, the reactor will initially be considered as two plug-flow reactors in series. Figure 2 and 3 depict the inlet conditions for the ATR model and results from the model, respectively.

Kinetic Measurements: Preliminary studies have been conducted for the kinetic model development for the autothermal reforming of diesel fuel. Three

different catalysts (g-alumina supported Pt, Pd, and Ru) were evaluated to obtain data for the ATR kinetic modeling.

A fixed bed reactor system was used to conduct the diesel ATR experiments. The reactor was operated continuously at steady state. The temperature was varied between 750 – 850°C, oxygen/carbon ratio was 0.6, steam/carbon ratio was 1.5, and the gasl hourly space velocity was 25,000 - 200,000 hr^{-1}. Table 2 shows the surface area, porosity, pore size distribution, metal loading, and metal dispersion of the catalysts used in the study.

Table 2. Physicochemical Properties of Catalyst used in Diesel ATR

Catalyst	N_2 BET Surface area (m^2/g)	Dispersion (%)	Pore Volume (cc/g)	Avg. Pore Size (A)
0.611 wt% Pt on γ-alumina	103	60	0.27	104
0.699 wt% Pd on γ-alumina	103	88	0.28	107
0.423 wt% Ru on γ-alumina	122	33	0.27	87

Figure 4 compares the product distribution from ATR of diesel from three different catalysts at 850 °C. The γ-Alumina supported ruthenium catalyst proved to be the most active catalyst in producing synthesis gas from diesel ATR.

Kinetic modeling of diesel autothermal reforming is extremely complicated. Diesel fuel consists of a complex variable mixture of hundreds of hydrocarbon compounds containing paraffins, isoparaffins, naphthenes, aromatics, and olefins. To simplify the model, a steady-state power law rate expression for the diesel reforming over each type of catalyst used in this study was developed. A linearized least-squares method of data analysis was used to determine the power law parameters from a series of diesel ATR experiments. The power law rate model for diesel autothermal reaction may be written as:

$$-r_{HC} = ke^{\frac{-E_A}{RT}} C^a{}_{HC} C^b{}_{H_2O} C^c{}_{O_2} \qquad \text{(I)}$$

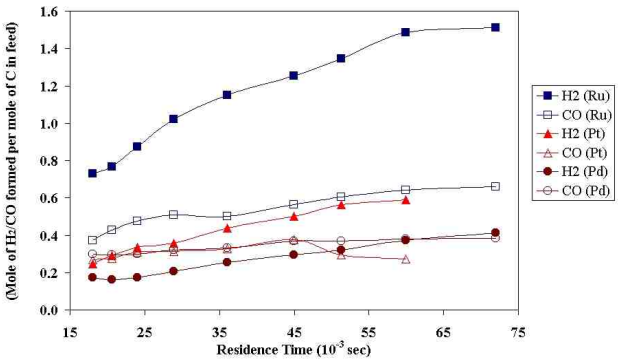

Figure 4. Product Distribution from ATR of Diesel (T=850°C, O_2/C=0.3, S/C=1.5)

Equation (I) is linearized so that a linear least square approach could be employed to solve for the activation energy, E_A, and the reaction orders in hydrocarbon (HC), a, H_2O, b, and O_2, c.

$$\ln(-r_{HC}) = \ln(k) - \frac{E_A}{RT} + a\ln(C_{HC}) + b\ln(C_{H_2O}) + c\ln(C_{O_2}) \qquad \text{(II)}$$

The resulting activation energy, preexponential factor, and the reaction order with respect to each reactant are presented in Table 3. A comparison of data predicted from the power law model to the experimental data shows the goodness of fit (correlation factor: ~92% for Pt and Pd, and ~72% for Ru). The ATR rate shows a non-monotonic dependence with respect to oxygen varying from positive to negative. By looking at the very low reaction orders with respect to oxygen from each kind of catalyst used in this study, it can also be concluded that the rate of diesel ATR is almost independent of oxygen. Good agreement has been found between Pd and Pt catalysts with respect to reaction order and activation energy. The negative order with respect to water shows that the water present in the system strongly inhibits the rate of reaction.

Autothermal reforming of single components such as n-hexadecane and toluene was also performed at the same reaction conditions as the diesel ATR to understand the reaction mechanisms and pathways for the ATR system.

Table 3. Kinetic Parameter for Diesel Reforming from Three Different Catalysts

Catalyst	Pre-Exponential Factor[1]	Activation Energy[2]	a	b	c
Pt/γ-Al_2O_3	18.4	16.5	0.87	1.02	0.13
Pd/γ-Al_2O_3	44.7	16.4	0.74	1.07	0.10
Ru/γ-Al_2O_3	0.02	9.7	0.50	1.39	0.03

Units: $^{1}(L/mol)^{a+b+c-1}/sec$; $^{2}kcal/mol$

Conclusions

A novel fuel processor is configured at NETL to integrate the fuel cell system for process optimization and system control. In the proposed system, startup occurs by firing an internal combustor in the dual reactor reformer, which provides heat to the ATR reformer via conduction as well as supplying heat to the fuel cell cathode via direct exhaust from the combustor.

A CFD model in Fluent was also developed by NETL to understand and address the heat and mass transfer issues and reactor performance for steady-state and transient analysis.

A power law-type kinetic model for diesel ATR has also been presented, which provides preliminary insight into reaction kinetics and will provide direction for future high level kinetic modeling.

FY 2002 Presentations/Publications

1. Gardner, T. H., Berry, D. A., James, R. E., Lyons, K. D., Monahan, M. J. "Fuel Processor Integrated H_2S Catalytic Partial Oxidation Technology for Sulfur Removal in Fuel Cell Power Plants". FUEL, Vol. 81, issue 17, September 2002.

2. Berry, D. A., Gardner, T. H., James, R. E., Rogers, W., Shekhawat, D., "Processing of Diesel for Fuel Cell Auxiliary Power Systems", 3rd Annual Department of Defense Logistic Fuel Reforming Workshop, Panama City, Florida, August 26 – 29, 2002.

3. Surdoval, W. A. and Berry, D. A, "Solid State Energy Conversion Alliance", 3rd Annual Department of Defense Logistic Fuel Reforming Workshop, Panama City, Florida, August 26 – 29, 2002.

4. Berry, D. A., Gardner, T. H., James, R. E., Rogers, W., Shekhawat, D., "Fuel Processing of Diesel Fuel for Fuel Cells", 2002 SECA Core Review Conference, Pittsburgh, Pennsylvania, June 18 – 19, 2002.

5. Berry, D. A., Gardner, T. H., James, R. E., Rogers, W., Shekhawat, D., "Fuel Processing of Diesel for Fuel Cells", 2002 Fuel Cells for Transportation Program / Lab R&D Review, Department of Energy Office of Transportation Technology, Denver, Colorado, May 6 – 10, 2002.

IV.C.10 Testing of Fuels in Fuel Cell Reformers

Rod Borup (Primary Contact), Michael Inbody, Troy Semelsberger, Lee Perry and Jerry Parkinson
P.O. Box 1663
Los Alamos National Laboratory
Los Alamos, NM 87545
(505) 667-2823, fax: (505) 665-6173, e-mail: Borup@lanl.gov

DOE Technology Development Manager: Nancy Garland
(202) 586-5673, fax: (202) 586-9811, e-mail: Nancy.Garland@ee.doe.gov

Objectives

- Explore effects of fuels, fuel components, additives and impurities on the performance of hydrogen generation technologies
  - Examine fuel composition effect on energy efficiency, durability, cold startup, transients, NH_3 concentration, cost, and power density
  - Understand the parameters that affect fuel processor and fuel cell lifetime and durability

Approach

- Examine fuel effects on fuel processing by testing fuels in automotive scale, adiabatic reactors
  - Examine individual fuel components
  - Examine fuel component blends
  - Examine 'real' fuels (reformulated gasoline, naptha)
  - Examine fuel additives (anti-oxidants, detergents, impurities)
- Model fuel reforming chemistry
  - Model carbon formation
  - Model equilibrium gas composition
  - Model thermodynamic properties

Accomplishments

- Tested iso-octane, iso-octane/xylene, methylcyclohexane, naptha, reformulated gasoline, diesel components, anti-oxidants, and nitrogen containing hydrocarbons; monitored ammonia formation with
  - Aliphatic and napthenic hydrocarbons
  - Catalytic and homogeneous oxidation
  - Nitrogen bound compounds (anti-oxidants)
- Monitored carbon formation with *in situ* laser diagnostics
  - Monitored carbon formation for various fuel components
  - Monitored carbon formation during start-up and shut-down

Future Directions

- Evaluate effects of fuel constituents on fuel processor operation
  - Monitor carbon formation *in situ* with an adiabatic reactor and laser scattering

  - Monitor carbon formation during start-up and reactor transients
  - Define methods of operation for fast, repetitive start without carbon formation
- Develop capabilities to monitor carbon formation with *in situ* gravimetric analysis steam reforming apparatus
  - Delineate carbon formation mechanisms
  - Measure carbon effect on reforming kinetics
  - Measure carbon formation kinetics
- Measure fuel additive and impurity effects on performance and carbon formation
  - Sulfur effect
  - Oxygenated hydrocarbons

• Integrate fuel cell stack testing with fuel processor operation to evaluate system integration effects of fuels

---

Introduction

This report describes our FY02 technical progress in examining the effects of fuel on hydrogen generation for proton exchange membrane (PEM) fuel cells for transportation. The goal of this research is to explore the effects of fuels, fuel constituents, additives and impurities on the performance of on-board hydrogen generation devices and, consequently, on the overall performance of a PEM fuel cell system using a reformed hydrocarbon fuel. Understanding the fuel effects on the durability of PEM fuel cell systems is key for their commercial use.

Different fuels and components have been tested in automotive scale, adiabatic reactors to observe their relative reforming characteristics with various operating conditions. Ammonia (NH_3) formation was monitored, and conditions were varied to observe under what conditions NH_3 is made. Nitrogen-bound hydrocarbons were added to fuels to determine their effect on NH_3 formation. Carbon formation was monitored during fuel processor operation by *in situ* laser measurements of the effluent reformate. Fuel composition effects on carbon formation were measured.

Approach

To examine the effect of the fuel on hydrogen production devices, various fuel components and real fuels have been tested in autothermal reformers (ATRs) and fuel reforming systems. Fuel reformers used for these experiments are automotive-scale reactors, and are operated adiabatically, such as systems likely will operate in vehicles. The analysis of the fuel effect on the product composition stream is conducted by various analytical techniques, specifically laser scattering and laser flourescence, gas chromatography, FTIR (fourier transform infrared), NDIR (non-dispersive infrared), paramagnetic oxygen and GC/MS (gas chromatography/mass spectrometry). Ammonia formation from various fuels and for different operating conditions was measured by FTIR. Carbon formation for different operating conditions and fuel components was monitored by *in situ* laser scattering. Mapping of the onset of carbon formation for different fuel components as a function of operating conditions has been conducted with these techniques. The reactor with catalyst observation windows, laser extinction, and scattering facilities is shown in Figure 1. Expected outlet concentrations of the fuel reformer and the relative fuel component effects on the fuel reformer outlet have been modeled. In particular, modeling of equilibrium carbon formation has been used to predict the operating conditions for the onset of carbon formation for various fuel blends.

Specific fuel compositions and components measured include iso-octane, xylene, methylcyclohexane, naptha and California reformulated gasoline. Additives examined include anti-oxidant No. 29 (2,6-Di-Tert-Butyl-4-methylphenol), anti-oxidant No. 22 (N, N'-Di-Sec-Butyl-P-Phenylenediamine) and DMA-548.

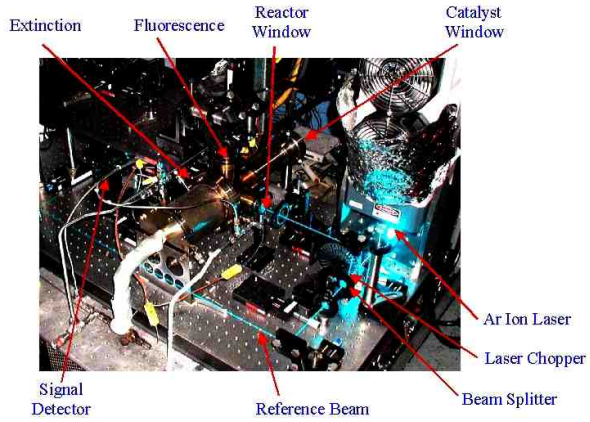

Figure 1. Catalytic partial oxidation with facilities for laser extinction and scattering measurements with catalyst observation.

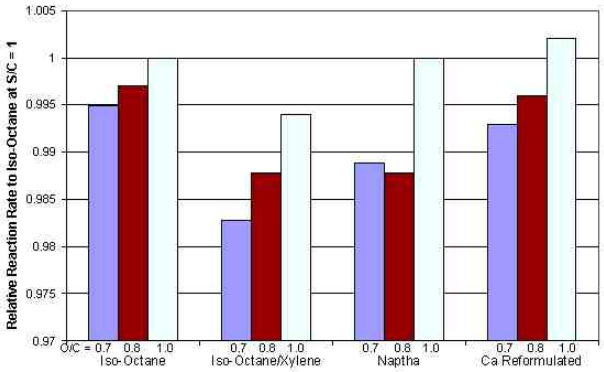

Figure 2. Relative oxidation rates of iso-octane, iso-octane/20% xylene, Phillips Naptha and California reformulated gasoline.

Results

Fuel Effects Comparisons in Catalytic Partial Oxidation

The relative rates for catalytic partial oxidation for different fuels have been measured for various operating conditions. Figure 2 shows relative reaction rates for various fuel components, mixtures, and a Phillips Petroleum Hydrotreated Naptha stream at a S/C of 1.0. The relative reaction rates vary as the O/C ratio varies due to temperature changes. At lower O/C ratios, the adiabatic temperature rise is lower, thus the overall reaction rate is lower. The reaction rate for all components are higher at higher O/C, and subsequently, higher temperatures. The oxidation rates for O/C's of 0.7 and 0.8 are fastest for iso-octane. The addition of aromatics such as xylene slows the kinetics and conversion. Real fuel composition mixtures such as the Phillips Naptha and California reformulated gasoline show an oxidation rate faster than that of iso-octane/xylene mixtures even though the relative aromatic concentration is approximately the same. At high O/C ratios (O/C = 1.0), the real fuel mixtures show an equal or faster oxidation rate compared with pure iso-octane. The resulting decrease in kinetics due to the presence of aromatic hydrocarbons indicates that the fuel composition will have an effect on the required size (and cost due to catalyst loading) of the fuel processor. If it is possible to make a non-aromatic containing fuel available, the fuel processing size and cost would be positively effected.

Ammonia Formation

Ammonia formation in the fuel processor is a concern, as NH_3 is a poison to PEM fuel cell membranes and ionomer.[1] As ammonia is known to degrade the performance of fuel cells, the DOE has targeted the outlet concentration for ammonia formation is < 0.5 ppm for 2005 and < 0.1 ppm by 2010. However, little has been published about the generation of NH_3 in ATR reactors. To examine this issue, an FTIR was set up to monitor the reactor effluent and calibrated to a detection limit of 400 ppb (parts-per-billion) of NH_3 with the presence of ethylene. Without the presence of ethylene, the detection limit of NH_3 is significantly lower, < 100 ppb. Figure 3 shows FTIR spectra for NH_3 calibration and of reformate from the partial oxidation and reforming of MCH (methylcyclohexane). Small amounts of NH_3 are easily measured in a pure N_2 background with the major peak at 967 cm^{-1}; however, with the addition of ethylene, the sensitivity is greatly reduced, since ethylene has a minor peak near 967 cm^{-1}. With the addition of 100 ppm ethylene, the NH_3 sensitivity is reduced to about 400 ppb. Normal catalytic partial oxidation of fuel components does not show a measureable NH_3 concentration (see curve 3(c)).

Precombustion can occur in a reformer due to mixing air/fuel at high temperatures; this is essentially homogeneous combustion before the catalyst surface and typically an operation mode

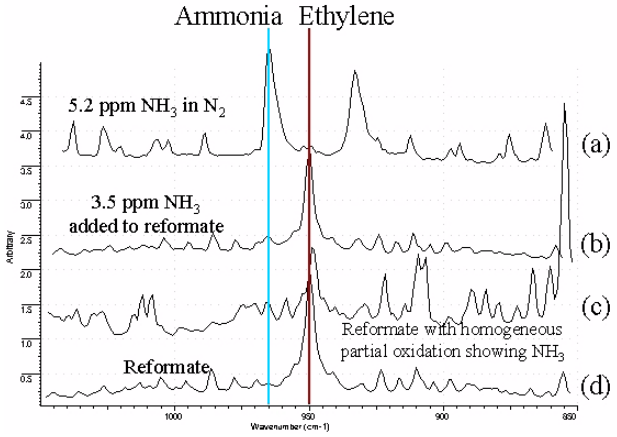

Figure 3. FTIR spectra of (a) 5.2 ppm NH_3 in N_2, (b) 3.5 ppm NH_3 added to MCH reformate, (c) reformate from homogeneous partial oxidation of MCH showing ethylene and 11 ppm NH_3, and (d) reformate from the catalytic partial oxidation of MCH showing ethylene and 0 ppm NH_3.

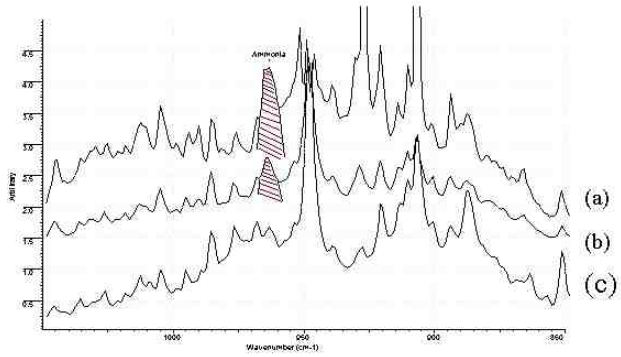

Figure 4. FTIR spectra of reformed (a) MCH (methylcyclohexane) with 10% pyridine, (b) MCH with 1% pyridine, and (c) MCH with 50 ppm of anti-oxidant.

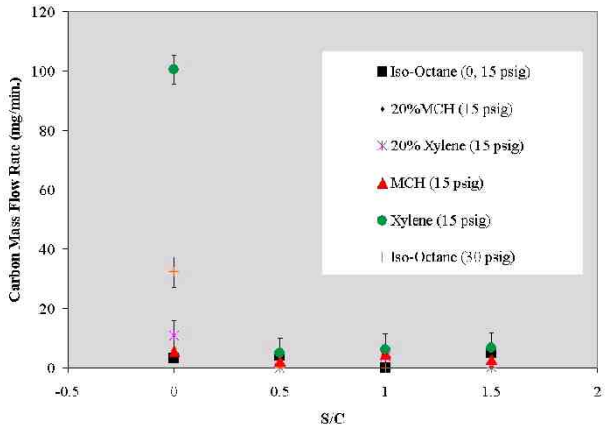

Figure 5. Equilibrium modeling of carbon formation for various fuels and conditions. The dashed conditions are potential start-up scenarios, depending upon whether water is available during reactor start-up.

which is avoided. However, when pre-combustion of fuels occurs (homogeneous combustion upstream of the catalyst) as in 3(c), NH_3 is observed, in this case at a concentration of 11 ppm.

Nitrogen-containing hydrocarbons are present in gasoline fuels. These can be small amounts of naturally occurring hydrocarbons, or they can be anti-oxidants or detergents with amine groups added to the fuel, such as Anti-oxidant No. 22 (N, N'-Di-Sec-Butyl-P-Phenylenediamine). To determine the conversion products of nitrogen-containing hydrocarbons, 50 ppm of Anti-oxidant No. 22 was added to MCH to observe potential NH_3 formation. In addition, pyridine was added to a pure fuel to observe whether NH_3 formation would occur at higher concentrations of nitrogen-containing hydrocarbons. Figure 4(a) shows FTIR spectra of reformed MCH with 10% pyridine added. The measured NH_3 in the reformate was 414 ppm NH_3. When 1% pyridine was added to MCH, the reformate analysis measured 54 ppm NH_3. When 50 ppm of the nitrogen containing anti-oxidant was added, no NH_3 was observed (Figure 4(c)).

Carbon Formation

Carbon formation is recognized to be a potential limiter of fuel processor ATR durability. Equilibrium calculations can identify proper operating conditions to prevent carbon formation; however, during the start-up of the fuel processor, avoiding non-zero carbon equilibrium is difficult. Laser extinction measurements have been conducted to observe carbon formation for different fuel components. An example of this is shown in Figure 5. The residence time of this reactor was short, about 10 msec. As the S/C ratio is decreased, carbon formation is detected by a decrease in the laser extinction signal, which is converted to a mass flow rate of carbon formed. Little measurable carbon was formed until equilibrium conditions predicted carbon formation.

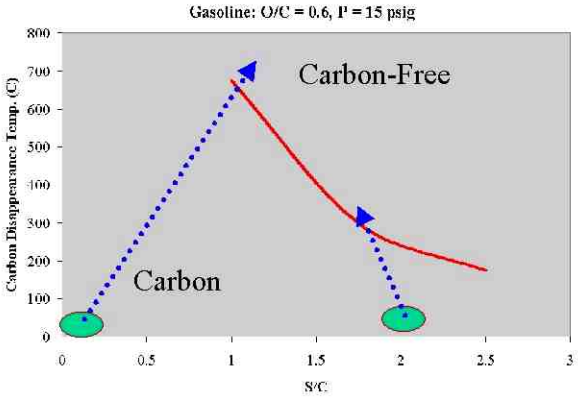

Figure 6. Mass flow rate of carbon formation for various fuel components and component blends. O/C = 0.65.

Aliphatic hydrocarbons such as iso-octane could be reformed without significant carbon formation even when equilibrium predicted carbon formation. However, the addition of aromatic hydrocarbons caused significant carbon formation. The addition of anti-oxidants to the fuel stream did not make any measurable difference in carbon formation.

Figure 6 shows the minimum temperature at which the equilibrium concentration of carbon is zero as a function of S/C ratio. During start-up, water may not be available to suppress carbon formation. In this case, lighting off a partial oxidation reactor without water could result in large amounts of carbon formation. Figure 7 shows the lightoff of a partial oxidation reactor with low amounts of water. As the temperature approaches normal operating conditions, large amounts of carbon are observed via laser scattering.

Carbon formation has been observed to occur both in the partial oxidation/steam reforming catalyst and in the reformate after it exits the catalyst. Analysis of carbon formed in the steam reformer catalyst found that the carbon was mostly carbonaceous carbon with an approximate H/C ratio of 0.2 – thus about 97% carbon. Carbon that formed in the reformate after it exited the catalyst (probably from unconverted hydrocarbons) has been analyzed to contain 30% by weight solidified hydrocarbons.

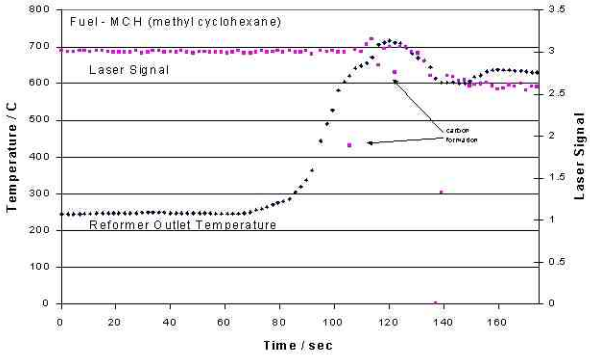

Figure 7. Carbon formation during ATR start-up. Reactor was preheated to 250°C, and started up with an O/C=1.0 and S/C = 0.0.

Conclusions

Fuel component effects are being examined to determine their effect on hydrogen generation technologies. Measurements show that the fuel composition does effect the design and operation of the fuel reformer, and fuel blends low in aromatic content show higher reforming kinetics, which result in a reduced fuel processor size (and thus cost). The fuel composition effect also effects the relative carbon formation, which will effect the fuel processor durability.

Various fuel components and fuels have been tested with various O/C and S/C ratios in partial oxidation/steam reforming reactors. The addition of aromatics slows the overall reaction rate for catalytic oxidation. Real fuels have similar oxidation rates at high O/C compared with iso-octane, but lower oxidation rates at O/C < 1.0.

Ammonia formation was not observed at a measurable concentration for normal operating conditions with expected fuel compositions. Pre-combustion of fuels lead to the formation of NH_3 measured at 11 ppm NH_3. Large concentrations of nitrogen-containing hydrocarbons lead to higher amounts of NH_3 formation.

Laser extinction measurements mapping the onset of carbon formation have been conducted. Carbon formation was quantified by the laser extinction measurement. Post analysis of carbon formed indicates the method and cause of carbon formation lead to different carbonaceous species.

Carbon formed in the steam reformer was mostly carbonaceous carbon with an approximate H/C ratio of 0.2, while carbon formed downstream from the reformer consisted of high amounts of solidified hydrocarbons.

Acknowledgments

The authors would like to thank Fred Cornforth of Philips Petroleum for supplying the fuels and anti-oxidants used in this testing.

References

1. Francisco Uribe, Oakridge TN, June 2001 DOE Fuel Cells for Transportation Program Review

Presentations/Publications

1. Fuel Effects on Startup for Automotive Fuel Cell Systems, Troy A. Semelsberger, Rodney L. Borup, Lee F. Brown and Michael A. Inbody, AIChE Meeting, Spring 2002, New Orleans, LA, Los Alamos National Laboratory publication, LAUR-02-1619, March 2002.

2. Fuel Processing for Fuel Cells: Fuel Effects on Carbon Formation, Lee Perry, Rod Borup, Michael Inbody, Byron Morton, and Troy Semelsberger, AIChE Meeting, Spring 2002, New Orleans, LA, March 2002.

3. Fuels for Fuel Cells for Transportation Applications, Rod Borup, Lee Perry, Mike Inbody, Byron Morton, Troy Semelsberger and Jose Tafoya, AIChE Meeting, Spring 2002, New Orleans, LA, Los Alamos National Laboratory publication, LAUR-02-1207, March 2002.

4. Fuel Processing for Fuel Cells: Fuel Effects on Carbon Formation, Lee Perry, Rod Borup, Michael Inbody, Byron Morton, and Troy Semelsberger, AIChE Meeting, Fall 2001, Reno NV, Los Alamos National Laboratory publication, LAUR-01- 6479, November 2001.

5. Fuel Processing for Fuel Cells: Effects on Durability and Carbon Formation, Rod Borup, Michael Inbody, Byron Morton, Lee Perry and Lee Brown, American Chemical Society, Chicago, IL, Los Alamos National Laboratory publication, 01-4413, August 2001.

IV.C.11 Sulfur Removal from Reformate

Xiaoping Wang, Theodore Krause (Primary Contact) and Romesh Kumar
Argonne National Laboratory
9700 South Cass Avenue
Argonne, IL 60439
(630) 252-4356, fax: (630) 972-4463, e-mail: krause@cmt.anl.gov

DOE Technology Development Manager: Nancy Garland
(202) 586-5673, fax: (202) 586-9811, e-mail: Nancy.Garland@ee.doe.gov

Objectives

- Adapt proven technologies for on-board fuel processing to be capable of reducing the H_2S concentration to <1 ppm in reformate.
- Develop new technologies or improve existing technologies to meet the DOE targets for H_2S removal: (1) H_2S concentration of <10 ppb in reformate (FY 2010), (2) a reactor size of <0.06 L/kWe (<0.06 kg/kWe), and (3) GHSV of 50,000 h^{-1}.

Approach

- Predict the H_2S equilibrium partial pressure for candidate adsorbents (metal sulfide-H_2S equilibrium) and identify candidate materials.
- Synthesize mixed metal oxides consisting of CuO/Cu_2O and another first-row transition metal oxide based on thermodynamic calculations.
- Conduct experimental studies in a microreactor system to evaluate the H_2S concentration in the effluent as a function of temperature and the gas composition for candidate mixed metal oxides.

Accomplishments

- Synthesized various mixed metal oxides consisting of CuO/Cu_2O and screened them for H_2S uptake in a microreactor system.
- Determined that competitive adsorption between H_2O and H_2S inhibits H_2S uptake by these mixed metal oxides.

Future Directions

- Work to improve the H_2S uptake performance of mixed metal oxides containing predominantly Cu oxides.
- Evaluate the use of metal doping to increase the rate of H_2S uptake by ZnO.
- Evaluate the impact of using liquid-phase sulfur adsorption on the H_2S removal requirements of the fuel processor.
- Better define the sulfur removal requirements for the fuel processor based on sulfur tolerance studies for the ATR and WGS catalysts.

Introduction

New EPA regulations will significantly lower the sulfur content of gasoline from the current average of 300 ppmw to an average of 30 ppmw with a maximum of 80 ppmw by the year 2006. For on-board fuel processing for transportation applications, reformate produced by autothermal reforming of these gasolines will contain 3-8 ppmv of H_2S. Even at these low concentrations, H_2S is known to poison many of the catalysts being developed for use in the fuel processor and in the fuel cell anode for PEMFC systems. For example, an H_2S concentration of <50 ppb is recommended for copper-zinc oxide water-gas shift catalysts. Studies have shown that the Pt-anode catalyst in the PEMFC is irreversibly poisoned at an H_2S concentration as low as 50 ppb (Uribe et al. 2002).

Two different approaches are being considered for on-board sulfur removal. The first approach involves liquid-phase desulfurization of the fuel prior to reforming using a nickel-based adsorbent to remove organosulfur compounds (Bonville et al. 2000). While liquid-phase desulfurization can significantly reduce the sulfur content of the fuel, it is not clear whether the extent of desulfurization achieved by this process will meet the requirements for the fuel processor and fuel cell stack without additional removal of sulfur in the fuel processor. The second approach involves gas-phase desulfurization of reformate in the fuel processor using a metal oxide adsorbent, typically ZnO, to remove H_2S. Gas-phase desulfurization requires that the reforming catalyst be sulfur tolerant at least to the concentration of sulfur present in the fuel.

Gas-phase desulfurization using ZnO is the approach that we have pursued in past years. ZnO is an attractive adsorbent for on-board fuel processing because of its favorable sulfidation thermodynamics (<1 ppmv). The sulfidation equilibrium for ZnO ($ZnO + H_2S \Leftrightarrow ZnS + H_2O$) is a function of the temperature and the ratio of the partial pressure of H_2O/H_2S. To reduce the H_2S concentration to <0.1 ppmv requires a temperature of 300-350°C based on the typical range of H_2O concentrations present in the reformate (Carter et al. 2001). However, it has been observed that although the equilibrium becomes more favorable as the temperature is lowered, the concentration of H_2S in the reformate after contacting ZnO actually increases with decreasing temperature because of a significant decrease in the rate of H_2S uptake (Carter et al. 2001).

We have begun to investigate mixed metal oxide systems predominantly based on copper oxide. Copper oxides (CuO and Cu_2O) have sulfidation equilibrium constants among the highest of all metal oxides and could potentially achieve sub-ppb concentrations of H_2S in reformate, as shown in Figure 1. Unfortunately, CuO/Cu_2O is readily reduced to metallic Cu in reformate, which significantly reduces the desulfurization efficiency. In order to maintain Cu in the +1/+2 oxidation state, researchers have focused on combining CuO/Cu_2O with other metal oxides (Li and Flytzani-Stephanopoulos 1997), which is the approach that we are investigating.

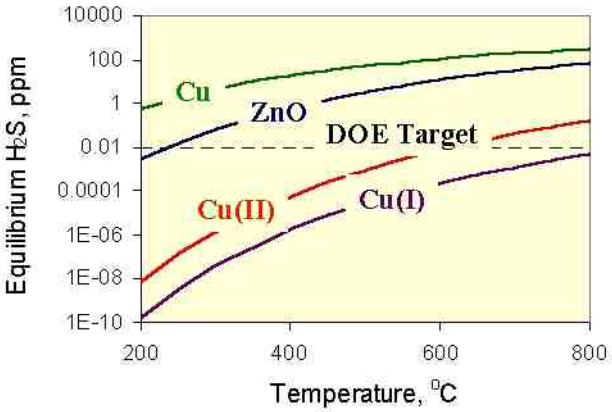

Figure 1. Equilibrium concentration of H_2S as a function of temperature in the presence of 20 vol% H_2O or H_2 for Cu_2O, CuO, Cu and ZnO.

Approach

Mixed metal oxides consisting of a combination of Cu and another first-row transition metal oxide, such as Co, Mn, and Ni, were synthesized by various techniques, including coprecipitation and glycine-nitrate combustion. Some of the mixed metal oxides were dispersed on a high-surface-area δ-alumina. The H_2S uptake of the candidate metal oxides was evaluated using a microreactor system with an on-line gas chromatograph equipped with a flame

photometric detector and an on-line H_2S analyzer equipped with a lead acetate detector. The typical experimental protocol involved exposing a sample of the mixed metal oxide to four different gas compositions (50 ppm H_2S/N_2, 50 ppm H_2S/ reformate [dry], 10 ppm H_2S/10%H_2O/reformate, and 50 ppm H_2O/20% H_2O/reformate) at temperatures ranging from 150 to 550ºC using a heating rate of 2ºC/min. The GHSV was 5,000 h^{-1}. The gas composition was varied to study the effect of the various components in reformate (H_2O, CO, and CO_2) on the uptake of H_2S by the mixed metal oxide.

Results

Figure 2 shows the H_2S concentration in the effluent from the microreactor for the four different gas compositions as a function of temperature for a Cu-Co oxide. The H_2S concentration in the effluent was <1 ppm over a temperature range of 250-450ºC for the gas composition containing only H_2S and N_2. When the gas composition was changed to a dry reformate containing CO, CO_2, and H_2 in addition to N_2, an H_2S concentration of ~1-2 ppm was observed at 330-380ºC. At 240-280ºC, the H_2S concentration was ~5 ppm, which is slightly higher than at 330-380ºC; however, it appears that a significant portion of the H_2S was converted to COS (Figure 3). It is not known whether COS is produced by the reaction with CO ($CO + H_2S \Leftrightarrow COS + H_2$) or with CO_2 ($CO_2 + H_2S \Leftrightarrow COS + H_2O$); however, assuming that some of the oxidized Cu or Co is reduced to metallic Cu or Co, the CO pathway is more probable due to the higher affinity of these metals for CO than CO_2. The presence of H_2O in reformate (10 or 20 vol%) resulted in higher H_2S concentrations in the effluent than in the absence of H_2O (Figure 2). The observation that the H_2S concentration in the effluent increased with increasing H_2O concentration suggests that competitive adsorption between H_2O and H_2S inhibits H_2S uptake by the oxide. As shown in Figure 3, the presence of water inhibits the formation of COS.

Although H_2S uptake data are presented for only one Cu-containing composition, i.e., Cu-Co, similar behavior has been observed, in terms of the effect of

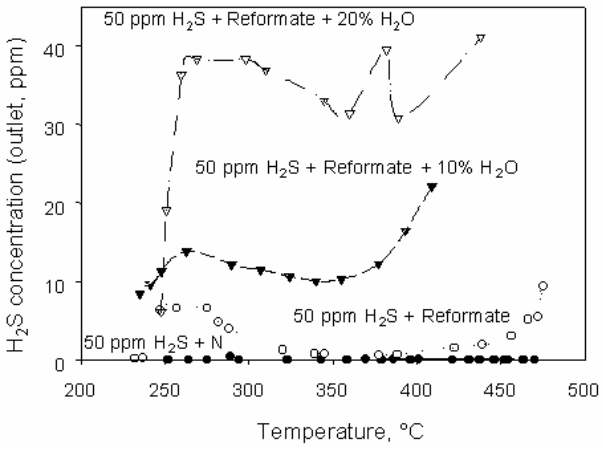

Figure 2. Concentration of H_2S in the effluent as a function of temperature for four different gas compositions, each containing 50 ppm H_2S. The adsorbent is a Cu-Co oxide.

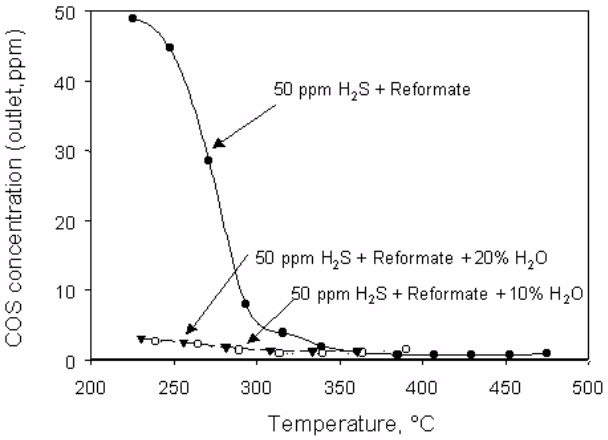

Figure 3. Concentration of COS in the effluent as a function of temperature for four different gas compositions, each containing 50 ppm H_2S. The adsorbent is a Cu-Co oxide.

H_2O and CO/CO_2 on H_2S uptake, for other Cu-containing oxides investigated.

Conclusions

Although the sulfidation equilibria suggest that CuO/Cu_2O should be able to reduce the H_2S concentration in reformate below the 10 ppb DOE target, initial screening of various Cu-containing mixed metal oxides suggests that competitive adsorption between H_2O and H_2S may inhibit H_2S uptake. As a consequence, the H_2S concentration that

is predicted by the sulfidation equilibrium may not be achieved. Future work will focus on confirming that (1) oxidized Cu can be stabilized in reformate under fuel processing conditions, (2) sulfidation is occurring at oxidized Cu, and (3) competitive adsorption between H_2O and H_2S inhibits H_2S uptake.

References

1. F. Uribe, T. Zawodzinski, J. Valerio, G. Bender, F. Garzon, A. Saab, T. Rockward P. Adcock, J. Xie, and W. Smith, "Fuel Cell Electrode Optimization for Operation on Reformate and Air," presented at the DOE Fuel Cells for Transportation National Laboratory R&D Meeting, May 8-10, 2002, Golden, CO.

2. L.J. Bonville, Jr., C.L. DeGeorges, P.F. Foley, J. Garow, R.R. Lesieur, J.L. Reston, Jr., and D.F. Szydlowski, U.S. Patent 6,159,256, 2000.

3. J. D. Carter, T. Krause, J. Mawdsley, R. Kumar, and Michael Krumpelt, "Sulfur Removal from Reformate," presented at the DOE Fuel Cells for Transportation National Laboratory R&D Meeting, June 6–8, 2001, Oak Ridge, TN.

4. Z. Li and M. Flytzani-Stephanopoulos, *Ind. Eng. Chem. Res.* **1997**, *36*, 187-196.

IV.C.12 Nanoscale Water Gas Shift Catalysts

Scott L. Swartz, Ph.D. (Primary Contact)
NexTech Materials, Ltd.
720-I Lakeview Plaza Boulevard
Worthington, OH 43085-4733
(614) 842-6606, fax: (614) 842-6607, e-mail: swartz@nextechmaterials.com

DOE Technology Development Manager: Patrick Davis
(202) 586-8061, fax: (202) 586-9811, e-mail: Patrick.Davis@ee.doe.gov

Main Subcontractors: University of Pennsylvania, Catalyte, LLC, Süd-Chemie, Inc.

Objectives

- Develop synthesis methods for highly active water-gas-shift (WGS) catalysts based on platinum supported on nanoscale ceria-based oxides.
- Develop and scale up washcoating process for depositing Pt/ceria catalysts on monolithic supports, and demonstrate high WGS activity in monolith-supported catalysts.
- Demonstrate that Pt/ceria catalysts can meet application-specific requirements for the WGS reactors of automotive fuel processors, which include: resistance to degradation by exposure to air; ability to withstand repeated temperature cycles during operational transients; and stable operation over a wide temperature range.
- Demonstrate that DOE technical targets for size, weight and cost of water-gas-shift reactors can be met using monolith-supported Pt/ceria catalysts.

Approach

- Use wet-chemical synthesis methods to prepare aqueous suspensions of nanoscale ceria-based oxides and to incorporate platinum onto ceria nano-particle surfaces.
- Optimize of catalyst synthesis methods and formulations through extensive micro-reactor testing and use of characterization techniques such as temperature programmed reduction and CO chemisorption.
- Collect of long-term micro-reactor test data to assess catalyst deactivation rates, and correlate catalyst activity and deactivation rates with catalyst formulation and synthesis methods.
- Collect micro-reactor data at different temperatures and gas compositions to determine kinetics of Pt/ceria WGS catalysts. Use these kinetic data in a model for estimating the size, weight and cost of monolith-supported catalysts for 50-kW scale WGS reactors.
- Modify Pt/ceria catalyst suspensions with surfactants and binders, and washcoat catalysts onto ceramic honeycomb monoliths.
- Conduct extensive sampling of Pt/ceria catalyst powders, pellets, and washcoated monoliths for evaluation by Süd-Chemie, HydrogenSource, and other fuel processor developers.

Accomplishments

- A number of highly active and stable Pt/ceria catalyst formulations have been demonstrated, with performance sufficient for the automotive fuel processor application.
- A washcoating process has been developed for monoliths with catalyst loadings up to 400 grams per liter, and excellent performance has been demonstrated in these monoliths.

- A fundamental understanding of WGS kinetics for Pt/ceria catalyst system has been established, and a kinetic model has been developed to allow realistic comparisons of data obtained under different test conditions.
- Based on the kinetic model, it is estimated that for a 50-kW scale WGS reactor, CO levels can be reduced to less than one percent using a monolith with a weight of less than a kilogram, a volume of less than a liter, and a cost of less than $150.

Future Directions

- This project ends March 31, 2003. Plans for the remainder of the project include scale-up of the monolith washcoating process and testing of a 10-kW scale monolith at HydrogenSource.

Introduction

A major technical barrier to commercialization of PEM fuel cells in automobiles is the need for a fuel processing system to convert liquid fuels, including gasoline into a hydrogen-rich gas. The fuel processor must be small enough to fit into the confined spaces of a vehicle. The system must also be able to perform reliably under highly variable power loads, be capable of rapid start up, and deliver a gas stream containing very low levels of carbon monoxide. The water-gas shift (WGS) reactor is a critical component of the fuel processor. Its function is to reduce carbon monoxide levels to intermediate levels, which can then be further reduced in a subsequent preferential oxidation step. Commercial copper-based WGS catalysts are unsuitable for transportation applications because of the tendency of the catalysts used in these reactors to degrade under the severe conditions encountered in an automotive system.

NexTech Materials is collaborating with the University of Pennsylvania, Süd-Chemie, Catalyte, HydrogenSource, and McDermott Technology to develop catalytic water-gas-shift reactors that meet the needs of the automotive PEM fuel cell systems. The catalyst being developed is based on nanoscale mixtures of ceria-based oxides and uniformly incorporated platinum. Compared to existing copper-based catalysts, the Pt/ceria system offers several advantages: (1) operation at higher temperatures (where kinetics are more favorable); (2) no need for activation prior to use; (3) no degradation upon exposure to air; and (4) availability of conventional washcoating technologies for ceria-based catalysts (reduced size and weight, improved ruggedness).

Approach and Results

Results of work performed during the past year are summarized below:

Catalyst Characterization and Testing: NexTech's micro-reactor was refined to allow collection of reliable test data over extended time periods. Much of the catalyst testing work focused on long-term catalyst performance, to support the development of high-activity and stable catalysts. In parallel, catalysts were characterized by surface area, temperature-programmed reduction (TPR), and CO chemisorption methods. The results suggest that optimization of platinum dispersion (as measured by CO chemisorption) is important to achieving high activity and suppressing deactivation. Reducibility of the precious metal (as measured by TPR) does not appear to be related to WGS activity.

Formulation Development: Improvements in WGS performance were achieved by optimizing the ceria composition, synthesis processes for the nanoscale ceria support, and platinum incorporation methods. Long-term micro-reactor test results suggest that proper synthesis conditions are required to produce highly active and stable catalysts (Figures 1 and 2). Low de-activation rates were achieved by modifying the ceria support composition and by optimizing the precious metal dispersion. Pt/ceria catalysts can be regenerated by heating in air (Figure 3).

Monolith Washcoating and Testing: A process was developed for applying Pt/ceria catalyst coatings onto ceramic honeycomb monoliths (see Figure 4), and high catalyst loadings (>350 grams per liter) were achieved. Results obtained at Süd-Chemie indicate that these monoliths provide exceptional

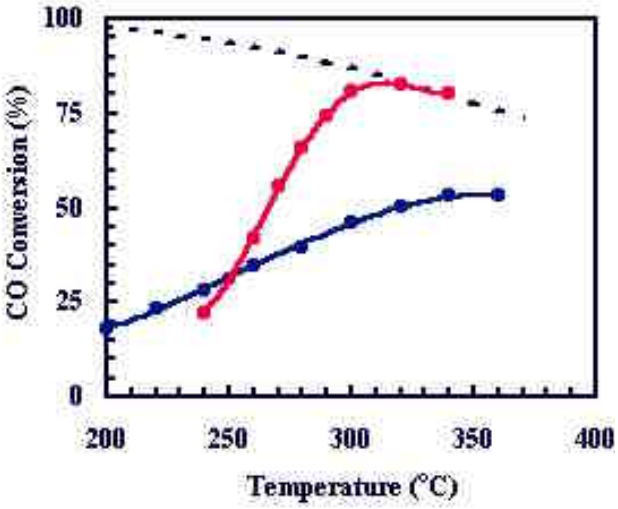

Figure 1. Comparison of temperature dependence of Pt/ceria and commercial (Cu/ZnO) catalysts.

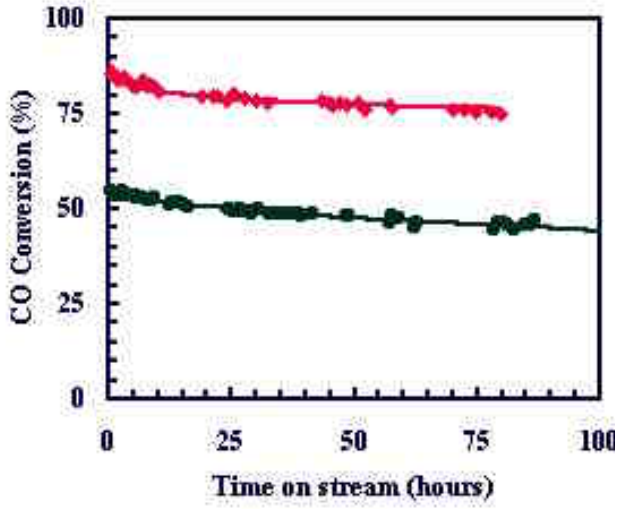

Figure 2. Comparison of long-term performance of Pt/ceria and commercial (Cu/ZnO) catalysts at 300ºC.

performance (Figure 5). The construction and commissioning of NexTech's WGS monolith-testing reactor also was completed, with design support provided by Catalyte.

Size/Weight/Cost Modeling: A kinetic model was established for estimating the size, weight and cost of monolith reactors with washcoated Pt/ceria catalysts, using Arrhenius data obtained from micro-reactor tests. A reaction rate expression for Pt/ceria catalysts was derived from kinetic data, which was

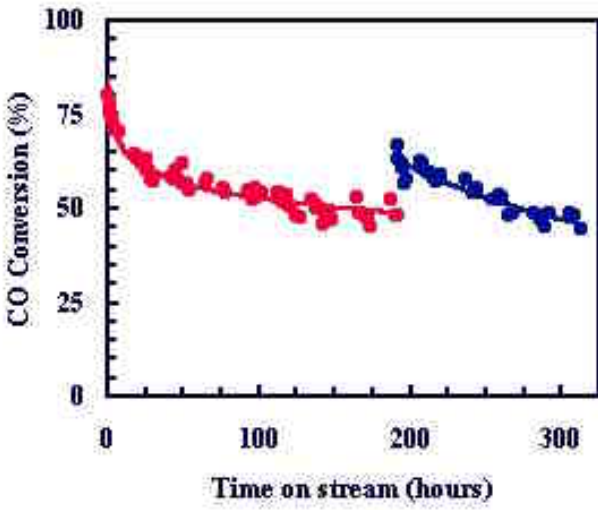

Figure 3. CO conversion versus time at 300ºC for a Pt/ceria catalyst sample, before and after regeneration by annealing in air at 375ºC.

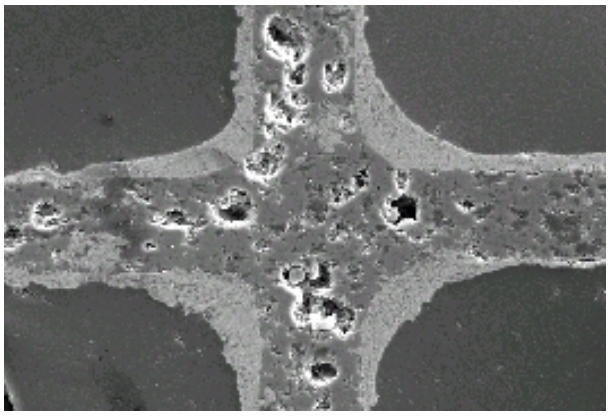

Figure 4. SEM micrograph of a washcoated Pt/ceria catalyst layer on a cordierite monolith.

used to estimate the amount of catalyst required to achieve equilibrium conversions at a given temperature for any input reformate gas composition. This model (Figures 6 and 7) suggests that a WGS monolith reactor scaled to 50 kilowatts will have a volume of less than 1 liter, a weight of less than 1 kilogram, and a cost of less than $150. This reactor will operate at 350ºC and will provide an exit CO content of less than 0.9 percent.

Conclusions

- Pt/ceria water-gas-shift catalysts are sufficiently active and offer a number of

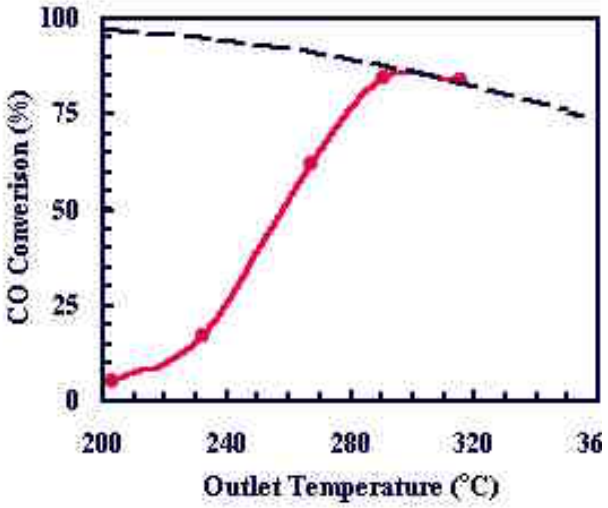

Figure 5. WGS performance of a Pt/ceria monolith

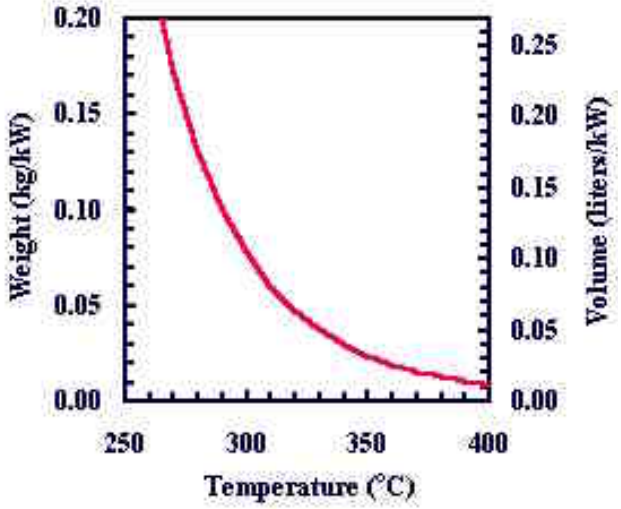

Figure 6. Estimated weight and volume of a WGS monolith washcoated with Pt/ceria catalysts.

practical advantages for automotive fuel processors for PEM fuel cell systems.

- Pt/ceria catalysts are substantially more active than commercially available copper-based catalysts at temperatures above about 270ºC.
- Careful synthesis and processing is required to minimize long-term de-activation of Pt/ceria catalysts. Regeneration of deactivated catalysts can be achieved by heating in air.
- Washcoating of monoliths with Pt/ceria catalysts provides a viable path for achieving rugged and volumetrically efficient packaging of catalysts in WGS reactors of automotive fuel processors.
- Based on current performance levels, modeling suggests that a WGS reactor based on monoliths loaded with Pt/ceria catalysts will exceed DOE technical targets for reactor volume and weight. The reactor cost will be less than $3.00 per kilowatt.

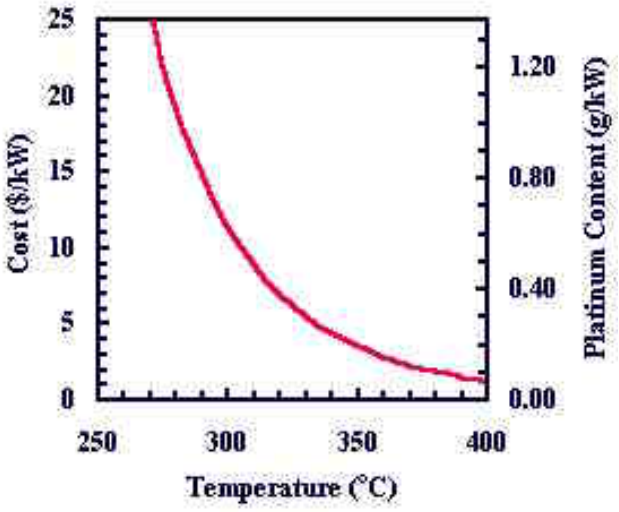

Figure 7. Estimated cost and platinum content of a WGS monolith washcoated with Pt/ceria catalysts.

IV.C.13 Water-Gas Shift Catalysis

Deborah J. Myers (Primary Contact), John F. Krebs, Sara Yu, Michael Krumpelt
Argonne National Laboratory, Argonne, IL 60439-4837
(630) 252-4261, fax: (630) 252-4176, e-mail: Myers@cmt.anl.gov

DOE Technology Development Managers:
JoAnn Milliken: (202) 586-2480, fax: (202) 586-9811, e-mail: JoAnn.Milliken@ee.doe.gov
Nancy Garland: (202) 586-5673, fax: (202) 586-9811, e-mail: Nancy.Garland@ee.doe.gov

Objectives

- Develop water-gas shift catalysts that:
  - Meet the DOE goals of 90% CO conversion,
  - 99% selectivity, 30,000 hr^{-1} gas hourly space velocity (GHSV), <$1/kilowatt electric (kWe)
  - Eliminate the need for careful in situ catalyst activation
  - Are tolerant to temperature excursions
  - Have operating lifetimes of >5000 hours

Approach

- Develop metal-support combinations to promote bifunctional mechanism of catalyst action:
  - One component to adsorb carbon monoxide (CO), e.g., metal with intermediate CO adsorption strength
  - Another component to adsorb and dissociate water (H_2O), e.g., oxides with redox properties or oxygen vacancies under reformate conditions

Accomplishments

- Fabricated copper/mixed oxide catalyst as extrudates with no loss in activity
- Demonstrated <1% CO at 20,000 per hour) with Cu/mixed oxide vs 16,000 hr^{-1} for iron oxide-chromium oxide + copper/zinc oxide (Fe-Cr + Cu/ZnO)
- Determined sulfur tolerance of copper (Cu)/mixed oxide catalyst; catalyst loses all WGS activity after 45 hours on 4.5 ppm hydrogen sulfide (H_2S)
- Improved activity of ruthenium (Ru) and Co catalysts while suppressing methanation by using a promoter

Future Directions

- Demonstrate <1% CO out at 30,000 hr^{-1} using a structured non-precious metal catalyst
- Determine lifetime and durability of catalysts under actual reformate conditions
- Improve low-temperature activity (<300°C) of catalysts to >50 μmoles CO/sec-g catalyst (currently 11 at 230°C)
- Develop a catalyst that is tolerant to 3-4 parts per million volume (ppmv) H_2S in reformate

Introduction

The water-gas shift (WGS) reaction,

$CO + H_2O \quad CO_2 + H_2$,

is used to convert the bulk of CO in the raw reformate to carbon dioxide (CO_2) and additional hydrogen (H_2). In the chemical process industry, e.g., in the manufacture of ammonia, the shift reaction is conducted at two distinct temperatures. The high-temperature shift (HTS) is carried out at 350-450°C using an iron-chrome (Fe-Cr) catalyst. The low-temperature shift (LTS) is carried out at 160-250°C with the aid of a copper/zinc oxide catalyst (Cu/ZnO).

The commercial HTS and LTS catalysts require activation by careful pre-reduction in situ and, once activated, lose activity very rapidly if they are exposed to air. Further, the HTS catalyst is inactive at temperatures <300°C, while the LTS catalyst degrades if heated to temperatures >250°C. The automotive application, because of its highly intermittent duty cycle, requires alternative water-gas shift catalysts that (1) eliminate the need to sequester the catalyst during system shutdown; (2) eliminate the need to activate the catalyst in situ; (3) increase tolerance to temperature excursions; and (4) reduce the size and weight of the shift reactors. Another desirable property for an automotive WGS catalyst is tolerance to ppm levels of sulfur in the feed stream because sulfur species are present as contaminants or additives in conventional fuels (30 parts per million weight [ppmw] in future gasoline gets converted to 3 ppmv H_2S in reformate).

Approach

We are investigating bifunctional catalysts in which one component of the catalyst adsorbs or oxidizes CO and the other component dissociates water. Our present research is focusing on metal-support combinations to promote this bifunctional mechanism. The metallic component is chosen to adsorb CO at intermediate adsorption strengths (platinum [Pt], Ru, palladium [Pd], PtRu, PtCu, cobalt [Co], ruthenium [Ru], silver [Ag], iron [Fe], copper [Cu], and molybdenum [Mo]). The support is chosen to adsorb and dissociate water, typically a mixed-valence oxide with redox properties or oxygen vacancies under the highly reducing conditions of the reformate.

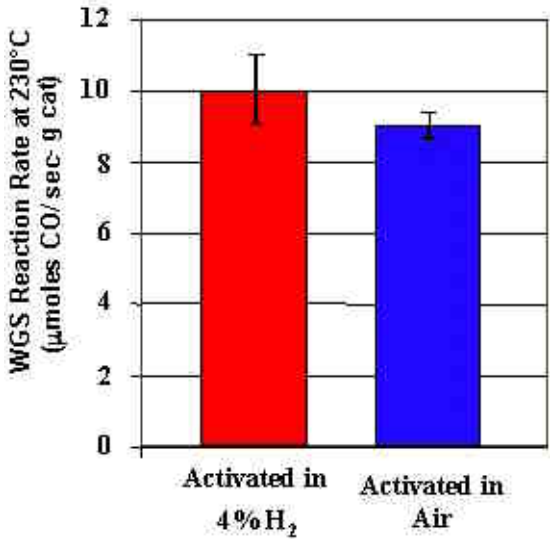

Figure 1. ANL's copper/mixed oxide catalyst can be activated in air rather than dilute hydrogen with no loss of WGS activity (within the error of the measurement). GHSV = 200,000 hr^{-1}, "High CO" reformate

Tests of the candidate catalysts' activities were conducted with simulated reformate using a micro-reactor. The micro-reactor was operated as a differential reactor for determining kinetic parameters and as an integral reactor for overall CO conversions. The concentrations of reactant gases were chosen to simulate the composition and concentrations of gases exiting an auto-thermal reformer ("High CO", dry composition: 10% CO, 13% CO_2, 43% H_2, balance diatomic nitrogen [N_2]) and exiting an HTS stage ("Low CO", dry composition: 5% CO, 15% CO_2, 45% H_2, balance N_2. A steam-to-dry gas ratio of 0.45 was chosen to simulate the additional amount of water necessary to cool the autothermal reforming gases to 400°C. Sulfur tolerance testing was conducted using simulated reformate containing 11% CO, 7.5% CO_2, 45.5% H_2, 6 ppmv H_2S, balance N_2, and a steam-to-dry gas ratio of 0.45.

Results

Last year a copper/mixed oxide catalyst was identified as a potential WGS catalyst with several desirable properties. As opposed to copper/zinc

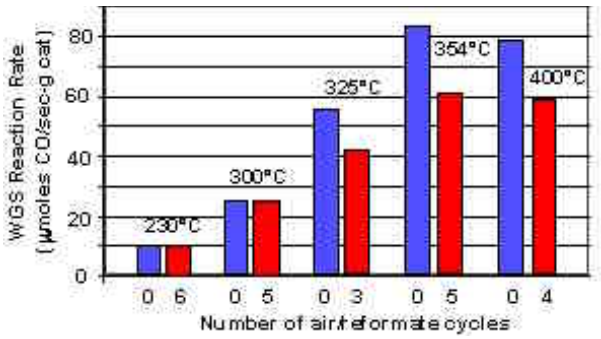

Figure 2. ANL's copper/mixed oxide catalyst does not lose WGS activity with multiple cycles between reformate and air at temperatures up to 300°C. GHSV = 200,000 hr^{-1}, "High CO" reformate

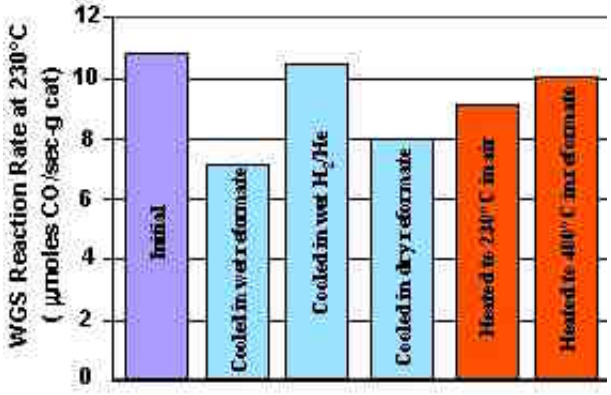

Figure 3. ANL's copper/mixed oxide catalyst does not lose WGS activity when exposed to water condensate in hydrogen/helium and reversibly loses activity when cooled to room temperature in wet or dry reformate. GHSV = 200,000 hr^{-1}, "High CO" reformate

oxide, this catalyst can operate above 260°C without loss of activity, does not have to be reduced in situ (Figure 1) and does not lose activity upon exposure to air up to 300°C (Figure 2). This catalyst also does not lose activity upon exposure to water condensate. It does lose activity when cooled down to room temperature in reformate; however, the activity can be regenerated by heating the catalyst to reaction temperature in air or to 400°C in reformate (Figure 3).

A WGS bed composed of the copper/mixed oxide catalyst powder was tested for its ability to reduce the CO in reformate from an inlet

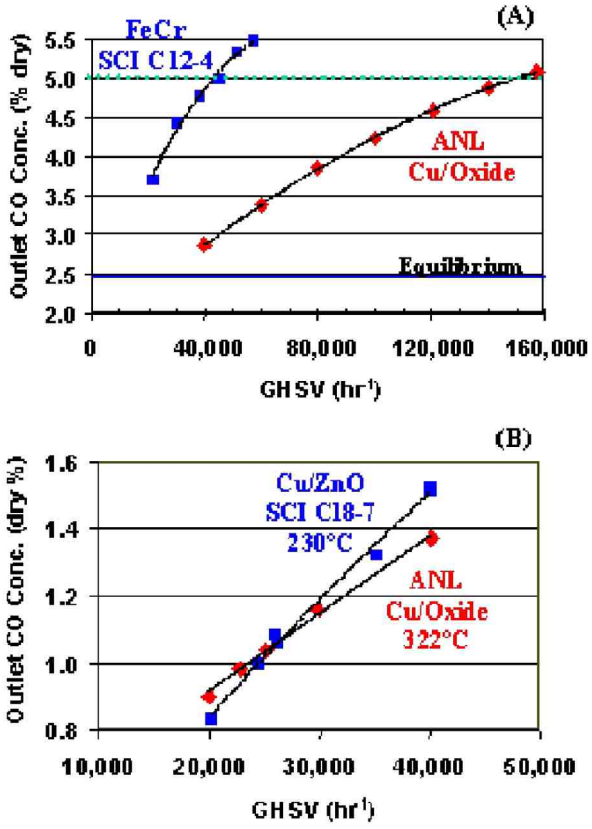

Figure 4. ANL's copper/mixed oxide catalyst can achieve CO conversions from (A) 10.2% in to <5% out at 400°C and 158,000 hr^{-1} (vs 45,000 hr^{-1} for Fe-Cr) and (B) 5% in to <1% out at 322°C and 23,000 hr^{-1} (vs 25,000 hr^{-1} at 230°C for Cu/ZnO).

concentration of 10.2% (dry basis) to an outlet concentration of 1% (dry basis). This was accomplished in two steps, by first reducing the CO concentration to 5% and then to <1%. Figure 4A shows that the copper/mixed oxide bed can achieve 5% CO out (dry basis) at a temperature of 400°C and a gas hourly space velocity (GHSV) of 158,000 hr^{-1} compared with 45,000 hr^{-1} for the commercial iron-chrome catalyst. A dry outlet CO concentration of <1% can be achieved by the copper/mixed oxide catalyst at a temperature of 322°C and a GHSV of 23,000 hr^{-1} compared with 230°C and 25,000 hr^{-1} for the commercial copper/zinc oxide (Figure 4B). The temperature of the copper/zinc oxide bed was held at 230°C in order to avoid the deactivation of the catalyst that occurs above 260°C. Therefore, the copper/mixed oxide catalyst can achieve an outlet

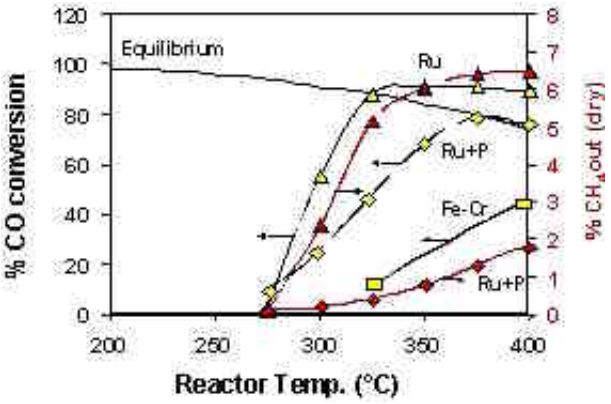

Figure 5. The addition of a promoter (P) to ANL's ruthenium/mixed oxide catalyst diminishes the conversion of CO to methane while maintaining WGS activity higher than commercial iron-chrome (Fe-Cr). GHSV = 30,000 hr^{-1}, "High CO" reformate

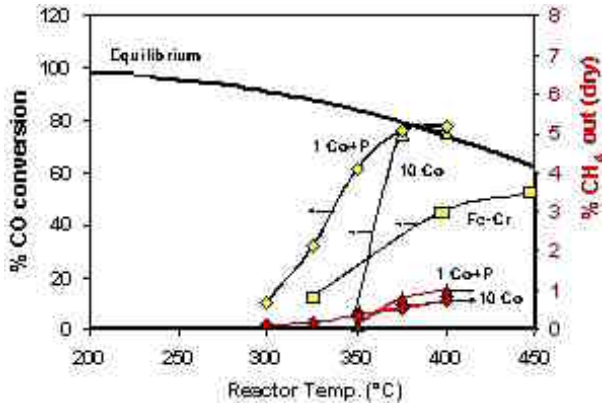

Figure 6. The addition of a promoter (P) to ANL's cobalt/oxide catalyst improves its WGS activity at temperatures below 350°C to give it higher activity than commercial iron-chrome (Fe-Cr). GHSV = 30,000 hr^{-1}, "High CO" reformate

CO concentration of <1% (90% conversion) at an overall GHSV of 20,000 hr^{-1} whereas a combination of iron-chrome and copper/zinc oxide requires a lower GHSV of 16,000 hr^{-1}.

The higher GHSV that can be achieved with the Argonne National Laboratory (ANL) copper/mixed oxide translates into a 20% reduction in the WGS catalyst volume compared with the commercial catalysts. The projected size, weight, and cost of copper/mixed oxide catalyst for an automotive fuel processor are 0.15 liter/kilowatt electric (L/kWe), 0.14 kg/kWe, and $0.9/kWe. The projected size and weight fall short of the DOE goals. Iprovements are needed in the catalyst's activity. Improvements are also needed in the sulfur tolerance of the catalyst, as it showed total deactivation after 45 hours on a stream of 4.5 ppmv H_2S in reformate.

We improved the WGS activity of cobalt- and ruthenium-based catalysts while suppressing the methanation activity by adding a promoter. As shown in Figures 5 and 6, these catalysts are more active than commercial iron-chrome at temperatures >300°C. Our results indicate that the cobalt and ruthenium catalysts would be suitable replacements for iron-chrome as an HTS catalyst.

Conclusions

We further developed a temperature-stable copper/mixed oxide catalyst by fabricating it in a structured form that has the same activity as the powder. This catalyst can be activated in air and does not lose activity after exposure to air at temperatures up to 300°C. The ANL copper/mixed oxide catalyst has the potential to reduce the volume of the WGS reactor by 20% compared with the commercial catalysts. The copper catalyst showed susceptibility to poisoning by H_2S in the reformate feed. We have also developed cobalt and ruthenium catalysts with higher activity than commercial iron-chrome (325-400°C) by using a promoter to suppress methane formation.

FY 2002 Publications/Presentations

1. D. J. Myers, J. F. Krebs, J. D. Carter, R. Kumar, and M. Krumpelt, "Metal/Ceria Water-Gas Shift Catalysts for Automotive Polymer Electrolyte Fuel Cell Systems," Presentation, Abstract, and Presentation Record, American Institute of Chemical Engineers, 2002 Spring Meeting, Fuel Processing Session III, New Orleans, LA, March 10-14, 2002.

2. D. J. Myers, J. F. Krebs, J. D. Carter, R. Kumar, and M. Krumpelt, "Metal/Ceria Water-Gas Shift Catalysts for Automotive Polymer Electrolyte Fuel Cell Systems," Presentation and Preprint, 224th American Chemical Society Fall National Meeting, Boston, MA, August 18-22, 2002.

IV.C.14 Transition Metal Carbide Water Gas Shift Catalysts

Levi Thompson (Primary Contact)
University of Michigan
Department of Chemical Engineering
3026 H.H. Dow Building
Ann Arbor, MI 48109-2136
(734) 647-7150, fax: (734) 763-0459, e-mail: ltt@umich.edu

DOE Technology Development Manager: Nancy Garland
(202) 586-5673, fax: (202) 586-9811, e-mail: Nancy.Garland@ee.doe.gov

ANL Technical Advisor: William Swift
(630) 252-5964, fax: (630) 972-4473, e-mail: swift@cmt.anl.gov

Subcontractors: Süd Chemie, Louisville, KY; Catalyte LLC, Arlington, MA; Union Miniere Inc., New Brunswick, NJ

Objectives

The objective of the project is to demonstrate water gas shift (WGS) catalysts with:

- Rates in the absence of sulfur that are twice those for Cu-based shift catalysts,
- Activities in the presence of sulfur that are >85% of activities in the absence of sulfur,
- Projected stabilities and durabilities that are compatible for use in automobiles, and
- Costs that are competitive with Cu-based catalysts.

Approach

Tasks devised to accomplish the program objectives included:

- Develop monolith washcoat procedure.
- Optimize carbide formulation, microstructure and pretreatment.
- Fabricate prototype catalyst.
- Evaluate and model catalyst performance.
- Demonstrate performance in prototype fuel processor.
- Access commercial potential.

Accomplishments

- Methods were demonstrated to washcoat the carbide catalysts onto cordierite monoliths and ceramic foams. The adhesion of the carbides to the substrates was very good.
- Our best performing carbide catalysts outperformed the commercial Cu-Zn-Al catalyst by a factor of more than 2. Ninety percent CO conversion was achieved with an hourly space velocity in excess of 70,000 hr^{-1}, exceeding the present DOE WGS catalyst performance target.

Future Directions

- Evaluate carbide catalysts in the presence of sulfur.
- Produce >1 kg of catalyst for prototype work and third-party testing.
- Produce monolith supported prototype catalysts.
- Assess cost competitiveness via evaluations by an established fuel processor developer.

Introduction

Fuel cells are being developed to enable the commercialization of cleaner, more fuel efficient vehicles. The fuel cell technology favored by many vehicle manufacturers is proton exchange membrane (PEM) cells operating with H_2 from hydrocarbon steam reforming and/or partial oxidation. The water gas shift (WGS) is a critical step during fuel processing, and the associated reactor constitutes about a third of the mass, volume and cost of the fuel processor. While presently available catalysts work well in industrial petroleum refining and chemical plants, significantly improved catalysts are required to meet the transient operation and size constraints imposed by vehicular applications. Rather than seeking incremental improvements through the modification of existing formulations (e.g., Fe-Cr and Cu-Zn catalysts), we are developing new WGS catalysts based on transition metal carbides. Significant reductions in the WGS reactor size and cost are anticipated as a consequence of *high activities, durabilities and sulfur tolerance*.

The focus of Phase II of this project is to optimize formulations for the carbide catalysts and produce monolith supported prototype catalysts that substantially out-perform the commercial catalysts. In addition, we will evaluate the cost competitiveness of the monolith supported carbide catalysts. The performance of new monolith supported catalysts demonstrated in this effort will be confirmed by independent evaluations by established fuel processor developers.

Approach

The carbide catalysts were synthesized and washcoated onto substrates using a proprietary method. Water gas shift rates and product selectivities for the carbide powders were measured in a plug flow reactor using a feed gas that simulates the exhaust from the partial oxidation of gasoline. The individual gas phase constituents were delivered by mass flow controllers, and H_2O was added by bubbling the dry gas mixture through a heated saturator vessel. The CO was passed through a bed of alumina to remove any carbonyls. The resulting reactant contained 38.6% H_2, 15.9% N_2, 5.7% CO, 6.3% CO_2, and 30.0% deionized H_2O. The WGS rates were measured at 175-240°C and atmospheric pressure with CO conversions that typically ranged up to 30%. Prior to the rate measurements, the catalyst bed was pretreated either in H_2 or a mixture of 15% CH_4 in H_2 for 4 hours at 400-590°C.

Results

The reaction rates reached steady-state after approximately three hours on-stream and were reproducible to within 10% during subsequent runs. Small amounts of methane were produced over some catalysts; however, there was no evidence of methanation activity at steady-state.

The performance of selected catalysts that were pretreated at 450°C in the CH_4/H_2 mixture is illustrated in Figure 1 (the Cu-Zn-Al catalyst was pretreated at 200°C in a mixture of 2% H_2 in N_2 for 4 hours as recommended by the manufacturer). Several of the formulations substantially outperformed the commercial Cu-Zn-Al catalyst.

The performance of the carbide catalysts was a function of the pretreatment conditions employed. For example, pretreatment in the CH_4/H_2 mixture typically resulted in catalysts that were more active than those same catalysts pretreated in pure H_2 (Figure 2). For some materials, increasing the pretreatment temperature also resulted in significant improvements in the performance. The improved activities appear to be linked to the production of

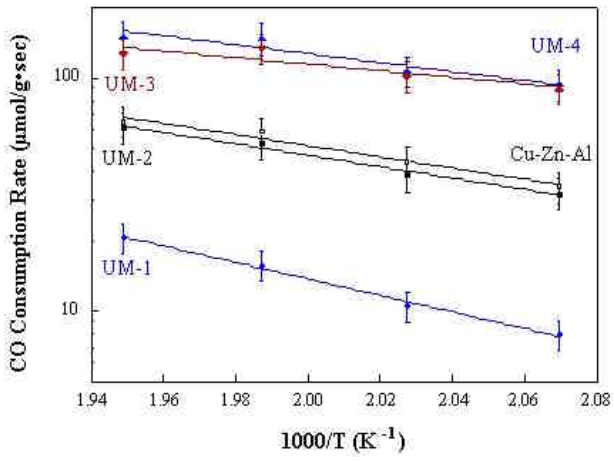

Figure 1. Comparison of Reaction Rates for the Carbide and Cu-Zn-Al Catalysts

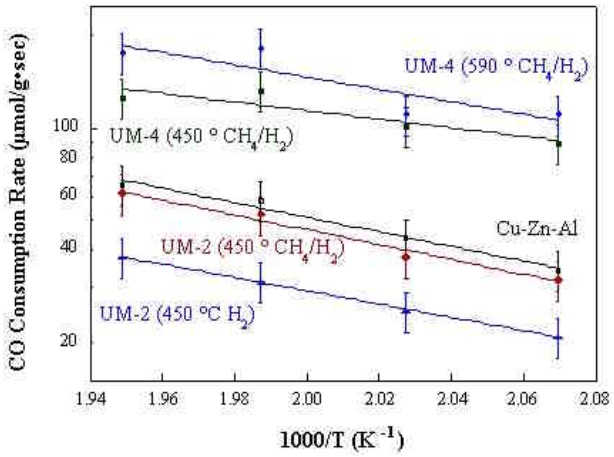

Figure 2. Effects of Pretreatment Gas and Temperature on Rates for the Carbide Catalysts

additional carbide sites based on the results of *in situ* x-ray photoelectron spectroscopic characterization.

We recently compared characteristics of the carbide catalysts to the DOE targets. As one can see from Table 1, the performance of one of our best catalysts, UM-3, exceeded important DOE targets.

Characteristic	Target	Cu-Zn-Al	UM-3
GHSV (hr^{-1})	30,000	30,800	>70,000
CO Conversion (%)	>90	76	89
H_2 Selectivity (%)	>99	>99	>99
Volume (L/kW_e)	<0.1		
Weight (kg/kW_e)	<0.1		
Durability (Hrs.)	5000		
Cost ($/$kW_e$)	<1		
*Rates measured at 240°C. The equilibrium CO conversion under these conditions is 96.5%.			

Table 1. Progress Against DOE Performance Targets*

We demonstrated that the carbide catalysts could be washcoated onto cordierite monoliths and ceramic foams. Details regarding the methods are proprietary and were not disclosed. Examples of the monolith and foam supported catalysts are illustrated in Figures 3 and 4.

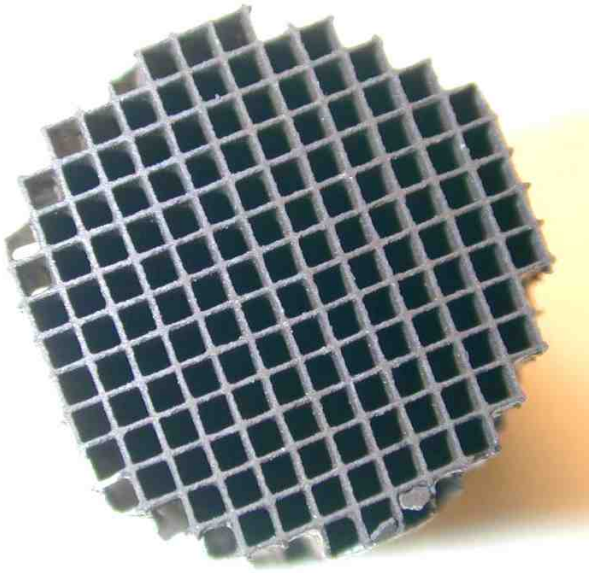

Figure 3. Carbide Washcoated Cordierite Monolith

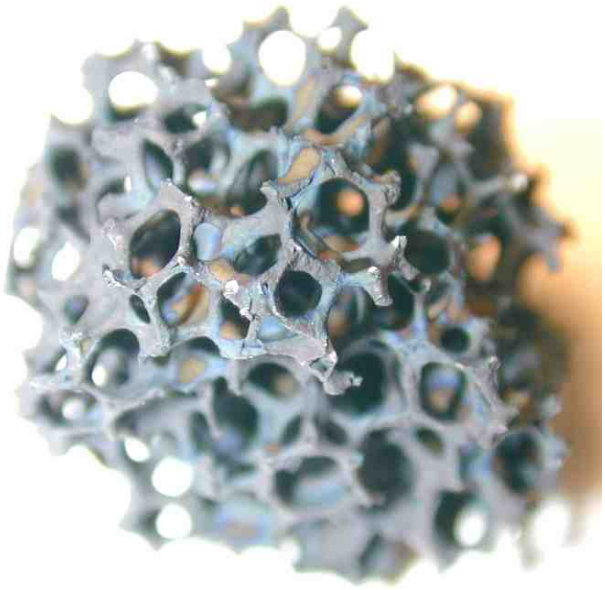

Figure 4. Carbide Washcoated Ceramic Foam

Conclusions/Future Work

The carbides have been demonstrated to be highly active WGS catalysts and are able to be washcoated onto monolith and foam substrates. To further differentiate the carbide catalysts and enhance their commercial potential, we will demonstrate that they are:

- more durable than the Cu-Zn-Al catalysts that are used commercially,
- much more tolerant to sulfur than other types of WGS catalysts, and
- cost effective.

Future work will focus on producing larger quantities (>1 kg) of the most active carbide catalysts, preparing and evaluating monolith supported prototype catalysts, and determining the cost competitiveness of the catalysts.

IV.C.15 Development of Novel Water-Gas-Shift Membrane Reactor

W.S. Winston Ho (Primary Contact)
Department of Chemical Engineering
The Ohio State University
140 West 19th Avenue
Columbus, OH 43210-1180
(614) 292-7907, fax: (614) 292-3769, e-mail: ho@che.eng.ohio-state.edu

DOE Technology Development Manager: Nancy Garland
(202) 586-5673, fax: (202) 586-9811, e-mail: Nancy.Garland@ee.doe.gov

ANL Technical Advisor: Thomas G. Benjamin
(630) 252-1632, fax: (630) 252-4176, e-mail: benjamin@cmt.anl.gov

Objectives

- Develop a mathematical model for the novel water-gas-shift (WGS) membrane reactor with a carbon dioxide (CO_2)-selective membrane to elucidate the effects of system parameters on the reactor and to show the feasibility of achieving hydrogen (H_2) enhancement via CO_2 removal and carbon monoxide (CO) reduction to 10 parts per million (ppm) or lower from the modeling study.
- Synthesize CO_2-selective membranes for the reactor.
- Develop the membrane reactor for achieving H_2 enhancement and <10 ppm CO.

Approach

- Develop a non-isothermal model for the novel WGS membrane reactor by taking material and energy balances and reaction into account.
- Use the model to study the effects of system parameters on the reactor, to carry out the technical analysis of the reactor for synthesis gases from steam reforming and autothermal reforming, and to guide/minimize experimental work.
- Synthesize and characterize of CO_2-selective membranes containing amino groups.
- Incorporate the membrane synthesized in the reactor to demonstrate H_2 enhancement via CO_2 removal and CO reduction to 10 ppm or lower.

Accomplishments

- Developed a one-dimensional non-isothermal model for the novel WGS membrane reactor with a CO_2-selective membrane in the hollow-fiber configuration using air as the sweep gas.
- Elucidated the effects of system parameters on the membrane reactor for synthesis gases from steam reforming and autothermal reforming.
- Showed the feasibility of achieving H_2 enhancement via CO_2 removal and CO reduction to 10 ppm or lower based on the modeling study.

Future Directions

- Analyze the effects of feed pressure on the membrane reactor for synthesis gases from steam reforming and autothermal reforming.
- Synthesize and characterize CO_2-selective membranes for the reactor.

- Conduct the proof-of-concept demonstration using the laboratory membrane reactor.
- Carry out the prototype membrane reactor demonstration for a 50 kilowatt (kW) fuel cell.

Introduction

A WGS reactor for the conversion of carbon monoxide and water to hydrogen and carbon dioxide is widely used in chemical and petroleum industries. The reactor is also critically needed for the conversion of fuels, including gasoline, diesel, methanol, ethanol, natural gas, and coal, to hydrogen for fuel cells. Since the WGS reaction is reversible, the reaction is not efficient, resulting in a high concentration of unconverted CO (about 1%) in the H_2 product and a bulky, heavy reactor.

The WGS reaction can be enhanced significantly through a CO_2-selective membrane, which removes the reaction product, CO_2, in order to beat the reaction equilibrium and shift the reaction towards the product side. The CO_2-selective WGS membrane reactor has advantages including (1) a high-purity H_2 product is recovered at the high pressure (feed gas pressure) and (2) air can be used as the sweep gas to remove the permeate, CO_2, on the low-pressure side of the membrane to have a high driving force for the separation. These advantages are especially important for fuel cell vehicles. The first advantage eliminates the need for an unwanted compressor. With the second advantage, the high driving force created by the air sweep can result in low CO concentration and high H_2 purity and recovery.

We have developed a mathematical model for the countercurrent WGS membrane reactor with a CO_2-selective membrane in the hollow-fiber configuration using air as the sweep gas. With this model, we have elucidated the effects of system parameters on the novel WGS membrane reactor for synthesis gases from steam reforming and autothermal reforming. The modeling results show that H_2 enhancement via CO_2 removal and CO reduction to 10 ppm or lower are achievable. For comparison and the completeness of the modeling work, we have also developed a similar model for the cocurrent WGS membrane reactor.

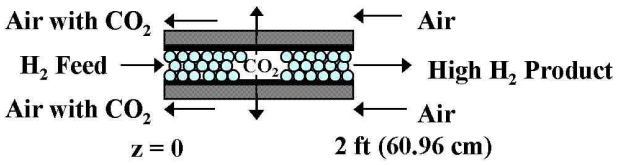

Figure 1. Schematic of a Countercurrent CO_2 Selective Membrane Reactor Containing Catalyst Particles

Results

Development of Mathematical Model

We have developed a one-dimensional non-isothermal model for the countercurrent WGS membrane reactor with a CO_2-selective membrane in the hollow-fiber configuration using air as the sweep gas. Figure 1 shows the schematic of each hollow-fiber membrane with catalyst particles in the reactor. The modeling study of the membrane reactor is based on: (1) the CO_2 / H_2 selectivity and CO_2 permeance reported by Ho [1, 2] and (2) low-temperature WGS reaction kinetics for the commercial catalyst copper oxide, zinc oxide, aluminum oxide (CuO/ZnO/Al_2O_3) reported by Moe [3] and others [4]. In this modeling study, the model that we have developed has taken into account critical system parameters including temperature, pressure, feed gas flow rate, sweep gas (air) flow rate, CO_2 permeance, CO_2 /H_2 selectivity, CO concentration, CO conversion, H_2 purity, H_2 recovery, CO_2 concentration, membrane area, water (H_2O)/CO ratio, and reaction equilibrium.

For a 50 kW fuel cell system, two types of synthesis gases, one from the steam reforming of methane and the other from the autothermal reforming of gasoline with air, have been considered. The syngas from steam-reforming of methane consists of 18.63% CO (theoretical maximum value), 58.23% H_2, 0.78% CO_2, and 22.36% water (24% CO, 75% H_2, and 1% CO_2 on a dry basis). The syngas from autothermal reforming of gasoline with air consists of 18.63% CO (maximum), 20.96% H_2,

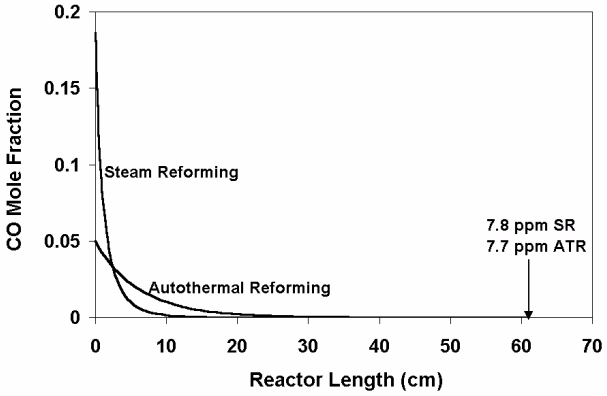

Figure 2. Profiles of Carbon Monoxide Mole Fractions in the Hydrogen Products Along the Countercurrent Membrane Reactors for the Synthesis Gases With (1) 18.63% CO from Steam Reforming and (2) 5% CO from Autothermal Reforming

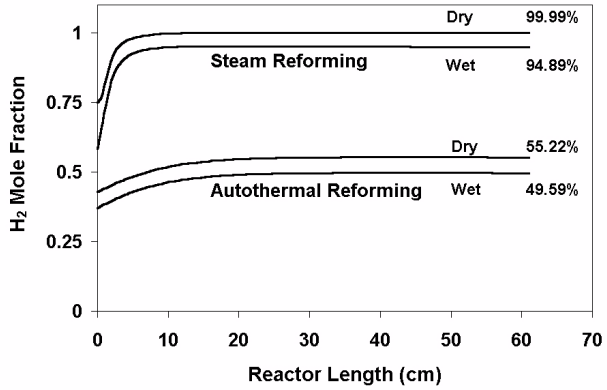

Figure 3. Profiles of Hydrogen Mole Fractions in the Hydrogen Products on Dry and Wet Bases Along the Countercurrent Membrane Reactors for the Synthesis Gases with (1) 18.63% CO from Steam Reforming And (2) 5% CO from Autothermal Reforming

0.78% CO_2, 37.27% diatomic nitrogen (N_2), and 22.36% water (24% CO, 27% H_2, 1% CO_2, and 48% N_2 on a dry basis).

Modeling for Syngas from Steam Reforming of Methane

For the syngas at 3 atm from steam reforming of methane, the modeling of the membrane reactor containing 20,500 hollow fibers was conducted. Figure 2 shows the profile of the CO concentration in the H_2 product in the reactor with an inlet feed temperature of 180°C for a total reactor length of 61 centimeters (24 inches). The syngas flow on the high-pressure side of the membrane (3 atmospheres [atm]) was countercurrent to the flow of air sweep at 1 atm on the low-pressure permeate side of the membrane (with 22°C inlet air). The molar flow rate ratio of the air sweep to the syngas was 0.75. As shown in this figure, the CO concentration in the H_2 product at the exit of the reactor was 7.8 ppm, which was better than the desired concentration of 10 ppm for fuel cells. The H_2 recovery was very good at 90.3%. A CO conversion of 99.997% was achieved.

Figure 3 depicts the profiles of the H_2 mole fraction in the H_2 product both on a dry basis and on a wet basis in the same membrane reactor. A high H_2 concentration of 99.99% on a dry basis resulted in the H_2 product, which was significantly higher than the original concentration of 75% in the syngas. In other words, the novel membrane reactor has given not only significant H_2 enhancement but also a H_2 product with a CO concentration of less than 10 ppm.

For the same membrane reactor, the effects of inlet feed temperature and sweep-to-feed molar ratio on CO and CO_2 concentrations and H_2 recovery were studied. For the inlet feed temperatures ranging from 160°C to 220°C at a sweep-to-feed molar ratio of 0.75, the CO concentrations in the H_2 product were all below 10 ppm, and the H_2 recoveries were about 90%. As the sweep-to-feed molar ratio increased from 0.5 to 1.25 at an inlet feed temperature of 180°C, the CO concentration in the H_2 product decreased from 12.5 ppm to 2.2 ppm as a result of a more favorable equilibrium at a lower outlet feed temperature. As shown in Figure 4, the H_2 recovery decreased significantly as the ratio increased. The H_2 loss to the sweep gas was a result of the higher H_2 driving force created from the higher ratio.

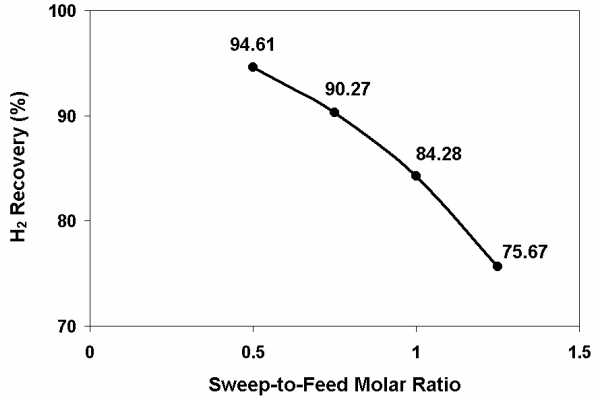

Figure 4. Effect of Sweep-To-Feed Molar Flow Rate Ratio on Hydrogen Recovery for the Countercurrent Membrane Reactor With the 18.63% CO Syngas From Steam Reforming

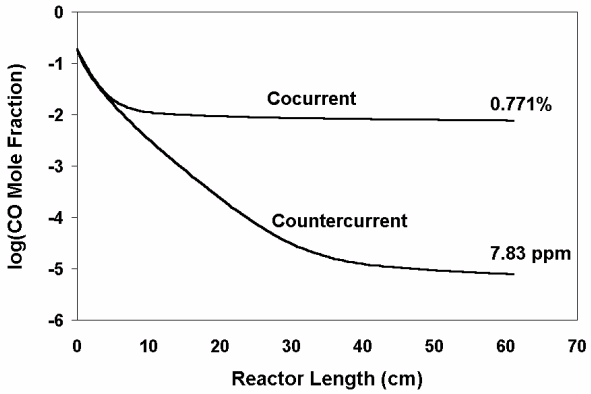

Figure 5. Comparison Between Cocurrent And Countercurrent Membrane Reactors in Terms of the Profiles of Carbon Monoxide Mole Fractions in the Hydrogen Products along the Reactors

However, the CO_2 concentration (~100 ppm) in the H_2 product hardly changed with either the ratio or the inlet feed temperature since the CO_2 concentration was nearly equivalent to that in the sweep gas.

Modeling for Syngas from Autothermal Reforming of Gasoline with Air

Similarly, significant H_2 enhancement and a H_2 product with 10 ppm CO or lower were also obtained for the synthesis gases at 3 atm from the autothermal reforming of gasoline with air containing CO at concentrations of 18.63%, 10%, 5%, and 1%. As the CO concentration of the feed gas decreased, the temperature rise in the membrane reactor due to the WGS reaction decreased. At the feed gas CO concentration of 5% or lower, there was no temperature rise. For the feed gas CO concentration of 5% (5% CO, 37% H_2, 11% CO_2, 33.5% N_2, and 13.5% water), Figure 2 illustrates the profile of the CO concentration in the H_2 product for the reactor containing 20,000 hollow fibers with an inlet feed temperature of 180°C. The molar flow rate ratio of the air sweep to the syngas was 1. As shown in this figure, the CO concentration in the H_2 product at the exit of the reactor was 7.7 ppm. The H_2 recovery was excellent at 98.4%.

Figure 3 depicts the profiles of the H_2 mole fraction in the H_2 product both on a dry basis and on a wet basis in the same membrane reactor. A H_2 concentration of 55.22% on a dry basis resulted in the H_2 product, which was significantly higher than the original concentration of 42.8% in the syngas.

Comparison with Cocurrent WGS Membrane Reactor

For comparison and the completeness of the modeling work, we have also developed a similar model for the cocurrent WGS membrane reactor. Figure 5 illustrates the comparison between the cocurrent and countercurrent WGS membrane reactors in terms of the profiles of CO mole fractions in the H_2 products along the reactors under the same conditions. As shown in this figure, the CO concentration in the H_2 product was 7.8 ppm for the countercurrent reactor whereas that was 0.77% (7,700 ppm) for the cocurrent reactor. Thus, the countercurrent reactor was much more effective than the cocurrent one. Future work will be on the countercurrent reactor only.

Conclusions

We have developed a one-dimensional non-isothermal model for the countercurrent WGS membrane reactor with a CO_2-selective membrane in the hollow-fiber configuration using air as the sweep gas. With this model, we have elucidated the effects of system parameters, including feed CO concentration, feed temperature, and sweep-to-feed molar ratio, on the reactor for synthesis gases from steam reforming and autothermal reforming. The

modeling results have shown that H_2 enhancement (>99.9% H_2 for the steam reforming of methane and >49% H_2 for the autothermal reforming of gasoline with air on a dry basis) via CO_2 removal and CO reduction to 10 ppm or lower are achievable for both synthesis gases investigated. For comparison and the completeness of the modeling work, we have also developed a similar model for the cocurrent membrane reactor. The countercurrent reactor is much more effective than the cocurrent one.

References

1. W. S. Ho, "Membranes Comprising Salts of Aminoacids in Hydrophilic Polymers", U. S. Patent 5,611,843 (1997).

2. W. S. Ho, "Membranes Comprising Aminoacid Salts in Polyamine Polymers and Blends", U. S. Patent 6,099,621 (2000).

3. J. M. Moe, "Design of Water-Gas-Shift Reactors", Chem. Eng. Progress, 58, 33 (1962).

4. N. E. Amadeo and M. A. Laborde, "Hydrogen Production from the Low-Temperature Water-Gas-Shift Reaction: Kinetics and Simulation of the Industrial Reactor", Int. J. Hydrogen Energy, 20 (12), 949 (1995).

FY 2002 Presentations/Publications

1. Louei El-Azzami and W.S. Winston Ho, "Modeling of Water-Gas-Shift Membrane Reactors with a CO_2-Selective Membrane for Fuel Cells", AIChE Annual Meeting, Reno, NV, November 4 – 9, 2001.

2. W.S. Winston Ho, "Engineering Membranes for Environmental and Energy Applications", Invited Talk at the Ohio State University, Columbus, OH, March 14, 2002.

3. W.S. Winston Ho, "Engineering Membranes for Environmental and Energy Applications", Invited Talk at the Colorado State University, Fort Collins, CO, March 29, 2002.

Patent Filed

1. W.S. Winston Ho, "CO_2-Selective Membranes Containing Amino Groups", U. S. Patent Application Serial No. 10/145,297, filed on May 14, 2002.

IV.D Fuel Cell Stack Subsystem and Components

IV.D.1 R&D of a 50 kW, High Efficiency, High Power Density, CO-Tolerant PEM Fuel Cell Stack System

Tim Rehg (Primary Contact), Nguyen Minh (Program Manager)
Honeywell International
2525 W. 190th Street, MS-36-1-93193
Torrance, CA 90504-6099
(310) 538-7220, fax: (310) 512-3432, e-mail: Timothy.Rehg@ ps.ge.com

DOE Technology Development Manager: Patrick Davis
(202) 586-8061, fax: (202) 586-9811, e-mail: Patrick.Davis@ee.doe.gov

ANL Technical Advisor: William Swift
(630) 252-5964, fax: (630) 972-4473, e-mail: swift@cmt.anl.gov

Objectives

- Research, develop, assemble, and test a 50 kW net polymer electrolyte membrane (PEM) fuel cell stack system comprised of a PEM fuel cell stack and the supporting gas, thermal, and water management subsystems. The PEM fuel cell stack system will be capable of integration with at least one of the fuel processors currently under development by Hydrogen Burner Technology (HBT) and Arthur D. Little, Inc.

Approach

This phased program includes the fabrication and testing of three 10-kW subscale PEM fuel cell stacks leading up to the final 50 kW system. Stack technology development and system analysis were conducted iteratively to identify pertinent technology advances to be incorporated into successive subscale stack builds. The final system analysis will define the 50 kW stack and system configuration.

Phase I:

- PEM stack R&D to demonstrate multi-fuel capability and CO tolerance
- PEM stack R&D to advance technologies toward DOE targets

Phase II:

- Subscale integration, electronic control system development, transient characteristics, and durability testing

Phase III:

- Testing of the 50 kW PEM fuel cell stack system
- Hardware delivery of 50 kW PEM fuel cell stack system to Argonne National Laboratory

Accomplishments

- Testing of the balance-of-plant with the integrated turbocompressor has been completed.
- A 3rd generation 10-kW class PEM stack with compression molded bipolar plates has been completed and tested, and anode stoichiometry of 1.15 has been demonstrated.
- The 50-kW class PEM fuel cell stack has been built and integrated into the brassboard system.

Future Directions

- Conduct performance testing of the 50 kW net PEM fuel cell stack system brassboard at nominal load, peak load, and different intermediate partial loads and determine system efficiency.
- Deliver 50 kW net PEM fuel cell stack system brassboard to Argonne National Laboratory at the conclusion of the project (07/02).

Introduction

Fuel cell power plants will become viable substitutes for the internal combustion engine (ICE) in automotive applications only when their benefits of increased fuel efficiency and reduced emissions are accompanied by performance and cost comparable to the ICE. Meeting these requirements is a significant technical challenge that requires an integrated systems approach. This effort encompasses the technical and developmental activities required to incorporate innovations necessary to develop a 50 kW fuel cell stack system to meet the requirements set forth by the DOE.

Approach and Results

Fuel Cell Stack System

The PEM fuel cell stack system consists of the fuel cell stack and supporting gas, thermal and water management systems as shown in Figure 1. Overall system performance depends on the careful integration of these subsystems. The system developed under this contract was designed to accept reformed gasoline from a fuel processor. Development of the fuel processor was not part of this program.

The 50 kW fuel cell stack brassboard system design has been completed. The three-dimensional layout including six hexagonally shaped stacks can be seen in Figure 2. During this reporting period, all major components have been procured, and the balance of plant has been assembled. A photograph of the system is shown in Figure 3. The brassboard has been designed for 50 kW electric power output, operating at high-efficiency on simulated gasoline reformate. It incorporates full integration and management of on-board thermal, water and air subsystems, and makes use of off-the-shelf components to minimize cost and assembly time.

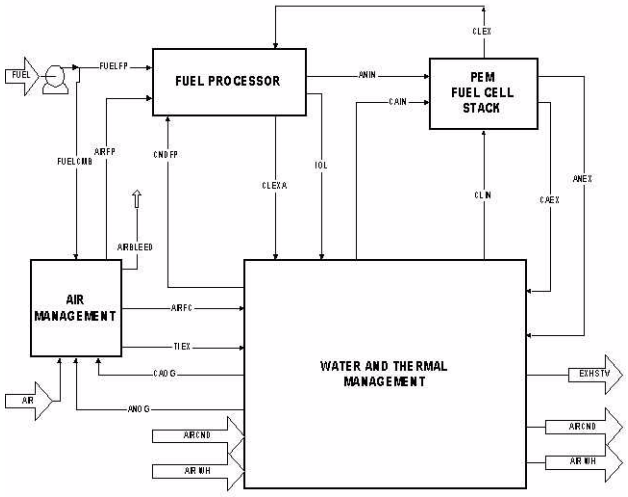

Figure 1. PEM Fuel Cell Stack System Diagram

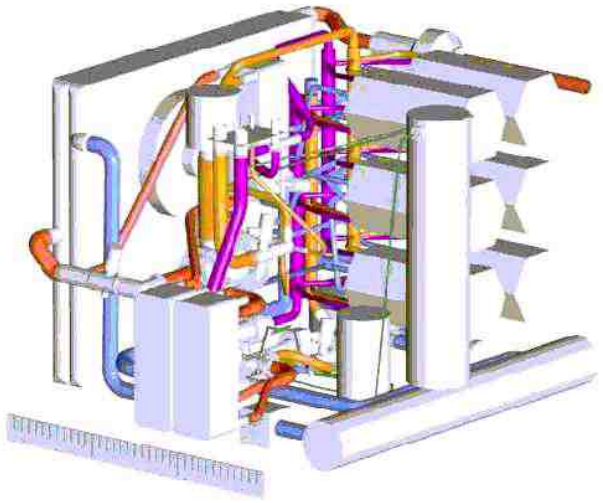

Figure 2. 50 kW Brassboard System Design

For air delivery, the fuel cell stack system is equipped with a Honeywell turbocompressor developed under separate DOE funding (see Figure 4). The turbocompressor delivers enough air for the fuel cell stack system and the fuel processor at an

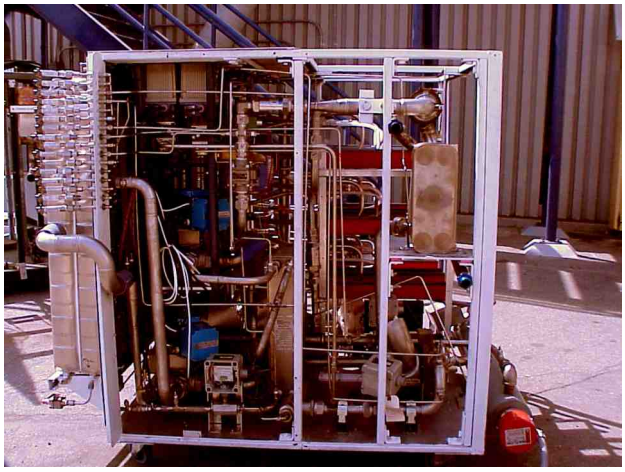

Figure 3. 50 kW Brassboard System

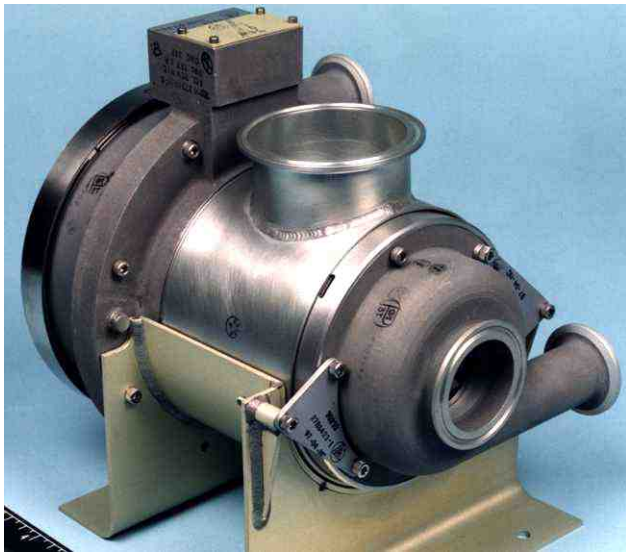

Figure 4. Honeywell Phase II Turbocompressor

operating pressure of up to 3 atmospheres at peak condition. During this reporting period the balance-of-plant with the integrated turbocompressor and its controller has been tested to verify adequate performance. Six 10-kW class PEM fuel cell stacks have been built using compression molded bipolar plates. These stacks have been integrated into the balance-of-plant for final system performance testing.

10-kW PEM Fuel Cell Stack With Molded Bipolar Plates

For the fabrication of the 50-kW PEM fuel cell stack, compression-molded composite bipolar plates have been employed. These plates are made in a single step, which will help to reduce the manufacturing cost substantially in the future. During this reporting period, Honeywell has received final delivery of all molded bipolar plates and has completed the assembly and testing of six 10-kW size PEM fuel cell stacks.

In order to test the performance of the compression-molded bipolar plates, a 63-cell subscale stack was built initially and tested. The performance of the subscale stack at the nominal power condition is shown in Figure 5. The test conditions are described in detail in Table 1. At a current density of 0.115 A/cm^2, the stack was able to stably operate at an anode stoichiometry of 1.15. The single cell voltage at this point was measured at 0.74 V. This results in slightly higher performance than previously seen with machined bipolar plates.

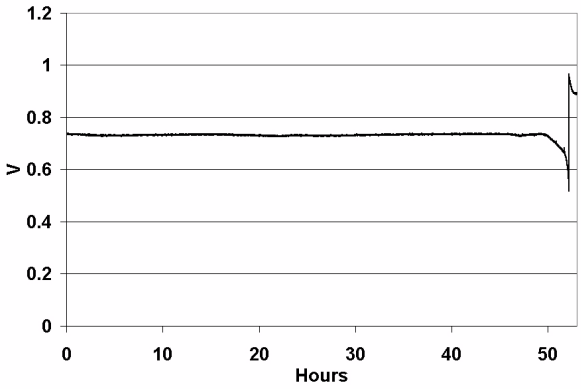

Figure 5. Performance of 63-cell PEM Fuel Cell Stack with Compression Molded Composite Bipolar Plates

	Anode	Cathode
Gas	Reformate	Air
Stoich	1.15	2.15
RH	100%	50%
Temperature	80°C	80°C
Pressure	1.25 atm	1.25 atm

Table 1. Test Conditions for 63-cell PEM FC Stack with Molded Composite Bipolar Plates

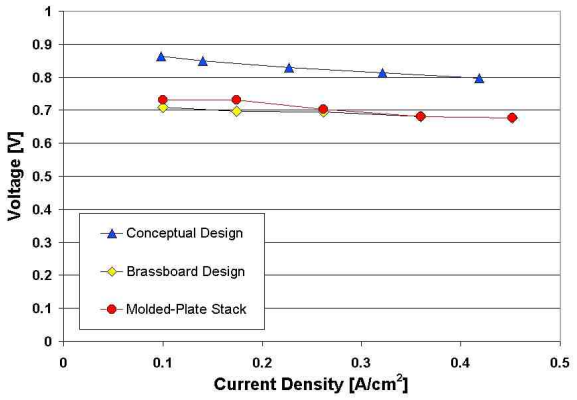

Figure 6. PEM Fuel Cell Stack Performance at Different System Operating Points

After completion of the testing of the 63-cell stack, the first 10-kW size stack was built and tested. Figure 6 compares the performance of this stack with the conceptual design performance and the originally predicted performance for the 50-kW brassboard system. The results show that the single-cell voltage remains slightly below the desired performance for the conceptual design, but has improved over the predicted brassboard performance for the lower power conditions. At the higher power conditions, including peak power, the voltage is identical to the prediction. In addition, the results show that the stack was able to operate at an anode stoichiometry of 1.25 for all power settings above 12.5 kW. At the nominal power setting, the overall pressure drop through the anode flowfield of the molded bipolar plates at flows below 1.35 stoichiometry is too low to remove liquid water. Anode stoichiometry below 1.25 at the nominal condition were demonstrated in later testing by reducing the anode relative humidity to 50%.

After successful testing of the first 10-kW size stack with molded bipolar plates, five more stacks were assembled and tested. Successively, all six stacks were integrated into the balance-of-plant, and the system is ready for performance testing.

Conclusions

In this reporting period Honeywell has completed the assembly and testing of the balance-of-plant with the turbocompressor and fuel cell stacks. Our attention is now focussed on the final performance testing of the 50 kW brassboard system and delivery to Argonne National Laboratories. Results from a 63-cell sub-scale PEMFC stack test with compression-molded composite bipolar plates demonstrated a low anode stoichiometric flow of 1.15 at nominal conditions. A full size 10-kW PEM fuel cell stack demonstrated stable performance at all system power points for an anode stoichiometric flow of 1.25.

The current projected brassboard system nominal efficiency is 45% (assuming 1.25X stoichiometric flow of reformate), and the projected power densities are ~0.2 kW/kg and ~ 0.15 kW/L, versus the CY 2002 DOE targets established for this project of 55%, 0.35 kW/kg and 0.35 kW/L. It should be noted that the above numbers include contributions from off-the-shelf components for the brassboard, i.e. oversized heat exchangers and valves. The main contributers to the loss of efficiency are increased flow stoichiometry and parasitic loads. Some of the key reasons for increased parasitic loads are compressor motor power and increased pressure drop for some components (heat exchangers, valves, etc.).

IV.D.2 Development of Comprehensive Computer Models for Simulation of Fuel Cell Systems

Hongtan Liu
Department of Mechanical Engineering
University of Miami, Coral Gables, FL 33214
(305) 284-2019, fax: (305) 284-2580, e-mail: hliu@miami.edu

DOE Technology Development Manager: Donna Lee Ho
(202) 586-8000, fax: (202) 586-9811, e-mail: Donna.Ho@ee.doe.gov

ANL Technical Advisor: William Swift
(630) 252-5964, fax: (630) 972-4473, e-mail: Swift@cmt.anl.gov

Objectives

- Develop comprehensive computer model for Polymer Electrolyte Membrane (PEM) fuel cells.
- Demonstrate the feasibility of unified model approach to eliminate errors due to approximate boundary conditions at various interfaces.
- Develop reliable tools for design and optimization of fuel cells, fuel cell stacks, and fuel cell energy systems (long-term).

Approach

- Develop general mathematical models valid in different elements of a fuel cell .
- Eliminate boundary conditions at the various interfaces between different elements of a fuel cell.
- Develop models with flexibility, adaptability and different levels of complexity, so that they can be used for different purposes. The model must be easy to update and revise to incorporate custom code.
- Develop independent packages (not based on any CFD package) that are economical, robust and high-speed.

Accomplishments

- Demonstrated the feasibility of the unified approach.
- Developed sub-model A: 2D single-phase flow model – down the channel and across the FC sandwich.
- Developed sub-model B: 2D single-phase flow model – across the channel and across the FC sandwich.
- Developed a 3-D model for hydrogen feed with constant over-potential across the catalyst layer.
- Developed a 2D two-phase flow model with variable over-potential across the catalyst layer.
- Substantially extended and improved the 3-D single phase model, including the variation of over-potential across the catalyst layers.
- Developed a 3-D single-phase model for reformate feed in the anode.
- Developed a preliminary fuel cell stack model.
- Performed systematic experimental tests to calibrate and improve the models.
- Worked closely with industry to customize and improve the models.

Future Plans

- Further develop the 3-D single-phase model: improve on reformate feed and for different flow fields.
- Improve the fuel cell stack model.
- Couple the stack model with a system model.
- Extend the models to other types of fuel cells.
- Further interactions with industry.

Introduction

A fast, reliable, and specialized CFD model for PEM fuel cell simulation can be very useful in fuel cell design optimization and operation control. In this project, a unified PEM fuel cell simulation model has been successfully established. This project started in FY 2000 with 2-D single-phase models. In FY 2001, the 2-D models were successfully transformed into a unified 3-D model for hydrogen feed. In FY 2002, this established 3-D model was extended to include reformate feed, accounting for the poisonous effect of carbon monoxide as well as the dilution effect of the reformate gas stream on the anode side. Based on this 3-D model with the geometry of a single fuel cell, a preliminary stack model was established. Extensive experiments in our lab and industry interactions were carried out to improve and calibrate the computation model.

Approach

The geometry of a single fuel cell is shown in Figure 1. The PEM fuel cell is divided into 9 regions according to the material properties and flow characteristics. In FY 2000, this project started with 2-D single-phase models that included 2 sub-models [1, 2]. One of the 2-D models has a geometry comprised of flow direction and the plane across the fuel cell sandwich (on the xy-plane). The other one includes the region across the channel and across the fuel cell sandwich (on the xz-plane).

In FY 2001, a general 3-D model was developed [3]. This general mathematical model consists of the equations of continuity, momentum, energy, and species concentrations in different elements of the fuel cell sandwich, as well as the equations for phase potential in the membrane and the catalyst layer. This set of governing equations is coupled with chemical reaction kinetics by introducing various

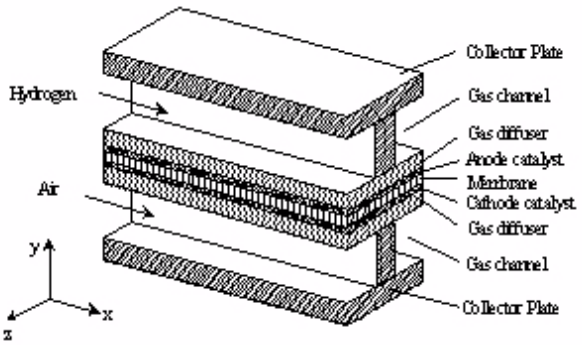

Figure 1. Single Fuel Cell Geometry

source terms. The generality of the model lies in its independence of chemical kinetic models, since the kinetics are incorporated in the source terms. One can choose any kinetics model, and any new development in the electrochemistry can easily be incorporated in this general model. To solve the mathematical model, an in-house computer code has been developed. Compared with some commercial CFD packages, this self-produced code was designed for a specific purpose so that the computation time could be significantly reduced. The output results from this 3-D model include oxygen concentration variations in different planes, local current density distributions, reaction rate, temperature distributions, water vapor distributions along anode and cathode, etc. Details about the model and results can be found in Zhou and Liu [3]. In FY 2001, a preliminary 2-phase, 2-D model was also developed [4]. It was found that a single-phase model is sufficient when the current density is low, when the current density is larger and approaching the current density limit, phase changing of water becomes significant.

In FY 2002, the 3-D single-phase model was significantly improved in several aspects. Specifically, instead of assuming constant overpotential across the catalyst layer, the variation

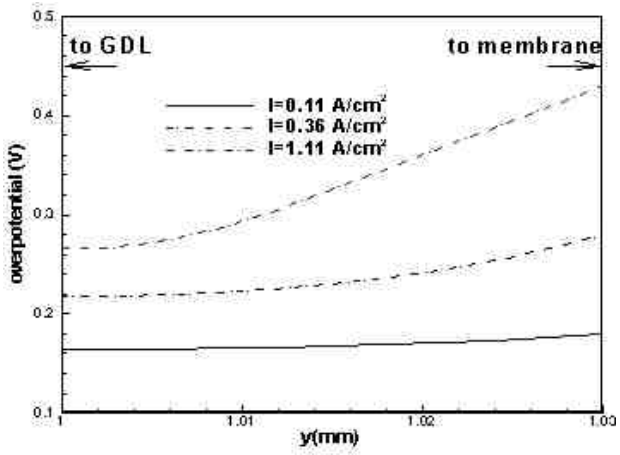

Figure 2. Variation of Overpotential Inside the Catalyst Layer

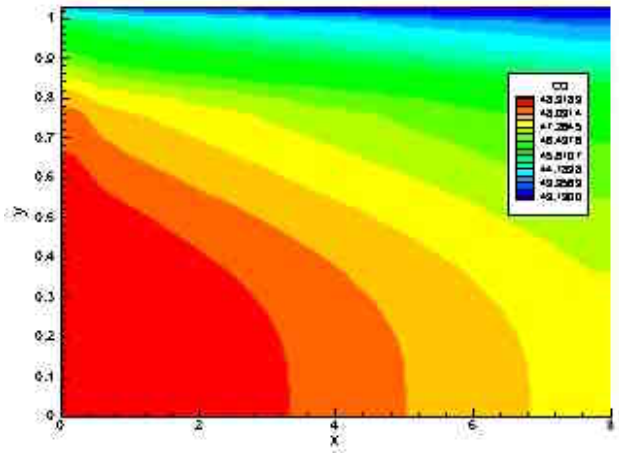

Figure 3. CO Concentration Along the Flow Direction

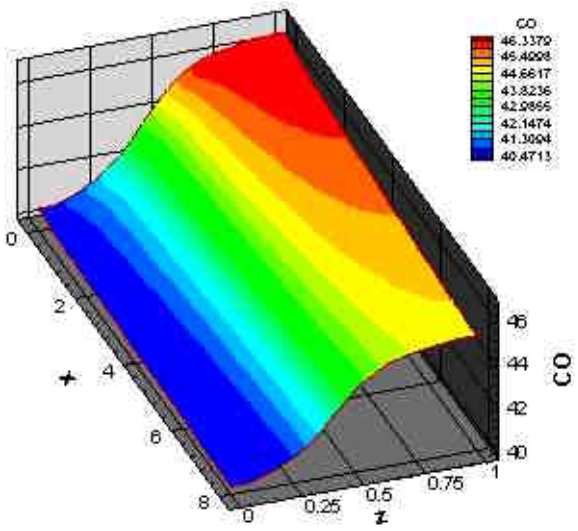

Figure 4. CO Concentration Across the Fuel Cell (Half of Z Over the Shoulder Plate)

of over-potential across the catalyst layer was added to the model [5]. Figure 2 shows the variation of the overpotential within the catalyst layer at different current densities. When the current density is low, variation of overpotential is not significant, but when the current density is high, the overpotential variation is significant and cannot be neglected. In order to reduce computation time and ensure the accuracy of the model, systematic analysis and reductions of the model have been conducted, some highlights of which can be found in [5].

Reformate feed is expected to be the viable intermediate fuel for fuel cell applications, and a PEM fuel cell operating on reformate gas has unique characteristics. Two of the characteristics are the dilution effect of the inert gases and the variation of hydrogen content at different locations of a fuel cell. The third is the poisoning effect of the carbon monoxide (CO) present in the reformate. The previous 3-D model has been extended and modified to account for these extra characteristics. The kinetic equations for CO poisoning effects that were presented by Springer et al. [6] were used. With those adjustments, the 3-D model now can successfully demonstrate some features not revealed by 1-D kinetic models in the literature [6]. The reduction of CO at larger current density due to reaction consumption is shown by the CO contours in Figures 3 and 4. The model results of CO affecting PEM fuel cell performance is shown in Figure 5. Figure 6 shows that the computation results compared very well with the test data available from the literature [7].

Based on the single fuel cell model, a preliminary stack model is set up as shown by Figure 7. This modeled region includes 5 channels and 3 cells. Cooling plates were inserted into the stack at an interval of 3 cells. (This choice is just used as an example.) The model can easily accommodate different numbers of cells and channels, and different stack designs can also be easily handled. With this stack model, computational investigations of the temperature distributions were carried out. Some sample temperature contours are shown in Figures 8

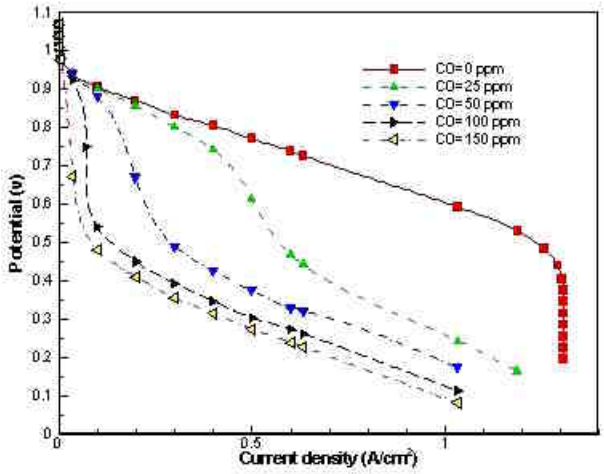

Figure 5. Polarization Curves at Different CO

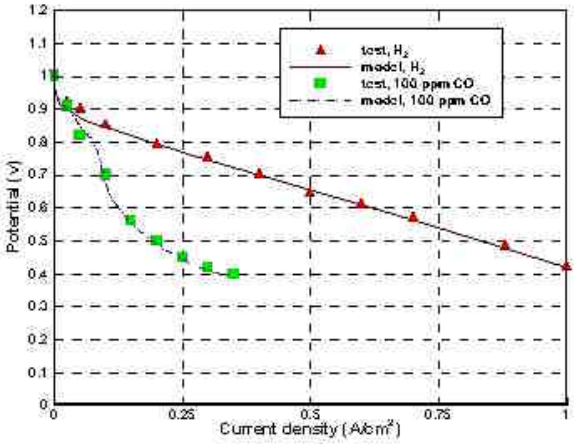

Figure 6. Comparison of Modeling Results With Experimental Data for CO Poisoning

and 9. While the cooling plates and the convection along the border cool the fuel cells, some locations of the fuel cells inside the stack can experience very high temperature. The modeling results can be used to devise better ways for fuel cell stack thermal management.

To calibrate the model, extensive experiments were conducted in our Fuel Cell Laboratory at the University of Miami [8]. Close interaction with the fuel cell industry was also carried out.

Conclusions

During the past 3 years, a generalized 3-D PEM fuel cell simulation model was developed at the

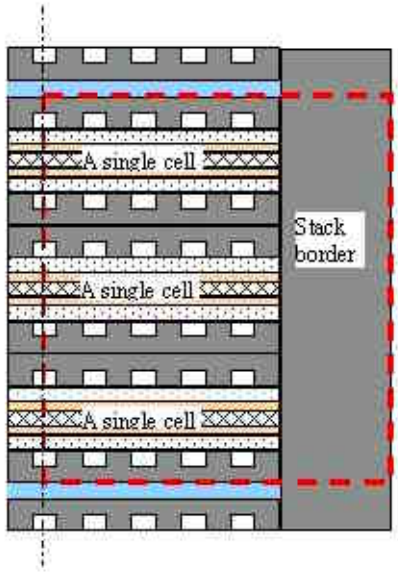

Figure 7. Geometry for the Fuel Cell Stack Model

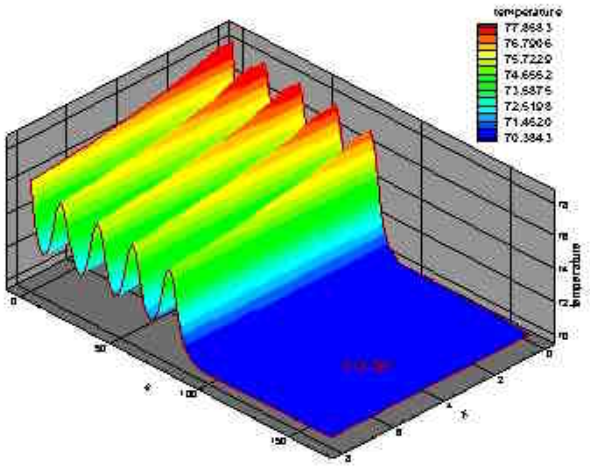

Figure 8. Temperature Contours Across the Flow Channels

University of Miami. This generalized model started from the basic fluid flow and electro-chemical principles. This generalization makes it easily adaptable to include choices of different flow fields, different fuel cell materials and flow design, and different fuels used. A computation code specifically designed for this mathematical model was produced and proved accurate and efficient. In FY 2002, the 3-D model has been significantly improved by adding the variation of overpotential across the catalyst layer. It was also extended to include the reformate feed at the anode. Extension of this single-cell model to study various stack design choices has also been

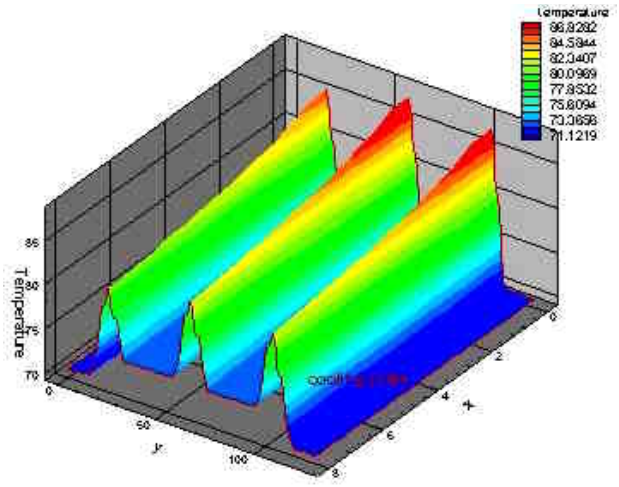

Figure 9. Temperature Distribution Within the 3 Cells Along the Flow Direction

proven feasible. The great potential of the models for industrial applications has been demonstrated, especially through the close collaborations with industry partners. Our future research plans include extending this generalized 3-D model to other types of fuel cells and coupling the stack model to a fuel cell system model.

References

1. Gurau, V., Liu, H.T. and Kakac, S., *AIChE*, Vol. **44**, pp. 2410-2422, 1998.

2. Kazim, A., Liu, H.T. and Forges, P., *J. Applied Electrochem.*, Vol. **29**, pp. 1409-1416, 1999.

3. Zhou, T. and Liu, H.T., *Int. J. Transport Phenomena*, Vol. **3** (3), pp. 177-198, 2001.

4. You, L. and Liu, H.T., *Int. J. Heat and Mass Transfer*, Vol. **45**, pp. 2277-2287, 2002.

5. Zhou, T. and H.T. Liu, *6th Biennial Conf. on Engineering Systems Design and Analysis*, Istanbul, Turkey, July 8-11, 2002.

6. Springer, T.E., Rockward, T., Zawodzinski, T.A., *J. Electrochemi. Soc.*, Vol.**148** (1), pp. A11-A23, 2001 .

7. Divisek, J., Oetjen, H.-F., Schmidt, V.M. and Stimming, U., *Electrochem. Acta*., Vol. **43**, pp. 3811-3815, 1998.

8. Wang, L., Husar, A., Zhou, T., and Liu, H., Zhou, T, "Parametric Study of PEM Fuel Cell Performances," to be presented at ASME Congress, New Orleans, November 17 – 22, 2002.

FY 2002 Publications and Presentations

1. Zhou, T. and Liu, H.T., "A General Three Dimensional Model for PEM Fuel Cells," in *Int. J. Transport Phenomena*, Vol. **3** (3), pp. 177-198, 2001.

2. You, L. and Liu, H.T., "A Parametric Study of the Cathode Catalyst Layer of PEM Fuel Cells Using a Pseudo-Homogeneous Model," *Int. J. Hydrogen Energy*, Vol. 26, pp. 991-999, 2001.

3. Liu, H.T., Zhou, T. and You, L., "CFD Modeling of Proton Exchange Membrane Fuel Cells," in *Proc. 9th Annual Conference of the CFD Society of Canada*, Kitchener, Ontario, Canada, May 27-29, 2001.

4. Zhou. T. and Liu, H.T., "Numerical Simulation Of Performance Of PEM Fuel Cells," in *Proc. of the 2nd Int. Conference on Computational Heat and Mass Transfer*, COPPE/UFRJ – Federal University of Rio de Janeiro, Brazil, October 22-26, 2001.

5. You, L. and Liu, H.T., "A Two-Phase Flow And Transport Model For The Cathode Of PEM Fuel Cells," *Int. J. Heat and Mass Transfer*, Vol. **45**, pp. 2277-2287, 2002.

6. Zhou, T. and Liu, H.T., "Heat Transfer Enhancement in Fuel Cells with Interdigitated Flow Field Design," *Int. J. Computer Applications in Technology*, in publication, 2002.

7. Zhou, T. and Liu, H.T., "Development and Simplification of a Three-Dimensional PEM Fuel Cell Model," *6th Biennial Conference on Engineering Systems Design and Analysis*, Istanbul, Turkey, July 8-11, 2002.

8. Zhou, T. and Liu, H.T., "Effects of Heat and Mass Transfer Enhancements on PEM Fuel Cell Performances," *12th International Heat Transfer Conference,* France, August 18-23rd, 2002.

9. Zhou, T. and Liu, H.T., "Simulation of Performance of PEMFC Operated by Reformed Gas," accepted for the *2002 Fuel Cell Seminar*, Palm Springs, California, November 18-21, 2002.

10. Wang, L., Husar, A., Zhou, T., Liu, H., and Zhou, T, "Parametric Study of PEM Fuel Cell Performances," accepted to the ASME Congress, New Orleans, November 17 - 22, 2002.

11. Higier, A., Husar, A., and Liu, H., "Design of a Fuel Cell Fixture with Precise Compression Control and Preliminary Experimental Results," accepted for the *2002 Fuel Cell Seminar*, Palm Springs, California, November 18-21, 2002.

IV.D.3 High Performance, Matching PEM Fuel Cell Components and Integrated Pilot Manufacturing Processes

Mark K. Debe (Principal Investigator), Judith B. Hartmann (Primary Contact)
3M Company
3M Center, Building 0201-01-C-30
St. Paul MN 55144-1000
(651) 736-1772, fax: (651) 575-1187, e-mail: jbhartmann@mmm.com

DOE Technology Development Manager: Valri Lightner
(202) 586-0937, fax: (202) 586-3237, e-mail: Valri.Lightner@ee.doe.gov

DOE Technology Development Manager: JoAnn Milliken
(202) 586-2480; fax: (202) 586-9811; e-mail: JoAnn.Milliken@ee.doe.gov

ANL Technical Advisor: Thomas Benjamin
(630) 252-1632, fax: (630) 252-4176, e-mail: benjamin@cmt.anl.gov

Subcontractor: GM - GAPC, Rochester, NY

Objectives

- Develop a set of high performance, matched proton exchange membrane (PEM) fuel cell components and pilot manufacturing processes to facilitate high volume, high yield stack production.
- Demonstrate the matched component performance in a 1-kW fuel cell stack.

Approach

- Phase 1
  - Increase surface area of the 3M-patented, nanostructured, thin film catalyst support system consistent with high volume manufacturing process.
  - Develop anode catalyst compositions and structures with higher reformate tolerance and/or a non-precious metal replacement for Ru, using a catalyst deposition process that easily generates new compositions and structures.
  - Investigate binary and ternary catalyst compositions and structures to produce higher activity cathodes.
  - Develop carbon electrode backing (EB) media, optimized for performance with the catalyst system and flow field.
  - Optimize the fuel cell flow field design for optimized water management and air bleed utilization with the catalyst and EB components.
  - Define pilot manufacturing scale-up of the processes for fabrication of catalysts, catalyst coated membrane (CCM) assemblies, and electrode backing media.
- Phase 2
  - Optimize pilot scale manufacturing of roll-good fabricated catalyst support films and catalyst deposition.
  - Specify membrane electrode assembly (MEA) component parameters and conduct final pilot scale runs to generate process statistics.

- Fabricate, test, and deliver a 1-kW stack to subcontractor for evaluation using optimized flow field and matched MEAs fabricated by pilot processes.

Accomplishments

- Developed a new Pt ternary cathode catalyst that gives the same performance with one-half the amount of Pt, producing 0.4 A/cm^2 at 0.8 V under 30/30 psig H_2/air with 0.2 mg/cm^2 total precious metal per MEA.
- Identified a non-precious metal replacement for Ru on the anode for reformate tolerance, which, with air bleed, gives equivalent performances within ±10-20 mV.
- Integrated multiple process steps for generating the nanostructured catalyst support films into a single pass, dry web-coating, pilot plant process. Completed MEA fabrication cost model based on existing pilot production process and equipment.
- Developed a unique flow field design via modeling and basic principles of gas transport that optimizes the uniformity of hydrogen and air mass flow velocities for the matched EB media and increases high current density performance over conventional designs.
- Developed a roll-good processed electrode backing/gas diffusion layer component having matched properties to the nanostructured thin film catalyst and flow field; generated pilot scale production quantities for statistical analysis of variance and demonstration of process capability.

Future Directions

- Complete pilot scale fabrication of multiple lots of roll-good, nanostructured support films, anode and cathode catalyst deposition on those substrates, and roll-good CCM fabrication to generate statistical process and performance data.
- Complete fuel cell testing of statistically sampled, roll-good fabricated, coated EB materials and CCMs having matched properties for optimum performance.
- Complete evaluation of roll-good fabricated MEAs from pilot processed material lots in 1-kW stacks at 3M and subcontractor facilities.

Introduction

The membrane electrode assembly (MEA) is the core component set of a PEM fuel cell (PEMFC) stack. An MEA consists of five basic components: anode and cathode catalysts, ion exchange polymer membrane, and anode and cathode gas diffusion layers. The functions of these basic components are intimately related, and their properties must be matched for optimum performance. For large-scale volume fabrication at the cost and quality targets required by transportation applications, very high yields and in-line process control of integrated processes based on cost effective materials are required. This project is directed towards demonstrating high performance, matching PEM fuel cell components manufacturable by integrated pilot processes, utilizing a patented nanostructured thin film catalyst support system.

Approach

Our approach to developing high performance, matching PEMFC components and integrated pilot manufacturing processes has several facets. These include optimization of the individual components, such as the anode and cathode catalysts and their supports, and electrode backing and gas diffusion layers, all made by processes consistent with high volume manufacturing methods.

For the anode and cathode catalyst development, the unique nanostructured support and catalyst coating methods offer many combinations of materials and process conditions to generate new

catalyst compositions and structures. The major focus areas have been generating higher surface area supports, fabricating and testing new Pt_xM_y binary and ternary constructions for anodes and cathodes, and reducing air bleed - all with goals of increasing performance and stability and reducing precious metal loading.

Development of carbon electrode backing (EB) media has included evaluation of different types of electrode backing materials, coatings, coating configurations, and coating processes. Evaluation involves measurement of a variety of physical properties and of fuel cell performance under a broad range of controlled conditions using nominally identical catalyst coated membranes (CCMs).

The flow field is an integral component of the MEA system. Matching it to the EB material is particularly important in order to obtain uniform gas flow velocity and pressure distributions that in turn will yield the most uniform current density distributions. The gas permeability properties of the various electrode backing and gas diffusion layers were key inputs for fluid dynamic modeling used to devise a unique flow field design that gives optimized mass flow uniformity while enhancing performance at high current densities and matching pressure drop specifications supplied by the subcontractor.

Scale-up and integration of the processes for producing the nanostructured catalyst support films via a single pass, dry web process with on-line monitoring has been a major focus during the past year to demonstrate process control, determine the pilot production equipment limits, increase material yields, and reduce costs. The catalyst coating processes have also been scaled up to give the required cross-web uniformities and apply the new multi-element catalysts. A detailed cost model for several different final integrated process scenarios was developed.

Results

Cathode Catalysts

In the past year, screening of a wide range of binary Pt_xM_y catalysts to find a cathode catalyst with greater mass activity and/or stability than pure Pt was completed. The process for fabricating the nanostructured catalysts allows a wide range of new constructions to be easily made and tested.

Figure 1 compares the performance of three different Pt binaries and two different Pt ternary constructions with the pure Pt cathode catalyst. The test uses high-pressure hydrogen/oxygen to best reflect the oxygen reduction reactivity of the cathode catalysts. As can be seen, all the combinations outperform the pure Pt catalyst. All the samples contained 0.1 mg/cm^2 of precious metal, except for the second ternary, PtAB-2, which contained 0.15 mg/cm^2. PtAB-2 was selected for scale-up during Phase 2 and became the focus for 50-cm^2 fuel cell testing.

As discussed in Reference 1, it is well documented that, with our standard nanostructured support particles, the baseline pure Pt catalyst has a mass specific surface area of about 7 m^2/g. For our standard loadings of 0.22 mg/cm^2, this corresponds to an effective surface roughness factor (or SEF, surface enhancement factor) of 12-15 cm^2/cm^2. Figure 2 shows duplicate measurements (Series A, Series B) of the SEF for the PtAB-2 ternary catalyst at three different loadings compared to the standard Pt at 0.22 mg/cm^2. It is seen that the ternary has the same surface area with half the amount of Pt as the standard pure Pt catalyst. This doubling of the mass

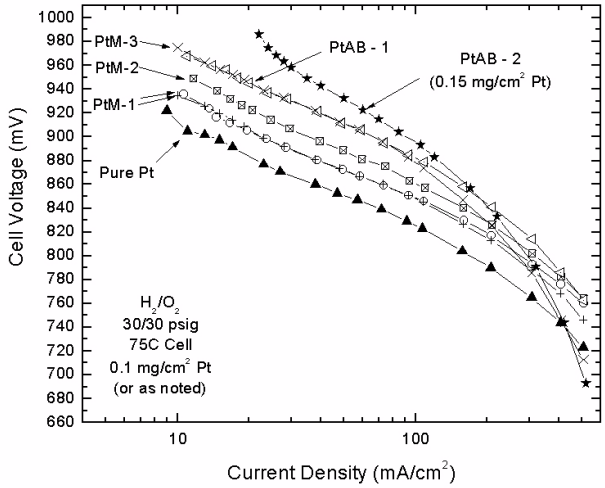

Figure 1. Comparison of the oxygen reduction activity of various binary and ternary catalysts with pure Pt, using 30-psig oxygen test conditions to enhance the differentiation.

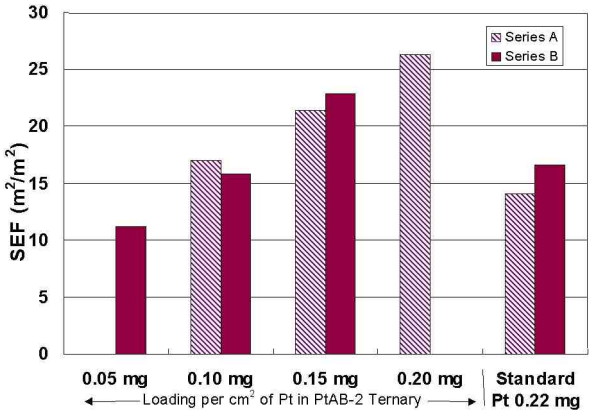

Figure 2. Comparison of the measured surface area, using hydrogen adsorption-desorption cyclic voltammetry, from pure Pt and the PtAB-2 ternary containing varying amounts of Pt.

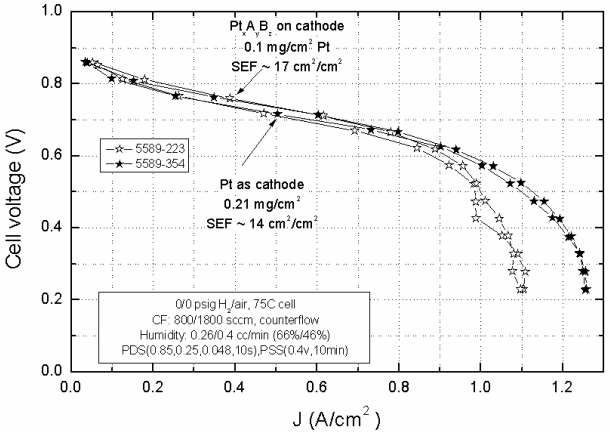

Figure 3. Comparison of PDS polarization curves from a single MEA tested in two orientations, first with the PtAB-2 ternary (with 0.1 mg/cm^2 Pt) as a cathode and the pure Pt (0.21 mg/cm^2) as the anode (5589-223), and second with the PtAB-2 as the anode and the pure Pt as the cathode (5589-354). The ternary with half the amount of Pt outperforms the pure Pt.

specific surface area to ~ 15 m^2/g allows the same fuel cell performance to be obtained with half the precious metal content.

This is best shown by comparing polarization curves for the same MEA, taken in two orientations. The first orientation has the PtAB-2 catalyst, with 0.1 mg/cm^2 Pt, as the cathode and the standard Pt catalyst, with 0.2 mg/cm^2, as the anode. In the

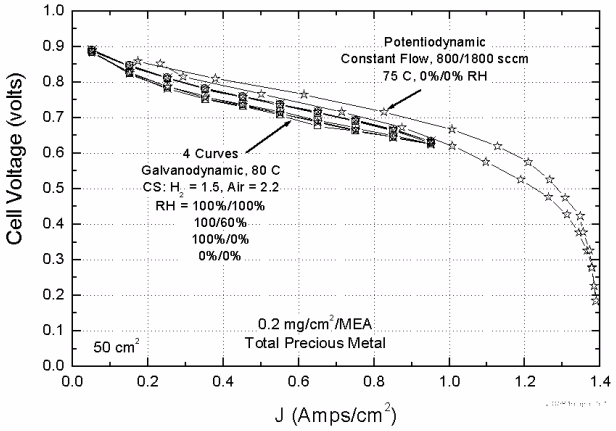

Figure 4. PDS-CF and GDS-CS polarization curves at 30 psig inlet pressure from an MEA having a total of 0.2 mg/cm^2/MEA of total precious metal (Pt).

second orientation, the hydrogen, air, and voltage leads are reversed so the ternary becomes the anode and the standard Pt is on the cathode. Figure 3 compares potentiodynamic (PDS) constant flow polarization curves at ambient pressure for these two MEA orientations and clearly indicates the improved kinetic behavior of the ternary over the standard Pt catalyst.

Figure 4 shows two types of polarization scans from an MEA having a total of 0.2 mg Pt/cm^2/MEA. This MEA has the same PtAB-2 catalyst on the cathode as in Figure 3, but the standard Pt on the anode reduced to 0.1 mg/cm^2. In Figure 4, the single potentiodynamic scan (PDS) polarization curve was obtained with constant flow (CF) conditions at 75ºC, while the lower four galvanodynamic scan (GDS) curves were obtained with constant stoichiometric flow (CS) conditions and varying humidification at 80ºC. All were obtained with H_2/air at 30/30 psig inlet pressures. The 30-psig constant flow conditions can achieve close to the DOE technical target of 0.4 A/cm^2 at 0.8 V for MEAs on hydrogen/air. This performance with this total loading of 0.2 mg/cm^2/MEA of Pt corresponds to the 2005 target of 0.6 g/kW at 0.8 V and 0.3 g/peak kW of precious metal.

Anode Catalysts

Screening for better or less costly anode catalysts is also a major task area. Finding a replacement for

Ru was a primary goal, along with reducing the amount of Pt required for adequate reformate tolerance. To facilitate the rapid screening of many new catalyst constructions having different compositions and structures, anode over-potential (AOP) and AC impedance measurements were used. Reference 1 discussed results from two new binary anode catalysts containing 0.1 mg/cm^2 of Pt and non-precious metal replacements for Ru, which had less AOP than the PtRu control. This past year led to development of still another PtM binary, where M is a non-precious metal replacement for Ru, which was down-selected for scale-up during Phase 2. Figure 5 compares 75ºC, 30 psig, constant flow polarization curves under H_2/air, reformate with 2% air bleed, and reformate with 4% air bleed from an MEA having this binary as the anode (0.20 mg/cm^2 Pt) and a standard Pt cathode (0.21 mg/cm^2). There is little difference between 2% and 4% air bleed and about a 35 mV loss compared to pure hydrogen at 0.5 A/cm^2. The curves suggest the DOE reformate target of 125 mA/cm^2 at 0.83 V and 9 psig are close to being met, but the rated power targets under reformate of 500 mA/cm^2 at 0.75 V and 30 psig fall short by about 35 mV.

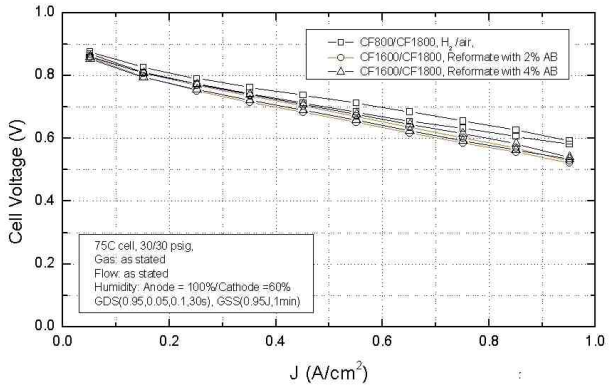

Figure 5. GDS-CF polarization curves under hydrogen and reformate with 2% and 4% air bleed, from an MEA having a PtM binary on the anode containing no Ru and 0.2 mg/cm^2 of total precious metal (Pt).

Roll-Good Electrode Backing Media

The EB materials and configurations demonstrating the highest potential for meeting project goals were selected for optimization. This past year, the work focused on demonstrating the EB/GDL process capability. Rolls of EB material were processed and the EB coatings applied in multiple pilot scale coating runs. Two types of on-line measurements were successfully used for characterization of two key physical properties. All lots were characterized off-line as well for these two plus a third critical property. All three parameters were demonstrated to be in process control. Analysis of variance within and between rolls did show some statistically significant differences, but total variability was small. Fuel cell characterization of MEAs having EB/GDL samples taken across all the produced rolls are underway using CCMs having standard Pt anodes and cathodes. Fuel cell tests of EB/GDL media sampled from one 450-lineal-yard roll are also underway with CCMs having the new PtAB-2 ternary cathode catalyst. This matched CCM/EB combination is giving the best performance to date and excellent statistical reproducibility, as shown in Figure 6. This shows the galvanodynamic, constant stoichiometry polarization curves from the first seven tested MEAs of 12 statistically sampled EB/GDLs from the fully processed 450-lineal-yard roll-good.

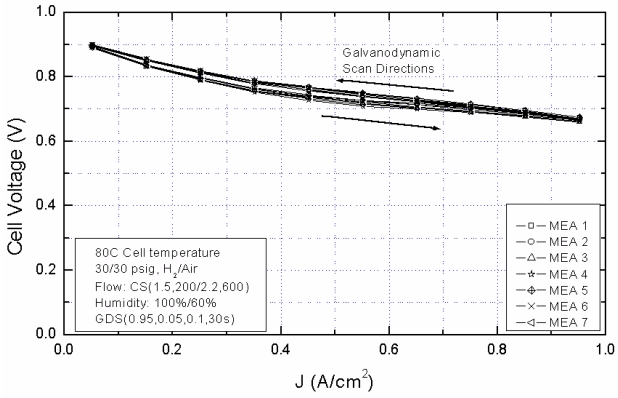

Figure 6. Seven GDS-CS polarization curves of EB/GDL samples taken from a pilot-scale processed 450-lineal-yard roll. The excellent reproducibility also reflects uniformity of the CCM. The galvanostatic (GSS) current density between scans was 0.95 A/cm^2.

Flow Field

The flow field and EB/GDL must be matched for optimum performance and durability. Designing for the most uniform gas flow distributions and effective water management should translate into the most

uniform current distributions. This year, computational fluid dynamics (CFD) modeling at 3M has led to a unique flow field design targeted for the EB roll-good materials discussed above. This design was refined as well to meet the desired in-cell pressure drops for the pressure-flow rate curves suggested by our subcontractor. Figure 7 shows a series of comparison polarization curves from different MEAs, each tested first in a cell having a commercially available quad-serpentine flow field, and then after transferring to a cell having the optimized flow field. By design, the gas flow distributions should be significantly more uniform in our new optimized flow field. As Figure 7 shows, there is also better performance in the high current density regime, as expected due to the operating principle of the new flow field.

Nanostructured Catalyst Process Scale-Up

A key aspect of demonstrating an integrated MEA manufacturing process has been development of a single pass, dry web coating process for generating the nanostructured catalyst support films with their catalyst coating. This overall process involves several separate sub-processes, which previously were done individually. Reduced cost and improved yields are greatly facilitated by sequentially carrying out these individual process steps during a single web coating run. This year significant progress was made on demonstrating a single pass pilot process with online control of the nanostructured support films. Scanning electron microscopy (SEM) imaging allows off-line characterization of the catalyst coated support films to document the nanostructured element feature dimensions, number density, and geometric surface area as a function of cross-web and down-web position. Figure 8 shows SEM cross-sectional and plan view images of Pt-coated nanostructured features at 50, 125, and 240 ft respectively, down-web of a single pass 250-lineal-ft coating run. The nanostructured support whiskers are essentially identical both cross-web and down-web. Twelve nominally identical coating runs have been completed for statistical characterization of this integrated process.

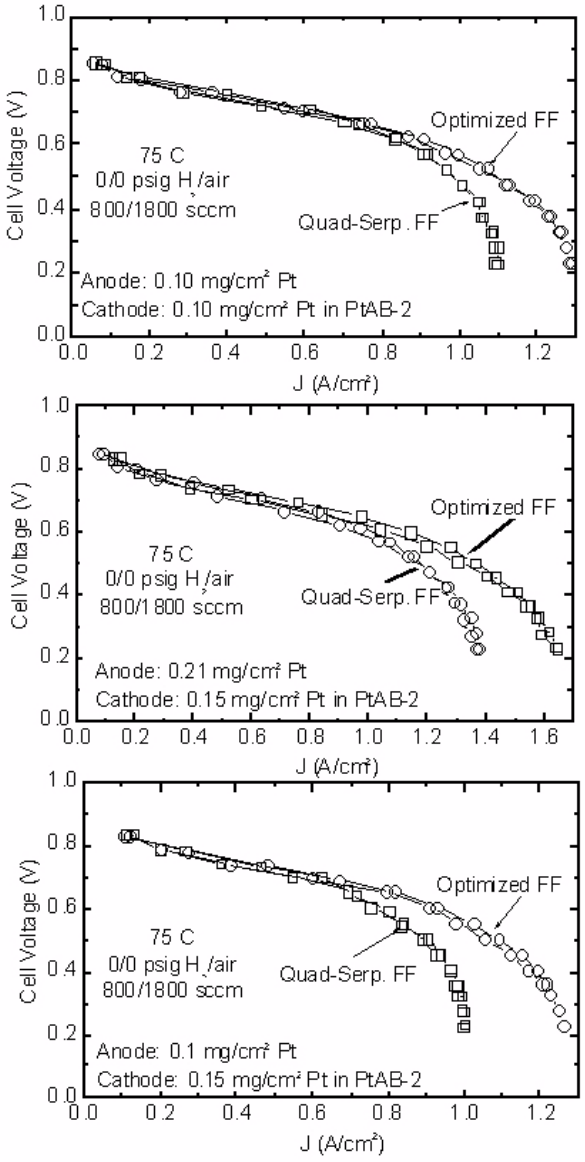

Figure 7. Comparison of PDS-CF polarization curves from three MEAs, each evaluated first in the standard quad-serpentine flow field, and

Stack Testing

The MEAs fabricated with the matched components and integrated manufacturing processes are to be evaluated in a 1-kW stack at the subcontractor's facilities. Development of the stack with the proprietary flow fields is being done at 3M

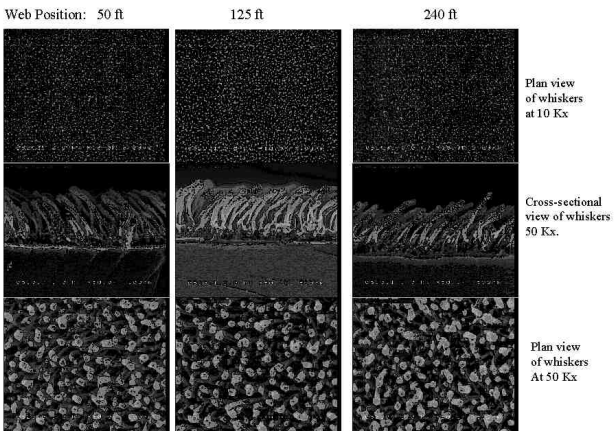

Figure 8. Scanning electron micrographs of the nanostructured catalyst support films at beginning (50 ft), middle (125 ft) and end (240 ft) locations of a 250-lineal-ft pilot scale run in which the support films were produced in a single pass, dry process.

with consultation from the subcontractor. The first H_2/air tests with 200-cm^2 MEAs incorporating the new cathode ternary catalysts and optimized EB/GDL were started on June 28, 2002, in this first stack and currently show excellent cell-to-cell uniformity.

Conclusions

Significant progress has been made in all aspects of the objectives of developing high performance, matched PEM fuel cell components and integrated pilot manufacturing processes. Results to date indicate that, with the new ternary cathode catalyst, the potential is good for meeting the project performance objectives on hydrogen air in a 1-kW stack while exceeding the precious metal loading targets. Similarly, the progress on development of the integrated manufacturing processes indicates the potential for meeting volume and quality objectives. Future work includes finishing the generation of multiple lots of roll-good fabricated CCM and subsequent characterization and fuel cell testing to determine the statistical variance of the processes, completion of a similar fuel cell evaluation of the EB/GDL roll-good media, and completion of the 1-kW stack development and testing of the pilot manufactured MEAs at the subcontractor facilities.

References

1. FY 2001 Progress Report for Fuel Cells for Transportation, page 113.

IV.D.4 Design and Installation of a Pilot Plant for High-Volume Electrode Production

James Arps (Primary Contact)
Southwest Research Institute
P.O. Drawer 28510
San Antonio, TX 78228-0510
(210) 522-6588, fax: (210) 522-6220; e-mail: jarps@swri.org

DOE Technology Development Manager: JoAnn Milliken
(202) 586-2480, fax: (202) 586-9811, e-mail: JoAnn.Milliken@ee.doe.gov

DOE Technology Development Manager: Valri Lightner
(202) 586-0937, fax: (202) 586-3237, e-mail: Valri.Lightner@ee.doe.gov

ANL Technical Advisor: Thomas Benjamin
(630) 252-1632, fax: (630) 252-4176, e-mail: Benjamin@cmt.anl.gov

Subcontractors: General Motors, Warren, MI; W.L. Gore and Associates, Inc., Elkton, MD

Objectives

- Demonstrate proofs of concept for the large-scale preparation of high performance electrodes for membrane electrode assemblies (MEAs) and assess electrode and MEA architecture against FreedomCAR cost targets.
- Design, build, and install equipment for a high-volume pilot plant capable of catalyzing tens of thousands of square meters of electrode material per year.
- Complete process development and qualification of the pilot plant.
- Benchmark MEAs fabricated at SwRI against commercially available products.
- Incorporate MEAs into two ”short stack” fuel cells built by General Motors and deliver to Argonne National Laboratory for testing and evaluation.

Approach

- Prepare MEAs using ultra-low load Pt and Pt-alloy deposition technologies that exceed DOE 2005 precious metal loading targets, and test the MEAs under hydrogen-air and reformate-air operating conditions.
- Determine the impact of large-scale catalyzation methods on MEA performance, if any, and develop approaches to minimize them.
- Establish *in situ* process control methods for catalyst deposition and demonstrate high-efficiency metal recovery approaches.
- Complete equipment shakedown and initiate regular operations at the pilot plant.
- Fabricate sufficient ultra-low load MEAs from catalyzed electrode material for incorporation into two short stacks.

Accomplishments

- Completed construction, acceptance testing, installation, and shakedown of pilot manufacturing system at SwRI.
- Catalyzed several thousand square feet of anode and cathode electrode materials at feed rates up to 40 feet per minute using the pilot system.
- Confirmed that materials manufactured using the pilot system exhibit similar performance to electrodes catalyzed on a laboratory scale.
- Developed robust, off-line methods for spot-checking loading and uniformity of catalyzed material.
- Fabricated more than fifty 800-cm^2 MEAs to date as part of the development effort for the GM stacks.

Future Directions

- Complete trials to optimize electrode catalyzation rates, catalyst utilization, material throughput, and production yield.
- Continue efforts to optimize catalysts for improved CO tolerance and long-term durability.
- Complete fabrication of hydrogen-air and reformate-air MEAs for GM stacks.
- Assemble, test, characterize, and deliver stacks to Argonne National Laboratory.

Introduction

Broad commercial acceptance of fuel cell technology for use in automotive applications is expected to require a fuel cell stack that meets FreedomCAR target costs of $35/kW by 2010. One of the most critical components impacting overall system performance and economics is the membrane electrode assembly (MEA). It is anticipated that the MEA must be available for less than $10/kW in order to meet these overall cost targets. Central to achieving these economics is the reduction of the amount of precious metal catalyst in the MEA, specifically platinum (Pt) and related alloys such as Platinum Ruthenium (Pt-Ru), without degrading power density or system longevity. To this end, a target of 0.2 g per rated kW or approximately 0.1 mg/cm^2 total platinum loading in the MEA has been established for 2010.

Work at Southwest Research Institute (SwRI) has been directed at addressing this issue through the development of large-area, high-throughput, vacuum-based coating technologies to reduce the overall precious metal content of finished electrodes. Specifically, "ultra-low" Pt and Pt-Ru catalyzed electrodes with loadings of 0.10 mg/cm^2 or less have been fabricated using state-of-the art electrode substrates procured from W.L. Gore and Associates. A pilot manufacturing facility has now been completed which has the capability to catalyze more than 100,000 square meters of electrode material per year on a two-shift basis – enough to allow the fabrication of MEAs for potentially several thousand fuel cell-powered vehicles.

Approach

The centerpiece of this project, a highly automated system for catalyzing fuel cell electrode materials, was installed in April; acceptance testing was completed in May 2002. A photograph of the system in operation is shown in Figure 1. In general, the system has performed to design specifications, with material feed rates up to 40 feet per minute having been demonstrated in recent trials at precious metal deposition rates of ~0.02 mg/cm^2/sec. Cycle time from loading of a roll of electrode material to catalyzation and removal is typically less than 2 hours. Additional features of note include the ability to account for and adjust to changes in the material such as splices, wrinkles, and edge shifts, and the incorporation of removable, recyclable shielding that should allow for the recovery of more than 90% of any unused catalyst.

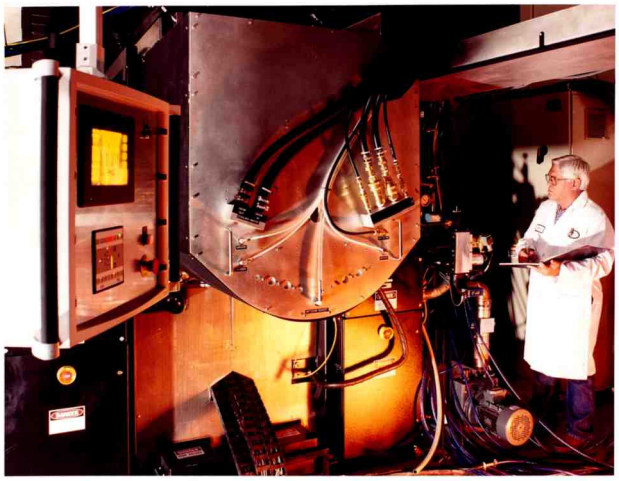

Figure 1. Photograph of Pilot System

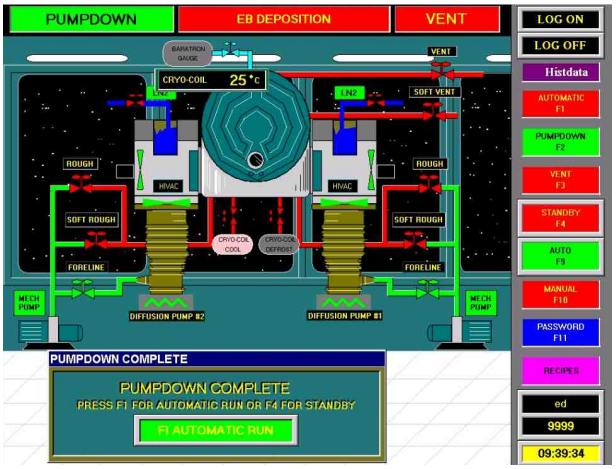

Figure 2. Sample Control Screen

One of the control screens developed for the system is illustrated in Figure 2. Notable data acquisition and control features include fully computerized, touch-screen control of the entire process sequence, including one-touch pump down, automated run, and vent cycles.

Data logging of all critical deposition and vacuum system parameters is available to ensure optimal run-to-run quality control, correlate material and system performance, and assess long term machine stability.

Several thousand linear feet of additional intermediate electrode material has been supplied by Gore over the past year for use with this system

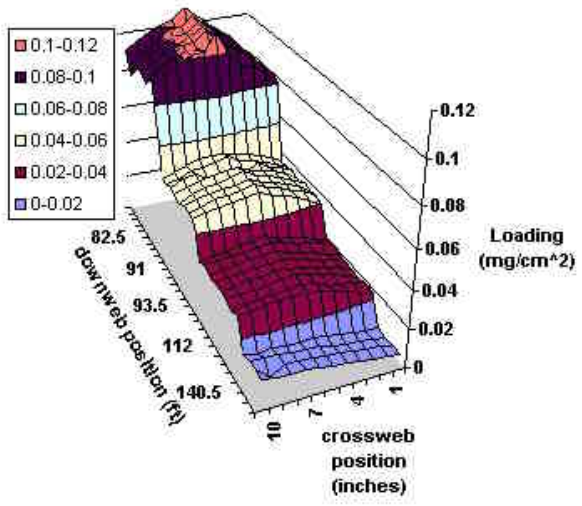

Figure 3. Catalyst Loading Contour Plot at Different Deposition and Feed Rates

during extensive production optimization trials. Pilot quantities of catalyzed electrode material, up to 500 linear feet per run, have been prepared and evaluated using standardized test methods. A hand-held spectrophotometer has also been implemented for rapid inspection of catalyst loading and uniformity (few seconds per point). A section of electrode material intentionally catalyzed at different platinum loadings from approximately 0.01 to 0.10 mg/cm^2 is presented in Figure 3. The catalyst uniformity is better than +/-10% both parallel and perpendicular to the machine direction.

Small scale (25-100 cm^2 active area) MEAs have been fabricated using electrode materials with the pilot system. Sample MEAs have been test evaluated in both hydrogen-air and simulated reformate-air with 10-50 ppm CO at H_2/air stoichiometries of 1.2/2.0 and 2.0/3.5 at pressures ranging from ambient to 30 psig. MEAs tested on hydrogen-air have produced beginning-of-life performance in the range of ~200 mA/cm^2 at 0.8 V and ~700 mA/cm^2 at 0.7 V at a total loading of ~0.1 mg Pt/cm^2. MEAs tested on reformate (40% H_2)-air have generated initial current densities in the range of up to ~150 mA/cm^2 at 0.8 V and ~500 mA/cm^2 at 0.7 V at a total loading of ~0.2 mg Pt/cm^2. Given the particularly good performance on neat H_2 at ultra-low loadings, it was agreed that two smaller stacks, ~10 kW each, optimized to run on neat hydrogen and

Figure 4. Photograph of a General Motors "Short" Stack that Will Utilize SwRI-Manufactured MEAs

reformate, respectively, would be constructed with MEAs fabricated at SwRI as the final deliverables for the project. Figure 4 is a photograph of a GM stack similar to the ones scheduled for construction.

Conclusions

The primary objective, construction and demonstration of a pilot-scale system for catalyzing ultra-low load electrodes for polymer electrolyte fuel cells, has been achieved. The system has nominally met major design targets for material feed rates and catalyst deposition rates. It is estimated that, in two-shift operation, the system is capable of catalyzing sufficient electrode material to fabricate stacks for as many as 10,000 vehicles. MEAs fabricated with electrodes produced by this system significantly exceed 2005 FreedomCAR targets for catalyst loading and approach the requirements set for 2010. Continued work is planned to further optimize material throughput, yield, and catalyst utilization on the pilot system. Additional efforts to evaluate the performance of SwRI-manufactured MEAs at higher CO concentrations and over longer durations are also anticipated.

IV.D.5 Integrated Manufacturing for Advanced Membrane Electrode Assemblies

Emory S. De Castro
De Nora N.A., E-TEK division
39 Veronica Ave
Somerset, NJ 08873
(732) 545-5100 ext 114, fax: (732) 545-5170, e-mail: emory.decastro.etek@denora.com

Mark G. Roelofs
DuPont Company
Chestnut Run
Wilmington, DE
(302) 695-7342, fax: (302) 695-2503, e-mail: mark.g.roelofs@usa.dupont.com

DOE Technology Development Managers:
Valri Lightner: (202) 586-0937, fax: (202) 586-3237, e-mail: Valri.Lightner@ee.doe.gov
JoAnn Milliken: (202) 586-2480, fax: (202) 586-9811, e-mail: JoAnn.Milliken@ee.doe.gov

ANL Technical Advisor: Thomas Benjamin
(630) 252-1632, fax: (630) 252-4176, e-mail: Benjamin@cmt.anl.gov

Subcontractors: DuPont Company, Wilmington, DE; Nuvera Fuel Cell, Cambridge, MA; Northeastern University, Boston, MA

Objectives

- Create improved cathode structures and catalysts for proton exchange membrane fuel cells (PEMFCs) at temperatures <100°C that allow a significant reduction of precious metal without loss in performance
- Discover and develop proton exchange membranes (PEMs) capable of extended fuel cell operation at higher temperatures of 120 to 150°C, at low relative humidity (RH), and without leachable components
- Incorporate the advances of the efforts described above with advanced MEA fabrication processes that are amenable to mass production

Approach

- Fabricate highly controlled gas diffusion layers through fine gradient machine coating methods; exploit a new structure-function approach to designing improved catalysts and catalyst alloys
- Investigate additives to extend the stable performance of Nafion® membranes to 120°C; create a new class of ionizable materials that enable proton transport in the absence of water (150°C operation)
- Develop new machine-based or ion beam coating methodologies to create very low loaded precious metal MEAs

Accomplishments

- Identified a preparation for platinum on carbon black catalyst that provides ~60% reduction in precious metal grams/kW compared to current commercial preparations
- Established “proof of principle” for catalyst structure-function approach

- Set up basis for constructing fine-gradient ELAT® materials
- Developed a new base material into a gas diffusion layer (GDL) with lower resistance and improved mass transport at high current density
- Synthesized and screened approximately twenty electrolyte and monomer compounds for high temperature membranes
- Identified several model liquid electrolytes with >100 mS/cm conductivity at 150°C and low RH
- Fabricated a candidate composite membrane with 60% increase in conductivity vs. Nafion® N117 at 120°C and low RH

Future Directions

- Further develop catalyst structure-function approach and implement to create designed catalysts with anticipated reduced metal loads
- Link ink morphology to GDL structure; establish relationship between GDL structure and FC performance; build fine gradient ELAT® with increased precious metal (PM) utilization
- Continue exploration of alternate polymeric backbones and acid groups (high temperature membrane)
- Create and test hypotheses as to required functionality and utilize these to narrow and focus the synthetic effort (high temperature membrane)
- Evaluate FC lifetime and performance of benchmark Nafion® and candidate membranes (high temperature membrane)

Introduction

A significant challenge for PEMFC technology is precious metal thrift and creating new ion exchange membranes that are capable of stable operation at temperatures exceeding 120°C and preferably 150°C. The greatest barrier to reduction of platinum metal in the MEA is due to the cathode half reaction. For membranes to operate at over 120°C, a new class of materials employing alternative proton transport mechanisms is necessary. Current platinum or alloy catalysts have a distribution of crystal facets, and some of these crystal planes exhibit higher activity for oxygen reduction. If one could selectively synthesize catalysts with a greater number of the desired planes, a more potent catalyst would result. However, advances in catalyst structure are not enough; the utilization of the catalyst and also proton and oxygen transport must improve to realize the full potential of the activity and ultimately reduce PM loading. Proton and oxygen transport may be improved through the realization of a fine gradient structure for the GDL. A satisfactory answer to these technical challenges would reduce the barrier to commercialization by reducing precious metal cost, allow a significant reduction in heat exchangers, and provide a vast simplification for systems operating with hydrogen derived from hydrocarbon sources.

Approach

A series of innovative catalyst preparation techniques has been identified. Each technique is surveyed, and the resulting catalyst is subjected to electrochemical and spectroscopic evaluation. Spectroscopic data are reintegrated in a sophisticated computer model that allows detailed bulk structural information to be derived. For this modeling, the methods are ranked according to the likelihood of selectively fabricating highly active crystal faces. Thus, the model provides a link to design catalysts based on a structure-function approach.

For the fine-gradient ELAT®, we first establish the relationship between ink formulation parameters and how they impact key architectural quantities such as pore size distribution and hydrophobicity. Next, the architectural quantities are linked to actual fuel cell test results. Finally, fine gradients of porosity and hydrophobicity are constructed using the relationship(s) previously established.

For high temperature membranes, three avenues are being pursued: a) synthesis of new ionomers, b) covalent modification of Nafion®, and c) polymer-inorganic composites. Some of the approaches aim to increase the attractive forces holding water within the membrane, enabling operation at low RH. Others seek to embody Brønstead bases as an alternative to water, which allow for proton mobility in the absence of water. This mechanism is exemplified by proton conductivity in e.g. H_3PO_4 or $CsHSO_4$, in which the protons hop and the protonated base need not move macroscopic distances.

Results

A summary of catalyst synthesis methods investigated for both activity and potential to control the crystal face population(s) is shown in Table 1. Of these, the methodology indicated as "Shows Promise" appears to provide a wide range of structures over only a moderately small range of tested parameters. Due to this unexpected result, additional efforts were directed to this method.

Catalyst	Pt on carbon	Alloys on carbon
Organic Method	XXX	XX
Controlled Environment	⊕	---
Simultaneous vs. Sequential	NA	XX
New Carbons	⊕	---
Temperature	⊕	---

Key	Symbol
Preliminary Evaluation	⊕
Shows Promise	XXX
Interesting Results	XX
No Potential	X
Not Evaluated to date	---
Not Applicable	NA

Table 1. Methods Evaluated to Control Crystal Face Population

Table 2 summarizes some preliminary results in testing these new platinum catalysts. Using our rapid catalyst screening protocol (70°C, 43 psig cathode, 36 psig anode), we record a reduction in precious metal usage of around 60% as measured by power.

Preparation Method	"High Efficiency Hydrogen" at 0.8V	"Reformate Target" at 0.75V
Commercial	4.25 g/kW	2.84 g/kW
Organic Method	1.76 g/kW	1.02 g/kW
Percent Reduction in PM	59%	64%

Table 2. Comparison of "Organic Method" Platinum on Carbon Black vs. Commercial Catalyst (cathode metal only)

In developing the fine-gradient ELAT®, one activity is incorporating new carbon cloth or paper materials as the support web for the microporous carbon black/catalyst coatings. Figure 1 shows the consequences of converting a new type of web to the ELAT® configuration. We were able to build an assembly with lower overall electrical resistances that can facilitate transport at high current density.

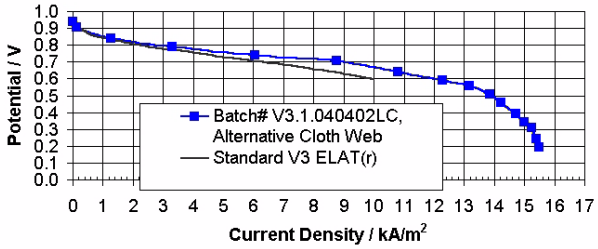

Figure 1. Evaluation of Alternative Web (Cathode/ Anode: 1.5 Bar A, 70°C; Anode hydrator T = Cathode hydrator T = Cell: 70°C)

An example of the process behind building a GDL is shown in the metrics of Figure 2. Here we are evaluating a 2 x 2 matrix of formulation (1 and 2) vs. coating method (A and B), and plotting the total solids deposited on the web versus the position of the layer. In addition to the differences in deposition rate listed here, most notable is the instability induced at the fifth position for Formulation 1, Coating method

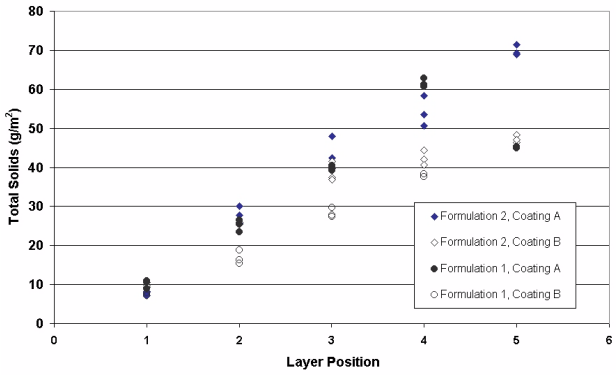

Figure 2. Comparison of Formulations and Coating Parameters

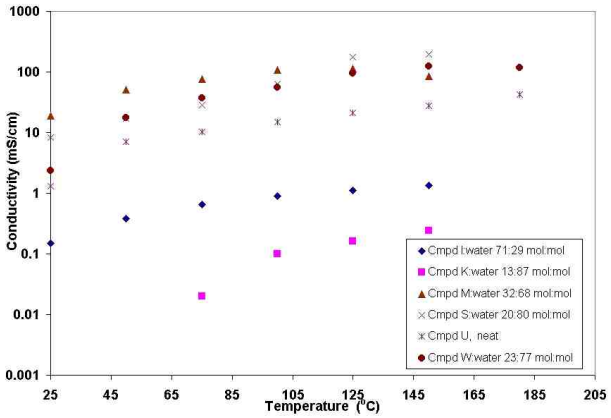

Figure 3. Conductivity vs. Temperature

A: instead of a linear increase in solids, we actually start to remove solids under these conditions. In addition to solids, we also measure through-plane conductivity, permeability, and numerous other characteristics as a function of the position in the gradient. The correlation of these characteristics to the formulation morphology is the goal of these experiments.

A series of model electrolyte compounds and monomers has been synthesized with the aim of understanding which functionalities can engender conductivity at low RH for high temperature membranes. The working hypothesis is that ionomers are in general less conductive than their constituent monomers, so that chemistries may be screened using model compounds prior to investment in polymer synthesis and membrane fabrication. A cell was constructed of quartz, ceramic, PTFE, and Pt materials, allowing measurement of the conductivity of 800 microliter liquid samples at temperatures up to 200°C. Conductivities of several liquid organic electrolyte model compounds are shown in Figure 3, with a few samples attaining 50 to 200 mS/cm at 150-180°C. The water contents indicated are the starting compositions and are chosen to correspond to significantly lower water contents (acid:water mole:mole) than is required by Nafion®. Though water vapor pressure was not explicitly controlled, the cell was not pressurized and the water vapor partial pressure was less than 1 atm. The maximum conductivity, followed by a decrease in conductivity at higher temperatures, observed for some samples is believed to be due to evaporation of water.

Compound U is one of the very few electrolytes investigated in which the neat liquid without added water generates appreciable conductivity. For comparison, the conductivity of Nafion® 117 membrane was measured as 7 mS/cm at 150°C and a water vapor partial pressure of 1.1 atm (23% RH).

The electrolytes investigated so far cover a range of aliphatic and aromatic compounds, fluorinated and non-fluorinated, with sulfonic and non-sulfonic acid groups. Our challenge now is to learn to incorporate these acid functionalities into ionomers without losing the conductivity as they are diluted and immobilized with polymer scaffolding.

Another potential method for achieving a high temperature membrane utilizes composites of ionomers with hydrophilic inorganic compounds. The desire is for the inorganic compounds to alter the microstructure of the ionomer, perhaps by holding open the ionic pores or by increasing the attractive force with which the water is held in the membrane. A further function of the filler is to decrease the creep of the ionomer and prolong membrane life. The most promising results have been obtained with an ionomer/inorganic composite membrane, where the conductivity at 120°C, 23% RH has been increased from ~5 mS/cm for N117 to ~9 mS/cm (Table 3). The goal resistance of 0.1 ohm cm^2 would, however, require 50 mS/cm, assuming a 50 micron thick membrane. Thus, we still need a much larger increase in conductivity to achieve very thin membranes.

Conclusions

Although quite early in our program, the use of the structure-function approach for catalyst design has yielded great improvements to the platinum on carbon black design. The further development of this methodology, when combined with the anticipated increase in performance of the fine-gradient ELAT®, should result in greatly enhanced cathode structures for normal temperature operation (up to 100°C).

For the high temperature membrane, achieving high conductivity at low relative humidity is one of the most challenging requirements. However, given that low resistance is the germane need, low conductivity may be ameliorated with very thin membranes. If such a compromise proves necessary, it will then place the onus back on achieving excellent puncture, creep, and fuel permeation properties. Our future path includes work to further increase conductivity and to incorporate the existing liquid electrolyte leads into ionomers without losing the conductivity as they are made into solid membranes.

Membrane	Conductivity (mS/cm)		
	@ 80°C, 95% RH	@ 80°C, 20% RH	@ 120°C, 23% RH
N117, sample 1	86	3.3	4.5
N117, sample 2	85	5.5	6.1
Candidate V, sample 1	89	5.8	10.0
Candidate V, sample 2	105	4.3	8.4

Table 3. Conductivities measured with AC-impedance, 4-point probe for N117 and a candidate composite membrane. Metered dry air and water are mixed in a vaporizer then fed to a pressurized flow cell in an oven. The 80°C, 95% RH data are for membranes which had been previously exposed to low RH. Freshly-boiled expanded membranes which have not been exposed to low RH give much higher conductivities of the order of 180 mS/cm @80°C, 95% RH.

IV.D.6 Development of High Temperature Membranes and Improved Cathode Catalysts

Dr. Shari Bugaj (Primary Contact)
UTC Fuel Cells
195 Governor's Highway
South Windsor, CT 06074
(860) 727-2808, fax: (860) 727-2750, e-mail: Shari.Bugaj@utcfuelcells.com

DOE Technology Development Manager: Valri Lightner
(202) 586-0937, fax: (202) 586-3237, e-mail: Valri.Lightner@ee.doe.gov

Main Subcontractors:
High Temperature Membrane
Virginia Polytechnic Institute and State University (Virginia Tech), Blacksburg, Virginia
Pennsylvania State University, University Park, Pennsylvania
Stanford Research Institute International, Menlo Park, California
IONOMEM, Marlborough, Connecticut
Princeton University, Princeton, New Jersey
Cathode Catalysts
Northeastern University, Boston, Massachusetts
University of South Carolina, Columbia, South Carolina
United Technologies Research Center, East Hartford, Connecticut
Case Western Reserve University, Cleveland, Ohio

Objectives

- Develop and demonstrate an advanced polymeric membrane able to operate at near ambient (1-1.5 atmospheres) pressure in the temperature range of 120~150^{o}C and able to meet DOE's program goals for performance.
- Develop and demonstrate improved high-concentration platinum (Pt) cathode catalysts that will enable the reduction of Pt loading to 0.05 milligrams per centimeter squared (mg/cm^2) and meet DOE's goals for performance.

Approach

- Phase 1: High Temperature Membranes (HTMs) and improved Pt catalysts will be synthesized, characterized and compared with issued specifications.
- Phase 2: Laboratory-scale catalyst-coated membranes (CCMs) will be fabricated, optimized and tested using the Phase 1 down-selected membranes and catalysts.
- Phase 3: Full-size CCMs with the down-selected and optimized HTMs and catalysts will be fabricated and tested in two individual multi-cell stacks.

Accomplishments

- This project was initiated during the first quarter of 2002. Eight out of the nine subcontractors have initiated membrane and catalyst synthesis. Technical accomplishments for the four months since the initiation are given below.
- At Virginia Tech., high yields (>80%) of 3,3'-disulfonate, 4,4'-dichlorodiphenylsulfone were obtained by sulfonating commercially available monomers. Films (>40,000 molecular weight) drawn from these co-monomers showed negligible degradation in boiling water and acceptable proton conductivity at room temperature in water.
- United Technologies Corporation Fuel Cells (UTCFC) has developed and applied a new and novel in-situ electrochemical technique to quantify hydrogen crossover in membranes.
- High-concentration (40 weight percent [wt%]) ternary Pt alloy samples prepared using the carbothermal technique have yielded surface area and activity values comparable to commercial Pt samples. Platinum/Carbon (Pt/C) prepared by pulse-electrodeposition showed superior surface area and activity when compared to direct current deposited Pt/C electrodes.

Future Directions

- Continue polymer synthesis and evaluation of the fabricated films per membrane screening specifications. Initiate the fabrication of initial promising candidates into CCMs.
- Continue evaluation of Pt catalysts being synthesized using the colloidal sol, carbothermal and the electrodeposition techniques and compare results against catalyst screening specifications. Debug rotating disk electrode technique.

Introduction

Two main challenges in the PEMFC arena are the reduction of cathode Pt loading and development of membranes that can operate over 120^{o}C. Surmounting these two challenges will directly affect the cost, performance and the size of PEMFC stacks. On the HTM project, new polymeric materials with negligible thermal degradation and acceptable proton conductivity in the 120-150^{o}C range are required. On the improved catalyst project, a combination of higher activity catalysts and thinner catalyst layers is required to achieve the aggressive DOE performance targets.

Approach

To develop HTMs, UTCFC has teamed with research groups that possess competencies in the fields of polymer chemistry and engineering. The subcontractors on the HTM project are investigating modified Nafion® and new non-Nafion® based membrane systems (see Table 1). The subcontractors on the improved catalyst project and their individual approaches are given in Table 2.

Table 1. High Temperature Membrane Program Approach

Group	Principal Investigator	Approach
IONOMEM	Mr. Leonard Bonille	Hygroscopic solid ion conductor (e.g., zirconium phosphate, etc.) filled Nafion®
Penn State University	Prof. Digby Macdonald	Sulfones and sulfoxides of aromatic PPBP and aliphatic PVA. Covalent sulfonic acid bonded PEEK, PBI and PPBP
Princeton University	Prof. Andrew Bocarsly	Layered sulfonated Polystyrene/Fluoropolymer system
Stanford Research Institute	Dr. Susanna Ventura	Sulfonated PEEK-PBI-PAN
Virginia Tech	Prof. James McGrath	Sulfonated Poly(arylene ether sulfone)

Results

This project was initiated during the first quarter of 2002. Since then, all the subcontractors have hired appropriate personnel and initiated membrane/catalyst synthesis. A majority of the required processes are in place, and eight of the nine

Table 2. Advanced Cathode Catalyst Program Approach

Group	Principal Investigator	Approach
North Eastern University (NEU)	Prof. Sanjeev Mukerjee	Micellar Pt nano cluster synthesis, colloidal sol synthesis of binary Pt alloys
University of South Carolina (USC)	Prof. Branko Popov	Pulse electro-deposition of Pt and Pt alloys on Carbon [Pt and Pt-X, X=Fe, Ni, Co, Mn, Cu]
UTC Fuel Cells	Dr. Shari Bugaj	Carbothermal synthesis of ternary Pt alloys [Pt-Ir-X and Pt-Rh-X, [X=Ni, Co and V]]
Case Western Reserve University (CWRU)	Prof. Al Anderson	Quantum chemical modeling of Pt alloys and ORR
UT Research Center (UTRC)	Dr. Ned Cipollini	Reproducible and stack size CCM fabrication

subcontractors have reported preliminary results. At Case Western, the catalyst modeling work will start in September 2002, when Dr. Jerome Roques will start as a post doctoral associate. Some of the preliminary results obtained during the past four months are presented here.

High Temperature Membranes

To measure the gas crossover in HTMs, UTCFC developed a new in-situ electrochemical test. The test involves oxidizing the hydrogen that is transported across the membrane and measuring the limiting currents. Typical crossover limiting currents for two membranes of different thicknesses are depicted in Figure 1.

At VirginiaTech, 3,3'-disulfonate, 4,4'-dichlorodiphenylsulfone co-monomers with varying degrees of sulfonation were prepared from commercially available monomers. Nuclear magnetic resonance (NMR) spectroscopy was conducted on selected polymeric films to investigate the level of sulfonation. The NMR results showed that the sulfonation levels could be quantified very accurately. The water uptake of bi-phenol sulfone (BPSH) films increased with an increase in the degree of sulfonation. The membrane samples drawn from BPSH40 with 20, 30 and 40 K molecular

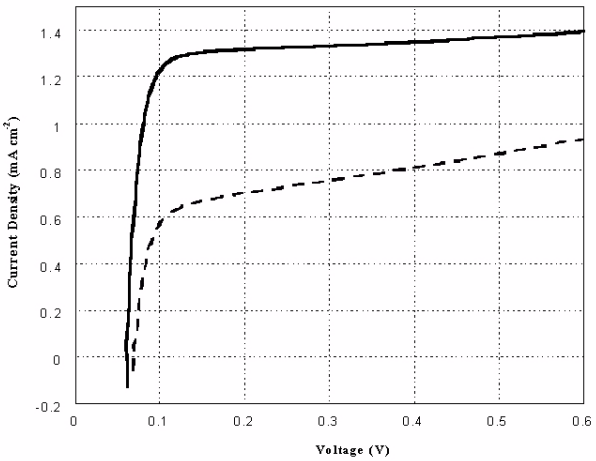

Figure 1. In-situ Limiting Hydrogen Crossover Currents for Two Membranes of Different Thicknesses

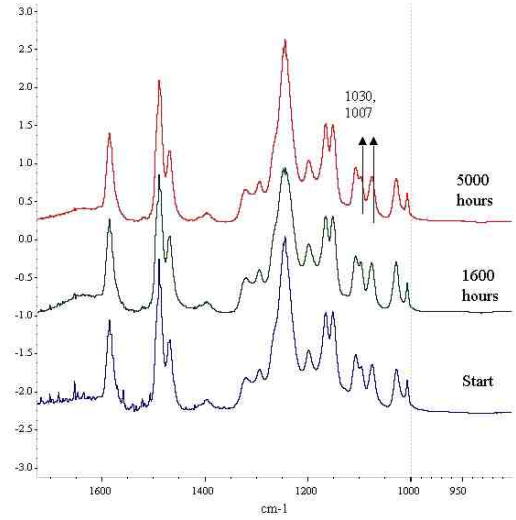

Figure 2. Influence of Hot Water Soxhlet Extraction on the FTIR of Sulfonated Poly(arylene ether) Copolymers BPSH40

weights showed proton conductivity values on the order of 0.09 S/cm. To evaluate the thermal degradation of the polymers, BPSH40 films were exposed to boiling water extractions using the Soxhlet technique in conjunction with Fourier transform infrared (FTIR) spectroscopy. The spectra were collected as a function of exposure time (see Figure 2). As seen from the figure, there is negligible change in the spectra up to 3,500 hours,

indicating that the hydrolytic stability of the films is excellent. No noticeable change in the nature or the ion exchange capacity of the membrane was noted during the Soxhlet experiment.

Penn State has modified electrochemical instrumentation that operates above 100°C. The accuracy of the instrumentation was confirmed by Nafion® 117 characterization. Princeton has initiated the synthesis of laminar membranes and anticipates initial characterization results on these materials over the next quarter. IONOMEM possesses a HTM that was shown to operate at 120°C prior to the start of this program. Since the initiation of this program, IONOMEM's efforts have been focused on electrode structure and catalyst modifications to establish a performance base.

Advanced Cathode Catalysts

UTCFC has modified the carbothermal synthesis process (U.S. Patent 4,677,092, US 4,806,515, US 5,013,618, US 4,880,711, US 4,373,014, etc.) to prepare 40 wt% ternary Pt alloy catalysts. Various high-concentration Pt catalyst systems were synthesized and the electrochemical surface area (ECA) and electrochemical activity values compared to commercially available catalysts (see Table 3). The UTCFC catalysts showed ECA and activity values comparable to the commercial catalysts. A rotating disk electrode technique for catalyst activity measurements has been developed and is currently being debugged at UTCFC.

Table 3. Preliminary ECA and Activity Data of Synthesized Pt Alloys

Catalysts	Catalysts ECA (m^2/Pt)	Catalyst Activity (A/gPt)
Commercial 50% Pt/C	98	25.1
Comercial 50% PTFE/C alloy	63	37.7
40% PT/Carbon C	110	27
40% $Pt_{50}Ir_{23}Co_{25}$	75/62	33
40% $Pt_{50}Ir_{23}Ni_{25}$	60	23

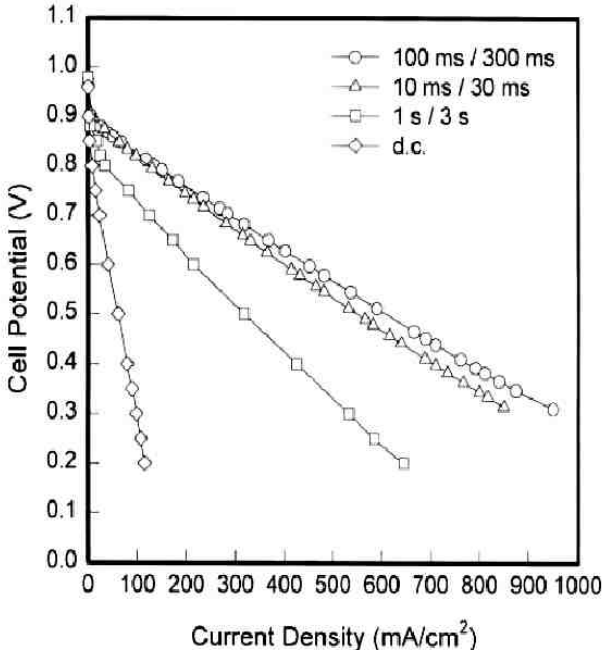

Figure 3. Polarization Curves at 50 milliamps/cm^2 and Duty Cycle of 0.25

At the University of South Carolina, Pt/C electrodes were fabricated by using direct current (DC) and pulse current electrodeposition methods. With the use of current pulses rather than DC, a higher deposition current density could be used and Pt deposits with a higher surface area were possible. Figure 3 compares the polarization performance of electrodes prepared by pulse electrodeposition (current density=50 mA/cm^2 and duty cycle=0.25) and DC deposition. Electrodes fabricated under pulse deposition conditions display better performance than the DC-plated electrode. The best performance is obtained when the ON time is 100 ms and OFF time is 300 ms.

At NEU, a series of electrocatalysts were synthesized based on classical colloidal sol synthesis techniques. These included platinum nickel/carbon (PtNi/C), platinum chromium/carbon (PtCr/C), and platinum cobalt/carbon (PtCo/C) together with the control Pt/C. All of the above electrocatalysts were prepared with 20% metal loading on carbon support (Vulcan XC-72, Cabot Corp). Ohmic corrected Tafel

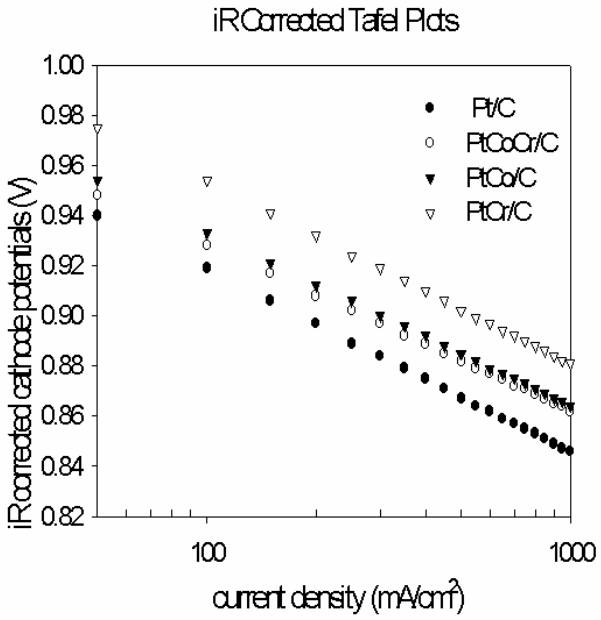

Figure 4. Ohmic Corrected Tafel Plots for Oxygen Reduction on Pt and Pt Alloy Electrocatalysts Prepared at Northeastern (note that PtCr/C is a system being considered only for ORR fundamentals; it will not be under consideration for down-selection)

plots for PtCr/C, PtCo/C, PtCoCr/C and PtNi/C are shown in Figure 4. As seen from the figure, the alloy catalysts are inherently more active than the Pt/C control. The data shows a lowering of the overpotential for oxygen reduction by up to 50 millivolts. At a potential of 0.9 volts, this translates to an eight-fold enhancement in oxidation-reduction reaction (ORR) activity. Stability and surface analysis of the Pt alloys was also performed using x-ray techniques.

Conclusions

The project is in its early stages and processes are in place for making progress. Preliminary results show that the HTM team is ramping up by initiating polymer synthesis processes and also by modifying instrumentation to perform high temperature measurements. On the advanced catalyst program, Pt and Pt alloys prepared using the colloidal sol, carbothermal and pulse electrodeposition processes are being characterized and compared with commercial Pt catalysts.

References

1. S. Kocha, P.Plasse, L.Onishi, D. Wheeler, J. Bett, AIChE Spring Meeting Proceedings- Fuel Cell Technology: Opportunities and Challenges, March 10-14, 2002, New Orleans.

IV.D.7 High-Temperature Membranes

Thomas A. Zawodzinski (Primary Contact), Hayley Every
Department of Chemical Engineering
Case Western Reserve University
Cleveland, OH 44106
(216) 368-5547, fax: (216) 368-3016, e-mail: taz5@po.cwru.edu

Michael Eikerling, Lawrence Pratt, Antonio Redondo, Tom Springer, Judith Valerio, Francisco Uribe, Michael Hickner and Tommy Rockward
Los Alamos National Laboratory
Electronic and Electrochemical Materials and Device Research Group
Los Alamos, NM 87545

DOE Technology Development Managers:
JoAnn Milliken: (202) 586-2480, fax: (202) 586-9811, e-mail: JoAnn.Milliken@ee.doe.gov
Nancy Garland: (202) 586-5673, fax: (202) 586-9811, e-mail: Nancy.Garland@ee.doe.gov

Objectives

- To develop new membranes and membrane electrode assemblies (MEAs) for operation at temperatures substantially in excess of 120°C

Approach

- Simultaneously carry out R&D on:
  - Physical chemistry of polymer electrolytes
  - New polymeric electrolytes
  - New approaches to proton transport in polymer electrolytes
  - Development of MEAs based on new polymer electrolytes

Accomplishments

Physical Chemistry

- Computational studies revealed key intermediate states in proton transfer processes; showed that water plays a role in 'bridging' and organizing acid groups to facilitate proton transfer

New Membranes

- Synthesized new polymers with higher acidity
- Developed several strategies targeting 'water replacements'

Catalyst-Coated Membranes (CCMs)/Electrodes

- Successfully fabricated MEAs for one class of new membrane materials; achieved performance comparable to that of Nafion-based MEAs

Industrial and Other Collaborative Interactions

- Worked directly with several university partners in developing and testing high-temperature membranes
- Assisted DOE industry partners in CCM development for high-temperature membranes

- Developed draft Roadmap for High Temperature Polymer Membranes
- High-Temperature Polymer Membrane Working Group (HTPMWG) was expanded and strengthened through several meetings

Future Directions

- Perform more extensive computational studies on novel systems
- Continue to develop methods for screening new membrane concepts at a higher rate; test new electrolytes in fuel cells on a 4 month cycle starting in the fall of 2002
- Expand initial tests on enhancing electrode performance; develop capability for probing oxidation reduction reaction (ORR) at temperature ex situ; develop understanding of interactions at buried interfaces within electrodes
  - Develop reliable CCM fabrication approaches
  - Continue to develop means for scale-up of polymers, film-making and CCM production to modest scale
- Industry and Other Collaborations
  - Continue to make industrial and academic contacts from Case Western Reserve University (CWRU) to enable technology transfer and dissemination of ideas
  - Organize the HTMWG (streamline funding mechanism, improve meeting scheduling); evolve toward a discussion group format, idea exchange

---

Introduction

The need to operate at temperatures exceeding 100°C presents difficult new challenges for the polymer electrolytes used in fuel cells. This difficulty stems from the decrease in water content of the polymer electrolytes in the desired temperature range. There is a need for detailed understanding of the impact of poor or zero hydration on membrane and electrode processes in the fuel cell. Water plays a key facilitating role in proton transport; thus, lower water content leads to lower conductivity. Lack of water also has important negative consequences for electrode behavior.

Approach

At this point, we do not know which of several approaches is most promising. Thus, our membrane development efforts involve (1) a full-fledged effort to explore approaches involving polymer synthesis and development, as well as implementation of new "carrier" media to replace the function of water in Nafion, and (2) a study of proton transfer dynamics. We are using theoretical approaches to explore specific possibilities for new acid group types or for acid-base interactions that could lead to progress in proton transfer media. We are also working to establish better understanding of the energetics of proton transfer to inform synthetic efforts. We also are working to incorporate new polymers in fuel cells by developing catalyst-coated membranes from the new materials. Finally, we have assisted DOE in setting up a range of polymer electrolyte development efforts, involving several universities and with significant industrial input.

Results

Physical Chemistry

As a starting point for our efforts, proton solvation and transfer in water-containing polymer electrolytes will provide some clues on critical steps in the approach. We are studying the energetics and dynamics of these processes. The tools we develop allow us to compare strengths of various target acids and assess the efficacy of water 'replacements.' We continue to expand the range of acid types studied as hydrates using density functional computational methods. These studies give us insight into the relative importance of solvation and dissociation

processes for various highly delocalized anions. The most interesting work this year used a sophisticated *ab initio*/molecular dynamics method to identify some surprising aspects of the proton transport dynamics. Specifically, we found that sidechain-to-sidechain hopping of protons could occur, albeit with the 'cooperation' of certain water configurations bridging between sidechain groups. This finding is highly suggestive regarding possible water replacements and their structural requirements for facilitating proton transport.

Additional work is underway to use computational methods to (i) tailor bases to mimic water, perhaps using substituted imidazoles or other proton carriers; (ii) understand proton transport in phosphoric acid/basic polymer systems; and (iii) augment other experiments on new polymers and additives of various types.

New Membranes

Three classes of membrane materials are presently in preparation and testing. These are (i) polymers and inorganic materials with controlled pore size to be modified with acid groups lining pores, (ii) polymeric systems with intrinsically stronger acid groups, and (iii) polymer systems swollen or imbibed with tailored proton acceptors. These are useful both intrinsically and as test or model systems. At least two more types of materials are 'on the drawing board.' Details of our ideas and approaches will be provided as the materials are tested later this year.

CCMs

We are forming CCMs from new polymers, often with radically different properties than those to which we are accustomed. Observed difficulties in achieving good performance with new CCMs stem from processes occurring at several different length scales:

- Macro scale (CCM level): adhesion phenomena, polymer segregation in catalyst layer, mechanical properties of electrode and membrane
- Meso scale (agglomerate level): mass transport of gases, continuous proton and electron conducting pathways
- Nano scale (local level): proton accessibility to site, electrocatalysis, polymer adsorption, polymer mobility

We have successfully catalyzed the Virginia Tech membranes and obtained performance comparable to that obtained with Nafion membranes of comparable thickness. Results are shown in Figures 1 and 2. The importance of these results lies in our ability to overcome difficulties inherent in catalyzing many of the emerging new membranes. Achieving good performance required some treatment of the CCM under operating conditions in the cell. The cells thus prepared appear to be robust in lifetests over hundreds of hours.

A more fundamental problem that arises in the high temperature regime is the necessity of good proton accessibility to electrodes. Many new polymer types proposed involve a sulfonated aromatic polymer. Microelectrode studies of the ORR on such materials indicate a significant loss of activity with decreasing water content in the polymer, far exceeding that observed with Nafion. This is likely due to the lower acidity of the aromatic sulfonates compared with that of the perfluorinated material. Our best results to date have been obtained using Nafion as the ionomer in the cathode catalyst layer.

We are actively studying the impact of the range of environments local and corresponding different

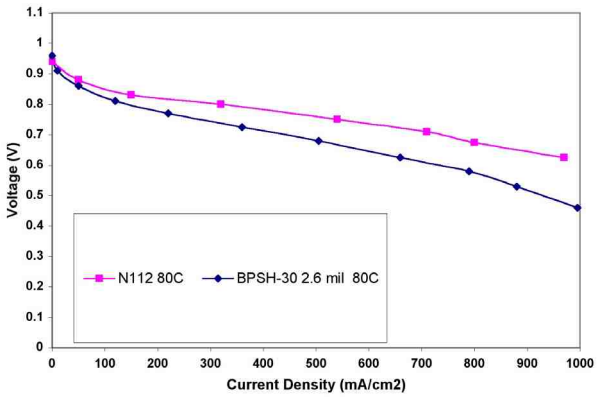

Figure 1. Polarization curves showing comparison of performance at 80°C of CCMs prepared from Nafion 112 and biphenyl sulfone (BPSH-30, 2.6 mil thick) membranes. Catalyst loading: 0.2 mg/cm^2 Pt anode, 0.4 mg/cm^2 cathode.

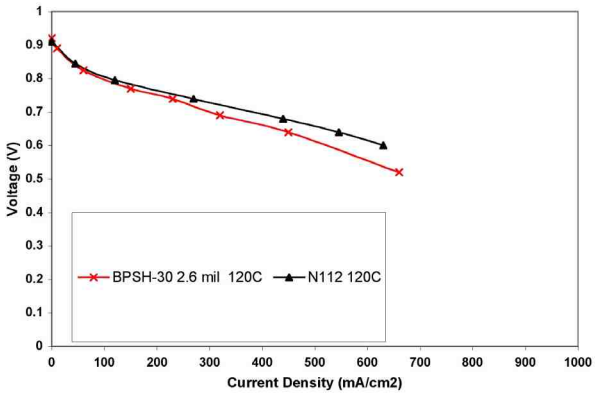

Figure 2. Polarization curves showing comparison of performance at 120°C of CCMs prepared from Nafion 112 and BPSH-30 (2.6 mil thick) membranes. Catalyst loading: 0.2 mg/cm^2 Pt anode, 0.4 mg/cm^2 cathode.

degrees of proton access to surface. Given the constrained dynamics of the polymer system, acid access to the catalyst surface is a key issue. Various additives, such as low molecular weight acids, have been and are being used to augment catalyst layer acidity and the mobility of acidic groups. Results to date have been inconclusive.

Industrial and Other Collaborative Interactions

We are engaged in a series of collaborative efforts with industry, national laboratories, and universities to facilitate efforts to achieve the targets for high-temperature polymer membranes. We have organized the High-Temperature Polymer Membrane Working Group, which has met four times to date. Bi-annual meetings allow us to assess progress and to communicate issues and needs to the high-temperature membrane community at large.

Conclusions

The development of new polymer electrolytes for operation at elevated temperature is under way. However, this is a long-term project. Replacement of water is the most difficult problem, but adequate stability and cathode activity are not trivial objectives to achieve. We have developed several different approaches to address this problem. Fundamental work, including computational and experimental studies of new acid-functionalized materials, can provide useful insights into the conduction process to guide synthetic efforts. The first polymers geared for temperatures in excess of 100°C are emerging, and testing is showing that, although promising, there are definite shortcomings. Work on making viable new materials continues.

IV.D.8 Bacterial Cellulose Membranes

Hugh O'Neill (Primary Contact), Barbara R. Evans, and Jonathan Woodward
Chemical Sciences Division, Oak Ridge National Laboratory
P.O. Box 2008
Oak Ridge, TN 37831-6194
(865) 574-5004, fax: (865) 574-1275, e-mail: oneillhm@ornl.gov

DOE Technology Development Managers:
JoAnn Milliken: (202) 586-2480, fax: (202) 586-9811, e-mail:JoAnn.Milliken@ee.doe.gov
Nancy Garland: (202) 586-5673, fax: (202) 586-9811, e-mail: Nancy.Garland@ee.doe.gov

ORNL Technical Advisor: David Stinton
(865) 574-4556, fax: (865) 241-0411, e-mail: stintonp@ornl.gov

Objectives

- To synthesize a low cost proton conductive membrane from bacterial cellulose for polymer electrolyte membrane (PEM) fuel cells.
  - This membrane must be stable at temperatures greater than 120^{o}C.
  - It must maintain the conditions conducive to proton conductance from the anode to the cathode through the polymeric medium, while operating at high temperatures. The area specific resistance must be no greater than 0.1 ohm-cm^2.

Approach

- Bacterial cellulose has several properties that have been identified as useful for PEM fuel cell development, including thermal stability and low hydrogen crossover characteristics.
- Bacterial cellulose membranes were modified with acid groups to produce a proton conductive membrane without compromising the structure of the cellulose membrane.

Accomplishments

- Different strategies to confer ion-exchange properties on bacterial cellulose were investigated. The synthesis of a cellulose phosphate membrane was the most successful.
- Several properties of the cellulose phosphate membrane were evaluated, including hydrogen crossover, ion-exchange capacity and thermal stability.

Future Directions

- Complete the characterization of phosphate membranes, especially the determination of the proton conductivity of the membranes.
- Test the performance of ion-exchange membranes in a membrane electrode assembly (MEA).
- Revisit and evaluate other strategies for chemical modification of cellulose.
- Modify cellulose *in vivo* by using activated glucose monomers.

Introduction

Bacterial cellulose is produced by *Gluconoacetobacter sp*. bacteria during growth on carbohydrate sources. Nascent cellulose strands, synthesized by the bacteria, are secreted and form layers at the air-liquid interface (Figure 1A, 1B). This network of cellulose fibrils resembles a sponge and is called a pellicule. After cleaning to remove cellular debris, the pellicule typically contains greater than 99% H_2O, the remainder being cellulose. On drying the pellicules to remove water, the layers of cellulose collapse on top of each other to produce a very thin membrane (< 50 μm thick).

Of particular interest to the DOE fuel cell program is the development of thermostable membranes that will facilitate the transfer of protons from the anode to the cathode during operation of a PEM fuel cell at high temperatures (>120^{o}C). At higher operating temperatures, the electrode kinetics is improved, resistance to poisoning by carbon monoxide is increased, and the catalyst cost is minimized. In addition, higher operating temperatures would facilitate the thermal management of the system and stack.

Bacterial cellulose has several unique properties that potentially make it a valuable material for the development of PEM fuel cells (Reference 1): (1) it is an inexpensive and non-toxic natural resource; (2) it has good chemical and mechanical stability; (3) it is very hydrophilic; and (4) it doesn't re-swell after drying. Additionally, its thermal stability and gas crossover characteristics are superior to Nafion 117®, a material currently widely used as a proton conductive membrane in PEM fuel cells.

Approach

There is a wealth of data, both in the scientific and patent literature, on the chemical modification of plant cellulose. All of these methods are equally applicable to bacterial cellulose given that the two types of cellulose are chemically identical. However, it is the physical structure of bacterial cellulose membranes that make them a potential material for PEM fuel cells. Therefore, the aim is to modify bacterial cellulose pellicules in a manner that retains the structure of the cellulose and does not compromise the physical properties, such as thermal stability, gas crossover characteristics, and resistance to re-swelling after drying.

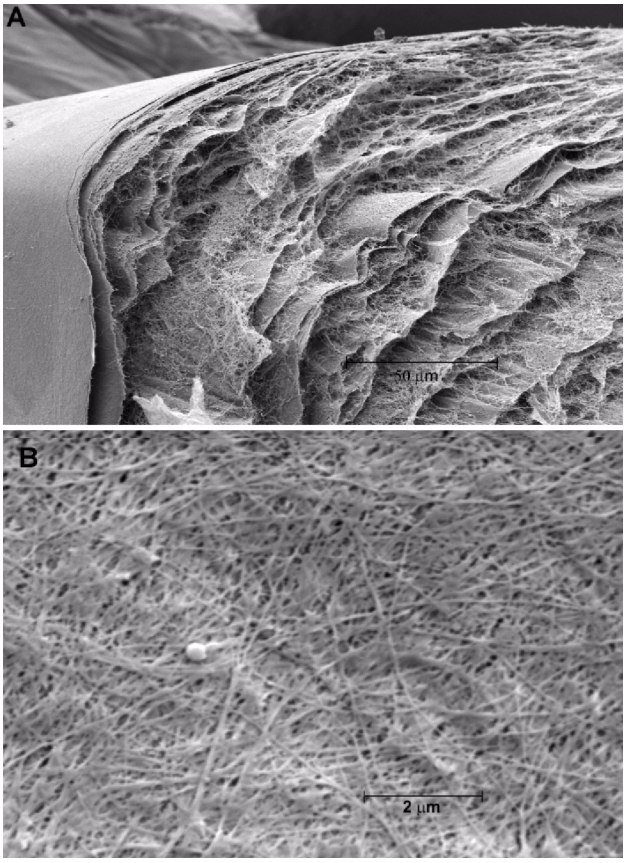

Figure 1. SEM Micrographs of Freeze Dried Bacterial Cellulose (A: transverse section, B: top view)

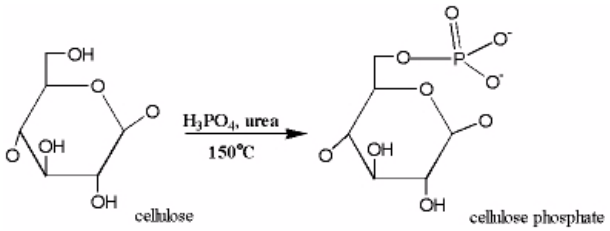

Figure 2. Synthesis of Cellulose Phosphate

Results

Several different strategies were employed to modify bacterial cellulose with ion-exchange groups. Of the methods attempted, modification of native bacterial cellulose with phosphate groups was the most successful (Figure 2). The properties of the

Membrane Characteristics		Native Cellulose	Cellulose Phosphate	Nafion 117®
Physical Properties	Dry membrane thickness (mm)	0.010	0.023	0.199
	Wet membrane thickness (mm)	0.032	0.081	0.225
	H_2O content / g dry membrane (g/g)[1]	3.47	3.16	0.31
	Thermal stability (^oC)	130	245	<90
	Ion exchange capacity (mequiv/g)	0	1.3	0.9
	H_2 crossover (nmol.mil/h.cm^2.atm)[2]	n.d.	267.2	2039.4
Mechanical stability	Resistance to crease/crack: dry	Yes	No	Yes
	hydrated	Yes	Yes	Yes
	Resistance to tearing: dry	No	No	Yes
	hydrated	Yes	Yes	Yes
	Resistance to gas pressure (dry)	n.d.	30 psi	>50 psi
Chemical stability	Acid stability (% weight loss)[3]	12	39	2.5

Table 1. Comparison of the Properties of Cellulose Phosphate with Native Bacterial Cellulose and Nafion 117®

native and modified membrane compared with Nafion 117® are presented in Table 1.

Thermogravimetric analysis of cellulose phosphate in an oxygen atmosphere indicated that it started to degrade at 245°C, compared to less than 90°C for Nafion 117®. This marked increase in the thermal stability of cellulose phosphate over native cellulose was not unexpected given that this material was first developed as a flame retardant. Cellulose phosphate has only 13% of the H_2 permeability of Nafion. Unlike Nafion, cellulose phosphate is prone to swelling in H_2O. However, at temperatures greater than 120^{o}C this may not pose a problem during operation of the fuel cell. The density of ion-exchange groups available for proton transport is similar in both materials. The superior mechanical properties of Nafion are most probably due to the difference in thickness between the materials.

The acid stability of the cellulose phosphate membrane was determined at 95^{o}C in 1N sulfuric acid. After 45 hours cellulose phosphate lost 39% of its original weight. This increase in sensitivity to acid attack is most probably an artifact of the reaction conditions employed in the synthesis. Modifications on the reaction procedure will be investigated to minimize this unwanted side reaction.

Conclusions

Several properties of cellulose phosphate have been evaluated. The material has good thermal stability and low hydrogen crossover, two requirements that are important to meet DOE fuel cell program targets. Further characterization of the material is required, especially the determination of proton conductivity. In addition, testing of the material in an MEA will allow the effect of acid stability and swelling properties of cellulose phosphate be evaluated under typical PEM fuel cell operating conditions.

References

1. O'Neill, H., Evans, B.R., and Woodward, J. (2001) in Fuels Cells for Transportation Annual Progress Report pp 141-145

Publications/ Presentations

1. Evans, B.R., O'Neill, H., Malyvanh, V.P., Woodward, J. "Palladium-bacterial cellulose membranes for fuel cells" Biosensors and Bioelectronics, submitted

2. O'Neill, H., Evans, B.R., and Woodward, J. (2002) "Bacterial Cellulose in Energy Conversion Applications" A poster presentation at the 24th Symposium on Biotechnology for Fuels and Chemicals, April 28th to May 1st, Gatlinburg, TN.

3. O'Neill, H., Evans, B.R., and Woodward, J. (2002) "Micro-fuel cell development based on bacterial cellulose" An oral presentation at the 14th World Hydrogen Conference, June 9th- 13th, Montréal, Canada.

Special Recognitions & Awards/Patents Issued

1. Evans, B.R., O'Neill, H., Malyvanh, V.P., and Woodward, J. (2001) "Metallization of bacterial cellulose for electronic and electrical devices" Patent Pending ID 0869, S-96, 631

2. O'Neill, H., Evans, B.R., and Woodward, J. (2002) "Synthesis of a novel ion-exchange/ proton conductive membrane" Invention disclosure, submitted ID 1099, S-99, 279

IV.D.9 Nano-particulate Porous Oxide Electrolyte Membranes (POEMs) as Proton Exchange Membranes

M. Isabel Tejedor, Marc A. Anderson, and Walt Zeltner
Environmental Chemistry and Technology Program, University of Wisconsin
Room 109, 660 North Park Street, Madison, WI 53706
(608) 262-2674, fax:(608) 262-0454, e-mail: nanopor@facstaff.wisc.edu

Mark A. Janney and James O. Kiggans
Metals and Ceramics Division, Oak Ridge National Laboratory
P.O. Box 2008, MS 6087, Oak Ridge, TN 37831-6087
(865) 574-8863, fax:(865) 574-8271, e-mail: kigganssjo@ornl.gov

DOE Technology Development Manager: JoAnn Milliken
(202) 586-2480, fax: (202) 586-9811, e-mail: JoAnn.Milliken@ee.doe.gov

ORNL Technical Advisor: David Stinton
(865) 574-4556, fax: (865) 241-0411, e-mail: stintondp@ornl.gov

ANL Technical Advisor: Thomas Benjamin
(630) 252-1632, fax: (630) 252-4176, e-mail: benjamin@cmt.anl.gov

Objectives

- Develop microporous inorganic oxide-based membranes of TiO_2 with high proton conductivity that can operate at above 100°C with minimal water management problems.
- Develop processes to fabricate porous nickel or graphite paper electrodes that support the membrane.
- Demonstrate fuel cell behavior in porous oxide electrolyte membrane- (POEM-) based membrane electrode assemblies (MEAs).

Approach

- Phase 1: (a) Determine conditions under which nanoparticle sols of candidate oxides yield microporous gels; (b) Measure proton conductivities of these gels as a function of temperature and relative humidity; (c) Chemically adsorb anionic or cationic functional groups onto oxide particles contained in xerogels or membranes in order to enhance proton conductivity.
- Phase 2: (a) Develop methods for depositing platinum on asymmetric mesoporous electrodes; (b) Deposit crack-free films of POEMs on mesoporous electrodes; (c) Characterize permeabilities of H_2 and O_2 through the resulting supported membranes under desired conditions of relative humidity and temperature; (d) Fabricate and test an entire inorganic MEA containing a POEM deposited on mesoporous electrodes.

Accomplishments

- Demonstrated proton conductivity of 0.022 S/cm in POEMs (membranes <1 μm thick) at temperatures up to 135^{o}C at a relative humidity (RH) of 81%.
- Better defined the effects of pore size and pH on proton conductivity in POEMs.

- Collected initial data concerning open circuit potential and current-voltage relationships for an oxide-based anode/POEM configuration (i.e., 2/3 of an MEA). (Pt loading in anode = 0.003 mg/cm^2)

Future Directions

- Develop a better understanding of the relationships and interactions among the various layers in the MEA (particularly the cathode layer) and how they control the performance of the overall fuel cell system.
- Characterize and subsequently optimize the performance of fuel cells that contain POEMs.
- Develop testing techniques for measuring proton conductivity at temperatures approaching 150°C at ≥ 40% RH.
- Investigate POEMs using the nickel substrate as the support for the cathode instead of the anode in an inorganic MEA.
- Further develop graphite fiber paper supports as a potential substitute for nickel substrates.

Introduction

Nano-particulate porous oxide electrolyte membranes (POEMs) are being developed as a radical alternative to polymeric proton exchange membranes (PEMs) for fuel cells. These new membranes can operate at temperatures over 100°C, retain water at these elevated temperatures, and provide proton conductivities of the same order of magnitude as the presently employed Nafion membranes. In addition, inorganic membrane electrode assemblies (MEAs) that incorporate POEMs should reduce the cost of fuel cells by substantially reducing the amount of Pt catalyst required to operate the fuel cell, and by minimizing CO poisoning of the Pt and facilitating heat rejection when operating at elevated temperatures.

One constraint in using POEMs is that they must be supported on a structural substrate because the membranes are thin (≤ 500 nm), porous (~40 vol% void space), and brittle (an inherent property of ceramic membranes). The porous substrate provides both electrical conductivity and gas distribution. Because the POEM itself is composed of 5-10 nm particles, an intermediary sandwich layer (particle diameter 50 to 500 nm) is required to provide geometric compatibility.

These membranes are made of nanoparticle oxides, which represent hydrophilic, higher temperature alternatives to polymeric proton exchange membranes (PEMs). These membranes are supported on either tape cast porous nickel or porous graphite paper electrodes – to date, we have only examined the porous nickel supports.

Approach

The objective of this effort is to develop MEAs for H_2 fuel cells based on POEMs. These membranes are made of nanoparticle oxides such as TiO_2, SiO_2, ZrO_2, or Al_2O_3 that are hydrophilic and offer higher temperature stability and operation than polymeric PEMs. These membranes are supported on tape cast porous nickel.

The POEM MEA is a complex materials system, not just a collection of individual components. This oxide-based MEA (anode / membrane electrolyte (separator) / cathode) is a composite material that simultaneously performs a variety of operations. One cannot consider any particular aspect of this materials system in isolation; all functions must operate in concert with one another. The anode must conduct electrons and at the same time convert hydrogen gas to protons at one interface with the POEM. The POEM itself must conduct protons but not electrons, which would cause a short, while also preventing crossover of hydrogen and oxygen across the POEM. Lastly, the cathode must convert gaseous oxygen to O^{-2} ions that then combine, at the other interface with the POEM, with protons that have migrated through the POEM. This cathode reaction is

a four-electron-transfer reaction that is quite difficult to perform efficiently. More will be said about the cathode layer and reasons for improving its performance later in this report.

Results and Discussion

Membrane Development – pH Effects

Proton conductivity in fluid-filled, hydrophilic, mesoporous, inorganic membranes such as these POEMs derives from the movement of H^+ ions (1) by hopping along surface sites from particle to particle, (2) by migrating through the electrical double layer in the pores near the surface of the particles, or (3) by migrating through the bulk pore fluid. As shown in Figure 1, proton transport and the resulting conductivity drastically change with the pH at which the membrane is equilibrated. Note that "Nafion" type membranes are often soaked in strong acids to protonate their acid groups. In this regard POEMs are similar, although full protonation of the surfaces of these inorganic membranes may be reached at higher pH values than required for Nafion.

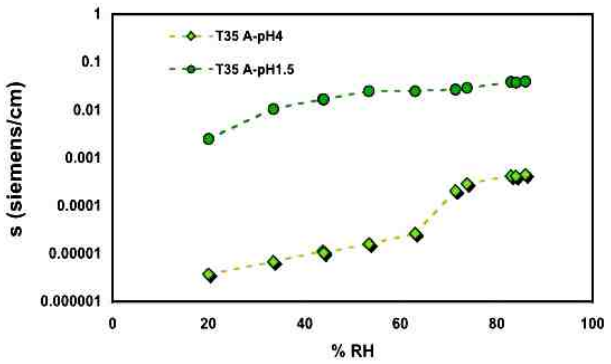

Figure 1. Dependence of Proton Conductivity on pH at 40°C

This behavior also greatly depends upon the nature of the oxide as shown in Figure 2. Note that at lower relative humidities, TiO_2/ZrO_2 and Al_2O_3 membranes have conductivities that are two to three orders of magnitude higher than SiO_2 even though the silica membranes are more acidic. The reason for this behavior is that these membranes were preequilibrated at pH 1.5. This pH is very close to the isoelectric pH (i.e., the pH at which the surface of the oxide is electrically neutral) of SiO_2, which is ≈ 2-3, but 4 to 7 pH units more acidic than the isoelectric

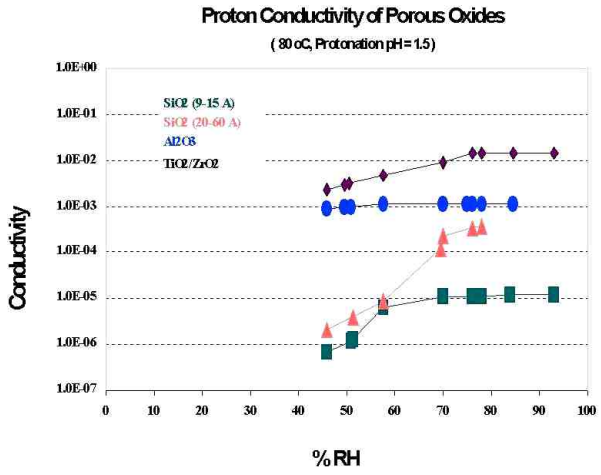

Figure 2. Proton Conductivity (in S/cm) for Various Oxides as a Function of Relative Humidity at 80°C [diamonds are TiO_2/ZrO_2, ovals are Al_2O_3, triangles are SiO_2 (20-60 A), squares are $Si0_2$ (9-15 A)]

pH values of TiO_2/ZrO_2 and Al_2O_3, respectively. As a result, the SiO_2 membranes are NOT highly protonated at pH 1.5 whereas the other two membranes have almost achieved maximum charging and therefore maximum proton conductivity.

Membrane Development – Pore Size Dependence

The conductivity of a particular membrane depends on the conditioning of the surfaces within the pores as well as the relative humidity. These two factors interact to determine how much water resides inside the pores. In the as-fired condition, the pore surfaces are poorly protonated. Conditioning the membrane material by exposing the membrane to an aqueous solution tends to increase the degree of protonation depending on the pH of the solution, as noted above. However, as can be seen in Figure 3, proton conductivity for TiO_2 at 40°C also depends upon pore size, increasing one order of magnitude at low RH values as pore diameter decreases from 35 to 25 Angstroms. We can lower the pore size in this membrane even further to ca. 15 Angstroms, which may further enhance its proton conductivity.

Initial Evaluation of an Inorganic MEA

Because these POEMs are not self-standing materials like organic polymer membranes such as

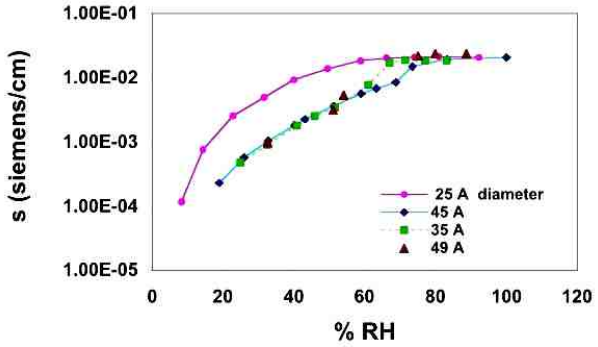

Figure 3. Dependence of Proton Conductivity on RH for Various Pore Size TiO_2 Membranes

Nafion, an MEA cannot be fabricated unless the membranes are cast on a rigid but porous support. Furthermore, the support must be electrically conducting and must already be coated with a porous catalyst layer before the membrane is cast. The resulting composite MEA will be activated by imbibing an acid solution into the MEA before it is used.

Enable Fuel Cell Corp. (Middleton, WI) fabricated a passive test chamber to evaluate the performance of the materials. For these initial room temperature tests, we fabricated 2/3 of an inorganic MEA (i.e., porous nickel support / nanoparticle TiO_2 membrane loaded with Pt catalyst to serve as one electrode / TiO_2 POEM). We used a carbon fabric loaded with Pt as the second electrode. We ran the inorganic MEA as either an anode or a cathode depending on the polarity of the test circuit. When hydrogen contacted the inorganic MEA (i.e., the MEA was operated as a working anode), we achieved open circuit voltages between 0.74 and 1.02 V. When the inorganic MEA was operated as a cathode, we obtained slightly lower voltages (0.76 – 0.88 V).

Unfortunately, it was difficult to seal the cell to prevent hydrogen leaks. In addition, it was difficult to test individual layers of the MEA system because the carbon fabric glued itself to the inorganic MEA and could not be detached without delaminating the MEA. To resolve these issues, we built a new test cell, as shown in Figure 4. As shown, the MEA is now sealed in a metal "O" ring using ceramic cement. This cell proved to be easily sealed without

Figure 4. Teflon Test Cell and the Inorganic MEA System

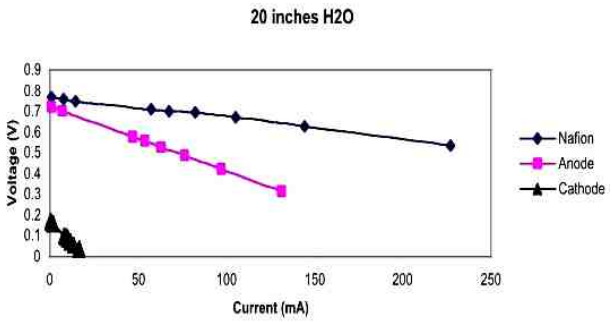

Figure 5. Current-Voltage Curves for the Inorganic MEA versus a Nafion System

hydrogen leaks and, furthermore, it could be readily disassembled. However, we still need to improve the ohmic contacts to the anode and cathode layers. We utilized copper wool to provide contacts in this apparatus. However, copper wool easily oxidizes when in contact with acids and does not provide a uniform contact with the electrodes.

Test Performance

Shown in Figure 5 are initial current-voltage curves for the 2/3 of an inorganic MEA system described above versus a similar Nafion-based system in tests at room temperature. As can be seen, the Nafion system performs somewhat better than our initial prototype when the inorganic MEA operates as an anode. When we invert the contacts so that the inorganic MEA operates as a cathode, the inorganic MEA system performs much worse. A positive side to this performance is that the Pt content of the inorganic MEA is 0.003 mg/cm^2.

Cathodes and the Total MEA

Shown in Figure 6 is a diagram of a nickel support and a Pt-loaded nanoparticulate oxide acting as a porous cathode. Organic-based fuel cell cathodes often have some Nafion added to improve proton conductivity but at the cost of electrical conductivity. However, we have the reverse problem – we have excellent proton conductivity in the inorganic cathode, but the oxides are electrical insulators. We need to boost the electrical conductivity of the cathode in order to fabricate a total inorganic MEA. This is a major objective of our future work.

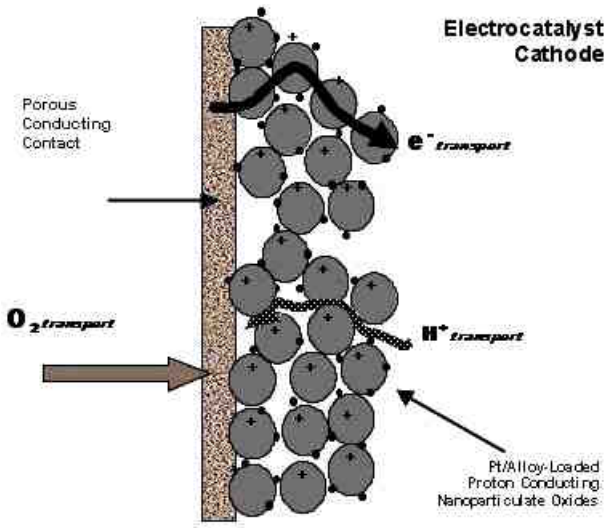

Figure 6. Diagram of an Inorganic Fuel Cell Cathode

Conclusions/Future Directions

- We have successfully fabricated and tested 2/3 of an inorganic MEA consisting of a porous nickel support, a nanoparticle TiO_2 membrane containing platinum catalyst that served as an effective anode, and a nanoporous TiO_2 porous oxide electrolyte membrane. A novel test cell was built to facilitate testing, but additional modifications are needed. Although the performance of this prototype inorganic MEA was not as good as a corresponding Nafion-based system at room temperature, the inorganic MEA required only a small amount of platinum to function. In order to prepare this inorganic MEA, a novel method had to be developed for applying a ceramic sandwich layer to the porous, electrically conducting nickel substrate. This method should be useful in other membrane applications.
- Efforts will continue to fabricate a full inorganic MEA and to test these systems at high temperatures. It appears that a functional inorganic MEA will require a cathode with higher electrical conductivity than available in our initial tests. In addition, we are attempting to develop a graphite fiber-based substrate having the requisite chemical compatibility with the PEM environment. As part of this development, POEM fuel cell assembly using standard, multilayer manufacturing technologies will be investigated.

FY 2002 Publications/Presentations

1. Results were presented at the national meeting of the American Institute of Chemical Engineers in New Orleans in March 2002.

IV.D.10 Low-Platinum Catalysts for Oxygen Reduction at PEMFC Cathodes

Karen Swider Lyons (Primary Contact), Gregory B. Cotten, and Jason A. Stanley
Naval Research Laboratory
Code 6171
4555 Overlook Ave, SW
Washington, DC 20375-5342
(202) 404-3314, fax: (202) 767-3321, e-mail: karen.lyons@nrl.navy.mil

Wojtek Dmowski and Takeshi Egami
Department of Materials Science and Engineering
University of Pennsylvania
3231Walnut Street
Philadelphia, PA 19104

DOE Technology Development Managers:
JoAnn Milliken: (202) 586-2480, fax: (202) 586-9811, e-mail: JoAnn.Milliken@ee.doe.gov
Nancy Garland: (202) 586-5673, fax: (202) 586-9811, e-mail: Nancy.Garland@ee.doe.gov

Objective

- Decrease the platinum content of the oxygen reduction reaction catalysts in fuel cell cathodes to meet the DOE 2010 precious-metal-loading goals of 0.2 g/rated kW.
- The new catalysts must cost less than $35/kW and be stable for at least 5000 hours.

Approach

- Low-platinum catalysts are prepared in combination with amorphous, hydrous transition-metal oxides. The catalysts are dispersed in carbon inks, and their electrocatalytic activity is screened in half-cell measurements.
- The physical properties of the catalysts are determined from thermal analysis, surface-area measurements, X-ray photoelectron spectroscopy, and transmission electron microscopy.
- Atomic pair-density function analysis of X-ray diffraction patterns is used to resolve the local structure of the catalysts from 0.15 to 2 nanometers (nm).
- Catalyst performance is confirmed by testing in fuel cells in collaboration with Los Alamos National Laboratory (LANL).

Accomplishments

- Half-cell measurements on catalysts of a Pt-doped iron-oxide phase have approximately 20 times the activity of the standard 10 weight % Pt on Vulcan carbon.
- Pair-density function analysis of X-ray diffraction patterns shows that active iron oxide (FeO_x) catalysts are disordered at the nanoscale by the platinum and also have micropores, while inactive catalysts do not share these features.
- Platinum supported on niobium oxide phases also exhibits high activity for oxygen reduction, despite a 50 to 150 fold decrease in platinum compared to the standard 10 weight % platinum on Vulcan carbon.
- The Pt-loading goals for the DOE 2008 program will be met if the half-cell performance of the new catalysts is matched in fuel cell measurements and the catalysts prove to be stable.

Future Directions

- Correlate the half-cell catalysis results to fuel cell performance.
- Improve corrosion resistance of catalysts.
- Improve activity and test stability of platinum-niobium oxide catalysts.
- Develop Pt-free catalysts by using transition-metal oxide mixtures that mimic Pt performance.
- Develop fuel-cell testing capabilities at the Naval Research Laboratory (NRL).

Introduction

State-of-the-art proton exchange membrane fuel cells (PEMFCs) contain high loadings of Pt, making the fuel cells costly and subject to fluctuations in the market availability of the noble metal. The cost of the fuel cells and imports of noble metals can be drastically reduced by using little or no Pt in fuel cell cathodes. This would improve the commercialization potential of fuel cells.

The catalytic activity of the oxygen reduction reaction (ORR) at the fuel cell cathode is known to be relatively slow, presumably because it is a 4-electron (e^-) mechanism:

$$O_2 + 4H^+ + 4e^- = 2\ H_2O$$

*Note: O_2 = Oxygen gas, H^+ = proton, H_2O = water

The cathode must be catalytically active, and the catalyst site must have a supply of oxygen, protons, and electrons, and must be able to transport away water. The reaction above becomes limited when the transport of any of these four species is slow.

We are designing new low-Pt electrocatalysts for oxygen reduction at PEMFC cathodes. Catalysts are targeted based on their ability to transport the following species: (1) molecular oxygen, (2) protons, (3) electrons, and (4) water. We have selected "amorphous" hydrous oxides with low amounts of platinum to fulfill these transport criteria. All catalysts are transition-metal oxide based, because hydrous transition-metal oxides are good proton and water conductors. Oxides are also less prone to poisoning (electro-chemical activity degradation) than metals, and some mixed-oxide catalysts also have the ability to mimic Pt. Some oxide catalysts may also be resistant to dissolving under the highly corrosive conditions at the PEMFC cathode.

Although the catalysts are termed amorphous, they can have nanoscale order in their atomic structures that can have a significant bearing on their activity and transport properties. These nanoscale structural properties are not easily discerned with conventional materials science tools, but can be elucidated using an emerging technique: atomic pair-density function analysis of X-ray diffraction (PDF-XRD).[1,2]

We analyzed the physical and structural properties of hydrous oxide materials having high ORR activity to determine the factors leading to high-performance PEMFC cathode catalysts. Last year, we reported 20 times the ORR activity per weight Pt when Pt-iron oxide (Pt-FeO_x) catalysts are compared to 10 weight % Pt/Vulcan carbon standards. The nanoscale structural properties that lead to this high activity are reported here.

Approach

Catalyst powders are prepared from aqueous solutions in ambient conditions and then heated at various temperatures to adjust their water contents. The water content of the final materials is determined via thermal analysis.

The catalytic activity of the catalysts for the ORR is screened using a rotating-disk electrode (RDE) method.[3] The activity of the new transition metal oxide catalysts is estimated by comparison to a standard RDE of 10 weight % platinum/Vulcan carbon, XC-72 (Pt/VC) catalyst (Alfa). The electrocatalytic activity of the catalysts are compared in Tafel plots of potential vs. current, calculated from the electrochemical data as described in the literature.

Because conventional structural analysis methods (e.g., X-ray diffraction and transmission electron microscopy) are not effective on amorphous

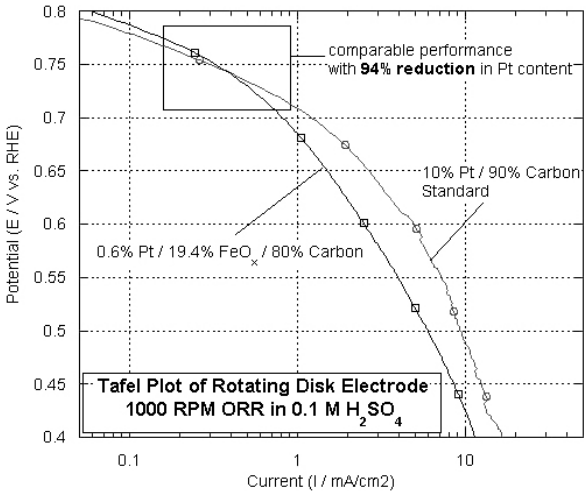

Figure 1. Tafel plot of standard 10% Pt on Vulcan carbon compared to the new catalysts of 20% Pt (~5% Pt-Fe_x) on Vulcan carbon (0.6 weight % Pt total).

Conditions: sweep rate = 10 millivolts; electrolyte: 0.1 M sulfuric acid (H_2SO_4); rotation rate = 1000 rpm; temperature = 60°C. Data from argon gas sweep subtracted from that of O_2 sweep.

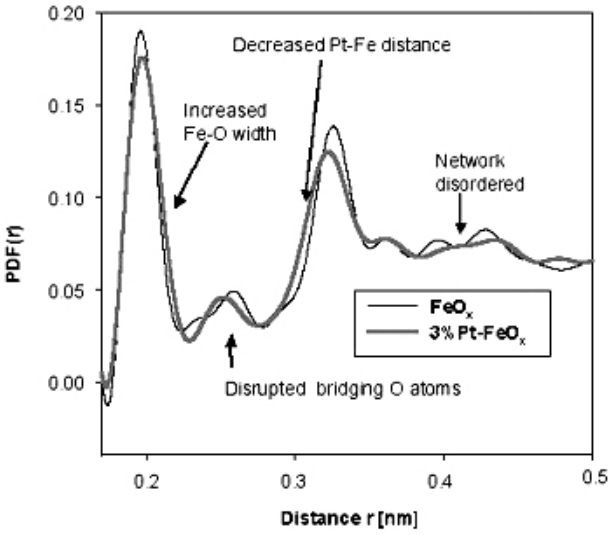

Figure 2. PDF-XRD of 3% Pt-FeO_x vs. FeO_x. The addition of 3% Pt to the FeO_x structure causes four significant changes: (1) an increase in the distance between the iron and oxygen atoms, (2) a decrease between the platinum and iron atoms, (3) disruption of the bridging oxygen, and (4) disorder to the network beyond 0.4 nm.

materials, the nanoscale structures are best resolved via atomic pair-density function (PDF) analysis of the X-ray diffraction patterns of the catalysts. High-energy X-ray diffraction is carried out at beamline X7-A of the National Synchrotron Light Source.

Results

As reported last year, Pt-FeO_x catalysts have the same ORR activity with 20 times less Pt than a 10 weight % Pt/VC standard. These results of an active catalyst are shown in a Tafel plot of current vs. voltage in Figure 1.

The Pt-FeO_x samples with the highest ORR activity are heated at 150°C in air. Samples heated at higher or lower temperatures, or under oxygen, argon or hydrogen have lower electrocatalytic activity. The procedures for adding the Pt to the FeO_x also have a significant impact on their activity.

Conventional XRD measurements show that all of the active and inactive samples are strongly disordered (i.e, amorphous solids or dispersed nanocrystals). However, the PDF-XRD measurements show significant differences between the active and inactive catalysts. When 3% Pt is added to the FeO_x, it distorts the entire FeO_x structure. The PDF-XRD data for a 3% Pt-FeO_x sample is compared to a pure FeO_x sample in Figure 2. The atomic structure of the best performing Pt-FeO_x sample is best described as glassy corner linked polyhedral (CLP) network. A schematic of this structure is shown in Figure 3. The iron (Fe) atoms are coordinated in a tetrahedral oxygen cage. In comparison, the inactive samples do not have this nanoscale structure and are partially crystalline.

The most active samples have only local order (to 1.0 nm) and also have cage-like structures, or ones with micropores. The micropores (sized on the order of 0.4 to 1.0 nm) are likely filled with water or hydroxyl groups and are therefore conducive for proton conduction. The iron in the active samples also exists in mixed valence states, which is likely to contribute to the electrochemical activity of the Pt-FeO_x. Furthermore, the Pt atoms are uniformly distributed throughout the structure.

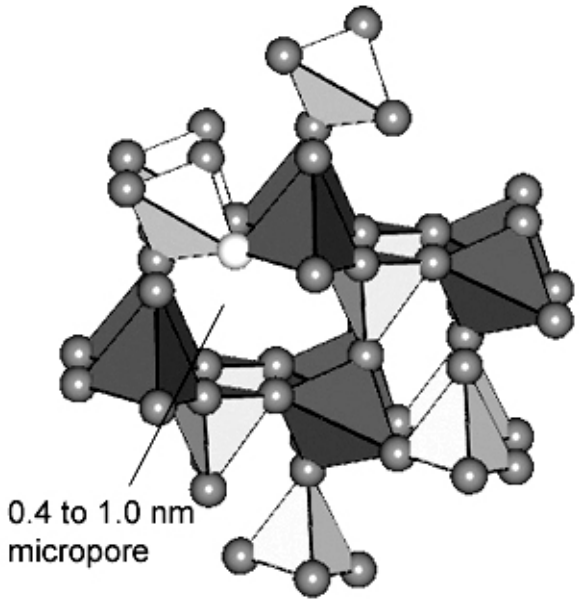

Figure 3. Schematic of a CLP framework. The micropores in the structure are ideal for proton conduction.

The Pt-FeO_x catalysts are not stable to corrosion, as has been confirmed in our laboratory and during fuel cell testing at LANL.

However, we can use our understanding of the Pt-FeO_x materials to design new, stable catalysts. Pt-niobium oxide (Pt-NbO_x) catalysts are currently under development. Preliminary studies show that despite having 150 times less Pt than the 10% Pt/VC standard, the Pt-NbO_x samples have high activity. NbO_x is a more stable oxide than FeO_x, and studies are underway to confirm its long-term activity.

Conclusions

The ORR activity of Pt is greatly enhanced by dissolving it in a matrix that is a good protonic conductor. PDF-XRD structural measurements show that the addition of low amounts of Pt (~3%) to FeO_x can lead to a material with high ORR activity and a unique structure. Active materials are disordered beyond ~1.0 nm and also have micropores. Disruption of the microporous structure causes a decrease in catalyst activity. Although the Pt-FeO_x catalysts are not stable to corrosion, new niobium-based catalysts are being investigated and already show higher stability.

Other transition-metal oxide systems having little or no Pt will continue to be developed. A fuel cell test station is also being acquired by NRL, so that new materials can be tested rapidly and effectively.

If the results from the half-cell measurements are matched in the actual fuel cell operation, the DOE goals to reduce the Pt loading of the fuel cell by 10X by 2008 will be met. The decreased amount of Pt in the fuel cell will also result in a significant decrease in the cost of the PEMFCs.

References

1. K. E. Swider-Lyons, K. M. Bussmann, D. L. Griscom, C. T. Love, D. R. Rolison, W. Dmowski, and T. Egami, in *Solid State Ionic Devices II Ceramic Sensors*, E. D. Wachsman, W. Weppner, E. Traversa, P. Vanysek, N. Yamazoe, M. L. Liu, Editors, The Electrochemical Proceedings Series, Pennington, NJ , 2000, PV2000-32, p. 148.

2. T. Egami, *Mater. Trans.,* 31 (1990) 163.

3. S. Lj. Gojkovic, S. K. Zecevic, and R. F. Savinell, *J. Electrochem. Soc.,* 145 (1998) 3713.

FY 2002 Publications/Presentations

1. K. E. Swider-Lyons, "Mixed-Conducting Oxides in Electrochemical Power Sources," in High Temperature Materials In Honor of the 65th Birthday of Professor Wayne L. Worrell, ed. S. Singhal, The Electrochemical Proceedings Series, 2002, PV 2002-5, p. 124.

2. K. E. Swider-Lyons, "Mixed-Conducting Oxides in Electrochemical Power Sources," Symposium on High Temperature Materials In Honor of the 65th Birthday of Professor Wayne L. Worrell, 100th Meeting of the Electrochemical Society, 12-17 May 2002, Philadelphia, PA.

3. W. Dmowski, T. Egami, K. E. Swider-Lyons, and C. T. Love, "Nanocrystalline or Amorphous? Structure of Hydrous RuO_2 from X-ray Scattering" Conference on Crystal Chemistry of New Materials and Soft Matter Studied by

Synchrotron and Neutron Diffraction and Scattering. August 2002, Grenoble, FRANCE.

4. Karen E. Swider-Lyons, Jason A. Stanley, Gregory B. Cotten, Wojtek Dmowski, and Takeshi Egami, "Low-Platinum Oxide-Based Electrocatalysts For Oxygen Reduction In Proton Exchange Membrane Fuel Cells," Symposium on Recent Advances in Fuel Cells and Fuel Processing, 224th National Meeting of the American Chemical Society,18-22 August 2002, Boston, MA.

IV.D.11 Low Platinum Loading Catalysts for Fuel Cells

Radoslav Adzic (Primary Contact), Jia Wang, Stanko Brankovic, Kotaro Sasaki
Brookhaven National Laboratory, Bldg. 555
Upton, NY 11973-5000
(631) 344-4522, fax : (631) 344-5815, e-mail: adzic@bnl.gov

DOE Technology Development Managers:
JoAnn Milliken: (202) 586-2480, fax: (202) 586-9811, e-mail: JoAnn.Milliken@ee.doe.gov
Nancy Garland: (202) 586-5673, fax: (202) 586-9811, e-mail: Nancy.Garland@ee.doe.gov

Objectives

- Develop a new catalyst with a considerably lower Pt loading, to reach the 2004 DOE target of 300 μg/cm^2 total noble metal loading (150 μg/cm^2 for anode) and improved carbon monoxide (CO) tolerance compared with the commercial platinum Ruthenium (Pt-Ru) catalysts.
- Characterize Pt/Ru electrocatalysts prepared by a new method involving a spontaneous deposition of Pt on Ru nanoparticles.

Approach

- Synthesize electrocatalysts having a submonolayer Pt loading on Ru nanoparticles by spontaneous deposition of Pt on a Ru surface.
- Determine the catalytic properties of the new catalyst for hydrogen (H_2) and H_2 + CO oxidation and improve the thin layer rotating disk electrode method.
- Characterize new electrocatalysts by high-resolution transmission electron microscopy (HRTEM), in-situ fourier transform infrared (FTIR) spectroscopy and extended x-ray absorption fine structure (EXAFS) techniques.
- Test the new electrocatalyst in the membrane electrode assembly (MEA) at Los Alamos National Laboratory.
- Explain the catalytic activity and function of the new electrocatalyst.

Accomplishments

- Electrocatalysts with a 1/8 of monolayer Pt loading on Ru nanoparticles have been synthesized by spontaneous deposition of Pt on a Ru surface, each of which have at least three times larger mass-specific activity for H_2 oxidation than two commercial catalysts and a larger CO tolerance, as determined by thin film rotating disk electrode measurements.
- The carbon-supported catalysts with 1% Pt on 10% Ru (18 μg Pt/cm^2) tested in the MEA at Los Alamos National Laboratory by Dr. Francisco Uribe exhibited a high CO tolerance and the same activity for H_2 oxidation as commercial catalysts with 10 times larger Pt loadings. This catalyst has the noble metal loading close to the 2004 DOE target (200 vs. 150 μg/cm^2), which can be reached by a small decrease of Ru content.
- The possibility of having a catalyst for diatomic oxygen (O_2) reduction with a monolayer of Pt on Ru that approaches the activity of carbon-supported Pt has been demonstrated.
- A method of synthesizing carbon-supported W nanoparticles has been developed with D. Mahajan from Brookhaven National Laboratory (BNL). These nanoparticles will be tested as the *core* for new catalysts containing low coverages of noble metals in the shell.

Future Directions

- Further optimization of the catalyst prepared by spontaneous deposition of Pt and further catalyst characterization with electrochemical and EXAFS techniques.
- Further testing of the catalyst in the MEAs.
- Investigation of possibilities to reduce or replace Ru in the catalyst by non-noble metals.
- Investigations of low Pt loading catalysts for O_2 reduction.

Introduction

In June 2001 we initiated this project to explore the possibilities of decreasing the Pt loading in Pt-Ru catalysts for H_2/CO oxidation in the polymer electrolyte membrane fuel cells (PEMFCs). We have demonstrated a new method for the preparation of the Pt-Ru catalysts involving spontaneous deposition of Pt on Ru nanoparticles that we explored first with single crystal Ru surfaces. The resulting catalysts have a high CO tolerance with considerably lower Pt loading than the commercial catalysts.

Approach

Pt is deposited only at the surface of Ru nanoparticles rather than throughout the Pt-Ru nanoparticles. The method facilitates tuning of the electronic and catalytic properties of Pt-Ru catalysts by controlling the Pt cluster size. In contrast to the Pt-Ru alloy catalysts, this structure has all the Pt atoms available for the catalytic reaction, which decreases the Pt loading.

Results

Characterization of the Electrocatalyst

HRTEM has been used to investigate the type of Pt deposited on Ru nanoparticles. For the $PtRu_{20}$ catalyst, the dominant features, both in symmetry and lattice spacing, are consistent with the hexagonally close-packed Ru single crystal structure. An example of the images with different resolutions obtained with the help of Y. Zhu (BNL) is shown in Figure 1. Figure 1e is a pattern Fourier transferred from the boxed area in Figure 1d, where the particle is viewed along the $(\bar{1}01)$ direction.

The distribution of the lattice spacing and the lattice fringes obtained from 170 particles fit well with the low index spacings of the hexagonally close-packed Ru single crystal. Pt is selectively deposited

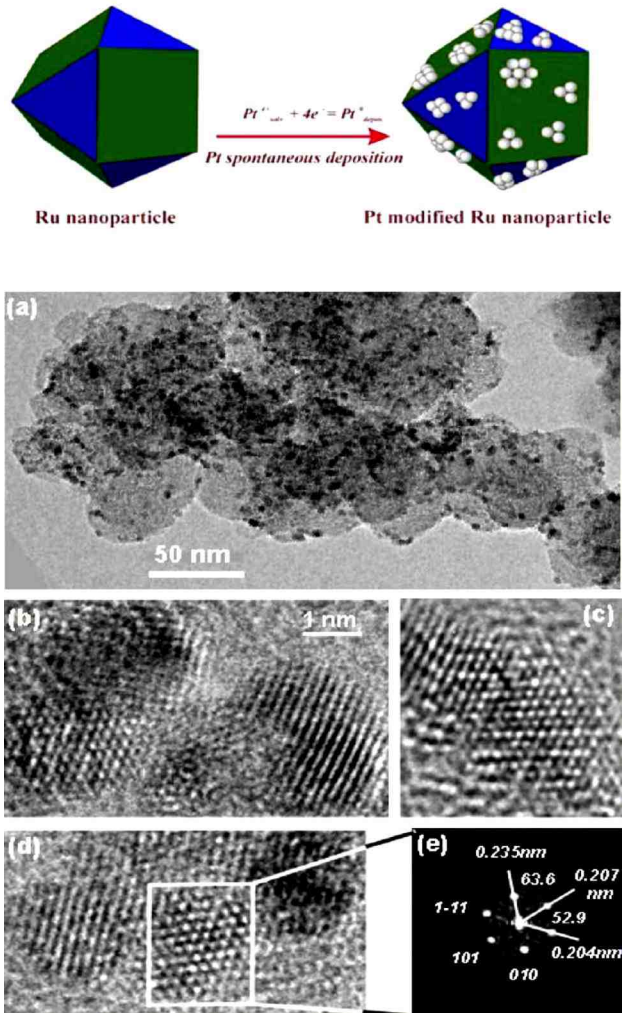

Figure 1. Upper panel: model of Pt islands on a Ru cubooctahedron nanoparticle. Lower panel: Electron micrographs of the $PtRu_{20}$ catalyst. (a) Low magnification morphology of the metal particles (black dots, average size 2.5 nm) on carbon spheres (average size 50 nm). (b-d) High-resolution images showing atomic resolved lattice structures. (e) Diffractogram obtained from the high-resolution image shown in (d).

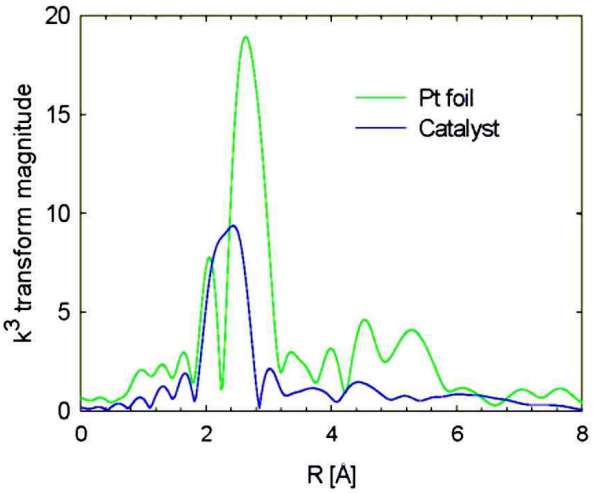

Figure 2. In situ EXAFS data for the $PtRu_{20}$ electrocatalyst at 0.05 V vs. reversible hydrogen electrode in 0.5 M H_2SO_4 solution. The curve for a Pt foil is given for comparison.

on Ru nanoparticles and not on carbon because a metallic Ru surface acts as a reducing agent for Pt deposition. For low Pt:Ru atomic ratios the small Pt clusters are expected, and these probably acquire the Ru lattice spacing upon small contraction.

In-situ EXAFS data obtained with the help of M. Subramanian and J. McBreen (BNL) are shown in Figure 2. The radial structure functions of Pt foil and Pt/Ru catalysts are compared. The spectrum for the Pt/Ru catalyst is dominated by Ru. The analysis shows that the smaller peak can be fitted by the one Pt atom coordinated to four Ru atoms. The Pt-Ru bond length is 2.69Å, as in the Pt-Ru alloys. The Pt-Pt coordination is being analyzed. First results indicate that the Pt islands on Ru are very small, which is consistent with the HRTEM data.

Catalytic Activity

The thin-film rotating disk electrode has been used for determination of the catalytic activity. The catalyst was attached to the glassy carbon electrode by careful deposition from aqueous dispersion and *no Nafion® film was used* to cover the deposit. This can significantly improve the tests of supported electrocatalysts. Kinetic parameters for the oxidation of H_2 and H_2 + CO have been determined by

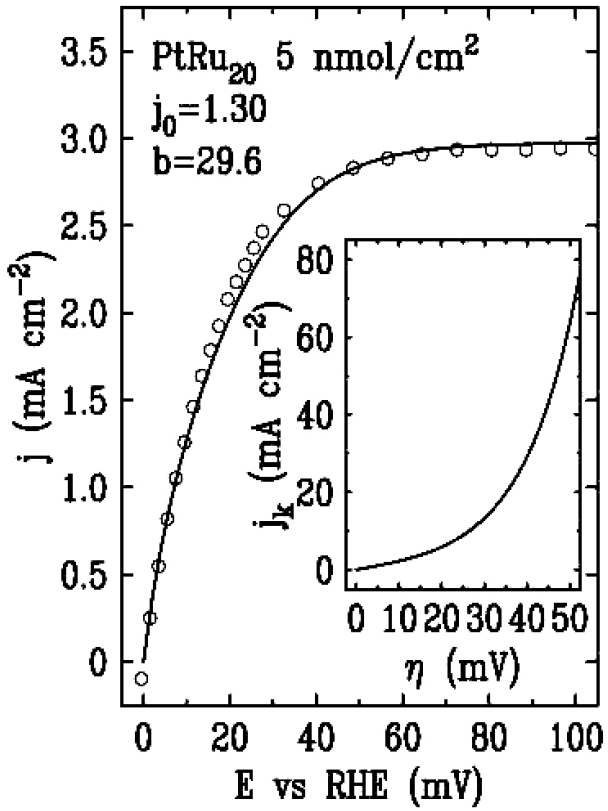

Figure 3. Polarization curves for H_2 oxidation on $PtRu_{20}$/C prepared by spontaneous Pt deposition in 0.5 M H_2SO_4 solution. The parameters of the best fits are given in the graph. Insert: Calculated kinetic current vs. potential with b=29.6 mV and j_0=1.30 mA/cm^2.

nonlinear fitting of the entire polarization curve. Mass-specific activities of the catalysts were determined by finding the minimum Pt loading needed to obtain the Tafel slope, exchange current density, and the Levich slope comparable to those found for the polycrystalline Pt electrode. In this way, a full utilization of the catalyst is verified. Figure 3 shows H_2 oxidation on the $PtRu_{20}$ catalyst; the curve is the fit to the experiment (points) for j_0 = 1.3 millamps per centimers squared (mA/cm^2) and b = 29.6 millivolt (mV), which are the values for polycrystalline Pt. The insert shows the calculated kinetic current in the absence of diffusion control.

For the $PtRu_{20}$, $PtRu_{10}$, and $PtRu_5$ samples prepared by spontaneous deposition of 1/9 to 4/9

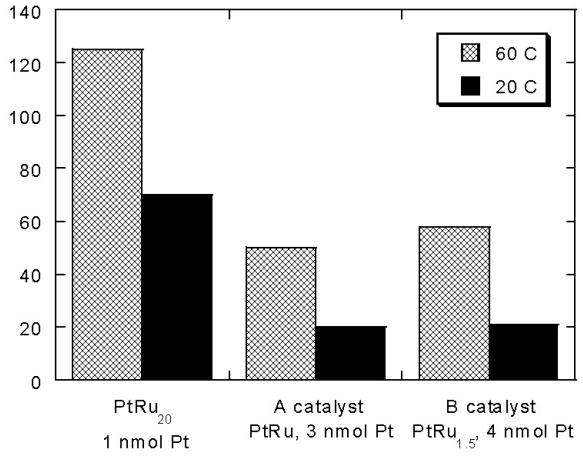

Figure 4. Mass-specific activities of the three electrocatalysts for the oxidation of H_2 at 0.05 V in 0.5M H_2SO_4 at 25 and 60º C at 2500 rpm.

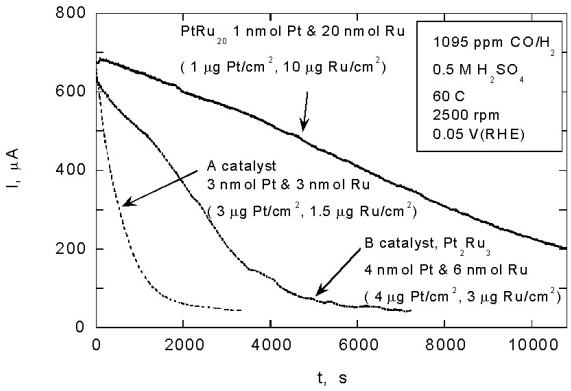

Figure 5. CO tolerance of the three electrocatalysts from a time dependence of the current for the oxidation of H_2 with 1095 ppm CO in 0.5M H_2SO_4 at 60º C at 2500 rpm.

monolayer Pt on Ru, the minimum Pt loading is 5 nmol/cm^2 (1 μg Pt/cm^2). This is only 1/3 of that for Pt or PtRu (Commercial A) catalysts and only twice of the atomic density of a Pt(111) surface, indicating that the high activity of Pt metal for hydrogen oxidation is retained when the atomic assemblies are reduced to submonolayer levels on Ru. The enhanced CO tolerance was studied at low potentials by correlating the loss of activity in 0.1% CO/H_2 and the CO coverage on Pt and Ru sites.

Figure 4 displays a mass-specific activity of $PtRu_{20}$ catalyst in comparison to Commercial A's PtRu 1:1 alloy and Commercial B's Pt_3Ru_2 electrocatalysts for the oxidation of H_2 in 0.5M H_2SO_4. A considerably higher mass-specific activity of the $PtRu_{20}$ electrocatalyst has been observed.

CO Tolerance

Figure 5 displays a comparison of the CO tolerance of three catalysts based on the current as a function of time for the oxidation of H_2 with 1095 ppm of CO at 60º C for the $PtRu_{20}$, Commercial A's PtRu and Commercial B's Pt_3Ru_2 catalysts with the loadings indicated in the graph obtained with rotating disk electrode at 2500 rpm. A considerably larger CO tolerance is seen for the $PtRu_{20}$ electrocatalyst.

Conclusions

The new electrocatalyst has higher mass-specific activity and CO tolerance than commercial electrocatalysts with several times larger Pt loadings. The Pt islands on Ru have lower CO coverage than that of the Pt-Ru alloy, as inferred from the CO stripping charges. Lower Pt-CO bond strength and an efficient CO spillover to RuOH are the likely causes of enhanced CO tolerance. The new catalyst facilitates reaching the limiting value for Pt dispersion, and thus, full catalyst utilization becomes possible.

For Pt, the loading of the new catalyst is below the DOE target (150 μg/cm^2) for precious metals for 2004. For Ru, it is at the present level of the state-of-the-art catalysts.

Preliminary data for O_2 reduction on ½ monolayer of Pt on Ru nanoparticles (not shown) indicates that a very active catalyst for O_2 reduction can be designed with low Pt loadings.

FY 2002 Publications

1. S. R. Brankovic, J.X. Wang, and R.R. Adzic, 2. Pt submonolayers on Ru nanoparticles - a novel low Pt loading, high CO tolerance fuel cell electrocatalyst , Electrochem. Solid State Lett., 4, A217-A220 (2001).

3. S.R. Brankovic, J McBreen, R.R. Adzic, Spontaneous Deposition of Pt on a Ru(0001) Surface, J. Electroanal. Chem., 503, 99-104 (2001).

4. S.R. Brankovic, J. McBreen, R.R. Adzic, Spontaneous deposition of Pd on a Ru(0001) Surface, Surf. Sci., 479, L363-L368 (2001).

5. S.R Brankovic, J.X Wang, R.R. Adzic, Metal monolayer deposition by replacement of metal adlayers on electrode surfaces, Surf. Sci., 477, L173- L179 (2001).

IV.D.12 Development of High-Performance, Low-Pt Cathodes Containing New Catalysts and Layer Structure

Paolina Atanassova (Primary Contact), David Dericotte, Paul Napolitano, Rimple Bhatia, Jim Brewster, Mark Hampden-Smith (SMP), Cynthia Lundgren, Lin Wang (DuPont) and Sandip Mazumder (CFDRC)
Superior MicroPowders, LLC
3740 Hawkins Dr. NE
Albuquerque, NM 87109
(505) 342-1492, fax: (505) 342-2168, e-mail: paolina@smp1.com

DOE Technology Development Managers:
JoAnn Milliken: (202) 586-2480, fax: (202) 586-9811, e-mail: JoAnn.Milliken@ee.doe.gov
Valri Lightner: (202) 586-0937, fax: (202) 586-3237, e-mail: Valri.Lightner@ee.doe.gov

Contractor: Superior MicroPowders, LLC, Albuquerque, NM
Subcontractors: DuPont, Wilmington, DE; CFDRC, Huntsville, AL

Objectives

- Develop and apply combinatorial powder synthesis platform based on spray pyrolysis for discovery of high-performance low-Pt cathode electrocatalysts.
- Develop engineered cathode layer structures containing the new electrocatalysts.
- Demonstrate enhanced performance of membrane electrode assemblies (MEAs) with low Pt content towards the DOE goals of 0.6 g Pt/kW in automotive applications for the year 2005.

Approach

- Design and build a combinatorial powder synthesis system (CPSS) capable of generating a large number of electrocatalyst powders with variable composition and microstructure.
- Test benchmark catalysts with half-cell rapid screening technique for their activity in the oxygen reduction reaction (ORR) and compare ranking of catalysts with their performance in polymer electrolyte membrane MEAs.
- Synthesize binary and ternary Pt-alloy electrocatalysts by spray pyrolysis and test their performance in MEAs.
- Optimize the MEA structure with benchmark Pt-based supported catalysts with various Pt loadings in the catalysts and in the cathode layer.
- Improve the software for modeling the operation of fuel cells to account for the effect of liquid water on the performance of the cell, and perform validation studies.

Accomplishments

- Combinatorial Powder Synthesis System (CPSS) designed and assembled on schedule.
- Half-cell rapid screening technique for screening electrocatalysts for their ORR activity in place and benchmarked for various Pt-based electrocatalysts.

- Various binary and ternary Pt-alloy catalysts synthesized by spray pyrolysis and improved performance demonstrated in terms of lower g Pt/kW at 0.8 V – up to 40% reduction of Pt loading demonstrated for ternary Pt-alloy catalysts compared to supported Pt catalysts.
- Strategy and workflow for future combinatorial synthesis in place.
- MEA structure and printing approach improvements demonstrated in comparison with initial test data.
- Improvements in the fuel cell performance modeling developed and validation studies in progress.

Future Directions

- Install and apply the CPSS for production, in a combinatorial mode, of a large number of electrocatalyst powders with variable composition and microstructure.
- Increase capacity of half-cell rapid screening technique to match the screening needs of CPSS powder generation capability.
- Continue to improve the structure and performance of the cathode layer and test the performance of newly discovered electrocatalyst compositions in MEA configuration that are identified by the rapid screening technique to have enhanced kinetic performance.
- Use modeling to predict trends in the MEA performance as a function of variables in the electrode structure and operating conditions.
- Demonstrate the performance of combined features derived from the best performing low-Pt electrocatalyst and the optimal MEA structure in a short stack fuel cell.

Introduction

One vital issue delaying mass production of PEMFCs is the availability of a low-cost, high-performance oxygen reduction catalyst. Superior MicroPowders (SMP) has developed a spray-based process for low-cost, high-volume manufacturing of high-performance, highly reproducible electrocatalyst powders for PEMFC applications (1). This powder production process serves as the platform for this project to achieve the aggressive low-Pt DOE targets of 0.6 g Pt/kW by the year 2005.

The project goals are to significantly improve both the kinetic performance of the electrocatalyst powder at low noble metal loading and its utilization in the cathode layers through layer structure development. Limitations in the catalyst performance will be addressed through combinatorial discovery of supported catalyst compositions and microstructures. The discovery of these new catalyst formulations will be carried out under conditions that have been scaled for commercial powder production. A large variation of binary, ternary and quaternary noble metal - transition metal alloys and mixed metal-metal oxide catalyst compositions will be screened. To improve the utilization/performance of the catalyst in MEAs, the electrocatalyst-containing formulations will be applied to proton-conductive membranes where the chemical composition of the formulation and the nature of the coating will be varied to uncover the optimum cathode layer performance.

Approach

Effort 1: *Combinatorial discovery of low Pt compositions with microstructure optimization using spray based catalyst manufacturing.* This effort is focused on the combinatorial discovery of new low Pt electrocatalyst formulations. A large variation of multi-component catalysts will be produced by SMP in a combinatorial discovery mode. Initially, the powder synthesis will be performed with existing equipment and then on a new system designed and built at SMP. Samples generated at SMP, will be tested by DuPont in a half-cell rapid screening device for their electrochemical performance. The optimum compositions will be scaled up for testing in single MEAs and stacks.

Effort 2: *Development of engineered particles and layers.* This effort is focused on the ability of the spray-based generation approach to tailor electrocatalyst structure to minimize polarization

losses. SMP will engineer and produce novel composite particles and MEA structures and test them in single 50 cm^2 cell MEA configuration to optimize the cathode layer structure and performance. In parallel, Computational Fluid Dynamics Research Corporation (CFDRC) will model MEA processes on microscopic (primary and secondary particle structure) and macroscopic (layer, MEA) scales. Using the results from the single cell testing and the data from the CFDRC model, SMP will further optimize the MEA structure to obtain maximum performance with a focus on high-throughput manufacturing and cost reduction.

Stack testing. Ultimately, MEAs designed and fabricated by SMP that combine the best scaled up novel catalysts (Effort 1) and the optimal cathode structure (Effort 2) will be tested in full scale short stack operation modules. The stack building and testing will be performed by leading automotive PEMFC developers, such as General Motors. The end-users will also provide valuable feedback in terms of performance and cost targets from a perspective of commercial implementation in the market.

Results

In order to execute a combinatorial approach for discovery of novel electrocatalyst materials, several key workflow components need to be in place, including the ability to generate a large number of electrocatalyst powders with variation in the composition and microstructure and to test their activity in the ORR by a rapid screening technique.

Combinatorial Synthesis. The conceptual design of the CPSS was completed during the current report period and its installation is on schedule. Figure 1 illustrates the overall configuration of the CPSS, which is based on current R&D scale unit at SMP.

Rapid screening of the electrochemical performance. DuPont has developed rapid half-cell screening techniques to evaluate catalyst activity for methanol oxidation, CO tolerance and oxygen reduction. These measurements are performed in liquid sulfuric acid electrolytes, and up to 32 electrodes can be screened in parallel using a variety of electrochemical techniques in a 3-electrode

Figure 1. Combinatorial Powder Synthesis System

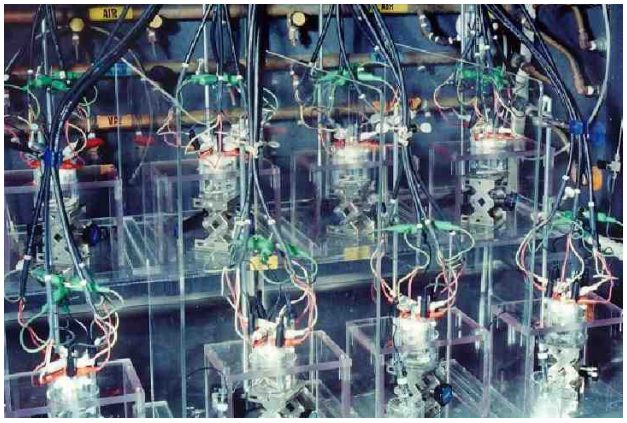

Figure 2. DuPont's Experimental Set-Up for Rapid Half-Cell Screening of Electrocatalysts

configuration. A picture of the experimental setup is shown in Figure 2. With this capability, DuPont can rapidly evaluate many electrocatalyst samples and map their activity for electrochemical reactions. Using this set-up, DuPont evaluated a series of benchmark Pt-based catalysts supplied by SMP for the oxygen reduction reaction using linear polarization techniques in a sulfuric acid medium. The catalysts were tested at various loadings in the electrodes, and the normalized currents at various voltages were compared to the current densities observed in the kinetic region for MEAs made and tested at SMP. We have been able to correlate the ranking of the activity by the rapid screening approach and the MEA performance for different classes of catalysts. Further optimization of the electrode formulation is needed for accurate ranking of catalysts supported on different types of carbons.

Binary and ternary Pt alloys. A large variety of Pt-based catalysts were tested for their performance in test conditions relevant to automotive applications and to benchmark their performance for further comparison with the newly discovered electrocatalyst compositions. Significant effort was placed on finding alternative platinum precursors to support the synthesis of complex alloy and metal-metal oxide electrocatalyst compositions, where metal precursor compatibility becomes important. Several platinum precursors were identified as yielding high performance Pt-based catalysts and being compatible with a variety of alloying metal precursors. The precursors are also more cost-effective for large-scale production.

In order to establish a baseline for our systems and methodologies, several binary and ternary compositions supported on Vulcan XC-72 were evaluated. Among these were Pt_xRu_y, Pt_xCo_y, Pt_xCr_y, Pt_xPd_y, $Pt_xCr_yCo_z$, and $Pt_xNi_yCo_z$. Initial efforts were directed towards variation of the spray conversion processing conditions to ensure conversion of metals, crystallite size and alloying. Post processing of the powders was attempted in several cases and consisted of annealing the electrocatalysts in varying H_2/N_2 atmospheres, temperatures and times. Conversion of the metal precursors and alloying of different species were monitored via x-ray diffraction (XRD). Figure 3 illustrates the effect of various processing conditions on the structural characteristics of $Pt_xNi_yCo_z$/Vulcan XC-72 electrocatalysts. A selected ternary alloy, 20 and 40 wt.% PtNiCo/Vulcan XC-72 electrocatalysts were tested in MEAs at identical total metal loadings and test conditions and compared to pure Pt supported catalyst. Improvement of up to 40% in terms of g Pt/kW at 0.8 V was observed when alloyed catalysts were compared to pure Pt ones. Figure 4 compares the performance of 40 wt.% PtNiCo/Vulcan XC-72 catalysts prepared at different conditions and 40 wt.% Pt/Vulcan XC-72 catalyst deposited at the same total metals loading of 0.45 mg Me/cm^2 (Me – total metals loading) in the MEA.

Test conditions. For the evaluation, 50 cm^2 test MEAs with Nafion 112 (DuPont) membrane were used. The MEAs were tested at 80°C, with flows corresponding to 1A/cm^2 at 1.5 stoichiometry for hydrogen and 2.5 stoichiometry for air on the anode

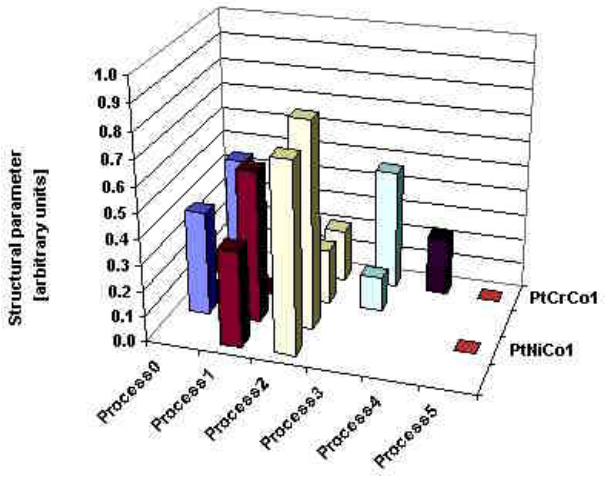

Figure 3. Synthesis of Ternary Pt-alloy Electrocatalysts: Effect of Composition and Processing Conditions on Structural Parameters

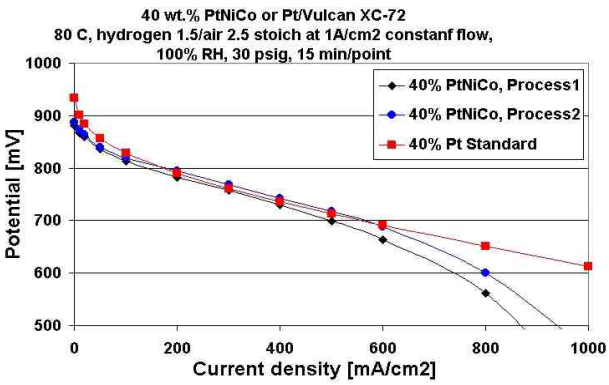

Figure 4. Performance Comparison of Ternary 40 wt.% $Pt_xNi_yCo_z$/Vulcan XC-72 and 40 wt.% Pt/ Vulcan XC-72 Electrocatalysts

and cathode, respectively. Humidified H_2 (100%) and air were used, at 30 psig pressure on both the anode and cathode sides.

MEA structure development. The development of the electrode structure was focused on finding optimal combinations of electrocatalyst loadings, layer thicknesses and ionomer-to-catalyst ratios. Figure 5a shows the polarization curves for MEAs with 60 wt.% Pt/Carbon used as cathode catalyst at Pt loadings in the range of 0.25 to 0.65 g Pt/cm^2. Figure 5b compares the performance of these MEAs in terms of g Pt/kW at 0.8 V. For all these benchmark Pt loadings, a performance around 2 g Pt/ kW was demonstrated.

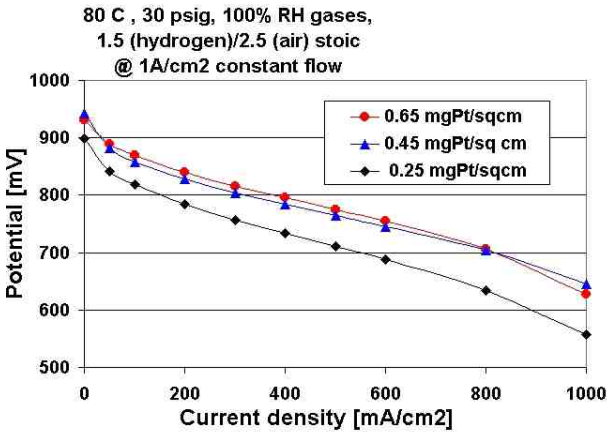

Figure 5a. Effect of Pt Loading on Performance Using 60 wt.% Pt/Carbon as Cathode Catalyst

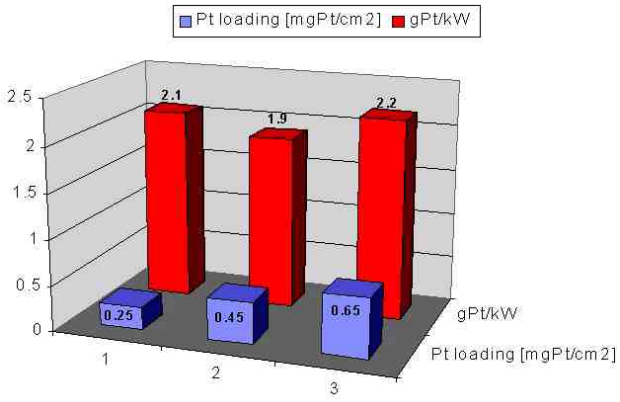

Figure 5b. Performance of MEAs with 60 wt.% Pt/ Carbon Cathode Electrocatalyst at 0.8 V

Various types of Nafion membranes and gas diffusion layers were compared as well. The electrode deposition technique was optimized to achieve performance comparable to the "state-of-the-art" for ink deposition approach. Several deposition techniques were investigated for printing the electrode layers, Figure 6 compares the performance achieved with two MEAs, printed by method A and method B with otherwise identical composition. Improved Method B yields performance of 1.9 g Pt/ kW at 0.8 V and the above stated test conditions. Further optimization of the electrode structure is in progress for catalysts with various loadings on high-surface-area carbon supports.

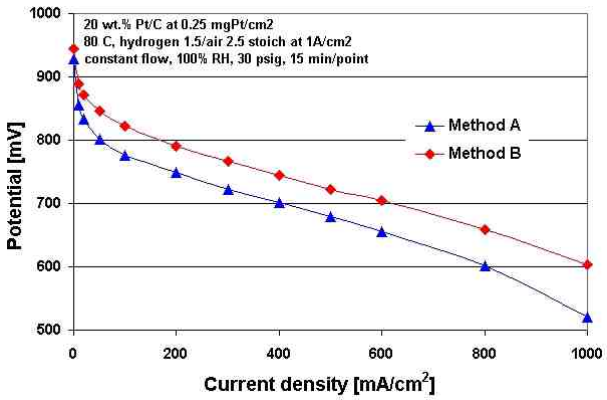

Figure 6. Effect of Deposition Method on the MEA Performance

Modeling effort. CFDRC has made several generic improvements to their existing software for modeling fuel cells and performed several validation studies. These are listed below:

- A comprehensive water transport model was developed to account for effect of liquid water on the performance of the cell. This involved solution of an additional transport equation for liquid water saturation. Effects of convection, surface tension, electro-osmotic drag, gravity and surface tension are taken into account in this model.
- Several new models to compute effective diffusivity in porous regions were implemented.
- Several validation studies were performed against data reported in the literature.

Validation of the code against data generated in-house at SMP is underway. Upon completion of these validation studies (expected by September, 2002), much of the focus will be on using the model as a predictive tool to identify better MEA designs. Further development of the model to account for variables in the structure on a microscopic level is in progress.

Conclusions

Significant progress has been made in implementing all necessary components for successful execution of both the combinatorial

discovery approach and electrode structure optimization. Results on the synthesis of benchmark alloy catalyst compositions demonstrate the ability of the SMP's spray approach to generate complex electrocatalyst formulations with improved electrochemical performance. Future work will expand on the compositions screened according to a combinatorial strategy in place. The advances in the two parallel efforts, i.e. improvements in kinetic performance and MEA structure optimization, will be combined to reveal the overall achievements in performance at reduced Pt loadings.

References

1. Kodas, T.T., M.J. Hampden-Smith, J. Caruso, D.J. Skamser, and Q.P. Powell, *Metal-carbon composite powders, methods for producing powders and devices fabricated from same*. 2000, Superior MicroPowders: US 6,103,393.

IV.D.13 New Electrocatalysts for Fuel Cells

Philip N. Ross, Jr. (Primary Contact), Nenad Markovic
Lawrence Berkeley National Laboratory
Materials Sciences Division
1 Cyclotron Rd., MS 2-100
Berkeley, CA 94720
(510) 486-6226, fax: (510) 486-5530, e-mail: pnross@lbl.gov

DOE Technology Development Managers:
JoAnn Milliken: (202)586-2480, fax: (202)586-9811, e-mail: JoAnn.Milliken@ee.doe.gov
Nancy Garland: (202) 586-5673, fax: (202) 586-9811, e-mail: Nancy.Garland@ee.doe.gov

Objectives

- Conduct research on the kinetics and mechanism of electrode reactions in low temperature fuel cells. Develop new electrocatalysts using a materials-by-design approach.

Approach

- Study the kinetics of fuel cell electrode reactions on well-characterized model electrodes and high surface area fuel cell electrocatalysts using modern electroanalytical methods. Study the mechanisms of the reactions using state-of-the art in-situ spectroscopes.
- Use ultra-high vacuum methods of surface preparation and surface analyses to form tailored surfaces. Synthesize nanoclusters to have the tailored surface.
- Characterize the microstructure of the nanoclusters by high-resolution electron microscopy.
- Transfer technology to catalysts developers/vendors.

Accomplishments

- Proof-of-principle experiments demonstrated that a Au-Pd alloy with <50 wt. % Pd can replace Pt as the hydrogen electrode catalyst without any loss in performance.
- Proof-of-principle experiments demonstrated that “Pt skin” structures with a non-precious metal core can be stable under PEMFC air cathode operating conditions

Future Directions

Cathode side

- Create “skin” nanostructures of Pt on non-noble substrates and determine their activity and stability as novel low-Pt air cathode electrocatalysts. Select the most promising substrate for synthesis as high surface area catalyst.
- Develop and optimize a new class of non-Pt model catalysts. Synthesize and test new non-Pt high surface area catalysts at fuel cell conditions.

Anode side

- Synthesize and characterize Pd-Au bimetallic nanoparticles and conduct preliminary testing of these nanoparticles as anodes in PEMFC hydrogen-air cells.
- Determine CO-tolerance of tailored electrodes consisting of thin films (1-10 monolayer) of Pd on the close-packed single crystal surfaces of Ta, Re, and W.

Introduction

It is known from the theory of surface segregation in bimetallic alloys that, in certain systems, preferential surface enrichment in one element is so strong that it leads to a "skin" structure, i.e. the outermost layer is a "skin" of one element. Theoretically, for nanoparticles, such a segregating alloy system could form particles having a "grape" microstructure, a skin of one element over a core of the other. In principle, one could use this thermodynamic property to replace the "buried" atoms in Pt nanoparticles with a non-precious metal, e.g. Fe or Co, resulting in 100% Pt dispersion (all Pt atoms are surface atoms) without the need to create extremely small particles, e.g. <2 nm. For example, if a standard pure Pt catalyst consists of particles having on average a dispersion of 20%, replacement of the buried atoms in those particles with a base metal would enable the Pt loading to be reduced by a factor of 5, all other factors being the same. This is the basic strategy we are currently pursuing to reduce Pt loading in PEMFC cathodes.

Approach

Pt_3Ni and Pt_3Co are classical examples of alloys of Pt having a skin surface structure, a pure Pt skin. In this case, enrichment occurs by interchange of Pt and Co atoms between the first two atomic layers, the subsequent layers having the bulk composition (75% Pt). The thermodynamic driving force in this case is for the larger atom to be at the surface, since, in face-centered cubic metals, the surface is generally relaxed outward and the second layer contracted. The Pt_3Ni and Pt_3Co systems do not represent cases of extreme segregation we need for replacing buried Pt atoms, but they do serve as a useful test case for the concept of a skin structure, and there may be, by serendipity, a beneficial electronic effect. The most important aspect of the study of this system was the stability of the skin structure when used as an oxygen reduction electrode under PEMFC conditions.

Results

Cathode Catalysts

Pt_3Ni and Pt_3Co solid electrodes were prepared using conventional metallurgy and pre-treated in a surface analytical vacuum chamber equipped with various instruments for surface preparation and analysis. For each alloy, either a pure Pt skin or a 75 at.% Pt surface was prepared and tested as an oxygen reduction catalyst. The resulting activity for oxygen reduction as a function of composition is shown in Figure 1. The Pt skin structure is both more and less active than the pure Pt reference surface, depending on whether the subsurface is Co or Ni, suggesting there is an electronic effect that can be either beneficial or deleterious. The most important result represented in Figure 1 is the stability of the skin structure under the conditions of use as an oxygen reduction electrode, e.g. continuous cycling between 0.1 – 1.0 V under 1 bar O_2 in acid electrolyte (1 M trifluoromethane sulfonic acid) at 60^{o}C produced no change in the curves.

Anode Catalysts

The catalytic activity of Pd for the hydrogen oxidation reaction (HOR) can be modified by preparing the Pd in the form of an ultrathin film, e.g. 1 monolayer (ML). This result is summarized in Figure 2. A 1 ML film of Pd on Pt(111) has about 5 times the catalytic activity of a multilayer of Pd. Pt(111) was chosen for the substrate because of the lattice match with Pd. Preliminary results with a Re(0001) substrate look equally promising. According to thermodynamic predictions, Pd should form a pure monatomic skin on the surface of a Re_3Pd (25% Pd) alloy. If this Pd skin has the same catalytic activity as the monolayer shown in Figure 2, then the Pd loading in the hydrogen anode of a H_2-air PEMFC can be as low as 0.05 g per kW, e.g. about the same as in current conventional gasoline vehicle catalytic converters.

Conclusions

Proof-of-principle experiments indicate that synthesis of Pt as surface enriched nanoparticles could enable Pt loadings in the PEMFC air cathode to be lowered by as much as a factor of 5 from present (optimized) levels, e.g. from 1 g per kW to the DOE target of 0.2 g per kW. Comparable experiments with Pd thin films indicate an even greater reduction in Pt Group Metal (PGM) loading is possible for the hydrogen electrode, comparable to the PGM content of the catalytic converter in current conventional gasoline vehicles.

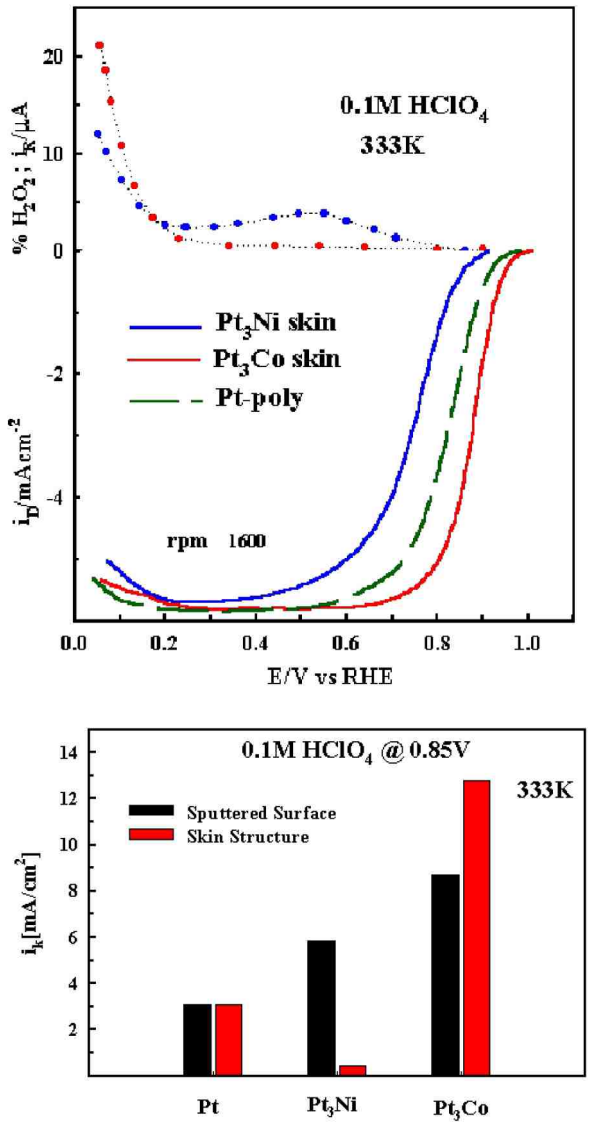

Figure 1. (top) Current-potential curve for a rotating disk electrode (1600 rpm) under 1 bar O_2 in 0.1 M $HClO_4$ for different disk electrodes: Pt skin on Pt_3Ni, Pt skin on Pt_3Co, and pure Pt. (bottom) Steady-state current densities (per unit geometric area) at 0.85 V (vs. reversible hydrogen electrode [RHE]) for the five different electrodes: pure Pt, Pt skin on Pt_3Ni and Pt_3Co, the 75% Pt surfaces on Pt_3Ni and Pt_3Co. 333 K.

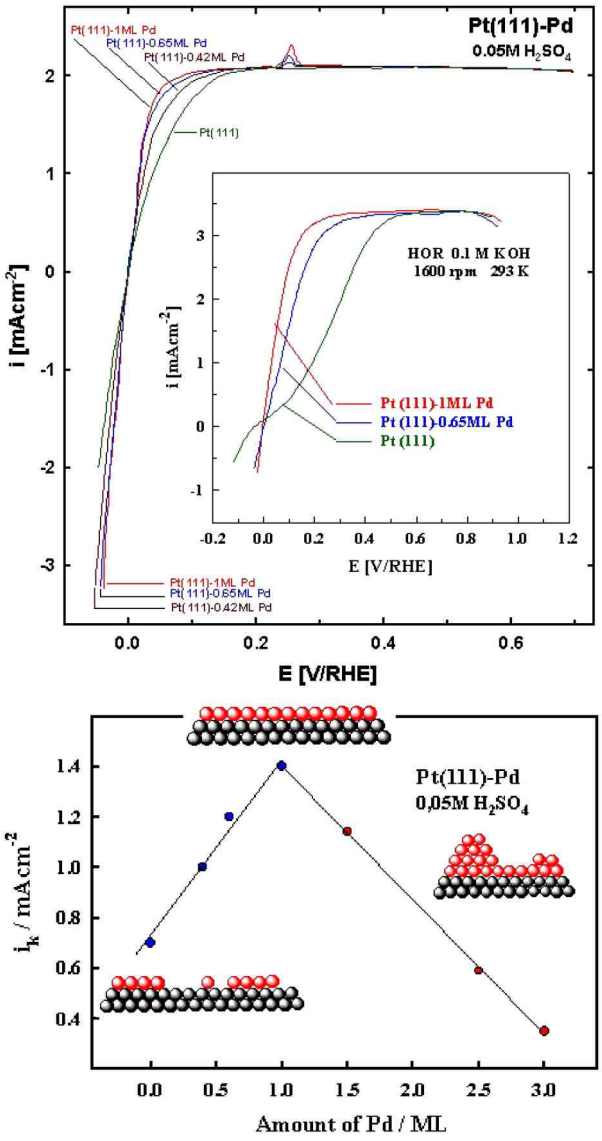

Figure 2. (top) Current-potential curve for a rotating disk electrode (1600 rpm) under 1 bar H_2 in 0.1 M $HClO_4$ for different disk electrodes as indicated in the labels. (bottom) Exchange-current densities in acid electrolyte (pH = 1) for the hydrogen oxidation reaction as a function of Pd coverage on the Pt(111) substrate. 293 K.

Publications

1. Markovic, N. M. and P. N. Ross, "Electrocatalysts by Design: From the Tailored Surface to a Commercial Catalyst", *Electrochim. Acta*, **45**, 4101, 2000.

2. Markovic, N. M. and P. N. Ross, "New Electrocatalysts for Fuel Cells: From Model Surfaces to Commercial Catalysts", *CATTECH* **4** (2000) 110.

3. V. Stamenkovi_, N. M Markovi_, P. N. Ross, "Structure-Property Relationships in Electrocatalysis: Oxygen Reduction and Hydrogen Oxidation Reactions on Pt(111) and Pt(100) in Solution Containing Chloride Ions", *J. Electroanal. Chem.* **500** (2001) 43.

4. T.J. Schmidt, B. N. Grgur, N.M. Markovi, and P.N. Ross, "Oscillatory Behavior in the Electrochemical Oxidation of Formic Acid on Pt(100): Rotation and Temperature Effects", *J. Electroanal. Chem.* **500** (2001) 43.

5. N. M Markovic, T.J. Schmidt, V. Stamenkovic, P.N. Ross, "Oxygen Reduction Reaction on Pt and Pt Bimetallic Surfaces: A Selective Review", *Fuel Cells-From Fundamentals to Systems* , **1** (2001)105-116.

6. T.J. Schmidt, V. Stamenkovic, C.A. Lucas, N.M. Markovi, and P.N. Ross, "Surface Processes and Electrocatalysis of the Pt(hkl)/Bi –Solution Interface", *Physical Chemistry Chemical Physics* **3** (2001)3879.

7. T.J. Schmidt, P.N. Ross, N.M. Markovi, "Temperature-Dependent Surface Electrochemistry of Pt Single Crystal Surfaces in Alkaline Solution" Part I. CO Oxidation", *J. Phys. Chem*, B **105** (2001)12082.

8. U.A. Paulus, A. Wokaun, G.G. Scherer, T.J. Schmidt, V. Stamenkovic, V. Radmilovic, N.M. Markovi, and P.N. Ross, "Oxygen Reduction on Carbon Supported Pt-Ni and Pt-Co Alloy Catalysts", *J. Phys. Chem. B* **106** (2002) 4181.

IV.D.14 Electrodes for Polymer Electrolyte Membrane Fuel Cell Operation on Hydrogen/Air and Reformate/Air

Francisco A. Uribe (Primary Contact), Tom Zawodzinski, Judith Valerio, Guido Bender, Fernando Garzon, Andrew Saab, Tommy Rockward, Peter Adcock, Jian Xie, Wayne Smith
Los Alamos National Laboratory
PO Box 1663, MS D429
Los Alamos, NM 87545
(505) 667-3964, fax: (505) 665-4292, e-mail: uribe@lanl.gov

DOE Technology Development Managers:
JoAnn Milliken: (202) 586-2480, fax: (202) 586-9811, e-mail: JoAnn.Milliken@ee.doe.gov
Nancy Garland: (202) 586-5673, fax: (202) 586-9811, e-mail: Nancy.Garland@ee.doe.gov

Objectives

- Optimize existing polymer electrolyte membrane (PEM) fuel cell technology for use with H_2 and reformed hydrocarbons.
- Improve overall PEM fuel cell operating efficiency.
- Improve the efficiency of the fuel cell cathode while lowering the dependence on precious metal loading.
- Achieve 0.4 amps per centimeters squared (A/cm^2) @ 0.8 volt (V) on hydrogen (H_2) with <0.25 milligrams platinum per centimeters squared (mg Pt/cm^2) on cathode
- Demonstrate 0.4 A/cm^2 @ 0.8 V on Reformate with <0.40 mg Pt/cm^2 on cathode
- Initiate Cooperative Research & Development Agreement with Donaldson for studying the effect of ambient air impurities on fuel cell performance.
- Establish the effect of 50 parts per billion hydrogen sulfide on anode performance

Approach

- Investigate the use of a reconfigured anode to improve fuel cell performance in the presence of trace levels of carbon monoxide (CO) impurities.
- Evaluate new anode catalysts for CO tolerance.
- Study the effect of other potential reformate impurities on fuel cell performance.
- Evaluate new cathode catalyst and materials for higher operating efficiencies at lower precious metal loadings.
- Evaluate new membrane electrode assembly (MEA) fabrication protocols to enhance catalyst utilization and overall fuel cell efficiency.

Accomplishments

- Demonstrated the effectiveness of using the reconfigured anode in reformate fuel streams containing up to 250 parts per million (ppm) CO impurity with air bleed.
- Obtained good performances with a new CO tolerant 90:10 ruthenium:platinum anode catalyst.
- Determined the effects of hydrogen sulfide, a potential reformate impurity, on fuel cell performance.
- Screened potential cathode catalysts with reduced platinum loadings.

- Developed new MEA fabrication protocols leading to enhanced catalyst utilization and overall fuel cell performance.

Future Directions

- Investigate alternative catalyst materials for use in reconfigured anodes.
- Evaluate new potential CO tolerant catalysts.
- Further study hydrogen sulfide fuel stream impurity effects and develop technologies to minimize associated performance reduction.
- Screen new potential cathode catalyst materials.
- Continue to develop modified MEA fabrication protocols.

Introduction

The reforming of hydrocarbon fuels is one of the leading processes under consideration for producing hydrogen to power PEM fuel cells. However, the hydrogen stream generated by the reforming process can contain volatile chemical compounds that significantly diminish the fuel cell performance. Two approaches to solving this problem are to lower the level of impurity resulting from the reformation process, or to modify the fuel cell itself to be more tolerant toward those compounds. This study has taken the latter approach; ways were investigated to improve the anode performance in the presence of anticipated reformate impurities.

Fuel cell operation depends not only on hydrogen oxidation at the anode but also on oxygen reduction at the cathode. The oxygen reduction reaction plays a very significant role in limiting the operating efficiency of the fuel cell, and is very dependent on high precious metal loadings in the catalyst layer. Improving the efficiency of this reaction while lowering the precious metal loadings is critical to commercialization of fuel cell technology to automotive applications.

Approach

The predominant deleterious impurity anticipated in the reformate fuel stream is CO. This gas is more strongly absorbed on the surface of the catalyst than hydrogen, effectively blocking the sites where hydrogen oxidation should occur. One method to prevent this from happening is to remove the CO by oxidizing it to harmless carbon dioxide before it can reach and react with the anode surface. This can be accomplished by using the Los Alamos National Laboratory (LANL) reconfigured anode, shown schematically in Figure 1. The reconfigured anode has an outer, non-precious metal catalyst layer added to the standard MEA. Bleeding a low level of air into the fuel stream results in preferential oxidation of the CO at this outer layer.

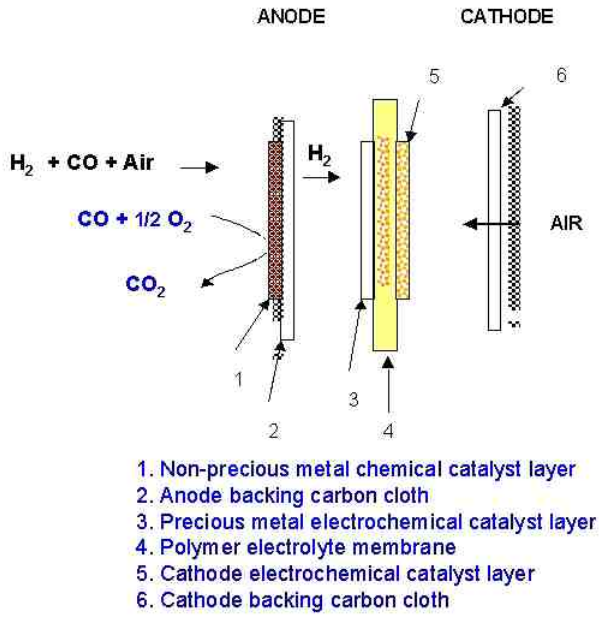

Figure 1. Fuel Cell Schematic with Reconfigured Anode

A second approach to solving the CO problem is to use an anode catalyst that is intrinsically more CO tolerant and that may contain a lower percentage of precious metals. In a given period of time, we receive many new potential catalysts from both commercial and non-commercial sources. These materials are

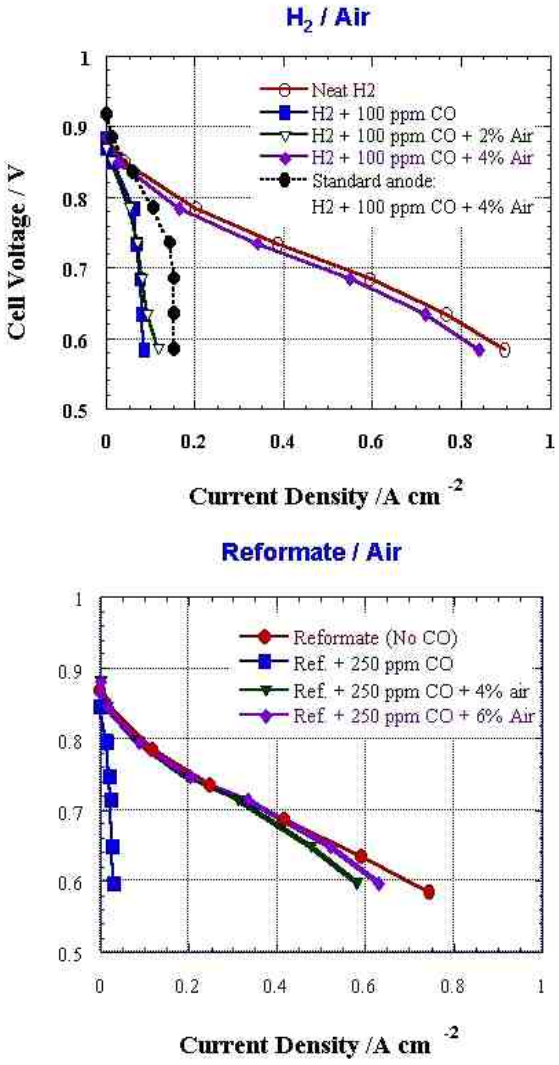

Figure 2. Fuel cell performance at 80°C with reconfigured anode containing a non-precious metal-based chemical catalyst. (0.2 mg Pt/cm^2 at each electrode)

fabricated into MEAs, using a protocol established at LANL, then placed in fuel cells and tested under standard operating conditions.

A third approach to developing better fuel cell anodes is to study the kinetics and mechanisms associated with the reactions of suspected impurities in the reformate stream and various catalysts. The mechanism for CO poisoning of the anode catalyst is fairly well understood, but for other potential poisons that may not necessarily be the case. During this past year such a study has been initiated for hydrogen sulfide, a very likely by-product in reformed fuels initially containing sulfur bearing compounds.

An approach similar to that used to improve anode performance was also applied to the study of the cathode reaction and included the following:

- Develop new MEA fabrication methods to improve catalyst utilization.
- Work with vendors to develop and test new catalyst formulations.
- Study the dependence of performance on catalyst layer structure.
- Study the effects of suspected impurities present in air (sulfur dioxide, nitrogen oxides, particulates) on cathode performance.

Results

Results obtained with the LANL reconfigured anode and platinum anode catalyst are shown in Figure 2. The graph on the top shows the effect of a small amount of CO on the operating characteristics of the fuel cell, with pure hydrogen as a fuel source. There is an almost catastrophic loss of performance when 100 ppm of CO is added to the hydrogen. However, using the reconfigured anode and adding 4% air to the mixture results in essentially complete CO oxidation and restores the performance of the fuel cell. The graph on the bottom shows similar results for a synthetic reformate fuel stream containing 40% hydrogen, 35% nitrogen and 25% carbon dioxide. In this case the effects of adding 250 ppm of CO are fully mitigated with the addition of 6% air.

The second approach of building CO tolerance directly into the anode catalyst has also been confirmed. The most promising results to date were obtained with a catalyst provided by R. Adzic from Brookhaven National Laboratory, composed of 10% ruthenium and 1% platinum on a carbon support. As shown in Figure 3, a significant fraction of the fuel cell performance is restored with the addition of small amounts of air to the fuel stream. Perhaps even more significant is that the total platinum loading of this catalyst is only 18 micrograms per square centimeter, approximately 1/10 that normally used in operating fuel cell anodes.

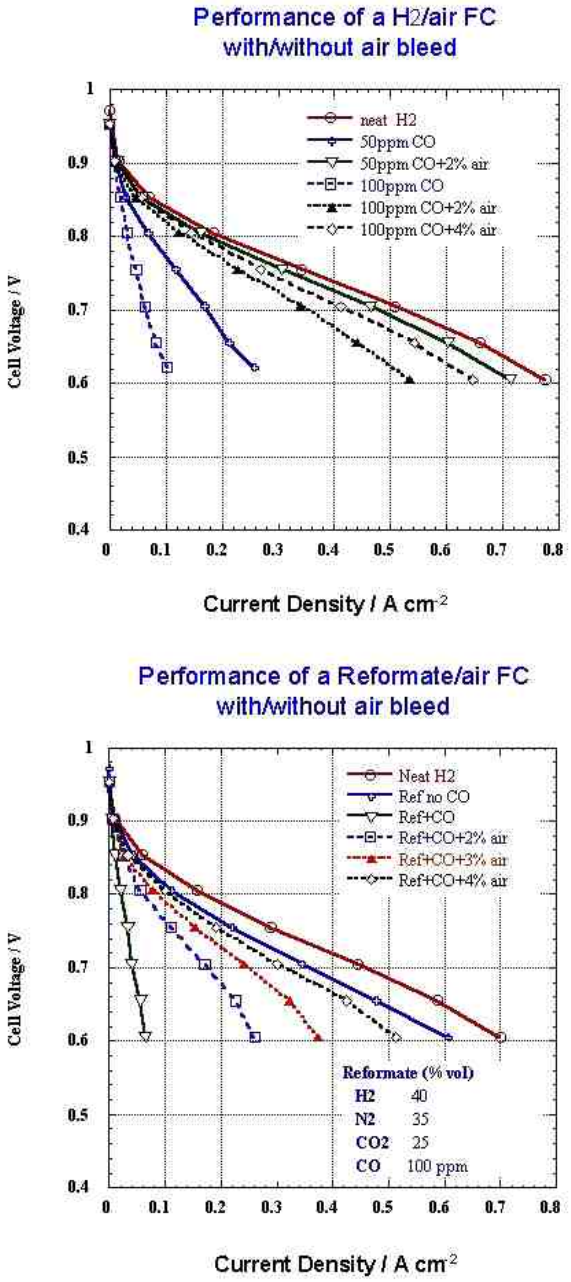

Figure 3. Low Pt Content Anode Catalyst for CO Tolerance (Anode: 0.2 mg Ru-Pt/cm^2; Cathode: 0.2 mg Pt/cm^2)

Preliminary data obtained with hydrogen sulfide, another anticipated reformed fuel impurity, show this compound has an even more serious effect on fuel cell performance than CO. Hydrogen sulfide appears to poison the platinum catalyst irreversibility.

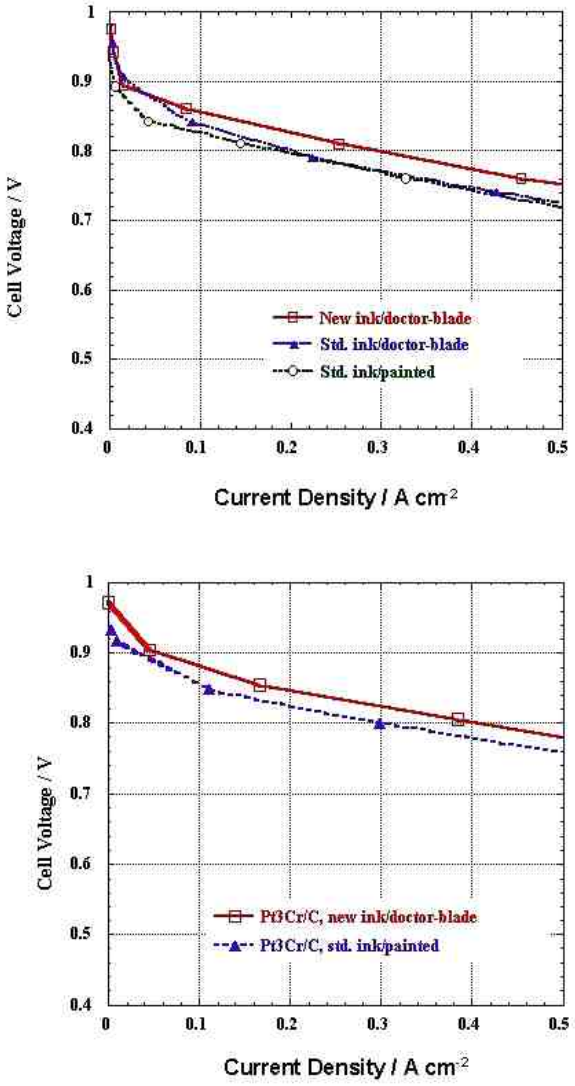

Figure 4. Cathode Optimization: New Catalyst and MEA Preparation (0.2 mg Pt/cm^2 at each electrode)

Results obtained from studies on improving the cathode/oxygen reduction reaction are summarized in Figure 4. This figure shows the effect of changing the catalyst from pure platinum to a platinum-chromium alloy, and of changing the MEA preparation method from the standard painted/decal method to using an automated doctor blade approach. The new catalyst and new preparation method both enhance fuel cell performance.

Conclusions

The performance of fuel cells operating on reformed hydrocarbon fuels is seriously affected by the presence of trace impurities present in the fuel stream. However, a significant fraction of performance losses can be regained by using either a reconfigured anode design or an alternative anode catalyst material. This has been clearly demonstrated for a CO impurity level of up to 250 ppm in the fuel stream. Studies also indicate that using alternative cathode catalyst materials and new MEA preparation methods can still result in further fuel cell performance gains.

FY 2002 Publications\Presentations

1. F. Uribe, S. Gottesfeld and T. Zawodzinski, "The Effect of Ammonia as Potential Fuel Impurity on Proton Exchange Membrane Fuel Cell Performance", J. Electrochem. Soc., 149, A293 (2002).

2. F. Uribe and T. Zawodzinski, "A Study of Polymer Electrolyte Fuel Cell Performance at High Voltages. Dependence on Cathode Catalyst Layer Composition and on Voltage Conditioning". Accepted in Electrochimica Acta. (2002).

3. P. A. Adcock, S. Pacheco, E. Brosha, T. Zawodzinski, and F. Uribe, "Maximization of CO Tolerance of PEMFC Systems Using Reconfigured Anodes". To be presented at the Electrochemical Society Meeting, Salt Lake City, UT (Fall 2002).

4. F. Uribe and T. Zawodzinski, "PEMFC Reconfigured Anodes for Enhancing CO Tolerance with Air Bleed", 201st Electrochemical Society Meeting, Philadelphia (2002). Abstract No. 806.

5. P. Adcock, F. Uribe, J. Valerio and T. Zawodzinski, "New Results for Maximization of CO Tolerance of Hydrogen and Reformate Fuel Cells", 201st Electrochemical Society Meeting, Philadelphia (2002). Abstract No. 814.

6. J. Xie, F. Garzon, T. Zawodzinski, "The Microstructure of the Cathode Catalyst Layer in PEFC's", 201st Electrochemical Society Meeting, Philadelphia (2002). Abstract No. 808.

7. J. Xie, S. Pacheco, K. Wilson, C. Zawodzinski and T. Zawodzinski, "Influence of Ionomer Content in the Cathode Catalyst Layer on the Performance of PEM Fuel Cells", 201st Electrochemical Society Meeting, Philadelphia (2002). Abstract No. 810.

8. E. Brosha, S. Pacheco, P. Zelenay, F. Uribe, F. Garzon and T. Zawodzinski, "Development of Freeze-Dried Catalysts for Hydrogen and Direct Methanol Fuel Cells", Electrochemical Society Meeting, San Francisco, CA (2001). Abstract No. 322.

9. F. Uribe and T. Zawodzinski, "The Effects of Fuel Impurities on PEM Fuel Cell Performance", Electrochemical Society Meeting, San Francisco, CA (2001). Abstract No. 339.

Patent Applications

1. F. Uribe and T. Zawodzinski, "Fuel Cell Anode Configuration for CO Tolerance" (2001).

2. F. Uribe and T. Zawodzinski, "Method for Improving High Cell Voltage Performance for Polymer Electrolyte Membrane Fuel Cell". 2001/0044040 (2001).

IV.D.15 Nondestructive Study of the Water Transport Mechanism Inside Operating PEM Fuel Cells Using Neutron Imaging Techniques

Muhammad Arif (Primary Contact), David Jacobson, Rahul Satija (now at Duke University)
National Institute of Standards and Technology
Gaithersburg, MD 20899
(301) 975-6303, fax: (301) 926-1604, e-mail: arif@nist.gov

DOE Technology Development Manager: Nancy Garland
(202) 586-5673, fax: (202) 586-9811, e-mail: Nancy.Garland@ee.doe.gov

Objectives

Neutron imaging may be the only technique available today that has the realistic possibility of mapping water distribution in flow channels and membranes inside operating PEM fuel cells. This information can be very important to fuel cell developers for designing more robust and efficient fuel cells. Our research objectives are as follows.

- Development of a neutron-imaging facility for studying PEM fuel cell water transport.
- Two-dimensional imaging of time-dependent bulk water distribution in an operating PEM fuel cell and quantification of the results.

Approach

- Phase 1. Define neutron beam characteristics most sensitive to water distribution in fuel cells. Define spatial and temporal resolution parameters for visualization of water/vapor distribution.
- Phase 2. Based on parameters defined in Phase 1, design a new beam line and a charge-coupled device (CCD)-based neutron imaging instrument at the National Institute of Standards and Technology (NIST) nuclear reactor. Make special considerations for easy accessibility and user friendliness of the facility for non-NIST fuel cell researchers.
- Phase 3. Carry out neutron measurements on a working 4-stack PEM fuel cell to define the operating parameters of the new setup and test the limits of achievable spatial and temporal resolution of water distribution and flow dynamics inside a working fuel cell.

Accomplishments

- Designed a state-of-the-art new neutron imaging facility for fuel cell research. This facility will be used for critical water transport studies in the MEA and the flow channels, for the measurement of the hydrogen diffusion co-efficient across the MEA and water/vapor phase, and for evaluation of the integrity of various interfaces. The facility is expected to be operational in October, 2002.
- Using existing facilities, non-destructively imaged and quantified time-dependent water distribution in an operating fuel cell. A near 1 second time resolution was achieved. The total water content inside the fuel cell as a function of time was also quantified.

Future Directions

Three-dimensional imaging of the fuel cell is needed to allow independent measurement of water/vapor distribution parameters within any section or part of the fuel cell.

- Develop neutron-imaging methods to accurately measure water gradients across a fuel cell PEM membrane.
- Determine diffusion coefficient and hydrophobic characteristics of the gas diffusion layer.
- Characterize two-phase flow mechanism in the fuel cell flow field.
- Study the time-dependent membrane-catalyst-gas diffusion layer interface integrity.

Introduction

Compared to most other forms of radiation, neutrons are highly efficient in probing complex structures because of their tremendous penetration capability in almost all known materials and due to their unique ability to distinguish different materials with very similar physical properties. They are particularly effective in detecting hydrogenous materials and other light elements. As a result, neutron imaging is ideally suited for ***non-destructive, in situ visualization and quantification*** of water transport phenomena in operating PEM fuel cells.

Approach and Results

The new setup is being constructed at the BT6 high intensity thermal beam line at the NIST Center for Neutron Research (NCNR) nuclear reactor (Figure 1) to non-destructively characterize water transport mechanism in single or multi-stack PEM fuel cells. The high neutron flux will allow attainment of a time resolution of about 1 sec and a nominal detector spatial resolution of about 30 μm. The imaging process consists of a neutron beam passing through a sample. The beam is attenuated by the presence of hydrogenous material (water vapor/ water) present in the sample (fuel cell as an example). Consequently, an image of the hydrogenous material is formed and recorded by a CCD camera (Figure 2). The digital image is then analyzed to determine the quantity and distribution of water/water vapor inside the fuel cell.

At the imaging station, the largest fuel cell that can be imaged is about 20 cm x 20 cm. A sample of larger length can be imaged section by section through translation of the sample. The fuel cells also can be single- or multi-cell. The facility will operate as a user facility; a proposal will be required and will be reviewed for merit before allocating beam time. A generic fuel cell test station will be available for

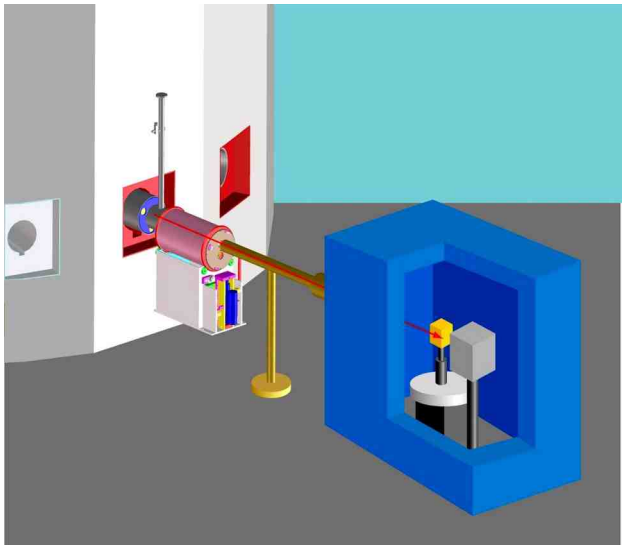

Figure 1. Schematic of New Fuel Cell Imaging Station

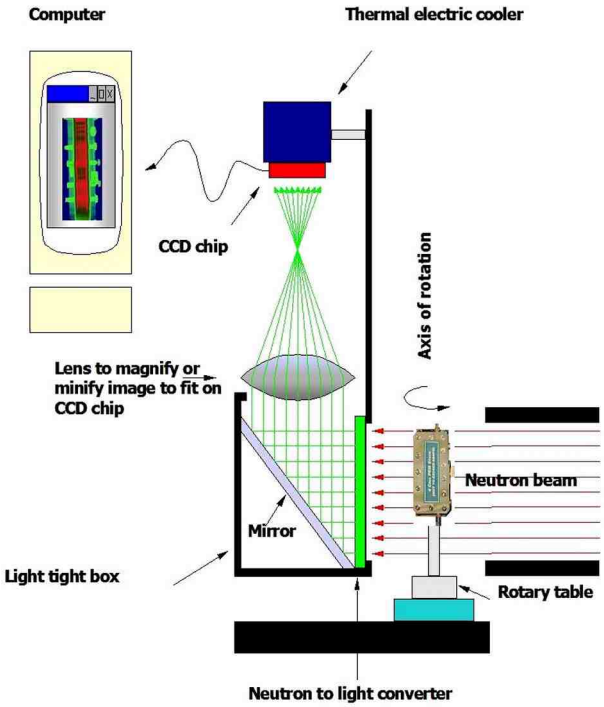

Figure 2. Schematic of Neutron Imaging Setup

general use, but users will be free to bring their own if needed.

To establish operating parameters for the new imaging station, we rotated a 4-cell stack in a high intensity thermal beam at the NCNR reactor and obtained three-dimensional images of the fuel cell as normally done during a medical imaging CAT scan. The cell was imaged while operating with a typical output of about 2.5 A at 3.5 V, and the water (and water vapor) profile in the flow channels was recorded as a function of time (about 1 frame a second). A sample of the water distribution is shown in Figure 3. A graph of the total water content as a function of time is shown in Figure 4. The water content shows periodic behavior with time. From time-lapse images it appears that the water drains only when it reaches a certain volume. The periodic drainage also seems to be un-correlated with the temperature fluctuation and hydrogen flow variations (which were small and random; inconsistent with observed periodicity). The most likely explanation is surface adhesion of water and/or capillary action by the flow channels. We plan to repeat these experiments in a more controlled environment in the near future. The quantification of time-dependent water distribution like this can be very useful in theoretical modeling of fuel cell water transport characteristics.

Conclusions

- A new imaging facility for fuel cell research is expected to be operational in October, 2002. It is a user facility open to researchers from fuel cell manufacturers and automotive companies as well as academic institutions and national laboratories.
- We have been able to observe time dependent water distribution in an operating fuel cell. The result should be useful in modeling water transport mechanism and design of flow channels. We plan to collaborate with University of Miami (among others) in this regard.

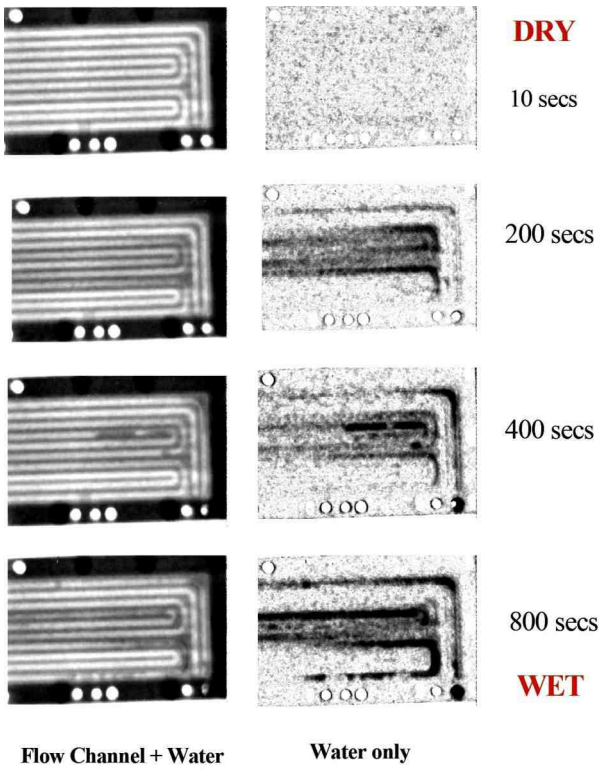

Figure 3. Water Distribution in Flow Channels

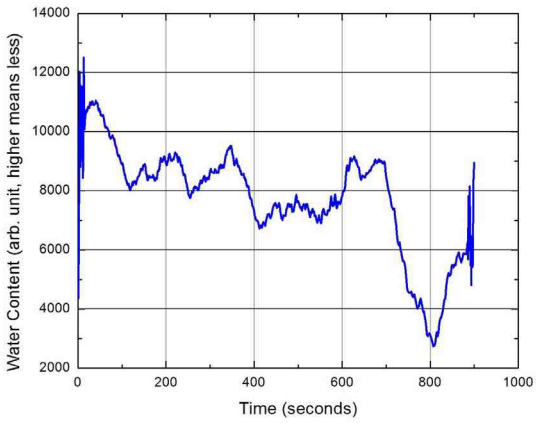

Figure 4. Total Water Content in the Fuel Cell as a Function of Time

IV.D.16 Direct Methanol Fuel Cells

Piotr Zelenay (Primary Contact), Eric Brosha, John Davey, Christian Eickes, Robert Fields, Michael Hickner, Don McMurry, Bryan Pivovar, Geraldine Purdy, John Ramsey, John Rowley, Mahlon Wilson, Christine Zawodzinski, Thomas Zawodzinski, and Yimin Zhu
Materials Science and Technology Division
Los Alamos National Laboratory
Los Alamos, New Mexico 97545
(505) 667-0197, fax : (505) 665-4292, e-mail : zelenay@lanl.gov

DOE Technology Development Managers: Nancy L. Garland and JoAnn Milliken
(202) 586-5673, fax: (202) 586-9811, e-mail: Nancy.Garland@ee.doe.gov
(202) 586-2480, fax: (202) 586-9811, e-mail: JoAnn.Milliken@ee.doe.gov

Objectives

- Develop materials, components and operating conditions of direct methanol fuel cells (DMFCs) for transportation and portable applications optimizing power density, overall fuel conversion efficiency and cost. In particular:
- Design and optimize membrane-electrode assemblies (MEAs) to enhance cell performance.
- Advance electrocatalysis of methanol oxidation and oxygen reduction, thus allowing lower total precious metal loading and/or better cell/stack performance.
- Demonstrate viability of cell components in short- and long-term operation of single cells and stacks.

Approach

- Build and operate single cells and prototype DMFC stacks with different anode and cathode catalysts, membrane materials, flow patterns and optimized MEAs to maximize performance and demonstrate stability.
- Perform complete electrochemical and non-electrochemical testing to gain insight into key factors impacting performance and durability of direct-methanol fuel cells.
- Model, design and fabricate hardware components to optimize performance of single cells and short stacks.

Accomplishments

Catalyst Research

- Identified an alternative binary platinum- patent pending/Carbon (Pt-X/C) cathode catalyst allowing DMFC operation at a voltage 60-80 millivolts (mV) higher than state-of-the-art platinum/carbon (Pt/C) catalysts.
- Established in-house catalyst fabrication capability, by which otherwise unavailable catalysts can be synthesized, e.g., 80 weight percent Pt/C catalyst for the DMFC cathode.
- Optimized composition of cathodes with significantly reduced Pt loading, thus achieving 0.15 watt per centimeter squared (W cm^{-2})with a total precious metal loading of 1.2 milligrams (mgs) cm^{-2} (80°C).
- Completed study of the effect of platinum-to-ruthenium (Pt-to-Ru) ratio on anode performance, demonstrating optimum performance with 55±5 atomic percent of Ru in the anode catalyst layer.

Membrane Research

- Determined sulfonation level and processing method as key to the performance of new sulfonated poly (arylene ether sulfone) membranes (BPSH membranes).
- Developed fabrication techniques and demonstrated BPSH MEAs with relative in-cell selectivity up to 2.5 times that of Nafion®-based MEAs.

Stack Research and Development

- Designed and fabricated components for a new 22 W stack for portable power applications and a new 500 W stack for auxiliary power unit (APU) applications.
- Tested novel hardware designs in single cells and prototype stacks with very good results.

Future Directions

- Continue fundamental research and development of electrocatalysts for methanol oxidation and oxygen reduction.
- Improve performance by optimizing hydrophilic/hydrophobic properties of the cathode.
- Determine the effect of sulfonation on performance of BPSH membranes in DMFCs; narrow the gap between bench-top and fuel cell selectivity of alternative membranes.
- Demonstrate durability of Nafion®-based MEAs in short stacks for 500 hours and alternative MEAs in single cells for 100 hours.
- Investigate composition of the DMFC cathode exhaust at various operating conditions.
- Complete 500 W stack for auxiliary power applications.

Introduction

Direct methanol fuel cell research at Los Alamos National Laboratory (LANL) has focused on developing materials, components and operating conditions relevant to potential applications in portable power (commercial electronics, battery replacement for the military) and transportation (vehicular propulsion, on-board auxiliary power units). The main objective of the LANL research effort in the area of direct methanol fuel cells has been to demonstrate that DMFC-based systems stand a good chance of meeting power-density, overall energy-conversion efficiency and cost targets outlined in the DOE Hydrogen, Fuel Cells and Infrastructure Technologies Program.

Results

In our FY 2002 research, we have focused on the performance of carbon-supported cathode catalysts, especially at low Pt loading. A major achievement has been the introduction of a new binary catalyst, Pt-X (patent application pending). In addition to showing higher activity towards oxygen (concluded from hydrogen/air fuel cell testing), this catalyst appears to be less susceptible to the detrimental action of the crossover methanol than regular Pt/C catalyst. As a consequence of higher activity in the oxygen reduction reaction and improved methanol tolerance, the Pt-X/C catalyst allows DMFC operation at a voltage 60-8-mV high than the voltage achievable with a state-of-the-art commercial PT/C catalyst (De Nora) at the same Pt loading of 0.6 mg cm^{-2} (Figure 1).

We have found that cathodes with significantly reduced Pt loading seem to benefit from the use of carbon-supported catalysts. A comparison of the activity of unsupported Pt cathode catalyst with the activity of carbon-supported Pt catalyst (40% Pt by weight) indicates that carbon-supported catalysts outperform unsupported catalysts as long as Pt loading remains below *ca.* 1 mg cm^{-2}. Also, carbon-supported Pt and Pt-X cathodes both require careful optimization of the ionomer content in the catalyst layer, with the best results obtained at a weight fraction of recast Nafion® between 30 and 40%. Once the anode and cathode catalyst layers are optimized, a very good DMFC performance can be

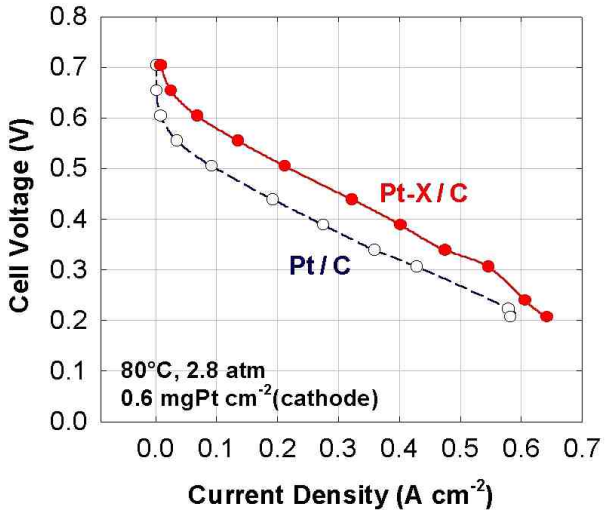

Figure 1. DMFC Performance of Pt-X/C and Pt/C Cathode Catalysts at 80°C - Cathode Pt Loading 0.6 mg cm^{-2}.

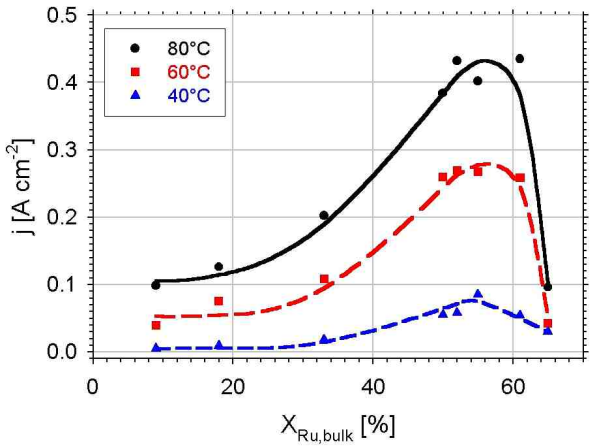

Figure 2. Performance of unsupported Pt-Ru anode catalyst as a function of atomic content of ruthenium in the bulk catalyst phase; current density determined from the anode polarization plots at a potential of 0.35 V *vs.* dynamic hydrogen electrode.

achieved with even moderate Pt loading. One of the highlights of our DMFC research in FY 2002 has been reaching 0.15 W cm^{-2} in aerial power density with a total (anode + cathode) Pt loading of only 1.2 mg cm^{-2} (80°C).

Continuing our anode catalyst effort, we have completed a performance study of unsupported Pt-Ru catalysts, with a Pt-to-Ru atomic ratio ranging from 9:1 to 1:2. This study, conducted in collaboration with Johnson Matthey, has shown that, regardless of the cell operating temperature, the highest activity towards methanol is achieved with catalysts containing 55±5 at% of Ru in the bulk phase (Figure 2). Voltammetric stripping of surface CO has further revealed that the corresponding surface composition of the best-performing catalysts is approximately 30 at% of Ru.

In the past year, we have come considerably closer to the introduction of new ionomeric membranes into direct methanol fuel cells. Most of our membrane/MEA research has focused on the BPSH polymer (collaboration with Virginia Tech). We have found that membrane processing, such as boiling in acidic aqueous solutions, greatly affects the polymer morphology, ability to partially block methanol crossover and, consequently, selectivity in DMFC operation. Once processed, membranes with somewhat lower sulfonation level, BPSH-35 rather than BPSH-40, have been found to perform better in an actual DMFC. A very significant accomplishment of the membrane research in FY 2002 has been successful fabrication and testing of BPSH-based MEAs in direct methanol fuel cells. As shown in Figure 3, these MEAs are capable of performing comparably, if not better, than state-of-the-art MEAs using Nafion®. In addition to offering good cell performance, BPSH MEAs has been found to reduce methanol crossover by as much as 58%, from ~0.12 A cm^{-2} (Nafion® 117) to ~0.05 A cm^{-2} (processed BPSH-35),

Although fundamental research has remained the focal point of the DMFC project at LANL, we have continued prototyping DMFC stacks for the portable power applications and auxiliary power units to prove practical viability of core technology developed at LANL, identify possible scale-up issues, and verify adaptability of the technology to complete systems developed by our partner, Ball Aerospace & Technologies Corporation.

Cell components for a portable power stack have been optimized in single-cell and short-stack testing. The first twenty-two-cell 22 W stack has been built and tested, showing respectable performance at ambient cathode pressure (0.75 atmospheres [atm]),

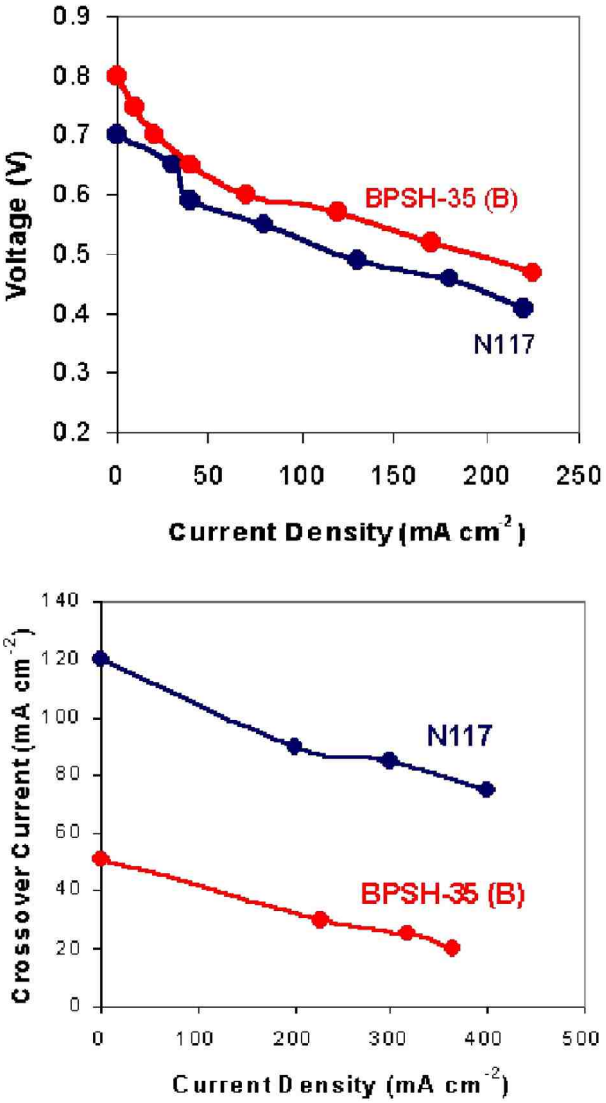

Figure 3. Cell Polarization and Methanol Crossover Plots Obtained with BPSH-35 (pre-processed by boiling) and Nafion® 117 at 80°C - Cell Polarization Data Taken at Ambient Cathode Pressure C_{MeOH}=1.0 mol per liter

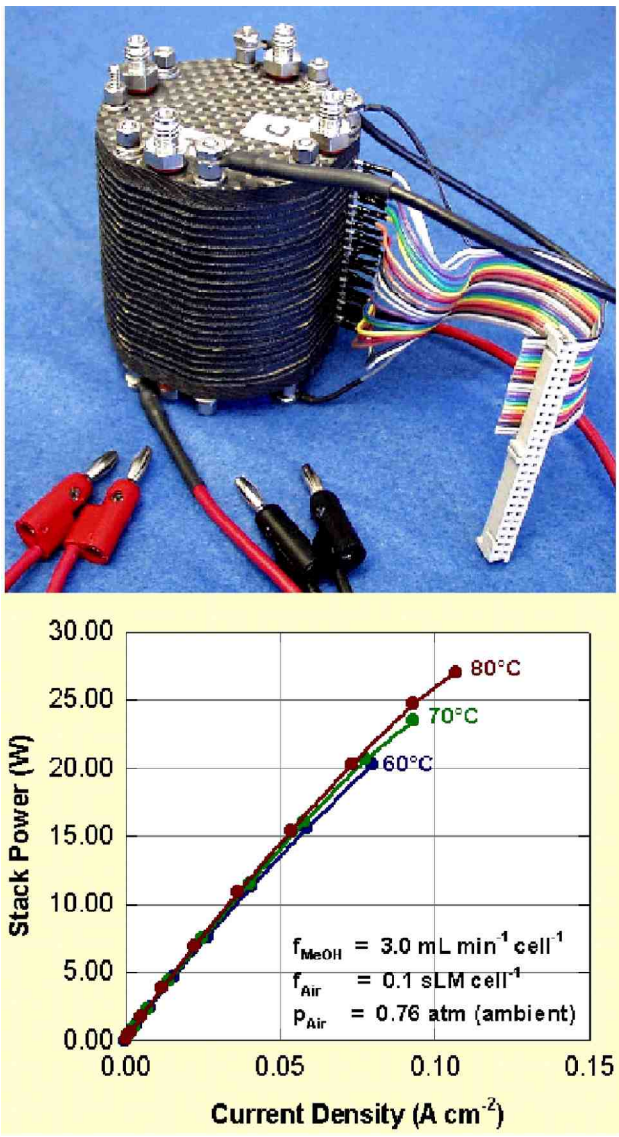

Figure 4. 22 W Portable Power DMFC Stack and selected Performance Data

low air flow (stoichiometry below 3) and relatively high voltage of 0.55 V/cell (Figure 4).

The first-generation APU hardware for MEAs with 100 cm^2 in the active area has been based on high-conductivity graphite plates. The maximum power generated by a single APU cell has been 21 W at a total cathode pressure of 2.8 atm and air stoichiometry of 2.1 (Figure 5). The same cell has delivered *ca.* 11 W at a cathode pressure of 0.76 atm (ambient) and air stoichiometry of only 1.3 (without accounting for the air needed to handle methanol crossover).

Conclusions

DMFC research at LANL in FY 2002 has focused primarily on fundamental issues relevant to potential portable and transportation applications of direct methanol fuel cells, such as cathode and anode electrocatalysis, electrode composition and structure, membrane properties and MEA design. Substantial progress has been achieved in cathode research,

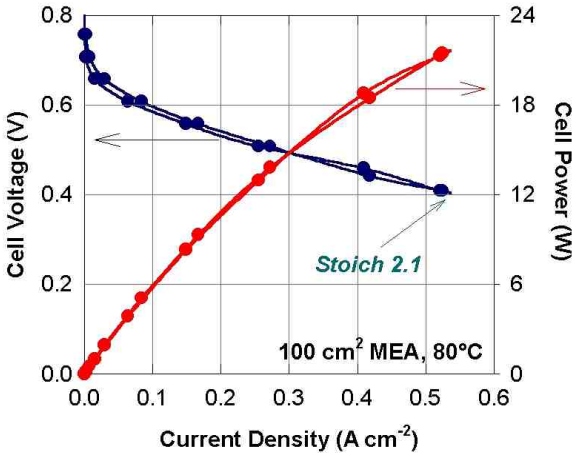

Figure 5. Development of 500 W DMFC stack for auxiliary power system: Single cell polarization and power plots.

which includes the introduction of a highly promising binary catalyst and optimization of catalyst layers at a low Pt loading. The most active composition of the unsupported Pt-Ru anode catalyst has been identified. Major progress has been made in membrane/MEA research, with alternative membrane materials exhibiting greatly reduced crossover rates and in-cell performance at the same, or higher, level as obtained with Nafion® 117. The core MEA technology and fuel cell hardware developed at LANL over the past few years has been incorporated into components for the prototype 22 W and 500 W DMFC stacks for prospective portable and APU use, respectively. The first 22 W stack has been built and tested at ambient cathode pressure and low flow of air, with results clearly demonstrating significant practical potential of DMFCs.

FY 2002 Publications/Presentations

1. Adsorption on Fuel Cell Nanoparticle Electrodes: A Radioactive Labeling Study," P. Waszczuk, A. Wieckowski, P. Zelenay, S. Gottesfeld, C. Coutanceau, J.-M. Léger and C. Lamy, *J. Electroanal Chem.*, 511, 55-64 (2001).

2. Direct Methanol Fuel Cells at Reduced Catalyst Loadings," P. Zelenay, F. Guyon and S. Gottesfeld, in *Direct Methanol Fuel Cells*, S. R. Narayanan, S. Gottesfeld and T. Zawodzinski (Eds.), ECS Proceedings, Electrochemical Society, Pennington, New Jersey, vol. 2001-4, pp. 123-135 (2001).

3. 80 Watt Direct Methanol Fuel Cell Stack for Portable Power Applications", X. Ren, J. Davey, H. Dinh, B. Pivovar, C. Rice, S. Gottesfeld, and P. Zelenay, in *Fuel Cell Technology: Opportunities and Challenges*, Topical Conference Proceedings, 2002 AIChE Spring National Meeting, March 10-14, 2002, New Orleans, Louisiana.

4. Direct Methanol Fuel Cell Performance Using Sulfonated Poly(arylene ether sulfones) Random Copolymers as Electrolytes", B. Pivovar, M. Hickner, J. McGrath, P. Zelenay, and T. Zawodzinski, in *Fuel Cell Technology: Opportunities and Challenges*, Topical Conference Proceedings, 2002 AIChE Spring Meeting, March 10-14, 2002, New Orleans, Louisiana.

5. Influencing the Transport of Water, Methanol and Protons through a Fuel Cell Ion Exchange Membrane", M. Hickner, F. Wang, Y. Kim, B. Pivovar, T. Zawodzinski and J. McGrath, in *Fuel Cell Technology: Opportunities and Challenges*, Topical Conference Proceedings, 2002 AIChE Spring Meeting, March 10-14, 2002, New Orleans, Louisiana.

6. Joint 200th Meeting of the Electrochemical Society and 52nd Meeting of the International Society of Electrochemistry, San Francisco, CA, September 2-7, 2001. Title: "Development of Freeze-Dried Catalysts for Hydrogen and Direct Methanol Fuel Cells"; E. L. Brosha*, S. Pacheco, F. Uribe, H. Garzon, T. A. Zawodzinski.

7. Joint 200th Meeting of the Electrochemical Society and 52nd Meeting of the International Society of Electrochemistry, San Francisco, CA, September 2-7, 2001. Title: "Problems with Membrane Electrode Assemblies for Non-Nafion® Based Membranes"; B. S. Pivovar*, M. Hickner, J. E. McGrath, P. Zelenay and T. A. Zawodzinski.

8. 4th Hawaii Battery Conference 2002, Waikoloa, HI, January 8-11, 2002. Title: "Direct Methanol Fuel Cell Research and Development at Los Alamos National Laboratory" P. Zelenay (*invited lecture*).

9. 2002 Spring National Meeting of American Institute of Chemical Engineers, New Orleans, LA, March 10-14, 2002. Title: "80 W Direct Methanol Fuel Cell Stack for Portable Power Applications"; X. Ren, J. Davey, B. S. Pivovar*, H. N. Dinh, C. Rice, S. Gottesfeld, P. Zelenay.

10. 2002 Spring National Meeting of American Institute of Chemical Engineers, New Orleans, LA, March 10-14, 2002. Title: "Direct Methanol Fuel Cell Performance Using Sulfonated Poly(arylene ether sulfone) Random Copolymers as Electrolytes"; B. S. Pivovar*, M. Hickner, F. Wang, J. McGrath, P. Zelenay, T. A. Zawodzinski.

11. MRS Spring Meeting, San Francisco, CA, April 2, 2002. Title: "System and Material Issues in Direct Methanol Fuel Cells"; B. S. Pivovar (*invited talk*).

12. 223rd Meeting of American Chemical Society, April 7-11, Orlando, FL. Title: "Electrocatalysis in Direct Methanol Fuel Cells"; P. Zelenay (*keynote lecture*).

13. 223rd Meeting of American Chemical Society, April 7-11, Orlando, FL. Title: "DMFC Activity of Pt:Ru Blacks of Different Composition"; C. Eickes*, P. Zelenay, T. Morita and D. Thompsett.

14. 223rd Meeting of American Chemical Society, April 7-11, Orlando, FL. Title: "Novel Pt/Ru Catalyst for the DMFC Anode: Electrochemical Cell and DMFC Testing"; P. Waszczuk, H.-S. Kim, A. Wieckowski, Y. Zhu, P. Zelenay*.

15. 201st Meeting of the of the Electrochemical Society, Philadelphia, Pennsylvania, May 12-17, 2002. Title: "DMFC Cathode Catalyst with Improved Methanol Tolerance"; Y. Zhu*, P. Zelenay.

16. Annex XI Meeting of International Energy Agency Meeting, May 17-18, 2002, Philadelphia, Pennsylvania, Title: "80 W DMFC Stack and Performance Data"; X. Ren, J. Davey, B. S. Pivovar, H. N. Dinh, C. Rice, S. Gottesfeld, P. Zelenay*.

IV.D.17 Development of Advanced Catalysts for Direct Methanol Fuel Cells

S. R. Narayanan
Jet Propulsion Laboratory
California Institute of Technology
Pasadena, California 91109
(818) 354-0013, fax: (818) 393-6951, e-mail: s.r.narayanan@jpl.nasa.gov

DOE Technology Development Managers:
JoAnn Milliken: (202) 586-2480, fax: (202) 586-9811, e-mail: JoAnn.Milliken@ee.doe.gov
Nancy Garland: (202) 586-5673, fax: (202) 586-9811, e-mail: Nancy.Garland@ee.doe.gov

Objectives

- Reduce catalyst cost for direct methanol fuel cells (DMFCs).
- Demonstrate feasibility of reducing Pt-Ru catalyst loading to 0.5 mg/cm^2 using thin film deposition techniques.
- Develop a low-cost manufacturing technique for MEA fabrication.
- Prepare and identify low-cost alternatives to Pt-Ru based on Ni, Zr, and Ti catalysts.

Approach

- Utilize direct current (DC) magnetron sputter-deposited multi-component catalyst layers.
- Employ reactive sputter-deposition of alloys and oxides.
- Characterize half-cells and full cell MEAs electrochemically.
- Characterize structural and electronic properties.

Accomplishments

- Platinum-Ruthenium alloy films of various compositions have been sputter-deposited and characterized in half-cells and full cells.
- Fuel cell performance has been improved from 100 mW/mg to 800 mW/mg at 0.1 mg/cm^2 of catalyst at the anode.
- Effect of reactive co-sputtering of RuO_x has been studied and determined not to have any beneficial effect.
- A unique metal nanostructure has been developed by pretreatment of Nafion films.

Future Directions

- Prepare and characterize ternary Pt M_x M_y films by December 2002.
- Deposit corrosion resistant alloy films of base metals by June 2003.
- Demonstrate 2000 mW/mg by June 2003.
- Characterize metal/metal oxide systems by December 2003.
- Demonstrate 2500 mW/mg by June 2004.

Introduction

Fuel cells offer the possibility of reduced emissions and high efficiency for transportation applications. Of the various fuel cells being considered, the direct methanol fuel cell (DMFC) is very attractive due to the key advantages of reducing system complexity and potentially improving transient response compared to reformate-air fuel cell systems. However, DMFCs currently require unsupported noble metal catalysts at high loadings of 2.5 – 4.0 mg/cm^2, leading to a high catalyst cost of $100-150/kW. Also, to keep the overall fuel cell cost low, the preferred method of catalyst application must be designed for manufacturing. Thus, cost presents a major obstacle to commercialization of DMFCs. Enhancement of the efficiency of this fuel cell is also necessary to achieve the required weight and volume required for transportation applications. This research effort aims at addressing these key issues of cost and efficiency.

The overall objective is to develop new methods of preparing electrocatalysts, novel electrode structures, and new-low cost electrocatalysts that will result in overall cost reduction and improved performance of direct methanol fuel cells.

The specific objectives are:

- Reduce the catalyst loading levels of Pt-alloy in DMFCs to 0.5 mg/cm^2 or less
- Develop new low-cost methods of fabricating membrane-electrode assemblies
- Prepare catalysts with enhanced activity for methanol electro-oxidation
- Develop non-noble metal methanol oxidation catalysts.

Approach

The Jet Propulsion Laboratory (JPL) has researched the stated objectives by investigating sputter-deposition (SD) of designed anode and cathode nanostructures of Pt-alloys, and electronic structures and microstructures of sputter-deposited catalyst layers. JPL has used the information derived from these investigations to develop novel catalysts and membrane electrode assemblies (MEAs) that will meet the DOE objectives of lower fuel cell cost and high performance.

SD is routinely used to deposit thin films and has proven benefits from economies of scale in the metallization of plastics. The technique has already been used to create enhanced and unique MEAs for H_2-air proton exchange membrane fuel cell (PEMFC) systems. In this project, JPL is pursuing the use of SD to create DMFC membrane electrode assembly structures with highly electro-active catalyst layers that will reduce the amount and cost of the Pt-alloy catalyst at the fuel cell anode.

The research involves the development of techniques for deposition of porous catalyst layers by defining the conditions of pressure, sputter rates, and target configurations that will result in appropriate compositions and morphology for the catalyst layer. The effect of catalyst structure and composition on the activity of the catalyst layers will be characterized by x-ray diffraction (XRD), x-ray photoelectron spectroscopy (XPS), scanning electron microscopy (SEM), x-ray absorption spectroscopy (XAS), and electrochemical polarization studies in half cells and full cells. New base metal and noble metal alloys and oxides will also be studied with an aim to identify new compositions that will result in enhanced activity. The catalyst activity target is 2500 mW/mg of anode catalyst.

Results

The main focus of this year's effort has been on the deposition and characterization of platinum-ruthenium films of various compositions produced by co-sputtering of the individual elements. The effect of ruthenium deposited by reactive co-sputtering has also been studied. The sputtering chamber was modified with a linear drive to be able to produce films on graphite foils, porous carbon structures, and on membranes. Thin films were deposited on graphite foil electrodes and characterized by XRD, XPS, SEM and polarization experiments.

XRD results indicate that the alloy phase exhibits continuous change in lattice parameter and a change in structure from a face-centered cubic (fcc) to a hexagonal close pack (hcp) lattice consistent with the

formation of a solid solution. The alloy deposit exhibits fine grain characteristics with crystallite size of about 15-25 nanometers. These grain sizes are about 3 to 4 times smaller than those observed in chemically prepared materials. Electrochemical activity as measured in half-cells and full-cells increases with platinum content, and the lowest Tafel slopes were obtained for a bulk composition of 50/50 atomic weight % of Pt/Ru. XPS analysis indicated small amounts of oxides of platinum and ruthenium on the surface. The oxide content was approximately 30% and did not seem to depend on the metal composition.

Cyclic voltammetric studies indicated that the activity of the Pt-Ru films increased with operating temperature just as in conventional catalyst layers produced from unsupported catalyst inks. Membrane electrode assemblies were fabricated from Pt-Ru films of the most active compositions, and a power density of 800 mW/mg was realized for anodes that were deposited with about 0.1 mg/cm^2 of Pt-Ru (see Figure 1). Applying the catalyst layers by sputter deposition on the electrode was found to yield better performance than applying them on the membrane. This was attributed to the enhanced electrical connectivity achieved when the catalyst layer is applied on the electrode. However, this is only true for very thin films. When thicker composite films are produced, such as those planned later in this project, good electrical connectivity may be achieved even with membrane deposition.

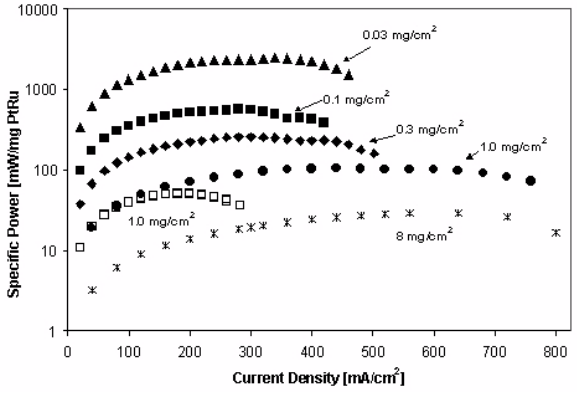

Figure 1. Catalyst Utilization Curves for Sputter-Deposited (filled symbols), Carbon Supported (□, 1.0 mg/cm^2), and Conventional (∗, 8.0 mg/cm^2) Pt-Ru

SEM photographs of sputtered films show that the layers are fairly dense and appear to crack into platelets when subjected to MEA fabrication. The dense films do not lend themselves to high surface areas; therefore, there is substantial scope for enhancement of performance if the surface area can be increased. This may be achieved by producing porous 3-D Pt-Ru layered structures. One such method for creating such 3-D structures, that seem to be extremely promising, involves the pre-treatment of the membrane surface by ion-beam etching, which is then followed by sputter-deposition of the metal. This results in substantially enhanced surface area and very rough nanostructures. Next year's effort will include characterization of such films.

Electrodes were fabricated with catalyst layers containing platinum-ruthenium alloys and platinum-ruthenium oxide. Membrane electrode assemblies were fabricated with such cells, and the performance was evaluated in a full cell configuration. Although ruthenium oxide is a proton conductor and is expected to enhance the rate of proton transport from the interface during methanol oxidation, no noticeable improvement in activity of the catalyst layer was observed by addition of ruthenium oxide. The role of other metal oxides such as tungsten oxide will be investigated next year, along with evaluation of non-noble metal catalysts based on nickel, titanium, and zirconium.

Conclusions

High catalyst activity and utilization of sputtered thin films was demonstrated in operating fuel cells. Optimal sputter-deposition conditions for platinum-ruthenium alloys have been determined. The effect of composition on the performance of Pt-Ru films was studied, and optimal composition has been determined. Novel methods of enhancing surface area and improving porosity have been identified. Co-sputtered ruthenium oxide has been demonstrated not to have any significant beneficial effect on the activity of the catalyst layers. While cost presents a major obstacle to commercialization of DMFCs for mobile applications, this project demonstrates novel means to reduce the catalyst costs in DFMC fuel cells. Efficiency enhancements that are also necessary for DMFCs to be viable will be addressed

in the subsequent phases of the project under the development of new catalysts.

Publications and Presentations

1. C. K. Witham,T.I. Valdez, and S. R. Narayanan, "Nanostructured Catalysts for Direct Methanol Fuel Cells", 200th Electrochemical Society Meeting, Philadelphia, May 2002

2. C. K. Witham, T. I. Valdez, and S. R. Narayanan, "Methanol Oxidation Activity of Co-Sputter Deposited Pt-Ru Catalysts", Proceedings of the Symposium on Direct Methanol Fuel Cells, Electrochemical Society, PV 2001-4, p.123

IV.D.18 Carbon Composite Bipolar Plates

T. M. Besmann (Primary Contact), J.W. Klett, and J. J. Henry, Jr.
Surface Processing and Mechanics Group and Carbon and Insulating Materials Group
Oak Ridge National Laboratory, P.O. Box 2008, MS 6063, Bldg. 4515
Oak Ridge, TN 37831-6063
(865) 574-6852, fax: (865) 574-6198, e-mail: besmanntm@ornl.gov

DOE Technology Development Managers:
JoAnn Milliken: (202) 586-2480, fax: (202) 586-9811, e-mail: JoAnn.Milliken@ee.doe.gov
Nancy Garland: (202) 586-5673, fax: (202) 586-9811, e-mail: Nancy.Garland@ee.doe.gov

ORNL Technical Advisor: David Stinton
(865) 574-4556, fax: (865) 574-6918, e-mail: stintondp@ornl.gov

Objectives

- Develop a slurry molded carbon fiber material with a carbon chemical vapor infiltrated sealed surface as a bipolar plate.
- Collaborate with potential manufacturers with regard to testing and manufacturing of such components.

Approach

- Fabricate fibrous component preforms for the bipolar plate by slurry molding techniques using carbon fibers of appropriate lengths.
- Fabricate hermetic plates using a final seal with chemical vapor infiltrated carbon.
- Develop commercial-scale components for evaluation.

Accomplishments

- Developed carbon composite material with graphite particulate filler to control pore size and speed surface sealing.
- Further characterized and measured mechanical properties of carbon composite plate material.
- Significantly improved wetting of bipolar plate surface.
- Determined surface roughness of finished bipolar plate components.
- Supported scale-up efforts at licensee Porvair Fuel Cell Technology.

Future Direction

- Develop bipolar plate materials/configurations to meet various users' unique requirements.
- Improve wetting properties of carbon surfaces.
- Decrease component thickness.
- Transfer technology and aid in scale-up with Porvair.

Introduction

In FY 2002, the Oak Ridge National Laboratory (ORNL) carbon composite bipolar plate effort has achieved several programmatic goals in measuring plate properties and improving wetting. It is necessary to have accurate mechanical property information for the bipolar plates in order to assure they will survive handling, assembly, and service. These measurements need to go beyond simple tensile or flexure strength, since the relatively thin plates will be subjected to combined tension-torsion loading in assembly and to potentially high rates of stress during handling and service. Thus, torsion behavior and fracture toughness are particularly important to understand. Measurements of these properties, along with methodologies to demonstrate material uniformity through thermal imaging, have been developed.

Approach

Fibrous component preforms for the bipolar plate are prepared by slurry molding techniques using 100-µm carbon fibers (e.g., Fortafil) in water containing phenolic resin followed by curing. Molds are used to impress channels and other features into the preform, and the surface of the preform was sealed using a chemical vapor infiltration (CVI) technique in which carbon is deposited on the near-surface fibers sufficient to make the surface hermetic. In the current work, differing amounts of carbon flake filler were used and the effects on properties determined. Infrared imaging to identify defects and inhomogeneities was performed by heating one side of the samples and imaging the opposite side. Shear stress is a good measure of torsion behavior. Thus, the Iosipescu method was used to measure shear properties, whereby the shear strength of one of the different material shear planes of a composite may be determined by loading a coupon in the form of a rectangular flat strip with symmetric centrally located V-notches using a mechanical testing machine and a four-point asymmetric fixture. Failure of the specimen occurs by shear between the V-notches. The efforts to improve wetting of the carbon surface consisted of briefly heating the components to 1000°C in air.

Results

Slurry-molded preforms 2.5 mm in thickness were produced and cut into 5-cm squares. Illustrative results of the thermal imaging are seen in Figure 1. The relative uniformity indicates little density difference within the plates and between plates. There is some indication of delamination along the edges, although this is likely due to cutting of a larger plate into the 5 cm samples.

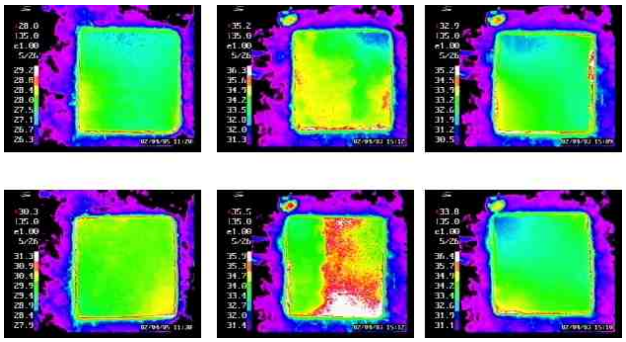

Figure 1. Infrared Images of Carbon Composite Bipolar Plate Material Samples

The Iosipescu torsion measurement results are given in Table 1, with an example stress-displacement curve shown in Figure 2. These values are indicative of a relatively torsion-resistant material, particularly given the low density of the carbon composite. The stress-displacement curves indicate little delamination or other failures until ultimate failure.

Sample (% Filler)	Strength Measurement
PMP10R (0%)	25.9±9.9 MPa
PMP10T (0%)	19.3 MPa (1 test)
PMP09K (15%)	24.4±11.8 MPa
PMP11E (30%)	43.3±2.7 MPa
PMP11G (30%)	17.1±1.1 MPa
PMP11H (30%)	18.7±4.7 MPa

Table 1. Measurements of Shear Stress by the Iosipescu Method for Carbon Composite Samples with Differing Amounts of Carbon Flake Filler

The dramatic improvement in wetting of the carbon composite surface with treatment is seen in Figure 3. Whereas, prior to oxidative treatment, water appeared to have a small wetting angle on the surface of the carbon composite, water readily spread

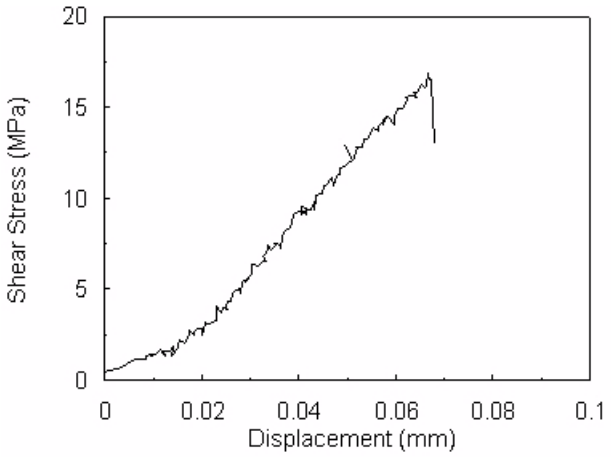

Figure 2. Typical Stress-Displacement Curve for the Iosipescu Torsion Measurement of the Carbon Composite Bipolar Plate Material

on the surface after treatment with an apparent large wetting angle.

Conclusions

During this period, the mechanical properties of the carbon composite bipolar plate material were assessed, including measurements of uniformity and defect distribution by infrared imaging. The results indicate good material uniformity and substantial resistance to torsional stresses. Significant improvement in the wetting of the material was demonstrated after a simple oxidation treatment.

FY 2002 Publications/Presentations

1. T. M. Besmann, J. W. Klett, J. J. Henry, Jr., and T. D. Burchell, "Carbon Composite Bipolar Plates for PEMFC," 26th Annual International Conference on Advanced Ceramics and Composites, January 13-18, Cocoa Beach, FL.

2. T. M. Besmann, J. W. Klett, J. J. Henry, Jr., and E. Lara-Curzio, "Carbon/Carbon Composite Bipolar Plate for PEM Fuel Cells," National Meeting of the American Institute of Chemical Engineers, March 10-14, New Orleans, LA.

3. T. M. Besmann, J. W. Klett, J. J. Henry, Jr., and T. D. Burchell, "Carbon Composite Bipolar Plate for PEMFC," Future Car Congress, June 3-5, Arlington, VA.

Figure 3. Water Illustrates a Much Larger Wetting Angle on the Carbon Composite after Oxidative Treatment

IV.D.19 Cost-Effective Surface Modification for Metallic Bipolar Plates

M.P. Brady
MS 6115, Oak Ridge National Laboratory
P.O. Box 2008, Oak Ridge, TN 37831-6115
(865) 574-5153, fax: (865) 241-0215, e-mail: bradymp@ornl.gov

DOE Technology Development Managers:
JoAnn Milliken: (202) 586-2480, fax: (202) 586-9811, email: JoAnn.Milliken@ee.doe.gov
Nancy Garland: (202) 586-5673, fax: (202) 586-9811, e-mail: Nancy.Garland@ee.doe.gov

ORNL Technical Advisor: David Stinton
(865) 574-4556, fax: (865) 574-6918, e-mail: stintondp@ornl.gov

Objective

- Develop a low-cost metallic bipolar plate alloy that will form an electrically conductive and corrosion resistant nitride surface layer during thermal nitriding to enable use in a PEM fuel cell environment.

Approach

- Conduct a study of the nitridation behavior of a series of model Ni-X and Fe-X base alloys (X = nitride forming elements such as Cr, Nb, Ti, V) that can potentially meet DOE bipolar plate cost goals.
- Identify the most promising combination of X additions, ternary and higher order alloying addition(s), and nitridation reaction conditions that result in the formation of an adherent, dense nitride surface layer.
- Evaluate corrosion behavior in 80°C sulfuric acid solutions to simulate PEM fuel cell environments (in collaboration with K. Weisbrod and C. Zawodzinski of Los Alamos National Laboratory and I. Paulauskas and R.A. Buchanan of the University of Tennessee)
- Characterize nitride layer microstructure and composition by x-ray diffraction, electron probe microanalysis, scanning electron microscopy, and transmission electron microscopy. Use this information in a feedback loop to modify alloy chemistry and nitridation processing conditions to optimize the protectiveness of the nitride surface layer.
- Measure electrical conductivity of select nitrided alloys by D.C. four-point probe.
- Down-select model Ni-Fe-X alloy for in-cell performance evaluation and begin modification and optimization of alloy composition/nitridation conditions for commercial scale up and/or identify nitridation conditions suitable for commercially available alloys (if feasible).

Accomplishments

- A model nitrided Ni-50Cr wt% alloy exhibited no discernible degradation after 1 week immersion in pH 2 sulfuric acid at 80°C and a corrosion current density of less than 1 x 10^{-6} A/cm^2 up to ~ 0.9 V vs. standard hydrogen electrode (SHE) in pH 3 sulfuric acid at 80°C. This level of corrosion resistance is in the range of the goal for metal bipolar plates and warrants scale-up to in-cell testing and evaluation. Further, the Cr-nitride layers formed on the Ni-50Cr alloy grow in a very robust manner such that lack of coverage over features such as stamped flow fields does not appear to be a major issue. Preliminary measurement of electrical properties of a nitrided coupon indicated an electrical conductivity in the $10^4\Omega^{-1}cm^{-1}$ range, which is two orders of magnitude greater than the DOE target.

- Coupons of nitrided Ni-50Cr were delivered to Los Alamos National Laboratory for further corrosion testing and evaluation. Preliminary feedback from ongoing exposure in the Corrosion Test Cell indicate stable electrical resistance (collaboration with K. Weisbrod).
- A United States provisional patent disclosure was submitted in April 2002 for nitrided Ni-Cr and related base alloys.

Future Directions

- Pursue in-cell testing of nitrided Ni-50Cr to determine if the promising corrosion resistance translates to in-cell performance.
- Optimize nitridation conditions and reduce the level of Cr to below 40-42 wt.% in order to improve the cold formability of the alloy and reduce processing and raw material costs (based on input from commercial alloy producers).
- Investigate the nitriding characteristics of existing commercial high-Cr-, Ni- and Fe- base alloys to determine if a similar corrosion resistant Cr-nitride layer can be formed in order to facilitate scale-up and transfer of this technology.
- Establish partnerships with alloy producers and fuel cell manufacturers.

Introduction

The bipolar plate is one of the most expensive components in proton exchange membrane (PEM) fuel cells. Thin metallic bipolar plates offer the potential for significantly lower cost than conventional machined graphite bipolar plates and reduced weight/volume and better performance than developmental carbon fiber and graphite bipolar plates currently under consideration. However, inadequate corrosion resistance can lead to high electrical resistance and/or can contaminate the proton exchange membrane. Metal nitrides (e.g. TiN or Cr_2N) offer electrical conductivities up to an order of magnitude greater than that of graphite and are highly corrosion resistant. Unfortunately, most conventional coating methods for metal nitrides are too expensive for PEM fuel cell stack commercialization or tend to leave pin-hole defects, which result in accelerated local corrosion and unacceptable performance.

Approach

The goal of this effort is to develop a bipolar plate alloy that will form an electrically conductive and corrosion resistant nitride surface layer during thermal (gas) nitriding. There are three advantages to this approach. First, because the nitriding is performed at elevated temperatures, pin-hole defects are not expected because thermodynamic and kinetic factors favor complete conversion of the metal surface to nitride. Rather, the key issues are nitride layer cracking, adherence, and morphology (discrete internal precipitates vs. continuous external scales), which can potentially be controlled through proper selection of alloy composition and nitridation conditions. Second, thermal nitridation is an inexpensive, well-established industrial technique. Third, the alloy can be formed into final shape by inexpensive metal forming techniques such as stamping prior to thermal nitridation.

Results

A series of model Ni-base alloys with additions of (5-15)Ti, (5-10)Nb, (10-15)V, (5-10)Nb + (5-15)V and (35-50)Cr wt%, to form external Ti, Nb, V, Nb+V, or Cr based nitride layers, was studied (Table 1). Ni was selected as the initial alloy base because it is relatively inexpensive ($2-4/lb), has good ductility, doesn't compete with Cr during thermal nitridation, and exhibits a relatively low permeability to nitrogen, which favors external nitride layer formation.

Corrosion behavior was screened by a 1 week immersion in pH 2 sulfuric acid at 80°C in order to optimize alloy composition and nitridation conditions. Anodic polarization testing was then conducted on the most promising nitrided alloys in aerated pH 3 sulfuric acid at 80°C to quantify

Alloy Base (wt.%)	Nitridation Conditions (high-purity nitrogen)		Nitrogen Uptake (mg/cm^2)
	Temperature	Time (h)	
Ni-(5-15)Ti	1000-1100°C	8-48	0.1-1
Ni-(5-10)Nb	900-1100°C	1-48	0.1-2
Ni-(10-15)V	1100°C	24-48	0.5-1
Ni-(5-10)Nb-(5-15)V	1100°C	24-48	0.5-1
Ni-(35-50)Cr	1100°C	1	1.5-2

Table 1. Summary of Nitriding Conditions

corrosion resistance. A corrosion current density of less than 1 x 10^{-6} A/cm^2 up to a range of approximately 0.9 V vs. standard hydrogen electrode (SHE) was considered indicative of sufficiently promising behavior to warrant further development and future in-cell stack testing.

Nitrided Ni-(5-10)Ti base alloys (to form an external TiN base layer) exhibited relatively low corrosion currents (Figure 1). However, regions of through thickness local attack of the TiN surface layer were evident in most of the coupons. Nitrided Ni-(5-10)Nb + (5-15)V wt% base alloys formed external Ni-Nb-V-N and Nb-V-N scales which resulted in good corrosion resistance in the 1 week immersion screening in pH 2 sulfuric acid at 80°C (weight loss <-0.05 mg/cm^2) but exhibited high corrosion currents in the anodic polarization testing (10^{-5}– 10^{-4} A/cm^2 range at 0.9 V vs. SHE). The Ni-(10-15)V wt% alloys formed external V-N layers after the nitridation treatment, but exhibited relatively high weight losses in the sulfuric acid immersion screenings (3-5 mg/cm^2 loss after 1 week). External Nb-N layers could not be formed on Ni-(5-10)Nb wt.% alloys under the nitridation conditions used in the present work (Table 1).

Of the nitrided alloys examined, Ni-50Cr wt.% exhibited the most corrosion resistance and met the target corrosion current of less than 1 x 10^{-6} A/cm^2 up to ~ 0.9V vs SHE in pH 3 sulfuric acid at 80°C (Figure 1 and Table 1). The post-nitridation microstructure of all the Ni-Cr alloys (35Cr, 45Cr, 50Cr wt.%) examined, nitrided for 1-2 h at 1100°C in nitrogen, consisted of external Cr_2N overlying a

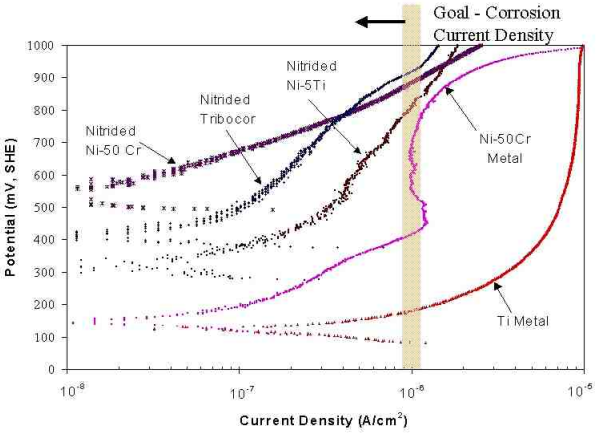

Figure 1. Anodic polarization data in aerated pH 3 sulfuric acid at 80°C (scan rate of 0.1 mV/s)

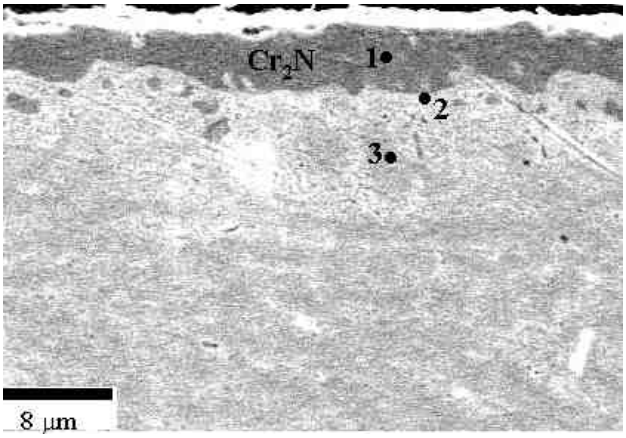

Figure 2. Scanning electron microscopy cross-section of Ni-50Cr wt% nitrided for 2 h at 1100°C in N_2. point 1- external Cr_2N scale: 69Cr-30N-1Ni atomic percent (at.%), point 2- Cr-depleted Ni(Cr) metal (light): 68Ni-32Cr at.% (71Ni-29Cr wt%), point 3- subscale ternary Ni-Cr-N phase (dark): 52Cr-14N-34Ni at.%. Compositions determined by electron probe microanalysis using pure element standards for Ni, Cr and a Cr_2N standard for nitrogen.

mixed zone of Cr-depleted Ni(Cr) and a ternary Ni-Cr-N subscale nitride (Figure 2) (occasional examples of internal Cr_2N were also observed in the lower Cr alloys). The degree of continuity, and hence protectiveness, of the external Cr_2N improved with increasing alloy Cr content, with a dense nearly continuous or continuous layer formed on Ni-50Cr. Optical analysis after testing revealed no evidence of significant corrosion or breaching of the nitride layer

formed on the Ni-50Cr. Uncoated Ni-50Cr metal also exhibited relatively low corrosion currents (Figure 1) but showed evidence of pitting after the test exposure.

The nitridation of the Ni-50Cr alloys was very robust, with no evidence of inadequate coverage at sharp corners or edges. Figure 3 shows a coupon of Ni-50Cr that was hand stamped with the letters "ORNL", nitrided, and then immersed in pH 2 sulfuric acid at 80°C for 1 week; there was no attack evident in the stamped regions. These results suggest that the present approach is amenable to coverage and protection of stamped flow field features in a bipolar plate. Bulk electrical conductivities were in the range of 1-2 x 10^4 $\Omega^{-1}cm^{-1}$ after nitriding, which surpasses the DOE electrical conductivity target by two orders of magnitude.

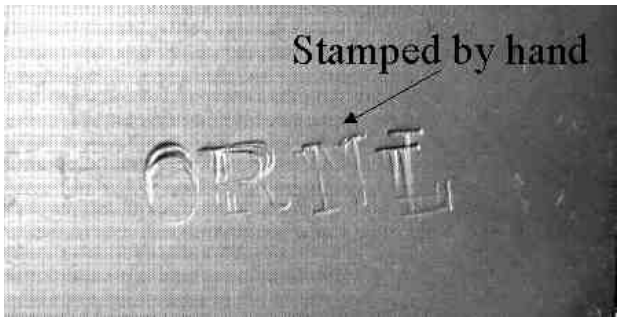

Figure 3. Macrograph of stamped and nitrided Ni-50Cr coupon after 1 week exposure in pH 2 sulfuric acid at 80°C (coupon dimensions 1" X ½").

Conclusions/Future Work

These results indicate that nitrided Ni-Cr base alloys show potential for use as bipolar plates in PEM fuel cells. Future work will focus on in-cell testing of nitrided Ni-50Cr to determine if the promising corrosion resistance demonstrated in the anodic polarization testing translates to good in-cell performance. From a cost and alloy processing perspective, lower levels of Cr are needed, ≤ ~ 40-42 wt% range [1], particularly in terms of the rate of work hardening during cold rolling, to allow the economical production of alloy sheet. The critical level of Cr needed to form an external nitride layer on binary Ni-Cr alloys is in the range of 30-40 wt% Cr [2], so a reduction below 50 wt% Cr appears feasible with proper adjustment of nitridation conditions (e.g. temperature, N_2 vs. NH_3 environments, initial surface condition) to form a sufficiently continuous and dense Cr_2N (or possibly CrN) layer. Reduction in Cr level may also be achievable through ternary alloying additions that form nitrides of intermediate thermodynamic stability between those of Cr and Ni, ie. secondary gettering [e.g. 3]. For example, the level of Al needed to form an external alumina layer on Cu-Al alloys can be significantly reduced by additions of Zn [e.g. 3]. It may also be possible to form similar corrosion resistant nitride layers on Fe-Cr or Ni(Fe)-Cr base alloys, which would also further reduce alloy cost. Investigation of the nitriding characteristics of existing commercial Ni-Fe-Cr alloys will also be performed. Emphasis in the next year will be placed on establishing collaborations with commercial alloy producers and fuel cell manufacturers to facilitate technological assessment (particularly in-cell testing) and scale-up of this approach.

References

1. G. Smith and M. Harper, Special Metals Corp., private communication (2002)

2. R.P. Rubly and D.L Douglass, Oxid. Met., 35, 259 (1991)

3. M.P. Brady, B. Gleeson, I.G. Wright, JOM, 52(1) 16 (2000).

FY 2002 Publications

1. "Assessment of Thermal Nitridation to Protect Metal Bipolar Plates in PEM Fuel Cells", M.P. Brady, K. Weisbrod, C. Zawodzinski, I. Paulauskas, R.A. Buchanan, and L.R. Walker, submitted to *Electrochemical and Solid State Letters*.

Patents

1. "Metallic Bipolar Plate Alloys Amenable to Inexpensive Surface Modification for Corrosion Resistance and Electrical Conductivity", M.P. Brady, J.H. Schneibel, B.A. Pint, and P.J. Maziasz, United States Provisional Patent Disclosure, April 2002.

IV.D.20 Scale-Up of Carbon/Carbon Composite Bipolar Plates

David Haack (Primary Contact), Ken Butcher, Earl Robert Torre
Porvair Fuel Cell Technology, Inc.
700 Shepherd Street
Hendersonville, NC 28792
(800) 843-6105, fax: (828) 697-7960; e-mail: dhaack@pamus.com

DOE Technology Development Manager: Donna Ho
(202) 586-8000, fax: (202) 586-9811, e-mail: Donna.Ho@ee.doe.gov

ANL Technical Advisor: Thomas Benjamin
(630) 252-1632, fax: (630) 252-4176, e-mail: Benjamin@cmt.anl.gov

Main Subcontractor: UTC Fuel Cells, Inc., South Windsor, Connecticut

Objectives

- Develop carbon/carbon composite materials for bipolar plates that meet or exceed target property criteria
- Evaluate the performance of the bipolar plate materials through fuel cell stack testing
- Design and construct a research-scale production line for materials development efforts
- Design and construct a pilot-scale production line to demonstrate high volume, low-cost bipolar plate manufacturing

Approach

Phase I

- Design, construct and install material forming, pressing and thermal treatment equipment
- Systematically investigate material forming techniques and composition ingredients
- Systematically investigate material processing variables and test material properties
- Perform fuel cell testing to evaluate plate performance at UTC Fuel Cells
- Investigate forming techniques aimed at rapid, low-cost production

Phase II

- Design, construct and install a pilot-scale production line for 300 plates per hour capacity
- Design and implement quality assurance system for pilot line
- Evaluate pilot line performance and estimate pilot and mass bipolar plate production costs
- Evaluate pilot line bipolar plates for fuel cell performance and deliver fuel cell stack

Accomplishments

- Developed two-sided embossed bipolar plates with excellent material properties, exhibiting the potential for low-cost production
- Designed, constructed and installed research material forming and processing equipment
- Developed improved bipolar plate materials, exhibiting improved material properties and low-cost ingredients

- Began investigation into rapid-forming techniques
- Began fuel cell testing at UTC Fuel Cells

Future Directions

- Continue material development efforts for improved material properties and reduced raw materials
- Continue rapid-forming investigations
- Continue fuel cell testing

Introduction

In April 2001, Porvair Fuel Cell Technology, Inc. (PFCT) licensed a carbon/carbon composite bipolar plate formation technology from Oak Ridge National Laboratory (ORNL). The goal of PFCT is to transfer this technology from the laboratory to full-scale, low-cost mass production to meet the emerging need of the rapidly developing fuel cell industry. This program is directed at further developing the carbon/carbon bipolar plate material to meet the performance, durability and cost demands of the fuel cell industry, and to demonstrate a pilot-scale manufacturing line to produce this material in reasonable pilot quantities (300 plates per hour).

The process involves formation of a carbon perform by a low-cost slurry molding process. The pre-form is pressed and a flow field pattern is embossed in the surfaces. The porosity of the plate is then filled to the desired density by chemical vapor infiltration.

Approach

The path to final production demonstration is split into two major parts in this program. Phase I focuses upon material and composition refinement to satisfy the fuel cell property and performance requirements. Also in Phase I, investigations and demonstrations of research-scale rapid material formation techniques will be performed.

The approach in material development is to systematically perform statistically designed experiments. Techniques include fractional factorial designs, Grecko-Latin squares, and self-directed optimization. Data collected is statistically evaluated to determine primary and combined effects of the variables of investigation. Properties of importance will be measured using standard techniques; they include material electrical conductivity, strength, flexure, hydrogen permeability, and corrosion rate. Our commercial partner in this endeavor, UTC Fuel Cells, will measure bipolar plate performance in out-of-cell testing and in-cell testing (both single and multiple cell stacks).

Phase II focuses upon process development to result in a pilot production line capable of producing 300 bipolar plates per hour. Our goal is a complete functional pilot line, including all relevant quality assurance, failure mode and effects analysis, and statistical manufacturing characterization processes. This will be completed by transferring the most promising mass-production technique to larger-scale and continuous equipment operation in a dedicated production line.

Results

The project to this point has focused primarily upon process design and equipment installation, although some material and process development has been performed. A laboratory space has been arranged for the bipolar plate development activities. A research vacuum forming system (Figure 1) has been installed for use in manufacturing experimental material. Material pressing equipment, material property testing equipment, and thermal processing equipment has also been installed. Figure 2 shows the laboratory-scale CVI furnace used for preliminary materials development efforts. Because the capacity of this furnace limits productivity, a larger furnace has been designed and installed (Figure 3) to provide capacity suitable to produce an average of 10 plates per hour (a Phase I productivity goal).

Figure 1. Photograph of carbon/carbon composite vacuum forming equipment.

Materials development activities have focused upon improving material properties and reducing the costs of the raw materials composing the bipolar plate. The original work done at ORNL focused primarily upon the use of short graphite fibers as the backbone of the bipolar plate. The fiber material utilized, however, is quite expensive (projected high volume costs of ~$5/lb) and may limit the achievement of desirable material properties. A two-level fractional factorial design investigating fiber type and content was undertaken to reduce the quantity of fiber in the product or to displace the expensive fiber material with lower cost alternatives. Results showed that much of the fiber within the material could be displaced, resulting in a lower-cost product with superior material properties.

The potential of embossing flow field patterns in the preform materials has also been investigated. A two-sided proprietary flow field pattern has been successfully transferred to the carbon/carbon material yielding near-net-shape bipolar plates. Subsequent materials property testing has confirmed adequate material properties.

Table 1 shows preliminary materials properties measured on non-optimized bipolar plate materials produced through initial development work at PFCT. Comparisons with published DOE goals are made in the table. Sealing of the plate through - through plate permeability is accomplished through the application

Figure 2. Photograph of laboratory-scale chemical vapor infiltration (CVI) furnace

of a thin non-permeable layer on the exterior surface of the material. Figure 4 is an SEM micrograph of such a surface. Permeability testing with nitrogen gas at room temperature has been performed (ASTM D1434), showing no detectable permeability. The experimental setup to allow testing with hydrogen is still under development.

Table 1. Carbon/Carbon Material Properties

Property	Value	DOE Target
Electrical Conductivity (S/cm) (ASTM C611)	> 300	> 100
Density (g/cc)	1.00 - 1.30	-
Flexural Strength (psi)	5700	> 600 (crush)
Flexibility (%) (deflection at mid-span)	1.5 - 3.5	3 - 5
Nitrogen Permeability (cc/cm^2/sec) (ASTM D1434)	Not detected	< $2x10^{-6}$ (Hydrogen)

Figure 3. Photograph of Phase I development CVI furnace in assembly.

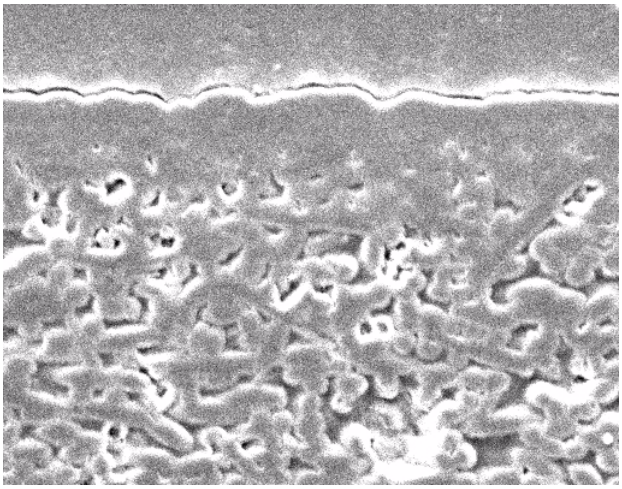

Figure 4. SEM micrograph of a molded carbon/carbon composite material. Figure shows thin skin coating on plate exterior to provide plate sealing.

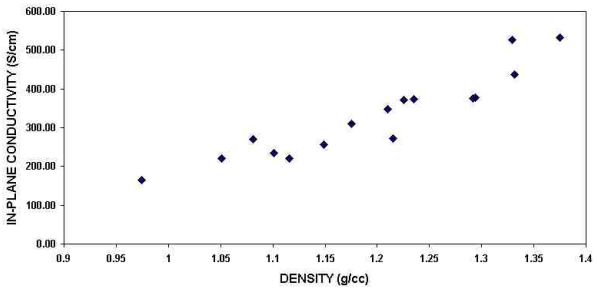

Figure 5. Density influence on through-plane electrical conductivity from an array of experimental compositions.

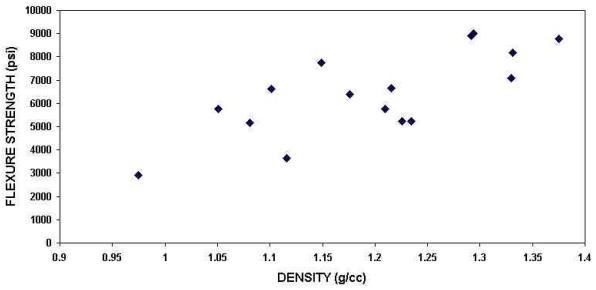

Figure 6. Density influence on flexural strength from an array of experimental compositions.

Some material trends have been established through continued experimental investigation. Figure 5 is a chart of material conductivity as a function of material density. Figure 6 is a similar chart showing material flexure strength. The process and material developed to date shows considerable flexibility to tailor material properties to desired levels. As seen in Figures 5 and 6, a trade-off exists between material density and material properties - a lightweight material will not be as strong or conductive as a heavier material. However, material properties measured appear to be well above the DOE targets, even with low-density materials. Further material optimization is continuing.

UTC Fuel Cells, Inc. is testing both machined and pattern-embossed materials in single fuel cell operation. Initial results, although not ready for publishlication, appear promising.

Conclusions

Preliminary work completed in this project includes laboratory and equipment setup and installation, and preliminary rounds of material optimization and process development. Full size bipolar plate prototypes have been produced with full double-sided flow patterns, demonstrating the potential of the manufacturing process. Process and material development has resulted in the characterization of material properties under a variety of composition levels. Material properties meeting or exceeding DOE targets have been measured, and bipolar plates, both machined and pattern-embossed, have been submitted to UTC Fuel Cells for in and out of cell testing. Phase I work will

continue this year in the optimization of the material composition for cost and performance, in the development of potential mass-production techniques, and in expanded in-cell testing.

IV.D.21 Carbon Foam for Fuel Cell Humidification

J. W. Klett (Primary Contact), Nidia Gallego, April McMillan, Lynn Klett
Carbon Materials Technology Group
Oak Ridge National Laboratory, P.O. Box 2008, MS 6087, Bldg. 4508
Oak Ridge, TN 37831-6087
(865) 574-5220, fax: (865) 576-8424, e-mail: klettjw@ornl.gov

DOE Technology Development Managers:
JoAnn Milliken: (202) 586-2480, fax: (202) 586-9811, e-mail: JoAnn.Milliken@ee.doe.gov
Nancy.Garland: (202) 586-5673, fax: (202) 586-9811, e-mail: Nancy.Garland@ee.doe.gov

ORNL Technical Advisor: David Stinton
(865) 574-4556, fax: (865) 241-0411, e-mail: stintondp@ornl.gov

Objectives

- Determine how graphite foams can be used to enhance the humidification of the fuel cell inlet air.
- Determine what characteristics of the foam require optimization to allow the combination of power electronics cooling with humidification of the inlet air.

Approach

- Design and construct a humidification test cell to utilize different foam structures to aid evaporation of water.
- Perform tests to characterize the humidification potential of the foam and develop optimized designs to minimize pumping power while maximizing humidification with heat generated from power electronics.

Accomplishments

- Foam was demonstrated to successfully humidify dry inlet air to 87% saturation at 60°C using a simulated power electronic device.
- Optimization of foam density uniformity, batch consistency, and thermal properties was performed and showed that a foaming rate of 3.5°C/min and a graphitization rate of 1°C/min produced the best foam structures.
- A mathematical model for heat transfer in foams was developed, which can simulate power electronics cooling by fluid flow through the foam.

Future Directions

- Apply optimized foam structures to humidification systems to show improvement in humidification potential.
- Apply mathematical model to design optimized humidification systems (i.e., lowest pressure drop, highest humidity, and lowest heater temperature).
- In collaboration with a fuel cell manufacturer, develop a full-scale prototype humidifier for fuel cell applications.

Introduction

The efficiency of the automotive proton exchange membrane (PEM) fuel cell is dependent on many factors, one of which is the humidification of the inlet air. If the inlet air is not sufficiently humid (saturated), then the stack can develop dry spots in the membrane and efficiency and voltage will drop. Therefore, it is necessary to ensure that humid inlet air at the proper elevated temperature is supplied to the stack. Current methods involve utilizing a spray nozzle to atomize water droplets onto a cloth or wire mesh substrate. As the ambient inlet air passes over the cloth it picks up moisture; however, the relative humidity drops as the air is heated in the fuel cell. If heat could be supplied to the water efficiently, the system would become independent of the ambient conditions, the inlet air could become more humid at the proper temperatures, and the overall stack could maintain a high level of efficiency. Previous work with power electronic heat sinks and automotive radiators has demonstrated the high efficiency of carbon foam for heat transfer. Utilizing the carbon foam in the PEM fuel cell may reduce the inlet air humidification problems.

The unique graphite foam, shown in Figure 1, has a ligament conductivity greater than 1500 W/m·K, equivalent to artificial diamond. The high thermal conductivity of the foam combined with the very high surface area (>4 m^2/g) result in heat transfer coefficients that are two orders of magnitude greater than those of conventional heat exchangers. Therefore, we believe that graphite foam can be effectively utilized to capture waste heat from power electronics to heat and humidify ambient air entering the fuel cell. To characterize the behavior of the foam in a humidification system, a test chamber normally used for evaluating heat sinks is utilized (see Figure 2). A block of carbon foam is brazed onto an aluminum plate and placed in a cavity through which cooling air flows. A simulated power inverter capable of generating up to 800 W, or 30 W/cm^2, is mounted to the back of the aluminum plate. As cooling air passes through the system, the temperature of the heater and the inlet and outlet air can be measured.

Several tests were run to determine the efficacy of using waste heat from power electronics to heat and humidify ambient inlet air. Testing was initiated by flowing 5 SCFM of ambient (~20°C) air through the heat sink (test system) that was dissipating 10 W/cm^2 of heat. The temperature of the outlet air increased to about 104°C. The test was repeated with the addition of 10 cm^3/min of water to not only heat but also humidify the air. The temperature of the outlet air increased to 73°C at a relative humidity of 24%. The test was repeated a second time with the addition of 20 cc/min of water for humidification. The temperature of the outlet air increased to ~59°C at a relative humidity of 87%.

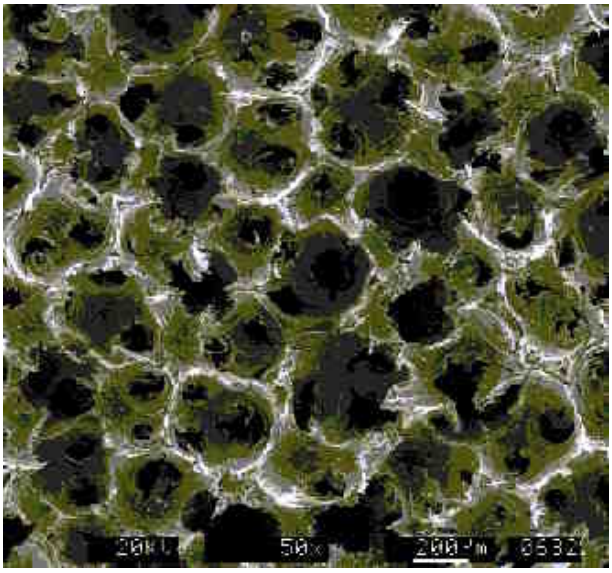

Figure 1. ORNL Graphite Foam

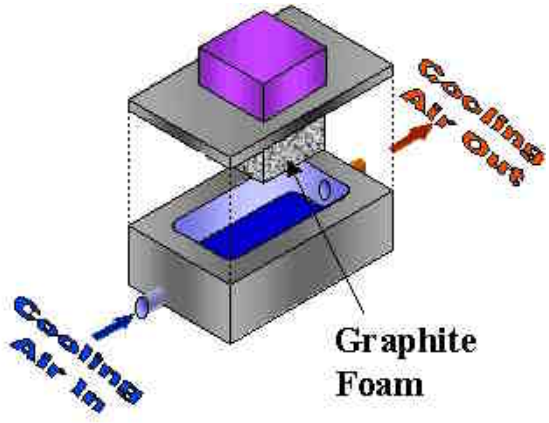

Figure 2. Schematic of Test Rig to Evaluate Heat Sink Geometries

The successful operation of a fuel cell vehicle will likely require about 4.5 m^3/min or 160 SCFM of inlet air at a temperature of about 80°C. Our calculations show that there should be sufficient heat generated by the power electronics to adequately heat and humidify this volume of air. Unfortunately, very large quantities of water would be required to humidify this large volume of air. In fact, a hybrid electric vehicle would consume more water per mile or per hour than gasoline. In order to make humidification systems practical, very efficient systems that recycle moisture from the exhaust stream will be required. Hence, understanding the structure-processing relationship of the foam as a means of tailoring the foam properties will be required to optimize the humidification system. In addition, developing a model that can predict heat transfer and developing better joining methods to reduce thermal resistance will be critical to the success of this project. Therefore, efforts were initiated in several of these areas.

Approach and Results

Foam Optimization

For many carbon materials the heat treatment rate during graphitization is critical to optimizing the material properties. Commercial heating rates of approximately 0.1°C/minute to 2800°C are typically used for graphitization. Because graphitization takes so long, it is expensive and energy intensive; thus, finding the maximum heating rate which yields the desired properties is critical to minimizing costs. Therefore, the influence of heating rate during graphitization on key properties of the foam such as density, thermal diffusivity and crystalline parameters was examined in this research.

Density Uniformity: The first characterization of the foams was the measurement of the density uniformity after carbonization. Several billets of foams were made with two different foaming rates: 3.5°C/min and 10°C/min. Test billets were heat treated in the top and bottom positions in the furnace, as illustrated in Figure 3. This provides an understanding of the temperature uniformity within the furnace and its effects on the resulting foam. Table 1 reports the density uniformity for the billets processed at different foaming rates and positions in the furnace. The density of samples heat treated at the top of the furnace is much more uniform than samples heat treated at the bottom of the furnace. While there appears to be a slight effect on density uniformity due to the foaming rate, this effect is small comared to the effect of the position of the pan in the furnace. This implies that the temperature at the bottom of the furnace (most likely a lower temperature) during the foaming is not sufficient to produce uniform temperature profiles in the foam, thereby leading to non-uniform foam density plots.

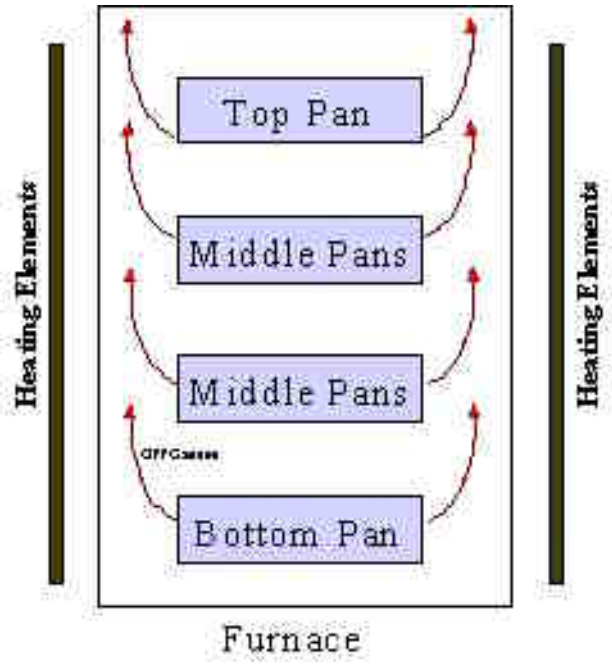

Figure 3. Furnace Diagram with Locations of Billets of Foam

	Bottom Pan		Top Pan	
Foaming Rate [°C/min]	Avg. Density	Max Deviation	Avg. Density	Max Deviation
3.5	0.474	10.6%	**0.448**	**3.7%**
10	0.434	13.1%	**0.430**	**3.8%**

Table 1. Density (in g/cc) Uniformity of Billets

Thermal Properties: Cubes cut from each billet were separated into groups of four and fired to

2800°C at five different heating rates (0.5, 1, 5, 10, and 15°C/min). The thermal properties of the samples were then measured in x, y, and z directions with a Xenon flash diffusivity apparatus. The thermal conductivity of the samples was calculated from their thermal diffusivity. Table 2 lists the Z-direction thermal conductivity values for each graphitization heating rate and position within the furnace. From these data, it is clear that the thermal conductivity is directly related to the graphitization heating rate. A similar trend was observed in the crystal properties of the foams determined from X-ray diffraction (not shown here for brevity). However, it is not understood why there is a maximum at 1°C/min.

Graphitization Heating Rate	Bottom Pan		Top Pan	
	Foaming Rate		Foaming Rate	
	3.5°C/ min	10°C/ min	3.5°C/ min	10°C/ min
0.5	118.6	85.8	132.9	109.4
1.0	134.7	111.9	148.9	115.5
5	130.7	104.3	133.9	114.1
10	123.7	96.6	126.4	112.7
15	98.7	88.4	125.1	115.3

Table 2. Z-direction Thermal Conductivity (in W/m·K) after Graphitization

The effect of the location of the samples in the foaming furnace on the final thermal properties is also noteworthy. It is clear that in the Z-direction (the direction with the highest conductivity), both billets that were located in the top of the furnace exhibited the highest overall thermal conductivity, irrespective of foaming rate. However, it is also evident that the foaming rate does affect the final thermal properties, with the lower foaming rate yielding graphitized foam with the higher thermal conductivity. While these trends are also true for the x and y directions, the effects are less pronounced due to the lower thermal conductivities in these directions.

Modeling of Heat Transfer

A mathematical model was developed to predict the thermal transfer in the foams. This is critical to developing engineered structures which provide both humidification and electronic cooling. This model uses the equations of energy, motion, and continuity to develop a finite element solution with a commercial package, FLEXPDE. For the hypothetical model, heat is assumed to be added to the top of the foam (simulating a heater), and the fluid flows perpendicular to the heat flow (see Figure 4). The following equations were input to the model:

Darcy-Forcheimer Equation for flow through porous media

$$0 = -\nabla p - \frac{\mu}{\kappa}\mathrm{v} + \frac{\mu\rho}{\sqrt{\kappa}}|\mathrm{v}|\mathrm{v}$$

Equation of Continuity

$$0 = -\nabla^2 P - \left(\frac{\mu}{\kappa} - \frac{\mu\rho}{\sqrt{\kappa}}|\mathrm{v}|\mathrm{v}\right)(\nabla\cdot\mathrm{v})$$

Heat Equation in Fluid

$$0 = \nabla\cdot\left(-k_w\nabla T_w\right) - \rho C_p DT + \dot{q}_{gained}$$

Heat Equation in Foam

$$0 = \nabla\cdot\left(-k_f\nabla T_f\right) - \dot{q}_{loss}$$

Model heat transfer from foam to fluid as a source/ loss term - q

$$\dot{q}_{loss} = \dot{q}_{gained} = -h_{loc}\cdot A_{spec}\cdot(T_f - T_w)$$

The results were exceptional, as shown in Table 3. The model adequately predicts the output fluid temperature and heater temperatures for various conditions in power input and flow rates. Now that the model is validated, it can be applied to engineering concepts to easily predict and design the optimum configurations to produce humid inlet air while cooling devices such as power electronics.

Figure 4 illustrates the results of the simulations. First, the model can predict the flow field of the fluid, in this case a plug flow, which is optimum for heat transfer. Next, the model predicts the isotherms of the foam and water, giving the designer important visualization of the system, thereby allowing easier engineering of optimum designs.

Power Input (W)	**300**	**300**	**600**	**600**
Water Flow Rate [gph]	**25**	**45**	**25**	**45**
Pressure Drop [psi]	**3.5**	**7.0**	**3.5**	**7.0**
Measured Base Plate Temperature [C]	**300.3**	**296.8**	**308.7**	**303.4**
Predicted Base Plate Temperature [C]	**299.6**	**297.2**	**308.4**	**303.6**
Measured Outlet Water Temperature [C]	**293.8**	**292.6**	**296.3**	**293.9**
Predicted Outlet Water Temperature [C]	**293.7**	**292.4**	**295.8**	**293.9**

Table 3. Heat Transfer Model Results

Conclusions

It was shown that carbon foam is beneficial to humidification systems for fuel cells. The foam has demonstrated the ability to utilize waste heat from power electronics to both heat and humidify ambient inlet air to ~80°C and 80% relative humidity.

The foaming process was characterized to optimize both the foaming rate and the graphitization rate of the foams. It was found that the temperature uniformity of the foaming furnace is critical to the density uniformity and batch consistency of the foam billets. It was found that a foaming rate of 3.5°C/min produced foams with more uniform densities and higher thermal conductivities than a higher foaming rate. It was also found that a graphitization rate of less than 1°C/min produces foams with the highest thermal conductivities.

Last, a mathematical model was developed which accurately predicts heat transfer from the foam to a fluid flowing through the pores of the foam. This is critical to developing optimized designs for humidification devices that both humidify and provide cooling potential.

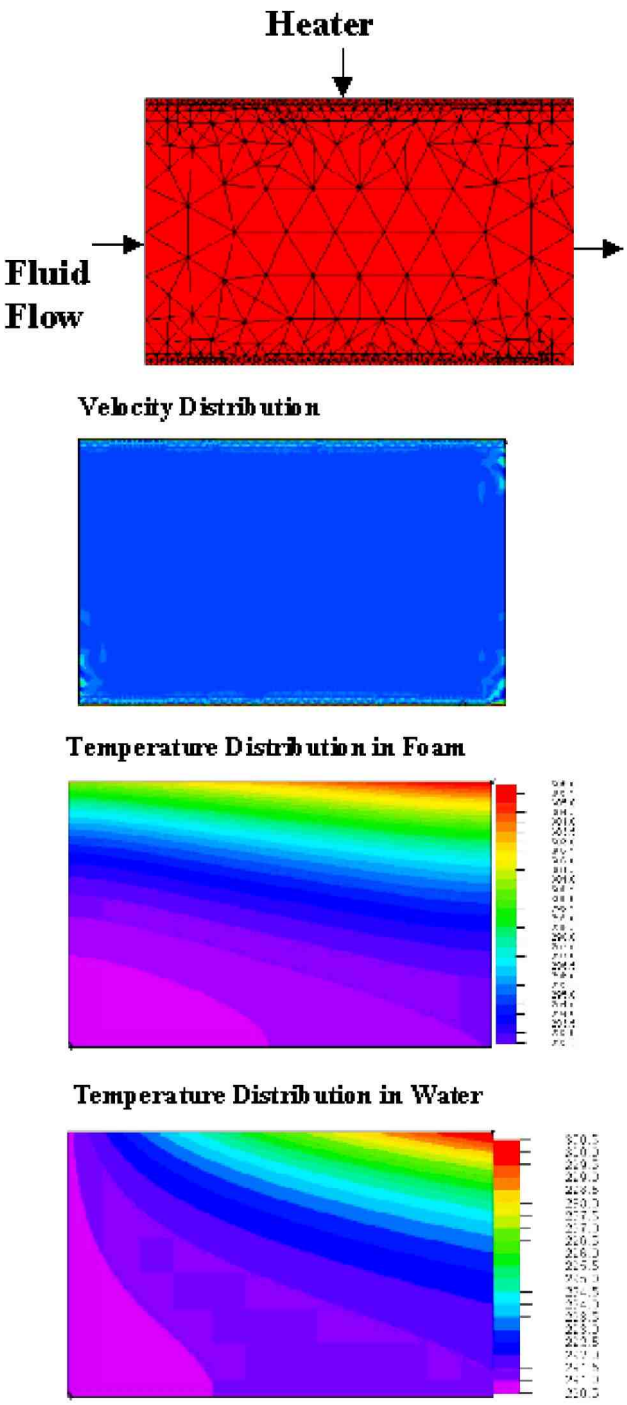

Figure 4. Model and Results of Simulated Heat Transfer from Foam to Fluid Flowing through Foam

IV.D.22 Carbon Monoxide Sensors For Reformate Powered Fuel Cells

Fernando Garzon (Primary Contact), Eric Brosha and Rangachary Mukundan
MS D429, MST-11 Group
Los Alamos National Laboratory
Los Alamos, New Mexico, 87545
(505) 667-6643, fax: (505) 665-4292, e-mail: garzon@lanl.gov

DOE Technology Development Managers:
Nancy Garland: (202) 586-5673, fax: (202) 586-9811, e-mail: Nancy.Garland@ee.doe.gov
JoAnn Milliken: (202) 586-2480, fax: (202) 586-9811, e-mail: JoAnn.Milliken@ee.doe.gov

Objectives

- Hydrogen reformate gas powered fuel cell systems require sensors for carbon monoxide level monitoring and feedback control.
  - Develop a high temperature sensor for measurement of 0.1 to 2% carbon monoxide in reformate gas for fuel processor control.
  - Develop a low temperature sensor for measuring 10-100 ppm range concentrations for stack poisoning control.

Approach

- Two electrochemical sensor types are being investigated for high and low temperature carbon monoxide sensing:
  - An oxide solid electrolyte device based on the kinetics of the electrode reactions is being developed for the high temperature application.
    - Yttria-doped zirconia and gadolinia-doped ceria oxygen ion conductors and strontium yttrium zirconium oxide proton conductors are being investigated as the solid electrolyte.
    - Several metals including Pt, Pd, Au, Ru and Ni are being evaluated as the sensing and reference electrodes.
  - A amperometric device based on carbon monoxide inhibition of hydrogen oxidation kinetics using either a perfluorosulfonic acid polymer electrolyte or an inorganic acid electrolyte is being evaluated for the low temperature application.

Accomplishments

- A cerium oxide based high temperature sensor has been developed. The sensor responds well to 10-500 parts per million of carbon monoxide in air.
- Strontium zirconate proton conducting thin film electrolytes have been successfully synthesized and characterized.
- Amperometric low temperature carbon monoxide sensors have been developed and tested under a variety of conditions. These devices respond well at ambient temperature to carbon monoxide in hydrogen streams.

Future directions

- Modify the electrodes in the cerium (or zirconium) oxide devices to detect CO in the presence of hydrogen.

- Increase the operating temperature of the low temperature devices from room temperature to approximately 80^{o}C.
- Optimize low temperature amperometric devices for fast response time.
- Evaluate catalyst composition, loading and particle size effects on sensor performance.
- Investigate alternative electrolytes.
- Test the sensor prototypes in actual reformate gas streams.

Introduction

The detection and measurement of carbon monoxide in high temperature reformate streams is of vital importance to the successful implementation of fuel cells for transportation. Much research is being performed to optimize low-cost fuel reformer systems that convert liquid hydrocarbon fuels to hydrogen gas containing fuel streams. This hydrogen gas typically feeds a polymer electrolyte membrane (PEM) fuel cell utilizing a platinum based anode. It is well known that low concentrations of carbon monoxide (~10-100) ppm impurities in hydrogen can severely degrade the performance of PEM fuel cell anodes. This performance degradation is due to strong adsorption of carbon monoxide on the electro-active platinum surface sites where hydrogen is normally oxidized to protons.

The proper design of fuel reformer systems must pay careful attention to the minimization of carbon monoxide before the processed fuel stream enters the fuel cell stack. Many reformer systems use a secondary preferential oxidation reactor that selectively oxidizes the carbon monoxide present in reformate streams. In most transportation applications the steam reformer and the selective oxidation reactors do not operate under steady state conditions; large transients may occur which produce relatively large amounts of carbon monoxide. It is highly desirable to have a low-cost real-time carbon monoxide measurement system that provides feedback control to the fuel processing system in order to protect the PEM fuel cells from performance degrading concentrations of carbon monoxide.

Current fuel cell systems use air-bleeding methods to reduce the carbon monoxide poisoning of the Pt anode. Since this method involves the mixing of 2-6% air with the fuel stream, it results in a decrease in the energy efficiency of the fuel cell system and thus should only be used for carbon monoxide transients. Hence, a CO sensor that measures the CO content of the anode stream can be used for feedback control of the air-bleeding system thus allowing these systems to operate at maximum energy efficiency. We are designing and developing solid-state electrochemical sensors meeting these criteria, including the demonstration of prototype sensors.

Approach

High temperature carbon monoxide sensors

Los Alamos is developing high temperature zirconia- and ceria-based electrochemical sensors to measure 0.1-2% CO in hydrogen streams. These sensors would operate at 400-600^{o}C and can be used for feedback control of the reformer system. We have successfully developed novel mixed-potential sensors that are capable of measuring ppm levels of CO in air[1]. We are currently working on modifying the electrodes of these devices to enable them to work in a hydrogen atmosphere. We are also exploring the possibility of using proton-conducting electrolytes and using these sensors in an amperometric mode.

Low temperature carbon monoxide sensors

Low temperature carbon monoxide sensors based on the reversible carbon monoxide adsorptive poisoning of precious metal electrodes are also being developed by Los Alamos National Laboratory. The addition of metals such as ruthenium to the platinum electrode material greatly improves the hydrogen oxidation kinetics in the presence of CO. An amperometric sensor that senses the CO inhibition of the hydrogen oxidation can be fabricated from a platinum electrode, a proton conductor and a platinum ruthenium alloy electrode. While the

current density of the platinum electrode will be influenced by the surface coverage of carbon monoxide, the current density at the Pt/Ru alloy electrode should be relatively unaffected. This difference in the electrode current density in the presence of CO can be used to fabricate a low temperature CO sensor.

Results

During FY 2002 we prepared several low temperature sensors based on a Nafion® electrolyte and various metal electrodes. We evaluated the CO response of Pt, Pt/Ru and Ru metal electrodes at various loadings. Figures 1 and 2 illustrate the current vs. voltage curves from two sensors using precious metal loadings of approximately 0.2 mg/cm^2. These electrodes were carbon supported electrodes and were prepared using a decal technique similar to typical fuel cell electrodes. Figure 1 illustrates that the Pt and Pt/Ru electrodes are poisoned by CO at room temperature, and the hydrogen-oxidation current is greatly decreased. However, this process was found to be difficult to reverse and the original current vs. voltage curves could not be obtained even after the CO was removed from the gas stream. It is seen from Figure 2 (inset) that the CO poisoning of the Ru electrode is

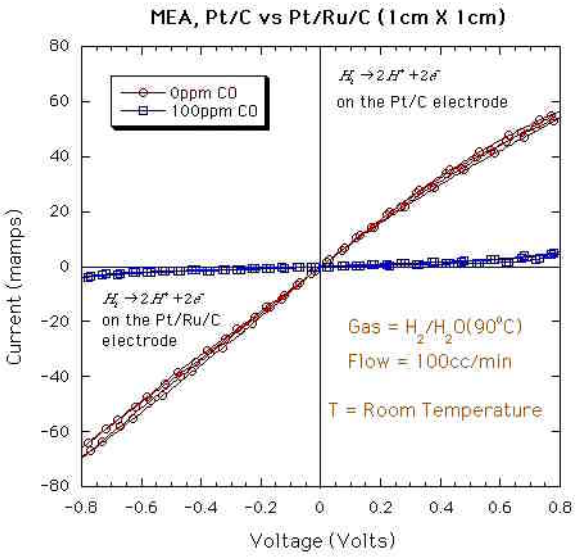

Figure 1. Current-Voltage Characteristics of a "0.22 mg/cm^2 Pt/C // Nafion® // 0.25 mg/cm^2 Pt/Ru/C" sensor at room temperature.

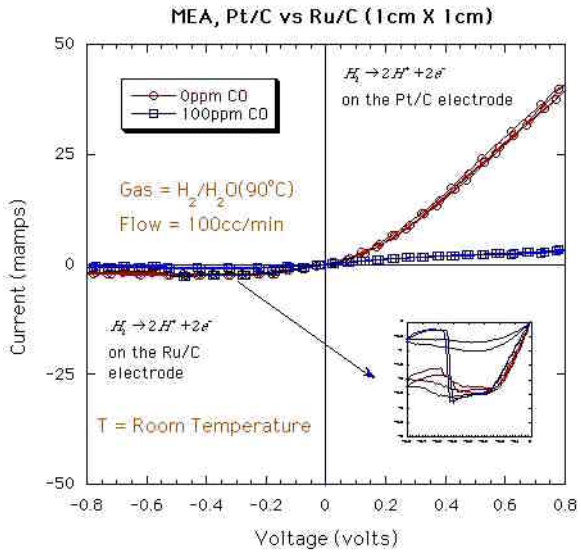

Figure 2. Current-Voltage Characteristics of a "0.22 mg/cm^2 Pt/C // Nafion® // 0.12 mg/cm^2 Ru/C" sensor at room temperature.

reversible, and the CO can be cleaned by the application of a voltage <-0.5 V. However, due to the low hydrogen-oxidation kinetics of this electrode, a sensor based on this electrode would have very little sensitivity to CO.

In order to improve the reversibility of the CO adsorption, several electrodes with higher catalyst loadings were evaluated. Pt, Ru and Pt/Ru black catalysts mixed with Nafion® and without carbon support were painted onto Nafion® membranes at approximately 10 mg/cm^2 loadings. The current vs. voltage curves of a "Pt/ Nafion®/ Pt-Ru " device are shown in Figure 3, where the Pt/Ru alloy electrode is relatively unaffected by the presence of 100 ppm of CO while the Pt electrode is poisoned. Moreover the CO from the Pt electrode can be easily cleaned by the application of a voltage >0.4 V. Therefore, this device, when biased at a voltage <0.4 V can be used as a CO sensor. The CO response obtained from this device at a bias of 0.3 V is illustrated in Figure 4.

Figure 5 illustrates the current vs. voltage curve of a "Pt/ Nafion® /Ru" device and indicates that the CO poisons both the Pt and the Ru electrodes in a reversible manner. The poisoning of the Ru electrode can also be used to yield a sensor response when the bias is >-0.6 V. Figure 6 illustrates the

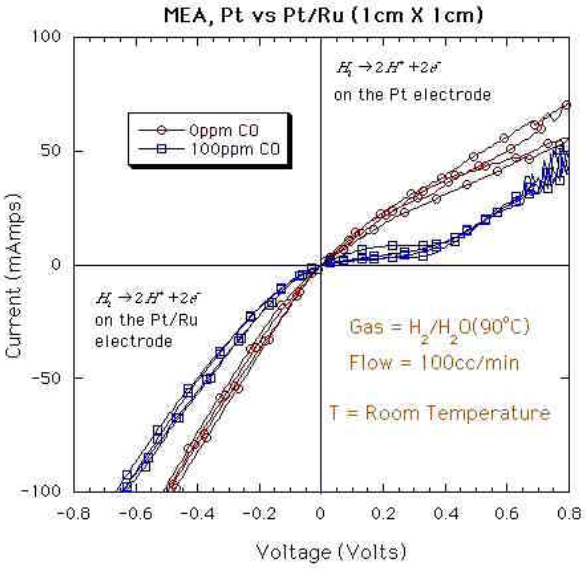

Figure 3. Current-Voltage Characteristics of a "10 mg/cm^2 Pt // Nafion® // 10 mg/cm^2 Pt/Ru" sensor at room temperature.

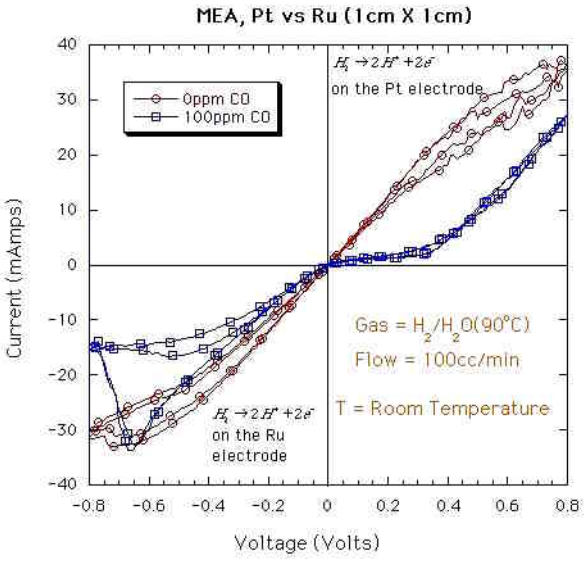

Figure 5. Current-Voltage Characteristics of a "10 mg/cm^2 Pt // Nafion® // 10 mg/cm^2 Ru" sensor at room temperature.

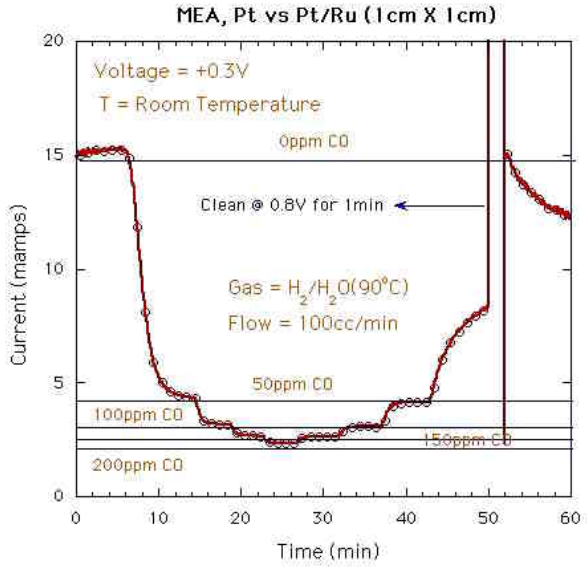

Figure 4. Response of the "10 mg/cm^2 Pt // Nafion® // 10 mg/cm^2 Pt/Ru" sensor to 0, 50, 100, 150, 200 ppm of CO in H_2.

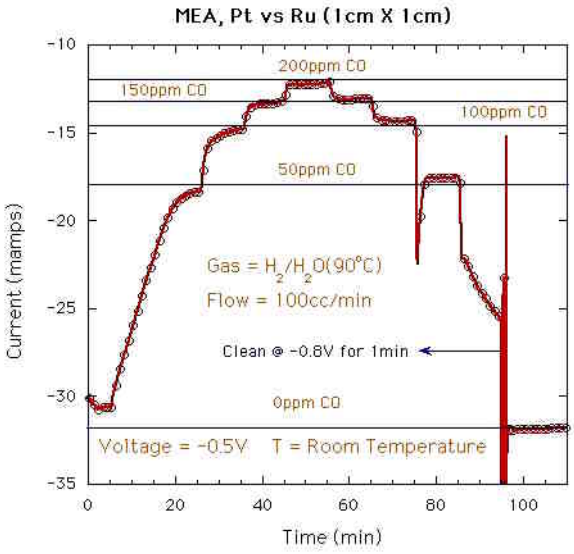

Figure 6. Response of the "10 mg/cm^2 Pt // Nafion® // 10 mg/cm^2 Ru" sensor to 0, 50, 100, 150, 200 ppm of CO in H_2.

response of this device to CO when the bias is set at –0.5 V. This sensor shows excellent sensitivity to CO and can be used to measure CO concentration in the 10-100 ppm range in a hydrogen stream. Although the CO desorption is fast at most CO levels, a bias of –0.8 V was found to restore the baseline of the sensor upon removal of the CO.

Conclusions

We have successfully developed low temperature sensors for the monitoring of carbon monoxide gas in a hydrogen stream. The sensors can detect parts per million concentrations of carbon monoxide in either a pure hydrogen or a hydrogen/carbon-dioxide

stream. Future work includes the raising of the operating temperature of the sensor to approximately 80^{o}C (fuel-cell operating temperature) and the optimization of the sensor response time and sensitivity.

References

1. R. Mukundan, E. L. Brosha, D. R. Brown, and F. H. Garzon. A mixed potential sensor based on a $Ce_{0.8}Gd_{0.2}O_{1.9}$ electrolyte and platinum and gold electrodes. *Journal of the Electrochemical Society,* **V 147(4)**, 1583-1588 (2000)

IV.D.23 Electrochemical Sensors for PEMFC Vehicles

Ai-Quoc Pham (Primary Contact)
Lawrence Livermore National Laboratory
P.O. Box 808, L-350
Livermore, CA 94550
(925) 423-3394, fax: (925) 422-6892, e-mail: pham2@llnl.gov

DOE Technology Development Managers: JoAnn Milliken and Nancy Garland
(202) 586-2480, fax: (202) 586-9811, e-mail: JoAnn.Milliken@ee.doe.gov
(202) 586-5673, fax: (202) 586-9811, e-mail: Nancy.Garland@ee.doe.gov

Objectives

- Develop a hydrogen safety sensor operating at 500°C or below, having 1s response time and being insensitive to humidity and hydrocarbons.
- Develop a hydrogen sensor for reformate fuel monitoring for hydrogen concentrations ranging between 10 to 100%.
- Develop a carbon monoxide (CO) sensor for reformate fuel monitoring.

Approach

- Use proven technology, i.e., solid state electrochemical sensors similar to the well-know oxygen sensor used in automobile exhaust gas
- Use mixed potential signal to eliminate the need for a reference gas compartment
- Use nanocrystalline electrode material for faster response time
- Develop micro-sensors for minimum power consumption

Accomplishments

- Data were obtained on temperature effect on sensor response
- Sensors with nanocrystalline electrodes were fabricated and tested
- Sensors with response time of a few seconds at 500°C were demonstrated
- Preliminary testing indicated no baseline drifting over several hundred hours

Future directions

- Complete characterization of hydrogen safety sensor
- Investigate limiting current type hydrogen fuel sensors
- Develop mixed potential CO sensors
- Develop micro-sensors with incorporated self heating device
- Transfer to industrial partners

Introduction

Proton exchange membrane fuel cells (PEMFCs) are among the most promising clean power system technologies being developed for transportation applications. The introduction of this new transportation technology implies important changes in vehicle design as well as incorporation of new features that do not currently exist in internal combustion engine automobiles. For example, the use of hydrogen, in particular, and combustible gases in general, requires additional safety devices to

prevent fire and explosion hazards. In addition, if hydrogen fuel is supplied by an on-board fuel reformer that delivers a hydrogen stream containing several other gases, additional control and monitoring devices are needed in order to protect and to efficiently operate the PEMFCs.

The purpose of this project is to design, develop, and demonstrate solid state electrochemical sensors for the various controls and monitoring on PEMFC vehicles. During this first phase of the project, we focus on the development of a hydrogen safety sensor.

Approach

A number of hydrogen and combustible gas sensors are commercially available. However, none of them appears to straightforwardly satisfy all the stringent requirements for automobile applications. In particular, the commercial hydrogen safety sensors suffer from significant long-term drifting as well as cross-sensitivity. Our approach is to use solid-state electrochemical sensor technology which has proven to be robust and reliable in automobile applications. Our sensor consists of an oxygen-conducting electrolyte membrane sandwiched between two electrodes, one serving as reference and one as working electrode. The working electrode has mixed potential response when exposed to an atmosphere containing hydrogen, i.e., due to the competing oxidation-reduction reactions of hydrogen and oxygen on the electrode surface, the potential of the mixed potential electrode departs from the actual thermodynamic value. The reference electrode, which is designed to reach thermodynamic equilibrium, will thus have a different potential. The potential difference between the two electrodes is thus the sensor voltage. This sensor voltage is dependent on the hydrogen concentration. This type of sensor does not require a separate reference gas compartment.

Accomplishments

This project started in January 2001. During FY01, we successfully developed a mixed potential type sensor with response time as fast as 1 second. However, a fairly high operating temperature (600°C or higher) was needed in order to have fast reaction kinetics. While this high operating temperature is not a major issue if a micro-sensor with enough insulation is used, the power consumption to maintain that temperature could still be fairly high. Therefore, our goal was to lower the operating temperature to 500°C or below.

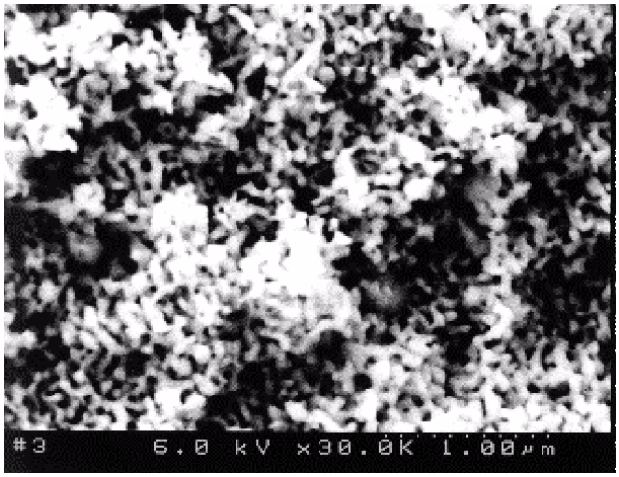

Figure 1. Micrograph of the Porous Nanocrystalline Electrode

We studied the effect of temperature on the sensor response. It was found that the lower the temperature, the higher was the signal amplitude while the response time became longer. We also found that the smaller the particle size of the electrode material, the faster was the sensor response. It was then concluded that using nanocrystalline material would be beneficial to accelerate sensor response, especially at low temperatures. Figure 1 shows the scanning electron microscopy picture of such a porous nanocrystalline electrode. The electrode was deposited using the colloidal spray deposition technique. The average particle size is less than 100 nm. At 500°C, the sensor response to hydrogen in air was 2 seconds for a flow rate of 2 liters per minute. A fast response to hydrogen was also observed at 400°C, however, the signal tended to overshoot before stabilizing at steady state.

Some of the characteristics of the new sensor are: no humidity effect on sensor response, high selectivity versus methane (see Figure 2) and virtually no baseline drifting over several hundred hours of operation. However, some issues still need to be improved, including the over-shooting that was

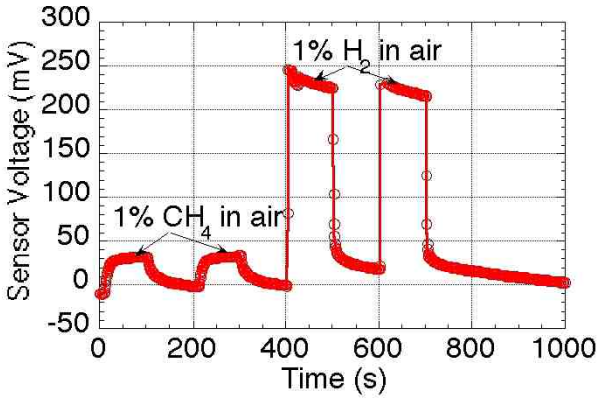

Figure 2. Sensor Response to Methane and Hydrogen

observed at time and the slow recovery upon removal of hydrogen from ambient air.

Conclusion and Future Work

We have demonstrated the possibility to reduce the sensor operating temperature from 600°C to 500°C. The sensor has some highly viable characteristics such as stability and selectivity.

Further work is needed in order to demonstrate a commercially viable device. For practical use, we will develop a self-heated micro-sensor for reduced power consumption as well as for minimum heat generation.

IV.D.24 Development of Sensors for Automotive Fuel Cell Systems

Brian A. Knight (Primary Contact)
United Technologies Research Center
411 Silver Lane Mail Stop 129-30
East Hartford, CT 06108
(860) 610-7293, fax: (860) 610-7669, e-mail: knightba@utrc.utc.com

DOE Technology Development Manager: Nancy Garland
(202) 586-5673, fax: (202) 586-9811, e-mail: Nancy.Garland@ee.doe.gov

Main Subcontractors: ATMI, Inc., Danbury, Connecticut; Illinois Institute of Technology, Chicago, Illinois; NexTech Materials, LTD, Worthington, Ohio

Objectives

- Develop technology and a commercial supplier base capable of supplying physical and chemical sensors required to optimize the operation of proton exchange membrane (PEM) fuel cell power plants in automotive applications.

Approach

- Obtain representative samples of physical parameter sensors currently available.
- Determine the suitability of state of the art physical parameter sensors for the extreme environment of a PEM fuel cell power plant by testing them in a combination of laboratory and simulated fuel cell flow stream environments.
- Assist the sensor manufacturers, where necessary, to modify the sensors to achieve the requisite performance, cost, and durability goals.
- Modify baseline chemical sensing technology to create sensors capable of making the measuring the parameters of Table 3.2 in a PEM fuel cell operating environment.
- Validate and document the performance and durability of the developed sensors by exposing them to a combination of laboratory and simulated fuel cell flow stream environments.
- Install the developed sensors on a breadboard PEM fuel cell at United Technologies Company fuel cell (UTCFC) for final testing.

Accomplishments

- This contract is still under negotiation; there has been no technical progress to date.

Introduction

The present state of the art in fuel cell powerplant sensor technology is embodied in the UTCFC PAFC PC 25 and PEM S200 powerplants. However, none of the chemical sensors, and only a very few of the physical sensors are "on-board" the powerplant. Furthermore, only temperature and stack differential pressure, in the S200, are measured continuously for control purposes. Production automotive fuel cell powerplants require all of these sensors to be on-board the powerplant, and to provide data signals on a continuous basis to optimize fuel cell operation and protect the cell stack from damage.

The measurement technology used by the PC 25 and S200 "off-line" chemical analyzers cannot be adapted to provide the basis for on-board, continuously measuring chemical sensors. IFC and

its team members have identified three candidate technologies that have the potential to achieve these goals.

Approach

Table 1 identifies the two technologies and the specific parameters the technologies will be targeting during the development effort. The sections below discuss each technology that we plan to use to develop the required capability.

Table 1.

Technologies	CO	H_2	SO_2	H_2S	NH_3	O_2
Electrochemical	X		X	X	X	X
MEMS		X	X	X	X	

CO = carbon monoxide, H_2 = hydrogen, SO_2 = sulfur dioxide, H_2S = hydrogen sulfide, NH_3 = Ammonia, O_2 = diatomic oxygen

Electrochemical

Electrochemical sensing is based on the interaction of an electrically conductive film with a molecular species in its environment. Typically an inorganic film is deposited on a semiconducting film, which, in turn is deposited over a series of interdigitated electrodes. The temperature of the device is maintained at a predetermined temperature to facilitate the desired interaction. As the target compound adsorbs to the sensing film, a change in the conductance of the semiconducting film between the interdigitated electrodes is produced, sensed and a signal is generated for external use.

NexTech Materials is pursuing the development of low-cost electrochemical carbon monoxide (CO) sensors that will meet the requirements of the fuel cell application. NexTech has recently demonstrated detection of parts per million (ppm) CO in a 50% hydrogen stream using copper/chlorine (CuCl) thick films. Figure 1 shows the response of NexTech's sensor when cycling between 50:50 vol% nitrogen/ hydrogen (N_2/H_2) and 1000 ppm CO in N_2/H_2. The hydrogen content was varied between 25 and 75 vol% (balanced with nitrogen) with no change in the baseline resistance noted. The sensing approach is based on the change in electrical resistance that occurs when carbon monoxide is selectively adsorbed by an inorganic film of a semiconducting

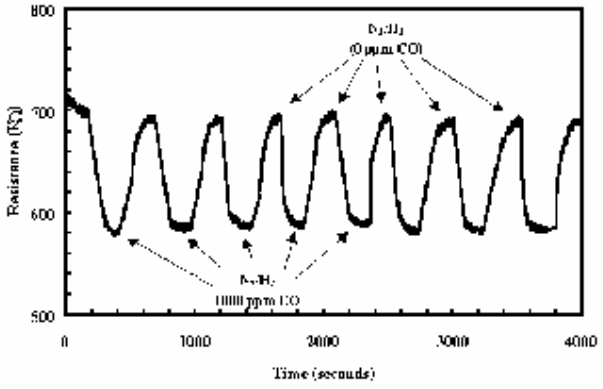

Figure 1. Effect of carbon monoxide (1000 ppm) on resistance of NexTech sensor in a baseline gas composition of 50% hydrogen and 50% nitrogen.

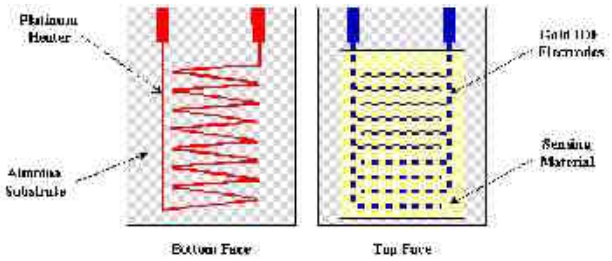

Figure 2. Sensor Construction Detail

material. The sensing material is deposited onto a substrate with interdigitated electrodes, with temperature being controlled by a thick-film heater deposited on the underside of the substrate, as shown in Figure 2. NexTech's results have demonstrated that this resistance change occurs rapidly (with either increasing or decreasing CO content), varies with the amount of CO from the gas stream, is insensitive to the presence of hydrogen, and can be used to detect low carbon monoxide levels. This type of sensor has the potential to be manufactured at a cost of $5 to $10 in volume. However, these sensors were used at a single temperature and CO concentration in the range of 100 -1500 ppm. More work is needed to determine the capability of this material for sensing CO at higher temperatures and/or higher CO concentration. Effort to explore the range of operation of the sensors will accelerate under this project.

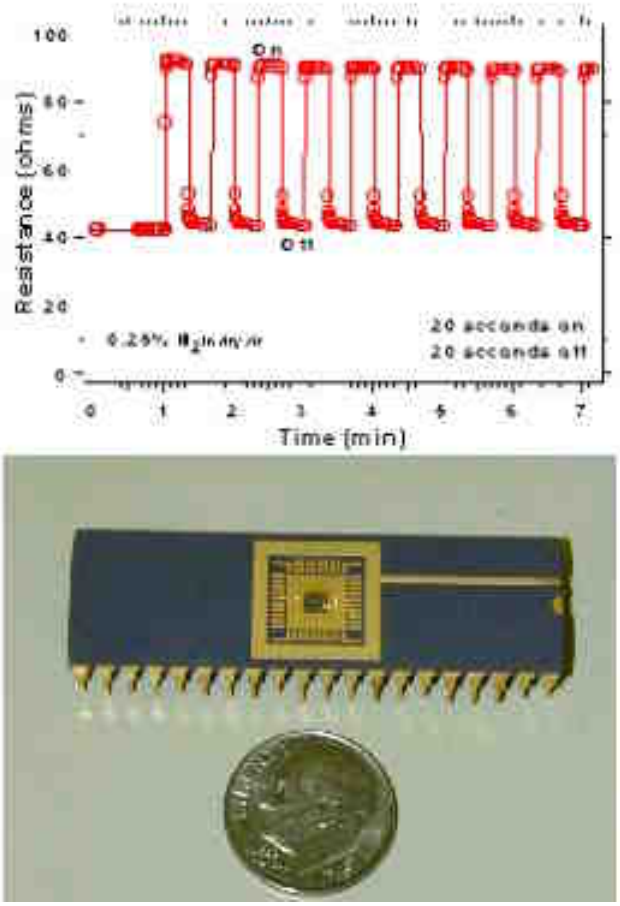

Figure 3. MEMS Hydrogen Sensor

Micro Electro Mechanical Systems (MEMS)

MEMS is a method to produce microscopic three-dimensional sensor arrays from a solid substrate. Sensing mechanisms such as the hydrogen-induced transition from a metallic di-hydride to a semiconducting tri-hydride can be deposited on a MEMS substrate. The reduced size, mass, subsequent thermal rise and fall times of the tiny devices, often called microhotplates, makes it possible to pulse the sensor to a desired operating temperature in milliseconds, make a measurement, and step to another measurement condition. Power consumption of such devices can be brought to very low values, response times can be in the sub second range, and sensitivity can be controlled by the actual reaction taking place in the uppermost sensing film.

The micro-hotplate gas sensor is a conductometric MEMS-based sensor that uses the change in conductance of the sensing layer as a function of temperature and time to measure the gases present. A critical step in developing these gas sensors is the selection of a specific chemi-resistive reactive layer for each target gas. ATMI has demonstrated the development of a high performance-low cost MEMS based H_2 gas sensor, (U.S. Patent, 09/231277, Allowed 2000) using palladium (Pd) alloy coated metal hydrides as the gas sensitive layer.

Figure 3 shows a typical unit of this design and the response to 0.25% hydrogen in dry air. These sensors have shown over a 100% change in resistivity to 0.25% H_2 in air, at speeds of response of less than 0.5 second.

UTCFC and its team members will investigate each of these platforms as a technology for part of the chemical-sensing requirement. No single platform is believed capable of addressing the entire chemical sensing requirement; therefore, each of the team members will develop its platform toward the requirement indicated in Table 3 1. The goal is to develop at least one applicable technology for each species and demonstrate them on an on-line S300 system

Current Technology for Physical Sensing

The state of development of physical sensor technology is dramatically different from that of the chemical sensors. Demand for high performance temperature, humidity and pressure sensors by the automotive and heating, ventilating, air conditioning and refrigeration (HVAC) industries have resulted in a large variety of different sensors. Consequently, the primary goal of this section of the effort will be to evaluate and modify, as necessary, commercial off-the-shelf sensors to fill the need. The physical sensors used by the PC 25 and S200 physical powerplants can be used as the basis of on-board continuously measuring sensors. Additionally, it is possible that more recently developed sensors for measuring the same parameters may be a better starting platform than the PC25/S200 sensors. The team will continually monitor the evolution of new physical sensors during the performance of this project.

The UTCFC team will select a baseline device for each sensor and to confirm its ability to fully meet the DOE specification. If there are deficiencies, we will work with the manufacturer to modify the sensor to conform. Table 2 identifies current sensors and the properties expected to limit their application. The potential limitations will be carefully evaluated in lab testing and subsequent on-line testing if they successfully complete the lab-testing phase.

Table 2.

Physical Sensor	Current Manufacturer	Operating Range	Items to be Confirmed in Testing
Temperature	Gulf Sensors Inc.	0 - 1900^{o}F	Corrosion resistance; repeatability
P Cell Stack	Atmos Engineering	1-3 atm; -50^{o}C to +100^{o}C	Survivability in gas stream; linearity; drift; accuracy, cost
Relative Humidity	General Eastern	0 to 100% RH; -10^{o}C to 100^{o}C gas stream	Corrosion resistance; sensor drift; repeatability, cost
Mass Flowmeter	Sierra Instruments	30 - 300 SLPM @ 80^{o}C	Accuracy, corrosion resistance; repeatability, cost

UTCFC will evaluate these sensors in the appropriate test facilities, supplying a synthesized gas stream of known inlet gas composition, and determine the response accuracy of each sensor at the required operating temperature. By controlling the inlet gas composition and mass flow, a fixed reference will be established to which the sensor response will be compared as a function of time. This effort will be conducted in United Technologies Research Center (UTRC), IIT and UTCFC facilities. Baseline sensor technology taken from a combination of production PC25, S200 and fuel cell development laboratory applications will be subjected to a series of performance, durability and cost reduction studies. Concurrent with this portion of the task, a detailed review of alternate sensors will be conducted. Appropriate sensors will be ranked according to probability of successful test outcome. This ranking will be used to identify replacement candidates should any baseline sensor fail the full suite of evaluations. Initial qualification tests will be conducted by IIT in the PEM Fuel Cell Benchmark Facility. These tests will consist of installation and exposure of baseline sensor technology to precisely controlled temperature, humidity, pressure, and gas mixture conditions. Sensor response versus these parameters will be logged.

Second level testing will be conducted at UTRC. During these tests, the sensors will be installed in a chamber through which gases simulating an ATR exhaust stream (created by mixing gases, heating, and humidifying as necessary to obtain the desired composition) will flow. The sensors will be evaluated for accuracy, speed of response, cross sensitivity to non-target parameters and test gas parameters. The tests will operate continuously for 40 hours, during which time a PC utilizing National Instruments LabView software will control and log all test parameters, including gas composition, sensor output, and control safety systems.

It is assumed that repetition of the above testing cycle will be required due to non-performance of some sensors. If baseline sensors cannot demonstrate superior performance, alternates will be selected.

References

1. J.N. Huiberts, et al, Nature 380 231(1996).

IV.D.25 Design and Development of New Glass-Ceramic Proton Conducting Membranes

Steve W. Martin (Primary Contact), Steven A. Poling, Jacob T. Sutherland
Iowa State University, Materials Science and Engineering Department
3053 Gilman Hall
Ames, Iowa, 50011
(515) 294-0745, fax: (515) 294-5444, e-mail: swmartin@iastate.edu

DOE Technology Development Manager: Roxanne Danz
(202) 586-7260, fax: (202) 586-9811, e-mail: Roxanne.Danz@ee.doe.gov

Objectives

- Investigate a new class of proton conducting membranes using thio-acids for hydrogen fuel cell applications.
- Produce anhydrous solid membranes having minimal fuel crossover capability and address many of the problems associated with current hydrogen fuel cell technologies.
- Optimize thio-acid membranes to yield high proton conductivities (10^{-6} to 10^{-3} Siemens per centimeter [S/cm]).
- Demonstrate performance, thermal stablility, and chemical stability with exposusre to water (H_2O) and diatomic oxygen (O_2) in a typical fuel cell setup.

Approach

- Synthesize new thio-acids.
- Synthesize membrane materials from thio-acids; final product may be a glass, glass/ceramic, or ceramic structure with stable sulfur-hydrogen groups.
- Measure the proton conductivity between -70^{o}C and 500^{o}C.
- Determine thermal stability.
- Determine chemical stability with respect to H_2O and O_2.
- Determine electrochemical properties, including reduction and oxidation potentials, and cyclic voltammetry.
- Cooperatively fabricate and test membrane electrode assembly (MEAs) using the most promising membranes. This is to be done in partnership with an external company specializing in fuel cells.

Accomplishments

- Two new thio-acids have been synthesized, a thiogermanic acid and a thiomolybdic acid. Additionally, the synthesis route is able to produce hydrosulfides and sulfides from many different hydroxide and oxide precursors.
- Thiogermanic acid, dihydrogen tetragermanium sulfide ($H_2Ge_4S_9$), is the thermally stable form of nanostructured tetrahydrogen tetragermanium sulfide ($H_4Ge_4S_{10}$). Tetrahydrogen tetragermanium sulfide with n molecules of H_2S ($H_4Ge_4S_{10} \bullet nH_2S$) has a measurable conductivity of 10^{-5}S/cm at room temperature; at higher termperatures it decomposes to $H_2Ge_4S_9$ with a reduced conductivity and greater thermal stability.
- Thiomolybdic acid H_2MoS_4 appears to conduct both protons and electrons. Possible catalytic behavior, electrode application, and storage capability of this acid are undetermined at this time.

- Thermally and chemically stable membranes have been synthesized from thio-acids. Conductivities of 10^{-7} S/cm at ~ 352°C were achieved with materials thermally stable to at least 500°C and chemically stable with H_2O for prolonged exposures.

Future Directions

- Reaction kinetics involving liquid hydrogen sulfide (H_2S) solution are being studied for the germanium oxide (GeO_2) and germanium sulfide (GeS_2) systems. This study is exploring the effects of water, temperature, time, and pressure on the kinetics of these types of reactions. At this point, it is clear that hydration by water speeds the reaction. A high pressure phase, which is more thermally stable, is also realized from long reaction times.
- Investigation into new thio-acid compounds from oxide, hydroxide, and sulfide precursors is being excuted. One new compound has recently demonstated 10^{-3}S/cm at 100°C.
- Efforts to thermally stabilize these thio-acids with large alkali metal cations are underway. This may also produce primitive rotating phases with higher proton conduction values.
- Work is now underway to produce thermally and chemically stable membranes from these thio-acids. This involves bonding thio-acid units to known chemically and thermally durable compounds.

Introduction

Hydrogen-based fuel cells are becoming increasingly popular as an alternative to petroleum-fueled internal combustion engines. Specifically, hydrogen can be converted to electricity through the use of a (H_2-O_2) fuel cell. The by-product of this type of a fuel cell is water, making this a "green" or environmentally friendly technology. At the heart of the fuel cell is the proton exchange membrane (PEM), which transports the proton from the anode to the cathode while providing electronic insulation between them. There are many types of PEMs, each with specific limitations [1].

With current PEMs, there remains a temperature region between ~200°C and ~700°C that currently no one membrane can provide for optimum performance. We propose the use of chalcogenide glass-ceramic proton conducting membranes to help fill this temperature performance regime. These membranes are being developed to be highly conducting to protons, anhydrous in nature, thermally stable up to ~500°C, and chemically stable with respect to H_2O and O_2. Being solid in nature, these membranes are not expected to exhibit fuel cross-over problems. Proton conductivities of these membranes are expected to be orders of magnitude higher than their oxide counterparts, assuming they follow the trend exhibited by alkali cations such as lithium (Li) and silver (Ag) in chalcogenide verses oxide host materials [2].

Approach

Oxide, hydroxide, and sulfide compounds capable of forming thio-acids in liquid H_2S solution are being identified. As an example, the reaction of GeO_2 with liquid H_2S at room temperature produces the thio-acid ($H_4Ge_4S_{10} \bullet xH_2S$). Membranes may be produced by bonding thio-acid units with known thermally and chemically stable sulfide or oxide compounds. Taking a glass or ceramic material that has one or more thio-acid analogs and reacting it in a liquid H_2S solution is one way to accomplish this.

Proton conductivity in the glasses and glass-ceramics is being determined through impedance measurements as a function of temperature and frequency. Direct current polarization experiments have been used to determine the electronic verses ionic conductivity of the samples. Physical properties of the glass-ceramic proton conducting materials have been determined, including decomposition, sublimation, crystallization, and glass transition temperatures. Structural comparisons have been used to examine stability with exposure to H_2O and O_2.

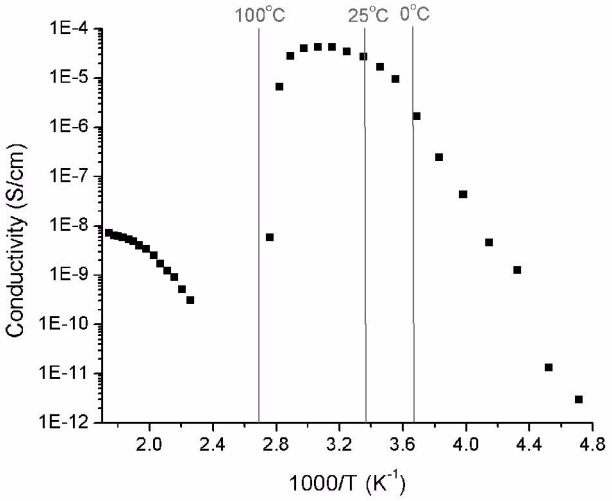

Figure 1. Proton Conductivity Values for the Thiogermanic Acid between -61°C and 300°C

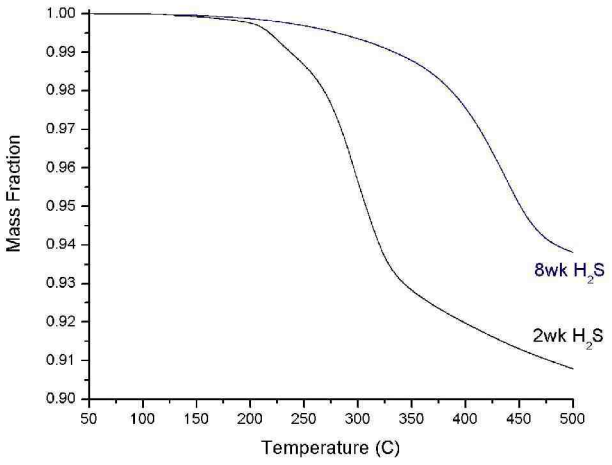

Figure 2. TGA Scan at 10°C/min of the Thiogermanic Acid

A cooperative effort to fabricate and test MEAs using our most promising membranes is being carried out in partnership with an external company specializing in fuel cells.

Results

Proton conduction has been demonstrated for our anhydrous thio-acid materials. Figure 1 shows the resulting proton conductivity values for

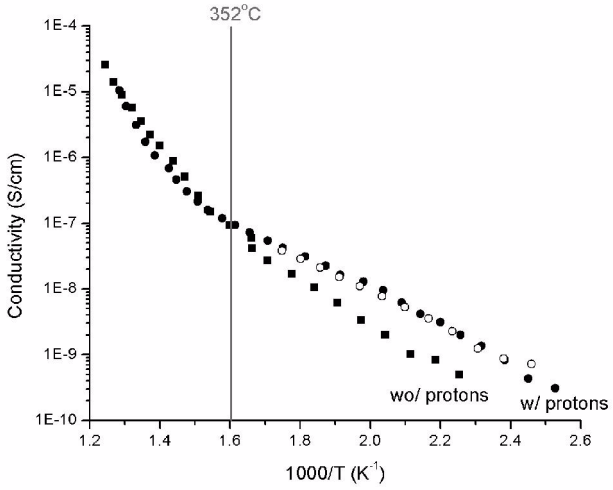

Figure 3. Proton Conductivity Values of the 0.14 Ga_2S_3 + 0.86 GeS_2 + H_2S System between 110°C and 500°C

nanostructured $H_4Ge_4S_{10} \bullet nH_2S$ produced by reacting GeO_2 with liquid H_2S for four weeks. The data is presented in the temperature range of 61°C to 300°C; a conductivity of 10^{-5}S/cm is realized at room temperature before the nanostructured $H_4Ge_4S_{10}$ material decomposes to the thiogermanic acid $H_2Ge_4S_9$. Effort is currently underway to stabilize the nanostructured $H_4Ge_4S_{10}$ material, thereby increasing the conductivity and useable temperature range.

Figure 2 illustrates thermogravimetric analyzer (TGA) spectra of the thiogermanic acid $H_2Ge_4S_9$. Longer reaction times, i.e. eight weeks versus two weeks, with liquid H_2S appears to produce a more thermally stable crystal phase.

Figure 3 demonstrates proton conduction for one of our thermally and chemically stable thio-acid membranes. A conductivity of 10^{-7}S/cm at ~ 352°C as achieved in the 0.14 gallium sulfide (Ga_2S_3) + 0.86 GeS_2 + H_2S system. This material is thermally stable to at least 500°C and chemically stable with prolonged H_2O exposures.

Figure 4 presents preliminary proton conduction for one of our new thio-acid compounds. Conductivity of 10^{-3}S/cm at ~100°C was achieved (this is close to the commercial PEM Nafion® ~

10^{-2} S/cm). Beyond 100°C this compound decomposes. Effort is currently underway to

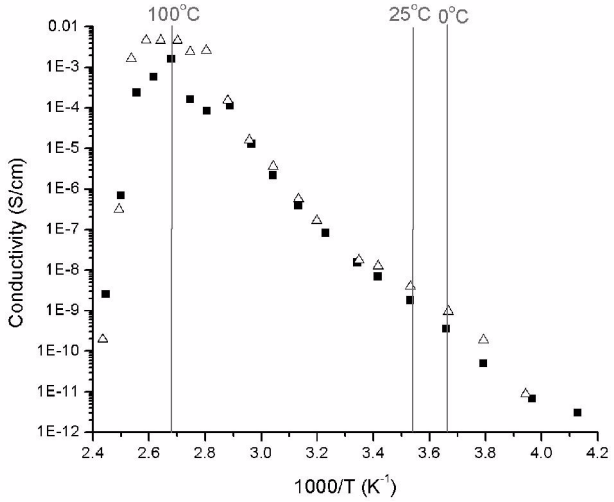

Figure 4. Preliminary Conductivity Values for a Newly Synthesized Compound between -31°C and 136°C

thermally stabilize this new thio-acid compound, and to increase its proton conductivity and useable temperature range.

Conclusions

- A synthesis route for producing thio-acids, hydrosulfides, and sulfides has been identified; effort to decrease production time is underway.The structure, conductivity, thermal and chemical stability of many potential thio-acids have been investigated; many more are being pursued.
- Two new thio-acids have been identified and synthesised for the first time, namely thiogermanic acid and thiomolybdic acid.
- Preliminary ionic conductivity as high as 10^{-3}S/cm at ~100°C has been realized from one new compound; this is close to the commercial membrane material Nafion®.
- Structural modifications to thio-acid compounds and thio-acid membranes are underway to increase thermal stability and conductivity.

References

1. Martin, S.W., Poling, S.A., Sutherland, J.T., "Design and Development of New Glass-Ceramic Proton Conducting Membranes." DOE Hydrogen Program Annual Review, Proceedings (2002): NREL/CP-610-32405.

2. Angell, C.A. 1992. "Mobile Ions in Amorphous Solids." Annual Review of Physical Chemistry, 43:693-717.

FY 2002 Publications/Presentations

1. "Design and Development of New Glass-Ceramic Proton Conducting Membranes," Steve W. Martin, Steven A. Poling, and Jacob T. Sutherland, DOE Hydrogen Program Annual Review, Proceedings (2002): NREL/CP-610-32405.

2. "Synthesis and Structure of Thiogermanic Acid $H_2Ge_4S_9$," Steven A. Poling, Steve W. Martin, and Jacob T. Sutherland, to be submitted.

3. "Design and Development of New Glass-Ceramic Proton Conducting Membranes," Steve W. Martin, Steven A. Poling, and Jacob T. Sutherland, DOE Hydrogen Program Annual Review, Golden, CO, May 6-10, 2002.

4. "Synthesis and Characterization of a New Class of Ceramic Proton Conducting Solid Electrolytes," Steve W. Martin, Steven A. Poling, and Jacob T. Sutherland, 201st Meeting of The Electrochemical Society, Philadelphia, PA, May 12-17, 2002.

5. Invited Talk, "Preparation and Characterization of New Proton Conducting Chalcogenide Glasses and Glass-Ceramics," University of Muenster, Muenster, Germany, July, 2002.

6. Invited Talk, "Preparation and Characterization of New Proton Conducting Chalcogenide Glasses and Glass-Ceramics," University of Dortmund, Dortmund, Germany, July, 2002.

7. "Invited Talk, "Preparation and Characterization of New Proton Conducting Chalcogenide Glasses and Glass-Ceramics," University of Montepellier II, Montepellier, France, July, 2002.

8. "Protonated Chalcogenide Materials for Fuel Cell Electrolyte Membranes," poster at the104th Annual Meeting and Exposition of the American Ceramic Society, Steve W. Martin, Steven A. Poling, and Jacob T. Sutherland, St. Louis, MO, April 29-May 1, 2002.

Special Recognitions & Awards/Patents

1. Provisional Patent: "Synthesis and Uses of Thio Acids" Steve W. Martin, Steven A. Poling, Jacob T. Sutherland, Iowa State University, ROI ISURF 2894, February 8, 2002. Provisional filing date of July 26, 2002.

IV.D.26 Fuel Cell System Durability

Rod Borup (Primary Contact), Michael Inbody, Troy A. Semelsberger, Francisco Uribe, and José Tafoya
P.O. Box 1663
Los Alamos National Laboratory
Los Alamos, NM 87545
(505) 667-2823, fax: (505) 665-9507, e-mail: Borup@lanl.gov

DOE Technology Development Managers:
JoAnn Milliken: (202) 586-2480, fax: (202) 586-9811, e-mail: JoAnn.Milliken@ee.doe.gov
Nancy Garland: (202) 586-5673, fax: (202) 586-9811, e-mail: Nancy.Garland@ee.doe.gov

Objectives

- Achieve DOE system durability target of 5,000 hours on reformate.
- Quantify fuel cell component durability
  - Fuel processor durability reforming liquid hydrocarbons (gasoline)
  - Fuel cell durability on reformed gasoline
  - Fuel cell durability on hydrogen
- Quantify fuel reformate effects on fuel cell system (fuel processor and fuel cell stack) durability
  - Determine stack durability limits of operation with reformed fuel
    - Determine reformate effect on electrocatalyst durability
    - Determine reformate effect on proton exchange membrane durability
  - Determine fuel and fuel impurity effects on fuel processor catalyst durability
  - Identify reformate species which limit fuel cell anode durability

Approach

- Measure single cell fuel cell performance with hydrogen and gasoline reformate
  - Measure stack component durability with hydrogen
  - Measure stack component durability with gasoline reformate from fuel processor
- Operate modular fuel processor system with liquid hydrocarbons to generate real reformate
  - Measure fuel processor operation and reformate composition over long operational period (1000 hrs)
    - Analyze fuel processor catalysts to determine structural and elemental changes
    - Analyze reformate to determine low level of impurities
  - Characterize membrane electrode assemblies (MEAs) during operation
    - Electrochemical polarization curves, high frequency measurements
    - Hydrogen adsorption/desorption

Accomplishments

- Operated fuel processor system with liquid hydrocarbon fuels for over 1000 hrs
  - Measured fuel reformate impurities
    - Near-zero NH_3 formation (<0.5 ppm) with normal operating conditions

  - Measured catalyst surface area after extended operation (~1,200 hours)
    - Decrease of 20% to 90% observed in autothermal reforming (ATR) and preferential oxidation (PrOx) catalysts, including loss in activity and CO conversion in PrOx
- Improved fuel processor subsystem (carbon formation and fuel processor hydrocarbon breakthrough)
  - Carbon formation limited by precious metal steam reforming catalysts, high steam-to-carbon (S/C) ratio (1.3), and high reforming temperature (>725^{o}C)
  - Hydrocarbon breakthrough limited by additional S/C and reforming catalysts (<20 ppm C_2 compounds)
- Measured hydrogen proton exchange membrane (PEM) performance
  - Operated single cells with reformate and hydrogen – low performance observed with reformate

Future Directions

- Improve fuel processor conversion to eliminate high molecular weight hydrocarbon formation
- Study stack operation on reformed petroleum-based fuels to evaluate reformate effects:
  - Pure fuel components and components blends
  - Real fuels such as reformulated gasoline
- Measure fuel cell stack durability with hydrogen and reformate for direct comparison of reformate effects

---

Introduction

This report describes our FY02 technical progress in examining the durability of fuel cell systems to support the DOE target for 5,000 hour durability of these systems. The goal of this research is to identify the factors limiting the durability of fuel cells and fuel processors. This includes PEM fuel cell durability issues for operating on pure hydrogen, as well as those that arise from the fuel processing of liquid hydrocarbons (e.g., gasoline) as a function of fuel composition and impurity content. Benchmark comparisons with the durability of fuel cells operating on pure hydrogen are used to identify limiting factors unique to fuel processing.

We describe the design, operation and operational results of the durability system, including the operating conditions for the system, fuel processor subsystem operation over 1000 hours, post-mortem characterization of the catalysts in the fuel processor, and single cell operation.

Approach: Durability Gasoline Reformate Production and Single Cell Fuel Cells

Our approach to identify the limiting factors on fuel cell system durability is, first, to develop and operate a modular fuel processor system to examine the fuel composition and impurity effects on fuel processor durability and to generate reformate for testing the durability of fuel cell components. Second, we examine the effects of the reformate on the fuel cell components, primarily the membrane electrode assembly (MEA), by testing MEAs in single-cell fuel cells operating on both reformate and pure hydrogen. Third, we use a combination of fuel processor gas analysis, fuel processor catalyst characterization, and MEA characterization during and after operation to quantify performance losses and to identify limiting factors on durability such as poisons. The modular fuel processor subsystem, shown in Figure 1, was designed and constructed to simulate conventional methods of hydrogen generation for PEM fuel cell stacks. The fuel processor consists of a sequence of reactors: a partial oxidation/steam reformer (POx/SR) or autothermal reformer (ATR), sulfur removal, high-temperature shift (HTS), low-temperature shift (LTS), and preferential oxidation reactor (PrOx). Typical commercial and semi-commercial noble metal oxidation catalysts and noble metal or non-noble metal steam reforming catalysts are used in the ATR. Conventional commercial catalysts also are used in the HTS, LTS, and PrOx to allow full

Figure 1. Fuel Processor System Showing the Stages for POx/SR, HTS, LTS and PrOx

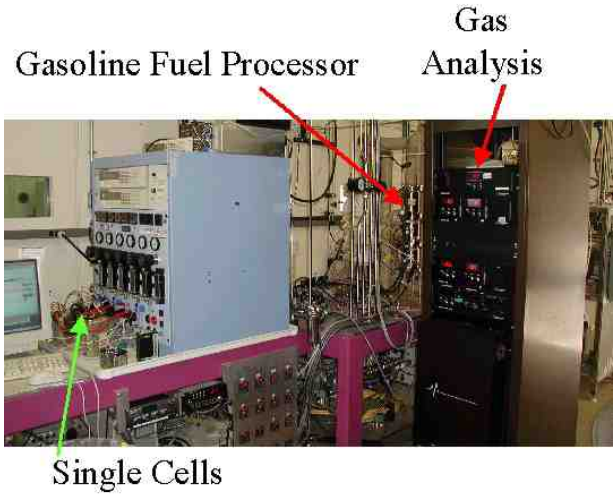

Figure 2. Fuel Processor Coupled with Fuel Cell Test Station and Two PEM Fuel Cell Single Cells

characterization of the catalysts without violating proprietary concerns. The ATR atomic O/C (oxygen/carbon - O from air only) is 0.8 to 0.85, while typical S/C (steam/carbon) is from 1.0 to 1.25. Additional downstream liquid water injection increases the overall S/C ratio to a typical S/C of 2.5 to 3.0. A slipstream of the reformate flow from the fuel processor is routed to the fuel cell test station.

Figure 2 shows the fuel cell test station and single cells coupled with the fuel processor. The fuel

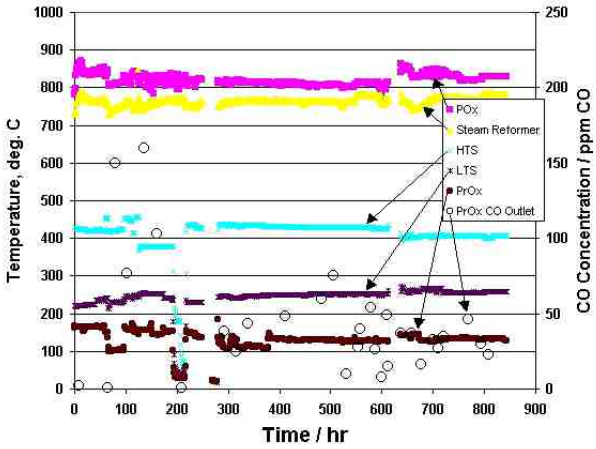

Figure 3. Temperature and PrOx Outlet CO Concentration of Fuel Processor System during ~ 800 hrs Operation with Isooctane

cell test station can operate 3 single-cell fuel cells with either pure hydrogen or with the gasoline reformate. The direct comparison of pure hydrogen and reformate feeds to the single cells is used to identify the effects that fuel processing reformate has on the fuel cell durability. Currently, 50 cm^2 single cell components are being tested. Performance during the durability test is measured with continual monitoring of the voltage/current performance along with periodic polarization curve, AC Impedance, and hydrogen adsorption/desorption (HAD) measurements to monitor the anode catalyst surface area. Following the durability testing, MEAs will be characterized to evaluate degradation mechanisms.

Results: Fuel Processor Operation

The fuel processor subsystem was operated with pure iso-octane to verify its performance. Figure 3 shows 800 hours of the fuel processor operation on iso-octane, showing the temperatures in the different stages, and the CO outlet concentration. The temperature in the partial oxidation stage is about 800 – 825°C, and the outlet temperature of the steam reforming section is 775°C. The average residence time for the ATR section is about 0.5 sec (GHSV ~ 10,000), which should be sufficient for complete hydrocarbon conversion.

The HTS is operated at 400°C, the LTS is operated at 250°C, and the PrOx is controlled to a temperature of 125°C. The outlet CO concentration

from the ATR was typically about 10%; the outlet CO concentration from the LTS was <1%; and the outlet CO concentration from the PrOx varied initially from 0 to 150 ppm, with improved controls keeping the CO concentration below 100 ppm and typically below 40 ppm.

Figure 4 shows operation of the fuel processor subsystem on iso-octane for 11 days, after which the fuel was switched to a simulated gasoline of 74% iso-octane, 20% xylene, 5% methylcyclohexane and 1% 1-pentene. After only two days of operation on this simulated gasoline, the pressure drop between the ATR and HTS increased due to carbon formation. Post characterization of the carbon formed showed that a high concentration of solidified hydrocarbons were present in the carbon (30% by weight). To prevent carbon formation between these reactor sections, the HTS water injection was moved from the inlet to the HTS to the outlet of the steam reformer section.

After extended operation, the catalysts present in the fuel processor were characterized to observe any potential degradation of the catalysts. The relative catalyst surface areas of the ATR, HTS, LTS and PrOx catalysts all decreased after extended operation. The initial portion of the ATR catalyst, where the fuel oxidation occurs, showed a large decrease in surface area, over an order of magnitude decrease from about 3 m^2/g to <0.2 m^2/g (note that the surface area is low because the support material is included in the measurement). Other portions of the ATR catalyst did not show as big a decrease in surface area. The LTS catalyst surface area decreased about 50%, which appears to be independent of the catalyst location in the LTS section. The measured PrOx catalyst surface area, shown in Figure 5, decreased as a function of the axial location in the reactor catalyst volume. The measured PrOx catalyst surface area shows a high decrease in the upstream section, while in downstream sections of the PrOx, approximately 75% of the original surface area is maintained.

Current results indicate operational issues for the fuel processor subsystem to meet the DOE durability target of 5000 hours due to carbon formation and catalyst surface area. Upon post-analysis of the fuel processor, carbon formation was observed regardless

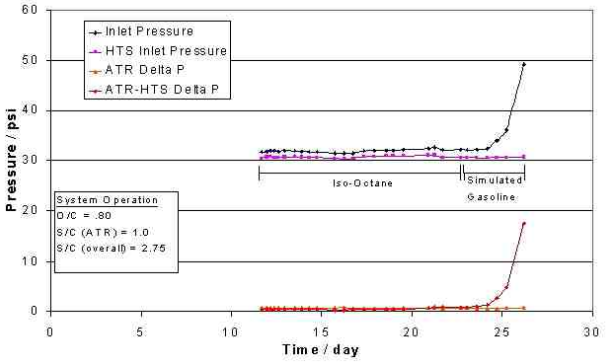

Figure 4. Operation of fuel processor with isooctane and simulated fuel. Inlet pressures and pressure drops are shown, demonstrating the build-up of carbon in between the ATR and HTS.

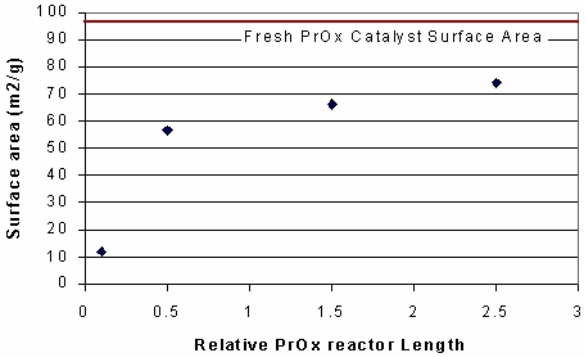

Figure 5. PrOx Catalyst Surface Area after Total On-Stream Time of ~1200 hrs of Operation

of fuel composition and operating condition. When aromatics were present in the fuel, carbon formation was a much a larger issue, such that the amount of carbon formed caused increases in the system pressure drop. Various improvements in the ATR design, including the water injection for the HTS, decreased the amount of carbon formation. In addition, elimination of any nickel steam reforming catalysts has helped decrease carbon formation.

Results: Single Cell Operation

Figure 6 shows a single cell operation for Nafion 112 MEAs on pure hydrogen, and with reformate produced from the fuel processor. The steady state performance of the MEA on pure hydrogen was about 0.9 A/cm^2 at 0.62 V. At hour 48, the pure hydrogen feed was switched to the gasoline

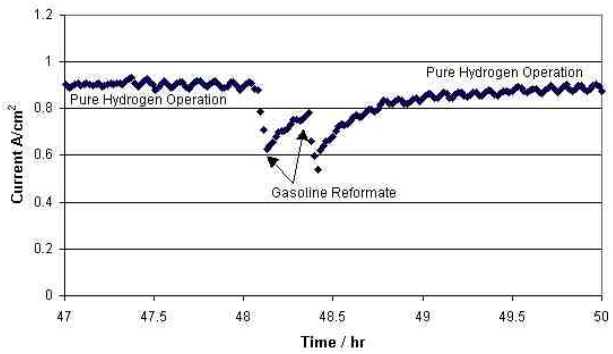

Figure 6. Single Cell Operation on H_2, Followed by Operation on Gasoline Reformate

reformate. Even though the CO content of the fuel processor was below 50 ppm, and air injection was used for the anode of the fuel cell, the performance of the fuel cell was poor, as shown by the rapidly dropping current density of the MEA. As the reformate was switched back to pure hydrogen, the performance recovered quickly, within a few minutes.

Analysis of the fuel processor condensate showed that hydrocarbons were present. The hydrocarbons found in the condensate include hydrocarbons with molecular weights higher than those present in the original fuel, over 150. This could mean that some polyaromatic hydrocarbons are formed. Changes to the catalyst used in the fuel processor ATR section have been made to reduce the hydrocarbon output of the fuel processor section to improve performance of the fuel cells.

Hydrocarbon breakthrough from the fuel processor appears to have limited the durability of the PEM fuel cell anode. The loss of MEA humidification has also been observed to limit MEA durability. Hydrocarbon breakthrough has been eliminated by using small amounts of nickel catalyst in the ATR portion of the fuel processor; however, this resulted in carbon formation, which limited the fuel processor operational durability. Increasing the ATR S/C ration, adding precious metal steam reforming catalyst, and increasing the steam reforming temperature has also eliminated the hydrocarbon breakthrough. Modification of the MEA humidification should eliminate loss of gas feed humidification. These improvements should greatly improve the PEM MEA durability.

Conclusions

Fuel processor operation producing hydrogen with low carbon monoxide content has been demonstrated for over 1000 operational hours. Current results indicate difficulties in operating the fuel processor subsystem continuously for the DOE target of 5000 hours due to carbon formation and reduced catalyst surface area. The catalyst surface decreased in all the stages of the fuel processor, with the amount of decrease depending on the catalyst and its axial location in the catalyst volume. Although the carbon monoxide concentration in the outlet of the fuel processor is low, the performance of the single cells is poor, apparently due to small amounts of hydrocarbons present in the reformate stream. Carbon formation over relatively long periods of time was also an issue between the ATR and HTS stages when fuels containing aromatics were used.

Future work is being conducted to examine fuel processor durability, PEM cell durability on reformate, and operation of PEM fuel cells on hydrogen. The durability of fuel processor catalysts and reactor materials will be examined with 'real' fuel blends with operation and design modified to help prevent carbon formation. This work will evaluate the fuel processor catalyst durability, carbon formation, and changes to the mechanical properties of ATR materials. PEM cell durability studies will concentrate on the operation and causes of degradation of the MEA portion of the fuel cell.

Presentations/Publications

1. Fuels for Fuel Cells for Transportation Applications, Rod Borup, Lee Perry, Mike Inbody, Byron Morton, Troy Semelsberger and Jose Tafoya, AIChE Meeting, Spring 2002, New Orleans, LA, Los Alamos National Laboratory publication, LAUR-02-1207, March 2002.

IV.E Air Management Subsystems

IV.E.1 Turbocompressor for PEM Fuel Cells

Mark K. Gee
Honeywell Engines & Systems
2525 W. 190th Street, MS-36-2-93084
Torrance, CA 90504
(310) 512-3606, fax: (310) 512-4998, e-mail: mark.gee@honeywell.com

DOE Technology Development Manager: Patrick Davis
(202) 586-8061, fax: (202) 586-9811, e-mail: Patrick.Davis@ee.doe.gov

ANL Technical Advisor: Bob Sutton
(630) 252-4321, fax: (630) 252-4176, e-mail: sutton@cmt.anl.gov

Objectives

- Develop an optimum turbocompressor configuration by working with fuel cell system manufacturers and by improving upon previous project results.
- Reduce turbocompressor/motor controller costs while increasing design flexibility.
- Develop and integrate the turbocompressor/motor controller into a fuel cell system.

Approach

- Use automotive and aerospace turbomachinery technology to reduce cost and weight/volume.
- Use VNT® variable nozzle turbine inlet geometry to improve performance across the desired flow range.
- Use a mixed flow type compressor to improve low flow performance.
- Use contamination/oil free and zero maintenance compliant foil air bearings.
- Use a modular approach to improve design flexibility.
- Use a high efficiency, low cost two pole toothless motor.
- Use a low cost, no sensor required, variable speed motor-controller topology design.

Accomplishments

- Accomplished numerous start/stop cycles with no appreciable wear.
- Continued demonstration of a modified turbocompressor with increased turbine inlet temperature (315°C) capability and aerospace quality variable speed brassboard motor controller in the 50-kW DOE/Honeywell fuel cell brassboard system.
- Completed the analysis, design, and fabrication of the turbocompressor with a mixed flow compressor and VNT® variable nozzle turbine.
- Completed the analysis, design, and fabrication of a vehicle ready motor controller.
- Completed testing of the mixed flow compressor.
- Completed integration testing of the turbocompressor and vehicle-ready motor controller.

Future Directions

- Complete testing of the turbocompressor VNT® variable nozzle turbine.
- Complete analysis, design, fabrication, and testing of a reduced cost and enhanced performance turbocompressor.
- Complete analysis, design, fabrication, and testing of a reduced cost and enhanced performance motor.
- Complete analysis, design, fabrication, and testing of a reduced cost and enhanced performance motor controller with no sensor requirements.

Introduction

The objective of this work is to develop an air management system to pressurize a light-duty vehicle fuel cell system. The turbocompressor is a motor-driven compressor/expander that pressurizes the fuel cell system and recovers subsequent energy from the high-pressure exhaust streams. Honeywell designed and developed the motor driven compressor/expander and evaluated performance, weight and cost projection data. As compared to a positive displacement technology, the turbocompressor approach offers high efficiency and low-cost potential, in a compact and lightweight package.

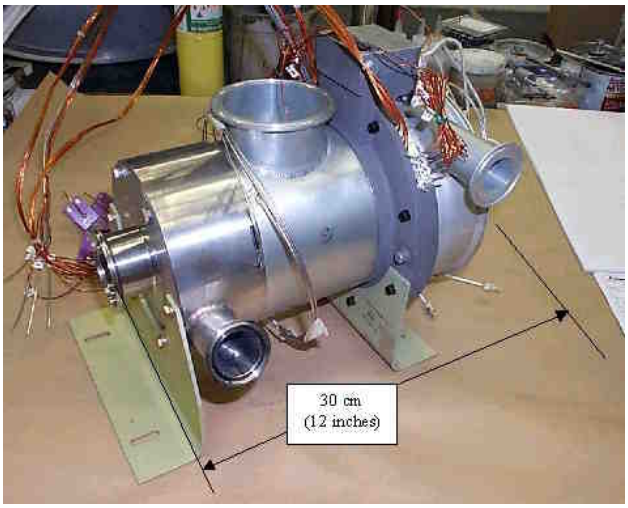

Figure 1. Honeywell Fuel Cell Turbocompressor with Mixed Flow Compressor and VNT® Variable Nozzle Turbine

Approach

The turbocompressor design depicted in Figures 1 and 2 consists of a compressor impeller, an expander/turbine wheel, and a motor magnet rotor incorporated onto a common shaft operating up to a speed of 110 krpm on compliant foil air bearings. A motor controller drives and controls the motor, which is capable of driving the turbocompressor to the maximum design speed. The air bearings are lubrication free in addition to being lightweight, compact, and self-sustaining. Thus, no pressurized air is required for operation. The current turbocompressor operates by drawing in ambient air through the motor/bearing cavities, where it is pressurized by the compressor, delivered to the fuel cell stack, used to oxidize any excess fuel in a tailgas combustor, then expanded through the turbine to aid in the overall turbocompressor/fuel cell system efficiency.

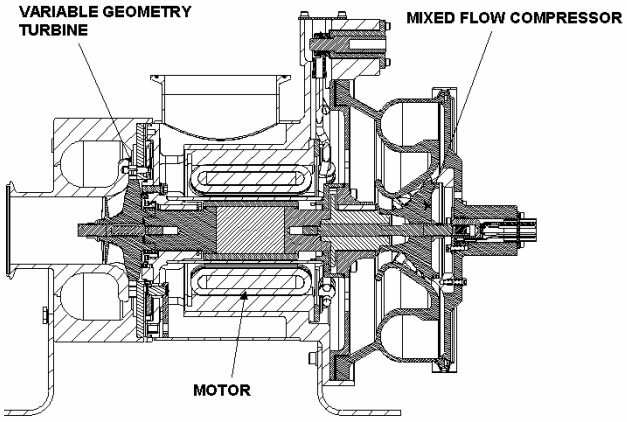

Figure 2. Cross Section of Fuel Cell Turbocompressor with Mixed Flow Compressor and VNT®

Results

The current turbocompressor has operated for more than 450 hours at varying conditions. To date, a maximum speed of 110 krpm has been attained.

To support the DOE/Honeywell fuel cell brassboard system testing, the turbocompressor was modified to handle increased turbine inlet temperatures. In addition, a modified aerospace quality motor/controller was assembled and used in the DOE/Honeywell fuel cell brassboard system, replacing a previously used motor/controller commercial unit. Testing of the DOE/Honeywell fuel cell brassboard system was initiated in late 2000 and is expected to be completed in mid 2002.

The turbocompressor and vehicle-ready motor controller was analyzed, designed, fabricated, and tested (see Figures 1, 2, and 3, and Table 1). The turbocompressor incorporates a mixed flow compressor and a VNT® variable nozzle turbine. These features were incorporated to improve the low-flow performance while maintaining efficiency across the flow range. These changes included the following: the redesigned mixed flow compressor improved low flow performance with an improved surge line; however, the VNT® variable nozzle turbine, which would have further improved performance and, consequently, lowered overall power consumption, was not tested due to program constraints. The vehicle-ready motor controller is of reduced size. Although its new technology requiring no sensors was not incorporated due to project constraints, the controller topology is configured to reduce production costs. Predicted performance of the turbocompressor and motor controller with the mixed flow compressor test results is presented in Figure 4.

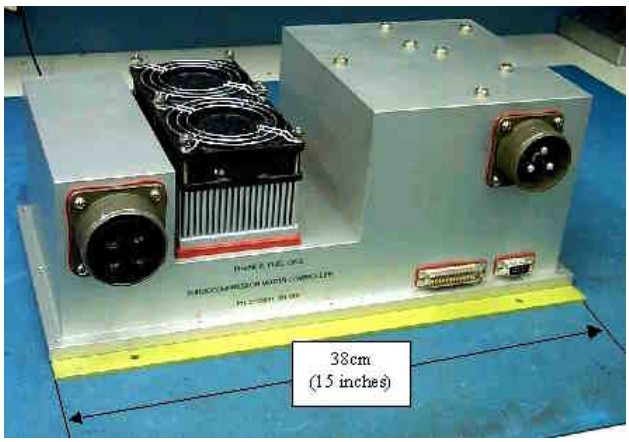

Figure 3. Fuel Cell Turbocompressor Motor Controller

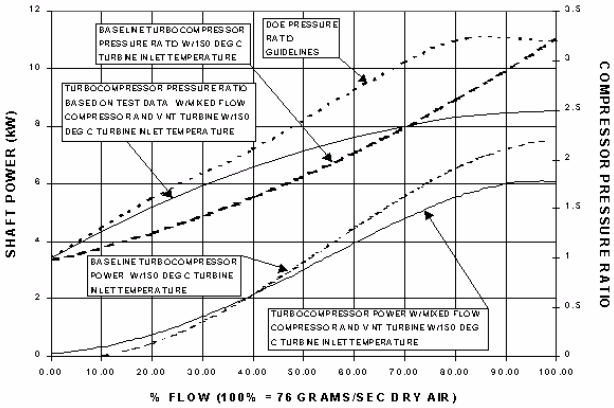

Figure 4. Turbocompressor Shaft Power/Compressor Outlet Pressure Ratio vs. % Flow

DOE Parameters	DOE Guidelines	Honeywell Turbocompressor
Volume	4 liters total (w/o heat exchangers)	Turbocompr.: 6 liters Controller: 13 liters
Weight	3 kg total (w/o heat exchangers)	Turbocompr.: 9 kg max Controller: 6.5 kg max

Table 1. Fuel Cell Turbocompressor Physical Parameters

Conclusions/Future Work

The turbocompressor concept using self-sustaining compliant foil air bearings has demonstrated low power consumption and moderate pressure ratio at low flow rates in a compact lightweight package. Predicted power consumption, which includes the predicted effects of the VNT® variable turbine nozzle can be further reduced if increased expander/turbine temperatures can be provided by the fuel cell system. The turbocompressor, capable of increased expander/turbine temperatures, continues to be demonstrated in the DOE/Honeywell 50-kW fuel cell brassboard system. The latest turbocompressor with mixed flow compressor and variable inlet nozzle turbine technology, which, however, has not been utilized to date, demonstrated improved low-flow performance,

while the latest variable speed motor/controller demonstrated reduced size, weight, reliability, and cost. Future work will investigate turbocompressor designs that incorporate flexibility to better meet the various vehicle fuel cell system developers' needs in the rapidly changing vehicle fuel cell system market, while continuing to improve performance and reduce cost.

IV.E.2 Development and Testing of a High Efficiency Integrated Compressor/ Expander Based on Toroidal Intersecting Vane Machine Geometry

Sterling Bailey (Primary Contact), Steve Chomyszak
Mechanology, LLC
453 South Main Street
Attleboro, MA 02703
(408) 356-5520, fax: (408) 358-4012, e-mail: sterling@mechanology.com

DOE Technology Development Manager: Patrick Davis
(202) 586-8061, fax: (202) 586-9811, e-mail: Patrick.Davis@ee.doe.gov

ANL Technical Advisor: Robert Sutton
(630) 252-4321, fax: (630) 252-4176, e-mail: Sutton@cmt.anl.gov

Objectives

- Develop a Toroidal Intersecting Vane Machine (TIVM)-based air management system that satisfies DOE's 50-kWe automotive fuel cell system requirements and is readily adaptable to alternate user requirements.
- Select and demonstrate design features to assure adequate sealing, minimum porting pressure loss, and low friction operation.
- Measure the performance of the TIVM compressor/expander across the operating range.
- Fabricate and deliver a compressor/expander/motor prototype for independent testing.

Approach

- Test candidate materials for friction and wear using standard laboratory tribilogical methods.
- Test candidate seal and port designs as well as low friction materials in simplified test configurations to select the best performing options for the TIVM compressor/expander.
- Optimize the vane surface solution methodology to provide a more efficient design process.
- Fabricate a TIVM compressor/expander prototype using seals, porting, and materials selected from the simplified feature tests and evaluations.
- Conduct performance tests of the prototype covering the full operating range.
- Refine the prototype features as necessary to obtain optimal performance.
- Integrate a high efficiency motor with the TIVM prototype and test the combined unit across the operating range.
- Deliver a TIVM compressor/expander/motor prototype to ANL for testing.

Accomplishments

- Initial friction and wear tests have identified one suitable material pair for the TIVM operating conditions and lifetime requirement. Additional tests are underway.
- A simplified single vane test rig has been designed for screening of seal and port designs and low friction materials. Hardware has been procured and assembly is in progress.
- CFD calculations have been initiated to guide seal and port designs.
- Analyses have been performed to determine port flow area and timing requirements.

- Design optimization has reduced maximum speed from 4800 rpm to 3500 rpm with no increase in volume.
- A Linear Intersecting Vane Machine test device has been designed to allow simplified testing of vane interaction features.
- Experimental expander vanes are being fabricated to potentially qualify a unique powder metallurgy process that provides net shape, finish, and hardness without secondary operations.
- A theoretical mathematical analysis of the surface solution methodology has been initiated.
- Initial thermal analyses have been performed to evaluate geometric changes caused by differential thermal expansion.

Future Directions

- Screening tests will be performed in the single vane test device using candidate seals and ports as well as low friction materials. Results will be evaluated to select the best options and to identify additional options to be tested.
- The Linear Intersecting Vane Machine test device will be fabricated and used with selected seals, ports, and low friction materials to provide basic performance data applicable to the TIVM and to further down-select options.
- The best performing design and material options will be implemented in a fully functional TIVM compressor/expander prototype, which will be tested across the operating range using Mechanology's automated test stand.
- The TIVM prototype will be refined based on empirical and analytical data to optimize performance.
- A high efficiency motor will be integrated with the TIVM compressor/expander and a prototype compressor/expander/motor unit will be fabricated and delivered to ANL for independent testing.

Introduction

The Toroidal Intersecting Vane Machine (TIVM) is an innovative mechanical concept, invented and patented by Mechanology, that can be configured as an integrated, positive displacement compressor/expander or compressor/compressor. In FY99 DOE investigated the TIVM concept for potential application to automotive fuel cell systems and determined that the inherent efficiency, compactness and thermodynamic attributes of this concept might be of significant benefit. Mechanology developed a prototype design specifically for the 50-kWe automotive system and evaluated its potential performance. Based on the encouraging results obtained, a first generation compressor/expander prototype was built and tested. Figure 1 illustrates this prototype partially assembled to show the compressor and expander. The compressor/expander prototype tests indicated that the TIVM runs smoothly with no mechanical problems; however,

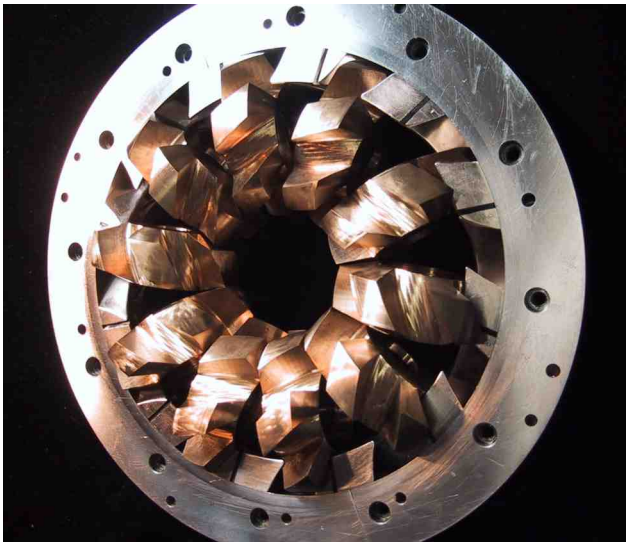

Figure 1. Partially Assembled First Generation TIVM Compressor/Expander Prototype

improvements are required to limit air leakage. Additional tests using the generic prototype with temporary seals demonstrated the capability of the TIVM to produce the necessary flow and pressure. The TIVM compressor/expander development plan was subsequently refocused on development and demonstration of seals, ports, and low friction materials. These are necessary to satisfy the functional performance requirements with low parasitic power. Although not the main focus of the current development program, the requirements for air management system packaging, noise, and cost are also considered critical for a successful TIVM based system and are carefully considered as development progresses.

Approach

The basic functions of the TIVM compressor/expander (kinematics, pressure, flow) have been demonstrated; however, development and qualification of specific seals, flow ports, and low friction materials are required to meet the performance requirements.

During 2002 Mechanology has focused on the use of simplified feature tests to allow rapid, efficient characterization of a broad range of design options for later inclusion in a full TIVM device. The initial simplified tests use a single vane test device to measure the leakage and friction characteristics of candidate vane seal designs and the effectiveness of alternate flow port designs. Computational Fluid Dynamics (CFD) analysis of the vane/housing/air interactions will be used to guide the design and testing of these features. Additional tests will be performed using a Linear Intersecting Vane Machine (LIVM) which introduces the vane interactions in simplified geometry. These tests will be used to further screen seal, port, and material candidates.

Definition of the vane surface configurations required for a specific TIVM can be accomplished through an iterative process developed by Mechanology. With sufficient iterations, a very good meshing surface solution can be obtained, as evidenced by the generic TIVM prototype vanes. However, this process is quite time consuming. Mechanology is exploring alternate mathematical approaches to develop a more efficient surface design methodology.

Low friction materials are necessary for the intersecting vanes to realize the predicted energy efficiency of the TIVM compressor/expander. Additionally, these materials must have sufficiently low wear under the TIVM operating conditions to perform acceptably during a 6,000-hour lifetime. Several candidate material pairs and potential coatings have been identified based on published data. To qualify materials for the TIVM, standard laboratory friction and wear tests are being performed. Successful materials will be tested in the single vane and LIVM devices, and the best materials will be used in a TIVM prototype.

One or more full TIVM compressor/expander prototypes will be fabricated by Mechanology and tested across the full operating range. Modifications will be made as necessary to optimize performance. Subsequently, a high efficiency electric motor will be integrated with the TIVM to form a complete compressor/expander/motor (CEM) component. This unit will be tested by Mechanology and then delivered to ANL for independent testing.

Results

ANL has constructed a tribology test rig that operates at the speed and interface pressure of the TIVM compressor/expander vanes at full power. This test rig is depicted in Figure 2. Initial dry friction and wear tests with stainless steel and low friction engineered polymer samples provided by Mechanology have indicated an acceptable friction coefficient at the TIVM operating conditions and wear rate consistent with the lifetime requirement. Additional tests are being conducted with high humidity and different material combinations.

A simplified single vane test rig has been designed for screening of seal and port designs and testing of low friction materials with vanes traveling at speeds in the planned operating range. The single vane test device design with the pressure cover removed is illustrated in Figure 3. This device is designed to permit parametric variation of clearances and seal preloads as well as rapid change out of materials and seal designs. Test hardware and

Figure 2. ANL Tribology Test Equipment

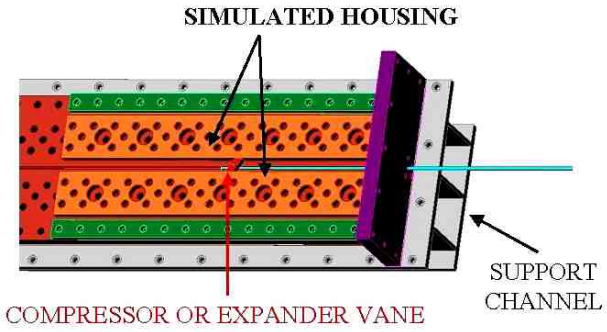

Figure 3. Single Vane Test Apparatus Design

instrumentation have been procured, and assembly is in progress. A computer control and data acquisition program has been written to allow testing at specified speeds and pressure differentials with automated data logging.

CFD calculations have been initiated at ANL using Mechanology's single vane test configuration. These analyses will be used to understand the interaction of the vane/seal/air system as a function of operating conditions and to guide seal and port designs.

Optimization of the geometry detail has reduced the speed required for 100% flow from 4800 rpm for the first generation TIVM to 3500 rpm for later generations with no increase in the component

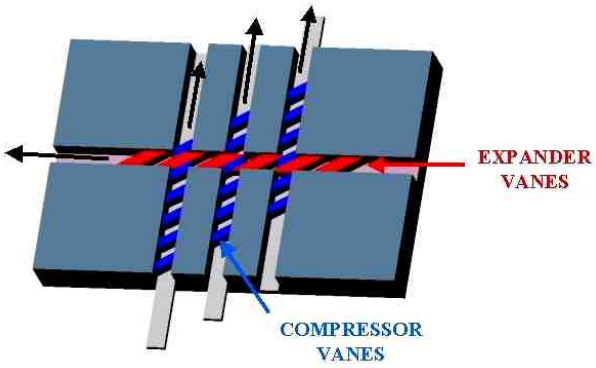

Figure 4. Linear Intersecting Vane Machine Design

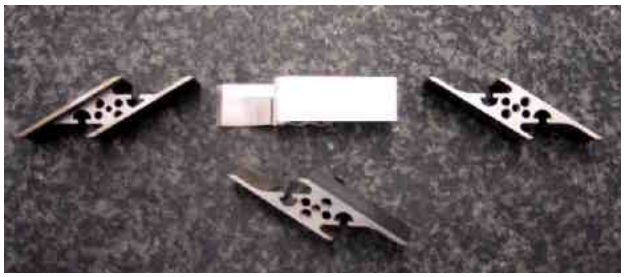

Figure 5. Vanes for Linear Intersecting Vane Machine Testing

overall dimensions. This has reduced the peak vane interaction speed by 25%.

A Linear Intersecting Vane Machine (LIVM) test device has been designed to allow simplified, rapid testing of vane interaction features. The LIVM design is shown schematically in Figure 4. The expander vanes in the LIVM, just as in the actual TIVM, drive the compressor vanes. The LIVM is instrumented to measure flows and pressures in the compression and expansion chambers as well as the force required as a function of time. Figure 5 shows an initial set of compressor vanes, with cutouts to accommodate various seal design inserts, to be tested in the LIVM.

Conclusions/Future Work

Design and analysis of the first generation TIVM compressor/expander has shown that this concept has the potential to meet the DOE requirements for automotive fuel cell applications with better performance than many other options. Testing of the compressor/expander and generic TIVM prototypes

has demonstrated correct kinematic functioning and the capability to produce the required pressure and flow. These tests have also highlighted the need for efficient seals and flow ports in the TIVM. Laboratory tribology measurements have indicated acceptably low friction and wear for one of the material pair candidates for the intersecting vanes. The ongoing development program is focusing on selection of seals, porting, and material options through simplified feature tests and then, sequentially, more prototypic TIVM tests. A full prototype TIVM compressor/expander/motor will be fabricated and tested to measure actual performance with the selected options. Subsequent work will include development and qualification of cost efficient manufacturing methods for high volume production and development of features to assure compliance with noise requirements. Additional testing will focus on the operating environment and reliability/endurance issues.

FY 2002 Publications/Presentations

1. Toroidal Air Management System Development and Testing Status, presented to the FreedomCAR Technical Team, April 17, 2002.

IV.E.3 Turbocompressor for Vehicular Fuel Cell Service

P. Fonda-Bonardi
Meruit, Inc.
1450 23rd Street,
Santa Monica, CA 90404-2902
(310) 453-3259, fax: (310) 828-5830, e-mail: fbarch@concentric.net

DOE Technology Development Manager: Patrick Davis
(202) 586-8061, fax: (202) 586-9811, e-mail: Patrick.Davis@ee.doe.gov

ANL Technical Advisor: Dr. Robert Sutton
(630) 252-4321, fax: (630) 252-4176, e-mail: sutton@cmt.anl.gov

Subcontractors: MarNor Enterprises, Newport Beach, CA (instrumentation); FD Contours, Costa Mesa, CA; Prestige Mold, Santa Ana, CA (fabrication)

Objectives

- Test the design and performance of air bearings for turbocompressors.
- Test the performance of the expander and compressor for fuel cell system service.
- Test the endurance of Argonne National Laboratory's (ANL's) near-frictionless carbon (NFC) coatings in air bearings.

Approach

- Design, build, and test a specialized, instrumented test rig for measuring the performance of a new, high performance air bearing.
- Measure the performance of the DOE/Argonne near-frictionless carbon coating.
- Design, build, and test the prototype of a turbocompressor system supplying 76 g/sec of air for a fuel cell rated for 50-kWe output.

Accomplishments

- Demonstrated a mechanically simple (leafless) journal bearing for small (~1 kg weight, ~2 cm shaft diameter) rotors with lift-off and landing speeds of about 900 RPM, corresponding to a rubbing speed of about 1 m/s and a total rub of about 2 m per start-stop cycle.
- Completed over 10,000 start-stop cycles with minimal NFC wear during NFC endurance testing; also demonstrated 3,700 start-stop cycles with DuPont Vespel journals and 1,300 start-stop cycles with DuPont Delrin journals.
- Demonstrated radial bearing take-off and landing without any low friction coatings (i.e. steel-on-steel surfaces) using a low-acceleration startup.
- Demonstrated radial and thrust bearing rotordynamic stability to 27,000 RPM.
- Demonstrated a mechanically simple self-centering thrust bearing with a stiffness of 1.92 kilo-Newton/mm (11.0 klb/in) at 20,000 RPM and 6 psig bearing feed pressure, increasing to 4.50 kn/mm (25.7 klb/in) at 20,000 RPM and 12 psig bearing feed pressure.
- Integrated prototype air bearing turbocompressor with commercial automotive positive-displacement compressor, instrumentation, and test bench.

- Demonstrated turbocompressor expander, radial bearing, thrust bearing, and compressor performance to 33,000 RPM.

Future Directions

- Complete performance testing of bearings and turbocompressor prototype to design speed.

Introduction

Meruit Inc. has developed a novel air bearing for use in a small high-performance automotive fuel cell turbocompressor. A suitable air bearing must be inexpensive, durable, stable, and stiff enough to survive the automotive environment. Meruit has one main task: to validate its air bearing for automotive compressor/expander use. Development of an air bearing turbocompressor meeting DOE's specifications was also pursued under the project.

Approach

A specialized test rig was designed, built and instrumented to investigate the radial (journal) lift-off and landing performance, radial bearing longevity with low-friction coatings, radial bearing rotordynamic stability, and thrust bearing stiffness. Meruit's mechanically simple (i.e. cost effective) bearing demonstrated floating, non-contact operation, low lift-off and landing speeds, over 10,000 start-stop cycles, high stiffness, and rotordynamic stability to the test rig limit of 27,000 RPM.

A prototype turbocompressor using this air bearing system, designed to deliver the DOE-specified mass flows and pressure ratios, was built, integrated into an instrumented turbocompressor test bench simulating an automotive air system with an in-line positive-displacement compressor, and demonstrated to 33,000 RPM (35% of design speed).

Results

Radial (Journal) Bearing Lift-off

It was experimentally determined that while a large diameter (>75 mm) radial (journal) gas bearing would easily float a steel bearing in steel journals, the scaled-down (~20 mm) gas bearings intended for the DOE application would not lift off ("float") satisfactorily. This condition, present only when the shaft begins to turn from rest, could be remedied by lowering the coefficient of friction between the journal and gas bearing, and several low friction remedies were found to work: DuPont *Vespel,* DuPont *Delrin,* and ANL's *Near Frictionless Carbon* (NFC). Since the Meruit bearing only suffers wear on take-off or landing, the longevity of the bearing is measured in number of start-stop cycles (rather than operating hours). A bearing test rig was configured as an endurance tester to cycle the tested materials. For one start-stop cycle, the drive air is turned on, accelerating the rotor past the lift-off point; the air is turned off; and the coasting rotor floats until it lands and slows to a stop. Steel bearings with Vespel bushings in the journal were tested to 3,700 cycles; steel bearings with Delrin bushings were tested to 1,300 cycles; and both bearings could have continued for more cycles.

ANL applied a NFC to the bearing shaft, which was tested with uncoated steel bushings. It was found that the bearing floated the ~1 kg rotor at just over 900 RPM with about 1 m of sliding contact and a rubbing speed of about 1 m/s. One NFC trial coating reached 5,800 cycles, and another reached 10,200 start-stop cycles.

Modeling of the take-off process revealed that another way to achieve a clean take-off was to reduce angular acceleration ("slow start"). This was experimentally confirmed with bare steel bearings on bare steel journals.

Radial Bearing Rotordynamic Stability

It was determined that while the large diameter (>75 mm) three-lobe gas bearing could be accelerated to 30,000 RPM with no evidence of rotordynamic instability, the scaled-down ~20 mm bearing became unstable at about 14,000 RPM. This

instability was not a resonance that could be accelerated through; higher speed operation led to repeated bearing contact with the journal and eventual bearing destruction. CFD modeling suggested that at the smaller diameter, a four-lobe design would be stable over the entire design speed range. Several shafts with four lobes were designed, built, and tested with and without NFC coating. A ~20 mm four-lobe shaft, otherwise identical to the three-lobe shaft, floated at a slightly higher (~950) RPM than the three-lobe shaft, but was shown to be stable to the test rig limit of 27,000 RPM (almost twice the critical speed of the three-lobe bearing). A 23-mm shaft demonstrated stability to 33,000 RPM in the turbocompressor test rig.

Axial (Thrust) Bearing Stiffness

Another aspect of the bearing test program was the experimental measurement of the thrust bearing's stiffness, force, and damping properties. The thrust bearing's stiffness is computed to increase with bearing feed air pressure, air temperature, and RPM; any increase in these values leads to a stiffer bearing with a more strongly damped response to shocks. Even a slight air flow through the bearing at zero RPM will center the bearing in its clearance and provide some stiffness. The test rig was configured with a thrust piston to apply controlled axial loads and instrumented to measure the resultant axial displacement as a function of bearing feed air pressure at speeds ranging from zero to 27,000 RPM.

The measured stiffness at about 20,000 RPM was found to range from 1.92 kn/mm (11,000 lbs/in) at a feed pressure of 41.3 kPa (6 psig) to 4.50 kn/mm (25,700 lb/in) at 82.7 kPa (12 psig). The measured stiffness at a constant feed pressure of 6 psig at speeds of 21,000 and 27,000 RPM was found to be 1.92 kn/mm (11,000 lb/in) and 2.24 kn/mm (12,800 lb/in) respectively. These speeds are low compared to the design turbocompressor speed of 95,000 RPM, and yet the bearing still generates substantial and useful centering forces that resist thrust loads. Bearing air consumption was measured at about 0.08 g/sec, which is negligible in comparison to the 76 g/sec design air flow of the DOE turbocompressor.

Air System and Turbocompressor Design/ Performance Testing

To make up the difference between the expected expander returned power and the required compressor input power, Meruit designed an air system using a commercially available positive-displacement compressor driven by an electric motor in tandem with Meruit's turbocompressor. Meruit designed a family of compressor and expander wheels with varying characteristics (specific speed, dimensional ratios, etc.) representing different compromises in providing performance compatible with the DOE specifications. After extensive evaluation, a compressor wheel was chosen to provide a desired pressure curve over a wide range of mass flows, and a turbine wheel was matched to it. The chosen compressor wheel is intended to trade peak efficiency for extended turndown performance.

The basic expander configuration comprises variable inlet vanes (nozzle segments) for the control of back pressure and mass flow for matching the performance of the compressor. Figure 1 presents the geometry of the inlet vanes and their relationship to the blades of the turbine wheel. The turbocompressor uses Meruit's radial and thrust gas bearings with ANL's NFC coating; the rotor is illustrated in Figure 2, and the turbocompressor body without the expander and compressor housings is presented in Figure 3.

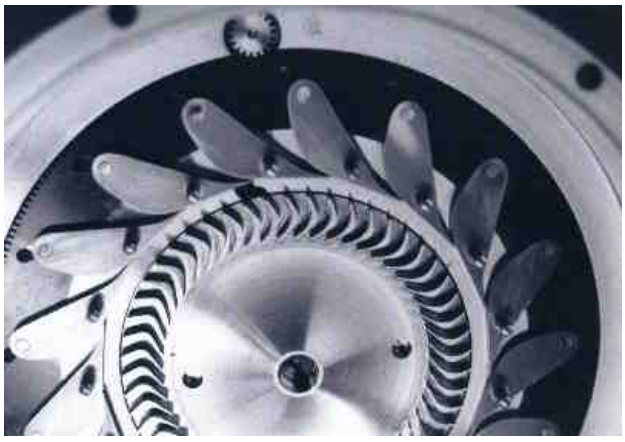

Figure 1. Meruit Variable Nozzle Expander

Figure 2. Meruit Turbocompressor Rotor

Figure 3. Meruit Turbocompressor Body

Using the valving of the test rig and the variable nozzles of the turbocompressor, the expander can be tested through a full range of nozzle openings from zero to 115% at various turbine feed pressures and mass flows. The compressor can be independently evaluated over a range of mass flows at each value of RPM. After the four-lobe bearing was demonstrated in the bearing test rig, the turbocompressor was fitted with a 23-mm four-lobe bearing. At the speeds tested to date (i.e. one-third of design speed), the compressor generates very little pressure (i.e. about one-ninth of design pressure), but all of the compressor performance data available so far indicate the designed pressure-to-mass flow performance with increases in mass flow at each speed.

Conclusions/Future Directions

Meruit's leafless radial air bearing for small shafts has demonstrated low-speed lift-off and landing, trouble-free take-off, longevity, stiffness, and stability to moderate speeds. The leafless thrust bearing has demonstrated self-centering at zero speed and adequate stiffness at moderate speeds for automotive applications. Meruit's turbocompressor using these air bearings has demonstrated the desired flat pressure performance to the speeds tested so far. Work continues to demonstrate rotordynamic stability and turbocompressor performance at higher speeds.

References

1. Ajayi, O.O. et al. 2002. *"Low Friction Coatings for Fuel Cell Turbocompressors"*, in *DOE 2002 Review OTT Fuel Cells Program*, U.S. Department of Energy Office of Transportation Technology, May 2002.

IV.E.4 Motor Blower Technologies for Fuel Cell Automotive Power Systems

Thomas Clark (Primary Contact) and Michael Arner
UTC Fuel Cells
195 Governors Highway
South Windsor, CT 06074
(860) 727-2287, e-mail: tom.clark@utcfuelcells.com

DOE Technology Development Manager: Patrick Davis
(202) 586-8061, fax: (202) 586-9811, e-mail: Patrick.Davis@ee.doe.gov

Subcontractors: Phoenix Analysis and Design Technologies (PADT), Phoenix, AZ; R&D Dynamics, Bloomfield, CT

Objectives

- Develop small, lightweight, motor driven blowers to provide cathode air and fuel processor air for a near ambient pressure fuel cell operating on gasoline.
- Demonstrate the performance of various types of air blowers via integration into a power plant.
- Evaluate both fuel processor air blower approaches, regenerative and centrifugal, and identify which technology is superior.
- Identify and develop manufacturing methods that will allow the blowers to be produced at low cost in large production volumes.

Approach

- Define performance requirements, flows, pressures, and temperatures, as well as cost and life targets, for both the cathode and fuel processor air blowers.
- PADT will develop and build a mixed flow type blower to meet requirements for cathode air and a regenerative type blower to meet fuel processor air requirements. Prototypes will be used to evaluate aerodynamic performance as well as life and durability.
- R&D Dynamics will develop and build a high-speed centrifugal machine supported by air bearings to meet the fuel processor air requirements.
- UTC Fuel Cells will demonstrate operability and performance of both approaches by integrating the units into a power plant.

Accomplishments

- Requirements for both the cathode air blower and fuel processor air blowers have been defined and documented.
- PADT has completed design of the mixed flow axial cathode and regenerative fuel processor air blowers.
- PADT has developed and calibrated a regenerative wheel performance model.
- R&D Dynamics has completed design of a high-speed centrifugal machine for the fuel processor air blower utilizing air bearings.

Future Directions

- Complete the prototype production of all three machines.
- Complete performance and endurance testing of all three blower types.
- Integrate blowers into a fuel cell power plant and test for operability.

Introduction

Near ambient pressure fuel cells running on gasoline require two sources of air, one for the fuel cell cathode and one for the gasoline fuel processor, which generates hydrogen. Due to the relative pressure differences required by the two applications, it is not energy efficient to fulfill the two air requirements with a single blower/compressor as is commonly utilized in pressurized type fuel cell systems. This project will define different types of machines to meet each air supply requirement; specifically, one type of machine will be evaluated for the low-pressure cathode air blower, and two other different types of machines will be evaluated for the higher-pressure fuel processor air blower. Air blower development targets are presented in Table 1.

Capabilities	Cathode Air Blower	Fuel Processor Air Blower
Max Flow Rate (cfm)	170	70
Pressure Rise	1 psi	12 psi
Ambient Temperature (F)	-40 – 140	-40 – 140
Overall Efficiency[a] 100% flow 25% flow	 60% 35%	 50% 30%
Production Unit Cost[b] @100,000 units/yr	$75	$75
Service Life (hrs)	5000	5000
Power Supply	200 Vdc	200 Vdc

a Includes motor, controller, mechanical and isentropic efficiency
b Includes motor controller and blower

Table 1. Blower Development Targets

Approach

For the near ambient pressure cathode air blower application, the best machine is clearly a mixed flow type of axial blower. This type of machine, illustrated in Figure 1, yields excellent overall efficiency in a very compact package and can be produced, in quantity, at a relatively low cost. Specific speed analysis indicates that a mixed flow machine will yield a high efficiency machine at reasonable rotational speeds. In this project, PADT will design, build, and test an optimized mixed flow blower which meets the performance requirements established and is readily producible using standard manufacturing processes.

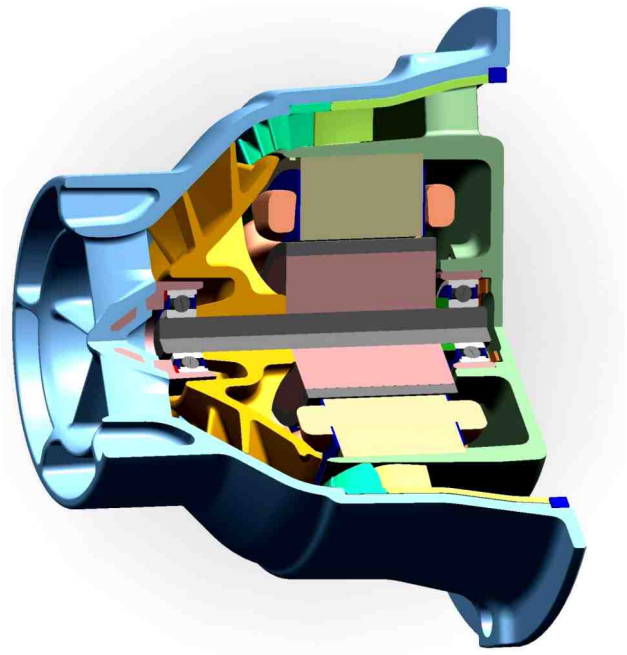

Figure 1. Solid Model of PADT Designed Cathode Air Blower

For the higher pressure fuel processor air blower application, the optimal type of machine is not as clear. As part of the preliminary sizing, a variety of machines were evaluated, including rotary lobe, sliding vane, radial, centrifugal, and regenerative. Although the rotary lobe and sliding vane type machines could be developed to yield high overall efficiencies, they were eliminated as a result of other,

non-aerodynamic requirements, primarily concerns regarding excessive size and weight, limited life capability due to wear, and higher production cost due to the need for more precise control of part dimensions and clearances.

A radial type centrifugal machine was viewed to be an excellent overall choice because parts can be mass-produced at a low cost and life should be acceptable. However, in order to achieve peak efficiency and small size, the rotational speed needs to be high, far exceeding the capability of conventional low cost bearings. R&D Dynamics is presently working to develop a machine utilizing air bearings, thereby eliminating the life and speed limitation of conventional grease packed bearings. We believe that R&D Dynamics's proprietary air bearing design can be mass produced at costs consistent with our overall goals and thus have begun development of a high speed (150,000 rpm) radial type, centrifugal machine as shown in Figure 2.

Another equally viable approach to the fuel processing system (FPS) air blower is the regenerative type machine being developed by PADT. The regenerative machine as shown in Figure 3 allows for higher-pressure generation at lower rotational speed. This machine is presently being designed to run at 26,000 rpm and will utilize traditional, low cost, grease packed roller bearings. The theoretical maximum efficiency is not as high as the high-speed radial machine, but the low speed approach minimizes concerns with bearing life, thereby mitigating risk. Two critical tasks in the design of this machine will be to optimize the impeller geometry to obtain peak isentropic efficiencies while minimizing the number of critical clearances and tolerances, and to evaluate cooling schemes and their effect on the overall efficiency and cost of the machine.

Results

Work to date has resulted in evolving designs for all three blowers, as shown in Figures 1, 2 and 3. All three designs utilized a typical turbo-machine design process that included tasks such as specific speed analysis, blade optimization, rotor-dynamic analysis, bearing analysis, thermal analysis, and motor optimization studies. Each machine has been

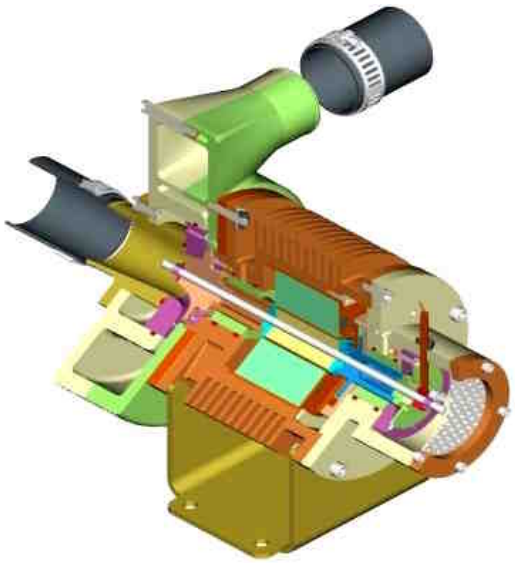

Figure 2. Solid Model of R&D Dynamics Designed Fuel Processor Air Blower

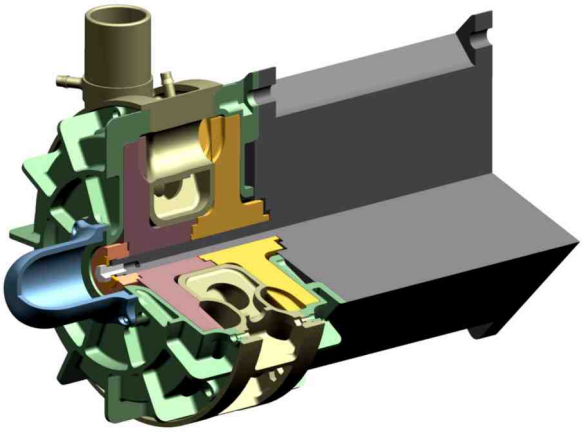

Figure 3. Solid Model of PADT Designed Fuel Processor Air Blower

designed to be small, yield high efficiency, and be manufacturable utilizing standard production methods commonly found in industry today.

Due to the low weight and small volume requirements dictated by a transportation application, power density is much higher in these machines than in equivalent performing, commercially available machines. Thus, removal of heat from the motor becomes a challenge. This issue of motor cooling has been a particularly troublesome task for all of the blower designs. Heat rejection in the PADT designed regenerative impeller FPS air blower has been particularly challenging, primarily due to the

	Motor Winding Temp	*Motor Housing Temp*	*Pump Head Temp*
Air Cooling	295°C	155°C	155°C
With thermal isolation	267°C	127°C	161°C
Thermal isolation & potted windings	197°C	127°C	160°C
Water Cooling	282°C	142°C	142°C
With thermal isolation	226°C	86°C	160°C
Thermal isolation & potted windings	156°C	86°C	160°C

Note: The above numbers presume a 90%-92% efficient motor and a pump head isentropic efficiency of 40%. These efficiencies are critical to selecting the proper cooling approach and will be validated by testing by the motor and pump head design.

Table 2. Results of PADT Fuel Processor Blower Thermal Analysis

relatively low efficiency of the pump head. This low efficiency requires the motor to produce more shaft power and thus results in a larger amount of motor waste heat that needs to be rejected. A thermal model has been developed and is being used as a tool to evaluate water cooling and a variety of air cooling techniques. Some of the output from this model, using conservative estimates for motor efficiency, is presented in Table 2. This data was evaluated and the following conclusions were made:

- Sustained operation at the maximum power condition may require water cooling. The water temperature will need to be less than 40°C.
- Thermal isolation between the pump and motor housings will reduce motor winding temperature but increase the forward bearing temperature in excess of 140°C, which is detrimental to the bearing lube.
- Motor windings, which are thermally potted to the motor casing, will decrease the winding temperature and may allow air cooling if motor efficiency is 90%-92%.
- Motor efficiencies greater than 92% may allow air cooling without thermally potting the motor windings.

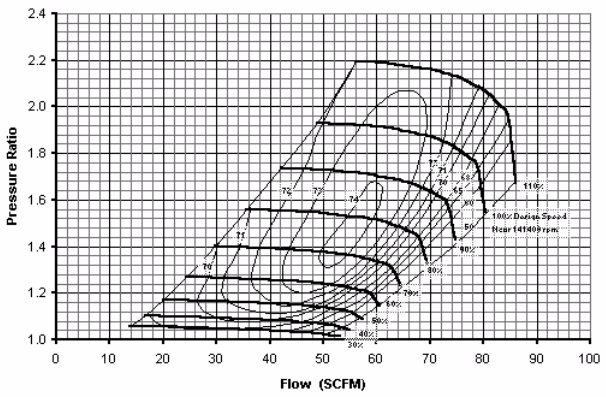

Figure 4. Predicted Performance of R&D Dynamics Fuel Processor Blower

In the case of the R&D Dynamics machine, the isentropic efficiency of the machine is high; therefore, the shaft power required is lower than that required for the regenerative unit, and the amount of waste heat generated by the motor is lower. The predicted performance of this machine is presented in Figure 4. Because of this, placing fins on the motor casing and ducting air over the fins can cool the motor. The amount of cooling air is expected to be minimal and will be verified through thermal testing of the first prototype unit.

For the near ambient pressure PADT cathode air blower machine, depicted in Figure 1, heat rejection is accomplished by rejecting energy from the motor housing directly to the process air, utilizing the mixed flow cathode air blower design itself. This technique is possible for several reasons. The axial geometry of the blower lends itself to this type of approach; the amount of work done on the process fluid is fairly small and the volumetric flow rate relatively high; thus, the temperature rise of the process air is very small, and a large temperature differential exists between the motor housing and the process air.

Conclusions/Future Directions

PADT is presently building an aerodynamic development rig that will be used to validate a model that was developed to predict aerodynamic performance of their fuel processor blower. Prototype motors have been designed and will be

tested to establish "real-world" efficiencies. R&D Dynamics has manufactured blowers with both radial and thrust air bearings and is preparing to run these units in a test rig to determine the load capability of each bearing.

All three designs are nearly completed and production of parts for the prototype units has begun. Two prototype units for all three designs will be complete by November 2002. Performance testing of the units will commence immediately thereafter to verify aerodynamic performance and efficiency of each design.

IV.E.5 Hybrid Compressor/Expander Module

George E. Selecman (Primary Contact) and Paul E. McTaggart
TIAX LLC
Acorn Park
Cambridge, MA 02140-2390
(617) 498-6083, fax: (617)-498-7250, e-mail: selecman.g@tiax.biz

DOE Technology Development Manager: Patrick Davis
(202) 586-8061, fax: (202) 586-9811, e-mail: Patrick.Davis@ee.doe.gov

ANL Technical Advisor: Robert D. Sutton
(630) 252-4321, fax: (630) 252-4176, e-mail: sutton@cmt.anl.gov

Subcontractors: Concepts NREC, White River Junction, VT; Scroll Corporation, Carlisle, MA

Objective

- Based on the experience of two previous generations of scroll-based compressor/expander modules developed with DOE, design and build a hybrid compressor/expander module using both turbomachinery and scroll compression.
- Develop the algorithms and hardware to ensure stable and effective control of the hybrid system.
- Deliver a system with equivalent thermodynamic performance, at significantly lower weight and volume, when compared to previous generations of scroll compressor/expander modules.

Approach

- In the first year, develop system architecture and subsystem designs consistent with the overall goals of maintaining thermodynamic performance while reducing weight and volume relative to previous generations.
- In the second year, complete detailed engineering and initiate fabrication of subsystem components, and develop the control system hardware and algorithms.
- In the third and final year, complete fabrication of components and conduct subsystem assembly and test, followed by system integration and performance verification.

Accomplishments

- Defined basic system architecture, including preliminary allocation of performance requirements to subsystems.
- Initiated detailed design tradeoff studies for scroll machinery.

Future Directions

- Refine subsystem-level performance allocations.
- Initiate detailed design tradeoff studies for turbomachinery.
- Initiate breadboard scroll drive mechanism development and testing.

Introduction

Most current automotive fuel cell systems are designed for pressurized operation in order to reduce system size, boost stack efficiency, and improve water management. Applications for automobiles also require significant partial load capability, since the anticipated level of electrical energy storage is minimal. Due to the aggressive efficiency goals driving fuel cell development, the compressor must operate efficiently over a wide flow range, and efficient waste energy recovery in an expander or turbine is required to offset the compression load.

Traditionally, high-speed centrifugal technology, such as that used in automotive turbochargers, has resulted in a compact high-speed package that delivers high efficiency at the design point, but with performance that falls off dramatically under off-design conditions. Scroll technology, a type of positive displacement machinery, provides high efficiency across a broad range of operating conditions, but results in a package that is significantly larger and heavier than that of high-speed centrifugal technology.

The objective of this project is to develop a hybrid compressor/expander module, based on both scroll and high-speed centrifugal technologies, which will combine the strengths of each technology to create a concept with superior performance at minimal size and cost. The resulting combined system will have efficiency and pressure delivery capability comparable to that of a scroll-only machine, at significantly reduced system size and weight when compared to scroll-only designs.

Approach

The design approach for the Hybrid TurboScroll Compressor/Expander Module (CEM) exploits the experience of developing the first two generations of scroll CEMs, in combination with the substantial experience of our turbomachine subcontractor, Concepts NREC. (Figure 1 shows the Second Generation Scroll CEM on its test stand.) By combining the performance attributes of a positive displacement scroll compressor (electrically driven) with those of a turbocharger (driven by fuel cell exhaust gases), we expect to be able to very closely match the pressure and flow requirements of the DOE guidelines in a package that is smaller and lighter than previous generations. Table 1 shows the weight and volume design goals for the program; with acknowledgement that these goals are still somewhat short of the DOE guidelines, they are clearly an improvement over the Second Generation Scroll.

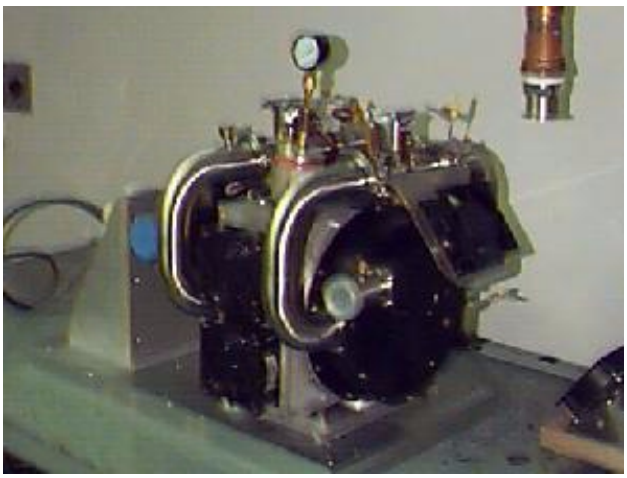

Figure 1. Second Generation Scroll Compressor/ Expander Module

Param.	Hybrid				2nd Gen. CEM
	Turbo	Scroll	Motor	Total	
Dia. (in)	6	7	7	7	12
Len. (in)	5	8	5	18	20
Vol. (l)	2.3	5	3	10.3	30
Wgt. (lb)	10	17	10	37	90

Table 1. Key Envelope Performance Goals for the Hybrid TurboScroll CEM

Our first step was the construction and testing of a breadboard model of the system, as shown in Figure 2. In this configuration, a conventional automotive turbocharger (in the foreground) was coupled to the scroll compressor portion of the First Generation Compressor/Expander Module (in the

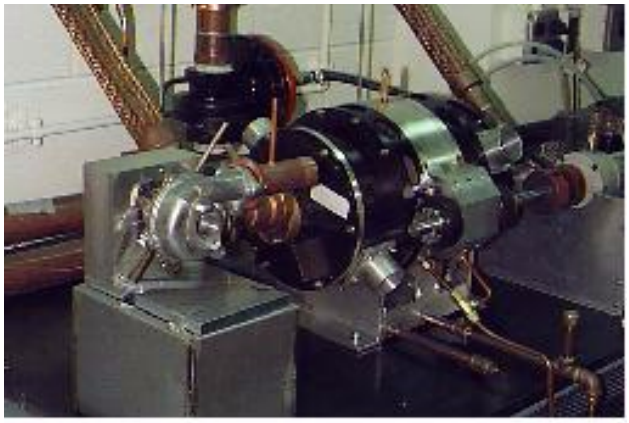

Figure 2. Breadboard Version of Hybrid TurboScroll CEM Configuration

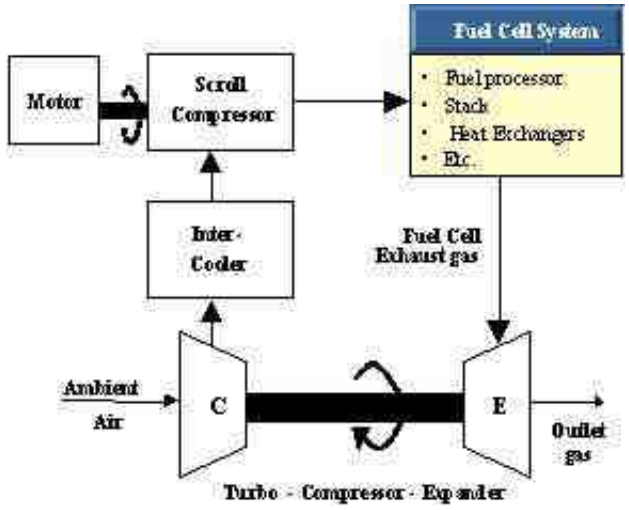

Figure 3. System Architecture of Hybrid TurboScroll CEM

background). The results of that preliminary exploratory testing, while not delivering the desired efficiency, were sufficiently promising to justify the system concept.

Next, the development of an appropriate system architecture resulted in the block diagram shown in Figure 3. In this configuration, the turbocompressor draws in atmospheric air and compresses it to an intermediate pressure. (Note that the specification of this intermediate pressure is a key element in assigning performance requirements to the subsystems.) In order to reduce both the size and operating temperature of the scroll compressor, an intercooler is provided to reject at least part of the heat of compression to the atmosphere. The partially compressed gas, now cooler and denser, is then fed into the scroll compressor, which uses electrical power to achieve the final compression of the gas. Finally, the compressed air is fed into the fuel cell, which increases its temperature and reduces its pressure slightly. The exhaust gas from the fuel cell drives the turbine (through controllable inlet guide vanes) and, with the bulk of its energy extracted, is expelled to the atmosphere. The turbine provides the shaft power to drive the compressor by direct coupling.

This architecture offers some important advantages:

- The turbocompressor is powered only by the turbine, eliminating the issues associated with coupling power into a high-speed rotating shaft.
- Turbine inlet guide vanes provide both inlet control and control of fuel cell stack pressure.
- The scroll compressor provides pressure and flow characteristics that enable efficient operation across a broad range of flow rates.

Capturing these advantages entails overcoming certain challenges:

- Control of coupled turbomachinery and positive displacement machinery,
- Power and waste heat management,
- Isolation of lubricants from the process gas stream, and
- Reduction of size, weight and cost.

Starting with the turbocharger, pictured in Figure 4, the approach to design involves balancing competing elements. Although clearly representing an increase in complexity and parts count, controllable inlet guide vanes for the turbine are considered a necessary minimum. Similar controls on compressor flow will be considered as part of the overall component design tradeoff study. In the interest of simplicity and conventionality, the initial design studies have focused on conventionally lubricated roller bearings. Management of the lubricant, though challenging, is considered more tractable at the present time that the integration of gas

Figure 4. Concepts NREC Baseline Turbocharger Design

bearings or other technologies. The intercooler between the turbocompressor and the scroll compressor has conventional performance requirements, and indeed the preliminary approach is to select an available automotive intercooler of the appropriate size and integrate it into the system.

For the scroll, the design approach has involved the detailed evaluation of three competing configuration options, shown in Figure 5. The first alternative was a conventional crank-driven orbiting scroll, supported on a roller-Oldham bearing system, with grease lubrication. This configuration has the substantial advantage of conventionality, enabling the direct utilization of knowledge gained in dozens of scroll compressor design programs. In the second configuration, the two opposing elements of the scroll both rotate, on offset axes, coordinated in such a way that their relative motion is orbital. The primary advantage of this configuration lies in the relatively conventional bearing configuration, offset in part by a relatively unconventional drive mechanism requirement. The third design gangs multiple scrolls on a common drive mechanism, offering the possibility of reduced noise with the accompanying penalty of a relatively complex drive mechanism.

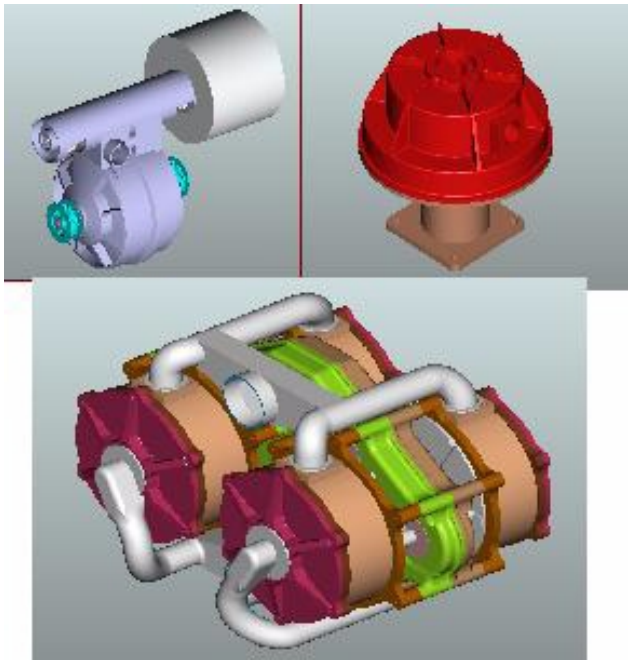

Figure 5. Three Alternate Scroll Compressor Preliminary Design Configurations

Each of the above alternatives was carried to the point of preliminary drive system sizing and overall subsystem layout. Based on that information, our evaluation of the alternatives has led to the selection of the conventional crank-driven orbital scroll as the primary design direction. This represents a conservative choice in the design of this system element, consistent with the overall need embodied in the program objectives to demonstrate the performance of the overall system concept.

The control and data management system configuration depends on both the data acquisition requirements and the control measurement and actuation means configured into the individual subsystems. Design of the hardware and algorithms are to commence following the completion of the preliminary subsystem designs. The test regimen for the subsystems, and ultimately the system as a whole, are anticipated to represent not merely a data acquisition phase, but an integration, test, and debugging phase.

Results

Having conducted a body of preliminary concept feasibility work, the design activities conducted in

the first active quarter of this project have focused on the system configuration and the definition of key subsystem requirements. Preliminary designs have been completed for three alternative scroll compressor configurations, and a down-select to the primary configuration has been accomplished. Upcoming work will involve the refinement of key system interface definitions and initiation of detailed design activity for the turbocharger.

Conclusions

Continued, and progressively more detailed, investigation of the Hybrid TurboScroll CEM concept indicates no issues that seem to threaten the viability of the selected system architecture. A substantial degree of additional detailed system and component design work is required to fully explore the issues of practicality and performance, but the design team still believes that the promise of thermodynamic performance substantially equal to that of the Second Generation Scroll CEM, at a substantially reduced weight and volume, is not only achievable, but within reach.

IV.F Crosscutting Fuel Cell Analysis and Demonstration

IV.F.1 Precious Metal Availability and Cost Analysis for PEMFC Commercialization

Eric J. Carlson (Primary Contact) and Dr. Johannes H.J. Thijssen
TIAX LLC
Acorn Park
Cambridge, MA 02140-2390
(617) 498-5903, fax: (617) 498-7012, e-mail: carlson.e@tiax.biz

DOE Technology Development Manager: Arlene Anderson
(202) 586-3818, fax: (202) 586-9234, e-mail: Arlene.Anderson@ee.doe.gov

ANL Technical Advisor: Thomas Benjamin
(630) 252-1632, fax: (630) 252-4176, e-mail: Benjamin@cmt.anl.gov

Objectives

- Assess current and projected demand for platinum group metals (PGMs) exclusive of fuel cell applications
- Estimate the relationships between supply capacity/reserves and long-term growth in demand for PGMs
- Develop an econometric model to simulate the impact of fuel cell market growth scenarios on PGM supply and pricing
- Perform a sensitivity analysis on supply and pricing to critical parameters in the model related to fuel cell markets and technology advances
- Obtain critical feedback from the important participants in the PGM value chain on the model assumptions and projections
- Develop a cost projection for the recycling of PGMs from fuel cells, and assess the impact on PGM supply and price

Approach

The project has been broken into five tasks as follows:

- Task 1: Collect historical PGM supply, demand, pricing and resource data
- Task 2: Develop fuel cell market commercialization scenarios
- Task 3: Develop PGM recycling scenarios including a high level PGM proten exchange membrane fuel cell (PEMFC) recycling cost model
- Task 4: Develop econometric model for the simulation of the impact of fuel cell introduction on PGM supply and price
- Task 5: Solicit feedback from PGM industry and automotive OEMs

Tasks 1 and 4 were scheduled for the fiscal years 2001 and 2002. The balance of the tasks will be completed in 2003.

Accomplishments

- Completed PGM data collection with inputs from literature sources, PGM industry reports, precious metal trading companies, and geology experts
- Developed econometric modeling approach and presented to PGM industry for feedback

Future Directions

- During the balance of 2002, complete development of the econometric model
- During 2003, develop fuel cell market and recycling scenarios for input to PGM supply and pricing simulation
- Run simulation to project impact of fuel cell commercialization on platinum pricing and supply
- During 2003, obtain feedback from PGM industry and automotive OEMs

---

Introduction

Platinum group metals are critical to the commercialization of fuel cells, but they also represent a significant contribution to overall system cost. Depending on operating design parameters, platinum would represent 10 - 20% of the cost of a gasoline fuel cell system produced in high volume. PGMs (primarily platinum and some ruthenium) are critical to catalyzing reforming/shift reactions in the fuel processor and electrochemical oxidation and reduction in the fuel cell, with the fuel cell requirements presently dominating the demand.

Successful adoption of fuel cells in transportation applications over the long-term could create markets on the order of ten million vehicles, leading to significant pressure on PGM suppliers to increase production capacity and supply. Consideration of stationary and portable applications for fuel cells further increases the demands on PGM supplies. Clearly, the combination of stationary, portable and transportation markets for fuel cells will create pressure on the PGM industry to increase supplies and might cause rapidly escalating prices (thereby threatening fuel cell market viability) unless action is taken to guide the process.

The commercialization of fuel cells will also depend on the amount of economically mineable PGM resources and the ability of the PGM value chain to supply the PGM materials in the needed forms at reasonable markups above the London Metals Exchange (LME) price.

The relationship between supply, demand, and price of the PGMs is complicated by several factors, including: the geographical concentration of ore bodies in South Africa and Russia, the control of production by a limited number of companies in these regions, the impact of politics, and the impact of the world economy on demand and price. Significant new demands for PGMs can lead to price increases in the short-term and potentially in the long-term if supply capacity does not increase.

The large layered intrusions that host all the world's major PGM deposits can be easily identified even if covered to depths of a few kilometers by using regional gravity surveys. These rocks have high density and are easily recognizable in such studies. Hence, the likelihood of finding significant new deposits is not high. The discovery of new resources of PGM is likely to be limited to smaller intrusions that may provide small mining activities, but will not influence global production in a significant way.

Approach

The overall goal is not only to develop projections of PGM availability and cost, but also to identify and quantify the industry and market drivers influencing these parameters. On the demand side, we will break down the demand between existing markets and the potential applications of fuel cells. We will identify underlying trends in the industrial/ chemical and lifestyle markets with attention to growth of demand and potential for substitution of alternative materials. In the fuel cell markets, the

impact of technology on PGM demands will also be considered.

The modeling approach starts with construction of an econometric model based on historic supply, demand, and price data. A simulation will then be run to study the impact of introduction of fuel cell vehicles on the supply and price of platinum. Figure 1 illustrates the steps in the modeling approach, and Figure 2 shows the structure and outputs of the econometric model.

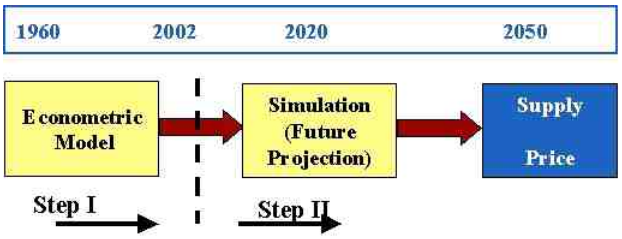

Figure 1. Overview of Modeling Steps in Development of Future Projections of Supply and Price of Platinum

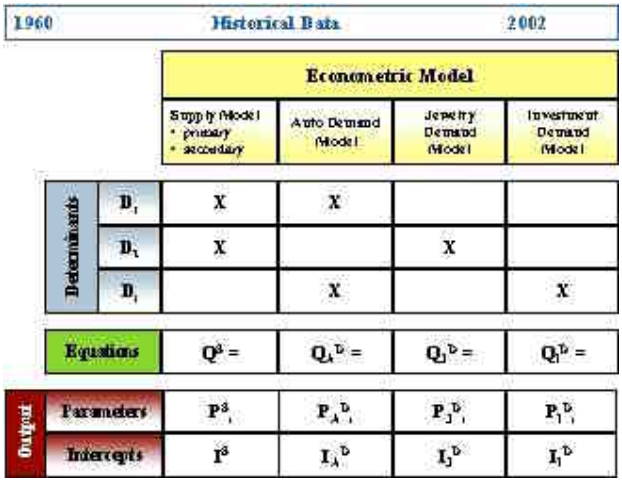

Figure 2. Structure of the Econometric Model and Outputs

Automotive catalysts and jewelry are the two dominant markets for platinum (approximately 80%) and are important elements in the econometric model. The investment industry consumes a minor amount of material but can exert significant influence on short-term price. However, over long periods of time, investment should have zero impact on supply and demand.

The model will be developed to provide at least the following information:

1. *Price Elasticity of Demand:* A measure of the sensitivity of quantity demanded to a change in the price of platinum. It provides a quantitative measure of the price responsiveness of quantity demanded along a demand curve. The greater the elasticity, the greater the effect that a price change will have on the quantity demanded.
2. *Income elasticity:* A measure of how responsive consumption of platinum is to a change in personal income when the price of platinum itself is not changed.
3. *Price Elasticity of Supply:* A measure of the responsiveness of quantity supplied to a change in price. It provides a quantitative measure of the price responsiveness of quantity supplied along a supply curve. The greater the elasticity, the greater the effect that a price change will have on the quantity supplied.

The validity of the model will be assessed first by examining it for theoretical consistency - that is, we will confirm that estimated coefficients have the correct signs as economic theory predicts. Second, we will examine the model's "goodness of fit". "Goodness of fit" refers to a quantitative measure of the extent to which the explanatory variables in the model "explain" the change in the dependent variables (i.e., the quantity of demand and supply of platinum).

After completion and validation of the econometric model, future demand scenarios will be input into the econometric model to project the impact of fuel cell commercialization on supply and pricing. The scenarios for stationary, portable, and transportation applications of fuel cells will range from optimistic to pessimistic and contain volume and time estimates. Economic growth, catalyst technology development, and shifts in automotive powertrain technology will be some of the factors considered in development of the demand scenarios (see Figure 3). The model and the scenarios can be used to conduct sensitivity analyses to the various factors. Recycling will play a significant role as platinum consumption increases further. Recycling of automotive catalysts is now between 10 and 20% depending on the prices of platinum and palladium.

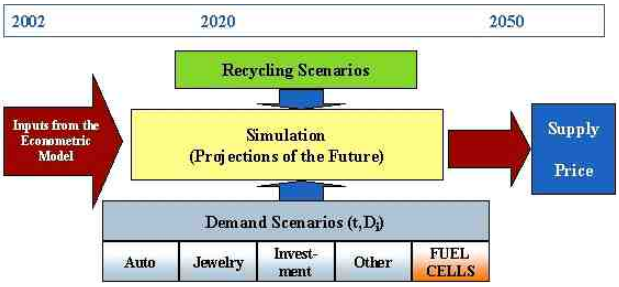

Figure 3. Demand and Recycling Scenarios Will Input to the Econometric Model to Develop Projections of Supply and Price of Platinum

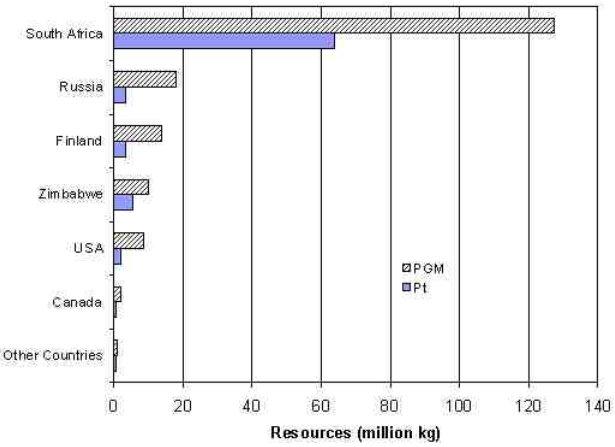

Figure 4. Platinum Resources Summary (Total PGM: 181 million kg, Total Pt: 80 million kg)

Results

Figure 4 summarizes the available resource data for PGMs and platinum. The assumptions and definitions underlying the reported data are critical to selection of values for the resource prediction. The increase in South African resources is based on the revised estimate by G. Cawthorn (2001). Technology advances now allow mining to greater depths, and Cawthorn's increased resource amount assumes a depth of 2 kilometers in all areas of South Africa. The geology of the South African deposits is well characterized and can be extrapolated with confidence.

In contrast, the information about precious metals in Russia is considered a state secret, and much greater variation exists in reported values. Data from a variety of sources were compiled to arrive at the values for the other countries.

Model development started with analysis of the behavior of the real price of platinum over time. The nominal price was deflated by the consumer price index. Preliminary analysis indicates that the mean real price may be constant over a 100 year span; however, statistical tests are being performed to validate this result (see Figure 5). Excursions from the mean real price can be accounted for by specific events, for example, World War I and the U.S. regulations on automotive emissions. However, over time, the supply and demand come back into balance through increases in production or substitution of non-PGM materials.

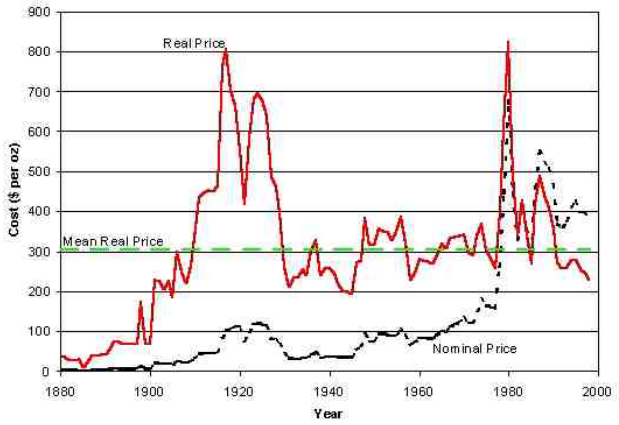

Figure 5. U.S. Geological Survey Platinum Prices with Consumer Price Index (CPI) Deflator

Conclusions

- South Africa will continue to dominate supply of platinum and, in the estimate shown, has 80% of the projected resources.
- If statistical tests support the hypothesis of a constant real platinum price and historical behavior is repeated, then one could expect the introduction of fuel cells to increase the short term price of platinum; however, the platinum prices will then return to traditional values as supply increases.

Reference

1. Cawthorn RG (2001), "Global Platinum and Palladium Deposits," August 2001 Presentation, copy from the author

IV.F.2 Assessment of Fuel Cell Auxiliary Power Systems for Onroad Transportation Applications

Dr. Carole J. Read (Primary Contact), Dr. Johannes Thijssen
TIAX, LLC
20 Acorn Park
Cambridge, MA 02140-2390
(617) 498-6162, fax: (617) 498-7054, e-mail: read.carole@tiax.biz

DOE Technology Development Manager: John Garbak
(202) 586-1723, fax : (202) 586-9811, e-mail: John.Garbak@ee.doe.gov

Main Subcontractors: University of California-Davis, Institute of Transportation Studies

Objectives

- The objective of this cooperative study is to determine the viability of the use of proton exchange membrane fuel cells (PEMFCs) and electrode supported solid oxide fuel cells (SOFCs) as auxiliary power units (APUs) for on-road vehicles. The overall objectives of the program are:
- Assess viability considering:
  - Fuel flexibility
  - Start-up time
  - Power level
  - Duty cycle
  - Overall vehicle efficiency
  - Weight and volume
  - Capital and operating & maintenance (O&M) cost
  - Reliability, maintainability, "ease of repair"
- Determine research and development (R&D) needs and possible DOE roles
- Project potential benefits to the Nation
  - Barrels of oil displaced
  - Criteria pollutants avoided
  - Safety improvement & noise reduction benefits

Approach

- Task 1. Project kick-off Summarize the impact of system operating parameters on the design and performance of PEM and solid oxide fuel cells.
- Task 2. Identify APU Requirements Finalize the segmentation of the vehicle APU market by vehicle class and application. For key segments, develop "straw-man" duty cycles, capital cost, O&M cost, and weight & volume targets. Confirm and adjust "straw-man" APU specifications via telephone interviews with industrial contacts. Choose 2 to 3 (total) PEM and SOFC APU applications to advance to Task 3.
- Task 3. Develop Design Concepts Develop system layouts and conceptual designs for the 2 or 3 options selected in Task 2. Conduct a trade-off analysis for the critical design and performance factors.

Address vehicle integration issues. Compare the most promising fuel cell systems with other APU approaches (e.g. internal combustion engines, battery APUs, Stirling engines).

- Task 4. R&D Gap Analysis Determine the current gaps among fuel cell cost, performance and application requirements (look at 2005-2006 technology). Develop a timeline for technology development and commercialization, and extract R&D needs and opportunities for DOE involvement. Project benefits to the nation from technology introduction (e.g. oil displaced, emission reductions, noise reduction, and safety benefits)
- Task 5. Updatea Analysis Update the performance specifications and the implications on system design, after 6 months to a year from the delivery of the draft final report.

Accomplishments

- Held kick-off meeting at Acorn Park headquarters of Arthur D. Little on January 23, 2002.
- Refined scope of project.
- Finalized selection of fuel cell types for analysis. Determined that PEM and planar anode-supported SOFC are the most attractive fuel cell technologies to assess for onroad transportation APU applications.
- Initiated characterization and preliminary selection of fuel cell/APU applications.
- Completed inventory of data gaps in promising APU applications (e.g. capacity, fuel capability, duty cycle).
- Selected long-haul heavy-duty truck cab load application using diesel fuel with a solid oxide fuel cell for conceptual design, layout and vehicle integration analysis.

Future Directions

- Incorporate 21st Century Truck Industry Working Group feedback on heavy-duty truck APU requirements and cost and performance targets.
- Conduct telephone interviews with interested industrial stakeholders on APU applications and their respective specifications for refrigeration applications, utility truck, police car applications, and future passenger car/light-duty vehicle applications.
- Commence design work on heavy-duty truck cab application using planar electrode supported solid oxide fuel cell and diesel fuel. Finalize specifications (e.g. capacity, duty cycle, volume and weight, vehicle integration issues).
- Finalize selection of remaining 1 to 2 systems for detailed study (leading candidates a refrigeration truck and a police car or contractor/utility truck application)

Introduction

Thus far, most of the interest in fuel cell transportation applications has focused on the use for propulsion, a very challenging task. Over the last two years, interest in the use of fuel cells for vehicle APUs has risen. The requirements of APU applications are thought to better match the initial performance and cost characteristics of fuel cells. APUs are also a possible initial fuel cell market application in the transportation sector and a step towards introduction of hybrid and fuel cell propulsion systems. The objective of this cooperative study is to determine the viability of the use of PEM and planar anode-supported SOFCs as APUs for on-road vehicles. In this context, the viability is defined in terms of achieving cost and performance targets.

Approach

Our team combines TIAX LLC and the Institute of Transportation Studies, University of California at Davis. We are concentrating on the application of PEM and anode-supported planar SOFC

Expected Fuel Cell Characteristics						
	Fuel Cell Type	Electrolyte	Operating Temperature (°C)	Power Density (mW/cm²)	Electrical Efficiency[1] (%, LHV)	Startup Time (hours)
Low Temperature	Proton Exchange Membrane[2] (PEMFC)	Fluorinated-sulfonic acid polymer membrane	70–90[3] 100-160	400-700	30–40% (Low temp.) 35–45% (High temp.)	<0.2
Low Temperature	Phosphoric Acid (PAFC)	Phosphoric acid	160 - 220	200	35–45%	1-4
High Temperature	Molten Carbonate (MCFC)	Lithium, potassium carbonate salt	600–650	120-160	45–55% (FC system only)	5-10
High Temperature	Solid Oxide (SOFC)[4]	Yttria-stabilized zirconium oxide	900–1,100 (tubular) 650–850 (planar)	150-200 (tubular) 200-600 (planar)	45–55% (FC system only) 65–70% (Gas turbine hybrid)	5-10 (tubular) 1-5 (planar)

1. Net electrical efficiency based on natural gas fuel. LHV = Lower heating value. Includes gas compression and other ancillaries
2. Also sometimes called a solid polymer electrolyte fuel cell (SPFC).
3. Recent developments in PEMFC are pushing temperature up to 160°C
4. Solid oxide technology describes both tubular and planar and both electrolyte-supported and electrode-supported technology.

Figure 1. Fuel Cell Performance Characteristics

Potential Fuel Cell APU Loads	
Hotel loads & Telematics	• Power truck cab/sleeper appliances • Provide AC when parked • Telecommunications, navigational equipment
Refrigeration loads	Replacement of diesel generators to increase efficiency and cut noise
Light-duty idling	Powers accessories during driving cycle, allowing engine-off while stopping
Start-up	Avoid cold-start problems
Engine redesign (Vehicle electrification)	• Redesign of engine • Electric breaking, steering, pumps, etc

Figure 2. Potential Fuel Cell APU Loads

technologies. With agreement of DOE, the scope has been refined to focus on technologies available in the 2005-2006 timeframe. Applications will be those available from the present time to 2010. We will address applications that use existing fuel infrastructure (namely gasoline and petroleum diesel), alternative fuels (e.g. propane), and future fuel (hydrogen).

We will look at passenger cars, class 1 and 2 light-duty trucks and SUVs, class 3-8 trucks, recreational vehicles, transit buses, and specialized vehicle applications. Military applications are not part of the current scope of work.

Our project is being carried out in five tasks. This first task (completed) confirmed the scope and approach with DOE. Task 2, currently underway, is developing a list and ranking of promising current and future applications for APUs. Sources are publicly available data and input from industry and government contacts. Task 3 will produce conceptual designs and vehicle integration layouts of 2-3 fuel cell APU systems. Task 4 will identify the R&D gaps and possible roles for DOE. Benefits to the Nation will be projected including oil displacement and emission reductions. Task 5 will provide an update 6 to 12 months from the submittal of the draft final report.

Results

Based upon current publicly available data, PEM and anode-supported SOFC technologies are the most promising technologies for transportation APUs, and thus will be the focus of this project. The performance specifications of fuel cell technologies are summarized in Figure 1. The key factors that influence fuel cell applicability as transportation APUs are power density, efficiency and system volume. Other important factors are fuel capability (and associated complexity of a fuel reformer), startup time and fuel cell stack life. A high-level ranking system yielded that PEM (both current and future high-temperature technology) and planar electrode-supported SOFC technologies appear to be the most applicable technologies for transportation APUs. These fuel cell technologies will be the focus of our study.

The team completed a high-level characterization of potential fuel cell APU applications. The overall process for this selection entailed four steps:

- Identify long list of potential fuel cell APU applications;
- Screen out options unlikely to be of interest based on DOE objective of achieving national benefits directly with APUs themselves or indirectly by facilitating introduction of fuel cells in vehicles for propulsion;
- Characterize applications at a high level; and
- Develop straw-man selection.

The types of loads considered were identified and classified in categories that represent increasing integration with the vehicle's propulsion system. These loads are summarized in Figure 2. The loads can be classified as those associated with hotel loads and telematics; refrigeration; loads during engine idling; aid to cold start; and integration with propulsion (e.g. complete vehicle electrification).

	Vehicles Meeting Market & Price Criteria	
	Annual Sales (thousands)	Starting Cost (thousands)
Luxury passenger cars	900 [1]	$34
Luxury light trucks	300 [1]	$40
Law enforcement large cars	70 [2]	$25
Contractor Special pick-ups	300 [3]	$30
W PTO/utility trucks (Class 3-8)	74 [4]	Highly variant
Recreational Vehicles	193 [5]	$50
Refrigeration units (Class 3-8)	60 [6]	$35
Heavy-duty trucks long-haul	105 [4]	$67

[1]J.D. Power & Associates, 2001 and Davis, Stacy, 2001; [2]Kelly, 2001and NAFA, 2000; [3]Kurylko, 2000; [4]VIUS, 2000; [5]RVIA, 2002 (http://www.rvia.org/consumers/recreationvehicles/types.htm); [6]U.S. Department of Commerce, 2001

Figure 3. Potential Fuel Cell APU Applications - Vehicles Meeting Market and Cost Criteria

The complete list of APU applications considered included:

- Passenger Cars
  - Minicompact
  - Subcompact
  - Compact
  - Midsize (Luxury and Standard)
  - Large (Luxury, Standard and Law Enforcement)
  - 2-Seater
- Light-Duty Trucks
  - Small pickup (<3,500 lbs.)
  - Small van (<4,500 lbs.)
  - Small utility (<3,500 lbs.)
  - Large pickup (3,500-8,500 lbs.; Contractor vehicle and Standard)
  - Large van (4,500-8,500 lbs.)
  - Medium utility (3,500-4,799 lbs.; Luxury and Standard)
  - Large utility (4,800-8,500 lbs.; Luxury and Standard)
- Medium-Duty Trucks (Class 3-6)
  - PTO/Utility (e.g. lift, dump, wrecker, service)
  - Delivery (Refrigerated and Standard)
  - Recreational vehicle
- Heavy-Duty Trucks (Class 7-8)
  - Local (Standard, Refrigerated and PTO/ Utility)
  - Line-haul (Standard, Refrigerated, PTO/ Utility)
  - Recreational vehicle
  - Motor coach & transit buses

The characterization and selection of systems addressed the following aspects of fuel cell APU applications:

- Potential national benefits, which are the product of the achievable market and the benefit per vehicle:
  - Economic (cost savings)
  - Energy savings
  - Environmental benefits (e.g. carbon dioxide, nitrogen oxides reduction)
  - Noise reduction and safety improvement
- The possibility to either be introduced into the market in the near-term, i.e. an existing APU application (e.g. replacement of existing less-efficient APU technology), or have significant national and user benefits but require longer-term market introduction, e.g. future APU application that may require redesign of vehicle.
- Compatibility with either current or possible future fuel infrastructure.

Screening criteria were used to narrow the initial market analysis of possible APU applications for fuel cells:

- Duty cycle - the duty cycle of the vehicle should be suited to APU use, e.g. long idle times
- Market size - the market potential must be adequate to support investment in APU technology
- Vehicle cost - the initial cost of the vehicle must be high enough that an APU would likely represent a reasonably small portion of total vehicle cost (<15%, assuming a fuel cell APU cost of $5000)

The vehicles meeting the initial criteria are shown in Figure 3.

Subsequent screening criteria used have both a short and long-term outlook:

- Energy savings
- Emissions savings
- Cost savings
- Acceleration of fuel cell introduction

Conclusions

Based on our first-pass APU application characterization and screening, hotel loads for long-haul heavy-duty truck / recreational vehicles, refrigerated trucks, police car and contractor utility trucks appear to be good candidates for further analysis. We will start detailed analysis of the long-haul truck cabin loads using petroleum diesel as a fuel. We will work with DOE to agree on the next 1 to 2 applications for detailed study as part of Task 3.

References

1. Davis, Stacy C. (2001). Transportation Energy Data Book Edition 21—2001 ORNL-6966. Oak Ridge National Laboratory. October.

2. J.D Power and Associates (2001). "Luxury crossover SUVs Gaining Market Share at Expense of Midsize SUVs." http://www.jdpa.com/pdf/0143.pdf. August 15. Visited April 8, 2002.

3. Kelly, K. (2001). "Battle for Police Market Heats Up." WardsAuto.com. Website, http://industryclick.com/microsites/newsarticle.asp?newsarticleid=269083&siteid=26&magazineid=1004&instanceid=8578&pageid=1126&srid=10250. Dec 27. Visited March 3, 2002.

4. Kurylko, Diana T. (2001). "DCX plans Hybrid pickup for 2005." Automotive News, May 7. http://www.autonews.com/article.cms?articleId=1894&a=a&bt=contractor+special. Visited April 14, 2002.

5. North American Fleet Association (NAFA), 1997. "NAFA's 1998 Model Year New Vehicle Acquisition Survey Results" http://www.nafa.org/public/searchidx.html. Fleet Executive, Volume 11, Number 12, December.

6. Recreational Vehicles Industry Association (RVIA), (2002). "RV Info." http://www.rvia.org/consumers/recreationvehicles/types.htm. Visited March 7.

7. U.S. Department of Commerce (2001). "Truck Trailers: Summary." Current Industry Report. Website, http://www.census.gov/ftp/pub/industry/1/m37l0013.pdf. M336L(00)-13. August.8. U.S. Department of Commerce's Vehicle Inventory & Use Survey (VIUS), (1997). U.S. Department of Commerce, Economics and Statistics Administration, U.S. Census Bureau. CD-ROM CD-EC97-VIUS. February.

FY 2002 Publications/Presentations

1. Presentation to 21st Century Truck Industrial Working Group in conjunction with SAE Government & Industry meeting, Washington, DC, May 15, 2002.

IV.F.3 Guidance for Transportation Technologies: Fuel Choice for Fuel Cell Vehicles

Stephen Lasher (Primary Contact), Johannes Thijssen, Stefan Unnasch
TIAX, LLC
Acorn Park
Cambridge MA, 02140
(617) 498-6108, fax: (617) 498-7054, e-mail: lasher.stephen@tiax.biz

DOE Technology Development Manager: Peter Devlin
(202) 586-4905, fax: (202) 586-9811, e-mail: Peter.Devlin@ee.doe.gov

ANL Technical Advisor: Robert Sutton
(630) 252-4321, fax: (630) 972-4430, e-mail: sutton@cmt.anl.gov

Objectives

- Support refined R&D targets for direct-hydrogen fuel cell vehicles (FCV) based on an analysis of well-to-wheel energy use, greenhouse gas (GHG) emissions, cost, and safety of direct-hydrogen FCVs and competing vehicle technologies.
- Assess opportunities and risks of various FCV and fuel choices, specifically hydrogen, comparing the technical, efficiency, economic, safety and financial risks of each option with onboard reforming of gasoline.

Approach

- In Phases 1 and 2, TIAX developed detailed well-to-wheel performance and cost calculations, taking into account technology options, system integration and efficiencies, hybridization, vehicle weight, and drive cycle. Last year's annual report included some of the results from these Phases; in this report, we present those results which were not previously reported.
- In Phase 3, we are evaluating the financial risks of various FCV options and potential triggers that may reduce the risks compared to conventional vehicles.
  - Perform detailed analysis of market introduction issues.
  - Evaluate the effect that potential triggers may have on the various stakeholders using a net present value (NPV) analysis.

Accomplishments

- Completed Phases 1 and 2.
- Developed a NPV analysis framework and a preliminary analysis of hydrogen and gasoline FCV options.

Future Directions

- Verify and refine NPV assumptions and analysis and use it to identify low-cost options for introduction of hydrogen or other fuel infrastructures.
- Evaluate the technology risk, financial exposure, and safety and regulatory risks associated with the various fueling options for each respective stakeholder.

Introduction

The focus of this project is to assess the potential impact of on-board storage of hydrogen, rather than on-board reforming of gasoline as a means of supplying fuel to FCVs. The overall risk involved in each of the fuel options for FCVs varies, and the risk may shift from one player in the value chain to another. This risk trade-off is the focus of Phase 3.

Approach

Phase 2

The approach to Phase 2 was described in detail in the full report (Arthur D. Little 2002), as well as in last year's annual report (Lasher, et al 2001). Key points are:

- Fuel cell system and vehicle analysis based on detailed performance and drive-cycle models, but based on a future fuel cell technology scenario, assuming success in current R&D efforts.
- Hydrogen costs based on detailed on-site hydrogen fueling station cost analysis.
- Vehicle cost estimates based on a detailed bottom-up analysis consistent with TIAX's automotive fuel cell costing study.

Phase 3

In Phase 3, we are performing NPV calculations to determine overall and individual stakeholder investment risks for various fuel and FCV options. Minimizing risks will require managing utilization factors, FCV introduction strategies, and infrastructure options. The NPV analysis is being used to evaluate the effect that potential triggers and drivers may have on the various stakeholders for each fuel chain and FCV option. Potential factors include:

- Crude oil and gasoline price increases
- FCV cost reduction
- Value of emissions reduction
- Subsidies and R&D funding and timing
- FCV fuel economy improvements
- Energy and capital cost improvements for hydrogen generation

Results

Phase 2

An overview of the well-to-wheels energy, GHG emissions, and fuel cost results were presented in last year's annual report (Lasher, et al 2001). Complete results can be found in the full report at: http://www.cartech.doe.gov/pdfs/FC/192.pdf. Last year's presentation of vehicle and ownership cost results was preliminary, and the final results are presented herein.

Vehicle Factory Cost Results

- Based on our scenario analysis, hydrogen-fueled FCV factory costs are around 30% ($4,000 per vehicle) higher than hybrid electric vehicles (HEVs).
- Fuel processor-based FCVs are projected to cost about 10% ($1,000-$2,000 per vehicle) more than compressed-hydrogen vehicles - roughly the same as metal hydride-based FCVs.
- However, FCV costs, even reformer-based FCVs, would be lower than battery EV costs while offering longer range.

Vehicle Ownership Cost Results (Figure 1)

- Vehicle ownership costs are dominated by vehicle depreciation, representing over 70% of annual cost for all vehicles.
- Fuel costs typically amount to less than $500 per year.
  - High efficiency of direct hydrogen and methanol-based FCVs compensates for higher hydrogen and methanol costs, bringing annual fuel costs on par with ICEVs.
- Sensitivity analysis shows that cost differences between FCVs and petroleum ICEVs are statistically significant.
  - Differences among FCV options are not statistically significant.

Safety Analysis Results

- Hydrogen transportation, fueling station, and on-board safety issues can likely be resolved without onerous cost increases.
- However, fuel cell vehicles will require modifications to garages, maintenance facilities,

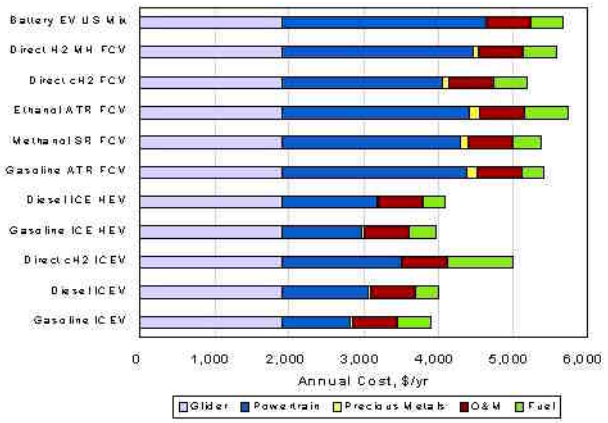

Notes: Assumes 14,000 mi/yr driving and 350 mile range (except the Battery EV that has 120 mile range); vehicle costs are adjusted for resale value with monthly payments over 5 years at 4% finance rate; insurance, tax, and license costs are excluded.
Assumes identical O&M costs for all vehicles.
Hydrogen is assumed to cost $20/GJ.

Figure 1. Estimated Vehicle Ownership Costs for Various Types of Vehicles

and on-road infrastructure that could be costly and difficult to implement.

Phase 3

We are currently refining our preliminary analysis based on existing information and using the on-site generated hydrogen FCV and gasoline FCV cases as the first examples. We started from the results of the previous phase and made the necessary updates and assumptions needed to perform NPV calculations. Progress towards the preliminary analysis includes:

- An initial set of NPV variables and outputs has been established.
- We have incorporated two FCV introduction scenarios and the associated R&D funding levels, consistent with scenarios used in DOE's Vision Model.
- We have estimated the fueling station capacity requirements based on FCV introduction, utilization factors, and infrastructure limitations.
- High and low production volume FCV and hydrogen fueling station equipment costs have been estimated using progress ratios.
- Large and small fueling station costs have been estimated using scaling factors for individual equipment based on vendor quotes or internal analysis.
- Preliminary costs and revenues of the major stakeholders have been estimated.

Conclusions

FCVs are expected to be able to achieve the lowest well-to-wheel energy consumption, provided efficient fuel chains are used. Direct-hydrogen FCVs carrying compressed hydrogen produced from natural gas can offer well-to-wheel energy consumption of approximately half that of conventional gasoline-fueled vehicles. However, substantial additional technology breakthroughs will be required to achieve FCV cost competitiveness with ICEVs.

Alternative fuels, especially hydrogen, will require significant up-front investment, representing a risk to both vehicle manufacturers and fuel providers. Dealing with this risk represents a formidable barrier to the use of hydrogen for FCVs.

References

1. Arthur D. Little, "Guidance for Transportation Technologies: Fuel Choice for Fuel Cell Vehicles, Phase II Final Report", available at http://www.cartech.doe.gov/pdfs/FC/192.pdf, February 2002

2. Lasher, S., J. Thijssen, S. Unnasch, "Guidance for Transportation Technologies: Fuel Choice for Fuel Cell Vehicles", *2001 Annual Progress Report – Fuels for Advanced CIDI Engines and Fuel Cells,* EERE OTT, November 2001

Publications/Presentations

1. Arthur D. Little, "Guidance for Transportation Technologies: Fuel Choice for Fuel Cell Vehicles, Phase II Final Report", available at http://www.cartech.doe.gov/pdfs/FC/192.pdf, February 2002

2. Thijssen, J., "Fuel Choice for Fuel Cell Vehicles", presented at 2002 Future Car Congress, Arlington VA, June 3-5, 2002

3. Weber, B., "Economics/Commercialization Issues and Opportunities", presented at ASME Workshop on Fuel Cell Technologies for Advanced Vehicles, Rochester Institute of Technology, Rochester NY, April 22-24, 2002

4. Weber, B., "Future of Hydrogen Fuels, Fuel Cells and Alternative Energy Technology", presented at 7th ASCOPE (ASEAN Council on Petroleum), Kuala Lumpur, Malaysia, November 5-8, 2001

IV.F.4 Fuel Cell R&D and Demonstration

Robert E. Fields, E. John Rowley, Mahlon S. Wilson (Primary Contact), Christine Zawodzinski
Los Alamos National Laboratory
PO Box 1663, MS D429
Los Alamos, NM 87545
(505) 667-9178, fax: (505) 665-4292, e-mail: mahlon@lanl.gov

DOE Technology Development Manager: Neil Rossmeissl
(202) 586-8668, fax: (202) 586-5860, e-mail: Neil.Rossmeissl@ee.doe.gov

Objectives

- Develop a fuel cell test bed to enhance understanding of fuel cell operation under real-world conditions.
- Develop a hybrid fuel cell-powered demonstration vehicle.
- Develop specialized circuitry that can be used to monitor fuel cell stack performance on the benchtop while mimicking real-world loading conditions.
- Develop a fuel cell stack system that operates under both active and passive modes for optimal overall efficiency.

Approach

- Determine power requirements of a standard battery-powered three-wheeled personal mobility vehicle (scooter).
- Design, build, and test a 4-cell, 35 cm^2 active/passive short fuel cell stack to verify performance, heating, and water balance issues.
- Design, build, and test a 40-cell, 35 cm^2 active area active/passive fuel cell stack to power the three-wheeled scooter.
- Design, build, write software/firmware for, and test a custom electronics package to monitor, control, and protect the fuel cell stack and associated electronics.
- Refine the design based on results to enhance performance, accomplish automatic fuel cell stack startup, and incorporate automatic phase-in of power delivery from the fuel cell stack.

Accomplishments

- Determined the power requirements of a standard three-wheel scooter.
- Verified performance, heating, and water issues with a 4-cell short fuel cell stack.
- Demonstrated active/passive dual-mode fuel cell operation on a stack level.
- Built, tested, and installed a 40-cell fuel cell stack in a three-wheeled scooter.
- Designed, built, and wrote software for a custom electronics package to monitor, control, and protect the fuel cell stack.
- Demonstrated fuel cell-powered scooter at public demonstrations and to visiting scientists and DOE officials.
- Incorporated electronics package into other DOE fuel cell project testing equipment.

Future Directions

- Refine software/firmware to accomplish transparent fuel cell stack startup and drive-off and enhance reliability.
- Incorporate additional circuitry to more efficiently control fuel cell stack and power conditioning circuitry and efficiently switch between active and passive modes of fuel cell stack operation.
- Build lifetime and power use profile data for the scooter under real-world operating conditions.
- Incorporate lifetime and power use profile data into benchtop stack testing procedures.
- Develop and build higher power output fuel cell stack to provide enhanced power reserves for severe loading and faster startup transition to all-fuel cell power.

Introduction

Hydrogen fuel cells have yet to have any meaningful commercial success. Obstacles include cost, reliability, fuel supply/storage and entrenched competition. The first market entry points will probably be those areas where the extra cost and fuel inconvenience are offset by the advantages of the fuel cell over the previous technology. A power range where this may apply is on the several-hundred watt level, where batteries are unwieldy and internal combustion engines are inefficient and noisy. A potentially interesting commercial application for several-hundred watt fuel cells is in powering personal mobility vehicles (PMVs). These include powered wheelchairs and three-wheeled electric powered "scooters" often used by the elderly or infirm. The users of PMVs are often located in environments where hydrogen supply could be established (e.g., nursing homes or hospitals) or routine customers of medical supply houses. The usefulness and benefits of PMVs to many users are often limited by battery considerations. The additional range (and possibly life and reliability) offered by fuel cells may more than compensate for higher cost and fuel supply issues.

To this end, we have modified a Victory® personal mobility vehicle (Pride Mobility Products Corporation, Exeter, PA), as shown in Figure 1, to accept a mid-range fuel cell system with a custom monitoring, control, and data logging electronics package. The control system consists of two components - a main monitor and control board which handles low-level monitoring and near real-time protection features, and a Handspring (Mountain View, CA) Visor Pro personal digital assistant that acts as an operator display and data logger and provides manual systems control. The electronics protect the fuel cell stack and store operational information that can be used to further optimize stack installation and operation.

Figure 1. A Pride Mobility Products Corporation Victory® Personal Mobility Vehicle (scooter)

Approach

To adapt a personal mobility scooter to fuel cell-powered operation, it was first necessary to determine peak and average power requirements of a standard battery-equipped scooter. A battery-powered scooter was equipped with current and voltage monitoring circuitry and was driven under common operating conditions. A minimum power output requirement for the fuel cell stack was found. The scooter electrical system and physical

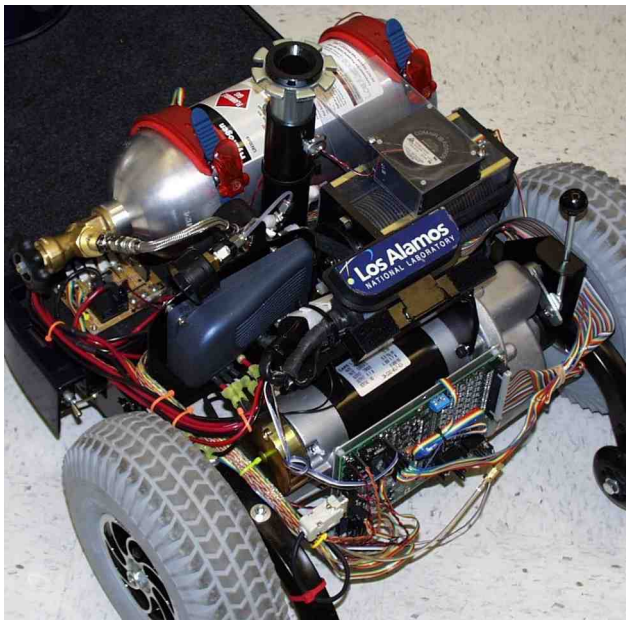

Figure 2. Overview of hydrogen fuel cell installation. The scooter body shroud has been removed for photographs.

Figure 3. The 40-cell hydrogen stack installed on the scooter chassis. Ribbon cable allows monitoring all cell voltages.

configuration were inspected to find the best way to equip it with a hydrogen fuel cell, hydrogen storage system, and control and monitoring electronics with minimum modification to the scooter and while maintaining the original mechanical outline. Hydrogen storage methods were investigated, and it was determined that a metal hydride would provide the optimum solution without adding significantly to the overall scooter weight.

An initial monitoring and control strategy was determined and suitable electronic circuitry was designed, constructed, tested, and installed. Preliminary testing of the fuel cell system revealed an issue with power distribution between the fuel cell stack and the lead-acid batteries used to supply power during peak loading during acceleration or hill climbing. This issue was addressed and solved to a first approximation with rudimentary additional circuitry. Stack protection methods were further optimized over the initial strategy. A more optimum power distribution and stack protection method that will also significantly increase overall system efficiency was determined.

The original design for passive "air-breather" fuel cell stacks developed under a Hydrogen Program Cooperative Research and Development Agreement was scaled-up and modified to accommodate active (fan-supplied air) operation. Single-cell and short stack testing of various component permutations were used to design the eventual 40-cell stack. While it was necessary to restrict air access in the 40-cell design to prevent dryout, the stack exhibited stable performance and operated well in both active and passive modes.

Results

A hybrid fuel cell powered personal mobility research, development, and demonstration vehicle was constructed based on a commercially available standard three-wheeled scooter and fuel cell designs developed at Los Alamos National Laboratory. The fuel cell-powered scooter required minimal modification to the standard scooter aside from the actual fuel cell, metal hydride cylinder, and electronics installation (Figures 2-5). The electronics package developed for the project has proven valuable in providing insight into operational, gas flow, and temperature issues with the fuel cell developed for the scooter and in testing other fuel cell stacks developed for other DOE projects. The scooter has been used in several successful private and public demonstrations highlighting the utility and advantages of fuel cell power.

Figure 4. Metal Hydride Hydrogen Storage Tank Mounted in Stock Scooter Battery Location

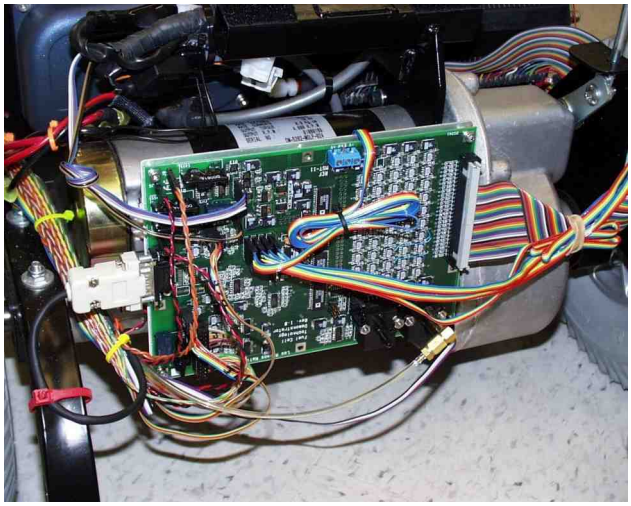

Figure 5. Fuel Cell Monitoring and Control Electronics Circuit Board Mounted on Scooter Drive Unit

Conclusions

The fuel cell-powered scooter project has provided valuable insights into fuel cell operation under real-world conditions as well as monitoring and control strategies to maximize power and efficiency. The electronics developed for the project have found dual use with other fuel cell testing systems. Additionally, the fuel cell-powered scooter has proven valuable as a way to illustrate and demystify fuel cell systems, and as a public relations tool to promote alternative energy research at Los Alamos National Laboratory.

FY 2002 Publications/Presentations

1. R. Fields, E.J. Rowley, M. Wilson, and C. Zawodzinski, "A Fuel Cell Monitoring and Control System for a Personal Mobility Vehicle". To be presented at the Electrochemical Society Meeting, Salt Lake City, UT (Fall 2002).

2. Robert E. Fields, E. John Rowley, Mahlon S. Wilson and Christine Zawodzinski, "Fuel Cell R&D and Demonstration" U.S. DOE Hydrogen and Fuel Cells Annual Program/Lab R&D Review, Golden, Colorado (May 2002).

IV.F.5 Advanced Underground Vehicle Power and Control Fuel Cell Mine Locomotive

David L. Barnes (Primary Contact), Arnold R. Miller
Vehicle Projects, LLC
621 Seventeenth Street, Suite 2131
Denver, Colorado 80293-2101
(303) 296-4218, fax: (303) 296-4219, e-mail: david.barnes@vehicleprojects.com

DOE Technology Development Manager: Sigmund Gronich
(202) 586-1623, fax: (202) 586-5860, e-mail: Sigmund.Gronich@ee.doe.gov

Main Subcontractors: Canada Center for Mineral and Energy Technology, Ottawa, ON, Canada; Hatch Associates Ltd, Sudbury, ON, Canada; Sandia National Laboratories, Livermore, California; University of Nevada, Reno, Nevada; Kappes, Cassiday & Associates, Reno, Nevada

Objectives

- Develop a zero-emissions, fuel cell-powered metal-mining locomotive
- Evaluate its safety and performance, primarily in surface tests
- Evaluate its productivity in an underground mine in Canada

Approach

- Design 14 kilowatts (kW) fuel cell powerplant
- Design metal-hydride storage
- Integrate powerplant and hydride storage onto locomotive base vehicle
- Conduct preliminary tests and evaluate
- Refine final design
- Perform safety and risk analysis and complete documentation to meet regulatory approval
- Evaluate productivity performance in an underground metal mine

Accomplishments

- Designed 14 kW fuel cell powerplant and metal-hydride storage
- Integrated powerplant and metal-hydride storage onto locomotive base vehicle
- Performed preliminary testing and evaluation in Nevada
- Conducted safety and risk assessment

Future Directions

- Integrate recommended safety improvements into final design
- Complete documentation for final regulatory approval
- Evaluate performance on surface and underground in a metal mine

Introduction

Underground mining is one of the most promising applications in which fuel cell vehicles can compete strictly on economic merit (1). The mining industry, one of the most regulated, faces economic losses resulting from the health and safety deficiencies of conventional underground traction power. Conventional power technologies - tethered (including trolley), diesel, and battery - are not simultaneously clean, safe, and productive. Fuel cell power would solve the challenges by providing large cost savings relative to the high capital cost of current underground traction power. Lower recurring costs, reduced ventilation costs, and higher vehicle productivity could make the fuel cell vehicle cost-competitive years before surface applications. The fuel cell locomotive is shown in Figure 1.

Figure 1. Fuel Cell Mine Locomotive

Approach

A joint venture between the Fuel Cell Propulsion Institute (a nonprofit consortium of industry participants) and Vehicle Projects LLC (project management) provided the basis for the 2 phase project. In phase 1, Sandia National Laboratories was tasked with the design of the fuel cell powerplant and the metal-hydride storage, as well as system integration. Phase 2 includes system evaluation, safety and risk assessment, and underground testing in a production environment.

To ensure the locomotive was designed with industry in mind, various industry participants were involved in assessing the design for risk and functionality. When the locomotive is tested underground, all regulatory requirements will have been met.

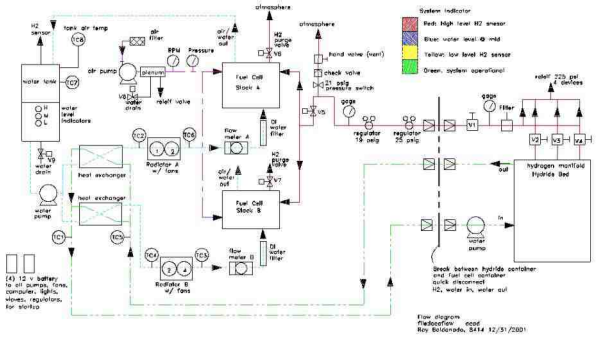

Figure 2. Schematic Layout of Fuel Cell Powerplant and Metal-Hydride Storage

Comparison of Battery and Fuelcell Locomotives		
Parameter	**Battery**	**Fuelcell**
Power, rated continuous	7.1 kW (gross)	14 kW (gross)
Current, rated continuous	76 A	135 A
Voltage at continuous rating	94 V (estimated)	104 V
Energy capacity, electrical	43 kWh	48 kWh
Operating time	6 h (available)	8 h
Recharge time	8 h (min)	1 h (max)
Vehicle weight	3,600 kg	2,500 (without ballast)

Figure 3. Battery and Fuel Cell Specifications

Results

The locomotive's fuel cell power system uses proton exchange membrane fuel cells. No traction battery is employed: thus, the vehicle is a pure fuel cell vehicle. Two stacks in electrical series provide 104 volts and 135 amps at the continuous rated power of 14 kW gross. Waste heat from the stacks provides the heat to desorb hydrogen from the metal-hydride bed. A heat exchanger links the two isolated thermal systems: (a) the hydride-bed heating/cooling loop and (b) the stack cooling loop. Figure 2 depicts the schematic layout of the powerplant and metal-hydride storage. Specifications of the fuel cell and battery versions of the locomotive are compared in Figure 3.

The hydride storage system stores 3 kg of hydrogen, sufficient for eight hours of locomotive operation at the predicted 6 kW average power of its

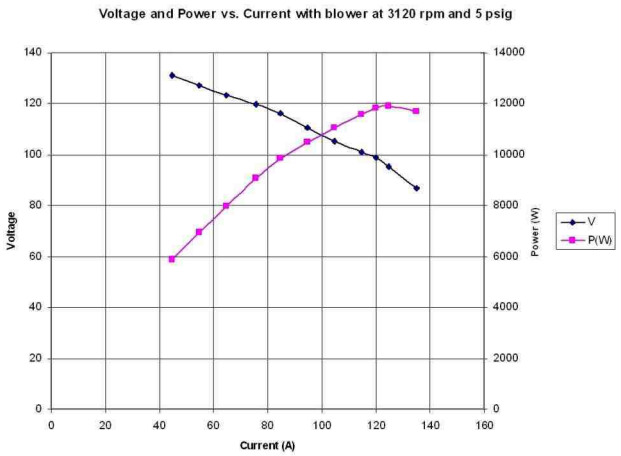

Figure 4. Fuel Cell Power Curve Showing 12 kW Gross Power

duty cycle. Hydride subsystem design allows forrapid change-out (swapping) of a discharged bed with a freshly charged unit. Recharging will utilize gaseous hydrogen and has been measured at approximately one hour.

Bench performance data for the powerplant are shown in Figure 4. Both voltage versus current and gross power versus current are shown. Maximum observed power in the test was 12 kW gross due to air pressure of 5 psig, rather than 7 psig as specified for 14 kW gross power. Parasitic losses are less than 10%, a very good performance result.

Mine Safety and Health Administration (MSHA) focused on possible hazards of hydrogen underground, including detailed review of process piping and electrical routing. The assessment indicated few changes required to meet existing standards and will help establish new standards for hydrogen-fueled underground mine vehicles.

MSHA measured noise levels (Table 1) of the locomotive under a number of operating conditions, including acceleration (2). Unlike some fuel cell vehicles, our locomotive is very quiet under all conditions. It emanates a pleasant, low frequency purring, and normal conversation can easily be carried out while standing beside the operating powerplant. Consequently, the steel-wheel-to-steel-track generated noise will be the most prevalent.

Table 1. Average Recorded Sound Levels

Average Sound Levels for the Locomotive		
Location/Condition	**dBA***	**Linear****
Operator Position/Traveling Forward, Run 1 (Full Throttle)	75.3	80.1
Operator Position/Traveling Forward, Run 2	76.6	85.1
Operator Position/Traveling in Reverse, Run 1 (Full Throttle)	76.6	85.1
Operator Position/Traveling in Reverse, Run 2	76.2	82.2
Operator Position/Idle	74.4	81.2
6 Inches from Blower on Right Side/Idle	78.9	85.3
6 Inches from Top Vent on Right SIde/Idle	80.0	84.3
6 Inches from Control Panel on Left Side/Idle	79.5	84.0
1 Foot in Front of Locomotive/Idle	75.3	81.9
Background Near Area of Tests	73.4	78.3

* Sound Level Using an "A-weighted"network
** Sound Level using and unweighted network (flat response)

Conclusions

The problems of vehicle emissions and noise have negative economic consequences for underground vehicle applications. Fuel cells coupled with reversible metal-hydride storage, by solving these problems, offer cost offsets - higher productivity and lower operating costs - that can make underground fuel cell vehicles cost-competitive sooner than surface applications. Our hydride-fuel cell locomotive, like the battery version, is a zero-emissions vehicle. However, the fuel cell locomotive has greater net power, greater energy storage, higher gravimetric energy and power density, higher volumetric power density, and substantially faster recharging. Because weight is not an issue, safe and compact metal-hydride storage is an ideal storage technology for underground locomotive applications.

References

1. A. R. Miller, Tunneling and Mining Applications of Fuel Cell Vehicles. Fuel Cells Bulletin, July 2000, pp. 5-9.

2. Special Acoustical Field Investigation, Hydrogen Fuel Cell Powered Locomotive. Investigative Report PP-025-02O, Mine Safety and Health Administration, Pittsburgh, PA, 17 May 2002.

Presentations

1. R. Sage, "Fuel Cell Mine Loader and Prototype Locomotive", Canadian Institute of Mining Annual Conference & Exhibition, Vancouver, British Columbia (2002)

2. A. Miller, "Fuel Cell Locomotives", European Fuel Cell Forum, Lucerne, Switzerland (2002)

Section V. Integrated Hydrogen and Fuel Cell Demonstration/Analysis

V.A System Analysis

V.A.1 Analysis of Hydrogen Production Using Ammonia and Ammonia-Borane Complex for Fuel Cell Applications

Ali T-Raissi (Primary Contact)
University of Central Florida
Florida Solar Energy Center
Cocoa, FL 32922-5703
(321) 638-1446, fax: (321) 638-1010, e-mail: ali@fsec.ucf.edu

DOE Technology Development Manager: Roxanne Danz
(202) 586-7260, fax: (202) 586-4753, e-mail: Roxanne.Danz@ee.doe.gov

Objectives

- Analyze the viability (i.e. cost, safety, and performance) of ammonia-based chemical hydrides as hydrogen (H_2) storage compounds for fuel cell applications.
- Identify the pros and cons of using ammonia (NH_3) as a chemical carrier for H_2.
- Evaluate the viability of autothermal NH_3 reformation on-board fuel cell vehicles.
- Analyze the viability (cost and performance) of using ammonia-borane complex (H_3BNH_3) as a chemical hydrogen storage medium on-board fuel cell vehicles.
- Identify technoeconomic barriers to the implementation and use of amine borane complexes, in general, and H_3BNH_3, in particular, as prospective chemical hydrogen storage media on-board fuel cell vehicles.

Approach

- Review all published papers, reports, patents, etc. in the past 50 years related to the development of ammonia-based chemical hydrides as H_2 storage compounds.
- Develop contacts with and inquire about information from the researchers and/or companies involved with the development of ammonia-based chemical hydrides.
- Use FactSage Program to calculate and optimize the performance parameters for the autothermal reformation of ammonia to hydrogen gas.
- Compile information on the physiochemical properties and synthesis of ammonia-borane complex.
- Compare the characteristics and costs of H_3BNH_3 as a hydrogen storage media to that of sodium borohydride ($NaBH_4$) and ionic hydrides such as lithium hydride (LiH) and calcium hydride (CaH_2).
- Identify possible approaches that have potential to significantly reduce the cost of ammonia-borane synthesis.

Accomplishments

- Reviewed and evaluated more than 120 published papers, reports, patents and other archival records related to ammonia-based chemical hydrides, including amine borane complexes, as prospective chemical hydrogen storage compounds.
- Completed an assessment of the pros and cons of ammonia-based hydrogen storage compounds for vehicular fuel cell power applications.

- Used FactSage 5.1 Program for Computational Thermochemistry to determine the performance parameters for the autothermal reformation of NH_3 gas to hydrogen.
- Evaluated a number of ammonia adducts, including H_3BNH_3, as non-toxic, non-cryogenic alternatives to ammonia for use in vehicular fuel cell applications.
- Completed a tentative evaluation of the production costs of ammonia- and amine borane-based hydrogen storage compounds.
- Identified the current high costs of ammonia-borane complex production as the main drawback to the successful implementation of H_3BNH_3 as a H_2 storage compound for the vehicular fuel cell applications.

Future Directions

- Complete technoeconomic analysis of ammonia-borane complex as a hydrogen storage compound for fuel cell applications.
- Conduct a thorough literature search to identify and evaluate new, more advanced and potentially lower cost chemical processes for the synthesis of H_3BNH_3.

Introduction

The aim of this project is to assess the issues of cost, safety, performance, and environmental impact associated with the production of hydrogen (H_2) by several methods, not presently funded by the U.S. DOE Hydrogen, Fuel Cell and Infrastructure Program. Three technology areas being evaluated are: 1) thermochemical reformation of methane (CH_4) and hydrogen sulfide (H_2S) gas with and without using solar energy; 2) ammonia (NH_3) and ammonia adducts as hydrogen storing chemical hydrides for fuel cell applications; and 3) thermochemical water-splitting cycles suitable for solar power interface.

A report on the first topic involving an assessment of the thermochemical reformation of CH_4/H_2S has been submitted previously. This second report is concerned with the prospects of NH_3 and ammonia-borane as hydrogen storage media for fuel cell applications.

Advantages and Drawbacks to Ammonia Use

Ammonia is the second largest synthetic commodity product of the chemical industry, with world production capacity exceeding 140 million metric tons. In 2000, the U.S. consumed in excess of 20 million metric tons of NH_3. Anhydrous ammonia costs about $150 per short ton (f.o.b. U.S. Gulf Coast) or less than $6.25 per million BTU of H_2 contained. Besides the large volume of production and use, and relatively low cost, NH_3 has the following advantages as a hydrogen-rich fuel for fuel cell applications:

- Energy density - contains 17.8 weight % hydrogen (liquid ammonia stores 30% more energy per unit volume than liquid hydrogen).
- Infrastructure for NH_3 transportation, distribution, storage and use already exists.
- Simplicity - its use requires no shift converter, selective oxidizer or co-reactants.
- No purification is needed for NH_3 use with alkaline fuel cells (AFCs).
- Only 16% of the energy stored in NH_3 is needed for its conversion to N_2 and H_2.
- There are good NH_3 decomposition catalysts such as: ICI-47-1 (10 weight % nickel on alumina); Haldor Topsøe DNK-2R (triply promoted iron-cobalt); SÜD-Chemie 27-2 (nickel oxide on alumina); various supported nitrided catalysts (e.g. molybdenum nitride and nickel molybdenum nitride on - α alumina); and ruthenium modified nickel oxide on alumina.
- Flammability range for ammonia -air (at 0°C and 1 atm) is much narrower than that for hydrogen-air mixtures (i.e. 16-27 volume % NH_3 vs. 18.3-59 volume % H_2).

- Using ammonia in fuel cell power plants does not generate carbon dioxide (CO_2) or nitrogen oxides (NO_2) emissions.

There are several drawbacks to ammonia as a fuel and chemical carrier for H_2, especially in vehicular applications, including safety concerns with the widespread transportation, utilization and use of ammonia as a transportation fuel; storage requirements for sub-ambient temperatures and/or elevated pressures; and requirements for on-board reformation to liberate H_2. These limitations make the widespread ammonia use as a transportation fuel problematic. Furthermore, cost and energy efficiency considerations dictate that any chemical hydride employed as a vehicular hydrogen storage medium, including ammonia, not require complicated on-board reformation in order to generate hydrogen.

To mitigate ammonia's shortcomings, our approach involved complexing NH_3 with other hydrides to form compounds that are stable but not toxic or cryogenic. In particular, our approach considered a class of compounds (with generalized formula amine boranes [B_xN_xHy]) known as amine-boranes that contain H_2 at gravimetric and volumetric densities comparable to that of anhydrous ammonia. The simplest known stable compound in this class is ammonia-borane, H_3BNH_3 (or borazane). Borazane is a white crystalline solid that when heated releases hydrogen in a sequence of reactions that occur at distinct temperature ranges. H_3BNH_3 contains about 20 weight % hydrogen and is stable in water and ambient air.

Physiochemical Properties and Synthesis of Ammonia-Borane Complex

Pyrolysis of ammonia-borane is a complex process, and the products of the decomposition reaction markedly depend on the conditions employed. Furthermore, the initial process is a solid-state reaction for which the onset of decomposition is a function of heating rate of the substrate (β). In thermogravimetric analyzer-Fourier transform infrared (TGA-FTIR) and thermogravimetric analyzer-differential scanning (TGA-DSC) analysis, heating a borazane sample to 90°C at a rate of 0.5°C/min and then holding it at that temperature for 200 min resulted in a loss of about 10.2% of initial sample mass. FTIR analysis of the evolved gases has shown approximately one mol of H_2 forming per mol of BH_3NH_3 reacted. Reaction products, in addition to hydrogen, have included monomeric aminoborane (BH_2NH_2) and a small amount of volatile borazine ($B_3N_3H_6$). The monomeric aminoborane is unstable at room temperature, oligomerizing to form a non-volatile white solid residue of poly (aminoboranes) $(BH_2NH_2)_x$. The inorganic analog of polyethylene, polymeric $(NH_2BH_2)_x$, is still not fully characterized. Crystalline cyclic oligomers, $(NH_2BH_2)_n$ (where, n = 2, 3, 4, 5) have been prepared, and an amorphous $(NH_2BH_2)_x$ consisting of solvated linear chains with x= 3-5 has also been produced by gas-phase pyrolysis of ammonia-borane.

Unlike aminoborane oligomers, borazine (isoelectronic with benzene) is a volatile colorless liquid that boils at 55°C. Based on the TGA and DSC analysis, pyrolysis of ammonia-borane begins with a sharp endothermic peak that appears just above the melting point of BH_3NH_3 (112-114°C depending on the sample heating rate). Near 117°C, a steep exothermic peak occurs, reaching a maximum at about 130°C with rapid evolution of gas. A final broad exotherm appears near 150°C. Although processes other than step-wise decomposition and hydrogen loss are involved to some extent in H_3BNH_3 and its intermediate compounds, nonetheless the following sequence of events occur (BN = boron nitride, g = gas phase, $[HBNH]_x$ = polyborazine, $[HBNH]_3$ = borazine, H_2BNH_x = monomeric aminoborane, $[H_2BNH_x)_x$ = polymeric aminoborane, kJ/mol = kilo Joule per mole, s = solid phase, ΔH_r = heat of reaction, β = heating rate):

$$H_3BNH_3\ (l) \rightarrow H_2BNH_2\ (s) + H_2\ (g)\ \sim 137°C,$$

$$\beta = 5\text{-}10°C/min,\ \Delta H_r = -(21.7 \pm 1.2)\ kJ/mol$$

$$x\ (H_2BNH_2)\ (s) \rightarrow (H_2BNH_2)_x\ (s)\ at \sim 125°C$$

$$(H_2BNH_2)_x\ (s) \rightarrow (HBNH)_x\ (s) + x\ H_2\ (g)\ at \sim 155°C$$

$$(HBNH)_x\ (s) \rightarrow borazine + other\ products$$

$$(HBNH)_3 \rightarrow 3\ BN + 3\ H_2\ at\ above\ 500°C$$

$$(H_2BNH_2)_x\ (s) \rightarrow (BN)_x\ (s) + 2x\ H_2\ (g)\ at \sim 450°C,\ \beta = 10°C/min$$

Due to the large amount of evolved H_2 and the exothermicity of the process, ammonia-borane appears to be a more effective chemical carrier for H_2 than anhydrous NH_3. Other physicochemical

properties of ammonia-borane complex are given in Table 1 below.

Table 1. Selected Physiochemical Properties of Ammonia-Borane Complex

Property	Description
Formula	NH_3BH_3
Molecular weight	30.86
X-ray structure	C_{4V} symmetry; unit cell is tetragonal
Odor	Ammonia-like
Density, kg/L	0.74
Melting point	112-114°C, slow decomposition at approx. 70°C
Heat of formation	ΔH_f°= -178 ± 6 kJ/mol
Heat of combustion	ΔH_c°= -1350 ± 3 kJ/mol
Water stability	10% solution stored at ambient temperatures: Dormancy — % hydrogen loss 4 days — 1.8 11 days — 3.6 1 month — 4.8 2.5 months — 9.3 18 months — 45.0

Another important factor is interaction with water and other solvents. Unlike ionic hydrides, NH_3BH_3 does not react violently with water. Table 2 depicts the solubilities of borazane in water and a number of organic solvents.

Borazane can be prepared through several indirect procedures including the reaction with lithium borohydride, $LiBH_4$, in diethyl ether by either of the following two methods (LiCl = lithium chloride, Li_2SO_4 = lithium sulfate, NH_4Cl = ammonium chloride, $[NH_4]_2SO_4$ = ammonium sulfate :

$$LiBH_4 + NH_4Cl \text{ – in diethyl ether} \rightarrow LiCl + H_3BNH_3 + H_2$$

$$2\ LiBH_4 + (NH_4)_2SO_4 \text{ – in diethyl ether} \rightarrow Li_2SO_4 + 2\ H_3BNH_3 + 2\ H_2$$

Alternatively, H_3BNH_3 is prepared directly from the gases by reacting diborane with ammonia in polar organic solvents (e.g. ether and dioxan) and in aqueous media:

$$\text{(diborane) } B_2H_6 + 2\ NH_3 \text{ – in ether or dioxan} \rightarrow 2\ H_3BNH_3$$

Table 2. Solubilities of Ammonia-Borane Complex in Various Solvents

Solvent	Weight %	Temper-ature, °C	Density of saturated solution, kg/L
Water	26	23	0.89
Methanol	23	23	0.78
Ethyl Ether	0.80	24	0.71
Hexane	0.003	25	0.56
Benzene	0.03	25	0.87
Methylene Chloride	0.08	21	1.32

For vehicular fuel cell applications, the main drawback to the use of amine-boranes, in general, and H_3BNH_3, in particular, is the present high cost of these compounds and lack of a suitable reformer design for the on demand generation of hydrogen. No data could be found for the large-scale production costs of ammonia-borane. However, the Callery Chemical Co manufactures large quantities of dimethylamine borane (DMAB), which has significant use in the electroless plating industry. Depending on the volume, the price of DMAB is in the range of about $75-100/lb. It can be expected that the large volume price of ammonia-borane would also be in this range. The issue of the cost of ammonia-borane can be highlighted by comparing its price to the bulk material prices for other chemical hydrides under consideration as hydrogen storage compounds. The feasibility of using various ionic hydrides as potential H_2 storage compounds for AFC applications has been analyzed. This application requires a hydrogen storage system capable of supplying H_2 to an AFC producing 1 kW of electrical power for 8 h. The fuel cell is assumed to operate at 57% efficiency (at 0.7 volt), requiring 231 mol of H_2

(assuming 100% utilization). Table 3 depicts the cost of several H_2 storage media including H_3BNH_3.

Table 3. Required Mass, Volume and Cost of Chemical Hydrides for 8 hours/1 kW Duty

Storer	Mass, kg	Volume, Liters	Cost, US$
LiH	1.7	3.7	109
CaH_2	4.5	4.0	104
$NaBH_4$ (35 Weight % aqueous)	6.21	6.21	102
H_3BNH_3	2.38	3.21	390-525

New chemical synthesis techniques and/or processes are needed to reduce the H_3BNH_3 production costs. In addition to the cost issues, new processes must be developed to allow recycling of the by-products of ammonia-borane decomposition on-board fuel cell powered vehicles. For example, if an on-board ammonia-borane based hydrogen storage system is to be developed for maximum H_2 delivery, then it will be desirable, if not necessary, to be able to retrieve and recycle the boron nitride residue. Here, the challenge is to develop a chemical route for activating the boron-nitrogen bond in a manner analogous to dinitrogen bond activation in the Haber-Bosch process for ammonia synthesis. In a modern ammonia plant, steam reformation of natural gas is used as the primary source of hydrogen. A simple stoichiometric equation for ammonia production by steam methane reformation (SMR) is as follows:

$$CH_4 + 0.3035\ O_2 + 1.131\ N_2 + 1.393\ H_2O \rightarrow CO_2 + 2.262\ NH_3$$

$$\lfloor\ 1.4345\ AIR\ \rfloor$$

In practical processes, a high degree of irreversibility exists, and a considerable amount of energy is needed to produce ammonia from methane, air and water. The stoichiometric quantity of methane required in the equation above is about 583 m^3 per ton of NH_3 produced. Energetically, this corresponds to approximately 20.9 giga-joule (GJ) per ton of NH_3 (lower heating value). This is the minimum amount of energy needed per ton of ammonia produced using the SMR process. It is interesting to note that the best energy figure reported for commercial ammonia production is about 27 giga Joule per metric ton (GJ/t) NH_3. This figure corresponds to a rather high efficiency of around 75% with respect to the theoretical minimum of 20.9 GJ/t NH_3, calculated as stoichiometric methane demand discussed above.

In a like manner, an idealized process for ammonia-borane synthesis from recycled BN (or borazine) may be written as:

$$CH_4 + 1.33\ BN + 2\ H_2O \rightarrow CO_2 + 1.33\ H_3BNH_3$$

Or,

$$CH_4 + 0.667\ (HBNH)_3 + 2\ H_2O \rightarrow CO_2 + 2\ H_3BNH_3$$

If similar processes could be developed at energy conversion efficiency levels that are comparable to the present day SMR-based NH_3 synthesis plants, then it would be possible to realize a major reduction in the production costs of ammonia-borane complex. We note that a concept similar to that discussed above has already been developed for nitric acid synthesis process based on boron nitride analogous to the Haber-Bosch route for nitric acid production from NH_3. Finally, recent results have shown that unusual parallel behavior exists between hydrocarbons and their corresponding B-N analogues. Thus, hydrogenation of benzene to cyclohexane may also provide a model for the reformation of borazine to other amine-boranes.

Conclusions

There are many advantages to the use of NH_3 as hydrogen source for vehicular fuel cell vehicle applications. However, a major drawback is ammonia's extreme toxicity and adverse health effects. By complexing NH_3 with diborane, a stable, non-toxic and non-cryogenic material (H_3BNH_3) can be prepared. This ammonia-borane complex is stable in water and ambient air and when heated liberates H_2 in a sequence of reactions between 137°C and 400°C that reaches about 20% of the initial mass of H_3BNH_3. Successful implementation of ammonia-borane as a potential future transportation fuel, however, requires new chemical techniques and/or processes for its synthesis that promise substantial reduction in its production costs.

FY 2002 Publications/Presentations

1. A. T-Raissi, "Ammonia and Ammonia Adducts as Hydrogen Energy Storers for Fuel Cell Applications," Proceedings of the 14th WHEC, Montreal, Canada, June 9-13 (2002).

2. C.A. Linkous, C. Huang, J. Fowler, G. Scott, A. T-Raissi, and N.Z. Muradov, "Closed Cycle Photochemical Methods for Deriving Hydrogen from Hydrogen Sulfide," Proceedings of the 14th WHEC, Montreal, Canada, June 9-13 (2002).

3. A. T-Raissi, "Technoeconomic Analysis of Area II Hydrogen Production, Part II - Hydrogen from Ammonia and Ammonia-Borane Complex for Fuel Cell Applications," Proceedings of the U.S. DOE Hydrogen Program Annual Review, Golden, CO, May 7 (2002), URL: http://erendev.nrel.gov/hydrogen/pdfs/ 32405b15.pdf.

4. A. T-Raissi, "Ammonia and Ammonia-Borane Complexes as Hydrogen Energy Storers for Fuel Cell Applications," at Session A2.8: Hydrides II, 14th WHEC, Montreal, Canada, June 10 (2002).

5. A. T-Raissi, "Technical Analysis of Hydrogen Production," Hydrogen Program Annual Review, Session B: Storage, Utilization, Analysis, Golden, CO, May 7 (2002).

Patent Applications

1. A. T-Raissi, N.Z. Muradov and E.D. Martin, "Method and Apparatus for Low Flux Photocatalytic Pollution Control," Serial No. 09/782,427, Feb. 12 (2001).

2. A. T-Raissi, N.Z. Muradov and E.D. Martin, "Apparatus and Method for Decoupled Thermo-Photocatalytic Pollution Control," U.S. Pat. No. 6,342,128 B1, Jan. 29 (2002).

3. A. T-Raissi, N.Z. Muradov and E.D. Martin, "Apparatus and Method for Decoupled Thermocatalytic Pollution Control," U.S. Pat. No. 6,334,936 B1, Jan. 1 (2002).

4. A. T-Raissi, N.Z. Muradov and E.D. Martin, "Method for High Flux Photocatalytic Pollution Control," U.S. Pat. No. 6,315,870 B1, Nov. 13 (2001).

5. A. T-Raissi, N.Z. Muradov and E.D. Martin, "Apparatus for Low Flux Photocatalytic Pollution Control," U.S. Pat. No. 6,309,611 B1, October 30 (2001).

V.A.2 Well-to-Wheels Analysis of Energy and Emission Impacts of Fuel Cell Vehicle Fuels

Michael Wang
Argonne National Laboratory
ESD362/B215
9700 S. Cass Avenue
Argonne, IL 60439
(630) 252-2819, fax: (630) 252-3443, e-mail: mqwang@anl.gov

DOE Technology Development Manager: Peter Devlin
(202) 586-4905, fax: (202) 586-9811, e-mail: Peter.Devlin@ee.doe.gov

Objectives

- Evaluate well-to-wheels (WTW) energy and emission impacts of various potential fuels for fuel-cell vehicles.
- Update and upgrade Argonne's GREET (Greenhouse gasses, Regulated Emissions, and Energy use in Transportation) model to analyze new fuels and new fuel production pathways for fuel-cell vehicle applications.
- Characterize production pathways of various fuel-cell fuels, such as gaseous hydrogen, liquid hydrogen, methanol, gasoline, ethanol, and Fischer-Tropsch (FT) naphtha.
- Analyze key issues in production and distribution of fuel-cell fuels and evaluate their impacts on WTW energy use and emissions.

Approach

- Revise Argonne's GREET model to accommodate fuel-cell fuels for WTW analyses.
- Estimate emissions of greenhouse gases (CO_2, CH_4, and N_2O) and criteria pollutants [VOCs, CO, NO_x, PM_{10} (particulate matter with diameter less than 10 microns), and SO_x] and energy use for all energy sources, fossil fuels (petroleum, natural gas, and coal), and petroleum.
- Specify production and distribution pathways for individual fuel-cell fuels.
- Obtain data on new technologies, energy efficiencies, and emissions associated with key WTW activities (e.g., fuel production and fuel-cell vehicle operations).
- Evaluate and process the data obtained for application to the GREET model.
- Conduct GREET simulations to generate WTW energy and emission results for various fuel-cell fuels.

Accomplishments

- Evaluated energy use and greenhouse gas (GHG) emissions impacts of central gaseous hydrogen (GH_2) from natural gas (NG), central liquid hydrogen (LH_2) from NG, station GH_2 from NG, station LH_2 from NG, solar photovoltaic (PV) GH_2, solar PV LH_2, station GH_2 via electrolysis, station LH_2 from electrolysis, gasoline, methanol, cellulosic ethanol, and naphtha from both crude and NG.
- Specified production and distribution pathways for each of the above fuels and fuel production pathways.
- Revised GREET 1.6. The version is posted at the GREET website for download and evaluations (http://greet.anl.gov).
- Reviewed completed studies on energy and emission impacts of fuel-cell vehicle fuels.

Future Directions

- Continue to revise key assumptions in GREET l.6 to reflect technology developments related to hydrogen production, distribution, and storage.
- Review completed studies on the topic of fuel-cell fuel energy and emission impacts and summarize differences and similarities among the reviewed studies.
- Add additional hydrogen production pathways as needed.
- Seek feedbacks from GREET users to further improve the functionality of the GREET model.
- Continue to evaluate WTW energy and emission impacts of fuel-cell fuels.

Introduction

Fuel-cell vehicles (FCVs) are being promoted for their energy efficiency gains and zero or near-zero emissions. Although experts agree that hydrogen is the ultimate fuel-cell fuel in the long term, it may not be available on a large scale for FCV applications in the foreseeable future, mainly because of hydrogen production and distribution infrastructure constraints. Intensive R&D efforts are being focused on hydrocarbon fuels, besides hydrogen, for FCV applications. Because production and distribution of various fuel-cell fuels are subject to different energy efficiencies and emissions, WTW analysis is necessary to obtain impartial evaluations of fuel-cell vehicle/fuel systems.

Approach

For a given vehicle technology/transportation fuel combination, the GREET model separately calculates the following items on the WTW basis:

1. Energy consumption for three energy categories (total energy, fossil fuels, and petroleum)
2. Emissions of three greenhouse gases (CO_2, CH_4, N_2O)
3. Emissions of five criteria pollutants (total and urban emissions, VOCs, CO, NO_x, PM_{10}, and SO_x)

Figure 1 shows the stages covered in GREET simulations. A WTW analysis includes the feedstock, fuel, and vehicle operation stages. The feedstock and fuel stages together are called well-to-pump stages, and the vehicle operation stage is called the pump-to-wheels stage. In GREET, WTW energy and emission results are presented separately for each of the three stages.

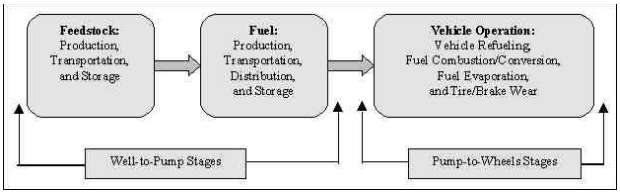

Figure 1. Stages Covered in GREET Well-to-Wheels Analysis

GREET includes a variety of vehicle propulsion technologies and transportation fuels, of which fuel-cell vehicle technologies and fuel-cell fuels are a sub-set. Table 1 lists the fuel-cell fuels included in the GREET model. GREET can simulate multiple options for a given pathway. For example, GREET 1.6 includes 48 options for GH_2 and LH_2 pathways.

Results and Conclusions

Argonne applied GREET 1.6 to estimate WTW energy and emission impacts of various fuel-cell fuels. We cannot include all the results here, but Figures 2-5 provide a snapshot of WTW total energy use, fossil energy use, petroleum use, and CO_2-equivalent GHG emission impacts of some key fuel-cell fuels. (For each figure, the bars represent average values while the lines superimposed on the bars represent uncertainty ranges.)

For total energy use (including both nonrenewable and renewable energy sources), use of electrolysis hydrogen, liquid hydrogen from NG, and cellulosic ethanol may increase total energy use, relative to baseline gasoline internal combustion engine vehicles (GVs) (Figure 2). However, when one considers fossil energy use (petroleum, natural gas, and coal), cellulosic ethanol, solar PV hydrogen, and station electrolysis hydrogen from renewable

Fuel-Cell Fuel	Production Pathways
GH_2 & LH_2	Central plant production from North American (NA) and Non-North American (NNA) NG Central plant production from NNA FG Refueling station production from NA and NNA NG Refueling station production from NNA FG Solar photovoltaic Electrolysis of water with conventional electricity
Methanol	Production from NA and NNA NG Production from NNA FG
Gasoline	Federal RFG California RFG
Diesel	Low-sulfur diesel
Ethanol	Production from corn Production from woody biomass Production from herbaceous biomass
CNG & LNG	Production from NA and NNA NG Production from NNA FG
LPG	Production from crude oil Production from NG
Naphtha	Production from NA and NNA NG via the FT process Production from NNA FG via the FT process Production from crude oil

Table 1. Fuel-Cell Fuels and Production Pathways

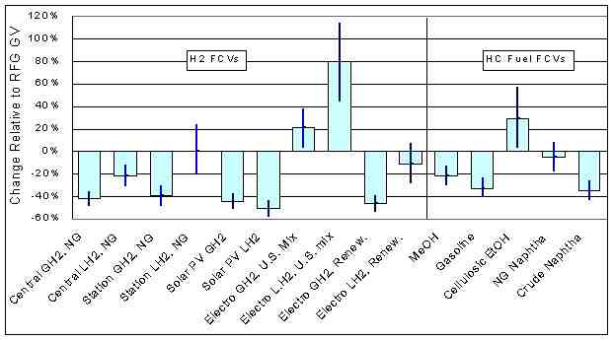

Figure 2. WTW Total Energy Use Changes by Fuel-Cell Vehicles (Relative to GVs)

electricity are superior to any other fuel-cell fuels (Figure 3). Furthermore, if one is concerned about petroleum use of motor vehicles, all non-petroleum-based fuel pathways almost eliminate petroleum use (Figure 4). The two petroleum pathways, gasoline and crude naphtha, result in significant reductions in

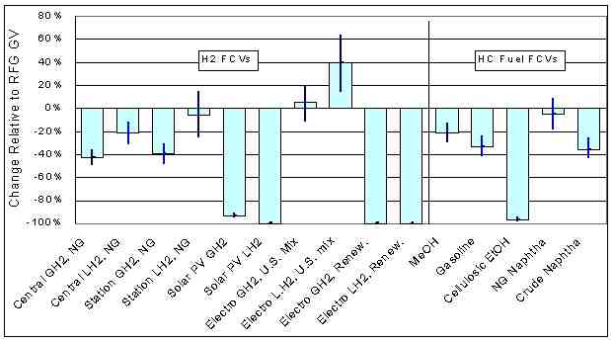

Figure 3. WTW Fossil Energy Use Changes by Fuel-Cell Vehicles (Relative to GVs)

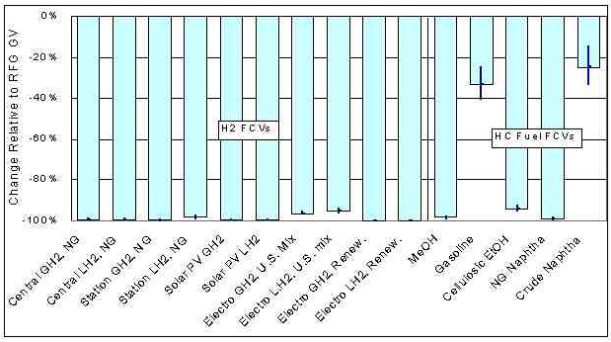

Figure 4. WTW Petroleum Use Changes by Fuel-Cell Vehicles (Relative to GVs)

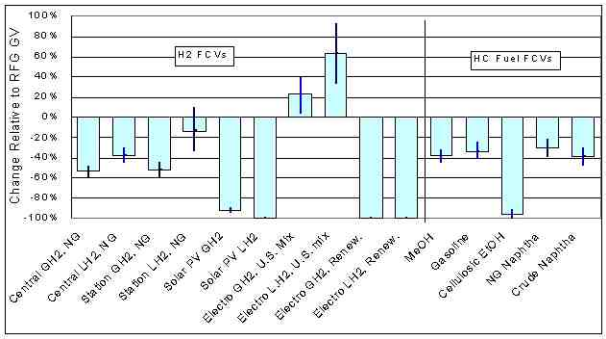

Figure 5. WTW Greenhouse Gas Emissions Changes by Fuel-Cell Vehicles (Relative to GVs)

petroleum use because of the high energy efficiency of FCVs.

Except for electrolysis hydrogen generated with the U.S. average electricity mix and station-produced liquid hydrogen from NG, all fuel-cell fuels provide GHG emission reduction benefits (Figure 5). Not surprisingly, renewable ethanol, solar PV hydrogen, and electrolysis hydrogen from renewable electricity achieve the largest GHG emission benefits.

Notes for Table 1 and Figures 2-5:

Central GH_2, NG	gaseous hydrogen produced in centralized plants with NA NG
Central LH_2, NG	liquid hydrogen produced in centralized plants with NA NG
Station GH_2, NG	gaseous hydrogen produced in refueling stations with NA NG
Station LH_2, NG	liquid hydrogen produced in refueling stations with NA NG
Solar PV GH_2	gaseous hydrogen produced in central locations from solar photovoltaic via electrolysis
Solar PV LH_2	liquid hydrogen produced in central locations from solar photovoltaic via electrolysis
Electro GH_2, U.S. Mix	gaseous hydrogen produced in refueling stations via electrolysis with U.S. average electricity
Electro $L.H_2$, U.S. Mix	liquid hydrogen produced in refueling stations via electrolysis with U.S. average electricity
Electro GH_2, Renew.	gaseous hydrogen produced in refueling stations via electrolysis with renewable electricity
Electro $L.H_2$, Renew.	liquid hydrogen produced in refueling stations via electrolysis with renewable electricity
MeOH	methanol produced from NA NG
NG naphtha	naphtha produced from NNA NG via the FT process
Crude naphtha	naphtha produced from crude oil in petroleum refineries
HC	hydrocarbon
RFG	reformulated gasoline
NA	North American
NNA	non-North American
FG	flared gas
CNG	compressed natural gas
LNG	liquefied natural gas
LPG	liquefied petroleum gas (propane)
EtOH	ethanol

WTW results depend heavily on the assumptions regarding fuel production efficiencies and fuel-cell vehicle fuel economy. The GREET model can readily test alternative assumptions and provide WTW energy and emission results.

Reference

1. Wang, M., 2001, *Development and Use of GREET 1.6 Fuel-Cycle Model for Transportation Fuels and Vehicle Technologies,* ANL/ESD/TM-163, Center for Transportation Research, Argonne National Laboratory, Argonne, Ill., June.

V.A.3 Hydrogen and Fuel Cell Vehicle Evaluation

Richard Parish (Primary Contact), Leslie Eudy, and Ken Proc
National Renewable Energy Laboratory
1617 Cole Blvd.
Golden, CO 80401
(303) 275-4453, fax: (303) 275-4415, e-mail: richard_parish@nrel.gov

DOE Technology Development Manager: John Garbak
(202) 586-1723, fax: (202) 586-9811, e-mail: John.Garbak@ee.doe.gov

Objectives

- Gather performance information on hydrogen fuel cell vehicles to establish their operating characteristics and applicability to fleet service and the general transportation marketplace.
- Gather and evaluate information on establishing a hydrogen fueling and maintenance infrastructure.

Approach

- Continue working with SunLine Transit Agency and Alameda-Contra Costa Transit District (AC Transit) to define the hydrogen fuel cell bus evaluation process and required fueling infrastructure at the AC Transit site.
- Evaluate the performance and operational characteristics of a hydrogen fuel cell bus in revenue service at SunLine Transit Agency.
- Establish an effective relationship with the California Fuel Cell Partnership (CaFCP) and define the value added tasks that the National Renewable Energy Laboratory (NREL) can provide to their fuel cell vehicle testing and evaluation program.

Accomplishments

- Contract with AC Transit and ISE Research-Thunderbolt to provide fuel cell buses for AC Transit in Oakland, California was approved, with delivery of the first bus scheduled for June 2004.
- NREL, AC Transit, and University of California-Davis have completed a preliminary vehicle evaluation plan for the AC Transit fuel cell bus demonstration.
- Identified products that NREL could provide as a partner in the California Fuel Cell Partnership (CaFCP), e.g., status reports on partnership activities and fueling technologies, and a web-based “suggestion box”.

Future Directions

- Continue evaluation of ISE/UTC Fuel Cells fuel cell bus operation at SunLine Transit Agency.
- Define AC Transit hydrogen fueling infrastructure.
- Develop hydrogen reference guide documents: (1) Hydrogen Fuel Systems for Vehicles, and (2) Hydrogen Fueling Systems.
- In cooperation with CaFCP, characterize existing hydrogen fueling stations and define critical elements for designing and implementing new stations.

Introduction

Government- and industry-sponsored research regarding hydrogen as a transportation fuel—particularly in mobile fuel cells—is growing rapidly. One of the first fuel cell applications in the transportation arena will be powering transit buses. This is due to their capacity for handling the extra volume currently required for the fuel cell and the associated hydrogen fuel storage tanks. The NREL Fleet Test & Evaluation (FT&E) team in Golden, Colorado, is dedicated to evaluating and documenting the performance and operational characteristics of advanced vehicle technologies that use alternative fuels or other concepts that reduce dependency on conventional petroleum fuels. The NREL FT&E team is investigating the status of fuel cell technology and hydrogen as key elements in a future transportation scenario. Specifically, FT&E is developing plans for evaluating prototype fuel cell buses; near-production light-, medium-, and heavy-duty fuel cell vehicles; and the hydrogen fueling and maintenance infrastructure required to make the vehicles fully operational.

Approach

The California Fuel Cell Partnership (CaFCP) is a focal point for fuel cell development and demonstration activity, and one of its tasks will be to evaluate fuel cells used in transit bus applications. The CaFCP is also evaluating fuel cells in light-duty vehicles and looking at a variety of feedstock fuels for the hydrogen required for the fuel cells. Based on past experience of developing and evaluating alternative fuel and hybrid electric vehicles, NREL has taken the initiative to establish a relationship with the CaFCP to determine how it could assist the partnership with its fuel cell vehicle and hydrogen infrastructure development and evaluation. To gain experience and knowledge with fuel cell performance and operation characteristics, SunLine Transit Agency and the Alameda-Contra Costa Transit District (AC Transit), both associate members of the CaFCP, will acquire fuel cell buses for evaluation in normal operation. NREL will assist these agencies in acquiring data to evaluate the bus performance and prepare the transit agency for its fully commercial fuel cell buses. The XCELLSIS

Figure 1. The XCELLSIS Bus being Fueled at SunLine Transit Agency in 2001

fuel cell bus shown in Figure 1 was demonstrated at SunLine Transit Agency in 2001.

Results

In April 2002, AC Transit announced the purchase of four fuel cell buses using compressed hydrogen. The 40-foot buses will be built on a Van Hool (from Belgium) bus platform in a hybrid electric configuration using fuel cells from UTC Fuel Cells, and will be integrated by ISE Research. The buses will not be delivered until mid-2004. In the interim, a prototype fuel cell bus from ISE Research will be operated by SunLine to evaluate the bus performance and prepare the transit agency for its fully commercial fuel cell buses. Evaluation of the ISE prototype fuel cell bus performance is expected to occur during FY 2003. The design and construction of a hydrogen fueling station and necessary maintenance facility modifications is on hold until a contract can be placed. The FT&E team produced a preliminary vehicle evaluation plan. NREL will conduct the evaluation with AC Transit and University of California, Davis (UC Davis). Finalization of the evaluation plan will occur as the delivery date of the fuel cell buses approaches.

NREL met with the CaFCP Light-Duty Vehicle (Vehicle Operation or VeOps) and Fuels Teams to define activities in which NREL/DOE could become involved to increase the amount of information available. NREL has developed a web-based "suggestion box" for the VeOps Team to identify problems, issues, and development needs they might be reluctant to identify in a meeting with other manufacturers or fuel providers. NREL is also developing a web-based fleet information database to gather information on California fleets to identify

good candidates for evaluation and testing of light-duty fuel cell vehicles. For the Fuels Team, NREL will develop fact sheets on existing hydrogen fueling stations that could be used by partnership auto manufacturers, and on the process of hydrogen fueling station siting and implementation. The existing hydrogen fueling station at the California Fuel Cell Partnership's facility in Sacramento, California is shown in Figure 2.

Figure 2. A Fueling Demonstration of the Nissan Xterra Fuel Cell Vehicle at the California Fuel Cell Partnership's Hydrogen Fueling Station

Conclusions

- NREL's FT&E Team is working to develop a strong role in the CaFCP, providing creative options for gathering and disseminating information about hydrogen fuel cell vehicles and associated hydrogen infrastructure, without revealing prototypic and proprietary information about the vehicle technology.
- In collaboration with the CaFCP, once the fuel cell buses are delivered and the hydrogen fueling and vehicle maintenance facilities are completed, NREL will begin collecting and evaluating data that will help to demonstrate that fuel cell buses can be fueled and maintained efficiently and perform consistently.

FY 2002 Publications/Presentations

1. Levin, J., Miller, M., and Eudy, L. "Fuel Cells for the Transportation Industry: Developing a Credible Demonstration Program on the Path to Commercialization," Presented to the *14th World Hydrogen Energy Conference held June 9-13, 2002 in Montreal, Quebec, Canada*.

V.A.4 Power Parks System Simulation

Andrew Lutz (Primary Contact)
Sandia National Laboratories
MS 9053
Livermore, CA 94551-0969
(925) 294-2761, fax: (925) 294-1004, e-mail: aelutz@sandia.gov

DOE Technology Development Manager: Sigmund Gronich
(202) 586-1623, fax: (202) 586-5860, e-mail: Sigmund.Gronich@ee.doe.gov

Objectives

- Develop a system model to simulate distributed power generation in power parks.
- Demonstrate the potential of hydrogen technologies for power generation.
- Analyze the dynamic performance of the system to examine the thermal efficiency, power availability, and cost.

Approach

- Develop a library of Simulink modules for the various components being proposed for power parks.
- Assemble the components into a sample power park to demonstrate the model's ability to analyze thermal efficiency and supply an electric load.

Accomplishments

- The library of components includes a fuel cell stack, a steam-methane reformer, a multi-stage compressor, and hydrogen storage in a high-pressure vessel.
- In the initial power park, a reformer operates at a steady rate to produce hydrogen, which feeds a fuel cell to provide an electric load. When excess hydrogen is available, it is compressed and stored.
- The model evaluates the combined efficiency of the power system.

Future Directions

- Continue to develop additional modules in the Simulink library, including a photovoltaic array, an electrolyzer, a battery, a wind turbine, and an autothermal reformer.
- Implement a control strategy to direct the power within the park to meet the internal load while optimizing the energy efficiency and cost.
- Develop a layer of analysis to compute the cost of the power and hydrogen generated, including the initial capital costs of the components and the continuous operation costs during the life of the simulation.
- Compare the simulations of dynamic performance with data collected from demonstration sites.

Introduction

Power parks are distributed energy sites where power generation is co-located with businesses or industrial energy consumers. Proposed power parks use combinations of technologies. A local power source is often combined with a storage technology to adapt the dynamic nature of the source to the load. In some cases, the system operates completely separate from the utility grid. Alternatively, the power park may use the utility grid as a storage device, selling power to the utility when there is

excess and drawing power when the local source cannot meet the load.

Often, power parks are sited in order to take advantage of a renewable energy source. Generation by photovoltaic collectors or wind turbines can be combined with energy storage technologies. Power parks provide an excellent opportunity for using hydrogen technologies. Electricity from the renewable source can be used to generate hydrogen by electrolysis, which is stored for use in fuel cells or to refuel vehicles. Similarly, heat from a renewable source can be used to reform hydrocarbon fuels into hydrogen.

The variety of technologies and their combinations that are being proposed for power parks suggests that each system will be novel, at least in some aspect of its design. Consequently, a simulation tool will be very useful in evaluating the various systems and optimizing their performance with respect to efficiency and cost.

Approach

The deliverable of this project will be a tool for simulation of the local power generation system, constructed in the language of the Simulink software [1]. Simulink provides a graphical workspace for block diagram construction. The workspace provides the flexibility to quickly assemble components into a system. Simulink performs dynamic simulation by integrating the system in time using a collection of ordinary differential equation solvers. After the simulation is completed, the solution can be examined by plotting variables at various states in the system. Simulink also contains modules for dynamic control and solution of iterative loops within the system.

The system design begins with development of a library of Simulink modules that represent components in the power system. The component models are based on fundamental physics to the extent practical. These models are generic in that they are not customized to represent a specific brand or manufacturer's features for the component. However, the generic components from the library can be tied to a specific unit by relying on performance data. The library components can be quickly modified to represent new or specialized components, thereby expanding the library's collection.

Many of the basic modules that represent hydrogen and other gas mixtures use the Chemkin [2] software package to provide thermodynamic properties of the species and mixtures. For example, the mixer component accepts two gas streams and adiabatically mixes them to yield an output stream. The temperature of the new stream depends on the temperatures, compositions, and relative flow rates of the two inlet streams. Solution for the outlet temperature uses Newton iteration over Chemkin calls, which returns the updated enthalpy of the mixture. Another example is the Equil module, which computes the equilibrium composition at a given temperature and pressure. This module is coupled to a Chemkin-implementation of the Stanjan [3] equilibrium solver. The Equil module is used to represent chemical reactions in either a reformer or a combustor component. These modules are combined in a sub-system to form a module for the steam-methane reformer.

Results

We have developed a library of Simulink modules for some of the various components being proposed for power parks. Existing components include a fuel cell stack, a steam-methane reformer, a multi-stage compressor, a high-pressure storage vessel, and an internal electric load. The load versus time is read from a file, so it can be changed quickly.

The reformer takes an input flow rate of methane and computes the hydrogen output. The reformer module balances energy by combusting the reformate stream with air and exchanging the heat released to the catalyst reactor. Parameters on the reformer are the steam-to-carbon ratio and the outlet temperature of the exhaust products from the internal burner. The temperature at which the equilibrium reforming occurs depends on these parameters. Figure 1 shows the variation in thermal efficiency of the reformer with temperature and steam-to-carbon ratio. The minimum steam-to-carbon ratio is 2; however, reformers are often operated with excess steam to improve the efficiency and prevent coking problems.

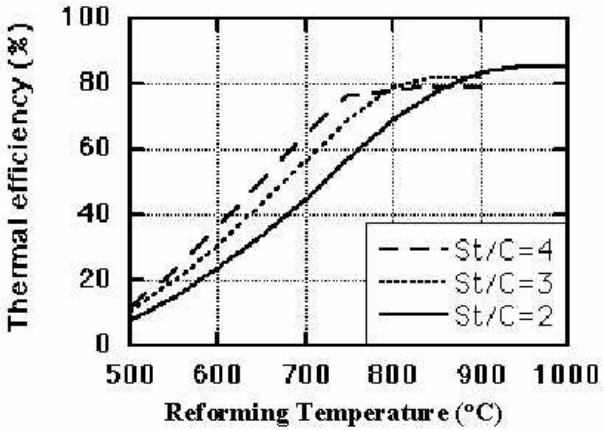

Figure 1. Thermal Efficiency of the Steam-Methane Reformer Module Versus the Temperature and Steam-to-Carbon Ratio, Computed at Chemical Equilibrium

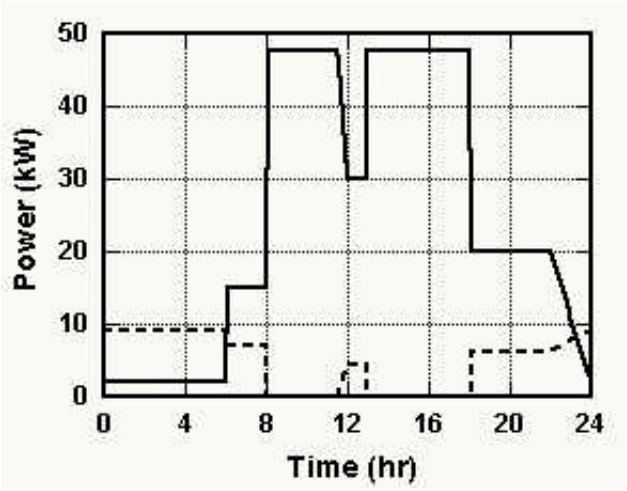

Figure 2. Power Output of the Fuel Cell (solid line) and Power Consumed by the Compressor (dashed line) for a Sample Simulation over a Daily Cycle

More detailed analysis of the reformer sub-system is presented in reference [4].

The fuel cell module takes a hydrogen inlet flow rate and a requested power, then determines if sufficient power can be supplied. The stack model uses a simple map of efficiency versus power. This data is read from an input file to allow the fuel cell to be calibrated to real performance data. If sufficient

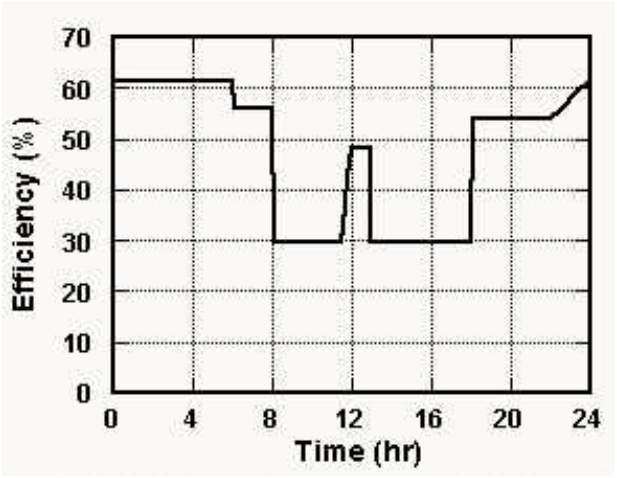

Figure 3. Thermal Efficiency of the Power System for a Sample Simulation over a Daily Cycle

power can be provided, the excess hydrogen flow is returned for compression and storage. A compressor module represents an ideal two-stage compressor that assumes isentropic compression in each stage. The power required by the compressor is included in the analysis of the overall thermal efficiency of the system.

The simulation in this example runs over a daily load cycle. The power output by the fuel cell, which in this case matches the demand, is shown by the solid line in Figure 2. The power consumed by the hydrogen compressor is shown by the dotted line in Figure 2. During the night, when the load is low, the compressor load is large because most of the hydrogen produced by the reformer is being compressed for storage. During the peak daytime loads, the compressor is not operating because there is no excess hydrogen.

The model evaluates the overall thermal efficiency of the power system, as shown in Figure 3. The system efficiency is the hydrogen stored and electric power supplied to the load, divided by the methane input to the reformer and the power consumed by the compressor. The system efficiency is highest when the reformer is producing hydrogen to be stored during the low-load periods. In contrast, the system efficiency drops when the combined reformer and fuel cell are working at capacity to supply the peak load.

Conclusions and Future Directions

The demonstration of the sample power park shows the usefulness of system simulations in evaluating the overall performance. The flexibility provided by the block diagram structure will allow for rapid construction of various system configurations.

Future efforts will continue to develop modules for the Simulink library, adding modules for electricity generation by a photovoltaic array, temporary electricity storage in batteries, and hydrogen generation by an electrolyzer and an autothermal reformer. The final stages of the work will implement a control strategy to direct the power within the park to balance meeting internal load with supplying external power to the grid. We will also include a layer of analysis to compute the cost of the power and hydrogen generated. The cost analysis will accept input of the initial capital costs of the components, as well as the continuous operation costs during the life of the simulation, and add the costs using time-value adjustments. We expect the simulation tool will provide valuable assistance in the planning and design of hydrogen technologies in distributed power systems. In addition, the simulations of dynamic performance can be compared with data collected from demonstration sites.

References

1. Simulink. The MathWorks, Inc, MA (www.mathworks.com) 2002.

2. The CHEMKIN program and subroutine library are part of the Chemkin Collection. R. J. Kee, F. M. Rupley, J. A. Miller, M. E. Coltrin, J. F. Grcar, E Meeks, H. K. Moffat, A. E. Lutz, G. Dixon-Lewis, M. D. Smooke, J. Warnatz, G. H. Evans, R. S. Larson, R. E. Mitchell, L. R. Petzold, W. C. Reynolds, Caracotsios, M., Stewart, W. E. and Glarborg, P., Chemkin Collection, Release 3.5, Reaction Design, Inc., San Diego, CA (1999).

3. "Stanjan: Interactive Computer Programs for Chemkin Equilibrium Analysis", W C Reynolds, Stanford University report, January (1981).

4. Lutz, A. E., Bradshaw, R. W., Keller, J. O., and Witmer, D. E., "Thermodynamic Analysis of Hydrogen Production by Steam Reforming," accepted for publication in the *International Journal of Hydrogen Energy*, 2002.

FY 2002 Publications/Presentations

1. Lutz, A. E., Bradshaw, R. W., Keller, J. O., and Witmer, D. E., "Thermodynamic Analysis of Hydrogen Production by Steam Reforming," *Int. J. of Hydrogen Engy*, accepted for publication, 2002.

2. Lutz, A. E., Larson, R. S., and Keller, J. O., "Thermodynamic Comparison of Fuel Cells to the Carnot Cycle," *Int. J. of Hydrogen Engy*, 27 (10), (2002) pp. 1103-1111.

V.A.5 Process Analysis Work for the DOE Hydrogen Program - 2001

Pamela L. Spath, Wade A. Amos, and Margaret K. Mann (Primary Contact)
National Renewable Energy Laboratory
1617 Cole Blvd.
Golden, CO 80401
(303) 275-2921, fax: (303) 275-2905, e-mail: margaret_mann@nrel.gov

DOE Technology Development Manager: Matthew Kauffman
(202) 586-5824, fax: (202) 586-5860, e-mail: Matthew.Kauffman@ee.doe.gov

Objectives

- Add to the suite of technoeconomic analyses (TEAs) performed on hydrogen research projects.
- Update previous analyses using recent experimental results.
- Determine delivered hydrogen costs by incorporating storage and transportation costs into previous analyses.
- Provide information to DOE and task researchers, to guide ongoing and proposed research projects.

Approach

- Identify the hydrogen production, storage, and utilization projects and processes to be analyzed.
- Using available data (technical literature, laboratory data, pilot-scale data, etc.), generate process flow sheets, material and energy balances, and equipment capital costs using ASPEN Plus process simulation computer software.
- Determine hydrogen selling price and conduct sensitivity analyses to determine the largest cost drivers and areas for continued cost reduction.
- Use the results of these analyses to guide ongoing and proposed research projects.

Accomplishments

- Completed analyses and produced reports in the following areas:
  - Technoeconomic Analysis of the Thermocatalytic Decomposition of Natural Gas, May 2001.
  - Assessment of the Mass Production of Nanotubes, August 2001.
  - Economic Analysis of the Biological Water Gas Shift Process for the Production of Hydrogen from Synthesis Gas, October 2001.
  - Assessment of Hydrogen from Small-Scale Reformers-Available Technologies and Costs, October 2001.
  - Assessment of Natural Gas Splitting with a Concentrating Solar Reactor for Hydrogen Production, April 2002.
- Drafted analysis plan at DOE workshop held in March 2002.

Future Directions

- Evaluate water requirements for large-scale hydrogen use.
- Complete a Monte Carlo sensitivity analysis of hydrogen storage and transportation costs.
- Evaluate the market potential of coproducts from biomass pyrolysis oil reforming.

- Integrate various renewable forms of hydrogen production to supply future transportation needs into TEA models.
- Continue to coordinate analysis work for the DOE Hydrogen, Fuel Cells, and Infrastructure Technologies Program.

Introduction

The goal of the process analysis work conducted at the National Renewable Energy Laboratory (NREL) for the DOE's Hydrogen, Fuel Cells, and Infrastructure Technologies Program is to provide direction, focus, and support to the development of renewable hydrogen through evaluation of technical, economic, and environmental aspects of hydrogen production and storage technologies. The primary purpose of this work is to identify those areas of research in which improvements will result in the largest reductions in system costs. This helps to define research goals and moves novel technologies more quickly to commercialization. Additionally, this project provides information to DOE on the long-term technical and economic feasibility of ongoing and proposed research projects.

This year, areas of analysis included (1) hydrogen production via natural gas splitting with a solar reactor, (2) biological water gas shift for hydrogen production from synthesis gas, and (3) assessment of the mass production of carbon nanotubes for hydrogen storage.

Approach

Technoeconomic analyses are performed to determine the potential economic viability of a research process. The selection of projects to be analyzed is made in conjuction with DOE program management. Detailed TEAs begin with discussions between researchers and analysts, to obtain experimental data and a common understanding of project goals. Experimental results are used to develop material and energy balances in ASPEN Plus, a chemical engineering process simulator that contains extensive thermodynamic data. The material and energy balance results are used to determine the size, and subsequently, the capital cost, of major pieces of process equipment. Along with operating costs, these are used in a cash flow spreadsheet to determine the necessary hydrogen selling price to obtain a 15% after-tax internal rate of return. Storage and transportation costs are integrated with process costs to obtain a delivered hydrogen selling price. Monte Carlo sensitivity analyses are used to determine the largest cost drivers and areas for continued cost reduction. These results are used to make focused recommendations to the researchers and to DOE.

Results

Hydrogen Production via Natural Gas Splitting with a Solar Reactor

This study analyzed hydrogen production via thermal decomposition of methane using a solar reactor for two different applications: (1) a fueling station and (2) power production. The analysis shows that for either application, the production of carbon black plays a key role in the economics of the process. In addition, the net greenhouse gas emissions and overall fossil energy consumption are lower for the solar processes than for the conventional fossil system.

In the stand-alone fueling station application, there are many times when the storage capacity is reached and the hydrogen production system must be shut down. For this reason, only 54%-66% of the total possible hydrogen production can actually be realized. Increasing the size of the hydrogen storage results in a small increase in useable hydrogen, which does not outweigh the large cost associated with storing the hydrogen. Supplying hydrogen directly to a pipeline network was examined as one option to overcome these physical and economic limitations. The reduction in the hydrogen selling price is 68% from the stand-alone base case ($18/giga-Joule [GJ] compared to $57/GJ). Another option that was examined to improve the productivity of the solar process was adding a small electric heater that can be turned on when the hydrogen supply gets

low to provide heat to the solar reactor. The hydrogen selling price with the supplemental heater is considerably less than the stand-alone base case at $42-$46/GJ, compared to $57/GJ.

For the power production scenario, the hydrogen is co-fired in a turbine at a natural gas combined-cycle (NGCC) plant. Two options were examined: (1) selling the carbon black and (2) burning the carbon to produce more power. Because of its value, it is more profitable to sell the carbon instead of burning it. In order for the electricity produced from the hydrogen to be less than the base electricity production cost of the NGCC plant, the price of the carbon must be greater than $0.80/kilogram (kg). However, even if the power produced from hydrogen is more that the base power production price, overall it would not significantly increase the price of power from the NGCC power plant. This is because the fraction of electricity generated from the solar process is small compared to the total (0.2%-1.1% of the total output of a 500-MW NGCC plant).

Biological Water-Gas Shift for Hydrogen Production

The biological water-gas shift (WGS) reaction uses photosynthetic bacteria to convert CO into CO_2 and H_2. After successful proof-of-concept tests showed that high CO to H_2 rates were possible, researchers focused on collecting reliable kinetic data for the biological WGS process. Based on this laboratory kinetic data, a preliminary process design was proposed for shifting the CO from a biomass gasification process into hydrogen. The capital and operating costs were estimated for such a system and showed that the WGS reactor was a significant cost, nearly $3 million for a small facility (2.5 million standard cubic feet per day [scf/d]) and over $10 million for a larger facility (10.0 million scf/d). The projected costs were cut nearly in half by redesigning the system. Two important conclusions came out of the economic analysis:

- Pressurizing the system reduces the size of the WGS reactor, thereby reducing the capital cost of the system.
- An increase in shift rate by a factor of 2 decreases the reactor size enough that the reactor then becomes a relatively small cost compared to the balance of plant costs. Increasing the shift rate beyond this point has diminishing returns.

These two results have shifted the course of the laboratory research. Rather than concentrating on getting large improvements in the shift rate, the researchers have designed a high-pressure reactor for testing the biological WGS reaction at pressures up to 400 pounds per square inch gauge (2,900 kilopascal).

Assessment of the Mass Production of Carbon Nanotubes

Neoterics International was contracted by NREL to assess the mass production of carbon nanotubes for hydrogen storage applications. The technology base for this analysis is the single-wall nanotubes extrusion concept being developed at NREL, in which carbon nanotubes are produced using methane decomposition chemistry. The design basis is a grassroots facility producing 75,000 metric tons per year of active material. Hydrogen is also produced as a coproduct from this manufacturing facility.

Four scenarios were evaluated. The high and low conversion cases assumed a per-pass conversion of 44.48% (corresponds to thermodynamic equilibrium at the reactor outlet) and 30% (accounts for the possibility that mass transfer or other mechanisms could limit the reaction), respectively. Lab experiments to date have only been able to demonstrate 7% per pass conversion, but these experiments were designed to demonstrate catalyst activity rather than high per pass conversion. The high and low levels assumed for selectivity were 100% and 80%, respectively, reflecting the fact that very high selectivity has already been demonstrated in the lab.

Fixed capital ranged from $164.1 million to $208.2 million for the four cases considered. This translates into $2.2 to $2.8 per annual kg of capacity. Natural gas is the dominant component of the cash operating costs. The hydrogen coproduct is a significant source of revenue, contributing approximately one-third of the revenue for all cases considered. The selling price for the carbon nanotubes varied from $0.8 to $1.1 per kg.

Conclusions

Hydrogen Production via Natural Gas Splitting with a Solar Reactor

- Hydrogen storage is costly. If the hydrogen can be consumed directly or used in another application where storage is eliminated and compression is moderate, then the hydrogen selling price decreases significantly.
- The price of carbon black has the greatest effect on the economics of hydrogen production from a solar reactor, regardless of application. Thus, higher value carbon markets should be pursued as a way to improve the process economics.
- There is a significant environmental benefit from carbon black production via the solar route compared to the conventional route.

Biological Water-Gas Shift for Hydrogen Production

- The WGS system must be operated under pressure to be economical. If the process cannot be operated at high pressures, an incremental improvement in shift rate alone will not significantly reduce hydrogen production costs.

Assessment of the Mass Production of Carbon Nanotubes

- The concept of using carbon nanotubes for hydrogen storage is still at relatively early stage of development. Further fundamental studies on the mechanism of hydrogen adsorption are needed to assess whether carbon nanotubes are capable of meeting DOE's technical storage goals (greater than 5.5 weight % and 50 kg/m^3).
- The current analysis shows that the hydrogen coproduct is a significant source of revenue in the large-scale nanotube production process.

V.B Integrated Hydrogen and Fuel Cell Demonstration

V.B.1 Real-World Demonstration of Fuel Cell Vehicles and Refueling Technology

Joseph J. Irvin
California Fuel Cell Partnership
3300 Industrial Boulevard, Suite 1000
West Sacramento, CA 95691
(916) 371-2870, fax: (916) 375-2008, e-mail: jirvin@cafcp.org

DOE Technology Development Manager: Christopher Bordeaux
(202) 586-3070, fax: (202) 586-5860, e-mail: Christopher.Bordeaux@ee.doe.gov

Objectives

- Demonstrate fuel cell technology by operating and testing vehicles on California's roads.
- Demonstrate alternative fuel infrastructure technology.
- Explore the path to commercialization for fuel cell-powered vehicles.
- Increase public awareness through a coordinated outreach plan.

Approach

- Adopt a California Fuel Cell Partnership (CaFCP) organizational structure consisting of an Executive Committee, Working Group and Communications Team to provide and implement a decision-making structure for developing a workplan, budget, headquarters facility, and outreach strategy under the following timetable:
  - Phase I — through 1999, project development and planning, adding new partners, and preparing vehicle and refueling facilities;
  - Phase II — 2000-2001, demonstrate cars and buses using hydrogen fuel;
  - Phase III — 2002-2003, demonstrate more cars and buses using hydrogen, methanol, gasoline or other fuels as determined by the Partnership.

Accomplishments

- Established and opened the West Sacramento headquarters facility as an operations base for on-road vehicle usage and fueling.
- Established a "safety first" policy and culture at the facility.
- Dedicated 16 vehicles to the project by the end of the year – together these vehicles accumulated over 34,000 miles, conducted 754 refueling events, and totaled 1,880 persons who rode or drove in the vehicles.
- Conducted 25 public outreach events to increase awareness among media, stakeholder groups, educators, and the general public – together, these events directly reached more than 176,000 people.
- Accommodated more than 80 headquarters tours, tallying more than 1,500 headquarters visitors.
- Staged a Technology Forum at the headquarters facility, bringing fuel cell industry suppliers and consultants together with CaFCP members for business-to-business discussions – the 2001 event featured more than 30 exhibitors and 300 attendees.

- Released a "Fuel Scenarios Study" examining four potential fuel sources for fuel cells and the challenges to their commercialization.
- Established strong ties with the environmental and legislative communities through the Environmental Team and stakeholder outreach activities.
- Tested one fuel cell bus, the Ballard/XCELLSiS ZEbus, in the Palm Springs area.
- Participated as a team entry in the third annual Michelin Bibendum Challenge, and drove from Los Angeles to Las Vegas in relay fashion.
- Hosted the Electric Vehicle Association of the Americas' "Electric Transportation Industry Conference" for a daylong tour and Ride 'n' Drive event at CaFCP's demonstration center.

Future Directions

- Operate twenty (20) CaFCP vehicles, together accumulating 60,000 miles in calendar year 2002.
- Install a methanol fueling station at the West Sacramento headquarters.
- Install a satellite hydrogen fuel station in Richmond, California, as well as two additional hydrogen stations at appropriate locations.
- Commence a second joint study that examines hydrogen vehicle facility construction and use issues.
- Educate two regional emergency response agencies about how to address potential health and safety issues in the event of vehicle/fuel station accidents.
- Determine and announce the membership's plans for beyond 2003 [current CaFCP plans have been announced through 2003].
- Through multiple public outreach events, familiarize 250,000 people with fuel cell technology.
- Distribute 1,000 Teacher Learning Kits to middle and high school science teachers.

Introduction

California is the home to the California Fuel Cell Partnership (CaFCP), a unique collaboration between auto manufacturers, energy companies, fuel cell technology companies, and government agencies. This partnership is advancing a new vehicle technology that could move the world toward practical and affordable environmental solutions. For the first time ever, automobile companies and fuel suppliers have joined together to demonstrate fuel cell vehicles under real day-to-day driving conditions.

The California Fuel Cell Partnership expects to place up to 60 fuel cell passenger cars and fuel cell buses on the road by 2003. In addition to testing the fuel cell vehicles, the partnership is examining fuel infrastructure issues and beginning to prepare the California market for this new technology.

The members include companies and organizations from around the world: DaimlerChrysler, Ford, General Motors, Honda, Hyundai, Nissan, Toyota, and Volkswagen; Ballard Power Systems, UTC Fuel Cells; BP, ExxonMobil, Shell Hydrogen, and ChevronTexaco; and the California Air Resources Board, the California Energy Commission, the United States Department of Energy, the United States Department of Transportation and the South Coast Air Quality Management District.

Additionally, there are nine Associate Partners who assist with specific areas of expertise to help meet the CaFCP's goals: hydrogen gas suppliers (Air Products and Chemicals, Inc. and Praxair); hydrogen fueling stations (Pacific Gas & Electric, Proton Energy Systems, Inc., and Stuart Energy Systems); a methanol fuel supplier (Methanex); and bus transit agencies (AC Transit and Santa Clara Valley Transportation Authority which operate in the

Greater San Francisco Bay area, and SunLine Transit Agency in the Palm Springs area).

Approach

The CaFCP is testing and demonstrating fuel cell electric vehicles in California through 2003 under day-to-day driving conditions; demonstrating alternative fuel infrastructure technology; exploring the path to commercializing fuel cell electric vehicles by examining such issues as fuel infrastructure requirements, vehicle and fuel safety, market incentives, and consumer acceptance; and working to increase public awareness of fuel cell vehicle technology and the benefits it can offer.

Results

For the California Fuel Cell Partnership, the past year could be summarized as a year of "taking it to the streets" -- that is, driving fuel cell-powered electric vehicles on California's roadways in real-world conditions. Together, members worked hard in many ways to raise public awareness; gain experience with fuel cell technology, vehicles and fuels; and evaluate the commercialization of fuel cell vehicle technology for the 21st Century.

A functional headquarters facility in West Sacramento, California serves as an operations base for demonstrating and housing vehicles and their fuel supplies. Automotive partners are test-driving full scale fuel cell-powered vehicles on California roadways in real-world conditions -- in traffic, up and down hills, and in wide-ranging weather conditions. A few years ago, there wasn't a single running fuel cell vehicle on the road; today, there are eighteen operating in the Partnership.

Energy providers are working through the challenges of developing fuel infrastructure for fuel cell vehicles. They are providing the fuel needed for the partnership's demonstration program. During this early stage, all of the vehicles have been powered by hydrogen stored and dispensed onsite at the facility. CaFCP will also test liquid fuels rich in hydrogen – methanol and a cleaner form of gasoline – in order to learn more and determine what will best serve a successful commercial launch. (A methanol fueling station was installed in April 2002.)

Photo 1. FCVs and Staff Next to the Hydrogen Fueling Station at the CaFCP Headquarters Facility in West Sacramento, California

Photo 2. The Methanol Fueling Station – West Sacramento, California

Fuel cell makers have achieved remarkable success developing smaller, better and more powerful fuel cell systems. Their progress has stimulated an entirely new fuel cell supply industry – and prompted the Partnership's formation of a Technology Forum to provide an opportunity for non-member companies to meet the partners in a business-to-business environment.

Because success will require the active cooperation and assistance of the public sector, CaFCP's state and federal government partners are helping to build awareness and support among key stakeholders and the public, as well as identify

Photo 3. CaFCP Participated in the Michelin Bibendum Challenge

Photo 4. CaFCP Takes Vehicles and Displays into Local Communities to Increase Awareness

possible roles for government participation in the promotion of fuel cell technology.

One of the remaining challenges to commercialization is fuel choice. On one hand, fuel cells are ideal because they can be operated on a number of fuels; on the other, there are serious

Photo 5. A Hands-on Fueling Demonstration Exhibit Was Created to Familiarize People with Hydrogen Fueling and Fuel Choice Issues

factors to be considered with each fuel – infrastructure cost, environmental tradeoffs, technological readiness, and, perhaps most importantly, consumer comfort and acceptance.

To help address these issues, the CaFCP commissioned a consultant-prepared study to examine how to bring fuel cell vehicles to actual showrooms as quickly as possible, taking into account the challenges and potential solutions in using several fuel options, including hydrogen, methanol, gasoline, and ethanol. The "Fuel Scenarios Study" can be found on the partnership's website at

http://fuelcellpartnership.org/event_roundtable.html.

The members have also formalized safety standards for headquarters vehicle and fueling operations, including the safe management of thousands of visitors.

Dozens of public outreach events featuring vehicle, fuel, and fuel cell displays were conducted to increase awareness. Highlights included participation in the Michelin Bibendum Challenge by six of the CaFCP's automotive companies and the Ballard ZEbus. This alternative fuel vehicle event included a road rally drive from Los Angeles to Las Vegas. The Partnership also developed a unique, portable exhibit that simulates refueling with hydrogen and presents fuel choice issues in DVD format.

The ZEbus was the first Partnership fuel cell-powered bus to be demonstrated in real-world conditions. The successful year-long test was conducted through the work of SunLine Transit Agency, located in the Palm Springs area.

Conclusion

The third year of the project featured new, measurable achievements in vehicle and fuel demonstrations. The construction of a headquarters facility has boosted the effort to provide hands-on, visible evidence of the fuel cell in operation – a necessary step on the road to commercialization.

CaFCP members continue to gain real-world experience driving vehicle miles, refueling with hydrogen and now methanol, and participating in public outreach events. There is a very unique strength within the California Fuel Cell Partnership, as members work cooperatively and competitively at the same time in a stimulating environment, exchanging experiences, learning from each other and exploring the pathways to commercialization.

The world is watching what happens with fuel cell transportation technology in the Sacramento area. The work of the California Fuel Cell Partnership has the potential to bring about revolutionary change to transportation systems worldwide – change that is beneficial for the environment, for the economy, and for future generations.

FY 2002 Publications/Presentations

1. Bringing Fuel Cell Vehicles to Market: Scenarios and Challenges with Fuel Alternatives (Oct. 2001)

2. EVS-18: Driving for the Future: An Update on the California Fuel Cell Partnership Experience

V.B.2 Filling Up With Hydrogen 2000

Matthew Fairlie (Primary Contact), Paul Scott, Alex Lambert
Stuart Energy USA
7949 Woodley Ave.
Van Nuys, CA 91406
(818) 375-5052, fax: (818) 780-0515, e-mail: mfairlie@stuartenergy.com

DOE Technology Development Manager: Sigmund Gronich
(202) 586-1623, fax: (202) 586-5860, e-mail: Sigmond.Gronich@ee.doe.gov

Objectives

- Design and build fuel appliances based on new low-cost electrolyser technology.
- Demonstrate hydrogen vehicle re-fueling using fuel appliance systems.
- Obtain 'third party operating experience feedback' in refueling applications.
- Establish precedents for development of codes and standards.
- Determine cost effectiveness of fuel supply pathway.

Approach

- Conduct prototype development project involving building eight different appliances; each appliance project has five phases:
  - Design
  - Build
  - Test
  - Customer Evaluation
  - Tear-down and post mortem

Accomplishments

- Seven fleet fuel appliance prototypes have been constructed, featuring different technical advances. Three units have been placed in the field at the following sites: SunLine Transit, Powertech, and Southwest Research Institute; two units are built and being tested prior to delivery to the Fuel Cell Propulsion Institute and Alemeda County Transit; one additional unit is in testing un-deployed at this time. In addition, two smaller fueling systems called personal fuel appliances were built under this project, one of which is under evaluation with Ford Motor Company, supporting their fuel cell car program.

Future Directions

- Complete prototype deployment. P4-1B unit will be moved from Southwest Research Institute, where it is supplying fuel to a hydrogen motor generator set (joint development with Ford Power Products), to Wind Site at South Coast Air Quality District.
- Analyze performance of systems in the field; determine operating and manufacturing costs.
- Commercialize systems within market potential; establish market and product support systems.
- Project scheduled to be complete by March 31, 2003. Report results and recommend improvements for next cycle of fuel appliance development.

Introduction

"Filling Up with Hydrogen 2000" is a prototyping development project intended to validate the Stuart Fuel Appliance Model for hydrogen vehicle fuel supply infrastructure. Stuart fuel appliances are on-site electrolytic hydrogen generators for refueling gaseous hydrogen vehicles. Using only electricity and water and having no emissions beyond oxygen, electrolytic fuel appliances can be readily deployed to create a highly distributed fuel supply network.

The objective of the Stuart/DOE project is to design, build and deploy a variety of fuel appliances. Two types of appliance are being built under this project: Fleet Fuel Appliances and Personal Fuel Appliances, both of which target the needs of nascent hydrogen vehicle commercialization. The Fleet Fuel Appliance targets buses, trucks and other centrally fuelled fleet vehicles, where fuel production rates in excess of 400 standard cubic feet per hour (scfh) are required. The Personal Fuel Appliance is geared towards consumers' vehicles at the home or office, and can be powered by the utilities found in the typical North American home. The production rate of these units is in the range of 50 scfh. Both types of appliances are capable of delivering gaseous hydrogen at high pressure (up to 5000 pounds per square inch gauge [psig]) to the vehicle.

Approach

The successful development and demonstration of fuel appliance technology will enable a cost effective pathway for building a hydrogen fuel supply infrastructure to support hydrogen vehicles in their early commercialization. The fuel appliance addresses the issue of fuel delivery by providing point of use fuel generation using existing energy utilities. Using the existing electricity grid, a full service infrastructure can be built up as a distributed network of small electricity-to-hydrogen fuel converters.

Key to meeting the market requirements is reducing the cost of electrolysis. Stuart's patented alkaline water electrolysis cell technology is designed to achieve the cost targets demanded by transportation fuels. The Double Electrode Plate

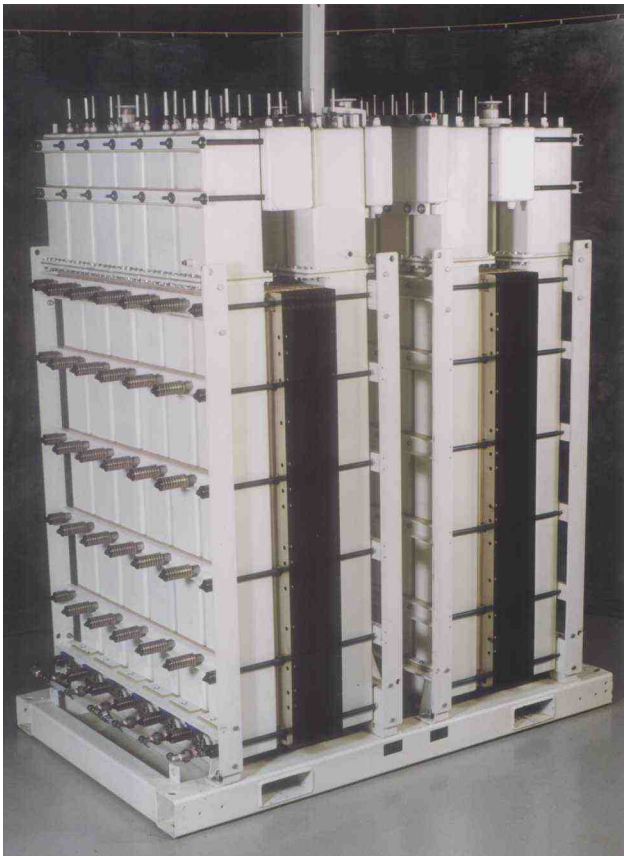

Figure 1. P3-5 Bus Fueler Appliance Cell Stack

(DEP®) technology uses low-cost polymer and metal sheets, which are easily assembled in a stack. The DEP® electrolyser can be configured either as a single stack or multi-stack electrolyser. The multi-stack electrolyser, having multiple cells in parallel, can run cell currents up to 30,000 amps and is suitable for large fueler applications. All the prototypes built under "Filling Up With Hydrogen 2000" use DEP® technology. The electrolyser packaged with the power system, compressor, purification and controls needed in a refueling application make up the fuel appliance.

"Filling Up With Hydrogen 2000" will provide an experience base with the cell stack technology for later commercialization and is a cost effective approach for equipment testing in that the user/ customer picks up operating costs for the benefit of the hydrogen produced. In addition to testing the cell technology, the prototype development plan provides public exposure to the fuel appliance concept,

Figure 2. P3-1A Fuel Appliance at SunLine Transit, 1000 Palms, California

Figure 3. P3-1B Fuel Appliance at Powertech, Vancouver, BC

introducing customers to the idea of distributed on-site hydrogen production as well as providing valuable precedents for the development of codes and standards and hydrogen project risk assessment. The operation of the bus fuel appliance (P3-1A) at SunLine Transit provides public access to the technology through SunLine. The low-pressure fueler (P3-1B LP) provides a demonstration of a system which can refuel metal hydride gas storage. The high-pressure fueler (P3-1B HP) demonstrates the concept of a distributed "community fueler". The design of the bus fueler, P3-5, demonstrates the large format cell technology which could be used in large bus fleet fueling applications (Figure 1). The P4 prototypes are being used to test different configurations of the cell stack integration with the compressor, including a pressurized stack configuration and integration with a wind turbine in a semi-stand-alone energy system. Prototyping of the personal fuel appliance (PFA P1 Model 25) at major automakers will provide the auto industry the opportunity to evaluate the concept of a small onsite hydrogen generator and potential home-based fueling appliance.

Results

Highlights of progress made in the past year in the prototyping project include the following:

- P3-1A: Bus Fuel Appliance, which produces up to 1,400 scfh at 4,000 psig, has operated for over 2,000 hours and produced over 2.5 million SCF of hydrogen fuel. The appliance has been used to fuel a variety of hydrogen and Hythane vehicles operated at SunLine (Figure 2).
- P3-1B (HP): Community Fuel Appliance, which produces up to 400 scfh at 5,000 psig, has operated for over 1500 hours, producing 650,000 SCF. The appliance has been used to test/certify hydrogen vehicle fuel tanks and fuel a fleet of Hythane vehicles (Figure 3). An identical version of this appliance will be provided to the California Fuel Cell Partnership.
- P3-1B(LP): Community Fuel Appliance, which produces up to 400 scfh at 200 psig. This unit has operated in-house for 3,000 hours has been refitted for refueling the metal hydride – hydrogen fuel cell mining locomotive in a joint project with the Fuel Cell Propulsion Institute. The siting of the appliance is approved and installation is expected to occur in September 2002.
- P4-1A: This fuel appliance, capable of 400 scfh at 6,000 psig, incorporating a higher-pressure stack, is being tested in house. Problems have arisen because of contamination of sensors used to control pressure in the cell. The approach to pressurize the cell is under review.
- P4-1B: Community Fuel Appliance, which produces up to 900 scfh, is currently being used to test a hydrogen internal combustion

Figure 4. Personal Fuel Appliance in Public Demonstration

engine generator set at Southwest Research Institute. After tests are

- complete, the unit will be moved to Palm Springs for the South Coast Air Quality Management District wind-hydrogen project.
- PFA Model 25: The Personal Fuel Appliance is on tour with the Ford Think fuel cell vehicle to demonstrate the household fuel supply system (Figure 4).

Conclusions

Fuel appliances can reliably meet needs of hydrogen vehicle refueling, delivering gas up to 5000 psig. Prototyping has indicated further work is required to reduce equipment and installation costs and refine process automation.

References

1. Stuart Energy USA, Filling Up With Hydrogen, 1998, under DOE Cooperative Agreement No. DE-97GO10221

V.B.3 Hydrogen Reformer, Fuel Cell Power Plant, and Vehicle Refueling System

Venki Raman (Primary Contact)
Air Products and Chemicals Inc.
7201 Hamilton Boulevard
Allentown, PA 18195
(610) 481-8336, fax: (610) 706-7463, e-mail: ramansv@apci.com

DOE Technology Development Manager: Chris Bordeaux
(202) 586-3070, fax: (202) 586-5860, e-mail: Chris.Bordeaux.ee.doe.gov

Main Subcontractors: Plug Power Inc., Latham, New York, City of Las Vegas, Las Vegas, Nevada

Objectives

- Resolve design issues and demonstrate small, on-site hydrogen (H_2) production for fuel cells and H_2 fuel stations
- Design, construct, and operate a multipurpose refueling station
- Dispense compressed natural gas (CNG), H_2/CNG blends, and pure H_2 to up to 27 vehicles
- Design, construct, and operate a stationary 50 kW fuel cell on pure H_2
- Evaluate operability, reliability, and economic feasibility of integrated power generation and vehicle refueling designs
- Maintain safety as a top priority in the refueling station and fuel cell design and operation
- Obtain adequate operational data on the fuel station to provide a basis for future commercial fueling station designs; develop appropriate "standard" designs for commercial applications
- Expand the current facility to serve as the first commercial facility when sufficient hydrogen demand develops. Ultimately serve as a link in a national H_2 corridor

Approach

- Further develop an existing small-scale (1,000 standard cubic feet per hour [scfh] H_2) natural gas-based autothermal reformer (ATR) prototype and test in conjunction with pressure swing adsorption (PSA) for on-site production of hydrogen
- Design and develop a scaled-up H_2 generator (3,000 scfh H_2)
- Develop a 50 kW proton exchange membrane (PEM) fuel cell capable of operating on pure hydrogen, based on 7 kW modules developed for a residential fuel cell product
- Design and develop a multi-purpose fuel station capable of dispensing various blends of H_2 and CNG and pure H_2 at pressures of 3,600 pounds per square inch (psi) and 5,000 psi for vehicle fueling
- Achieve integrated operation of the complete system and conduct a nominal two-year test program to determine reliability and maintainability
- Operating modes for the integrated system will be developed for testing various operational scenarios of the overall system

Accomplishments

- The ATR prototype unit was fully characterized at the Air Products and Chemicals, Inc. (APCI) labs after extensive changes necessitated by various operational issues

- Conclusions of economic analysis, which indicated that steam-methane reforming was the more appropriate choice for the scaled-up H_2 generator, and recurring maintenance issues lead to decision not to install the prototype unit in Las Vegas in FY 02
- Constructed scaled-up H_2 generator, and completed performance testing in the lab; shipped unit to Las Vegas (June 2002)
- Completed detailed design, fabrication, and testing on Plug Power's first large scale stationary fuel cell system (50 kW); shipped 50 kW fuel cell systems to Las Vegas (October 2001)
- All subsystems (vehicle refueling system, hydrogen generator and fuel cell power generator) currently being installed (August 2002)

Introduction

A part of the strategy for implementing hydrogen infrastructure for fuel cells, particularly in the early years of fuel cell vehicle introduction, involves the development of very small reformers that can use natural gas to produce hydrogen on-site at the fuel station. These reformers will need to have about a ten-fold lower production capacity than current economically sized hydrogen plants. Furthermore, their utilization factors will be very poor due to the limited number of vehicles and their sporadic filling demands, in turn leading to poor economics. An approach to improving the economics of hydrogen fuel production at these scales may be to integrate a fuel cell power plant with the fuel station to produce power and sell it back to the electricity grid when there is low fuel demand by vehicles. This co-production of electric power and hydrogen fuel is referred to as the "Energy Station" concept.

This project involves the development and validation of small-scale hydrogen reformer technology, a 50 kW PEM fuel cell power plant, and a multipurpose vehicle fuel station capable of dispensing hydrogen; hydrogen enriched natural gas; and CNG.

Approach

The project is a combined effort of three organizations: Air Products (prime contractor) with responsibility for the overall project and specifically for the hydrogen reformer and the multipurpose fuel station; Plug Power Inc. with responsibility for the 50 kW PEM fuel cell development; and the City of Las Vegas with responsibility for providing the project site, for installing a CNG fuel station (outside the scope of this project), for providing several vehicles operating on hydrogen/CNG blend fuels, and for facility operations support during the test period. Figure 1 shows a schematic of the overall integrated system configuration.

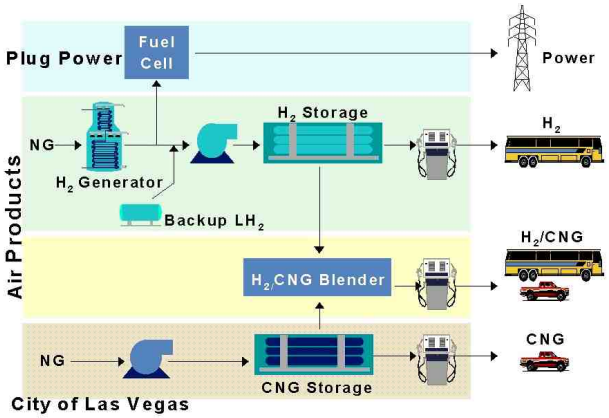

Figure 1. Overall System Integration Configuration

The project got started by testing an existing prototype small-scale (1,000 scfh) natural gas ATR previously under development by Air Products in conjunction with PSA for on-site production of hydrogen. Simultaneously, technical and economic studies of new small-scale reformer technologies were undertaken, outside the scope of this project, to select appropriate technology for a scaled-up hydrogen reformer (3,000 scfh) capable of meeting the hydrogen demands of up to 27 vehicles, and the 50 kW fuel cell.

The fuel station draws natural gas from a separate CNG fuel station installed by the City of Las Vegas. The multi-purpose fuel station was designed and developed by Air Products and utilized dynamic

blending of hydrogen and CNG to achieve various ratios and with the capability of dispensing the fuels at pressures of 3,600 psi and 5,000 psi.

Plug Power Inc. undertook the design and development of a 50 kW PEM fuel cell capable of operating on pure hydrogen, based on multiple 7 kW modules developed for a residential fuel cell product.

Results

Significant progress was made in the development of this project in the current year as described below.

H_2 Generator

The fully integrated ATR prototype H_2 generator that was completed last year and successfully tested at the Air Products laboratories in Allentown, PA, experienced ongoing operational issues requiring several changes. Major changes included replacement of the air blower to obtain additional capacity, steam generation coil and waste gas combustion chamber modifications due to failures, change of recycle water system to once-through due to solids build up, and PSA adsorbent change-out. Following these changes, a full characterization of the ATR was completed at the Air Products laboratories. However, based on an economic analysis that concluded that SMR technology was more economical than ATR technology to generate pure hydrogen at this size range (1000-3000 scfh H_2), and the recurring maintenance issues, it was decided not to install it in Las Vegas in FY 02.

A SMR (3,000 scfh H_2) based on technology from Harvest Energy Technologies was developed and tested at the Harvest facilities in California. Lessons learned in the previous ATR development were incorporated in the SMR development, including one button start capability, improved PSA recovery, and recycle of off-gas. The unit was moved to Las Vegas site**.**

Fuel Station

Air Products completed the fuel station design, and fabrication of all the equipment components such as the compressor, storage tubes, blender, and dispenser in November 2000. The integration of a metal hydride "thermal" compressor to compress hydrogen for the fuel station was evaluated but dropped from the project since it was determined that there was insufficient waste heat from the reformer to provide the thermal energy required by the metal hydride compressor.

Installation of the fueling equipment at the project site was delayed by one year awaiting completion of the CLV CNG station, which was completed in March 2002. The required permits for installation of the hydrogen station were issued and site work initiated in late March 2002.

Fuel Cell

The 50 kW fuel cell stack system comprised of eight 7.5 kW stack modules was fully assembled and tested at Plug Power's Latham, New York facility. This is Plug Power's first large scale stationary system. Initial startup and qualification testing yielded a number of design changes related to component selection, control and electronic equipment, software algorithms, and gas delivery systems. Plug Power first qualified individual subsystems, followed by final system configuration testing. Test data provided an operational baseline and validation of the interface conditions to support integration into the refueling station.

The 50 kW fuel cell system was shipped to the Las Vegas site in October 2001. Figure 2 is a photograph of the complete 50 kW fuel cell power plant.

Figure 2. 50 kW Fuel Cell Power Plant

Conclusions

- Studies indicated that SMR technology was the more economical option than ATR technology for production of pure hydrogen in the size range of interest and was selected for the scale-up hydrogen generator.
- As of this writing (August 2002), all equipment items have been installed at the site and individual equipment checkout is underway.
- Current progress indicates that target start-up of fully integrated operations by September 1, 2002 will be met.

FY2002 Presentations

Presentations on the "Energy Station" concept and the Las Vegas project have been given to various audiences separately or in conjunction with a discussion of developing hydrogen infrastructure, including:

1. Merrill-Lynch Global Energy Technology Conference – New York City, May 2001

2. California Fuel Cell Partnership Steering Team – Diamond Bar, CA, October 2001

3. The EVAA Electric Transportation Industry Conference & Exposition – Sacramento, CA, December 2001

4. NRC Hydrogen Study Team Meeting - Washington D.C. CHALLENGES FOR THE CHEMICAL SCIENCES IN THE 21ST CENTURY – January 2002

5. Globe 2002 – Vancouver, Canada, March 2002

6. H_2 Investor Forum – Washington, D.C., April 2002

Outreach efforts have been made to auto participants of the California Fuel Cell Partnership with a view to promote the Las Vegas site as a link in a California-Nevada hydrogen corridor.

Section VI. Safety and Codes & Standards

VI.A Safety

VI.A.1 Gallium Nitride Integrated Gas/Temperature Sensors for Fuel Cell System Monitoring for Hydrogen and Carbon Monoxide

Steve Pyke (Primary Contact)
Peterson Ridge LLC
PO Box 1257
Sisters, OR 97759
(541) 318-8265, fax: (541) 330-0073, e-mail: spyke@empnet.com

DOE Technology Development Manager: Neil Rossmeissl
(202) 586-8668, fax: (202) 586-5860, e-mail: Neil Rossmeissl@ee.doe.gov

Objectives

- Adapt catalytic gate field effect transistor (FET) sensors to resolve and detect carbon monoxide (CO) contamination levels from 1-100 ppm in reformer produced hydrogen (H_2) fuel for (proton exchange membrane (PEM) fuel cells
- Use FET sensors on gallium nitride (GaN) for increased sensitivity and faster response in high temperature
- Compare performance against industry requirements to assess outcome and opportunity
- Improve measurement precision and accuracy
- Field test for reliability and lifetime

Approach

- Design catalytic gate FET sensor for high temperature applications
- Build 1st generation FETs with platinium (Pt), rhodium (Rh) and palladium silver (PdAg) gates for evaluation
- Determine the performance requirements against which to measure performance
- Test and determine the population statistics for sensitivity, interferent resolution and temperature coefficients (electrical and chemical) for 1st generation devices
- Redesign for improved performance and build and evaluate 2nd generation test articles

Accomplishments

- Built GaN MODFET sensors with Pt, Rh and PdAg gate metallization
- Demonstrated CO sensitivity enhancement at $T \geq 150^{o}C$ for Pt and Rh GaN FET sensorss
- Demonstrated Pt sensitivity to CO from 0-100 ppm at 150, 250, 350 and $450^{o}C$ in 10%, 35 and 50% H_2 in diatomic nitrogen (N_2)
- Demonstrated Pt sensitivity to H_2 from 0-100% at $450^{o}C$ in N_2 background

Future Directions

- Fabricate 2nd generation sensors with high surface area gate metal films and architectures for greater sensitivity, adhesion layers under the gate metal for a higher yield of working devices, insulating nitride layers between the catalytic metal and the GaN substrate for reduced gate-drain leakage current

and device protection, chromium/gold (Cr/Au) cap layers for protecting source and drain ohmic contacts and Ir and other new gate metals for greater resolution and interference rejection

- Design and build five low-cost prototypes including digital sensor control electronics for improved precision (ca. 1 millivolt)
- Adapt high temperature ceramic "spark plug" packaging for field testing
- Field test prototypes at Idatech, H_2Gen, Teledyne Energy Systems and National Renewable Energy Laboratory

Introduction

The need addressed by this project is for a sensor to detect the presence of CO in the H_2 produced from hydrocarbon feedstocks in reformers and used to power PEM fuel cells. Low-cost sensors are not available for measuring CO at 1-100 ppm levels in a fuel cell environment. The primary goal of this project is to develop a low-cost microelectronic gas sensor for detecting CO (1-100 ppm) in the fuel stream. The sensors must operate in hydrogen (30-75%), with carbon dioxide (CO_2) (15%), CO (0-10,000 ppm), H_2O (30%), percent levels hydrocarbons, and N_2 (balance), from 1-3 atm total pressure and temperatures as high as 800^{o}C (Glass et. al. 2000). There is also a need for hydrogen sensors that can also be addressed by this technology and must be part of the CO measurement in order to remove the confounding effect of H_2.

Approach

The technical approach is a catalytic-gate (Pt, Rh and PdAg) GaN FET sensor for operating in high H_2 and at high temperature. The detection of hydrogen was reported first by Lundstrom (Lundstrom 1975) on a palladium gate FET sensor on silicon, but high temperature operation of silicon-based FETs is limited to <150^{o}C. A higher bandgap semiconductor FET specifically, GaN, was proposed to extend this range for potential improvements in sensitivity and response times. Recent reports on GaN Schottky diode sensors (Schalwig et al 2001) and silicon carbide (SiC) FET based sensors show enhanced sensitivity at high temperature to combustion gases and suggest the potential of the technology in automotive exhaust gas monitoring applications. These and other sensor developments for automotive and aerospace applications have been recently reviewed (Mueller et. al. 2001).

Results

The results reported previously were for CO dependence at constant hydrogen concentration (35%). The data demonstrated CO sensitivity that increased with increasing temperature, but potentially interfering effects of changing H_2 concentration were not explored. The Rh gate FET sensor was sensitive to CO above 200^{o}C with apparent sensitivity only above 200 ppm. The Pt sensor was sensitive to CO between 50 and 500 ppm at 150^{o}C. The interfering effects of O_2 on the Pt sensor are substantial. The scanning and transmission electron microscopy and X-ray analysis shows no interdiffusion of contact metallization with GaN at the resolution limit of the analysis (<125Å) for process temperatures to 600^{o}C for all of the gate metals and the Ti/Al source/drain metallization. The yield of working devices was <25% due to the poor adhesion of the gate metal to the gallium nitride.

Recent testing of Pt sensors extended sensitivity studies for CO and H_2 to 450^{o}C and suggested substantial confounding effects for changes in H_2 concentration from 30-75%. Device failure occurred in the range 550^{o}C-750^{o}C probably due to oxidation of the ohmic contact metallization. Preliminary indications are sensitivity to CO is high at low levels (0-20 ppm) (see Figure 1), but more experimental precision is necessary to confirm the results. The response is nonlinear and dependent on both temperature and H_2 and measurement precision is crude (Signal to noise ~3) with the first generation electronics. In addition, gas chromatography analysis using the helium ionization detector does not have sufficient precision below about 20 ppm CO for an accurate measurement of concentration. A more sensitive detector will be needed to accurately measure CO at levels below 20 ppm. Results show H_2 sensitivity of the Pt sensor is high below 5% H_2 and no saturation to 100% (see Figure 2).

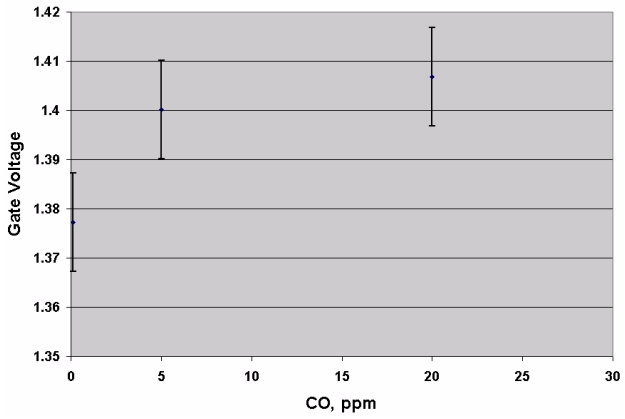

Figure 1. Pt Sensor Response with Low and Changing Concentrations CO in 35% H_2 at 450°C

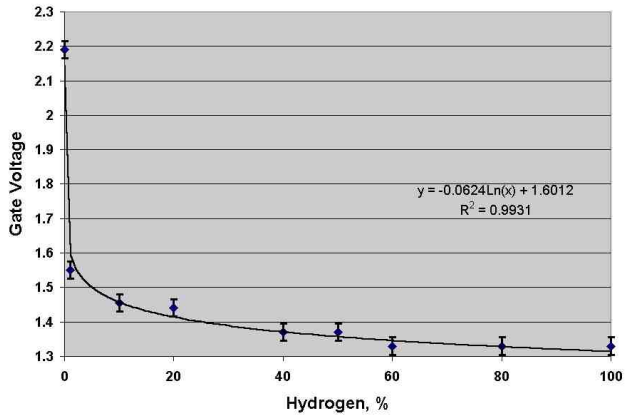

Figure 2. Pt Sensor Response with Changing H_2 at 450°C

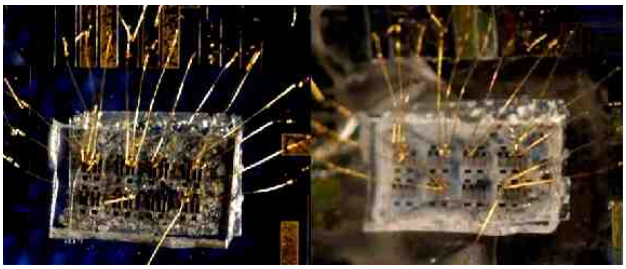

Figure 3. Comparison of Pt Sensor before and after Heating to 750°C shows the Black Rectangular Source and Drain Metallization Has Become Transparent Consistent

Sensor failure was promoted by increasing the temperature from 450°C to higher temperatures in 100°C increments in an oxidizing background gas consisting of 2% O_2, 10% CO_2, 100 ppm CO, and 100 ppm nitric oxide (NO), chosen for a more aggressive environment characteristic of combustion gas. The damage to the sensor and package is shown in a comparison of the sensor before and after heating in Figure 3.

Conclusion

- The Pt and Rh gate GaN FET sensors can be used to detect CO in the 0-100 ppm level in H_2 above 150°C
- The Pt sensor is sensitive to H_2 below 1% in N_2 and can be used for H_2 safety (0-4% in air)
- The lack of H_2 saturation suggest the Pt sensor could be useful H_2 monitoring and control
- Low CO sensitivity on Rh below 200 ppm at 200°C can be used to provide a measure of H_2 and correct the measurement of CO by Pt for changes in H_2
- Sensor failure results from oxidation of the source and drain contact metallization

References

1. Glass, R.S., J. Milliken, K. Howden and R. Sullivan (eds), 2000. "Sensor Needs and Requirements for Proton-Exchange Membrane Fuel Cell Systems and Direct-Injection Engines", LLNL, (http://www.ott.doe.gov/pdfs/sensors_report.pdf).

2. Lundstrom, I., M.S. Shivaraman, C. Svensson, and L. Lundqvist, 1975. J. Appl. Phys., 26:55.

3. Mueller, G., G. Krotz and J. Schalk, 2001. "New Sensors for Automotive and Aerospace Applications", Phys. Stat. Sol. (a) 185, No. 1, pages 1-14.

4. Schalwig, J., G. Mueller, O. Ambacher and M. Stutzman, 2001. "Group III-Nitride Based Gas Sensing Devices", Phys. Stat. Sol., (a) 185, No. 1, pages 39-45.

5. Lloyd Spetz, A., L. Uneas, H. Svenningstorp, P. Tobias, L.-G. Ekedahl, O. Larsson, A. Goras, S. Savage, C. Harris, P. Martensson, R. Wigren, P. Salomonsson, B. Haggendahl, P. Liung, M.

Mattsson and I. Lundstrom, 2001. "SiC Based Field Effect Gas Sensors for Industrial Applications", Phys. Stat. Sol., (a) 185, No. 1, pages 15-25.

FY 2002 Publications/Presentations

1. Pyke, S.C. and L. Sadwick, 2002. "Gallium Nitride Integrated Gas/Temperature Sensors for Fuel Cell System Monitoring for Hydrogen and Carbon Monoxide", Annual Review of the DOE Hydrogen/Fuel Cell Program, Golden, CO.

VI.A.2 Interfacial Stability of Thin Film Hydrogen Sensors

J. Roland Pitts (Primary Contact), Se-Hee Lee, Ping Liu, R. Davis Smith and Ed Tracy
National Renewable Energy Laboratory
1617 Cole Blvd.
Golden, CO 80401
(303) 384-6485, fax: (303) 384-6655, e-mail: roland_pitts@nrel.gov

DOE Technology Development Manager: Neil Rossmeissl
(202) 586-8668, fax: (202) 586-5860, e-mail: Neil.Rossmeissl@ee.doe.gov

Objectives

- Make available the technology to produce safe, reliable, sensitive, fast, lightweight, and inexpensive hydrogen sensors.
- Determine the factors affecting the stability and performance of thin film sensors in practical environments.
- Find solutions for extending the lifetime and functionality of thin film hydrogen sensors.

Approach

- Study service lifetime of sensors in ambient environments and in the presence of suspect contaminant gases.
- Investigate the effects of variations in temperature and relative humidity on sensor performance.
- Continue research on fundamental properties of sensor materials.

Accomplishments

- Constructed gas manifold with mass flow controllers (MFCs) for accurate gas proportioning.
- Investigated new protective layers to enhance protection from liquid water.
- Fundamental studies have yielded new chemochromic materials produced from electrochemical deposition techniques with controlled morphologies.
- Lifetime studies with protected sensor films indicate functional sensor lifetime has been extended to 12 months.

Future Directions

- Continue documentation of lifetimes of current sensors for realistic exposure conditions.
- Continue to optimize the thin film constructions for the protection of the palladium (Pd) catalyst.
- Improve large area sensors for visible detection and bio-hydrogen applications.

Introduction

The goal of this project is to develop safe, low cost, lightweight, reliable hydrogen sensors that can be used as safety sensors where hydrogen is used, stored, or transported. These sensors must be inexpensive enough to use several of them on a hydrogen powered vehicle, and they must be sensitive and fast enough to provide early leak detection so that action can be taken before the flammability limit in air is reached. We have chosen to work on a fiber-optic sensor configuration that stands the best chance of meeting all of these goals.

The National Renewable Energy laboratory (NREL) fiber-optic sensor consists of chemochromic (a color change produced as a result of a chemical reaction) coatings at the end of an optical fiber that

sense the presence of hydrogen in air. When the coating reacts with the hydrogen, its optical properties are changed. Light from a central electro-optic control unit is projected down the optical fiber, where it is either reflected from the sensor coating back to a central optical detector, or is transmitted to another fiber leading to the central optical detector. A change in the reflected or transmitted intensity indicates the presence of hydrogen. The fiber-optic detector offers inherent safety by removing all electrical power from the test site, and it reduces signal-processing problems by minimizing electromagnetic interference. Critical detector performance requirements include high selectivity, response speed, and durability as well as potential for low-cost fabrication, meeting or exceeding most of the proposed criteria for safety sensors.

The NREL sensor shares a common link with many other hydrogen sensor concepts in that they all use Pd or one of its alloys as a catalyst. Molecular hydrogen dissociates on the catalyst surface sites forming atomic hydrogen that diffuses rapidly through the film, reacting with the underlying chemochromic layer. All the sensor configurations utilizing Pd have the potential for degradation in their performance over time as a result of their cyclic interaction with hydrogen or contamination from impurities in the environments in which they will be used. Therefore, we have chosen to focus on stability issues related to ambient exposure of Pd and cyclic exposure of Pd to hydrogen.

Approach

A number of strategies for protecting the Pd catalyst were investigated in fiscal year (FY) 2001. The most effective of these was the application of novel inorganic coatings, which could offer effective protection to the hydrogen dissociation sites. Work continued in FY 2002 on the most effective of these strategies. Tests were conducted to determine the response of the sensor films with varying temperature and relative humidity (RH). For the latter work, a new gas manifold and proportioner was constructed, as well as an environmental chamber to allow control of gas and sensor temperature.

Work was also undertaken in the application of polymeric films that provide protection against water

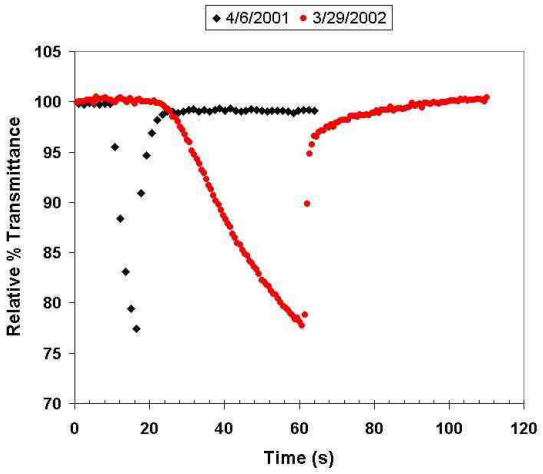

Figure 1. Response of Pd/WO_3 Sensor with Protectiv Coating, after One Year of Aging in Pollutec Atmospheres and Cycling in Hydrogen

condensation on the Pd surface, in particular for the sensors used by the NREL bio-hydrogen group. Interaction with representatives of GVD Corporation resulted in a short-term collaboration to test the efficacy of their proprietary polymer coatings. These coatings are deposited using a chemical vapor deposition technique, which results in a substantial amount of control of the film composition, density, and morphology.

In addition to innovative coatings for the protection of the hydrogen dissociation catalyst, mesoporous metal oxide layers for enhanced performance of the sensor elements were investigated. The results demonstrated the suitability of an electrodeposited tungsten oxide (WO_3) as a chemochromic layer for hydrogen detection, providing a valuable alternative to vacuum deposition.

Results

Inorganic Coatings

The study of inorganic coatings was focused mainly on the coating strategy that was found to be most effective during FY 2001. Samples made during this period were continually tested and have survived more than one year with some degradation in performance noted. An example of this performance is illustrated in Figure 1.

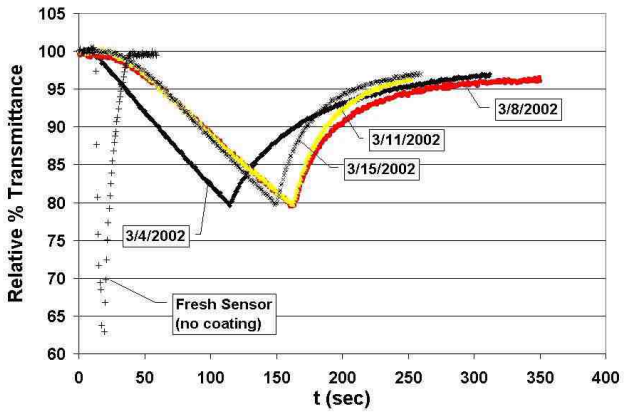

Figure 2. Response of Pd/WO_3 Sensor Coated with GVD Film after Ambient Exposure

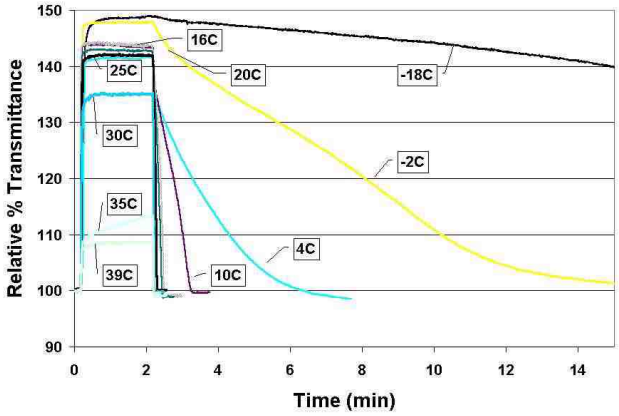

Figure 3. Pd/VO_x Sensor Tested with 4% H_2 in Air as a Function of Temperature

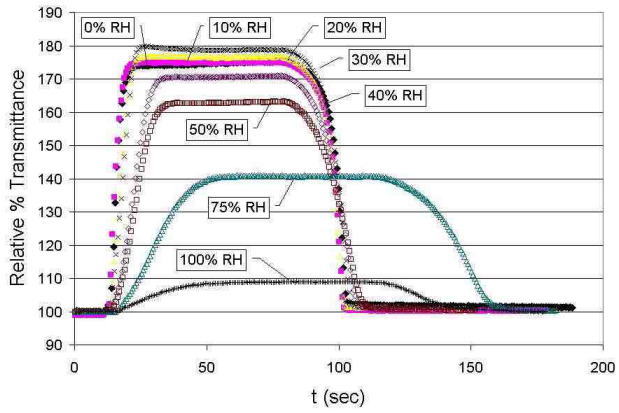

Figure 4. Pd/VO_x Sensor Response to 4% H_2 in Air as a Function of Relative Humidity

Organic Coatings

Sensor films were fabricated at NREL and sent to GVD Corporation for application of a variety of polymeric films. After coating, the films were returned to NREL for testing, and these films showed good resistance to pollutants in ambient air. Figure 2 illustrates the resistance to contamination of a sensor film over 2 months of testing. This represents a remarkable degree of protection for a polymer film and gives us an attractive avenue for exploration in the future, especially to control the ingress of water into the optically active elements of the sensor.

Sensor Response as a Function of Temperature/ Relative Humidity

The construction of a gas manifold incorporating four mass flow controllers allowed the mixing of water saturated air with dry air to produce test streams of gas with accurate RH. Measured amounts of hydrogen were then added to the test stream. An environmental test chamber was also constructed from an insulated cooler. A heating element on the test chamber and a proportional temperature controller allowed control of the gas temperature and thus the thin film temperature to within 0.1°C.

Experiments were conducted on the sensor films at various temperatures and RH values. The response of a Pd/vanadium oxide (VO_x) sensor to changes in temperature and RH is illustrated in Figures 3 and 4. The sensor exhibits degradation in performance at temperatures below 0°C and above 40°C. Response of the sensor is also slowed significantly by the presence of water vapor when the relative humidity exceeds 50%.

Mesoporous Metal Oxides

Figure 5 shows the optical response of a Pd/ electrodeposited-WO_3 sensor to 0.1% hydrogen/ nitrogen. The sensor exhibits a fast response that is comparable to that of an evaporated tungsten oxide-based sensor.

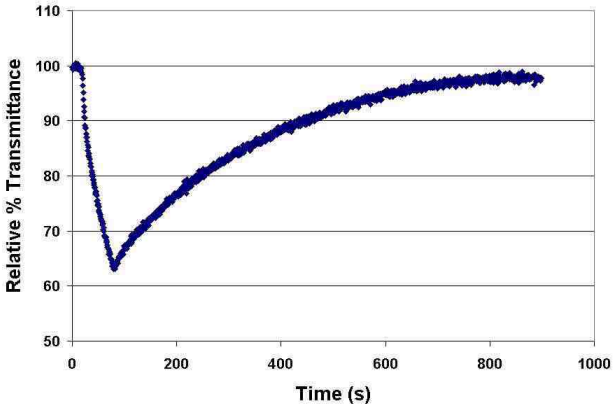

Figure 5. Optical Response of a Pd/WO_3 Sensor in which the Tungsten Oxide is an Electrodeposited Mesoporous Film

Conclusions and Future Direrctions

- Primary goals of speed, sensitivity, weight, and inherent safety have been met.
- Some sensor films have been demonstrated to be functional over one year.
- Collaboration with GVD Corporation produced promising results on organic protective coatings.
- Electrodeposited mesoporous metal oxides were investigated as chemochromic hydrogen sensor films.
- An environmental chamber was constructed to test sensor films at various temperatures.
- A gas manifold for proportioning gases and controlling relative humidity was constructed.
- Preliminary experiments indicate that both the speed and sensitivity of the sensor films vary with both temperature and relative humidity.
- Work continues on functional lifetime and response to variations in environmental conditions.

FY 2002 Publications/Presentations

1. S.-H. Lee, H. M. Cheong, P. Liu, D. Smith, C. E. Tracy, A. Mascarenhas, J. R. Pitts, and S. K. Deb, "Raman Spectroscopic Studies of Gasochromic a-WO_3 Thin Films," Electrochimica Acta, 46, 1995 (2001).

2. R. D. Smith II, D. K. Benson, J. R. Pitts, D. L. Olson, and T. R. Wildeman, Diffusible Weld Hydrogen (Measurement by Fiber Optic Sensors)," MP (Materialprüfung), Jahrg. **43**, 26 (2001).

3. Ping Liu, Se-Hee Lee, C. E. Tracy, J. R. Pitts and R. D. Smith, "Stable Pd/V_2O_5 Optical H_2 Sensor," J. Electrochem. Soc., 149, H76 (2002).

4. E. Ozkan, S.-H. Lee, P. Liu, C. E. Tracy, F. Z. Tepehan, J. R. Pitts, and S. K. Deb, "Electrochromic and Optical Properties of Mesoporous Tungsten Oxide Films," Solid State Ionics, in press.

5. R. D. Smith II, Ping Liu, Se-Hee Lee, C. Edwin Tracy and J. Roland Pitts, "Low-cost Fiber Optic Hydrogen Sensors", to be presented at the 224th ACS National Meeting, Boston, MA, August 18-22, 2002.

Patents Issued

1. P. Liu, C. E. Tracy, J. R. Pitts, and S.-H. Lee, "H_2O Doped WO_3, Ultra-Fast, High-Sensitivity Hydrogen Sensors," PCT/US01/14375, published Nov. 15, 2001.

2. S.-H. Lee, C. E. Tracy, J. R. Pitts, and P. Liu, "Pd/Ni-WO_3 Anodic Double Layer Gasochromic Device," PCT/US01/14381, published Nov. 15, 2001.

3. P. Liu, C. E. Tracy, J. R. Pitts, S.-H. Lee, and D. Smith, "Pd/V_2O_5 Device for H_2 Detection," PCT/US0114411, published Nov. 15, 2001.

4. P. Liu, C. E. Tracy, J. R. Pitts, and S.-H. Lee, "Protective Coating for Gasochromic-Based Sensors Used in Sensing the Presence of Hydrogen," ROI, NREL #01-41, application submitted.

VI.A.3 Micro-Machined Thin Film H_2 Gas Sensors

Frank DiMeo, Jr. (Primary Contact), Ing-Shin Chen, Philip Chen, Jeffrey Neuner, Michele Stawasz, James Welch, and Andreas Rohrl
ATMI, Inc.
7 Commerce Drive
Danbury, Connecticut 06810
(203) 794-1100, fax: (203) 830-2123, e-mail: fdimeo@atmi.com

DOE Technology Development Manager: Neil Rossmeisel
(202) 586-8668, fax: (202) 586-5860, e-mail: Neil.Rossmeisel@ee.doe.gov

Objectives

- Optimize micro-hotplate based H_2 sensor design and fabrication processes
- Investigate potential sensor cross sensitivities and degradation mechanisms
- Demonstrate an extrapolated sensor lifetime greater than 3 years

Approach

- Investigate the use of alternative micro-hotplate geometries to increase power density and reduce heat loss
- Develop surface treatment processing to minimize the contact resistance between the sensing layer and the underlying metal contact
- Construct test manifolds and signal-conditioning circuitry for advanced sensor testing
- Study sensor response to H_2 in the presence of contaminant gases
- Evaluate sensor response performance for an extended time period

Accomplishments

- Designed new micro-hotplates for low voltage (5 V), low power (5 mW) operation
- Evaluated the effectiveness of protective coatings against high-level H_2 exposure
- Demonstrated working sensors in atmospheres containing low-level contaminant gas - 100 ppm CO, 20 ppm H_2S, or 600 ppm isopropyl alcohol (IPA)
- Collected long-term sensor performance data over a three-month period

Future Directions

- Implement advanced micro-fabrication processing methods and statistical process control
- Evaluate environment-tolerant protective coatings
- Investigate catalytic chemistry at sensor surface
- Examine the phase transformation mechanism of the sensing materials
- Develop integrated system solution

Introduction

The reputation of hydrogen as the next generation energy delivery agent, supplementing today's electricity, is firmly established. Multifaceted use of hydrogen will play a crucial role in future communities. However, hydrogen is a gas at atmospheric conditions and can escape from its containment to cause an explosion hazard. Safe storage and delivery of hydrogen is a necessity for public acceptance of hydrogen as an energy medium.

The ability to detect and quantify the amount of gaseous hydrogen present is fundamental to all aspects of hydrogen processes. In addition to safety needs, hydrogen sensing is also required as a means of monitoring and controlling hydrogen-based processes used in fuel cells. The demand for hydrogen sensors is very great in terms of quantity and variety because each application may have specific requirements for sensor characteristics. The quantity demand also translates into a requirement for low production cost so that needs, rather than costs, are the determining factor for sensor use.

Approach

Essential features required for H_2 sensor applications include fast response, high sensitivity, and amenability to large-volume manufacturing, to name a few. Micro-machined thin film hydrogen gas sensors were developed at ATMI to meet these needs. These sensors combine novel H_2 responsive materials and micro-hotplate structures based on proven silicon technology. Our implementation of the micro-hotplate is a surface micro-machined thermal isolation structure with an embedded polycrystalline silicon resistive heater where elevated temperature can be achieved with ease (Semancik, et al., 2001). A typical ATMI micro-hotplate structure is shown in Figure 1.

A rare earth metal thin film over-coated with a palladium-based capping film serves as the active sensing layer. Detection of H_2 is based on the phase transformation induced by hydrogenation of rare earth metals. The rare earth metal reacts with hydrogen upon exposure, leading to a change in electrical resistance that scales with hydrogen concentration in the gas phase. When this sensing layer is coated on the surface of a micro-hotplate, as shown in Figure 2, the reaction kinetics can be engineered by the micro-hotplate temperature.

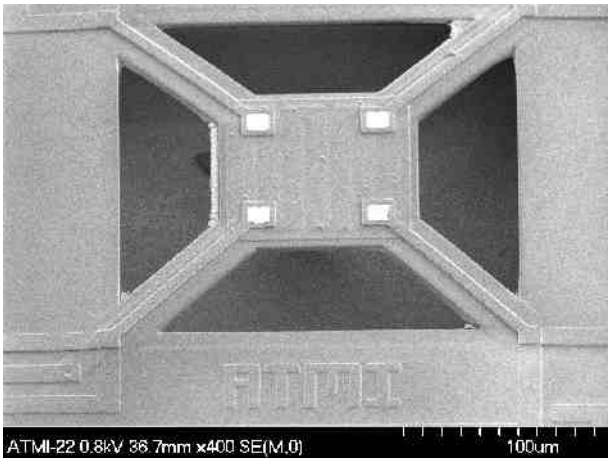

Figure 1. SEM Photo of a Released Micro-Hotplate Thermal Isolation Structure

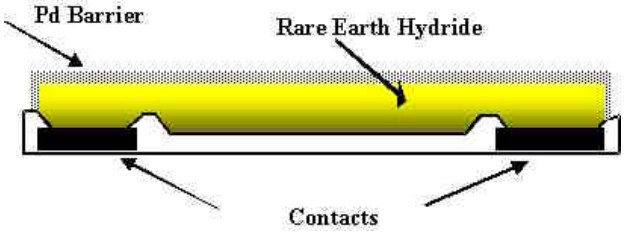

Figure 2. Schematic of Functional Layer Stack on a Micro-Hotplate Platform

Results

Designed for safety applications, our micro-machined thin film H_2 sensors have been tailored for H_2 concentrations at half of the lower explosive limit (4% in air for H_2) or lower. In this concentration range, we have demonstrated an extremely fast response and large signal-to-noise ratio.

Sensor operation in real applications is usually affected by the interference from common contaminant gases. These contaminant gases are known to cause false alarms or outright failure of sensors based on existing technology. To examine sensor performance in the presence of contaminant gases, sensors were exposed to low-level contaminant gases in a background of air. The first experiment was performed without H_2 in the gas stream. Dry air was used as the purge gas, and low-

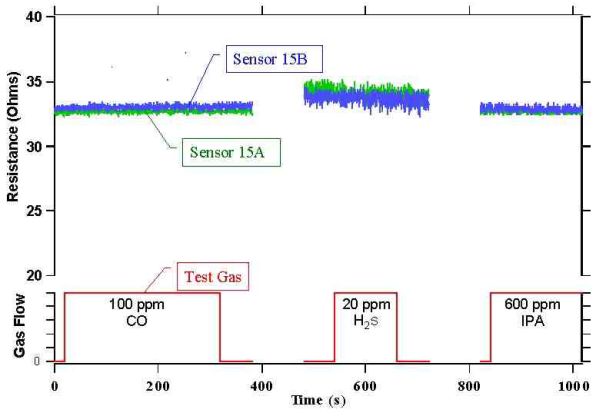

Figure 3. Response of a Sensor to Low-Level Contaminant Gases in Air

level contaminant gas was blended in air as test gas. A set of representative data is shown in Figure 3. The sensors did not respond to the presence of the contaminant test gas in the absence of hydrogen and thus caused no false alarms.

The next experiment was performed with H_2 in the gas stream during the test cycle. Low-level contaminant gas - 100 ppm CO, 20 ppm H_2S, or 600 ppm IPA - was blended with 0.5% H_2 as the test gas. A set of representative data is shown in Figure 4. The first, third, fifth, and the last subsets of data were collected with 0.5% H_2 in dry air with no contaminant gas, providing a reference background. The sensor exhibited enhanced response in the presence of CO and H_2S. The sensor remains functional during and after repeated exposure to any of these contaminant gases.

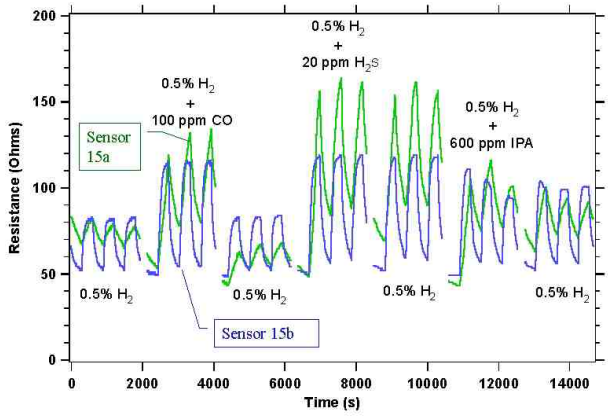

Figure 4. Response of a Sensor to 0.5% H_2 in the Presence of Contaminant Gases in Air

An experiment was carried out where a sensor was exposed to H_2 over a three-month period. The temporal sequence of the gas stream included a 24-hour dry air purge followed by a 10-minute exposure to 1% H_2. Figure 5 shows the long-term test results. The sensor remains fully functional after approximately three months of repeated exposure to H_2. This observation, while it does not directly provide a measure of sensor lifetime, is encouraging.

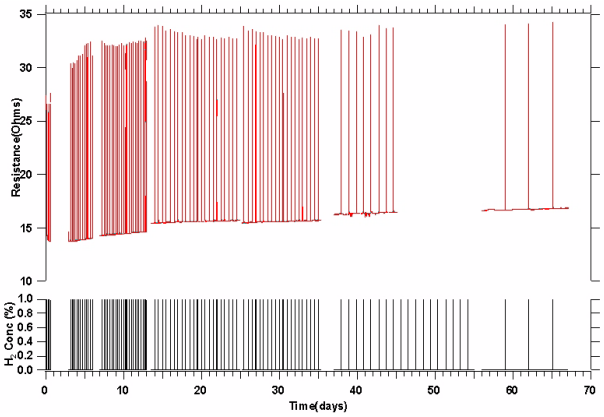

Figure 5. Response of a Sensor Under Repeated Exposure to 1% H_2 Over a 3-Month Period

Conclusions

- The sensors tested do not respond to contaminant gases
- The sensors exhibited enhanced response to H_2 in the presence of CO and H_2S
- The sensors continued to operate after exposure to contaminant gases
- Long-term performance at low-level H_2 exposure shows no intrinsic failure mode during normal operation

References

1. S. Semancik, R.E. Cavicchi, M.C. Wheeler, J.E. Tiffany, G.E. Poirier, R.M. Walton, J.S. Suehle, B. Panchapakesan, D.L. DeVoe, "Microhotplate platforms for chemical sensor research," Sensors and Actuators B 77, 579-591 (2001).

Presentations

1. "Advanced Gas Sensor R&D at ATMI" presented at ATMI's Emerging Technologies

Lunch at SESHA (Semiconductor Environmental, Safety, and Health Association) 24th Annual Symposium, April 4-6, 2002, Palm Springs, California.

2. "MEMS Based H_2 Gas Sensors" presented at symposium AL1 (Sensing In Industrial And Extreme Applications) of The Electrochemical Society 201st Meeting in Philadelphia, Pennsylvania, May 12-17, 2002.

VI.B Codes & Standards

VI.B.1 Hydrogen Infrastructure Activities Codes and Standards: Hydrogen Codes and Standards Outreach

Karen Miller
The National Hydrogen Association
1800 M Street NW, Suite 300
Washington, DC 20036-5802
(202) 223-5547, fax: (202) 223-5537, e-mail: kmiller@ttcorp.com

DOE Technology Development Manager: Neil Rossmeissl
(202) 586-8668, fax: (202) 586-5860, e-mail: Neil.Rossmeissl@ee.doe.gov

Technical Advisor: Robert L. Mauro
(202) 223-5547, fax: (202) 223-5537, e-mail: rmauro@ttcorp.com

Objectives

- Bring industry experts together to establish technical criteria for hydrogen energy components and systems nearing commercialization.
- Continue to advance U.S. industry positions in the international arena, including the International Standards Organization Technical Committee 197 (ISO TC 197) and the International Electrochemical Committee Technical Committee for Fuel Cells (IEC TC 105).
- Work closely with the International Code Council (ICC) Ad Hoc Hydrogen Committee (AHC) to include hydrogen and hydrogen energy systems in the model codes in the United States.
- Identify code and standard organizations that can begin to or are in the process of developing hydrogen codes and standards.
- Pull industry experts together to assure technical accuracy and consistency of these codes and standards.
- Report on the activities to a wide audience, assuring information transfer regarding the status of efforts and technical (and sometimes political) issues remaining.
- Working with the National Renewable Energy Laboratory (NREL), the National Hydrogen Association (NHA) also seeks to facilitate the coordination of hydrogen codes and standards activities through the Hydrogen Codes and Standards Coordination Committee (HCSCC), and disseminate timely information about these efforts through a monthly electronic publication, the "Hydrogen Safety Report".

Approach

- Hold technical conferences with industry, academia, national laboratories, government laboratories, code officials and code organizations to develop and write new standards for hydrogen technologies, including storage tanks, fueling nozzles, connectors, safety equipment, and other key components and integrated systems needed to move hydrogen into the energy sector.
- Participate in the International Standards Organization and its Technical Committee 197, which is responsible for the presentation and approval of the developed standards.
- Publish Codes and Standards (C&S) Workshop Proceedings online - available to the public.

- Support the International Code Council in their efforts to review, develop and promulgate new codes for the use of hydrogen. This includes providing experts, technical reports, data and other information needed by the code officials to complete the development of these new codes.
- Present the U.S. hydrogen positions at international forums and participate in international meetings that are of benefit to the whole hydrogen community in the areas of hydrogen safety, codes and standards.
- Publish and present pertinent hydrogen safety, codes and standards information at a variety of forums, including Global Parks conference to be held in September in Michigan; American Society of Nondestructive Testing (ASNT) conference held in March in Portland, Oregon; and SAE (Society of Automotive Engineers) Fuel Cell Transportation Technology Summit II in Michigan in April.
- Keep its members informed of progress in the development of hydrogen safety, codes and standards through publication in its Quarterly Newsletter, the *NHA News* and by posting sensitive draft information, including draft standards, on the NHA *Members Only* website.
- Conduct safety codes and standards outreach in an open, non-competitive manner by conducting workshops; participate in the development efforts of other organizations; work with the HCSCC to coordinate the efforts; present hydrogen safety, codes and standards activities at conferences and workshops; and make information available in a timely manner to all interested parties.

Accomplishments

- The NHA hosts two Hydrogen Safety Codes and Standards Workshops per year. The most recent one was held February 26, 2002. Proceedings were available on-line through the electronic newsletter and on the NHA website within 2 weeks of the workshop. The "Hydrogen Safety Report" has been published by the 15th of each month since December 2001, and it is free to all interested parties through the NHA website (www.HydrogenUS.com) and on its own site at (www.HydrogenSafety.info).
- The ICC AHC has proposed changes for including hydrogen energy systems and the NHA participated in all the hydrogen-related hearings. The two proposed code changes to the International Fire Code were approved, with modifications.
- ISO TC 197 and IEC TC 105 working group meetings and plenaries were held in June, 2002 in Montreal in conjunction with the World Hydrogen Energy Conference (WHEC). NHA has organized three technical sessions at WHEC on hydrogen safety, codes and standards.
- The U.S. TAG meeting for ISO TC 197 was held in Washington, DC during the third week of May, 2002. NHA discussed and proposed a new work item on charged metal hydrides.
- The NHA presented hydrogen codes and standards activities at the DOE Fuel Cell Summit at the end of May.
- The ICC process has recently brought a number of associations that serve the petroleum and natural gas industries to the fold, all in support of developing codes and standards for hydrogen energy systems.
- In October 2001, the NHA had a large article published in the U.S. General Services Administration (GSA) publication "Vehicle News".

Future Directions

- The next NHA C&S Workshop is to be held in Fort Worth, Texas on September 30, 2002 -in conjunction with the BOCA - ICBO - SBCCI Joint Annual Conference.

- Information dissemination remains crucial to building consensus and developing a national and international dialog. The NHA would like to expand on these efforts to develop informational materials, presentations, and forums for targeted audiences, such as code officials; regulators; early adopters for transportation, stationary, and portable power applications; and the public. It is important to educate the public on several levels. For example, the tax payers must understand hydrogen in order to support efforts to purchase and operate hydrogen buses, then the general public must feel safe and good about riding in them. The benefits of hydrogen technologies need to be clearly articulated. For example, with hydrogen fuel cells running auxiliary power in a vehicle, it is possible to have air conditioning running without the engine operating. There are many value-added benefits that can help prepare the market for these emerging technologies.

Introduction

The mission of the National Hydrogen Association (NHA) is to foster the development of hydrogen technologies and their use in commercial and industrial applications and to promote the role of hydrogen as a major energy carrier of the future.

The NHA holds technical conferences with industry, academia, national laboratories, government laboratories, code officials and code organizations to bring experts together in a focused activity to develop and write new standards for hydrogen technologies. This includes such items as storage tanks, fueling nozzles, connectors, safety equipment, and other key components and integrated systems needed to move hydrogen into the energy sector. The NHA has members and staff who are active participants in the International Standards Organization and its Technical Committee 197, which is responsible for the presentation and approval of the developed standards.

Approach

The NHA works with DOE, NREL, and others to coordinate codes and standards activities to avoid duplication of effort and enable hydrogen systems to be sited. This requires coordination with industry groups and standards organizations such as the International Organization for Standardization, American Society of Mechanical Engineers, IEC TC 105, the U.S. Fuel Cell Council, the Society of Automotive Engineers, Fuel Cell Propulsion Institute, National Fire Protection Association, and the DOE Fuel Cell Codes and Standards Summit.

NHA staff publishes and presents pertinent hydrogen safety, codes and standards information at a variety of forums, including Global Parks conference to be held in September in Michigan; ASNT conference held in March in Portland, Oregon; and SAE Fuel Cell Transportation Technology Summit II in Michigan in April.

The NHA keeps its members informed of progress in the development of hydrogen safety, codes and standards through publication in its Quarterly Newsletter, the *NHA News* and by posting sensitive draft information, including draft standards, on the NHA *Members Only* website. This allows NHA members an opportunity to review the work of other organizations who have requested collaboration with the hydrogen community but can not make these items publicly available. The general articles published in the newsletter are made available to the public on the NHA website and mailed to NHA members. In addition, we produce a monthly electronic newsletter dedicated to hydrogen safety issues. It is available on the NHA website, and also has its own dedicated site. Anyone can sign up to receive email notification each month when it is posted online. In this way, the information is distributed broadly, and interested parties are given an opportunity to get involved in the standards development process.

Results

The NHA presented hydrogen codes and standards activities at the DOE Fuel Cell Summit at the end of May, 2002. The NHA has successfully encouraged industry experts to join the NHA C&S Committee and the US TAG for ISO TC 197. The ICC process has recently brought a number of

Figure 1. Next Generation Fuel Cell ZEBus

Figure 2. Ford Focus Fuel Cell Vehicle

associations that serve the petroleum and natural gas industries to the fold, all in support of developing codes and standards for hydrogen energy systems. In October 2001, the NHA had a large article published in the GSA publication "Vehicle News". Photos from that article showed sample demonstration vehicles and refueling station projects for which safety codes and standards are needed.

Figure 1 shows the XCELLSiS Zebus (Zero Emission Bus) and Honda's FCX fuel cell vehicle at the SunLine Transit Agency hydrogen refueling station in the Coachella Valley. SunLine plans to have a number of fuel cell buses by 2003.

Ford Motor Company delivered the world's first production prototype, direct-hydrogen powered fuel cell vehicle (Ford Focus, Figure 2) to the California Fuel Cell Partnership in November 2000.

Figure 3 depicts the hydrogen fueling station at the California Fuel Cell Partnership's West

Figure 3. CaFCP Hydrogen Refueling Station

Sacramento Headquarters Facility, which was jointly designed and installed by five of the world leaders in energy and industrial gas supply: Air Products and Chemicals, BP, Praxair, Shell, and Texaco. The station is used to fill vehicles with gaseous hydrogen.

The NHA hosts two Hydrogen Safety Codes and Standards Workshops per year. The most recent one was held February 26, 2002, in conjunction with a WSRC Hydrogen Storage Workshop. Over thirty experts gathered to exchange information on the status of these efforts and how to participate in them. Proceedings were available on-line through the electronic newsletter and on the NHA website within 2 weeks of the workshop. The "Hydrogen Safety Report" has been published by the 15th of each month since December 2001 and is free to all interested parties through the NHA website (www.HydrogenUS.com), and on its own site at (www.HydrogenSafety.info). Over 300 interested parties receive email notification when a new issue is posted, with a hotlink to the information.

In December 2001, the National Hydrogen Association launched a monthly electronic newsletter on hydrogen safety, called the Hydrogen Safety Report (Figure 4). It is available to all interested parties on the Internet at www.HydrogenSafety.info.

Figure 4. Hydrogen Safety Report

Another major effort has been garnering industry support for the ICC hearings in Pittsburgh in April, 2002. The ICC AHC has proposed changes for including hydrogen energy systems. The NHA participated in all the hydrogen-related hearings. The two proposed code changes to the International Fire Code were approved, with modifications. There was huge support for the need to put something in the code now, knowing we have the next 18 months to work out the details, and include exceptions as appropriate. Only one person stood up in opposition claiming "hydrogen is a very dangerous gas and scares the living daylights out of me". It was a very touch-and-go situation, and we all learned quite a bit about process, and how important it is to have built support across communities, and have assistance, real-time, from those familiar with procedure. F176-02 was approved as modified. The modifications are consistent with SE/SW Fire Chiefs' recommendations to AHC. In addition, all four (4) exceptions to Section 2209.3 were deleted. F-177-02 also passed as amended, with issues of venting to be worked out. F177-02 was approved as modified. IFC Committee Chair ruled AHC modification 'editorial'.

All International Fuel Gas Code proposals were disapproved by the IFGC committee; however floor action was taken on each. Support for the changes was overwhelming, and the committee recommendation along with the floor action will go on to the Final Action Consideration at the end of September. The NHA is working with the HCSCC to coordinate information dissemination to voting members and industry as well as technical support to the ICC AHC.

Some interesting developments in Europe have necessitated an open dialog on the U.S. position in the development of international standards. This has implications both technically and politically, and relates to proposed European-wide regulations which are likely to be proposed as global regulations, despite lack of U.S. involvement in setting the framework.

ISO TC 197 and IEC TC 105 working group meetings and plenaries were held in June, 2002, in Montreal in conjunction with the World Hydrogen Energy Conference (WHEC). NHA organized three technical sessions at WHEC on hydrogen safety, codes and standards and actively participated by serving on the Technical Committee for these sessions, co-chairing a session, presenting a paper, and coordinating with speakers.

The U.S. TAG meeting for ISO TC 197 was held in Washington, DC during the third week of May. NHA proposed a new work item on charged metal hydrides.

Conclusions

The need to develop a U.S. position on the international level must go well beyond the current efforts. The NHA supports efforts to assure that decisions are made by consensus using international standards bodies and that U.S. interests are not disadvantaged.

In addition, with such excellent cooperation developing on a national level, the current efforts must continue, with additional support for coordinated activities, such as those of the HCSCC. The NHA is poised to lead efforts best led by the hydrogen industry, and play an active role in broader efforts.

There is a very meaningful international role for the U.S. Department of Energy (DOE):

- Make sure that U.S. interests are involved and adequately represented in the standards making process; and
- Make sure that the U.S. government speaks with the same voice in presenting U.S. interests internationally (WP29), as the consensus position of U.S. industry speaks with in international standards organizations.

The National Hydrogen Association will hold its next Hydrogen Safety, Codes and Standards Workshop on September 30, 2002 in Fort Worth, Texas (Figure 5). (For more information, visit www.HydrogenUS.org.) The NHA would like to expand on these efforts to develop informational materials, presentations, and forums for targeted audiences, such as code officials, regulators, early adopters for transportation, stationary, and portable power applications, and the public. The benefits of hydrogen technologies need to be clearly articulated.

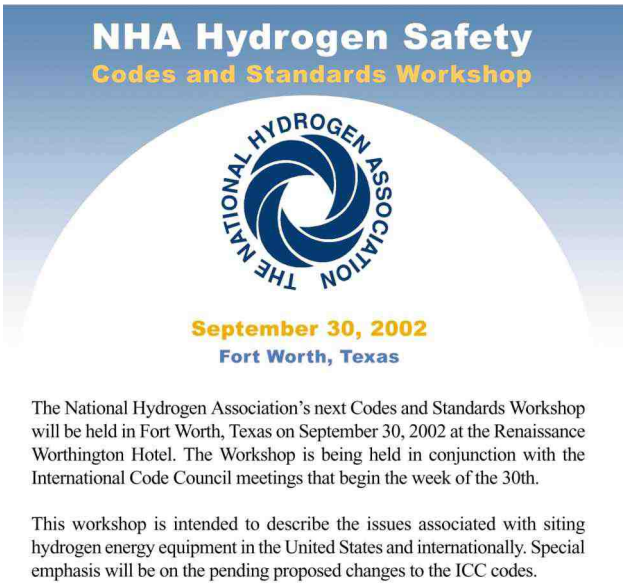

Figure 5. Workshop Announcement

References

1. Hydrogen Codes and Standards – NHA's presentation for the 2002 DOE Hydrogen Program Peer Review.

FY 2002 Publications/Presentations

1. Peer Review Presentation and Paper: NHA-DOE Cost Shared Activities: Hydrogen Codes and Standards Outreach

2. DOE Fuel Cell Summit Presentation: International Standards Activities in Hydrogen Technologies

3. Paper for Global Powertrain Conference: Hydrogen Power - Driving Our Future

4. AIAA Joint Propulsion Conference presentation: Safety Siting of Commercial Hydrogen Facilities

5. NHA Hydrogen Codes and Standards Workshop Proceedings – February 26, 2002

6. SAE Fuel Cell Transportation Summit II: NHA Fueling and Infrastructure

7. ASNT 2002 Spring Conference: NDE Issues for Hydrogen Energy Systems

8. HTAP Safety Summit: NHA Codes and Standards Activities

Special Recognitions

1. Outstanding Contribution to The Hydrogen Planet, 14th World Hydrogen Energy Conference

VI.B.2 Codes and Standards Analysis

Dr. Michael R. Swain (Primary Contact), Patrick Filoso, Dr. Matthew N. Swain
University of Miami
Coral Gables, FL 33124
(305) 284-3321, fax: (305) 284-2580,e-mail: mswain@miami.edu

DOE Technical Development Manager: Neil P. Rossmeissl
(202) 586-8668, fax: (202) 586-5860, e-mail: Neil.Rossmeissl@ee.doe.gov

Objectives

Task A - California Fuel Cell Partnership (CaFCP) Building Safety Analysis

- Determine whether garage door should be opened when hydrogen is detected.
- Quantify the risk of hydrogen ignition in the air conditioning (A/C) system during pressure relief device failure.
- Determine whether risk due to pressure relief device failure could be reduced by restricting vehicle location.
- Determine whether risk during pressure relief device failure could be reduced by relocating air conditioning return duct.
- Determine the severity of ignition of hydrogen leaking in bay.
- Determine the severity of ignition of hydrogen leaking under a large vehicle.

Task B - Development of Method to Determine Hydrogen Sensor Placement

- Develop a method to visualize the motion of gases from a hydrogen leak to aid in determining optimized hydrogen sensor locations for safety applications.

Task C - Safety and Analysis for Writing of Codes and Standards

- Determine the effect of hydrogen flame impingement on gypsum board.
- Determine the effect of hydrogen gas leakage from a residential refueler.

Approach

- Identify questions concerning safety of hydrogen installations or safety concerns of authors of codes and standards.
- Design tests or computer models to answer questions identified.
- Conduct tests to directly answer questions or verify computer model.

Accomplishments

- Implemented conclusion that CaFCP garage door should not be opened upon detecting hydrogen in bay.
- Determined that pressure relief device failure could cause hydrogen ignition in the CaFCP air conditioning system.
- Determined that restricting vehicle location to prevent the above scenario would reduce usable CaFCP bay space by 50%.

- Implemented conclusion that lowering air conditioning duct by eight feet would reduce the likelihood that pressure relief device failure would lead to hydrogen ignition in the CaFCP air conditioning system.
- Determined the maximum-recorded overpressure created by a 38.5 SCFM hydrogen leak in the bay was 0.17 psi at a distance of 1.5 ft from the centerline of the leak.
- Determined the maximum-recorded overpressure created by a 13 SCFM hydrogen leak under the full-scale model of the front half of a hydrogen-fueled bus was less than 0.03 psi.
- Developed a machine to produce a stream of helium-filled bubbles to track conservative path of rising gas.
- Determined maximum temperature rise on the backside of gypsum board during hydrogen flame impingement was 144°F.
- Determined residential garage could undergo 12 SCFM leak of hydrogen with proper venting and electrical restrictions.

Future Directions

- Determine proper separation distances for hydrogen facilities.
- Determine additional costs incurred when constructing hydrogen facilities.

Introduction

The goals and objectives of this work effort were developed anticipating the needs of various projects and authors of codes and standards. This work addresses potential safety concerns due to hydrogen leakage in three areas of hydrogen utilization. These safety concerns affect the widespread use of hydrogen in the private sector. The three areas of hydrogen utilization are as follows:

- Task A -- Safety Analysis of California Fuel Cell Partnership Building
- Task B -- Development of Method to Determine Hydrogen Sensor Placement
- Task C -- Safety Analysis for Writing of Codes

Approach

As noted in the above list of objectives, nine different questions were addressed in this year's work. The six questions of Task A dealt with potential modifications to the existing CaFCP building. Computer models of various accident scenarios involving hydrogen leaks inside the building resulted in two modifications. The models were used to define the problem and also to investigate potential solutions. Task B was the design and construction of a device to aid in hydrogen sensor placement. This was done by creating a helium soap bubble machine that created a stream of single helium soap bubbles. Running the machine, positioned at the location of a potential hydrogen leak, allows the operator to visualize a conservative estimate of how the gas cloud is affected by air circulation inside the enclosure. Task C employed experimental measurements of temperature rises produced by hydrogen flames impinging on gypsum board and the same computer modeling approach as used in Task A to aid in determining the effects of hydrogen gas leakage from a residential refueler.

Results

Examples of some of the results are shown in Figures 1 - 5. Figure 1 shows that a burnable cloud of hydrogen surrounds the electric motor, which opens the garage door, at the time the motor would be opening the door. The motor would likely ignite the cloud. The original hydrogen detection protocol was changed to prevent the problem. Figure 2 shows a burnable cloud of hydrogen filling the CaFCP A/C system (top of figure). Note the burnable mixture exiting the A/C vents on the floor. Since the A/C system would probably ignite the cloud, the A/C return duct was lowered to prevent the problem. Figure 3 shows the ignition of a 38.5 CFM leak of

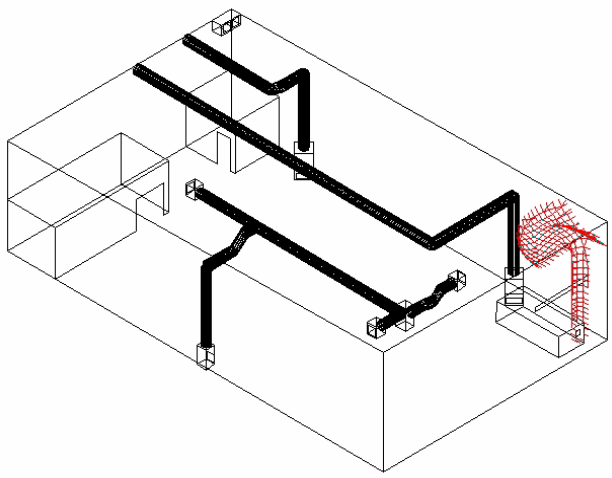

Figure 1. 4.1% Hydrogen Constant Concentration Surface for an 80 SCFM Leak after 16 Seconds with the A/C Off and 2100 SCFM

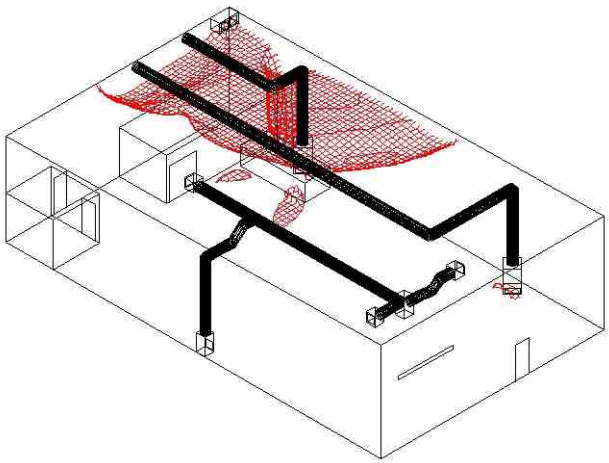

Figure 2. 4.1% Hydrogen Constant Concentration Surface for a PRD Failure after 10 Seconds with 4400 SCFM A/C Flow and 2100 SCFM Exhaust Fan Flow

hydrogen inside the bay. Resulting pressure rises were less than would result from bursting a child's balloon by overfilling it. Figure 4 shows the helium soap bubble machine designed to aid in visualizing hydrogen leakage and to assist in hydrogen sensor placement. Figure 5 shows hydrogen flames impinging on a gypsum board enclosure. Maximum temperature rise was 144°F.

Conclusions

- CaFCP Building - keep garage door in it's current position when hydrogen is detected

Figure 3. Ignition of 38.5 SCFM Hydrogen Leak in Bay

Figure 4. Helium Bubble Machine

to prevent motor from becoming ignition source.

- CaFCP Building - lower air-conditioning return duct to greatly reduce likelihood of hydrogen entering air-conditioning system.
- Hydrogen leaks up to 38.5 SCFM in buildings will not produce dangerous

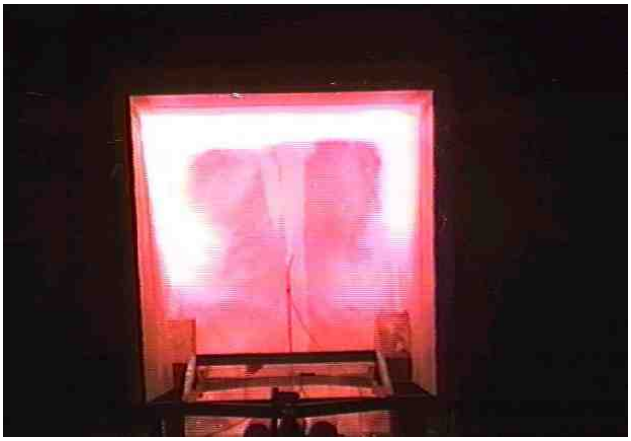

Figure 5. Gypsum Board Flame Impingement Test

overpressures if ignited as long as the building is ventilated well enough to prevent accumulation of hydrogen at the ceiling.

- Hydrogen leaks up to 13.0 SCFM under a vehicle will not produce dangerous overpressures if ignited as long as the hydrogen is not allowed to enter the vehicle and the undercarriage is properly shaped to vent hydrogen.
- A stream of helium filled soap bubbles can be utilized to visualize hydrogen leakage in an enclosure.
- Gypsum board resisted hydrogen flame impingement.
- Leakage of hydrogen from residential refueling system can be removed from garage with proper ventilation.

FY 2002 Publications/Presentations

1. "Hydrogen Leakage into Simple Enclosures", Swain, M.R., Filoso, P., Grilliot, E.S. and Swain, M.S., in publication in the International Journal of Hydrogen Energy

2. Invited Speaker, "The Safe Use of Hydrogen", National Fire Protection Association (NFPA), Anaheim California, May 12-16, 2001

3. Invited Panelist, "Hydrogen Venting" International Code Council (ICC) Ad hoc Committee, Denver Colorado, June 4-5, 2001

4. Invited Panelist, "CaFCP Building Safety Analysis", California Fuel Cell Partnership (CaFCP), Sacramento California, June 6-7, 2001

5. Invited Panelist, "Hydrogen Usage in Residential Garages", International Code Council (ICC) Ad Hoc Committee, Houston Texas, October 2-3, 2001

6. Invited Lecturer, for ICC Educational Session, Greensboro North Carolina, October 30-31, 2001

7. Invited Speaker, International Code Council draft code presentation, Pittsburgh Pennsylvania, April 18-19, 2002

VI.B.3 Hydrogen Codes and Standards

Jim Ohi (Primary Contact) and Russ Hewett
National Renewable Energy Laboratory
1617 Cole Blvd.
Golden, CO 80401
(303) 275-3706, fax: (303) 275-3886, e-mail: jim_ohi@nrel.gov

DOE Technology Development Manager: Neil Rossmeissl
(202) 586-8668, fax: (202) 586-5860, e-mail: Neil.Rossmeissl@ee.doe.gov

Objectives

- Expedite hydrogen infrastructure development.
- Coordinate infrastructure development activities, especially codes and standards, for the DOE Hydrogen, Fuel Cells, and Infrastructure Technologies Program.
- Incorporate hydrogen safety considerations into existing and proposed national and international codes and standards in order to facilitate market acceptance and penetration of the hydrogen technologies.

Approach

- Coordinate a collaborative national effort by government and industry to prepare, review, and promulgate hydrogen codes and standards.
- Bring together experts to address key issues and needs in national codes and standards workshops.
- Serve as a database repository, clearinghouse, and gatekeeper for the codes and standards activities being conducted within the DOE through the Hydrogen Codes and Standards Coordination Committee (HCSCC).

Accomplishments

- Established the DOE Hydrogen Codes and Standards Coordinating Committee (HCSCC) and conducted monthly conference calls and quarterly meetings.
- Aided the Hydrogen Ad Hoc Committee (HAHC) of the International Code Council (ICC) in developing and establishing support for the proposed changes to the ICC model codes regarding hydrogen.
- Completed first draft of a Hydrogen Codes and Standards Matrix and Database.
- Initiated work on a collaborative project with National Fire Protection Association (NFPA) to develop publications to assist local code officials.
- Assisted in the creation of the Hydrogen Technical Advisory Panel (HTAP) Hydrogen Safety Committee, contributing to the adoption of a charter, mission statement, and action plan.

Future Directions

- Continue the work of the HCSCC as the DOE focus for (a) coordinating codes and standards development efforts; (b) identifying and addressing codes and standards gaps and deficiencies; (c) identifying barriers with respect to getting codes and standards implemented; and (d) working with codes and standards development organizations to overcome such barriers.
- Facilitate incorporation of changes in the family of ICC model codes proposed by the HAHC.

- Continue working with the Society of Automotive Engineers (SAE) and NFPA to facilitate development and dissemination of standards for transportation and stationary applications, respectively.

Introduction

The development and promulgation of codes and standards are essential if hydrogen is to become a significant energy carrier and fuel; codes and standards are critical to establishing a market-receptive environment for commercializing hydrogen-based products and systems. DOE's Hydrogen, Fuel Cells, and Infrastructure Technologies Program and the National Renewable Energy Laboratory, with the help of some key stakeholders, are coordinating a collaborative national effort by government and industry to prepare, review, and promulgate hydrogen codes and standards needed to expedite hydrogen infrastructure development.

Approach

This project involves coordinating codes and standards development efforts on a number of fronts, including: (1) working collaboratively with codes and standards developing organizations; (2) keeping track of the development of hydrogen technology for various applications; (3) working collaboratively with technology developers to identify critical codes and standards needs; (4) articulating codes and standards needs, and working to get needed efforts underway; and (5) conducting technology transfer activities targeted at building-code and fire-safety officials, local/state/Federal policymakers and other strategic stakeholders.

Results

International Code Council's Hydrogen Ad-Hoc Committee

The International Code Council (ICC) is a joint venture of the three major code councils in the U.S., established to develop uniform national model building codes. The existing ICC model codes do not include hydrogen as an energy source or fuel cells as either power-generating devices or as appliances. To address this limitation, the ICC has established an Ad-Hoc Committee (HAHC) on hydrogen technologies. The HAHC is working with a diverse group of technical and advisory parties to review current codes and standards applicable to hydrogen, to determine the adequacy of its coverage in the ICC International Codes, and to propose changes as necessary. The HAHC has prepared proposed amendments to the ICC model Building, Fire, Electrical, Mechanical, and Fuel Gas codes for hydrogen that will be up for final consideration at the ICC Code Hearing in October 2002.

DOE Hydrogen Codes and Standards Coordination Committee

The DOE Hydrogen Codes and Standards Coordination Committee (HCSCC) was established with the mission of coordinating the development and implementation of a consistent set of hydrogen-related codes and standards that will ensure the safe production, delivery and use of hydrogen, and facilitate the accelerated commercialization of hydrogen technologies. Since its creation, the HCSCC has held monthly conference calls to update participants on current activities and to discuss key issues. The HCSCC has also convened two quarterly meetings in Washington, D.C. The HCSSC is planning to conduct workshops, which will provide a forum for organizations involved in hydrogen codes and standards development to identify the activities, gaps, and opportunities in this effort.

DOE Hydrogen Technical Advisory Panel

The Hydrogen Technical Advisory Panel (HTAP) Safety Committee was established in 2001 to provide a national forum to discuss critical issues in hydrogen safety, including codes and standards. Over the last year, the committee held both an annual and regional Hydrogen Safety Summit to define the current baseline on hydrogen safety capability and to identify critical codes and standards needs and priorities. At the national Hydrogen Safety Summit, scheduled for October 2002, the committee plans to present and discuss a National Hydrogen Safety Agenda.

Partnership for Advancing the Transition to Hydrogen

The DOE is sponsoring the Partnership for Advancing the Transition to Hydrogen (PATH) to coordinate codes and standards activities among key countries outside of the European Union. To date, Canada, Japan, and the U.S. have made commitments to join PATH. An organizational meeting was held at the World Hydrogen Energy Conference (WHEC) in June 2002. The DOE is funding the administrative costs for at least the first year of PATH and providing technical support.

Outreach

Public education and information dissemination on hydrogen safety are key components of the DOE hydrogen effort. As a continuing part of its coordination effort, the DOE is providing support to the National Hydrogen Association (NHA) to publish a monthly electronic letter covering codes and standards activities and issues for the U.S. hydrogen community. The DOE co-sponsored a new educational video, Hydrogen Energy: The Safe and Clean Alternative, which is targeted at the general public and was premiered at the WHEC. The DOE is also sponsoring outreach efforts to building and fire code officials by developing seminars, training, and handbooks on permitting hydrogen facilities.

Conclusions

- The DOE has supported a growing and increasingly important effort to coordinate the development and promulgation of hydrogen codes and standards.
- In addition to supporting specific projects to develop codes, such as that of the ICC/ HAHC, and standards, such as that of ISO TC197, the Program is supporting the coordination of many other efforts so that codes and standards can be developed and adopted as efficiently as possible and so that the lack of codes and standards will not be a barrier to the commercialization of hydrogen technologies.
- There are many government and non-government organizations independently involved in generating codes and standards, thus support of codes and standards efforts will remain an important part of the Hydrogen, Fuel Cells, and Infrastructure Technologies Program for many years to come.

VI.B.4 SAE Fuel Cell Codes and Standards Initiative

Anthony Androsky
SAE International
1300 Eye St. NW
Suite 1090 East Tower
Washington, DC 20005-3314
(202) 962-8684, fax: (202) 962-8692, e-mail: tandrosky@sae.org

DOE Technology Development Manager: Neil Rossmeissl
(202) 586-8668, fax: (202) 586-5860, e-mail: Niel.Rossmeissl@ee.doe.gov

ANL Technical Advisor: Walter Podolski
(630) 252-7558, fax: (630) 972-4430, e-mail: podolski@cmt.anl.gov

Objectives

- Facilitate and accelerate the development of codes, standards, and recommended practices for fuel cell powered vehicles in order to smoothly and uniformly transition fuel cell vehicles into the marketplace.

Approach

- Directly support the SAE Fuel Cell Committee and its seven working groups and establishment of new groups where required.
- Develop liaisons, collaborations, and cooperative working agreements with technical topic area organizations (e.g. U.S. Fuel Cell Council, National Fire Protection Association, The Methanol Institute).
- Directly support Cooperative Research Projects for development and verification of pre-competitive data for use in codes, standards and recommended practices.
- Support workshops and meetings to facilitate expert advisor input
- Support technical expert advisors as needed by the SAE Standards Committee, working groups and SAE Cooperative Research Projects.

Accomplishments

- J2572, Recommended Practice for Measuring the Exhaust Emissions, Energy Consumption and Range of Fuel Cell Powered Electric Vehicles Using Compressed Gaseous Hydrogen (draft)
- J2574, SAE Information Report - Fuel Cell Electric Vehicle Terminology (published)
- J2578, Recommended Practices for General Fuel Cell Vehicle Safety (published)
- J2579, Recommended Practices for Hazardous Fluid Systems in Fuel Cell Vehicles (draft)
- J2594, Fuel Cell Recyclability Guidelines (in ballot)
- J2600, Compressed Hydrogen Vehicle Fueling Connection Devices (published)
- J2601, Compressed Hydrogen Vehicle Fueling Communication Devices (draft)
- J2615, Performance Test Procedures of Fuel Cell Systems for Automotive Applications (final draft)
- J2616, Performance Test Procedures for the Fuel Processor Subsystem of Automotive Fuel Cell System (draft)
- J2617, Performance Test Procedures of PEM Fuel Cell Stack Subsystem for Automotive Applications (final draft)

- Agreement with the IEC TC105 WG-#6
- Memorandum of Understanding (MOU) with the JEVA (Japanese Electric Vehicle Association)
- Working Relationship with the EIHP-II (European Integrated Hydrogen Project)
- Inclusion of the SAE within the dialogue of the GCG (Global Cooperation Group)
- MOU with the National Fire Protection Association

Future Directions

- The intent of this activity is to assist in providing a safe, reliable product to the public by way of a responsible, industry friendly climate that is environmentally sound, i.e., development of Standards, Codes and Recommended Practices that enable commercialization of automotive fuel cell applications.

Introduction

As with any new technology that is attempting to move towards commercialization, the establishment of standards, codes and recommended practices is a major concern. If done through a widely accepted consensus process that leads credence to industry endorsed, globally accepted rule making-- then standards development becomes the leveraging shoehorn that allows for the perfect fit, and enables marketplace acceptance and ease of commercialization.

In early 1999, the fuel cell literate world had no clear, defined direction or globally accepted leadership in standards development for transportation applications of fuel cells. In fact, the major standards development organizations, both domestic and international, were anticipating a "not recommended landscape" of work duplication, mismatched data, non-consensus documents and chaos that would certainly inhibit commercialization and negatively impact rulemaking.

The introduction in mid-1999 of the SAE Fuel Cell Standards Initiative and establishment of the SAE Fuel Cell Standards Forum changed the climate of standards development for vehicles. Not only did the U.S. outlook take on a positive source of urgency, but also the SAE Fuel Cells Forum was quickly recognized as the global leader by the European and Pacific concerns.

Approach

The SAE will initiate, facilitate, develop and publish required standards and standards processes for fuel cell powered vehicles.

The SAE has formed and will form relationships with sectors, organizations and committees that effect or are affected by fuel cell technology for vehicles. These include, but are not limited to, vehicle manufacturers and their suppliers, fuel cell manufacturers and their suppliers, energy providers and their suppliers, national and international government agencies and other organizations involved with the development of the necessary and ancillary infrastructure and support facilities/ structures.

Deliverables will include draft recommended practices and codes and standards as applicable that are necessary for the operation of fuel cell powered vehicles (Figures 1 and 2).

SAE will utilize a fuel cell standards group and others to accomplish deliverables. The Fuel Cell Standards Group will be chartered on the following premise:

> To establish standards and test procedures for fuel cell powered vehicles. The standards will cover safety, performance, reliability and recyclability of fuel cell systems in vehicles with emphasis on efficiency and environmental impact. The standards will also establish test procedures for uniformity in test results for the

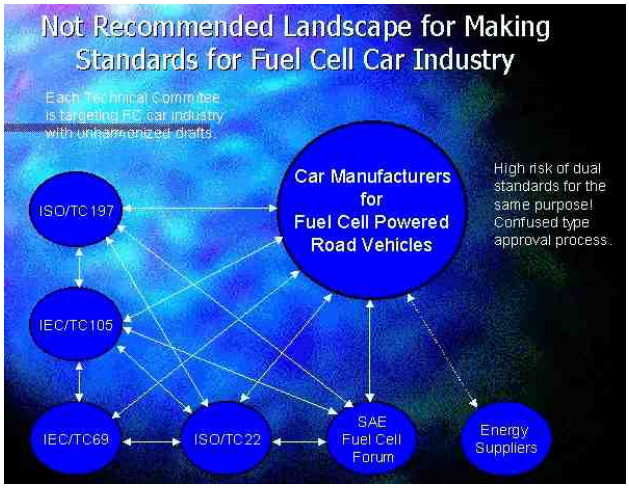

Figure 1. Not Recommended Landscape for Vehicle Standards Development

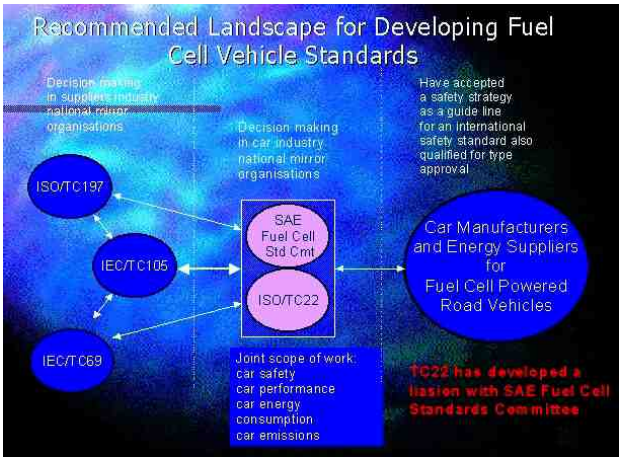

Figure 2. Recommended Landscape for Vehicle Standards Development

vehicles/systems/components performance, and define interface requirements of the systems to the vehicles.

The Fuel Cell Standards Group includes the following working groups: safety**,** performance**,** emissions, interface, terminology, and recyclability. These working groups include representatives from automotive original equipment manufacturers (OEMs), automotive OEM suppliers, fuel cell developers/manufacturers, fuel cell manufacturer suppliers, energy suppliers, energy supplier providers, government agencies and national and international organizations that are related to fuel cell industry and infrastructure.

The SAE Fuel Cell Standards Group will collaborate or liaison directly with ISO/TC22 and ISO/TC 22 SC21, IEC/TC105, IEC/TC105 WG6, IEC/TC 69, ISO/TC 197, and ISO/TC 58. The SAE Fuel Cell Standards Group will work cooperatively with U.S. Fuel Cell Council, National Hydrogen Association, Canadian Hydrogen Association, Japanese Electric Vehicle Association (JEVA), American Petroleum Institute, Underwriters Laboratory, CSA International, US Air Force, US Army, National Laboratories, US Air Force Research Labs, and the US Air Force Alternate Fuel Initiative among others directly or indirectly involved in fuel cells for transportation applications and its support infrastructures.

Results

The Emissions & Fuel Consumption working group's mission is to establish standards and test procedures for measuring emissions and fuel consumption for fuel cell powered vehicles. The standards and test procedures to be created will provide methods for measuring exhaust and evaporative emissions, plus the fuel consumption measurement for the fuel cell vehicle. The goal is to establish methodology for uniformity in test results for all designs of fuel cell vehicles, and allow a comparison with conventional vehicles. J2572 is the first document that this working group is completing. This document is for fuel cell vehicles using compressed hydrogen gas supplied by an off-board source and stored as a compressed gas onboard. The procedure includes hybrid (use of a storage battery for traction power) versions of fuel cell vehicles. The working group will address fuel cell vehicles that have a reformer on-board to produce hydrogen once J2572 is completed.

The Interface working group was created to develop standards to coordinate between fuel suppliers and vehicle manufacturers to ensure safe, efficient and customer friendly delivery of fuel to fuel cell powered vehicles. Topics to be covered include fuel supply, infrastructure, fuel storage, fuel processor and vehicle interface. The Interface working group has two draft standards in progress, J2600 and J2601. J2600, Compressed Hydrogen

Vehicle Fueling Connection Devices, defines the geometries of the receptacles for different pressure levels. It has been successfully balloted, with a 98% APPROVAL rating and NO DISAPPROVAL ballots. J2601, Compressed Hydrogen Vehicle Fueling Communication Devices, will define the different fueling strategies and document their advantages and disadvantages with respect to type III and IV tanks. It will also develop the strategies and protocols for what refueling with and without communications should look like. In addition, it will identify what technology wireless communication should utilize to be most effective in an automotive environment. Data is being collected for this draft standard. It is targeted is to be completed in the second quarter of 2003.

Developing a guidance document that incorporates and summarizes existing recyclability measurement techniques and identifies recyclability issues associated with fuel cells in End of Life Vehicles (ELVs) is the goal of the Recyclability working group. J2594, Fuel Cell Recyclability Guidelines is currently under final pre-ballot review by the Fuel Cell Standards committee.

To recommend design and construction, operation, emergency response and maintenance practices for the safe use of fuel cell vehicles by the general public is the goal of the Safety working group. J2578 is the first safety document that covers the general safety of the vehicle. J2578 has already been successfully balloted. However, in the attempt to address all participating comments, the committee has agreed to incorporate, where applicable, this new information. The document is currently under its second ballot and is expected to be APPROVED by a unanimous ballot (100% approval rating). J2579, Fuel Systems for Fuel Cell Vehicles, is the second document the safety working group currently has under work.

The first document of the SAE Fuel Cell Standards Committee to be completed was developed by the Terminology working group. J2574, Fuel Cell Terminology Report, was balloted in September 2001. It is used world wide as a reference source and foundation document for all of the Vehicle Fuel Cell Standards efforts. This report defines terminology for fuel cell powered vehicles.

The mission of the Performance working group is to develop procedures for testing the Proton Exchange Membrane (PEM) fuel cell system and its major subsystems for automotive applications. The working group currently has three draft standards under development, J2615, J2616 and J2617. The Performance task group is defining performance and measured parameters for three test subjects: PEM fuel cell system, fuel processor and PEM fuel cell stack. Major subsystems of the PEM fuel cell system are the following: fuel processor, fuel cell stack, air processor, thermal management, water management and electronic controller. Test procedures are being developed for both steady state and transient (start-up and load following) performance measurements. Instrumentation to be used, pre-test procedures to ensure safety in testing, limitations of test procedures and methods of calculating and reporting results will all be addressed in the documents. The target completion date for these three documents is 2002.

Conclusions

The continued work of the SAE Fuel Cell Standards committee and its working groups, has provided the single point of reference to all agencies, U.S. or global, in regards to standards pertaining to transportation/mobility applications. As the proliferation of fuel cell vehicles gains momentum, the need for standardization becomes critical. Regulation and rule-making, coupled with growing interest in global technical regulations (GTRs) in many countries, cause an urgent demand for foundation data and documents. The SAE committee remains the best near term solution to address and provide this needed data and source documentation.

Section VII. Conversion Devices

VII.A Conversion Devices - Turbines

VII.A.1 Reduced Turbine Emissions using Hydrogen-Enriched Fuels

Robert Schefer (Primary Contact), Joe Oefelein
Sandia National Laboratories
7011 East Ave
Livermore CA 94550
(925) 294-2681, fax: (925) 294-2595, e-mail: rwsche@sandia.gov

DOE Technology Development Manager: Neil Rossmeissl
(202) 586-8668, fax: (202) 586-5860, e-mail: Neil.Rossmeissl@ee.doe.gov

Objectives

- Quantify effect of hydrogen addition on flame stability, combustor acoustics, emissions and efficiency in a gas turbine.
- Establish a scientific and technological database for lean combustion of hydrogen-enriched fuels.
- Establish numerical simulation capabilities that will facilitate design optimization of hydrogen and hydrogen-enriched lean gas turbine combustors.
- Develop criteria for use of hydrogen addition as a control knob to eliminate instabilities related to varying product gas composition.

Approach

- Design and fabricate a lean premixed swirl burner that simulates the basic features of gas turbine combustors.
- Apply advanced experimental diagnostics to understand fluid dynamics, combustion chemistry, and pollutant formation.
- Develop a computational model for combustor performance in parallel with an experimental project based on next generation Large Eddy Simulation (LES) technique. Use experimental database for model validation.
- Identify problem areas in practical gas turbine combustors where hydrogen enrichment of hydrocarbon fuels could be beneficial.

Accomplishments

- Completed design and fabrication of lean premixed swirl burner that will be used to study combustion of H_2-blended hydrocarbon fuels in stationary gas turbine environment. (Collaboration with the National Energy Technology Laboratory).
- Completed design and fabrication of prototype H_2/air burner for aircraft gas turbine applications. Characterized relationship between flame and fluid dynamics and evaluated fuel/air mixing. (Collaboration with NASA Glenn.)
- Formed collaboration with General Electric Aircraft Engines (GEAE) to evaluate production fuel injector for use with hydrogen-blended fuels.
- Developed international effort through the International Energy Agency (IEA) to address aspects of H_2-enriched hydrocarbon fuels for low emission, high efficiency gas turbine combustion.

Future Directions

- Assess and verify the flow, flame characteristics and dynamic stability limits of the lean premixed hydrogen swirl burner.
- Establish a representation of the turbulent recirculating flow characteristics in the swirl burner using the LES model approach.
- Establish a framework for modeling hydrogen-enriched lean premixed combustion in the presence of acoustically active flame processes.
- Complete development of test matrix for GEAE swirlcup fuel injector and perform testing. Identify areas where hydrogen enrichment could be beneficial.
- Continue the formation of a broad consortium of industrial partners.
- Continue development of international collaborations, both directly and through the IEA.

Introduction

The development of advanced combustion capabilities for gaseous hydrogen and hydrogen-blended hydrocarbon fuels in gas turbine applications is currently an area of much interest. Driving this interest are several needs. One need is the cost-effective utilization of alternative fuels with a wide range of heating values. For example, fuels containing significant hydrogen are often produced as a by-product in Coal-Gasification Combined Cycle installations. These product gases could provide a significant source of cost-effective fuels for gas turbines. A second need is related to the recognition that ultra-lean premixed combustion is an effective approach to NO_x emissions reduction from gas turbine engines. Hydrogen blended with traditional hydrocarbon fuels significantly improves flame stability during lean combustion and allows stable combustion at the low temperatures needed to minimize NO_x production.

A longer-term need is to eliminate unburned hydrocarbon (UHC) and CO_2 emissions. Gas turbines account for 20% of U.S. CO_2 emissions, which is a significant fraction of the total current CO_2 emissions. This number will increase as natural gas turbines replace older coal-fired steam generation plants. The use of hydrogen-blended hydrocarbon fuels thus provides both a solution to the immediate need for NO_x reduction, and also provides a transition strategy to a carbon free energy system in the future.

Approach

The addition of hydrogen to hydrocarbon fuels affects both the chemical and physical processes occurring in flames. These changes affect flame stability, combustor acoustics, pollutant emissions, and combustor efficiency. Few of these issues are clearly understood. This project will investigate issues surrounding hydrogen and hydrogen-enriched hydrocarbon fuel use and will include studies of chemical kinetics, fluid dynamics and flame structure to better define and understand these issues. Both experimental and modeling approaches are being utilized. The experimental data will be obtained using an array of advanced laser diagnostic techniques that provide information on flame structure, fluid dynamics, combustion gas species concentrations and temperature. These measurements, in addition to providing direct insights into the effects of hydrogen enrichment on combustion and pollutant emissions, will provide the technological database needed for the parallel development of a numerical code, based on the LES technique, to simulate lean premixed combustion of hydrogen and hydrogen-enriched fuels. Close collaborations have been developed with industrial partners to provide a mechanism for the transfer of this technology to practical applications in stationary and aircraft gas turbines. These collaborations will facilitate the identification of problematic areas related to practical gas turbine design and hardware. Areas where hydrogen addition could prove beneficial will be identified, and the potential merits of hydrogen-enriched hydrocarbon fuels will be demonstrated.

Results

The design and fabrication of a lean premixed swirl burner representative of land-based industrial applications was completed. This burner will be used to study combustion of hydrogen and hydrogen-blended hydrocarbon fuels. The design emphasizes well-characterized flow and boundary conditions to facilitate the development of a database for LES model validation. Emphasis with regard to LES has been placed on providing support calculations for design purposes and establishing an initial baseline-modeling framework for treatment of hydrogen-enriched, premixed methane flames. This burner is shown in Figure 1. The burner design is operationally relevant to industrial devices and is optimally tuned for flow and diagnostic capabilities at the Sandia Combustion Research Facility.

The design and fabrication of a prototype hydrogen/air burner for aircraft gas turbine applications was completed in collaboration with NASA Glenn. The stability and burning characteristics of fuel-lean hydrogen/methane/air flames were characterized over a range of operating conditions. Figure 2 shows the effect of hydrogen addition on flame stability, where the variable n_{H2} is the fraction of hydrogen in the fuel (n_{H2}=0 corresponds to pure methane and n_{H2}=1 is pure hydrogen). The equivalence ratio is a measure of the fuel/air ratio. These measurements were obtained by igniting the flame and then decreasing the fuel/air ratio until the flame is completely extinguished, or is blown out. The flame typically becomes unstable as the blowout condition is approached. Increasing the hydrogen content from 70% to 100% results in a significant shift in flame blowout conditions to leaner fuel/air ratios. Since operation at leaner fuel/air ratios results in a lower flame temperature and reduced NO_x emissions, it is clear that hydrogen addition allows stable operation at the lean operating conditions needed to limit NO_x emissions. Mixing of the fuel and air is also important, since incomplete mixing leads to higher flame temperatures, increased NO_x and lower efficiency. Planar Laser Induced Fluorescence (PLIF) measurements of acetone, which was added as a fuel tracer, were obtained to evaluate the mixing of the fuel and air. Based on these measurements, design improvements will be identified and implemented. PLIF measurements of the hydroxyl (OH) radical, which is important to flame chemistry, were obtained to characterize the relationship between the flame and fluid dynamics.

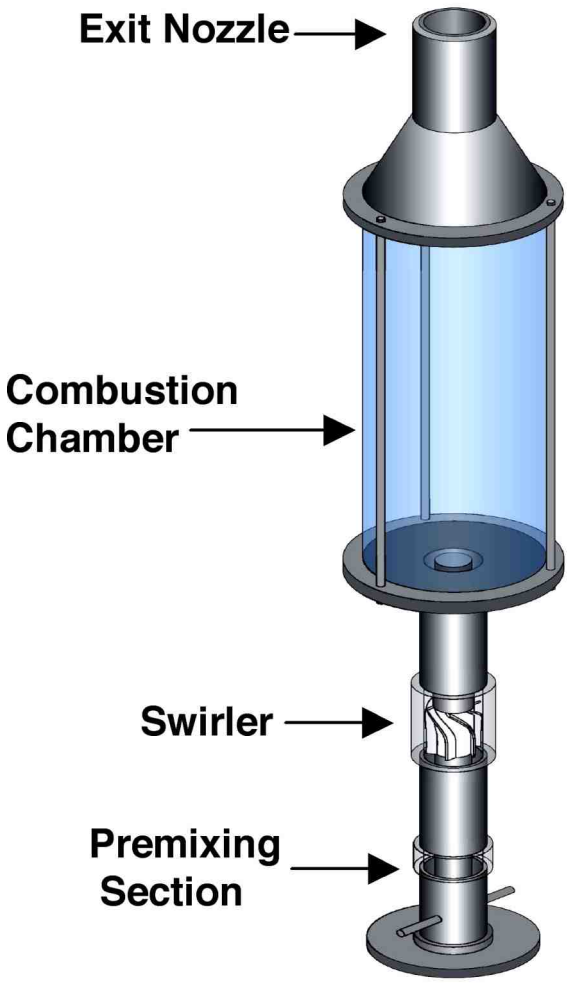

Figure 1. Lean premixed swirl burner designed to study combustion of hydrogen and hydrogen-blended hydrocarbon fuels.

The use of hydrogen addition to natural gas feedstocks of midsize (30-150 megawatt) gas turbines was analyzed as a method of reducing NO_x. Cost comparisons were made with current control technologies for both existing and new systems to determine its benefits and market feasibility. Less than 3 ppm NO_x should be achievable with 15% H_2 addition. The comparisons in Figure 3 show that 15% H_2 addition is cost competitive with both conventional Selective Catalytic Reduction (SCR) and high temperature SCR over a wide range of plant

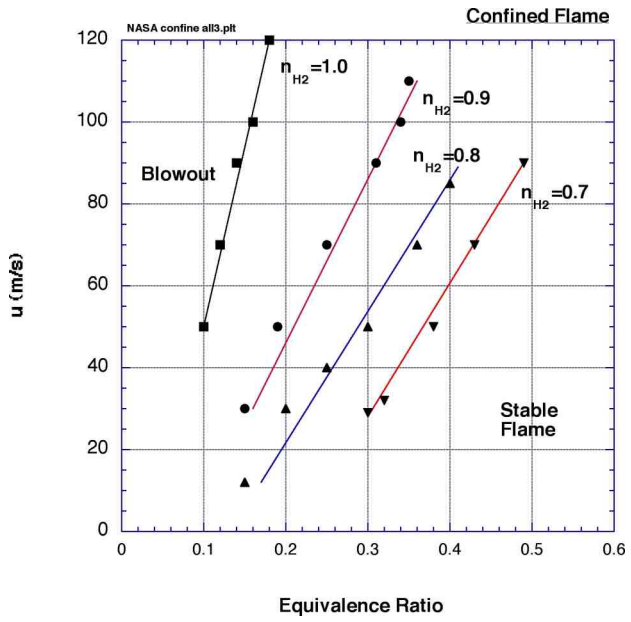

Figure 2. Effect of Hydrogen Addition on Flame Stability in Prototype Hydrogen/Air Burner

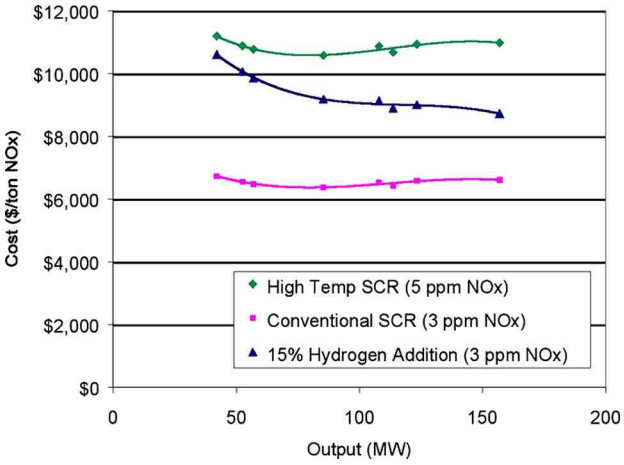

Figure 3. Cost Comparison of 15% Hydrogen Addition with Current NO_x Control Technologies

power outputs. Higher levels of hydrogen addition, while somewhat more expensive, should offer even lower NO_x emissions.

Conclusions

- Hydrogen addition significantly improves flame stability and allows stable burner operation at the lean fuel/air ratios needed for reduced NO_x emissions.
- Hydrogen addition for NO_x reduction to the 3 ppm level is cost competitive with current control technologies and has the potential to reduce NO_x emissions lower than any other control strategy.

Publications

1. R. W. Schefer, D. M. Wicksall and A. K. Agrawal: "Combustion of Hydrogen-Enriched Methane in a Lean Premixed Swirl-Stabilized Burner", Proceedings of the 29th Symposium (International) on Combustion, (2002).

2. R. W. Schefer: "Hydrogen Enrichment for Improved Lean Flame Stability", International Journal of Hydrogen Energy (accepted) 2002.

3. R. W. Schefer: "Reduced Turbine Emissions using Hydrogen-Enriched Fuels", Proceedings of the U.S. DOE Hydrogen Program Review, May 6-8, Boulder CO (2002).

Presentations

1. R.W. Schefer: "Reduced Turbine Emissions using Hydrogen-Enriched Fuel", 14th World Energy Conference, Montreal, Quebec, Canada, June 9-13, 2002.

2. C. Termaath, E. Skolnick, J. O. Keller and R. W. Schefer: "Emissions Reduction Benefits from H_2 addition to Midsize Gas Turbine Feedstocks", 14th World Energy Conference, Montreal, Quebec, Canada, June 9-13, 2002.

VII.B Internal Combustion Engines

VII.B.1 Internal Combustion Engines Research And Development

Peter Van Blarigan
Sandia National Laboratories
7011 East Ave
Livermore, CA 94550
(925) 294-3547, fax: (925) 294-1322, e-mail: pvanbla@sandia.gov

DOE Technology Development Manager: Neil Rossmeissl
(202) 586-8668, fax: (202) 586-5860, e-mail: Neil.Rossmeissl@ee.doe.gov

Objectives

- Design and demonstrate high efficiency, low emissions hydrogen fueled 30 kW electrical generator
  - 50% fuel to electricity conversion efficiency and near-zero emissions

Approach

- Utilize highly developed piston engine technology
- Combine free-piston, linear alternator and homogeneous charge compression ignition to achieve the following:
  - Ideal Otto cycle performance
  - Electronic compression ratio control
  - NO_x control by low equivalence ratio

Accomplishments

- Developed full-scale linear alternator test capability
- Designed two-stroke cycle scavenging system
- Completed analysis of power density and performance for aircraft applications (NASA funded)
- Evaluated 2 kW size combustion experiment (Sandia LDRD funded)

Future Directions

- Complete scavenging system experiment fabrication and testing
- Develop comprehensive system model
- Quantify linear alternator performance
- Form industrial consortium for commercial application

Introduction

Electrical generators capable of high conversion efficiencies and extremely low exhaust emissions will no doubt power advanced hybrid vehicles and stationary power systems. Fuel cells are generally considered to be ideal devices for these applications where hydrogen or methane is used as fuel. However, the extensive development of the internal combustion engine and the existence of repair and maintenance industries associated with piston engines provide strong incentives to remain with this technology until fuel cells are proven reliable and cost competitive. In addition, the fuel cell may not

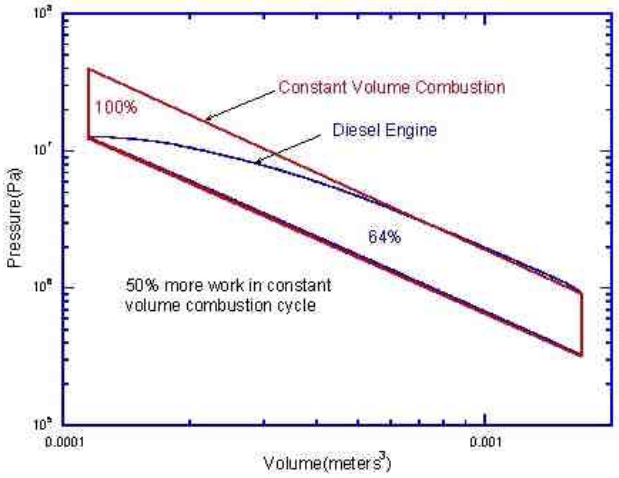

Figure 1. Modern 4-Stroke Heavy Duty Diesel Engine

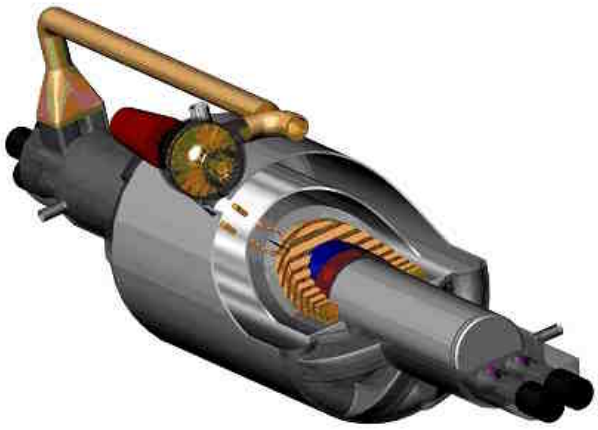

Figure 2. Free-Piston Linear Alternator

offer significant efficiency advantages relative to an optimized combustion system.

In Figure 1, the amount of work attained from a modern 4-stroke heavy-duty diesel engine is shown. The results indicate that under ideal Otto cycle conditions (constant volume combustion), 56% more work is available than from an ideal constant pressure combustion (ideal diesel) cycle. This extreme case of non-ideal Otto cycle behavior serves to emphasize how much can be gained by approaching constant volume combustion systems.

Approach

The free-piston linear alternator illustrated in Figure 2 has been designed in hopes of approaching ideal Otto cycle performance through homogeneous

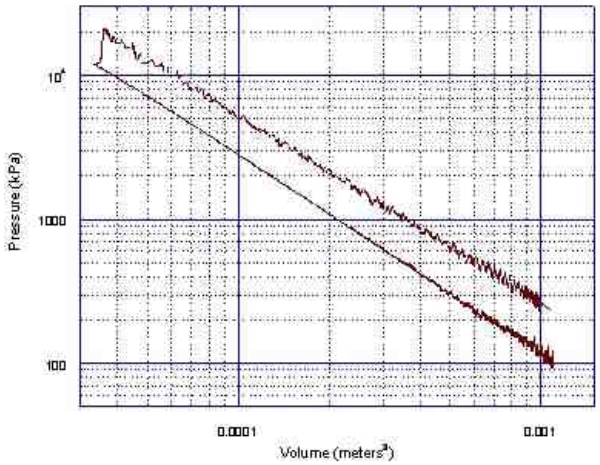

Figure 3. Hydrogen HCCI Combustion using the RCEM

charge compression ignition (HCCI) operation. In this configuration, high compression ratios can be used and rapid combustion can be achieved.

The linear alternator is designed such that electricity is generated directly from the piston's oscillating motion. Combustion occurs alternately at each end of the piston, and a modern two-stroke cycle scavenging process is used. The alternator component controls the piston's motion and, thus, the extent of cylinder gas compression. Compression of the fuel/air mixture is achieved inertially, and as a result, a mechanically simple, variable compression ratio design is possible with sophisticated electronic control.

The combination of the HCCI combustion process and the free-piston geometry is expected to result in significant improvements in the engine's thermal efficiency and its exhaust emissions.

Combustion System - Tests

Figure 3 shows the result of one of the HCCI combustion analyses. In this investigation, a single-stroke rapid compression-expansion machine (RCEM) was used to compression ignite homogeneous fuel/air mixtures. The piston, for all practical purposes, does not move during the combustion event. In the free-piston configuration, high pressure-rise rates can be handled without difficulty since there are no load-bearing linkages, as in crankshaft-driven engines.

Figure 4. Alternator Tester

Results - Linear Alternator

Two parallel paths are being pursued to develop the linear alternator. First, an alternator is being designed, built and tested in-house. In parallel, Magnequench, Inc. has designed and fabricated an alternator for this application. Both alternators will be tested under full design output conditions. A picture of the alternator tester is presented in Figure 4.

Two Stroke-Cycle Scavenging System

Our approach is to utilize multi-dimensional modeling (KIVA–3V) to design the scavenging system and then to validate the computational predictions for selected operating conditions with the use of a single-cycle scavenging experiment.

Important goals to be achieved with the scavenging design are high scavenging efficiency (η_{sc}>90%) and high trapping efficiency (η_{tr}>97%).

For the computational study, inverted-loop and uniflow scavenging methods were investigated. A loop-scavenged option was investigated first due to its potential for a mechanically simple system.

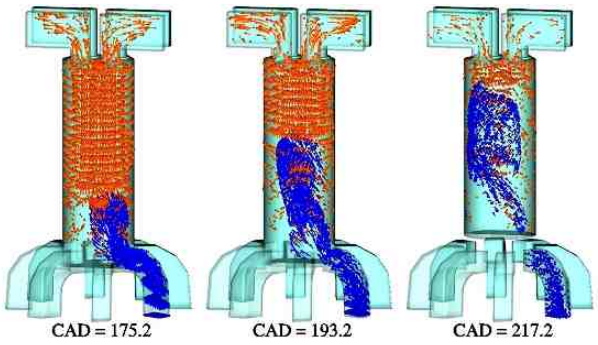

Figure 5. KIVA-3V Calculated Uniflow Scavenging

However, the mixing dynamics encourages fuel short-circuiting through the exhaust port. Additionally, for the configurations considered either high pumping losses or low power output must be accepted in order to achieve adequate cylinder charging.

An inverted-loop option was investigated next, with the intent of improving the trapping characteristics by placing the inlet ports above the exhaust ports. However, KIVA results showed the cylinder cannot be adequately charged, and a low scavenging efficiency (η_{sc}~0.45) and highly stratified charge result at the time of combustion.

The final scavenging option studied was a uniflow arrangement. In this configuration, four exhaust valves are located in the cylinder head, with intake ports located circumferentially around the bottom of the cylinder. Variation of the inlet port geometry and exhaust valve timing resulted in a more acceptable 83% scavenging efficiency with less than 1% short-circuiting of the inlet flow. Further, a low driving pressure can be used to adequately recharge the cylinder. An example of the in-cylinder flows for this arrangement is shown in Figure 5.

NASA Study

NASA-Langley requested assistance from Sandia to determine the feasibility of free-piston electrical generators in providing propulsive power for aircraft. The concept is to distribute generators throughout the aircraft and utilize electric motor powered fans to propel the aircraft.

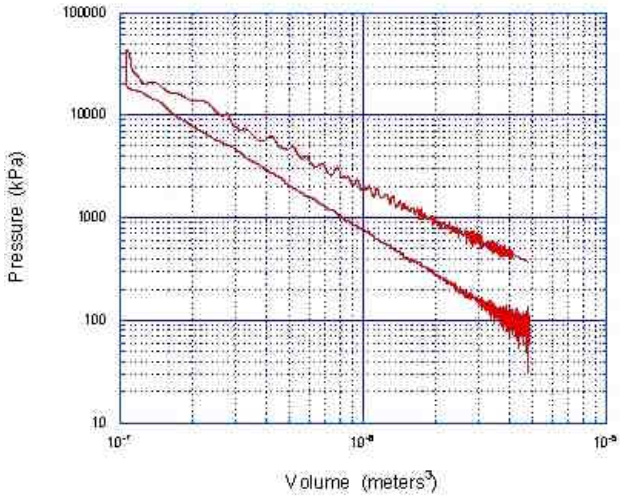

Figure 6. HCCI Combustion using the Small RCEM

One discovery made during this study was that while turbocharging the engine does not allow significantly increased power output per stroke due to peak pressure limitations, it does appear to be capable of providing all of the pumping work necessary to scavenge the combustion chamber. The result of this is that we will incorporate a turbocharger into the baseline 30 kW prototype design.

Another interesting discovery was that increased boost pressures with hotter fuel/air mixtures can maintain peak pressures similar to unboosted operation, but this results in significantly increased oscillation rates, which in turn increase the power output of the device.

Reduced-Size HCCI Combustion System

Another area for which the Advanced Generator Program has additional support is the investigation of a greatly reduced power output device. Funding is through internal laboratory sources with the objective of determining if the free-piston approach would work well for a single-occupancy vehicle that requires only 2 kW of output power. A small, rapid compression-expansion machine was fabricated with a bore of 1.2 cm, compared to the larger RCEM dimension of 7.6 cm. Figure 6 shows the near Otto cycle performance achieved, which is similar to that shown in Figure 3. Efficiencies were comparable to the 30 kW experiment.

Conclusions

A novel combustion-driven reciprocating electrical generator has been designed to produce 50% fuel to electricity conversion efficiency and essentially zero emissions. The prototype design is moving forward, with quantification of the performance of each piece of the prototype proceeding. To date no unsolvable technical barriers have materialized.

VII.B.2 HCNG Heavy Duty Vehicle Prime Mover

Kirk Collier (Primary Contact), Neal Mulligan, Ranson Roser
NRG Tech
681 Edison Way
Reno, NV 89502
(775) 857-1937, fax: (775) 857-1938, e-mail: kcollier@nrgtech.com

DOE Technology Development Manager: Sigmund Gronich
(202) 586-1623, fax: (202) 586-5860, e-mail: Sigmund.Gronich@ee.doe.gov

Objectives

- Develop a low-emissions heavy-duty vehicle engine package to seamlessly repower today's buses and trucks with existing natural gas and diesel engines.
- Exceed DOE's goal of reducing 1998 emission standards by 75% by achieving 99.5% reduction. Carbon monoxide (CO) emissions will be <1 ppm, non-methane hydrocarbon (NMHC) emissions will be <0.05 g/hp-hr, and oxides of nitrogen (NO_x) will be <0.15 g/hp-hr.
- Maintain or enhance current vehicle driveability by effective selection, matching, and configuring of off-the-shelf components.
- Maintain thermal efficiency of greater than 35%.
- Prove and enhance the engine design through in-service testing.
- Develop a public/private partnership to implement a commercialization plan that will bring new business and economic opportunities to Nevada.

Approach

- Use hydrogen added to the natural gas fuel mixture to achieve high charge dilution ratios to create near-zero NO_x emissions.
- Incorporate an alternative engine design from that of current heavy-duty engines which includes:
  - Nickel silicon carbide cylinder bores
  - Quiescent combustion
  - Higher rpm operation
  - Larger displacement
  - Mass air flow engine control

Accomplishments

- Demonstrated 0.22 g/hp-hr NO_x simulated driving cycle emissions
- Produced equivalent power and torque to natural gas engine
- Demonstrated 36% engine efficiency

Future Directions

- Expand the work to convert five additional City of Las Vegas Buses to HCNG

Introduction

The use of hydrogen as a fuel additive to extend the lean burn limit of conventional fuels has been repeatedly demonstrated to be a viable approach to achieving near-zero exhaust emissions from internal combustion engines. This technology is intended to be a near-term application for hydrogen and hydrogen infrastructure development given the current economic climate. Hydrogen fuel-related problems such as high fuel cost, high prime mover costs (fuel cells) and low energy density are largely overcome by supplementing natural gas, with hydrogen and using it in low-cost internal combustion engines.

Although lean-burn has been widely accepted as a viable approach to lowering exhaust emissions, achieving it with conventional fuels has not been as successful as exhaust catalyst systems. Finding the best application for hydrogen-supplemented lean-burn technology depends greatly on the nature of the engine loads and the standards used to test for exhaust emissions.

A significant philosophical difference between lean-burn and catalysts for controlling exhaust emissions is that lean-burn does not create the pollutants while catalysts chemically convert them. Understanding this basic difference is the key to recognizing the relative merits of each approach. Because pollutants are not created using the lean-burn technology, the types and frequency of engine loads are inconsequential to emission levels. With catalyst systems, the temperature of the catalyst is extremely important in determining the efficiency of emissions control. When catalyst temperatures are too low, as exists when a vehicle is first started, catalyst efficiency is poor. When catalyst temperatures are too high, the catalyst is degraded. Both scenarios result in high exhaust emissions. Therefore, engine loading and the frequency of those loads are very important in determining how catalyst systems work because they affect catalyst temperature. Given this technology base, heavy-duty transportation is the area where hydrogen-supplemented natural gas utilizing high charge dilution strategies can have the most significant impact on urban air quality.

Producing ultra-low exhaust emissions from heavy-duty vehicles differs markedly from that of light-duty vehicles. The most significant reason for this difference has to do with the relative power-to-weight ratios between the two. Light-duty engines typically produce much more ultimate power than is required by the emissions certification driving test. On the other hand, the engines used in heavy-duty applications typically are operated at their maximum power level most of the time, and the heavy-duty emissions test mirrors that use. Where this impacts emissions reduction technology is the effect that charge dilution (adding excess gases to the air-fuel mixture over what is required for stoichiometric combustion) has on engine power.

Charge dilution, whether it be excess air (lean-burn) or recirculated exhaust gases (EGR) or a combination of the two, is an extremely effective method of producing very low NO_x emissions. The support of complete combustion under these extreme charge diluted conditions is the rationale for using hydrogen in the fuel mix. The disadvantage to charge dilution is the reduction in the engine's maximum power output. This reduction in maximum power is the key to understanding why emissions control between light-duty and heavy-duty applications are significantly different.

The most effective way to recuperate lost engine power is to move more air through the engine. This is typically achieved by super/turbocharging or increasing engine rotational speed. Both of these techniques are readily implemented into light-duty engines. However, for heavy-duty engines, these techniques are not necessarily viable solutions. In the first place, heavy-duty engines are already turbocharged with significant levels of boost pressure to achieve high brake mean effective pressure (BMEP) at low rpm. Secondly, they are not readily adaptable to increased engine speed due to their extremely high reciprocating mass and low bore-to-stroke ratios. Therefore, using extremely high boost pressures (~ 2-3 bar) with existing heavy-duty engines would create large parasitic loads and reduce fuel efficiency. Increasing engine speed on these heavy pieces would seriously compromise reliability. These observations along with the fact that heavy-duty engines operate a great deal at maximum output, creates a serious problem for using charge dilution as

a technique for lowering heavy-duty vehicle emissions with existing engine platforms.

The solution to this problem is to create an alternative engine platform that is designed for high charge dilution with the ability to produce power characteristics equivalent to those of current engines. Equivalent power characteristics are an important consideration. Not only is maximum engine power output important, but the maximum engine torque and the rpm for maximum torque are also important.

Approach

NRG Technologies, Inc. is using charge dilution as the mechanism for controlling harmful exhaust emissions. The basic technique employed is to combine EGR and lean-burn. Cooled and dried EGR will be used to control NO_x emissions, and lean-burn will be employed to control CO and NMHC emissions. It is anticipated that lean-burn will be employed to achieve approximately 2 to 4% oxygen in the exhaust. This will allow an off-the-shelf oxidizing catalyst to achieve very high conversion rates for both CO and NMHC emissions. Because the exhaust gas temperatures will be comparatively very low (<1000^{o}F), catalyst lifetime will be extremely high (>100,000 miles).

To achieve near-zero NO_x emissions, (10 to 20 ppm) using charge dilution, the engine must operate with an overall lambda (including EGR) of between 1.8 and 2.0. To achieve this value, at least 30%, by volume, of the fuel must be hydrogen. Any less than that will not support sufficiently consistent combustion from cylinder-to-cylinder or from cycle-to-cycle. Any attempts to achieve this through mechanical means (high turbulence combustion chambers, etc.) will result in (1) loss of engine efficiency through increased combustion chamber heat transfer rates and (2) increased NO_x emissions compared to "quiescent" or open combustion chambers and hydrogen addition to the fuel. The result is that mechanical enhancement (swirl, tumble, etc.) for lean-burn will require higher values of lambda to achieve equivalent NO_x emissions to that achieved by hydrogen-enhanced fuel.

Given the constraints for modifying existing heavy-duty engines, NRG proposes to develop an engine platform specifically-designed for high charge dilution that will create the same power characteristics to the rear wheels as the original natural gas or diesel engine. This is accomplished as follows:

- Large displacement engine:
  - An 8.8L V8 engine
- Turbocharging to increase BMEP
- Increased engine speed with gear reduction:
  - Using 8 cylinders rather than 6 allows greater engine rpm for the same engine displacement.
  - A gearset mounted on the rear of the engine to match the torque and speed characteristics of the original natural gas or diesel engine. The existing transmission can be retained.

The main drawback to NRG's approach will be the tendency to increase the frictional horsepower of the engine. All other things being equal, this will result in increased fuel consumption. There are many ways to combat this problem. They include the following:

- Higher values of lambda result in higher thermodynamic performance.
- Ratio of specific heats is higher which results in higher theoretical Otto Cycle efficiency.
- Very light valve train utilizing low spring pressure valve springs and low friction components (roller rockers and lifters).
- Cylinder coatings with low friction coefficients.
- Nickel-Silicon Carbide (currently used by BMW, Mercedes, and Porsche).

The overall engine package is controlled by an engine control module. The same basic package that NRG has used for electronic fuel, ignition, and actuator controls on all of their light-duty vehicles will also be used for this heavy-duty engine.

The test project will include the evaluation of exhaust emissions, engine performance, engine reliability, and vehicle performance. During Phase I, exhaust emissions were verified using a steady-state simulation of the Federal Driving Test. For Phase II of the project, emissions will be verified by a vehicle

driving test conducted at CAVTEC, an independent testing laboratory in Oakland, CA. For the on-the-road testing to be conducted in Las Vegas, an on-board data acquisition system (Campbell Scientific) with cell phone access will be installed on the bus. The measurements anticipated to be monitored include:

- Engine oil, water, and intake air temperatures
- Turbocharger boost pressure
- Engine rpm
- Throttle position
- Vehicle speed

Fuel economy will be measured using records of gas usage vs. bus mileage.

The maintenance program for Phase II will include:

- Periodic oil analysis
- Training of city personnel for:
  - Engine oil usage
  - Gearbox oil usage
  - Filter replacements
  - Gearbox troubleshooting

Results

A 30-ft. transit bus was purchased by DOE and shipped to NRG Tech for conversion to HCNG operation. This bus came equipped with a Cummins 8.3L natural gas engine. The project called for characterizing the exhaust emissions from the current configuration so that the benefits of HCNG can be quantitatively assessed. Baseline exhaust emissions were taken from the engine using a steady-state emissions test protocol that is designed to simulate the heavy-duty driving test procedure. This protocol is as follows:

Engine rpm at Maximum Torque Value

Test Point 1	100% load	Emissions are 15% of weighted value
Test Point 2	75% load	Emissions are 15% of weighted value
Test Point 3	50% load	Emissions are 15% of weighted value
Test Point 4	10% load	Emissions are 10% of weighted value

Engine rpm at Maximum Power Value

Test Point 5	100% power	Emissions are 10% of weighted value
Test Point 6	75% power	Emissions are 10% of weighted value
Test Point 7	50% power	Emissions are 10% of weighted value
Test Point 8	Idle	Emissions are 15% of weighted value

The results of testing the Cummins engine that was installed in this bus using the protocol listed above are shown in Table 1.

Emissions results for the 8.8L NRG engine using the same testing protocol and using a 30/70 mixture of hydrogen and natural gas are shown in Table 2.

The final configuration for the 8.8L NRG engine consists of the following:

- 8.8L aluminum V8 engine
- Nickel-silicon carbide coated cylinder sleeves
- DIS ignition system
- Fuel injection system with feedback control
- Fully computer-controlled engine management system

Conclusions

Emissions, power, torque, and efficiency goals have been met. NO_x emissions have been reduced by a factor of 20 when compared to the existing engine without a loss of power, torque characteristics, or fuel efficiency. Major milestones for the remainder of the project will be to demonstrate drivability in an operating bus and verify exhaust emissions in a driving test.

Table 1. 8 Mode Steady State Emissions Summary
Cummins 8.3L Natural Gas Engine (as received)

Individual Modes	NOx g/hp-hr	THC g/hp-hr	NMHC (g/hp-hr)	CO g/hp-hr	Weighting Factor
1400 rpm - 100% Load	7.42	5.21	0.16	0.19	0.15
- 75% Load	4.70	2.57	0.08	0.22	0.15
- 50% Load	5.67	3.37	0.10	0.25	0.15
- 10% Load	5.77	7.70	0.23	0.59	0.10
2400 rpm - 100% Load	1.18	2.82	0.08	0.28	0.10
- 75% Load	0.80	4.26	0.13	0.32	0.10
- 50% Load	0.44	5.56	0.17	0.37	0.10
800 rpm - Idle	6.96	107.74	3.23	12.98	0.15
Weighted 8 Mode (g/hp-hr)	4.60	19.87	0.58	2.20	
Weighted 8 Mode (g/kw-hr)	6.16	26.63	0.78	2.95	

Table 2. 8 Mode Steady State Emissions Summary
NRG Hydrogen-Enriched Natural Gas Bus Engine

Individual Modes	NOx g/hp-hr	THC g/hp-hr	NMHC (g/hp-hr)	CO g/hp-hr	Weighting Factor
1800 rpm - 100% Load	0.37	3.70	0.07	0.00	0.15
- 75% Load	0.20	5.80	0.10	0.00	0.15
- 50% Load	0.10	5.48	0.10	0.00	0.15
- 10% Load	0.25	5.10	0.10	0.00	0.10
2800 rpm - 100% Load	0.10	5.63	0.26	0.00	0.10
- 75% Load	0.09	4.71	0.19	0.00	0.10
- 50% Load	0.11	6.01	0.26	0.00	0.10
800 rpm - Idle	0.40	17.44	0.36	0.00	0.15
Weighted 8 Mode (g/hp-hr)	0.22	7.00	0.18	0.00	
Weighted 8 Mode (g/kw-hr)	0.29	9.38	0.24	0.00	

Acronyms

A	Amp
AAS	Atomic Adsorption Spectroscopy
ACR	Autothermal Cyclic Reforming
ADVISOR	Advanced Vehicle Simulator
AES	Auger Electron Spectroscopy
AFC	Alkaline Fuel Cell
AFV	Alternative Fuel Vehicle
Ag	Silver
AHC	Ad Hoc Hydrogen Committee
AIAA	American Institute for Aeronautics and Astronautics
Al	Aluminum
Al/Si	Aluminosilicate
Al_2O_3	Aluminum Oxides
AMS	Accelerator Mass Spectrometry
ANL	Argonne National Laboratory
APCI	Air Products and Chemicals, Inc
APU	Auxiliary Power Unit
a-Si	Amorphous Silicon
a-Si:Ge	Amorphous Silicon/Germanium
a-SiC	Amorphous Silicon Carbide
ASNT	The American Society for Nondestructive Testing
ATDC	After Top Dead Center
atm	atmospheres
ATR	Autothermal Reformer
ATR	Auto-Thermal Reformer
Au	Gold
BDI	Boothroyd-Dewhurst, Inc.
BKI	Bevilacqua-Knight, Inc.
bmep	Brake Mean Effective Pressure
BN	Boron Nitride
BPSH	Bi-Phenol Sulfone
BTI	Breakthrough Technology Institute
C	Carbon
^oC	Degrees Celsius
C_2 plus	Hydrocarbon gases containing 2 or more carbon atoms
C_2H_4	Ethylene
CAD	Computer-Aided Drafting
CaFCP	California Fuel Cell Partnership
CaH_2	Calcium Hydride
CAM	Computer Aided Machining
CAM	Computer Aided Manufacture
CAO	Chlorophyll a Oxygenase
CARB	California Air Resources Board
CCD	Charge-Coupled Device
CCM	Catalyst Coated Membrane
CEM	Compressor Expander Module
CEM	Continuous Emissions Monitor
CESI	Catalystic Energy Systems, Inc.
CFD	Computational Fluid Dynamics
CGO	Gadolinium-Doped Ceria
CH_2	Compressed Hydrogen Gas
CH_2-ISS	Compressed Hydrogen Gas Integrated Storage System
CH_4	Methane
CIDI	Compressed Ignition Direct Injection
CIGS	Copper-Indium-Gallium-Diselenide
Chl	Chlorophyll
Cl	Chlorine
CLP	Corner Linked Polyhedral
cm	Centimeters
cm^2	Centimeters Squared
CMC	Carbonxymethylcellulose
CNG	Compressed Natural Gas
CO	Carbon Monoxide
Co	Cobalt
CO_2	Carbon Dioxide
COD	Chemical Oxygen Demand
CODH	Carbon Monoxide Dehydrogenase
Cr	Chromium
CSA	Canadian Standards Association
Cu	Copper
Cu/ZnO	Copper/zinc oxide
CVI	Chemical Vapor Infiltration
CWRU	Case Western Reserve University
DBM	Dibutyl Maleate
dc	Direct Current
DCM	Dichloromethane
DCSF	Diesel Combustion Simulation Facility
DECSE	Diesel Emission Control-Sulfur Effects
DEP®	Double Electrode Plate technology
DFMA	Design for Manufacturing and Assembly
DMAB	Dimethylamine Borane
DMFC	Direct Methanol Fuel Cell
DMI	Diversified Manufacturing Inc.
DOC	Diesel Oxidation Catalyst
DOE	Department of Energy
DPF	Diesel Particulate Filter

DPG	Distributed Power Generation
DSC	Differential Scanning Calorimeter
EC TC 105	International Electrotechnical Committee Technical Committee for Fuel
ECA	Electrochemical Surface Area
ECD	Energy Conversion Devices, Inc.
ECD-1	Emission Control Diesel-1
EDS	Energy Dispersive Spectroscopy
EDX	Electron Dispersive X-Ray
EGR	Exhaust Gas Recirculation
EIHP	European Integrated Hydrogen Project
ELV	End of Life Vehicle
EMC	Electro Magnetic Compatibility
EPAct	Energy Policy Act
ESR	Electron Spin Resonance
EtOH	Ethanol
eV	Electron Volts
EXAFS	Extended X-ray Absorption Fine Structure
^{o}F	Degrees Fahrenheit
FCC	Face-Centered Cubic
FCPS	Fuel Cell Power System
FCV	Fuel Cell Vehicle
Fe	Iron
FeO_2	Iron Oxide
FET	Field Effect Transistor
FG	Flared Gas
FHDS	Federal Highway Driving Schedule
Fl MH	Fluorinated Metal Hydride
FMEA	Failure Mode and Effects Analysis
FMEA	Failure Mode Evaluation and Analysis
FOS	Factor of Safety
FPS	Fuel Processing System
FreedomCAR	U.S. Department of Energy Automotive Research Partnership
FT	Fischer-Tropsch
FT100	Neat Fischer-Tropsch fuel
FTIR	Fourier Transform Infrared
FTP	Federal Test Procedure
FUDS	Federal Urban Driving Schedule
FY	Fiscal Year
g	Gas Phase
g/s	Gallons per Second
GA	General Atomics
Ga_2S_3	Gallium Sulfide
GeS_2	Germanium Sulfide
GeO_2	Germanium Oxide
GaN	Gallium Nitride
GC	Gas Chromatography
GC/MS	Gas Chromatography/Mass Spectrometry
GCG	Global Corporation Group
GDATP	General Dynamic Armaments and Technical Products
GDL	Gas Diffusion Layer
GE EER	GE Energy and Environmental Research Corporation
GHG	Greenhouse Gas
GHSV	Gas Hourly Space Velocity
GJ	Giga-Joule
GJ/t	Giga Joule per Metric Ton
gm	Gram
GRC	Global Research Center
GREET	Greenhouse gases, Regulated Emissions and Energy Use in Transportation
GTI	Gas Technology Institute
GTR	Global Technical Regulation
GV	Gasoline internal combustion engine Vehicle
h	Hours
H	Hydrogen
h^{-1}	per hour
$(H_2BNH_2)_x$	Polymeric Aminoborane
$(HBNH)_3$	Borazine
$(HBNH)_x$	Polyborazine
$H_2Ge_4S_9$	Dihydrogen Tetragermanium Sulfide
$H_4Ge_4S_{10}$	Tetrahydrogen Tetragermanium Sulfide
$H_4Ge_4S_{10}{\cdot}nH_2S$	Tetrahydrogen Tetragermanium Sulfide with n Molecules of H_2S
$H_4Ge_4S_{10}{\cdot}xH_2S$	Tetrahydrogen Tetragermanium Sulfide with x Molecules of H_2S
H_2-O_2	Hydrogen and Oxygen Gas Mixture
H_2	Hydrogen
H_2BNH_2	Monomeric Aminoborane
H_2O	Water
H_2S	Hydrogen Sulfide
H_2SO_4	Sulfuric Acid
H_3BNH_3	Ammonia-Borane Complex
HAD	Hydrogen Adsorption/Desorption
HALT	Highly Accelerated Life Testing
HAZOP	Hazardous Operations
HC	Hydrocarbon
ΔH_c°	Heat of Combustion
HCI	Hydrochloric Acid

HCN	Hydrochloric Cyanide
HCNG	Hydrogen Enriched Natural Gas
hcp	Hexagonal Close Pack
HCSCC	Hydrogen Codes and Standards Coordinating Committee
HDPE	High Density Polyethylene
HEV	Hybrid Electric Vehicle
ΔH_f°	Heat of Formation
HFA	Hydrogen Fueling Appliance
HFSF	High-Flux-Solar Furnace
HGS	Hydrogen Generating System
HHV	Higher Heating Value
H-ICE	Hydrogen- Internal Combustion Engine
HOGEN	Hydrogen Oxygen Generator
HOR	Hydrogen Oxidation Reaction
ΔH_r	Heat of Reaction
HRT	Hydraulic Retention Time
HRTEM	High-Resolution Transmission Electron Microscopy
HTAP	Hydrogen Technical Advisory Panel
HTM	High Temperature Membrane
HTM	Hydrogen Transport Membrane
HTPMWG	High-Temperature Polymer Membrane Working Group
HTS	High Temperature Shift
I^2R	Ohmic Resistances
ICC	International Code Council
ICE	Internal Combustion Engine
ICEV	Internal Combustion Engine Vehicle
INEEL	Idaho National Engineering & Environmental Laboratory
IPA	Isopropyl Alcohol
ISO TC 197	International Organization of Standardization Technical Committee for Hydrogen Technologies
ISS	Integrated Storage System
ITM	Ion Transport Membrane
JEVA	Japanese Electric Vehicle Association
JHU/APL	Johns Hopkins University Applied Physics Laboratory
JPL	Jet Propulsion Laboratory
K	Kelvin
K_2O	Potassium Oxide
kg	Kilogram
kj/mole	Kilo Joule
kJ/Mol-kilo	Joule per Mole
km	kilometers
KOH	Potassium Hydroxide
kPa	Kilopascal
Krpm	Thousands of Rotations per Minute
kW	Kilowatt
kWe	Kilowatt Electrical
L	Liter
LANL	Los Alamos National Laboratory
LCHPP	Low Cost Hydrogen Production Platform
LH_2	Cryogenic Liquid Hydrogen
LHV	Lower Heating Value
Li	Lithium
Li_2SO_4	Lithium Sulfate
$LiBH_4$	Lithium Borohydride
LiCl	Lithium Chloride
LiF	Lithium Flouride
LiH	Lithium Hydride
LII	Laser-Induced Incandescence
LME	London Metals Exchange
LNG	Liquefied Natural Gas
LPG	Liquefied Petroleum Gas (Propane)
LPM I	Liters Per Minute
LTS	Low Temperature Shift
M	Molar
M $HClO_4$	Molar Perchloric Acid
m^2Pa sec	Mole per Meter Squared Pascal Second (flux unit)
m^3/hr	Moles per hour cubed
mA	Milliamps
MBMS	Molecular-Beam Mass Spectrometer
MCH	Methylcyclohexane
MDSC	Modulated Differential Scanning Calorimetry
MEA	Membrane Electrode Assembly
MECA	Manufacturers of Emission Controls Association
MEMS	Micro Electro Mechanical Systems
MFC	Mass Flow Controller
Mg	Magnesium
mg	Milligram
MHSS	Metal Hydride Storage System
ML	Monolayer
mm	Millimeter
µm	Microns
MMSCFD	Million Standard Cubic Feet per Day Gas Flowrate
Mn	Manganese
Mo	Molybdenum
MOU	Memorandum of Understanding
MPR	Modular Pressurized Reformer

MSCFD	Thousand Standard Cubic Feet per Day Gas Flowrate
MSHA	Mine Safety and Health Administration
MSW	Municipal Solid Waste
MTS	Medium Temperature Shift
mV	Millivolt
mW	Megawatt
mW/mg	Milliwatts Per Milligram
N	Normal
N_2	Diatomic Nitrogen
NA	North American
NaCl	Sodium Chloride
NaF	Sodium Flouride
NADP	Nicotinamide Adenine Dinucleotide Phosphate
NaH	Sodium Hydride
$NaAlH_4$	Sodium Tetrahydroaluminate
Na_3AlH_6	TriSodium Hexahydroaluminate
Nb	Niobium
NCNR	NIST Center for Neutron Technology
NDIR	Non-Dispersive Infrared
NEDC	New European Drive Cycle
NETL	National Energy Technology Laboratory
NFC	Near Frictionless Carbon
NG	Natural Gas
NGASE	Natural-Gas-Assisted Steam Electrolyzer
NGCC	Natural Gas Combined-Cycle
NH_3	Ammonia
NH_4Cl	Ammonium Chloride
$(NH_4)_2SO_4$	Ammonium Sulfate
NHA	National Hydrogen Association
Ni	Nickel
NIST	National Institute of Standards and Technology
NL	Natural Luminosity
Nm	Nanometer
NMHC	Non-Methane Hydrocarbon
NMOG	Non-Methane Organic Gases
NMR	Nuclear Magnetic Resonance
NNA	Non-North American
NO_x	Nitrogen Oxides
NO_xEI	Nitrogen Oxide Index
NPD	Neutron Powder Diffractometer
NPV	Net Present Value
NREL	National Renewable Energy Laboratory
NRL	Naval Research Laboratory
O&M	Operating and Maintenance
O_2	Oxygen Gas or Diatomic Oxygen
OECD	Organization for Economic Cooperation and Development
OEM	Original Equipment Manufacturer
OEP	Octaethyl Porphyrin
ORNL	Oak Ridge National Laboratory
ORR	Oxygen Reduction Reaction
OTM	Oxygen Transport Membrane
P&ID	Piping and Instrumentation Diagram
PADT	Phoenix Analysis and Design Technologies
PAH	Polycyclic Aromatic Hydrocarbon
PCR	Polymerase Chain Reaction
Pd	Palladium
PDF	Pair Distribution Function
PDF	Pair-Density Function
PDU	Process Development Unit
PEC	Photoelectrochemical
PECVD	Plasma-Enhanced Chemical Vapor Disposition
PEM	Polymer Electrolyte Membrane
PEM	Proton Exchange Membrane
PEMFC	Proton Exchange Membrane Fuel Cell
PFA	Personal Fuel Appliance
PFCT	Porvair Fuel Cell Technology, Inc.
PFD	Process Flow Diagram
p-$GaInP_2$	Gallium Indium Phosphide
PGM	Platinum Group Metal
PHA	Personal Hazard Analysis
PM	Particulate Matter
PM	Precious Metal
PMV	Personal Mobility Vehicle
PNNL	Pacific Northwest National Laboratory
POEM	Porous Oxide Electrolyte Membrane
PO_x	Partial Oxidation
POx/SR	Partial Oxidation/Steam Reformer
ppm	Parts per Million
ppmv	Parts per Million Volume
ppmw	Parts per Million Weight
PQ	Plastoquinone
PROX	Preferential Oxidation
PrOx	Preferential Oxidizer
PSA	Pressure Swing Adsorption
PSI	Photosystem I
Psi	Pounds per Square Inch
PSIA	Pounds Per Square Inch Absolute

PSIG	Pounds Per Square Inch Gauge
PSII	Photosystem II
Pt	Platinum
Pt-FeO_x	Platinum-iron oxide
PV	Photovoltaic
R&D	Research and Development
RDE	Rotating-Disk Electrode
Re	Rhenium
RFG	Reformulated Gasoline
RH	Relative Humidity
Rh	Rhodium
ROI	Record of Invention
RPECS	Rapid Prototyping Electronic Control System
Ru	Ruthenium
$RuCl_3$	Ruthenium Chloride
Rx	Rubrivivax
s	Solid Phase
S/C	Steam/Carbon
S/cm	Siemens per centimeter
S_2	Sulfur
SAE	Society of Automotive Engineers
scc/hr/l	Standard Cubic Centimeters per Hour per Liter
sccm	Standard Cubic Centimeters per Minute
scfd	Standard Cubic Feet per Day
scfh	Standard Cubic Feet per Hour
scfm	Standard Cubic Feet per Minute
SCORE	Sandia/Caterpillar Optical Research Engine
SCP	Single Cell Protein
SD	Sputter Deposition
SECA	Solid State Energy Conversion Alliance
SEM	Scanning Electron Microscope
SEP	Subscale Engineering Prototype
SESHA	Semiconductor Environmental, Safety, and Health Association
SET	Sustainable Energy Technologies
SF_6	Sulfur Hexafluoride
SFTP	Supplemental Federal Test Procedure
SHE	Standard Hydrogen Electrode
S-HTS	Scrubber-High Temperature Shift
SiC	Silicon Carbide
SINL	Spatially Integrated Natural Luminosity
SiO_2	Silica Dioxide
slpm	Standard Liters per Minute
SMR	Steam Methane Reformer
SO_2	Sulfur Dioxide
SOFC	Solid Oxide Fuel Cell
SR	Steam Reformer
STAR	Substrate based Transportation application Autothermal Reformer
SUV	Sport Utility Vehicle
SWNT	Single Walled Nanotube
SWOP	Supercritical Water Partial Oxidation
SwRI	Southwest Research Institute
t/yr	tonnes/year
Ta	Tantalum
TBD	To Be Determined
TCD	Thermal Conductivity Detector
TCD	Thermocatalytic Decomposition
TCR	Thermocatalytic Reactor
TCR	Total Capital Requirement
TCUF	Thermochemical User's Facility
TEA	Technoeconomic Analysis
TEM	Transmission Electron Microscopy
TEM	Transmission Electron Photomicrograh
TGA-DSC	Thermogravimetric Analyzer-Differential Scanning
TGA-FTIR	Thermogravimetric Analyzer-Fourier Transform Infrared
TGC	Tail Gas Combustor
THC	Total Hydrocarbons
Ti	Titanium
($TiAl_{0.1}V_{0.04}$)	Metal Hydride Alloy
$TiCl_2$	Titanium Dichloride
$TiCl_3$	Titanium Trichloride
TiF_3	Titanium Triflouride
TiO_2	Titanium Dioxide
tla	truncated light-harvesting Chl antenna
TMI	Technology Management, Inc.
TPC	Total Plant Cost
TPGME	Tripropylene Glycol Monomethyl Ether
TPR	Temperature-Programmed Reduction
T-RFLP	Terminal Restriction Fragment Length Polymorphism
TVA	Thermovolumetric analyzer
UH	University of Hawaii
UIC	University of Illinois at Chicago
UTRC	United Technologies Research Center

V	Vanadium
V	Volt
VC	Vulcan carbon, XC-72
VFA	Volatile Fatty Acids
VNT®	Variable Nozzle Turbine
VO_x	Vanadium Oxide
VRA	Vehicle Refueling Appliance
W	Tungsten
W	Watt
WGS	Water-Gas Shift
WHEC	World Hydrogen Energy Conference
WHSV	Weekly Hourly Space Velocity
WO_3	Tungsten Oxide
Wt	Weight
Wt%	Weight Percent
WTW	Well-to-Wheels
XAS	X-ray Absorption Spectroscopy
XPS	X-ray Photoelectron Spectroscopy
XRD	X-ray Diffraction
XRF	X-ray Fluorescense
ZEV	Zero-Emission Vehicle
Zn	Zinc
ZnO	Zinc Oxide
Zr	Zirconium
ZrO_x	Zirconia Dioxide
Ωcm^2	Ohm-centimeter-squared

Appendix A. Draft DOE Technical Targets

Tables 1 through 3 list the DOE technical targets for PEM fuel cell stack systems, fuel-flexible fuel processors, and integrated fuel cell power systems operating on gasoline. Target values listed in these tables represent a self-consistent set and must be achieved simultaneously. Targets for 2010 are R&D milestones for the purpose of measuring progress, not necessarily the targets required for successful commercialization of the technology. Table 4 lists the DOE technical targets for integrated fuel cell power systems running on direct hydrogen. Table 5 shows the technical targets for on-board hydrogen storage, and Table 6 lists the technical targets for off-board hydrogen production and dispensing infrastructure. Tables 7 through 10 list technical targets for fuel cell stack and fuel processor components. All targets were developed with industry through preliminary vehicle system analyses and will be refined further as the technology matures and power system trade-offs are identified. Targets for hydrocarbon-based systems are based on operation with reformulated gasoline containing an average of 30 ppm sulfur (80 ppm maximum); except for the hydrogen storage targets in Table 5, all power target values indicate electric power (We).

Targets are reviewed on an annual basis and updated as necessary based on new information.

Table 1. Technical targets: fuel cell stack systems operating on hydrogen-containing fuel from a fuel processor (gasoline reformate) in 50 kWe (net) fuel cell systems

(Excludes fuel processing/delivery system)
(Includes fuel cell ancillaries: thermal, water, air management systems)
All targets must be achieved simultaneously and are consistent with those of FreedomCAR

Characteristics	Units	Calendar year		
		2001 status	2005	2010
Stack system power density[a,b]	W/L	200	400	550
Stack system specific power	W/kg	200	400	550
Stack system efficiency[c] @ 25% of rated power	%	45	50	55
Stack system efficiency[c] @ rated power	%	40	42	44
Precious metal loading[d]	g/rated kW	2.0	0.6	0.2
Cost[e]	$/kW	200	100	35
Durability[f]	hours	1000[g]	>2000[h]	>5000[i]
Transient response (time for 10% to 90% of rated power)	sec	3	2	1
Cold start-up time to rated power @ –20°C ambient temperature @ +20°C ambient temperature	 min min	 2 1	 1 0.5	 0.5 0.25
Survivability[j]	°C	–20	–30	–40
CO tolerance[k] steady state (with 2% maximum air bleed) transient	 ppm ppm	 50 100	 500 500	 500 1000

[a]Power refers to net power (i.e., stack power minus auxiliary power requirements).

[b]Volume is "box" volume, including dead space, and is defined as the water-displaced volume times 1.5 (packaging factor). Power density includes ancillaries (sensors, controllers, electronics, radiator, compressor, expander, and air, thermal and water management) for stand alone operation.

[c]Ratio of output DC energy to lower heating value of hydrogen-rich fuel stream (includes converter for 300 V bus); ratio of rated power to 25% of rated power efficiencies unchanged, assuming continued proportional reduction in stack efficiency at higher current and proportional increase in compressor efficiency at higher flow rates.

[d]Equivalent total precious metal loading (anode+cathode): 0.1 mg/cm^2 by 2010 at rated power. Precious metal target based on cost target of <$3/kW precious metals in MEA [@$450/troy ounce ($15/g), <0.2 g/kW]

[e]High-volume production: 500,000 units per year.

[f]Performance targets must be achieved at the conclusion of the durability period; durability includes tolerance to CO, H_2S and NH_3 impurities.

[g]Continuous operation (pertains to full power spectrum).

[h]Includes thermal cycling.

[i]Includes thermal and realistic driving cycles.

[j]Performance targets must be achieved at the end of 8-hour cold-soak at temperature.

[k]CO tolerance requirements assume capability of fuel processor to reduce CO. Targets for the stack CO tolerance are subject to trade-offs between reducing CO in the fuel processor and enhancing CO tolerance in the stack. It is assumed that H_2S is removed in the fuel processor.

Table 2. Technical targets: fuel processors[a] to generate hydrogen-containing fuel gas from reformulated gasoline containing 30 ppm sulfur, average, for 50 kWe (net) fuel cell systems

(Excludes fuel storage; includes controls, shift reactors, CO cleanup, heat exchangers)
All targets must be achieved simultaneously and are consistent with those of FreedomCAR

Characteristics	Units	Calendar year		
		2001 status[b]	2005	2010
Energy efficiency[c]	%	78	78	80
Power density	W/L	500	700	800
Specific power	W/kg	450	700	800
Cost[d]	$/kW	85	25	10
Cold start-up time to maximum power @ –20°C ambient temperature @+20°C ambient temperature	 min min	 TBD <10	 2.0 <1	 1.0 <0.5
Transient response (time for 10% to 90% power)	sec	15	5	1
Emissions[e]		<Tier 2 Bin 5	<Tier 2 Bin 5	<Tier 2 Bin 5
Durability[f]	hours	1000[g]	4000[h]	5000[i]
Survivability[j]	°C	TBD	–30	–40
CO content in product stream[k] steady state transient	 ppm ppm	 10 100	 10 100	 10 100
H_2S content in product stream	ppb	<200	<50	<10
NH_3 content in product stream	ppm	<10	<0.5	<0.1

[a]With catalyst system suitable for use in vehicles.
[b]Projected status for system to be delivered in late 2002: 80% efficiency, 900 W/L, 550 W/kg.
[c]Fuel processor efficiency = total fuel cell system efficiency/fuel cell stack system efficiency, where total fuel cell system efficiency accounts for thermal integration. For purposes of testing fuel-processor-only systems, the efficiency can be estimated by measuring the derated heating value efficiency (lower heating value of $H_2 \times 0.95$/ lower heating value of the fuel in) where the derating factor represents parasitic system power losses attributable to the fuel processor.
[d]High-volume production: 500,000 units per year.
[e]0.07 g/mile NO_x and 0.01 g/mile PM (particulate matter).
[f]Time between catalyst and major component replacement; performance targets must be achieved at the end of the durability period.
[g]Continuous operation.
[h]Includes thermal cycling.
[i]Includes thermal and realistic driving cycles.
[j]Performance targets must be achieved at the end of an 8-hour cold-soak at specified temperature.
[k]Dependent on stack development (CO tolerance) progress.

Table 3. Technical targets: 50 kWe (net) integrated fuel cell power systems operating on Tier 2 gasoline containing 30 ppm sulfur, average

(Including fuel processor, stack, auxiliaries)
(Excluding gasoline tank and vehicle traction electronics)
All targets must be achieved simultaneously and are consistent with those of FreedomCAR

Characteristics	Units	Calendar year		
		2001 status	2005	2010
Energy efficiency[a] @ 25% of rated power	%	34	40	45
Energy efficiency @ rated power	%	31	33	35
Power density	W/L	140	250	325
Specific power	W/kg	140	250	325
Cost[b]	$/kW	300	125	45
Transient response (time from 10 to 90% power)	sec	15	5	1
Cold start-up time to rated power @ –20°C ambient temperature @+20°C ambient temperature	 min min	 TBD <10	 2 1	 1 <0.5
Survivability[c]	°C	TBD	–30	–40
Emissions[d]		<Tier 2 Bin 5[e]	<Tier 2 Bin 5[e]	<Tier 2 Bin 5[e]
Durability[f]	hours	1000[g]	2000[h]	5000[i]
Greenhouse Gases	One-third reduction compared with conventional SI-IC engines in similar type vehicles			

[a]Ratio of dc output energy to the lower heating value of the input fuel (gasoline).
[b]Includes projected cost advantage of high-volume production (500,000 units per year) and includes cost for assembling/integrating the fuel cell system and fuel processor.
[c]Achieve performance targets at 8-hour cold-soak at temperature.
[d]Emissions levels will comply with emissions regulations projected to be in place when the technology is available for market introduction.
[e]0.07 NO_x g/mile and 0.01 PM g/mile.
[f]Performance targets must be achieved at the end of the durability time period.
[g]Continuous operation.
[h]Includes thermal cycling.
[i]Includes thermal and realistic drive cycles.

Table 4. Technical targets: 50 kWe (net) integrated fuel cell power systems operating on direct hydrogen[a]

All targets must be achieved simultaneously and are consistent with those of FreedomCAR

Characteristics	Units	Calendar year		
		2001 status	2005	2010
Energy efficiency[b] @ 25% of rated power	%	59	60	60
Energy efficiency @ rated power	%	50	50	50
Power density excluding H_2 storage including H_2 storage	 W/L W/L	 400 TBD	 500 150	 650 220
Specific power excluding H_2 storage including H_2 storage	 W/kg W/kg	 400 TBD	 500 250	 650 325
Cost[c] (including H_2 storage)	$/kW	200	125	45
Transient response (time from 10% to 90% of rated power)	sec	3	2	1
Cold start-up time to maximum power @ –20◦C ambient temperature @+20◦C ambient temperature	 sec sec	 120 60	 60 30	 30 15
Emissions		Zero	Zero	Zero
Durability[d]	hours	1000	2000[e]	5000[f]
Survivability[g]	◦C	-20	–30	–40

[a]Targets are based on hydrogen storage targets in an aerodynamic 2500-lb vehicle.
[b]Ratio of DC output energy to the lower heating value of the input fuel (hydrogen).
[c]Includes projected cost advantage of high-volume production (500,000 units per year).
[d]Performance targets must be achieved at the end of the durability time period.
[e]Includes thermal cycling.
[f]Includes thermal and realistic drive cycles.
[g]Achieve performance targets at 8-hour cold-soak at temperature.

Table 5. Technical targets for on-board hydrogen storage[a,b] subsystem

Characteristic	Units	Target	2001 Status Physical storage[c]	2001 Status Chemical storage[d]
Storage capacity[e]	wt%	6	5.2	3.4
Recoverable usable amount[f]	%	90	99.7	>90
Energy density[g]	Wh/L[h]	1100[h]	813	1300
Specific energy[i]	Wh/kg[h]	2000	1745	1080
Cost[j]	$/kWh	5	50[k]	18[l]
Cycle life	cycles	500	>500	20-50
Operating temperature[m]	°C	–40° to +50°C	–40° to +50°C	20°C to 50°C
Start-up time to full flow @+20°C @-20°C	 sec sec	 15 30	 <1 TBD	 <15 TBD
Refueling time	min	<5	TBD	TBD
Hydrogen loss	scc/hour/L	<1.0	<1.0	<1.0

[a]Based on lower heating value of hydrogen; includes both physical and chemical methods of hydrogen storage; enables greater than 300-mile range, based on an aerodynamic, 2500-lb vehicle.
[b]R&D carried out in collaboration with DOE Hydrogen Program.
[c]Includes compressed gas and cryogenic liquid tanks.
[d]Projected from laboratory-scale (100 g) test beds and proposed system designs.
[e]Weight percent H_2 is the weight of H_2 divided by the weight of (H_2 + tank).
[f]Recoverable stored hydrogen, e.g. in a 100-kg H_2 storage system containing 6 kg of stored hydrogen, at least 5.4 kg of useful hydrogen must be recoverable.
[g]Based on 5 kg hydrogen for >300 mile range at 10,000 psia (volume of stored hydrogen is 135 L). Allowing for 10% containment volume, system volume is 150 L..
[h]Watts thermal.
[i]Specific energy is the lower heating value energy of H_2 contained, divided by the weight of (H_2 + tank) .
[j]Based on high-volume production of 500,000 units per year.
[k]Based on individual tanks.
[l]Projected hydride material cost only; based on 100-200 kg alanate production.
[m]Hydrogen storage system must provide hydrogen to the fuel cell at these ambient temperatures.

Table 6. Technical targets for off-board hydrogen production and dispensing infrastructure					
Component	Characteristic (LHV Basis)	Units	Current Status[a]	2005	2010
Reforming	Cost	$/GJ H_2	9.9	8.8	7.7[b]
	WTW GHGs	g/km	75	70	65
	Primary Energy Eff.	% (LHV)	80[c]	82	85
Purification	Cost	$/GJ H_2	0.56	0.56	0.56[d]
	WTW GHGs[e]	g/km	1.1	1.1	1.1
	Primary Energy Eff.	% (LHV)	75[f]	82	90
Compression	Cost	$/GJ H_2	2.6	2.3	2.0[g]
	WTW GHGs	g/km	14	11	8
	Primary Energy Eff.	% (LHV)	82[h]	85	88
Storage & Dispensing	Cost	$/GJ H_2	2.7[i]	2.7	2.7[j]
	WTW GHGs	g/km	0	0	0
	Primary Energy Eff.	% (LHV)	100[k]	100	100
Total	Cost[l]	$/GJ H_2	19.2	17.2	16.2[m]
	WTW GHGs	g/km	90	82	75
	Primary Energy Eff.	% (LHV)	62	68	75

Notes: Well-to-wheel greenhouse gas (WTW GHG) emissions are weighted by their global warming potential. Assumes 84-mpeg fuel economy in a direct hydrogen FCV and on-site power from the US average grid mix. Primary energy efficiency is defined as Hydrogen Output LHV / Primary Energy Input LHV of the process step. Primary energy associated with on-site power use assumes a 35% production and transmission efficiency penalty (typical US grid mix).

[a] Assumes state-of-the-art technology that is feasible but not necessarily available in a complete system today. This assumption is consistent with the automotive fuel cell performance target assumptions.

[B] Assumes energy cost reductions by way of higher efficiency and a 50% equipment cost reduction from the current scenario. Small-scale reformers are assumed to come down significantly in price with projected advances in materials and designs.

[C] Assuming a steam methane reformer operating at 10 atm.

[D] Assumes no equipment cost reduction from the current scenario. Conventional equipment (PSAs) will not likely come down significantly in price, especially with higher efficiency requirements. Advanced technologies may provide higher efficiencies, but are unlikely to be cheaper.

[E] Assumes 100% of the purification purge stream (primarily CO2, H2, CH4, and CO) is recycled to the production step, where the purge stream is burned to generate heat for the reforming process. There may be some additional purification emissions in other system configurations, but the total sum of emissions from the production and purification steps will remain the same.

[F] Assuming a small-scale PSA system operating at reformer outlet pressure.

[G] Assumes energy cost reductions by way of higher efficiency but no equipment cost reduction from the current scenario. Conventional equipment (gas compressors) will not likely come down significantly in price, especially with higher efficiency requirements. Advanced technologies may provide higher efficiencies, but are unlikely to be cheaper.

[H] Assuming conventional compressors are used from the PSA outlet pressure to 3600-psi maximum on-site storage pressure and accumulator-type compressors are used from the storage pressure to 5000 psi on-board storage.

[I] Based on 3600-psi on-site gas storage.

[J] Assumes no equipment cost reduction from the current scenario. Conventional equipment (high-pressure gas storage tanks) will not likely come down significantly in price. Advanced technologies may provide higher overall efficiencies, but are unlikely to be cheaper.

[K] Assuming high-pressure gas storage with no leaks during storage or dispensing.

[L] Includes operation, site prep, and central control costs.

[M] Costs are based on a hydrogen fueling station serving 300 vehicles per day (~10,000 std m3 per day) with on-site production. Capital equipment costs assume mature production volumes of 100 units per year. Production volumes of 100 units/year were also studied by DTI with analgous economic predictions. Production volumes of 10,000 units per year will reduce capital costs substantially to $13/GJ (See "Integrated Vehicle Analysis" DTI, 1998). Energy costs assume a natural gas price of $5/GJ (HHV) and power price of $0.07/kWh.

Table 7. Technical targets for fuel cell stack components

Component	Requirement
Membranes	Cost: $5/kW Stability: <2 mV w/RH 20–100% , <10% swelling H_2 crossover: <1 mA/cm^2 O_2 crossover: <3 mA/cm^2 Area specific resistance: 0.1 ohm-cm^2
Electrodes	Cost: $5/kW CO tolerance: 500 ppm steady state, 1000 ppm transient with 0.2 g Pt/rated kW Durability: 5000 hours Utilization: 85% H_2, 60% O_2
Membrane-Electrode Assembly	Performance: On hydrogen 400 mA/cm^2 at 0.80 V (at rated power) 100 mA/cm^2 at 0.85 V (at quarter power) On gasoline reformate 500 mA/cm^2 at 0.75 V (at rated power, 30 psig) 125 mA/cm^2 at 0.83 V (at quarter power, 9 psig) Cost: $10/kW
Bipolar Plates	Cost: $10/kW; <1kg/kW H_2 permeation rate: <2 $\times$ 10^{-6} cm^3 sec^{-1} cm^{-2} @ 80°C, 3 atm (Equivalent to <0.1 mA/cm^2) Corrosion limit: <16 microamps/cm^2 Resistivity: 0.02 ohm/cm^2

Table 8. Technical targets for sensors for automotive fuel cell systems[a]	
Sensor	Requirements
Carbon Monoxide	(a) 1–100 ppm reformate pre-stack sensor • Operational temperature: <150◦C • Response time: 0.1–1 sec • Gas environment: high-humidity reformer/partial oxidation gas: H_2 30–75%, CO_2, CO, N_2, H_2O at 1–3 atm total pressure • Accuracy: 1–10% full scale (b) 100–1000 ppm CO sensors • Operational temperature: 250 ◦C • Response time: 0.1–1 sec • Gas environment: high-humidity reformer/partial oxidation gas: H_2 30–75%, CO_2, CO, N_2, H_2O at 1–3 atm total pressure • Accuracy: 1–10% full scale (c) 0.1–2% CO sensor 250–800◦C • Operational temperature: 250–800◦C. • Response time: 0.1–1 sec • Gas environment: high-humidity reformer/partial oxidation gas: H_2 30–75%, CO_2, CO, N_2, H_2O at 1–3 atm total pressure • Accuracy: 1–10% full scale
Hydrogen in fuel processor output	• Measurement range: 1–100% • Operating temperature: 70–150◦C • Response time: 0.1–1 sec for 90% response to step change • Gas environment: 1–3 atm total pressure, 10–30 mol % water, 30–75% total H_2 , CO_2, N_2 • Accuracy: 1–10% full scale
Hydrogen in ambient air (safety sensor)	• Measurement range: 0.1–10% • Temperature range: –30 to 80◦C • Response time: under 1 sec • Accuracy: 5% • Gas environment: ambient air, 10–98% RH range • Lifetime: 5 years • Interference resistant (e.g., hydrocarbons)
Sulfur compounds (H_2S, SO_2, organic sulfur)	• Operating temperature: up to 400◦C • Measurement range: 0.05–0.5 ppm • Response time: <1 min at 0.05 ppm • Gas environment: Hydrogen, CO, CO_2, hydrocarbons, water vapor
Flow rate of fuel processor output	• Flow rate range: 30–300 standard L/min • Temperature: 80◦C • Gas environment: high-humidity reformer/partial oxidation gas: H_2 30–75%, CO_2, N_2, H_2O, CO at 1–3 atm total pressure
Ammonia	• Operating temperature: 70–150◦C • Measurement range: 1–10 ppm • Selectivity: <1 ppm from matrix gases • Lifetime: 5–10 years • Response time: seconds • Gas environment: high-humidity reformer/partial oxidation gas: H_2 30–75%, CO_2, N_2, H_2O, CO at 1–3 atm total pressure

Table 8. Technical targets for sensors for automotive fuel cell systems[a]

Sensor	Requirements
Temperature	• Operating range: –40 to 150°C • Response time: in the –40 to 100°C range <O.5 sec with 1.5% accuracy; in the 100–150°C range, a response time <1 sec with 2% accuracy • Gas environment: high-humidity reformer/partial oxidation gas: H_2 30–75%, CO_2, N_2, H_2O, CO at 1–3 atm total pressure • Insensitive to flow velocity
Relative humidity for cathode and anode gas streams	• Operating temperature: 30–110°C • Relative humidity: 20–100% • Accuracy: 1% • Gas environment: high-humidity reformer/partial oxidation gas: H_2 30–75%, CO_2, N_2, H_2O, CO at 1–3 atm
Oxygen in fuel processor and at cathode exit	(a) Oxygen sensors for fuel processor reactor control • Operating temperature: 200–800°C • Measurement range: 0–20% O_2 • Response time: <0.5 sec • Accuracy: 2% of full scale • Gas environment: high-humidity reformer/partial oxidation gas: H_2 30–75%, CO_2, N_2, H_2O, CO at 1–3 atm (b) Oxygen sensors at the cathode exit • Measurement range: 0–50% O_2 • Operating temperature: 30–110°C • Response time: <0.5 sec • Accuracy: 1% of full scale • Gas environment: H_2, CO_2, N_2, H_2O at 1–3 atm total pressure
Differential pressure in fuel cell stack	• Range: 0–1 psi or (0–10 or 1–3 psi, depending on the design of the fuel cell system) • Temperature range: 30–100°C • Survivability: –40°C • Response time: <1 sec • Accuracy: 1% of full scale • Size: $\leq$1 in^2, usable in any orientation • Other: Withstand and measure liquid and gas phases

[a]Sensors must conform to size, weight, and cost constraints of automotive applications.

Table 9. Technical targets for compressor/expander (C/E) units for automotive fuel cell systems[a]

Characteristic	Units	Target
Input power[b] at full flow	kW	4.3
Efficiency at full flow Compressor (at 3.2 pressure ratio)[c] Expander	 % %	 75 90
Efficiency @ 20% of full flow Compressor (at 1.6 pressure ratio)[c] Expander	 % %	 65 80
Volume[d]	L	4
Weight[d]	kg	3
Cost[d,e]	$	200
Turndown ratio		10
Noise	db	<80

[a]Targets are being reviewed as a result of the Compressor Peer Review.

[b]Input power to the controller to power a compressor/expander system producing 76 g/sec (dry) maximum flow. This flow rate roughly corresponds to maximum power for a 50-kW fuel cell system. A 25% flow is 19 g/sec. Expander inlet conditions are assumed to be: 82 g/sec, 150°C, and 2.8 atm (at full flow).

[c]The pressure ratio is allowed to float as a function of load on the fuel cell system (i.e., as a function of the flow through the compressor/expander unit).

[d]Weight, volume, and cost do not include the motor/controller or heat rejection (if required).

[e]Cost target based on a manufacturing volume of 100,000 units per year.

Table 10. Technical targets for fuel processor catalysts and reactors (for reforming Tier II gasoline containing 30 ppm Sulfur)[a]

Characteristic	Units	Autothermal reformer	Sulfur removal	Water gas shift	CO preferential oxidation
GHSV[b]	per hour	200,000	50,000	30,000	150,000
Conversion[c]	%	>99.9	>99.95	>90	>99.8
H2 selectivity[d] (or consumption)	%	>80	<0.1	>99	<0.2
Volume[e]	L/kWe	<0.013	<0.06	<0.1	<0.02
Weight[e]	kg/kWe	<0.015	<0.06	<0.1	<0.03
Durability[f]	hours	5000	5000	5000	5000
Cost	$/kWe	<5	<1	<1	<1

[a]GHSV (gas hourly space velocity) = the volumetric flow rate of the product gases reduced to 25°C and 1 atm, divided by the bulk volume of the catalyst.

[b]Target values are guidelines for single reactor R&D; system/subsystem targets take precedence.

[c]Conversion: (moles of reactant in – moles of reactant out) × 100/(moles of reactant in).

[d]Selectivity: At the autothermal reformer: (moles of H_2 in product) × 100/(moles of H_2 "extractable" from the reformer feed); at the shift reactor: (moles CO converted to H_2) × 100/(total moles of CO converted).

[e]The volume and weight targets include only the catalysts, not the hardware needed to house the catalysts or any heat exchangers.

[f]Over standard driving cycles.

Index of Primary Contacts

Printed with a renewable-source ink on paper containing at least 50% wastepaper, including 20% postconsumer waste

Hydrogen, Fuel Cells and Infrastructure Technologies Program 2002 Annual Progress Report

WWW.EREN.DOE.GOV/HYDROGEN

DOE/EERE/HFIT - 2002/001